OCRWM	MODEL COVER SHEET	1. QA: QA Page 1 of 484

2. Type of Mathematical Model

☒ Process Model ☒ Abstraction Model ☐ System Model

Describe Intended Use of Model

The principal intentions of this model and analysis activity are:

- Evaluate the changes in the chemical environment that affect drip shield degradation, waste package degradation, and radionuclide migration through the invert.
- Provide valid models that will be used for the future integration of EBS thermal, hydrological, and chemcial (THC) processes, which directly support the TSPA model.
- Evaluate uncertainties associated with the model

3. Title

Engineered Barrier System: Physical and Chemical Environment Model

4. DI (including Rev. No. and Change No., if applicable):

ANL-EBS-MD-000033 Rev 02

5. Total Attachments	6. Attachment Numbers - No. of Pages in Each
4	I-10 (with attached CD ROM), II-68, III-60, IV-50

	Printed Name	Signature	Date
7. Originators	Darren M. Jolley Russell Jarek Paul Mariner	SIGNATURE ON FILE SIGNATURE ON FILE SIGNATURE ON FILE	2/5/04 2-5-04 2-5-04
8. CSO	Bruce Kirstein	SIGNATURE ON FILE	2/5/04
9. Checker	Charles Bryan (Lead)	SIGNATURE ON FILE	2/5/04
10. QER	Judy Gebhart	SIGNATURE ON FILE	2/6/04
11. Responsible Manager/Lead	Cliff Howard	SIGNATURE ON FILE	2-9-04
12. Responsible Manager for	Paul Dixon Ernest Hardin	SIGNATURE ON FILE	2-9-04

13. Remarks

The following individuals also contributed to portions of this document:

Patricia Bernot, Carlos Jove-Colon, Paul Cloke, Cliff Howard, Milton Hsieh, Susan LeStrange, Richard Metcalf, David Mirc, David Shields, Eric Sorensen, Terry Steinborn, Mary Turner, Yifeng Wang, and Kaveh Zarrabi.

This document also replaces the following technical reports, prepared previously for the site recommendation report:

ANL-EBS-MD-000040 Rev 00, *In-Drift Gas Flux and Composition*; ANL-EBS-MD-000041 Rev 00, *In-Drift Corrosion Products*; ANL-EBS-MD-000044 Rev 00, and *Physical and Chemical Environment Abstraction Model*

The following Condition Reports (CR's) can be closed with the issuance of this report:

CR 201, CR 197, CR 198, CR 199, CR 194, CR 195, CR 148, and CR 132

The following TBV's can be closed with the issuance of this report:

3904, 3905, 4476, 4477, 4478, 4479, 4480, 4481, 4482, 4586, 4587, 4588, 4621, 4623, 4931, 4947, 4950, and 4953

INTENTIONALLY LEFT BLANK

CONTENTS

Page

1. PURPOSE 1-1
   1.1 SCOPE OF MODEL 1-1
   1.2 INTENDED MODEL USE 1-2
   1.3 MODEL LIMITATIONS 1-2

2. QUALITY ASSURANCE 2-1

3. USE OF SOFTWARE 3-1
   3.1 EQ3/6 V8.0 3-1
   3.2 GETEQDATA V1.0.1 3-1
   3.3 EXEMPT SOFTWARE USE 3-1

4. INPUTS 4-1
   4.1 DATA AND PARAMETERS 4-1
      4.1.1 Engineered Barrier System Committed Materials Inventory 4-1
      4.1.2 Material Corrosion Rates and Materials Compositions 4-10
      4.1.3 Water and Gas Compositions 4-12
      4.1.4 Thermodynamic Databases 4-17
      4.1.5 In-Drift Evaporation 4-17
      4.1.6 Dust Leachate Compositions 4-17
      4.1.7 Steel Corrosion Chemistry 4-21
      4.1.8 Inputs used for Sensitivity Studies 4-22
   4.2 CRITERIA 4-23
      4.2.1 Degradation of Engineered Barriers Acceptance Criteria 4-24
      4.2.2 Quantity and Chemistry of Water Contacting Engineered Barriers and Waste Forms–Acceptance Criteria 4-26
   4.3 CODES AND STANDARDS 4-31
      4.3.1 Codes 4-31
      4.3.2 Standards 4-31
   4.4 INPUTS USED FOR MODEL VALIDATION 4-33
      4.4.1 THC Seepage Abstraction Validation Inputs 4-33
      4.4.2 Precipitates/Salts Model Validation Inputs 4-33
      4.4.3 Evaporation of Dilute Salt Solutions 4-34
      4.4.4 Evaporation of Waters to Form Concentrated Brines 4-35
      4.4.5 Deliquescence Point Comparison 4-36
      4.4.6 Chromium Calculation 4-36

5. ASSUMPTIONS 5-1
   5.1 DISCUSSION OF ASSUMPTIONS IN UPSTREAM DOCUMENTATION 5-1
      5.1.1 Standard State of Liquid Phase (Assumption 5.1 of the In-Drift Precipitates/Salts Model) 5-1
      5.1.2 Equilibrium Conditions (Assumption 5.2 of the IDPS Model) 5-2
   5.2 ASSUMPTIONS INTERNAL TO PHYSICAL AND CHEMICAL ENVIRONMENT MODEL 5-2

CONTENTS (Continued)

Page

5.2.1 Repository Location 5-2
5.2.2 Representative Distribution of Seepage Water Compositions 5-3
5.2.3 Representative Distribution of Dust and Dust Leachate Compositions 5-3

6. MODEL DISCUSSION 6.1-1
6.1 MODELING OBJECTIVES 6.1-1
6.2 ENGINEERED BARRIER SYSTEM PHYSICAL AND CHEMICAL ENVIRONMENT MODEL CONCEPTUAL MODEL 6.2-1
6.2.1 Integrated Perspective on the Evolution of the Engineered Barrier System Physical and Chemical Environments 6.2-1
6.2.2 Evolution of Engineered Barrier System Chemical Environments by Process 6.2-1
6.2.3 Evolution of Engineered Barrier System Chemical Environments by Spatial Location 6.2-5
6.2.4 Engineered Barrier System Physical and Chemical Environment Conceptual Model Locations 6.2-7
6.3 COUPLED PROCESSES 6.3-1
6.4 INTRODUCED MATERIALS 6.4-1
6.4.1 Material Corrosion Rates 6.4-1
6.4.2 Material Lifetimes 6.4-11
6.4.3 Materials Compositions 6.4-12
6.5 GEOCHEMICAL MODELING CONSTRAINTS 6.5-1
6.5.1 Mathematical Models Implemented by the Use of EQ3/6 V8.0 Geochemical Modeling Software 6.5-1
6.5.2 Geochemical Modeling Methodology 6.5-7
6.5.3 Equilibrium versus Kinetics 6.5-8
6.5.4 Engineered Barrier System Geochemical Equilibrium Modeling 6.5-9
6.5.5 Rationale for Including or Excluding Precipitating Minerals 6.5-13
6.6 INCOMING SEEPAGE COMPOSITION ABSTRACTION 6.6-1
6.6.1 Conceptual Framework Summary for the Thermal-Hydrological-Chemical Seepage Abstraction 6.6-1
6.6.2 Sort Waters by Point in Time, Quadrant, Fracture/Matrix, Zone, and Index (Step 1) 6.6-2
6.6.3 Evaporate Waters to a Common Degree of Concentration (Step 2) 6.6-4
6.6.4 Seepage Water Composition Bin Generation (Step 3) 6.6-6
6.6.5 Choice of Representative Seepage Water for Each Bin (Step 4) 6.6-8
6.6.6 Abstraction of THC Model Outputs - Defining Time-Sequences of Bins that Approximate Seepage Water Composition Time-Histories from THC Model Outputs (Step 5) 6.6-10
6.6.7 Impact Analysis Due to Errors Found During Check Process 6.6-12
6.7 EVOLUTION OF IN-DRIFT GAS AND TEMPERATURE 6.7-1
6.7.1 O_2 Mass Balance Evaluations 6.7-1
6.7.2 Thermal-Hydrological-Chemical Seepage Model In-Drift CO_2 Gas and Temperature Abstraction 6.7-4

CONTENTS (Continued)

Page

6.7.3 Thermal-Hydrological-Chemical Seepage Water Equilibrium Gas Fugacities 6.7-11
6.7.4 Dust Leachate Equilibrium Gas Fugacities 6.7-11
6.8 GROUND SUPPORT INTERACTIONS WITH SEEPAGE WATER 6.8-1
6.8.1 Corrosion Products Concepts 6.8-1
6.8.2 Definition of Base Case 6.8-5
6.8.3 Abstraction of 316L Stainless Steel and its Corrosion Rate 6.8-7
6.8.4 Abstraction and Base Case Limitations 6.8-8
6.9 IN-DRIFT SEEPAGE EVAPORATION 6.9-1
6.9.1 Seepage Water Inputs 6.9-1
6.9.2 Temperature and Carbon Dioxide 6.9-1
6.9.3 Lookup Tables 6.9-5
6.9.4 Illustration of Results 6.9-9
6.10 IN-DRIFT DUST LEACHATE ANALYSES 6.10-1
6.10.1 Conceptual Framework 6.10-1
6.10.2 Evaluation of U.S. Geological Survey Datasets 6.10-1
6.10.3 Equilibrium of Dust Leachate Waters 6.10-3
6.10.4 Calculation of Mineralogy at Dryout 6.10-4
6.10.5 Dust Leachate Abstraction 6.10-6
6.10.6 Development of Lookup Tables for Total Systems Performance Assessment - License Application 6.10-18
6.10.7 Illustration of Results 6.10-23
6.11 ALTERNATE CONCEPTUAL MODELS 6.11-1
6.11.1 Alternative Binning of Seepage 6.11-1
6.11.2 Transport Affected Salt Assemblages 6.11-11
6.11.3 Brine Compositions Due to Dust Deliquescence 6.11-12
6.12 EVALUATION OF KEY UNCERTAINTIES 6.12-1
6.12.1 Uncertainties and Variabilities in the Inputs from THC Model Calculations 6.12-2
6.12.2 Uncertainties in the In-Drift Precipitates/Salts Model that Affect Characterization and Binning of Seepage Water Compositions 6.12-4
6.12.3 Discretization Error Associated with Binning Abstractions 6.12-5
6.12.4 Factors Showing No Significant Impact on Water Chemistry 6.12-9
6.12.5 Implementing Uncertainties in the TSPA-LA Abstraction Look-Up Tables 6.12-23
6.13 ENGINEERED BARRIER SYSTEM CHEMICAL ENVIRONMENT 6.13-1
6.13.1 Engineered Barrier System Seepage Chemistry 6.13-7
6.13.2 Engineered Barrier System Dust Deliquescence Chemistry 6.13-11
6.13.3 Lookup Table Interpolation for Seepage and Deliquescence Conditions 6.13-14
6.13.4 Chemical Environments on the Drip Shield and Waste Package 6.13-15
6.13.5 The Chemical Environment in the Invert 6.13-19
6.14 FEATURES, EVENTS AND PROCESSES EVALUATION 6.14-1
6.15 IMPLEMENTATION INSTRUCTIONS FOR TOTAL SYSTEM PERFORMANCE ASSESSMENT-LICENSE APPLICATION MODEL 6.15-1

CONTENTS (Continued)

Page

6.15.1 Implementation of Engineered Barrier System Chemistry on Waste Package Surfaces 6.15-1
6.15.2 Implementation of Engineered Barrier System Chemistry in the Invert 6.15-5

7. VALIDATION 7-1
7.1 VALIDATION CRITERIA 7-1
7.2 MODEL ABSTRACTION VALIDATION CASES 7-2
7.2.1 Comparison of THC Seepage Abstraction with THC Seepage Model Output 7-2
7.2.2 Comparison of Lookup Table Interpolations with P&CE Model Results 7-3
7.3 IN DRIFT PRECIPITATES/SALTS MODEL VALIDATION DISCUSSION 7-4
7.3.1 Experimental Evaporation Data 7-5
7.3.2 Evaporation of Dilute Salt Solutions 7-8
7.3.3 Comparison of Data0.ypf and Data0.ymp.R2 Database Predictions 7-8
7.3.4 Validation for Mineral Outputs 7-9
7.4 EVAPORATION OF SIERRA NEVADA SPRING WATERS TO FORM CONCENTRATED BRINES 7-10
7.5 DELIQUESCENCE POINT COMPARISON 7-11
7.6 MINERAL PRECIPITATION 7-14
7.7 CHROMIUM CALCULATIONS 7-16

8. CONCLUSIONS 8-1
8.1 SUMMARY OF MODEL FINDINGS 8-1
8.2 SUMMARY OF MODEL ABSTRACTION FOR TOTAL SYSTEM PERFORMANCE ASSESSMENT 8-2
8.2.1 Summary of the Total System Performance Assessment Look-up Tables 8-2
8.2.2 Data Tracking Numbers for Data Generated in This Report 8-3
8.3 MODEL UNCERTAINTY AND RESTRICTIONS 8-8
8.4 YUCCA MOUNTAIN REVIEW PLAN CRITERIA ASSESSMENT 8-9
8.4.1 Degradation of Engineered Barriers Acceptance Criteria 8-9
8.4.2 Quantity and Chemistry of Water Contacting Engineered Barriers and Waste Forms–Acceptance Criteria 8-15

9. INPUTS AND REFERENCES 9-1
9.1 DOCUMENTS CITED 9-1
9.2 CODES, STANDARDS, AND REGULATIONS 9-16
9.3 DATA, LISTED BY DIRS 9-18
9.4 PROJECT SOFTWARE SOURCES 9-20
9.5 OUTPUT DATA, LISTED BY DATA TRACKING NUMBER 9-20

CONTENTS (Continued)

Page

ATTACHMENT I – SUPPORTING FILES ON CD ROM I-1

ATTACHMENT II – T-H-C SEEPAGE LOOKUP TABLE RESULTS II-1

ATTACHMENT III – DUST LEACHATE LOOKUP TABLE RESULTS III-1

ATTACHMENT IV – CRITIQUE OF EXCLUDED MINERALS IV-1

INTENTIONALLY LEFT BLANK

FIGURES

Page

4.4-1. Three-Species Model for Chromium Solubility F4-1

5.2-1. Piper Plot of Water Compositions (meq/L) from Proposed Repository Units F5-1

6-1-1. General Location of Engineered Barrier System Components and Materials F-6.1-3
FO/ 6.1-1. Major EBS Environment Process Flowchart, with Section References F-6.1-5
6.2-1. Simplified Chemical Divides Diagram Based on Evaporative Concentration of Dilute Starting Waters to Form a Suite of Naturally-Occurring Lake Waters F6.2-1
6.2-2. Schematic Illustration of Deliquescence and Evaporation F6.2-2
6.2-3. Calculated Solubilities Using the Pitzer Approach Compared to Experimental Data for the $MgCl_2$-H_2O Binary System F6.2-3
6.2-4. Experimental Relationship between Borehole Temperature and Volumetric Water Content for Borehole 79 During the Drift Scale Test Over a Two-Year Period During Heating F6.2-4
6.2-5. Locations of Important Interfaces and Fluxes in the Engineered Barrier System F6.2-5
6.4-1. Corrosion Rates for Mild Steel in Water, Plotted as a Function of Temperature F6.4-1
6.4-2. Titanium Longevity as a Function of Thickness F6.4-2
6.4-3. Alloy 22 Longevity as a Function of Thickness F6.4-3
6.4-4. 316L Stainless Steel Longevity as a Function of Thickness F6.4-4
6.4-5. 304 Stainless Steel Longevity as a Function of Thickness F6.4-5
6.4-6. Borated Stainless Steel Longevity as a Function of Thickness F6.4-6
6.4-7. Copper Alloy Longevity as a Function of Thickness F6.4-7
6.4-8. Aluminum Alloy Longevity as a Function of Thickness F6.4-8
6.4-9. Low Carbon Alloy Steel Longevity as a Function of Thickness F6.4-9
6.4-10. Lifetime of Solid Materials (1 inch Thickness), Based on Atmospheric/Steam and/or Fresh/Salt Water Corrosion Rates F6.4-10
6.5-1 A Simplified Roadmap of the Process Required to Give a Valid Technical Basis for Mineral Suppression or Inclusion in Geochemical Equilibrium Modeling F6.5-1
6.6-1. Quadrant Designations for Abstraction of Data from the THC Seepage Model F6.6-1
6.6-2. The Location of the Wetting Front in the Host Rock, as Calculated by the Thermal-Hydrological-Chemical-Seepage Model F6.6-2
6.6-3. Ca to Cl Ratio in thc6_w0_r.xls Fracture Top Front Waters F6.6-2
6.6-4. Fracture Saturation Level in thc6_w6_r.xls Fracture Top Front Waters F6.6-3
6.6-5. Selected Molal Ratios from the Evaporation of the 368 Seepage Waters to 65 Percent Relative Humidity, Used in the Binning Analysis to Establish Binning Criteria F6.6-4
6.6-6. Selected Molal Ratios from the Evaporation of the 368 Seepage Waters to 65 Percent Relative Humidity, Used in the Binning Analysis to Establish Binning Criteria F6.6-4

FIGURES (Continued)

Page

6.6-7. Mineral Assemblages of the 368 Selected Seepage Waters after Evaporation to 65 Percent Relative Humidity F6.6-5
6.6-8. Evaporated Water Compositions for All Bins Sorted by Bin After Evaporation to 65 Percent Relative Humidity F6.6-5
6.6-9. Evaporated Water Compositions for Bin 1 After Evaporation to 65 Percent Relative Humidity F6.6-6
6.6-10. Evaporated Water Compositions for Bin 2 After Evaporation to 65 Percent Relative Humidity F6.6-6
6.6-11. Evaporated Water Compositions for Bin 3 After Evaporation to 65 Percent Relative Humidity F6.6-7
6.6-12. Evaporated Water Compositions for Bin 4 After Evaporation to 65 Percent Relative Humidity F6.6-7
6.6-13. Evaporated Water Compositions for Bin 5 After Evaporation to 65 Percent Relative Humidity F6.6-8
6.6-14. Evaporated Water Compositions for Bin 6 After Evaporation to 65 Percent Relative Humidity F6.6-8
6.6-15. Evaporated Water Compositions for Bin 7 After Evaporation to 65 Percent Relative Humidity F6.6-9
6.6-16. Evaporated Water Compositions for Bin 8 After Evaporation to 65 Percent Relative Humidity F6.6-9
6.6-17. Evaporated Water Compositions for Bin 9 After Evaporation to 65 Percent Relative Humidity F6.6-10
6.6-18. Evaporated Water Compositions for Bin 10 After Evaporation to 65 Percent Relative Humidity F6.6-10
6.6-19. Evaporated Water Compositions for Bin 11 After Evaporation to 65 Percent Relative Humidity F6.6-11
6.6-20. Bins for Evaporated Crown Seepage: Case w0tf4 ..... F6.6-11
6.6-21. Bins for Evaporated Invert Seepage: Case w0bf4 ..... F6.6-12
6.6-22. Bins for Evaporated Crown Seepage: Case w4tf4 ..... F6.6-13
6.6-23. Bins for Evaporated Invert Seepage: Case w4bf4 ..... F6.6-13
6.6-24. Bins for Evaporated Crown Seepage: Case w5tf4 ..... F6.6-14
6.6-25. Bins for Evaporated Invert Seepage: Case w5bf4 ..... F6.6-14
6.6-26. Bins for Evaporated Invert Seepage: Case w6tf4 ..... F6.6-15
6.6-27. Bins for Evaporated Invert Seepage: Case w6bf4 ..... F6.6-15
6.6-28. Bins for Evaporated Invert Seepage: Case w7tf4 ..... F6.6-16
6.6-29. Bins for Evaporated Invert Seepage: Case w7bf4 ..... F6.6-16
6.7-1. Gas Flux per Meter of Drift F6.7-1
6.7-2. Oxygen (O_2) Consumption Due to Degradation of Components External to the Waste Package F6.7-2
6.7-3. Oxygen (O_2) Consumption in a 21 PWR Waste Package F6.7-3
6.7-4. Oxygen (O_2) Consumption in a N Reactor Co-Disposal Waste Package F6.7-4
6.7-5. P_{CO_2} Concentration in the Drift and Near-drift Environment Through Time (Log Scale) F6.7-5

FIGURES (Continued)

Page

6.7-6. *P*co$_2$ Concentration in the In-Drift Environment Through Time (Normal Scale) F6.7-5
6.7-7. Comparison of Temperatures at Various Locations Within and Around the Drift as Determined by the Thermal-Hydrological-Chemical Model Output F6.7-6
6.8-1. Eh-pH Diagram for Part of the System Fe-C-Si-O-H at 25°C F6.8-1
6.8-2. Eh-pH Diagram for Part of the System Ni-O-H at 25°C F6.8-2
6.8-3. The pe-pH Diagram for Aqueous Inorganic Chromium Hydrolysis Species. Hatched Area Indicates Predominance Region for Cr(OH)3(s) F6.8-3
6.9-1. Predicted Compositional Evolution as Bin 11 Waters Evaporate at 70ºC and 10^{-3} CO_2 Fugacity, Plotted Versus Relative Humidity F6.9-1
6.9-2. Predicted Compositional Evolution as Bin 11 Waters Evaporate at 70ºC and 10^{-3} CO_2 Fugacity, Plotted Versus Concentration Factor F6.9-1
6.9-3. The Predicted Concentrations of ANC Species During Evaporative Evolution of Bin 11 Water at 70ºC and 10^{-3} atm CO_2 Fugacity, Plotted Versus Relative Humidity F6.9-2
6.9-4. The Predicted Concentrations of ANC Species During Evaporative Evolution of Bin 11 Water at 70ºC and 10^{-3} atm CO_2 Fugacity, Plotted Versus Concentration Factor F6.9-2
6.9-5. Predicted Mineral Precipitation as Bin 11 Waters Evaporate at 70°C and 10^{-3} CO_2 Fugacity, Plotted Versus Relative Humidity F6.9-3
6.9-6. Predicted Mineral Precipitation as Bin 11 Waters Evaporate at 70°C and 10^{-3} CO_2 Fugacity, Plotted Versus Concentration Factor F6.9-3
6.9-7. Predicted Compositional Evolution as Bin 11 Waters are Diluted at 70ºC and 10^{-3} CO_2 Fugacity, Plotted Versus Relative Humidity F6.9-4
6.9-8. Predicted Compositional Evolution as Bin 11 Waters are Diluted at 70ºC and 10^{-3} CO_2 Fugacity, Plotted Versus Concentration Factor F6.9-4
6.9-9. The Predicted Concentrations of ANC Species During Dilution of Bin 11 Water at 70ºC and 10^{-3} atm CO_2 Fugacity, Plotted Versus Relative Humidity F6.9-5
6.9-10. The Predicted Concentrations of ANC Species During Dilution of Bin 11 Water at 70ºC and 10^{-3} atm CO_2 Fugacity, Plotted Versus Dilution Factor F6.9-5
6.10-1. Flow Chart Representing the Dust Leachate Analysis Abstraction Process F6.10-1
6.10-2. EQ6 Dust Leachate Water Mineralogy at the Dryout End Point at 25°C and Atmospheric *P*co$_2$ F6.10-2
6.10-3. Total Elemental Molalities and pH of All Waters Used in the Binning Analysis After Evaporation to 65 Percent Relative Humidity F6.10-3
6.10-4. Molar Ratios in Brines after Evaporation to 65 Percent Relative Humidity (Plot 1) F6.10-3
6.10-5. Molar Ratios in Brines After Evaporation to 65 Percent Relative Humidity (Plot 2) F6.10-4
6.10-6. Mineral Assemblages After Evaporation to 65 Percent Relative Humidity F6.10-4
6.10-7. Evaporated Water Compositions for Dust Leachate Bin 1 After Evaporation to 65 Percent Relative Humidity F6.10-5
6.10-8. Evaporated Water Compositions for Dust Leachate Bin 2 After Evaporation to 65 Percent Relative Humidity F6.10-5

FIGURES (Continued)

Page

6.10-9. Evaporated Water Compositions for Dust Leachate Bin 3 After Evaporation to 65 Percent Relative Humidity F6.10-6
6.10-10. Evaporated Water Compositions for Dust Leachate Bin 4 After Evaporation to 65 Percent Relative Humidity F6.10-6
6.10-11. Evaporated Water Compositions for Dust Leachate Bin 5 After Evaporation to 65 Percent Relative Humidity F6.10-7
6.10-12. Evaporated Water Compositions for Dust Leachate Bin 6 After Evaporation to 65 Percent Relative Humidity F6.10-7
6.10-13. Predicted Compositional Evolution as Dust Leachate Bin 5 Waters Evaporate at 70ºC and 10^{-3} CO_2 Fugacity, Plotted Versus Relative Humidity F6.10-8
6.10-14. Predicted Compositional Evolution as Dust Leachate Bin 5 Waters Evaporate at 70ºC and 10^{-3} CO_2 Fugacity, Plotted Versus Concentration Factor F6.10-8
6.10-15. The Predicted Concentrations of ANC Species During Evaporative Evolution of Dust Leachate Bin 5 Water at 70ºC and 10^{-3} bar CO_2 Fugacity, Plotted Versus Relative Humidity. F6.10-9
6.10-16. The Predicted Concentrations of ANC Species During Evaporative Evolution of Dust Leachate Bin 5 Water at 70ºC and 10^{-3} bar CO_2 Fugacity, Plotted Versus Concentration Factor. F6.10-9
6.10-17. Predicted Mineral Precipitation as Dust Leachate Bin 5 Waters Evaporate at 70°C and 10^{-3} CO_2 Fugacity, Plotted Versus Relative Humidity F6.10-10
6.10-18. Predicted Mineral Precipitation as Dust Leachate Bin 5 Waters Evaporate at 70°C and 10^{-3} CO_2 Fugacity, Plotted Versus Concentration Factor F6.10-10
6.12-1. Uncertainty in Bin 11 Br Concentrations Using the Br Values from Pore Water F6.12-1
6.12-2. Uncertainty in Bin 11 Ionic Strength Due to Adding Br F6.12-1
6.12-3. Uncertainty in Bin 11 pH Due to Adding Br F6.12-2
6.12-4. Uncertainty in Bin 11 Molar Ratios Due to Adding Br F6.12-2
6.12-5. Comparative Evaporative Concentration of Br in Dust Leachate Water Lookup Tables F6.12-3
6.12-6. Change in Predicted pH Due to Adjustment of Dust Leachate Bin 1 Br Concentration F6.12-3
6.12-7. Change in Predicted Ionic Strength Due to Adjustment of Dust Leachate Bin 1 Br Concentration F6.12-4
6.12-8. Change in Predicted N Concentrations Due to Adjustment of Dust Leachate Bin 1 Br Concentration F6.12-4
6.12-9. Change in Predicted Br Concentrations Due to Adjustment of Dust Leachate Bin 1 Br Concentration F6.12-5
6.12-10. Change in Predicted Cl Concentrations Due to Adjustment of Dust Leachate Bin 1 Br Concentration F6.12-5
6.12-11. Variation in Bin 11 Base Case File pH as a Function of Pco_2 ..... F6.12-6
6.12-12. Variation in Bin 11 Base Case File Ionic Strength as a Function of Pco_2 ..... F6.12-6
6.12-13. Variation in Bin 11 Base Case File Total Elemental Cl as a Function of Pco_2 ..... F6.12-7
6.12-14. Variation in Bin 11 Base Case File Total Elemental N as a Function of Pco_2 ..... F6.12-7
6.12-15. Variation in Bin 5 Base Case File pH as a Function of Pco_2 ..... F6.12-8

FIGURES (Continued)

Page

6.12-16. Variation in Bin 5 Base Care Ionic Strength as a Function of Pco_2 ..... F6.12-8
6.12-17. Variation in Bin 5 Base Case File Total Elemental Cl as a Function of Pco_2 ..... F6.12-9
6.12-18. Variation in Bin 5 Base Case File Total Elemental N as a Function of Pco_2 ..... F6.12-9
6.12-19 Comparison of Base Case EQ6 Results with those of the Cryolite-Suppressed Modeling Run F6.12-10
6.12-20. Comparison of Base Case Results to those of the Same Modeling Run with Glaserite Unsuppressed F6.12-10
6.13-1. Color Coded Bin History Maps Showing Differences Between Crown Seepage and Invert Wicking F6.13-1
6.13-2. Aqueous Composition Predictions Versus Relative Humidity for All Seepage Evaporation Lookup Tables for Bin 1 (IS = Ionic Strength) F6.13-2
6.13-3. Aqueous Composition Predictions Versus Relative Humidity for All Seepage Evaporation Lookup Tables for Bin 2 (IS = Ionic Strength) F6.13-2
6.13-4. Aqueous Composition Predictions Versus Relative Humidity for All Seepage Evaporation Lookup Tables for Bin 3 (IS = Ionic Strength) F6.13-3
6.13-5. Aqueous Composition Predictions Versus Relative Humidity for All Seepage Evaporation Lookup Tables for Bin 4 (IS = Ionic Strength) F6.13-3
6.13-6. Aqueous Composition Predictions Versus Relative Humidity for All Seepage Evaporation Lookup Tables for Bin 5 (IS = Ionic Strength) F6.13-4
6.13-7. Aqueous Composition Predictions Versus Relative Humidity for All Seepage Evaporation Lookup Tables for Bin 6 (IS = Ionic Strength) F6.13-4
6.13-8. Aqueous Composition Predictions Versus Relative Humidity for All Seepage Evaporation Lookup Tables for Bin 7 (IS = Ionic Strength) F6.13-5
6.13-9. Aqueous Composition Predictions Versus Relative Humidity for All Seepage Evaporation Lookup Tables for Bin 8 (IS = Ionic Strength) F6.13-5
6.13-10. Aqueous Composition Predictions Versus Relative Humidity for All Seepage Evaporation Lookup Tables for Bin 9 (IS = Ionic Strength) F6.13-6
6.13-11. Aqueous Composition Predictions Versus Relative Humidity for All Seepage Evaporation Lookup Tables for Bin 10 (IS = Ionic Strength) F6.13-6
6.13-12. Aqueous Composition Predictions Versus Relative Humidity for All Seepage Evaporation Lookup Tables for Bin 11 (IS = Ionic Strength) F6.13-7
6.13-13. Selected Aqueous Molal Ratios Useful for Corrosion Analysis Versus Relative Humidity for All Seepage Evaporation Lookup Tables for All Bins F6.13-7
6.13-14. Flow Diagram Showing Some of the Precipitating Minerals that are Associated with Each of the 11 Seepage Bins F6.13-8
6.13-15. Range of pH Versus Relative Humidity for the Seepage Evaporation Lookup Tables Representing Bins 3 through 11 ..... F6.13-9
6.13-16. Range of pH Versus Relative Humidity for the Seepage Evaporation Lookup Tables Representing Bins 1 and 2 ..... F6.13-9
6.13-17. Range of H_2O Vapor Pressure vs Activity of Water Resulting in Wet Conditions for All Dust Leachate Lookup Tables at or above 100°C F6.13-10
6.13-18. Aqueous Composition Predictions Versus Relative Humidity for All Dust Leachate Lookup Tables for Bin 1 (IS = Ionic Strength) F6.13-11

FIGURES (Continued)

Page

6.13-19. Aqueous Composition Predictions Versus Relative Humidity for All Dust Leachate Lookup Tables for Bin 2 (IS = Ionic Strength) F6.13-11
6.13-20. Aqueous Composition Predictions Versus Relative Humidity for All Dust Leachate Lookup Tables for Bin 3 (IS = Ionic Strength) F6.13-12
6.13-21. Aqueous Composition Predictions Versus Relative Humidity for All Dust Leachate Lookup Tables for Bin 4 (IS = Ionic Strength) F6.13-12
6.13-22. Aqueous Composition Predictions Versus Relative Humidity for All Dust Leachate Lookup Tables for Bin 5 (IS = Ionic Strength) F6.13-13
6.13-23. Aqueous Composition Predictions Versus Relative Humidity for All Dust Leachate Lookup Tables for Bin 6 (IS = Ionic Strength) F6.13-13
6.13-24. Selected Aqueous Molal Ratios Versus Relative Humidity for All Dust Leachate Lookup Tables for All Bins F6.13-14
6.13-25. Flow Diagram Showing Some of the Precipitating Minerals that are Associated with Each of the 6 Dust Leachate Brine Evaporation Bins F6.13-14
6.13-26. Variation of pH with Relative Humidity for All Six Dust Leachate Bins F6.13-15
6.13-27. Range of F Versus Relative Humidity for the Seepage Evaporation Lookup Tables Representing Bins 3 through 11 ..... F6.13-15
6.13-28. Range of Cl Versus Relative Humidity for the Seepage Evaporation Lookup Tables Representing Bins 3 through 11 ..... F6.13-16
6.13-29. Range of Cl to N Molal Ratios for the Seepage Evaporation Lookup Tables Representing Bins 3 through 11 ..... F6.13-16
6.13-30. Range of Total Elemental Ca for the Seepage Evaporation Lookup Tables Representing Bins 3 through 11 ..... F6.13-17
6.13-31. Range of Total Elemental S for the Seepage Evaporation Lookup Tables Representing Bins 3 through 11 ..... F6.13-17
6.13-32. Range of Total Elemental C for the Seepage Evaporation Lookup Tables Representing Bins 3 through 11 ..... F6.13-18
6.13-33. Range of Ionic Strength Versus Relative Humidity for the Seepage Evaporation Lookup Tables Representing Bins 3 through 11 ..... F6.13-18
6.13-34. Mass of Water Versus Ionic Strength for the Seepage Evaporation Lookup Tables Representing Bins 3 through 11 ..... F6.13-19
6.13-35. Variation of F Concentration with Relative Humidity for All Six Dust Leachate Bins F6.13-19
6.13-36. Variation of Ionic Strength with Relative Humidity for All Six Dust Leachate Bins F6.13-20
6.13-37. Variation of Cl Concentration with Relative Humidity for All Six Dust Leachate Bins F6.13-20
6.13-38. Variation of Cl/NO_3 with Relative Humidity for All Six Dust Leachate Bins .. F6.13-21
6.13-39. Variation of NO_3 with Relative Humidity for All Six Dust Leachate Bins F6.13-21
6.13-40. Mass of Water Versus Ionic Strength for All 6 Dust Leachate Bins F6.13-22
6.13-41. Schematic Representation of the Sources of Different Chemical Fluxes Into the Invert and Subsequent Radionculide Release from the Engineered Barrier System F6.13-23

FIGURES (Continued)

Page

6.13-42. Range of F Versus Relative Humidity for the Seepage Evaporation Lookup Tables Representing Bins 1 and 2 ..... F6.13-24
6.13-43. Range of Cl Versus Relative Humidity for the Seepage Evaporation Lookup Tables Representing Bins 1 and 2 ..... F6.13-24
6.13-44. Range of Ionic Strength Versus Mass of Water (kg) for the Seepage Evaporation Lookup Tables Representing Bins 1 and 2 ..... F6.13-25
6.13-45. Range of Total Elemental Ca for the Seepage Evaporation Lookup Tables Representing Bins 1 and 2 ..... F6.13-25
6.13-46. Range of Total Elemental S for the Seepage Evaporation Lookup Tables Representing Bins 1 and 2 ..... F6.13-26
6.13-47. Range of Total Elemental C for the Seepage Evaporation Lookup Tables Representing Bins 1 and 2 ..... F6.13-26
6.15-1. Roadmap for Total Systems Performance Assessment - License Application Implementation of Engineered Barrier System Chemistry on the Waste Package Surface Under the "Dripping Scenario" 6.15-1
6.15-2. Roadmap for Total Systems Performance Assessment - License Application Implementation of Engineered Barrier System Chemistry on the Waste Package Surface Under the "No Dripping Scenario" 6.15-2

7.2-1. Comparison of Thermal-Hydrological-Chemical Seepage pH with Abstraction Results for w0bf4 ..... F7-1
7.2-2. Comparison of Thermal-Hydrological-Chemical Seepage Ca^{2+} with Abstraction Results for w0bf4 ..... F7-1
7.2-3. Comparison of Thermal-Hydrological-Chemical Seepage pH with Abstraction Results for w0tf4 ..... F7-2
7.2-4. Comparison of Thermal-Hydrological-Chemical Seepage Mg^{2+} with Abstraction Results for w0tf4 ..... F7-2
7.2-5. Comparison of Thermal-Hydrological-Chemical Seepage pH with Abstraction Results for w4bf4 ..... F7-3
7.2-6. Comparison of Thermal-Hydrological-Chemical Seepage Na^{+} with Abstraction Results for w4bf4 ..... F7-3
7.2-7. Comparison of Thermal-Hydrological-Chemical Seepage pH with Abstraction Results for w4tf4 ..... F7-4
7.2-8. Comparison of Thermal-Hydrological-Chemical Seepage Cl^{-} with Abstraction Results for w4tf4 ..... F7-4
7.2-9. Comparison of Thermal-Hydrological-Chemical Seepage pH with Abstraction Results for w5bf4 ..... F7-5
7.2-10. Comparison of Thermal-Hydrological-Chemical Seepage $SiO_{2(aq)}$ with Abstraction Results for w5bf4 ..... F7-5
7.2-11. Comparison of Thermal-Hydrological-Chemical Seepage pH with Abstraction Results for w5tf4 ..... F7-6
7.2-12. Comparison of Thermal-Hydrological-Chemical Seepage $HCO3^{-}$ with Abstraction Results for w5tf4 ..... F7-6
7.2-13 Comparison of Thermal-Hydrological-Chemical Seepage pH with Abstraction Results for w6bf4 ..... F7-7

FIGURES (Continued)

Page

7.2-14. Comparison of Thermal-Hydrological-Chemical Seepage SO_4^{2-} with Abstraction Results for w6bf4 ..... F7-7
7.2-15. Comparison of Thermal-Hydrological-Chemical Seepage pH with Abstraction Results for w6tf4 ..... F7-8
7.2-16. Comparison of Thermal-Hydrological-Chemical Seepage K^+ with Abstraction Results for w6tf4 ..... F7-8
7.2-17. Comparison of Thermal-Hydrological-Chemical Seepage pH with Abstraction Results for w7bf4 ..... F7-9
7.2-18. Comparison of Thermal-Hydrological-Chemical Seepage F^- with Abstraction Results for w7bf4 ..... F7-9
7.2-19. Comparison of Thermal-Hydrological-Chemical Seepage pH with Abstraction Results for w7tf4 ..... F7-10
7.2-20. Comparison of Thermal-Hydrological-Chemical Seepage NO_3^- with Abstraction Results for w7tf4 ..... F7-10
7.2-21. Comparison of Model Results (Ionic Strength at 98% RH) with Look-up Table Interpolation Values ($Pco_2 = 10^{-3.2}$ Bars and Temperature = 56°C) F7-11
7.2-22. Comparison of Model Results (pH at 98% RH) with Look-up Table Interpolation Values ($Pco_2 = 10^{-3.2}$ Bars and Temperature = 56°C) F7-11
7.2-23. Comparison of Model Results (Cl^- at 86% RH) with Look-up Table Interpolation Values ($Pco_2 = 10^{-3.2}$ Bars and Temperature = 56°C) F7-12
7.2-24. Comparison of Model Results (NO3- at 64% RH) with Look-up Table Interpolation Values ($Pco_2 = 10^{-3.2}$ Bars and Temperature = 56°C) F7-12
7.3-1. Predicted Versus Measured Concentrations for Synthetic J-13 Water Evaporation Experiments of Rosenberg et al. (1999 [125338]) F7-13
7.3-2. Predicted Versus Measured pH Values for Synthetic J-13 Water Evaporation Experiments of Rosenberg et al. (1999 [125338]) F7-13
7.3-3. Predicted Versus Measured Concentrations for 100x Synthetic J-13 Water Evaporation Experiments of CRWMS M&O (2000 [146460]) F7-14
7.3-4. Predicted Versus Measured Concentrations for Synthetic Topopah Spring Tuff Pore Water from Evaporation Experiments of Rosenberg et al. (1999 [125339]) F7-14
7.3-5. Predicted Versus Measured pH Values for Synthetic Topopah Spring Tuff Pore Water from Evaporation Experiments of Rosenberg et al. (1999 [125339]) F7-15
7.3-6. Predicted Versus CRC Handbook Mineral Solubilities at 25°C F7-16
7.3-7. Predicted Versus CRC Handbook Mineral Solubilities at 100°C F7-17
7.3-8. YPF Versus Set 1 YMP.R2 Aqeuous Predictions for Average In Situ J-13 Well Water at 70°C and $CO_{2(g)}$ Fugacity of 10^{-3} Bar F7-18
7.3-9. YPF Versus Set 1 YMP pH and Ionic Strength Predictions for Average In Situ J-13 Well Water at 70°C and $CO_{2(g)}$ Fugacity of 10^{-3} Bar F7-18
7.3-10. YPF Versus Set 2 YMP Aqeuous Predictions for Average In Situ J-13 Well Water at 70°C and $CO_{2(g)}$ Fugacity of 10^{-3} Bar F7-19
7.3-11. YPF Versus Set 2 YMP pH and Ionic Strength Predictions for Average In Situ J-13 Well Water at 70°C and $CO_{2(g)}$ Fugacity of 10^{-3} Bar F7-19

FIGURES (Continued)

Page

7.4-1. Published Results (Garrels and Mackenzie, 1967) for Modeled Evaporation of Typical Sierra Nevada Spring Water at 25°C in Equilibrium with Atmospheric CO_2 at $10^{-3.5}$ Bar F7-20

7.4-2. IDPS Model Results for Evaporation of Typical Sierra Nevada Spring Water at 25°C in Equilibrium with Atmospheric CO_2 at $10^{-3.5}$ Bar F7-21

7.7-1. EQ3/6 Calculated Chromium Solubility in Equilibrium with $Cr(OH)_{3(am)}$ (Blue Diamonds with Lines) Compared to the 3-Species Model of Rai et al. (1987, 2, Solid Black Lines) with Their Detection Limit Shown by the Red Dashed Line F7-22

F/O 8.2-1. Engineered Barrier System Environment Water Chemistry Derivations for Total System Performance Assessment-License Application on the Waste Package and Drip Shield 8-5

INTENTIONALLY LEFT BLANK

TABLES

Page

4.1-1. Masses of Ground Support Materials per Meter of Repository Drift 4-1
4.1-2. Masses of Drip Shield and Waste Package Pallet per Meter of Repository Drift 4-2
4.1-3. Masses of Invert and Gantry Rail Components per Meter of Repository Drift 4-2
4.1-4. Masses of 24 BWR Waste Package Components 4-3
4.1-5. Masses of 21 PWR Waste Package Components 4-4
4.1-6. Masses of 5-DHLW/DOE SNF Short Waste Package Components 4-5
4.1-7. Masses of 5-DHLW/DOE SNF Long Waste Package Components 4-6
4.1-8. Masses of 2-MCO/2-DHLW Waste Package Components 4-7
4.1-9. Masses of 12-PWR Long Waste Package Components 4-8
4.1-10. Masses of 44-BWR Waste Package Components 4-9
4.1-11. Source Data/Input Information Used for Corrosion Rate Determinations of Metallic Materials 4-10
4.1-12. Source Data/Input Information Used for Corrosion Rate Determinations of Waste Forms 4-11
4.1-13. References for Input to Binning Analysis 4-13
4.1-14. References for Input Gas Chemistry Analyses 4-13
4.1-15. Time-Varying Inputs for the Gas Flux Calculation in Section 6.7.1 4-14
4.1-16. Constant Inputs for Gas Flux and Oxygen Demand Calculations from Section 6.7.1 4-15
4.1-17. Inputs for Calculation of Oxygen Consumption by Corrosion Processes 4-16
4.1-18. In-Drift Precipitates Salts Model General File Formats 4-18
4.1-19. Water Soluble Cations and Anions Leached from Dust Collected Throughout the Exploratory Studies Facility 4-18
4.1-20. Water Soluble Cations and Anions Leached from Dust Collected Throughout the Exploratory Studies Facility 4-19
4.1-21. Partial Pressure of CO_2 at Atmospheric Conditions 4-21
4.1-22. Dimensional Information for 316L Stainless Steel Sheets and Rock Bolts 4-21
4.1-23. Parameters Used to Abstract 316L Stainless Steel Ground Support Corrosion 4-22
4.1-24. Dissolution Data for Amorphous Chromium(III) Hydroxide $Cr(OH)_3$ and Eskolaite (Cr_2O_3) at 25°C 4-22
4.1-25. Pore Water Compositional Data Used to Evaluate the Relative Importance of Br 4-23
4.4-1. Measured Concentrations for Synthetic J-13 Water Evaporation Experiments 4-33
4.4-2. Measured Concentrations for 100X Synthetic J-13 Water Evaporation Experiments 4-34
4.4-3. Measured Concentrations for Synthetic Topopah Spring Tuff Pore Water from Evaporation Experiments 4-34
4.4-4. Aqueous Solubilities of Na, K, Ca, and Mg Salts 4-35
4.4-5. Composition of Sierra Nevada Spring Water Used in Validation Tests for the EBS Seepage Evaporation Model 4-36
4.4-6. Measured Deliquescence Relative Humidity Values for Salts and Salt Mixtures 4-36

TABLES (Continued)

Page

6.4-1. Typical Activity Ranges for SO_X and Chlorides in Various Environments 6.4-2
6.4-2. Titanium Corrosion Rates from Laboratory Experiments at Near 100 Percent Relative Humidity and High Temperature 6.4-3
6.4-3. Possible Corrosion Rates of Ti-Alloys at Lower Temperatures 6.4-3
6.4-4. Corrosion Rates of Titanium Grade 7 ..... 6.4-3
6.4-5. Corrosion Rates of Alloy-22 in Various Environmental Conditions 6.4-4
6.4-6. Corrosion Rates of Alloy-22 ..... 6.4-4
6.4-7 Corrosion Rates of Inconel Alloys in Various Aqueous Environments 6.4-5
6.4-8. Corrosion Rates of Copper Under Various Environmental Conditions 6.4-5
6.4-9. Corrosion Rates of Aluminum Alloys in Aqueous Environments 6.4-6
6.4-10. Atmospheric Corrosion Rates of Aluminum Alloy 6061 ..... 6.4-6
6.4-11. Corrosion Rates of 316L Stainless Steel Under Various Environmental Conditions 6.4-7
6.4-12. Corrosion Rates of 316L Stainless Steel 6.4-7
6.4-13. Corrosion Rates of 304L Stainless Steel in Various Environmental Conditions 6.4-8
6.4-14. Corrosion Rates of Borated Stainless Steels Under Various Environmental Conditions 6.4-9
6.4-15. Corrosion Rates of Carbon and Low Alloy Steels in Various Environmental Conditions 6.4-10
6.4-16. Aqueous Corrosion Rates for Mild Carbon Steel 6.4-10
6.4-17. Comparison of N-Reactor to Total U.S. Department of Energy Spent Nuclear Fuel 6.4-11
6.4-18. Selected Corrosion Rates of Metallic and Alloy Materials for Use in Engineered Barrier System Chemical Environment Calculations 6.4-14
6.4-19. Longevity of 1.0-Inch of Introduced Material in the Drift 6.4-15
6.4-20. Materials Compositions 6.4-16
6.5-1. Compositions of Fluoride and Trace Elements in ECRB Pore Water Samples 6.5-14
6.5-2. Mineral Suppressions that are Used in the Engineered Barrier System Physical and Chemical Environment Geochemical Modeling 6.5-15
6.5-3. Minerals Allowed to Precipitate in the Engineered Barrier System Physical and Chemical Environment Geochemical Modeling 6.5-16
6.6-1. Locations and Identification of Seepage Water Compositions to be Binned 6.6-5
6.6-2. Additional Mineral Suppressions Included During Evaporation to 65 Percent Relative Humidity 6.6-6
6.6-3. Binning Criteria Answer Key 6.6-8
6.6-4. Median Water Identifier for Each Bin and Percentage in Each Bin 6.6-9
6.6-5. Initial Compositions of the 11 Binned THC Seepage Waters 6.6-11
6.6-6. Calculated Statistics for All Values within Each Bin (a_w = 0.65) 6.6-13
6.6-7. Calculated Statistics for All Values on the Data and Plots Worksheet 6.6-15
6.6-8. Bin Map for "Water 0" Incoming Seepage Waters 6.6-16
6.6-9. Bin Map for "Water 4" Incoming Seepage Waters 6.6-17
6.6-10. Bin Map for "Water 5" Incoming Seepage Waters 6.6-18
6.6-11. Bin Map for "Water 6" Incoming Seepage Waters 6.6-19

TABLES (Continued)

Page

6.6-12. Bin Map for "Water 7" Incoming Seepage Waters 6.6-20
6.6-13. Details of Impact Analysis on Binning Due to Endpoint a_w 6.6-21
6.6-14. Details of Impact Analysis on CO_2 Pressure Correction..... 6.6-22
6.7-1. Look-up Tables for Total System Performance Assessment-License Application Analysis of In-Drift and Invert Pco_2 for W0 (HD-PERM) Seepage Water 6.7-6
6.7-2. Look-up Tables for Total System Performance Assessment-License Application Analysis of In-Drift and Invert Pco_2 for W4 (CS2000) Seepage Water 6.7-7
6.7-3. Look-up Tables for Total System Performance Assessment-License Application Analysis of In-Drift and Invert Pco_2 for W5 (CS1000) Seepage Water 6.7-8
6.7-4. Look-up Tables for Total System Performance Assessment-License Application Analysis of In-Drift and Invert Pco_2 for W6 (SD-9) Seepage Water 6.7-9
6.7-5. Look-up Tables for Total System Performance Assessment-License Application Analysis of In-drift and Invert Pco_2 for W7 (CS500) Seepage Water 6.7-10
6.7-6. Equilibrium Gas Fugacities, Temperatures, pH, and Ionic Strengths from the 11 Bin Waters..... 6.7-12
6.7-7. Equilibrium Gas Fugacities, Temperatures, pH and Ionic Strengths from the 6 Bin Dust Leachate Waters..... 6.7-13
6.8-1. Typical Oxidation-Reduction Reactions and Potential Fe Minerals..... 6.8-2
6.8-2. EQ3/6 Input/Output Files for 316L Stainless Steel Corrosion Abstraction Model 6.8-8
6.8-3. Additional EQ3/6 Mineral Suppressions Included for Seepage Ground Support Interactions 6.8-9
6.8-4. Aqueous Species Suppressions Included for Seepage Ground Support Interactions..... 6.8-10
6.8-5. Absolute (Percent Relative) Differences Due to SS316L Dissolution in Bin 11 Seepage Water at 100 and 98 Percent Relative Humidity 6.8-11
6.9-1. Total EQ3NR Equilibrated Aqueous Elemental Compositions for the 11 Bins 6.9-2
6.9-2. EQ3NR Equilibrium Speciation of the 11 Bins 6.9-3
6.9-3. List of Species Used to Charge Balance the Individual Water Chemistries 6.9-4
6.9-4. EQ3NR Input/Output Files for TSPA-LA Abstraction..... 6.9-4
6.9-5. EQ6 Input/Output Files for TSPA-LA Abstraction 6.9-6
6.9-6. Lookup Tables for TSPA-LA Abstraction..... 6.9-7
6.9-7. Relative Humidity Boundaries Between Evaporation and Dilution Lookup Tables 6.9-8
6.10-1. Rationale for the Suppression of Cryolite and K-Wadeite in Dust Leachate Model Analyses..... 6.10-4
6.10-2. EQ3NR Input/Output Files for Dust Leachate Analyses 6.10-5
6.10-3. EQ6 Input and Output Files Used for Determination of the Mineralogy at Dryout..... 6.10-6

TABLES (Continued)

Page

6.10-4. EQ6 Dust Leachate Water pH, a_w, Ionic Strength (I) Cl, N, and Cl:N Ratios at the Dryout End Point at 25°C and Atmospheric Pco_2 ..... 6.10-7
6.10-5. Binning Criteria Answer Key 6.10-12
6.10-6. Median Waters and Percentage of Waters in Each Bin 6.10-12
6.10-7. Calculated Statistics for Evaporated Dust Leachate Waters (a_w = 0.65) Within Each Bin 6.10-15
6.10-8. Calculated Statistics for all 52 Evaporated Dust Leachate Waters Evaluated in the Binning Analysis (a_w = 0.65) 6.10-16
6.10-9. Total EQ3NR Equilibrated Aqueous Elemental Compositions for the 6 Bins 6.10-17
6.10-10. EQ3NR Equilibrium Speciation of the Six Bins 6.10-17
6.10-11. EQ3NR Input/Output Files for TSPA-LA Dust Leachate Abstraction 6.10-19
6.10-12. EQ6 Input/Output Files for TSPA-LA Abstraction 6.10-20
6.10-13. Additional Suppressions and Inclusions in EQ3/6 Runs Involving Dust Leachate Evaporation as a Function of Temperature 6.10-21
6.10-14. Dust Leachate Evaporation Lookup Tables for TSPA-LA Abstraction 6.10-23
6.11-1. Statistica 5.1 Files Saved from Generated Data 6.11-3
6.11-2. Clusters 1-11 with Associated Minerals 6.11-4
6.11-3. pH Statistics for Mineral Clustering and Aqueous Binning 6.11-5
6.11-4. Al Statistics for Mineral Clustering and Aqueous Binning 6.11-5
6.11-5. C Statistics for Mineral Clustering and Aqueous Binning 6.11-6
6.11-6. Ca Statistics for Mineral Clustering and Aqueous Binning 6.11-6
6.11-7. Cl Statistics for Mineral Clustering and Aqueous Binning 6.11-7
6.11-8. F Statistics for Mineral Clustering and Aqueous Binning 6.11-7
6.11-9. K Statistics for Mineral Clustering and Aqueous Binning 6.11-8
6.11-10. Mg Statistics for Mineral Clustering and Aqueous Binning 6.11-8
6.11-11. N Statistics for Mineral Clustering and Aqueous Binning 6.11-9
6.11-12. Na Statistics for Mineral Clustering and Aqueous Binning 6.11-9
6.11-13. S Statistics for Mineral Clustering and Aqueous Binning 6.11-10
6.11-14. Si Statistics for Mineral Clustering and Aqueous Binning 6.11-10
6.12-1. Estimated Model Uncertainty Ranges for In-Drift Precipitates/Salts Model Outputs 6.12-5
6.12-2 Spreadsheets Containing Log Transformed Data and Statistics for Each of the Uncertainty RH Locations Evaluated 6.12-6
6.12-3. Relative Humidity Point with the Most Variability for Bins 1 through 11 for pH, Cl, and Cl:NO_3 ..... 6.12-7
6.12-4. The Error Applied to the THC Seepage Lookup Tables for pH, I, Cl, and Cl:NO_3 Based on the RH with the Highest Variability in Bins 1 through 11 (Errors are Based on 2s Values) 6.12-7
6.12-5. Dust Leachate Variability Calculations at 85 and 98 Percent RH 6.12-8
6.12-6. Spreadsheets Containing Log Transformed Data and Statistics for Each of the RH Locations Evaluated for Uncertainty 6.12-8
6.12-7. Table Giving the Relative Humidity with the Most Uncertainty in Bins 1 through 5 for pH, Cl, and Cl:NO_3 ..... 6.12-8

TABLES (Continued)

Page

6.12-8. The Error Applied to the Dust Leachate Lookup Tables for pH, I, Cl, and Cl:NO_3, Based on the RH with the Highest Uncertainty within Bins 1 through 5 (Errors are Based on 2s Values) 6.12-9
6.12-9. Base Case EQ3/6 Input Files for Uncertainty Analysis 6.12-10
6.12-10. EQ6 Input/Output Files for 316L Stainless Steel Corrosion Rate Uncertainty Case 6.12-10
6.12-11. Comparison of pH and Ionic Strength for Corrosion Rate Uncertainty Case 6.12-11
6.12-12. EQ3/6 Input/Output Files for 316L Stainless Steel Cr(VI) Uncertainty Case 6.12-11
6.12-13. Comparison of pH and Ionic Strength for Cr(VI) Uncertainty Case 6.12-11
6.12-14. EQ3/6 Input/Output Files for 316L Stainless Steel Bin 07 Uncertainty Case 6.12-12
6.12-15. Comparison of pH and Ionic Strength for Bin 07 Uncertainty Case 6.12-12
6.12-16. EQ3/6 Input/Output Files for 316L Stainless Steel $Pco_2 = 10^{-2}$ Uncertainty Case 6.12-13
6.12-17. Comparison of pH and Ionic Strength for $Pco_2 = 10^{-2}$ Uncertainty Case 6.12-13
6.12-18. EQ3/6 Input/Output Files for 316: Stainless Steel $Pco_2 = 10^{-4}$ Uncertainty Case 6.12-13
6.12-19. Comparison of pH and Ionic Strength for $Pco_2 = 10^{-4}$ Uncertainty Case 6.12-14
6.12-20. Cl and Br Data for Pore Waters Collected in the ECRB 6.12-15
6.12-21. Mean, Minimum, and Maximum Cl:Br Ratios Present in Drift Samples, Calculated from the Data in DTN: GS020408312272.003 [DIRS 160899] 6.12-16
6.12-22. Bromide Values Used as Input into EQ3 Input Files 6.12-16
6.12-23. Br Uncertainty Analysis EQ3/6 Input and Output Files 6.12-16
6.12-24. Cl:Br Ratios of Dust Leachate Samples 6.12-18
6.12-25. Br Dust Leachate Uncertainty Analysis EQ3/6 Input and Output Files 6.12-20
6.12-26. Input and Output Files for Seepage Bin 11 Analysis of Pco_2 ..... 6.12-20
6.12-27. Input and Output Files for Dust Leachate Bin 5 Analysis of Pco_2 ..... 6.12-21
6.12-28. Traceability Roadmap for Mineral Suppression EQ6 Sensitivity Cases 6.12-22
6.12-29. Cl:NO_3 Molal Ratio for Seepage at the Halite Chemical Divide 6.12-25
6.12-30. Cl:NO_3 Molal Ratio for Dust at the Halite Chemical Divide 6.12-28
6.13-1. Time Integrated Bin Probability for Any Given Crown Seepage Bin (20,000 Year Case) 6.13-2
6.13-2. Time Integrated Bin Probability for Any Given Invert Wicking Seepage Bin (20,000 Year Case) 6.13-3
6.13-3. Water Bins Associated with Different Periods in the Repository Thermal History 6.13-4
6.13-4. Bin Probabilities for Crown Seepage as a Function of Time 6.13-5
6.13-5. Bin Probabilities for Invert Seepage as a Function of Time 6.13-6
6.13-6. Summary Table of Precipitating Minerals in Each of the Eleven Bins 6.13-9
6.13-7. Summary Table of Precipitating Minerals in Each of the Six Dust Leachate Evaporation Bins 6.13-13
6.13-8. Engineered Barrier System Seepage Lookup Table End Point Relative Humidity and Brine Evolution 6.13-17
6.13-9. Dust Leachate Lookup Table End Point Relative Humidity and Brine Evolution 6.13-20

TABLES (Continued)

Page

6.14-1. Features, Events and Processes Included in This Model Report and Their Disposition in Total Systems Performance Assessment - License Application..... 6.14-1
6.14-2. Features, Events and Processes Excluded in This Model Report and Their Disposition in Total Systems Performance Assessment - License Application... 6.14-10

7.3-1. Specific In-Drift Precipitates Salts Model Output Validation Objectives 7-7
7.5-1. Input/Output Files EQ3/6 (Version 8.0) Used to Calculate the Equilibrium Deliquescence Points of Binary and Mixed Salts 7-12
7.5-2. Comparisons of Relative Humidity Values for Equilibrium Deliquescence Points of Selected Salts Between EQ3/6 (Version 8.0–data0.ypf Pitzer Database) and Experimental Data 7-13
7.6-1. Natural Analog Information for the Inclusion of Minerals Not Reported in Section 6.5 7-15

8.2-1. Engineered Barrier System Physical and Chemical Environment Model Output DTNs Derived for use in the Total System Performance Assessment-License Application Model 8-3
8.2-2. Engineered Barrier System Physical and Chemical Environment Model Supplemental Output DTNs 8-7

ACRONYMS

ANC	acid neutralizing capacity
DIRS	Document Input Reference System
DRH	deliquesce relative humidity
DTN	data tracking number
EBS	engineered barrier system
ESF	Exploratory Studies Facility
FEPs	features, events, and processes
IDPS	in-drift precipitates/salts
IED	Information Exchange Drawings
LA	licensing agreement
P&CE	physical and chemical environment model
RH	relative humidity
SAW	Simulated Acidified Water
SCW	Simulated Concentrated Water
SDW	Simulated Dilute Water
SNF	spent nuclear fuel
THC	thermal-hydrological-chemical
TSPA	total system performance assessment
TSPA-LA	total system performance assessment-licensing agreement
UZ	unsaturated zone
YMP	Yucca Mountain Project

INTENTIONALLY LEFT BLANK

1. PURPOSE

The conceptual and predictive models documented in this Engineered Barrier System: Physical and Chemical Environment Model report describe the evolution of the physical and chemical conditions within the waste emplacement drifts of the repository. The modeling approaches and model output data will be used in the total system performance assessment (TSPA-LA) to assess the performance of the engineered barrier system and the waste form. These models evaluate the range of potential water compositions within the emplacement drifts, resulting from the interaction of introduced materials and minerals in dust with water seeping into the drifts and with aqueous solutions forming by deliquescence of dust (as influenced by atmospheric conditions), and from thermal-hydrological-chemical (THC) processes in the drift. These models also consider the uncertainty and variability in water chemistry inside the drift and the compositions of introduced materials within the drift.

This report develops and documents a set of process- and abstraction-level models that constitute the engineered barrier system: physical and chemical environment model. Where possible, these models use information directly from other process model reports as input, which promotes integration among process models used for total system performance assessment. Specific tasks and activities of modeling the physical and chemical environment are included in the technical work plan *Technical Work Plan for: In-Drift Geochemistry Modeling* (BSC 2004 [DIRS 166519]). As described in the technical work plan, the development of this report is coordinated with the development of other engineered barrier system analysis model reports.

1.1 SCOPE OF MODEL

This model report focuses on abstractions of seepage and gas inflow values, based on inputs from the *Drift-Scale Coupled Processes (DST and THC Seepage) Models* report (BSC 2003 [DIRS 162050]), and predicts in-drift aqueous solution compositions due to seepage and deliquescence of dust using the *In-Drift Precipitates/Salts Model* (BSC 2003 [DIRS 162529]).

As seepage waters percolate into the drift, their chemical composition will change by evaporation and mineral precipitation. Under higher temperature conditions when seepage does not occur, deliquescence of salts in dust will control the chemistry of any in-drift waters. Evaporation causes aqueous species' concentrations to increase, minerals to precipitate, and the most soluble components to become concentrated in the brine. When minerals (salts) precipitate, the relative concentrations of dissolved components change.

Within this model, chemical speciation calculations allow equilibrium and reaction-path modeling of evaporation to highly concentrated brines for potential water compositions of the system Na-K-H-Mg-Ca-Al-Cl-F-NO_3-SO_4-Br-CO_3-SiO_2-CO_2-O_2-H_2O, at temperatures from 0ºC to more than 100ºC, pressures in the atmospheric range, and relative humidities from 0 to 100 percent. These geochemical modeling results are used to determine the conditions that govern development of aqueous solutions on the waste package and drip shield.

Seepage water and gas composition inputs for in-drift chemistry modeling are abstracted from THC model outputs of time-dependent seepage water compositions and gas-phase compositions in the host rock (near-field environment) adjacent to the drift wall. An abstraction method is

used to generate look-up tables for possible in-drift water compositions, incorporating the effects of seepage water evaporation and deliquescence of salt minerals (in dust on the drip shield and waste package) as a function of environmental conditions.

This is accomplished by sorting seepage water and dust leachate compositions into bins. Each bin contains a group of seepage water or dust leachate compositions that yield chemically similar solutions when they are concentrated by evaporation. Then, a median water composition in each bin is identified that serves to approximate all of the water compositions in the group.

In addition to the water composition tables, tables for defining in-drift and invert carbon dioxide partial pressure (Pco_2), which is controlled by the seepage compositions, were prepared using THC model output. An appropriate in-drift temperature range is determined by examining time-temperature curves for four locations: the waste package surface, the drift wall surface at the crown of the drift, the base of the invert, and within the rock above the crown of the drift.

The evaporative evolution of seepage waters is affected by relative humidity (*RH*), Pco_2, and temperature. Thus, it is necessary to specify these conditions to predict equilibrium chemistries for in-drift aqueous solutions. To accomplish this, look-up tables are prepared to enable selection of predicted water chemistry as a function of seepage or leachate water chemistry (bin number), *RH*, Pco_2, and temperature.

In addition, an evaluation of the corrosion of the ground support materials and its effects on sequestration of oxygen is performed to determine whether there is sufficient flux of oxygen into the drifts to maintain an oxic environment throughout the evolution of the engineered barrier system chemical environments.

1.2 INTENDED MODEL USE

The principal intentions for the use of this model and analysis are to:

- Evaluate the evolution of in-drift chemical environments that affect drip shield and waste package durability, and control solubility and colloidal stability of radionuclides in the invert

- Provide inputs to total system performance assessment to enable quantification of ionic strength, chloride and nitrate concentration, and pH as a function of *RH*, Pco_2, and temperature. These chemical parameters are archived in look-up tables.

1.3 MODEL LIMITATIONS

The ranges for the TSPA look-up tables that quantify the chemical parameters of interest for seepage water or dust deliquescence are defined using three sets of Pco_2 (10^{-2}, 10^{-3}, and 10^{-4} bars of pressure) and multiple temperatures (40, 70, and 100°C for seepage chemistries and 40, 70, 100, 120, and 140°C for dust deliquescence), and are evaluated at approximately every two *RH* units. The main limitations of the physical and chemical environment model involve Pco_2 and temperature as inputs to total system performance assessment.

When selecting chemical parameters for either seepage waters or dust deliquescence under conditions that fall between look-up tables, the parameters should be estimated using linear interpolation of temperature and log linear interpolation of Pco_2. Chemistry values should be extrapolated for pH, ionic content, chloride, and nitrate if the Pco_2 exceeds the range of $1x\ 10^{-4}$ to $1\ x\ 10^{-2}$ atmospheres established in the look-up tables (up to $2\ x\ 10^{-2}$ and down to $1\ x\ 10^{-5}$ atmospheres).

When selecting chemical parameters for seepage waters, for temperatures above 100ºC and below 40ºC, no extrapolation is allowed and values should be taken directly from the 100ºC or 40ºC look-up tables, respectively. A comparable limitation is placed on the dust deliquescence water compositions—extrapolation below 40ºC or above 140°C is not allowed. The lowest *RH* values at which chemistries are provided in the look-up tables for both seepage water or dust deliquescence do not always correspond to the final eutectic point for the mixture of salt minerals present, or to dryness. This is especially true when the deliquescence relative humidity falls below 40 percent.

INTENTIONALLY LEFT BLANK

2. QUALITY ASSURANCE

Development of this model report and the supporting analyses has been determined to be subject to the Office of Civilian Radioactive Waste Management quality assurance program (BSC 2004, Section 8 [DIRS 166519]). Approved quality assurance procedures identified in the technical work plan (BSC 2004, Section 4 [DIRS 166519]) have been used to conduct and document the activities described in this analysis report. The technical work plan also identifies the methods used to control the electronic management of data (BSC 2004, Section 8 [DIRS 166519]) during the analysis and documentation activities.

This report does not directly address either engineered or natural barriers as defined in the *Q-List* (BSC 2003 [DIRS 165179]). However, it does provide information to other modeling activities that are important to meeting the performance objectives in 10 CFR 63.113 [DIRS 156605].

INTENTIONALLY LEFT BLANK

3. USE OF SOFTWARE

The following software was used in the preparation of this model report:

3.1 EQ3/6 V8.0

EQ3/6 Version 8.0 (STN: 10813-8.0-00 [DIRS 162228]) is a software package utilized to perform geochemical modeling computations encompassing fluid-mineral interactions and/or solution-mineral-equilibria in aqueous systems. Hereafter, the code will be referred to as EQ3/6, EQ3, or EQ6 depending on the specific use in the calculations described in later sections of this document.

3.2 GETEQDATA V1.0.1

GETEQDATA V1.0.1 (STN: 10809-1.0.1-00 [DIRS 161900]) is a software routine that operates as a Microsoft Excel (97 or 2000) macro to post-process data found in EQ3/6 *.3o or *.6o output files. Hereafter, the code will be referred to as GETEQDATA.

3.3 EXEMPT SOFTWARE USE

The following commercial, off-the-shelf software is used in this model report in an exempt manner to do basic calculations and statistical operations based on the internal functions of the codes:

- Microsoft Excel 97
- Statistica 5.1

Excel is used throughout the document. The individual spreadsheets are called out in the section where they were used. Statistica is only used in Section 6.11.

INTENTIONALLY LEFT BLANK

4. INPUTS

4.1 DATA AND PARAMETERS

If not otherwise indicated, data and parameters used in this section are specifically selected for use in this model.

4.1.1 Engineered Barrier System Committed Materials Inventory

Several Information Exchange Drawings (IED), considered to be the most current design information available, are information sources for the Physical and Chemical Environment model report, including 800-IED-WIS0-00302-000-00A (BSC 2003 [DIRS 164101]), 800-IED-WIS0-00301-000-00A (BSC 2003 [DIRS 164052]), 800-IED-WIS0-00401-000-00B (BSC 2003 [DIRS 165304]), 800-IED-WIS0-00201-000-00C (BSC 2003 [DIRS 165406]), and 800-IED-WIS0-00202-000-00A (BSC 2003 [DIRS 163855]). The inputs from the IEDs and supporting documents are presented below. In addition, the reader of this document should refer to the IED source documents for assumptions and details that support the information presented.

Tables 4.1-1 through 4.1-10 are used as input to the introduced materials evaluation documented in Section 6.4 of this report. These tables list the masses of introduced materials per meter of repository drift. Thickness is taken from the IED tables by comparing the width, flange thickness, thickness, and other detail columns, and selecting the thickness that will control the lifetime of the material when applying corrosion rates. The mass and thickness of 21 PWR waste package components are used for the naval short and long waste packages (USN 1996 [DIRS 101941]).

Table 4.1-1. Masses of Ground Support Materials per Meter of Repository Drift

Component	Mass (Kg/m)	Thickness (mm)
Steel Sets W6x20[1]	409.0	9.3
Pipe Spacers 1-1/4"[1]	37.2	3.6
Tie Rods 5/8"[1]	18.5	15.9 (dia.)
Steel Wire Fabric 3"x3" grid[1]	62.3	5.7 (dia.)
Rock Bolts (Swellex)	86.09	3[2]
Steel Sheets (Bernold)	374.41	3.0

Source: BSC 2003 [DIRS 164101], Table 3

NOTES: [1] Used only on an as needed basis, not part of baseline design.
[2] See note 1 for Table 3 BSC 2003 [DIRS 164101].

Table 4.1-2. Masses of Drip Shield and Waste Package Pallet per Meter of Repository Drift

Component	Mass[1] (Kg/m)	Thickness (mm)
Drip Shield[2]		
Drip Shield (Plates and Conductor (Connector) Guides)	592.38	15[3]
Drip Shield (Bulkheads, Posts, and Lifting Connectors)	150.49	38[4]
Drip Shield (Base Alloy C-22)	19.96	10
Drip Shield Weld Metal	19.96	-
Emplacement Pallet[5]		
Emplacement Pallet (316L SS)	127.74	9.525
Emplacement Pallet (Alloy C-22)	277.28	6.35
Emplacement Pallet Weld Metal	4.09	-

Source: BSC 2003, Table 1 [DIRS 164052] and BSC 2003, Tables 5 and 6 [DIRS 165304]

NOTES: For those spaces indicated with a "-" the value is not available.
[1] Mass values from BSC 2003, Table 1 [DIRS 164052].
[2] Thickness values from BSC 2003, Table 5 [DIRS 165304].
[3] Value is for plate.
[4] Value is for bulkhead.
[5] Thickness values from BSC 2003, Table 6 [DIRS 165304].

Table 4.1-3. Masses of Invert and Gantry Rail Components per Meter of Repository Drift

Component	Mass (Kg/m)	Thickness (mm)
Invert		
Transverse Beams w/ Stiffeners	228.0	14.6
Longitudinal Support Beams	89.2	9.3[1]
Stiffener Brackets	82.0	Varies
Base Plates	43.0	50.8 (2")
Structural Bolts	37.0	22.23 (7/8") Diameter
Longitudinal Support Beam Rock Anchor Bolts	12.0	34.93 (1-3/8") Diameter
Ballast – Crushed Tuff	3095	-
Gantry Rail Assembly		
Gantry Runway	Combined: 313.3	23.75
Cap Plate		19.05 (3/4") Diameter
Guide Beams	59.5	9.27
Miscellaneous Plates	37.0	Varies
Gantry Rail	133.9	31.75
Rail Fittings	13.4	28.58 (Bolt Diameter)
Conductor Bar (Copper)	4.0	-
Conductor Bar Fittings (Steel)	0.3	-

Source: BSC 2003, Table 3 [DIRS 164101]

NOTES: The value is not available for those spaces indicated with a dash.
[1] Value from AISC 1997 [DIRS 107063].

Table 4.1-4. Masses of 24 BWR Waste Package Components

Component	Mass (Kg)	Thickness (mm)
Basket A – Sideguide (x16)	27	10
Basket B – Sideguide (x16)	1.3	10
Basket Corner Guide (x32)	22	10
Basket Stiffener (x64)	1.6	10
Fuel Basket A – Plate (x4)	89	10
Fuel Basket B – Plate (x4)	89	10
Fuel Basket C – Plate (x8)	90	10
Fuel Basket D – Plate (x8)	90	10
Fuel Basket E – Plate (x16)	30	10
Fuel Basket Tube (x24)	113	5
Inner Shell	6731	50
Inner Shell Lid (x2)	489	65
Inner Shell Lid Lifting Feature	12	27
Outer Shell	3268	20
Extended Outer Shell Lid	103	25
Extended Outer Shell Lid Base	221	25
Outer Shell Lid Lifting Feature (x2)	13	27
Extended Lid Reinforcement Ring	75	50
Outer Shell Flat Closure Lid	98	10
Outer Shell Flat Bottom Lid	245	25
Upper Trunnion Collar Sleeve	404	40
Lower Trunnion Collar Sleeve	396	40
Inner Shell Support Ring	32	20
Total Alloy 22 Welds	194	-
Total 316 Welds	59	-
Waste Package Assembly	19437	-
BWR Fuel Assembly (x24)	328.4	-
WP Assembly with SNF	27318	-

Source: BSC 2003, Table 9 [DIRS 163855]

NOTE: The value is not available for those spaces indicated with a dash.

Table 4.1-5. Masses of 21 PWR Waste Package Components

Component	Mass (Kg)	Thickness (mm)
Basket A – Side Guide (x32)	27	10
Basket A – Stiffener (x64)	0.72	10
Basket B – Side Guide (x16)	36	10
Basket B – Stiffener (x32)	1.5	10
Basket C – Stiffener (x32)	2.3	10
Basket Corner Guide (x16)	42	10
Fuel Basket A – Plate (x8)	85	7
	86#	7
Fuel Basket B – Plate (x8)	85	7
	86#	7
Fuel Basket C – Plate (x16)	44	7
	45#	7
Fuel Basket D – Plate (x8)	21	5
Fuel Basket E – Plate (x8)	21	5
Fuel Basket Tube (x21)	164	5
Inner Shell	8709	50
Inner Shell Lid (x2)	1200	95
Inner Shell Lid Lifting Feature	12	27
Outer Shell	4193	20
Extended Outer Shell Lid	132	25
Extended Outer Shell Lid Base	366	25
Outer Lid Lifting Feature (x2)	13	27
Extended Lid Reinforcement Ring	97	50
Outer Shell Flat Closure Lid	159	10
Outer Shell Flat Bottom Lid	396	25
Upper Trunnion Collar Sleeve	507	40
Lower Trunnion Collar Sleeve	497	40
Inner Shell Support Ring	41	20
Total Alloy 22 Welds	249	-
Total 316 Welds	128	-
Waste Package Assembly	26035	-
	26059#	-
PWR Fuel Assembly (x21)	773.4	-
WP assembly with SNF	42277	-
	42301#	-

Source: BSC 2003, Table 2 [DIRS 163855]

NOTES: # In 21-PWR waste package assembled with stainless steel/boron plates.
The value is not available for those spaces indicated with a dash.

Table 4.1-6. Masses of 5-DHLW/DOE SNF Short Waste Package Components

Component	Mass (Kg)	Thickness (mm)
Divider Plate (x5)	66	12.7
Inner Bracket (x5)	195	25.4
Outer Bracket (x5)	247	12.7
Support Tube	1265	31.75
Inner Shell	7621	50
Inner Shell Lid (x2)	1765	80
Inner Lid Lifting Feature	12	27
Outer Shell	4692	25
Extended Outer Shell Lid	172	25
Extended Outer Shell Lid Base	629	25
Extended Outer Lid Reinforcement Ring	129	50
Outer Lid Lifting Feature (x2)	13	27
Outer Shell Flat Closure Lid	268	10
Outer Shell Flat Bottom Lid	669	25
Upper Trunnion Collar Sleeve	655	40
Lower Trunnion Collar Sleeve	642	40
Inner Shell Support Ring	53	20
Total Alloy 22 Welds	325	-
Total Stainless Steel Welds	133	-
5 DHLW DOE SNF – Short Waste Package	23360	-
HLW Glass Assembly (x5)	2500	-
18" SNF Canister Short	2270	-
WP Assembly with SNF	38130	-

Source: BSC 2003, Table 5 [DIRS 163855]

NOTE: The value is not available for those spaces indicated with a dash.

Table 4.1-7. Masses of 5-DHLW/DOE SNF Long Waste Package Components

Component	Mass (Kg)	Thickness (mm)
Divider Plate (x5)	100	12.7
Inner Bracket (x5)	296	25.4
Outer Bracket (x5)	375	12.7
Support Tube	1924	31.75
Inner Shell	11507	50
Inner Shell Lid (x2)	2314	105
Inner Lid Lifting Feature	12	27
Outer Shell	6918	25
Extended Outer Shell Lid	172	25
Extended Outer Shell Lid Base	629	25
Extended Lid Reinforcement Ring	129	50
Outer Lid Lifting Feature (x2)	13	27
Outer Shell Flat Closure Lid	268	10
Outer Shell Flat Bottom Lid	669	25
Upper Trunnion Collar Sleeve	655	40
Lower Trunnion Collar Sleeve	642	40
Inner Shell Support Ring	53	20
Total Alloy 22 Welds	325	-
Total Stainless Steel Welds	194	-
Waste Package Assembly	32610	-
HLW Glass Assembly (x5)	4200	-
18" Canister Long	2721	-
WP assembly with SNF	56331	-

Source: BSC 2003, Table 6 [DIRS 163855]

NOTE: The value is not available for those spaces indicated with a dash.

Table 4.1-8. Masses of 2-MCO/2-DHLW Waste Package Components

Component	Mass (Kg)	Thickness (mm)
A-Plate (x2)	571	10
Inner Shell	9743	50
Inner Shell Lid (x2)	1641	105
Inner Lid Lifting Feature	12	27
Outer Shell	5897	25
Extended Outer Shell Lid	146	25
Extended Outer Shell Lid Base	450	25
Extended Outer Lid Reinforcing Ring	108	50
Outer Lid Lifting Feature (x2)	13	27
Outer Shell Flat Closure Lid	194	10
Outer Shell Flat Bottom Lid	484	25
Upper Trunnion Collar Sleeve	561	40
Lower Trunnion Collar Sleeve	550	40
Inner Shell Support Ring	45	20
Total Alloy 22 Welds	276	-
Total 316 Welds	164	-
Waste Package Assembly	23081	-
HLW Glass Assembly (x2)	4200	-
Mass HLW Glass Canister as a Percent of HLW Glass Assembly	13.3%[b]	
MCO (x2)	8909.6	12.7[a]
Average U in Mark IV Fuel Element	22.73%[c]	-
WP Assembly with SNF	49300	-

Source: BSC 2003, Table 7 [DIRS 163855]

NOTES: The value is not available for those spaces indicated with a dash.

[a] Thickness of MCO shell (DOE 2000 [DIRS 150095], p. 23).

[b] Source is DOE 2002 [DIRS 161752], Section 1.4.3.1.

[c] Source is DOE 2000 [DIRS 150095], Table 3-1.

Table 4.1-9. Masses of 12-PWR Long Waste Package Components

Component	Mass (Kg)	Thickness (mm)
Basket Side Guide (x32)	28	10
Basket Side Guide Stiffener (x64)	0.5	10
Basket Corner Guide (x16)	48	10
Basket Corner Guide Stiffener (x32)	2.5	10
Fuel Basket A – Plate (x4)	76	7
Fuel Basket B – Plate (X4)	76	7
Fuel Basket C – Plate (x16)	34	7
Fuel Basket D – Plate (x4)	19	5
Fuel Basket E – Plate (x4)	19	5
Fuel Basket Tube (x12)	187	5
Inner Shell	7589	50
Inner Shell Lid (x2)	538	70
Inner Shell Lid Lifting Feature	12	27
Outer Shell	3666	20
Extended Outer Shell Lid	104	25
Extended Outer Shell Lid Base	226	25
Extended Lid Enforcement Ring	76	50
Outer Lid Lifting Feature (x2)	13	27
Outer Shell Flat Closure Lid	100	10
Outer Shell Flat Bottom Lid	250	25
Upper Trunnion Collar Sleeve	408	40
Lower Trunnion Collar Sleeve	400	40
Inner Shell Support Ring	32	20
Total Alloy 22 Welds	196	-
Total 316 Welds	67	-
Waste Package Assembly	19541	-
PWR Fuel Assembly (x12)	882.2	-
WP Assembly with SNF	30127	-

Source: BSC 2003, Table 8 [DIRS 163855]

NOTE: The value is not available for those spaces indicated with a dash.

Table 4.1-10. Masses of 44-BWR Waste Package Components

Component	Mass (Kg)	Thickness (mm)
Basket B – Side Guide (x32)	19	10
Basket B – Stiffener (x64)	0.31	10
Basket Corner Guide (x32)	46	10
Basket Stiffener (x64)	2.7	10
Fuel Basket A – Plate (x4)	63	5
Fuel Basket B – Plate (x4)	63	5
Fuel Basket C – Plate (x16)	15	5
Fuel Basket D – Plate (x16)	44	5
Fuel Basket E – Plate (x16)	44	5
Fuel Basket F – Plate (x8)	21	5
Fuel Basket G – Plate (x8)	21	5
Fuel Basket Tube (x44)	113	5
Inner Shell	8886	50
Inner Shell Lid (x2)	1251	95
Inner Shell Lid Lifting Feature	12	27
Outer Shell	4275	20
Extended Outer Shell Lid	135	25
Extended Outer Shell Lid Base	381	25
Outer Shell Lid Lifting Feature (x2)	13	27
Extended Lid Reinforcement Ring	99	50
Outer Shell Flat Closure Lid	165	10
Outer Shell Flat Bottom Lid	412	25
Upper Trunnion Collar Sleeve	517	40
Lower Trunnion Collar Sleeve	507	40
Inner Shell Support Ring	42	20
Total Alloy 22 Welds	253	-
Total 316 Welds	131	-
Waste Package Assembly	28068	-
BWR Fuel Assembly (x44)	328.4	-
WP assembly with SNF	42517	-

Source: BSC 2003, Table 3 [DIRS 163855]

NOTE: The value is not available for those spaces indicated with a dash.

4.1.2 Material Corrosion Rates and Materials Compositions

Ranges in corrosion rates for the committed materials listed on Tables 4.1-1 through 4.1-10 are required to determine material lifetimes in the in-drift environments and the potential chemical impacts of water-material interactions, as evaluated in Sections 6.4, 6.7, and 6.8 of this report. Tables 4.1-11 and 4.1-12 list the inputs used to determine maximum, minimum, and mean or median corrosion rates (humid air, atmospheric, and aqueous) for the committed materials. Documents produced within the Project are considered appropriate sources of technical information for this report. The non-Project sources, such as journal articles and engineering handbooks, are also considered suitable information for three reasons:

- Journals are peer-reviewed, with rigorous screening processes
- Data in handbooks are rigorously reviewed and widely accepted
- In some instances, such as with stainless steels, published information is sparse and these references give the only information available on the subject.

Table 4.1-11. Source Data/Input Information Used for Corrosion Rate Determinations of Metallic Materials

Parameter		Source
Titanium - Humid Air and Atmospheric Corrosion Rates		McCright 1998, Section 2.2.6, Supplements 1 and 2 [DIRS 114637] Covington and Schutz 1981 [DIRS 151102]
Alloy 22	Humid Air Corrosion Rates	McCright 1998, Section 2.2.6, Supplements 1 and 2 [DIRS 114637]
	Aqueous Corrosion Rates	DTN: MO0401SPAMCRAE.000 [DIRS 166801]
Inconel Alloys X-750 and 600 - Aqueous Corrosion Rates		DTN: MO0401SPAMCRAE.000 [DIRS 166801]
Copper Alloy - Humid Air and Atmospheric Corrosion Rates		Southwell et al. 1976, Table 3 [DIRS 100927] Forgeson et al. 1958, Table 7 [DIRS 159343] Townsend and Zoccola 1982, Table 3 [DIRS 100937] Guttman and Sereda 1968, Tables 3, 4, 7, and 8 [DIRS 100895] McCright et al. 1987, Table 13 [DIRS 159336] Boyer and Gall 1984, Table 7 [DIRS 155318] Southwell and Bultman 1982, Table 64.5 [DIRS 100928] Beavers and Durr 1991, Tables 4.4, 6.2, 6.3, and 7.2 [DIRS 159341]
Aluminum Alloy	Atmospheric Corrosion Rates	American Society for Metals International 1987, Tables 8 and 11 [DIRS 103753]
	Aqueous Corrosion Rates	DTN: MO0401SPAMCRAE.000 [DIRS 166801]
316L SS	Humid Air and Atmospheric Corrosion Rates	Southwell et al. 1976, Tables 5 and 7 [DIRS 100927] Alexander et al. 1961, Table 2 [DIRS 162265] Bomberger et al. 1954, Table 11 [DIRS 163699] McCright et al. 1987, Table 6 [DIRS 159336] Copson 1955, Table IX [DIRS 162451] Johnson and Pavlik 1982, Tables 32.6 and 32.7 [DIRS 162292] Southwell and Bultman 1982, Table 64.6 [DIRS 100928] Merz 1982, Table 3.18 [DIRS 162290]
	Aqueous Corrosion Rates	DTN: MO0401SPAMCRAE.000 [DIRS 166801]

Table 4.1-11. Source Data/Input Information Used for Corrosion Rate Determinations of Metallic Materials (Continued)

Parameter		Source
304L SS	Aqueous Corrosion Rates	DTN: MO0401SPAMCRAE.000 [DIRS 166801]
Borated SS	Aqueous Corrosion Rates	DTN: MO0401SPAMCRAE.000 [DIRS 166801] Van Konynenburg et al. 1998, Table 3 [DIRS 100948]
Carbon and Low Alloy Steels	Humid Air and Atmospheric Corrosion Rates	Dutra and de O. Vianna 1982, Tables 53.3 and 53.4 [DIRS 162266] McCright 1998, Section 2.2.6, Supplements 1 and 2 [DIRS 114637] Larrabee and Coburn 1961, Table 3 [DIRS 162288] Wei 1991, Tables 2 and 4 [DIRS 100945] Haynie and Upham 1974, Table 3 [DIRS 100900] Haynie and Upham 1971, Tables 2 and 3 [DIRS 100899] Komp 1987, Table 2 [DIRS 100908] Guttman and Sereda 1968, Tables 3 through 8 [DIRS 100895]
	Aqueous Corrosion Rates	DTN: MO0401SPAMCRAE.000 [DIRS 166801] DTN: LL980704605924.035 [DIRS 147298]

NOTE: Due to the large amount of data used to calculate atmospheric corrosion rates, these rates are not individually presented here but may be found in "atmospheric.xls."

The input used to determine the corrosion rate for the N-Reactor waste form and the COMMERCIAL SNF waste form can be found in Table 4.1-12. The COMMERCIAL and N-Reactor SNF degradation rates are calculated in "Oxygen demand.xls," archived in output DTN: MO0312SPAPCEGF.002 (see Section 6.7.1).

Table 4.1-12. Source Data/Input Information Used for Corrosion Rate Determinations of Waste Forms

Description	Source	Value
Dissolution Rates for N-Reactor	BSC 2003, Table 6 [DIRS 163693]	$k=2.52 \times 10^{10} \exp[-66{,}400/RT]$ $mg/cm^2 \cdot hr$; R=8.314 J/mol·K, T=temperature, Kelvin
Inputs to CSNF waste form degradation rate equation	BSC 2003, p. 94, Table 8.1-2 [DIRS 163824]	$a_0 = 4.705$ $a_1 = -1093.826$ $a_2 = -0.102$ $a_3 = -0.338$

CSNF = commercial spent nuclear fuel

The American Society for Testing and Materials (ASTM) standards listed on the IEDs (800-IED-WIS0-00302-000-00A (BSC 2003 [DIRS 164101]), 800-IED-WIS0-00301-000-00A (BSC 2003 [DIRS 164052]), 800-IED-WIS0-00401-000-00B (BSC 2003 [DIRS 165304]), 800-IED-WIS0-00201-000-00C (BSC 2003 [DIRS 165406]), and 800-IED-WIS0-00202-000-00A (BSC 2003 [DIRS 163855])) in Section 4.3.2 and on Table 6.4-20 are used to provide the compositional information found on Table 6.4-20. The locations from which the inputs were taken are listed below:

- ASTM A53/A53M-02, Table 1 [DIRS 162719]
- ASTM A240/A240M-02a, Table 1 [DIRS 162720]
- ASTM A276-03, Table 1 [DIRS 165006]
- ASTM A307-02, Section S1.5.1 [DIRS 162722]
- ASTM A490-02, Table 2 [DIRS 158937]

- ASTM A516/A516M-01, Table 1 [DIRS 162723]
- ASTM A572/A572M-01, Table 2 [DIRS 158661]
- ASTM A588/A588M-01, Table 1 [DIRS 162724]
- ASTM A759-00, Table 1 [DIRS 159971]
- ASTM B209M-02e1, Table 1 [DIRS 162727]
- ASTM B265-02, Table 2 [DIRS 162726]
- ASTM B575-99a, Table 1 [DIRS 147465].

The 316L stainless steel composition specified by ASTM A240/A240M-02a, Table 1 [DIRS 162720], is modified by the use of *Corrosion* (Volume 13 of *Metals Handbook*, ASM International 1987, p. 931 [DIRS 103753]) for use in the inner waste package barrier. No ASTM standard exists for the fuel basket plate; therefore, the source for the composition of Neutronit A 987 used in Table 6.4-20 can be found in DTN: MO0109RIB00049.001 [DIRS 155964] under section "Material Properties of Neutronit A976/A978."

The compositions for the conductor bar and fittings and communications cables can be found in BSC (2003, Table 3 [DIRS 164101]).

4.1.3 Water and Gas Compositions

The seepage water compositions used in the physical and chemical environment (P&CE) model, and their equilibrium CO_2 fugacities, are listed in DTN: LB0302DSCPTHCS.002 [DIRS 161976]. This DTN consists of five complete drift scale seepage coupled thermal-hydrological-chemical (THC) modeling results, each representing a different starting pore water taken from the *Drift Scale Coupled Processes (DST and THC Seepage) Models* (BSC 2003 [DIRS 162050]). The THC seepage model output for each water is in Microsoft Excel spreadsheet format:

- CS500/12.0 (thc6_w7_r.xls)
- CS2000/16.5 (thc6_w4_r.xls)
- CS1000/7.3 (thc6_w5_r.xls)
- SD-9/990.4(thc6_w6_r.xls)
- HD-PERM water (thc6_w0_r.xls)

These five waters were selected to represent the spread of potential pore water data that serve as starting water compositions for the drift scale THC seepage model. The rationale for the initial selection of these five waters is discussed in Section 6.2.2.1 of *Drift Scale Coupled Processes (DST and THC Seepage) Models* (BSC 2003 [DIRS 162050]).

Table 4.1-13 lists the outputs from the THC seepage model that were used as inputs to the binning analysis (see Section 6.6) and identifies these inputs by starting water composition. Throughout the remainder of this report, the waters will be referred to by their abbreviated water name.

Table 4.1-13. References for Input to Binning Analysis

Abbreviated Water Name	Filename	Starting Water Composition	Informational Reference for Starting Water Itself
W0	thc6_w0_r.xls	HD-PERM water (Alcove 5)	BSC 2003, Table 6.2-1 [DIRS 162050]
W4	thc6_w4_r.xls	Cross-drift water CS2000/16.5	DTN: GS020408312272.003 [DIRS 160899]
W5	thc6_w5_r.xls	Cross-drift water CS1000/7.3	DTN: GS020408312272.003
W6	thc6_w6_r.xls	Cross-drift water SD-9/990.4	DTN: GS020408312272.003
W7	thc6_w7_r.xls	Cross-drift Water CS500/12.0-16.7	DTN: GS020408312272.003

Source of THC seepage model: DTN: LB0302DSCPTHCS.002 [DIRS 161976]

The files shown in Table 4.1-14 are used as inputs for the in-drift gas analyses.

Table 4.1-14. References for Input Gas Chemistry Analyses

Filename	Starting Water Composition	Informational Reference for Starting Water Itself
thc6_w0_r.xls thc6_w0_drift_r.xls	HD-PERM water (Alcove 5)	BSC 2003, Table 6.2-1 [DIRS 162050]
thc6_w4_r.xls thc6_w4_drift_r.xls	Cross-drift water CS2000/16.5	DTN: GS020408312272.003 [DIRS 160899]
thc6_w5_r.xls thc6_w5_drift_r.xls	Cross-drift water CS1000/7.3	
thc6_w6_r.xls thc6_w6_drift_r.xls	Cross-drift water SD-9/990.4	
thc6_w7_r.xls Thc6_w7_drift_r.xls	Cross-drift Water CS500/12.0-16.7	

Source of THC seepage model: DTN: LB0302DSCPTHCS.002 [DIRS 161976]

The gas flux across the drift wall and into the drift is estimated using input from the *Drift-Scale Coupled Processes (DST and THC Seepage) Models* (BSC 2003 [DIRS 162050]), as listed in Table 4.1-15. The complete set of results in the dataset (DTN LB0302DSCPTHCS.002, spreadsheet "thc6_w0_drift_r.xls" [DIRS 161976]) includes gas flux at the base, side, and the crown. To maximize the estimated gas flux, however, only the largest value of flux, regardless of its position in the drift (crown, base, or side), is used at each time step in the calculations (spreadsheet gas flux.xls, output DTN MO0312SPAPCEGF.002). The maximum gas flux is used in the calculations to ensure that the oxygen supply to the drift and the resulting corrosion of drift materials would be maximized. Table 4.1-15 summarizes the position in the drift where the max flux occurred, the CO_2 volume fraction, the gas flux, and air mass fraction. Additional inputs required to make the gas flux calculations are provided on Table 4.1-16.

Table 4.1-15. Time-Varying Inputs for the Gas Flux Calculation in Section 6.7.1

TIME (Postclosure-Years)	Position in Drift (at the Wall)	CO_2(g) Volume fraction	Gas Flux (kg/s)	Air Mass Fraction
0.0027	Base	9.29E-04	-5.09E-09	9.80E-01
1	Side	1.33E-03	2.15E-09	9.40E-01
5	Side	1.26E-03	4.56E-09	9.03E-01
10	Side	1.20E-03	4.83E-09	8.92E-01
20	Side	1.09E-03	3.89E-09	8.94E-01
30	Side	9.98E-04	2.88E-09	9.02E-01
40	Side	9.97E-04	2.08E-09	9.10E-01
50	Side	9.75E-04	1.50E-09	9.17E-01
51	Side	5.01E-04	1.05E-07	2.75E-01
53	Crown	2.10E-04	1.12E-07	9.19E-03
55	Side	1.17E-04	2.71E-08	2.75E-03
60	Crown	2.58E-05	9.51E-08	3.49E-05
75	Crown	9.33E-05	3.70E-08	1.56E-03
100	Crown	2.59E-04	2.03E-08	1.81E-02
150	Crown	5.19E-04	2.94E-08	5.18E-02
200	Crown	5.99E-04	5.10E-08	6.71E-02
250	Crown	4.92E-04	3.52E-08	7.04E-02
300	Crown	3.60E-04	2.22E-08	6.49E-02
350	Crown	2.95E-04	1.59E-08	5.99E-02
400	Crown	2.95E-04	1.31E-08	5.37E-02
500	Crown	4.46E-04	1.12E-08	4.31E-02
600	Crown	8.09E-04	1.07E-08	3.96E-02
650	Crown	1.13E-03	1.38E-08	3.30E-02
700	Crown	1.48E-03	1.42E-08	3.46E-02
751	Crown	1.87E-03	1.36E-08	4.02E-02
790	Crown	2.10E-03	1.34E-08	4.57E-02
801	Crown	2.30E-03	1.33E-08	4.75E-02
1001	Crown	4.13E-03	1.20E-08	9.23E-02
1201	Crown	5.24E-03	1.14E-08	1.29E-01
1401	Crown	6.37E-03	9.90E-09	1.83E-01
1601	Crown	7.19E-03	8.47E-09	2.42E-01
1801	Crown	7.74E-03	7.37E-09	2.86E-01
2001	Side	7.71E-03	4.37E-08	2.17E-01
2202	Base	7.94E-03	3.29E-08	3.01E-01
2402	Base	8.34E-03	3.34E-08	3.57E-01
3002	Base	7.94E-03	2.80E-08	4.84E-01
5003	Base	6.81E-03	2.13E-08	7.01E-01

Table 4.1-15. Time-Varying Inputs for the Gas Flux Calculation in Section 6.7.1 (Continued)

TIME (Postclosure-Years)	Position in Drift (at the Wall)	CO_2 (g) Volume fraction	Gas Flux (kg/s)	Air Mass Fraction
7005	Base	7.02E-03	1.87E-08	8.00E-01
10007	Base	7.15E-03	1.67E-08	8.73E-01
12310	Base	6.69E-03	1.59E-08	9.01E-01
15010	Base	5.92E-03	1.51E-08	9.23E-01
20013	Base	4.59E-03	1.42E-08	9.46E-01
27355	Base	3.42E-03	1.34E-08	9.61E-01
30020	Base	3.02E-03	1.32E-08	9.64E-01
50035	Base	2.24E-03	1.24E-08	9.74E-01
77206	Base	1.92E-03	1.19E-08	9.79E-01
100067	Base	1.68E-03	1.17E-08	9.80E-01

Source: DTN: LB0302DSCPTHCS.002 [DIRS 161976], File "thc6_w0_drift_r.xls" tabs "fractures-ch" and "fractures-th"

NOTE: Negative gas flux means flux is away from the drift.

Table 4.1-16. Constant Inputs for Gas Flux and Oxygen Demand Calculations from Section 6.7.1

Parameter	Value	Location in Report	Source
Atomic Weight of O	15.9994 g/mol	Section 6.7.1, spreadsheet "gas flux.xls"	Parrington, et al. 1996, pp. 62-63 [DIRS 103896]
Atomic Weight of C	12.0107 g/mol		
Atomic Weight of N	14.00674 g/mol		
Atomic Weight of H	1.00794 g/mol		
Atomic Weight of Ar	39.948 g/mol		
Volume fraction of O_2 in atmospheric air	0.20946	Section 6.7.1, spreadsheet "gas flux.xls"	Weast and Astle 1979, p. F-211 [DIRS 102865]
Volume fraction of N_2 in atmospheric air	0.78084		
Volume fraction of Ar in atmospheric air	0.00934		
Cross-sectional area at wall (crown and side)	0.3605 m^2	Section 6.7.1, spreadsheet "gas flux.xls"	LB0302DSCPTHCS.002 [DIRS 161976], spreadsheet "thc6_w0_drift_r.xls" tab "notes"
Cross-sectional area at wall (base)	0.5417 m^2		
Drift diameter	5.5 m	Section 6.7.1, spreadsheet "gas flux.xls"	BSC 2003, Figure 2 [DIRS 164101]
N-Reactor waste package length (2-MCO/2-DHLW)	5.217 m	Section 6.7.1, spreadsheet "Oxygen Demand.xls"	BSC 2003, Table 1 [DIRS 165406]
21 PWR waste package length	5.165 m	Section 6.7.1, spreadsheet "Oxygen Demand.xls"	BSC 2001, Table 1 [DIRS 165406]
Spacing between waste packages	0.1 m	Section 6.7.1, spreadsheet "Oxygen Demand.xls"	BSC 2003 [DIRS 164069]

The effects of corrosion of engineered barrier system (EBS) committed materials on the concentration of oxygen in the drift atmosphere through time are evaluated by combining the material inputs from Section 4.1.2 with the additional information in Table 4.1-16 and Table 4.1-17. For this methodology, see Section 6.7.1.

Table 4.1-17. Inputs for Calculation of Oxygen Consumption by Corrosion Processes

N-Reactor WP			
Item	**Value**	**Source**	**Location in Report**
Surface Area of Mark IV Fuel element	3152 cm^2	DOE 2000 [DIRS 150095], p. 51	Section 6.7.1, Spreadsheet "Oxygen Demand.xls" Output DTN: MO0312SPAPCEGF.002
Elements per basket	54	DOE 2000 [DIRS 150095], p. 26	
Baskets per MCO	5		

21- PWR CSNF WP						
Material	**Mass (g)**	**Surface Area (cm^2)**	**Source and Location in Report**	**Density (g/cm^3)**	**Source**	**Location in Report**
A516 Fuel Basket Tube	3.48E+06	1.78E+06	Source: DTN: MO0210MWDEXC01.008 [DIRS 163531] Location: Section 6.7.1, Spreadsheet "Oxygen Demand.xls" Output DTN: MO0312SPAPCEGF.002	7.85	ASME 1998, SA-20/SA-20M, Section 14.1, p. 67 [DIRS 145103]	Section 6.7.1, Spreadsheet "Oxygen Demand.xls" Output DTN: MO0312SPAPCEGF.002
A516 Guides	2.43E+06	6.14E+05		7.85		
Neutronit	2.10E+06	5.29E+05		7.76	DTN: MO0109RIB00049.001 [DIRS 155964] (Under Section "Material Properties of Neutronit A976/A978")	
Al-6061	3.42E+05	2.59E+05		2.7	ASTM G 1-90, p. 7, Table X1.1 (A96061) [DIRS 103515]	
316NG Inner Shell	1.05E+07	5.00E+05		8	DTN: MO0003RIB00076.000 [DIRS 153044]	
CSNF Fuel	1.08E+07	2.28E+07				

4.1.4 Thermodynamic Databases

Two datasets have been developed by the Project for geochemical modeling calculations using EQ3/6. These are:

- Data0.ymp.R2: This database is found in DTN: MO0302SPATHDYN.000 [DIRS 161756] and is documented in Data Qualification: Update and Revision of the Geochemical Thermodynamic Database, Data0.ymp (Steinborn et al. 2003 [DIRS 161956]). This dataset is used for non-Pitzer type calculations, and includes updated equilibrium constants (e.g., log K, ΔH, ΔG, and S) for temperatures above 25°C and additional mineral phases, including zeolites, clays, cement phases, and radionuclides.

- Data0.ypf: This database is found in DTN: SN0302T0510102.002 [DIRS 162572]. Its development is documented in the In-Drift Precipitates/Salts Model (BSC 2003 [DIRS 162529]). This dataset is used for EQ3/6 Pitzer type calculations such as those done to calculate evaporative brine compositions and includes updated equilibrium constants (e.g., log K, ΔH, ΔG, and S) and Pitzer interaction parameters for temperatures above 25°C, and additional mineral phases, including zeolites, clays, cement phases, and minerals associated with salt deposits.

In other sections of this document, these datasets are referred to as the Data0.ymp.R2 and the Data0.ypf data files.

4.1.5 In-Drift Evaporation

The *In-Drift Precipitates/Salts Model* (BSC 2003 [DIRS 166031]) is documented independently of this model report. The in-drift precipitates/salts model, its assumptions, and validation are a direct feed into this model. The reader is referred to the document above for the specifics on model development and is the source for the first DTN listed in Table 4.1-18.

The model validation range for the current in-drift precipitates/salts model is for temperatures up to 140°C (see BSC 2003 [DIRS 166031]).

The second DTN listed in Table 4.1-18 is being developed in the *In-Drift Precipitates/Salts Model* (BSC 2003 [DIRS 166031]) and is used as input for the uncertainties quantified in the P&CE model.

4.1.6 Dust Leachate Compositions

Two data sets have been provided by the U.S. Geological Survey to evaluate the impacts of the dusts that could be deposited on waste packages and other in-drift components. These data sets (DTN: MO0207EBSDUSTS.020 [DIRS 162556] and DTN: MO0209EBSDUST2.030 [DIRS 162557]) contain the dust leachate chemical compositions, particle size distributions for the dust, and quantities of accumulated dust per unit area of the exposed surface.

The data in Tables 4.1-19 and 4.1-20 were used to develop EQ3 input files that are used for analyses in Section 6.10.

Table 4.1-18. In-Drift Precipitates Salts Model General File Formats

DTN	Description	Location in Text
MO0303SPAMEQ36.000 [DIRS 162549]	General Formats for EQ3/6 Input Files Simulating the In-Drift Precipitates Salts Model	Sections 6.6.5, 6.9, 6.10.4, 6.10.5
MO0312SPAESMUN.002 [DIRS 166329]	Estimated Model Uncertainties in the In-Drift Precipitates Salts Model	Section 6.12

Table 4.1-19. Water Soluble Cations and Anions Leached from Dust Collected Throughout the Exploratory Studies Facility

Lab No.	Field No.	Cl ppm	F ppm	NO_3 ppm	SO_4 ppm	Br ppm	Ca ppm	K ppm	Mg ppm	Na ppm	Si ppm
C-186077	SPC00573607	260	8	1820	2200	14	2490	350	12.8	455	173
C-186080	SPC00573610	162	24	220	640	34	430	221	19.4	304	89.2
C-186081	SPC00573611	200	30	340	840	56	941	242	6.32	378	213
C-186082	SPC00573612	154	10	340	1060	50	630	231	28.3	388	95.1
C-186084	SPC00573614	130	12	380	1160	24	939	219	27.1	343	121
C-186085	SPC00573615	162	12	380	740	22	863	220	25.9	369	134
C-186086	SPC00573616	130	12	400	1480	26	893	248	35.7	374	107
C-186087	SPC00573617	140	18	440	1180	20	919	221	32.8	332	96.4
C-186088	SPC00573618	114	12	300	400	16	439	479	13.7	345	120
C-186089	SPC00573619	200	24	420	720	22	635	214	43.6	397	100
C-186090	SPC00573620	56	4	82	162	6	226	101	10.6	157	79.1
C-186091	SPC00573622	182	6	800	1120	10	980	183	83.6	358	43.5
C-186092	SPC00573623	180	6	580	980	22	638	193	79.7	431	46.6
C-186093	SPC00573624	240	10	280	340	54	332	128	35.7	386	14.9
C-186094	SPC00573625	300	8	680	1340	26	974	260	79.1	617	58.7
C-186095	SPC00573626	200	14	400	660	26	575	206	34.3	415	94.9
C-186096	SPC00573627	260	32	420	1020	34	394	237	53.4	511	65.0
C-186097	SPC00573628	160	8	380	620	18	480	142	34.8	287	61.2
C-186098	SPC00573629	184	10	240	360	38	268	126	26.7	346	34.5
C-186099	SPC00573630	196	8	280	480	28	392	149	42.0	344	27.9
C-186100	SPC00573631	220	40	260	640	64	630	150	31.4	389	82.5
C-186101	SPC00573632	220	8	114	300	28	229	101	18.9	262	42.3
C-186102	SPC00573633	114	18	62	320	22	543	80	9.76	158	97.5

Source: DTN: MO0207EBSDUSTS.020, Table S02163_009 [DIRS 162556]

Table 4.1-20. Water Soluble Cations and Anions Leached from Dust Collected Throughout the Exploratory Studies Facility

Lab. No./ Sample No.	Mesh Size	ESF Local (m)	Element-Oxide (ppm)									
			Ca	Mg	K	Na	Si	Cl	Br	F	NO_3	SO_4
C-203135/ 00574986C	60-200	0.00	147	16.3	159	55.4	161	<24	<1.6	8	<7	<32
C-203113/ 00574979B	200-325		91.7	9.47	127	46.4	96.5	<24	<1.6	4	10	<32
C-203114/ 00574979C	<325		119	12.6	174	66.0	144	<24	<1.6	8	24	<32
C-203115/ 00574980A	60-200	223.7	270	34.3	193	115	169	76	<1.6	18	220	220
C-203116/ 00574980B	200-325		466	49.3	181	124	76.6	98	4	4	400	360
C-203117/ 00574980C	<325		1080	80.1	206	195	176	154	8	12	640	840
C-203118/ 00574981A	60-200	613.0	772	44.1	280	188	33.4	74	4	8	116	3800
C-203119/ 00574981B	200-325		1060	39.5	389	471	287	280	44	22	360	1000
C-203120/ 00574981C	<325		2340	130	389	392	42.8	320	6	8	1760	4600
C-203121/ 00574982A	60-200	861.0	246	39.6	196	262	164	86	4	20	240	320
C-203122/ 00574982B	200-325		458	64.1	244	339	51.6	118	6	4	520	520
C-203123/ 00574982C	<325		1010	99.6	345	556	99.2	170	12	6	1000	1060
C-203124/ 00574983A	60-200	1263.2	262	23.7	281	296	94.9	114	8	12	198	380
C-203125/ 00574983B	200-325		770	50.8	303	425	57.3	260	10	4	540	720
C-203126/ 00574983C	<325		1240	85.9	369	666	62.7	360	10	10	980	1200

Table 4.1-20. Water Soluble Cations and Anions Leached from Dust Collected Throughout the Exploratory Studies Facility (Continued)

Lab. No./ Sample No.	Mesh Size	ESF Local (m)	Element-Oxide (ppm)									
			Ca	Mg	K	Na	Si	Cl	Br	F	NO_3	SO_4
C-203127/ 00574984A	60-200	2207.5	335	49.4	339	265	87.3	128	10	10	220	440
C-203128/ 00574984B	200-325		-	-	-	-	-	-	-	-	-	-
C-203129/ 00574984C	<325		-	-	-	-	-	220	18	10	500	1040
C-203130/ 00574985A	60-200	5405.4	994	65.4	303	349	248	170	20	18	340	880
C-203131/ 00574985B	200-325		1260	52.4	333	461	181	168	14	22	480	1180
C-203132/ 00574985C	<325		1030	54.7	275	480	130	166	16	22	500	1220
C-203133/ 00574986A	60-200	4013.5	248	23.4	234	222	75.4	96	6	6	146	320
C-203134/ 00574986B	200-325		806	38.0	220	292	131	170	10	12	300	740
C-203135/ 00574986C	<325		1190	51.4	260	408	159	220	14	18	440	1140
C-203136/ 00574987A	60-200	3007.0	1290	84.6	257	201	21.8	188	2	8	600	5800
C-203137/ 00574987B	200-325		1180	64.1	313	564	135	360	42	22	540	1400
C-203138/ 00574987C	<325		1280	70.5	288	570	143	320	32	24	520	1480
C-203139/ 00574990A	60-200	6515.2	274	19.8	186	149	44.7	88	10	8	170	500
C-203140/ 00574990B	200-325		434	25.9	151	186	38.9	102	16	6	220	760
C-203141/ 00574990C	<325		689	34.7	251	370	82.2	136	22	14	300	940
C-203142/ 00574991A	60-200	7050.0	281	55.4	139	128	161	88	12	22	122	440
C-203143/ 00574991B	200-325		319	56.8	114	121	79.4	76	10	4	156	520
C-203144/ 00574991C	<325		622	53.6	177	196	215	82	12	10	164	700
C-203145/ 00574992A	60-200	7622.2	122	10.3	155	171	57.4	98	6	8	70	116
C-203146/ 00574992B	200-325		110	9.48	121	126	12.3	82	<1.6	2	68	124
C-203147/ 00574992C	<325		305	19.8	173	187	60.2	166	2	6	150	280

Source: DTN: MO0209EBSDUST2.030, Table 4 [DIRS 162557]

The partial pressure of CO_2 in the Earth's atmosphere (Table 4.1-21) is used in Section 6.10.3 in performing geochemical speciation calculations for the dust leachate waters.

Table 4.1-21. Partial Pressure of CO_2 at Atmospheric Conditions

Partial Pressure of CO_2 in Atmosphere	$10^{-3.5}$ Atmospheres	Weast 1984, p. F.157 [DIRS 106170]

4.1.7 Steel Corrosion Chemistry

This section provides inputs to Section 6.8, which examines the chemical impact of the steel ground support system and its resulting corrosion products on seepage waters entering the drift. The current design calls for using 316L stainless steel sheets and rock bolts (BSC 2003, Note 6 [DIRS 164101]) as the drift ground support system. The metallic elements contained within this steel are presented here.

The IED 800-IED-WIS0-00302-000-00A (BSC 2003, Table 3 [DIRS 164101]) contains the relevant compositional and dimensional information for the 316L stainless steel "Bernold brand type S" sheets and rock bolts that are currently planned for use as in-drift ground support. The relevant dimensional information is presented in Table 4.1-22.

Table 4.1-22. Dimensional Information for 316L Stainless Steel Sheets and Rock Bolts

Parameter	Value	Source in BSC 2003 [DIRS 164101]
Sheet Thickness	3.0 mm	Table 3
Rock Bolt Component	10 Bolts/Row 2.8 m long	Table 3
Rock Bolt Thickness (Diameter)	54 mm	Table 3
Rock Bolt Thickness	3 mm	Note 1
Rock Bolt Row Spacing	1.25 m	Note 4

The abstracted calculation for 316L stainless steel corrosion is performed in Sections 6.8.3 and 6.8.4. Table 4.1-23 summarizes the specific inputs utilized to abstract the degree of corrosion as a function of time.

Table 4.1-23. Parameters Used to Abstract 316L Stainless Steel Ground Support Corrosion

Parameter	Value	Units	Source
316L Density	7.98	g/cc	ASTM G 1-90, Table XI [DIRS 103515]
Cr and Fe weight composition of 316L	Fe - 65.545 Cr - 16.0-18.0 (17 avg)	Weight Percent	ASTM A 240/A 240M-02a [DIRS 162720]
Time dependent infiltration rates	Various	mm/year	DTN: LB0302DSCPTHCS.002 [DIRS 161976]
Transition time from dry to wet drift wall conditions	2000	years	DTN: LB0302DSCPTHCS.002 [DIRS 161976]

NOTE: The weight percent of Fe was calculated from Table 1 of ASTM A 240/A 240M-02a [DIRS 162720] by subtracting all alloying elements from 100. When a range was given, the average of that range was used.

The addition of an amorphous chromium(III) hydroxide mineral species is required to model the effects of corrosion on incoming seepage waters; otherwise, there is no controlling solid phase available for Cr in the Data0.ymp.R2 database (DTN: MO0302SPATHDYN.000 [DIRS 161756]). The rationale for selecting the amorphous chromium hydroxide mineral species is discussed in Section 6.8.2 of this report. In addition, the formation reaction for the mineral Eskolaite (Cr_2O_3) in the current non-Pitzer database has been recast to match that described in the source for the thermodynamic data for amorphous chromium hydroxide. The source for these species is a peer-reviewed journal article with rigorous screening processes, in the highly respected *Journal of Chemical and Engineering Data*, authored by experts in this field. The solubility parameters are listed in Table 4.1-24.

Table 4.1-24. Dissolution Data for Amorphous Chromium(III) Hydroxide $Cr(OH)_3$ and Eskolaite (Cr_2O_3) at 25°C

Mineral	Parameter	Value	Source
$Cr(OH)_{3\ (am)}$	Log *K*	-9.35	Ball and Nordstrom (1998), Table 8 [DIRS 163015]
Cr_2O_3	Log *K*	-8.52	Ball and Nordstrom (1998), Table 8 [DIRS 163015]

4.1.8 Inputs used for Sensitivity Studies

In the THC seepage model, Bromide (Br^-) is a trace component that is not modeled. Because halides are of concern to corrosion modeling, it is important to know to what levels they will concentrate. As Br^- is not a modeled species, no direct output for Br^- concentration is available. Measured pore water Br^- concentrations listed in Table 4.1-25 are used in Section 6.12.4 to estimate the uncertainty that the presence of Br^- adds to the seepage water composition.

Table 4.1-25. Pore Water Compositional Data Used to Evaluate the Relative Importance of Br

	Local Sample Name	SPC Number	Cl mg/L	Br mg/L
1	ECRB-SYS-CS400/3.8-4.3/UC	SPC00554610	29	<1
2	ECRB-SYS-CS400/5.6-6.2/UC	SPC00554611	21	<1
3	ECRB-SYS-CS600/3.6-4.0/UC	SPC00554612	22	<1
4	ECRB-SYS-CS1000/7.3-7.7/UC	SPC00554613	21	<1
5	ECRB-SYS-CS750/6.2-6.5/UC	SPC00554614	73	<1
6	ECRB-SYS-CS2150/5.5-6.1/UC	SPC00554615	27	<0.2
7	ECRB-SYS-CS900/5.4-5.9/UC	SPC00554616	37	<0.2
8	ECRB-SYS-CS850/5.1-5.6/UC	SPC00554617	32	<0.2
9	SD-9/990.4-991.7/UC	SPC00554618	23	<0.2
10	ECRB-SYS-CS900/3.5-4.1/UC	SPC00554619	53	0.3
11	ECRB-SYS-CS1000/12.9-14.0/UC	SPC00554620	22	<0.1
12	ECRB-SYS-CS450/5.3-6.0/UC	SPC00554621	66	0.4
13	ECRB-SYS-CS2300/4.3-4.9/UC	SPC00554622	23	<0.1
14	ECRB-SYS-CS500/12.0-16.7/UC	SPC00554800	54	0.4
15	ECRB-SYS-CS2000/16.5-21.1/UC	SPC00554801	26	<0.2
16	ECRB-SYS-CS2000/16.3-16.5/UC	SPC00554802	24	<0.2
17	ECRB-SYS-CS950/5.2-5.3/UC	SPC00554803	19	<0.2
18	ECRB-SYS-CS950/4.8-5.5/UC	SPC00554804	30	<0.2
19	SD-9/991.7-992.1/UC	SPC00554805	26	0.1
20	ECRB-SYS-CS1250/5.0-5.7/UC	SPC00554806	50	0.2
21	ECRB-SYS-CS1250/3.4-4.0/UC	SPC00554807	25	M
22	SD-9/670.5-670.6/UC	SPC00554808	46	0.3
23	ECRB-SYS-CS800/4.9-5.6/UC	SPC00554809	20	M
24	ECRB-SYS-CS700/5.5-5.8/UC	SPC00554810	64	<0.1
25	NRG-7/7A/839.3-839.8/UC	SPC00554811	31	0.1

Source: DTN: GS020408312272.003 [DIRS 160899]

NOTE: M indicates not measured.

4.2 CRITERIA

The *Project Requirements Document* (Canori and Leitner 2003 [DIRS 166275]) contains three criteria that are relevant to the work documented in this report. They are:

1. PRD-002/T-014 Performance Objectives for the Geologic Repository After Permanent Closure; see 10 CFR 63.113 [DIRS 156605] for compete requirement text.

2. PRD-002/T-015 Requirements for Performance Assessment; see 10 CFR 63.114 for compete requirement text.

3. PRD-002/T-016 Requirements for Multiple Barriers; see 10 CFR 63.115 for compete requirement text.

Work described in this document will support these requirements, but more specific criteria exist in the *Yucca Mountain Review Plan, Final Report* (Yucca Mountain Review Plan) (NRC 2003 [DIRS 163274]). Selected Yucca Mountain Review Plan acceptance criteria are presented to supplement or clarify the *Project Requirements Document* citation.

The following Yucca Mountain Review Plan acceptance criteria were identified as applicable to this technical product. Several parts of the criteria are not included because they are not relevant to this model report.

4.2.1 Degradation of Engineered Barriers Acceptance Criteria

These criteria are from the Yucca Mountain Review Plan, Final Report (NRC 2003, Section 2.2.1.3.1.3 [DIRS 163274] which are based on meeting the requirements of 10 CFR 63.114(a)–(c) and (e)–(g) [DIRS 156605]).

4.2.1.1 Acceptance Criterion 1–System Description and Model Integration Are Adequate

(1) The total system performance assessment adequately incorporates important design features, physical phenomena, and couplings, and uses consistent and appropriate assumptions throughout the degradation of engineered barriers abstraction process;

(2) Assessment abstraction of the degradation of engineered barriers uses assumptions, technical bases, data, and models that are appropriate and consistent with other related U.S. Department of Energy (DOE) abstractions. For example, the assumptions used for degradation of engineered barriers should be consistent with the abstractions of quantity and chemistry of water contacting waste packages and waste forms (Section 2.2.1.3.3), climate and infiltration (Section 2.2.1.3.5), mechanical disruption of waste packages (Section 2.2.1.3.2). The descriptions and technical bases provide transparent and traceable support for the abstraction of the degradation of engineered barriers;

(3) The descriptions of engineered barriers, design features, degradation processes, physical phenomena, and couplings that may affect the degradation of the engineered barriers are adequate. For example, materials and methods used to construct the engineered barriers are included, and degradation processes, such as uniform corrosion, pitting corrosion, crevice corrosion, stress corrosion cracking, intergranular corrosion, microbially influenced corrosion, dry-air oxidation, hydrogen embrittlement, and the effects of wet and dry cycles, material aging and phase stability, welding, and initial defects on the degradation modes for the engineered barriers are considered;

(4) Boundary and initial conditions used in the total system performance assessment abstractions are propagated consistently throughout the abstraction approaches. For example, the conditions and assumptions used

in the degradation of engineered barriers abstraction are consistent with those used to model the quantity and chemistry of water contacting waste packages and waste forms (Section 2.2.1.3.3); climate and infiltration (Section 2.2.1.3.5); and mechanical disruption of waste packages (Section 2.2.1.3.2);

(5) Sufficient technical bases for the inclusion of features, events, and processes (FEPs) related to degradation of engineered barriers in the total system performance assessment abstractions are provided;

(7) Guidance in NUREG–1297 (Altman et al. 1988 [DIRS 103597] and NUREG–1298 (Altman et al. 1988 [DIRS 103750]), or other acceptable approaches, is followed.

4.2.1.2 Acceptance Criterion 2–Data Are Sufficient for Model Justification

(1) Parameters used to evaluate the degradation of engineered barriers in the license application are adequately justified (e.g., laboratory corrosion tests, site-specific data such as data from drift-scale tests, in-service experience in pertinent industrial applications, and test results not specifically performed for the Yucca Mountain site, etc.). DOE describes how the data were used, interpreted, and appropriately synthesized into the parameters;

(2) Sufficient data have been collected on the characteristics of the engineered components, design features, and the natural system to establish initial and boundary conditions for abstraction of degradation of engineered barriers;

4.2.1.3 Acceptance Criterion 3–Data Uncertainty Is Characterized and Propagated Through the Model Abstraction

(1) Models use parameter values, assumed ranges, probability distributions, and/or bounding assumptions that are technically defensible, reasonably account for uncertainties and variabilities, and do not result in an under-representation of the risk estimate;

(2) For those degradation processes that are significant to the performance of the engineered barriers, DOE provides appropriate parameters, based on techniques that may include laboratory experiments, field measurements, industrial analogs, and process-level modeling studies conducted under conditions relevant to the range of environmental conditions within the waste package emplacement drifts. DOE also demonstrates the capability to predict the degradation of the engineered barriers in laboratory and field tests;

(3) For the selection of parameters used in conceptual and process-level models of engineered barrier degradation that can be expected under repository conditions, assumed range of values and probability distributions are not

likely to underestimate the actual degradation and failure of engineered barriers as a result of corrosion;

4.2.1.4 Acceptance Criterion 4–Model Uncertainty Is Characterized and Propagated Through the Model Abstraction

(1) Alternative modeling approaches of FEPs are considered and are consistent with available data and current scientific understanding, and the results and limitations are appropriately considered in the abstraction;

(2) Consideration of conceptual model uncertainty is consistent with available site characterization data, laboratory experiments, field measurements, natural analog information and process-level modeling studies; and the treatment of conceptual model uncertainty does not result in an under-representation of the risk estimate; and

(3) DOE uses alternative modeling approaches, consistent with available data and current scientific understanding, and evaluates the model results and limitations, using tests and analyses that are sensitive to the processes modeled. For example, for processes such as uniform corrosion, localized corrosion, and stress corrosion cracking of the engineered barriers, DOE considers alternative modeling approaches, to develop its understanding of environmental conditions and material factors significant to these degradation processes.

4.2.1.5 Acceptance Criterion 5–Model Abstraction Output Is Supported by Objective Comparisons

(1) Models implemented in this total system performance assessment abstraction provide results consistent with output from detailed process-level models and/or empirical observations (laboratory and field testing and/or natural analogs);

(5) Accepted and well-documented procedures are used to construct and test the numerical models that simulate the engineered barrier chemical environment and degradation of engineered barriers; and

(6) Sensitivity analyses or bounding analyses are provided to support the abstraction of degradation of engineered barriers that cover ranges consistent with the site data, field or laboratory experiments and tests, and industrial analogs.

4.2.2 Quantity and Chemistry of Water Contacting Engineered Barriers and Waste Forms–Acceptance Criteria

These criteria are from the *Yucca Mountain Review Plan, Final Report* (NRC 2003, Section 2.2.1.3.3.3 [DIRS 163274] which is based on meeting the requirements of 10 CFR 63.114(a)–(c) and (e)–(g) [DIRS 156605]).

4.2.2.1 Acceptance Criterion 1–System Description and Model Integration are Adequate

(1) Total system performance assessment adequately incorporates important design features, physical phenomena, and couplings, and uses consistent and appropriate assumptions throughout the quantity and chemistry of water contacting engineered barriers and waste forms abstraction process;

(2) The abstraction of the quantity and chemistry of water contacting engineered barriers and waste forms uses assumptions, technical bases, data, and models that are appropriate and consistent with other related DOE abstractions. For example, the assumptions used for the quantity and chemistry of water contacting engineered barriers and waste forms are consistent with the abstractions of "Degradation of Engineered Barriers" (Section 2.2.1.3.1); "Mechanical Disruption of Engineered Barriers" (Section 2.2.1.3.2); "Radionuclide Release Rates and Solubility Limits" (Section 2.2.1.3.4); "Climate and Infiltration" (Section 2.2.1.3.5); and "Flow Paths in the Unsaturated Zone" (Section 2.2.1.3.6). The descriptions and technical bases provide transparent and traceable support for the abstraction of quantity and chemistry of water contacting engineered barriers and waste forms;

(3) Important design features, such as waste package design and material selection, backfill, drip shield, ground support, thermal loading strategy, and degradation processes, are adequate to determine the initial and boundary conditions for calculations of the quantity and chemistry of water contacting engineered barriers and waste forms;

(4) Spatial and temporal abstractions appropriately address physical couplings (thermal-hydrological-mechanical-chemical). For example, DOE evaluates the potential for focusing of water flow into drifts, caused by coupled thermal-hydrological-mechanical-chemical processes;

(5) Sufficient technical bases and justification are provided for total system performance assessment assumptions and approximations for modeling coupled thermal-hydrological-mechanical-chemical effects on seepage and flow, the waste package chemical environment, and the chemical environment for radionuclide release. The effects of distribution of flow on the amount of water contacting the engineered barriers and waste forms are consistently addressed, in all relevant abstractions;

(6) The expected ranges of environmental conditions within the waste package emplacement drifts, inside of breached waste packages, and contacting the waste forms and their evolution with time are identified. These ranges may be developed to include:

(i) the effects of the drip shield and backfill on the quantity and chemistry of water (e.g., the potential for condensate formation and dripping from the underside of the shield);

(ii) conditions that promote corrosion of engineered barriers and degradation of waste forms;

(iii) irregular wet and dry cycles;

(iv) gamma-radiolysis; and

(v) size and distribution of penetrations of engineered barriers;

(7) The model abstraction for quantity and chemistry of water contacting engineered barriers and waste forms is consistent with the detailed information on engineered barriers design and other engineered features. For example, consistency is demonstrated for:

(i) dimensionality of the abstractions;

(ii) various design features and site characteristics; and

(iii) alternative conceptual approaches.

Analyses are adequate to demonstrate that no deleterious effects are caused by design or site features that DOE does not take into account in this abstraction;

(12) Guidance in NUREG–1297 (Altman et al. 1988 [DIRS 103597] and NUREG–1298 (Altman et al. 1988 [DIRS 103750]), or other acceptable approaches, is followed.

4.2.2.2 Acceptance Criterion 2–Data are Sufficient for Model Justification

(1) Geological, hydrological, and geochemical values used in the license application are adequately justified. Adequate description of how the data were used, interpreted, and appropriately synthesized into the parameters is provided;

(2) Sufficient data were collected on the characteristics of the natural system and engineered materials to establish initial and boundary conditions for conceptual models of thermal-hydrological-mechanical-chemical coupled

processes, that affect seepage and flow and the engineered barriers chemical environment;

4.2.2.3 Acceptance Criterion 3–Data Uncertainty Is Characterized and Propagated Through the Model Abstraction

(1) Models use parameter values, assumed ranges, probability distributions, and bounding assumptions that are technically defensible, reasonably account for uncertainties and variabilities, and do not result in an under-representation of the risk estimate;

(2) Parameter values, assumed ranges, probability distributions, and bounding assumptions used in the total system performance assessment calculations of quantity and chemistry of water contacting engineered barriers and waste forms are technically defensible and reasonable, based on data from the Yucca Mountain region (e.g., results from large block and drift-scale heater and niche tests), and a combination of techniques that may include laboratory experiments, field measurements, natural analog research, and process-level modeling studies;

(3) Input values used in the total system performance assessment calculations of quantity and chemistry of water contacting engineered barriers (e.g., drip shield and waste package) are consistent with the initial and boundary conditions and the assumptions of the conceptual models and design concepts for the Yucca Mountain site. Correlations between input values are appropriately established in the DOE total system performance assessment. Parameters used to define initial conditions, boundary conditions, and computational domain in sensitivity analyses involving coupled thermal-hydrological-mechanical-chemical effects on seepage and flow, the waste package chemical environment, and the chemical environment for radionuclide release, are consistent with available data. Reasonable or conservative ranges of parameters or functional relations are established;

(4) Adequate representation of uncertainties in the characteristics of the natural system and engineered materials is provided in parameter development for conceptual models, process-level models, and alternative conceptual models. DOE may constrain these uncertainties using sensitivity analyses or conservative limits. For example, DOE demonstrates how parameters used to describe flow through the EBS bound the effects of backfill and excavation-induced changes;

4.2.2.4 Acceptance Criterion 4–Model Uncertainty Is Characterized and Propagated Through the Model Abstraction

(1) Alternative modeling approaches of FEPs are considered and are consistent with available data and current scientific understanding, and the results and limitations are appropriately considered in the abstraction;

(2) Alternative modeling approaches are considered and the selected modeling approach is consistent with available data and current scientific understanding. A description that includes a discussion of alternative modeling approaches not considered in the final analysis and the limitations and uncertainties of the chosen model is provided;

(3) Consideration of conceptual model uncertainty is consistent with available site characterization data, laboratory experiments, field measurements, natural analog information and process-level modeling studies; and the treatment of conceptual model uncertainty does not result in an under-representation of the risk estimate;

(4) Adequate consideration is given to effects of thermal-hydrological-mechanical-chemical coupled processes in the assessment of alternative conceptual models. These effects may include:

(i) thermal-hydrologic effects on gas, water, and mineral chemistry;

(ii) effects of microbial processes on the engineered barriers chemical environment and the chemical environment for radionuclide release;

(iii) changes in water chemistry that may result from the release of corrosion products from the engineered barriers and interactions between engineered materials and ground water; and

(iv) changes in boundary conditions (e.g., drift shape and size) and hydrologic properties, relating to the response of the geomechanical system to thermal loading

4.2.2.5 Acceptance Criterion 5–Model Abstraction Output is Supported by Objective Comparisons

(1) The models implemented in this total system performance assessment abstraction provide results consistent with output from detailed process level models and/or empirical observations (laboratory and field testing and/or natural analogs);

(2) Abstracted models for coupled thermal-hydrological-mechanical-chemical effects on seepage and flow and the engineered barriers chemical environment, as well as on the chemical environment for radionuclide release, are based on the same assumptions and approximations demonstrated to be appropriate for process-level models or closely analogous natural or experimental systems. For example, abstractions of processes, such as thermally induced changes in hydrological properties, or estimated diversion of percolation away from the drifts, are adequately justified by comparison to results of process-level modeling, that are consistent with direct observations and field studies; and

(3) Accepted and well-documented procedures are used to construct and test the numerical models that simulate coupled thermal-hydrological-mechanical-chemical effects on seepage and flow, engineered barriers chemical environment, and the chemical environment for radionuclide release. Analytical and numerical models are appropriately supported. Abstracted model results are compared with different mathematical models, to judge robustness of results.

4.3 CODES AND STANDARDS

4.3.1 Codes

This model documentation was prepared to comply with the U.S. Nuclear Regulatory Commission high-level waste rule 10 CFR Part 63 [DIRS 156605]. Subparts of this rule that are applicable to data include Subpart B, Section 15 (Site Characterization) and Subpart E, Section 114 (Requirements for Performance Assessment). The Subpart applicable to models is also Subpart E Section 114. The sections applicable to FEPs are 10 CFR 63.114(d), (e), and (f).

4.3.2 Standards

As discussed in BSC (2003 [DIRS 166519], Section 3), ASTM C 1174-97 [DIRS 105725], *Standard Practice for Prediction of the Long-Term Behavior of Materials, Including Waste Forms, Used in Engineered Barrier Systems (EBS) for Geological Disposal of High-Level Radioactive Waste*, was used as guidance in the preparation of this model.

The following standards are also applicable to this report, as they have been used as direct input in Section 4.1.2.

ASTM A53/A53M-02 [DIRS 162719], *Standard Specification for Pipe, Steel, Black and Hot-Dipped, Zinc-Coated, Welded and Seamless*, was used to determine the chemical composition of the material to be used in the fabrication of pipe spacers for the ground support.

ASTM A240/A240M-02a [DIRS 162720], *Standard Specification for Chromium and Chromium-Nickel Stainless Steel Plate, Sheet, and Strip for Pressure Vessels and for General Applications*, was used to determine the chemical composition of the material to be used in the fabrication of the emplacement pallet (316L SS , see Table 4.1-24).

ASTM A276-03 [DIRS 165006], *Standard Specification for Stainless Steel Bars and Shapes*, was used to determine the chemical composition of the material to be used in the fabrication of the steel wire fabric for the ground support, inner lid and pallet for the waste package.

ASTM A307-02 [DIRS 162722], *Standard Specification for Carbon Steel Bolts and Studs, 60 000 PSI Tensile Strength*, was used to determine the chemical composition of the material to be used in the fabrication of the tie rods for the ground support, and the invert-anchor bolts.

ASTM A490-02 [DIRS 158937], *Standard Specification for Structural Bolts, Alloy Steel, Heat Treated, 150 ksi Minimum Tensile Strength*, was used to determine the chemical composition of the material to be used in the fabrication of the structural bolts for the invert.

ASTM A516/A516M-01 [DIRS 162723], *Standard Specification for Pressure Vessel Plates, Carbon Steel, for Moderate- and Lower-Temperature Service*, was used to determine the chemical composition of the material to be used in the fabrication of the basket for the waste package.

ASTM A572/A572M-01 [DIRS 158661], *Standard Specification for High-Strength Low-Alloy Columbium-Vanadium Structural Steel*, was used to determine the chemical composition of the material to be used in the fabrication of the steel sets for the ground support.

ASTM A588/A588M-01 [DIRS 162724], *Standard Specification for High-Strength Low-Alloy Structural Steel with 50ksi [345Mpa] Minimum Yield Point to 4-in. [100-mm] Thick*, was used to determine the chemical composition of the material to be used in the fabrication of the invert-transverse beams with stiffeners, invert-longitudinal support beams, invert-stiffener brackets, invert-base plates, invert-structural bolts, and the rail runway beams, cap plate, and guide beams for the gantry rail assembly.

ASTM A759-00 [DIRS 159971], *Standard Specification for Carbon Steel Crane Rails*, was used to determine the chemical composition of the material to be used in the fabrication of the gantry rail for the gantry rail assembly.

ASTM B209M-02 [DIRS 162727], *Standard Specification for Aluminum and Aluminum-Alloy Sheet and Plate [Metric]*, was used to determine the chemical composition of the material to be used in the fabrication of the thermal shunt for the waste package.

ASTM B265-02 [DIRS 162726], *Standard Specification for Titanium and Titanium Alloy Strip, Sheet, and Plate*, was used to determine the chemical composition of the material to be used in the fabrication of the drip shield (plates and conductor guides, bulkheads posts and lifting connectors).

ASTM B575-99a [DIRS 147465], *Spec for Low-Carbon Nickel-Molybdenum-Chromium, Low-Carbon Nickel-Chromium-Molybdenum, Low-Carbon Nickel-Chromium-Molybdenum-Copper, Low-Carbon Nickel-Chromium-Molybdenum-Tantalum, Low-Carbon Nickel-Chromium-Molybdenum-Tungsten Alloy Plate, Sheet and Strip*, was used to determine the chemical composition of the material to be used in the fabrication of the drip shield (base alloy C-22), and outer shell for the waste package.

ASTM G 1-90 (1999) [DIRS 103515], *Standard Practice for Preparing, Cleaning, and Evaluating Corrosion Test Specimens* was used to provide input found on Tables 4.1-17 and 4.1-24.

4.4 INPUTS USED FOR MODEL VALIDATION

This section summarizes the inputs used for model validation (Section 7).

4.4.1 THC Seepage Abstraction Validation Inputs

Five complete drift scale seepage THC modeling results, taken from the *Drift Scale Coupled Processes (DST and THC Seepage) Models* (BSC 2003 [162050]), represent the sources of seepage water entering the drift (DTN: LB0302DSCPTHCS.002 [DIRS 161976]). Due to the large amount of information contained within this DTN, specific values are not cited here (see Table 4.1-13).

4.4.2 Precipitates/Salts Model Validation Inputs

To help validate the precipitates/salts model, laboratory evaporation experiments from Lawrence Livermore National Laboratory are compared against model results in *In-Drift Precipitates/Salts Model* (BSC 2003 [DIRS 162529]). The laboratory experiments include the evaporation of simulated J-13 well water, simulated concentrated J-13 (100X concentration), and a synthetic solution designed to simulate Topopah Spring pore water. The data from these experiments are presented for reference only in Tables 4.4-1 through 4.4-3. Section 7.3.1 summarizes the validation comparisons in *In-Drift Precipitates/Salts Model* (BSC 2003 [DIRS 162529]) that use these experimental data.

Table 4.4-1. Measured Concentrations for Synthetic J-13 Water Evaporation Experiments

Constituent (mg/kg)	Initial Synthetic J-13	J-13 (956X Concentration)	Initial Synthetic J-13	J-13 (157X Concentration)
pH	7.84	not reported	8.33	10.18
HCO_3	108	24878	103	4295
Ca	6.4	29.86	5.3	1.2
Cl	6.9	4835	7.5	849
F	2.2	1550	2.4	247
K	5.3	4792	4.9	560
Mg	2.2	0.14	2.1	0.05
NO_3	8	5532	8	1050
Na	46	44082	45.4	5298
SO_4	18.1	12926	19	2162
$SiO_{2\,(aq)}$	11.3	18008	10	999

Source: Rosenberg et al. 1999, Tables 3 and 6 [DIRS 125338]

Table 4.4-2. Measured Concentrations for 100X Synthetic J-13 Water Evaporation Experiments

Constituent (mg/L)	Initial J-13 (100X Concentration)	J-13 (2070X Concentration)
HCO_3	4142	54614
Ca	5	36
Cl	730	14419
F	208	3630
K	513	10832
Mg	2	0
NO_3	732	14085
Na	4032	76314
SO_4	1632	29783

Source: DTN: LL000202905924.117, Table S00134_003 [DIRS 144913]

Table 4.4-3. Measured Concentrations for Synthetic Topopah Spring Tuff Pore Water from Evaporation Experiments

Constituent (mg/kg)	SPW (No Evaporation)	Concentrated 1243 Times
pH*	7.68	6-6.5
Na	8.2	5961
K	4.2	2779
Mg	11.7	5478
Ca	57.2	15629
$SiO_{2(aq)}$	9.8	513
HCO_3	16.2	<35
SO_4	81.7	2077
Cl	78.0	53084
NO_3	11.0	Not measured
F	2.3	<577

Source: Rosenberg et al. 1999, Table 3 [DIRS 125338]

NOTE: *Semi-quantitative, measurement made with pH paper.

4.4.3 Evaporation of Dilute Salt Solutions

To demonstrate model validation for simple salt systems, the in-drift precipitates/salts model and the Pitzer database are used in *In-Drift Precipitates/Salts Model* (BSC 2003 [DIRS 162529]) to evaporate dilute solutions of simple Na, K, Ca, and Mg salts to mineral saturation at 25°C and 100°C. The final aqueous compositions are then compared to the published, experimentally-derived salt solubilities listed for reference only in Table 4.4-4. The validation results in BSC (2003 [DIRS 162529]) are summarized in Section 7.3.2.

Table 4.4-4. Aqueous Solubilities of Na, K, Ca, and Mg Salts

Salt	Aqueous Solubility at 25ºC (mass percent of solute)	Aqueous Solubility at 100ºC (mass percent of solute)
NaCl	26.45%	28.05%
KCl	26.22%	36.05%
$CaCl_2$	44.83%	59.94%
$MgCl_2$	35.90%	42.15%
$NaHCO_3$	9.32%	19.10%
$KHCO_3$	26.6%	40.45% at 70°C
Na_2CO_3	23.5%	30.09%
K_2CO_3	52.7%	61.0%
NaF	3.97%	4.82%
KF	50.4%	60.0% at 80°C
CaF_2	0.0016%	not reported above 25°C
MgF_2	0.013%	not reported above 25°C
Na_2SO_4	21.94%	29.67%
K_2SO_4	10.7%	19.3%
$CaSO_4$	0.205%	0.163%
$MgSO_4$	26.3%	33.3%
NaBr	48.6%	54.9%
KBr	40.4%	50.8%
$CaBr_2$	61.0%	73.0% at 60°C
$MgBr_2$	50.6%	55.7%
$NaNO_3$	47.7%	63.8%
KNO_3	27.7%	70.8%
$Ca(NO_3)_2$	59.0%	78.5%
$Mg(NO_3)_2$	41.6%	72.0%

Source: Lide 2000 [162229] pp. 8-102 to 8-110

4.4.4 Evaporation of Waters to Form Concentrated Brines

To validate the approach for the EBS seepage evaporation model calculations, a classic model presented by Garrels and McKenzie (1967 [DIRS 123636]) for the evaporation of Sierra Nevada spring water is used. The EBS model simulates evaporation and concentration of these waters by a factor of 1000, and the results are compared against the original results of Garrels and McKenzie. Table 4.4-5 gives the initial spring water composition used in this validation test. Figure 4 from Garrels and Mckenzie (1967 [DIRS 123636]) has been reproduced as Figure 7.4-1 for comparison against the EBS model results.

Table 4.4-5. Composition of Sierra Nevada Spring Water Used in Validation Tests for the EBS Seepage Evaporation Model

Parameter	ppm	Moles/Liter X 10^4
SiO_2	24.6	4.10
Ca	10.4	2.60
Mg	1.7	0.71
Na	5.95	2.59
K	1.57	0.40
HCO_3	54.6	8.95
SO_4	2.38	0.25
Cl	1.06	0.16
pH	6.8	
Ionic strength	0.0013 moles/Liter	

Source: Garrels and McKenzie 1967, Table VI [DIRS 123636]

NOTE: At 25°C and $Pco_2 = 10^{-3.5}$ atm.

4.4.5 Deliquescence Point Comparison

To validate the equilibrium deliquescence point calculations, comparisons of the values predicted by EQ6 calculations using Data0.ypf Pitzer database are made with the experimental data of Greenspan (1977 [DIRS 104945]) and Pabalan et al. (2002 [DIRS 163067]). The published values are shown in Table 4.4-6; in Section 7.5, those from Greenspan are recalculated to the same single temperature as presented in Pabalan et al.

Table 4.4-6. Measured Deliquescence Relative Humidity Values for Salts and Salt Mixtures

Reference	Salt Composition	Temperature (°C)				
		23.0	38.1	48.0	69.0	85.8
Pabalan et al. 2002, Table 5-1	$NaNO_3$	74.9	---------	69.7	62.7	---------
	$MgCl_2$	33.9	31.7	31.0	29.1	---------
Pabalan et al. 2002, Table 5-2	$NaCl + NaNO_3$	74.7	66.4	67.2	59.6	56.0
	$NaCl + NaNO_3 + KNO_3$	67.8	60.7	61.3	51.8	43.4
Reference	**Salt Composition**	**Temperature (°C)**				
		20-25	**35-40**	**45-50**	**65-70**	**85-90**
Greenspan, 1977, Table 2	$NaNO_3$	75.36-74.25	72.06-71.00	69.99-69.04	66.64-66.04	65.03-65.00
	$MgCl_2$	33.07-32.78	32.05-31.60	31.10-30.54	28.54-27.77	25.11-24.12

Sources: Pabalan et al. 2002 [DIRS 163067], Greenspan 1977 [DIRS 104945]

4.4.6 Chromium Calculation

Figure 2 from Rai et al. 1987 [DIRS 163369], has been used to validate the $Cr(OH)_{3(am)}$ solubility log K value obtained from Ball and Nordstrom (1998 [DIRS 163015]) in Section 7.7. This figure is reconstructed in Figure 4.4-1.

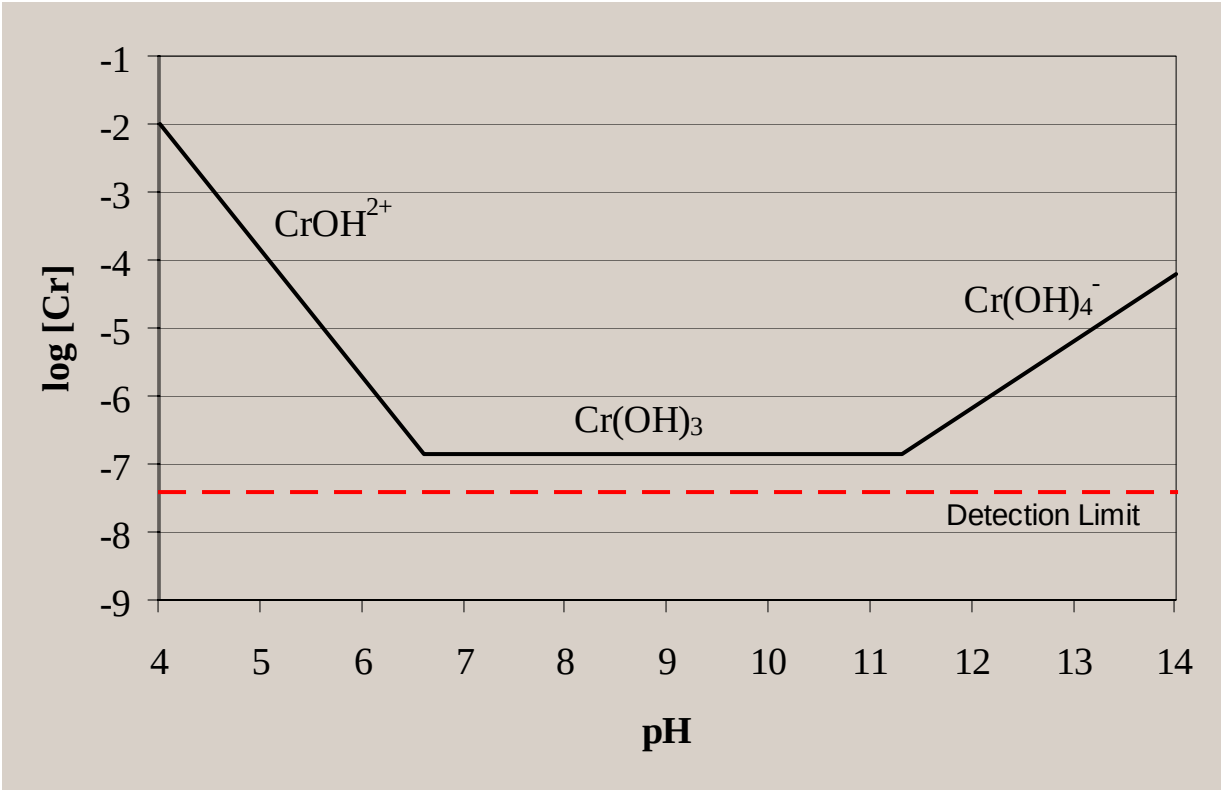

Source: Rai et al. 1987 [DIRS 163369]

NOTE: The lines represent best-fit linear regressions (see Rai et al. 1987 [DIRS 163369] for the regression equations) through 77 experimentally measured solubility data points (not shown).

Figure 4.4-1. Three-Species Model for Chromium Solubility

INTENTIONALLY LEFT BLANK

5. ASSUMPTIONS

This section addresses the assumptions built into the engineered barrier system physical and chemical environment model and those passed into it from upstream documentation that may have significant impact on the results of this model.

5.1 DISCUSSION OF ASSUMPTIONS IN UPSTREAM DOCUMENTATION

The assumptions listed in the three primary modeling reports that feed this model were reviewed and evaluated for their potential consequences. The two reports are:

- *Drift-Scale Coupled Processes (DST and THC Seepage) Models* report (BSC 2003, Section 6.8 [DIRS 162050])
- *In-Drift Precipitates Salts Model* report (BSC 2003 [DIRS 162529]).

Those assumptions having a potentially significant impact are addressed below.

5.1.1 Standard State of Liquid Phase (Assumption 5.1 of the In-Drift Precipitates/Salts Model)

Assumption: Liquid phase is at standard state

Basis: As discussed in *In-Drift Precipitates Salts Model* report (BSC 2003 [DIRS 162529]), an aqueous solution at standard state has an equilibrium relative humidity that is equivalent to the activity of water in the aqueous solution. Standard state in this sense implies that the water-air interface is flat (i.e., that the boundary between water and air is a plane) and that the behavior of the water molecule (H_2O) is not influenced by solid surfaces in contact with the water. Adsorption and air-water interface curvature, such as the curvature of menisci caused by capillary forces, create non-standard state conditions with respect to vapor pressure and equilibrium relative humidity near the air-water interface (Walton 1994 [DIRS 127454]; Koorevaar et al. 1983, pp. 67-68 [DIRS 125329]).

For the in-drift precipitates/salts (IDPS) model, non-standard state aqueous solutions are not considered. Only dissolved salts and temperature are considered to affect liquid-vapor equilibrium. The small amounts of water held in double layers and adsorbed to solid surfaces have negligible roles in radionuclide transport and waste package corrosion due to their near immobility. Water held by the surface tension effects of capillary binding are more mobile than water in double layers or adsorbed to solids; however, even capillary forces under very dry conditions (in the range of negative 500 meters water pressure head) have a limited effect on H_2O activity in solution (Walton 1994, pp. 3480-3481 [DIRS 127454]).

Confirmation Status: No further confirmation is required. Because of this limited effect, uncertainties due to the assumption that the liquid phase in the IDPS model is at standard state are negligible compared to the more sizable uncertainties in the IDPS model and model inputs.

Use in the Model: This assumption is used throughout.

5.1.2 Equilibrium Conditions (Assumption 5.2 of the IDPS Model)

Assumption: The system is in a state of local metastable equilibrium. All aqueous and gas constituents in the model achieve and maintain local equilibrium, and most mineral phases achieve and maintain local equilibrium upon saturation. Several slow-forming and unlikely minerals identified in *In-Drift Precipitates Salts Model* report (BSC 2003 [DIRS 162529]) will not precipitate upon saturation or supersaturation. The model can be used, however, to make steady-state non-equilibrium predictions with respect to relative humidity, provided the appropriate inputs are used.

Basis: Most chemical reactions included in the model occur rapidly compared to the modeling timeframe. Redox reactions, which generally are not rapid, are not included in the model. Similarly, certain mineral precipitation reactions are not expected to be rapid enough to occur to a considerable degree for the anticipated applications of the model. Mineral precipitation reactions that fall into this category are suppressed, as explained in in-drift precipitates salts report (BSC 2003 [DIRS 162529]), permitting the formation of metastable mineral phases in the model.

Confirmation Status: No further confirmation is required because mineral precipitation reactions that fall into this category are suppressed, as explained in in-drift precipitates salts report (BSC 2003 [DIRS 162529]), permitting the formation of metastable mineral phases in the model.

Use in the Model: This assumption is used throughout.

5.2 ASSUMPTIONS INTERNAL TO PHYSICAL AND CHEMICAL ENVIRONMENT MODEL

5.2.1 Repository Location

Assumption: Analysis and results of this model are assumed to apply across the lithology of the entire repository drift, although the current thermal-hydrological-chemical (THC) model results (BSC 2003, Section 6.8 [DIRS 162050]) that were provided in the input listed on Tables 4.1-13 and 4.1-14 only provide output from the Tptpll lithologic unit.

Basis: This assumption is consistent with the *Drift-Scale Coupled Processes (DST and THC Seepage) Models* report (BSC 2003, Section 1.3 [DIRS 162050]), which states: "The THC seepage model was developed with data for specific hydrogeologic units, the Tptpmn and Tptpll. Although many aspects of the model are applicable to other host rock units of the repository, differences in the mineralogy, geochemistry, and thermal-hydrological properties must be considered before the results can be directly applied elsewhere. These differences, however, are expected to be reflected in the range of pore water compositions input into the model (Section 6.2.2.1), such that results of the THC seepage model as a whole (i.e., including the variability introduced by using various input water compositions) could be reasonably applied to other locations within the repository footprint." For the TSPA-License Application model to apply the results of the THC seepage model abstraction within repository drifts outside the Tptpll, this assumption is made so that possible spatial dependency of the THC seepage model output will not affect the use of the look-up table results within other rock units (such as the

upper lithophysal zone (Tptpul), middle nonlithophysal zone (Tptpmn), or the lower nonlithophysal zone (Tptpln)).

Confirmation Status: No further confirmation is required because the variability in chemistries that are provided in the other lithologies are on the same order of magnitude as the variability in chemistry provided by the range of pore water compositions. This assumption allows the TSPA-License Application model to implement the lookup tables derived in Section 6.9.3.

Use in the Model: This assumption is used throughout.

5.2.2 Representative Distribution of Seepage Water Compositions

Assumption: The 368 seepage waters used to develop the incoming seepage abstraction is representative of the population of waters passing across the drift wall through time.

Basis: The five selected pore waters used as input to the THC model were selected to cover a broad range of observed cross-drift, alcove, and borehole pore waters (see Figure 5.2-1). These five starting waters were used to generate 18,000 specific time- and spatially- dependent THC seepage model output waters, which were then abstracted down to 368 starting waters (see Section 6.6). The 368 modeled seepage water compositions selected for use from the THC model are then believed to represent a reasonable range of seepage waters that could enter into the drift through time. For additional basis, see Assumption 5.2.1 and Section 6.12.1.

Confirmation Status: No further confirmation is required because the range of input waters is representative of the waters in the host rock.

Use in the Model: This assumption is used throughout but is explicitly referenced in Section 6.13.4

5.2.3 Representative Distribution of Dust and Dust Leachate Compositions

Assumption: The distribution of the aqueous leachate from 52 dust samples corresponds to a representative distribution of previously suspended dust in the Exploratory Studies Facility (ESF) drift and is representative of repository dust.

Basis: Excavation activity should generate the majority of the repository dust (see Section 6.10.2), and, as this dust has a common source, it should be of similar composition to those U.S. Geological Survey samples taken from the ESF. Peterman et al. (2003, Figure 3 [DIRS 162819]) indicate that the major source of the dust collected in the ESF is from the rhyolite of the Topopah Spring tuff. The dust samples themselves are similar with respect to leachate chemistries, and only six abstraction bins are needed to separate them into their major chemical groups (see Section 6.10.5).

Confirmation Status: No further confirmation is required because the generally similar leachate chemistries reported in Section 6.13.4.2 indicate that the chemical variability is minor and is adequately represented by the existing data set.

Use in the Model: This assumption is used in Section 6.10.

INTENTIONALLY LEFT BLANK

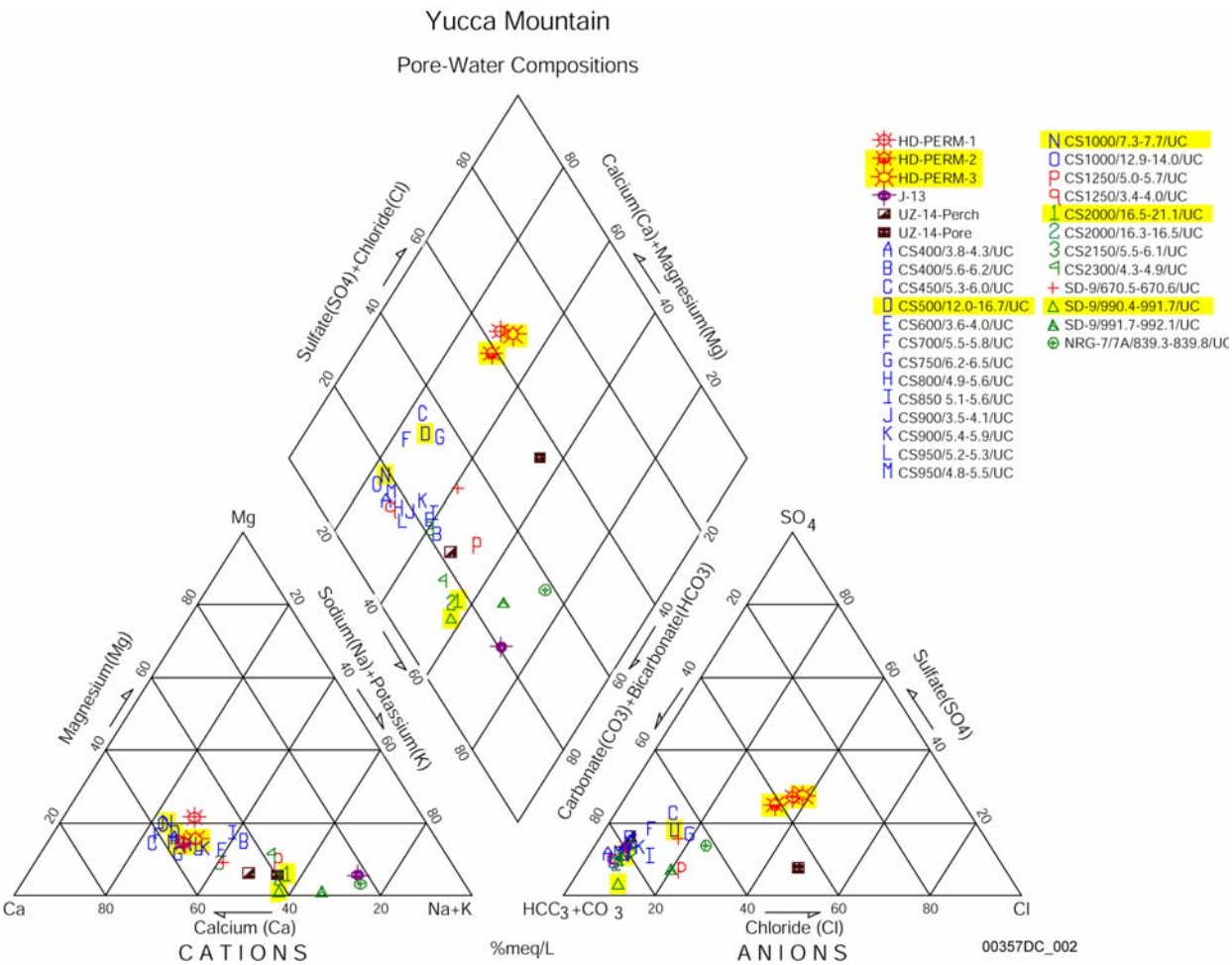

NOTE: Samples labeled HD-PERM are pore-waters from the Tptpmn unit in Alcove 5 of the ESF. Samples ID's starting with CS represent pore waters from the ECRB cross drift and are listed in order of increasing distance (ft) into the drift (down stratigraphy), with labels reflecting hydrogeologic units as follows: Tptpul (capitals A-O), Tptpmn (lower case p-q), and Tptpll (numbers 1-4). Sample ID's starting with SD-9 and NRG-7 represent pore waters from boreholes with the same names and show the sampling interval in feet from ground surface. The first SD-9 sample at 670 ft is from the base of the Tptpul, and the others are from the Tptpll. The NRG7 sample is from the Tptpmn.

Source: Drift Scale Coupled Processes (DST and THC Seepage) Models (BSC 2003, Figure 6.2-4 [162050])

Figure 5.2-1. Piper Plot of Water Compositions (meq/L) from Proposed Repository Units

INTENTIONALLY LEFT BLANK

6. MODEL DISCUSSION

6.1 MODELING OBJECTIVES

The main purpose of the engineered barrier system (EBS) physical and chemical environment (P&CE) model is to predict the evolution of the environment in the disposal drifts in response to the chemical and physical processes shaping it following repository closure. The chemical conditions can affect drip shield and waste package durability and radionuclide solubility and colloidal stability. The conceptual model (see Section 6.2) for the evolution of water chemistry in the EBS includes the consideration of seepage evaporation effects, interactions with engineered materials dust deliquescence, and reactions with in-drift gases.

In general, Section 6 can be broken down into two major areas of focus. First, a set of screening analyses are conducted to evaluate the effects of introduced materials (see Foldout Figure 6.1-1) on the EBS geochemical environment. Second, models are developed and abstracted for use by the TSPA-LA model in evaluating engineered barrier performance and radionuclide mobility (see Foldout Figure 6.1-1).

One of the screening analyses provided in Section 6 consists of evaluating the engineered material types, compositions and lifetimes (Section 6.4). Section 6.4 establishes corrosion rates for, and evaluates the longevity of, the steel and alloy materials. Once the longevity has been determined, most of the materials are screened out as having little potential to affect seepage compositions. A graphical presentation of the introduced materials (Foldout Figure 6.1-1) indicates that the rock bolts and the perforated stainless steel sheets are the engineered items that could react with, and affect the chemical composition of, any potential seepage before it makes contact with the drip shield or waste package. These two items are made of stainless steel. Stainless steel-seepage interactions are evaluated in Section 6.8, and do not significantly affect the composition of seepage entering the drift.

Also included in the screening analyses is an evaluation of the effect of the degradation of introduced materials on the in-drift gas composition (particularly O_2 and CO_2; Section 6.7). This analysis investigates whether corrosion of the introduced materials has the potential to affect one of the main boundary conditions established in the main model calculations, that oxic conditions will be maintained in the drift. This analysis concludes that oxygen availability will potentially limit the general rate of corrosion for about 500 years after permanent closure although truly anoxic conditions are unlikely. Thereafter, there should be sufficient oxygen entering the drifts to maintain an oxic environment.

In the remainder of section 6 three different models are developed:

- Lookup tables to represent the partial pressure of CO_2 (P_{CO_2}) in the drift through time (see Section 6.7.2.1)
- An abstraction model to represent potential seepage through time (Section 6.6 and 6.9)
- A model to evaluate the deliquescence of dusts (Section 6.10).

Foldout Figure 6.1-1 diagrams the main process steps that generate the abstractions and lookup tables feeding the TSPA-LA model.

The main software tool used in the development of the seepage abstraction and the dust deliquescence model is the EQ3/6 Version 8.0 software package. Section 6.5 gives a brief discussion of the mathematics used by the EQ3/6 calculations and some of the modeling constraints required to produce the model results used in developing the look-up tables for seepage and deliquescent dusts. The main modeling tool used in these calculations is the *In-Drift Precipitates/Salts Model* (BSC 2003 [DIRS 162529].

The results of the modeling calculations are summarized in two sections: Section 6.12 details the uncertainties associated with key inputs, the *In-Drift Precipitates Salts Model* and the development of the lookup tables. Section 6.12 also documents several additional sensitivity analyses, including:

- Use of alternate mineral suppressions
- Model sensitivity to $P\mathrm{co}_2$
- The presence of bromine in seepage and dusts
- Variations in the geochemical model for stainless steel-seepage interactions.

Section 6.13 summarizes the model results and discusses them in terms of the potential environment on waste packages and drip shields, and in the invert. This section also discusses the potential evolution of brines, the controlling mineral phases for each brine, and the types of water probabilities that could contact waste packages, drip shields, and the invert. Finally, there are specific instructions important to the TSPA so the lookup tables can be properly implemented in the TSPA-LA model. These instructions are located primarily in Section 6.15. Three main TSPA abstraction models are outlined in this section:

- First, the implementation of seepage conditions on the waste package

- Second, in the absence of seepage, the dust deliquesence model implements the dust chemistries on the waste package

- Third, the instructions for the abstraction model in the invert are provided to utilize the seepage chemistry lookup tables.

Instructions for implementing uncertainty on each of these abstractions are outlined in Section 6.12.5. Some discussion on the implementation of interpolation and extrapolation between the lookup tables is discussed in Section 6.13. Features, events, and processes (FEPs) and alternate conceptual models are also discussed in Sections 6.14 and 6.11, respectively.

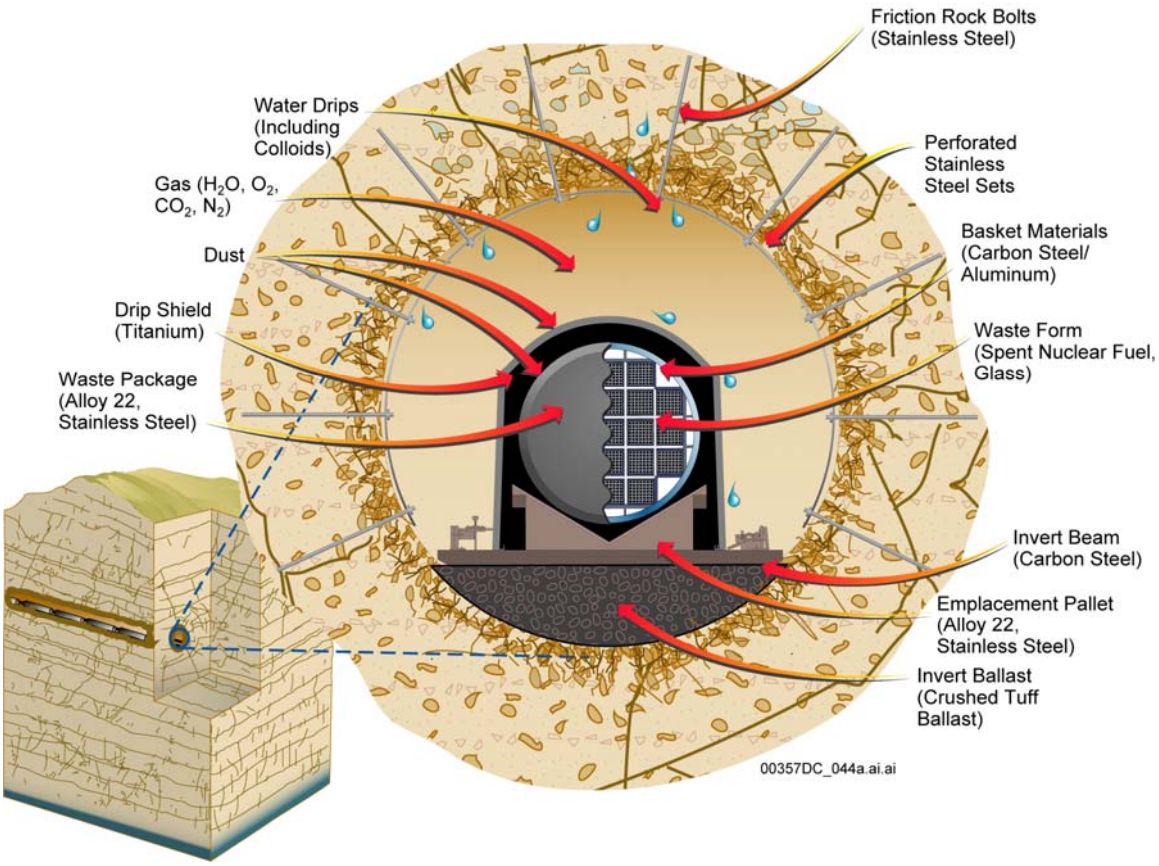

Figure 6.1-1. General Location of Engineered Barrier System Components and Materials

INTENTIONALLY LEFT BLANK

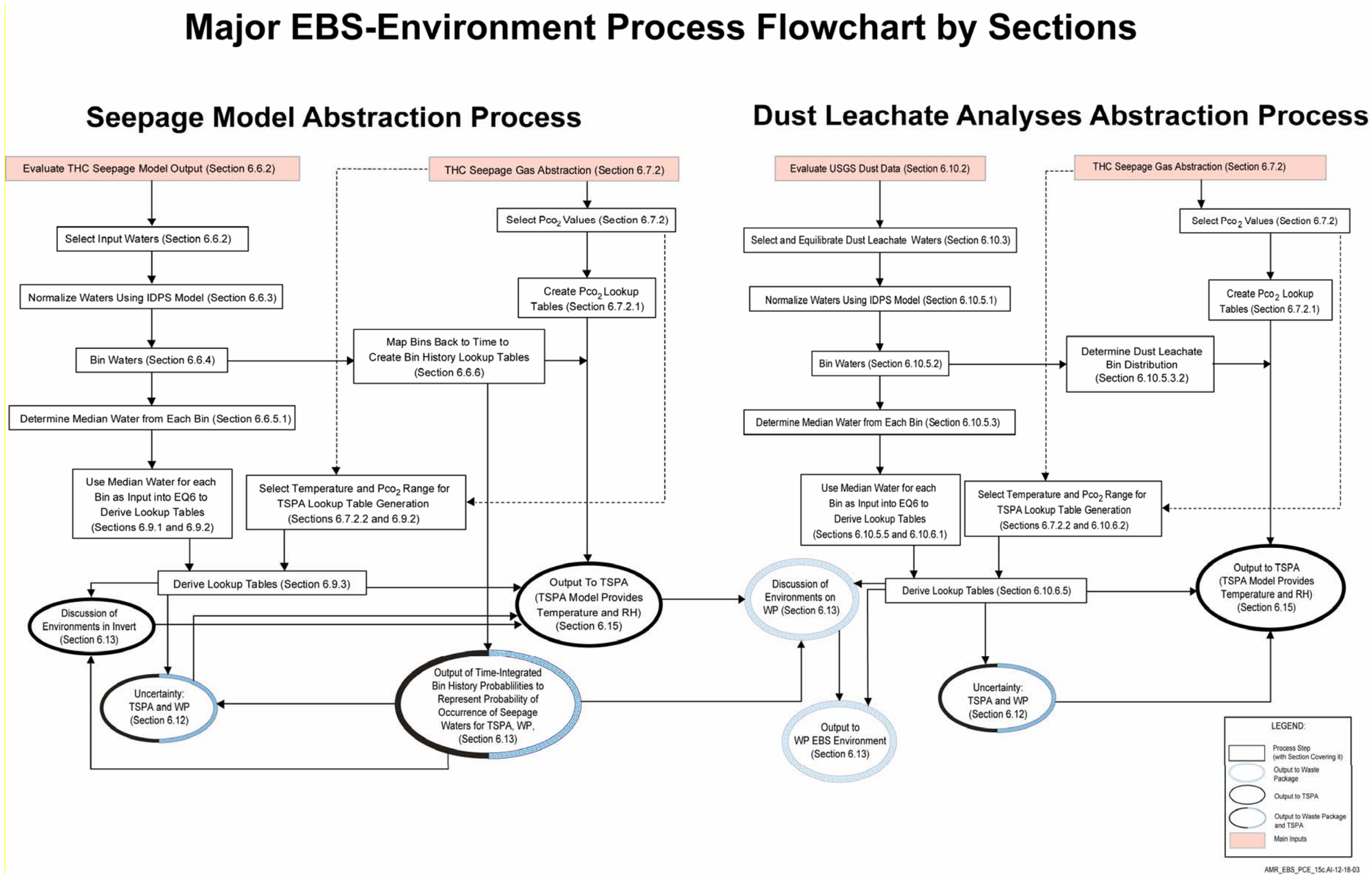

Fold Out 6.1-1. Major EBS Environment Process Flowchart, with Section References

INTENTIONALLY LEFT BLANK

6.2 ENGINEERED BARRIER SYSTEM PHYSICAL AND CHEMICAL ENVIRONMENT MODEL CONCEPTUAL MODEL

6.2.1 Integrated Perspective on the Evolution of the Engineered Barrier System Physical and Chemical Environments

The EBS P&CE model describes the mechanical, thermal, hydrological, and geochemical environments within the emplacement drifts. Included in the EBS environments are the physical characteristics and configuration of the EBS components (such as drip shields, waste packages, the invert; conditions due to degradation of the drift itself [including rockfall into the drifts]), potential seepage (via dripping and imbibition) into the drift; compositions of in-drift aqueous solutions and gases including relative humidity; and in-drift temperatures. These environmental conditions control the composition and evolution of aqueous solutions in the drift, and how they react with the engineered components of the repository. Thermal effects on water flux and solute flux outside the drifts potentially affect inputs to the EBS geochemical models because they may influence the amount and composition of water and gas that enter the drifts.

The EBS environments are important to repository performance to the extent that they help determine engineered barrier component degradation rates, quantities and species of mobilized radionuclides, and transport rates for radionuclides and fluids through the drift into the unsaturated zone (UZ). The drip shield and the waste package are the principal performance-related engineered barrier components that initially prevent water contact with waste forms and determine fluid transport paths. Waste form degradation determines quantities and species of mobilized radionuclides. The EBS chemical environments affect radionuclide solubility and colloid stability in the invert, all of which affect the mobile radionuclide source term for transport. Fluid transport paths and rates, coupled with the source term, determine radionuclide transport rates to the UZ.

The main purposes of this report are to provide:

- Geochemical conditions on the waste package and drip shield, where concentrated brines could potentially form through the evaporation of seepage waters and deliquescence of salt minerals in dust deposited on the metal surface

- Geochemical conditions in the invert, which may be used to determine the solubility and colloidal stability of radionuclides.

The evolution of the EBS environment is discussed in terms of both process (Section 6.2.2) and spatial location (Section 6.2.3). Descriptions by process are often independent of exact spatial location in the drift. On the other hand, descriptions by spatial location may encompass multiple processes taking place within centimeters to meters of each other within the drift. The *In-Drift Precipitates Salts Model* (BSC 2003 [DIRS 162529]) also discusses many of these same concepts and processes.

6.2.2 Evolution of Engineered Barrier System Chemical Environments by Process

EBS chemical environments can vary vertically, horizontally, or transversely with respect to the longitudinal axis of the drift. Vertically and transversely varying processes change over the scale

of a few meters across the drift's cross-section. Longitudinally, EBS chemical processes are similar on the scale of a waste package's length. Two assumptions (see Sections 5.2.1 and 5.2.2) have been made that discuss the variability of the waters selected for use in this model. Thus, a two-dimensional model of the repository, describing the processes that occur in a cross section of the drift, is generally applicable. The following discussion conceptualizes potential seepage and evaporation, dust deposition and deliquescence, and the influence of temperature changes over time on the chemical environment within the drift.

6.2.2.1 Seepage

Surface waters, originating as surface precipitation and snow melt, gradually make their way downwards through both fractures and the matrix of the tuffaceous rocks in the UZ to the level of the drift. Infiltration fluxes can be concentrated in zones of increased fractures or higher permeability as they seep into the drift from above. These processes are accounted for by the "Flow Focusing Model" in the TSPA-LA model.

During the initial radioactive heating pulse (extending approximately 2,000 years after the permanent closure of the repository), areas of the drift can rise significantly in temperature above 96°C, the boiling point of water for the drift elevation (see Figure 6.7-7). This 2,000-year long heating pulse drives away residual water in the unsaturated tuff matrix (where permeability allows transport), and percolation flux as steam, resulting in some parts of the drift that do not have macro-scale liquid water available for chemical reactions. This process is important because it limits corrosion that can occur on the waste package and drip shield. The process also limits the water that is available to transport soluble and colloidal radionuclides from the waste form during early waste package failures that may occur as a result of rockfall, igneous activity, or seismic events. Another potential result of the early radioactive heat pulse is the evaporation of seepage and deposition of solutes as deliquescent (water-absorbing) minerals on the surface of the waste package and drip shield. These deliquescent minerals have the potential to affect localized corrosion of the titanium and C-22 alloys in the drip shield and waste package, respectively (see Section 6.2.2.4).

After the maximum temperature in the drift is reached during the radioactive heat pulse, water can potentially flow into the lower part of the drift from the host rock. Depending on the percolation fluxes, the contact between the host rock and crushed tuff, and the amount and rates of heating and cooling, water can imbibe into the lower parts of the drift through permeable tuffaceous formations.

6.2.2.2 Chemical Divides

As seepage waters make their way into the drift, their chemical composition can significantly change by evaporation and mineral precipitation. Evaporation causes aqueous species' concentrations to increase, minerals to precipitate, and the most soluble components to concentrate in brine.

When minerals (salts) precipitate, the relative concentrations of dissolved components change. This effect is a result of chemical divides encountered whenever a mineral precipitates. The chemical divide is explained by Drever (1988, p.235 [DIRS 118564]): "Whenever a binary salt is

precipitated during evaporation, and the effective ratio of the two ions in the salt is different from the ratio of these ions in solution, further evaporation will result in an increase in the concentration of the ion present in greater relative concentration in solution and a decrease in the concentration of the ion present in lower relative concentration." There are six common geochemical divides for natural lakes (Figure 6.2-1). These geochemical divides largely control the types of waters that can develop by evaporation in these lakes.

In the seepage abstraction, potential seepage waters were grouped based on the composition of the concentrated brines that form upon each water's evaporation (Section 6.6). In accordance with geochemical divide theory, the composition of the water changes due to the sequence of minerals that precipitate from solution. That sequence is a function of the initial water composition, the thermal conditions, and gas the composition at the location where the evaporation occurs. Evaporation to concentrated brines is simulated using geochemical speciation calculations (EQ3/6, Sections 6.5 and 6.6). These modeling results provide the suite of concentrated brine compositions that could potentially form on the waste package and drip shield.

Analogous evaporite minerals are commonly found on desert playa lakes in Nevada as the result of evaporative concentrations of relatively dilute and low-solute content rainwater and snowmelt (Papke 1976, Table 1 [DIRS 162274]). For these reasons, model calculation runs simulating the evaporation of Sierra snowmelt were carried out to validate the EQ6 Pitzer brine evaporation modeling (see Section 7.4). In addition, the presence of the same evaporite minerals in Nevada playas provides corroboration for the mineral assemblages predicted by the EQ3/6 software evaporative concentration computer simulations (Section 6.13.1).

6.2.2.3 Dust Deposition

During construction, ventilation, and waste package emplacement, and after sealing the primary entrances to the repository, dust will accumulate in the drift. Dust on the drip shields and waste packages is of primary concern for its potential influence on the corrosion of metals.

Most of the dust is formed from the tuff bedrock during excavation and construction of the repository (see Section 6.10). Some may be surface dust, carried into the drifts via ventilation, which may contain native evaporitic minerals, blown in from the surrounding countryside and playas, possibly up to hundreds of kilometers in distance (Reheis et al. 2002 [DIRS 163132]). Some of the dust may contain bromide, used as a tracer in construction waters near, and inside, the drift. The effect of bromine in the dust on the expected chemical environment is evaluated in Section 6.12.4.2. The bromide-containing dust is of interest for possible effects on the corrosion of metals after rehydration by condensation or potential seepage waters. Some dust is expected to be generated by evaporation of potential seepage waters (see Sections 6.6 and 6.9) during and after the heat pulse, and may involve transport from its original place of deposition.

Atmospheric dust has not been characterized directly as part of this project, but information in the literature on the general properties of this dust, on relevant atmospheric processes, and on materials from desert playas in Nevada, has been summarized in *Environment on the Surfaces of Drip Shield and Waste Package Outer Barrier* (BSC 2003, Section 6.7.2.8 [DIRS 164872]). In general, nitrate is an important component of atmospheric dusts, primarily due to its production

in the upper atmosphere by electrical phenomena as previously noted. Nitrate salts are recognized as an important component of atmospheric dusts and aerosols, and their properties (including deliquescence) are considered important to the understanding of certain weather and climatic phenomena. Anthropogenic sources add to the nitrate burden of atmospheric dust. The extent to which playa dusts add to this burden is not well known. Nitrate minerals are not commonly described as components of surficial playa salts, so playas are probably not a significant source of nitrate in atmospheric dust.

6.2.2.4 Deliquescence

Some minerals absorb water from the air and incorporate this liquid as waters of hydration within their mineral lattice structure. Common examples of such a material are the sodium-silicate-gel desiccants that are used as packing for transoceanic shipping.

Deliquescent minerals in drift dust (or evaporated salts from seepage) are of consequence because of their potential ability to change the microscale liquid environment around dust as they absorb water vapor from the air (see Figure 6.2-2). The presence of liquid water and mineral saturation in solution are both required for the relative humidity (expressed as a unit fraction) of the drift's atmosphere to equal the activity of water for the solution. Campbell and Smith (1951, p. 237 [DIRS 163817]) state, "It is clear that if the pressure of the aqueous vapor in the atmosphere is greater than that of the saturated solution of a salt, that salt will, on being placed in the air, form a solution: it will deliquesce." Where deliquescing minerals (salts) are present in the dust, the minerals will dissolve to form a small drop or puddle of liquid water. As shown in Figure 6.2-2, the evaporative process is the reverse of deliquescence.

One other general characteristic of deliquescent minerals is that, at ambient temperature, these minerals hold more waters of hydration within the mineral lattice structure than they do at higher temperatures. Figure 6.2-3 illustrates this with $MgCl_2$. At 1 atm total pressure, solid $MgCl_2$ has six waters of hydration below a temperature of 117°C, four waters of hydration from 117ºC to 180ºC, and, two waters of hydration above about 180°C. The same pattern occurs with the $CaCl_2$ minerals. This means more total water vapor may be adsorbed from the air by deliquescence at lower temperatures than at higher temperatures. It is important to recognize that the mass of salts in the dust is small compared to the total mass of dust and therefore, the total mass of deliquesced water will be small in comparison to the total mass of dust.

6.2.2.5 Temperatures Limiting the Amount of Liquid Water Available for Chemical Reactions in the Drift

The determination of when these scenarios are operative or dominate the chemistry is important to the type of chemical conditions that could be expected on the waste package or drip shield. As shown in Figure 6.2.2.2-7b of the *Drift-Scale Coupled Processes (DST and TH Seepage) Models* BSC 2003 [DIRS 166512]), the thermal seepage constraints indicate that there can be no seepage at drift temperatures above about 100°C due to the presence of a vaporization barrier. In addition to this limitation, the results of the DST corroborate the absence of macroscale liquid water available in the host rock at temperatures above about 105°C (Figure 6.2-4). Figure 6.2-4, which shows results of the Drift Scale Test, illustrates the observed *in situ* relationship between temperature and volumetric water content (from neutron logging) in borehole

EFS-HD-79-TEMP1 (also known as borehole 79) from February 1998 to May 2000 (see DTNs listed as source for Figure 6.2-4). These data are used to screen out elevated temperatures for processes that depend on the inflow of liquid water. These data also limit the maximum temperatures needed for high-temperature equilibrium constants in geochemical modeling.

Literature data and measured laboratory core sample saturations (Flint 1998, pp. 32 to 33 [DIRS 100033]) are in close agreement with observations from the Drift Scale Test (Figure 6.2-4), and show that at 60°C and 65 percent relative humidity, rock saturation becomes low enough that liquid flow stops and vapor flow becomes the dominant process. In measuring volumetric water content, Flint (1998, pp. 32 to 38) used the standard drying heat of 105°C, which normally is considered to remove most pore waters, but noted that "some, but not all, water was removed from the zeolites, clays, and pore spaces." The literature surveyed by Flint (1998, p. 38) suggested that most of the water released from 105°C to 180°C is from thermal dehydration of zeolites, clays, and interstitial waters.

These constraints indicate that the seepage scenario or environment will not occur above temperatures of about 100ºC.

6.2.3 Evolution of Engineered Barrier System Chemical Environments by Spatial Location

Evolution of the chemical environments includes the changing compositions of gas, water, and solids within the emplacement drifts under repository conditions (see Figure 6.1-1). The major compositional changes are caused by the changing thermal conditions in the drift—the initial rapid heating, followed by a slow cool down as the thermal activity of the waste package's decrease—and variation of gas and water compositions potentially flux into the drift. Thermal perturbation will affect the composition and movement of gas and water through the unsaturated system. These fluids may enter the drifts and react with the materials emplaced during construction of the repository. Most of these emplaced materials will be compositionally different from the host rock, and reactions with these materials, such as metals, may alter water and gas compositions before they react with the engineered barriers.

Figure 6.2-5 depicts several representative locations along a vertical flow path from the crown of the drift to the base of the invert where the chemical compositions of water and gas can directly affect degradation rates of the engineered barrier components, quantities and species of mobilized radionuclides, and transport rates for radionuclides and fluids through the drift into the UZ. These conditions and processes exist in the context of the EBS design.

A generalized representation of EBS design features, and processes that may occur (e.g. water movement, rockfall) within the emplacement drifts, is given in Figure 6.1-1 diagram. Waste forms are contained in metal waste packages. These packages lie on pallets that rest on a flat invert composed of crushed host rock and metal beams. Titanium alloy drip shields, resting on the invert, cover the waste packages. Drip shields are intended to divert entering water, preventing it from contacting the waste packages. Eventually, some drip shields may degrade and develop gaps. If a drip shield is breached, it only partially shields the waste packages from potential seepage water. Waste packages may be breached by corrosion, which may lead to

degradation of the waste forms and release of radionuclides to the invert and the UZ of the host rock.

The most direct way that the EBS chemical environments may impact long-term performance is by degradation of the EBS components that inhibit access to and limit the release of radionuclides to the UZ. Chemical changes to the in-drift environment may affect the amounts and types of mobile radionuclides and the properties of the solids through which they are transported.

Several processes potentially affect the in-drift chemical environments and are relevant to performance assessment:

- Gas, water, and EBS materials interactions (see Sections 6.4, 6.5, 6.6, 6.7, 6.8, 6.9, 6.10, and 6.13)
- Evaporation of water and condensation of water vapor (see Sections 6.9, 6.10)
- Salts precipitation and dissolution (see Section 6.9, 6.10).

Flow and transport paths among the EBS components (see Figure 6.2-5) define critical locations where chemical compositions of water and gas can directly affect degradation rates of the engineered barrier components, quantities and species of mobilized radionuclides, and transport rates for radionuclides and fluids through the drift into the UZ. It is at the critical locations that performance-related water compositions may change (to concentrated brines in some instances) due to the processes previously described.

When conditions for seepage exist, potential seepage water may enter the drift by gravity (i.e., by dripping, see Figure 6.2-5). The composition of this water may have been chemically influenced by reactions with ground support materials (e.g., rock bolts, and other ground support components) and with gases in the host rock. The water then falls through the air gap above the drip shield where further reactions with in-drift gases can occur. Interactions with ground support materials and reactions with gases are considered to be part of Location 1 (see Figure 6.2-5).

After passing through the air gap above the drip shield, the water contacts the surface of the drip shield (see Figure 6.2-5, Location 2) where it is diverted away from the waste package. On the drip shield, water evaporation, salt precipitation, and aqueous solution formation by rewetting and deliquesence of precipitated salts may occur. Aqueous solutions can initiate and maintain corrosion. Corrosion products on the surface of the drip shield can further alter the water composition. As long as it is intact, the drip shield will divert water fluxes around the waste packages to the invert and the UZ.

If the drip shield is breached, seepage water can pass through the breaches and contact the surface of the waste package (see Figure 6.2-5, Location 3) where it is diverted to the invert until the waste package is breached. Potential evaporation, condensation, and chemical processes at the surface of the waste package are the same as those for the drip shield. Aqueous solutions can initiate corrosion that can breach the waste package and corrosion products can further alter the water composition. Under appropriate conditions, water can condense under the drip shield, and

water reflux can occur between hotter and cooler locations. Thus, drip shield breaches are not a necessary condition for waste package corrosion.

Water that passes through breaches in the waste package will contact the waste forms (see Figure 6.2-5, Location 4). As the cladding and waste forms degrade, radionuclides will be mobilized in the water as dissolved or colloidal species. Water may also condense from water vapor onto waste forms. Water composition will also be modified by chemical reactions with the waste and other internal waste package components. Further discussion of these issues is provided in *In-Package Chemistry Abstraction* (BSC 2003 [DIRS 161962]), *Dissolved Concentration Limits of Radioactive Elements* (BSC 2003 [DIRS 163152]), and *Waste Form and In-drift Colloids-Associated Radionuclide Concentrations: Abstraction and Summary* (BSC 2003 [DIRS 161620]).

Advection and diffusion in flowing water and condensed water films can transport radionuclide-containing species through materials inside the waste package, through breaches in the waste package, and across waste package and pallet surfaces, to the invert (see Figure 6.2-5, Location 5).

Water can enter the invert (Figure 6.2-5, Location 5) from:

- Direct seepage
- Diversion by the drip shield
- Diversion by the waste package
- Reflux
- Flow from the waste package
- Imbibition or wicking from host rock (not shown in Figure 6.2-5)
- Flow directly from the host rock below the surface of the invert.

Dissolved constituents can also diffuse through water and water films from the waste package to the invert.

The composition of waters entering the invert (see Figure 6.2-5, Location 5) determines the stable concentrations of dissolved and colloidal radionuclides, based on solubility and colloid stability models (see *Dissolved Concentration Limits Of Radioactive Elements*, BSC 2003 [DIRS 163152], and *Waste Form And In-drift Colloids-Associated Radionuclide Concentrations: Abstraction And Summary*, BSC 2003 [DIRS 161620]). The interactions of these waters and resulting chemical environments are not evaluated in this report; however, the implications of such phenomena are considered in the TSPA.

6.2.4 Engineered Barrier System Physical and Chemical Environment Conceptual Model Locations

The EBS P&CE model can be summarized by a discussion of the locations identified in the conceptual model (see Figure 6.2-5). The model can be described as a series of either mixing or reaction cells that are found at the various spatial locations along the flow path, as discussed in Section 6.2.2. The various process model calculations documented in, or reported in, Sections 6.4 through 6.10 utilize these reaction cells. Outputs from these sections are applied to

other existing models, such as in-drift colloids and radionuclide solubility in the invert. The following subsections describe the development, application, and use of the P&CE model calculations. The actual flow and transport calculations that determine the fluxes within the drift can be found in *EBS Radionuclide Transport Abstraction* (BSC 2003 [DIRS 166466]).

6.2.4.1 Flux into Drift

The first step in developing the P&CE model is the selection of the incoming gas and water compositions for potential seepage entering through the crown of drift. This is described in Section 6.6. Water compositions representing fluids wicking into the invert for the same spatial and boundary conditions are also provided for direct input into Location 5.

6.2.4.2 Location 1 (Drift Wall and Air Gap)

The selected potential seepage water and gas chemistries can be modified by interactions with rock bolts and steel sheets, or directly flow (drip) onto the surface of the drip shield (Location 2). In general, potential seepage water interactions with the corrosion products themselves should not significantly alter the major ion composition of the water entering the drift. Given the limited longevity of most ground support materials (gantry rail, invert support beams, etc), as reported in Table 6.4-19, this effect would be short-lived for most of the materials emplaced within the drift (hundreds of years). However, the effect would be longer lived for the stainless steel components (steel sheets and rock bolts). Sensitivity analyses of the effects of chromium released during the corrosion of 316L stainless steel have been conducted (Section 6.8).

6.2.4.3 Location 2 (Surface of the Drip Shield)

A portion of the water coming from Location 1 may be diverted directly to the invert (Location 5) by the drip shield, or it may undergo evaporative processes, be influenced by any biofilms present, and/or react with dust and debris sitting on the drip shield. These fluids could flow onto the surface of the waste package (Location 3) at many times but could only flow into the package (Location 4) if a pathway becomes available. The effects of evaporative processes on the potential seepage composition are modeled and discussed in Sections 6.9 and 6.13. These process model results are the primary source of chemistry for fluids contacting the waste package.

The corrosion products associated with the drip shield are not expected to adversely effect the compositions of any waters flowing off or through the drip shield due to the very slow corrosion rates for titanium and to the insoluble nature of titanium oxides (see Section 6.4.2). For the same reasons, removal or addition of trace elements by sorption or dissolution processes associated with the active corrosion of the alloy was not considered.

6.2.4.4 Location 3 (Surface of the Waste Package)

Although the composition of the waste package alloy differs from that of the drip shield, it too, is highly corrosion-resistant (see Section 6.4.2), and the processes occurring at Location 2 are also applicable to this location.

6.2.4.5 Location 4 (Inside Waste Package)

This portion of the conceptual process is reported in other modeling reports such as *Summary of In-Package Chemistry Abstraction* (BSC 2003 [DIRS 161962]). The results of the model developed in that report are used as input into Location 5.

6.2.4.6 Location 5 (Invert)

The in-drift colloids model and the radionuclide solubility model require compositional parameters for water in the invert as discussed in Section 6.13. Three incoming water sources are considered--from Locations 2 or 3 (i.e., potential seepage was modified by evaporative processes and diverted around the waste package), from Location 4, and waters wicking directly into the invert. These are provided to the TSPA-LA (see Sections 6.13 and 6.15) in order to evaluate radionuclide solubility and colloid stability in the TSPA model for the invert.

INTENTIONALLY LEFT BLANK

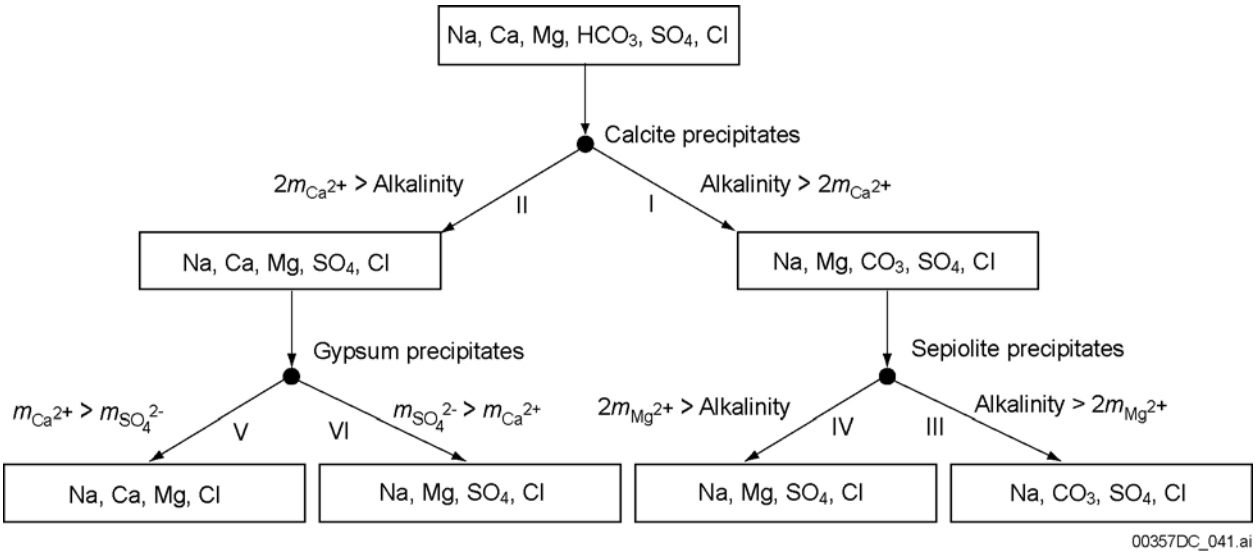

Source: Drever 1988, p.236 [DIRS 118564]

Figure 6.2-1. Simplified Chemical Divides Diagram Based on Evaporative Concentration of Dilute Starting Waters to Form a Suite of Naturally-Occurring Lake Waters

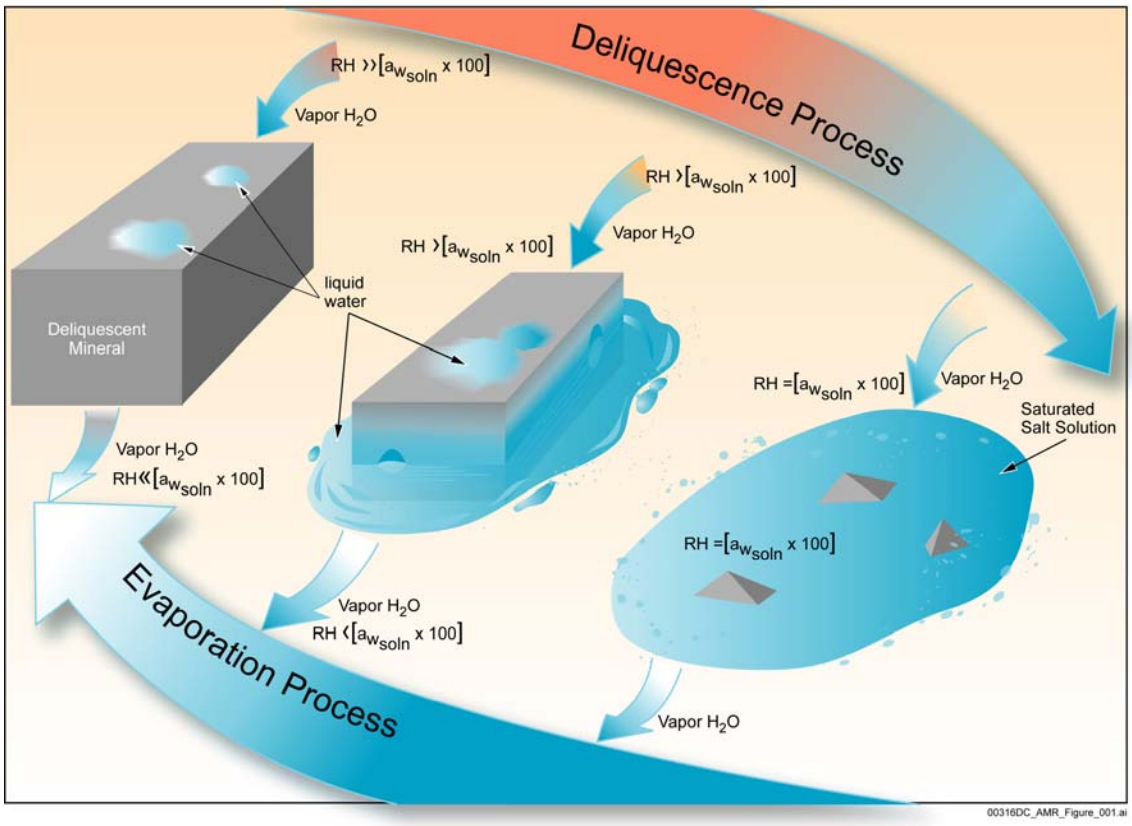

Figure 6.2-2. Schematic Illustration of Deliquescence and Evaporation

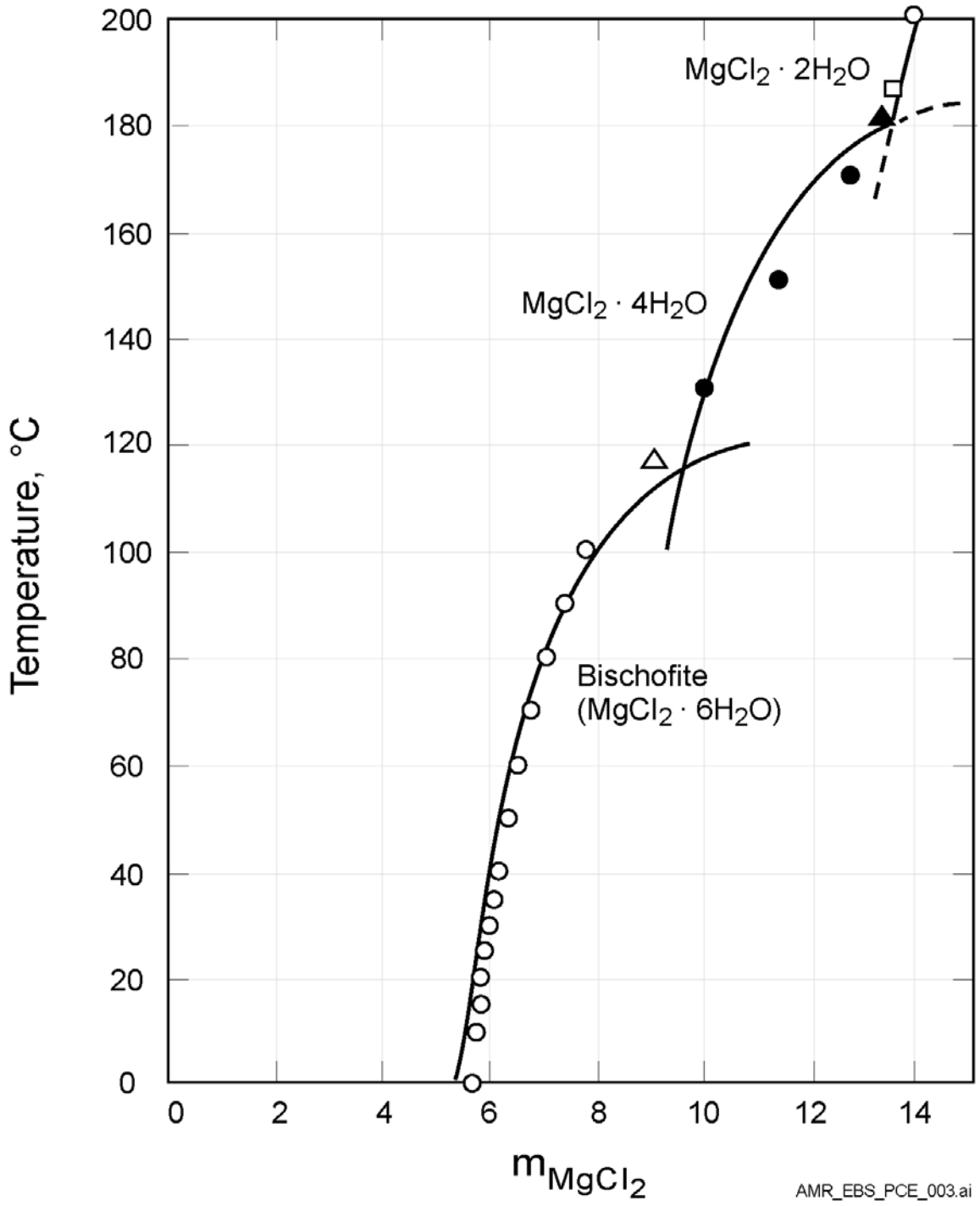

Source: Pitzer 1987, p.118 [DIRS 162481]

Figure 6.2-3. Calculated Solubilities Using the Pitzer Approach Compared to Experimental Data for the $MgCl_2$-H_2O Binary System

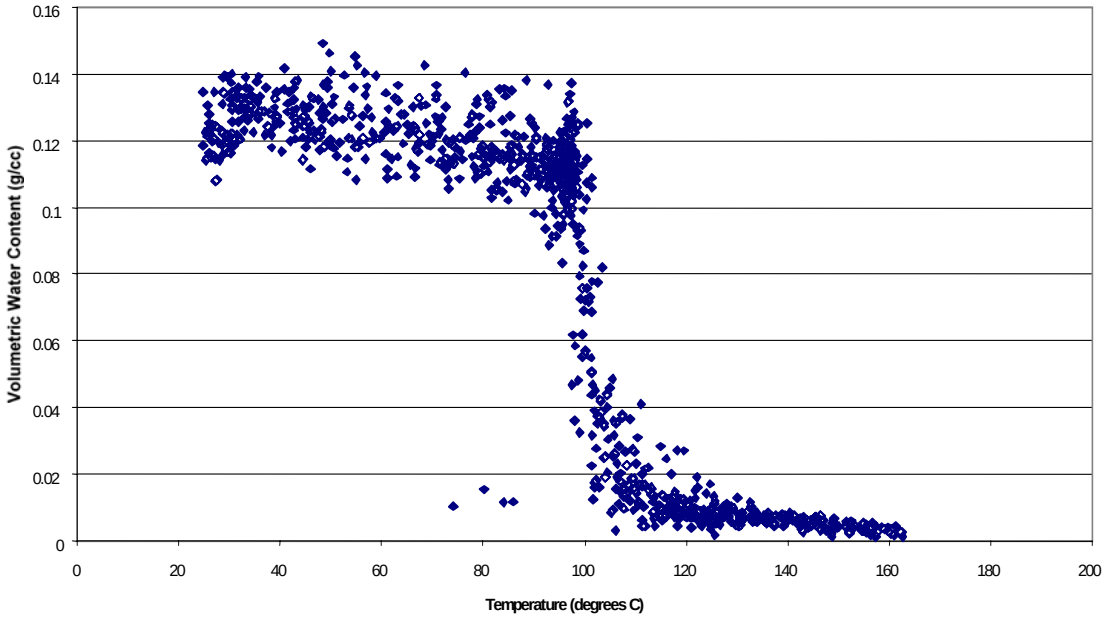

DTNs: MO9807DSTSET01.000 [DIRS 113644], MO9810DSTSET02.000 [DIRS 113662], MO9906DSTSET03.000 [DIRS 113673], MO0001SEPDSTPC.000 [DIRS 153836], MO0007SEPDSTPC.001 [DIRS 153707], and LL020710223142.024 [DIRS 159551]

NOTE: This borehole is almost level over an instrumented 40 m section, almost parallel and 9.5 m offset from the center of the drift, and about 3.5 m above the wing heaters that simulate the heat from a waste package. The test was conducted from February 1998 to May 2000.

Figure 6.2-4. Experimental Relationship between Borehole Temperature and Volumetric Water Content for Borehole 79 During the Drift Scale Test Over a Two-Year Period During Heating

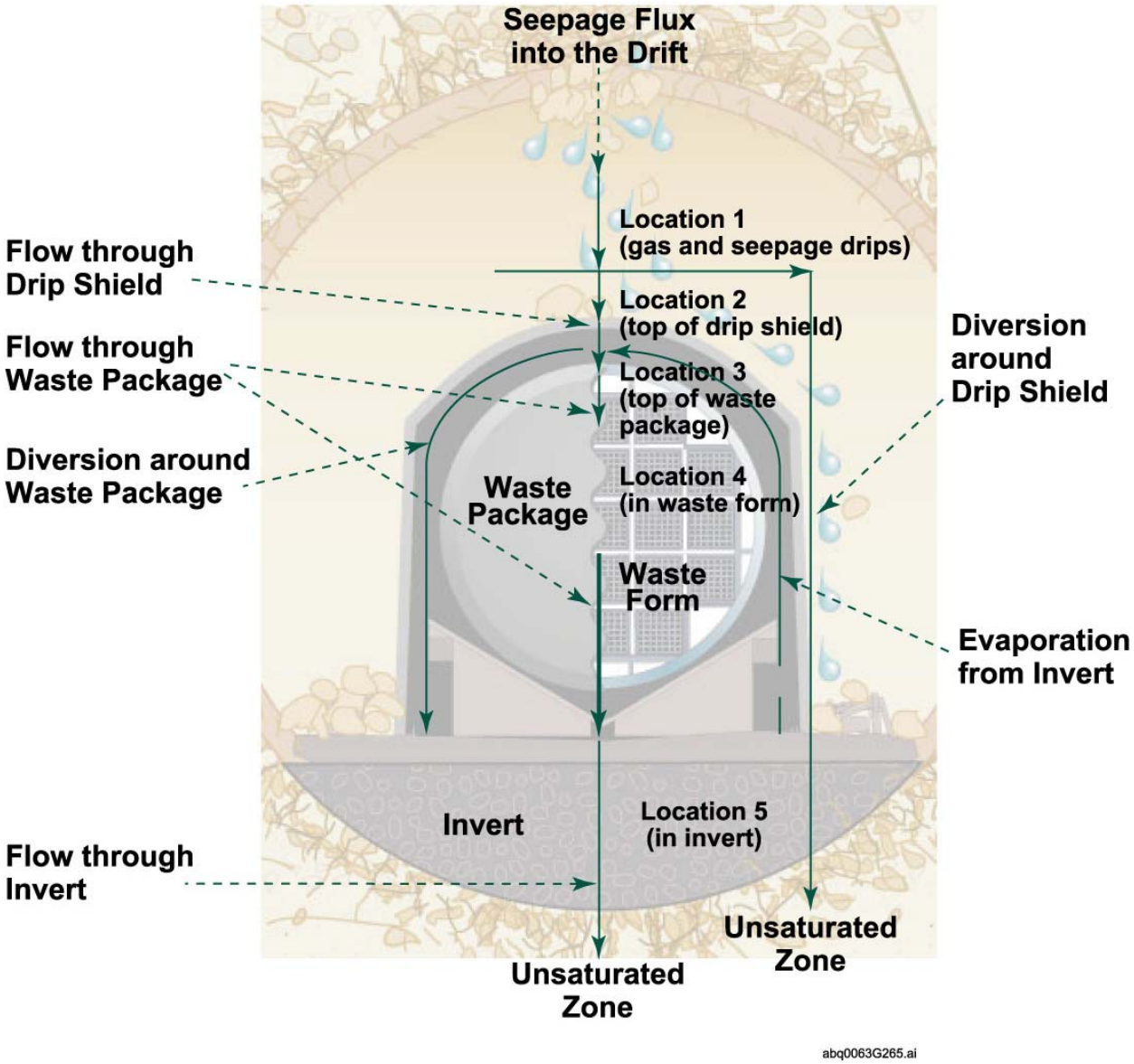

NOTE: Not shown is the wicking of water into the invert from the host rock.

Figure 6.2-5. Locations of Important Interfaces and Fluxes in the Engineered Barrier System

INTENTIONALLY LEFT BLANK

6.3 COUPLED PROCESSES

Coupled processes are those in which two or more physical and chemical processes simultaneously interact to produce a result, or in which a process is affected by physical and chemical variables at the same time. The coupled processes considered in the TSPA are those that can affect dose calculations such as the transport of aqueous species, including radionuclides. Onsager couplings are driven indirectly by gradients of thermodynamic state variables (e.g., temperature, pressure, chemical potential, and electrical potential) that affect chemical transport in aqueous solution. Direct transport processes are driven by the same thermodynamic-state variables in well-known relations such as Fourier's Law, Darcy's Law, Fick's Laws, and Ohm's Law. Diffusive processes dominate in Onsager-coupled processes. These processes are incorporated into the P&CE model implicitly through the THC seepage model output as well as through the abstraction methodology. This report describes the chemical processes at various locations in the drift, all of which are influenced by processes in the host rock, including coupled processes (e.g., BSC 2003 [DIRS 162050] and BSC 2003 [DIRS 166463]).

Other parts of the P&CE model also incorporate the effects of coupled processes. For example, the analysis of how corrosion products of ground support materials impact in-drift chemistry takes into account various thermal-hydrological-mechanical-chemical effects, as do the corrosion rates themselves.

The relative importance of different coupled processes, formally classified as FEPs, are discussed briefly in Section 6.14 and documented in more detail in various FEPs reports (such as the *Engineered Barrier System Features, Events, and Processes* report (BSC 2003 [DIRS 166464])). These reports contain straightforward screening arguments if the FEP is excluded from further consideration and a description of the TSPA disposition if it is included. The rationale for exclusion may be based upon regulatory requirements, low probability of occurrence, or low consequence in terms of impact on calculated dose.

INTENTIONALLY LEFT BLANK

6.4 INTRODUCED MATERIALS

Figure 6.1-1 shows the general configuration of materials introduced into a repository drift. These materials are expected to undergo chemical and physical changes in the repository environment, and they and their reaction products will affect the geochemical evolution of seepage infiltrating into the drift and of waters condensing or deliquescing within the drift.

This section analyzes the introduced materials of the current repository design (see Section 4.1) to establish boundary conditions and modeling constraints for this model. This section also describes the general evolution of introduced materials over time, or identifies documents where these materials have been evaluated. In general, waste package and drip shield material longevity is evaluated in documentation such as the *WAPDEG Analysis of Waste Package and Drip Shield Degradation* (BSC 2003 [DIRS 161317]). Evolution of in-package materials is evaluated in the *In-Package Chemistry Abstraction* (BSC 2003 [DIRS 161962]). The chemical effects and longevity of all other introduced materials is evaluated within this document. The waste package, drip shield, and waste form material lifetimes are only used here to perform general mass balance calculations associated with the evolution of the in-drift gaseous environment (see Section 6.7). The analyses in this section also are used to constrain boundary conditions and modeling constraints for the chemistry as it pertains to the drip shield, waste package, or the invert (e.g., 316L stainless steel corrosion in Section 6.8).

6.4.1 Material Corrosion Rates

To determine the effect of introduced materials on water and gas evolution in the drift, this section reviews corrosion rates relevant to determining the longevity of the introduced materials (see Section 4.1).

In the following sections and tables, corrosion rates under a variety of environmental conditions are discussed. These include corrosion rates measured under both humid air and immersed conditions. Experimental work for the Project was carried out using three waters, referred to as Simulated Dilute Water (SDW), Simulated Concentrated Water (SCW), and Simulated Acidified Water (SAW), respectively (McCright 1998 [DIRS 114637]). The SDW simulates J-13 well water at 10X concentration to account for minor effects of water evaporation and boiling. SCW simulates J-13 well water concentrated 1000X to account for long-term water evaporation and boiling in the repository environment. SAW represents J-13 well water that has been acidified and concentrated, which is intended to simulate the effect of possible microbial metabolic products. Corrosion tests were run on samples immersed in these waters, and in the humid air generated above these waters upon heating. Further information on these simulated solutions is provided in McCright (1998 [DIRS 114637]). The data from McCright form the original basis of the models used in waste package corrosion modeling done on the YMP.

In addition, outdoor atmospheric corrosion data are used. In Table 6.4-1, these data are designated by the column header word “Environment” following the type of outdoor environment (i.e., marine, industrial, urban, or rural).

The corrosion of metals in the atmosphere is primarily controlled by temperature, relative humidity, and the presence of atmospheric contaminants (which may specifically include aerosol

particles). Many other parameters can affect corrosion rates, including time of wetness, rainfall, fog, and hours of sunlight, but these will not be discussed here. Temperatures and relative humidity values are presented in the tables below. However, data on atmospheric contaminants is not available in many cases. Typical activity ranges for two of the more important contaminants (SO_X and chlorides) are presented in Table 6.4-1 (Money 1987 [DIRS 163007]); however, these values are not used as input parameters for determining the most likely corrosion rates.

Note that in many of the tables in this document there is inconsistent use of significant figures. An attempt was made to capture the data as it exists within each data source as opposed to providing a consistent number of significant figures. In the case of reporting values from EQ3/6 calculated data, rounding was usually done to two digits beyond the decimal.

Table 6.4-1. Typical Activity Ranges for SO_X and Chlorides in Various Environments

Environment	mg $SO_X/dm^2/day$	mg $Cl^-/dm^2/day$
Industrial	0.5-2.0	Nil
Urban	0.5-4.0	Nil
Rural (semi)	Nil-2.0	Nil
Marine	Nil-0.5	25-150

Source: Money 1987 [DIRS 163007]

The most corrosive environments are the marine and industrial atmospheres, which represent corrosion under conditions of high humidity, or of metal covered with a salt crust, or in the presence of high concentrations of atmospheric contaminants.

In the case of pooled water in or on materials, those values indicated by “Freshwater” and “Saltwater” are used for the corrosion rate. The freshwater rates are representative of those solutions that are dilute, such as lake water and J-13 well water. The saltwater rates are for ocean water with an average chloride content of 17,115-17,357 ppm (Forgeson et al. 1958 [DIRS 159343]), and are used when the natural waters have been concentrated due to evaporation or contact with engineered materials. Any modifications to these definitions will be discussed for each individual material in the following sections.

6.4.1.1 Titanium

Because a stable oxide film (rutile, anatase, or TiO_2) forms instantly upon exposure to air, titanium is generally resistant to corrosion. This is shown in Table 6.4-2, which lists corrosion rates of Ti-alloy over a one-year period in heated atmospheres at near 100 percent relative humidity. These values come from McCright (1998 [DIRS 114637]). It should be noted that, given the short duration of the tests, the values for the corrosion rates might be slightly high for long-term predictions of the metal’s lifetime (in general, corrosion rates decrease with time, as corrosion products build up on the metal surface and inhibit further reaction).

Table 6.4-2. Titanium Corrosion Rates from Laboratory Experiments at Near 100 Percent Relative Humidity and High Temperature

	SAW (60°C steam)	SAW (90°C steam)	SCW (60°C steam)
Maximum (μm/year)	0.02	0.07	0.02
Mean (μm/year)	0.00167	0.00292	0.00273
Minimum (μm/year)	0	0	0

Source: DTN: MO0312SPAPCEML.003

NOTE: Calculated in spreadsheet "atmospheric," "Titanium" sheet.

Covington and Schutz (1981 [DIRS 151102]) present data on the atmospheric corrosion of titanium alloys after 20 years exposure in varying environments. These values are presented in Table 6.4-3. However, these values should be used with caution as the specimens were cleaned for five minutes in boiling 10 percent nitric acid before and after exposure. As titanium is known to corrode in boiling nitric acid (Schutz 1986 [DIRS 151162] and Schutz and Thomas 1987 [DIRS 112147]), it is unclear if the observed small amount of metal loss is from the atmospheric corrosion of the metal or from the cleaning process itself.

Table 6.4-3. Possible Corrosion Rates of Ti-Alloys at Lower Temperatures

	Marine Atmosphere	Industrial Atmosphere	Rural Atmosphere
Maximum (μm/year)	0.0229	0.0254	0.0279
Mean (μm/year)	0.0116	0.0116	0.0121
Minimum (μm/year)	0.0025	0.0025	0.0025

Source: DTN: MO0312SPAPCEML.003

NOTE: Calculated in spreadsheet "atmospheric," "Titanium" sheet.

An alternate source containing Project data, DTN: MO0003SPASUP02.003 [DIRS 147299], contains values for corrosion of titanium (Grade 7) as a cumulative distribution function. Interpolation of the cumulative distribution function at the 5th, 50th, and 95th percentile levels is done to correspond to a minimum, mean, and maximum value (CRWMS M&O 2000, Table 25 [DIRS 151561]). These are presented in Table 6.4-4 and are on the same order as those presented above in Table 6.4-2 and Table 6.4-3, except in the maximum value case that likely represents a short-term deviation to the mean corrosion rate.

Table 6.4-4. Corrosion Rates of Titanium Grade 7

5th Percentile (Minimum-μm/year)	50th Percentile (Mean-μm/year)	95th Percentile (Maximum-μm/year)
0.0053	0.025	0.26

Source: DTN: MO0003SPASUP02.003 [DIRS 147299]

6.4.1.2 Alloy 22

Given the recent introduction (1982) of Alloy-22, published long-term corrosion studies of the material are sparse (Agarwal 2000, Section 20 [DIRS 163034]). The most extensive information is a one-year study of the corrosion of Alloy-22 from *Corrosion Data and Modeling Update for Viability Assessment* (McCright 1998 [DIRS 114637]). Given the short duration of the tests, the measured values for the corrosion rates, tabulated in Table 6.4-5, might be slightly high for long-term predictions of the metal's lifetime, as they tend to over-emphasize the high initial corrosion rates.

Table 6.4-5. Corrosion Rates of Alloy-22 in Various Environmental Conditions

Environment	Maximum (μm/year)	Mean (μm/year)	Minimum (μm/year)
60°C (SAW Steam)**	0.16	0.05	0.00
60°C (SDW Steam)**	0.10	0.07	0.00
60°C (SCW Steam)**	0.11	0.06	0.02
90°C (SAW Steam)**	0.12	0.04	0.00
90°C (SDW Steam**	0.08	0.06	0.03
90°C (SCW Steam)**	0.47	0.07	0.00
60°C (SAW)*	0.12	0.04	0.00
60°C (SDW)*	0.10	0.06	0.00
60°C (SCW)*	0.13	0.08	0.03
90°C (SAW)*	0.11	0.02	0.00
90°C (SDW)*	0.12	0.07	0.03
90°C (SCW)*	0.25	0.08	0.00

Sources: * DTN: MO0401SPAMCRAE.000 [DIRS 166801]
**Calculated in spreadsheet "atmospheric," "Alloy-22" sheet, DTN: MO0312SPAPCEML.003.

An alternate source containing Project data, DTN: MO0003SPASUP02.003 [DIRS 147299], contains the values for corrosion of Alloy-22 as a cumulative distribution function. Interpolation of the cumulative distribution function at the 5th, 50th, and 95th percentile levels is done to correspond to a minimum, mean, and maximum value (CRWMS M&O 2000, Table 25 [DIRS 151561]). These values are presented in Table 6.4-6. These values are in agreement with those presented in Table 6.4-5.

Table 6.4-6. Corrosion Rates of Alloy-22

5th Percentile (Minimum-μm/year)	50th Percentile (Mean-μm/year)	95th Percentile (Maximum-μm/year)
0.0038	0.029	0.11

Source: DTN: MO0003SPASUP02.003 [DIRS 147299]

6.4.1.3 Inconel Alloys X-750 and 600

Because there is a lack of corrosion data for Alloys X-750 and 600, alloy 625 was used as a surrogate for these alloys. It is compositionally similar to X-750 and 600, and all are highly corrosion-resistant. The best available information is a one-year study of the corrosion of Inconel Alloy 625 (*Corrosion Data and Modeling Update for Viability Assessment*, McCright 1998 [DIRS 114637]). It should be noted that, given the short duration of the tests, the corrosion rates listed in Table 6.4-7 might be slightly high for long-term predictions of the metal's lifetime, again due to relatively rapid initial corrosion.

Table 6.4-7. Corrosion Rates of Inconel Alloys in Various Aqueous Environments

Environment	Maximum (μm/year)	Mean (μm/year)	Minimum (μm/year)
60°C (SAW)	0.08	0.0268	0
60°C (SDW)	0.05	0.025	0
60°C (SCW)	0.10	0.08	0.05
90°C (SAW)	0.09	0.0108	0
90°C (SDW)	0.1	0.04	0
90°C (SCW)	0.24	0.08	0.03

Source: DTN: MO0401SPAMCRAE.000 [DIRS 166801]

6.4.1.4 Copper Alloy

The corrosion rates for copper under different environmental conditions are presented in Table 6.4-8. Under outdoor conditions, the main factors influencing corrosion of copper are the relative humidity and concentration of aerosol particles (Sequeira 2000 [DIRS 162970]).

Table 6.4-8. Corrosion Rates of Copper Under Various Environmental Conditions

Environment	Maximum (μm/year)	Mean (μm/year)	Minimum (μm/year)
90°C, J-13 Steam, near 100% relative humidity	4.15	2.86	1.67
95-100°C, J-13 Steam, near 100% relative humidity	6.60	4.79	3.15
150°C, J-13 Steam, near 100% relative humidity	1.78	1.09	0.46
90°C, Soln 7 steam, near 100% relative humidity (1000 ppm Cl)	5.90	1.6	0.39
Marine Atmosphere (70%-83% relative humidity)	4.14	1.68	0.43
Marine Atmosphere (60%-70% relative humidity)	1.38	1.33	1.27
Rural Atmosphere (wet-69.5-83% relative humidity)	2.01	0.94	0.42
Rural Atmosphere (dry-39% relative humidity)	0.13	0.13	0.13
Industrial Atmosphere (65-68% relative humidity)	1.90	1.50	1.30
Urban Atmosphere (74% relative humidity)	1.40	1.22	1.04

NOTE: Calculated in spreadsheet "atmospheric" "Copper" sheet in DTN: MO0312SPAPCEML.003.

6.4.1.5 Aluminum Alloy

Measured aqueous corrosion rates for aluminum alloy are presented in Table 6.4-9. Aluminum differs from other metals in that the main corrosion behavior is a form of localized corrosion called pitting. Because pitting does not allow for easy determination of material lifetimes, pitting weight loss data for aluminum are converted to general rates for use in this report.

Table 6.4-9. Corrosion Rates of Aluminum Alloys in Aqueous Environments

Environment	Maximum (μm/year)	Mean (μm/year)	Minimum (μm/year)
Fresh water	36.93	12.95	0.40
Saltwater	124.46	10.88	0.12

Source: DTN: MO0401SPAMCRAE.000 [DIRS 166801]

Atmospheric data on the corrosion of aluminum alloy come from American Society for Metals International (1987, Tables 8 and 11 [DIRS 103753]) and can be found in Table 6.4-10. The minimum value comes from 20-year atmospheric corrosion data, the median value from 10-year atmospheric corrosion data, and the maximum from the highest value of atmospheric corrosion.

Table 6.4-10. Atmospheric Corrosion Rates of Aluminum Alloy 6061

Maximum Rate (μm/year)	Median Rate (μm/year)	Minimum Rate (μm/year)
0.422	0.35	0.076

Source: American Society for Metals International 1987, Tables 8 and 11 [DIRS 103753]

6.4.1.6 316L Stainless Steel

In relatively uncontaminated environments, such as rural atmospheres or steam produced from dilute solutions such as J-13 well water, corrosion of 316 stainless steel is very minor. However, when the atmosphere contains contaminants, such as chlorides and metallic iron dust, the corrosion rate rises significantly (see Table 6.4-11). Chloride contamination can come from exposure to marine environments. The amount of corrosion depends on the distance of the test specimen from the chloride source (i.e., the tide line), showing that the more chlorides an environment contains, the more corrosive it will be. On the other hand, iron dust contamination can come from fabrication or erection of metal structures (Davison et al. 1987 [DIRS 162971]), such as when the repository is being constructed, and may enhance corrosion of the 316 stainless steel.

Table 6.4-11. Corrosion Rates of 316L Stainless Steel Under Various Environmental Conditions

Environment	Maximum (μm/year)	Mean (μm/year)	Minimum (μm/year)
100°C J-13 Steam**	0.099	0.099	0.099
150°C J-13 Steam**	0.064	0.064	0.064
Marine Atmosphere**	0.517	0.113	0.000
Industrial Atmosphere**	0.014	0.008	0.000
Rural Atmosphere**	0.00	0.00	0.00
207°C Brine Steam**	53	49.667	48
29.5°C Freshwater*	0.0475	0.0083	0.0007
50°C Freshwater*	0.2286	0.1614	0.1016
70°C Freshwater*	0.2540	0.2413	0.2286
80°C Freshwater*	0.2794	0.2141	0.1090
90°C Freshwater*	0.2540	0.2032	0.1524
100°C Freshwater*	0.5100	0.3247	0.0370
26.7°C Saltwater*	14.79	1.9391	0.0014

Source: *DTN: MO0401SPAMCRAE.000 [DIRS 166801]

NOTE: **Calculated in spreadsheet "atmospheric.xls," "316" sheet (DTN: MO0312SPAPCEML.003)

Additional corroborative data is available from the *In-Drift Microbial Communities* report (Table 25, CRWMS M&O 2000 [DIRS 151561]) (from DTN: MO0004SPASMA05.004 [DIRS 151049]), which tabulates median, maximum, and minimum values for corrosion of 316L stainless steel (presented in Table 6.4-12). The lower bound value is representative of general corrosion of 316L stainless steel. The median value is close to the mean value of 316 corrosion in saltwater. However, the upper bound value is three times higher than the maximum saltwater corrosion rate that was obtained from literature sources and used in this report.

Table 6.4-12. Corrosion Rates of 316L Stainless Steel

Upper Bound (μm/year)	Median (μm/year)	Lower Bound (μm/year)
45.5	2	0.0879

Sources: Upper and lower bounds: DTN: MO0004SPASMA05.004 [DIRS 151049], in spreadsheet "Corrosion rates.xls"
Median: from Section 6.5.2.3 of "In-drift Microbial Communities" (CRWMS M&O 2000 [DIRS 151561])

6.4.1.7 304L Stainless Steel

Like 316L stainless steel, 304L stainless steel displays excellent resistance to corrosion in freshwaters (Table 6.4-13). However, due to the absence of molybdenum, its susceptibility to more corrosive environments, such as saltwater, is increased (e.g., rates at 26.7°C saltwater in Tables 6.4-11 and 6.4-13).

Table 6.4-13. Corrosion Rates of 304L Stainless Steel in Various Environmental Conditions

Environment	Maximum (μm/year)	Mean (μm/year)	Minimum (μm/year)
28°C Freshwater	0.285	0.191	0.0811
50°C Freshwater	0.229	0.129	0.025
70°C Freshwater	0.203	0.203	0.203
80°C Freshwater	0.229	0.172	0.085
90°C Freshwater	1.57	0.291	0.02
100°C Freshwater	0.25	0.135	0.072
26.7°C Saltwater	36.902	9.934	1.588
90°C Saltwater	15.9	5.816	0.66
90°C Boil-down test	11.8	2.924	0.09

Source: DTN: MO0401SPAMCRAE.000 [DIRS 166801], spreadsheet "aqueous-304L.xls"

6.4.1.8 Borated Stainless Steel

No direct experimental data on the corrosion rate of borated stainless steel (Neutronit) in an environment similar to that expected in the repository have been found in the published literature. Kugler (1996 [DIRS 107760]) states that corrosion resistance has "proven satisfactory" and is similar to that of AISI (American Iron and Steel Institute) type 321 stainless steel. Like other stainless steel, it is corrosion resistant, especially in more dilute waters. A corrosion rate of 40 μm/year has been suggested in Van Konynenburg et al. (1998 [DIRS 100948]). This value is higher than the maximum saltwater rate found in various literature sources and may represent the upper bound for the corrosion of Neutronit in highly corrosive media.

Several waste package designs also propose a borated 304L stainless steel as the neutron absorber containing material. Unfortunately, most corrosion experiments have been conducted in extremely hostile environments, such as boiling nitric acid, sulfuric acid, and seven normal HNO_3 (Smith et al. 1992 [DIRS 103441]; EPRI 1986 [DIRS 159367]; and Butler 1963 [DIRS 159368]). *Corrosion of Stainless Steel Type 304 Alloyed with Boron or Gadolinium by Plant Process Solutions Containing HNO_3 and HF* (Cole 1976 [DIRS 159369]) was the only paper located giving any data on borated 304 stainless steel corrosion in more realistic corrosive environments. More information on how these corrosion rates were determined is provided in DTN: MO0401SPAMCRAE.000 [DIRS 166801]. These values are given in Table 6.4-14.

6.4.1.9 Carbon and Low Alloy Steels

The corrosion rates for carbon and low alloy steels in different environments are shown in Table 6.4-15. Under subaerial exposure, the highest corrosion rate of 1057.18 μm/year comes from a steel sample sitting directly on the beach at Cape Kennedy, Florida. This sample was fully exposed to constant sea spray and is a good indication of how salt buildup may affect the corrosion of metals. The lowest rate (0.4 μm/year) comes from a rural atmosphere at a relative humidity below 60 percent. These two values show how the corrosion rate for these steels can greatly differ depending on the atmospheric environment.

Table 6.4-14. Corrosion Rates of Borated Stainless Steels Under Various Environmental Conditions

Environment		Maximum (μm/year)	Mean (μm/year)	Minimum (μm/year)
Neutronit				
29.5°C Freshwater		0.01131	0.00438	0.00071
50°C Freshwater		0.17780	0.15240	0.12700
70-90°C Freshwater		0.33020	0.25400	0.20320
100°C Freshwater		0.20320	0.11430	0.02540
26.7°C Saltwater		29.22	11.0595	1.81
0.3% B in 304L Stainless Steel				
Fresh Acting Solutions	Ambient	12.19	7.62	3.05
	50°C	27.43	18.29	12.19
	Boiling	24.38	19.30	15.24
Saline Acting Solutions	Ambient	26.46	17.05	2.94
	50°C	147.00	94.67	38.22
	Boiling	58.80	29.77	11.76
1.5% B in 304L Stainless Steel				
Fresh Acting Solutions	Ambient	771.14	676.66	234.70
	Boiling	219.46	197.36	161.54
Saline Acting Solutions	Ambient	1805.16	1225.98	649.74
	50°C	1058.40	998.13	937.86
	Boiling	1893.36	531.41	164.64

Source: DTN: MO0401SPAMCRAE.000 [DIRS 166801]

Aqueous corrosion rates of carbon and mild steels are much lower than marine or industrial atmospheric corrosion rates. Temperature effects are also different. In atmospheric corrosion, there is generally a direct correlation between temperature and corrosion rate. However, in aqueous environments, corrosion at 60°C is greater than that at 90°C. This is corroborated by Brasher and Mercer (1968 [DIRS 100883]), who measured the relationship between corrosion and temperature (Figure 6.4-1). As shown in the worksheet titled "rate vs. temperature" in DTN: MO0401SPAMCRAE.000 [DIRS 166801], the highest corrosion rates occur at 60°C. The corrosion rate decreases with either increasing or decreasing temperature from this value (i.e., corrosion rates for both 25°C and 90°C will be lower than the 60°C rates). As can be seen from Figure 6.4-1, the rates for the mild steel are within the same range as those for the A516 from McCright (1998 [DIRS 114637]). Thus far, no specific data have been located for corrosion at 25°C of A516. The data plotted in Figure 6.4-1 shows that corrosion for mild steel the rates at 25°C are slightly lower than those at 90°C. Therefore, in the absence of 25°C data for A516, the values presented for 90°C can be used as a surrogate.

Table 6.4-15. Corrosion Rates of Carbon and Low Alloy Steels in Various Environmental Conditions

Environment	Maximum (μm/year)	Mean (μm/year)	Minimum (μm/year)
60C-SDW Steam**	74.25	41.97	18.60
90C-SDW Steam**	135.26	63.60	22.69
60C-SCW Steam**	360.78	177.16	76.38
90C-SCW Steam**	423.06	195.43	72.96
Marine Atmosphere (80% relative humidity and over)**	851.09	153.33	9.87
Marine Atmosphere (70 to 80% relative humidity)**	1057.18	101.94	6.39
Industrial Atmosphere (Over 80% relative humidity)**	123.00	102.5	85.50
Industrial Atmosphere (70-80% relative humidity)**	137.80	46.28	12.55
Industrial Atmosphere (60 to 70% relative humidity)**	164.54	20.58	3.77
Semi-Industrial Atmosphere (over 80% relative humidity)**	171.70	119.93	75.3
Semi-Industrial Atmosphere (60 to 70% relative humidity)**	60.88	35.23	17.33
Rural Atmosphere (over 80% relative humidity)**	60.10	39.19	21.60
Rural Atmosphere (70-79% relative humidity)**	59.00	26.63	10.68
Rural Atmosphere (60-69% relative humidity)**	75.50	19.37	3.93
Rural Atmosphere (less than 60% relative humidity)**	38.67	13.86	0.40
Urban Atmosphere (70-80% relative humidity)**	68.70	34.81	10.76
Urban Atmosphere (60-70% relative humidity)**	93.70	38.71	7.12
Urban Atmosphere (below 60% relative humidity)**	29.16	11.09	0.70
60°C-SDW*	130.70	88.79	41.31
90°C-SDW*	180.42	68.54	29.53
60°C-SCW*	104.20	39.95	6.77
90°C-SCW*	22.06	9.81	3.69

Source: *DTN: MO0401SPAMCRAE.000 [DIRS 166801], spreadsheet "aqueous-A516.xls"

NOTE: **Calculated in spreadsheet "atmospheric.xls," "mild-structural-carbon" sheet (DTN: MO0312SPAPCEML.003).

For comparison, additional aqueous corrosion rates for mild and carbon steels, from DTN: LL980704605924.035 [DIRS 147298], are presented in Table 6.4-16. These fall within the larger range of data obtained from literature sources previously mentioned and are in general agreement.

Table 6.4-16. Aqueous Corrosion Rates for Mild Carbon Steel

Maximum Rate (+1 STD) (μm/year)	Mean Rate (AVG) (μm/year)	Minimum Rate (-1 STD) (μm/year)
95.34	59.42	23.5

Source: DTN: LL980704605924.035 [DIRS 147298]

6.4.1.10 General Waste Form Dissolution Rate

In order to calculate the oxygen consumption (Section 6.7) in the repository, spent nuclear fuel (SNF) consumption of oxygen must be taken into account. To select a "general" waste form dissolution rate it is necessary to select a single fuel type to represent the waste forms. The most abundant waste form is commercial SNF. The degradation rate for the commercial SNF used in the oxygen consumption calculations are provided in Table 4.1-12

The U.S. Department of Energy (DOE) National Spent Fuel Program reports on the total inventory of DOE-owned SNF (DOE 2003 [DIRS 163377]) targeted for disposal. Table 6.4-17 summarizes the total ratio of DOE fuels to the N-reactor SNF. N-reactor spent fuel is a U-metal that constitutes a major sink for consumption of the oxygen in the drift. Therefore, N-reactor fuel dissolution is used as the major oxygen consumer discussed in Section 6.7. The rate applied to this fuel dissolution is 1.39×10^4 mg/m^2·day (Section 4.1.2)

Table 6.4-17. Comparison of N-Reactor to Total U.S. Department of Energy Spent Nuclear Fuel

End of Life Total Mass of DOE SNF (kg)	End of Life Mass of N-Reactor SNF (kg)	Percent N-reactor SNF to Total DOE SNF
2409455.05	2099824.04	87.14%

Source: Term Estimates for DOE Spent Nuclear Fuels. Excel program "all sites summary sheets.xls" worksheet "Nominal 2010". DOE/SNF/REP-078 REV. 0 [DIRS 163377]

6.4.2 Material Lifetimes

The expected lifetime of the introduced materials in the repository will be influenced by key environmental parameters such as temperature, relative humidity, and available oxygen.

The availability of oxygen to support corrosion in the drift is addressed in Section 6.7. There it is concluded that air flux through the closed repository will be sufficient to support an oxic environment in the drift at almost all times. Temperature extremes are addressed in *Repository Multiple Waste Package Thermal Calculation* (BSC 2001 [DIRS 156276]) by evaluating thermal loading of the waste package wall, the drift wall, 1-5 meters into the rock, and between drifts. Simulations predict that the drift components would not experience temperature regimes exceeding 250°C (if unventilated) or 90°C (if ventilated). Therefore, an upper bound for thermal loading is selected to be 250°C, although the duration of the high temperature regime is short and early in the lifetime of the waste packages (within first 500 years after emplacement). The lower bounding limit for temperature is selected to be the drift ambient temperature of 25°C.

Accordingly, material lifetimes of individual components have been estimated by establishing bounding conditions for possible environmental conditions in the drift.

6.4.2.1 Selection of Corrosion Rates

To calculate the longevity of each introduced material in the repository, a single rate for minimum, maximum, and mean corrosion rate was selected from Tables 6.4-2 through 6.4-17. The selected rates for the minimum, maximum, and mean were the maximum values reported for that material in each category. The maximum corrosion rates were selected as they would

represent the most corrosive possible conditions within the drift (although it may be of short duration), and would be most conservative (i.e., tend to overestimate corrosion rates). The selection of these rates is used to specifically represent the largest possible oxygen consumption rate during active corrosion as discussed in Section 6.7, or the largest degradation rate for ground support materials interacting with seepage (see Sections 6.8 and 6.12.4.1.1). These rates are applied at discrete locations, however it is recognized that corrosion rates will not be uniform throughout the repository. It is expected that most of the repository could see lower corrosion rates. Table 6.4-18 is the summary listing of the selected metal and metal alloy material corrosion rates.

6.4.2.2 Calculation of Material Lifetimes

The lifetimes (longevity) of materials committed to the drift are calculated using a material thickness of 1.0 inch. For each longevity plot, material thicknesses are calculated as a function of time and environmental conditions, assuming both one- and two-sided corrosion. The corrosion rates that are used are given in Table 6.4-18 and an Excel program is used to allow for a uniform corrosion of materials as a function of time. All longevity calculations are in Excel spreadsheet "Material Rates and Longevity.xls" archived in DTN: MO0312SPAPCEML.003. Figures 6.4-2 through 6.4-9 are longevity charts for different materials anticipated to be used in construction of the repository. Figure 6.4-10 is a lifetime comparison profile of solid materials (1-in. thickness) based on steam/hostile atmosphere and fresh and saltwater corrosion rates. Individual components of the introduced materials actually have variable nominal thicknesses (Section 4.1.1), and will have varying longevities, even if they are composed of the same material. A single mid-range value (1 inch) is used in these calculations because it allows direct comparison of the different material longevities.

Figure 6.4-10 and Table 6.4-19 summarize the longevity of introduced materials, assuming a 1-inch thickness. The table was generated from calculations listed in the Excel spreadsheet titled "Material Rates and Longevity.xls" (worksheet "material lifetime") archived in MO0312SPAPCEML.003. The materials that corrode away within a few hundred years (carbon steel and 1.5-3 percent borated stainless steel) will form oxides that will settle into the drift. It is anticipated that the remaining materials will last long enough to interact with seepage water entering the drift after temperatures drop below the boiling point and to influence the chemistry of those waters. The major elemental constituents of these long-lasting components are listed in Table 6.4-20. The major elements that could influence the chemistry in the invert, are Fe, Ti, Cr, Ni, Mo, Mn, Al, and Cu. The long- lasting components of primary interest specifically include the steel plate along the crown of the drift, the conductor bar in the invert, and the waste package pallet, in addition to the waste package and drip shield. The majority of the other ground support components are generally comprised of low carbon steel and are not predicted to have a sufficiently long life to impact the composition of seepage water.

6.4.3 Materials Compositions

To evaluate the impacts of the corrosion of introduced materials on seepage water chemistry and on oxygen availability, the composition of each introduced material is required. The information exchange drawings listed in Section 4.1.1 (e.g., BSC 2003 [DIRS 164101] and [DIRS 163855]) identify a conformance standard (i.e., A572/A 572M-01 for Steel Sets [DIRS 158661]) for most

introduced materials. However, conformance standards for certain materials are not provided and in these instances the grade used is based upon the maximum percentage of minor components allowable for each material as specified in the ASTM conformance specifications (all ASTM standards used below are listed in Sections 4.1.2 and 4.3.2). All other inputs are listed in Section 4.1.2. For example, for 316L stainless steel the ASTM range of Cr is given as 16-18 percent, its compositional value is, therefore, specified here as 18 percent. The amount of Fe is not specified in the ASTM standards; therefore, it is quantified as the residual amount when summing the relative weights to 100 percent. The value used for boron (1.6%) in the fuel basket plate composition is taken from DTN: MO0109RIB00049.001 [DIRS 155964] under the section titled "Material Properties of Neutronit A976/A978." The compositions used are summarized in Table 6.4-20.

Table 6.4-18. Selected Corrosion Rates of Metallic and Alloy Materials for Use in Engineered Barrier System Chemical Environment Calculations

Material	Environmental Conditions	Maximum Corrosion µm/year	Mean Corrosion µm/year	Minimum Corrosion µm/year	Reference	Comments
Titanium	Steam and atmospheric	0.07	0.012065	0.00254	Tables 6.4-2 and 6.4-3	SAW steam at 90°C and 100% relative humidity for Maximum and Ti in hostile atm at lower temp for Mean and Minimum
Alloy 22	Steam	0.47	0.07	0.03	Table 6.4-5	SCW 90°C for maximum, mean, and SDW 90°C for minimum
Alloy 22	Simulated water	0.25	0.08	0.03	Table 6.4-5	SCW 90°C for maximum, mean, and SCW 60°C for minimum
Inconel alloy X-750 and 600 SS	Simulated water	0.24	0.08	0.05	Table 6.4-7	Inconel Alloy 625 was used as surrogate. SCW 90°C for maximum, mean, and SCW 60°C for minimum
Copper Alloy	Steam and atmospheric	6.6	4.79	3.15	Table 6.4-8	J-13 steam, 95-100°C, near 100 relative humidity
Aluminum Alloy	Fresh/salt water	124.46	12.95	0.4	Table 6.4-9	saltwater for maximum, fresh water for mean, and minimum
316L SS	Steam and atmospheric	0.517	0.113	0.099	Table 6.4-11	marine atm for maximum and mean and 100°C J13 steam for minimum (data for 207°C brine steam not included)
316L SS	Brine Steam	53	49.667	48	Table 6.4-11	207°C Steamy Brine, Unlikely environmental conditions for the drift
316L SS	Fresh/salt water	14.79	1.9391	0.2286	Table 6.4-11	26.7°C saltwater for maximum and mean and 70°C fresh water for minimum
304L SS	Fresh/salt water	36.902	9.934	1.588	Table 6.4-13	26.7°C saltwater for maximum, mean and minimum
Borated SS (Neutronit)	Fresh/salt water	29.22	11.0595	1.81	Table 6.4-14	26.7°C saltwater for maximum, mean and minimum
Borated SS (0.3%B in 304L)	Fresh/salt water	147	94.67	38.22	Table 6.4-14	26.7°C saltwater for maximum, mean and minimum
Borated SS (1.5%B in 304L)	Fresh/salt water	1893.36	1225.98	937.86	Table 6.4-14	maximum boiling saline, mean ambient saline solution, and minimum 50°C saline solution
Carbon/Low Alloy Steels	Steam and atmospheric	1057.18	195.43	85.5	Table 6.4-15	maximum marine atm 70-80% RH, mean SCW 90°C steam, and minimum industrial atm. Over 80% RH
Carbon/Low Alloy Steels	Simulated water	180.42	88.79	41.31	Table 6.4-15	SCW 90°C for maximum, and SDW 60°C for mean and minimum

Source: DTN: MO0312SPAPCEML.003

Table 6.4-19. Longevity of 1.0-Inch of Introduced Material in the Drift

Introduced Materials	Environmental Conditions	Mean Longevity Assuming One-inch Thickness (One sided corrosion), years	Mean Longevity Assuming One-inch Thickness (Two sided corrosion), years
Titanium-steam	steam	2105263	1052632
Alloy 22-steam	steam	362857	181429
Alloy 22-water	simulated water	317500	158750
Inconel alloy X-750 and 600 SS-water	simulated water	317500	158750
316L SS-steam	steam/atmosphere	110435	55217.4
316L SS-water	fresh/salt water	220870	110435
304L SS-water	fresh/salt water	2557	1278
Borated SS (Neutronit)-water	fresh/salt water	2297	1148
Copper Alloy-steam	steam and atmosphere	5303	2651
Aluminum Alloy-water	fresh/salt water	1961	980.7
Carbon/Low Alloy Steels-water	simulated water	286	143.1
Borated SS (0.3%B in 304L)-water	fresh/salt water	268	134.1
Borated SS (1.5%B in 304L)-water	fresh/salt water	20.7	10.4
Carbon/Low Alloy Steels-steam	steam/atmosphere	130	65

Source: Calculated from Excel spreadsheet “Material Rates and longevity.xls” (worksheet “material lifetime”), DTN: MO0312SPAPCEML.003

Table 6.4-20. Materials Compositions

Component	Material Conformance ASTM Manual	Type of Material	Relative Percent by Weight Chemical Composition	Residual[A] (%)
Ground Support				
#Steel Sets W6x20	A572/A 572M-01 (Table 2) [DIRS 158661]	Grade 65 [450]	$Fe_{97.9}C_{0.26}Mn_{1.35}P_{0.04}S_{0.05}Si_{0.4}$	
#Pipe Spacers	A53/A 53M-02 (Table 1) [DIRS 162719]	Type S, Grade B	$Fe_{96.975}C_{0.3}Mn_{1.2}P_{0.05}S_{0.045}V_{0.08}Cu_{0.4}Ni_{0.4}Cr_{0.4}Mo_{0.15}$	
#Tie Rods	A307-02 (Page 5, Section S1.5.1) [DIRS 162722]	Bolts Suitable for Welding	$Fe_{98.11}C_{0.3}Mn_{1.0}P_{0.04}S_{0.05}Si_{0.5}$	
#Steel Wire Fabric 3"x3" Grid	A276-03 (Table 1) [DIRS 165006]	316L SS [S31603]	$Fe_{61.895}C_{0.03}Mn_{2.0}P_{0.045}S_{0.03}Si_{1.0}Ni_{14.0}Cr_{18.0}Mo_{3.0}$	
Rock Bolts (Swellex)	A276-03 (Table 1)	316L SS [S31603]	$Fe_{61.895}C_{0.03}Mn_{2.0}P_{0.045}S_{0.03}Si_{1.0}Ni_{14.0}Cr_{18.0}Mo_{3.0}$	
Stainless Steel Sheets (Bernold)	A276-03 (Table 1)	316L SS [S31603]	$Fe_{61.895}C_{0.03}Mn_{2.0}P_{0.045}S_{0.03}Si_{1.0}Ni_{14.0}Cr_{18.0}Mo_{3.0}$	
Invert				
Transverse Beams w/ Stiffeners	A588/A 588M-01 (Table 1) [DIRS 162724]	Grade B	$Fe_{96.16}C_{0.2}Mn_{1.35}V_{0.1}Cu_{0.4}P_{0.04}S_{0.05}Si_{0.5}Ni_{0.5}Cr_{0.7}$	
Longitudinal Support Beams	A588/A 588M-01 (Table 1)	Grade B	$Fe_{96.16}C_{0.2}Mn_{1.35}V_{0.1}Cu_{0.4}P_{0.04}S_{0.05}Si_{0.5}Ni_{0.5}Cr_{0.7}$	
Stiffener Brackets	A588/A 588M-01 (Table 1)	Grade B	$Fe_{96.16}C_{0.2}Mn_{1.35}V_{0.1}Cu_{0.4}P_{0.04}S_{0.05}Si_{0.5}Ni_{0.5}Cr_{0.7}$	
Base Plates	A588/A 588M-01 (Table 1)	Grade B	$Fe_{96.16}C_{0.2}Mn_{1.35}V_{0.1}Cu_{0.4}P_{0.04}S_{0.05}Si_{0.5}Ni_{0.5}Cr_{0.7}$	
Anchor Bolts	A307-02 (Page 5, Section S1.5.1)	Bolts Suitable for Welding	$Fe_{98.11}C_{0.3}Mn_{1.0}P_{0.04}S_{0.05}Si_{0.5}$	
Structural Bolts	A490-02 (Table 2) [DIRS 158937]	Type 3	$Fe_{97.635}C_{0.55}Mn_{0.37}Cu_{0.63}P_{0.04}S_{0.045}Ni_{0.17}Cr_{0.42}Mo_{0.14}$	
Miscellaneous Plates	A588/A 588M-01 (Table 1)	Grade B	$Fe_{96.16}C_{0.2}Mn_{1.35}V_{0.1}Cu_{0.4}P_{0.04}S_{0.05}Si_{0.5}Ni_{0.5}Cr_{0.7}$	
Gantry Rail Assembly				
Rail Runway Beams	A588/A 588M-01 (Table 1)	Grade B	$Fe_{96.16}C_{0.2}Mn_{1.35}V_{0.1}Cu_{0.4}P_{0.04}S_{0.05}Si_{0.5}Ni_{0.5}Cr_{0.7}$	
Cap Plate	A588/A 588M-01 (Table 1)	Grade B	$Fe_{96.16}C_{0.2}Mn_{1.35}V_{0.1}Cu_{0.4}P_{0.04}S_{0.05}Si_{0.5}Ni_{0.5}Cr_{0.7}$	
Guide Beams	A588/A 588M-01 (Table 1)	Grade B	$Fe_{96.16}C_{0.2}Mn_{1.35}V_{0.1}Cu_{0.4}P_{0.04}S_{0.05}Si_{0.5}Ni_{0.5}Cr_{0.7}$	
Gantry Rails	A759-00 (Table 1) [DIRS 159971]		$Fe_{97.47}C_{0.84}Mn_{1.1}P_{0.04}S_{0.05}Si_{0.5}$	
Conductor Bar (Copper)	Not Specified on IED (BSC 2003, Table 3 [DIRS 164101])		Solid Copper	

Table 6.4-20. Materials Compositions (Continued)

Component	Material Conformance ASTM Manual	Type of Material	Relative Percent by Weight Chemical Composition	Residual[A] (%)
Conductor Bar Fittings	Not Specified on IED (BSC 2003, Table 3 [DIRS 164101])		Steel	
Emplacement Pallet				
Emplacement Pallet (316L SS)	A240/A 240M-01 (Table 1) [DIRS 162720]	316L SS [S31603]	$Fe_{62.045}C_{0.03}Mn_{2.0}P_{0.045}S_{0.03}Si_{0.75}Ni_{14.0}Cr_{18.0}Mo_{3.0}N_{0.1}$	
Emplacement Pallet (Alloy C-22)	B575-99a (Table 1) [DIRS 147465]	C-22 Alloy [N06022]	$Fe_{6.0}C_{0.015}Mn_{0.5}P_{0.02}S_{0.02}Si_{0.08}V_{0.35}Ni_{50.02}Co_{2.5}W_{3.5}Cr_{22.5}Mo_{14.5}$	
Emplacement Pallet Weld Metal	B575-99a (Table 1)	SFA-5.14 N06022	$Fe_{6.0}C_{0.015}Mn_{0.5}P_{0.02}S_{0.02}Si_{0.08}V_{0.35}Ni_{50.02}Co_{2.5}W_{3.5}Cr_{22.5}Mo_{14.5}$	
Drip Shield				
Drip Shield	B265-02 (Table 2) [DIRS 162726]	Titanium Grade 7	$Ti_{98.675}Fe_{0.3}C_{0.08}H_{0.015}O_{0.25}Pd_{0.25}N_{0.03}$	0.4
Drip Shield (Bulkheads and Posts)	B265-02 (Table 2)	Titanium Grade 24	$Ti_{87.525}Fe_{0.4}C_{0.08}H_{0.015}O_{0.2}Pd_{0.08}N_{0.05}V_{4.5}Al_{6.75}$	0.4
Drip Shield (Base Alloy C-22)	B575-99a (Table 1)	C-22 Alloy [N06022]	$Ni_{50.02}Fe_{6.0}C_{0.015}Mn_{0.5}P_{0.02}S_{0.02}Si_{0.08}V_{0.35}Co_{2.5}W_{3.5}Cr_{22.5}Mo_{14.5}$	
Drip Shield Weld Metal	B265-02 (Table 2)	Titanium Grade 7	$Ti_{98.575}Fe_{0.3}C_{0.08}H_{0.015}O_{0.25}Pd_{0.25}N_{0.03}$	
Miscellaneous Materials				
Communications Cable	Not Specified on IED (BSC 2003, Table 3 [DIRS 164101])	50% Cu wire, 50% polyethylene sheath		
Waste Package Materials				
Inner Barrier	A240/A 240M-01 (Table 1)	SA-240 S31603 as modified by ASM 1987 p. 931 [DIRS 103753]	$Fe_{62.075}C_{0.02}Mn_{2.0}P_{0.045}S_{0.03}Si_{0.75}Ni_{14.0}Cr_{18.0}Mo_{3.0}N_{0.08}$	
Alloy 22 Welds	B575-99a (Table 1)	SFA-5.14 N06022	$Fe_{6.0}C_{0.015}Mn_{0.5}P_{0.02}S_{0.02}Si_{0.08}V_{0.35}Ni_{50.02}Co_{2.5}W_{3.5}Cr_{22.5}Mo_{14.5}$	
316 Welds	A240/A 240M-01 (Table 1)	316L SS	$Fe_{61.775}C_{0.03}Mn_{2.0}P_{0.045}S_{0.03}Si_{0.75}Ni_{14.0}Cr_{18.0}Mo_{3.0}N_{0.1}$	
Fuel Basket Plate	DTN: MO0109RIB00049.001 [DIRS 155964] under Section "Material Properties of Neutronit A976/A978"	Neutronit A 978	$Fe_{66.66}C_{0.04}Cr_{18.5}Co_{0.20}Ni_{13.00}B_{1.6}$	
Outer Barrier	B575-99a (Table 1)	SB-575 N06022	$Fe_{6.0}C_{0.015}Mn_{0.5}P_{0.02}S_{0.02}Si_{0.08}V_{0.35}Ni_{50.02}Co_{2.5}W_{3.5}Cr_{22.5}Mo_{14.5}$	

Table 6.4-20. Materials Compositions (Continued)

Component	Material Conformance ASTM Manual	Type of Material	Relative Percent by Weight Chemical Composition	Residual[A] (%)
Fuel Basket Plate	B209M-02e1 (Table 1) [DIRS 162727]	SB-209 A96061 T 4	$Al_{95.85}Fe_{0.7}Mn_{0.15}Mg_{1.2}Cu_{0.4}Si_{0.8}Ti_{0.15}Cr_{0.35}Zn_{0.25}$	0.15
Basket Stiffener, Basket Guides, and Fuel Basket Tubes	A516/A516M-01, Table 1 [DIRS 162723]	SA-516 K02700	$Fe_{97.87}C_{0.31}Mn_{1.3}P_{0.035}S_{0.035}Si_{0.45}$	
HLW Canisters, N-Reactor MCO	ASTM A240/ A240M-99b 2000, Table 1	304L SS	$Fe_{68.045}C_{0.03}Mn_{2.0}P_{0.045}S_{0.03}Si_{0.75}Ni_{10.0}Cr_{19.0}N_{0.1}$	

Source: DTN: MO0312SPAPCEML.003

NOTES: [#] Not part of the baseline design, only used on as needed basis.

[A] A residual is an element present in a metal or an alloy in small quantities and is inherent to the manufacturing process but not added intentionally. In titanium, these elements include aluminum, vanadium, tin, chromium, molybdenum, niobium, zirconium, hafnium, bismuth, ruthenium, palladium, yttrium, copper, silicon, cobalt, tantalum, nickel, boron, manganese, and tungsten.

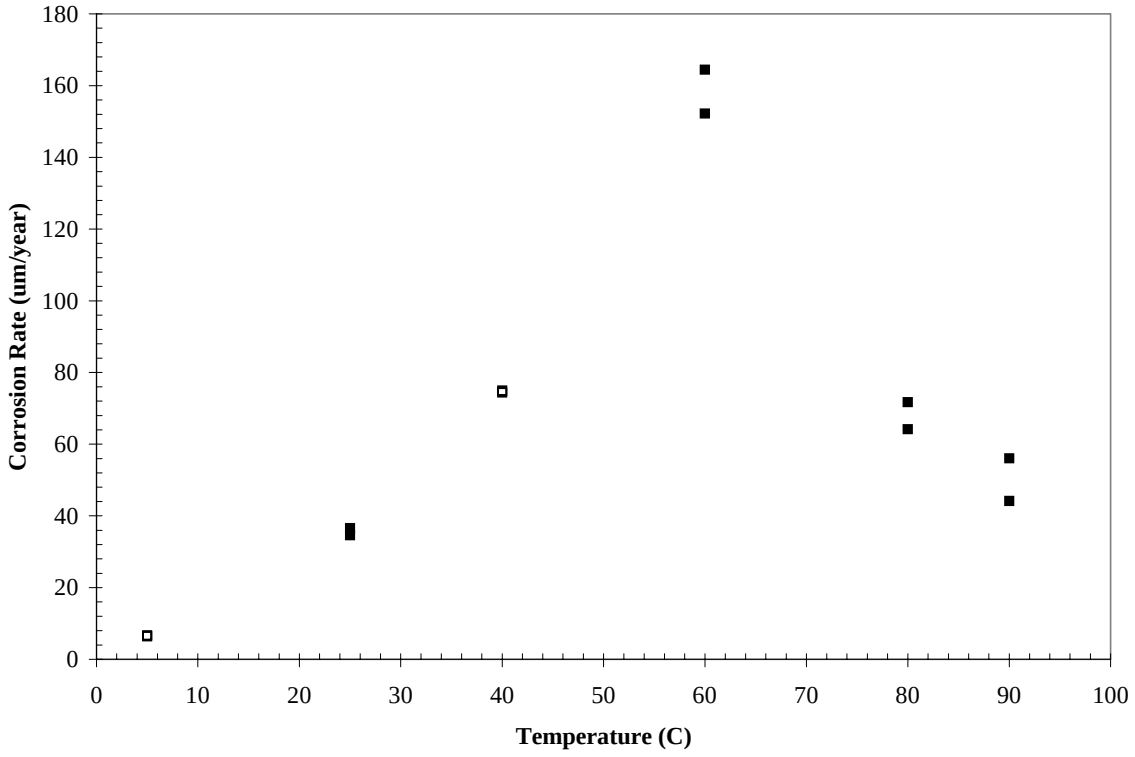

DTN: MO0303SPAMCRAQ.000 [DIRS162353]

Figure 6.4-1. Corrosion Rates for Mild Steel in Water, Plotted as a Function of Temperature

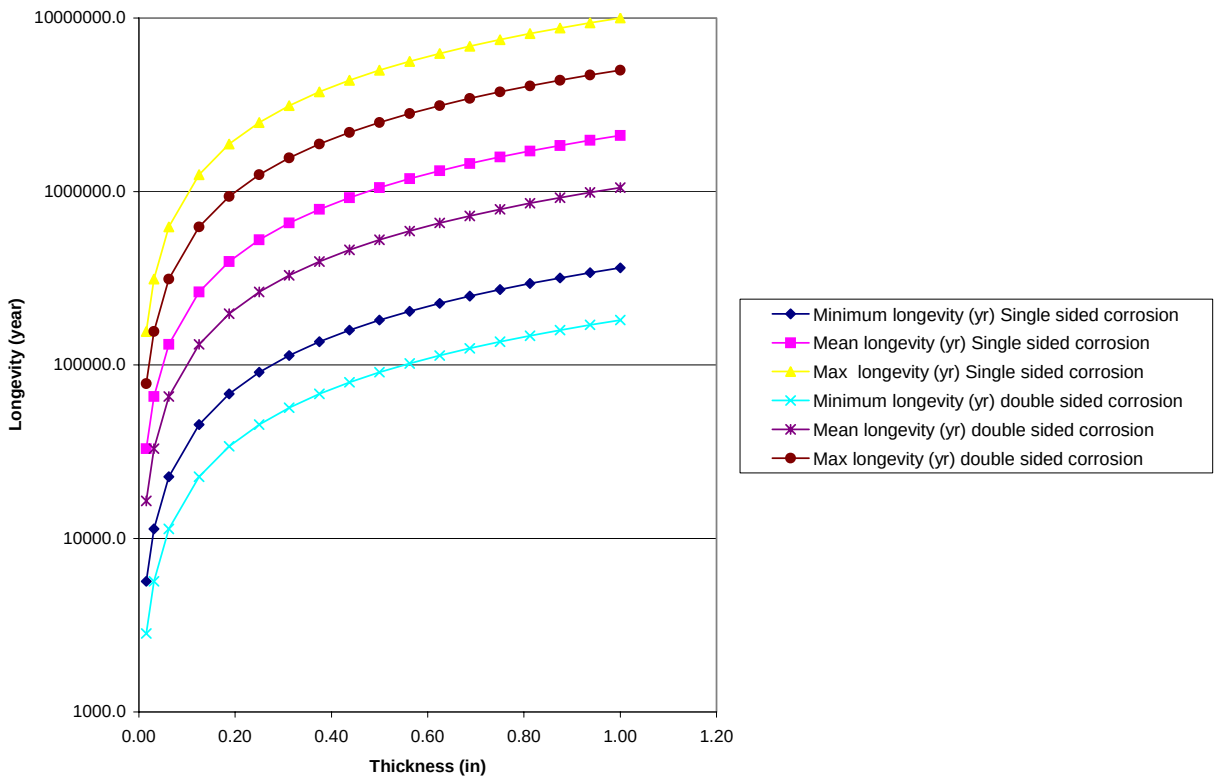

DTN: MO0312SPAPCEML.003

NOTE: Results for both single- and double-sided corrosion are shown, based on atmospheric and steam corrosion rates.

Figure 6.4-2. Titanium Longevity as a Function of Thickness

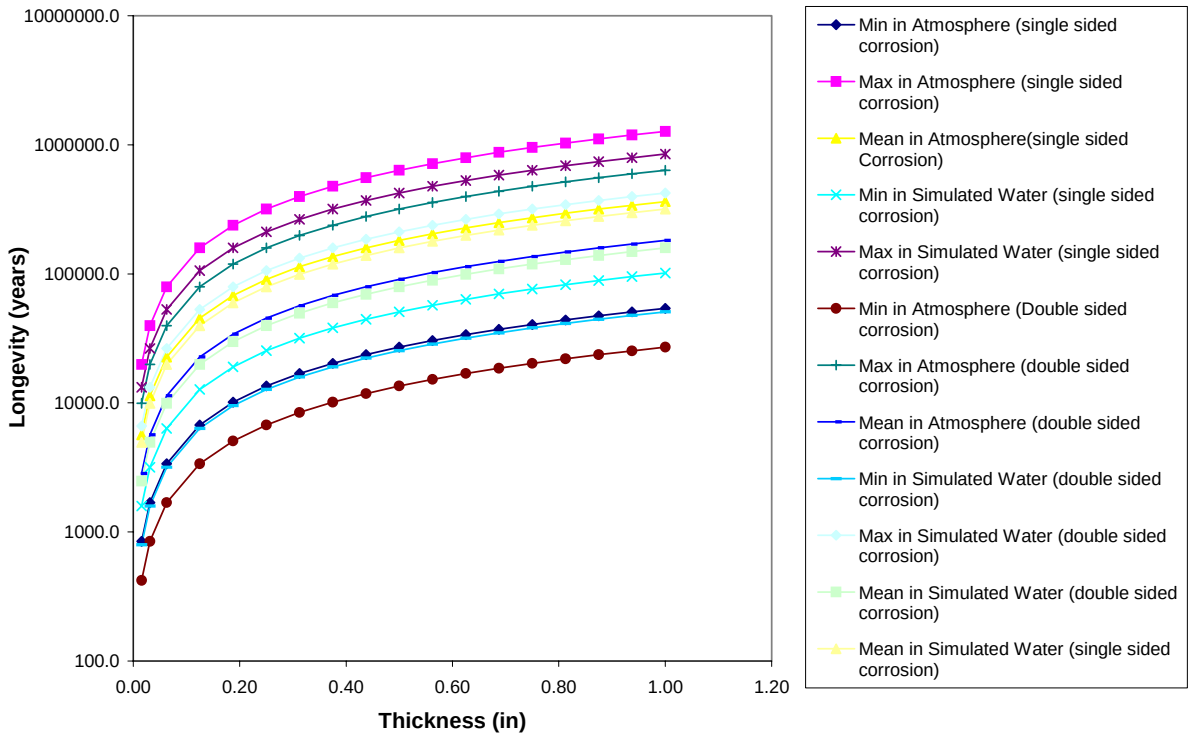

DTN: MO0312SPAPCEML.003

NOTE: Results for both single- and double-sided corrosion are shown, based on steam and simulated water corrosion rates.

Figure 6.4-3. Alloy 22 Longevity as a Function of Thickness

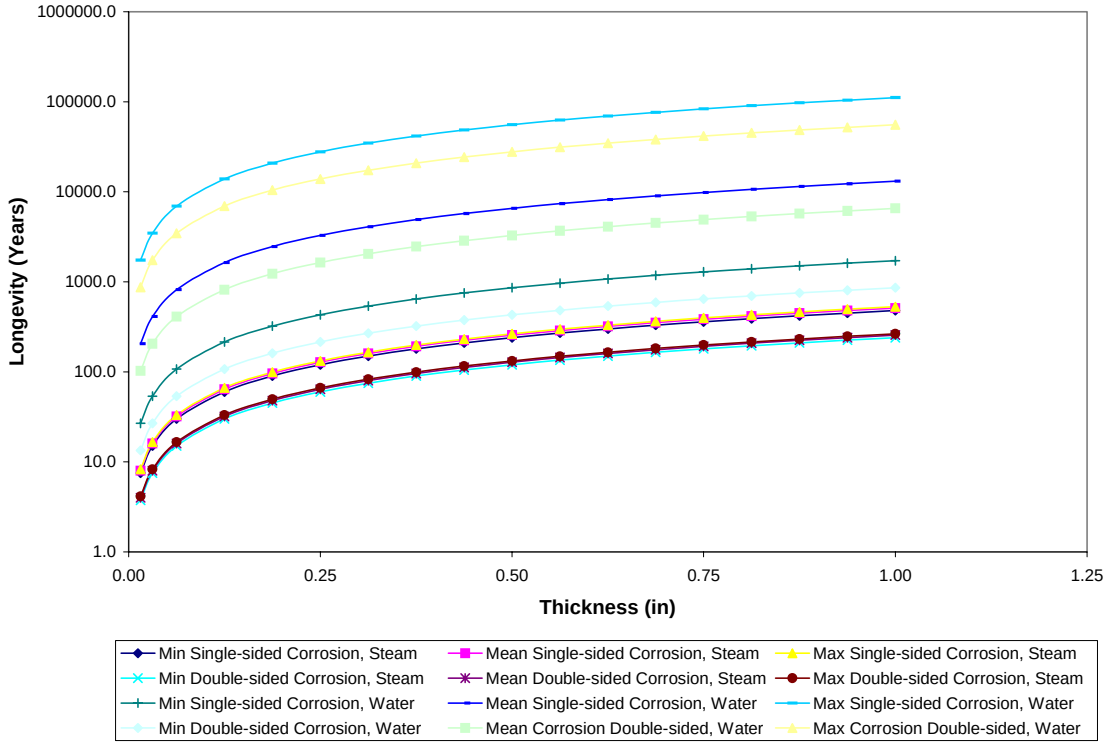

DTN: MO0312SPAPCEML.003

NOTE: Results for both single- and double-sided corrosion are shown, based on atmospheric/steam and fresh/salt water corrosion rates.

Figure 6.4-4. 316L Stainless Steel Longevity as a Function of Thickness

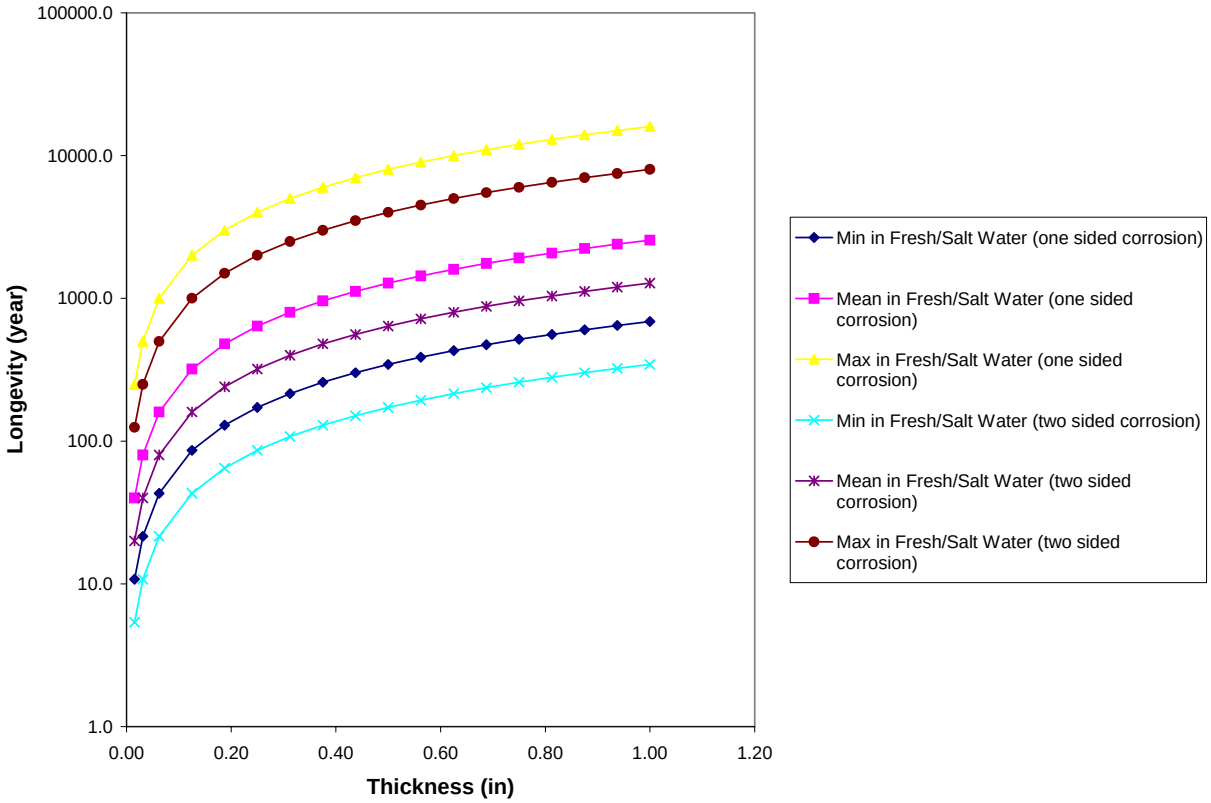

DTN: MO0312SPAPCEML.003

NOTE: Results for both single- and double-sided corrosion are shown, based on fresh and salt water corrosion rates.

Figure 6.4-5. 304 Stainless Steel Longevity as a Function of Thickness

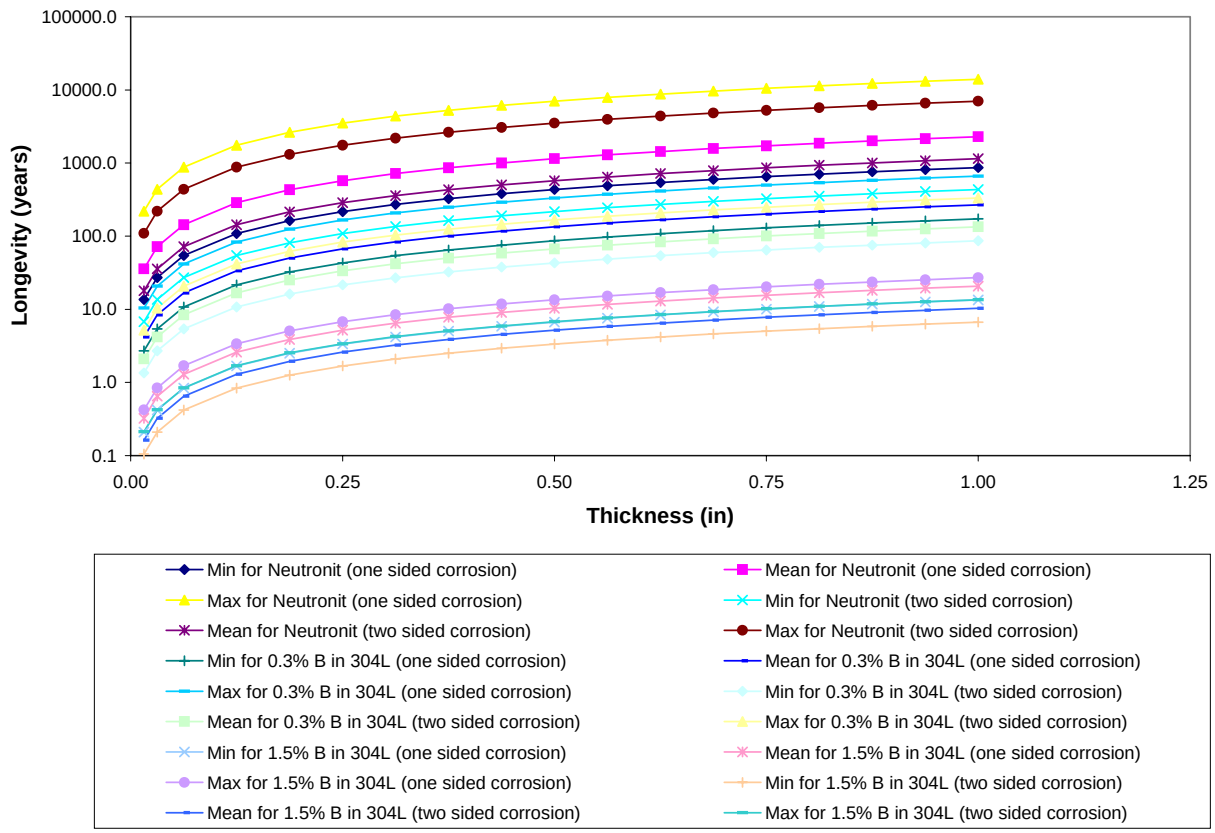

DTN: MO0312SPAPCEML.003

NOTE: Results for Both Single- and Double-Sided Corrosion are Shown, Based on Fresh and Salt Water Corrosion Rates.

Figure 6.4-6. Borated Stainless Steel Longevity as a Function of Thickness

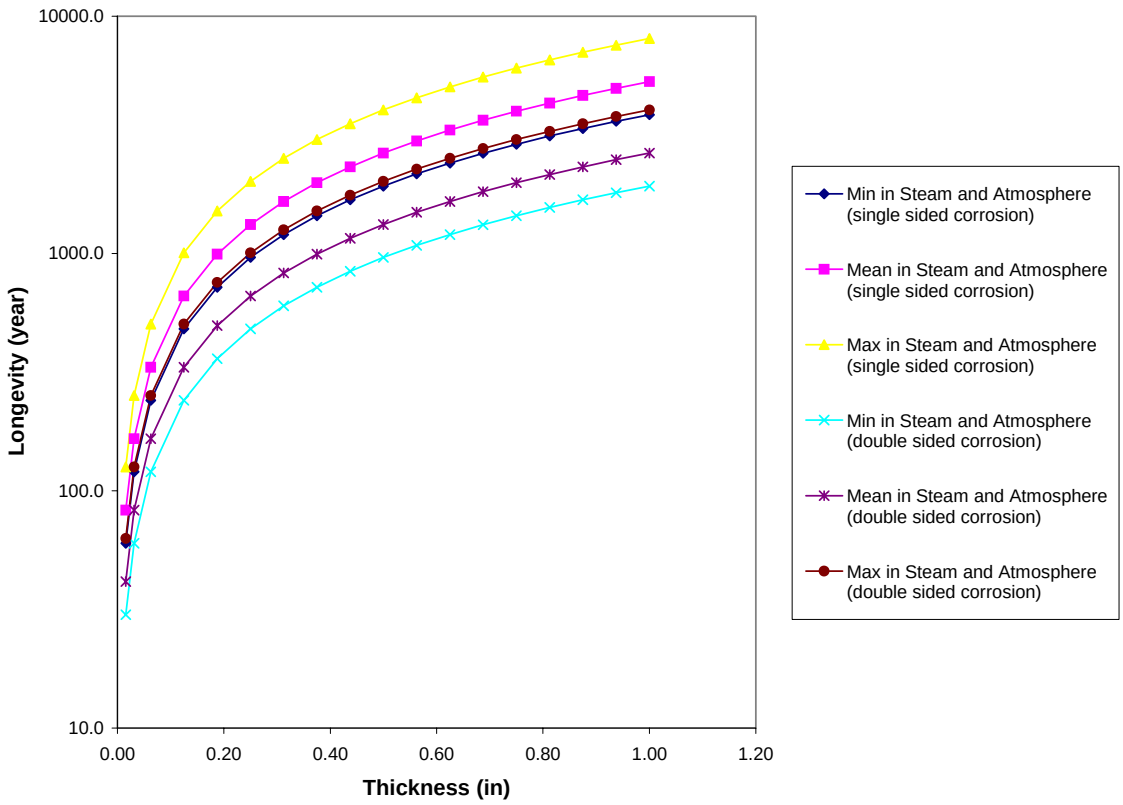

DTN: MO0312SPAPCEML.003

NOTE: Results for both single- and double-sided corrosion are shown, based on atmosphere and steam corrosion rates.

Figure 6.4-7. Copper Alloy Longevity as a Function of Thickness

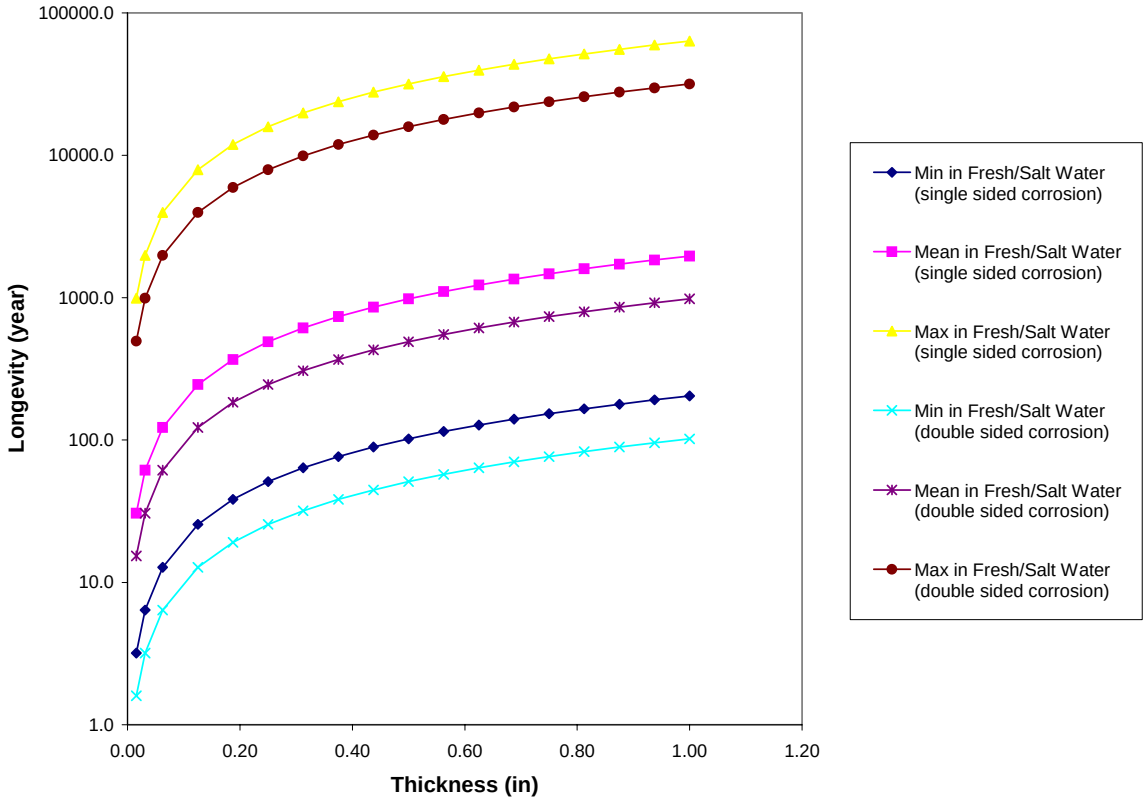

DTN: MO0312SPAPCEML.003

NOTE: Results for both single- and double-sided corrosion are shown, based on fresh and salt water corrosion rates.

Figure 6.4-8. Aluminum Alloy Longevity as a Function of Thickness

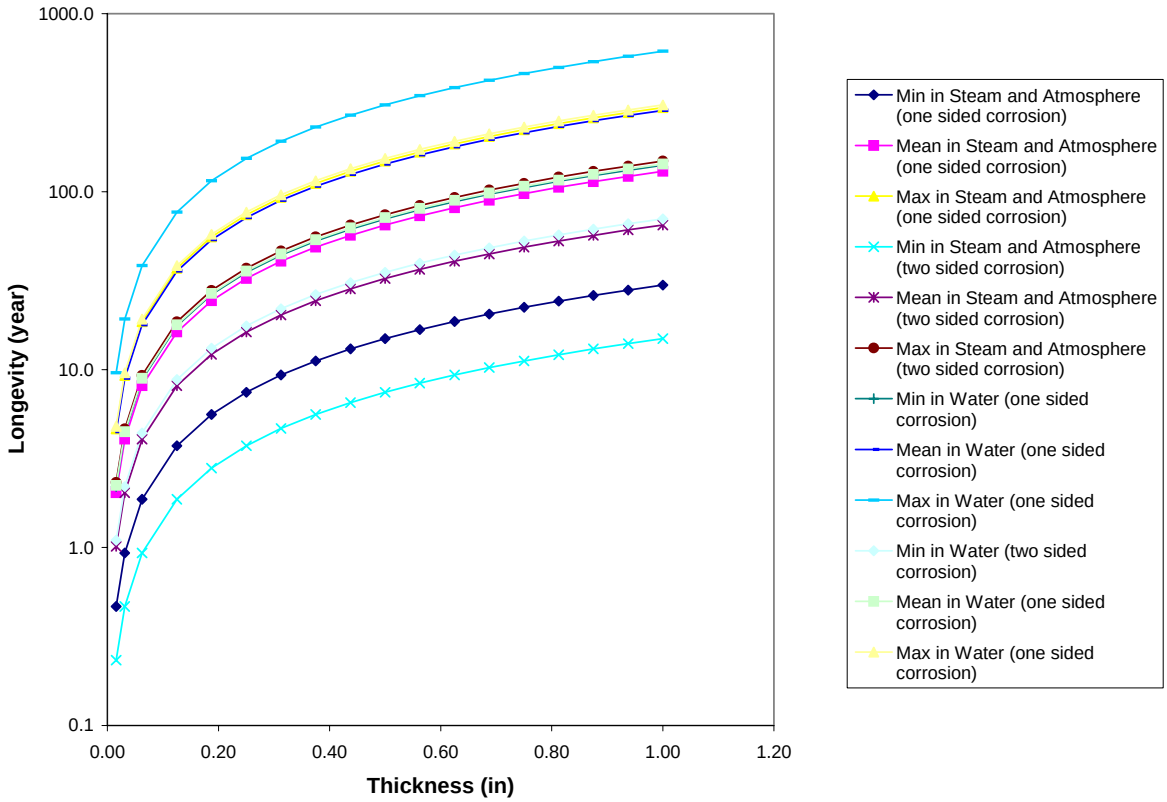

DTN: MO0312SPAPCEML.003

NOTE: Results for both single- and double-sided corrosion are shown, based on atmospheric/steam and fresh/salt water corrosion rates.

Figure 6.4-9. Low Carbon Alloy Steel Longevity as a Function of Thickness

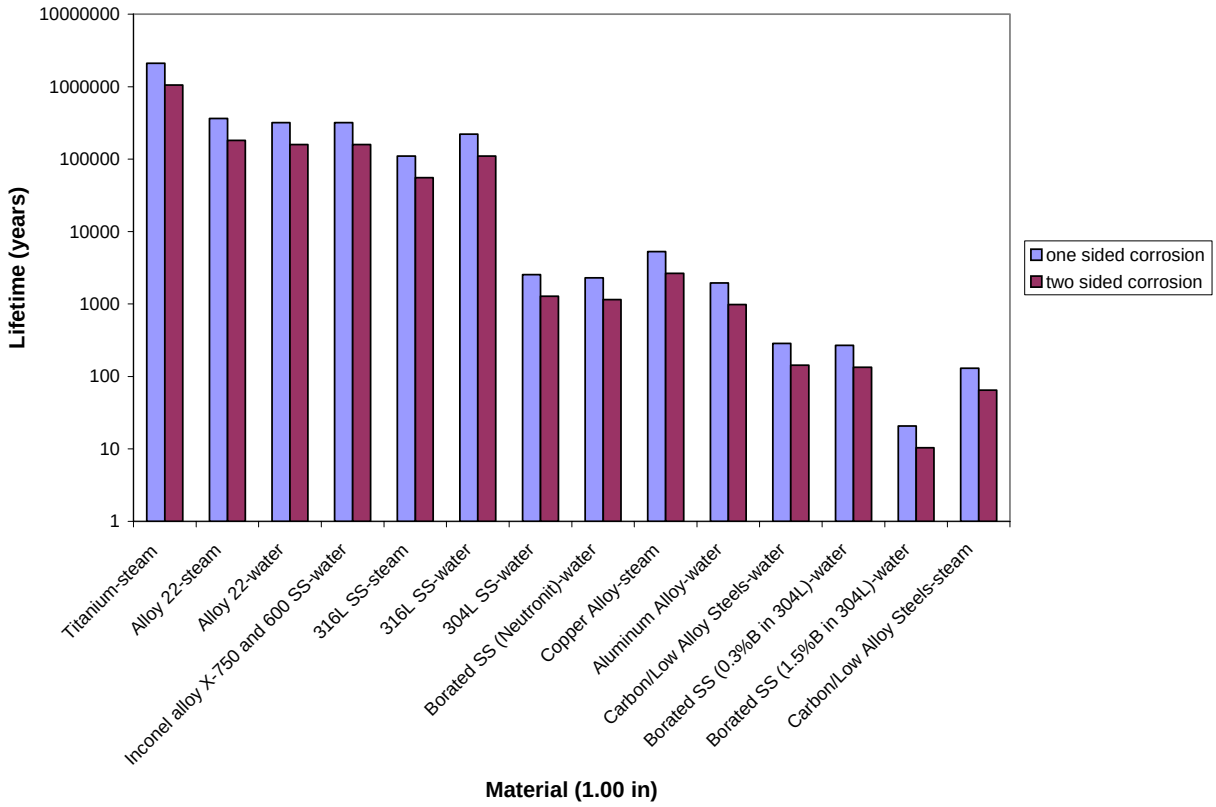

DTN: MO0312SPAPCEML.003

Figure 6.4-10. Lifetime of Solid Materials (1 inch Thickness), Based on Atmospheric/Steam and/or Fresh/Salt Water Corrosion Rates

6.5 GEOCHEMICAL MODELING CONSTRAINTS

This section summarizes the main set of mathematical models used in this report and establishes a modeling framework for developing equilibrium-type geochemical models in systems that are known or thought to be under metastable or partial equilibrium. This section can be thought of as a supplement to the conceptual model outlined in Section 6.2. It is also intended to demonstrate the importance of mineral and species suppression (i.e., the way equilibrium models are used to predict chemical conditions in metastable systems), which is a fundamental modeling concept of this model report. Some sensitivity studies discussing the uncertainties associated with this concept are further evaluated in Section 6.12.4.

6.5.1 Mathematical Models Implemented by the Use of EQ3/6 V8.0 Geochemical Modeling Software

Geochemical modeling constraints are imposed by the primary geochemical modeling software utilized in this report, *EQ3/6 Version 8.0* (STN: 10813-8.0-00 [DIRS 162228]). This software is composed of two independent codes: EQ3NR and EQ6. Both of these are described in general terms in the following subsections, much of which is derived from the *Software User's Manual EQ3/6 Version 8.0* (SNL 2003, SDN: 10813-UM-8.0-00; in particular, Appendices B and D [DIRS 162494]). The reader is referred to the EQ3/6 software users manual for a more detailed explanation of the concepts discussed in the following paragraphs.

6.5.1.1 EQ3NR: Speciation-Solubility Modeling of Aqueous Systems

EQ3NR is an equilibrium speciation-solubility code for aqueous systems. As such, given sufficient data for a chemical species to characterize a specific aqueous system, it computes a model of the solution that consists of two principal parts: the distribution of species in the solution and a set of saturation indices (SI = log *Q/K*) for various reactions of interest. The saturation indices measure the degree of disequilibrium of corresponding solution-mineral reactions. They provide a means for evaluating solubility controls on natural waters. For example, at equilibrium the SI = 0, but under close to equilibrium conditions where a series of related fluids all have a given mineral SI values close to zero, it is probable that this mineral is present and partial equilibrium with this mineral is maintained as the solutions evolve in composition.

EQ3NR is not a specific computerized geochemical model, but a software code that is useful in evaluating many different conceptual geochemical models, which are defined by the contents of a supporting data file (of which there are now several to choose from, including Data0.ymp.R2 and Data0.yfp) and by other user-defined inputs and constraints in the EQ3NR input file. The supporting data files differ not only in terms of data values, but also, more importantly, in terms of the identities of the components and chemical species represented, and in terms of the general approaches used in the estimation of activity coefficients. Because of various limitations (such as the use of the Pitzer model for estimation of activity coefficients), some problems may require the use of only certain data files, while others can be treated using any of the available data files. The user must choose the best data file (or files) with which to run a particular problem. The user must also understand both the particular problem and the code capabilities and limitations well enough to construct an adequate input file.

Although speciation-solubility models are commonly used as a means of testing whether heterogeneous reactions are in a state of thermodynamic equilibrium, they often just assume that all reactions occurring in aqueous solution are in such a state. Reactions most likely to be in disequilibrium are redox reactions or reactions for the formation or dissociation of large complexes that are more like small polymers, such as $(UO_2)_3(OH)_7^-$. Speciation-solubility models are better used when they are employed to test the degree of disequilibrium of these kinds of reactions than when these are assumed to be in equilibrium.

An equilibrium speciation-solubility model cannot, by itself, predict how aqueous solution composition will change in response to rock/water interactions. Nevertheless, this type of modeling can be a powerful tool for elucidating such interactions when it is applied to a family of related waters. Such a family might be a set of spring waters issuing from the same geologic formation, a sequence of groundwater samples taken along an underground flow path, or a sequence of water samples taken in the course of a rock/water interactions experiment in the laboratory. Jenne (1981 [DIRS 162479]) reviews several studies of this kind. Particularly interesting are Nordstrom and Jenne's (1977 [DIRS 162480]) study of fluorite solubility equilibria in geothermal waters and the Nordstrom et al. (1979 [DIRS 162508]) study of controls on the concentration of iron in acid mine waters. EQ3NR offers many options for the input file description of a given water chemistry's composition. Consequently, the code can be used in a variety of ways.

Many of the descriptive parameters of interest can be either model inputs or outputs. For example, the pH of a buffer solution can be calculated from the buffer recipe by adjusting the hydrogen ion concentration to satisfy charge balance. Alternatively, adjusting the concentration of a buffer component to satisfy the charge balance is a means of computing the complete recipe for a buffer having a desired pH. Some possible model inputs may be constraints, as in specifying equilibrium with one or more specified mineral phases. The use of some types of model inputs also pose special problems, some of which occur in particular contexts. The worst of these pertain to Eh, alkalinity, and pH and will be discussed in some detail later in this section.

6.5.1.1.1 Input Constraints, Governing Equations, and Outputs

Aqueous speciation models can be constructed to satisfy a variety of combinations of possible input constraints and governing equations. The input constraints may include:

- Total (analytical) concentrations
- An electrical balance requirement
- Mass balance
- Free ion concentrations
- Aqueous species activities
- pH
- Eh
- pe
- Oxygen fugacity

- Phase equilibrium requirements
- Homogeneous equilibria
- Run-specific values for equilibrium constants.

The governing equations are the corresponding mathematical expressions, such as the mass balance equation and the charge balance equation.

The choice of governing equations in large part depends on which parameters are to be inputs to the model, and which are to be outputs. This, in turn, is a function of what data on a given water are available, what form they are in, and what constraints the modeler would like to use.

Chemical analysis mainly provides a set of values for the so-called total concentrations of dissolved components. The analytical value for an ion such as calcium is an example. It does not discriminate between the various calcium species in solution, but rather estimates the dissolved calcium contributed by all of them. This leads to a mass balance equation of the form:

$$m_{T,Ca} = m_{Ca^{2+}} + m_{CaOH_{(aq)}} + m_{CaCO_{3(aq)}} + m_{CaHCO_3^{+}} + \ldots \qquad \text{(Eq. 6.5-1)}$$

where $m_{T,Ca}$ is the total or analytical concentration (on the molal scale) and m_i is the molality of any individual chemical species contributing to the mass balance. The summations must be weighted by the appropriate stoichiometric equivalences; e.g., in the case of F:

$$m_{T,F} = m_{F^-} + m_{HF_{(aq)}} + 2m_{H_2F_{2(aq)}} + 2m_{HF_2^-} + 3m_{AlF_{3(aq)}} + \ldots \qquad \text{(Eq. 6.5-2)}$$

The total concentration is the most common type of input parameter to an aqueous speciation model. Therefore, the most common governing equation is the mass balance constraint. As will be seen, there are situations in which a total concentration is replaced by another type of input such as the use of the input flag “heterogeneous equilibrium” where an aqueous concentration can be calculated from a gas fugacity. In these cases, the mass balance constraint is replaced by a different governing equation, and the total concentration becomes something to be calculated (an output parameter). Charge balance is also a common governing concept that will either calculate the apparent charge imbalance or force the aqueous solution to maintain electrical balance. Large charge imbalance errors indicate that there may be incomplete or erroneous chemical analysis or a mistake on the modeler’s part in interpreting reported analytical results.

From a mathematical point of view, there is no reason to discriminate among ion pairs (and ion-triplets, etc.) and complexes. For some investigators, the term “ion pair” implies a species in which an anion is separated from a cation by an unbroken hydration sheath about the latter, whereas the term “complex” implies direct contact and perhaps some degree of covalent bonding. Other investigators use these terms interchangeably. It is a general presumption in cases of geochemical interest that the concentrations of ion-pairs and complexes are governed by thermodynamic equilibrium.

Each case of this equilibrium can be represented by a mass-action equation for the dissociation of the ion-pair or complex. As an example, the calcium sulfate ion-pair dissociates according to the reaction:

$$CaSO_{4(aq)} = Ca^{2+} + SO_4^{2-} \qquad \text{(Eq. 6.5-3)}$$

where "=" is used as the sign for a reversible chemical reaction. The corresponding mass action equation is:

$$K_{CaSO_{4(aq)}} = \frac{a_{Ca^{2+}} a_{SO_4^{2-}}}{a_{CaSO_{4(aq)}}} \qquad \text{(Eq. 6.5-4)}$$

where K is the equilibrium constant and a_i represents the thermodynamic activity of each species. This may also be written in logarithmic form:

$$\log K_{CaSO_{4(aq)}} = \log a_{Ca^{2+}} + \log a_{SO_4^{2-}} - \log a_{CaSO_{4(aq)}} \qquad \text{(Eq. 6.5-5)}$$

The thermodynamic activity is related to the molal concentration by the relation:

$$a_i = m_i \gamma_i \qquad \text{(Eq. 6.5-6)}$$

where γ_i is the activity coefficient, a function of the composition of the aqueous solution. As the solution approaches infinite dilution, the value of γ_i for each species approaches unity. The user, in the EQ3/6 input calculation file, chooses the set of equations for computing the activity coefficients of aqueous species. The requisite supporting data are on the EQ3/6 database file. The activity of pure mineral phases is specified to be at unity.

6.5.1.1.2 Activity Coefficient Models of Aqueous Species

The thermodynamic activities (a_i) of aqueous solute species are usually defined on the basis of molalities. Thus, they can be described by the product of their molal concentrations (m_i) and their molal activity coefficients (γ_i) as shown in equation 6.5-6.

The thermodynamic activity of the water (a_w) is always defined on a mole fraction basis. Thus, it can be described analogously by product of the mole fraction of water (x_w) and its mole fraction activity coefficient (λ_w):

$$a_w = x_w \lambda_w \qquad \text{(Eq. 6.5-7)}$$

The activity coefficients, in reality, are complex functions of the composition of the aqueous solution. In electrolyte solutions, the activity coefficients are influenced mainly by electrical interactions. Much of their behavior can be correlated in terms of the ionic strength, defined by:

$$I = \frac{1}{2} \sum_i m_i z_i^2 \qquad \text{(Eq. 6.5-8)}$$

where the summation is over all aqueous solute species and z_i is the electrical charge. However, the use of the ionic strength as a means of correlating and predicting activity coefficients has been taken to extremes (e.g., in the mean salt method of Garrels and Christ 1965, p. 58–60 [DIRS 144877]). A comparison between the mean salt method of Garrels and Christ and Debye-Hückel (Fig 2.15, p. 63 of the same reference) shows a reasonable agreement up to an ionic strength 0.05 to 0.1 depending on the ion. In general, model equations that express the dependence of activity coefficients on solution composition only in terms of the ionic strength are restricted in applicability to dilute solutions.

The three basic options for computing the activity coefficients of aqueous species in EQ3/6 calculations are models based on the Davies equation (1962 [DIRS 162482]), the Hückel equation, also known as the "B-dot" equation (Helgeson 1969 [DIRS 137246]), and Pitzer's equations (1973 [DIRS 152738], 1975 [DIRS 152740], 1979 [DIRS 119530], 1987 [DIRS 162481]). The first two models, owing to limitations on accuracy, are only useful in dilute solutions (up to ionic strengths of 1 molal). The third basic model is useful in highly concentrated as well as dilute solutions, but is limited in terms of the components that can be accurately treated, as defined by the input database. Calculations of relevance to this model report were performed with either B-dot or Pitzer activity models.

With regard to temperature and pressure dependence, all of the following models are parameterized along the standard EQ3/6 curve, which is 1.013 bar up to 100°C and the steam/liquid water equilibrium curve at higher temperatures.

All EQ3/6 calculations in this model report, with the exception of the calculations performed in Section 6.8, use the Pitzer activity model, the usual formulation of which implies (in the absence of other action) a non-standard "Pitzer" pH scale. However, the results of this model report are presented in terms of National Bureau of Standards pH. The primary users of the output of this model are using the calculated pH values from this model to represent input parameters to models that have been established on laboratory measurements using National Bureau of Standards pH standards. The same measurement standard is true for values of pH that are input into EQ3/6 calculations (if you choose a scale for pH output, any pH input is thought to be on the same scale). This pH scale conversion is done internal to EQ3/6 software following the discussion outlined in Attachment B of *Software User's Manual EQ3/6 Version 8.0* (SNL 2003, Equation B-99 [DIRS 162494]).

6.5.1.2 EQ6: Reaction Path and Single-Point Modeling

EQ6 computations can first be broken down into "single-point" thermodynamic equilibrium calculations and irreversible mass transfer reaction path calculations. A single point thermodynamic calculation is essentially just the special case of a reaction path with no steps (e.g., used when precipitating supersaturated phases or making a temperature jump). Reaction paths may be calculated for titrations, irreversible reaction in closed systems, and irreversible reaction in certain well-defined types of open systems (e.g., a fluid-centered flow-through open system). Such calculations may be in reaction progress mode (time-independent) or time mode (explicit kinetic or time-dependent), depending on the rate law being implemented.

In EQ6, there are separate methodologies for treating equations that are intrinsically algebraic from those that are intrinsically differential. The former govern the thermodynamic calculations, and the latter are comprised of rate laws for irreversible processes. This numerical decoupling makes it possible to perform thermodynamic calculations, given the necessary inputs of total number of moles of components, the temperature, and the pressure, independently of the integration of rate equations. This decoupling permits making "single point" thermodynamic equilibrium calculations, such as the temperature jump problems, in which rate equations do not even appear.

In EQ6 reaction path models, the two types of equations are coupled in the mathematically formal sense, but the solution of each is performed semi-independently. Each type of calculation is performed alternately, the output of one becoming the input to the next execution of the other. For example, in moving a step forward in reaction progress (ξ), the rate equations are integrated. This defines new values for the temperature, pressure, and the total number of moles of the components, which are inputs to the following thermodynamic calculation. This, in turn, gives a new distribution of species from which may be calculated values for the rates of the irreversible processes at the new point. If accuracy tests on the ordinary differential equation integration are satisfied, these rate values are used in making the next integration step. Otherwise, the step size may be cut until those tests are satisfied.

When the rate chosen to constrain an irreversible process is a relative rate ($d\xi_j/d\xi$), the rate function is either a constant or a simple function of the overall reaction progress variable (ξ). When EQ6 operates in the mode of arbitrary kinetics (all irreversible processes constrained by relative rate expressions, no time variable in the model), these rates can be integrated by simple closed-form expressions. It is, therefore, possible to take arbitrarily large step sizes, subject only to the following conditions.

In the case of closed and open system calculations, the rate of an irreversible reaction is set to zero when the corresponding thermodynamic driving force, the affinity, is no longer positive. Affinities are outputs of the thermodynamic calculations. EQ6 locates the point of reaction progress where the affinity goes to zero. If the corresponding reactant is a mineral, this means that the aqueous solution has reached saturation. The code then changes the status of the reactant to inactive (meaning it is effectively removed from the set of reactants) and any remaining mass of the reactant is moved into the *equilibrium system*. Titration calculations are very similar to closed-system calculations, but the rate of an irreversible reaction is not set to zero when saturation is reached, and the remaining reactant mass continues to be added to the equilibrium system according to the rate law.

The rate of an irreversible reaction rate also becomes zero when the associated "reactant" becomes exhausted, no matter what kind of system model the code is dealing with. The user specifies how much of a reactant is available at the start of the calculation run. The code then finds the point of reaction progress at which exhaustion occurs.

6.5.1.2.1 Constraints on Thermodynamic Calculations

The following thermodynamic constraints are enforced in EQ6 calculations:

- Mass balance
- Charge balance
- Law of mass action
- Activity coefficients of aqueous species
- Activity coefficients of solid solution components
- Saturation indices and affinities.

Details on each of these can be found in the *Software User's Manual EQ3/6 Version 8.0* (SNL 2003, SDN: 10813-UM-8.0-00, Appendix D1.2 [DIRS 162494]).

6.5.1.2.2 Constraints on Reaction Path Calculations

The following reaction path constraints are enforced in EQ6 calculations:

- Reaction progress variable (ξ), which is a measure of the extent to which a reaction has proceeded

- Reaction rates and time for each irreversible reaction as a function for either the relative rate or the absolute rate

- Rate laws programmed into EQ6: relative rate, partial equilibrium, transition-state theory, and linear rate.

Details on each of these can be found in the *Software User's Manual EQ3/6 Version 8.0* (SNL 2003, SDN: 10813-UM-8.0-00, Appendix D1.3 [DIRS 162494]).

6.5.2 Geochemical Modeling Methodology

Generally, a reaction path geochemical equilibrium model is constructed using the steps outlined in Figure 6.5-1. First, a conceptual model is defined where the chemical system and state are defined. This system and state are tested and investigated to produce results. Those results are compared with independent experimental, natural analog, or other modeling data to ensure that the model is representative of the system and state to be analyzed.

Decisions about mineral suppression or inclusion require:

- A reasonable understanding of mineralogy and petrology

- A well researched conceptual model

- An understanding of how to develop a reaction path model using software codes like EQ3/6 (Wolery 1992 [DIRS 100836], Wolery and Daveler 1992 [DIRS 100097]), PHREEQC (Parkhurst 1995 [DIRS 142177]), or MINTEQA2 (HydroGeoLogic and Allison Geoscience Consultants 1999 [DIRS 158974])

- An understanding of how to ensure that confidence exists in the model and that model uncertainty has been appropriately addressed.

The following subsection contains a brief summary of the kinetics versus equilibrium relations rationale that must be considered in the selection of mineral phases for the model. For more detailed discussions on some aspects of modeling methodology Bethke (1996 [DIRS 162270]), Smith and Missen (1991 [DIRS 161602]), and Van Zeggeren and Storey (1970 [DIRS 161603]) may be consulted.

6.5.3 Equilibrium versus Kinetics

Bethke (1996, Chapter 2 [DIRS 162270]) reports that there are two main types of equilibrium end states that are important to recognize in reaction path modeling: complete equilibrium and metastable equilibrium. In complete equilibrium, the chemical state of the system attains stable equilibrium such that there is no chemical potential to drive any net chemical reaction. Usually, when an equilibrium model is first constructed, the first order model (see Figure 6.5-1) is allowed to go to complete equilibrium. When the initial system is constrained based on the end equilibrium state by determining variables such as the temperature, dissolved aqueous concentrations, quantity of given minerals in the system, or the fugacities of any gases, the calculation results in a fluid that is saturated with respect to the stable equilibrium mineral assemblage for the system.

Once this first-order model is constructed, the boundary conditions and the conceptual model are evaluated to determine whether various states of metastable equilibrium should be taken into account. The first-order model is then refined to account for these effects. For example, if the model predicts the complete equilibrium state to include minerals that do not occur in the actual system, this may imply that a metastable equilibrium situation exists in the actual system.

Metastable equilibrium occurs when one or more chemical reactions proceed toward equilibrium at a rate that is so small on the time scale of interest that the system does not reflect the consequences of reaction with that phase. In this case, the system can be considered not to include the reaction(s) involving that mineral. Such reactions are commonly heterogeneous reactions involving mineral precipitation. That is, the nucleation or growth of the mineral is subject to kinetic barriers that are large enough to preclude, or allow only negligible progress of, the reaction. In such a case, the mineral that should exert an equilibrium compositional constraint is supplanted by another, less stable, phase that is not kinetically constrained from forming and growing.

In other words, mineral suppression is used in equilibrium calculations to represent, in a simple manner, the fact that some solid phases are kinetically inhibited from precipitating or dissolving under equilibrium conditions in certain environments (e.g., quartz precipitation at low temperature). Because of the kinetic constraints, the chemical constituents commonly controlled

by the inhibited solid phase are controlled instead, if at all, by a somewhat less stable phase that reaches its metastable equilibrium rapidly compared to the inhibited phase. Inclusion of the explicit kinetic approaches would handle mineral dissolution or precipitation directly, but for simpler equilibrium calculations this is commonly handled by suppressing the occurrence of that phase in the model to represent the kinetic barrier and to achieve the same result found in real systems. Suppression of minerals, therefore, is a practical tool in being able to define the end-state equilibrium of a modeled system or to use an equilibrium-type model to mimic the effect of kinetic processes without having to know actual details about the kinetic rates of dissolution or precipitation.

Partial equilibrium and local equilibrium are specific cases or subsets of metastable equilibrium that can have relevance to a given geochemical problem. Partial equilibrium (also known as heterogeneous equilibrium) is defined by Wolery and Daveler (1992 [DIRS 100097]) in that some (usually most) reactions are in a state of equilibrium, while others, usually few in number and representing heterogeneous processes such as mineral dissolution or precipitation, are not. For example, the fluid in sandstone might be in equilibrium itself but may not be in equilibrium with the mineral grains in the sandstone or with just some of the grains. Local equilibrium, which is sometimes called mosaic equilibrium (i.e. temperature, mineralogy, or fluid chemistry vary across the system of interest), can be thought of as a system that is open to groundwater flow (Bethke 1996, p. 12 [DIRS 162270]). In this idealized flow through system, the aqueous phase moves over or through several different mineral assemblages and the water reacts with each of these and achieves some degree of equilibrium on the local scale with each assemblage, even though each location is at a different equilibrium state comparatively. All of these various types of equilibrium conditions can be combined into a single model, depending on the conceptual model.

Kinetics can be combined into reaction path modeling because the equilibrium point of a reaction is the point at which dissolution and precipitation rates balance. Bethke indicates that kinetic reactions fall into three groups (Bethke 1996, Chapter 2 [DIRS 162270]):

- Those in which reaction rates are so slow relative to the period of interest that the reaction can be ignored (i.e., accounting for metastable equilibrium). This slow reaction rate group commonly corresponds to what mineral suppression is used to represent.

- Those that are fast enough to maintain equilibrium (accounting for complete equilibrium).

- All other reactions that do not fall into the first two groups. These “all other reactions” are the only reactions that require a kinetic description.

6.5.4 Engineered Barrier System Geochemical Equilibrium Modeling

The equilibrium reaction path models used by the physical and chemical environment model are designed to predict long-term chemical processes within a potential repository drift. Although short-term occurrences (such as seepage water falling onto the drip shield) can cause transitory divergence from the conceptualized state of metastable equilibrium, an equilibrium approach is adopted because it provides valuable insight into long-term processes.

An equilibrium reaction path model, such as that implemented using the EQ6 software, relies on a thermodynamic database that contains standard-state thermochemical parameters of the different chemical species in a system to determine the chemical reaction equilibria as functions of the changing conditions. In addition to the homogeneous reactions that occur within each phase (e.g., water, gas, solid), there are heterogeneous reactions that involve more than one phase, such as mineral precipitation and degassing of volatile constituents from the aqueous phase. Most of the reactions in the equilibrium models employed by the engineered barrier system physical and chemical environment model are rapid relative to the timeframe of the modeling period; therefore, most reactions are allowed to reach equilibrium. However, there are many minerals in the thermodynamic database that will not form under the expected conditions of the repository. These minerals predominantly include those that require high pressures or very high temperatures to achieve the kinetic rates of formation that would produce a significant mass within the modeling time frame. Other minerals that could be excluded from consideration are those that form during the oxidation of pyrite or other sulfide minerals, which form only under redox conditions not thought possible in the repository (see Section 6.7.1).

The pressure in the repository is expected to remain near atmospheric, and the temperature at the drift wall is not expected to rise above 200°C (see Figure 6.7-7). These conditions limit those minerals in the database that can realistically be expected to form at a significant rate. As discussed previously, an equilibrium model ignores the use of kinetic rates; it predicts the most stable mineral phases at equilibrium except when those minerals are suppressed (i.e., ruled out) by the user. When precipitation is suppressed for a mineral, the equilibrium model does not allow the mineral to precipitate, resulting in a condition of supersaturation with respect to that phase. In this way, the equilibrium model can incorporate simplified kinetic constraints as metastable equilibrium conditions. Current conceptualization of postclosure drift conditions allows for conditions in the repository to be essentially dry. Any seepage entering the drift would be subject to conditions in which the relative humidity or activity of water would fall below one. Therefore, evaporative processes are expected to dominate during the evolution of in-drift seepage.

6.5.4.1 Modeling of Mineral Precipitation

The Pitzer thermodynamic database (Data0.ypf) currently includes more than 220 minerals, but only a small fraction of these have been suppressed in the modeling run calculations evaluated to date. It is unnecessary to identify *a priori* which of the more than 220 minerals should be suppressed for these calculations. The limited range of chemical compositions of the waters likely to occur within the drift dictates that a majority of the more than 220 minerals will never achieve a chemical potential favoring precipitation. This point is demonstrated by the results to date. So far, over 368 different observed and predicted water compositions at Yucca Mountain have been evaporated to dryness using Version 8.0 of the EQ3/6 software and the new Pitzer database (see Section 6.6), yet fewer than 40 minerals have become saturated or supersaturated with respect to the aqueous composition. Thus, it is not necessary to categorize the remaining 180-plus minerals according to their potential for precipitating under drift conditions.

Having some sort of simple criteria to appropriately suppress or include the approximately 40 minerals that have become saturated in the engineered barrier system models being developed for TSPA-LA facilitates determining the end equilibrium state in a model. Six criteria have been

developed to assist in determining the rationale for suppression or inclusion in the models to account for the kinetic or metastable equilibrium arguments stated previously. These six criteria are listed in the following paragraphs.

Criterion 1–Is the mineral of interest beyond or outside the defined chemical system of the model?

If the mineral lies outside or beyond the defined chemical system of the model, there is no reason to include the mineral. For example, while modeling mineral formation at low temperatures and pressures (near ambient), any mineral could be excluded that was known to form only at high temperatures or pressures.

Individuals trained in mineralogy or petrology can readily make these determinations. Example reference sources, used to make these decisions when combined with expert judgment, are Klein and Hurlbut's *Manual of Mineralogy* (1985 [DIRS 105907]), *Kerr's Optical Mineralogy* (1977 [DIRS 161606]), Roberts, et al., *Encyclopedia of Minerals, 2nd Ed.* (1990 [107105]), or any reference source that discusses the petrology or mineralogy of a given system or analogue system.

If a mineral is not included in the database, it is, in effect, suppressed. The formation conditions applicable to the great majority of the over 3,000 minerals included in Roberts et al. (1990 [107105]), lie outside the physicochemical boundaries of the repository system. Most of these can be excluded because they contain trace or minor elements that are of no interest to repository operations, or have been addressed through studies of corrosion and radionuclide solubility. Table IV-1 in Attachment IV provides details on the need in modeling for an additional 709 minerals that are not in data0.ymp.R2 or data0.ypf.

Criterion 2–Is the mineral of interest likely or unlikely to precipitate because of kinetic controls?

Langmuir (1997 [DIRS 100051]) gives a general rule of thumb for determining the need for a kinetic description of mineral dissolution or precipitation. When a reaction is irreversible or its rate is comparable to, or slower than, the system residence time (i.e., the half-life is greater than or equal to the residence time), a kinetic rate is needed to describe the state of reaction. When this rule of thumb is met and kinetic data are available, the data are used directly. Often however, rate data are not available for the system being modeled, or it is much simpler to invoke a state of metastable equilibrium and use a mineral suppression to simplify the model. Therefore, a modeler will make a mineral suppression that mimics the conceptualized state of metastable or localized equilibrium. As an example, one of the most common mineral suppressions used in geochemical modeling is that of considering the kinetic rates of reaction for amorphous silica, quartz, or one of its polymorphs (tridymite and chalcedony). In general, amorphous precipitates will tend to form first, and then a process of mineral re-crystallization will take place (Langmuir 1997, p 55 [DIRS 100051]). Therefore, the metastable phase that would generally be used in a reaction path model for quartz would be amorphous silica. If the conceptual model were to account for a longer system residence time or higher temperatures, the modeler would allow quartz or one of its polymorphs to precipitate. For iron oxides, it would be expected that either goethite or ferrihydrite would form first, depending on temperature and

relative humidity. Ferrihydrite re-crystallizes relatively quickly to form goethite or hematite, which may persist for eons.

Criterion 3–Is analytical or natural analog information available that warrants the inclusion or exclusion of the mineral?

Commonly, when doing geochemical modeling, information or data is found by researching the relevant literature used to develop the conceptual model. This information often comes from analytical data or natural analog information, and warrants the suppression or inclusion of minerals that could be dispositioned differently based on Criteria 1 and 2. This allows for inclusion of minerals that could form due to some unknown kinetic constraint that has not been accounted for directly in the model.

Although care is taken in constructing and attempting to "validate" a model as it is developed, conceptual model or thermodynamic database uncertainty must still be addressed. Therefore, three additional criteria are included to allow evaluation of the effect of mineral suppressions on model results.

Criterion 4–Do minerals need to be suppressed or included to test overall model uncertainty or sensitivity due to reported uncertainty in the supporting literature, database, or conceptual model?

Criterion 5–Does the suppression or inclusion of minerals that are highly uncertain drive the resulting chemical output to a more or less conservative modeling result?

Criterion 6–Do other minerals that are in a database provide an adequate surrogate or proxy for the mineral?

Certainly, Criteria 4 through 6 are not the normal types of mineral dispositions in models. However, they are of great use when conducting sensitivity studies or handling modeling uncertainties.

Although the six criteria are written to address mineral suppressions, they can and should be used to document the suppression of any aqueous species of concern (see Table 6.8-4).

6.5.4.2 Modeling of Trace Elements

The terms "minor" and "trace" used in reference to solutes in natural water cannot be precisely defined. Commonly, the terms are used for substances that always or nearly always occur in concentrations less than 1.0 mg/l (Hem 1985 [DIRS 115670], pp. 129–130). Trace elements from the natural system that are potentially present in the in-drift seepage waters that have been identified and considered to be potentially problematic for the waste package and drip shield degradation are lead (Pb), arsenic (As), and mercury (Hg). The chemical composition of the rhyolite tuff that makes up the repository horizon is well characterized and essentially uniform in composition (Peterman and Cloke 2002 [DIRS 162576]). Compositions of pore waters extracted from the tuff at the repository horizon have been characterized for trace element composition. Table 6.5-1 shows the composition of selected minor and trace elements in the pore waters extracted from cores collected in the enhanced characterization of the repository block cross

drift. As can be seen from Table 6.5-1, Pb and Hg concentrations and more than one third of the As concentrations are below the detection limit.

Fluoride, trace elements in seepage, and elements in introduced materials that are normally considered as trace species in natural waters may be important to certain in-drift processes, yet not be significant contributors to the major ion geochemistry. In-drift processes such as corrosion and radionuclide mobility may be particularly affected because of the possible local accumulation of these elements as chemical conditions evolve in response to changes in physical conditions such as temperature and relative humidity. Most analyses presented to date have focused on the chemical reactions among major constituents because these are considered to be the primary system drivers controlling the in-drift environmental conditions. Bruno et al (1998 [DIRS 110969]) also conclude in their studies of trace metals in natural systems that good characterization of the site mineralogy and a sound understanding of the main geochemical driving forces (i.e., bulk chemistry) are needed to further investigate the reactions of trace species; that is, the trace species will only have a small effect upon the bulk chemistry (e.g., pH, ionic strength, or major cation/anion concentrations).

Fluoride and bromide are explicitly included in the analyses and discussions of Sections 6.6, 6.12 and 6.13. The potential impacts of fluoride on corrosion processes have also been evaluated and found to not significantly enhance the general corrosion of the drip shield under repository conditions (BSC 2003 [DIRS 161236], Section 8.3). Chromium and iron, considered major constituents of introduced materials in the drift, and trace elements in the seepage waters entering the drift, are specifically considered in Sections 6.8 and 6.12.

6.5.5 Rationale for Including or Excluding Precipitating Minerals

Table 6.5-2 provides a listing of the minerals that have been suppressed in the engineered barrier system in-drift precipitates/salts and physical and chemical environment models; Table 6.5-3 provides a listing of the minerals that precipitated during modeling run calculations. In each case, a rationale for the decision to suppress or include each mineral is provided. In addition to the rationale listed in Tables 6.5-2 and 6.5-3, which are used to strengthen model validation, each engineered barrier system model is independently validated against natural analog data or experimental results, to ensure that the model is an appropriate representation. Minerals that are present in the thermodynamic database but did not precipitate during model development were not included on Table 6.5-3.

The relevant natural analogs for the in-drift precipitates/salts and physical and chemical environment conceptual models are saline lakes and playa deposits; the evaporite mineral assemblages that form in those environments are documented in sources such as Eugster and Hardie (1978 [DIRS 100743]) or Papke (1976 [DIRS 162274]). These minerals should reflect the mineral assemblages that could form in the low-temperature, low-pressure, in-drift environment; where the activity of water is below one and the solution compositions are comparable. These analogs are used, in conjunction with the model boundary conditions in the low-temperature, low-pressure, in-drift environment, to strengthen the mineral suppression and inclusion rationale listed in Tables 6.5-2 and 6.5-3.

Table 6.5-1. Compositions of Fluoride and Trace Elements in ECRB Pore Water Samples

SAMPLE DESIGNATION	F	Br	Mn	Co	Zn	Rb	Sr	As	Mo	Ba	Hg	Pb	U
ECRB-SYS-CS400/3.8-4.3/UC	3.7	<1	410	<2.5	<100	41	3580	8	13	420	<1.0	<2.0	6.9
ECRB-SYS-CS400/5.6-6.2/UC	1.7	<1	43	<2.5	<100	30	1480	<6.0	4.8	<30	<1.0	<2.0	<0.3
ECRB-SYS-CS600/3.6-4.0/UC	2	<1	39	<2.5	<100	16	1750	<6.0	5.3	<30	<1.0	<2.0	0.5
ECRB-SYS-CS1000/7.3-7.7/UC	3.4	<1	23	<2.5	<100	21	1040	<6.0	5.3	<30	<1.0	<2.0	0.8
ECRB-SYS-CS750/6.2-6.5/UC	1.2	<1	54	<2.5	<100	22	1160	<6.0	6.2	<30	<1.0	<2.0	10.3
ECRB-SYS-CS2150/5.5-6.1/UC	5.3	<0.2	38	<1.3	<100	16	1110	5.7	8.9	<15	<1.0	<1.0	4.1
ECRB-SYS-CS900/5.4-5.9/UC	1.7	<0.2	77	<1.3	<100	12	1980	5.4	7.4	<15	<1.0	<1.0	0.3
ECRB-SYS-CS850/5.1-5.6/UC	2.9	<0.2	14	<1.3	<100	9.3	1150	8.3	13	<15	<1.0	<1.0	2.7
ECRB-SYS-CS900/3.5-4.1/UC	2	0.3	470	1.1	<50	20	4090	3.4	9.5	<15	<1.0	<1.0	1.2
ECRB-SYS-CS1000/12.9-14.0/UC	2	<0.1	47	<1.0	<40	24	1110	5.4	11	61	<1.0	<1.0	6.9
ECRB-SYS-CS450/5.3-6.0/UC	1.1	0.4	100	<1.0	40	32	1240	5.7	5.1	46	<1.0	<1.0	0.1
ECRB-SYS-CS2300/4.3-4.9/UC	1.7	<0.1	260	<2.5	<100	22	590	<6.0	14	29	<1.0	<2.0	7.6
ECRB-SYS-CS500/12.0-16.7/UC	4.8	0.4	26	<2.5	<100	20	1100	7.6	14	<30	<1.0	<2.0	2.5
ECRB-SYS-CS2000/16.5-21.1/UC	11	<0.2	58	<1.3	<100	33	1390	5.9	22	<20	<1.0	<1.0	22.7
ECRB-SYS-CS2000/16.3-16.5/UC	6	<0.2	130	<1.3	<100	22	1260	<3.0	22	<15	1.2 [1]	<1.0	11.3
ECRB-SYS-CS950/5.2-5.3/UC	1.9	<0.2	62	<1.8	<100	10	1240	4	3.4	<25	<1.0	<1.6	<0.2
ECRB-SYS-CS950/4.8-5.5/UC	4.9	<0.2	130	<1.3	<100	11	2070	3.9	4.8	<15	<1.0	<1.0	0.2
ECRB-SYS-CS1250/5.0-5.7/UC	3	0.2	18	<1.3	<50	22	480	11	22	42	<1.0	<1.0	15
ECRB-SYS-CS1250/3.4-4.0/UC	2.1	M	200	<1.0	50	29	1390	<8.0	8	150	<1.0	<1.0	3.6
ECRB-SYS-CS800/4.9-5.6/UC	1.6	M	34	<1.0	<25	12	1140	6.7	6.3	36	<1.0	<1.0	0.9
ECRB-SYS-CS700/5.5-5.8/UC	6.2	<0.1	330	<7.5	<300	22	2970	<18	18	72	<2.5	<6.0	6.1

DTN: GS020408312272.003 [DIRS 160899]

NOTE: F and Br are in mg/l, all others are µg/l; M indicates not measured.
[1] Greater than 200 ppb tungsten in sample, resulting in possible interference for Hg

Table 6.5-2. Mineral Suppressions that are Used in the Engineered Barrier System Physical and Chemical Environment Geochemical Modeling

Mineral	Formula	Criteria Selected	Rationale	References
Cristobalite (alpha)	SiO_2	Criterion 2	Cristobalite forms at temperatures greater than 1470°C. At standard temperatures and pressures, cristobalite will slowly convert to quartz.	Krauskopf 1979 [DIRS 105909], Figure 14-1, Table 6.4.4-1
Dolomite	$CaMg(CO_3)_2$	Criterion 2	Although dolomite is a common mineral in evaporite deposits from springs derived from carbonate and tuffaceous waters in southern Nevada at Yucca Mountain, its growth mechanism is slow when compared to the precipitation calcite, opal and Mg-bearing minerals such as sepiolite.	Vaniman et al. 1992, Table 6.4.4-1 [DIRS 107066]
Glaserite	$NaK_3(SO_4)_2$	Criterion 4	Although glaserite is a mineral that is expected to form in evaporitic type deposits, at the time modeling runs for this document were initiated, the thermodynamic data for glaserite being considered for inclusion in the Pitzer database was in question.	This mineral was suppressed, subject to sensitivity analysis (see Section 6.12.4.4 for results of the sensitivity analysis).
Magnesite	$MgCO_3$	Criterion 4	Magnesite is commonly associated with metamorphic mineral assemblages, such as serpentine. There are instances where magnesite is associated with salt deposits, yet it is uncertain that it can form under standard temperatures and pressures as magnesite could be associated with the diagenesis of buried salt deposits.	Kerr 1977 [DIRS 161606] Eugster and Hardie 1978 [DIRS 100743] This mineral would be suppressed, subject to sensitivity analysis (see Section 6.12.4.4 for results of the sensitivity analysis).
Maximum Microcline	$KAlSi_3O_8$	Criterion 1	Microcline is generally associated with the formation of granite, syenite, and gneiss. Although it is often found as a common mineral in sandstone or arkose, the occurrence in these instances is detrital and not authigenic.	Kerr 1977 [DIRS 161606], p. 306, Table 6.4.4-1
Quartz	SiO_2	Criterion 2	Literature evidence suggests that amorphous silica is at metastable equilibrium with respect to quartz at low temperatures and pressures. This is also evidenced by the precipitation of opal-A (an amorphous silica phase) as opposed to quartz in evaporated carbonate and tuffaceous waters of southern Nevada.	Langmuir 1997 [DIRS 100051] Vaniman et al., 1992 [DIRS 107066]; Table 6.4.4-1

Table 6.5-2. Mineral Suppressions that are Used in the Engineered Barrier System Physical and Chemical Environment Geochemical Modeling (Continued)

Mineral	Formula	Criteria Selected	Rationale	References
Talc	$Mg_3Si_4O_{10}(OH)_2$	Criterion 1	Talc is characteristically associated with low-grade metamorphic rock and hydrothermal alteration of ultrabasic rocks.	Kerr 1977 [DIRS 161606], Table 6.4.4-1
Ca-saponite Mg-saponite Na-saponite H-saponite K-saponite	$Ca_{0.165}Mg_3Al_{0.33}Si_{3.67}O_{10}(OH)_2$ $Mg_{3.165}Al_{0.33}Si_{3.67}O_{10}(OH)_2$ $Na_{0.33}Mg_3Al_{0.33}Si_{3.67}O_{10}(OH)_2$ $H_{0.33}Mg_3Al_{0.33}Si_{3.67}O_{10}(OH)_2$ $K_{0.33}Mg_3Al_{0.33}Si_{3.67}O_{10}(OH)_2$	Criterion 1	Saponite is a montmorillonite or smectite clay. Smectite clays are commonly associated with fracture linings at Yucca Mountain. However, saponitic clays are associated with the weathering of basalt and not rhyolitic tuffs. Saponite does not generally form independently from its associated parent material, nor does it precipitate independently in soil environments.	Krauskopf 1979 [DIRS 105909] Carlos et al. 1995 [DIRS 105213] Deer et al 1966 [DIRS 162338] Borchardt 1989 [DIRS 156639]

Table 6.5-3. Minerals Allowed to Precipitate in the Engineered Barrier System Physical and Chemical Environment Geochemical Modeling

Mineral	Formula	Criteria Selected	Rationale	References
Calcite	$CaCO_3$	Criterion 3	Calcite is a common evaporite mineral formed from evaporated waters of southern Nevada.	Vaniman et al. 1992 [DIRS 107066]
SiO_2(am)	SiO_2	Criterion 2	Literature evidence suggests that amorphous silica is at metastable equilibrium with respect to quartz at low temperatures and pressures. This is also evidenced by precipitation of opal-A as opposed to quartz in evaporated carbonate and tuffaceous waters of southern Nevada	Langmuir 1997 [DIRS 100051] Vaniman et al. 1992 [DIRS 107066]
Fluorite	CaF_2	Criterion 3	Fluorite is associated with evaporite deposits in Nevada playas.	Papke 1976 [DIRS 162274], Table 1, Table 6.4.4-1
Sepiolite	$Mg_4Si_6O_{15}(OH)_2 \bullet 6H_2O$	Criterion 3	The precipitation of sepiolite is common in conjunction with calcite precipitation in calcrete deposits. Sepiolite is a common fracture-lining mineral above the basil vitrophyre of the Topopah Spring Member at Yucca Mountain. Sepiolite is also known to commonly form on evaporation of either carbonate-source or tuff-source waters in southern Nevada.	Hay and Wiggens 1980 [DIRS 162281] Carlos et al. 1995 [DIRS 105213] Vaniman et al. 1992 [DIRS 107066]

Table 6.5-3. Minerals Allowed to Precipitate in the Engineered Barrier System Physical and Chemical Environment Geochemical Modeling (Continued)

Mineral	Formula	Criteria Selected	Rationale	References
Celadonite	$KMgAlSi_4O_{10}(OH)_2$	Criterion 3	Although its occurrence is generally associated with hydrothermally altered mafic volcanic rocks and with illite-chlorite minerals, celadonite is also found as an authigenic silicate mineral in saline, alkaline, nonmarine environments such as playa deposits.	Li et al. 1997 [DIRS 159034] Hay et al. 1966 [DIRS 105965]
Thenardite	Na_2SO_4	Criterion 3	Thenardite is associated with evaporite deposits in Nevada playas.	Papke 1976 [DIRS 162274], Table 1
Halite	NaCl	Criterion 3	Halite is associated with evaporite deposits in Nevada playas.	Papke 1976 [DIRS 162274], Table 1; Kerr 1979 [DIRS 161606], p. 221, Table 6.4.4-1
Huntite	$CaMg_3(CO_3)_4$	Criterion 3	Huntite is an Mg carbonate mineral associated with cave and evaporite deposits as well as with meteoric (low-temperature) dissolution, and re-precipitation of calcite, dolomite, or magnitite. Huntite will precipitate instead of calcite when Mg^{2+} is concentrated in solutions with respect to Ca^{2+} due to evaporative processes.	Faust 1953 [DIRS 162282] Walling et al. 1995 [DIRS 162283], p. 360
Sellaite	MgF_2	Criterion 3	Sellaite is the Mg analog to fluorite that forms in evaporite deposits.	Palache et al. 1951 [DIRS 162280], pp. 37 to 39
Gypsum	$CaSO_4 \bullet 2H_2O$	Criterion 3	Gypsum is associated with evaporite deposits in Nevada playas.	Papke 1976 [DIRS 162274], Table 1 Kerr 1979 [DIRS 161606], p. 221, Table 6.4.4-1
Glauberite	$Na_2Ca(SO_4)_2$	Criterion 3	Glauberite is associated with evaporite deposits in Nevada playas.	Papke 1976 [DIRS 162274], Table 1
Niter	KNO_3	Criterion 3	Niter is associated with evaporite deposits in Nevada playas.	Papke 1976 [DIRS 162274], Table 1

Table 6.5-3. Minerals Allowed to Precipitate in the Engineered Barrier System Physical and Chemical Environment Geochemical Modeling (Continued)

Mineral	Formula	Criteria Selected	Rationale	References
Sylvite	KCl	Criterion 3	Sylvite is associated with evaporite deposits in Nevada playas.	Papke 1976 [DIRS 162274], Table 1 Kerr 1979 [DIRS 161606], p. 221
Arcanite	K_2SO_4	Criterion 3	Arcanite is a very soluble mineral belonging to the Mascagnite group and can be precipitated in the laboratory from the slow evaporation of water solutions. This mineral is related to thenardite and should have similar properties.	Palache et al. 1951 [DIRS 162280], pp. 398 to 400
Soda Niter	$NaNO_3$	Criterion 3	Soda Niter is associated with evaporite deposits in Nevada playas.	Papke 1976 [DIRS 162274], Table 1
Carnallite	$KMgCl_3 \bullet 6H_2O$	Criterion 3	Carnallite is associated with evaporite deposits in Nevada playas.	Papke 1976 [DIRS 162274], Table 1 Kerr 1979 [DIRS 161606], p. 221
Pentasalt (Gorgeyite)	$K_2Ca_5(SO_4)_6 \bullet H_2O$	Criterion 3	Gorgeyite occurs in association with glauberite, halite, and polyhalite in salt deposits.	Fleischer and Efremov 1954 [DIRS 162312]
Syngenite	$K_2Ca(SO_4)_2 \bullet H_2O$	Criterion 3	Syngenite is associated with salt deposits (especially halite) and precipitates in cavities created by volcanic action. It precipitates at room temperatures from solutions that contain K_2SO_4.	Palache et al. 1951 [DIRS 162280], pp. 442 to 444
Anhydrite	$CaSO_4$	Criterion 3	Anhydrite is associated with evaporite deposits in Nevada playas.	Papke 1976 [DIRS 162274], Table 1 Kerr 1979 [DIRS 161606], page 221
Natrite	Na_2CO_3	Criterion 3	Natrite is a highly soluble carbonate mineral associated with shortite, pirssonite, and gaylussite. These three minerals are also associated with the precipitation of trona, calcite, and montmorillonite and are found in clay beds that have deposited in borax lakes.	Fleischer and Pabst 1983 [DIRS 162284] Palache et al. 1951 [DIRS 162280]
Trona	$Na_3H(CO_3)_2 \bullet 2H_2O$	Criterion 3	Trona is associated with evaporite deposits in Nevada playas.	Papke 1976 [DIRS 162274], Table 1

Table 6.5-3. Minerals Allowed to Precipitate in the Engineered Barrier System Physical and Chemical Environment Geochemical Modeling (Continued)

Mineral	Formula	Criteria Selected	Rationale	References
Burkeite	$Na_6CO_3(SO_4)_2$	Criterion 3	Burkeite is a saline mineral associated with Na-CO_3-SO_4-Cl brines.	Eugster and Hardie 1978 [DIRS 100743], Table 3
Stellerite	$Ca_2Al_4Si_{14}O_{36} \bullet 14H_2O$	Criterion 3	Stellerite is a zeolite mineral commonly associated with fracture linings at Yucca Mountain.	Carlos et al. 1995 [DIRS 105213]
Phillipsite	$K_{0.7}Na_{0.7}Ca_{1.1}Al_{3.6}Si_{12.4}O_{32} \bullet 12.6H_2O$	Criterion 3	Phillipsite is a zeolite mineral commonly associated with evaporite deposits.	Hay et al. 1966 [DIRS 105965]
Kieserite	$MgSO_4 \bullet H_2O$	Criterion 3	Kieserite is an evaporite mineral commonly found in salt deposits. Often it is associated with halite or carnallite.	Palache et al. 1951 [DIRS 162280], page 477 to 479

INTENTIONALLY LEFT BLANK

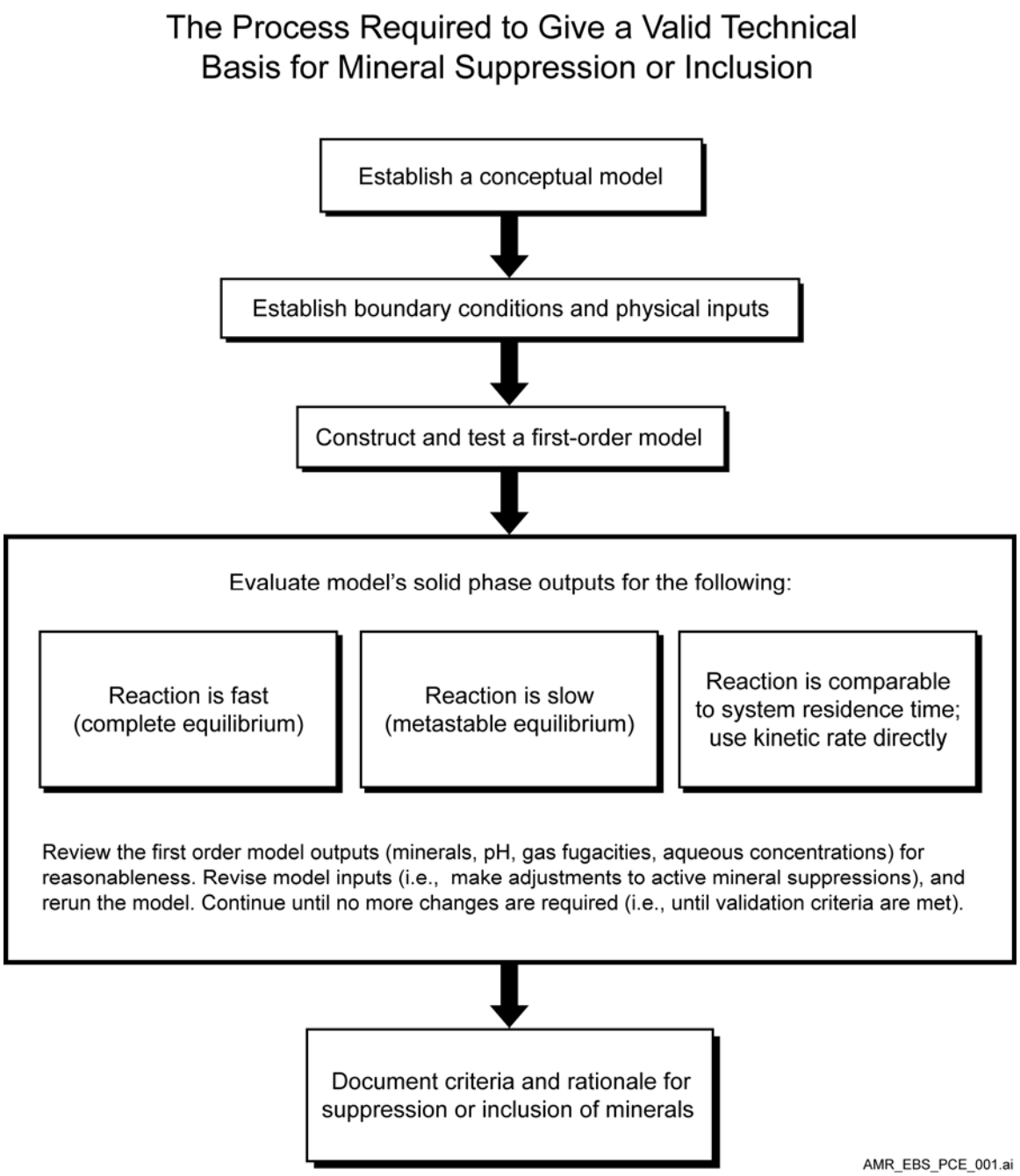

NOTE: A first order model Is a model that accounts for complete equilibrium (i.e., no metastable equilibrium or kinetic controls) with no active mineral suppressions.

Figure 6.5-1 A Simplified Roadmap of the Process Required to Give a Valid Technical Basis for Mineral Suppression or Inclusion in Geochemical Equilibrium Modeling

INTENTIONALLY LEFT BLANK

6.6 INCOMING SEEPAGE COMPOSITION ABSTRACTION

The required seepage water and gas compositions inputs for in-drift chemistry modeling were abstracted from THC model outputs of time-dependent seepage water compositions and gas-phase compositions in the host rock (near field environment) adjacent to the drift wall. A discussion of the model used to derive these compositions is presented in the *Drift-Scale Coupled Processes (DST and THC Seepage) Models* report (BSC 2003 [DIRS 162050]), hereafter referred to as the THC seepage model. The THC seepage model is based on a specific design basis thermal load and thermal decay rate, which are a function of repository loading and ventilation (see BSC 2003 [DIRS 162050], Section 4.1.7.3).

A time-history of seepage water compositions is calculated with the THC model for each of five compositions of pore water in the host rock, located far enough away from the drifts, at any given time interval, for liquid water presence. Those five pore water compositions, all given equal probability in the THC model, are designated as (*Drift-Scale Coupled Processes (DST and THC Seepage) Models* report (BSC 2003 [DIRS 162050]):

- w0 = HD-Perm water (Alcove 5)
- w4 = Cross-drift water CS2000/16.5
- w5 = Cross-drift water CS1000/7.3
- w6 = Cross-drift water SD-9/990.4
- w7 = Cross-drift water CS500/12.0.

The results of this model are abstracted (i.e., simplified) as described in this section to capture the time- and temperature-dependent changes in drift boundary conditions.

6.6.1 Conceptual Framework Summary for the Thermal-Hydrological-Chemical Seepage Abstraction

The composition of water potentially seeping into the drift is a primary influence on the type of brine that is produced after evaporation. For example, if the alkalinity of the water is more than twice the calcium concentration (molar basis), the water will tend to evaporatively evolve into a carbonate-rich brine (Eugster and Hardie 1978, p. 244 [DIRS 100743]). As evaporation continues, other chemical divides will be encountered, as phases precipitate containing, for example, Na, K, Ca, Mg, Cl, CO_3, SO_4, F, or NO_3. NO_3 is not necessarily conserved in a system that contains organics; however, the results of the in-drift microbial communities model (CRWMS M&O 2000 [DIRS 151561], Table 71) indicate that the total mass of organics in the system is limited and nitrate should be retained in the system. In the end, the composition of the resulting brine will depend heavily on the original ratios of dissolved components.

As described in Section 4.1.3, each of the five THC model runs produce time histories of changing water compositions for a large number of locations around the drift. The THC model calculates the time history at 72 locations and 50 discrete points in time over the 100,000-year modeling period. To capture the more rapid fluctuations at early times, these points in time are roughly log-normally distributed over the time period (i.e., durations between these points increase with time). In total, there are approximately 3,600 discrete water chemistries per THC output. Thus, the inputs listed on Table 4.1-13 contain 18,000 (5×72×50) water chemistries.

An abstraction method is used to generate look-up tables to represent the effects of evaporation within the drift for any given period. Five steps are required to abstract the THC results using this method. That sequence of steps is repeated for each of the five compositions of percolating water (w0, w4, w5, w6, and w7). The five steps are as follows:

- Step 1: Screen the waters by their time of occurrence and THC seepage model output parameters (i.e., location description: quadrant, fracture/matrix, zone, and index). In this way, the 300+ seepage water compositions are identified for binning (see Section 6.6.2).

- Step 2: Use the *In-Drift Precipitates Salts Model* (BSC 2003 [DIRS 162529]) to calculate compositions that result from the seepage waters evaporation identified in Step 1 to a common water activity equal to 0.65. This step characterizes the seepage compositions by chemical properties of the waters they yield when concentrated by evaporation, the in-drift process of concern (see Section 6.6.3).

- Step 3: Sort the evaporated seepage water compositions from Step 2 into groups that exhibit similar chemical characteristics, placing into a single bin those seepage water compositions from Step 1. The result is a set of seepage water composition bins, each populated with compositions that yield chemically similar solutions after they are concentrated by evaporation (see Section 6.6.4).

- Step 4: Identify the median water composition in each bin and use it as an approximation of all the seepage water compositions within the bin (see Section 6.6.5).

- Step 5: Approximate each THC output seepage water composition time history with a time-sequence of median bin compositions derived from Step 4 (see Section 6.6.6).

6.6.2 Sort Waters by Point in Time, Quadrant, Fracture/Matrix, Zone, and Index (Step 1)

The THC seepage model outputs used as input here are defined in Table 4.1-13. Several parameters are provided by the THC seepage model and include the QUADR (quadrant) ZONE, INDEX and DIST (distance). Figure 6.6-1 depicts the THC seepage model quadrant designators discussed in the following bulleted paragraphs. The DIST parameter is not used in developing the abstraction; however, a plot (see Figure 6.6-2) of the parameter through time from thc6_w4_r.xls shows the movement of the wetting front as the temperature in the drift increases and decreases. The following bulleted items describe the use of the remaining parameters and other specific outputs used in the abstraction.

- **Point in Time:** Each THC seepage model output contains 50 time output points covering a period of 0–100,000 years. Approximately 35 of the 50 time points are directly selected to cover the period of interest (51 through 20,013 years). This period represents the range of interest for the TSPA-LA. Two other points are selected (the 0–50 year pre-closure case can be approximated by the year 10 case, and the post 20,013 year, or ambient, case can be approximated by the 50,034 year case). The points for each of the five waters are coordinated so that water chemistries can be compared at equivalent times.

- **Quadrant:** The THC model provides waters that enter the drift from the top (drift crown), the side, and the bottom (invert base). When applied to the conceptual models under which the engineered barrier system is modeled, it is reasonable to neglect the data provided for the sides of the drift, as no direct drip shield/package seepage or invert uptake mechanisms are available for this water, and because the chemistry in the side of the drift is similar to the chemistry in the crown, therefore, only the drift crown and invert base waters are selected.

- **Fracture/Matrix:** There is water flowing in the fractures and in the matrix. Water entering the drift crown will come only from the fractures (CRWMS M&O 2000, Section 5.1.1 [DIRS 123916]). Water entering the invert base will come only from the matrix where matrix imbibition occurs via capillary suction from a higher saturated porous media into a porous media at a lower saturation (Jury et al. 1991, pp. 87–110 [DIRS 102010]). Gravity prohibits flow from the fractures into the invert. Therefore, the crown waters are selected from the THC seepage model output data worksheets labeled "fractures-ch" and the invert waters are selected from the data worksheets labeled "matrix-ch."

- **Zone:** The THC waters come from two zones: "Front" and "HiSat." The "Front" zone waters come from the cells closest to the drift center with saturation levels greater than zero. The "HiSat" zone waters come from cells having the highest saturation within 25 meters of the drift springline (crown of drift). The "Front" waters are more concentrated, but otherwise their chemistries are similar to the "HiSat" waters. The "Front" waters are shown in Figure 6.6-3. Figure 6.6-3 shows a comparison of concentration-sensitive species, which show differences during the dry-out period (50–200 years), but are otherwise similar. Therefore, "Front" waters are selected as being representative of both.

- **Index:** Index selection is performed to reduce spurious fluctuations in composition at the driest nodes that are due to numerical anomalies under the driest conditions, and to capture the chemical composition of the dry-out front. Index 4 is chosen to moderate the numerical artifacts at the driest nodes, but capture the chemical compositions of water in the dry-out front. The objective is to reflect the trends demonstrated by all front index waters, minimize any near field dry-out effects, and accommodate the EQ3/6 calculation runs, rather than using the THC model, to better control precipitation of abstracted waters. The dry-out effect is inherent to the discrete, numerical nature of the THC model, where a single cell may be virtually at an arbitrary phase approaching the dry-out cutoff, resulting in a wide range of relative concentration ratios as the THC model removes precipitates from the water. Figure 6.6-3 demonstrates this numerical fluctuation in the Ca/Cl ratio for fracture water from Top (i.e., crown) Front (spreadsheet thc6_w0_r.xls in DTN: LB0302DSCPTHCS.002 [DIRS 161976]). Index 1 data, having a Ca/Cl ratio of 1 at 650 years, show a large deviation from the other 5 Index waters having a Ca/Cl ratio of around 0.2. One source of this fluctuation is demonstrated by the saturation level (SL in spreadsheet) plot in Figure 6.6-4 for Top Front water, in which both Index 1 and Index 2 saturation levels deviate towards 0.001 at a time near 100 years. These order of magnitude deviations in water content affect the relative chemical concentrations in those waters as the THC model precipitates minerals and

possibly alter the results of the final EQ3/6 end-brine calculation. In addition to the abstraction rationale provided above, an independent evaluation of the THC seepage results was conducted in *Abstraction of Drift-Scale Coupled Processes* (BSC 2003, Section 8.1 [DIRS 164888]). This report also concluded that the selected waters in Table 6.6-1 are good candidates for in-drift seepage.

Table 6.6-1 is a summary of the seepage water selection process in Step 1. The right-hand column in Table 6.6-1 gives the points in time (which also coincides with the filenames) that are selected.

6.6.3 Evaporate Waters to a Common Degree of Concentration (Step 2)

The seepage water compositions from the THC model identified in Step 1 vary over time not only in terms of the molar ratios of the dissolved constituents, but also in terms of the absolute concentrations of these constituents. To group these calculated seepage water compositions into bins containing relatively homogeneous water types, these waters are normalized (based on same activity of water) to reflect the compositions of water by evaporating them to a common activity of water.

The in-drift precipitates/salts model (*In-Drift Precipitates Salts Model* report (BSC 2003 [DIRS 162529])) is used to calculate normalized seepage water compositions resulting from evaporation of the more than 300 waters identified in Step 1. This approach accounts for the effects of nearly all chemical divides important to a particular water. Other methods, such as dividing each concentration by the ionic strength, cannot accurately reveal the likely brine end-point for a given water, which is important to establishing corrosion rates germane to performance assessment. As determined by the in-drift precipitates/salts model evaporations, the waters evaporatively evolve to several different brine types, most commonly nitrate brines, chloride brines, and their combinations. An activity of water of 0.65 was chosen as the common end-point of these evaporation runs (at equilibrium, the water activity is equivalent to the relative humidity) because this is the lowest approximate value in which all runs are above the deliquescence point.

The EQ3/6 program input files used in the in-drift precipitates/salts model evaporation calculations are generated according to the protocol outlined in the *In-Drift Precipitates/Salts Model* report (BSC 2003 [DIRS 162529]) using the EQ3/6 programs template files found in DTN: MO0303SPAMEQ36.000 [DIRS 162549]. Temperature, pH, and concentrations of dissolved components tracked in the THC model (except for Fe) are taken directly from the THC model output listed on Table 6.6-1. Iron (Fe) is excluded as it is a relatively insoluble ($< 2 \cdot 10^{-10}$ molal) species and of no consequence to the evaporated brine composition. Electrical balancing is performed using the aqueous component whose molality (mole/kg. solution) would be least affected on a percentage basis. The minerals suppressed in these calculation runs are discussed in Section 6.5.5. In addition to the list of minerals provided on Table 6.5-2, three additional minerals (albite, k-feldspar and celadonite) that are not originally included in the in-drift precipitates/salts model mineral suppression list, are suppressed in a few of the calculation runs.

Table 6.6-1. Locations and Identification of Seepage Water Compositions to be Binned

Starting Water Composition	Worksheet: Quadrant: Zone: Index:	Case Abbreviation	Points in Time Specific to Case	Points in Time Common to All Cases
HD-PERM water (Alcove 5) thc6_w0_r.xls	"fractures-ch" "Top" "Front" "4"	w0tf4	789, 12310	10, 51, 53, 55, 60, 75, 100, 150, 200, 250, 300, 350, 400, 500, 600, 650, 700, 750, 800, 1000, 1200, 1400, 1601, 1801, 2001, 2201, 2401, 3002, 5003, 7004,10006, 15010, 20013, 50034
	"matrix-ch" "Base" "Front" "4"	w0bf4		
Cross-drift water CS2000/16.5 thc6_w4_r.xls	"fractures-ch" "Top" "Front" "4"	W4tf4	804, 2597, 12597	
	"matrix-ch" "Base" "Front" "4"	W4bf4		
Cross-drift water CS1000/7.3 thc6_w5_r.xls	"fractures-ch" "Top" "Front" "4"	w5tf4	784, 2392, 12304	
	"matrix-ch" "Base" "Front" "4"	w5bf4		
Cross-drift water SD-9/990.4 thc6_w6_r.xls	"fractures-ch" "Top" "Front" "4"	w6tf4	865, 3048, 13053	
	"matrix-ch" "Base" "Front" "4"	w6bf4		
Cross-drift water CS500/12.0 thc6_w7_r.xls	"fractures-ch" "Top" "Front" "4"	w7tf4	784, 2591, 12596	
	"matrix-ch" "Base" "Front" "4"	w7bf4		

Source: Starting water compositions: DTN: LB0302DSCPTHCS.002 [DIRS 161976]

NOTE: EQ3 and EQ6 input and output filenames are the same as the points in time with the extensions: *.3i, 3o, 6i, 6o respectively and are archived in DTN: MO0303MWDSCMAB.000 (Eq3) and DTN: MO0303MWDEBSSM.000 (EQ6).

The rationale for suppression of these three minerals is included on Table 6.6-2. These suppressions are also made in the modeling runs found in Section 6.9. The fugacity of carbon dioxide is set at the volume fraction value provided by the THC model output (see Section 6.6.7.2), and that of oxygen is set at the approximate atmospheric value of $10^{-0.7}$.

The only difference from the model protocol is that the evaporations are stopped when the activity of water reaches 0.65 (evaporations start with $a_w \approx 1.0$).

Table 6.6-2. Additional Mineral Suppressions Included During Evaporation to 65 Percent Relative Humidity

Mineral	Formula	Criteria Selected	Rationale	References
Albite	$NaAlSi_3O_8$	Criterion 2	Albite is a common mineral in felsic volcanic and plutonic rocks. It can also form in low-grade metamorphic greenschist facies. It forms at normal pressures at temperatures around 700°C. The formation of albite is kinetically retarded at low temperatures.	Frye 1981, p 538 [DIRS 161804] Deer et al. 1992, p 401 [DIRS 163286]
K-feldspar	$KAlSi_3O_8$	Criterion 2	K-feldspars such as sanidine and microcline are commonly found in plutonic rocks and pegmatites and are found in gneisses. K-feldspars generally form at temperatures between 700°C and 500°C. The formation of K-feldspar is kinetically retarded at low temperatures.	Frye 1981 [DIRS 161804], p 669-670 Deer et al. 1992 [DIRS 163286], Figure 130
Celadonite	$KMgAlSi_4O_{10}(OH)_2$	Criterion 2	Celadonite is a mica mineral similar to glauconite that occurs mostly in basalts. The occurrences are in vesicles or as replacements of ferromagnesian constituents.	Deer et al. 1992 [DIRS 163286], p 297

Table 6.6-1 lists the input and output files generated for use in EQ3/6 calculations, along with the DTNs in which the files are archived. The filenames correspond to the year for which the water composition prediction is documented by the THC model. With these approximations and the rationale for abstraction, the number of input waters is reduced from 18,000 to 368. The full set of input and output files generated is included in DTNs MO0303MWDSCMAB. and MO0303MWDEBSSM.000 [DIRS 162552].

6.6.4 Seepage Water Composition Bin Generation (Step 3)

The final equilibration results from each output file listed on Table 6.6-1 and archived in DTN: MO0303MWDEBSSM.000 [DIRS 162552], are tabulated using the GETEQDATA software to create an Excel spreadsheet entitled "Final Checked EBS Seepage Binning Abstraction Rev 4.xls." This spreadsheet is archived in DTN: MO0310SPAEBSCB.003 and contains the output variables: pH, activity of water ($a_w \approx 0.65$), ionic strength (I), total molalities of the aqueous constituents, and cumulative log moles of minerals precipitated. In addition, formulas are added to calculate various molar ratios and the hydrogen ion activity, and several graphs are inserted to illustrate the variability in the outputs and calculations (see Figures 6.6-5 to 6.6-7). These graphs are ordered primarily by the five different starting waters, and then each of those outputs ordered by time. This information is needed before the waters can be grouped by similarity.

Binning of the seepage water compositions identified in Step 1 is accomplished by group sorting, such that all the seepage waters in a group yield chemically similar solution compositions after they are concentrated by evaporation. Eight characteristic properties are identified for determining that chemical similarity. They are defined in such a way that they yield low intrabin composition ranges compared with the composition ranges existing among all of the waters.

The evaporated waters are binned based on the following eight criteria:

- Total aqueous Ca molality > 0.01 molal?
  - If yes, the water likely evaporatively evolves on the calcium side of the calcite and gypsum chemical divides, resulting in brine that is depleted of carbonate and sulfate. These brines also tend to have neutral to acidic pH and very low fluoride concentrations due to the low solubility of fluorite (CaF_2).
- Total aqueous CO_3 molality > 0.1 molal?
  - If yes, Ca is likely depleted by the precipitation of calcite. In some cases, both Ca and CO_3 have low concentrations, so this criterion further divides brines with Ca molality less than 0.1 molal. Waters having low concentrations of both of these components tend to maintain a neutral pH as they evaporate.
- Total aqueous Ca molality > total aqueous Na molality?
  - This criterion segregates bin 1 and bin 2 waters.
- Total aqueous Ca molality > total aqueous K molality?
  - This criterion segregates bin 2 and bin 3 waters. Without this criterion, K and Ca would have large variability ranges in a combined 2+3 bin.
- Total aqueous NO_3 molality > total aqueous CO_3 molality?
  - This criterion segregates bin 9 and bin 11 waters. Without this criterion, a combined 9+11 bin would have larger variations within the bin, especially for NO_3.
- Total aqueous F molality < 0.1 molal?
  - This criterion distinguishes waters in bin 6 from bin 9 and waters in bin 8 from bin 10. Without this criterion, combined 6+9 and 8+10 bins would have larger variabilities within the bins.
- Total aqueous F molality < 0.03 molal?
  - This criterion distinguishes waters in bin 7 from bin 8. Without this criterion, a combined 7+8 bin would have much larger variability within the bin for many of the components.

- Total aqueous SO_4 molality > 1 molal?
  - This criterion distinguishes waters in bin 6 from bin 8 and waters in bin 9 from bin 10. Without this criterion, combined 6+8 and 9+10 bins would have larger variabilities within the bins for many output parameters.

Columns containing "if/then/else" formulas are added to the spreadsheet to facilitate responding to each criterion for each water. Waters having identical answers to the questions listed on Table 6.6-3 are placed in the same bin. Eleven bins are defined in that way.

Table 6.6-3. Binning Criteria Answer Key

Bin	Ca > 0.01m	Ca > Na	CO_3 < 0.1m	Ca > K	NO_3 > CO_3	F < 0.1m	F < 0.03m	SO_4 > 1m
1	yes	yes	yes	yes	yes	yes	yes	no
2	yes	no	yes	yes	yes	yes	yes	no
3	yes	no	yes	no	yes	yes	yes	no
4	no	no	yes	no	yes	yes	yes	no
5	no	no	yes	no	yes	yes	yes	yes
6	no	no	no	no	yes	yes	no	no
7	no	no	no	no	yes	yes	yes	yes
8	no	no	no	no	yes	yes	no	yes
9	no	no	no	no	yes	no	no	no
10	no	no	no	no	yes	no	no	yes
11	no	no	no	no	no	no	no	no

Source: DTN: MO0310SPAEBSCB.003

Results are provided and plotted in the "Final Checked EBS Seepage Binning Abstraction Rev 4.xls" spreadsheet (DTN: MO0310SPAEBSCB.003). These are also shown in Figure 6.6-8 for all water compositions as sequentially sorted into bins 1 through 11, and Figures 6.6-9 through Figure 6.6-19 for each bin composition separately. A comparison of these plots with the previous plots showing all of the evaporated water compositions (Figures 6.6-5 to 6.6-7) illustrates that the binning process was successful in grouping waters with similar compositions in the same bin.

A second binning approach that uses characteristic properties of precipitating mineral assemblages to sort and generate the bins has also been evaluated. This approach is considered an alternate conceptual model and is documented in Section 6.11.

6.6.5 Choice of Representative Seepage Water for Each Bin (Step 4)

A median seepage water composition for each bin is chosen to represent all seepage water compositions in that bin. Table 6.6-4 provides the median water identifiers for each of the eleven bins defined in Section 6.6.4, and Table 6.6-5 provides the median seepage water compositions for each bin. A description of the method for that process is described as follows. All 368 unevaporated seepage water compositions corresponding to the evaporated waters binned in Step 3 are sorted by bin and copied into separate bin worksheets (e.g., Bin 11 abstract, Bin 10 abstract). This information is found in the data and plots worksheet of the "Final

Checked EBS Seepage Binning Abstraction Rev 4.xls" spreadsheet (DTN: MO0310SPAEBSCB.003). These worksheets are used to determine a representative median water for each bin, as well as individual bin statistics. In so doing, the abstraction further reduces from 368 to 11 the set of representative seepage waters. These 11 water compositions are then used as inputs into the model calculations performed in Section 6.9.

Table 6.6-4. Median Water Identifier for Each Bin and Percentage in Each Bin

Abstracted Water Compositions			Number of Waters In the Bin	% of All Evaporated Waters Represented by the Bin
Case	Water	Filename		
Bin 1	w7bf4	75.6o	5	1.36
Bin 2	w0bf4	250.6o	13	3.53
Bin 3	w0bf4	650.6o	12	3.26
Bin 4	w4bft	600.6o	43	11.68
Bin 5	w7tf4	300.6o	27	7.34
Bin 6	w0tf4	7004.6o	8	2.17
Bin 7	w4bf4	10006.6o	25	6.79
Bin 8	w5tf4	20013.6o	22	5.98
Bin 9	w6tf4	51.6o	58	15.76
Bin 10	w5bf4	10006.6o	10	2.72
Bin 11	w4tf4	300.6o	145	39.40

Source: DTN: MO0310SPAEBSCB.003

The selected bin chemistry is as close to the median chemistry within the bin as can be obtained without actually using the individual median, minimum, and maximum values calculated in each bin for each independent aqueous species. This approach is designed to maintain consistency with the evaporated EQ6 results, because the starting water used in the EQ3/6 evaluation is a specific time-dependent result from the THC model. In addition, this approach maintains charge balance (sum of cations versus anions), which is important in evaporation calculations.

6.6.5.1 Median Water

A flagging methodology is used to determine the median water from each of the 11 bins. The internal functions in Excel are used to determine the statistical rank for each set of twelve parameters. The selection of a median water is selected by determining which waters contain the median value for each parameter (e.g., pH, Ca, Cl), and then using the COUNTIF function, and summing the number of these median value parameters captured by each water in that bin. If two waters of a single bin contain equivalent numbers of median value parameters, then the number of "near median" values (parameter values on either side of the median) are next considered, with the water containing the greatest number of these then being designated as the median water to represent that bin. Table 6.6-4 lists the water selection results of the median water for each bin.

In addition, the distribution of all waters is calculated among the bins by counting the total number of waters contained within each bin and determining the percentage of waters represented in each bin; these results are also shown on Table 6.6-4. Bin 11 contains the largest

number of waters and thus is the most likely median water. Note that Bins 11, 4, and 9 make up the composition of over 66 percent of all of the waters. Each of the EQ6 filenames listed on Table 6.6-4 were mapped back to the values found on the THC spreadsheets listed on Table 6.6-1 to create Table 6.6-5 which contains the 11 complete starting water compositions and associated partial pressures of carbon dioxide.

6.6.5.2 Within Bin (Intrabin) Variability

Within each of the 11 "bin abstract" worksheets, the median, minimum, maximum standard deviation (s), count and two standard deviations (2s) are calculated. Table 6.6-6 contains the individual parameter statistics for each bin, which, when compared to similar statistics for data shown on the data & plots worksheet, indicate that the within bin statistics are generally much smaller than the entire group of data (Table 6.6-7).

6.6.6 Abstraction of THC Model Outputs - Defining Time-Sequences of Bins that Approximate Seepage Water Composition Time-Histories from THC Model Outputs (Step 5)

In this section, each THC model realization (time-history of seepage water compositions) is abstracted in the form of a time-sequence of the seepage water bin median compositions. For simplicity, the term "bin" henceforth refers to the median composition for a bin as well as to its contents, and the term "bin map" refers to time-sequences of seepage water bin median compositions that are abstracted from a THC model realization.

The bin maps for THC outputs are generated using the bin definitions given in Section 6.6.4 and the THC output time defined in Section 6.6.2 (Step 1). The following bin-mapping process was applied to each of the ten combinations of water composition parameter (QUADR, ZONE, and INDEX) values, and worksheets (fractures-ch and matrix-ch) from THC model outputs (defined in Section 6.6.2, Step 1, summarized in Table 6.6-1):

1. Define a time interval around each of the THC output time values that are identified in Step 1 of the binning process (see Section 6.6.2 and fourth and fifth columns of Table 6.6-1) for each of the combinations described above (e.g., the combination for case w0tf4). Begin and end the time intervals approximately midway between adjacent time values. For example, in Table 6.6-8 (applicable to water w0) for the THC output time value of 800 years (in EQ6 Output Filename 800.60), the time interval begins at 794.5 years (between 789 and 800 years) and ends at 900 years (between 800 and 1000 years).

Table 6.6-5. Initial Compositions of the 11 Binned THC Seepage Waters

Species	Bin 1	Bin 2	Bin 3	Bin 4	Bin 5	Bin 6	Bin 7	Bin 8	Bin 9	Bin 10	Bin 11
Water/ File Name	w7bf4/ 75.6o	w0bf4/ 250.6o	w0bf4/ 650.6o	w4bf4/ 600.6o	w7tf4/ 300.6o	w0tf4/ 7004.6o	w4bf4/ 10006.6o	w5tf4/ 20013.6o	w6tf4/ 51.6o	w5bf4/ 10006.6o	w4tf4/ 300.6o
T (°C)	111.9	109.1	104.3	104.9	95.62	6.51E+01	56.34	40.18	91.78	56.34	95.61
pH	7.407	7.583	7.615	7.896	7.634	7.70E+00	7.768	7.94	8.139	7.815	7.759
Ca^{+2}	1.75E-02	6.49E-03	2.14E-03	1.08E-03	1.36E-03	4.20E-04	4.46E-04	5.73E-04	7.24E-05	3.52E-04	3.34E-04
Mg^{+2}	1.70E-05	2.95E-06	4.13E-06	5.75E-07	1.13E-05	4.82E-05	5.52E-05	8.51E-05	2.54E-07	4.31E-05	6.34E-06
Na^{+}	3.89E-03	2.63E-03	2.67E-03	1.26E-03	5.53E-03	8.09E-03	7.65E-03	7.31E-03	4.27E-03	6.82E-03	4.80E-03
Cl^{-}	2.01E-02	5.02E-03	3.35E-03	1.03E-03	3.28E-03	3.32E-03	7.44E-04	5.61E-04	7.34E-04	6.00E-04	1.30E-03
$SiO_{2(aq)}$	9.42E-03	7.42E-03	6.96E-03	7.38E-03	1.22E-02	2.90E-03	2.46E-03	1.79E-03	4.15E-03	2.47E-03	1.19E-02
HCO_3^{-}	5.57E-05	9.06E-05	1.95E-04	1.64E-04	4.18E-04	2.93E-03	6.72E-03	6.92E-03	2.04E-03	5.74E-03	1.13E-03
SO_4^{-2}	8.87E-03	4.89E-03	1.50E-03	5.88E-04	1.77E-03	1.21E-03	4.12E-04	3.55E-04	1.18E-04	3.80E-04	7.29E-04
K^{+}	8.68E-04	5.40E-04	5.00E-04	2.38E-04	8.68E-04	6.25E-04	4.67E-04	2.76E-04	5.02E-04	4.17E-04	7.50E-04
AlO_2^{-}	3.27E-08	7.08E-08	5.02E-08	9.97E-08	8.03E-10	5.36E-09	3.62E-09	1.50E-09	6.09E-08	4.03E-09	1.42E-09
F-	1.93E-04	2.46E-04	3.48E-04	4.28E-04	1.00E-03	8.26E-04	7.81E-04	6.43E-04	9.77E-04	8.61E-04	1.38E-03
NO_3^{-}	1.30E-03	5.46E-04	1.83E-04	1.33E-04	2.22E-04	1.04E-04	6.87E-05	3.97E-05	3.10E-04	4.25E-05	1.26E-04
$CO_{2(g)}$ (atm)	3.89E-04	4.93E-04	1.04E-03	4.88E-04	1.88E-03	7.06E-03	1.19E-02	6.34E-03	2.94E-03	9.19E-03	4.06E-03
log $CO_{2(g)}$	-3.410	-3.307	-2.984	-3.312	-2.726	-2.151	-1.926	-2.198	-2.532	-2.037	-2.392

Source: DTN: MO0310SPAEBSCB.003

NOTE: Unless otherwise marked, units are in Moles/kg·H_2O.

2. Assign to that time interval the bin (bin median composition) that contains the seepage water composition from the THC output at the output time around which the time interval was defined. For example, in Table 6.6-8, Bin 11 is assigned to time interval 794.5 to 900 years for crown seepage (Quadrant = Top), because the THC seepage water output composition for case w0tf4 at 800 years (EQ6 Output Filename 800.6) is placed into bin 11 during the binning process.

3. Sequentially repeat items 1 and 2, directly above, for each THC output time.

Each combination is given a case abbreviation in the third column of Table 6.6-1. The first, second, and last periods for each case are special cases. The bin assigned to the 10-year output represents the period from 0 to 50 years. The 51-year output is binned for the period from 50 to 52 years. Lastly, the 50,034-year output is binned for the period from 35,023.5 to 100,000 years.

Tables 6.6-8 through 6.6-12 provide the maps for each seepage water in the binning analysis. The graphic plots of Figures 6.6-20 through 6.6-29 compare the binning assignments to the evaporated THC outputs. These figures graphically illustrate that the bins cover the changes in chemistry at 65 percent relative humidity through time. For example, peaks and valleys in the chemistry output correspond to a visible change in assigned bins.

6.6.7 Impact Analysis Due to Errors Found During Check Process

The binning process has been developed to facilitate an evaluation of whether any new input (such as a new THC seepage model output) would require a new type of chemistry (i.e., a new bin) that this abstraction has not investigated. Only if a potential water falls outside a defined bin area is re-analysis of potential seepage compositions necessary. The 11 bins are designed to cover a broad range of possible water chemistry within the drift. Likewise, if an error is found in any of the calculated chemistries, and an analysis of the error finds that the corrected chemistry falls within the same bin, then there is no real impact to the chemistries within that bin (i.e. the predicted evolution of the chemistry in the bin does not change), so the current median water is still sufficient to represent the corrected water.

During the check process, two errors in the binning abstraction were discovered. The first dealt with four of the 368 input waters not being completely normalized to an activity of water equaling 0.65. This occurred when the number of iterations EQ6 was allowed to perform was set too low for the calculation to reach the desired activity of water (a_w). The second error occurred when the $P\mathrm{CO_2}$ inputs used from the five THC seepage model outputs were not converted from dimensionless volume fractions to partial pressures in bars. Thus, the volume fractions in the model runs used for the binning process were treated as if they were partial pressures in bars. The impact evaluation of these two errors resulted in no changes to the assigned bins, therefore these errors have no impact on the look-up tables developed in Section 6.9. The details of the impact analyses are documented in the following section.

Table 6.6-6. Calculated Statistics for All Values within Each Bin (a_w = 0.65)

Bin	Statistic	pH	I	Al	C	Ca	Cl	F	K	Mg	N	Na	S	Si	Cl:N
1	Median	5.59	1.28E+01	3.20E-12	5.54E-04	3.58E+00	8.43E+00	6.31E-05	3.64E-01	9.16E-04	5.45E-01	1.63E+00	1.84E-03	1.48E-03	1.55E+01
	Min	5.53	1.23E+01	3.03E-12	4.03E-04	3.32E+00	6.52E+00	5.92E-05	1.76E-01	4.14E-04	2.73E-01	7.83E-01	1.82E-03	1.22E-03	2.37E+00
	Max	5.72	1.30E+01	3.60E-12	6.19E-04	4.01E+00	8.71E+00	6.99E-05	4.25E-01	1.27E-03	2.75E+00	1.92E+00	2.12E-03	1.61E-03	3.18E+01
	s	0.08	2.96E-01	2.22E-13	8.67E-05	2.88E-01	9.19E-01	4.18E-06	1.13E-01	3.55E-04	1.05E+00	5.00E-01	1.27E-04	1.86E-04	1.26E+01
	2s	0.15	5.93E-01	4.44E-13	1.73E-04	5.76E-01	1.84E+00	8.37E-06	2.25E-01	7.11E-04	2.11E+00	1.00E+00	2.55E-04	3.72E-04	2.53E+01
2	Median	5.69	1.15E+01	2.32E-12	5.74E-04	2.38E+00	8.30E+00	5.20E-05	9.28E-01	1.32E-03	7.62E-01	3.41E+00	1.93E-03	2.20E-03	1.09E+01
	Min	5.46	1.11E+01	1.33E-12	4.32E-04	1.86E+00	6.54E+00	4.41E-05	5.74E-01	4.66E-04	2.84E-01	2.82E+00	1.58E-03	1.90E-03	2.36E+00
	Max	5.79	1.17E+01	3.76E-12	8.94E-04	2.75E+00	8.83E+00	5.51E-05	1.58E+00	2.49E-03	2.83E+00	3.98E+00	2.03E-03	3.00E-03	3.11E+01
	s	0.11	1.98E-01	7.15E-13	1.52E-04	2.75E-01	6.77E-01	3.50E-06	3.32E-01	5.87E-04	8.35E-01	4.13E-01	1.29E-04	3.16E-04	7.74E+00
	2s	0.22	3.97E-01	1.43E-12	3.03E-04	5.51E-01	1.35E+00	6.99E-06	6.64E-01	1.17E-03	1.67E+00	8.27E-01	2.58E-04	6.31E-04	1.55E+01
3	Median	5.88	1.08E+01	1.09E-12	4.55E-04	1.10E+00	8.42E+00	3.79E-05	3.00E+00	1.26E-03	1.02E+00	4.24E+00	2.07E-03	2.29E-03	8.38E+00
	Min	5.62	1.03E+01	9.46E-14	1.56E-04	7.49E-02	7.74E+00	3.56E-05	1.93E+00	1.11E-04	7.05E-01	3.73E+00	1.54E-03	1.74E-03	3.43E+00
	Max	6.55	1.10E+01	3.54E-12	8.21E-04	1.74E+00	8.95E+00	8.47E-05	5.55E+00	2.50E-03	2.26E+00	4.76E+00	8.07E-03	3.27E-03	1.20E+01
	s	0.24	2.18E-01	9.64E-13	1.84E-04	4.24E-01	4.04E-01	1.36E-05	9.15E-01	7.39E-04	5.58E-01	3.22E-01	1.76E-03	5.22E-04	3.16E+00
	2s	0.49	4.35E-01	1.93E-12	3.67E-04	8.48E-01	8.08E-01	2.72E-05	1.83E+00	1.48E-03	1.12E+00	6.45E-01	3.52E-03	1.04E-03	6.33E+00
4	Median	7.13	1.17E+01	2.23E-13	4.23E-04	2.66E-03	7.17E+00	7.53E-04	5.64E+00	2.32E-06	3.64E+00	5.57E+00	3.76E-01	3.45E-03	1.97E+00
	Min	5.94	1.11E+01	4.07E-15	2.13E-04	9.33E-04	2.81E+00	3.28E-04	2.46E+00	2.20E-07	1.73E+00	5.07E+00	1.97E-01	8.22E-04	2.93E-01
	Max	7.62	1.41E+01	1.14E-12	2.10E-03	4.09E-03	8.28E+00	1.91E-03	6.17E+00	3.89E-04	9.90E+00	1.05E+01	8.61E-01	7.35E-03	4.79E+00
	s	0.34	1.02E+00	2.78E-13	3.15E-04	6.45E-04	1.87E+00	2.50E-04	9.45E-01	8.23E-05	2.79E+00	1.69E+00	9.58E-02	1.26E-03	1.41E+00
	2s	0.68	2.04E+00	5.56E-13	6.30E-04	1.29E-03	3.74E+00	5.00E-04	1.89E+00	1.65E-04	5.59E+00	3.38E+00	1.92E-01	2.51E-03	2.83E+00
5	Median	7.60	1.20E+01	1.26E-13	1.53E-03	8.57E-04	7.71E+00	2.29E-03	4.67E+00	9.30E-07	1.20E+00	6.22E+00	1.02E+00	5.51E-03	6.36E+00
	Min	7.26	1.17E+01	5.79E-14	7.97E-04	2.00E-05	6.98E+00	1.98E-03	4.60E+00	3.63E-08	6.30E-01	5.93E+00	1.00E+00	3.15E-03	2.84E+00
	Max	8.64	1.25E+01	3.44E-13	3.19E-02	9.78E-04	8.04E+00	1.91E-02	4.92E+00	7.68E-06	2.46E+00	6.77E+00	1.13E+00	2.45E-02	1.28E+01
	s	0.29	2.49E-01	8.09E-14	5.84E-03	1.72E-04	3.23E-01	3.24E-03	6.75E-02	2.37E-06	5.63E-01	2.39E-01	2.83E-02	3.95E-03	3.34E+00
	2s	0.58	4.97E-01	1.62E-13	1.17E-02	3.44E-04	6.46E-01	6.48E-03	1.35E-01	4.75E-06	1.13E+00	4.77E-01	5.66E-02	7.91E-03	6.68E+00
6	Median	9.01	1.24E+01	1.18E-13	5.03E-01	8.47E-06	6.36E+00	8.67E-02	4.30E+00	6.72E-08	1.45E+00	6.63E+00	8.53E-01	4.45E-02	4.37E+00
	Min	8.37	1.18E+01	1.13E-14	1.64E-01	7.54E-06	3.17E+00	4.91E-02	2.51E+00	2.59E-09	5.55E-01	6.28E+00	7.99E-01	2.03E-02	4.26E-01
	Max	9.68	1.40E+01	2.37E-13	7.96E-01	9.05E-06	7.79E+00	9.15E-02	4.49E+00	4.35E-07	7.43E+00	1.04E+01	9.30E-01	2.46E-01	1.34E+01
	s	0.37	8.46E-01	9.15E-14	2.52E-01	5.58E-07	1.65E+00	1.63E-02	6.66E-01	1.91E-07	2.73E+00	1.52E+00	4.38E-02	7.78E-02	4.87E+00
	2s	0.73	1.69E+00	1.83E-13	5.04E-01	1.12E-06	3.29E+00	3.26E-02	1.33E+00	3.83E-07	5.46E+00	3.04E+00	8.75E-02	1.56E-01	9.75E+00

Table 6.6-6. Calculated Statistics for All Values within Each Bin (a_w = 0.65) (Continued)

Bin	Statistic	pH	I	Al	C	Ca	Cl	F	K	Mg	N	Na	S	Si	Cl:N
7	Median	8.73	1.32E+01	3.94E-15	3.51E-01	1.00E-05	5.83E+00	4.42E-02	4.90E+00	1.30E-06	2.81E+00	6.81E+00	1.24E+00	8.04E-03	2.08E+00
	Min	8.52	1.28E+01	2.71E-15	2.57E-01	8.59E-06	4.08E+00	3.12E-02	4.15E+00	3.64E-07	2.33E+00	6.59E+00	1.03E+00	5.57E-03	7.31E-01
	Max	9.13	1.42E+01	5.87E-15	6.49E-01	1.11E-05	6.11E+00	7.08E-02	5.06E+00	2.31E-06	5.59E+00	8.59E+00	1.41E+00	2.00E-02	2.60E+00
	s	0.16	3.72E-01	1.08E-15	1.06E-01	7.70E-07	5.03E-01	1.15E-02	2.40E-01	5.78E-07	8.14E-01	4.96E-01	1.17E-01	4.00E-03	4.80E-01
	2s	0.32	7.44E-01	2.15E-15	2.11E-01	1.54E-06	1.01E+00	2.30E-02	4.81E-01	1.16E-06	1.63E+00	9.93E-01	2.34E-01	7.99E-03	9.60E-01
8	Median	8.58	1.43E+01	1.65E-15	2.08E-01	1.14E-05	4.57E+00	2.30E-02	4.63E+00	2.54E-06	3.86E+00	8.05E+00	1.64E+00	4.15E-03	1.19E+00
	Min	8.40	1.36E+01	6.86E-16	1.42E-01	9.56E-06	2.80E+00	1.36E-02	2.93E+00	1.08E-06	3.27E+00	6.99E+00	1.01E+00	2.10E-03	3.30E-01
	Max	8.98	1.49E+01	2.77E-15	2.65E-01	1.51E-05	5.59E+00	2.97E-02	5.23E+00	6.09E-06	8.48E+00	1.07E+01	1.87E+00	6.14E-03	1.71E+00
	s	0.14	3.07E-01	6.66E-16	3.28E-02	1.38E-06	7.31E-01	4.79E-03	6.63E-01	1.21E-06	1.43E+00	9.77E-01	2.38E-01	1.18E-03	3.52E-01
	2s	0.28	6.15E-01	1.33E-15	6.57E-02	2.75E-06	1.46E+00	9.57E-03	1.33E+00	2.43E-06	2.86E+00	1.95E+00	4.76E-01	2.36E-03	7.04E-01
9	Median	9.15	1.35E+01	1.22E-13	1.14E+00	2.57E-06	5.37E+00	2.39E-01	3.93E+00	3.28E-08	2.34E+00	7.51E+00	7.31E-01	9.34E-02	2.36E+00
	Min	8.78	1.23E+01	1.13E-14	5.95E-01	1.00E-06	3.83E+00	1.17E-01	2.75E+00	1.16E-09	8.18E-01	6.41E+00	6.03E-01	1.51E-02	7.51E-01
	Max	9.66	1.48E+01	1.16E-10	1.55E+00	7.53E-06	6.97E+00	2.64E-01	6.25E+00	5.48E-07	5.12E+00	9.58E+00	9.19E-01	3.01E-01	8.53E+00
	s	0.22	5.91E-01	1.52E-11	2.12E-01	1.98E-06	6.09E-01	4.11E-02	8.45E-01	1.65E-07	9.15E-01	9.65E-01	1.07E-01	7.03E-02	1.24E+00
	2s	0.43	1.18E+00	3.05E-11	4.24E-01	3.96E-06	1.22E+00	8.23E-02	1.69E+00	3.29E-07	1.83E+00	1.93E+00	2.14E-01	1.41E-01	2.49E+00
10	Median	8.75	1.32E+01	1.04E-14	4.12E-01	5.64E-07	5.33E+00	2.07E-01	4.60E+00	4.08E-07	3.37E+00	7.32E+00	1.09E+00	1.02E-02	1.58E+00
	Min	8.70	1.26E+01	4.28E-15	3.02E-01	3.39E-07	4.82E+00	2.05E-01	4.52E+00	3.32E-07	2.21E+00	6.70E+00	1.08E+00	7.76E-03	1.13E+00
	Max	8.97	1.38E+01	1.49E-14	5.06E-01	7.29E-07	6.08E+00	2.12E-01	4.67E+00	5.63E-07	4.25E+00	7.80E+00	1.32E+00	1.43E-02	2.74E+00
	s	0.10	4.62E-01	3.33E-15	7.77E-02	1.55E-07	4.98E-01	2.71E-03	4.66E-02	8.62E-08	8.54E-01	4.34E-01	1.02E-01	2.49E-03	6.78E-01
	2s	0.20	9.24E-01	6.66E-15	1.55E-01	3.10E-07	9.96E-01	5.42E-03	9.33E-02	1.72E-07	1.71E+00	8.67E-01	2.04E-01	4.98E-03	1.36E+00
11	Median	9.17	1.26E+01	1.04E-13	1.16E+00	2.65E-06	6.58E+00	2.42E-01	3.84E+00	3.91E-08	5.58E-01	7.06E+00	6.51E-01	8.12E-02	1.19E+01
	Min	8.85	1.21E+01	2.05E-14	7.35E-01	1.92E-06	3.56E+00	1.04E-01	2.96E+00	3.39E-09	3.27E-01	6.57E+00	6.06E-01	2.46E-02	5.55E+00
	Max	9.72	1.37E+01	2.46E-13	2.06E+00	7.85E-06	7.22E+00	3.34E-01	4.94E+00	3.82E-07	1.14E+00	7.84E+00	9.06E-01	2.98E-01	2.02E+01
	s	0.19	3.22E-01	4.21E-14	1.35E-01	1.81E-06	3.93E-01	4.22E-02	3.30E-01	8.18E-08	1.52E-01	2.61E-01	7.68E-02	5.56E-02	2.82E+00
	2s	0.38	6.44E-01	8.42E-14	2.70E-01	3.63E-06	7.86E-01	8.44E-02	6.60E-01	1.64E-07	3.04E-01	5.23E-01	1.54E-01	1.11E-01	5.63E+00

Source: DTN: MO0310SPAEBSCB.003

NOTE: Unless otherwise marked, units are in Moles/kg·H_2O.

Table 6.6-7. Calculated Statistics for All Values on the Data and Plots Worksheet

Statistic	pH	I	Al	C	Ca	Cl	F	K	Mg	N	Na	S	Si	Cl:N
Median	8.98	1.27E+01	1.08E-13	1.04E+00	6.93E-06	6.53E+00	1.48E-01	4.29E+00	2.04E-07	1.25E+00	6.93E+00	6.96E-01	3.79E-02	5.66E+00
Min	5.46	1.03E+01	6.86E-16	1.56E-04	3.39E-07	2.80E+00	3.56E-05	1.76E-01	1.16E-09	2.73E-01	7.83E-01	1.54E-03	8.22E-04	2.93E-01
Max	9.72	1.49E+01	1.16E-10	2.06E+00	4.01E+00	8.95E+00	3.34E-01	6.25E+00	2.50E-03	9.90E+00	1.07E+01	1.87E+00	3.01E-01	3.18E+01
s	1.12	8.88E-01	6.07E-12	5.39E-01	6.34E-01	1.21E+00	1.08E-01	1.09E+00	3.89E-04	1.94E+00	1.41E+00	3.81E-01	6.51E-02	5.72E+00
2s	2.23	1.78E+00	1.21E-11	1.08E+00	1.27E+00	2.42E+00	2.17E-01	2.17E+00	7.78E-04	3.87E+00	2.82E+00	7.61E-01	1.30E-01	1.14E+01

Source: DTN: MO0310SPAEBSCB.003

NOTE: All units are in Moles/kg·H_2O.

Table 6.6-8. Bin Map for "Water 0" Incoming Seepage Waters

Start (Year)	End (Year)	Bin for Invert Seepage (w0bf4)	Bin for Crown Seepage (w0tf4)	EQ6 Output Filename
0.0	50.0	4	4	10.6o
50.0	52.0	5	5	51.6o
52.0	54.0	11	5	53.6o
54.0	57.5	11	6	55.6o
57.5	67.5	2	6	60.6o
67.5	87.5	1	5	75.6o
87.5	125.0	1	5	100.6o
125.0	175.0	2	4	150.6o
175.0	225.0	2	4	200.6o
225.0	275.0	2	3	250.6o
275.0	325.0	2	3	300.6o
325.0	375.0	2	3	350.6o
375.0	450.0	2	3	400.6o
450.0	550.0	2	4	500.6o
550.0	625.0	3	4	600.6o
625.0	675.0	3	5	650.6o
675.0	725.0	4	11	700.6o
725.0	769.5	4	11	750.6o
769.5	794.5	4	11	789.6o
794.5	900.0	4	11	800.6o
900.0	1100.0	5	11	1000.6o
1100.0	1300.0	5	11	1200.6o
1300.0	1500.5	5	11	1400.6o
1500.5	1701.0	5	11	1601.6o
1701.0	1901.0	5	11	1801.6o
1901.0	2101.0	9	4	2001.6o
2101.0	2301.0	11	11	2201.6o
2301.0	2701.5	11	11	2401.6o
2701.5	4002.5	11	11	3002.6o
4002.5	6003.5	11	11	5003.6o
6003.5	8505.0	6	6	7004.6o
8505.0	11158.0	7	6	10006.6o
11158.0	13660.0	7	7	12310.6o
13660.0	17511.5	7	7	15010.6o
17511.5	35023.5	8	8	20013.6o
35023.5	100000.0	8	8	50034.6o

Source: DTN: MO0310SPAEBSCB.003

Table 6.6-9. Bin Map for "Water 4" Incoming Seepage Waters

Start (Year)	End (Year)	Bin for Invert Seepage (w4bf4)	Bin for Crown Seepage (w4tf4)	EQ6 Output Filename
0.0	50.0	10	10	10.6o
50.0	52.0	11	11	51.6o
52.0	54.0	11	11	53.6o
54.0	57.5	11	11	55.6o
57.5	67.5	4	11	60.6o
67.5	87.5	11	11	75.6o
87.5	125.0	11	11	100.6o
125.0	175.0	4	11	150.6o
175.0	225.0	4	11	200.6o
225.0	275.0	5	11	250.6o
275.0	325.0	4	11	300.6o
325.0	375.0	5	11	350.6o
375.0	450.0	5	11	400.6o
450.0	550.0	4	5	500.6o
550.0	625.0	4	5	600.6o
625.0	675.0	4	11	650.6o
675.0	725.0	5	11	700.6o
725.0	775.0	5	11	750.6o
775.0	802.0	11	11	800.6o
802.0	902.0	11	11	804.6o
902.0	1100.0	11	11	1000.6o
1100.0	1300.0	11	11	1200.6o
1300.0	1500.5	11	11	1400.6o
1500.5	1701.0	11	11	1601.6o
1701.0	1901.0	11	5	1801.6o
1901.0	2101.0	11	4	2001.6o
2101.0	2301.0	11	11	2201.6o
2301.0	2499.0	11	11	2401.6o
2499.0	2799.5	11	11	2597.6o
2799.5	4002.5	11	11	3002.6o
4002.5	6003.5	11	11	5003.6o
6003.5	8505.0	9	9	7004.6o
8505.0	11301.5	7	7	10006.6o
11301.5	13803.5	7	7	12597.6o
13803.5	17511.5	8	8	15010.6o
17511.5	35023.5	8	8	20013.6o
35023.5	100000.0	8	8	50034.6o

Source: DTN: MO0310SPAEBSCB.003

Table 6.6-10. Bin Map for "Water 5" Incoming Seepage Waters

Start (Year)	End (Year)	Bin for Invert Seepage (w5bf4)	Bin for Crown Seepage (w5tf4)	EQ6 Output Filename
0.0	50.0	7	7	10.6o
50.0	52.0	11	11	51.6o
52.0	54.0	11	11	53.6o
54.0	57.5	11	11	55.6o
57.5	67.5	3	11	60.6o
67.5	87.5	4	11	75.6o
87.5	125.0	2	11	100.6o
125.0	175.0	4	11	150.6o
175.0	225.0	4	11	200.6o
225.0	275.0	5	11	250.6o
275.0	325.0	4	11	300.6o
325.0	375.0	4	11	350.6o
375.0	450.0	4	11	400.6o
450.0	550.0	4	9	500.6o
550.0	625.0	5	11	600.6o
625.0	675.0	5	11	650.6o
675.0	725.0	11	11	700.6o
725.0	767.0	11	11	750.6o
767.0	792.0	11	11	784.6o
792.0	900.0	11	11	800.6o
900.0	1100.0	11	11	1000.6o
1100.0	1300.0	11	11	1200.6o
1300.0	1500.5	11	11	1400.6o
1500.5	1701.0	11	11	1601.6o
1701.0	1901.0	11	5	1801.6o
1901.0	2101.0	11	4	2001.6o
2101.0	2296.5	11	11	2201.6o
2296.5	2396.5	11	11	2392.6o
2396.5	2701.5	11	11	2401.6o
2701.5	4002.5	11	11	3002.6o
4002.5	6003.5	11	11	5003.6o
6003.5	8505.0	9	9	7004.6o
8505.0	11155.0	10	10	10006.6o
11155.0	13657.0	7	7	12304.6o
13657.0	17511.5	7	7	15010.6o
17511.5	35023.5	8	8	20013.6o
35023.5	100000.0	8	8	50034.6o

Source: DTN: MO0310SPAEBSCB.003

Table 6.6-11. Bin Map for "Water 6" Incoming Seepage Waters

Start (Year)	End (Year)	Bin for Invert Seepage (w6bf4)	Bin for Crown Seepage (w6tf4)	EQ6 Output Filename
0.0	50.0	7	7	10.6o
50.0	52.0	9	9	51.6o
52.0	54.0	9	9	53.6o
54.0	57.5	9	9	55.6o
57.5	67.5	2	9	60.6o
67.5	87.5	1	9	75.6o
87.5	125.0	2	9	100.6o
125.0	175.0	4	9	150.6o
175.0	225.0	4	9	200.6o
225.0	275.0	9	9	250.6o
275.0	325.0	4	9	300.6o
325.0	375.0	4	9	350.6o
375.0	450.0	9	9	400.6o
450.0	550.0	4	6	500.6o
550.0	625.0	4	9	600.6o
625.0	675.0	9	9	650.6o
675.0	725.0	9	9	700.6o
725.0	775.0	9	9	750.6o
775.0	832.5	9	9	800.6o
832.5	932.5	9	9	865.6o
932.5	1100.0	9	9	1000.6o
1100.0	1300.0	9	9	1200.6o
1300.0	1500.5	9	9	1400.6o
1500.5	1701.0	9	9	1601.6o
1701.0	1901.0	9	6	1801.6o
1901.0	2101.0	9	4	2001.6o
2101.0	2301.0	9	9	2201.6o
2301.0	2701.5	9	9	2401.6o
2701.5	3025.0	9	9	3002.6o
3025.0	4025.5	9	9	3048.6o
4025.5	6003.5	9	9	5003.6o
6003.5	8505.0	9	9	7004.6o
8505.0	11529.5	10	10	10006.6o
11529.5	14031.5	10	10	13053.6o
14031.5	17511.5	10	10	15010.6o
17511.5	35023.5	8	8	20013.6o
35023.5	100000.0	8	8	50034.6o

Source: DTN: MO0310SPAEBSCB.003

Table 6.6-12. Bin Map for "Water 7" Incoming Seepage Waters

Start (Year)	End (Year)	Bin for Invert Seepage (w7bf4)	Bin for Crown Seepage (w7tf4)	EQ6 Output Filename
0.0	50.0	7	7	10.6o
50.0	52.0	11	11	51.6o
52.0	54.0	11	11	53.6o
54.0	57.5	11	11	55.6o
57.5	67.5	3	11	60.6o
67.5	87.5	1	11	75.6o
87.5	125.0	2	11	100.6o
125.0	175.0	4	11	150.6o
175.0	225.0	4	11	200.6o
225.0	275.0	4	11	250.6o
275.0	325.0	3	5	300.6o
325.0	375.0	3	4	350.6o
375.0	450.0	3	4	400.6o
450.0	550.0	2	4	500.6o
550.0	625.0	3	4	600.6o
625.0	675.0	4	5	650.6o
675.0	725.0	4	11	700.6o
725.0	767.0	4	11	750.6o
767.0	792.0	5	11	784.6o
792.0	900.0	5	11	800.6o
900.0	1100.0	6	11	1000.6o
1100.0	1300.0	11	11	1200.6o
1300.0	1500.5	11	11	1400.6o
1500.5	1701.0	11	11	1601.6o
1701.0	1901.0	11	11	1801.6o
1901.0	2101.0	11	11	2001.6o
2101.0	2301.0	11	11	2201.6o
2301.0	2496.0	11	11	2401.6o
2496.0	2796.5	11	11	2591.6o
2796.5	4002.5	11	11	3002.6o
4002.5	6003.5	11	11	5003.6o
6003.5	8505.0	9	9	7004.6o
8505.0	11301.0	7	7	10006.6o
11301.0	13803.0	7	7	12596.6o
13803.0	17511.5	7	7	15010.6o
17511.5	35023.5	8	8	20013.6o
35023.5	100000.0	8	8	50034.6o

Source: DTN: MO0310SPAEBSCB.003

6.6.7.1 Endpoint a_w

Table 6.6-13 lists the files that do not normalize to an a_w of 0.65 and the results of the recalculation down to an a_w of 0.65.

Table 6.6-13. Details of Impact Analysis on Binning Due to Endpoint a_w

Water/File Name	Initial Endpoint a_w	Initial Bin	New Endpoint a_w	New Bin
W4bf4 2597.6o	0.72	11	0.65	11
W4bf4 3002.6o	0.706	11	0.65	11
W5bf4 3002.6o	0.695	11	0.65	11
W6bf4 3002.6o	0.675	9	0.65	9

Source: DTN: MO0303MWDEBSSM.000 [DIRS 162552]

Source: DTN: MO0310SPAEBSCB.003; Final Checked EBS THC Seepage Binning Abstraction Rev 4.xls

Source: DTN: MO0310SPAEBSCB.003; Bin Abstraction Rerun.xls

These four files were rerun to the correct water activity and the binning criteria discussed in Section 6.6.4 were reapplied. All of the waters fell within the original bins. Therefore, there was no impact to the look-up tables developed in Section 6.9. All recalculated EQ6 files and the rebinning spreadsheet (Bin Abstraction Rerun.xls) are archived in DTN: MO0310SPAEBSCB.003.

6.6.7.2 CO_2 Pressure Correction

To evaluate the impact of the error in units for the fugacity of CO_2, the median waters that are determined to represent the eleven bins were rerun with corrected CO_2 fugacities. The fugacities were corrected by multiplying the original volume fractions by the approximate average total atmospheric pressure at Yucca Mountain of 0.88 bars (see spreadsheet “gas flux.xls”, tab “fractures-ch” archived in DTN: MO0310SPAEBSCB.003). This action converts the volume fractions to partial pressures in bars.

After reapplying the binning criteria discussed in Section 6.6.4, all of the waters fall within the same bin as the original calculation runs (Table 6.6-14), showing that the error in the Pco_2 values has no effect on the binning analysis. All recalculated EQ6 files and the rebinning spreadsheet (Bin Abstraction Rerun.xls) are archived in DTN: MO0310SPAEBSCB.003.

Table 6.6-14. Details of Impact Analysis on CO_2 Pressure Correction

Water/File Name	Initial log CO_2 Value	Initial Bin	Corrected log CO_2 Value	New Bin
W7bf4/75.6o	-3.41	1	-3.466	1
W0bf4/250.6o	-3.307	2	-3.363	2
W0bf4/650.60	-2.984	3	-3.040	3
W4bf4/600.6o	-3.312	4	-3.368	4
W7tf4/300.6o	-2.726	5	-2.782	5
W0tf4/7004.6o	-2.151	6	-2.207	6
W4bf4/10006.6o	-1.926	7	-1.982	7
W5tf4/20013.6o	-2.198	8	-2.254	8
W6tf4/51.6o	-2.532	9	-2.589	9
W5bf4/10006.6o	-2.037	10	-2.093	10
W4tf4/300.6o	-2.392	11	-2.448	11

Source: DTN MO0303MWDEBSSM.000

Source: DTN: MO0310SPAEBSCB.003; Final Checked EBS THC Seepage Binning Abstraction Rev 4.xls

Source: DTN: MO0310SPAEBSCB.003; Bin Abstraction Rerun.xls

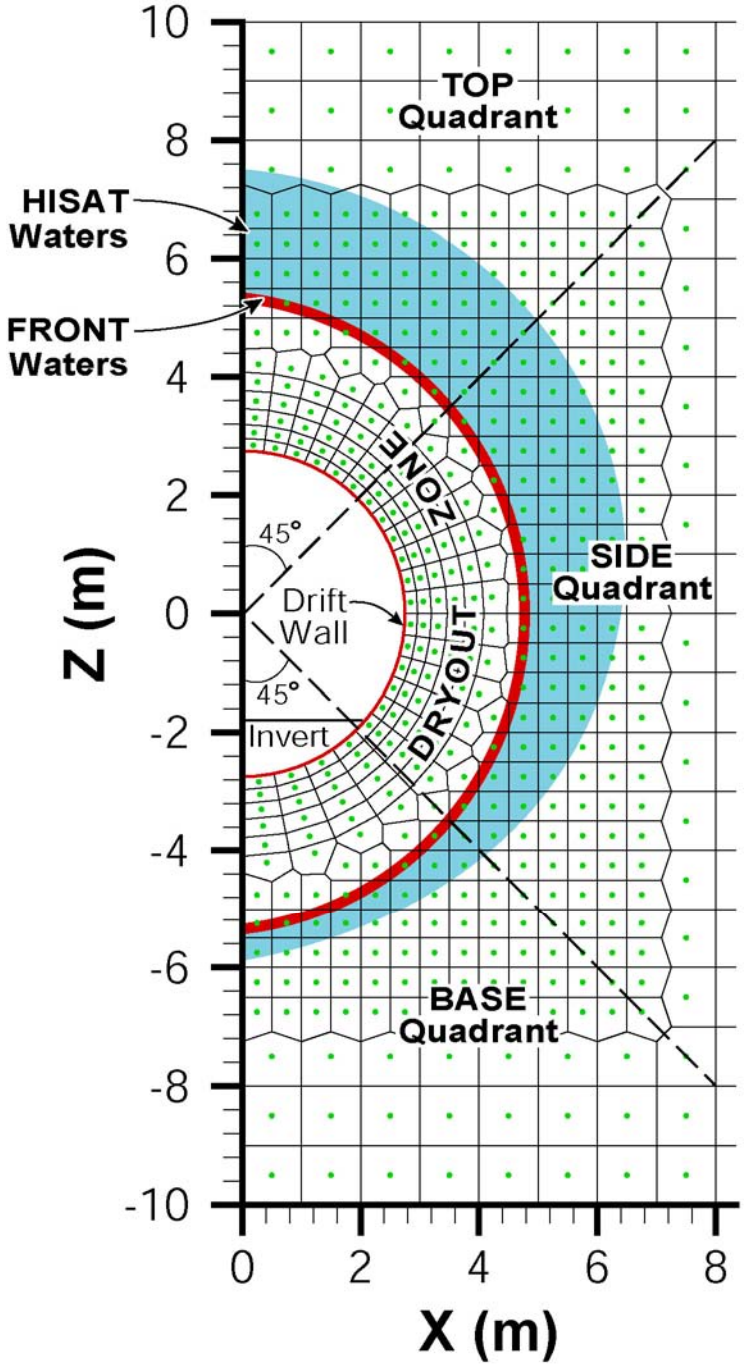

Source: BSC 2003 [DIRS 164888], Figure 6.2-2

Figure 6.6-1. Quadrant Designations for Abstraction of Data from the THC Seepage Model

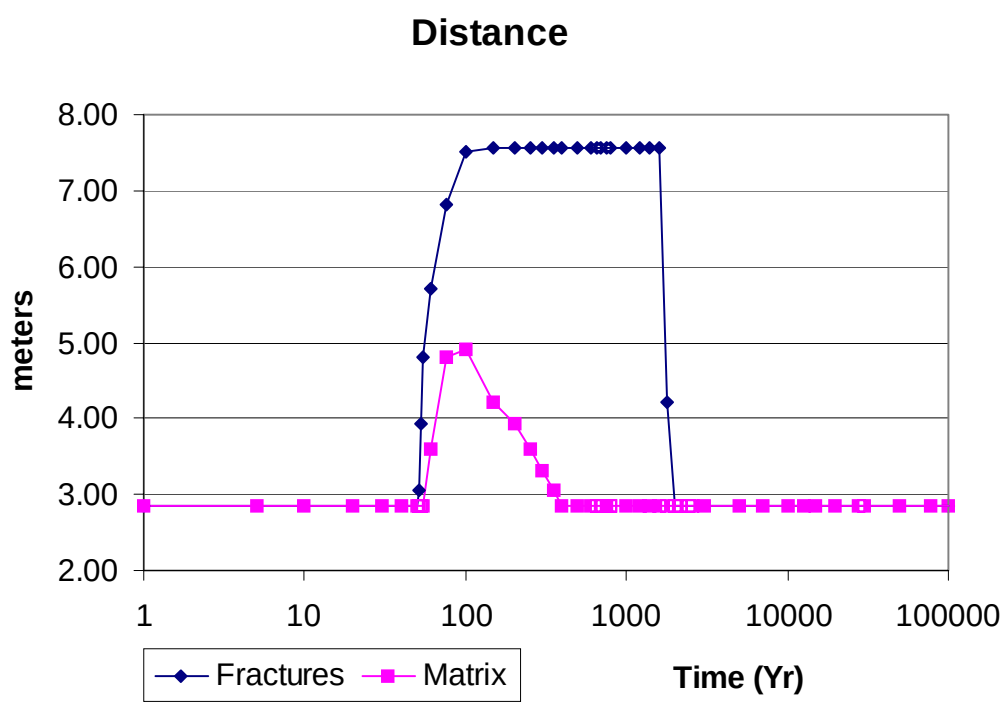

DTN: LB0302DSCPTHCS.002 [DIRS 161976]

Figure 6.6-2. The Location of the Wetting Front in the Host Rock, as Calculated by the Thermal-Hydrological-Chemical-Seepage Model

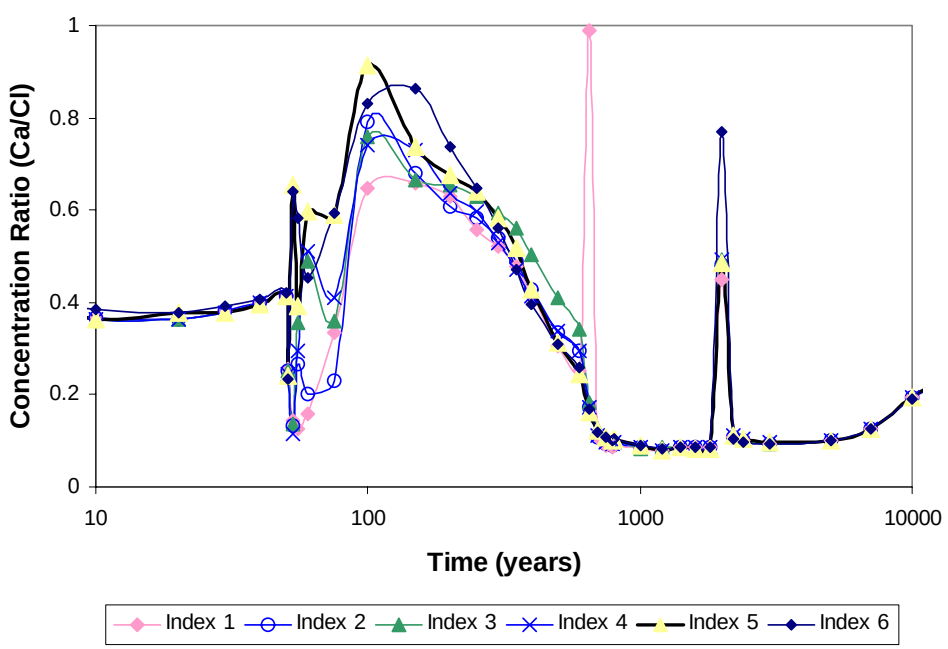

DTN: LB0302DSCPTHCS.002 [DIRS 161976]

Figure 6.6-3. Ca to Cl Ratio in thc6_w0_r.xls Fracture Top Front Waters

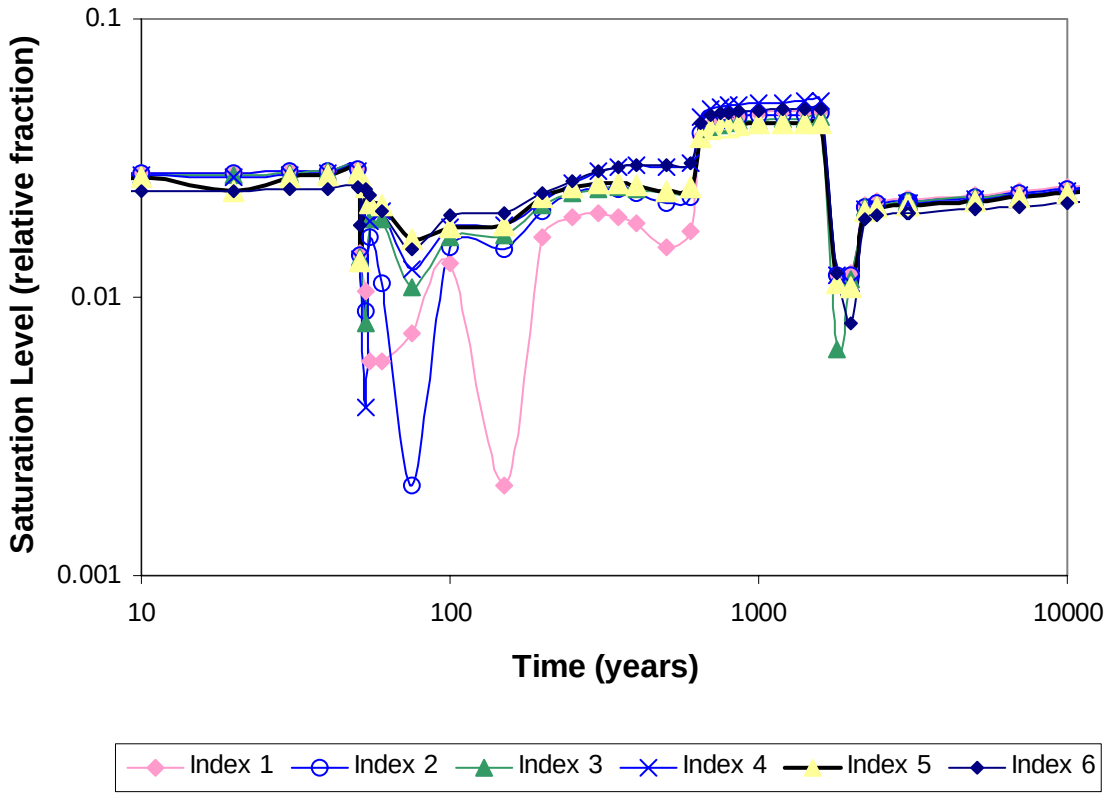

DTN: LB0302DSCPTHCS.002 [DIRS 161976]

Figure 6.6-4. Fracture Saturation Level in thc6_w6_r.xls Fracture Top Front Waters

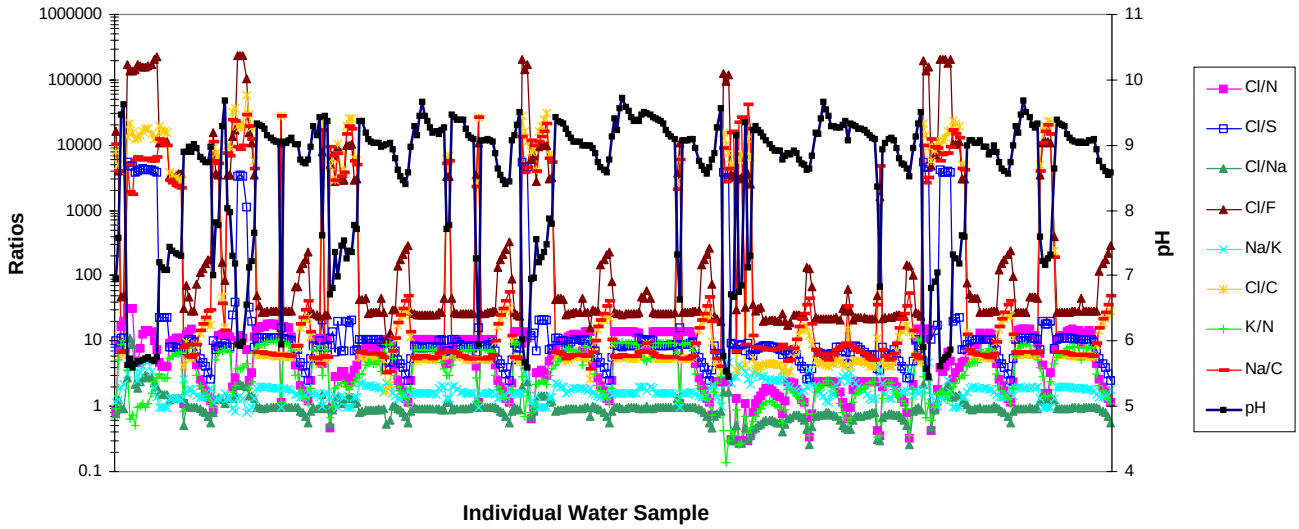

DTN: MO0310SPAEBSCB.003

Figure 6.6-5. Selected Molal Ratios (Cl/N, Cl/S, Cl/Na, Cl/F, Na/K, Cl/C, K/N, and Na/C) from the Evaporation of the 368 Seepage Waters to 65 Percent Relative Humidity, Used in the Binning Analysis to Establish Binning Criteria

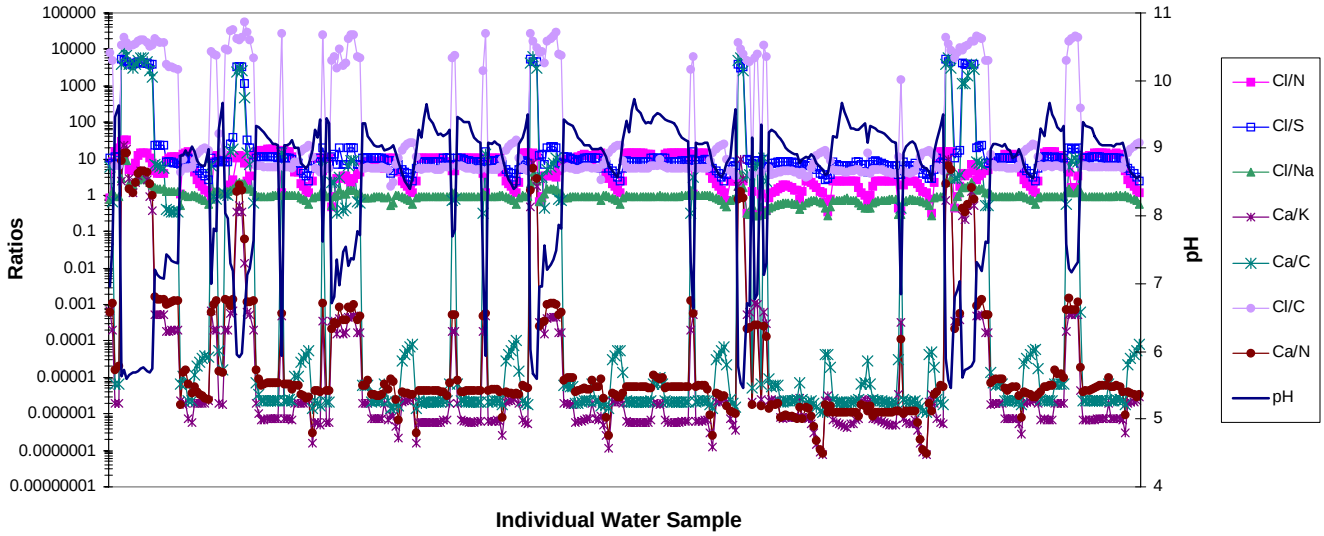

DTN: MO0310SPAEBSCB.003

Figure 6.6-6. Selected Molal Ratios (Cl/N, Cl/S, Cl/Na, Ca/K, Ca/C, Cl/C and Ca/N) from the Evaporation of the 368 Seepage Waters to 65 Percent Relative Humidity, Used in the Binning Analysis to Establish Binning Criteria

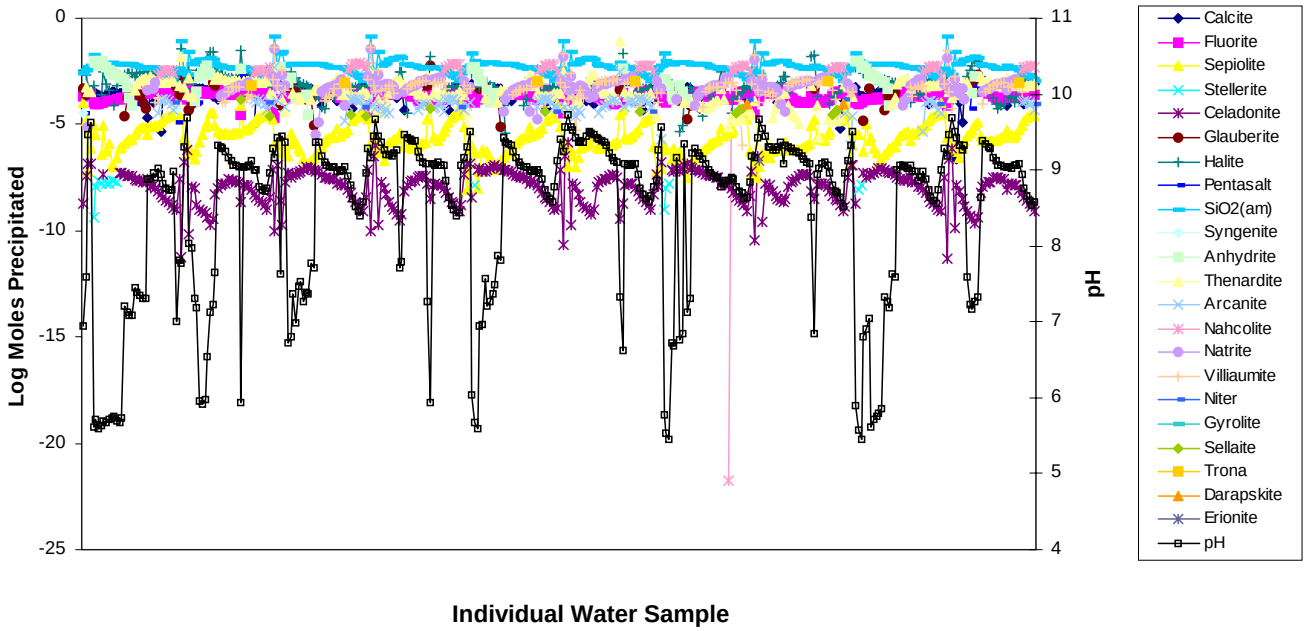

DTN: MO03108SPAEBSCB.003

Figure 6.6-7. Mineral Assemblages of the 368 Selected Seepage Waters After Evaporation to 65 Percent Relative Humidity

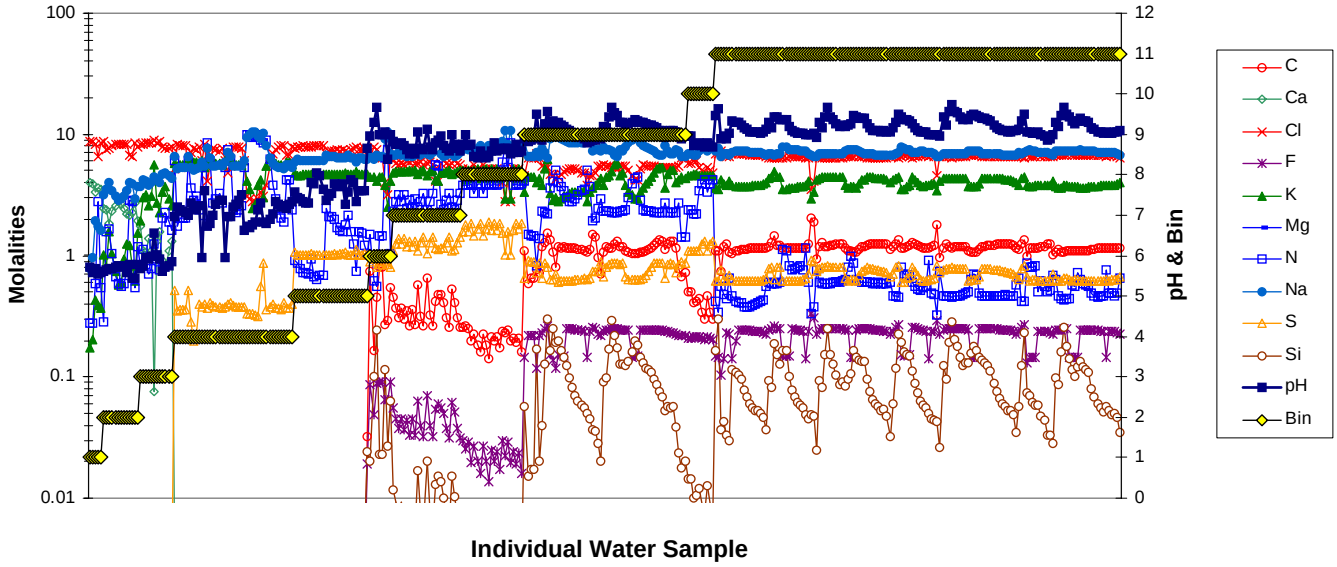

DTN: MO0310SPAEBSCB.003

Figure 6.6-8. Evaporated Water Compositions for All Bins Sorted by Bin After Evaporation to 65 Percent Relative Humidity

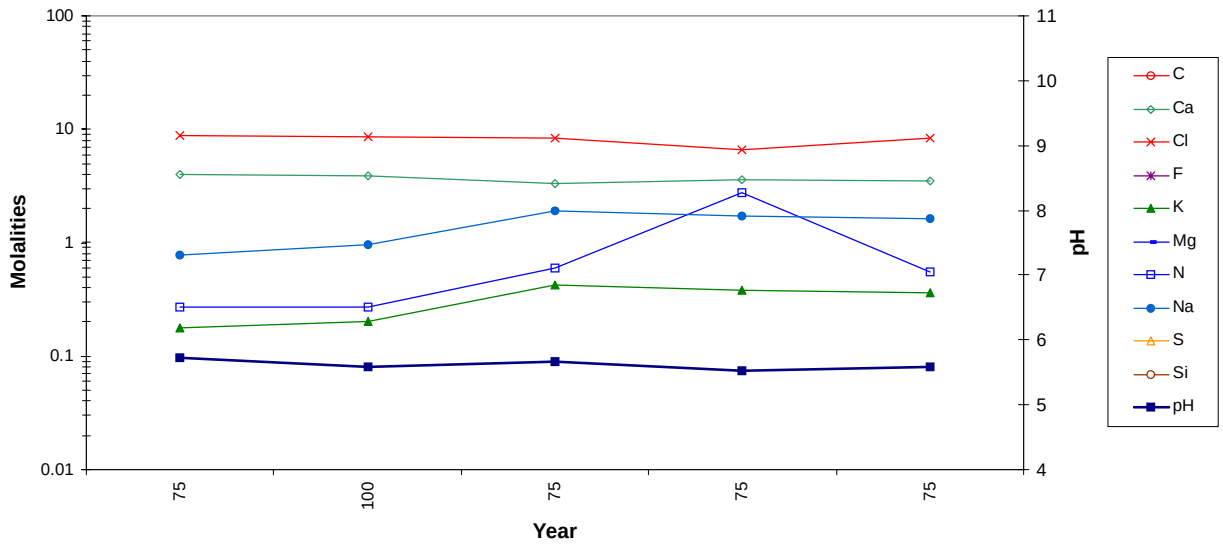

DTN: MO0310SPAEBSCB.003

Figure 6.6-9. Evaporated Water Compositions for Bin 1 After Evaporation to 65 Percent Relative Humidity

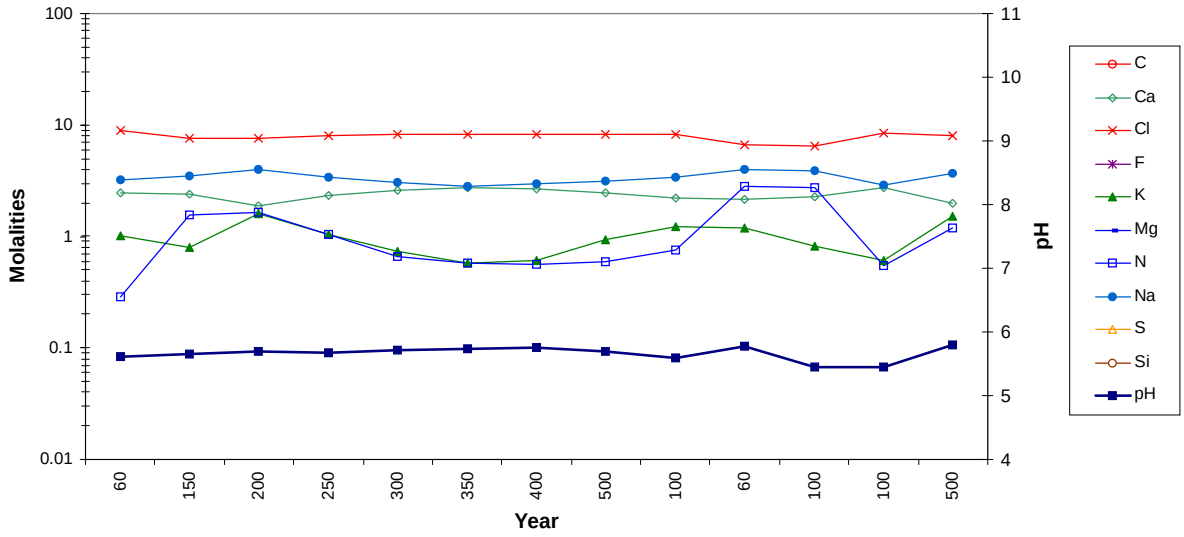

DTN: MO0310SPAEBSCB.003

Figure 6.6-10. Evaporated Water Compositions for Bin 2 After Evaporation to 65 Percent Relative Humidity

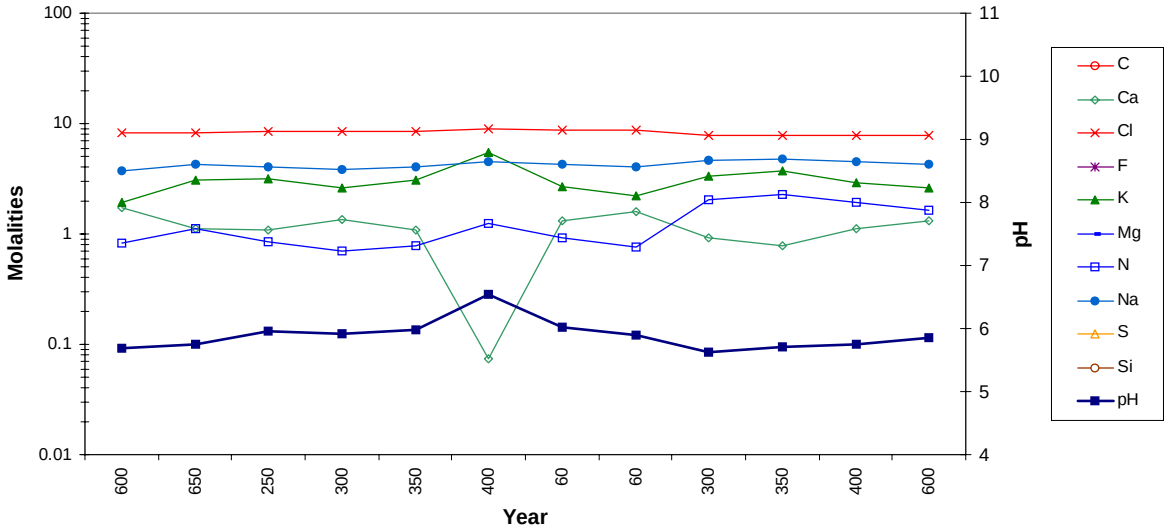

DTN: MO0310SPAEBSCB.003

Figure 6.6-11. Evaporated Water Compositions for Bin 3 After Evaporation to 65 Percent Relative Humidity

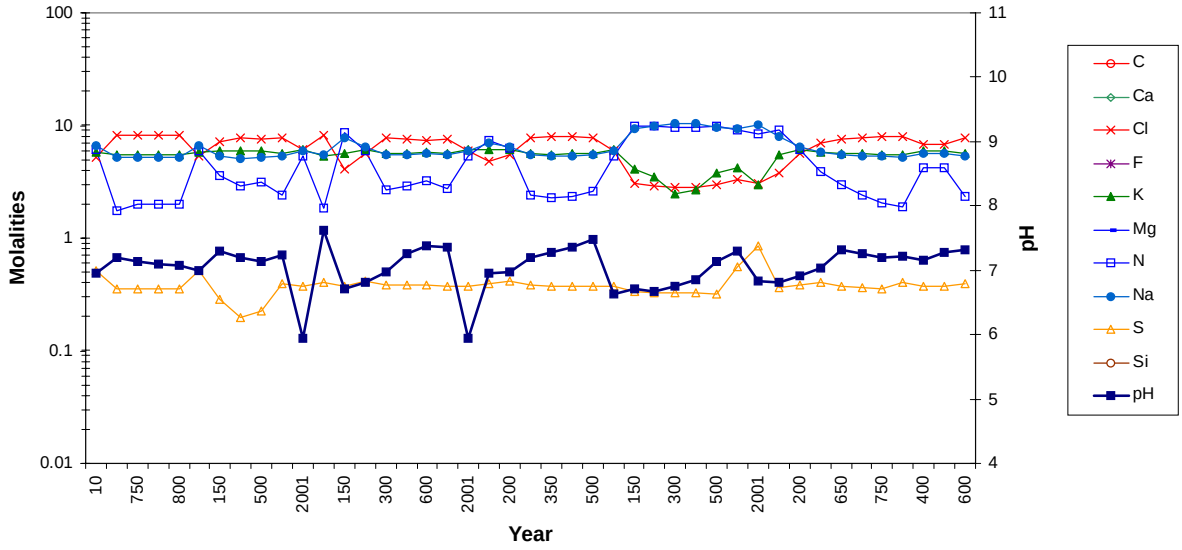

DTN: MO0310SPAEBSCB.003

Figure 6.6-12. Evaporated Water Compositions for Bin 4 After Evaporation to 65 Percent Relative Humidity

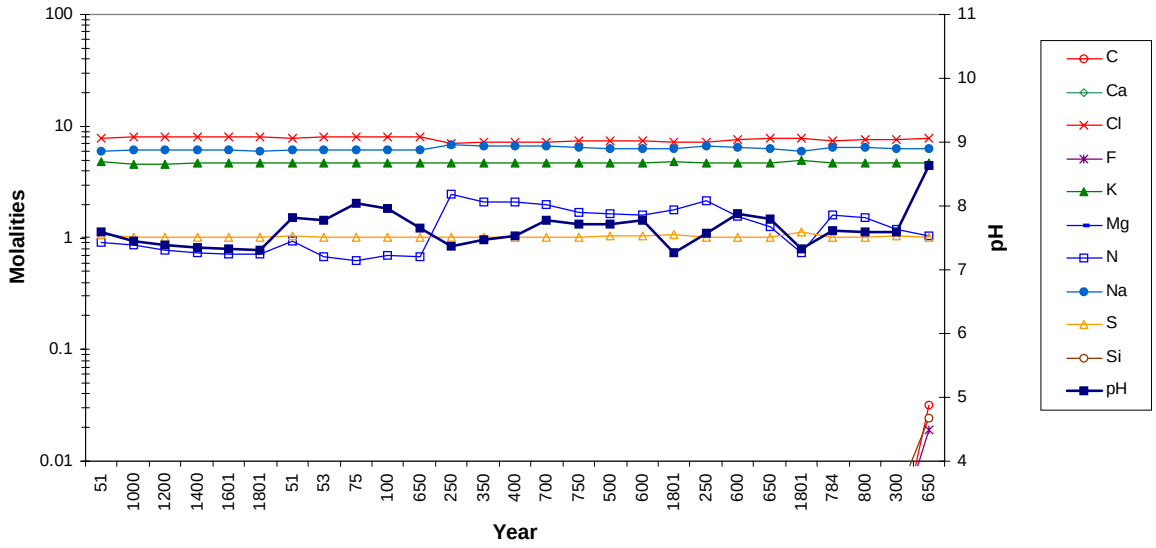

DTN: MO0310SPAEBSCB.003

Figure 6.6-13. Evaporated Water Compositions for Bin 5 After Evaporation to 65 Percent Relative Humidity

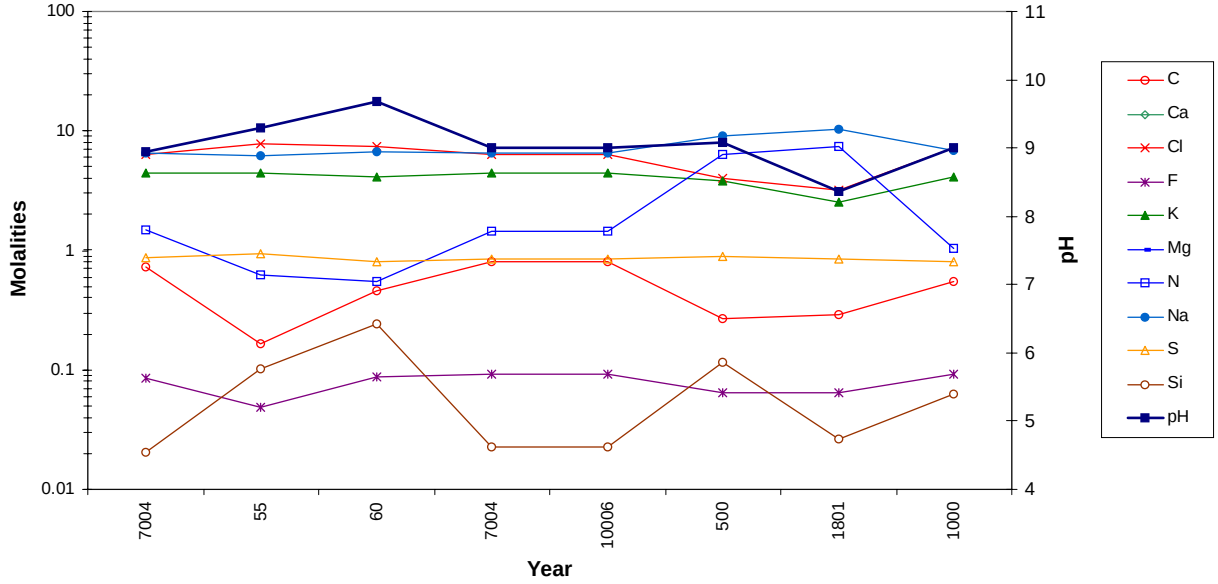

DTN: MO0310SPAEBSCB.003

Figure 6.6-14. Evaporated Water Compositions for Bin 6 After Evaporation to 65 Percent Relative Humidity

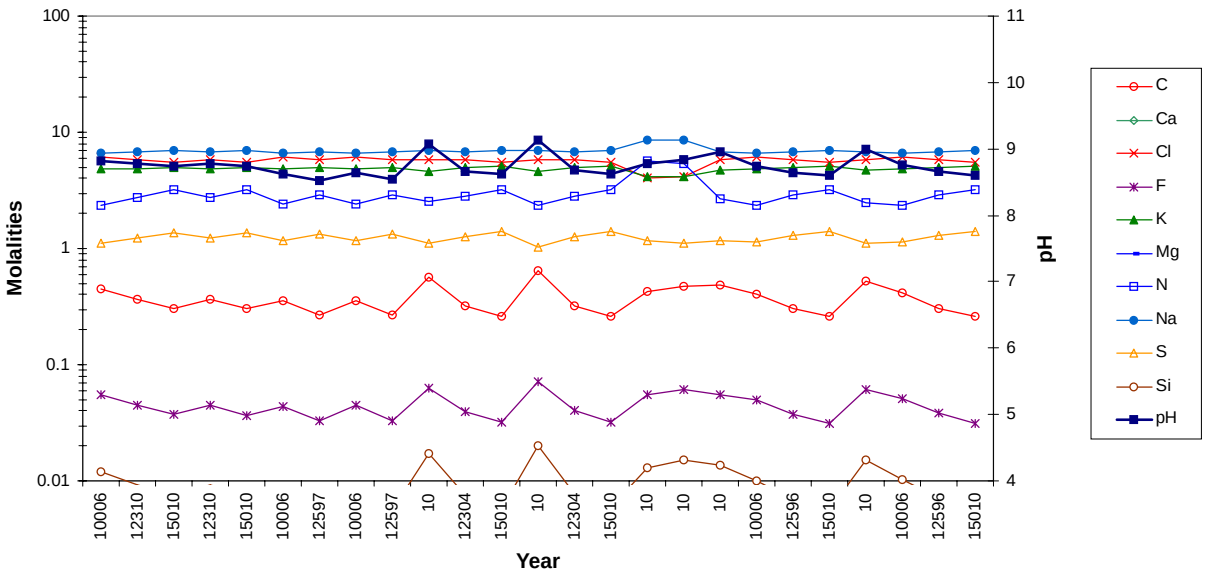

DTN: MO0310SPAEBSCB.003

Figure 6.6-15. Evaporated Water Compositions for Bin 7 After Evaporation to 65 Percent Relative Humidity

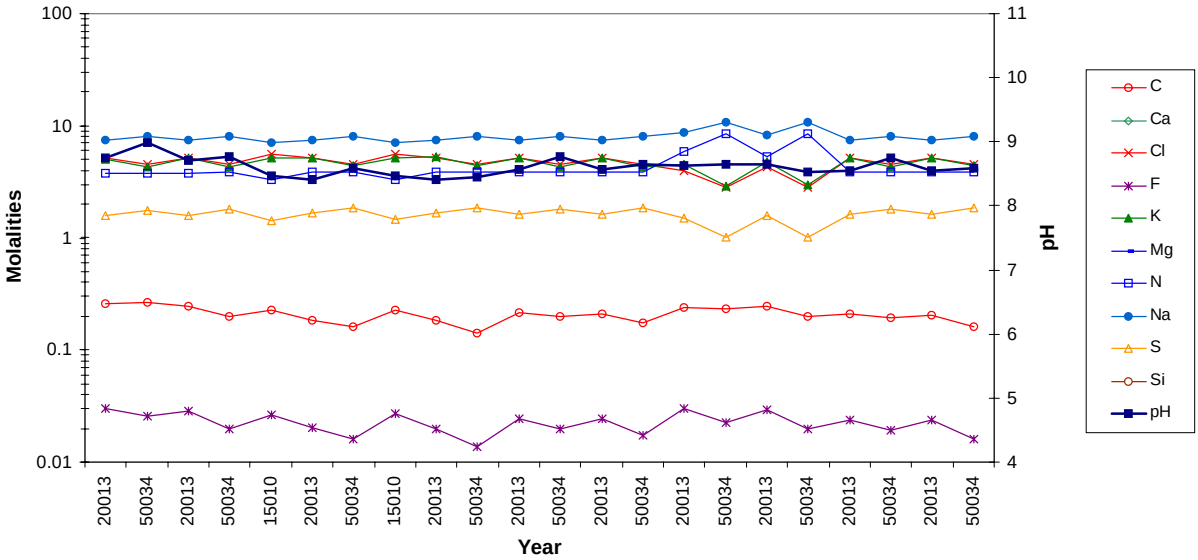

DTN: MO0310SPAEBSCB.003

Figure 6.6-16. Evaporated Water Compositions for Bin 8 After Evaporation to 65 Percent Relative Humidity

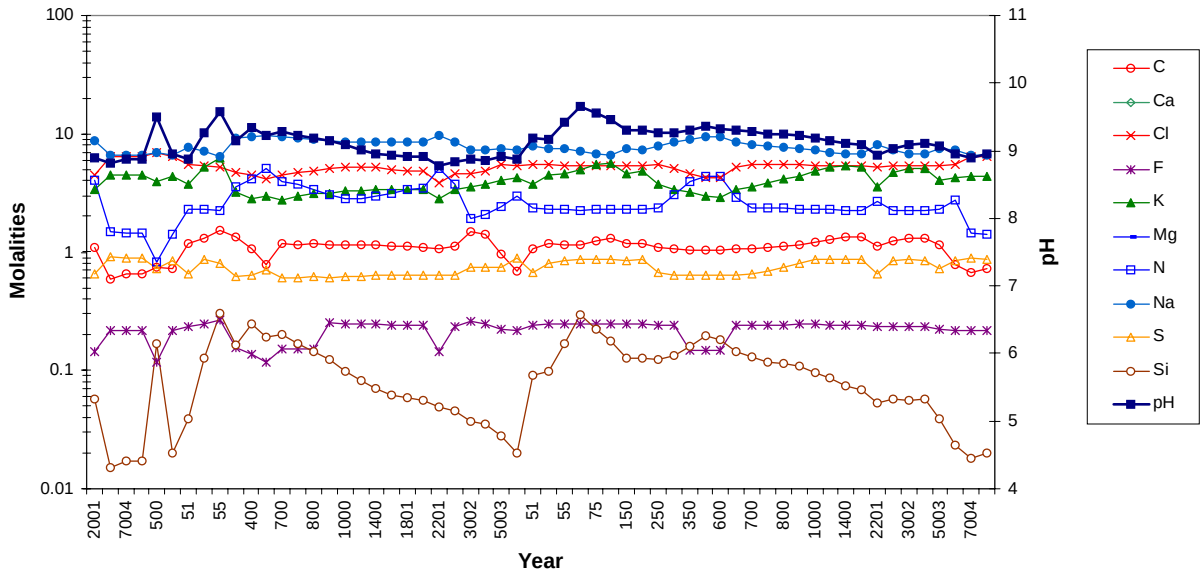

DTN: MO0310SPAEBSCB.003

Figure 6.6-17. Evaporated Water Compositions for Bin 9 After Evaporation to 65 Percent Relative Humidity

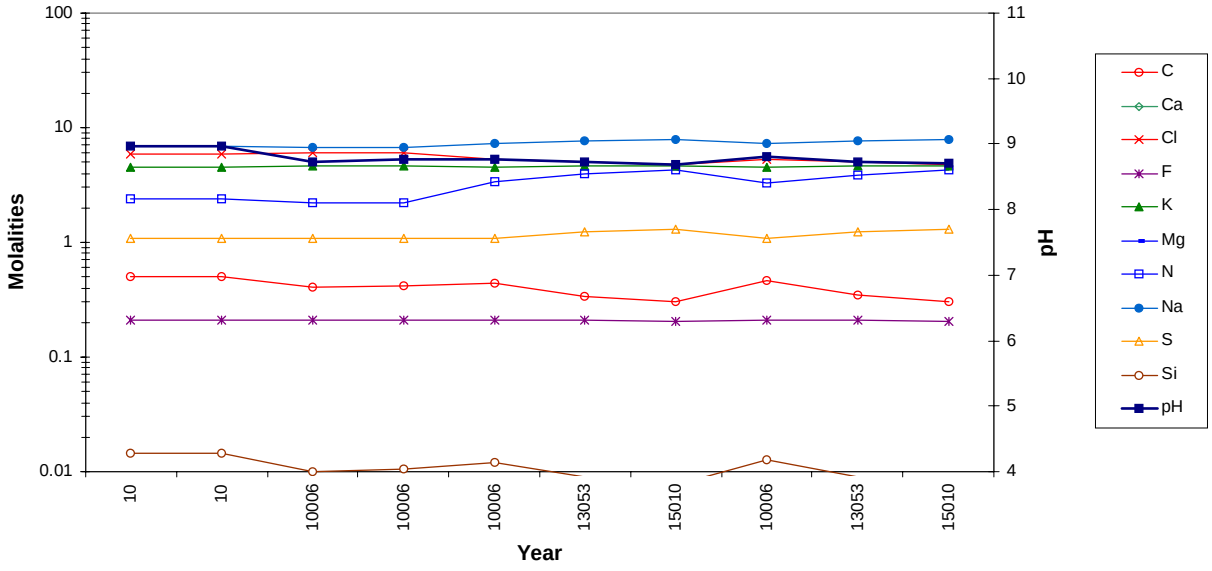

DTN: MO0310SPAEBSCB.003

Figure 6.6-18. Evaporated Water Compositions for Bin 10 After Evaporation to 65 Percent Relative Humidity

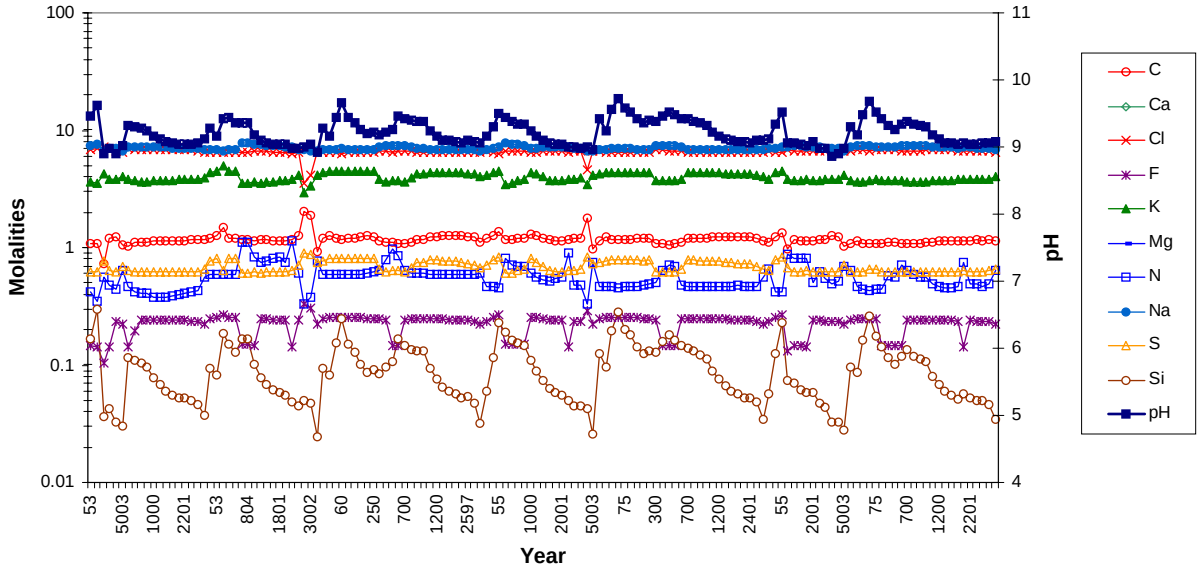

DTN: MO0310SPAEBSCB.003

Figure 6.6-19. Evaporated Water Compositions for Bin 11 After Evaporation to 65 Percent Relative Humidity

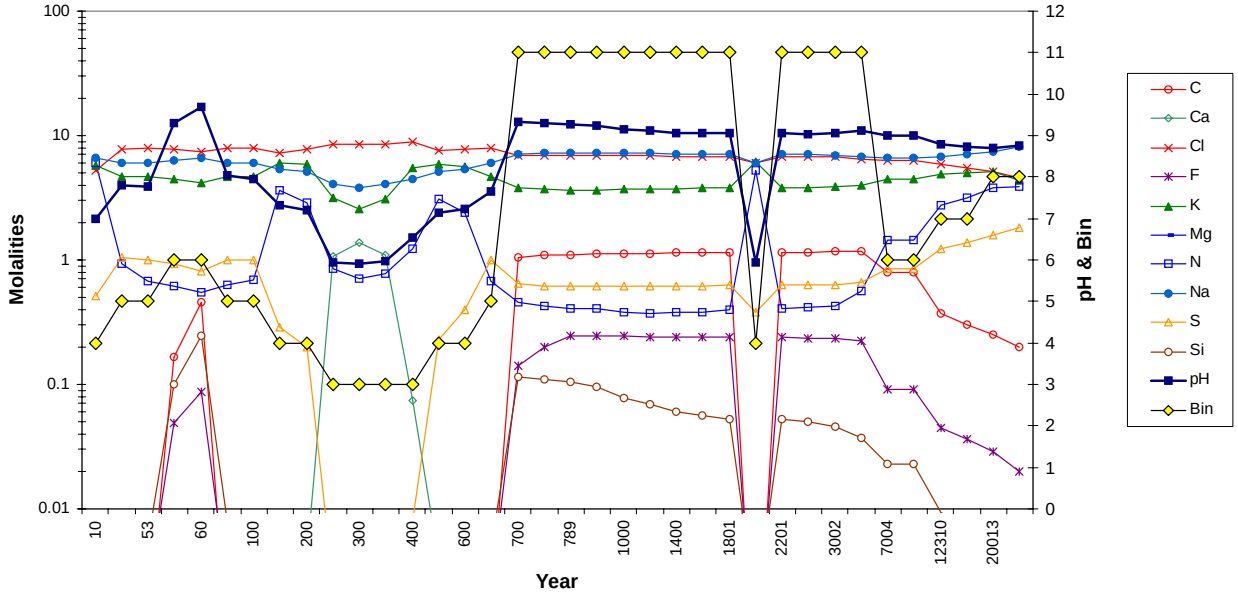

DTN: MO0310SPAEBSCB.003

Figure 6.6-20. Bins for Evaporated Crown Seepage: Case w0tf4

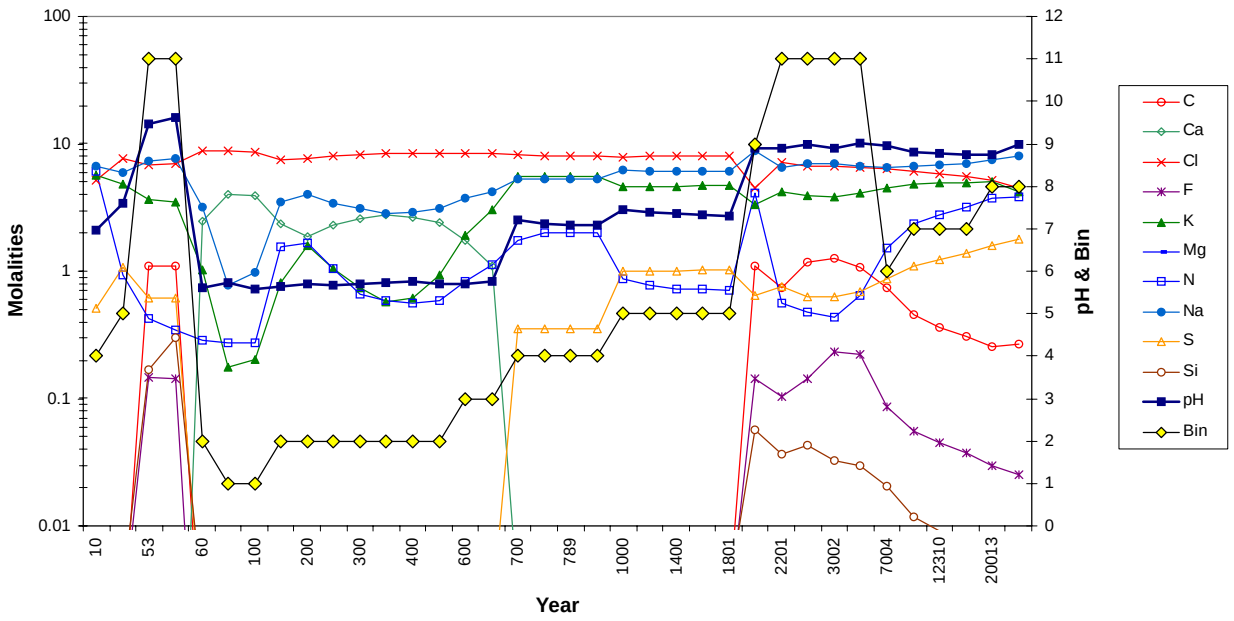

DTN: MO0310SPAEBSCB.003

Figure 6.6-21. Bins for Evaporated Invert Seepage: Case w0bf4

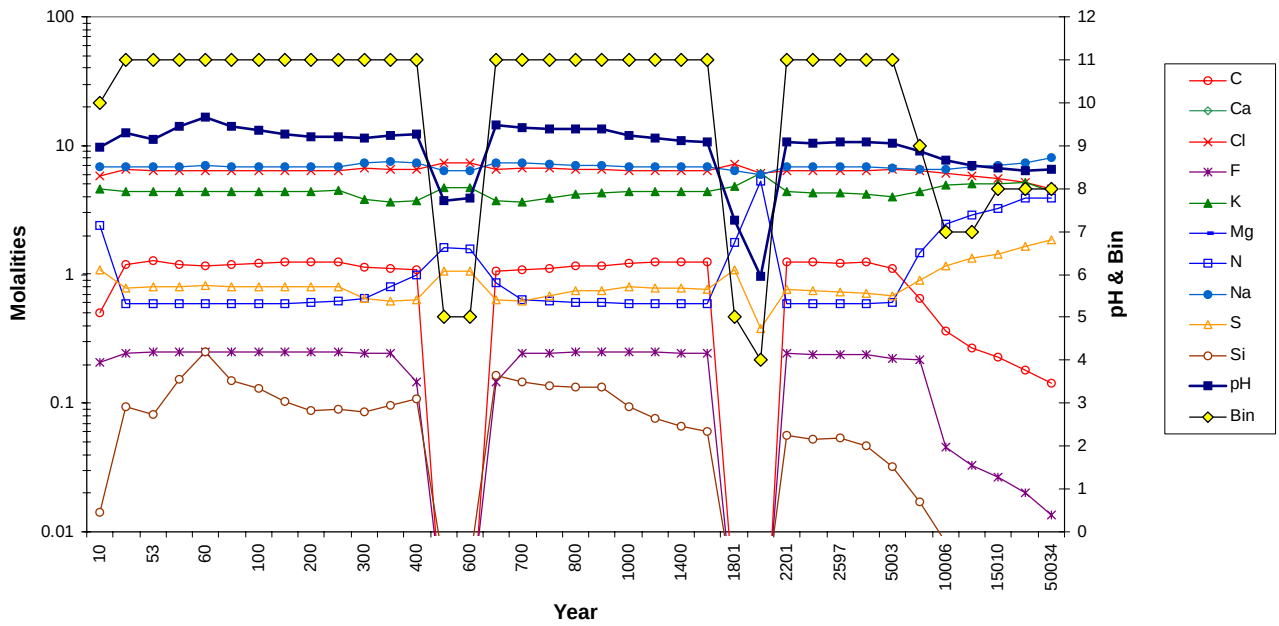

DTN: MO0310SPAEBSCB.003

Figure 6.6-22. Bins for Evaporated Crown Seepage: Case w4tf4

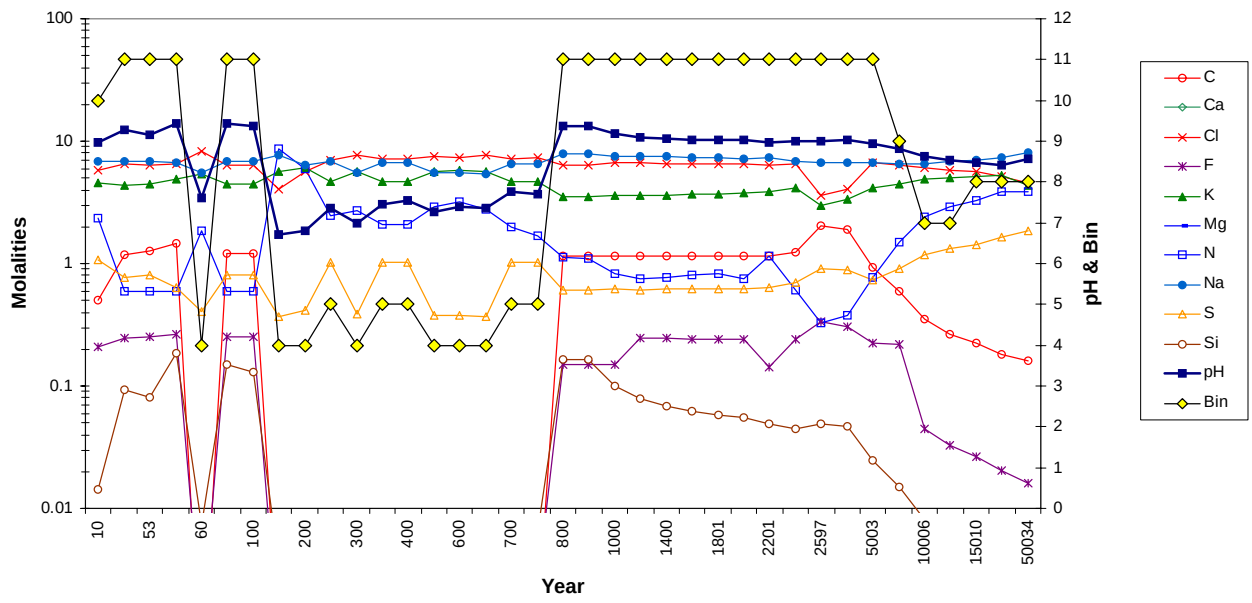

DTN: MO0310SPAEBSCB.003

Figure 6.6-23. Bins for Evaporated Invert Seepage: Case w4bf4

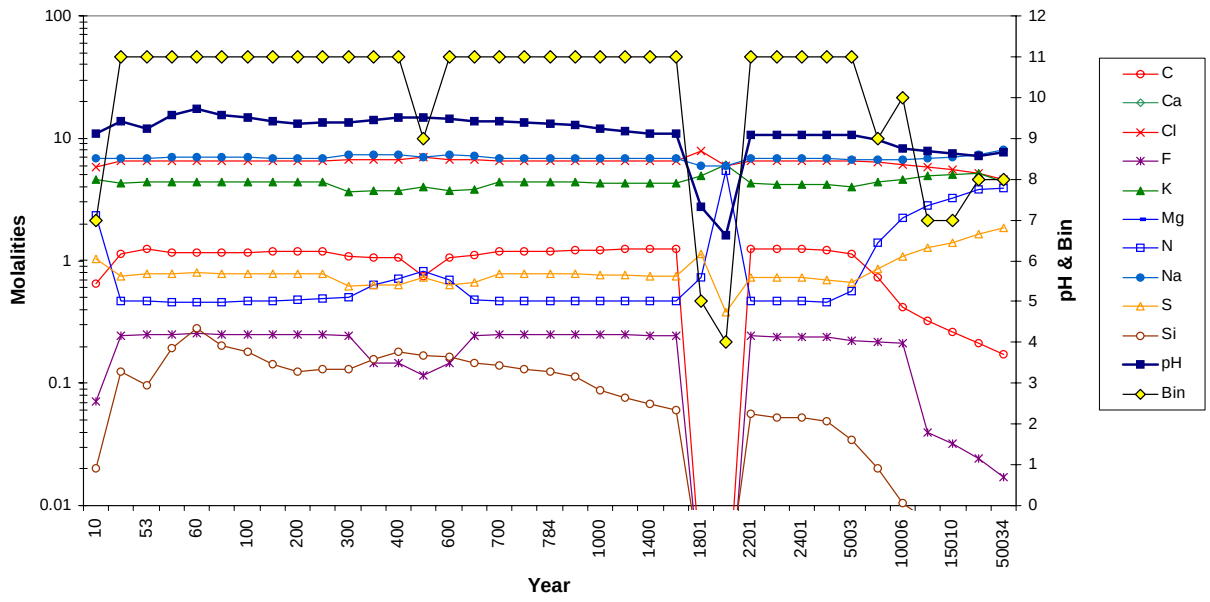

DTN: MO0310SPAEBSCB.003

Figure 6.6-24. Bins for Evaporated Crown Seepage: Case w5tf4

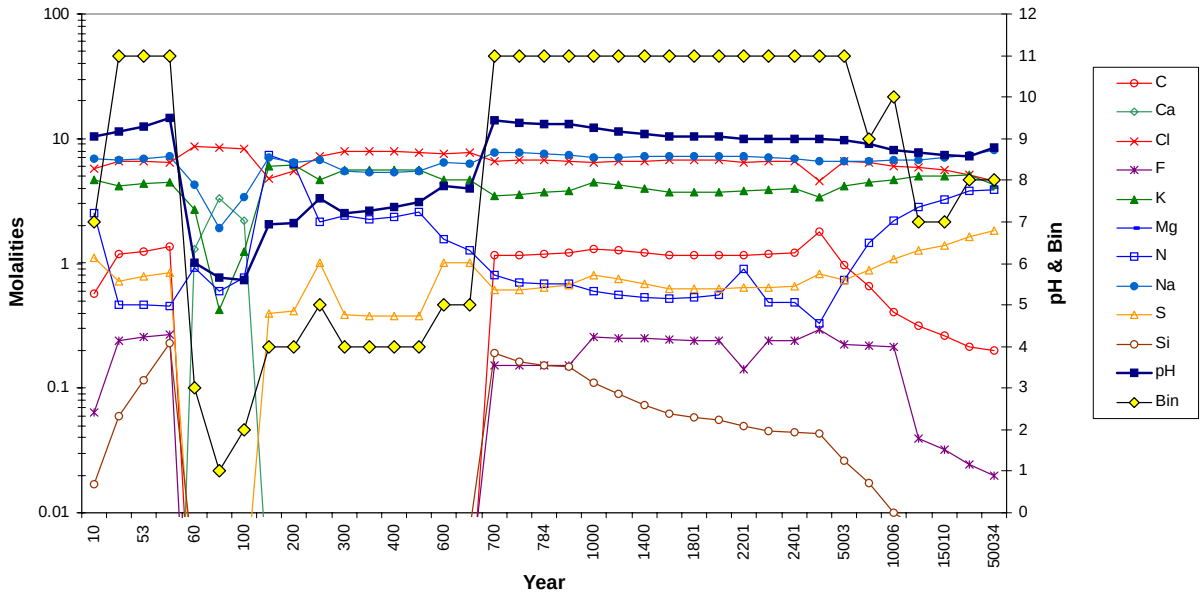

DTN: MO0310SPAEBSCB.003

Figure 6.6-25. Bins for Evaporated Invert Seepage: Case w5bf4

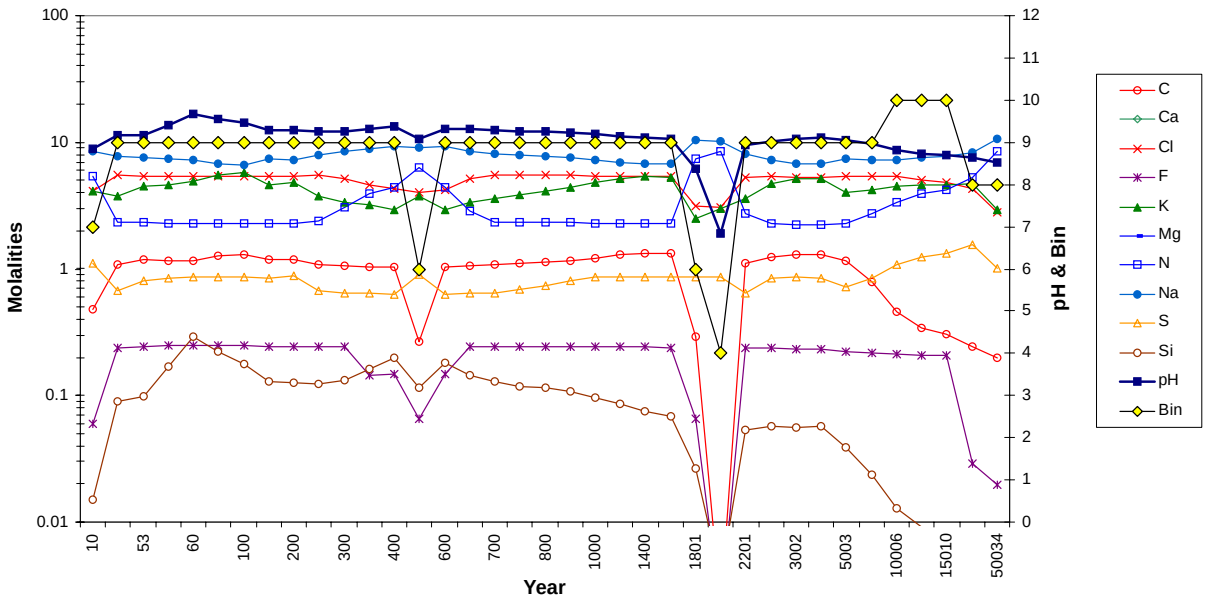

DTN: MO0310SPAEBSCB.003

Figure 6.6-26. Bins for Evaporated Invert Seepage: Case w6tf4

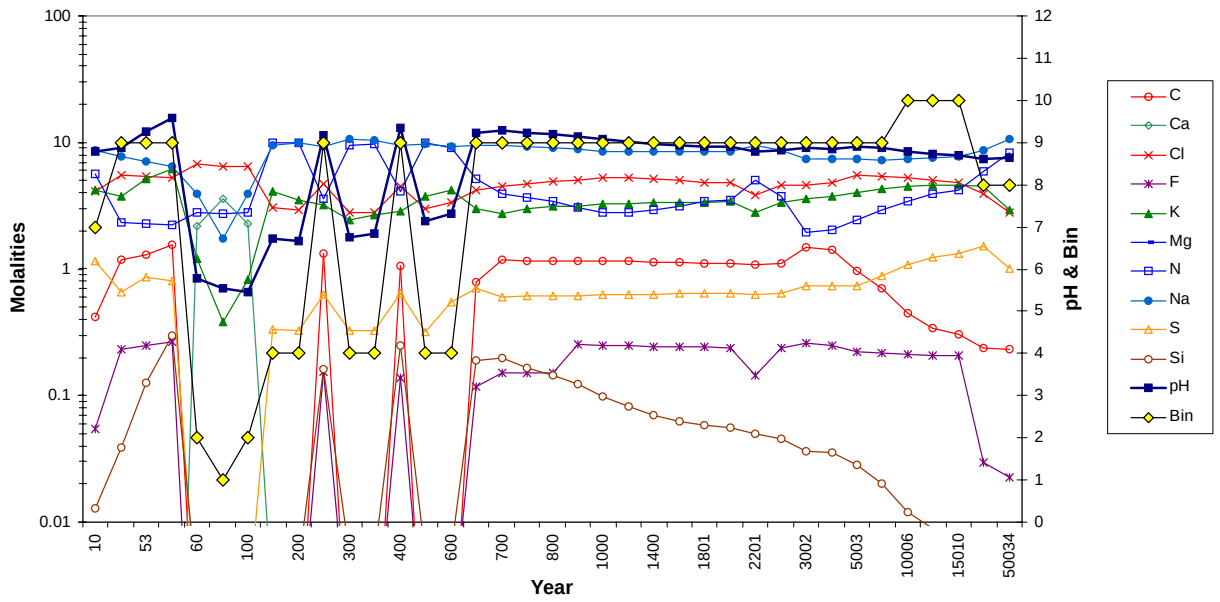

DTN: MO0310SPAEBSCB.003

Figure 6.6-27. Bins for Evaporated Invert Seepage: Case w6bf4

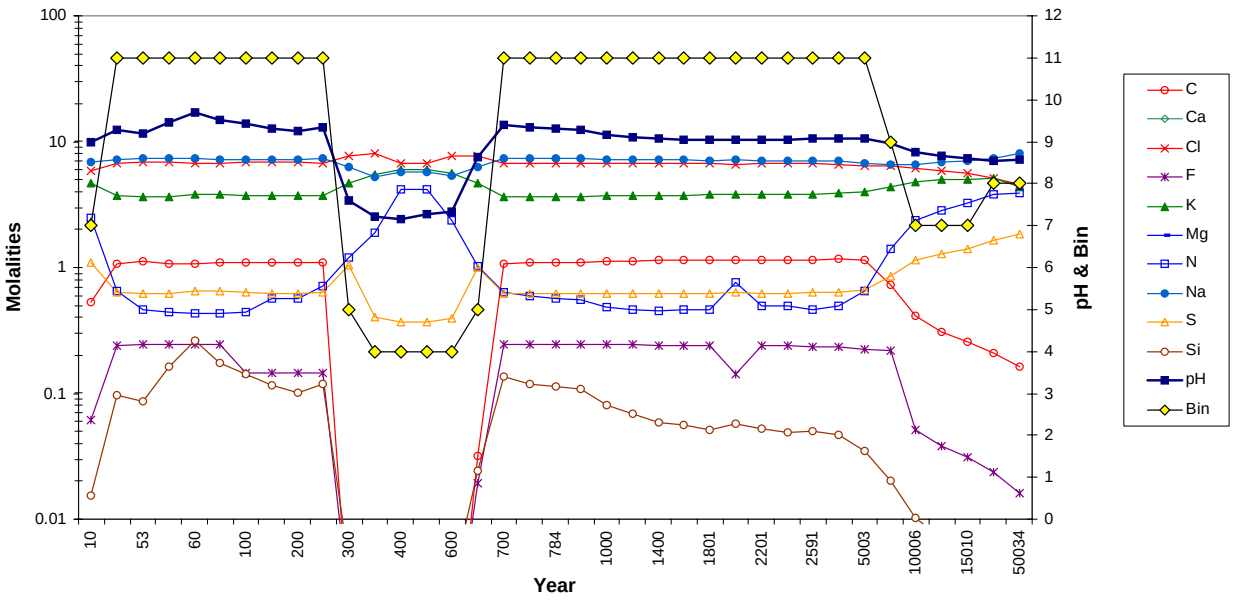

DTN: MO0310SPAEBSCB.003

Figure 6.6-28. Bins for Evaporated Invert Seepage: Case w7tf4

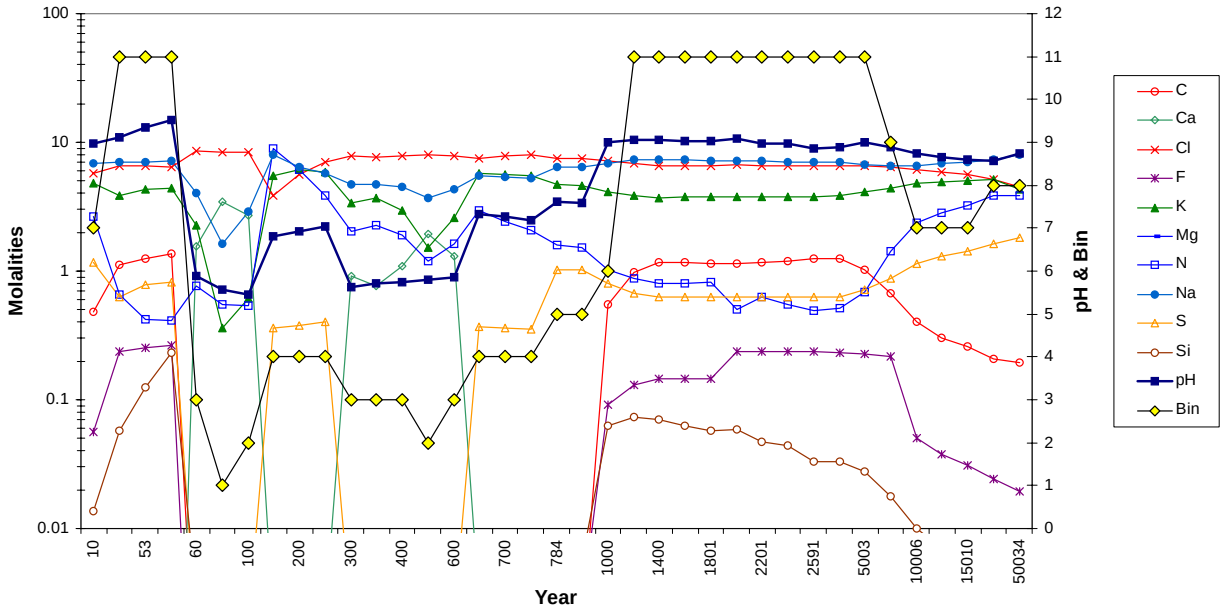

DTN: MO0310SPAEBSCB.003

Figure 6.6-29. Bins for Evaporated Invert Seepage: Case w7bf4

6.7 EVOLUTION OF IN-DRIFT GAS AND TEMPERATURE

The purposes of this section are:

- To analyze oxygen demand in the drift. This determines the potential (given the large masses of introduced materials in the drift) for the development of oxygen-deficient conditions.
- To establish the expected range of Pco_2 through time and derive look-up tables for this parameter for the TSPA-LA.
- To establish the expected range of in-drift temperatures, for use in deriving look-up tables.
- To report values of trace gas fugacities in equilibrium with the initial THC seepage and dust leachate waters used as inputs to this model.

6.7.1 O_2 Mass Balance Evaluations

A mass balance, based on one-meter length of drift, is calculated to determine the potential for the development of oxygen deficient conditions in the drift. The calculation involves (1) an estimate of oxygen flux into the drift through the walls and along the axis of the drift, and (2) estimates of oxygen consumption due to corrosion of the emplaced materials at corrosion rates specified in Section 6.4. Oxygen consumption due to microbial activity is expected to be low compared to oxygen consumption due to corrosion and is therefore not covered in the oxygen consumption calculation (CRWMS M&O 2000 [DIRS 151561], Section 6.6.5.4)

The estimate of oxygen flux begins with calculating the gas flux across the drift wall and into the drift, based on results from the *Drift-Scale Coupled Processes (DST and THC Seepage) Models* (BSC 2003 [DIRS 162050]). The THC model presents values of flux into (or out of) the drift at the crown, side, and base of the drift at each time step (DTN: MO0312SPAPCEGF.002, spreadsheet “gas flux.xls”, tab “fractures-th”, columns titled “Gflux”). At early times (250 - 1800 years after closure) the flow direction of the gas flux is *inward* at the crown and sides, and *outward* at the base. After 2000 years the direction changes, and the flow of gas is *inward* at the sides and base and *outward* at the crown. To estimate the gas flux into the drift, the location with the highest inward flux (for example, the base of the drift at time > 2000 years) was used to calculate the flux into the drift for the entire drift wall. Applying an inward flux to the entire wall, and not considering the outward flux was intended to more accurately represent the flux that would be available in the drift. The THC model does not take into account flow along the axis of the drift and therefore, taking the net flow into the drift (flow inward minus flow outward), would be an underestimation of the actual flux that would be expected in a three-dimensional drift. Additionally, diffusive flux of oxygen along the axis of the drift would be expected, because corrosive conditions would develop at different times and therefore, areas with corrosion occurring would likely be surrounded by oxygen-rich environments in which corrosion is not occurring.

The oxygen flux is calculated using the following values (DTN: LB0302DSCPTHCS.002 [DIRS 161976], spreadsheet "thc6_w0_drift_r.xls):

- Gas flux at the crown, base, and side of the drift
- Mass fraction of air in the gas (with the remainder being water vapor)
- Volume fraction of CO_2 in the gas
- The surface area of the drift wall for which the gas flux calculation was performed.

The following inputs are also needed:

- The volume fraction of oxygen, nitrogen, and argon in the earth's atmosphere (Weast and Astle 1979, p. F-211 [DIRS 102865])

- The atomic weights of the elements (Parrington et al. 1996, pp. 62-63 [DIRS 103896])

- The diameter of an emplacement drift (BSC 2003 [DIRS 162101]).

The results of these calculations are plotted in Figure 6.7-1, which shows the molar O_2 and CO_2 gas fluxes into the drift per year per linear meter of drift (DTN: MO0312SPAPCEGF.002, spreadsheet "gas flux.xls"). At 2,000 years, the gas flux increases, which also causes the O_2 and CO_2 to increase. This increase coincides with the temperature dropping significantly below 100°C (approximately 91°C) and, with the return of the liquid saturation in the rock, to values similar to pre-emplacement levels (Figures 6.8-4, 6.8-7 and 6.8-8 BSC 2003 [DIRS 162050]).

The second step in the mass balance is to calculate the oxygen consumption rate of the introduced materials as they corrode for three cases:

- Corrosion of materials outside of the waste package
- Corrosion of commercial waste packages (21 PWR)
- Corrosion of DOE SNF codisposal waste packages (N-Reactor)

The materials outside the waste package are expected to start corroding as soon as the repository is cooled enough to allow water to enter the drift. The materials inside the waste package are not expected to corrode until the corrosion-resistant (Alloy 22) outer shell is breached, long after the end of the regulatory period. However, the corrosion of materials in the waste package is included in the oxygen consumption calculations as an upper bound of oxygen consumption. Using the mass and nominal thickness values from Table 4.1-1 through Table 4.1-3 and the corrosion rates listed in Table 6.4-18, the oxygen consumption rate due to corrosion of all materials outside the waste package (ground support, invert, gantry rail, emplacement palate, and drip shield) is calculated (DTN: MO0312SPAPCEGF.002, spreadsheet "Oxygen Demand," tab "Non-Waste package"). A ratio of 1.5 moles of O per mole of metal is used in the calculation, based on the formation of hematite (Fe_2O_3)—the most thermodynamically stable form of iron oxide. This ratio is a maximum for Fe oxidation, which can also occur by reactions not requiring free oxygen, involving breakdown of water and generation of H_2. The O_2 consumption for materials outside the waste package is calculated using the mean and minimum corrosion rates listed in Table 6.4-18, and is plotted versus time after closure and cool-down (when conditions allow water to enter the drift) in Figure 6.7-2. The average oxygen supply rate that is expected

during the period from 100 to 10,000 years after closure is also plotted. This period was chosen because it is after the occurrence of major gas flux fluctuations in the first 100 years (Figure 6.7-1). The plots in Figure 6.7-2 shows that if minimum degradation rates are considered, the system will be oxygen-limited for the first 250 years after closure and cool-down of the repository. When the mean degradation rates are used, the repository system will be oxygen-limited for 100 years. Since corrosion proceeds much more slowly in an oxygen-deficient atmosphere, a more realistic plot is one in which the corrosion is limited by the O_2 supply. The minimum degradation rates are multiplied by a factor of 0.5 (found by trial and error) such that the O_2 consumption rate is equal to the supply. The Figure 6.7-2 plots also show that when corrosion is limited by the O_2 supply, the oxygen-limited period lasts for 500 years.

A calculation of oxygen consumption is performed for all components of the commercial SNF 21 PWR waste package. Of all the commercial SNF waste packages, the most common fuel type is 21 PWR. Therefore, this package has been chosen to represent all commercial SNF waste packages in the oxygen consumption calculation. The moles (based on 100 g/mole) and surface areas for all components in the 21 PWR waste package (DTN: MO0210MWDEXC01.008 [DIRS 163531], spreadsheet "CSNF WP Model Abstraction.xls") are used to calculate the oxygen consumption rate (DTN: MO0312SPAPCEGF.002, spreadsheet "Oxygen Demand," tab "21 PWR Summary"). As explained in the previous paragraph, a ratio of 1.5 moles of O per mole of metal is used in the calculation. Since the uranium in the UO_2 spent fuel is present in the (IV) state and can be oxidized to U(VI), a ratio of one mole of O per mole of UO_2 spent fuel was used to calculate the oxygen consumption of the fuel. The outer shell of the waste package, composed of Alloy-22, is not included in the calculations due to the low degradation rate. The calculated oxygen supply rate at 10,000 years after closure is plotted in Figure 6.7-3 for comparison with the oxygen consumption calculations. This time was chosen because the waste package is not expected to be breached until after the end of the regulatory period. The Figure 6.7-3 plots shows that, for the 21 PWR waste package, the oxygen-limited conditions will last less than 25 years after a waste package breach for the minimum degradation rate, and less than 100 years for the mean degradation rate. When the O_2 consumption is limited by the supply (multiplying the minimum degradation rates by 0.1), the oxygen-limited period lasts for just over 100 years.

The N-reactor waste package has been chosen to represent the DOE SNF waste packages since it contains the most uranium metal of all the DOE SNF waste packages, which could be a major contributor to oxygen consumption. The oxygen demand for N-reactor fuel is calculated based on information presented in Tables 4.1-8, 4.1-12, and 4.1-17, and is plotted in Figure 6.7-4. The N-reactor fuel is included in the calculation, along with the rest of the materials in the waste package, using a ratio of 1.5 moles of O per mole of metal for the steels and 3 moles of O per mole of uranium in the fuel (DTN: MO0312SPAPCEGF.002, spreadsheet "Oxygen Demand," tab "N-Reactor". The high-level waste glass and the outer shell of the waste package composed of Alloy-22, are not included in the calculations due to their low degradation rates. The calculated oxygen supply rate at 10,000 years after closure is plotted in Figure 6.7-4 for comparison with the oxygen consumption calculations. Figure 6.7-4 shows that for the N-reactor waste package, the oxygen-limited conditions will last less than 10 years after waste package breach for the minimum and mean degradation rates. When the O_2 consumption is limited by the supply (multiplying the minimum degradation rates by the factor 0.02), the oxygen-limited

period lasts for about 130 years. In this case, the factor is very small because the degradation rate of the N-reactor fuel is so rapid.

Figures 6.7-2 through 6.7-4 show that if oxygen deficient conditions are formed in the drift due to degradation of emplaced materials, the longest period of reduced oxygen conditions (corresponding to the data series titled "O2 consumption constrained by supply" on the figures) would last less than 500 years. Since the period is short, compared to the regulatory period, it is reasonable to use the atmospheric oxygen values for the EQ3/6 calculations used to generate the look-up tables for the TSPA-LA.

6.7.2 Thermal-Hydrological-Chemical Seepage Model In-Drift CO_2 Gas and Temperature Abstraction

The Pco_2 and temperature in the drift environment can affect chemical processes, such as radionuclide solubility. As an illustration, the uranium concentration in equilibrium with schoepite ($UO_3 \cdot 2H_2O$) is shown to be at least ten times higher for $Pco_2=10^{-2}$ bar compared to $Pco_2=0$ for pH>7 (Langmuir 1997 [DIRS 100051], Figure 13.5). Section 6.7.2.1 provides the look-up tables for in-drift and invert Pco_2 values, which correspond to the seepage compositions presented in Section 6.6.5. Section 6.7.2.2 provides a range of values of Pco_2 and temperatures for construction of water chemistry look-up tables presented in Section 6.9.3.

6.7.2.1 Total Systems Performance Assessment - License Application Look-up Tables for Drift and Invert Pco_2

In conjunction with the seepage binning and bin maps presented in Section 6.6.6 (see Tables 6.6-8 to 6.6-12), the TSPA-LA requires look-up tables to constrain the Pco_2 within the drift and invert for each of the five seepage compositions (Section 4.1.3). These look-up tables (Tables 6.7-1 to 6.7-5) are prepared using the ten THC seepage model output files listed in Table 4.1-14. The tables are found in the Excel spreadsheet entitled "THC CO2 GAS & TEMP COMPARE.xls" (archived in DTN: MO0308SPACO2GL.001). The files of the type "thc6_XX_drift_r.xls," (where XX is the abbreviated water name) are the source of the in-drift values; and the files of the type "thc6_XX_r.xls," are the source for the invert values. The in-drift values represent the Pco_2 values at the crown taken from worksheet "fracture-ch." The invert values represent the Pco_2 with the following designations: quadrant = bottom, zone = front, worksheet = "matrix-ch", index = 4. Section 6.6.2 provides additional information concerning these equations.

The Pco_2 values are plotted as a function of time in Figures 6.7-5 and 6.7-6. Figure 6.7-5 is a log-log plot of all the values; whereas Figure 6.7-6 is a linear plot of the in-drift values only. The atmospheric Pco_2 (Weast and Astle 1979, p. F-211 [DIRS 102865]) is also plotted for reference purposes. Both figures show the Pco_2 values for various spatial locations, namely, within the drift, in the rock near the drift wall crown, and near the base of the invert.

6.7.2.2 CO_2 and Temperature Values for Construction of Water Chemistry Abstraction Look-up Tables

The intent of the in-drift seepage evaporation abstraction (Section 6.9) is to take the 11 bin water values abstracted in Section 6.6 and calculate the resulting composition after evaporation using the in-drift precipitates (salts) model to generate look-up tables for use in the TSPA-LA. For the evaporation calculations, a range of temperatures and carbon dioxide fugacities is needed to capture the effects of these parameters on the evaporative evolution.

To determine the $P\mathrm{co}_2$ range, the $P\mathrm{co}_2$ values presented in the "THC CO2 GAS & TEMP COMPARE.xls" spreadsheet (DTN: MO0308SPACO2GL.001) were statistically analyzed using the built-in functions in the Microsoft Excel 97 software application. The overall fugacities range from a maximum of 1.75×10^{-2} bar (CS500, invert) to a minimum of 2.29×10^{-5} bar (HD-Perm, in-drift). The median value is determined to be 3.01×10^{-3} bar. The majority of values fall between 1.0×10^{-4} and 1.0×10^{-2} bar and only six values fall below 1.0×10^{-4} bar, or about 0.82 percent of all data points. The upper limit, or 95th percentile, value for all data points is 8.8×10^{-3} bar. Based on the statistical analysis, the three values selected for use are 1.0×10^{-2}, 1.0×10^{-3}, and 1.0×10^{-4} bar. Sensitivity cases have been run using a larger range of $P\mathrm{co}_2$ (see Section 6.12.4.3).

The in-drift temperature range (Figure 6.7-7) is constructed using the following four time-temperature curves: the waste package node, the drift wall surface at the crown of the drift, the base of invert, and within the rock above the crown of the drift (spreadsheet "THC CO2 GAS & TEMP COMPARE.xls" in DTN MO0308SPACO2GL.001). The plotted curves of Figure 6.7-7 indicate that the minimum temperature in the drift after 20,000 years is 40°C. The maximum in-drift temperature can be as great as 160°C on the waste package surface and 140°C at the drift wall during the peak thermal pulse. However, an evaluation of the Figure 6.7-7 curves shows that only in the period from 50 to approximately 2,000 years do temperatures go above 100°C, which is the time when liquid water available for macroscale reaction is limited by the temperature pulse in the drift (see Figure 6.2-4). Accurate modeling is also limited to temperatures of 100ºC or less because of the limits imposed by the boiling point at the elevation of the drift, uncertainties in the boiling point elevation due to concentration of pore water salts, and temperature limitations on the applicability of some thermodynamic data in the Data0.yfp database (DTN: SN0302T0510102.002 [DIRS 162572]). Therefore, an upper calculation limit of 100°C is within an acceptable range of calculational uncertainty. With an upper- and lower-bound determined, the midpoint between these two bounding points is selected (70°C). The three temperatures (40°C, 70°C, and 100°C) are used to construct the look-up tables for use in the analyses described in the following section and for the construction of the look-up tables for the TSPA-LA.

Table 6.7-1. Look-up Tables for Total System Performance Assessment-License Application Analysis of In-Drift and Invert Pco_2 for W0 (HD-PERM) Seepage Water

w0, HD-PERM		Drift	Invert
Start (year)	**End (year)**	**Partial Pressure $CO_{2(g)}$ bars**	**Partial Pressure $CO_{2(g)}$ bars**
1.00	2.50	1.21E-03	2.43E-03
2.50	7.50	1.12E-03	1.58E-03
7.50	15.00	1.05E-03	1.26E-03
15.00	25.00	9.51E-04	9.89E-04
25.00	35.00	8.82E-04	9.39E-04
35.00	45.00	8.80E-04	1.01E-03
45.00	50.50	8.61E-04	9.54E-04
50.50	52.00	4.25E-04	1.69E-03
52.00	54.00	1.86E-04	1.04E-03
54.00	56.00	1.01E-04	5.13E-04
56.00	61.00	2.29E-05	7.82E-04
61.00	71.50	8.25E-05	1.32E-04
71.50	101.50	2.29E-04	2.53E-04
101.50	150.00	4.58E-04	4.75E-04
150.00	200.00	5.28E-04	5.53E-04
200.00	250.00	4.34E-04	4.34E-04
250.00	300.00	3.18E-04	3.20E-04
300.00	350.00	2.60E-04	2.49E-04
350.00	412.50	2.60E-04	2.39E-04
412.50	500.00	3.93E-04	3.68E-04
500.00	588.50	7.12E-04	6.85E-04
588.50	651.00	9.97E-04	9.14E-04
651.00	713.00	1.30E-03	1.22E-03
713.00	770.00	1.65E-03	1.58E-03
770.00	795.00	1.85E-03	1.84E-03
795.00	900.50	2.02E-03	1.99E-03
900.50	1100.50	3.63E-03	3.59E-03
1100.50	1301.00	4.61E-03	4.62E-03
1301.00	1501.00	5.60E-03	5.57E-03
1501.00	1701.00	6.32E-03	6.32E-03
1701.00	1901.50	6.81E-03	6.79E-03
1901.50	2101.50	6.51E-03	6.29E-03
2101.50	2301.50	7.10E-03	8.81E-03
2301.50	2401.50	7.49E-03	1.03E-02
2401.50	2702.00	7.97E-03	1.52E-02
2702.00	4003.00	7.20E-03	8.28E-03
4003.00	6004.00	6.08E-03	7.20E-03
6004.00	8505.50	6.22E-03	6.69E-03
8505.50	11158.50	6.31E-03	6.04E-03
11158.50	13660.00	5.90E-03	5.16E-03
13660.00	17511.50	5.21E-03	3.81E-03
17511.50	100000.00	4.02E-03	2.02E-03

Source: DTN: MO0308SPACO2GL.001

Table 6.7-2. Look-up Tables for Total System Performance Assessment-License Application Analysis of In-Drift and Invert Pco_2 for W4 (CS2000) Seepage Water

w4, CS2000		Drift	Invert
Start (year)	**End (year)**	**Partial Pressure $CO_{2(g)}$ bars**	**Partial Pressure $CO_{2(g)}$ bars**
1.00	2.50	3.75E-03	5.27E-03
2.50	7.50	4.11E-03	5.11E-03
7.50	15.00	3.97E-03	4.42E-03
15.00	25.00	3.79E-03	3.78E-03
25.00	35.00	3.75E-03	3.73E-03
35.00	45.00	3.82E-03	3.89E-03
45.00	50.00	3.87E-03	3.92E-03
50.00	52.00	2.31E-03	8.78E-03
52.00	54.00	8.59E-04	3.96E-03
54.00	57.50	5.25E-04	2.44E-03
57.50	65.00	8.70E-05	3.60E-04
65.00	77.50	3.97E-04	5.05E-04
77.50	125.00	1.32E-03	1.51E-03
125.00	175.00	3.05E-03	3.22E-03
175.00	225.00	4.09E-03	4.20E-03
225.00	275.00	4.01E-03	4.07E-03
275.00	325.00	3.37E-03	3.39E-03
325.00	375.00	2.63E-03	2.65E-03
375.00	450.00	1.89E-03	1.89E-03
450.00	550.00	8.05E-04	8.01E-04
550.00	625.00	4.50E-04	4.29E-04
627.00	675.00	5.54E-04	5.02E-04
675.00	725.00	6.80E-04	6.31E-04
725.00	775.00	9.65E-04	8.85E-04
775.00	802.00	1.24E-03	1.18E-03
802.00	900.00	1.24E-03	1.19E-03
900.00	1100.00	2.98E-03	2.95E-03
1100.00	1300.00	4.63E-03	4.61E-03
1300.00	1500.50	5.69E-03	5.64E-03
1500.50	1700.50	6.48E-03	6.43E-03
1700.50	1900.50	6.55E-03	6.57E-03
1900.50	2100.50	6.60E-03	6.64E-03
2101.50	2300.50	7.47E-03	8.62E-03
2300.50	2498.00	7.89E-03	1.05E-02
2498.00	2701.00	6.96E-03	1.74E-02
2701.00	4002.50	7.82E-03	1.44E-02
4002.50	6003.50	7.63E-03	1.03E-02
6003.50	8505.00	8.55E-03	1.00E-02
8505.00	11301.50	9.87E-03	1.05E-02
12597.90	13804.50	1.01E-02	1.05E-02
15010.10	17511.50	9.63E-03	9.85E-03
17511.50	100000.00	8.19E-03	8.18E-03

Source: DTN: MO0308SPACO2GL.001

Table 6.7-3. Look-up Tables for Total System Performance Assessment-License Application Analysis of In-Drift and Invert Pco_2 for W5 (CS1000) Seepage Water

w5, CS1000		Drift	Invert
Start (year)	**End (year)**	**Partial Pressure $CO_{2(g)}$ bars**	**Partial Pressure $CO_{2(g)}$ bars**
1.00	2.50	3.73E-03	4.06E-03
2.50	7.50	3.00E-03	3.18E-03
7.50	15.00	2.75E-03	3.00E-03
15.00	25.00	2.50E-03	2.54E-03
25.00	35.00	2.35E-03	2.41E-03
35.00	45.00	2.31E-03	2.50E-03
45.00	50.50	2.26E-03	2.39E-03
50.50	52.00	1.12E-03	5.20E-03
52.00	54.00	4.47E-04	2.91E-03
54.00	57.50	2.82E-04	1.49E-03
57.50	67.50	8.33E-05	2.78E-04
67.50	87.50	2.10E-04	2.60E-04
87.50	125.00	6.49E-04	7.44E-04
125.00	175.00	1.47E-03	1.54E-03
175.00	225.00	1.85E-03	1.89E-03
225.00	275.00	1.67E-03	1.69E-03
275.00	325.00	1.29E-03	1.29E-03
325.00	375.50	9.04E-04	9.05E-04
375.50	450.50	5.82E-04	5.73E-04
450.50	550.50	3.27E-04	3.05E-04
550.50	625.50	4.86E-04	4.50E-04
625.50	675.50	7.01E-04	6.38E-04
675.50	725.50	9.52E-04	9.07E-04
725.50	767.50	1.28E-03	1.23E-03
767.50	792.50	1.52E-03	1.49E-03
792.50	900.50	1.70E-03	1.66E-03
900.50	1100.50	3.36E-03	3.28E-03
1100.50	1301.00	4.40E-03	4.41E-03
1301.00	1501.00	5.49E-03	5.50E-03
1501.00	1701.00	6.30E-03	6.34E-03
1701.00	1901.50	6.50E-03	6.52E-03
1901.50	2101.50	6.59E-03	6.70E-03
2101.50	2297.00	7.33E-03	8.32E-03
2297.00	2397.00	7.66E-03	9.40E-03
2397.00	2702.00	7.75E-03	1.00E-02
2702.00	4003.00	7.11E-03	1.56E-02
4003.00	6004.00	6.78E-03	9.75E-03
6004.00	8505.50	7.10E-03	8.56E-03
8505.50	11155.50	7.55E-03	8.11E-03
11155.50	13657.00	7.42E-03	7.72E-03
13657.00	17511.50	6.83E-03	6.93E-03
17511.50	100000.00	5.59E-03	5.54E-03

Source: DTN: MO0308SPACO2GL.001

Table 6.7-4. Look-up Tables for Total System Performance Assessment-License Application Analysis of In-Drift and Invert Pco2 for W6 (SD-9) Seepage Water

w6, SD-9		Drift	Invert
Start (year)	**End (year)**	**Partial Pressure $CO_{2(g)}$ bars**	**Partial Pressure $CO_{2(g)}$ bars**
1.00	2.50	3.36E-03	6.03E-03
2.50	7.50	3.81E-03	4.94E-03
7.50	15.00	3.77E-03	4.06E-03
15.00	25.00	3.69E-03	3.57E-03
25.00	35.00	3.73E-03	3.62E-03
35.00	45.00	3.82E-03	3.81E-03
45.00	50.50	3.88E-03	3.86E-03
50.50	52.00	1.99E-03	1.14E-02
52.00	54.00	7.56E-04	2.98E-03
54.00	57.54	4.48E-04	1.35E-03
57.54	67.55	9.07E-05	3.82E-04
67.55	87.56	3.26E-04	4.10E-04
87.56	125.08	9.72E-04	1.11E-03
125.08	175.00	1.76E-03	1.85E-03
175.00	225.00	1.98E-03	2.02E-03
225.00	275.00	1.69E-03	1.71E-03
275.00	325.00	1.22E-03	1.23E-03
325.00	375.00	8.07E-04	8.11E-04
375.00	450.50	4.89E-04	4.86E-04
450.50	550.50	2.50E-04	2.28E-04
550.50	625.50	4.10E-04	3.78E-04
625.50	675.50	6.09E-04	5.49E-04
675.50	725.50	8.76E-04	8.09E-04
725.50	775.50	1.18E-03	1.14E-03
775.50	833.00	1.60E-03	1.54E-03
833.00	933.00	2.08E-03	2.07E-03
933.00	1100.50	3.04E-03	3.03E-03
1100.50	1301.00	4.22E-03	4.23E-03
1301.00	1501.00	5.38E-03	5.34E-03
1501.00	1701.00	6.21E-03	6.20E-03
1701.00	1901.50	6.41E-03	6.47E-03
1901.50	2101.50	6.47E-03	6.58E-03
2101.50	2301.50	7.05E-03	7.68E-03
2301.50	2702.00	7.41E-03	9.13E-03
2702.00	3025.00	6.95E-03	1.66E-02
3025.00	4026.02	6.38E-03	1.63E-02
4026.02	6004.00	5.92E-03	8.98E-03
6004.00	8505.50	5.98E-03	7.25E-03
8505.50	11530.00	6.06E-03	6.51E-03
11530.00	14032.00	5.42E-03	5.55E-03
14032.00	17511.50	4.92E-03	4.97E-03
17511.50	100000.00	3.88E-03	3.87E-03

Source: DTN: MO0308SPACO2GL.001

Table 6.7-5. Look-up Tables for Total System Performance Assessment-License Application Analysis of In-drift and Invert Pco_2 for W7 (CS500) Seepage Water

w7, CS500		Drift	Invert
Start (year)	**End (year)**	**Partial Pressure $CO_{2(g)}$ bars**	**Partial Pressure $CO_{2(g)}$ bars**
1.00	2.50	4.73E-03	5.11E-03
2.50	7.50	4.04E-03	4.22E-03
7.50	15.00	3.72E-03	3.88E-03
15.00	25.00	3.38E-03	3.34E-03
25.00	35.00	3.19E-03	3.20E-03
35.00	45.00	3.12E-03	3.28E-03
45.00	50.50	3.04E-03	3.16E-03
50.50	52.00	1.69E-03	5.02E-03
52.00	54.00	5.97E-04	2.49E-03
54.00	57.50	3.36E-04	1.43E-03
57.50	67.50	7.83E-05	4.08E-04
67.50	87.50	2.69E-04	3.49E-04
87.50	125.00	8.20E-04	9.42E-04
125.00	175.00	1.82E-03	1.92E-03
175.00	225.00	2.30E-03	2.36E-03
225.00	275.00	2.10E-03	2.12E-03
275.00	325.00	1.63E-03	1.64E-03
325.00	375.00	1.17E-03	1.16E-03
375.00	450.00	7.66E-04	7.63E-04
450.00	550.00	3.55E-04	3.37E-04
550.00	625.00	4.25E-04	3.97E-04
625.00	675.00	6.34E-04	5.70E-04
675.00	725.50	8.95E-04	8.25E-04
725.50	767.00	1.24E-03	1.17E-03
767.00	792.00	1.42E-03	1.39E-03
792.00	900.50	1.64E-03	1.57E-03
900.50	1100.50	3.28E-03	3.26E-03
1100.50	1300.50	4.37E-03	4.38E-03
1300.50	1501.00	5.55E-03	5.50E-03
1501.00	1701.00	6.30E-03	6.32E-03
1701.00	1901.00	6.91E-03	6.87E-03
1901.00	2101.00	6.45E-03	6.05E-03
2101.00	2301.50	7.26E-03	9.04E-03
2301.50	2496.50	7.62E-03	9.86E-03
2496.50	2797.00	6.73E-03	1.75E-02
2797.00	4002.50	6.99E-03	1.51E-02
4002.50	6004.00	6.76E-03	8.96E-03
6004.00	8505.50	7.17E-03	8.26E-03
8505.50	11301.50	7.74E-03	8.14E-03
11301.50	13803.00	7.67E-03	7.96E-03
13803.00	17511.50	7.18E-03	7.26E-03
17511.50	100000.00	5.91E-03	5.79E-03

Source: DTN: MO0308SPACO2GL.001

6.7.3 Thermal-Hydrological-Chemical Seepage Water Equilibrium Gas Fugacities

EQ3 calculations are run to equilibrate and speciate the water compositions of the 11 bin waters abstracted in Section 6.6 (Table 6.6-5). The resulting water compositions and the corresponding gas fugacities are provided in Table 6.7-6. The fugacities represent values at the wetting front, which is defined as the closest cell to the drift center that has saturation levels above zero (i.e., the calculation cell is not completely dried out). The distance from the drift center ranges from about 2.7 to 7.5 m (Figure 6.6-2).

The complete set of fugacity values from all 368 waters listed in Table 6.6-1 (rather than the subset presented in Table 6.7-6) can be extracted from the calculated EQ3 3o files archived in DTN: MO0303MWDSCMAB.000 using the GETEQDATA V1.0.1 1 (BSC 2003, STN: 10809-1.0.1-0 [DIRS 162228]) data extraction tool. Values of gas fugacity as a function of time are available in the EQ6 output files listed in Table 6.6-1 and are archived in DTN: MO0303MWDEBSSM.000.

6.7.4 Dust Leachate Equilibrium Gas Fugacities

In conjunction with the aqueous chemical results produced in Section 6.10.6.4, equilibrium gas fugacities are available for the six binned dust leachate water compositions selected to represent the range of leachate water chemistries (see *6 bin EQ3 gas and dust leachate water extract.xls* in DTN: MO0310SPADLBU4.001). The values shown by the Table 6.7-7 graphical plots are representative of the equilibrium gas values at atmospheric $P\mathrm{co}_2$ ($10^{-3.5}$ bar), at or near ambient temperatures (25°C), and in equilibrium with solutions formed by dust deliquescence. For temperatures above this, the values that are found in the calculated EQ6 output files (Table 6.10-12) should be used.

Table 6.7-6. Equilibrium Gas Fugacities, Temperatures, pH, and Ionic Strengths from the 11 Bin Waters

	Bin01.3o	**Bin02.3o**	**Bin03.3o**	**Bin04.3o**	**Bin05.3o**	**Bin06.3o**	**Bin07.3o**	**Bin08.3o**	**Bin09.3o**	**Bin10.3o**	**Bin11.3o**
Temp (C)	112	109	104	109	95.6	65.1	56.3	40.2	91.8	56.3	95.6
pH	7.41	7.58	7.62	7.37	7.63	7.7	7.75	7.94	8.14	7.82	7.76
I (molal)	4.93E-02	2.05E-02	9.74E-03	1.39E-02	1.13E-02	1.12E-02	1.24E-02	9.77E-03	5.10E-03	8.71E-03	7.06E-03
H_2O(g)*	1.77E-01	1.34E-01	6.07E-02	1.34E-01	-6.92E-02	-6.02E-01	-7.77E-01	-1.13E+00	-1.30E-01	-7.77E-01	-6.91E-02
O_2(g)*	-7.00E-01	-7.00E-01	-7.00E-01	-7.00E-01	-7.00E-01	-7.00E-01	-7.00E-01	-7.00E-01	-7.00E-01	-7.00E-01	-7.00E-01
CO_2(g)*	-3.47E+00	-3.36E+00	-3.05E+00	-2.67E+00	-2.78E+00	-2.21E+00	-2.18E+00	-2.25E+00	-2.59E+00	-2.10E+00	-2.45E+00
HF(g)*	-9.82E+00	-9.91E+00	-9.91E+00	-9.57E+00	-9.69E+00	-1.07E+01	-1.11E+01	-1.19E+01	-1.03E+01	-1.11E+01	-9.67E+00
HCl(g)*	-1.23E+01	-1.32E+01	-1.35E+01	-1.32E+01	-1.38E+01	-1.49E+01	-1.53E+01	-1.69E+01	-1.51E+01	-1.61E+01	-1.43E+01
HNO_3(g)*	-1.38E+01	-1.44E+01	-1.51E+01	-1.42E+01	-1.53E+01	-1.67E+01	-1.70E+01	-1.82E+01	-1.57E+01	-1.75E+01	-1.56E+01
NO_3(g)*	-2.40E+01	-2.46E+01	-2.54E+01	-2.44E+01	-2.58E+01	-2.80E+01	-2.87E+01	-3.04E+01	-2.64E+01	-2.91E+01	-2.62E+01
H_2(g)*	-2.99E+01	-3.02E+01	-3.08E+01	-3.02E+01	-3.17E+01	-3.53E+01	-3.65E+01	-3.88E+01	-3.21E+01	-3.65E+01	-3.17E+01
N_2O_5(g)*	-3.28E+01	-3.40E+01	-3.53E+01	-3.36E+01	-3.57E+01	-3.84E+01	-3.92E+01	-4.16E+01	-3.66E+01	-4.01E+01	-3.64E+01

Source: DTN: MO0304SPAA11GC.000

NOTE: *Units are Log Fugacities in bars

Table 6.7-7. Equilibrium Gas Fugacities, Temperatures, pH and Ionic Strengths from the 6 Bin Dust Leachate Waters

Filename	**p25_25b.3o**	**p26_25b.3o**	**s80c25b.3o**	**s86a25b.3o**	**s90b25b.3o**	**s92a25b.3o**
Temp (°C)	25	25	25	25	25	25
pH	8.54	8.40	8.54	8.23	8.09	8.05
a_w	1.00	1.00	1.00	1.00	1.00	1.00
(I)	6.29E-03	3.80E-03	5.43E-03	2.01E-03	2.74E-03	1.15E-03
$O_{2(g)}$	-0.67	-0.67	-0.67	-0.67	-0.67	-0.67
$H_2O_{(g)}$	-1.50	-1.50	-1.50	-1.50	-1.50	-1.50
$CO_{2(g)}$	-3.50	-3.50	-3.50	-3.50	-3.50	-3.50
$HF_{(g)}$	-14.50	-14.11	-14.33	-14.30	-14.16	-13.99
$HCl_{(g)}$	-18.26	-18.29	-18.55	-18.42	-18.26	-18.23
$HNO_{3(g)}$	-18.31	-18.39	-18.34	-18.65	-18.34	-18.79
$HBr_{(g)}$	-22.23	-22.09	-22.74	-22.54	-21.98	-22.36
$NO_{3(g)}$	-30.99	-31.08	-31.02	-31.33	-31.02	-31.47
$H_{2(g)}$	-41.22	-41.22	-41.22	-41.22	-41.22	-41.22
$N_2O_{5(g)}$	-41.65	-41.83	-41.71	-42.34	-41.71	-42.61

Source: DTN: MO0310SPADLBU4.001

NOTE: *Units are Log Fugacities in bars

INTENTIONALLY LEFT BLANK

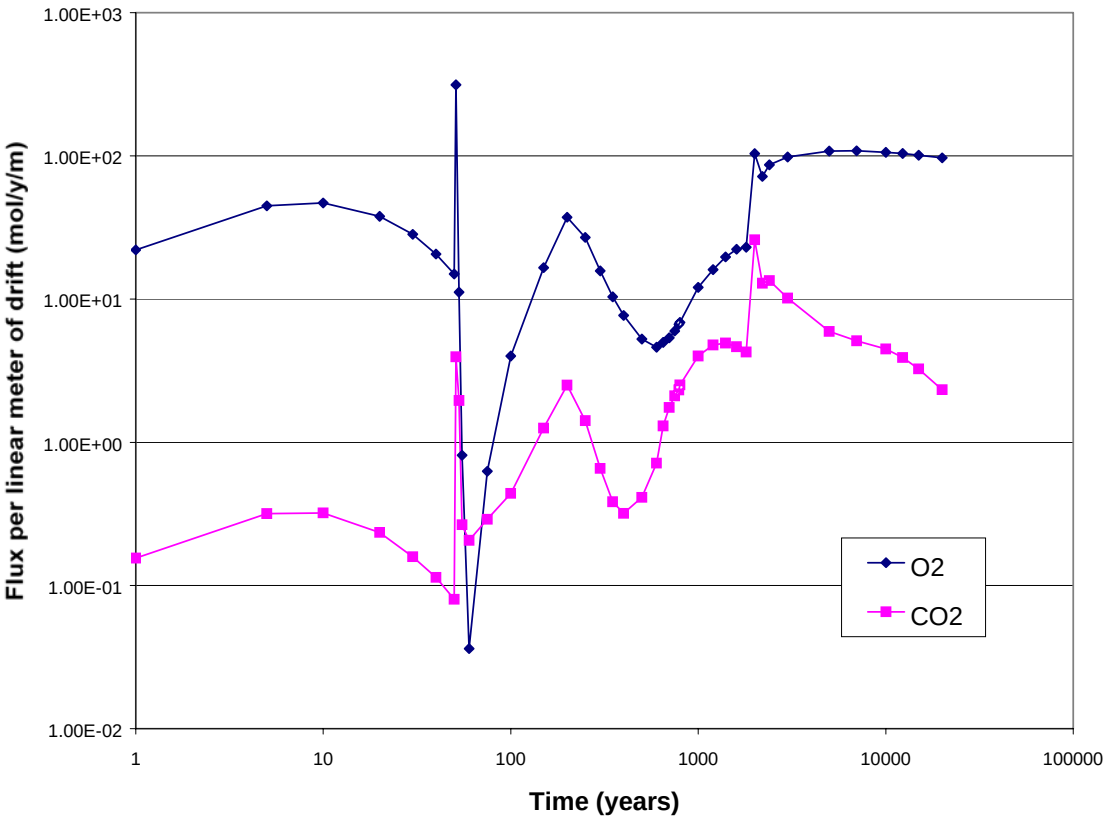

Note: Time = 0 represents the time at which waste package emplacement and forced ventilation begins.

DTN: MO0312SPAPCEGF.002

Figure 6.7-1. Gas Flux per Meter of Drift

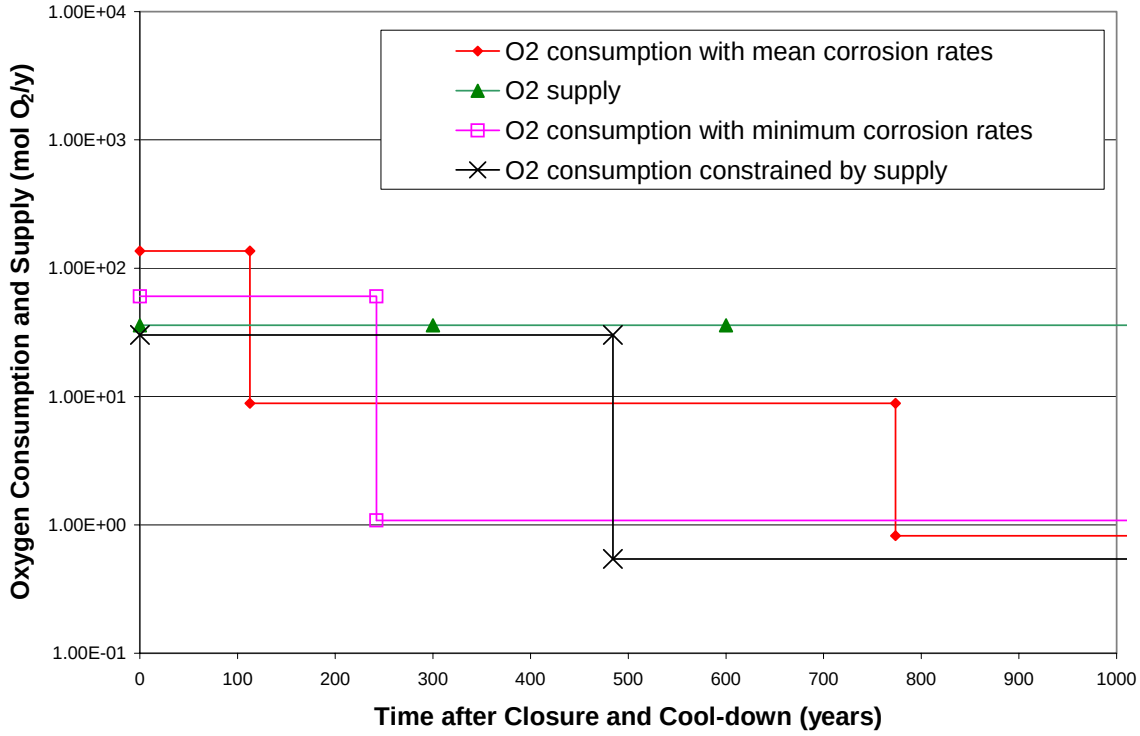

DTN: MO0312SPAPCEGF.002

Figure 6.7-2. Oxygen (O_2) Consumption Due to Degradation of Components External to the Waste Package

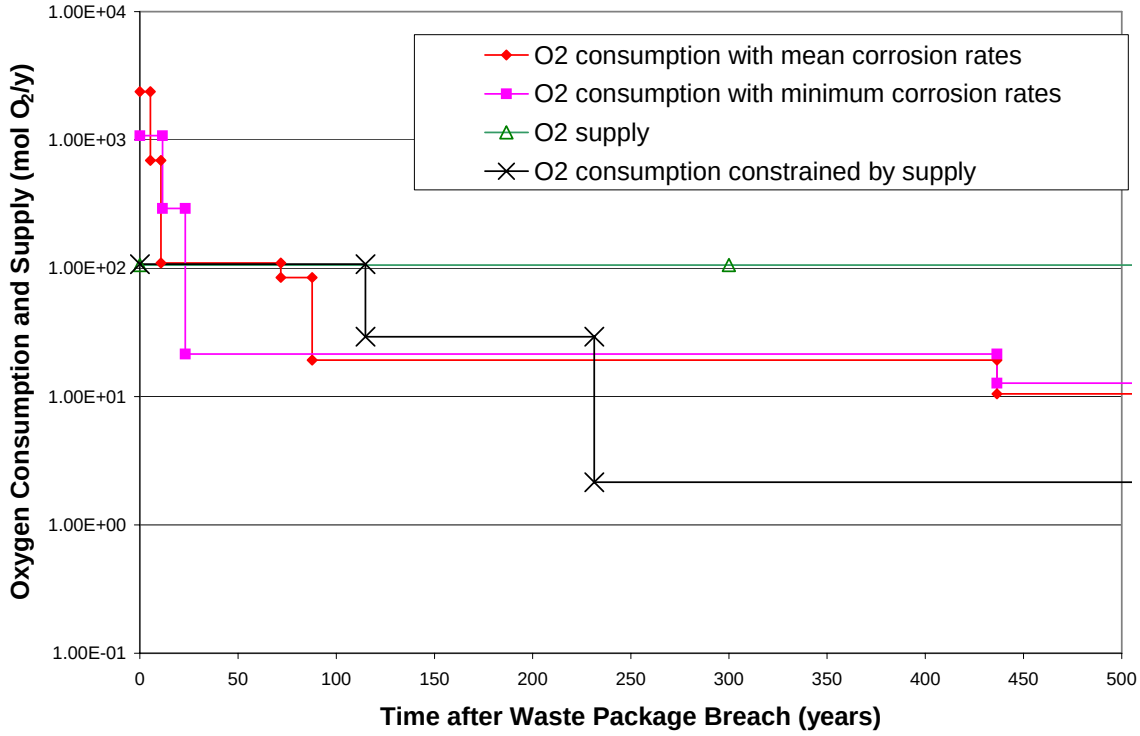

DTN: MO0312SPAPCEGF.002

Figure 6.7-3. Oxygen (O_2) Consumption in a 21 PWR Waste Package

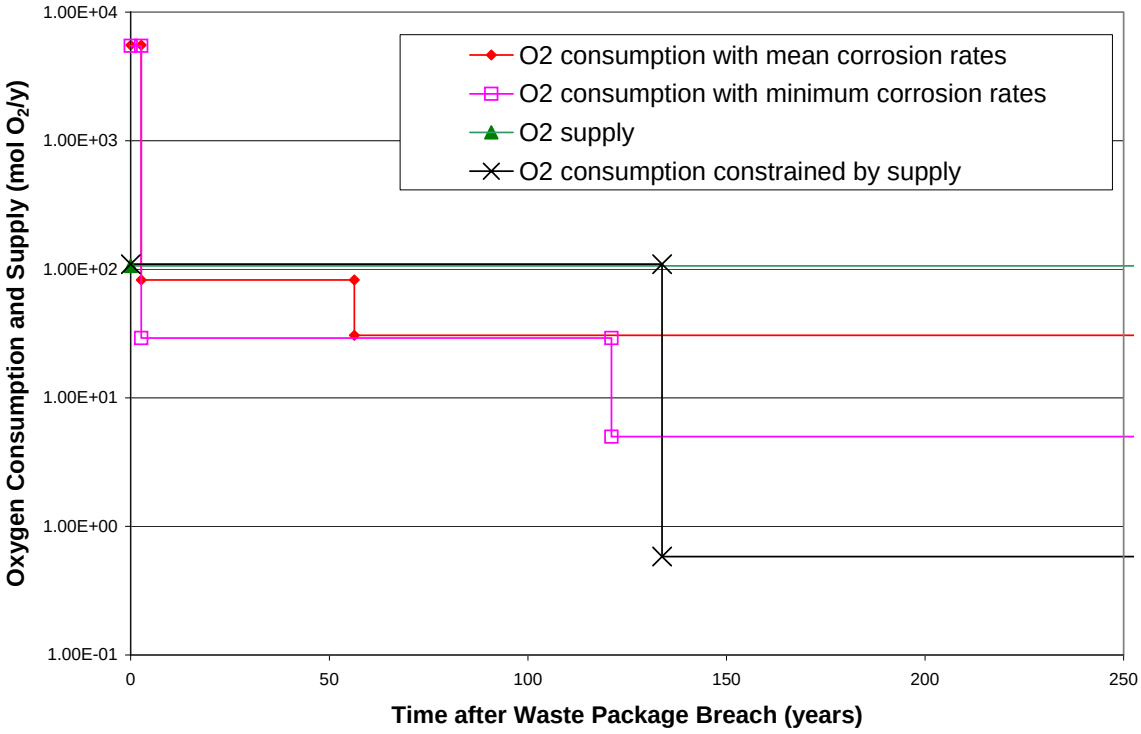

DTN: MO0312SPAPCEGF.002

Figure 6.7-4. Oxygen (O_2) Consumption in a N Reactor Co-Disposal Waste Package

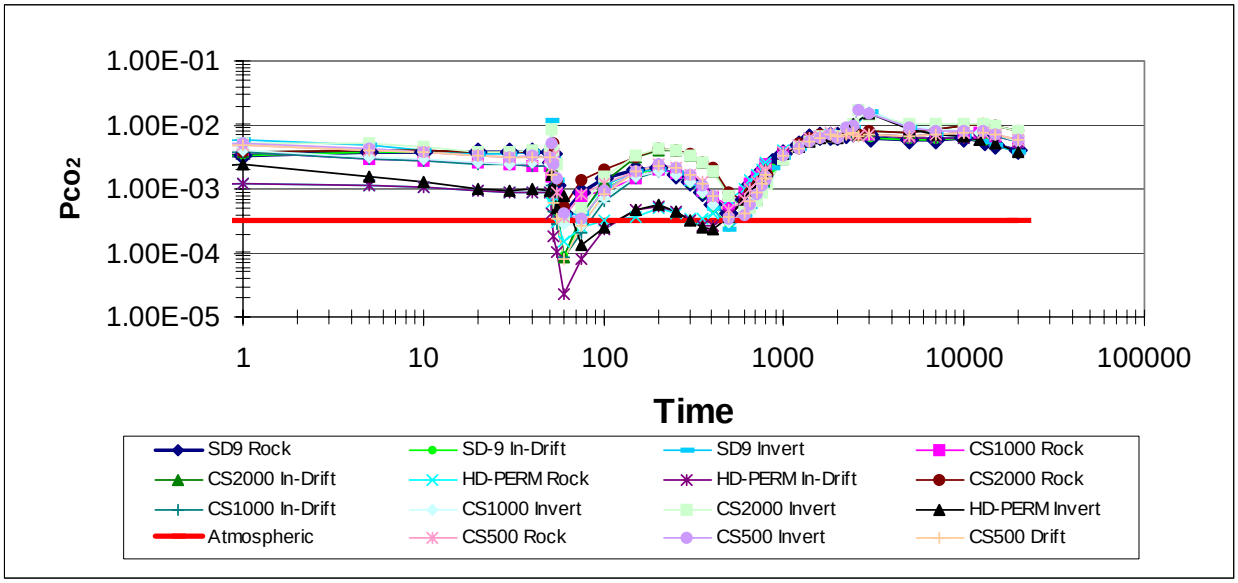

DTN: MO0308SPACO2GL.001

NOTE: See Table 4.1.3.1-1 for description of labels in the legend

Figure 6.7-5. Pco_2 Concentration in the Drift and Near-drift Environment Through Time (Log Scale)

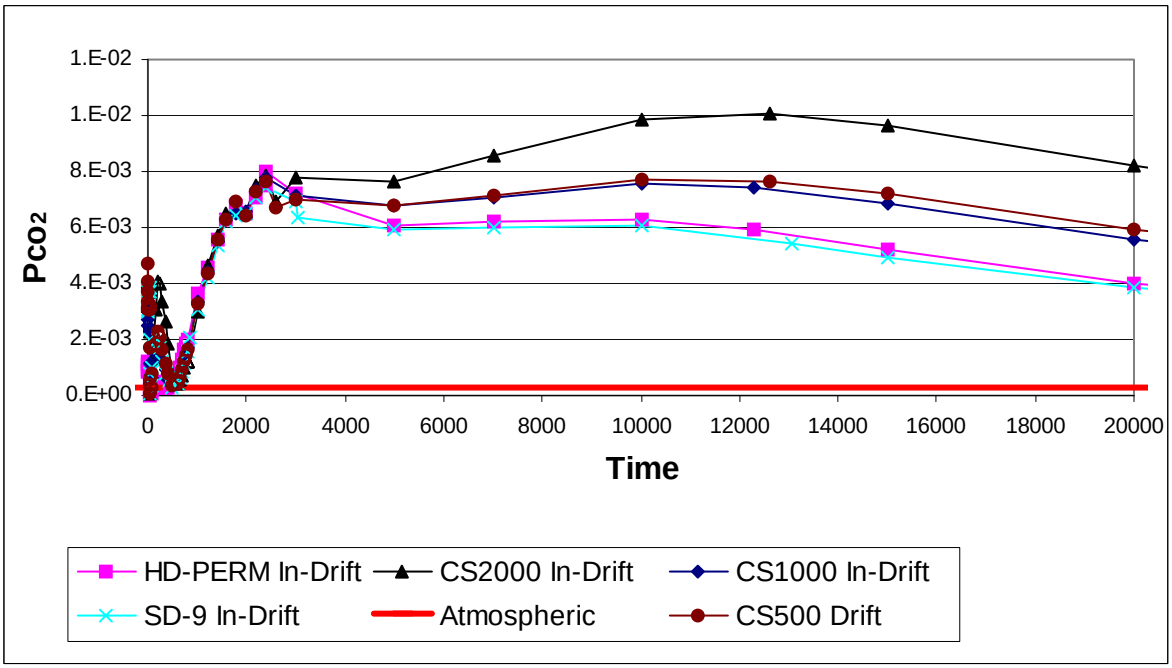

DTN: MO0308SPACO2GL.001

NOTE: See Table 4.1.3.1-1 for description of labels in the legend

Figure 6.7-6. Pco_2 Concentration in the In-Drift Environment Through Time (Normal Scale)

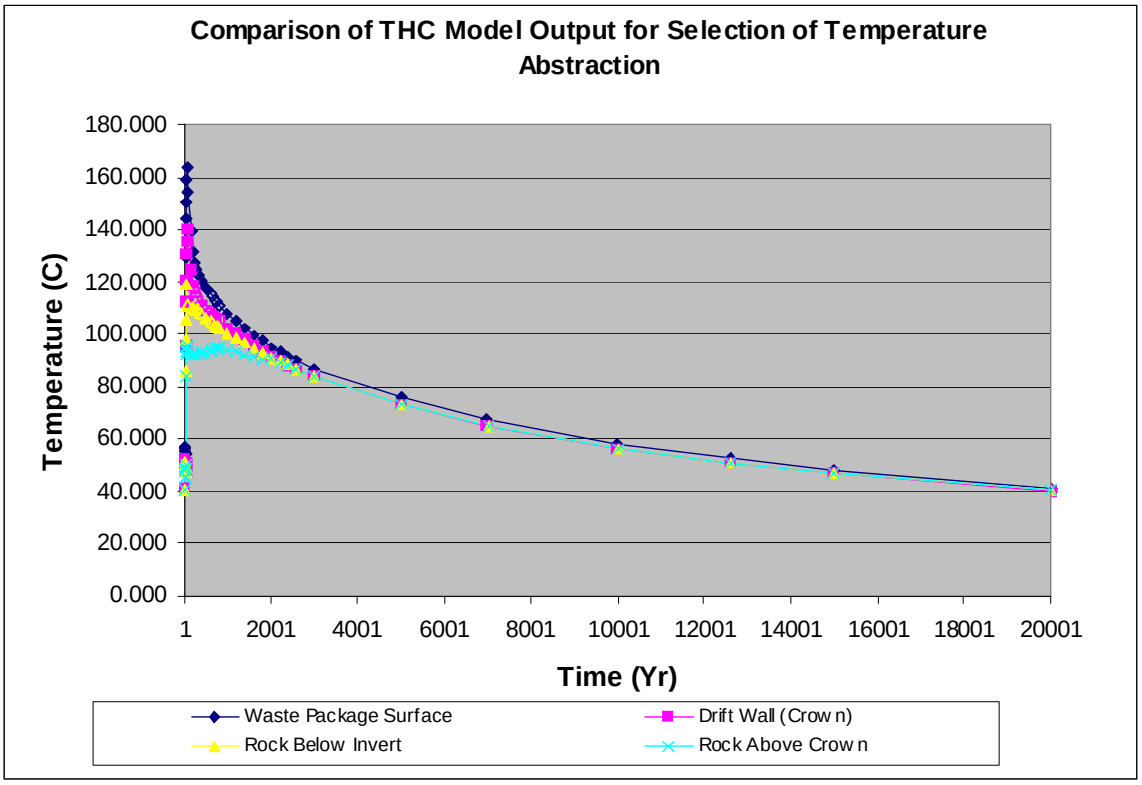

DTN: MO0308SPACO2GL.001

Figure 6.7-7. Comparison of Temperatures at Various Locations Within and Around the Drift as Determined by the Thermal-Hydrological-Chemical Model Output

6.8 GROUND SUPPORT INTERACTIONS WITH SEEPAGE WATER

This section evaluates the impact on seepage water chemistry from interactions with components of the ground support system and their resulting corrosion products. The ground support materials have been tabulated in Table 6.4-20, and are comprised of carbon steels and 316L stainless steel materials only. Based upon the short lifetime estimates of carbon/low alloy steels in steam environments such as that expected after closure, on the order of 100-300 years per inch of thickness (Table 6.4-19), any effects of carbon steel on seepage chemistry are short-lived and not to be further considered. However, 316L stainless steel has a significantly longer lifetime (relative per-inch thickness on the order of 100,000 years, Table 6.4-19) and therefore its effects upon the seepage water composition are considered.

Specifically, the present design calls for using 316L stainless steel perforated sheets and rock bolts (BSC 2003 [DIRS 164101] and Table 6.4-20) for the drift ground support system. Therefore, the elemental components of this steel are discussed, and this material is examined in detail with respect to its corrosion/precipitation and subsequent effect upon seepage water chemistry. The results presented here show that the 316L stainless steel corrosion process—the release of aqueous species and formation of corrosion products—has only negligible affects on the composition of incoming seepage waters.

6.8.1 Corrosion Products Concepts

Corrosion of the ground support materials is modeled as occurring by direct oxygen and proton consumption and can be generalized in Equation 6.8-1:

$$\mathrm{M}_{(s)} + \frac{n}{4}\mathrm{O}_{2\,(g)} + n\,\mathrm{H}^{+} \rightarrow \mathrm{M}^{n+}{}_{(aq)} + \frac{n}{2}\mathrm{H}_{2}\mathrm{O} \qquad \text{(Eq. 6.8-1)}$$

If this process alone occurs, the pH in the aqueous phase must increase. However, the magnitude of this effect is dependent upon the disposition of the metal ion released. If the ion is highly soluble, then the oxidation reaction shown in Equation 6.8-1 will dominate, and the pH of the seepage water will rise. However, if it is of low solubility then the resulting precipitation reaction must be accounted for. Typically, this reaction involves the formation of a hydroxide or oxide (or combined oxy-hydroxide). A general metal hydroxide formation reaction can be represented as shown in Equation 6.8-2:

$$\mathrm{M}^{n+}{}_{(aq)} + n\,\mathrm{H}_{2}\mathrm{O} \rightarrow \mathrm{M(OH)}_{n\,(s)} + n\,\mathrm{H}^{+} \qquad \text{(Eq. 6.8-2)}$$

This has the effect of releasing as many hydrogen ions as were consumed during corrosion, thereby negating any effect upon the water chemistry. This is also the general case for oxide formation, shown by Equation 6.8-3:

$$\mathrm{M}^{n+}{}_{(aq)} + \frac{n}{2}\,\mathrm{H}_{2}\mathrm{O} \rightarrow \mathrm{MO}_{\mathrm{n/2}\,(s)} + n\,\mathrm{H}^{+} \qquad \text{(Eq. 6.8-3)}$$

The following subsections will discuss the three primary metals comprising 316L stainless steel (Fe, Ni and Cr), that account for greater than 90 percent of this alloy by weight.

6.8.1.1 Iron (Fe)

Iron in the natural environment exists in two oxidation states. Fe(II) is the soluble form, but is not stable under the redox conditions postulated for the drift (i.e. atmospheric Po_2). Fe(III) primarily forms insoluble oxides and oxyhydroxides (e.g. Fe_2O_3 and FeOOH respectively); its solubility product ranges from 10^{-36} to 10^{-42} at 25°C and pH >3 based on the Pitzer Thermodynamic Database ([DIRS 162572]), and it is increasingly soluble with lower pH values (Pankow 1991, p. 231 [DIRS 105952]).

Table 6.8-1 shows the typical oxidation-reduction reactions for iron aqueous species and minerals. The Eh-pH diagram for iron plotted in Figure 6.8-1 shows that Fe(III) oxyhydroxides are the stable phase at the relatively high oxidation potentials expected at Yucca Mountain. The stability of the various forms of iron hydroxides and oxyhydroxides increases from amorphous $Fe(OH)_3$ to goethite to hematite (Fe_2O_3) at 25°C (Stumm and Morgan 1981, p. 434 [DIRS 100829]). However, predicting if goethite or hematite will be present in a given system is difficult, because geochemical conditions may favor nucleation and growth of one or the other phase, and because goethite may persist metastably for millions of years, as the conversion of goethite to hematite can be very slow (Krauskopf 1979, p. 208 [DIRS 105909]). However, in soils, goethite tends to form at low temperatures (in cool or temperate climate zones), at high H_2O activity, and with higher organic matter contents. The hematite-to-goethite ratio usually increases with increasing soil temperature (Schwertmann and Taylor 1995, pp. 398-400 [DIRS 105959]). pH also plays a role in the preferred formation of the two phases. Goethite is favored in soils with low pH (3-7), whereas hematite is favored above pH 7 (Schwertmann and Taylor 1995, pp. 401-402 [DIRS 105959]). However, if a small amount of Ti is present (<0.05 mol fraction) in the solution, it inhibits hematite formation and favors the formation of goethite (Fitzpatrick et al. 1978 [DIRS 105795]).

Given the slow rate of hematite formation, its suppression by high humidity conditions, and the presence of large quantities of Ti, goethite is expected to be the prevalent iron corrosion species for the period of regulatory interest. However, it is important to note that there is only a difference of <0.5 log units between the solubilities of goethite and hematite, so, for modeling purposes, the choice of mineral has little impact.

Table 6.8-1. Typical Oxidation-Reduction Reactions and Potential Fe Minerals

Reaction	Oxidation State	Minerals Formed
$2Fe^{2+} + ½O_2 + 2H_2O = Fe_2O_3 + 4H^+$ $Fe_3O_4 + 2H^+ = Fe_2O_3 + Fe^{2+} + H_2O$ $2FeOOH + 2H^+ + ½O_2 = Fe_2O_3 + Fe^{2+} + 2H_2O$	3	*Hematite* (α-Fe_2O_3)
$Fe^{2+} + ¼O_2 + {}^3/_2H_2O = FeOOH + 2H^+$ $Fe_3O_4 + H^+ + ½O_2 = Fe_2O_3 + FeOOH$	3	*Goethite* (α-FeOOH)
$3Fe^{2+} + ½O_2 + 3H_2O = Fe_3O_4 + 6H^+$	2.67	*Magnetite* (Fe_3O_4)

Source: Designed for Fe minerals using Tebo et al. (1997, Table 2 [DIRS 105960]), as an example.

Other minerals that could potentially form, based on the geochemical system at Yucca Mountain, are Fe carbonates and Fe-rich silicates. Given the low-temperature conditions, a likely iron-rich silicate mineral that may form would be a type of smectite clay [nontronite].

6.8.1.2 Nickel (Ni)

Only Ni(II) occurs at ambient environmental conditions. The higher oxidation states occur rarely and, even in those cases, it is not clear whether it is the ligand rather than the metal atom that is oxidized (Cotton and Wilkinson, 1988, p. 741 [DIRS 105732]). No other oxidation state would be expected under repository environmental conditions once Ni is released by oxidation of the metal alloys.

Once the Ni is released into an aqueous environment under oxidizing conditions, nickel hydroxides [$Ni(OH)_2$] are stable in a pH range between 8 and 12 (see Figure 6.8-2). Otherwise, either the Ni^{2+} ion or the $HNiO_2^-$ ions are in solution, indicating that nickel is relatively soluble under neutral-acidic conditions and under relatively alkaline conditions (Garrels and Christ 1990, pp. 244-245 [DIRS 144877]).

Nickel tends to substitute for iron and manganese in solid phases, and tends to be co-precipitated as $Ni(OH)_2$ with both iron oxides and manganese oxides (Hem 1985 [DIRS 115670]; Hem et al. 1989 [DIRS 105854]). Nickel will also adsorb to clays, iron and manganese oxides, and organic matter (McLean and Bledsoe 1992 [DIRS 108954]).

6.8.1.3 Chromium (Cr)

Unless otherwise indicated, the source of the following summary was taken from Palmer and Puls (1994 [DIRS 108991]).

Chromium exists in oxidation states ranging from +6 to –2; however, only the +6 and the +3 oxidation states are commonly encountered in the environment (refer to Eh/pH diagram in Figure 6.8-3). Cr(VI) exists in solution as the monomeric ions $H_2CrO_4^o$, $HCrO_4^-$ (bichromate), and CrO_4^{2-} (chromate), or as the dimeric ion $Cr_2O_7^{2-}$ (dichromate). The relative concentration of each of these species depends on both the pH of the chrome-laden water and the total concentration of Cr(VI).

Significant concentrations of $H_2CrO_4^o$ only occur at pH $\leq$ 1. Above pH 6.5, CrO_4^{2-} generally dominates. Below pH 6.5, $HCrO_4^-$ dominates when the Cr(VI) concentrations are low (<30mM), but $Cr_2O_7^{2-}$ becomes significant when concentrations are greater than 1mM, and may even dominate when the total Cr(VI) concentrations are greater than 30mM.

In the Cr(III)-H_2O system, Cr(III) exists predominantly as Cr^{3+} below a pH of 3.5. With increasing pH, hydrolysis of Cr^{3+} yields $Cr(OH)^{2+}$, $Cr(OH)_2^+$, $Cr(OH)_3^0$, and $Cr(OH)_4^-$ (corresponding to the species Cr+++, CrOH++, CrO+, HCrO2(aq) and CrO2-, respectively, in data0.R2.ymp). From under slightly acidic through alkaline conditions, Cr(III) can precipitate as an amorphous chromium hydroxide. Amorphous $Cr(OH)_3$ can crystallize to $Cr(OH)_3 \cdot 3H_2O$ or Cr_2O_3 [eskolaite] depending upon conditions. In the presence of Fe(III), trivalent chromium can precipitate as a solid solution, ($Fe_xCr_{1-x}(OH)_3$), with a lower solubility (Sass and Rai 1987, Figure 1 [DIRS 105957]). If the pH of the system is between 6 and 12, the aqueous solubility of

Cr(III) should be less than 1 μmole/l. In addition, when the pH of the groundwater is greater than 4, Cr(III) precipitates with the Fe(III) in a solid solution with the general composition $Cr_xFe_{1-x}(OH)_3$ (Sass and Rai 1987, pp. 2228-2229 [DIRS 105957]; Amonette and Rai 1990 [DIRS 105701]). This to should limit the concentration of Cr(III) to less than 10^{-6} molar, in the pH range from 6 to 12.

Cr(VI) is a strong oxidant and is reduced in the presence of electron donors. A common electron donor that could be present in the repository is ferrous iron. This reaction is very fast on the time scales of interest for most environmental problems, with the reaction going to completion in about five minutes even in the presence of dissolved oxygen (Eary and Rai 1988 [DIRS 105784]). When the pH is greater than 10, the rate of oxidation for Fe(II) by dissolved oxygen will exceed the rate of oxidation by Cr(VI) (Eary and Rai 1988 [DIRS 105784]).

Efficient Cr(VI) reduction in the presence of stainless steel, iron oxides, iron-containing silicates, and organic matter has been observed in several experiments. The reduction of Cr(VI) in the presence of hematite (Fe_2O_3) was demonstrated by Eary and Rai (1989 [DIRS 105788]). They attribute the reduction to the presence of a small amount of a FeO component in the hematite. They also suggest that the reaction occurs in solution after the FeO component has been solubilized. Reduction by biotite occurs when potassium ions are released to solution and Fe^{3+} ions are adsorbed onto the surface of the biotite. Potassium ions are released to maintain charge balance in the biotite structure. Reduction seems to occur even in oxygenated solutions. Lastly, experiments by Smith and Purdy (1995 [DIRS 162976]) addressing corrosion of 316L stainless steel and chromium speciation state in their abstract that: "Oxidation of chromium(III) to chromium(VI) was negligible at room temperature and only became significant in hot concentrated nitric acid. The rate of reduction of chromium(VI) back to chromium(III) by reaction with stainless steel or oxalic acid was found to be much greater than the rate of the reverse oxidation reaction."

Humic and fulvic acids are often associated with reduction by organic matter. The rate of reduction of Cr(VI) by the humic and fulvic acids will decrease with increasing pH. It increases with increasing initial Cr(VI) concentration and increases as the concentration of soil humic substances increases. At neutral pH, complete reduction of Cr(VI) may take many weeks. Sedlak and Chan (1997 [DIRS 105964]) studied the reaction of Cr(VI) with Fe(II) with respect to temperature and pH and determined that the reduction of Cr(VI) occurred on the time scale of minutes to months in sediments, soils, and waters that contained ferrous iron. Similar type experiments conducted in NaCl, $NaClO_4$, and seawater solutions showed a parabolic dependence on pH, and the influences of temperature, ionic strength, and reductant concentration showed various linearly dependent effects on reduction (Pettine et al. 1998 [DIRS 105955]). In low temperature soil environments that have been contaminated with chromate-laden solutions, $KFe_3(CrO_4)_2(OH)_6$ has been shown to precipitate and can reduce the amount of Cr(VI) in groundwater (Baron and Palmer 1996 [DIRS 105730]). This mineral, analogous to the sulfate mineral jarosite, is stable in oxidizing environments between a pH of 2 and 6.

Oxidation of Cr(III) to Cr(VI) has been achieved in three ways. The first requires dissolved oxygen, the second requires either manganese dioxide (MnO_2) (Eary and Rai 1987 [DIRS 105780]) or manganite (MnOOH) (Johnson and Xyla 1991 [DIRS 105878]), and the third is by using hot concentrated nitric acid (Smith and Purdy 1995 [DIRS 162976]). Eary and Rai

(1987, p. 1188 [DIRS 105780]) found that dissolved oxygen is not an especially effective nor likely way to oxidize Cr(III). However, interaction with manganese dioxide has been demonstrated to increase as pH decreases and the ratio of surface area to solution volume increases. Eary and Rai (1987 [DIRS 105780])) developed an empirical rate law for the oxidation of Cr(III) by β-MnO_2 [pyrolusite]. For manganite, the rate law has been determined to be independent of pH and ionic strength; however, it does proceed slower in the presence of organic ligands (Johnson and Xyla 1991 [DIRS 105878]).

Sorption of Cr(VI) onto goethite has been demonstrated to be a surface complexation mechanism dependent on pH. However, on magnetite, the mechanism has been determined to be reductive precipitation onto Fe(II) surface sites (Deng et al. 1996 [DIRS 105778]). Competition between common anionic groundwater ions ($CO_{2\,(g)}$, H_4SiO_4, and SO_4^{2-}) and the CrO_4^{2-} ion is known to occur, where the adsorption of CrO_4^{2-} onto amorphous iron oxides was suppressed between 50 to 80 percent (Zachara et al. 1987 [DIRS 105963]).

6.8.2 Definition of Base Case

The base case for 316L stainless steel corrosion is defined by the following:

- Material (sheets and rock bolts of 316L stainless steel) and dimensions as defined on 800-IED-WIS0-00302-000-00A (BSC 2003 [DIRS 164101])
- "Bin 11" seepage water (abstracted in Section 6.6.6, results in DTN: MO0304MWDSAB11.001) as it is the most likely water chemistry for this stainless steel corrosion period (51-5000 years, see Table 6.13-3)
- Oxidation corrosion products that include Fe(III) and Cr(III)
- Primary controlling mineral phases for stainless steel corrosion products: goethite and amorphous chromium hydroxide
- Temperature of 25ºC and fugacities of CO_2 and O_2 at 10^{-3} and $10^{-0.7}$ atm., respectively
- Abstracted 316L stainless steel corrosion rates based on DTN: MO0312SPAPCEML.003 (see Section 6.8.3).

The "maximum of the means" corrosion value for 316L stainless steel (Table 6.4-18) is used as the "Mean" to represent a relatively fast corrosion rate. As these corrosion rates are, in most experiments, based on weight loss, they include the effects of localized corrosion (if any) that occur during the experiments.

Interaction with the abstracted Bin 11 seepage water is chosen because this is the most likely water chemistry to exist during the period over which corrosion of stainless steel ground supports will occur (51–5000 years, see Table 6.13-3), and accounts for three of the four seepage water compositions shown in Tables 6.6-8 through 6.6-12. Bin 7 seepage water was selected as a sensitivity case in Section 6.12.4.

An Fe(III) phase has been selected as a corrosion end product that may influence seepage water chemistry because Fe(III), as opposed to Fe(II), is the oxidation state that would form under the relatively oxidizing conditions (atmospheric O_2 concentrations leading to significant dissolved oxygen content) and mild pH ranges of the seepage waters. The plotted diagram of Figure 6.8-1 shows that in the pH range of 6 through 9, with an O_2-fixed Eh range of ~0.8 through ~0.6 volts, the Fe(III) species are dominant.

Selection of Cr(III) over that of the more soluble Cr(VI) species is based on experimentally observed corrosion products, and on the kinetics and conditions required to obtain the fully oxidized Cr(VI) state (Smith and Purdy 1995 [DIRS 162976]). Smith and Purdy's examination of the actual chromium speciation as a result of corrosion of 316L stainless steel demonstrated a predominance of the less soluble Cr(III) species, except under the conditions of hot concentrated nitric acid (111°C and >7 molar HNO_3, see Smith and Purdy 1995, Figure 6). Other groups performing oxidation experiments, conducted under more ambient conditions, examined the oxidation of Cr(III) to Cr(VI) by dissolved oxygen. The experiments of Eary and Rai (1987, p. 1188 [DIRS 105780]) were performed from pH 4.0 to 12.5 without the detection of Cr(VI) formation in 24 days. Additionally, observed disequilibrium of dissolved oxygen in water correspond to the much more rapidly reacting O_2–H_2O_2 couple (see for example, Langmuir 1997 [DIRS 100051], Figure 11.5). The Eh values for this couple in the pH range from 6 to 9 are in the range of ~0.6 down to ~0.4 volts, corresponding to the Cr(III) field of Figure 6.8-3. However, Cr(VI) is examined as a sensitivity case in Section 6.12.4.

As discussed later in Section 6.8.4.2, goethite was selected as the iron controlling mineral phase and not the more thermodynamically stable hematite. Based on the review article of Ball and Nordstrom (1998 [DIRS 163015]) of the original work by Rai et al. (1987 [DIRS 163369]), the amorphous chromium hydroxide [$Cr(OH)_3$] was selected as the solubility limiting phase for Cr(III). The solubility constant was taken from Ball and Nordstrom (1998, Table 8 [DIRS 163015]). This constant at 25ºC is used as a modification to the data0.ymp.R2 database (DTN: MO0302SPATHDYN.000 [DIRS 161756]). In addition, Rai et al. (1987, p. 345 [DIRS 163361]) reiterate a previous review of literature (Rai and Zachara 1984 [DIRS 107060]) concluding that the Cr(III) solubility-controlling solids are thought to be either $Cr(OH)_3$ or Cr(III) co-precipitated with Fe oxides and hydroxides. This amorphous chromium phase end-member solubility represents a conservative upper solubility, as there exists a well-characterized solid solution of chromium(III)-iron(III) hydroxide with solubility decreasing as the iron content increases (Sass and Rai 1987 [DIRS 105957]).

The base case is limited to supporting calculations at 25ºC, because the primary mineral phase that controls Cr(III) solubility, $Cr(OH)_3$, has its solubility defined only at this temperature (Rai et al. 1987 [DIRS 163369]). Rai et al. (1987, Figure 4 [DIRS 163369]) only show that at 90°C the solubility of the $Cr(OH)_3$ solid decreases, lowering the concentration of aqueous Cr(III) species by about two orders of magnitude. A CO_2 fugacity of 10^{-3} atm. was chosen to be consistent with the median value from the ranges used for in-drift seepage evaporation (Section 6.9). Other fugacities of 10^{-2} and 10^{-4} atm. are examined to evaluate model uncertainty in Section 6.12.4.

6.8.3 Abstraction of 316L Stainless Steel and its Corrosion Rate

The development of the abstraction starts with a review of the standard specifications for 316L stainless steel, as determined by the American Society for Testing and Materials standard (ASTM A 240/A 240M-02a 2002, Table 1 [DIRS 162720]). This specification establishes weight-percentage values/limits or ranges for the various compositional elements. When ranges are specified, mean values are used to calculate the balance of Fe as 65.5 percent by weight (DTN: SN0312T0510102.013 –DegradationMolality.xls, sheet name: Composition). This compares to 17 percent Cr by weight, resulting in a molar ratio of Fe:Cr of 3.59:1.0 (DTN: SN0312T0510102.013– sheet: degradation) that is rounded off to 3.6:1.0 and implemented in the modified Data0.YMP.R2 EQ3/6 database file (original database DTN: MO0302SPATHDYN.000 [DIRS 161756]) as an abstracted mineral species titled SS316L.

The abstracted stainless steel species, whose molecular formula is $Fe_{3.6}Cr_{1.0}$, is defined by the dissociation reaction:

$$1.0\ SS316L + 13.8\ H^+ + 3.45\ O_2(g) \rightarrow 1.0\ Cr^{3+} + 3.6\ Fe^{3+} + 6.9\ H_2O \qquad \text{(Eq. 6.8-1)}$$

The reaction is not shown as being reversible because stainless steel will never precipitate. This is achieved operationally by providing an arbitrarily large solubility log *K* value of 266. The database text that was inserted into Data0.YMP.R2 is also in DTN: SN0312T0510102.013 (see filename Cr-database.zip).

The corrosion rate of 316L stainless steel controls the quantity of corrosion product and the extent to which corrosion affects the crown seepage water chemistry. The corrosion rate was estimated by determining the mean quantity of 316L stainless steel ground support over a one square meter section of crown drift wall. This quantity includes the 316L sheets and rock bolts (Bernold brand type S and Swellex brand, respectively) from 800-IED-WIS0-00302-000-00A (BSC 2003 [DIRS 164101]). A step-function for the corrosion rate was used to approximate the transition from dry to wet drift-wall conditions, which is estimated to occur around 2,000 years after emplacement as shown by the THC model results (DTN: LB0302DSCPTHCS.002 [DIRS 161976]). Seepage amounts, represented directly by the infiltration rates, were also taken from the THC spreadsheets (DTN: LB0302DSCPTHCS.002 [DIRS 161976], from “notes” sheet).

The rate of corrosion during the hot, dry period (up to 2000 years after closure) was taken as 0.113 µm/year, from the “316L SS” “Steam and atmospheric” “Mean” rate contained in Table 6.4-18 (DTN: MO0312SPAPCEML.003). At 2,000 plus years, a larger “fresh/salt water” corrosion rate was applied. The corrosion rate selected for wet conditions was 1.9391 µm/year, listed under Material “316L SS,” “fresh/salt water,” in Table 6.4-18 (DTN: MO0312SPAPCEML.003). To obtain the quantity (moles) of corroded steel in one year, the calculation multiplies the surface area with the corrosion rate, factoring in the density of 316L stainless steel (ASTM 1999 [DIRS 103515]) and its compositional makeup (ASTM 2002 [DIRS 162720]). This mole quantity of iron and chromium, as the amount released by corrosion per year, is then combined with the infiltration water amount used by THC

(DTN: LB0302DSCPTHCS.002 [DIRS 161976], in "notes" sheet) to generate a final molal quantity for input into the EQ3/6 speciation calculations.

These spreadsheet calculations, which are included in DegradationMolality.xls (DTN: SN0312T0510102.013, filename DegradationMolality.zip), provide a value for the corrosion rate in moles per year per square meter of the 316L stainless steel ground support.

6.8.4 Abstraction and Base Case Limitations

Details of the abstraction model calculation runs and results are supplied in the following subsections, concluding with a discussion on the limitations of this base case model.

6.8.4.1 EQ3/6 Model Runs

The abstracted model for stainless steel ground support interaction with seepage water consists of the following sequential EQ3/6 calculation runs:

1. Initial EQ3NR speciation of Bin 11 seepage water (DTN: MO0304MWDSAB11.001, a product output of this model) with trace quantities of "Fe++" (10^{-30} molal) and "Cr+++" (10^{-20} molal) added; output pickup file from this feeds into 2) and 3)

2. EQ6 evaporation to 98 percent relative humidity of the Bin 11 water for basis of comparison

3. EQ6 "titration" run dissolving abstracted SS316L mineral by corrosion quantity; output second half of pickup file from this feeds into 4)

4. EQ6 evaporation to 98 percent relative humidity of the steel corrosion product containing Bin 11 water.

The input and output files associated with these four EQ3/6 calculation runs are listed in Table 6.8-2 and are documented in the DTN: SN0312T0510102.013.

Table 6.8-2. EQ3/6 Input/Output Files for 316L Stainless Steel Corrosion Abstraction Model

Run	Input File Names	Output File Names	Pickup File Names
1	Bin11.3i	bin11.3o	bin11.3p
2	Bin11e.6i	bin11e.6o	bin11e.6p
3	SSbin11.6i	ssbin11.6o	ssbin11.6p
4	ssbin11e.6i	ssbin11e.6o	–

Source: DTN: SN0312T0510102.013

NOTE: These files are contained in Base case.zip

6.8.4.2 Mineral and Aqueous Suppressions

The mineral suppressions include those identified in Section 6.6.2.6.4 of *In-Drift Precipitates/Salts Analysis* (BSC 2003 [DIRS 162529]; see also Table 6.5-2 of this report) and the three minerals identified in Table 6.6-2 of this report (Albite, K-feldspar, and Celadonite). Due to the presence of ferric and chromium species, additional suppressions are required for these abstracted model calculation runs, and more silica species are suppressed as they saturated before amorphous silica in these 25ºC calculation runs. These extra mineral suppressions and the bases for their suppression are listed in Table 6.8-3.

Table 6.8-3. Additional EQ3/6 Mineral Suppressions Included for Seepage Ground Support Interactions

Mineral	Formula	Criteria Selected[a]	Rationale	References
Tridymite	SiO_2	Criterion 2	Tridymite forms at temperatures from about 700°C to 1470°C.	Deer et al. 1992, p. 465 [DIRS 163286]
Chalcedony	SiO_2	Criterion 6	Modeling choice uses amorphous silica to control the silica phase and provide adequate conservatism.	see Table IV-1
Coesite	SiO_2	Criterion 2	Coesite is a high pressure SiO_2 phase (>35 kbar) that will not form at atmospheric pressures.	Deer et al. 1992, p. 466 [DIRS 163286]
Cristobalite (beta)	SiO_2	Criterion 2	Cristobalite forms at temperatures from 330 to 440°C; beta quartz transforms into beta cristobalite at 1027°C and above 650 bars.	Deer et al. 1992 [DIRS 163286], p. 465-466
Hematite	Fe_2O_3	Criterion 3	Over long time frames, hematite is more stable than goethite, and the temperatures in the drift are elevated enough to warrant the precipitation of hematite, however if small amounts of Ti are present in solution, hematite is inhibited and goethite forms. Therefore, due to the large amount of Ti being emplaced in the repository drift, hematite will be suppressed (see discussion in Section 6.8.1.1).	Stumm and Morgan 1981, [DIRS 100829], p. 434 Fitzpatrick et al. 1978 [DIRS 105795]
Eskolaite	Cr_2O_3	Criterion 2	Eskolaite is a common chromium mineral that may precipitate from a cooling magma. Although details of its liquid precipitation curves are still emerging, present data shows that 0.5 to 1.0% by mass of eskolaite precipitates in the range from 1000 to 1150°C, and it is likely to begin precipitation above 920°C at atmospheric pressures.	Perez et al. 2001 [DIRS 163030], p. 4-31 Hrma et al. 2001 [DIRS 163031], Table 3.14, p. 3.27
Chromite	$FeCr_2O_4$	Criterion 2	Chromite is a spinel mineral that is one of the earliest minerals to form in a cooling magma. It does not form from aqueous solutions near or below 100°C.	Frye 1981 [DIRS 161804], p. 581
Magnesiochromite	$MgCr_2O_4$	Criterion 2	Magnesiochromite is a spinel mineral similar to chromite.	Frye 1981, [DIRS 161804], p. 581

NOTE: [a] The criteria used to include suppression of a mineral are defined in Section 6.5.4.

In calculation run 2 (see Table 6.8-2), the zeolite clinoptilolite-K (0.015 Fe content) is also suppressed, because trace amounts of Fe cause numerical EQ6 calculation run instabilities. This suppression is removed for calculation runs 3 and 4, and this zeolite is not seen to form.

The suppression of a set of aqueous species is also deemed necessary from these seepage-steel interaction run abstractions and is described in Table 6.8-4. Reasons for these suppressions range from incorrect oxidation states to overly stable polymeric aqueous species.

Table 6.8-4. Aqueous Species Suppressions Included for Seepage Ground Support Interactions

EQ3/6 Aqueous Species	Formula	Criteria Selected	Rationale	Reference(s)
Chromate	CrO_4^{2-}	Criteria 3	Oxidation of the initial Cr(III) corrosion species to this Cr(VI) basis species is very slow in the absence of strong oxidizing agent or extreme temperature and pH conditions	Eary and Rai 1987, [DIRS 105780], p. 1188 Smith and Purdy 1995, [DIRS 162976] abstract
CrO3Cl-	CrO_3Cl^-	Criteria 3	Cr(VI) species, see above	as above
CrO4---	CrO_4^{3-}	Criteria 3	Metastable Cr(V) species, not observable under near-equilibrium conditions	Niki 1985, [DIRS 163728], p. 460
Cr2(OH)2++++	$Cr_2(OH)_2^{4+}$	Criteria 3	Previous studies that determined the polymeric species used in the database are overly stable. "The polymeric species of Cr(III) are generally absent in solutions at room temperature"	Rai et al. 1987 [DIRS 163369], p. 345-346
Cr3(OH)4(5+)	$Cr_3(OH)_4^{5+}$	Criteria 3	as above	as above

6.8.4.3 Result of Introducing 316L SS to Bin 11

The effect of dissolving the abstracted 316L stainless steel species into Bin 11 water was negligible. Bin 11 water, with and without the $4.7 \cdot 10^{-3}$ moles of SS316L added, has only two differences in the water chemistries and then only at the 6th significant figure (ionic strength and C total molality). This is shown in the spreadsheet 316SS-base.xls (DTN: SN0312T0510102.013, in filename Base case.zip) under the heading "Dissolution of SS316L into Bin 11 water". The effect of 316L stainless steel dissolution in the Bin 11 crown seepage water is summarized in Table 6.8-5. Values in this table represent the values calculated with the SS316L dissolution, minus the values of pure Bin 11 seepage waters, as determined at 100 and 98 percent relative humidity. The largest differences are below 0.1 percent.

The results of sensitivity analyses (reported in Section 6.12.4.1) do not conflict, with the exception of the pH affecting case where Cr(VI) is allowed to form.

Table 6.8-5. Absolute (Percent Relative) Differences Due to SS316L Dissolution in Bin 11 Seepage Water at 100 and 98 Percent Relative Humidity

RH	ΔpH	Δ(Ionic Strength)	Δ(Cl moles/ kg H_2O)	Δ(Si moles/ kg H_2O)	Δ (C moles/ kg H_2O)
100	0.0001	1.5E–6 (2E–2)	3.6E–7 (3E–2)	1.7E–8 (8E–4)	3.6E–7 (3E–2)
98	–0.0001	–3.9E–4 (–0.05)	–1.1E–4 (–0.06)	–2.5E–5 (0.07)	–6.1E–5 (–0.05)

Source: DTN: SN0312T0510102.013 (in 316SS-base.xls within Base case.zip)

There are no significant differences in the amounts of the mineral phases that exist in both SS316L interacted and pure Bin 11 water at either 100 or 98 percent relative humidity; those minerals are: fluorite, sepiolite and $SiO_{2(am)}$. Goethite and $Cr(OH)_{3(am)}$ are found only in the SS316L interacted water. Several trace (< 10^{-8} moles) solid species are found only in one or the other of the waters; these consist of natronite (Ca and K derivatives), erionite, and stellerite.

6.8.4.5 Limitations to Base Case Results

Though there are several limitations discussed below, none are likely to affect the results of this section so much as to change the conclusion that stainless steel corrosion does not impact water chemistry.

Usage of only iron and chromium is considered a valid surrogate representation of stainless steel (encompassing ~85 percent by weight of total stainless steel composition), but is nonetheless a limitation. The next most abundant element is nickel at ~12 percent by weight. As nickel is more soluble than iron or chromium in mildly acidic conditions, it may be expected to effect pH slightly. However, not accounting for this effect is conservative as it would result in slightly higher pH solutions that are less likely to induce localized corrosion on the waste package outer barrier (BSC 2003 [DIRS 161235], see Figure 6-40). The higher pH results from the dissolution of metallic Ni to Ni^{2+} with consumption of H^+ during the corrosion process (Equation 6.8-1) without the corresponding production of H^+ during Ni hydroxide precipitation (Equation 6.8-2). Note as well that this is a self-limiting process; as one obtains higher Ni^{2+} aqueous species concentrations and higher pH, the solubility of Ni^{2+} decreases and more aqueous $Ni(OH)_2$ and solid are formed.

The temperature of 25ºC imposed by the Cr(III) solubility model is a limitation. Direct comparisons of the effect of the corrosion products on the seepage waters at operational temperatures are not possible. This is conservative in that Rai et al. (1987, Figure 4 [DIRS 163369]) show decreasing solubility with increasing temperatures.

The analysis run calculations are restricted to using the data0.ymp.R2 (DTN: MO0302SPATHDYN.000 [DIRS 161756]) non-Pitzer database and the B-dot activity model. Available Pitzer interaction parameters for Cr(III) species are limited, and the available pool was not deemed reliable enough to be implemented at this time.

INTENTIONALLY LEFT BLANK

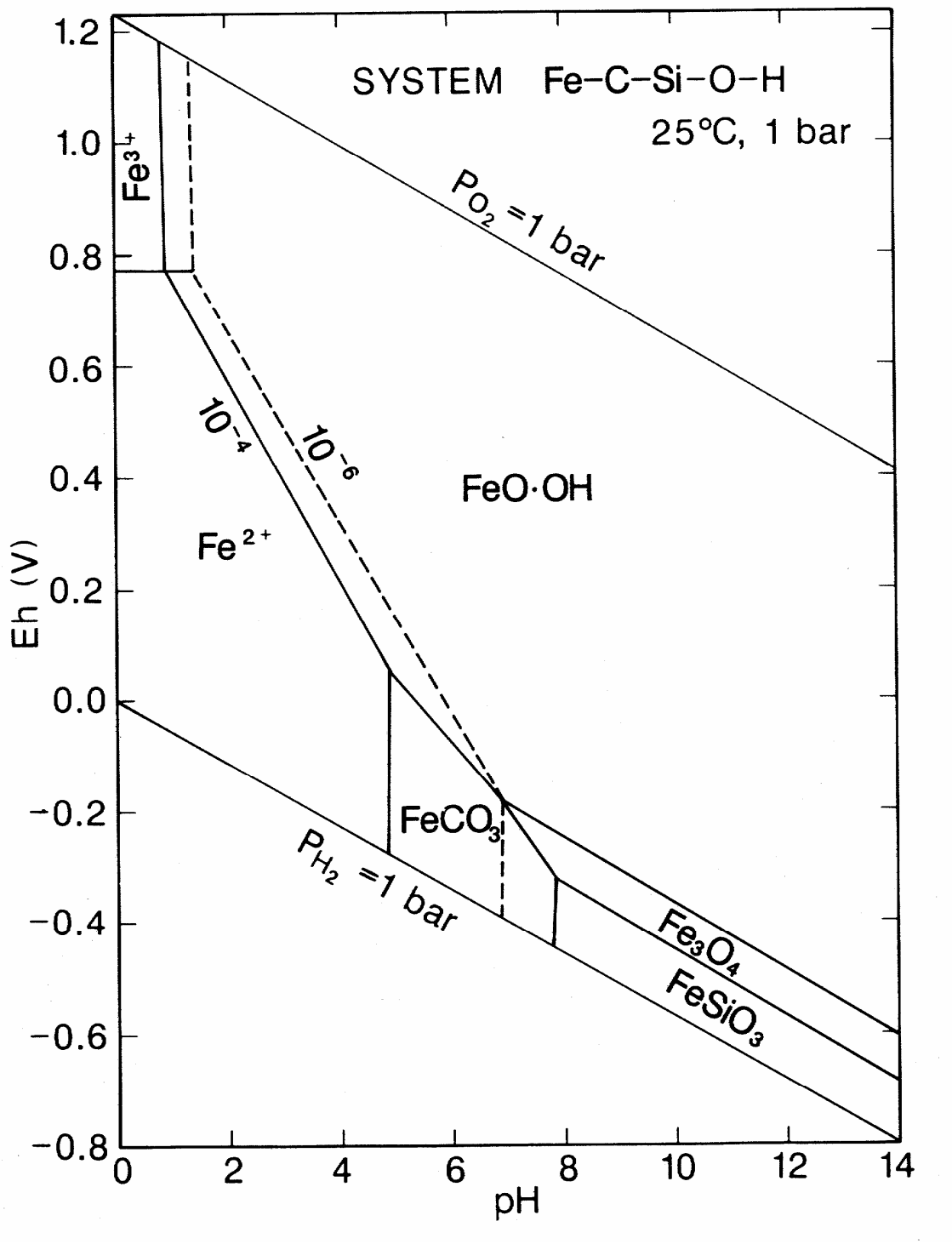

Source: Brookins 1988 [DIRS 105092]

NOTES: Approximated activities for dissolved species are: Fe = 10^{-6}, Si = 10^{-3}, C = 10^{-3}. Goethite and magnetite are considered Fe(III) solid phases.

Figure 6.8-1. Eh-pH Diagram for Part of the System Fe-C-Si-O-H at 25°C

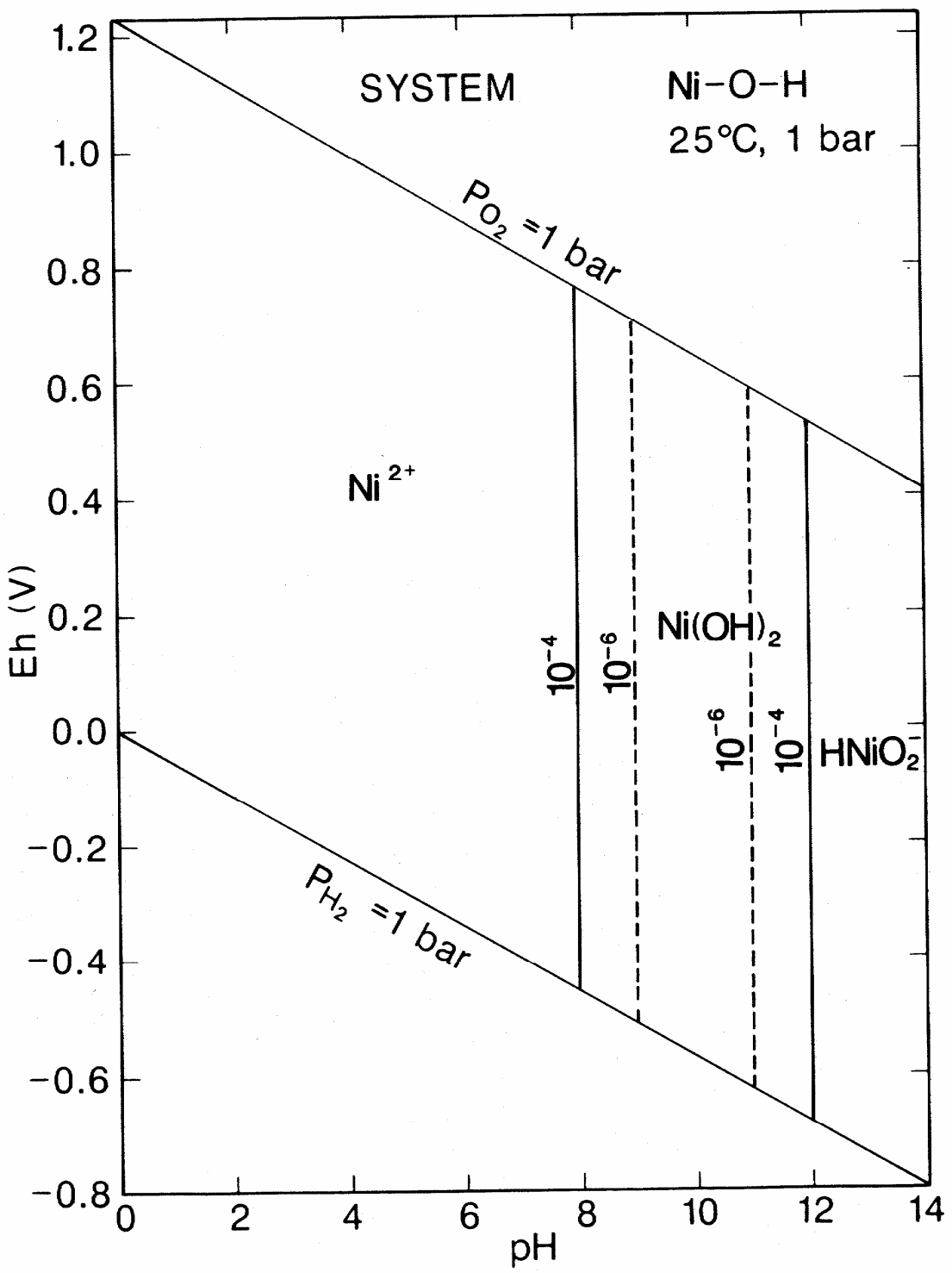

Source: Brookins 1988 [DIRS 105092]

NOTE: Estimated activity for Ni = 10^{-4}, 10^{-6}.

Figure 6.8-2. Eh-pH Diagram for Part of the System Ni-O-H at 25°C

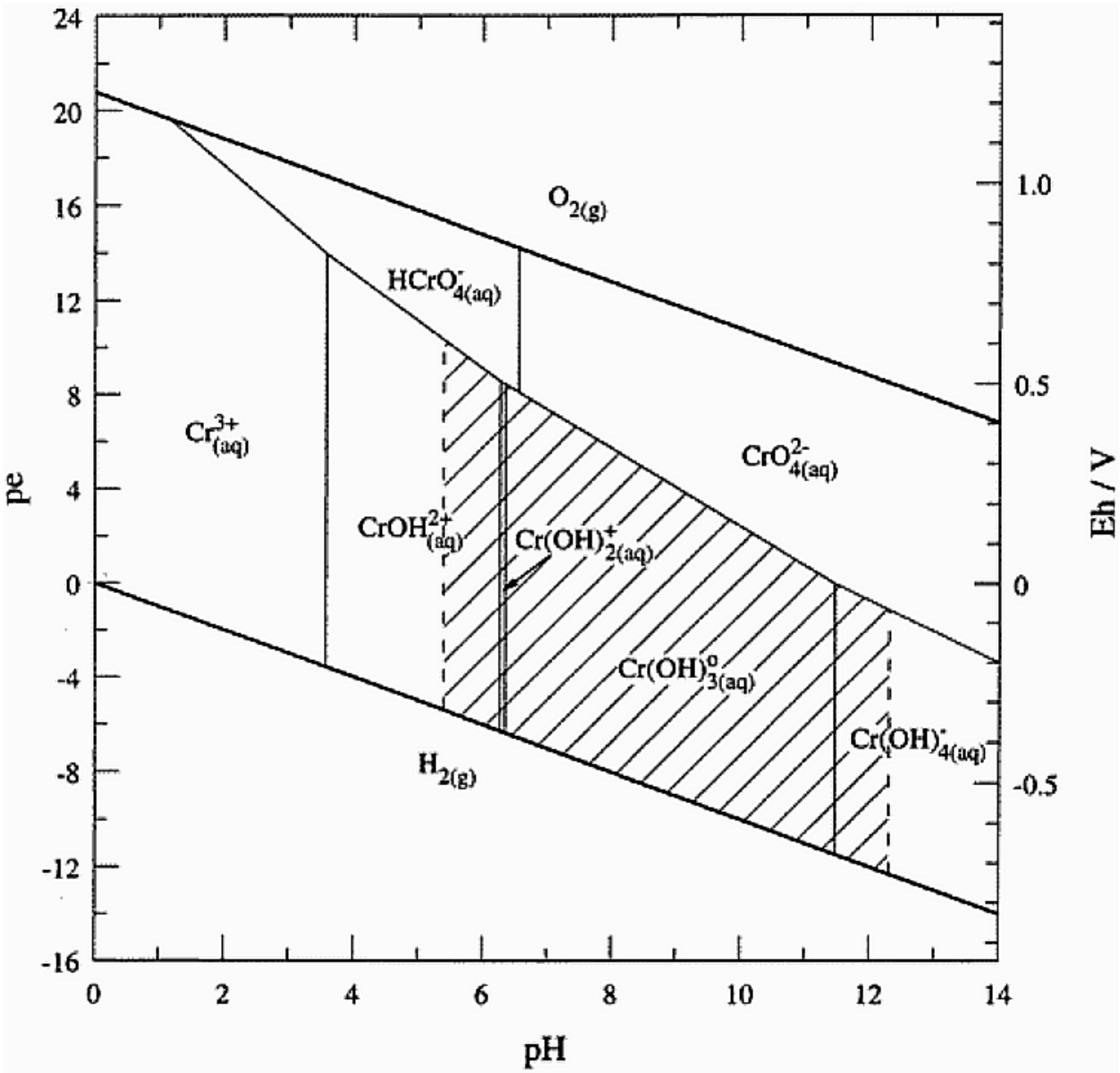

Source: Ball and Nordstrom 1998 [DIRS 163015]

Figure 6.8-3. The pe-pH diagram for aqueous inorganic chromium hydrolysis species. Hatched area indicates predominance region for $Cr(OH)_{3(s)}$.

INTENTIONALLY LEFT BLANK

6.9 IN-DRIFT SEEPAGE EVAPORATION

In-drift water compositions resulting from heating and evaporation of seepage are calculated with the in-drift precipitates/salts (IDPS) model (*In-Drift Precipitates/Salts Model* (BSC 2003 [DIRS 162529])). This model includes the chemical influence of the in-drift atmosphere. Calculated outputs from the IDPS model are abstracted in the form of lookup tables for use as inputs to TSPA-LA calculations.

6.9.1 Seepage Water Inputs

The 11 EQ3 input files associated with the EQ6 output files listed in Table 6.6-4 (archived in DTN: MO0303MWDSCMAB.000) were copied and renamed (Bin 01 through Bin 11), and three additional mineral suppression inputs are added (see Table 6.6-2). These 11 EQ3 3i files have been run and the results archived are available in DTN: MO0304MWDSAB11.001. Data from the 11 3o files are extracted using GETEQDATA V1.0.1 to produce an Excel spreadsheet: "11 bin EQ3 gas and water extract.xls" (archived in DTN: MO0304SPAA11GC.000). This spreadsheet is then used to produce Tables 6.9-1 and 6.9-2. These tables represent the EQ3NR equilibration and charge balancing of the 11 chemistries listed on Table 6.6-5. EQ3NR is used only to equilibrate the solution with respect to all aqueous species. It does not equilibrate the solutions with respect to minerals and gases. Subsequent EQ6 calculation runs are used for mineral and gas phase equilibration. Table 6.9-3 lists the species that are used to charge balance the 11 bin compositions. As noted in Section 6.6.3, charge balancing is done on the least affected species, as directed by Section 6.6.3.1 of the *In-Drift Precipitates/Salts Model* report (BSC 2003 [162529]). Comparison of Table 6.9-1 with the inputs found on Table 6.6-5 show that performing a charge balance does not impact the concentration of the given ion in the starting water.

The EQ3NR input and output files for the median bin waters that define the starting compositions of the 11 incoming seepage waters (Table 6.6-5) are documented in DTN: MO0304MWDSAB11.001 and are listed in Table 6.9-4.

6.9.2 Temperature and Carbon Dioxide

Temperature and carbon dioxide fugacity are varied to capture their effects on the compositional evolution of the bin waters during evaporation. Three values are chosen for each parameter, as described in Section 6.7.2. For temperature, the values are 40, 70, and 100ºC. The CO_2 fugacity values are 10^{-2}, 10^{-3}, and 10^{-4} bar. Each temperature is run for each CO_2 fugacity, resulting in nine combinations for each bin water. The input values for temperature and CO_2 fugacity are defined in the EQ6 input files of the in-drift precipitates/salts model. These input files are based on the EQ6 input file templates of DTN: MO0303MWDIOJ13.000 [DIRS 162841]. The EQ3NR pickup files identified in Table 6.9-4 provide the bottom halves of the input files.

Table 6.9-1. Total EQ3NR Equilibrated Aqueous Elemental Compositions for the 11 Bins

	Bin01.3o	**Bin02.3o**	**Bin03.3o**	**Bin04.3o**	**Bin05.3o**	**Bin06.3o**	**Bin07.3o**	**Bin08.3o**	**Bin09.3o**	**Bin10.3o**	**Bin11.3o**
Temp (°C)	112	109	104	105.00	95.6	65.1	56.3	40.2	91.8	56.3	95.6
pH	7.41	7.58	7.62	7.90	7.63	7.7	7.75	7.94	8.14	7.82	7.76
(I)	4.93E-02	2.05E-02	9.74E-03	4.92E-03	1.13E-02	1.12E-02	1.24E-02	9.77E-03	5.10E-03	8.71E-03	7.06E-03
Al*	3.27E-08	7.08E-08	5.02E-08	9.97E-08	8.03E-10	5.36E-09	3.71E-09	1.50E-09	6.09E-08	4.03E-09	1.42E-09
C*	5.57E-05	9.06E-05	1.95E-04	1.64E-04	4.18E-04	2.93E-03	4.15E-03	6.92E-03	2.04E-03	5.74E-03	1.13E-03
Ca*	1.75E-02	6.48E-03	2.15E-03	1.09E-03	1.36E-03	4.20E-04	6.40E-04	5.73E-04	7.24E-05	3.52E-04	3.34E-04
Cl*	2.01E-02	5.02E-03	3.35E-03	1.03E-03	3.28E-03	3.32E-03	3.33E-03	5.61E-04	7.34E-04	6.00E-04	1.30E-03
F*	1.93E-04	2.46E-04	3.48E-04	4.28E-04	1.00E-03	8.26E-04	6.73E-04	6.43E-04	9.77E-04	8.61E-04	1.38E-03
K*	8.68E-04	5.40E-04	5.00E-04	2.38E-04	8.68E-04	6.25E-04	5.37E-04	2.76E-04	5.02E-04	4.17E-04	7.50E-04
Mg*	1.70E-05	2.95E-06	4.13E-06	5.75E-07	1.13E-05	4.82E-05	6.94E-05	8.51E-05	2.54E-07	4.31E-05	6.34E-06
N*	1.30E-03	5.46E-04	1.83E-04	1.33E-04	2.22E-04	1.04E-04	1.05E-04	3.97E-05	3.10E-04	4.25E-05	1.26E-04
Na*	3.89E-03	2.63E-03	2.67E-03	1.26E-03	5.46E-03	8.08E-03	8.75E-03	7.30E-03	4.27E-03	6.81E-03	4.72E-03
S*	8.87E-03	4.89E-03	1.50E-03	5.88E-04	1.77E-03	1.21E-03	1.22E-03	3.55E-04	1.18E-04	3.80E-04	7.29E-04
Si*	9.42E-03	7.42E-03	6.96E-03	7.38E-03	1.22E-02	2.90E-03	2.35E-03	1.79E-03	4.15E-03	2.47E-03	1.19E-02

Source: DTN: MO0304SPAA11GC.000

NOTE: *Units are in Moles/kg H_2O.

Table 6.9-2. EQ3NR Equilibrium Speciation of the 11 Bins

Species*	Bin01.3o	Bin02.3o	Bin03.3o	Bin04.3o	Bin05.3o	Bin06.3o	Bin07.3o	Bin08.3o	Bin09.3o	Bin10.3o	Bin11.3o
Cl^-	2.01E-02	5.02E-03	3.35E-03	1.03E-03	3.28E-03	3.32E-03	3.33E-03	5.61E-04	7.34E-04	6.00E-04	1.30E-03
Ca^{2+}	1.33E-02	4.70E-03	1.79E-03	9.74E-04	1.12E-03	3.71E-04	5.68E-04	5.09E-04	6.02E-05	3.09E-04	2.88E-04
$SiO_{2(aq)}$	9.02E-03	7.02E-03	6.60E-03	6.70E-03	1.16E-02	2.80E-03	2.27E-03	1.73E-03	3.60E-03	2.38E-03	1.11E-02
SO_4^{2-}	4.66E-03	3.14E-03	1.16E-03	4.88E-04	1.55E-03	1.18E-03	1.19E-03	3.49E-04	1.17E-04	3.74E-04	6.98E-04
$CaSO_{4(aq)}$	4.21E-03	1.75E-03	3.35E-04	1.00E-04	2.22E-04	2.72E-05	3.16E-05	5.74E-06	1.12E-06	6.28E-06	3.11E-05
Na^+	3.89E-03	2.63E-03	2.67E-03	1.26E-03	5.46E-03	8.08E-03	8.75E-03	7.30E-03	4.27E-03	6.81E-03	4.72E-03
NO_3^-	1.30E-03	5.46E-04	1.83E-04	1.33E-04	2.22E-04	1.04E-04	1.05E-04	3.97E-05	3.10E-04	4.25E-05	1.26E-04
K^+	8.68E-04	5.40E-04	5.00E-04	2.38E-04	8.68E-04	6.25E-04	5.37E-04	2.76E-04	5.02E-04	4.17E-04	7.50E-04
$HSiO_3^-$	3.97E-04	3.95E-04	3.62E-04	6.82E-04	5.97E-04	1.01E-04	7.70E-05	6.18E-05	5.47E-04	9.28E-05	7.52E-04
F^-	1.93E-04	2.46E-04	3.48E-04	4.28E-04	9.99E-04	8.25E-04	6.72E-04	6.43E-04	9.76E-04	8.60E-04	1.38E-03
$O_{2(aq)}$	1.57E-04	1.57E-04	1.56E-04	1.56E-04	1.56E-04	1.67E-04	1.76E-04	2.03E-04	1.56E-04	1.76E-04	1.56E-04
HCO_3^-	3.92E-05	7.30E-05	1.71E-04	1.47E-04	3.82E-04	2.80E-03	3.97E-03	6.68E-03	1.97E-03	5.53E-03	1.07E-03
OH^-	2.93E-05	3.51E-05	3.05E-05	5.81E-05	2.28E-05	6.89E-06	4.88E-06	2.85E-06	6.08E-05	5.64E-06	3.00E-05
$CaOH^+$	2.75E-05	1.40E-05	4.88E-06	5.88E-06	1.75E-06	7.53E-08	6.23E-08	2.18E-08	2.64E-07	4.24E-08	6.48E-07
Mg^{2+}	1.68E-05	2.91E-06	4.06E-06	5.55E-07	1.11E-05	4.65E-05	6.64E-05	7.93E-05	2.32E-07	4.02E-05	6.11E-06
$CaHCO_3^+$	6.95E-06	5.43E-06	5.30E-06	2.83E-06	6.19E-06	9.87E-06	1.91E-05	2.68E-05	1.88E-06	1.56E-05	4.85E-06
$CaCO_{3(aq)}$	6.04E-06	7.42E-06	8.15E-06	8.66E-06	9.06E-06	1.17E-05	2.13E-05	3.16E-05	8.97E-06	2.10E-05	9.85E-06
$CO_{2(aq)}$	3.34E-06	4.37E-06	9.28E-06	4.37E-06	1.83E-05	9.30E-05	1.15E-04	1.32E-04	2.95E-05	1.39E-04	3.90E-05
CO_3^{2-}	2.05E-07	4.01E-07	8.72E-07	1.28E-06	2.02E-06	1.54E-05	2.34E-05	4.91E-05	2.96E-05	3.64E-05	7.02E-06
$MgOH^+$	1.42E-07	3.73E-08	5.41E-08	1.71E-08	9.05E-08	6.85E-08	5.89E-08	3.52E-08	5.92E-09	4.55E-08	7.49E-08
$NaF_{(aq)}$	1.21E-07	1.19E-07	1.80E-07	1.13E-07	9.46E-07	8.18E-07	6.45E-07	4.42E-07	7.52E-07	6.67E-07	1.19E-06
HSO_4^-	1.16E-07	6.44E-08	2.17E-08	5.46E-09	2.13E-08	5.27E-09	3.51E-09	4.22E-10	4.94E-10	9.90E-10	7.65E-09
H^+	4.94E-08	3.14E-08	2.72E-08	1.38E-08	2.67E-08	2.26E-08	2.02E-08	1.28E-08	7.93E-09	1.69E-08	1.93E-08
AlO_2^-	3.27E-08	7.08E-08	5.02E-08	9.97E-08	8.03E-10	5.36E-09	3.71E-09	1.50E-09	6.09E-08	4.03E-09	1.42E-09
$MgHCO_3^+$	7.58E-09	2.89E-09	1.13E-08	1.58E-09	5.73E-08	1.18E-06	2.12E-06	3.96E-06	7.27E-09	1.96E-06	1.00E-07
$MgCO_{3(aq)}$	1.49E-09	9.14E-10	4.16E-09	1.15E-09	2.13E-08	4.46E-07	8.15E-07	1.85E-06	9.03E-09	9.05E-07	5.15E-08
NO_2^-	5.53E-13	1.71E-13	3.68E-14	2.89E-14	2.13E-14	5.03E-16	1.94E-16	1.08E-17	2.08E-14	7.82E-17	1.20E-14
AlO^+	5.40E-14	6.57E-14	5.22E-14	2.69E-14	1.33E-15	5.16E-14	5.58E-14	3.58E-14	1.23E-14	4.37E-14	1.29E-15
$AlOH^{2+}$	1.49E-17	1.07E-17	7.87E-18	1.85E-18	2.75E-19	3.24E-17	4.88E-17	4.71E-17	8.01E-19	3.06E-17	1.83E-19
Al^{3+}	1.93E-21	6.81E-22	4.43E-22	4.29E-23	2.41E-23	1.16E-20	2.63E-20	3.90E-20	2.11E-23	1.25E-20	1.05E-23
ClO_4^-	9.85E-24	2.13E-24	1.18E-24	3.73E-25	8.53E-25	2.63E-25	1.82E-25	1.48E-26	1.65E-25	3.27E-26	3.37E-25
$H_{2(aq)}$	9.65E-34	4.76E-34	1.43E-34	1.82E-34	1.75E-35	3.83E-39	2.56E-40	1.25E-42	6.56E-36	2.56E-40	1.75E-35
$NH_{3(aq)}$	1.44E-49	1.54E-50	8.51E-52	4.76E-52	4.72E-53	8.89E-59	1.56E-60	1.65E-64	5.05E-54	5.45E-61	2.03E-53
NH_4^+	1.05E-49	8.13E-51	4.86E-52	1.32E-52	3.89E-53	2.91E-58	7.48E-60	1.33E-63	1.48E-54	2.19E-60	1.21E-53

Source: DTN: MO0304SPAA11GC.000

NOTE: *Units are in Molality.

Table 6.9-3. List of Species Used to Charge Balance the Individual Water Chemistries

Bin	Charge Balanced Ion
Bin 1	Ca^{2+}
Bin 2	Ca^{2+}
Bin 3	Ca^{2+}
Bin 4	Ca^{2+}
Bin 5	Na^{+}
Bin 6	Na^{+}
Bin 7	Na^{+}
Bin 8	Na^{+}
Bin 9	Na^{+}
Bin 10	Na^{+}
Bin 11	Na^{+}

Source: DTN: MO0304MWDSAB11.001

Table 6.9-4. EQ3NR Input/Output Files for TSPA-LA Abstraction

Bin	Input File Names	Output File Names	Pickup File Names
Bin 1	bin01.3i	bin01.3o	bin01.3p
Bin 2	bin02.3i	bin02.3o	bin02.3p
Bin 3	bin03.3i	bin03.3o	bin03.3p
Bin 4	bin04.3i	bin04.3o	bin04.3p
Bin 5	bin05.3i	bin05.3o	bin05.3p
Bin 6	bin06.3i	bin06.3o	bin06.3p
Bin 7	bin07.3i	bin07.3o	bin07.3p
Bin 8	bin08.3i	bin08.3o	bin08.3p
Bin 9	bin09.3i	bin09.3o	bin09.3p
Bin 10	bin10.3i	bin10.3o	bin10.3p
Bin 11	bin11.3i	bin11.3o	bin11.3p

Source: DTN: MO0304MWDSAB11.001

To cover the range of expected in-drift relative humidity values, the bin waters are evaporated to a water activity of 0.65 and diluted by a factor of 100. The starting bin waters are sufficiently dilute that they represented solutions in equilibrium with relative humidity between 99.9 and 99.99 percent. Dilution of water vapor is simulated for potential relative humidity values higher than the equilibrium relative humidity values of the starting bin water. Thus, for each temperature and CO_2 fugacity combination, two EQ6 input files are generated, one for evaporation and one for dilution.

The resulting EQ6 input and output data files for the bin waters are listed in Table 6.9-5 and documented in DTN: MO0304MWDEBSSA.000. The file nomenclature is ??c#t%$.6i or 6o, where:

- "??" is the two-digit bin number (01, 02, etc.)
- "#" is 2, 3, or 4 for fugacity of CO_2 equal to 10^{-2}, 10^{-3}, or 10^{-4} bar, respectively
- "%" is 4, 7, or 1 for temperature equal to 40, 70, or 100ºC, respectively, and
- "$" is "e" or "c" for evaporation or dilution.

For example, file 01c2t1c.6i is the EQ6 input file for bin 1 dilution at 100°C and a fugacity of CO_2 of 10^{-2} bar.

6.9.3 Lookup Tables

The abstracted results of the evaporation and dilution calculations that are provided as direct input into TSPA-LA calculations are summarized in a set of look-up tables documented in DTN: MO0304SPACSALT.000. These look-up tables, listed in Table 6.9-6, include stated boundary conditions, abstracted output, and results of supplemental calculations. Each evaporation or dilution look-up table corresponds to one of the in-drift precipitates/salts model output files identified in Table 6.9-5. Each row in these tables provides output parameter values as the water incrementally evolves due to evaporation or dilution, given the defined boundary conditions. Each value is defined by a unique equilibrium relative humidity, concentration factor, and relative evaporation rate.

The general look-up table format and the calculations placed in the look-up tables are developed and described in *In-Drift Precipitates/Salts Model* (BSC 2003, Sections 6.7.3 and 6.6.3.5 [DIRS 162529]). The first three columns of these tables are supplemental spreadsheet calculations for: concentration factor (*CF*), relative evaporation rate (*Qe*/*Qs*), and dilution factor (*DF*). The next column is the equilibrium *RH*, calculated by multiplying the activity of water (in column K) by 100 percent. The rest of the columns are filled using GETEQDATA software version 1.0.1 (BSC 2003 [161900]). Columns E through H show reaction progress and the boundary conditions for the starting water (i.e., the temperature and the fugacities of oxygen and carbon dioxide). Columns I through X show reaction progress, pH, ionic strength, mass of H_2O in the reactor, and the total concentrations of the aqueous components. Columns Y through AL present reaction progress, mass of H_2O, and the concentrations of potential acid-neutralizing species. Finally, columns AM through BD show the amounts of minerals accumulated. This last section is not included in the dilution look-up tables though small amounts of minerals (e.g., calcite) may be present, because mineral outputs from the in-drift precipitates/salts model are only needed from evaporation runs.

Table 6.9-5. EQ6 Input/Output Files for TSPA-LA Abstraction

Bin	Input File Names	Output File Names
1	01c2t1e.6i, 01c3t1e.6i, 01c4t1e.6i, 01c2t4e.6i, 01c3t4e.6i, 01c4t4e.6i, 01c2t7e.6i, 01c3t7e.6i, 01c4t7e.6i, 01c2t1c.6i, 01c3t1c.6i, 01c4t1c.6i, 01c2t4c.6i, 01c3t4c.6i, 01c4t4c.6i, 01c2t7c.6i, 01c3t7c.6i, 01c4t7c.6i	01c2t1e.6o, 01c3t1e.6o, 01c4t1e.6o, 01c2t4e.6o, 01c3t4e.6o, 01c4t4e.6o, 01c2t7e.6o, 01c3t7e.6o, 01c4t7e.6o, 01c2t1c.6o, 01c3t1c.6o, 01c4t1c.6o, 01c2t4c.6o, 01c3t4c.6o, 01c4t4c.6o, 01c2t7c.6o, 01c3t7c.6o, 01c4t7c.6o
2	02c2t1e.6i, 02c3t1e.6i, 02c4t1e.6i, 02c2t4e.6i, 02c3t4e.6i, 02c4t4e.6i, 02c2t7e.6i, 02c3t7e.6i, 02c4t7e.6i, 02c2t1c.6i, 02c3t1c.6i, 02c4t1c.6i, 02c2t4c.6i, 02c3t4c.6i, 02c4t4c.6i, 02c2t7c.6i, 02c3t7c.6i, 02c4t7c.6i	02c2t1e.6o, 02c3t1e.6o, 02c4t1e.6o, 02c2t4e.6o, 02c3t4e.6o, 02c4t4e.6o, 02c2t7e.6o, 02c3t7e.6o, 02c4t7e.6o, 02c2t1c.6o, 02c3t1c.6o, 02c4t1c.6o, 02c2t4c.6o, 02c3t4c.6o, 02c4t4c.6o, 02c2t7c.6o, 02c3t7c.6o, 02c4t7c.6o
3	03c2t1e.6i, 03c3t1e.6i, 03c4t1e.6i, 03c2t4e.6i, 03c3t4e.6i, 03c4t4e.6i, 03c2t7e.6i, 03c3t7e.6i, 03c4t7e.6i, 03c2t1c.6i, 03c3t1c.6i, 03c4t1c.6i, 03c2t4c.6i, 03c3t4c.6i, 03c4t4c.6i, 03c2t7c.6i, 03c3t7c.6i, 03c4t7c.6i	03c2t1e.6o, 03c3t1e.6o, 03c4t1e.6o, 03c2t4e.6o, 03c3t4e.6o, 03c4t4e.6o, 03c2t7e.6o, 03c3t7e.6o, 03c4t7e.6o, 03c2t1c.6o, 03c3t1c.6o, 03c4t1c.6o, 03c2t4c.6o, 03c3t4c.6o, 03c4t4c.6o, 03c2t7c.6o, 03c3t7c.6o, 03c4t7c.6o
4	04c2t1e.6i, 04c3t1e.6i, 04c4t1e.6i, 04c2t4e.6i, 04c3t4e.6i, 04c4t4e.6i, 04c2t7e.6i, 04c3t7e.6i, 04c4t7e.6i, 04c2t1c.6i, 04c3t1c.6i, 04c4t1c.6i, 04c2t4c.6i, 04c3t4c.6i, 04c4t4c.6i, 04c2t7c.6i, 04c3t7c.6i, 04c4t7c.6i	04c2t1e.6o, 04c3t1e.6o, 04c4t1e.6o, 04c2t4e.6o, 04c3t4e.6o, 04c4t4e.6o, 04c2t7e.6o, 04c3t7e.6o, 04c4t7e.6o, 04c2t1c.6o, 04c3t1c.6o, 04c4t1c.6o, 04c2t4c.6o, 04c3t4c.6o, 04c4t4c.6o, 04c2t7c.6o, 04c3t7c.6o, 04c4t7c.6o
5	05c2t1e.6i, 05c3t1e.6i, 05c4t1e.6i, 05c2t4e.6i, 05c3t4e.6i, 05c4t4e.6i, 05c2t7e.6i, 05c3t7e.6i, 05c4t7e.6i, 05c2t1c.6i, 05c3t1c.6i, 05c4t1c.6i, 05c2t4c.6i, 05c3t4c.6i, 05c4t4c.6i, 05c2t7c.6i, 05c3t7c.6i, 05c4t7c.6i	05c2t1e.6o, 05c3t1e.6o, 05c4t1e.6o, 05c2t4e.6o, 05c3t4e.6o, 05c4t4e.6o, 05c2t7e.6o, 05c3t7e.6o, 05c4t7e.6o, 05c2t1c.6o, 05c3t1c.6o, 05c4t1c.6o, 05c2t4c.6o, 05c3t4c.6o, 05c4t4c.6o, 05c2t7c.6o, 05c3t7c.6o, 05c4t7c.6o
6	06c2t1e.6i, 06c3t1e.6i, 06c4t1e.6i, 06c2t4e.6i, 06c3t4e.6i, 06c4t4e.6i, 06c2t7e.6i, 06c3t7e.6i, 06c4t7e.6i, 06c2t1c.6i, 06c3t1c.6i, 06c4t1c.6i, 06c2t4c.6i, 06c3t4c.6i, 06c4t4c.6i, 06c2t7c.6i, 06c3t7c.6i, 06c4t7c.6i	06c2t1e.6o, 06c3t1e.6o, 06c4t1e.6o, 06c2t4e.6o, 06c3t4e.6o, 06c4t4e.6o, 06c2t7e.6o, 06c3t7e.6o, 06c4t7e.6o, 06c2t1c.6o, 06c3t1c.6o, 06c4t1c.6o, 06c2t4c.6o, 06c3t4c.6o, 06c4t4c.6o, 06c2t7c.6o, 06c3t7c.6o, 06c4t7c.6o
7	07c2t1e.6i, 07c3t1e.6i, 07c4t1e.6i, 07c2t4e.6i, 07c3t4e.6i, 07c4t4e.6i, 07c2t7e.6i, 07c3t7e.6i, 07c4t7e.6i, 07c2t1c.6i, 07c3t1c.6i, 07c4t1c.6i, 07c2t4c.6i, 07c3t4c.6i, 07c4t4c.6i, 07c2t7c.6i, 07c3t7c.6i, 07c4t7c.6i	07c2t1e.6o, 07c3t1e.6o, 07c4t1e.6o, 07c2t4e.6o, 07c3t4e.6o, 07c4t4e.6o, 07c2t7e.6o, 07c3t7e.6o, 07c4t7e.6o, 07c2t1c.6o, 07c3t1c.6o, 07c4t1c.6o, 07c2t4c.6o, 07c3t4c.6o, 07c4t4c.6o, 07c2t7c.6o, 07c3t7c.6o, 07c4t7c.6o
8	08c2t1e.6i, 08c3t1e.6i, 08c4t1e.6i, 08c2t4e.6i, 08c3t4e.6i, 08c4t4e.6i, 08c2t7e.6i, 08c3t7e.6i, 08c4t7e.6i, 08c2t1c.6i, 08c3t1c.6i, 08c4t1c.6i, 08c2t4c.6i, 08c3t4c.6i, 08c4t4c.6i, 08c2t7c.6i, 08c3t7c.6i, 08c4t7c.6i	08c2t1e.6o, 08c3t1e.6o, 08c4t1e.6o, 08c2t4e.6o, 08c3t4e.6o, 08c4t4e.6o, 08c2t7e.6o, 08c3t7e.6o, 08c4t7e.6o, 08c2t1c.6o, 08c3t1c.6o, 08c4t1c.6o, 08c2t4c.6o, 08c3t4c.6o, 08c4t4c.6o, 08c2t7c.6o, 08c3t7c.6o, 08c4t7c.6o

Table 6.9-5. EQ6 Input/Output Files for TSPA-LA Abstraction (Continued)

Bin	Input File Names	Output File Names
9	09c2t1e.6i, 09c3t1e.6i, 09c4t1e.6i, 09c2t4e.6i, 09c3t4e.6i, 09c4t4e.6i, 09c2t7e.6i, 09c3t7e.6i, 09c4t7e.6i, 09c2t1c.6i, 09c3t1c.6i, 09c4t1c.6i, 09c2t4c.6i, 09c3t4c.6i, 09c4t4c.6i, 09c2t7c.6i, 09c3t7c.6i, 09c4t7c.6i	09c2t1e.6o, 09c3t1e.6o, 09c4t1e.6o, 09c2t4e.6o, 09c3t4e.6o, 09c4t4e.6o, 09c2t7e.6o, 09c3t7e.6o, 09c4t7e.6o, 09c2t1c.6o, 09c3t1c.6o, 09c4t1c.6o, 09c2t4c.6o, 09c3t4c.6o, 09c4t4c.6o, 09c2t7c.6o, 09c3t7c.6o, 09c4t7c.6o
10	10c2t1e.6i, 10c3t1e.6i, 10c4t1e.6i, 10c2t4e.6i, 10c3t4e.6i, 10c4t4e.6i, 10c2t7e.6i, 10c3t7e.6i, 10c4t7e.6i, 10c2t1c.6i, 10c3t1c.6i, 10c4t1c.6i, 10c2t4c.6i, 10c3t4c.6i, 10c4t4c.6i, 10c2t7c.6i, 10c3t7c.6i, 10c4t7c.6i	10c2t1e.6o, 10c3t1e.6o, 10c4t1e.6o, 10c2t4e.6o, 10c3t4e.6o, 10c4t4e.6o, 10c2t7e.6o, 10c3t7e.6o, 10c4t7e.6o, 10c2t1c.6o, 10c3t1c.6o, 10c4t1c.6o, 10c2t4c.6o, 10c3t4c.6o, 10c4t4c.6o, 10c2t7c.6o, 10c3t7c.6o, 10c4t7c.6o
11	11c2t1e.6i, 11c3t1e.6i, 11c4t1e.6i, 11c2t4e.6i, 11c3t4e.6i, 11c4t4e.6i, 11c2t7e.6i, 11c3t7e.6i, 11c4t7e.6i, 11c2t1c.6i, 11c3t1c.6i, 11c4t1c.6i, 11c2t4c.6i, 11c3t4c.6i, 11c4t4c.6i, 11c2t7c.6i, 11c3t7c.6i, 11c4t7c.6i	11c2t1e.6o, 11c3t1e.6o, 11c4t1e.6o, 11c2t4e.6o, 11c3t4e.6o, 11c4t4e.6o, 11c2t7e.6o, 11c3t7e.6o, 11c4t7e.6o, 11c2t1c.6o, 11c3t1c.6o, 11c4t1c.6o, 11c2t4c.6o, 11c3t4c.6o, 11c4t4c.6o, 11c2t7c.6o, 11c3t7c.6o, 11c4t7c.6o

Source: DTN: MO0304MWDEBSSA.000

Table 6.9-6. Lookup Tables for TSPA-LA Abstraction

Bin	Evaporation Lookup Tables	Dilution Lookup Tables
1	01c2t1e.xls.xls, 01c3t1e.xls.xls, 01c4t1e.xls.xls, 01c2t4e.xls.xls, 01c3t4e.xls.xls, 01c4t4e.xls.xls, 01c2t7e.xls.xls, 01c3t7e.xls.xls, 01c4t7e.xls.xls	01c2t1c.xls.xls, 01c3t1c.xls.xls, 01c4t1c.xls.xls, 01c2t4c.xls.xls, 01c3t4c.xls.xls, 01c4t4c.xls.xls, 01c2t7c.xls.xls, 01c3t7c.xls.xls, 01c4t7c.xls.xls
2	02c2t1e.xls.xls, 02c3t1e.xls.xls, 02c4t1e.xls.xls, 02c2t4e.xls.xls, 02c3t4e.xls.xls, 02c4t4e.xls.xls, 02c2t7e.xls.xls, 02c3t7e.xls.xls, 02c4t7e.xls.xls	02c2t1c.xls.xls, 02c3t1c.xls.xls, 02c4t1c.xls.xls, 02c2t4c.xls.xls, 02c3t4c.xls.xls, 02c4t4c.xls.xls, 02c2t7c.xls.xls, 02c3t7c.xls.xls, 02c4t7c.xls.xls
3	03c2t1e.xls.xls, 03c3t1e.xls.xls, 03c4t1e.xls.xls, 03c2t4e.xls.xls, 03c3t4e.xls.xls, 03c4t4e.xls.xls, 03c2t7e.xls.xls, 03c3t7e.xls.xls, 03c4t7e.xls.xls	03c2t1c.xls.xls, 03c3t1c.xls.xls, 03c4t1c.xls.xls, 03c2t4c.xls.xls, 03c3t4c.xls.xls, 03c4t4c.xls.xls, 03c2t7c.xls.xls, 03c3t7c.xls.xls, 03c4t7c.xls.xls
4	04c2t1e.xls.xls, 04c3t1e.xls.xls, 04c4t1e.xls.xls, 04c2t4e.xls.xls, 04c3t4e.xls.xls, 04c4t4e.xls.xls, 04c2t7e.xls.xls, 04c3t7e.xls.xls, 04c4t7e.xls.xls	04c2t1c.xls.xls, 04c3t1c.xls.xls, 04c4t1c.xls.xls, 04c2t4c.xls.xls, 04c3t4c.xls.xls, 04c4t4c.xls.xls, 04c2t7c.xls.xls, 04c3t7c.xls.xls, 04c4t7c.xls.xls
5	05c2t1e.xls.xls, 05c3t1e.xls.xls, 05c4t1e.xls.xls, 05c2t4e.xls.xls, 05c3t4e.xls.xls, 05c4t4e.xls.xls, 05c2t7e.xls.xls, 05c3t7e.xls.xls, 05c4t7e.xls.xls	05c2t1c.xls.xls, 05c3t1c.xls.xls, 05c4t1c.xls.xls, 05c2t4c.xls.xls, 05c3t4c.xls.xls, 05c4t4c.xls.xls, 05c2t7c.xls.xls, 05c3t7c.xls.xls, 05c4t7c.xls.xls
6	06c2t1e.xls.xls, 06c3t1e.xls.xls, 06c4t1e.xls.xls, 06c2t4e.xls.xls, 06c3t4e.xls.xls, 06c4t4e.xls.xls, 06c2t7e.xls.xls, 06c3t7e.xls.xls, 06c4t7e.xls.xls	06c2t1c.xls.xls, 06c3t1c.xls.xls, 06c4t1c.xls.xls, 06c2t4c.xls.xls, 06c3t4c.xls.xls, 06c4t4c.xls.xls, 06c2t7c.xls.xls, 06c3t7c.xls.xls, 06c4t7c.xls.xls
7	07c2t1e.xls.xls, 07c3t1e.xls.xls, 07c4t1e.xls.xls, 07c2t4e.xls.xls, 07c3t4e.xls.xls, 07c4t4e.xls.xls, 07c2t7e.xls.xls, 07c3t7e.xls.xls, 07c4t7e.xls.xls	07c2t1c.xls.xls, 07c3t1c.xls.xls, 07c4t1c.xls.xls, 07c2t4c.xls.xls, 07c3t4c.xls.xls, 07c4t4c.xls.xls, 07c2t7c.xls.xls, 07c3t7c.xls.xls, 07c4t7c.xls.xls
8	08c2t1e.xls.xls, 08c3t1e.xls.xls, 08c4t1e.xls.xls, 08c2t4e.xls.xls, 08c3t4e.xls.xls, 08c4t4e.xls.xls, 08c2t7e.xls.xls, 08c3t7e.xls.xls, 08c4t7e.xls.xls	08c2t1c.xls.xls, 08c3t1c.xls.xls, 08c4t1c.xls.xls, 08c2t4c.xls.xls, 08c3t4c.xls.xls, 08c4t4c.xls.xls, 08c2t7c.xls.xls, 08c3t7c.xls.xls, 08c4t7c.xls.xls

Table 6.9-6. Lookup Tables for TSPA-LA Abstraction (Continued)

Bin	Evaporation Lookup Tables	Dilution Lookup Tables
9	09c2t1e.xls.xls, 09c3t1e.xls.xls, 09c4t1e.xls.xls, 09c2t4e.xls.xls, 09c3t4e.xls.xls, 09c4t4e.xls.xls, 09c2t7e.xls.xls, 09c3t7e.xls.xls, 09c4t7e.xls.xls	09c2t1c.xls.xls, 09c3t1c.xls.xls, 09c4t1c.xls.xls, 09c2t4c.xls.xls, 09c3t4c.xls.xls, 09c4t4c.xls.xls, 09c2t7c.xls.xls, 09c3t7c.xls.xls, 09c4t7c.xls.xls
10	10c2t1e.xls.xls, 10c3t1e.xls.xls, 10c4t1e.xls.xls, 10c2t4e.xls.xls, 10c3t4e.xls.xls, 10c4t4e.xls.xls, 10c2t7e.xls.xls, 10c3t7e.xls.xls, 10c4t7e.xls.xls	10c2t1c.xls.xls, 10c3t1c.xls.xls, 10c4t1c.xls.xls, 10c2t4c.xls.xls, 10c3t4c.xls.xls, 10c4t4c.xls.xls, 10c2t7c.xls.xls, 10c3t7c.xls.xls, 10c4t7c.xls.xls
11	11c2t1e.xls.xls, 11c3t1e.xls.xls, 11c4t1e.xls.xls, 11c2t4e.xls.xls, 11c3t4e.xls.xls, 11c4t4e.xls.xls, 11c2t7e.xls.xls, 11c3t7e.xls.xls, 11c4t7e.xls.xls	11c2t1c.xls.xls, 11c3t1c.xls.xls, 11c4t1c.xls.xls, 11c2t4c.xls.xls, 11c3t4c.xls.xls, 11c4t4c.xls.xls, 11c2t7c.xls.xls, 11c3t7c.xls.xls, 11c4t7c.xls.xls

Source: DTN: MO0304SPACSALT.000

NOTE: TSPA-LA modelers should use DTN: MO0310SPAPCEGS.000 as the source for the lookup tables as discussed in Section 8.2.1. The filenames in DTN: MO0310SPAPCEGS.000 do not carry the extra ".xls."

The values in the look-up tables may be used to define response surfaces so that interpolations and extrapolations (Pco_2 parameter only, see Section 6.12.4.3) may be obtained for more precise input values not provided in the tables. Table 6.9-7 displays the maximum equilibrium relative humidity value in the evaporation look-up table for a given boundary condition at or below which the information remains valid. If the equilibrium relative humidity exceeds this maximum value, then the corresponding dilution look-up table is used instead.

Table 6.9-7. Relative Humidity Boundaries Between Evaporation and Dilution Lookup Tables

Bin	1E-2 CO_2 Fugacity			1E-3 CO_2 Fugacity			1E-4 CO_2 Fugacity		
	40°C	70°C	100°C	40°C	70°C	100°C	40°C	70°C	100°C
1	99.916%	99.915%	99.921%	99.917%	99.915%	99.921%	99.917%	99.915%	99.921%
2	99.962%	99.960%	99.957%	99.963%	99.961%	99.958%	99.963%	99.960%	99.957%
3	99.975%	99.973%	99.969%	99.976%	99.973%	99.970%	99.976%	99.973%	99.970%
4	99.985%	99.982%	99.978%	99.985%	99.983%	99.979%	99.986%	99.982%	99.978%
5	99.970%	99.967%	99.964%	99.971%	99.968%	99.965%	99.971%	99.968%	99.964%
6	99.964%	99.965%	99.966%	99.966%	99.967%	99.968%	99.968%	99.969%	99.969%
7	99.962%	99.964%	99.966%	99.965%	99.966%	99.967%	99.967%	99.968%	99.968%
8	99.969%	99.971%	99.971%	99.971%	99.972%	99.973%	99.974%	99.975%	99.974%
9	99.977%	99.975%	99.976%	99.978%	99.977%	99.978%	99.978%	99.979%	99.979%
10	99.969%	99.970%	99.971%	99.971%	99.972%	99.973%	99.974%	99.975%	99.975%
11	99.976%	99.973%	99.969%	99.976%	99.973%	99.970%	99.976%	99.973%	99.969%

Source: DTN: MO0304SPACSALT.000

6.9.4 Illustration of Results

Figures 6.9-1 through 6.9-6 graphically illustrate the results with plots of values from the 11c3t7e.xls.xls look-up table. These are Bin 11 evaporation results at a temperature of 70ºC and a CO_2 fugacity of 10^{-3} bar. Figures 6.9-1 and 6.9-2 plot the total elemental aqueous concentrations and pH as a function of relative humidity and concentration factor. Figures 6.9-3 and 6.9-4 plot the ANC (acid neutralizing capacity; ANC in this case represents those species that contribute to or influence the pH) aqueous species concentrations and pH as a function of relative humidity and concentration factor. Figures 6.9-5 and 6.9-6 plot pH, the fixed CO_2 and O_2 fugacities, and the moles of minerals precipitated from one kilogram of incoming water as a function of relative humidity and concentration factor.

Results of the corresponding dilution look-up table (11c3t7c.xls.xls) are displayed in Figures 6.9-7 through 6.9-10. The first two figures show plots of the total elemental aqueous concentrations and pH as a function of relative humidity and dilution factor. The last two plot the ANC aqueous species concentrations and pH as a function of relative humidity and dilution factor. The results from the remainder of the look-up tables are provided in Attachment II.

INTENTIONALLY LEFT BLANK

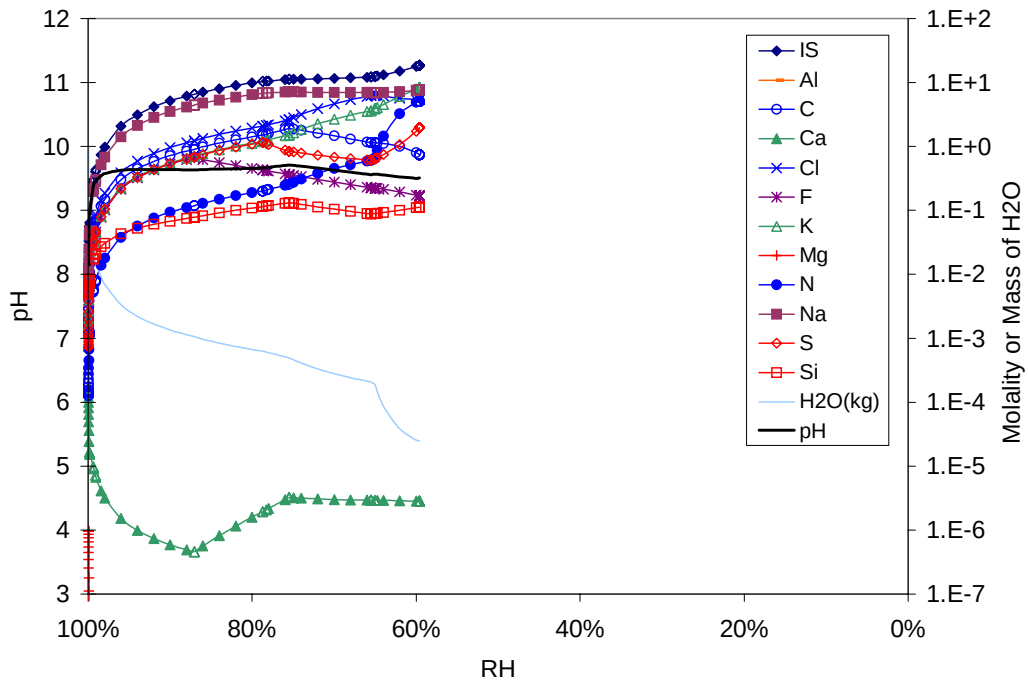

DTN: MO0304SPACSALT.000

Figure 6.9-1. Predicted Compositional Evolution as Bin 11 Waters Evaporate at 70ºC and 10^{-3} CO_2 Fugacity, Plotted Versus Relative Humidity

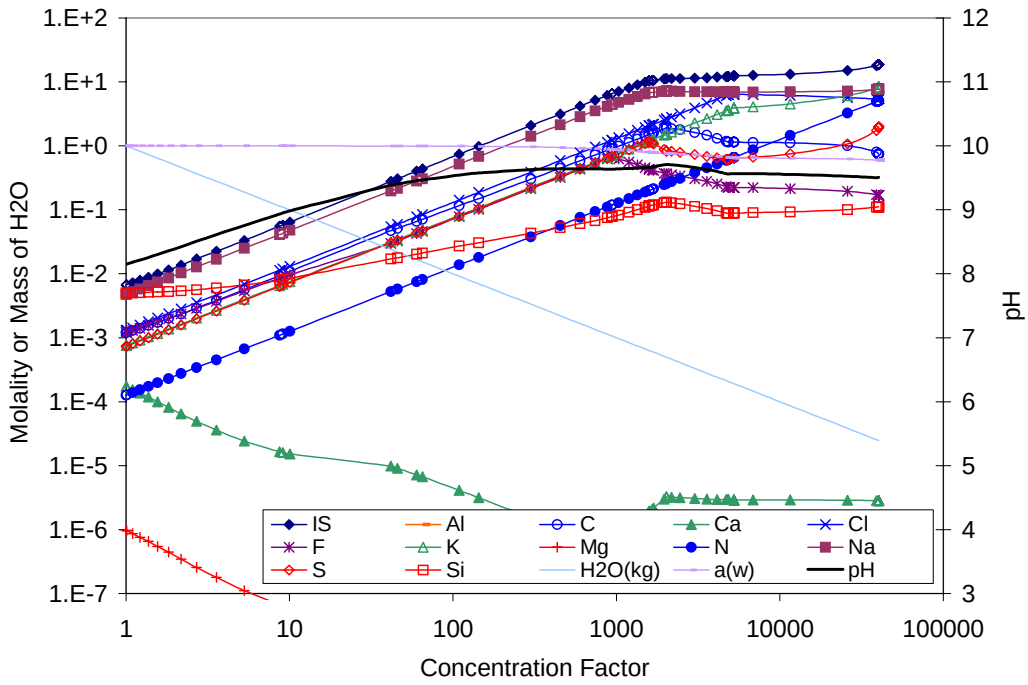

DTN: MO0304SPACSALT.000

Figure 6.9-2. Predicted Compositional Evolution as Bin 11 Waters Evaporate at 70ºC and 10^{-3} CO_2 Fugacity, Plotted Versus Concentration Factor

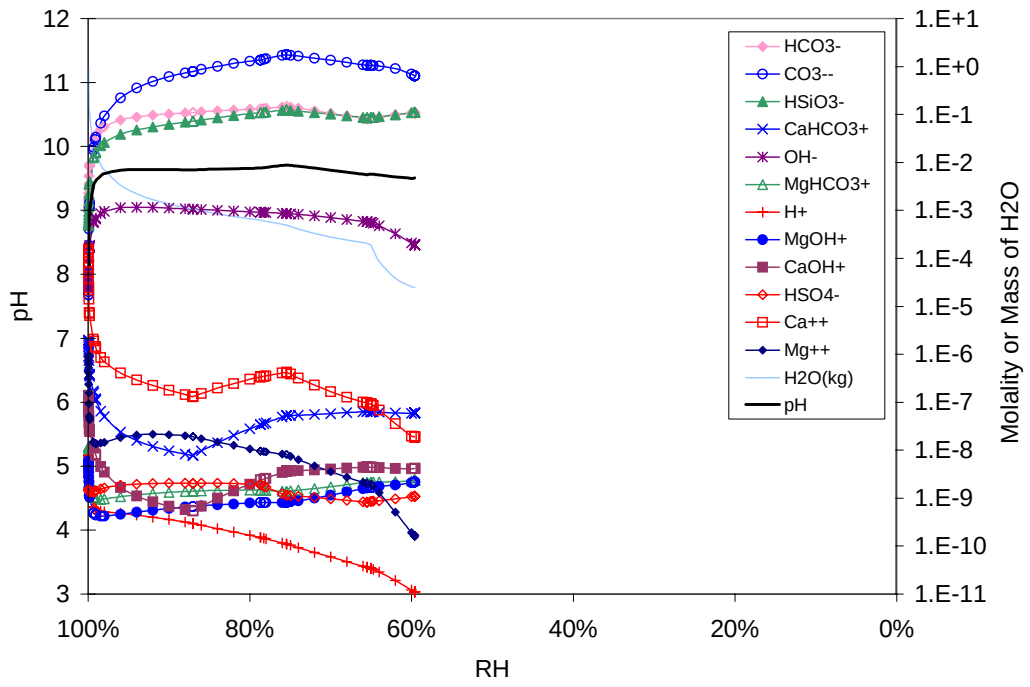

DTN: MO0304SPACSALT.000

Figure 6.9-3. The Predicted Concentrations of ANC Species During Evaporative Evolution of Bin 11 Water at 70ºC and 10^{-3} bar CO_2 Fugacity, Plotted Versus Relative Humidity

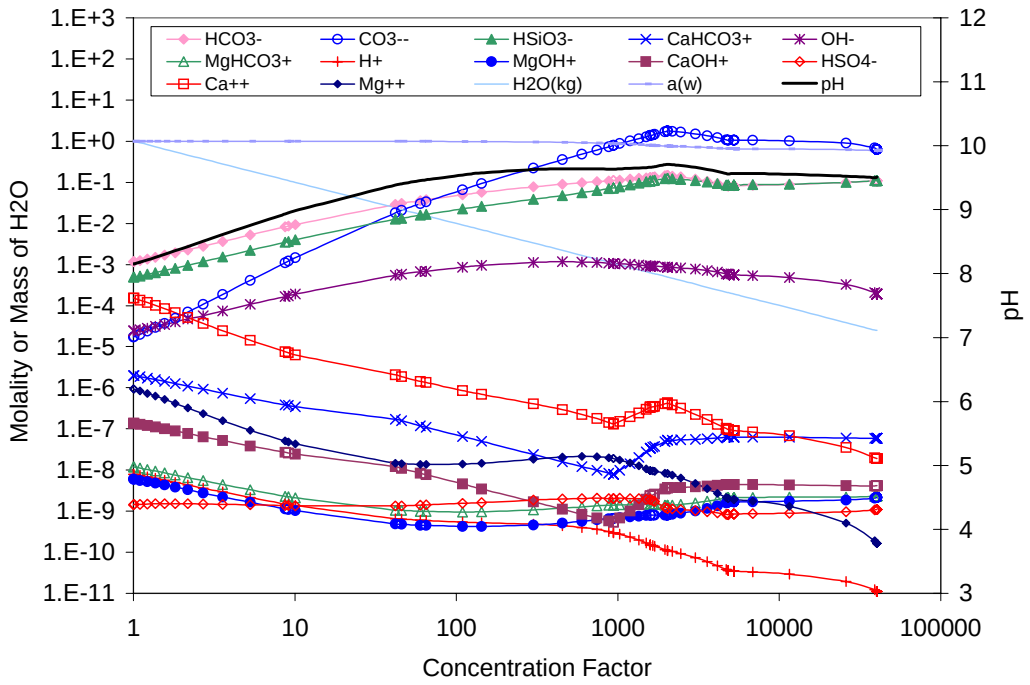

DTN: MO0304SPACSALT.000

Figure 6.9-4. The Predicted Concentrations of ANC Species During Evaporative Evolution of Bin 11 Water at 70ºC and 10^{-3} bar CO_2 Fugacity, Plotted Versus Concentration Factor

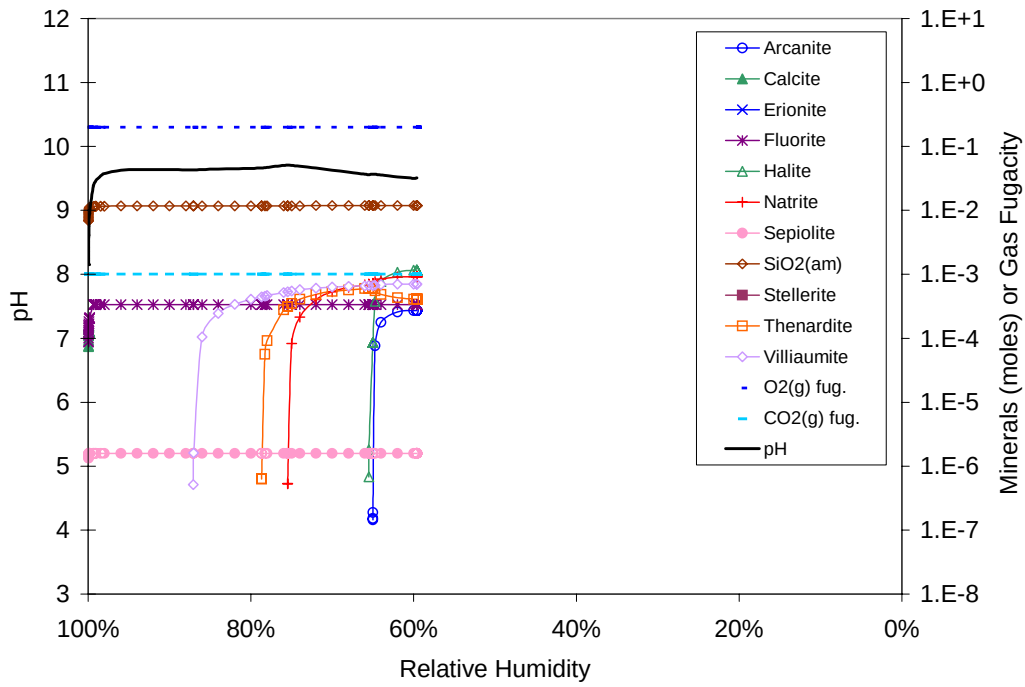

DTN: MO0304SPACSALT.000

Figure 6.9-5. Predicted Mineral Precipitation as Bin 11 Waters Evaporate at 70°C and 10^{-3} CO_2 Fugacity, Plotted Versus Relative Humidity

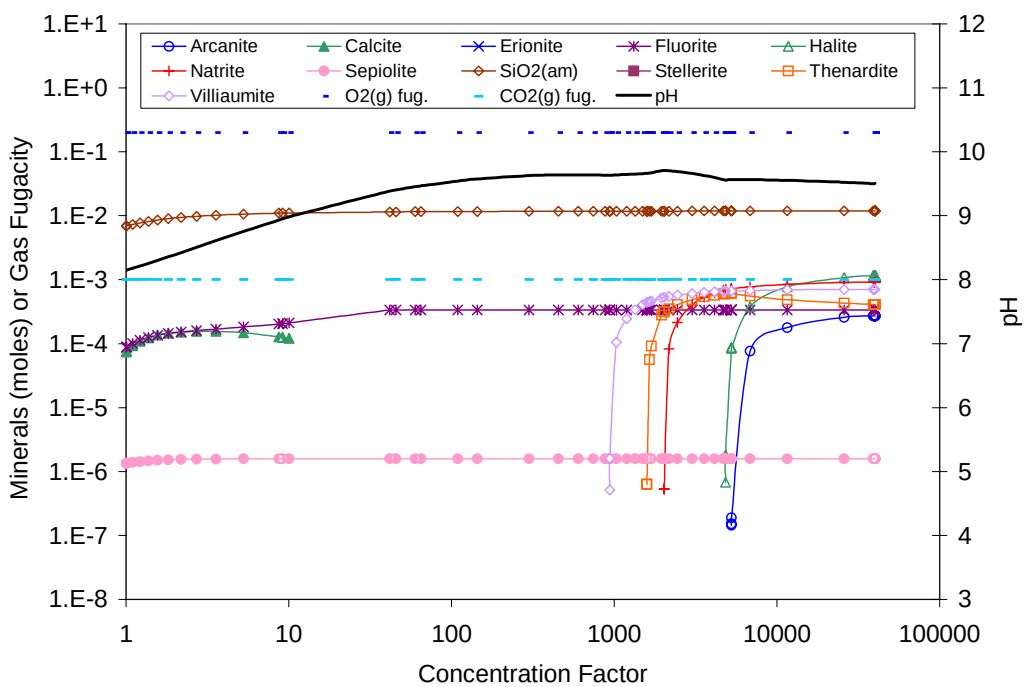

DTN: MO0304SPACSALT.000

Figure 6.9-6. Predicted Mineral Precipitation as Bin 11 Waters Evaporate at 70°C and 10^{-3} CO_2 Fugacity, Plotted Versus Concentration Factor

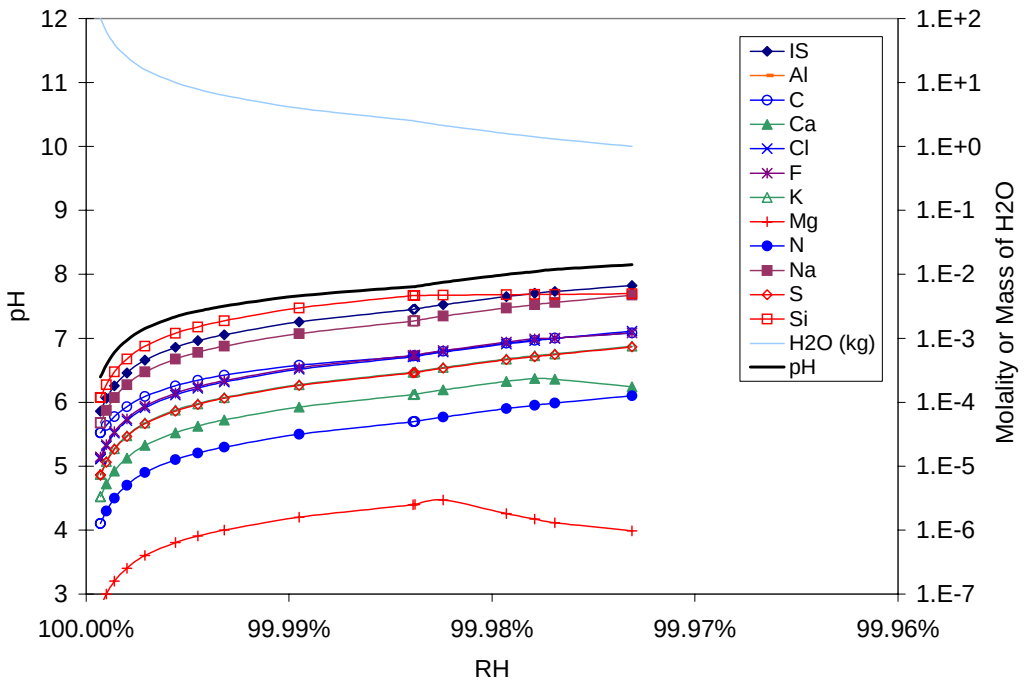

DTN: MO0304SPACSALT.000

Figure 6.9-7. Predicted Compositional Evolution as Bin 11 Waters are Diluted at 70ºC and 10^{-3} CO_2 Fugacity, Plotted Versus Relative Humidity

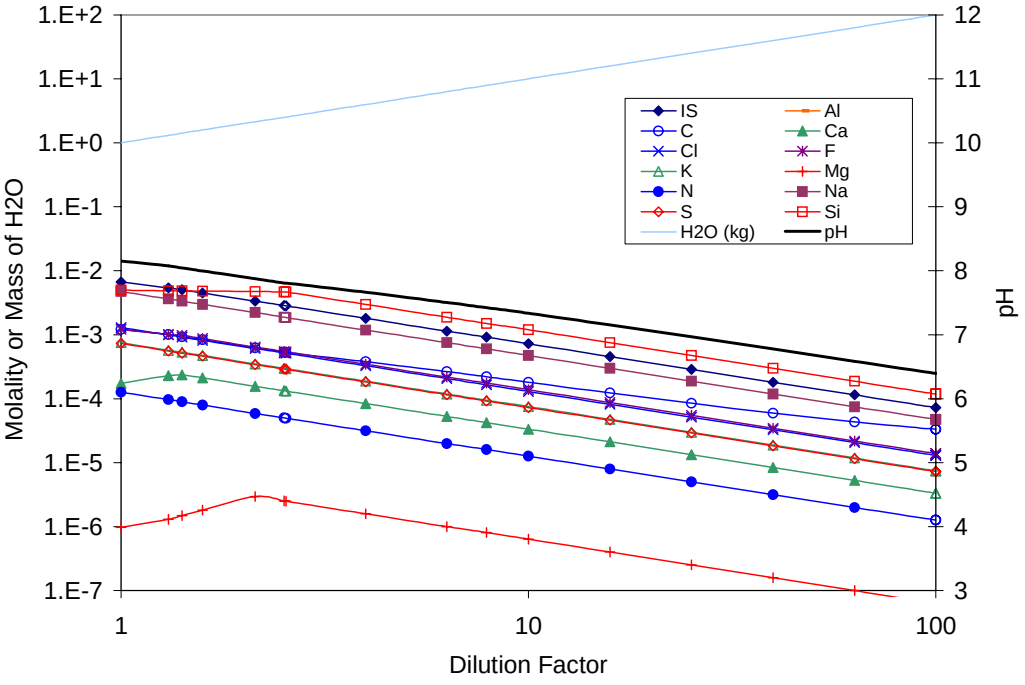

DTN: MO0304SPACSALT.000

Figure 6.9-8. Predicted Compositional Evolution as Bin 11 Waters are Diluted at 70ºC and 10^{-3} CO_2 Fugacity, Plotted Versus Concentration Factor

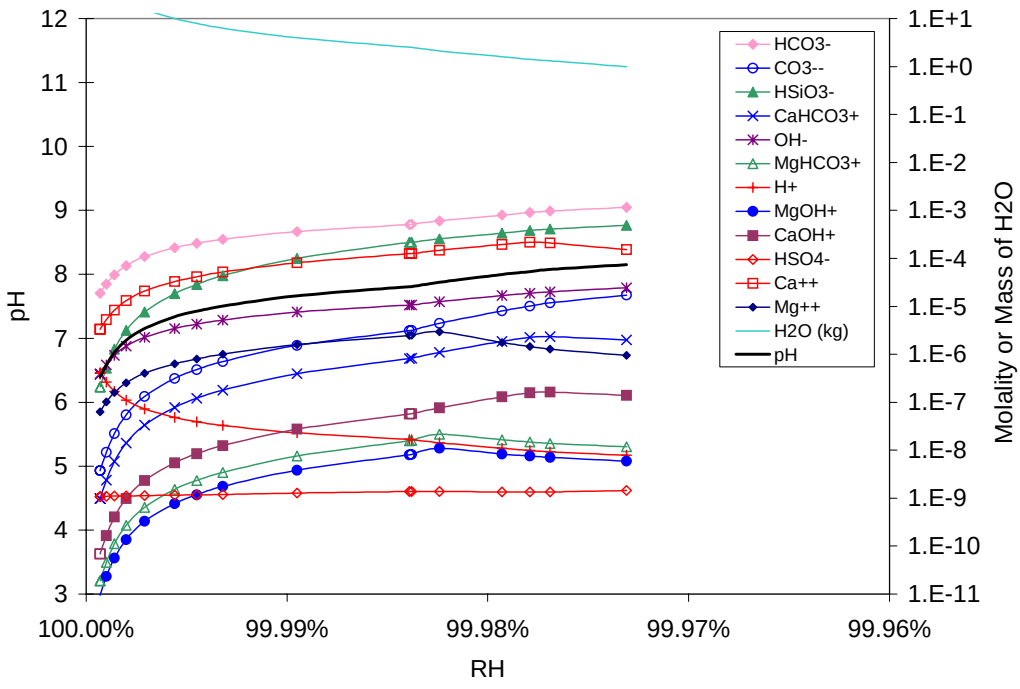

DTN: MO0304SPACSALT.000

Figure 6.9-9. The Predicted Concentrations of ANC Species During Dilution of Bin 11 Water at 70ºC and 10^{-3} bar CO_2 Fugacity, Plotted Versus Relative Humidity

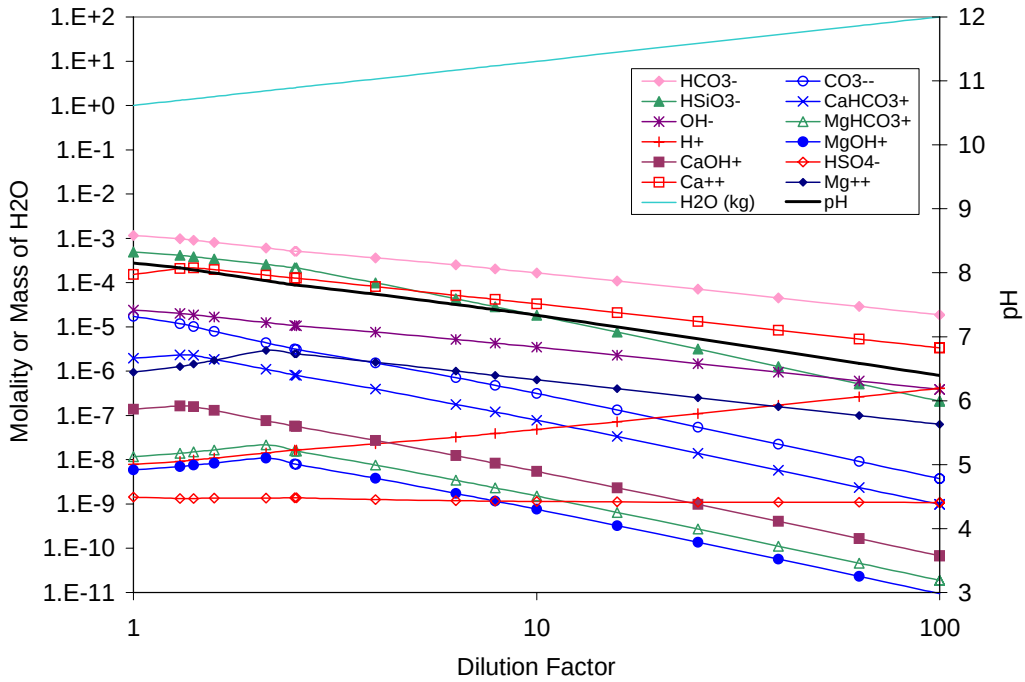

DTN: MO0304SPACSALT.000

Figure 6.9-10. The Predicted Concentrations of ANC Species During Dilution of Bin 11 Water at 70ºC and 10^{-3} bar CO_2 Fugacity, Plotted Versus Dilution Factor

INTENTIONALLY LEFT BLANK

6.10 IN-DRIFT DUST LEACHATE ANALYSES

This section presents the technical approach to evaluate dust leachate chemistry and construct a set of lookup tables for use in the TSPA-LA. Section 6.10.1 briefly discusses the physical processes that are evaluated, after which an assessment of the U.S. Geological Survey (USGS) ESF dust datasets is presented (Section 6.10.2). Finally, an evaluation of the dust leachate chemistry and its abstraction into lookup tables is performed (Sections 6.10.3 through 6.10.7). The lookup tables are constructed based on the EQ3/6 (v. 8.0) calculations using thermodynamic database data0.ypf (Section 4.1.4, DTN: SN0302T0510102.002 [DIRS 162572]) and the USGS data on dust leachate compositions (DTNs: MO0207EBSDUSTS.020 [DIRS 162556] and MO0209EBSDUST2.030 [DIRS 162557]). Figure 6.10-1 shows the flow of the dust leachate abstraction process as derived for implementation in the TSPA-LA.

6.10.1 Conceptual Framework

Dust accumulated on waste packages or drift shields during the operational period may contain some components of soluble salts, which will cause water condensation if the in-drift humidity is higher than the minimum deliquescence point of the salts. The resulting concentrated solution can potentially affect the degradation of the engineered barriers. Based on chemical equilibrium, the activity of water in the condensed (or deliquesced) solution (a_w) is set equal to the *RH* in the drift.

Based on the conceptual framework outlined in Section 6.2, the chemistry of the condensed water is mainly controlled by the:

- Type and relative amounts of soluble salts present in the dust deposited on the waste packages or drip shields
- Relative humidity, temperature, and partial pressure of CO_2 in the drift.

The amount of water that is expected to be present upon deliquescence of the system eutectic mineral assemblage is extremely small (at best a few nanolayers thick; see additional discussion on rock:water ratios in Section 6.11.3). Because of the randomness of the distribution of salt minerals within the dust, this water could be located anywhere in the dust and not in direct contact with the waste package. For TSPA-LA purposes the deliquesced water is modeled as being directly in contact with the waste package surface. See Section 6.11.3 for discussion of alternate conceptual models on salt and water distribution.

6.10.2 Evaluation of U.S. Geological Survey Datasets

The USGS has provided two sets of measurements on dust compositions, which constitute the basic input data for the dust deliquescence calculations (Section 4.1.6, DTNs: MO0207EBSDUSTS.020 [DIRS 162556] and MO0209EBSDUST2.030 [DIRS 162557]). The first set of measurements, presented in Table 4.1-19, was made on the samples collected throughout the ESF during site characterization activities. The second set of measurements, presented in Table 4.1-20, was made on samples sufficiently large for chemical analyses of size-classified aliquots. Three size distributions of dust samples were prepared for chemical

analysis: 60–200 mesh, 200–325 mesh, and less than 325 mesh (Peterman et al. 2003 [DIRS 162819]).

Data used in the dust leachate analysis were collected in ESF several years after initial construction of the tunnel. The following activities known to occur in the ESF could influence or alter the initial composition of dusts generated by the construction of potential emplacement drifts:

- Diesel emissions from trains
- Welding activities
- Conveyor belt operations
- Dust suppression activities
- Operation of construction equipment
- Drilling and blasting
- Accumulation of human and animal waste.

Each of these activities could have significant impact on both local and repository wide dust compositions. In all cases, trace elements and organics are possible constituents in airborne particulates. The dust composition measurements indicate that a large portion of the dust in the ESF comes from rock crushing during tunnel construction. The mean SiO_2, Al_2O_3, Na_2O, and K_2O values for the size-classified dust fractions are within about 10 percent of the Topopah Spring Tuff (Tptp) rhyolite values of the crystal-poor member of the Topopah Spring Tuff (Tptp). The water-soluble anions and cations (Ca, Mg, Na, PO_4, Na, Cl, Br, NO_3, and SO_4) are progressively enriched in the finer fractions of the dust, indicating that these components could be derived from atmospheric aerosols or from salts formed by evaporation of construction water and native pore water. The presence of salts formed from construction water is indicated by low Cl/Br ratios, reflecting construction water tagging with a LiBr tracer. See the detailed discussion by Peterman et al. (2003 [DIRS 162819]).

The variation in the compositions of dust samples collected and related leachates analyzed by the USGS (total of 59 leachate analyses) is used to represent their compositional variability within the potential repository (see Assumption 5.2.3). Of the 59 measurements, two analyses (#00574984B and 00574984C in Table 4.1-20) were excluded from the dust deliquescence calculations because they were incomplete. Three more were excluded (#00574979A, 00574979B, and 00574979C) because they were not collected inside the ESF but at the surface near the north portal.

The concentrations of soluble constituents in the dust samples analyzed by the USGS (DTNs: MO0207EBSDUSTS.020 [DIRS 162556] and MO0209EBSDUST2.030 [DIRS 162557]) are expressed in concentration units of micrograms of species per gram of dust (referred as ppm units in the source DTN – see Peterman et al. (2003 [DIRS 162819])). In order to use this data in the EQ3/6 equilibrium and reaction path calculations, these values were recalculated leachate solution compositions, with aqueous concentration units of micrograms of species per grams of H_2O. The conversion was done by dividing the values provided in the USGS DTNs by 20, which is the mass fraction factor (i.e., grams of H_2O/gram of dust) used in the dust leaching process. Conversions are given in DTN: SN0310T0510102.010 in the Excel file "Table_4_dust_leachate_Conv.xls."

6.10.3 Equilibrium of Dust Leachate Waters

Aqueous speciation calculations have been performed at 25°C with EQ3NR (BSC 2003 [DIRS 162228]) for 54 dust leachate samples. This set of calculations serves two purposes:

- Generating pickup files (*.3p) for subsequent evaporation calculations
- Selecting dust leachate samples for the evaporation calculations based on the calculated pH and the charge neutrality constraint.

The EQ3 input files (*.3i) used in the speciation calculations are generated according to the protocol outlined in the *In-Drift Precipitates/Salts Model* report (BSC 2003 [DIRS 162529]) using the EQ3/6 template files found in DTN: MO0303SPAMEQ36.000 [DIRS 162549].

Two deviations to the protocol outlined in the in-drift precipitates/salts model are necessary due to the lack of direct pH or alkalinity measurements on dust leachate samples. First, pH is estimated by charge balancing on H^+ ion and setting HCO_3^- concentration to be in heterogeneous equilibrium with a fixed $CO_{2(g)}$ fugacity, as a strict charge neutrality constraint must be maintained to obtain physically meaningful results for the intended evaporation calculations. Then, based on the calculated pH values, samples with pH values outside the range of 4 – 10 are screened out, because water-mineral interactions with finely comminuted rhyolitic rock plus equilibria between in-drift solutions and gases at ambient temperatures would buffer the leachate pH to within the range similar to that for seepage waters (pH = 7.4 – 8.1; see Table 6.9-1). Moreover, underlying analytical uncertainties of the dust leachate solutions coupled with dust components not considered in the fluid analysis can account for charge imbalances in the computational evaluation of aqueous solution concentrations. Therefore, the pH range chosen for screening is broad compared to expected values, allowing as many samples as possible to span a wide chemical parameter space. Based on the pH-screening criterion, two additional samples (#00574987A and 00574981A) have been excluded from the dust deliquescence calculations due to low pH, leaving 52 remaining samples.

All of the speciation calculations are performed at the temperature of 25°C, under the atmospheric CO_2 pressure ($10^{-3.5}$ bar, Weast 1984 [DIRS 106170]) and with the suppression of the following minerals:

- Maximum microcline
- Dolomite
- Quartz
- Cristobalite (alpha)
- Glaserite
- Talc
- Magnesite
- All saponites

The rationale and criteria for these mineral suppressions can be found on Table 6.5-2. These suppressions have also been documented in the In-Drift Precipitates/Salts Model report (BSC 2003, Section 6.6.2.6.4 [DIRS 162529]). In addition to the mineral suppressions advanced

by the in-drift precipitates/salts model, several more suppressions have been added. Three minerals (albite, K-feldspar, and celadonite) have been suppressed for the reasons documented in Section 6.6.3 (see Table 6.6-2). Two more minerals (cryolite and $K_2Si_4O_9$ [K-wadeite]) precipitating in preliminary models for this section and have been suppressed because of the rationale found in Table 6.10-1.

Table 6.10-2 lists the EQ3NR input files developed from the two original USGS dust leachate DTNs: (MO0207EBSDUSTS.020 [DIRS 162556] and MO0209EBSDUST2.030 DIRS 162557]) after converting the leachable salt values to conventional aqueous concentration units (ppm) calculated in DTN: SN0310T0510102.010. The associated output and pickup files to these calculation runs are given in this table. The values listed on these two tables are shown in micrograms per gram of H_2O, or ppm. The values used in the input EQ3 files are entered as mg/L; thus, the density of the leachate solution was taken to be 1.0 kg/L. This minor simplification should not appreciably affect the results of the calculations since these are dilute solutions. These files are archived in DTN: SN0310T050102.010.

Table 6.10-1. Rationale for the Suppression of Cryolite and K-Wadeite in Dust Leachate Model Analyses

Mineral	Formula	Criteria Selected	Rationale	References
Cryolite	Na_3AlF_6	Criterion 3	Associated with fluorite in pegmatite veins in granite and gneiss. This precipitation is normally at high temperatures and pressures.	Buhn and Rankin 1999 [DIRS 163753]
$K_2Si_4O_9$ (K-wadeite)	$K_2Si_4O_9$	Criterion 3	Appears to be a high-temperature, high-pressure mineral phase. The formation temperature for precipitation is about 770ºC.	Kracek and Clark 1966 [DIRS 163754], Figure 13-7

6.10.4 Calculation of Mineralogy at Dryout

The dryout calculations are designed to obtain a general idea about the evolution of chemical composition of dust leachate samples at different degrees of evaporation. In these calculations, water was continuously removed from the system using the titration mode of the code EQ6 (BSC 2003 [DIRS 162228]). The dryout is defined as the titration point where less than $\sim 10^{-10}$ kg of water remain from the initial 1 kg of water. However, the amount of water left in the calculation when the eutectic point is reached is generally between 10^{-5} to 10^{-6} kg (see Figures 6.13.18 to 6.13.22). This set of dryout calculations is performed at 25°C and atmospheric Pco_2. The EQ6 input files used in the dryout calculations are generated according to the protocol outlined in the *In-Drift Precipitates/Salts Model* report (BSC 2003 [DIRS 162529]), starting with the EQ6 evaporative template files found in DTN: MO0303SPAMEQ36.000 [DIRS 162549].

Table 6.10-2. EQ3NR Input/Output Files for Dust Leachate Analyses

Input Table	Field/Sample #	Input File Names	Output File Names	Pickup File Names
Table 4.1-19	SPC00573607	p07_25b.3i,	p07_25b.3o,	p07_25b.3p,
	SPC00573610	p10_25b.3i,	p10_25b.3o,	p10_25b.3p,
	SPC00573611	p11_25b.3i,	p11_25b.3o,	p11_25b.3p,
	SPC00573612	p12_25b.3i,	p12_25b.3o,	p12_25b.3p,
	SPC00573614	p14_25b.3i,	p14_25b.3o,	p14_25b.3p,
	SPC00573615	p15_25b.3i,	p15_25b.3o,	p15_25b.3p,
	SPC00573616	p16_25b.3i,	p16_25b.3o,	p16_25b.3p,
	SPC00573617	p17_25b.3i,	p17_25b.3o,	p17_25b.3p,
	SPC00573618	p18_25b.3i,	p18_25b.3o,	p18_25b.3p,
	SPC00573619	p19_25b.3i,	p19_25b.3o,	p19_25b.3p,
	SPC00573620	p20_25b.3i,	p20_25b.3o,	p20_25b.3p,
	SPC00573622	p22_25b.3i,	p22_25b.3o,	p22_25b.3p,
	SPC00573623	p23_25b.3i,	p23_25b.3o,	p23_25b.3p,
	SPC00573624	p24_25b.3i,	p24_25b.3o,	p24_25b.3p,
	SPC00573625	p25_25b.3i,	p25_25b.3o,	p25_25b.3p,
	SPC00573626	p26_25b.3i,	p26_25b.3o,	p26_25b.3p,
	SPC00573627	p27_25b.3i,	p27_25b.3o,	p27_25b.3p,
	SPC00573628	p28_25b.3i,	p28_25b.3o,	p28_25b.3p,
	SPC00573629	p29_25b.3i,	p29_25b.3o,	p29_25b.3p,
	SPC00573630	p30_25b.3i,	p30_25b.3o,	p30_25b.3p,
	SPC00573631	p31_25b.3i,	p31_25b.3o,	p31_25b.3p,
	SPC00573632	p32_25b.3i,	p32_25b.3o,	p32_25b.3p,
	SPC00573633	p33_25b.3i,	p33_25b.3o,	p33_25b.3p,
Table 4.1-20	00574979A	s79a25b.3i,	s79a25b.3o,	s79a25b.3p,
	00574979B	s79b25b.3i,	s79b25b.3o,	s79b25b.3p,
	00574979C	s79c25b.3i,	s79c25b.3o,	s79c25b.3p,
	00574980A	s80a25b.3i,	s80a25b.3o,	s80a25b.3p,
	00574980B	s80b25b.3i,	s80b25b.3o,	s80b25b.3p,
	00574980C	s80c25b.3i,	s80c25b.3o,	s80c25b.3p,
	00574981B	s81b25b.3i,	s81b25b.3o,	s81b25b.3p,
	00574981C	s81c25b.3i,	s81c25b.3o,	s81c25b.3p,
	00574982A	s82a25b.3i,	s82a25b.3o,	s82a25b.3p,
	00574982B	s82b25b.3i,	s82b25b.3o,	s82b25b.3p,
	00574982C	s82c25b.3i,	s82c25b.3o,	s82c25b.3p,
	00574983A	s83a25b.3i,	s83a25b.3o,	s83a25b.3p,
	00574983B	s83b25b.3i,	s83b25b.3o,	s83b25b.3p,
	00574983C	s83c25b.3i,	s83c25b.3o,	s83c25b.3p,
	00574984A	s84a25b.3i,	s84a25b.3o,	s84a25b.3p,
	00574985A	s85a25b.3i,	s85a25b.3o,	s85a25b.3p,
	00574985B	s85b25b.3i,	s85b25b.3o,	s85b25b.3p,
	00574985C	s85c25b.3i,	s85c25b.3o,	s85c25b.3p,
	00574986A	s86a25b.3i,	s86a25b.3o,	s86a25b.3p,
	00574986B	s86b25b.3i,	s86b25b.3o,	s86b25b.3p,
	00574986C	s86c25b.3i,	s86c25b.3o,	s86c25b.3p,
	00574987B	s87b25b.3i,	s87b25b.3o,	s87b25b.3p,
	00574987C	s87c25b.3i,	s87c25b.3o,	s87c25b.3p,
	00574990A	s90a25b.3i,	s90a25b.3o,	s90a25b.3p,
	00574990B	s90b25b.3i,	s90b25b.3o,	s90b25b.3p,
	00574990C	s90c25b.3i,	s90c25b.3o,	s90c25b.3p,
	00574991A	s91a25b.3i,	s91a25b.3o,	s91a25b.3p,
	00574991B	s91b25b.3i,	s91b25b.3o,	s91b25b.3p,
	00574991C	s91c25b.3i,	s91c25b.3o,	s91c25b.3p,
	00574992A	s92a25b.3i,	s92a25b.3o,	s92a25b.3p,
	00574992B	s92b25b.3i,	s92b25b.3o,	s92b25b.3p,
	00574992C	s92c25b.3i	s92c25b.3o	s92c25b.3p

Source: DTN: SN0310T050102.010, directory EQ3_runs

Temperature, pH, and aqueous concentrations of all dissolved components are copied from the EQ3NR pickup files (listed in Table 6.10-2) and appended to the bottom half of the associated EQ6 input files. These EQ6 input files are then run and the resulting output file calculations are produced. These input and output files are listed on Table 6.10-3 and are archived in DTN: SN0310T050102.010.

Table 6.10-3. EQ6 Input and Output Files Used for Determination of the Mineralogy at Dryout

EQ6 Input Files	EQ6 Output Files
p07_25b.6i, p10_25b.6i, p11_25b.6i, p12_25b.6i,	p07_25b.6o, p10_25b.6o, p11_25b.6o, p12_25b.6o,
p14_25b.6i, p15_25b.6i, p16_25b.6i, p17_25b.6i,	p14_25b.6o, p15_25b.6o, p16_25b.6o, p17_25b.6o,
p18_25b.6i, p19_25b.6i, p20_25b.6i, p22_25b.6i,	p18_25b.6o, p19_25b.6o, p20_25b.6o, p22_25b.6o,
p23_25b.6i, p24_25b.6i, p25_25b.6i, p26_25b.6i,	p23_25b.6o, p24_25b.6o, p25_25b.6o, p26_25b.6o,
p27_25b.6i, p28_25b.6i, p29_25b.6i, p30_25b.6i,	p27_25b.6o, p28_25b.6o, p29_25b.6o, p30_25b.6o,
p31_25b.6i, p32_25b.6i, p33_25b.6i, s79a25b.6i,	p31_25b.6o, p32_25b.6o, p33_25b.6o, s79a25b.6o,
s79b25b.6i, s79c25b.6i, s80a25b.6i, s80b25b.6i,	s79b25b.6o, s79c25b.6o, s80a25b.6o, s80b25b.6o,
s80c25b.6i, s81b25b.6i, s81c25b.6i, s82a25b.6i,	s80c25b.6o, s81b25b.6o, s81c25b.6o, s82a25b.6o,
s82b25b.6i, s82c25b.6i, s83a25b.6i, s83b25b.6i,	s82b25b.6o, s82c25b.6o, s83a25b.6o, s83b25b.6o,
s83c25b.6i, s84a25b.6i, s85a25b.6i, s85b25b.6i,	s83c25b.6o, s84a25b.6o, s85a25b.6o, s85b25b.6o,
s85c25b.6i, s86a25b.6i, s86b25b.6i, s86c25b.6i,	s85c25b.6o, s86a25b.6o, s86b25b.6o, s86c25b.6o,
s87b25b.6i, s87c25b.6i, s90a25b.6i, s90b25b.6i,	s87b25b.6o, s87c25b.6o, s90a25b.6o, s90b25b.6o,
s90c25b.6i, s91a25b.6i, s91b25b.6i, s91c25b.6i,	s90c25b.6o, s91a25b.6o, s91b25b.6o, s91c25b.6o,
s92a25b.6i, s92b25b.6i, s92c25b.6i	s92a25b.6o, s92b25b.6o, s92c25b.6o

Source: DTN: SN0310T050102.010, directory Evap.

A Microsoft Excel spreadsheet ("Dust Leach End Salt Assem Rev 01.xls," archived in DTN: MO0310SPADLBU4.001) is created using GETEQDATA Version 1.0.1 software (BSC 2003 [DIRS 161900]) by extracting data from the output files listed on Table 6.10-3. The endpoint equilibrium data listed in Table 6.10-4 are extracted, and within the spreadsheet, the Excel statistical tools are used to calculate the statistics found at the bottom of the table with results shown on Figure 6.10-2.

6.10.5 Dust Leachate Abstraction

As discussed in Section 6.5, chemical equilibrium is the basis for determining the resulting chemistry of the dust deliquescence process. Figure 6.2-2 illustrates that the aqueous solutions formed by deliquescence of soluble minerals in dry dust are the same composition as those that result as the solutions are evaporated.

Table 6.10-4. EQ6 Dust Leachate Water pH, a_w, Ionic Strength (I) Cl, N, and Cl:N Ratios at the Dryout End Point at 25°C and Atmospheric Pco_2

Output Filename	pH	EQ6 End Point a_w	(I)	Cl Moles/ kg. H_2O	N Moles/ kg. H_2O	Cl/N Molal Ratio
p07_25b.6o	7.59	0.39	18.56	1.87	4.50	0.41
p10_25b.6o	8.45	0.60	11.53	2.64	2.33	1.13
p11_25b.6o	8.45	0.60	11.53	2.64	2.33	1.13
p12_25b.6o	8.44	0.60	11.54	2.51	2.41	1.04
p14_25b.6o	7.82	0.55	11.73	1.49	3.55	0.42
p15_25b.6o	8.44	0.60	11.54	2.51	2.41	1.04
p16_25b.6o	7.82	0.55	11.73	1.49	3.55	0.42
p17_25b.6o	7.82	0.55	11.73	1.49	3.55	0.42
p18_25b.6o	10.21	0.61	12.13	3.18	2.04	1.56
p19_25b.6o	8.44	0.60	11.54	2.51	2.41	1.04
p20_25b.6o	10.21	0.61	12.13	3.18	2.04	1.56
p22_25b.6o	7.82	0.55	11.73	1.49	3.54	0.42
p23_25b.6o	7.82	0.55	11.73	1.49	3.54	0.42
p24_25b.6o	10.20	0.60	11.96	2.46	2.44	1.01
p25_25b.6o	7.82	0.55	11.73	1.49	3.54	0.42
p26_25b.6o	8.44	0.60	11.54	2.51	2.41	1.04
p27_25b.6o	8.44	0.60	11.54	2.51	2.41	1.04
p28_25b.6o	7.82	0.55	11.73	1.49	3.54	0.42
p29_25b.6o	10.20	0.60	11.96	2.46	2.44	1.01
p30_25b.6o	8.44	0.60	11.54	2.51	2.41	1.04
p31_25b.6o	8.44	0.60	11.54	2.51	2.41	1.04
p32_25b.6o	8.45	0.60	11.53	2.64	2.33	1.13
p33_25b.6o	8.45	0.60	11.53	2.64	2.33	1.13
s80a25b.6o	8.63	0.61	11.67	3.25	2.04	1.60
s80b25b.6o	7.82	0.55	11.73	1.49	3.54	0.42
s80c25b.6o	7.64	0.35	17.09	2.35	2.12	1.11
s81b25b.6o	8.45	0.60	11.53	2.64	2.33	1.13
s81c25b.6o	7.78	0.50	14.82	5.67	4.64	1.22
s82a25b.6o	10.21	0.61	12.13	3.18	2.04	1.56
s82b25b.6o	8.44	0.60	11.54	2.51	2.41	1.04
s82c25b.6o	8.11	0.55	11.94	1.47	3.60	0.41
s83a25b.6o	10.21	0.61	12.13	3.18	2.04	1.56
s83b25b.6o	8.44	0.60	11.54	2.51	2.41	1.04
s83c25b.6o	7.82	0.55	11.73	1.49	3.54	0.42
s84a25b.6o	10.21	0.61	12.12	3.19	2.04	1.56

Table 6.10-4. EQ6 Dust Leachate Water pH, a_w, Ionic Strength (I) Cl, N, and Cl:N Ratios at the Dryout End Point at 25°C and Atmospheric Pco_2 (Continued)

Output Filename	pH	EQ6 End Point a_w	(I)	Cl Moles/ kg. H_2O	N Moles/ kg. H_2O	Cl/N Molal Ratio
s85a25b.6o	8.45	0.60	11.53	2.64	2.33	1.13
s85b25b.6o	8.45	0.60	11.53	2.64	2.33	1.13
s85c25b.6o	8.44	0.60	11.54	2.51	2.41	1.04
s86a25b.6o	10.21	0.61	12.12	3.18	2.04	1.56
s86b25b.6o	8.45	0.60	11.53	2.64	2.33	1.13
s86c25b.6o	7.82	0.55	11.74	1.49	3.55	0.42
s87b25b.6o	7.82	0.55	11.73	1.49	3.54	0.42
s87c25b.6o	7.82	0.55	11.73	1.49	3.54	0.42
s90a25b.6o	8.45	0.60	11.53	2.64	2.33	1.13
s90b25b.6o	7.81	0.61	10.43	2.77	2.15	1.29
s90c25b.6o	8.45	0.60	11.53	2.64	2.33	1.13
s91a25b.6o	7.82	0.61	10.42	2.80	2.14	1.31
s91b25b.6o	7.81	0.61	10.43	2.77	2.15	1.29
s91c25b.6o	8.45	0.60	11.53	2.64	2.33	1.13
s92a25b.6o	10.20	0.62	11.61	3.71	1.79	2.07
s92b25b.6o	10.21	0.61	12.12	3.19	2.04	1.04
s92c25b.6o	8.634	0.61	11.67	3.26	2.04	0.41
Mean	8.56	0.58	11.93	2.48	2.67	0.99
Min	7.59	0.35	10.42	1.47	1.79	0.41
Max	10.21	0.62	18.56	5.67	4.64	2.07
S	0.86	0.05	1.33	0.77	0.70	0.42
2S	1.73	0.10	2.66	1.54	1.39	0.84

DTN: MO0310SPADLBU4.001

At equilibrium, deliquescence is reversible, and the reverse process is evaporation as defined in the considered conceptual model. The abstraction process and steps for dust deliquescence are similar to those used for in-drift seepage evaporation treated in Section 6.9. The selection of 52 dust leachate water compositions to be used to represent dust deliquescence was described in Section 6.10.3. Four steps are then followed to abstract water compositions potentially forming by deliquescence:

- Step 1: Use the in-drift salts/precipitates model (*In-Drift Precipitates/Salts Model* (BSC 2003 [DIRS 162529]) to calculate compositions that result from evaporating the dust leachate compositions to a common water activity equal to 0.65. This step characterizes the leachates by the chemical divides that the waters pass through as they are concentrated by evaporation. For convenience, the evaporated leachate compositions at a water activity equal to 0.65 are referred to as normalized compositions (Section 6.10.5.1).

- Step 2: Sort the normalized leachate compositions from Step 1 into groups that exhibit similar chemical characteristics. The chemical criteria used to sort the waters are discussed in Section 6.10.5.2. Then, the corresponding original leachate compositions from Section 6.10.3 that serve as precursors to the normalized seepage water compositions are placed into a bin. This process is repeated for all normalized leachate groups. The result is a set of leachate composition bins, each populated with compositions that yield chemically similar solutions after they are concentrated by evaporation (Section 6.10.5.2).

- Step 3: Identify a representative water for each bin, as close to the statistical median as possible, and use it as an approximation of all the leachate compositions in the bin (see Section 6.10.5.3.1).

- Step 4: Generate the probability distribution of the leachate compositions by determining the number of waters in each bin (see Section 6.10.5.3.2).

The six median water compositions chosen using the above procedure are used as inputs to the in-drift precipitates/salts model to generate lookup tables for water compositions produced by dust deliquescence for use in the TSPA-LA calculations.

6.10.5.1 Normalization of the Leachate Compositions (Step 1)

The compositions of dust leachates vary among different dust samples not only in terms of the molar ratios of the dissolved constituents, but also in terms of the absolute concentrations of these constituents. To group these waters into bins containing more or less homogeneous water types, these waters had to be normalized to reflect the compositions of water types at a common ionic strength or degree of concentration.

The method chosen to normalize these water compositions is identical to the method discussed in Section 6.6.3 and involves using the in-drift precipitates/salts model to evaporate the dust leachate waters to a common activity of water. This approach accounts for the effects of nearly every chemical divide important to a particular water. Other methods, such as dividing each

concentration by the ionic strength, cannot as accurately reveal the likely brine end-point for a given water. It is important to capture the likely evaporative evolution pathways in the binning analysis, because brine types can influence waste package and drip shield corrosion rates.

As determined by the in-drift precipitates/salts model evaporations reported in Section 6.10.4, the waters evaporatively evolve to several different brine types, most commonly nitrate brines, chloride brines, and their combinations. An activity of water (a_w) of 0.65 is chosen as the common end-point of these normalizing evaporation run calculations, because this is approximately the lowest value at which all calculation runs are above the deliquescence point. Also, the trend in solution constituent concentrations given by the extent of evaporation delineated up to this a_w value seems to define the predominant brine type expected with further evaporation. Therefore, a higher value of water activity is not chosen because the objective of the binning analysis is to classify the waters by the type of brine they will produce.

The same EQ6 input files as those for the dryout calculations in Section 6.10.4 (see Table 6.10-3) are used for the normalization calculations as well. The only difference from the model protocol is that the input files are modified so that the evaporations are stopped when the activity of water attains the value of 0.65. Therefore, refer to Table 6.10-3 for the list of input and output files generated for use in EQ6. These specific 65 percent evaporation files are found in DTN: SN0310T0510102.010, in subdirectory 65RH.

6.10.5.2 Bin Generation (Step 2)

Binning the leachate compositions is accomplished by sorting compositions into groups, such that all compositions in a group yield chemically similar solutions after they are concentrated by evaporation. Four properties are identified as criteria for determining chemical similarity. They are defined in such a way that they yield relatively low intrabin compositional ranges, compared with the compositional range of all the waters. Choices of the chemical characteristics are treated later in this section.

First, normalized leachate compositions from Step 1 are sorted into groups that exhibited similar chemical characteristics. Then each of the original leachate compositions from Section 6.10.3 that is a precursor to each of the normalized leachate compositions in a particular group is placed into a single bin; this process was repeated for all of the normalized leachate groups. The result is a set of leachate composition bins, each populated with compositions that yielded chemically similar solutions after they concentrated by evaporation.

The final equilibration results from each output file, archived in DTN: SN0310T050102.010 (subdirectory 65RH), have been extracted and tabulated in a single Excel spreadsheet using the GETEQDATA Version 1.0.1 (BSC 2003 [161900]) software. This spreadsheet, entitled “EBS Dust Leachate Binning Abstraction Rev 01.xls” is archived in DTN: MO0310SPADLBU4.001.

The variables selected for extraction included pH, activity of water ($a_w \approx 0.65$), ionic strength (I), total molalities of the aqueous constituents, and the log value of the cumulative number of moles of each mineral precipitated. Formulas were added to calculate various molar ratios and pH, and several graphs are inserted to illustrate the variability of these compositional parameters among different leachate samples (see Figures 6.10-3 to 6.10-6). This set of information was needed

before the waters can be grouped by similarity. Figures 6.10-3 to 6.10-6 are meant only to illustrate the general variation in results among dust leachate evaporations. The spreadsheet provides the actual values.

Grouping (or binning) of the normalized leachate waters is accomplished by sorting the waters by predominant traits. These four criteria resulted in the creation of six bins such that the compositional variation within each group is small compared to the variation between groups.

The evaporated waters are binned based on the following four criteria:

- Total aqueous Ca molality > 0.01 molal?
  - If yes, the water likely evaporates towards the calcium side of the calcite and gypsum chemical divides, resulting in a brine that is depleted of carbonate and sulfate. These brines also tend to have neutral to acidic pH and very low fluoride concentrations due to the low solubility of fluorite (CaF_2). This criterion is identical to one used in the THC seepage abstraction in Section 6.6.4.
- Total aqueous CO_3 molality > 0.1 molal?
  - If yes, Ca is likely depleted by the precipitation of calcite. In some cases, both Ca and CO_3 have low concentrations, so this criterion further divides the low Ca case above. Waters having low concentrations of both of these components tend to maintain a neutral pH as they evaporate. This criterion is identical to one used in the THC seepage abstraction in Section 6.6.4.
- Total aqueous Br molality > 2 molal?
  - This criterion segregates bin 2 from the other bins (see Table 6.10-5), thus reducing intra-bin variability.
- Total aqueous SO_4 molality > 1 molal?
  - This criterion distinguishes waters in bin 6 from bin 5 and waters in bin 3 from bin 4 (see Table 6.10-5), reducing intra-bin variability. This criterion is identical to one used in the THC seepage abstraction in Section 6.6.4.

Table 6.10-5. Binning Criteria Answer Key

Bin	Ca > 0.01 Molal	Br > 2 molal	CO_3 < 0.1 molal	SO_4 > 1 molal
Bin 1	yes	no	yes	no
Bin 2	no	yes	yes	no
Bin 3	no	no	no	yes
Bin 4	no	no	no	no
Bin 5	no	no	yes	yes
Bin 6	no	no	yes	no

Source: DTN: MO0310SPADLBU4.001

Columns containing "if/then/else" Excel-type commands are added to the spreadsheet to facilitate responding to each grouping criteria for each water. Waters having identical answers to the questions listed on Table 6.10-5 are placed in the same bin. Results are provided and plotted in the "EBS Dust Leachate Binning Abstraction Rev 01.xls" spreadsheet (DTN: MO0310SPADLBU4.001). They are also shown in Figures 6.10-7 through Figure 6.10-12. These Figures are presented only to illustrate the general variation in results among dust leachate evaporations. The spreadsheet provides the actual values.

Each leachate water composition is placed into the appropriate bin based on the above criteria. This process is repeated for all of the normalized leachate waters. The result is a set of six leachate composition bins, each populated with waters that yield chemically similar solutions after they are concentrated by evaporation.

6.10.5.3 Choice of Representative Leachate Water for Each Bin

The "median" leachate water composition in each bin is chosen to represent all waters in that bin using the flagging methodology detailed in the next section. The "median" leachate water is a representative water as near the statistical median as possible. That is, this "median" water should be regarded as a representative "near-median" water composition and does not correspond to the actual statistical median for each individual chemical parameter. Table 6.10-6 gives the identifiers for the six median water compositions. Median equilibrated (calculated with the code EQ3NR) leachate water compositions for the bins are given in Table 6.10-9.

Table 6.10-6. Median Waters and Percentage of Waters in Each Bin

Bin	Median Water File Name	Number of Waters In the Bin	% of All Evaporated Waters Represented by the Bin
Bin 1	s80c25b.6o	3	5.77
Bin 2	s90b25b.6o	4	7.69
Bin 3	s86a25b.6o	9	17.31
Bin 4	p25_25b.6o	12	23.08
Bin 5	p26_25b.6o	23	44.23
Bin 6	s92a25b.6o	1	1.92
Total		52	100.00

Source: DTN: MO0310SPADLBU4.001

All 52 waters found in the data and plots worksheet in the EBS Dust Leachate Binning Abstraction Rev 01.xls" spreadsheet (DTN: MO0310SPADLBU4.001) are sorted into six bins and copied into separate bin worksheets (e.g., Bin 1 abstract, Bin 2 abstract, etc.). These worksheets are used to determine the representative median water for each bin, as well as the individual bin statistics. In so doing, the 52 original waters are reduced to 6. These six water compositions are then used as inputs into Section 6.10.6 to create lookup tables for TSPA-LA analyses.

6.10.5.3.1 Median Water

The flagging methodology to determine the median water from each of the six bins uses the internal Excel functions of RANK and COUNTIF. These functions enable the selection of the median water by helping to determine and flag the actual middle value(s) for each parameter (e.g., pH, Ca, Cl) in each bin, and then counting the total number of these flagged values in each bin. Any ties are broken by flagging near-median values and summing the number of flags. This selection approach has the effect of maintaining consistency with the THC seepage abstraction outlined in Section 6.6. In addition, the selected bin chemistry is as close to the median chemistry within the bin as can be obtained without generating a hypothetical dust leachate water based on statistical averages of water constituent concentrations (see Section 6.6.5.1). This approach minimizes potential errors because speciation calculations are often charge balanced by adjusting ions such as Na^+ or Cl^-, and adjusting the concentration of these ions could produce a brine that does not appropriately represent the bin waters. Table 6.10-6 lists the median waters selected for each bin.

6.10.5.3.2 Bin Distribution

The distribution of waters between the bins is calculated by determining the percentage of waters in each bin; this is shown on Table 6.10-6. Bin 5 contains the largest number of values and thus is the most probable water. Table 6.10-6 can be used to determine the relative probability of each dust leachate waters being present on drip shield and waste package surfaces in the absence of dripping (i.e., under deliquescence conditions). This is based on assumption 5.2.3.

6.10.5.4 Within Bin Uncertainty

In each of the six "bin abstract" worksheets, the median, minimum, and maximum values for each compositional parameter are calculated, as well as the standard deviation (s) and two standard deviations (2s). Table 6.10-7 contains the individual parameter statistics for each bin. These statistics are compared to those for all 52 dust leachate waters presented in Table 6.10-8. Comparison of Tables 6.10-7 and 6.10-8 indicate that the variation within each bin is generally much smaller than that observed for all 52 dust leachate waters.

6.10.5.5 EQ3NR Equilibrated Water Compositions

The six EQ3 input files associated with the calculated EQ6 output files listed in Table 6.10-6 have been used to represent the dust leachate compositions in the lookup table generation (see Section 6.10.6.5). These six EQ3 3i files and the corresponding output files are archived in DTN: SN0310T050102.010. Data from the six 3o files have been extracted using GETEQDATA Version 1.0.1 (BSC 2003 [161900]) software to produce an Excel

spreadsheet "6 bin EQ3 gas and dust leachate water extract.xls" (archived in DTN: MO0310SPADLBU4.001). This spreadsheet was then used to produce Tables 6.10-9 and 6.10-10, which represent the EQ3NR equilibration and charge balancing of the six chemistries listed on Table 6.10-6. The charge balance is done in accordance with the discussion in Section 6.10.3. EQ3NR is used only to equilibrate the solution with respect to all aqueous species. It does not equilibrate the solutions with respect to minerals and gases other than those discussed in Section 6.10.3. Subsequent EQ6 runs are used for additional mineral and gas phase equilibration.

Table 6.10-7. Calculated Statistics for Evaporated Dust Leachate Waters (a_w = 0.65) Within Each Bin

Bin	Statistic	pH	Br	C	Ca	Cl	F	K	Mg	N	Na	S	Si	Ionic Strength	Cl:N
1	Median	7.45	6.96E-02	5.04E-03	1.05E+00	3.28E+00	2.25E-05	1.17E+00	1.88E-01	6.79E+00	6.09E+00	5.48E-03	1.47E-05	11.27	0.55
	Min	7.31	2.73E-02	1.04E-03	3.37E-01	2.91E+00	2.16E-05	8.77E-01	5.62E-03	5.97E+00	4.59E+00	4.70E-03	1.25E-05	11.19	0.39
	Max	7.49	1.01E-01	6.74E-03	1.61E+00	3.84E+00	2.35E-05	1.70E+00	8.58E-01	7.51E+00	8.00E+00	1.09E-02	3.00E-04	12.11	0.56
	s	0.10	3.69E-02	2.93E-03	6.39E-01	4.66E-01	9.50E-07	4.16E-01	4.49E-01	7.67E-01	1.71E+00	3.38E-03	1.66E-04	0.51	0.10
	2s	0.19	7.39E-02	5.85E-03	1.28E+00	9.31E-01	1.90E-06	8.33E-01	8.97E-01	1.53E+00	3.42E+00	6.75E-03	3.31E-04	1.02	0.20
2	Median	7.94	2.68E+00	9.91E-04	9.61E-03	3.84E+00	1.39E-04	2.49E+00	7.74E-03	2.82E+00	7.28E+00	2.32E-01	4.89E-05	10.05	1.36
	Min	7.94	2.55E+00	7.58E-04	9.52E-03	3.71E+00	1.13E-04	2.35E+00	4.54E-03	2.78E+00	7.26E+00	2.31E-01	3.74E-05	10.04	1.16
	Max	7.96	2.70E+00	1.22E-03	9.67E-03	3.86E+00	1.66E-04	2.52E+00	1.05E-02	3.20E+00	7.56E+00	2.39E-01	6.18E-05	10.18	1.39
	s	0.01	6.96E-02	2.69E-04	7.92E-05	6.76E-02	3.05E-05	7.52E-02	3.35E-03	1.97E-01	1.45E-01	3.80E-03	1.37E-05	0.07	0.11
	2s	0.02	1.39E-01	5.39E-04	1.58E-04	1.35E-01	6.09E-05	1.50E-01	6.71E-03	3.94E-01	2.91E-01	7.60E-03	2.74E-05	0.14	0.21
3	Median	10.33	1.16E+00	4.49E-01	7.97E-06	4.18E+00	3.73E-02	3.55E+00	1.60E-05	2.85E+00	7.99E+00	1.24E+00	8.63E-04	13.16	1.47
	Min	10.32	1.14E+00	4.47E-01	7.97E-06	3.64E+00	2.56E-02	2.94E+00	2.56E-07	2.84E+00	7.97E+00	1.19E+00	5.11E-04	13.13	0.99
	Max	10.36	1.17E+00	4.52E-01	7.97E-06	4.18E+00	3.73E-02	3.55E+00	3.39E-05	3.66E+00	8.77E+00	1.25E+00	1.36E-02	13.28	1.47
	s	0.02	1.18E-02	1.88E-03	1.36E-09	2.37E-01	6.00E-03	2.69E-01	1.68E-05	3.61E-01	3.46E-01	2.40E-02	6.88E-03	0.06	0.21
	2s	0.03	2.37E-02	3.75E-03	2.71E-09	4.75E-01	1.20E-02	5.38E-01	3.36E-05	7.22E-01	6.92E-01	4.79E-02	1.38E-02	0.12	0.42
4	Median	8.29	4.71E-01	1.11E-03	7.05E-03	2.95E+00	1.36E-04	2.40E+00	2.28E-03	8.10E+00	1.01E+01	4.90E-01	1.92E-05	12.99	0.36
	Min	8.06	1.01E-01	3.63E-04	3.72E-03	2.75E+00	1.22E-04	2.15E+00	4.38E-05	4.67E+00	8.40E+00	2.94E-01	1.68E-05	10.88	0.30
	Max	8.51	1.88E+00	1.19E-03	8.87E-03	3.43E+00	1.99E-04	2.60E+00	6.55E-03	9.16E+00	1.07E+01	7.82E-01	7.51E-04	14.09	0.73
	s	0.14	6.65E-01	2.49E-04	1.36E-03	2.46E-01	2.81E-05	1.66E-01	1.68E-03	1.66E+00	8.41E-01	1.38E-01	2.10E-04	1.13	0.15
	2s	0.27	1.33E+00	4.97E-04	2.73E-03	4.93E-01	5.62E-05	3.32E-01	3.35E-03	3.33E+00	1.68E+00	2.76E-01	4.20E-04	2.25	0.31
5	Median	8.62	1.73E+00	1.33E-03	1.14E-03	3.65E+00	6.81E-04	2.92E+00	4.09E-04	3.55E+00	8.24E+00	1.12E+00	6.52E-05	12.28	1.03
	Min	8.62	1.70E+00	1.21E-03	4.97E-04	3.65E+00	4.68E-04	2.85E+00	3.71E-06	2.74E+00	7.47E+00	1.11E+00	3.96E-05	12.16	1.03
	Max	8.78	1.82E+00	2.16E-03	1.14E-03	4.21E+00	1.04E-03	3.64E+00	8.66E-04	3.55E+00	8.25E+00	1.23E+00	1.10E-03	12.38	1.54
	s	0.05	2.61E-02	2.63E-04	2.04E-04	1.69E-01	1.62E-04	2.19E-01	3.67E-04	2.58E-01	2.41E-01	3.72E-02	4.86E-04	0.05	0.16
	2s	0.10	5.22E-02	5.27E-04	4.08E-04	3.38E-01	3.23E-04	4.39E-01	7.33E-04	5.16E-01	4.82E-01	7.45E-02	9.71E-04	0.09	0.31
6	Median	10.27	1.54E+00	4.49E-01	7.87E-06	4.68E+00	3.59E-02	3.70E+00	2.55E-07	2.19E+00	7.07E+00	7.43E-01	1.28E-02	11.89	2.14
	Min	N/A	N/A	N/A	N/A	N/A	N/A	N/A	N/A	N/A	N/A	N/A	N/A	N/A	N/A
	Max	N/A	N/A	N/A	N/A	N/A	N/A	N/A	N/A	N/A	N/A	N/A	N/A	N/A	N/A
	s	N/A	N/A	N/A	N/A	N/A	N/A	N/A	N/A	N/A	N/A	N/A	N/A	N/A	N/A
	2s	N/A	N/A	N/A	N/A	N/A	N/A	N/A	N/A	N/A	N/A	N/A	N/A	N/A	N/A

Source: DTN: MO0310SPADLBU4.001

NOTE: All units except for pH are in Moles/kg.H_2O. Bin 6 only has 1 water in it, therefore no statistics are calculated.

Table 6.10-8. Calculated Statistics for all 52 Evaporated Dust Leachate Waters Evaluated in the Binning Analysis (a_w = 0.65)

Statistic	pH	Br	C	Ca	Cl	F	K	Mg	N	Na	S	Si	Ionic Strength	Cl:N
Median	8.62	1.70E+00	1.33E-03	1.14E-03	3.65E+00	4.86E-04	2.92E+00	6.84E-04	3.55E+00	8.24E+00	1.12E+00	6.35E-05	1.23E+01	1.03E+00
Min	7.31	2.73E-02	3.63E-04	7.87E-06	2.75E+00	2.16E-05	8.77E-01	2.55E-07	2.19E+00	4.59E+00	4.70E-03	1.25E-05	1.00E+01	3.04E-01
Max	10.36	2.70E+00	4.52E-01	1.61E+00	4.68E+00	3.73E-02	3.70E+00	8.58E-01	9.16E+00	1.07E+01	1.25E+00	1.36E-02	1.41E+01	2.14E+00
s	0.84	6.93E-01	1.78E-01	2.67E-01	4.37E-01	1.31E-02	5.86E-01	1.21E-01	2.04E+00	1.09E+00	4.16E-01	3.94E-03	9.35E-01	4.16E-01
2s	1.69	1.39E+00	3.56E-01	5.34E-01	8.75E-01	2.61E-02	1.17E+00	2.42E-01	4.08E+00	2.18E+00	8.31E-01	7.89E-03	1.87E+00	8.31E-01

Source: DTN: MO0310SPADLBU4.001

NOTE: All units except for pH are in Moles/kg.H_2O.

Table 6.10-9. Total EQ3NR Equilibrated Aqueous Elemental Compositions for the 6 Bins

Bin	**1**	**2**	**3**	**4**	**5**	**6**
EQ3NR Filename	**s80c25b.3o**	**s90b25b.3o**	**s86a25b.3o**	**p25_25b.3o**	**p26_25b.3o**	**s92a25b.3o**
Temp (C)	25	25	25	25	25	25
Ph	8.54	8.09	8.23	8.54	8.40	8.05
a_w	1.00E+00	1.00E+00	1.00E+00	1.00E+00	1.00E+00	1.00E+00
(I)	5.43E-03	2.74E-03	2.01E-03	6.29E-03	3.80E-03	1.15E-03
Br	5.01E-06	1.00E-05	3.75E-06	1.63E-05	1.63E-05	3.75E-06
C	1.96E-03	6.50E-04	8.86E-04	1.94E-03	1.36E-03	5.81E-04
Ca	1.35E-03	5.41E-04	3.09E-04	1.22E-03	7.17E-04	1.52E-04
Cl	2.17E-04	1.44E-04	1.35E-04	4.23E-04	2.82E-04	1.38E-04
F	3.16E-05	1.58E-05	1.58E-05	2.11E-05	3.68E-05	2.11E-05
K	2.63E-04	1.93E-04	2.99E-04	3.32E-04	2.63E-04	1.98E-04
Mg	1.65E-04	5.35E-05	4.81E-05	1.63E-04	7.08E-05	2.14E-05
N	5.16E-04	1.77E-04	1.18E-04	5.48E-04	3.23E-04	5.64E-05
Na	4.24E-04	4.05E-04	4.83E-04	1.34E-03	9.03E-04	3.72E-04
S	4.37E-04	3.96E-04	1.67E-04	6.97E-04	3.44E-04	6.04E-05
Si	1.46E-04	3.25E-05	6.27E-05	4.89E-05	7.91E-05	4.78E-05

Source: DTN: MO0310SPADLBU4.001

NOTE: Except for pH and a_w, all Units are in Moles/kg H_2O.

Table 6.10-10. EQ3NR Equilibrium Speciation of the Six Bins

Bin	**1**	**2**	**3**	**4**	**5**	**6**
Filename	s80c25b.3o	s90b25b.3o	s86a25b.3o	p25_25b.3o	p26_25b.3o	s92a25b.3o
HCO_3^-	1.84E-03	6.29E-04	8.61E-04	1.82E-03	1.31E-03	5.65E-04
Na^+	4.24E-04	4.05E-04	4.83E-04	1.34E-03	9.03E-04	3.72E-04
Ca^{2+}	1.26E-03	5.30E-04	3.02E-04	1.13E-03	6.87E-04	1.50E-04
SO_4^{2-}	4.25E-04	3.90E-04	1.65E-04	6.80E-04	3.38E-04	6.01E-05
NO_3^-	5.16E-04	1.77E-04	1.18E-04	5.48E-04	3.23E-04	5.64E-05
Cl^-	2.17E-04	1.44E-04	1.35E-04	4.23E-04	2.82E-04	1.38E-04
K^+	2.63E-04	1.93E-04	2.99E-04	3.33E-04	2.63E-04	1.98E-04
$O_{2(aq)}$	2.68E-04	2.68E-04	2.68E-04	2.68E-04	2.68E-04	2.68E-04
Mg^{2+}	1.60E-04	5.31E-05	4.75E-05	1.58E-04	6.93E-05	2.12E-05
$CaCO_{3(aq)}$	5.49E-05	3.04E-06	3.41E-06	4.69E-05	1.62E-05	7.84E-07
$SiO_{2(aq)}$	1.33E-04	3.14E-05	6.00E-05	4.46E-05	7.39E-05	4.64E-05
CO_3^{2-}	3.90E-05	4.32E-06	7.96E-06	3.87E-05	1.92E-05	3.34E-06
F^-	3.16E-05	1.58E-05	1.58E-05	2.11E-05	3.68E-05	2.11E-05
$CaSO_{4(aq)}$	1.26E-05	5.79E-06	1.49E-06	1.73E-05	6.02E-06	2.96E-07
$CaHCO_3^+$	1.91E-05	2.96E-06	2.38E-06	1.66E-05	7.71E-06	8.13E-07
Br^-	5.01E-06	1.00E-05	3.75E-06	1.63E-05	1.63E-05	3.75E-06

Table 6.10-10. EQ3NR Equilibrium Speciation of the Six Bins (Continued)

Bin	1	2	3	4	5	6
$CO_{2(aq)}$	1.07E-05	1.07E-05	1.07E-05	1.07E-05	1.07E-05	1.07E-05
$HSiO_3^-$	1.32E-05	1.06E-06	2.77E-06	4.38E-06	5.20E-06	1.40E-06
OH^-	3.85E-06	1.31E-06	1.80E-06	3.82E-06	2.74E-06	1.18E-06
$MgCO_{3(aq)}$	3.04E-06	1.34E-07	2.38E-07	2.84E-06	7.19E-07	4.94E-08
$MgHCO_3^+$	2.29E-06	2.83E-07	3.61E-07	2.18E-06	7.43E-07	1.11E-07
$MgOH^+$	9.03E-08	1.11E-08	1.42E-08	8.58E-08	2.93E-08	4.39E-09
$CaOH^+$	5.17E-08	8.03E-09	6.46E-09	4.50E-08	2.09E-08	2.21E-09
H^+	3.10E-09	8.68E-09	6.24E-09	3.16E-09	4.25E-09	9.28E-09
$NaF_{(aq)}$	1.14E-09	5.70E-10	6.92E-10	2.38E-09	2.91E-09	7.29E-10
HSO_4^-	8.95E-11	2.54E-10	7.97E-11	1.43E-10	1.03E-10	4.54E-11
NO_2^-	1.85E-17	6.33E-18	4.19E-18	1.96E-17	1.15E-17	2.01E-18
ClO_4^-	3.05E-27	2.02E-27	1.90E-27	5.94E-27	3.96E-27	1.94E-27
$H_{2(aq)}$	4.78E-45	4.78E-45	4.78E-45	4.78E-45	4.78E-45	4.78E-45
NH_4^+	8.13E-67	2.29E-66	7.97E-67	8.87E-67	9.77E-67	8.65E-67
$NH_{3(aq)}$	1.51E-67	1.51E-67	7.33E-68	1.61E-67	1.32E-67	5.35E-68

Source: DTN: MO0310SPADLBU4.001

NOTE: Units are in Moles/kg H_2O.

6.10.6 Development of Lookup Tables for Total Systems Performance Assessment - License Application

The lookup tables have been constructed based on the EQ3/6 (v. 8.0) calculations using thermodynamic database data0.ypf (Section 4.1.4, DTN: SN0302T0510102.002 [DIRS 162572]) and the USGS data on dust leachate compositions (DTN: MO0207EBSDUSTS.020, Table 4.1-19 [DIRS 162556]; and MO0209EBSDUST2.030 [DIRS 162557], Table 4.1-20).

The model validation range for the current in-drift precipitates/salts model is for temperatures up to 140°C (BSC 2003 [DIRS 166031]). The data is split into the calculation runs at 100°C and below (DTN: SN0310T050102.011), and the calculation runs and lookup tables above this temperature (120°C and 140°C; DTN: SN03100T0510102.012).

6.10.6.1 Dust Leachate Water Inputs

Table 6.10-6 identifies the bin "median" composition inputs for the in-drift precipitates/salts model calculations of aqueous solution compositions produced by deliquescence.

The EQ3NR input and output files for lookup table calculations are documented in DTN: SN0310T050102.010. They are summarized in Table 6.10-11.

Table 6.10-11. EQ3NR Input/Output Files for TSPA-LA Dust Leachate Abstraction

Bin	Input File Names	Output File Names	Pickup File Names
1	s80c25b.3i	s80c25b.3o	s80c25b.3p
2	s90b25b.3i	s90b25b.3o	s90b25b.3p
3	s86a25b.3i	s86a25b.3o	s86a25b.3p
4	p25_25b.3i	p25_25b.3o	p25_25b.3p
5	p26_25b.3i	p26_25b.3o	p26_25b.3p
6	s92a25b.3i	s92a25b.3o	s92a25b.3p

Source: DTN: SN0310T050102.010, directory EQ3_runs

6.10.6.2 Temperature and Carbon Dioxide

Temperature and carbon dioxide fugacity are varied to capture the effects of these parameters on the evaporative evolution. Unlike the seepage lookup tables, deliquescence can occur at temperatures greater than 100°C in the repository. For temperature, the values are 40ºC, 70ºC, 100°C, 120°C, and 140°C. The CO_2 fugacity values were 10^{-2}, 10^{-3}, and 10^{-4} bar. Each temperature was run for each CO_2 fugacity, resulting in fifteen combinations for each bin water. The input values for temperature and CO_2 fugacity are defined in the EQ6 input files of the in-drift precipitates/salts model. These input files are based on the EQ6 input file templates of DTN: MO0303SPAMEQ36.000 [DIRS 162549]. The EQ3NR pickup files identified in Table 6.10-11 provided the bottom halves of the input files.

The in-drift precipitates/salts model is used to generate lookup tables of water compositions produced by dust deliquescence over the expected range of in-drift relative humidity values for use in TSPA-LA calculations. To cover this range, the bin waters are typically evaporated to dryness (see Section 6.10.4 for the operational definition of dryness). The two exceptions are for the low temperature cases that were calculated down to 50 percent and 30 percent *RH* at 40°C and 70°C, respectively. These lower *RH* limits were determined from the *Multiscale Thermohydrologic Model* (BSC 2003 [DIRS 166463]).

The starting bin waters are sufficiently dilute that they represented solutions in equilibrium with relative humidity between 99.9 and 99.99 percent. For potential relative humidity values higher than the starting bin water, condensation of water vapor is not simulated. The top value on any given lookup table should be sufficient to simulate the chemistry of the dilute waters above 99.99 percent. Thus, for each temperature and CO_2 fugacity combination, only one EQ6 input file is generated.

The resulting EQ6 input and output files for the bin waters are listed in Table 6.10-12 and documented in DTNs: SN0310T0510102.011 and SN0310T0510102.012. The file nomenclature is d?c#t%.6i or 6o, where "?" is the bin number (1, 2, etc.), "#" is 2, 3, or 4 for the partial pressure of CO_2 equal to 10^{-2}, 10^{-3}, or 10^{-4} bar, respectively, "%" is 04, 07, 10, 12, and 14, for temperature equal to 40, 70, 100, 120, and 140°C, respectively. For example, file d1c2t10.6i is the dust EQ6 input file for bin 1 at 100°C and a fugacity of CO_2 of 10^{-2} bar.

Table 6.10-12. EQ6 Input/Output Files for TSPA-LA Abstraction

Bin	Input File Names	Output File Names
1	d1c2t04.6i, d1c3t04.6i, d1c4t04.6i, d1c2t07.6i, d1c3t07.6i, d1c4t07.6i, d1c2t10.6i, d1c3t10.6i, d1c4t10.6i, d1c2t12.6i, d1c3t12.6i, d1c4t12.6i, d1c2t14.6i, d1c3t14.6i, d1c4t14.6i	d1c2t04.6o, d1c3t04.6o, d1c4t04.6o, d1c2t07.6o, d1c3t07.6o, d1c4t07.6o, d1c2t10.6o, d1c3t10.6o, d1c4t10.6o, d1c2t12.6o, d1c3t12.6o, d1c4t12.6o, d1c2t14.6o, d1c3t14.6o, d1c4t14.6o
2	d2c2t04.6i, d2c3t04.6i, d2c4t4.6i, d2c2t07.6i, d2c3t07.6i, d2c4t07.6i, d2c2t10.6i, d2c3t10.6i, d2c4t10.6i, d2c2t12.6i, d2c3t12.6i, d2c4t12.6i, d2c2t14.6i, d2c3t14.6i, d2c4t14.6i	d2c2t04.6o, d2c3t04.6o, d2c4t04.6o, d2c2t07.6o, d2c3t07.6o, d2c4t07.6o, d2c2t10.6o, d2c3t10.6o, d2c4t10.6o, d2c2t12.6o, d2c3t12.6o, d2c4t12.6o, d2c2t14.6o, d2c3t14.6o, d2c4t14.6o
3	d3c2t04.6i, d3c2t04b.6i, d3c3t04.6i, d3c4t04.6i, d3c2t07.6i, d3c3t07.6i, d3c4t07.6i, d3c2t10.6i, d3c2t10b.6i, d3c3t10.6i, d3c3t10b.6i, d3c4t10.6i, d3c4t10b.6i, d3c2t12.6i, d3c3t12.6i, d3c4t12.6i, d3c2t14.6i, d3c3t14.6i, d3c4t14.6i	d3c2t04.6o, d3c2t04b.6o, d3c3t04.6o, d3c4t04.6o, d3c2t07.6o, d3c3t07.6o, d3c4t07.6o, d3c2t10.6o, d3c2t10b.6o, d3c3t10.6o, d3c3t10b.6o. d3c4t10.6o, d3c4t10b.6o, d3c2t12.6o, d3c3t12.6o, d3c4t12.6o, d3c2t14.6o, d3c3t14.6o, d3c4t14.6o
4	d4c2t04.6i, d4c3t04.6i, d4c4t04.6i, d4c2t07.6i, d4c3t07.6i, d4c4t07.6i, d4c2t10.6i, d4c3t10.6i, d4c4t10.6i, d4c2t12.6i, d4c3t12.6i, d4c4t12.6i, d4c2t14.6i, d4c3t14.6i, d4c4t14.6i	d4c2t04.6o, d4c3t04.6o, d4c4t04.6o, d4c2t07.6o, d4c3t07.6o, d4c4t07.6o, d4c2t10.6o, d4c3t10.6o, d4c4t10.6o, d4c2t12.6o, d4c3t12.6o, d4c4t12.6o, d4c2t14.6o, d4c3t14.6o, d4c4t14.6o
5	d5c2t04.6i, d5c3t04.6i, d5c4t04.6i, d5c2t07.6i, d5c3t07.6i, d5c4t07.6i, d5c2t10.6i, d5c3t10.6i, d5c4t10.6i, d5c2t12.6i, d5c3t12.6i, d5c4t12.6i, d5c2t14.6i, d5c3t14.6i, d5c4t14.6i	d5c2t04.6o, d5c3t04.6o, d5c4t04.6o, d5c2t07.6o, d5c3t07.6o, d5c4t07.6o, d5c2t10.6o, d5c3t10.6o, d5c4t10.6o, d5c2t12.6o, d5c3t12.6o, d5c4t12.6o, d5c2t14.6o, d5c3t14.6o, d5c4t14.6o
6	d6c2t04.6i, d6c3t04.6i, d6c4t04.6i, d6c2t07.6i, d6c2t07b.6i, d6c3t07.6i, d6c4t07.6i, d6c2t10.6i, d6c2t10b.6i, d6c3t10.6i, d6c3t10b.6i, d6c4t10.6i, d6c4t10b.6i, d6c2t12.6i, d6c2t12b.6i, d6c3t12.6i, d6c3t12b.6i, d6c4t12.6i, d6c4t12b.6i, d6c2t14.6i, d6c2t14b.6i, d6c3t14.6i, d6c3t14b.6i, d6c4t14.6i, d6c4t14b.6i	d6c2t04.6o, d6c3t04.6o, d6c4t04.6o, d6c2t07.6o, d6c2t07b.6o, d6c3t07.6o, d6c4t07.6o, d6c2t10.6o, d6c2t10b.6o, d6c3t10.6o, d6c3t10b.6o, d6c4t10.6o, d6c4t10b.6o, d6c2t12.6o, d6c2t12b.6o, d6c3t12.6o, d6c3t12b.6o, d6c4t12.6o, d6c4t12b.6o, d6c2t14.6o, d6c2t14b.6o, d6c3t14.6o, d6c3t14b.6o, d6c4t14.6o, d6c4t14b.6o

Source: DTNs: SN0310T0510102.011 and SN0310T0510102.012

6.10.6.3 Calculation Using Additional Mineral and Aqueous Species Suppressions

Additional mineral and aqueous species suppressions were used in some evaporation simulations of dust leachate waters at various temperatures. It was noted that the $O_{2(aq)}$ concentration was reaching unreasonably high values at high levels of solute concentrations. This causes the EQ3/6 code calculation runs to terminate abruptly. This result seems to be a limitation of the data0.ypf Pitzer database regarding this neutral species where its model parameters are bounded to lower ionic strengths. Conceptually, there is no reason for $O_{2(aq)}$ to concentrate to such levels under in-drift conditions, and the calculation code runs use a constant fo_2 value at 0.212 bars. Therefore, in cases where $O_{2(aq)}$ poses a problem, this species is suppressed, allowing the code calculation runs to proceed normally without affecting the values used to constrain fo_2. Table 6.10-13 shows the dust leachate water bins where this suppression was applied.

Table 6.10-13. Additional Suppressions and Inclusions in EQ3/6 Runs Involving Dust Leachate Evaporation as a Function of Temperature

Bin	Temperature (°C)	Additional Suppressions	Comments
Bins 1 – 6	40	None	–
Bins 1 – 4	70	None	–
Bin 5	70	$O_{2(aq)}$	–
Bin 6	70	$O_{2(aq)}$, natrite, and trona[2]	
Bins 1, 2, 4, and 5	100	$O_{2(aq)}$	–
Bins 3 and 6	100	$O_{2(aq)}$, natrite, and trona[2]	Suppressions applied only to the extrapolation runs[1]
Bins 1, 2, 4, and 5	120	$O_{2(aq)}$	–
Bins 3 and 6	120	$O_{2(aq)}$, thermonatrite, and trona[2]	Suppressions applied only to the extrapolation runs[1]
Bins 1, 2, 4, and 5	140	$O_{2(aq)}$	–
Bins 3 and 6	140	$O_{2(aq)}$, thermonatrite	–

NOTES: [1]Extrapolation runs refer to those modified to attain the apparent eutectic nitrate salt assemblage (see Section 6.10.6.4), These represented by files labeled ###b.3i and ###b.6i in DTNs: SN0310T0510102.011 and SN0310T0510102.012.

[2]High temperature solubility data for Trona is absent from the database (only 25 °C log *K*) and extrapolation to >45°C are deemed unreliable.

Another suppression includes the mineral phases natrite and thermonatrite. These suppressions were applied to the code calculation runs only when these appear as saturated phases in the reaction path calculation. Natrite is suppressed in cases where it appears as part of the equilibrium mineral assemblage in reaction path calculations at temperatures below 100°C where thermonatrite is allowed to precipitate. Conversely, thermonatrite is suppressed in code calculation runs at 120ºC and 140ºC. The general rationale for this suppression is based on the occurrence and reported experimentally-determined stability (see e.g., Grønvold and Meisingset 1983 [DIRS 162069]) of these minerals at temperatures from 270 – 400 K. Table 6.10-13 indicates the dust leachate water bins where these inclusions/suppressions for these Na-carbonate phases were implemented. The DTNs containing the associated EQ3/6 input/output files for these runs encompassing a temperature range of 40 to 140 ºC are DTNs: SN0310T0510102.011 and SN0310T0510102.012.

6.10.6.4 EQ6 convergence Failures and Eutectic Point Estimation

Some evaporation simulations of the dust leachates fail to attain a eutectic point for the system K-Na-Cl-NO_3. Eutectic salt assemblages in this system represent the nearest point to dryout in the evaporation run calculations. Prior to reaching this eutectic a sulfate-chloride or sulfate-carbonate salt assemblage is observed in Bins 3 and 6, at which point the EQ3/6 calculation fails to proceed further. To obtain the eutectic salt assemblage comprising components in the system K-Na-Cl-NO_3 for the dust leachate evaporation run calculations in these bins, an extrapolation was done from the convergence failure by taking the end-point

chemistry for these cases and continuing the evaporation calculation from that point, but without the SO_4^{2-} species. The removal of this component, whose concentration is non-negligible at the sulfate salt saturation point, requires the removal of Na^+ and K^+ to avoid charge imbalances. As Na^+ and K^+ are the dominant cations, and the saturation points of Na_2SO_4 and K_2SO_4 are similar, sodium and potassium were decreased in amounts equivalent to the molality of SO_4^{2-}. Additional minor species were also dropped from the system at this point and charge balanced on K^+. The end-point water compositions are used in a subsequent EQ3NR calculation run to generate a pickup file in order to continue the EQ6 solution evaporation.

In order to closely match the remaining mass of aqueous phase relative to the prior run (e.g., see Figure III-03-05 in Attachment III), the value for the aqueous phase scale factor in the new EQ3 #b.3i file was approximated to the mass of H_2O (in kg) remaining in the last step of the previous EQ6 calculation run. The effect of this is to scale down the initial amount of H_2O in the subsequent EQ6 calculation run, which is by default 1 kg. When these continuation run calculations are combined for analysis with the initial evaporation results, the evaporation path is continued from the end-point activity water of the previous calculation run. This approach to extend from one salt equilibrium assemblage to another may be considered as a rough approximation. Nevertheless, the differences are relatively small when these are combined while closely matching the activity of H_2O in the preceding calculation. The solution compositions obtained by this method are within the compositional range of the observed values in the other evaporated water bins at the same temperature.

6.10.6.5 Lookup Tables

The results of the dust evaporation abstractions that are to be used as direct input into TSPA-LA calculations are summarized in a set of lookup tables documented in DTNs: MO0310SPADLALT.001 and MO0310SPADLHTL.000. These lookup tables, listed in Table 6.10-14, include boundary conditions, abstraction output, and results of supplemental calculations. Each lookup table corresponds to one of the in-drift precipitates/salts model output files identified in Table 6.10-12. Each row in these tables provides output parameter values as the water incrementally evolves due to evaporation or deliquescence given the defined boundary conditions. Each output row is defined by a unique equilibrium relative humidity.

The general lookup table format and the calculations in the lookup tables are developed and described in the *In-Drift Precipitates/Salts Model* report (BSC 2003, Sections 6.7.3 and 6.6.3.5 [DIRS 162529]). The first three columns are reserved for the THC seepage lookup tables discussed in Section 6.9 and are not relevant for the dust leachate table analysis. The next column is the equilibrium relative humidity, calculated by multiplying the activity of water (listed in column K) by 100 percent. The rest of the columns are filled using GETEQDATA Version 1.0.1 (BSC 2003 [161900]) software. Columns E through H show reaction progress and the boundary conditions for the starting water (i.e., the temperature and the fugacities of oxygen and carbon dioxide). Columns I through X show reaction progress, pH, ionic strength, mass of H_2O in the reactor, and the total concentrations of the aqueous components. Columns Y through AL present reaction progress, mass of H_2O in the reactor, and the concentrations of potential acid-neutralizing species. Finally, columns AM through BD are reserved to show the amounts of minerals accumulated in the reactor. The values in the lookup tables may be used to define response surfaces so that interpolations or extrapolations may be obtained for precise input

values not provided in the tables. Column E calculates the H_2O vapor pressure as a function of *RH* and the EQ6 calculated pressure (entered in Cell E1).

Table 6.10-14. Dust Leachate Evaporation Lookup Tables for TSPA-LA Abstraction

Bin	Lookup Tables
1	d1c2t04.xls, d1c3t04.xls, d1c4t04.xls, d1c2t07.xls, d1c3t07.xls, d1c4t07.xls, d1c2t10.xls, d1c3t10.xls, d1c4t10.xls, d1c2t12.xls, d1c3t12.xls, d1c4t12.xls, d1c2t14.xls, d1c3t14.xls, d1c4t14.xls
2	d2c2t04.xls, d2c3t04.xls, d2c4t04.xls, d2c2t07.xls, d2c3t07.xls, d2c4t07.xls, d2c2t10.xls, d2c3t10.xls, d2c4t10.xls, d2c2t12.xls, d2c3t12.xls, d2c4t12.xls, d2c2t14.xls, d2c3t14.xls, d2c4t14.xls
3	d3c2t04.xls, d3c3t04.xls, d3c4t04.xls, d3c2t07.xls, d3c3t07.xls, d3c4t07.xls, d3c2t10.xls, d3c3t10.xls, d3c4t10.xls, d3c2t12.xls, d3c3t12.xls, d3c4t12.xls, d3c2t14.xls, d3c3t14.xls, d3c4t14.xls
4	d4c2t04.xls, d4c3t04.xls, d4c4t04.xls, d4c2t07.xls, d4c3t07.xls, d4c4t07.xls, d4c2t10.xls, d4c3t10.xls, d4c4t10.xls, d4c2t12.xls, d4c3t12.xls, d4c4t12.xls, d4c2t14.xls, d4c3t14.xls, d4c4t14.xls
5	d5c2t04.xls, d5c3t04.xls, d5c4t04.xls, d5c2t07.xls, d5c3t07.xls, d5c4t07.xls, d5c2t10.xls, d5c3t10.xls, d5c4t10.xls, d5c2t12.xls, d5c3t12.xls, d5c4t12.xls, d5c2t14.xls, d5c3t14.xls, d5c4t14.xls
6	d6c2t04.xls, d6c3t04.xls, d6c4t04.xls, d6c2t07.xls, d6c3t07.xls, d6c4t07.xls, d6c2t10.xls, d6c3t10.xls, d6c4t10.xls, d6c2t12.xls, d6c3t12.xls, d6c4t12.xls, d6c2t14.xls, d6c3t14.xls, d6c4t14.xls

Source: DTNs: MO0310SPADLALT.001 and MO0310SPADLHTL.000

6.10.7 Illustration of Results

Figures 6.10-13 through 6.10-18 graphically illustrate the results with plotted values from the d5c3t7.xls lookup table. These figures are meant to illustrate the general output trends; for actual values, the reader should consult the lookup tables directly. These are bin 5 evaporation results at a temperature of 70°C and a CO_2 fugacity of 10^{-3} bar. The first two plot the total elemental

aqueous concentrations and pH as a function of relative humidity and concentration factor. The next two plot the ANC aqueous species concentrations (HCO_3^-, CO_3^{2-}, $HSiO_3^-$ $CaHCO_3^+$, OH^-, $MgHCO_3^+$, H^+, $MgOH^+$, $CaOH^+$, HSO_4^-, Ca^{2+}, and Mg^{2+}) and pH as a function of relative humidity and concentration factor. The last two results plot pH, the fixed CO_2 and O_2 fugacities, and the moles of minerals precipitated from one kilogram of dust condensate water as a function of relative humidity and concentration factor. The graphical results from the remainder of the lookup tables are provided in Attachment III.

6.10.8 Correction of SiO_2 Concentration Units: Sensitivity Analysis of Dust Leachate Evaporation

Concentration of Si content in the dust leachate waters is expressed in ppm (e.g., mg of solute per kg of solvent H_2O). However, Si concentration is entered as $SiO_{2(aq)}$ in the EQ3/6 input files. Therefore, a conversion from Si to SiO_2 in ppm units is needed to correctly represent the concentration of this component in the code run calculations. This step was inadvertently omitted during the calculation of input leachate concentrations for the EQ3/6 calculation runs given in DTN: SN0310T0510102.010 (see Sections 6.10.3 and 6.10.4). Because of this, a sensitivity analysis based on a comparison between corrected and uncorrected Si concentration units has been done using the six dust leachate median bin water values listed on Table 6.10.6. A comparison of resulting outputs is given in DTN: MO0311SPASADLS.000.

A priori, it is not expected that this change in Si concentration during evaporation down to an activity of water of ~0.65 would affect the output results in a significant way, because of its relatively low concentration in the starting water compositions, and this is generally true. Mg^{2+} concentrations are slightly different in most calculation runs due to sepiolite formation, except in the median waters p25 and S92a, where the resulting concentrations are similar. In water S80c, the predicted values for pH and the concentrations of Ca^{2+} and SO_4^{2-} differ in the calculation runs using the corrected and uncorrected $SiO_{2(aq)}$ concentrations. In both cases, similar Si phases with relatively low solubilities form early in the evaporation simulation. In both calculation runs, the common Si phase added to the equilibrium mineral assemblages in the early stages of the evaporation is sepiolite. However, due to the larger amount of Si in the calculation run with the corrected SiO_2 concentration (S80c_25bt), more sepiolite precipitates, resulting in the reduction of Mg in solution. This decrease in Mg prevents saturation with respect to huntite, a Ca-Mg carbonate phase which precipitates in the uncorrected $SiO_{2(aq)}$ run. In the uncorrected case, saturation with respect to this phase causes a further decrease in Ca, that in turn affects the SO_4^{2-} equilibrium concentration with respect to gypsum – a common phase in both calculation runs. Moreover, saturation with respect to huntite also affects the HCO_3^- concentration (because it affects the amount of $CaCO_3$ that precipitates), causing the pH to be slightly higher (~0.2 pH units, well within the uncertainty range in bin 1 pH values, see Table 6.12-8). In the S80c simulation using the corrected $SiO_{2(aq)}$ concentration, relatively larger amounts of sepiolite formed, reducing total Mg concentration and preventing the formation of huntite. The only median water affected by the change in the input values for $SiO_{2(aq)}$ is S80c, which is present in bin 1, and which only comprises ~5 percent of all the dust leachate waters. Therefore, it is not expected that the use of the incorrect Si content in the dust leachates will significantly impact chemical parameters relevant to TSPA-LA models, such as Cl/NO_3 ratios.

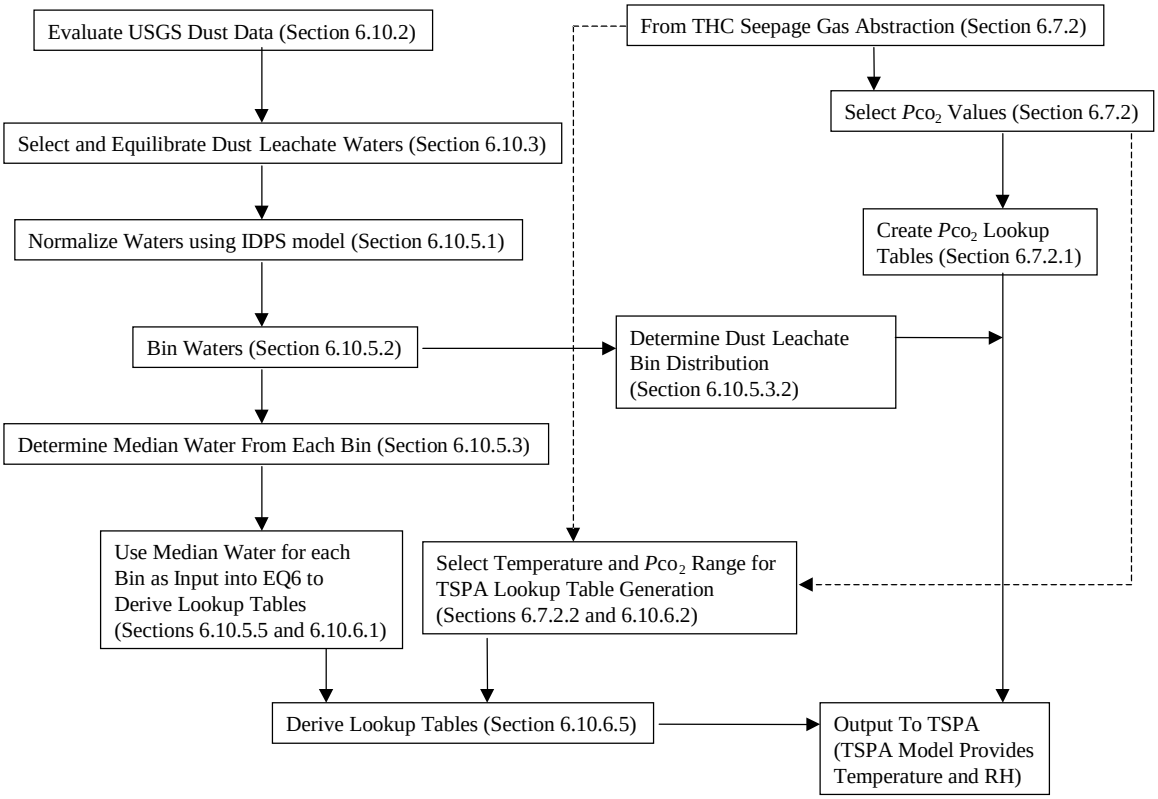

Figure 6.10-1. Flow Chart Representing the Dust Leachate Analysis Abstraction Process

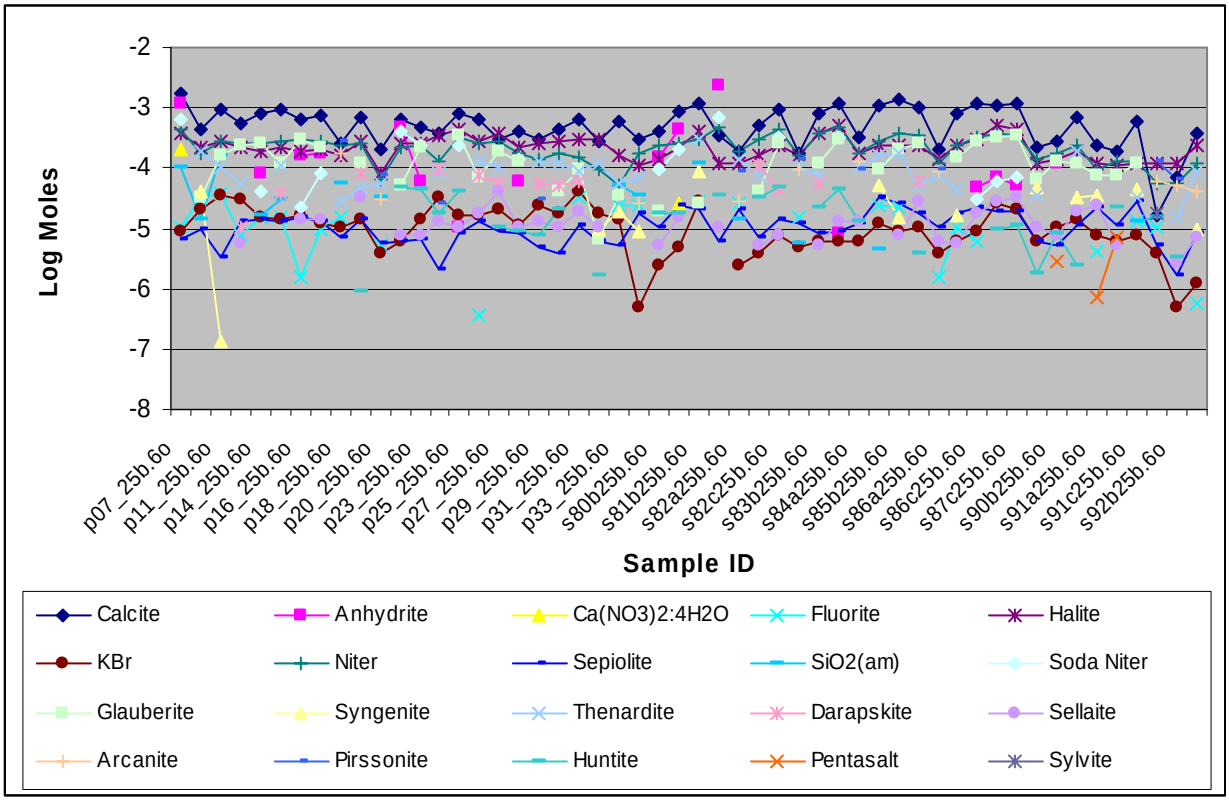

DTN: MO0310SPADLBU4.001

Figure 6.10-2. EQ6 Dust Leachate Water Mineralogy at the Dryout End Point at 25°C and Atmospheric Pco_2

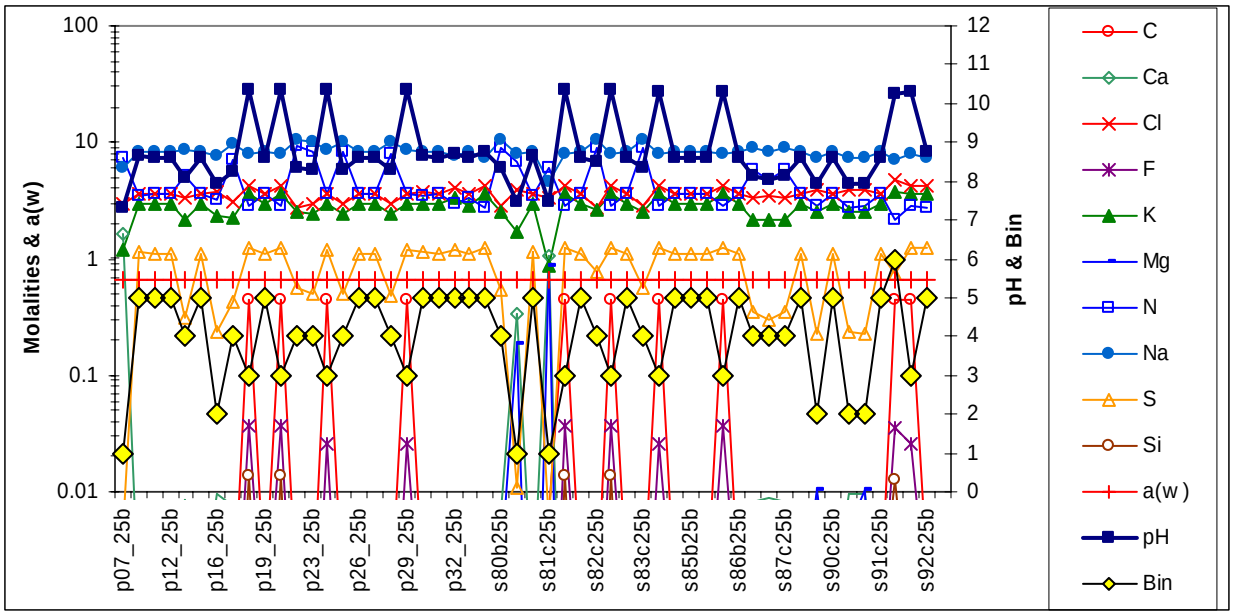

DTN: MO0310SPADLBU4.001

Figure 6.10-3. Total Elemental Molalities and pH of All Waters Used in the Binning Analysis After Evaporation to 65 Percent Relative Humidity

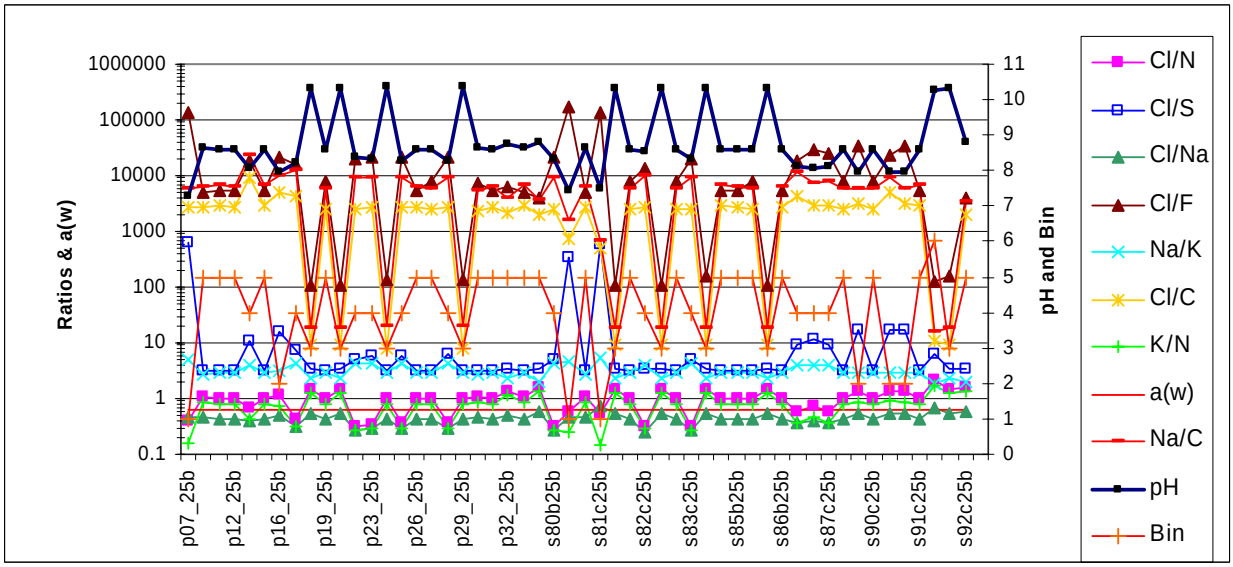

DTN: MO0310SPADLBU4.001

Figure 6.10-4. Molar Ratios in Brines After Evaporation to 65 Percent Relative Humidity (Plot 1)

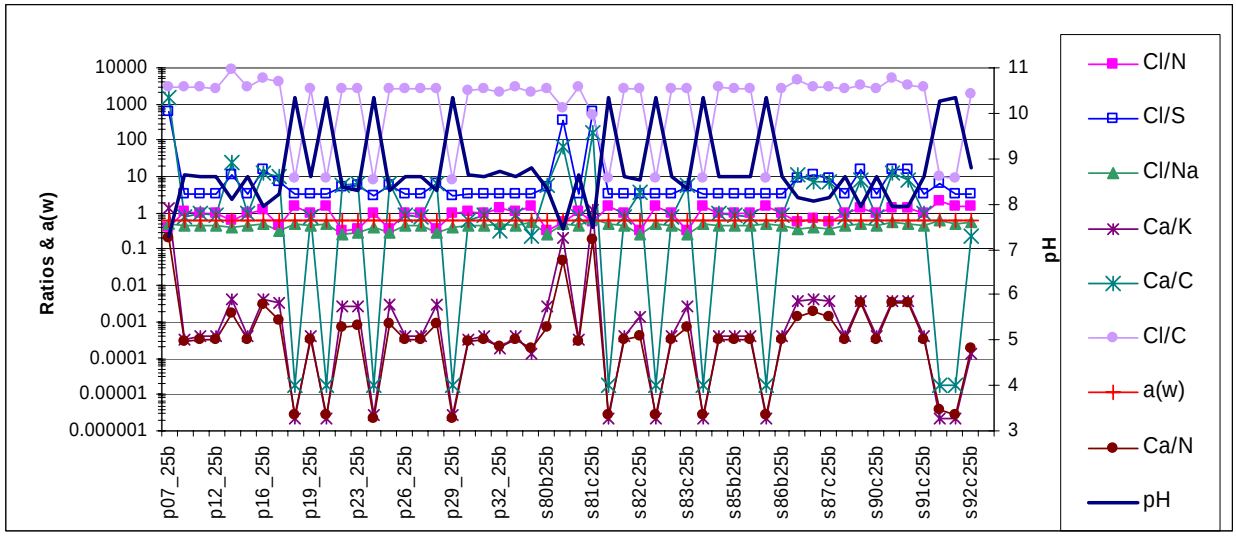

DTN: MO0310SPADLBU4.001

Figure 6.10-5. Molar Ratios in Brines After Evaporation to 65 Percent Relative Humidity (Plot 2)

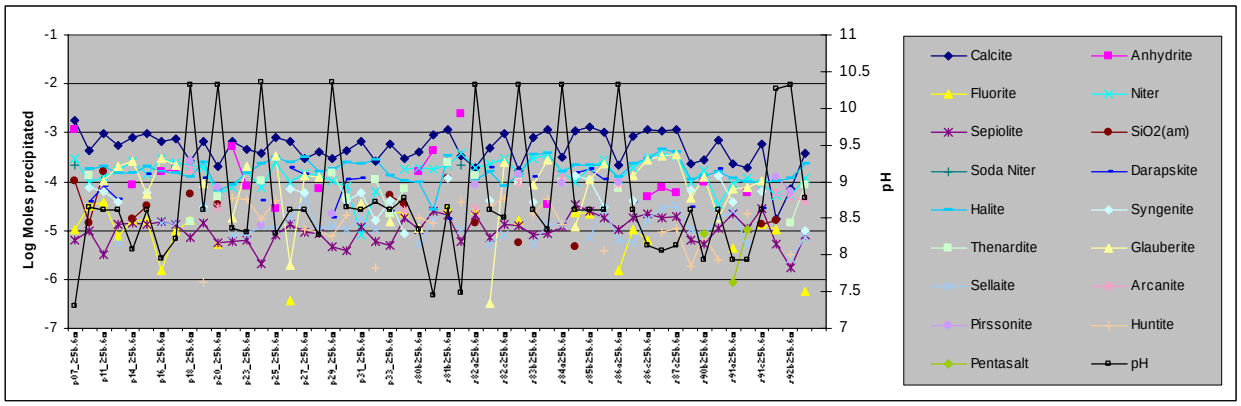

DTN: MO0310SPADLBU4.001

Figure 6.10-6. Mineral Assemblages After Evaporation to 65 Percent Relative Humidity

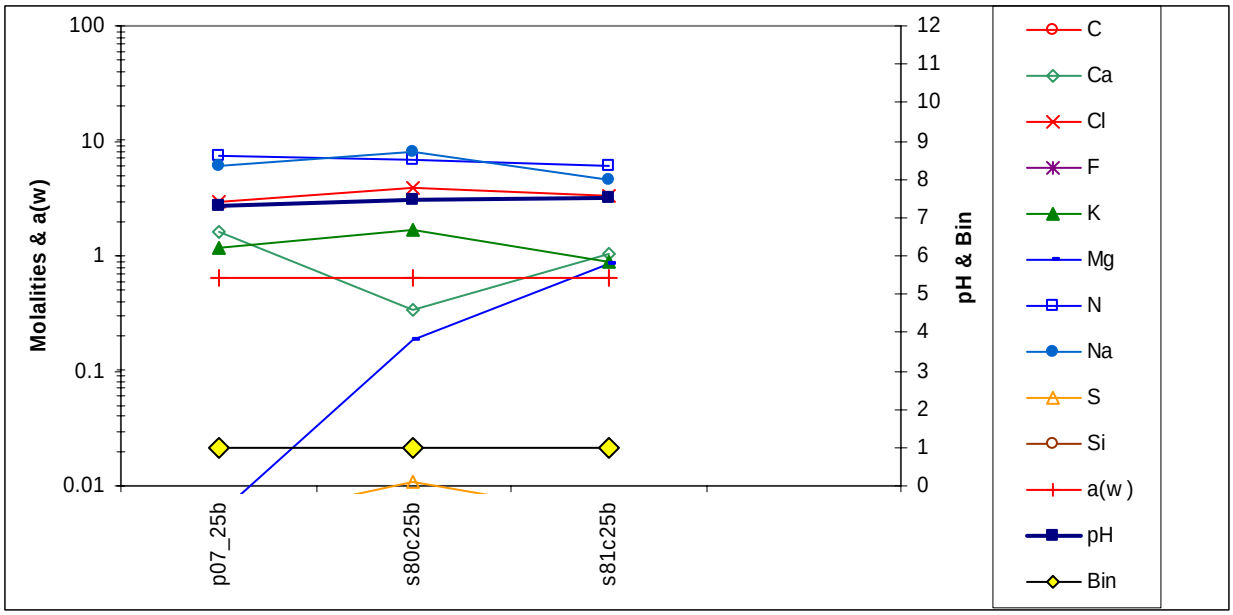

DTN: MO0310SPADLBU4.001

Figure 6.10-7. Evaporated Water Compositions for Dust Leachate Bin 1 After Evaporation to 65 Percent Relative Humidity

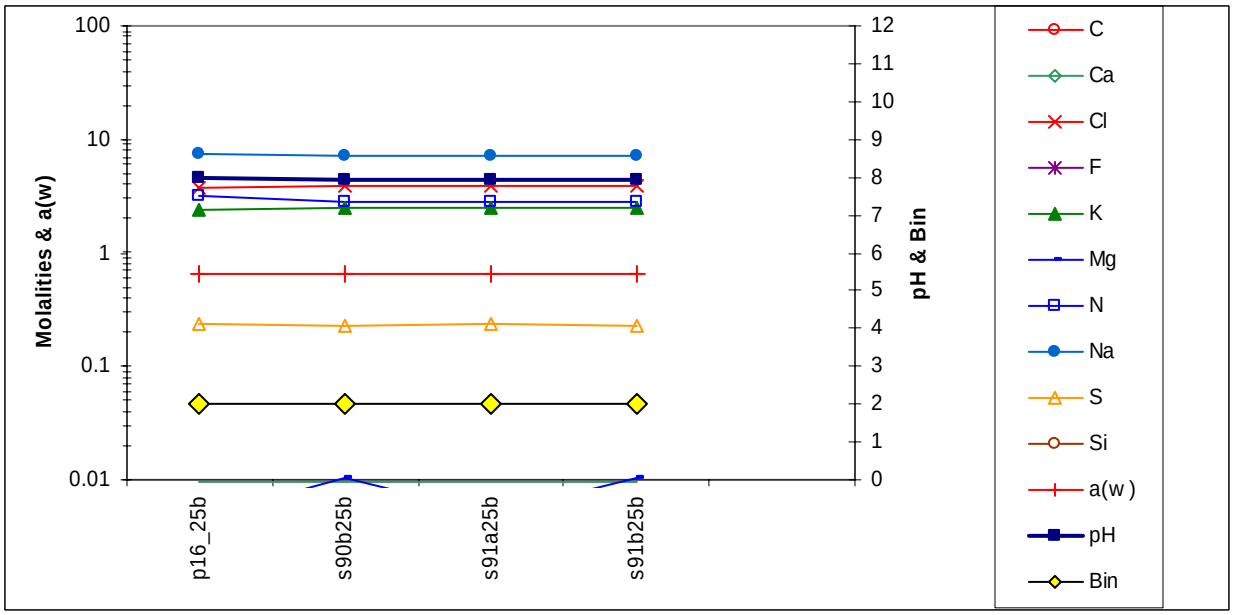

DTN: MO0310SPADLBU4.001

Figure 6.10-8. Evaporated Water Compositions for Dust Leachate Bin 2 After Evaporation to 65 Percent Relative Humidity

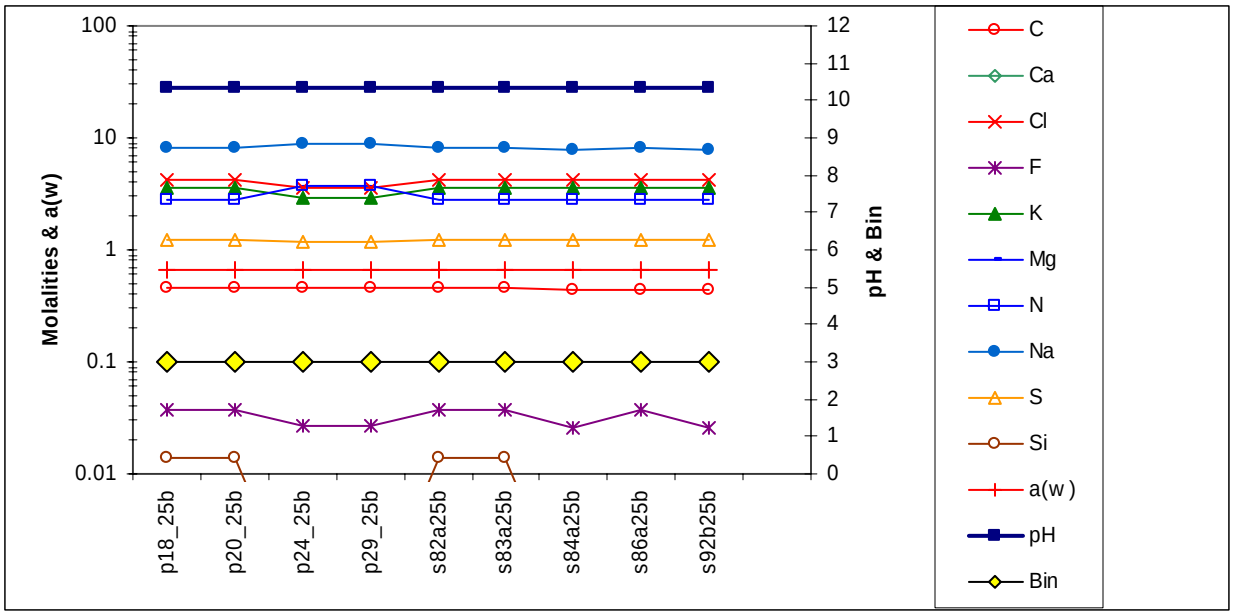

DTN: MO0310SPADLBU4.001

Figure 6.10-9. Evaporated Water Compositions for Dust Leachate Bin 3 After Evaporation to 65 Percent Relative Humidity

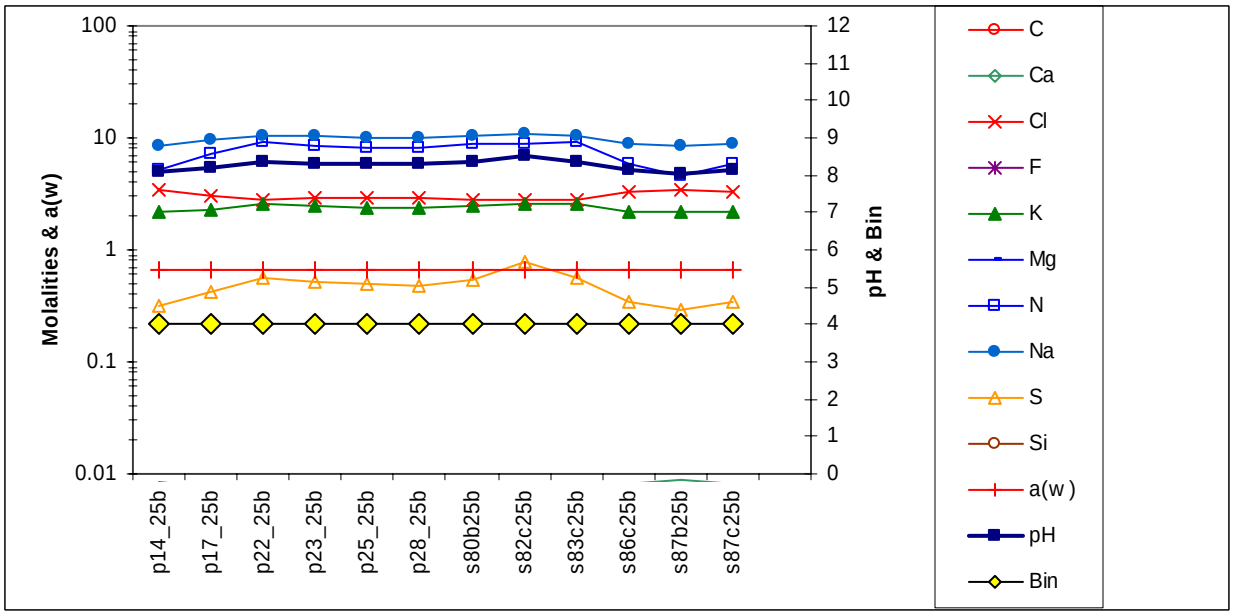

DTN: MO0310SPADLBU4.001

Figure 6.10-10. Evaporated Water Compositions for Dust Leachate Bin 4 After Evaporation to 65 Percent Relative Humidity

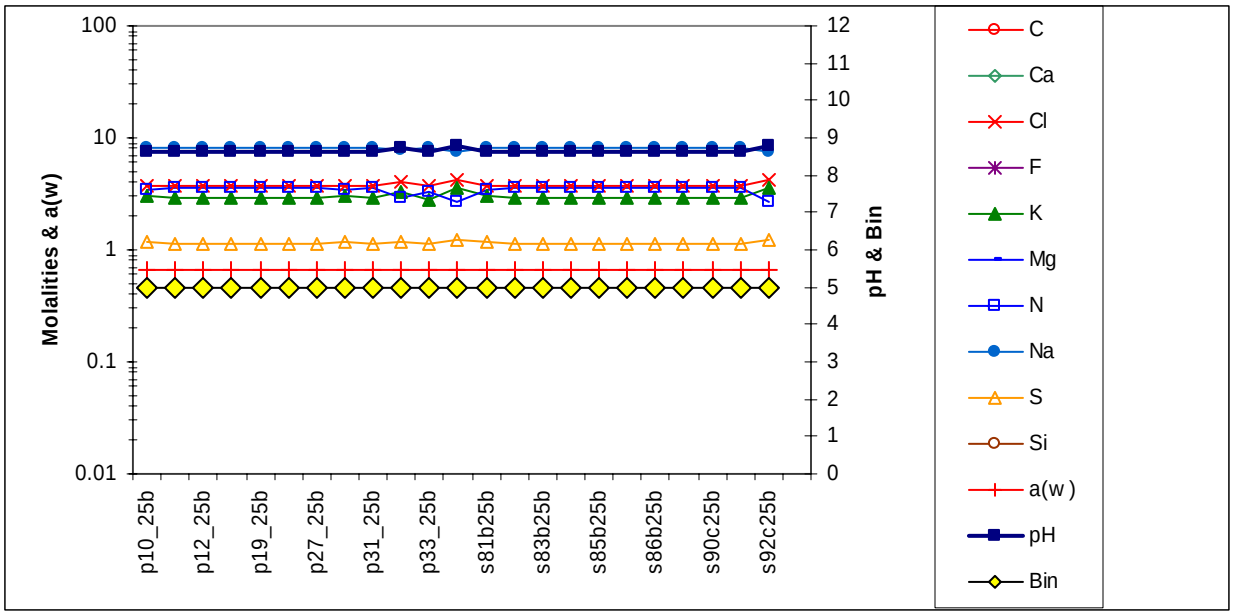

DTN: MO0310SPADLBU4.001

Figure 6.10-11. Evaporated Water Compositions for Dust Leachate Bin 5 After Evaporation to 65 Percent Relative Humidity

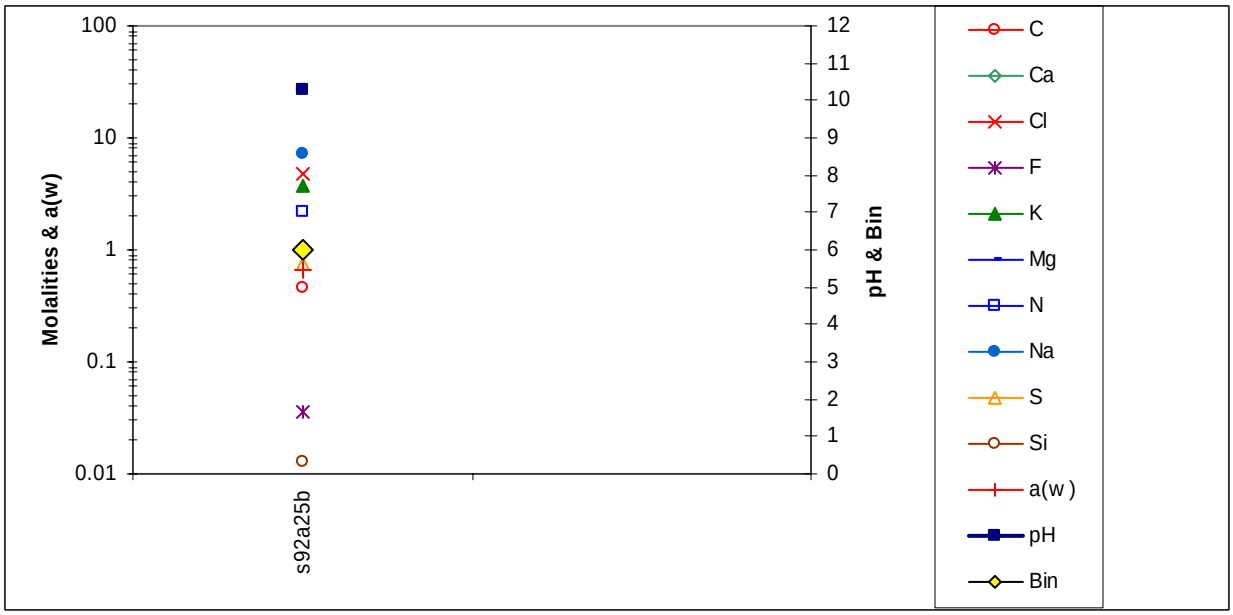

DTN: MO0310SPADLBU4.001

Figure 6.10-12. Evaporated Water Compositions for Dust Leachate Bin 6 After Evaporation to 65 Percent Relative Humidity

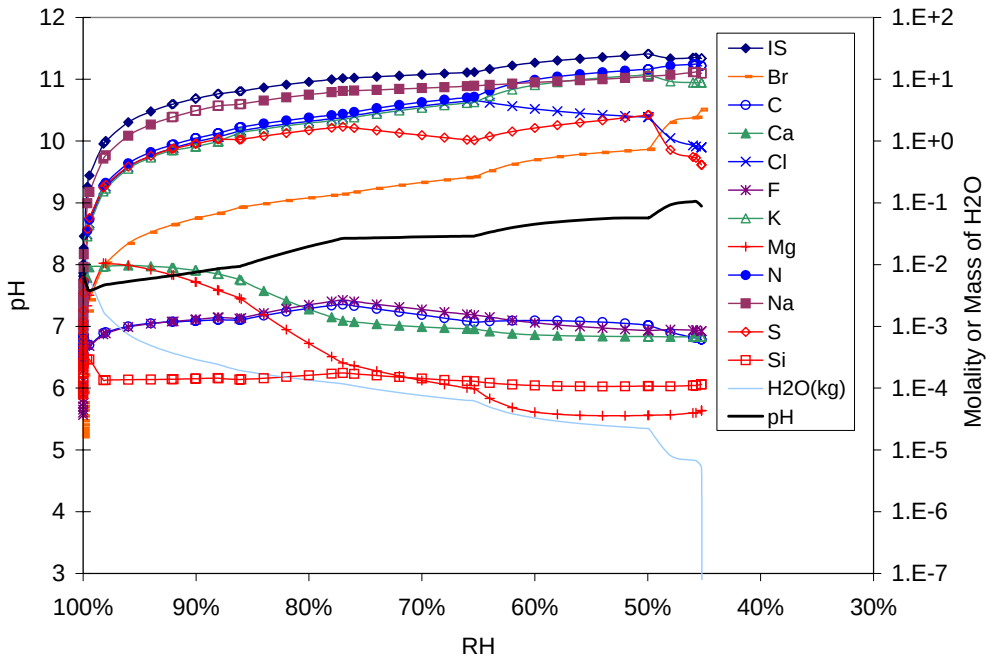

DTN: MO0310SPADLALT.001

Figure 6.10-13. Predicted Compositional Evolution as Dust Leachate Bin 5 Waters Evaporate at 70ºC and 10^{-3} Bar CO_2 Fugacity, Plotted Versus Relative Humidity

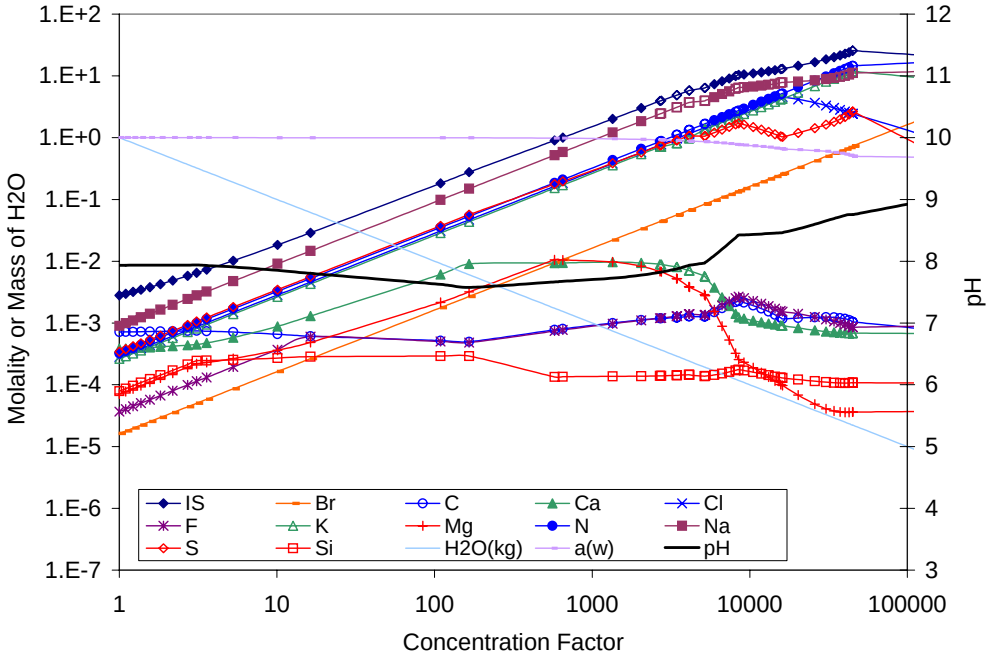

DTN: MO0310SPADLALT.001

Figure 6.10-14. Predicted Compositional Evolution as Dust Leachate Bin 5 Waters Evaporate at 70ºC and 10^{-3} Bar CO_2 Fugacity, Plotted Versus Concentration Factor

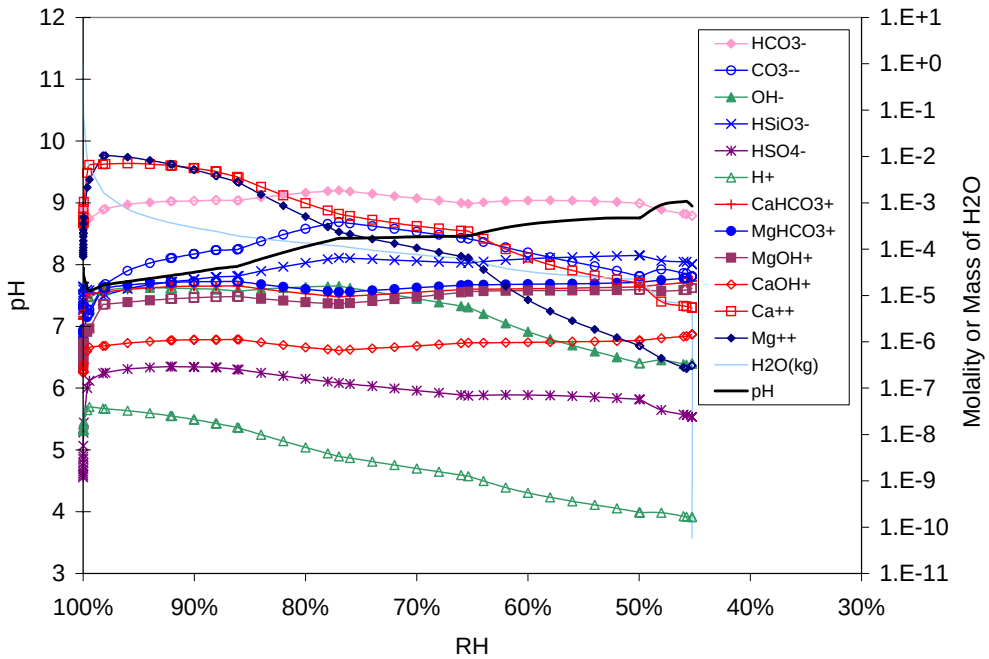

DTN: MO0310SPADLALT.001

Figure 6.10-15. The Predicted Concentrations of ANC Species During Evaporative Evolution of Dust Leachate Bin 5 Water at 70ºC and 10^{-3} Bar CO_2 Fugacity, Plotted Versus Relative Humidity.

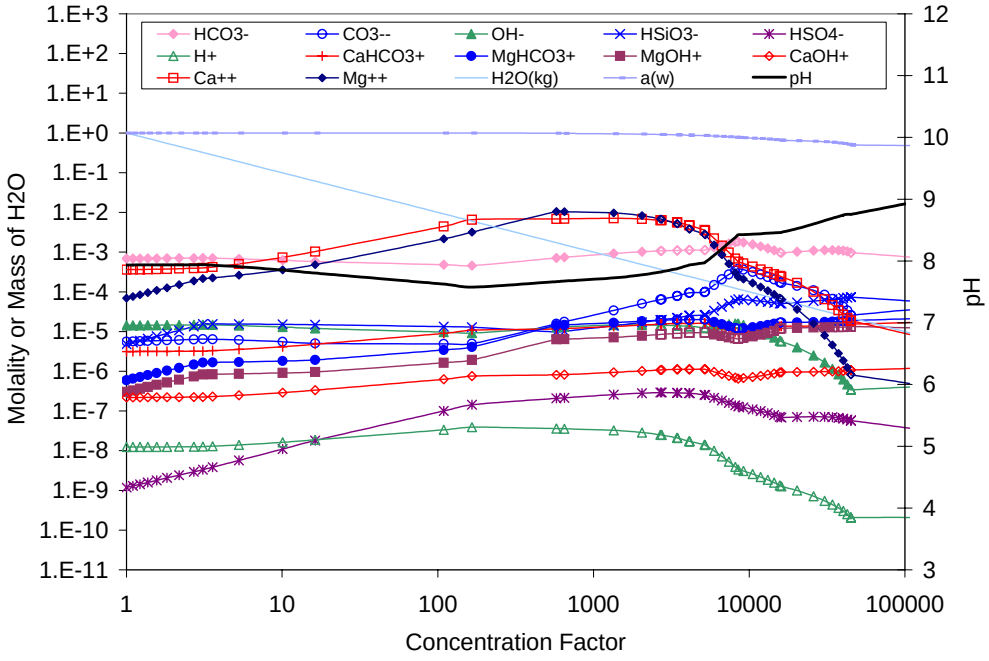

DTN: MO0310SPADLALT.001

Figure 6.10-16. The Predicted Concentrations of ANC Species During Evaporative Evolution of Dust Leachate Bin 5 Water at 70ºC and 10^{-3} Bar CO_2 Fugacity. Plotted Versus Concentration Factor.

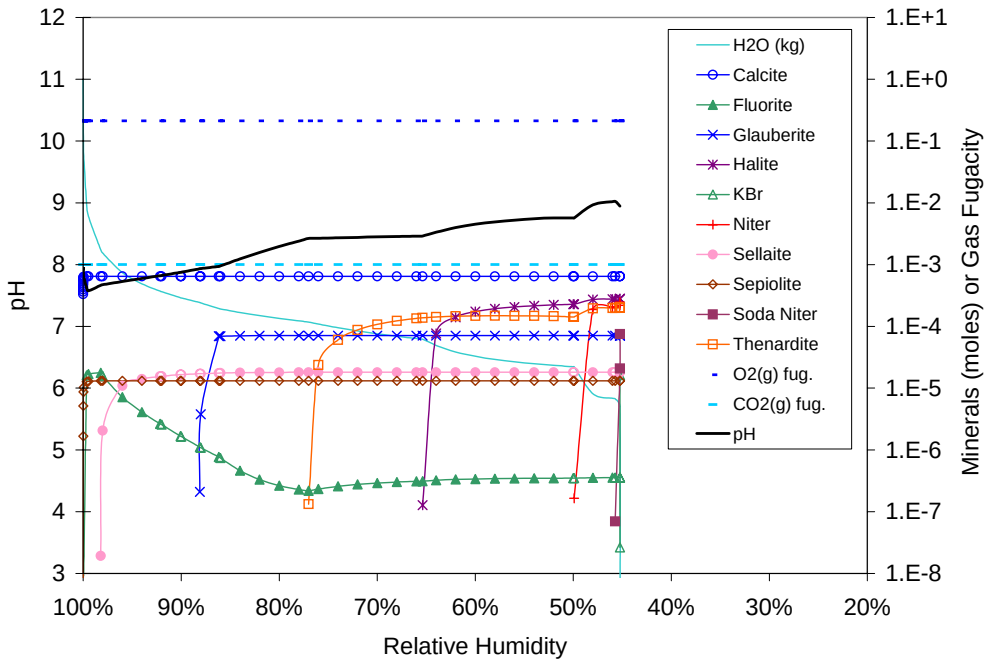

DTN: MO0310SPADLALT.001

Figure 6.10-17. Predicted Mineral Precipitation as Dust Leachate Bin 5 Waters Evaporate at 70°C and 10^{-3} Bar CO_2 Fugacity, Plotted Versus Relative Humidity

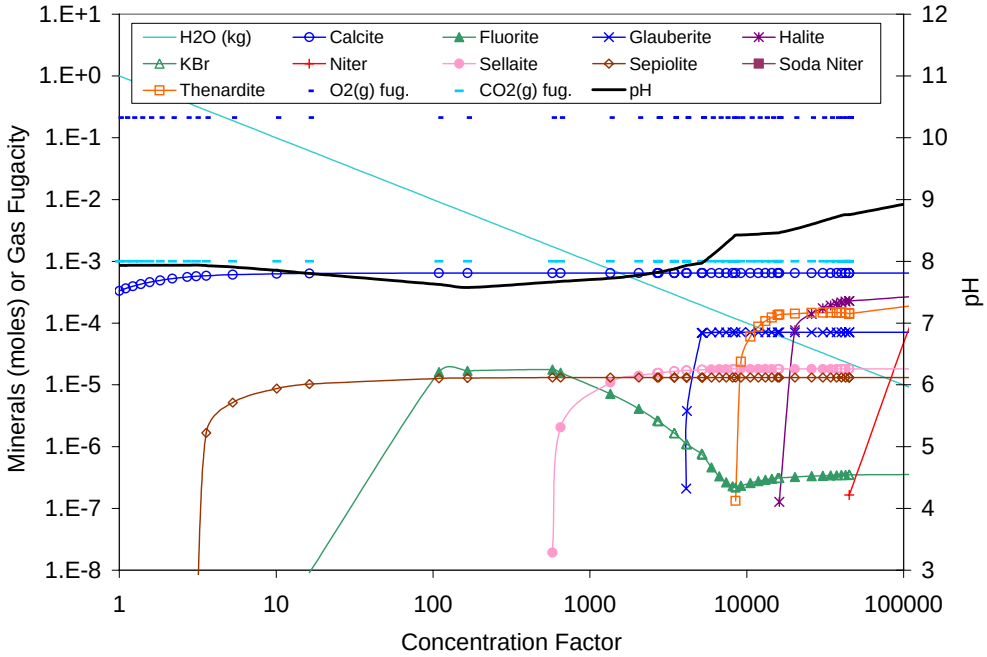

DTN: MO0310SPADLALT.001

Figure 6.10-18. Predicted Mineral Precipitation as Dust Leachate Bin 5 Waters Evaporate at 70°C and 10^{-3} Bar CO_2 Fugacity, Plotted Versus Concentration Factor

6.11 ALTERNATE CONCEPTUAL MODELS

Within the P&CE model, several sub-models are discussed and developed. Three alternate conceptual models were investigated, as discussed in the following subsections. The remaining alternative conceptual models for several sub-models in this document are screened out for the following three reasons:

- **In-Drift Gas**–The in-drift gas abstraction is consistent with the chemistry of the incoming seepage compositions as provided by the *Drift-Scale Coupled Processes (DST and THC Seepage) Models* (BSC 2003 [DIRS 162050], see Sections 4.1.3, 6.6, and 6.7 of this report)). For a discussion of alternative models of THC processes, see Section 6.3 of the THC seepage model. Analyses have shown that the repository is likely to remain an oxygen-rich environment throughout the repository lifetime (see Section 6.7).

- **Dust Deliquescence**–A decision was made to develop this sub-model to be consistent with both the THC seepage model and in-drift gas abstractions (see Sections 6.6, 6.7, 6.9, and 6.10). Because the in-drift precipitates/salts model (IDPS) is the primary analysis tool for investigating both in-drift deliquescence and seepage evaporation, for further discussion of alternative conceptual models concerning the use of the IDPS model are provided in the IDPS model report (BSC 2003 [DIRS 162529]).

- **Seepage/Introduced Materials Interactions**–Results of the abstracted model for 316L stainless steel indicate that the impacts to crown seepage chemistry from introduced materials are minimal (see Section 6.8). The interactions with materials such as carbon steel have not been investigated because of expected short corrosion lifetime of these materials (see Section 6.4). Interactions with Alloy-22 and titanium have not been investigated due to the limited potential for interaction with seepage waters because of extremely low corrosion rates (see Section 6.4).

6.11.1 Alternative Binning of Seepage

This alternate model discusses the abstraction of THC seepage waters based on clustering the waters by their identity and amount of precipitated carbonates, chlorides, nitrates, and sulfates present upon evaporation to dryness, rather than binning by aqueous elemental concentrations. Results of the alternate conceptual model are summarized in Section 6.11.2. The effectiveness of each approach was evaluated using the standard deviation as a percent of the mean (the coefficient of variation) for each bin. The mean value of the coefficient of variation is lower for the aqueous binning case for the pH and for the five solutes Ca, F, N, S, and Si, and is lower for the mineral clustering for the six solutes Al, C, Cl, K, Mg, and Na.

However, pH, Ca, N, and Cl are of primary importance when evaluating and determining corrosive properties and corrosion rates for the TSPA-LA. Aqueous binning gives a lower uncertainty (mean coefficient of variation) for all of these except Cl. Furthermore, the mean coefficient of variation for Cl in aqueous binning is only 0.24 percent higher than for mineral clustering (Table 6.11-7). Additionally, F and S can be inhibitors or enhancers of corrosion and it is desirable to have the least amount of uncertainty for these species, as with pH, Ca, N, and Cl. Aqueous binning gives less uncertainty (mean coefficient of variation) for both F and S.

Based on these findings it has been decided that aqueous binning will be used in the P&CE model.

In this alternate THC seepage model abstraction methodology, the output mineralogy extracted from the EQ6 calculation runs (Table 6.6-1) is used, instead of binning based on aqueous chemistry as discussed in Sections 6.6.4 and 6.6.5. The "normalized" mineral assemblages are used to classify or define a group of resulting output waters. The approach presented below relies entirely on the statistical analysis of the "normalized" output without considering any other geochemical parameters. If successful, the statistically-based model will analytically determine the best binning criteria to use for defining the bins. However, the intra-bin variances produced using this alternate method are generally larger than those reported in Section 6.6, so this alternate binning model will not be used.

In the analysis outlined in the following subsection, two terms are frequently used: bins and clusters. A bin is defined as a group of THC model output waters with similar physical/chemical characteristics (listed in Section 6.6.4), which appear to be from related geochemical groups, as determined by chemical divides or mineralogy of precipitates. A cluster is defined as "a group of THC model precipitated minerals," which is not chosen by physical/chemical criteria (as in "binning") but is instead chosen using "cluster analysis" in the Statistica 5.1 software.

6.11.1.1 Clustering Based on Mineralogy

The analysis begins by taking the mineral data from each EQ3/6 output from the *EBS THC Seepage Binning Abstraction REV 4.xls* spreadsheet developed in Section 6.6.4 and archived in DTN: MO0310SPAEBSCB.003. For abstraction purposes, only data from the carbonate, chloride, nitrate, and sulfate phases are used; the silicate and fluoride minerals are excluded from the clustering investigation. The mineral phases used for the clustering case are:

- anhydrite ($CaSO_4$)
- arcanite (K_2SO_4)
- calcite ($CaCO_3$)
- darapskite ($Na_3NO_3SO_4 \cdot H_2O$)
- glauberite ($Na_2Ca(SO_4)_2$)
- halite ($NaCl$)
- nahcolite ($NaHCO_3$)
- natrite (Na_2CO_3)
- niter (KNO_3)
- pentasalt ($K_2SO_4 \bullet 5CaSO_4 \cdot H_2O$)
- thenardite (Na_2SO_4)
- trona ($Na_3HCO_3CO_3 \cdot H_2O$)

Values for all of the selected minerals (moles precipitated) are cut and pasted from EBS THC Seepage Binning Abstraction REV 4.xls spreadsheet into a Statistica 5.1 main data file/spreadsheet, which is named NewQminbin.STA (archived in DTN: MO0310SPAPCEAC.002). This is the main data file from which the cluster analysis is developed. This data is binned using a "K-means cluster analysis." In cluster sampling, clusters

of individual units are chosen at random, and all units in the chosen clusters are measured (Gilbert 1987 [DIRS 163705] page 23). In a K-means cluster analysis, the user is allowed to select the number of clusters to form. Eleven clusters have been chosen for the model simply because 11 bins are used in the aqueous binning abstraction, thus a more direct comparison can be made between the uncertainty of the solute concentrations (including pH) in the waters of the 11 bins within the aqueous abstraction with the uncertainty of the solute concentration in the waters of each of the 11 clusters comprising the mineral abstraction. For the cluster analysis, output data is saved in Statistica 5.1 files (Table 6.11-1). All 368 waters (called case numbers by Statistica 5.1) from the EBS THC Seepage Binning Abstraction REV 4.xls are assigned a cluster (1-11) by cluster analysis in Statistica 5.1. For each specified cluster, case numbers are determined by checking the Statistica 5.1 output files WATERS OF CLUSTER NO 1.SCR to WATERS OF CLUSTER NO 11.SCR (archived in DTN: MO0310SPAPCEAC.002). The statistics mean and standard deviation are then calculated for each solute concentration and pH to determine the uncertainty for each cluster (see New Mineral Binning Stats2.xls). These uncertainties are then compared to the uncertainty of the 11-bin aqueous abstraction by determining the mean coefficient of variation for both the mineral clustering and aqueous binning for each solute and pH (see Tables 6.11-3 to 6.11-14). The associated precipitated minerals (excluding silicates and fluorides) for each of the 11 clusters are given in Table 6.11-2.

Table 6.11-1. Statistica 5.1 Files Saved from Generated Data

11-Cluster Model
NewQminbin.STA
WATERS OF CLUSTER NO 1.SCR to *WATERS OF CLUSTER NO 11.SCR*

Source: DTN: MO0310SPAPCEAC.002

6.11.1.2 Results

Results shown in Tables 6.11-3 to 6.11-14 indicate that the coefficients of variation are lower for aqueous binning in 6 cases and lower for mineral clustering in 6 cases. The mean value of the coefficients of variation is smaller for the solute species Ca, F, N, S, Si, and pH in the 11-bin aqueous abstraction. The mean value of the coefficient of variations is smaller for Al, C, Cl, K, Mg, and Na for the 11-cluster mineral case. On the basis of these results, where pH, Ca, N, F, and S uncertainties (mean coefficient of variations) are lower for the aqueous binning case and the Cl uncertainty (mean coefficient of variation) is very similar, the mineral clustering approach has been discarded in favor of the aqueous composition binning approach. However, because the results are similar, the alternative method corroborates the chosen method.

Table 6.11-2. Clusters 1-11 with Associated Minerals

Mineral	Cluster 1	Cluster 2	Cluster 3	Cluster 4	Cluster 5	Cluster 6	Cluster 7	Cluster 8	Cluster 9	Cluster 10	Cluster 11
Anhydrite	-	-	-	-	-	-	-	X	-	-	-
Arcanite	X	X	-	-	-	X	X	-	X	X	X
Calcite	-	-	X	-	X	X	-	X	X	-	X
Darapskite	-	-	-	-	-	-	-	-	-	-	X
Glauberite	-	-	-	-	-	X	-	X	-	-	-
Halite	X	-	X	-	-	X	X	X	X	-	X
Nahcolite	-	X	-	-	-	X	X	-	X	-	X
Natrite	-	X	X	X	X	X	X	-	-	X	-
Niter	-	-	-	-	-	-	-	-	-	-	X
Pentasalt	-	-	-	-	-	-	-	X	-	-	-
Thenardite	X	X	X	-	X	X	X	-	X	X	X
Trona	X	-	-	-	-	-	-	-	-	X	-

Source: DTN: MO0310SPAPCEAC.002; Filename: *New Mineral Binning Stats2.xls*

Table 6.11-3. pH Statistics for Mineral Clustering and Aqueous Binning

pH by Mineral Clustering					pH by Aqueous Binning				
Cluster	**Waters (n)**	**Mean**	**Standard Deviation**	**% Coefficient of Variation**	**Bin**	**Waters (n)**	**Mean**	**Standard Deviation**	**% Coefficient of Variation**
Cluster 1	4	9.09	0.02	0.26	Bin 1	5	5.62	0.08	1.35
Cluster 2	6	9.27	0.19	2.10	Bin 2	13	5.66	0.11	1.91
Cluster 3	80	9.15	0.17	1.88	Bin 3	12	5.89	0.24	4.14
Cluster 4	12	9.23	0.22	2.43	Bin 4	43	7.05	0.34	4.80
Cluster 5	32	9.24	0.18	1.97	Bin 5	27	7.64	0.29	3.82
Cluster 6	45	8.22	0.78	9.54	Bin 6	8	9.05	0.37	4.04
Cluster 7	24	8.86	0.10	1.15	Bin 7	25	8.74	0.16	1.81
Cluster 8	73	6.51	0.71	10.84	Bin 8	22	8.61	0.14	1.63
Cluster 9	36	8.70	0.19	2.15	Bin 9	58	9.13	0.22	2.36
Cluster 10	46	9.29	0.18	1.97	Bin 10	10	8.79	0.10	1.17
Cluster 11	10	8.67	0.15	1.77	Bin 11	145	9.21	0.19	2.05
Mean				3.28	Mean				2.64

Source: DTN: MO0310SPAPCEAC.002; Filename: *New Mineral Binning Stats2.xls*

Table 6.11-4. Al Statistics for Mineral Clustering and Aqueous Binning

Al by Mineral Clustering (Moles/Kg.H_2O)					Al by Aqueous Binning (Moles/Kg.H_2O)				
Cluster	**Waters (n)**	**Mean**	**Standard Deviation**	**% Coefficient of Variation**	**Bin**	**Waters (n)**	**Mean**	**Standard Deviation**	**% Coefficient of Variation**
Cluster 1	4	2.13E-14	1.62E-15	7.57	Bin 1	5	3.26E-12	2.22E-13	6.81
Cluster 2	6	1.22E-13	6.49E-14	53.13	Bin 2	13	2.52E-12	7.15E-13	28.36
Cluster 3	80	1.25E-13	6.43E-14	51.52	Bin 3	12	1.15E-12	9.64E-13	83.90
Cluster 4	12	9.96E-12	3.34E-11	335.89	Bin 4	43	3.28E-13	2.78E-13	84.62
Cluster 5	32	1.31E-13	7.11E-14	54.46	Bin 5	27	1.66E-13	8.09E-14	48.63
Cluster 6	45	1.61E-13	1.04E-13	64.81	Bin 6	8	1.10E-13	9.15E-14	83.18
Cluster 7	24	1.51E-14	1.09E-14	71.83	Bin 7	25	4.11E-15	1.08E-15	26.19
Cluster 8	73	1.05E-12	1.15E-12	108.82	Bin 8	22	1.33E-15	6.66E-16	50.25
Cluster 9	36	4.05E-15	2.59E-15	64.06	Bin 9	58	2.18E-12	1.52E-11	698.63
Cluster 10	46	9.54E-14	3.23E-14	33.90	Bin 10	10	9.78E-15	3.33E-15	34.06
Cluster 11	10	6.92E-16	4.62E-18	0.67	Bin 11	145	1.00E-13	4.21E-14	41.88
Mean				76.97	Mean				107.87

Source: DTN: MO0310SPAPCEAC.002; Filename: *New Mineral Binning Stats2.xls*

Table 6.11-5. C Statistics for Mineral Clustering and Aqueous Binning

C by Mineral Clustering (Moles/Kg.H_2O)					C by Aqueous Binning (Moles/Kg.H_2O)				
Cluster	**Waters (n)**	**Mean**	**Standard Deviation**	**% Coefficient of Variation**	**Bin**	**Waters (n)**	**Mean**	**Standard Deviation**	**% Coefficient of Variation**
Cluster 1	4	1.15E+00	9.50E-03	0.82	Bin 1	5	5.37E-04	8.67E-05	16.15
Cluster 2	6	1.32E+00	1.58E-01	11.95	Bin 2	13	6.04E-04	1.52E-04	25.12
Cluster 3	80	1.13E+00	4.41E-02	3.89	Bin 3	12	5.02E-04	1.84E-04	36.55
Cluster 4	12	1.29E+00	8.25E-02	6.40	Bin 4	43	5.04E-04	3.15E-04	62.43
Cluster 5	32	1.19E+00	1.71E-01	14.37	Bin 5	27	2.81E-03	5.84E-03	208.21
Cluster 6	45	2.62E-01	3.86E-01	147.17	Bin 6	8	5.07E-01	2.52E-01	49.71
Cluster 7	24	6.63E-01	2.85E-01	42.98	Bin 7	25	3.71E-01	1.06E-01	28.50
Cluster 8	73	5.24E-04	2.62E-04	50.02	Bin 8	22	2.08E-01	3.28E-02	15.82
Cluster 9	36	3.57E-01	1.68E-01	46.98	Bin 9	58	1.10E+00	2.12E-01	19.33
Cluster 10	46	1.25E+00	1.34E-01	10.72	Bin 10	10	4.03E-01	7.77E-02	19.26
Cluster 11	10	1.92E-01	3.64E-02	18.93	Bin 11	145	1.18E+00	1.35E-01	11.43
Mean				32.20	Mean				44.77

Source: DTN: MO0310SPAPCEAC.002; Filename: *New Mineral Binning Stats2.xls*

Table 6.11-6. Ca Statistics for Mineral Clustering and Aqueous Binning

Ca by Mineral Clustering (Moles/Kg.H_2O)					Ca by Aqueous Binning (Moles/Kg.H_2O)				
Cluster	**Waters (n)**	**Mean**	**Standard Deviation**	**% Coefficient of Variation**	**Bin**	**Waters (n)**	**Mean**	**Standard Deviation**	**% Coefficient of Variation**
Cluster 1	4	2.69E-06	4.98E-08	1.85	Bin 1	5	3.66E+00	2.88E-01	7.87
Cluster 2	6	2.49E-06	1.23E-07	4.93	Bin 2	13	2.37E+00	2.75E-01	11.63
Cluster 3	80	4.25E-06	2.15E-06	50.58	Bin 3	12	1.12E+00	4.24E-01	37.87
Cluster 4	12	2.60E-06	1.28E-07	4.91	Bin 4	43	2.63E-03	6.45E-04	24.54
Cluster 5	32	3.00E-06	1.26E-06	42.04	Bin 5	27	8.20E-04	1.72E-04	20.97
Cluster 6	45	4.95E-04	4.24E-04	85.51	Bin 6	8	8.31E-06	5.58E-07	6.72
Cluster 7	24	1.21E-06	7.20E-07	59.66	Bin 7	25	9.88E-06	7.70E-07	7.80
Cluster 8	73	8.58E-01	1.20E+00	140.33	Bin 8	22	1.15E-05	1.38E-06	11.97
Cluster 9	36	1.03E-05	1.22E-06	11.81	Bin 9	58	3.33E-06	1.98E-06	59.49
Cluster 10	46	2.62E-06	1.07E-07	4.09	Bin 10	10	5.46E-07	1.55E-07	28.40
Cluster 11	10	1.16E-05	1.75E-06	15.10	Bin 11	145	3.51E-06	1.81E-06	51.66
Mean				38.25	Mean				24.45

Source: DTN: MO0310SPAPCEAC.002; Filename: *New Mineral Binning Stats2.xls*

Table 6.11-7. Cl Statistics for Mineral Clustering and Aqueous Binning

Cl by Mineral Clustering (Moles/Kg.H_2O)					Cl by Aqueous Binning (Moles/Kg.H_2O)				
Cluster	**Waters (n)**	**Mean**	**Standard Deviation**	**% Coefficient of Variation**	**Bin**	**Waters (n)**	**Mean**	**Standard Deviation**	**% Coefficient of Variation**
Cluster 1	4	6.22E+00	5.48E-01	8.81	Bin 1	5	8.14E+00	9.19E-01	11.29
Cluster 2	6	6.27E+00	4.92E-01	7.85	Bin 2	13	7.93E+00	6.77E-01	8.53
Cluster 3	80	6.29E+00	7.83E-01	12.46	Bin 3	12	8.30E+00	4.04E-01	4.87
Cluster 4	12	5.31E+00	2.23E-01	4.21	Bin 4	43	6.32E+00	1.87E+00	29.57
Cluster 5	32	6.03E+00	7.74E-01	12.82	Bin 5	27	7.63E+00	3.23E-01	4.24
Cluster 6	45	6.81E+00	1.46E+00	21.44	Bin 6	8	6.08E+00	1.65E+00	27.07
Cluster 7	24	5.84E+00	6.45E-01	11.04	Bin 7	25	5.68E+00	5.03E-01	8.85
Cluster 8	73	7.06E+00	1.73E+00	24.50	Bin 8	22	4.67E+00	7.31E-01	15.67
Cluster 9	36	5.70E+00	3.70E-01	6.50	Bin 9	58	5.27E+00	6.09E-01	11.56
Cluster 10	46	6.40E+00	4.48E-01	7.00	Bin 10	10	5.42E+00	4.98E-01	9.19
Cluster 11	10	4.21E+00	7.41E-01	17.62	Bin 11	145	6.56E+00	3.93E-01	5.99
Mean				12.20	Mean				12.44

Source: DTN: MO0310SPAPCEAC.002; Filename: *New Mineral Binning Stats2.xls*

Table 6.11-8. F Statistics for Mineral Clustering and Aqueous Binning

F by Mineral Clustering (Moles/Kg.H_2O)					F by Aqueous Binning (Moles/Kg.H_2O)				
Cluster	**Waters (n)**	**Mean**	**Standard Deviation**	**% Coefficient of Variation**	**Bin**	**Waters (n)**	**Mean**	**Standard Deviation**	**% Coefficient of Variation**
Cluster 1	4	2.24E-01	5.25E-04	0.23	Bin 1	5	6.36E-05	4.18E-06	6.58
Cluster 2	6	2.52E-01	1.47E-02	5.83	Bin 2	13	5.07E-05	3.50E-06	6.89
Cluster 3	80	2.07E-01	4.51E-02	21.77	Bin 3	12	4.23E-05	1.36E-05	32.15
Cluster 4	12	2.44E-01	6.94E-03	2.84	Bin 4	43	7.66E-04	2.50E-04	32.64
Cluster 5	32	2.39E-01	3.27E-02	13.71	Bin 5	27	2.94E-03	3.24E-03	110.06
Cluster 6	45	3.98E-02	5.25E-02	131.75	Bin 6	8	7.83E-02	1.63E-02	20.81
Cluster 7	24	2.17E-01	9.52E-03	4.39	Bin 7	25	4.49E-02	1.15E-02	25.59
Cluster 8	73	4.71E-04	4.03E-04	85.49	Bin 8	22	2.26E-02	4.79E-03	21.18
Cluster 9	36	4.24E-02	1.91E-02	45.01	Bin 9	58	2.19E-01	4.11E-02	18.82
Cluster 10	46	2.51E-01	1.25E-02	4.99	Bin 10	10	2.09E-01	2.71E-03	1.30
Cluster 11	10	1.89E-02	3.42E-03	18.06	Bin 11	145	2.26E-01	4.22E-02	18.71
Mean				30.37	Mean				26.79

Source: DTN: MO0310SPAPCEAC.002; Filename: *New Mineral Binning Stats2.xls*

Table 6.11-9. K Statistics for Mineral Clustering and Aqueous Binning

K by Mineral Clustering (Moles/Kg.H_2O)					K by Aqueous Binning (Moles/Kg.H_2O)				
Cluster	**Waters (n)**	**Mean**	**Standard Deviation**	**% Coefficient of Variation**	**Bin**	**Waters (n)**	**Mean**	**Standard Deviation**	**% Coefficient of Variation**
Cluster 1	4	4.01E+00	3.04E-02	0.76	Bin 71	5	3.11E-01	1.13E-01	36.29
Cluster 2	6	4.74E+00	7.92E-01	16.70	Bin 2	13	9.75E-01	3.32E-01	34.08
Cluster 3	80	3.62E+00	2.42E-01	6.69	Bin 3	12	3.07E+00	9.15E-01	29.78
Cluster 4	12	5.06E+00	5.35E-01	10.58	Bin 4	43	5.38E+00	9.45E-01	17.57
Cluster 5	32	3.94E+00	4.02E-01	10.19	Bin 5	27	4.69E+00	6.75E-02	1.44
Cluster 6	45	4.33E+00	5.96E-01	13.76	Bin 6	8	4.05E+00	6.66E-01	16.44
Cluster 7	24	4.39E+00	2.35E-01	5.35	Bin 7	25	4.85E+00	2.40E-01	4.96
Cluster 8	73	3.87E+00	2.13E+00	54.99	Bin 8	22	4.61E+00	6.63E-01	14.39
Cluster 9	36	4.94E+00	2.16E-01	4.37	Bin 9	58	4.03E+00	8.45E-01	20.99
Cluster 10	46	4.31E+00	2.15E-01	4.98	Bin 10	10	4.59E+00	4.66E-02	1.02
Cluster 11	10	4.05E+00	5.89E-01	14.53	Bin 11	145	3.98E+00	3.30E-01	8.30
Mean				12.99	Mean				16.84

Source: DTN: MO0310SPAPCEAC.002; Filename: *New Mineral Binning Stats2.xls*

Table 6.11-10. Mg Statistics for Mineral Clustering and Aqueous Binning

Mg by Mineral Clustering (Moles/Kg.H_2O)					Mg by Aqueous Binning (Moles/Kg.H_2O)				
Cluster	**Waters (n)**	**Mean**	**Standard Deviation**	**% Coefficient of Variation**	**Bin**	**Waters (n)**	**Mean**	**Standard Deviation**	**% Coefficient of Variation**
Cluster 1	4	2.20E-07	1.89E-08	8.56	Bin 1	5	8.38E-04	3.55E-04	42.40
Cluster 2	6	6.95E-08	9.94E-08	143.07	Bin 2	13	1.39E-03	5.87E-04	42.27
Cluster 3	80	6.28E-08	6.17E-08	98.31	Bin 3	12	1.30E-03	7.39E-04	57.05
Cluster 4	12	6.70E-08	8.30E-08	123.87	Bin 4	43	2.16E-05	8.23E-05	381.32
Cluster 5	32	4.87E-08	6.35E-08	130.48	Bin 5	27	2.09E-06	2.37E-06	113.35
Cluster 6	45	1.36E-06	2.06E-06	151.46	Bin 6	8	1.66E-07	1.91E-07	115.42
Cluster 7	24	4.21E-07	8.96E-08	21.30	Bin 7	25	1.26E-06	5.78E-07	45.93
Cluster 8	73	5.30E-04	7.37E-04	139.01	Bin 8	22	2.72E-06	1.21E-06	44.52
Cluster 9	36	1.67E-06	1.05E-06	62.59	Bin 9	58	1.16E-07	1.65E-07	141.39
Cluster 10	46	5.50E-08	6.03E-08	109.72	Bin 10	10	4.30E-07	8.62E-08	20.03
Cluster 11	10	2.80E-06	1.45E-06	51.55	Bin 11	145	7.29E-08	8.18E-08	112.26
Mean				94.54	Mean				101.45

Source: DTN: MO0310SPAPCEAC.002; Filename: *New Mineral Binning Stats2.xls*

Table 6.11-11. N Statistics for Mineral Clustering and Aqueous Binning

N by Mineral Clustering (Moles/Kg.H_2O)					N by Aqueous Binning (Moles/Kg.H_2O)				
Cluster	**Waters (n)**	**Mean**	**Standard Deviation**	**% Coefficient of Variation**	**Bin**	**Waters (n)**	**Mean**	**Standard Deviation**	**% Coefficient of Variation**
Cluster 1	4	1.01E+00	8.44E-01	83.35	Bin 1	5	8.88E-01	1.05E+00	118.66
Cluster 2	6	8.46E-01	6.79E-01	80.26	Bin 2	13	1.16E+00	8.35E-01	72.23
Cluster 3	80	1.22E+00	1.22E+00	99.31	Bin 3	12	1.25E+00	5.58E-01	44.56
Cluster 4	12	2.25E+00	9.52E-02	4.24	Bin 4	43	4.76E+00	2.79E+00	58.72
Cluster 5	32	1.32E+00	9.88E-01	74.85	Bin 5	27	1.28E+00	5.63E-01	43.89
Cluster 6	45	2.02E+00	1.92E+00	95.30	Bin 6	8	2.55E+00	2.73E+00	106.79
Cluster 7	24	2.25E+00	1.15E+00	51.00	Bin 7	25	3.00E+00	8.14E-01	27.17
Cluster 8	73	3.28E+00	2.83E+00	86.25	Bin 8	22	4.37E+00	1.43E+00	32.69
Cluster 9	36	2.93E+00	6.74E-01	23.00	Bin 9	58	2.70E+00	9.15E-01	33.89
Cluster 10	46	5.13E-01	7.58E-02	14.78	Bin 10	10	3.22E+00	8.54E-01	26.50
Cluster 11	10	4.78E+00	1.92E+00	40.21	Bin 11	145	5.71E-01	1.52E-01	26.63
Mean				59.32	Mean				53.79

Source: DTN: MO0310SPAPCEAC.002; Filename: *New Mineral Binning Stats2.xls*

Table 6.11-12. Na Statistics for Mineral Clustering and Aqueous Binning

Na by Mineral Clustering (Moles/Kg.H_2O)					Na by Aqueous Binning (Moles/Kg.H_2O)				
Cluster	**Waters (n)**	**Mean**	**Standard Deviation**	**% Coefficient of Variation**	**Bin**	**Waters (n)**	**Mean**	**Standard Deviation**	**% Coefficient of Variation**
Cluster 1	4	6.94E+00	3.21E-01	4.62	Bin 1	5	1.41E+00	5.00E-01	35.51
Cluster 2	6	6.75E+00	1.94E-01	2.87	Bin 2	13	3.38E+00	4.13E-01	12.21
Cluster 3	80	7.58E+00	6.74E-01	8.89	Bin 3	12	4.24E+00	3.22E-01	7.60
Cluster 4	12	6.97E+00	2.52E-01	3.61	Bin 4	43	6.47E+00	1.69E+00	26.14
Cluster 5	32	7.44E+00	5.08E-01	6.83	Bin 5	27	6.28E+00	2.39E-01	3.80
Cluster 6	45	7.00E+00	1.19E+00	17.02	Bin 6	8	7.38E+00	1.52E+00	20.58
Cluster 7	24	7.00E+00	4.38E-01	6.25	Bin 7	25	6.97E+00	4.96E-01	7.12
Cluster 8	73	5.21E+00	2.10E+00	40.43	Bin 8	22	8.02E+00	9.77E-01	12.19
Cluster 9	36	6.95E+00	2.89E-01	4.16	Bin 9	58	7.82E+00	9.65E-01	12.35
Cluster 10	46	6.87E+00	9.80E-02	1.43	Bin 10	10	7.26E+00	4.34E-01	5.97
Cluster 11	10	8.60E+00	1.10E+00	12.84	Bin 11	145	7.08E+00	2.61E-01	3.69
Mean				9.90	Mean				13.38

Source: DTN: MO0310SPAPCEAC.002; Filename: *New Mineral Binning Stats2.xls*

Table 6.11-13. S Statistics for Mineral Clustering and Aqueous Binning

S by Mineral Clustering (Moles/Kg.H_2O)					S by Aqueous Binning (Moles/Kg.H_2O)				
Cluster	**Waters (n)**	**Mean**	**Standard Deviation**	**% Coefficient of Variation**	**Bin**	**Waters (n)**	**Mean**	**Standard Deviation**	**% Coefficient of Variation**
Cluster 1	4	6.75E-01	3.00E-02	4.44	Bin 1	5	1.89E-03	1.27E-04	6.74
Cluster 2	6	7.49E-01	7.25E-02	9.67	Bin 2	13	1.90E-03	1.29E-04	6.80
Cluster 3	80	6.26E-01	9.53E-03	1.52	Bin 3	12	2.58E-03	1.76E-03	68.27
Cluster 4	12	8.53E-01	3.60E-02	4.22	Bin 4	43	3.84E-01	9.58E-02	24.93
Cluster 5	32	7.07E-01	8.02E-02	11.34	Bin 5	27	1.03E+00	2.83E-02	2.76
Cluster 6	45	9.64E-01	1.98E-01	20.57	Bin 6	8	8.59E-01	4.38E-02	5.10
Cluster 7	24	9.59E-01	1.97E-01	20.49	Bin 7	25	1.24E+00	1.17E-01	9.43
Cluster 8	73	2.27E-01	2.03E-01	89.31	Bin 8	22	1.62E+00	2.38E-01	14.65
Cluster 9	36	1.31E+00	2.31E-01	17.58	Bin 9	58	7.45E-01	1.07E-01	14.34
Cluster 10	46	7.79E-01	3.47E-02	4.45	Bin 10	10	1.16E+00	1.02E-01	8.77
Cluster 11	10	1.67E+00	3.47E-01	20.78	Bin 11	145	6.91E-01	7.68E-02	11.12
Mean				18.58	Mean				15.72

Source: DTN: MO0310SPAPCEAC.002; Filename: *New Mineral Binning Stats2.xls*

Table 6.11-14. Si Statistics for Mineral Clustering and Aqueous Binning

Si by Mineral Clustering (Moles/Kg.H_2O)					Si by Aqueous Binning (Moles/Kg.H_2O)				
Cluster	**Waters (n)**	**Mean**	**Standard Deviation**	**% Coefficient of Variation**	**Bin**	**Waters (n)**	**Mean**	**Standard Deviation**	**% Coefficient of Variation**
Cluster 1	4	3.63E-02	2.00E-03	5.51	Bin 1	5	1.42E-03	1.86E-04	13.14
Cluster 2	6	1.30E-01	9.81E-02	75.67	Bin 2	13	2.26E-03	3.16E-04	13.97
Cluster 3	80	9.13E-02	4.71E-02	51.61	Bin 3	12	2.33E-03	5.22E-04	22.40
Cluster 4	12	1.18E-01	7.69E-02	65.12	Bin 4	43	3.49E-03	1.26E-03	35.96
Cluster 5	32	1.13E-01	4.84E-02	42.83	Bin 5	27	6.08E-03	3.95E-03	65.00
Cluster 6	45	4.61E-02	7.57E-02	164.06	Bin 6	8	7.71E-02	7.78E-02	100.86
Cluster 7	24	1.79E-02	7.77E-03	43.28	Bin 7	25	9.58E-03	4.00E-03	41.72
Cluster 8	73	2.94E-03	1.21E-03	41.25	Bin 8	22	4.16E-03	1.18E-03	28.36
Cluster 9	36	8.95E-03	5.51E-03	61.58	Bin 9	58	1.03E-01	7.03E-02	67.99
Cluster 10	46	1.12E-01	5.92E-02	52.71	Bin 10	10	1.07E-02	2.49E-03	23.16
Cluster 11	10	3.50E-03	1.04E-03	29.69	Bin 11	145	9.70E-02	5.56E-02	57.33
Mean				57.57	Mean				42.72

Source: DTN: MO0310SPAPCEAC.002; Filename: *New Mineral Binning Stats2.xls*

6.11.2 Transport Affected Salt Assemblages

At some point during the repository cooldown, there may be seepage onto the drip shield or waste package surfaces. These surfaces are at a higher temperature than the seepage source on the drift wall and therefore evaporation of the seepage water will occur. At some point, the evaporation rate, as compared to the seepage rate, will slow and allow accumulated liquid to travel down the surface slope towards the invert. As the water traveling upon the invert surface is undergoing evaporation, a potential for precipitation to occur along the transportation path exists. This precipitation will occur in the same order as that statically modeled within the P&CE (as implemented from the IDPS model). That is, when the traveling water has reached saturation with respect to a mineral phase, that phase will begin to form from that point onward, where the kinetics of its formation will control how much is actually deposited. For the sake of discussion here we are primarily concerned with the potentially deliquescent salt minerals that form with relative rapidity. This leads to a potential fractionation of salt minerals from the top to the bottom of the surface seeing seepage transport, where the highly soluble components in the seepage will be transported from the upper part of the transport path and preferentially redeposited at the lower part of the path.

For the potential crown seepage waters (Section 6.6), this fractionation will initially precipitate the chloride salts as opposed to the nitrates; this is due to the dominance of chloride in seepage and the lower solubility of chloride salts as compared to the nitrate salts. The nitrate-enriched seepage may either precipitate lower down the surface or complete its travel into the invert. The potential results of this process depends upon how future conditions evolve after seepage-salts are deposited:

- If temperature conditions remain constant, and seepage is constant or ceases, then this conceptual fractionation model leads to two results: first, the lowest deliquescent point salts deposited are nitrate-enriched, and will accumulate towards the invert; second, the chloride-dominant salts (primarily halite, NaCl) would be precipitated closer to the point of initial seepage contact. Because the concentration of nitrate is low relative to Cl^- in seepage waters, this is not likely to result in a significant difference in the chemical environment from the P&CE static equilibrium model.

- If the seepage remains constant, or increases, and the surface temperature cools (and *RH* accordingly increases), then the relative evaporation rate will decrease allowing flow to the invert. This will redissolve the more highly soluble salts precipitated on the metal surfaces and transport them to the invert. The less soluble chloride-dominant salts that would have been precipitated higher up on the metal surfaces would also remobilize, this would tend to redistribute the higher chloride salts down the metal surfaces, remixing and redistributing them with previously precipitated nitrate salts. This remixing and redistribution will continue to transport previously precipitated solutes towards the invert. This process should only result in slight deviations in the chemical environment as predicted in the P&CE model.

- If seepage ceases for a long period, then as the temperature cools and the *RH* increases, the salts will eventually deliquesce. Under these conditions the first to deliquesce will be those nitrate-enriched salts that were precipitated closer to the invert, resulting in

nitrate-enriched waters. As temperatures further cool the deliquescence wetting-front will travel up the surface to the more chloride-dominant salts. This could significantly change the local chemical environment from that modeled in the P&CE, as it allows formation of chloride-rich deliquescent brines.

The most likely evolutionary path will proceed from the first case above to the second, with the third not likely to occur because seepage into the drift is predicted to increase through time (BSC 2003 [DIRS 166512], Figure 6.2.2-7b).

6.11.3 Brine Compositions Due to Dust Deliquescence

In the P&CE model, the compositions of brines formed by dust deliquescence are estimated using the IDPS model and a Pitzer-based thermodynamic model generally applicable to bulk solutions. The model does not take into account the effects of surface interactions and interfacial forces, which are likely to be important in the case of dust deliquescence, where the brine volume can be very small, and the corresponding solid:water ratio is very large. Here, the possibility of using alternative conceptual models for modeling deliquescent brine compositions in the dust is examined.

The amounts of soluble anions in the dust (represented in the model by soluble salts) are small (Section 4.1.6), and the volume of brine that is likely to form by dust deliquescence is limited. In the calculated EQ3/6 dust leachate evaporation modeling runs described in Section 6.10, the eutectic point is not reached until the amount of water remaining in the model system is around 10^{-5} kg, or about 10 µL (Figure 6.13-40). Thus, brines forming initially, by deliquescence at the system eutectic, will have a very small volume. Because water compositions in the calculated dust leachate modeling runs represent leachate from a 20-gram aliquot of dust, water/solid ratios in the dust will be on the order of 10 µL/20 g. (This typical amount of water is only that which is associated with crystals of the deliquescent salts, and does not include moisture that is adsorbed on the surfaces of dust grains or held in the micropores by capillarity. The latter occurrences of moisture are considered to have no effect on the corrosion environment and are not further considered.)

At such low solid:water ratios, the brine exists in close proximity to the mineral grains of the dust, so that solid-liquid interface processes may be important. Water in close enough proximity to silicate mineral surfaces tends to be ordered by hydrogen bonding between the molecules and the surface, and has a lower activity than for bulk solution conditions. Capillary effects on the activity of the water may also be significant, depending on the geometry of brine droplets.

The effects previously described serve to lower the activity of water in the dust, without necessarily lowering the solute activities. Thus, the model may overpredict the relative humidity at which particular equilibrium solution conditions occur.

Another unmodeled concept is related to the homogeneity in the dust. The deliquescence calculations in Section 6.10 use homogeneously distributed soluble salt mineral phases in the dust, and presume that all phases are in contact with each other. These salt minerals constitute a minor fraction of the dust, and individual grains of salt minerals must be very small, for homogenous distribution. The grain size and distribution homogeneity of soluble salt minerals in

the dust are not known, which allows the possibility for more chemical heterogeneity in the dust layer than is accommodated in the model.

Finally, in the EBS model for deliquescent brine evolution, brine composition is only a function of the RH and the starting composition. Corrosion reactions are neglected, or, equivalently, consume only water. As the minute volumes of brine are in equilibrium with the atmosphere, the supply of water is relatively infinite. Salt components in the brine are conserved (with respect to corrosion) and they are treated as catalysts rather than reactants. In actuality, some fraction of the salt components will be incorporated into the corrosion products, and, because the total mass of salts (and the volume of brine) is very small, the brine composition may change significantly with time, even at constant RH. This process may be important in limiting the amount of corrosion that could occur due to dust deliquescence, and is currently not implemented in the P&CE model.

INTENTIONALLY LEFT BLANK

6.12 EVALUATION OF KEY UNCERTAINTIES

There are five primary inputs to the EBS P&CE model, and each has uncertainty associated with it. These inputs are the:

- Amounts and characteristics of engineered materials to be placed in the drift (ground support, emplacement rails, etc.). Though there may be minor changes in the mass and composition of the committed materials as the repository design evolves, the largest uncertainty associated with these materials is their potential impact, through corrosion reactions, on the composition of in-drift waters and atmosphere.

- Composition of seepage water entering the drift. A set of potential seepage waters is abstracted from the suite of possible water compositions determined by the *Drift-Scale Coupled Processes (DST and THC Seepage) Models* report (BSC 2003 [DIRS 162050]), and uncertainty in the water compositions is propagated into the P&CE model. Additional uncertainty is associated with the binning process used within the P&CE model to further abstract the water compositions into 11 representative waters.

- Composition of dust that is predicted to settle on the drip shield and waste package, and of the brines that form by deliquescing salt minerals within the dust. As with the seepage waters, the uncertainty in this input is associated with the binning process, in which the possible brines are abstracted into six representative waters.

- *In-Drift Precipitates/Salts Model* (BSC 2003 [DIRS 162529]) and its associated databases (thermodynamic data, modeling assumptions, and other technical information not specific to the site) used in the geochemical modeling of seepage water evaporation and brine formation by dust deliquescence that produces the model output.

- Composition and flux of in-drift gases.

The atmosphere in the drift, in particular the concentration of CO_2, will affect in-drift water compositions.

These inputs are used in the P&CE model to estimate the compositions of potential in-drift waters, which in turn are used in the TSPA-LA to evaluate drip shield and waste package corrosion, radionuclide solubility, and colloid stability. The following five parameters are extracted from the P&CE model output and passed as direct input to the TSPA-LA:

- Chloride ion concentration

- Chloride to nitrate ion molar ratio

- Ionic strength

- pH

- Deliquescence relative humidity—the RH value at which salt minerals in the dust will deliquesce and an aqueous phase forms.

Of the five P&CE model inputs, three have uncertainties that must be propagated into the parameters that are passed to the TSPA-LA: the composition of seepage waters, composition of aqueous solutions that could form due to dust deliquescence, and the in-drift precipitates/salts model. The other two, the composition of the in-drift atmosphere and the engineered materials placed in the drift, have been screened out. . Potential factors affecting composition and flux of in-drift gasses, including corrosion of the committed materials, are evaluated in Sections 6.7. The effects of corrosion are transient; following a short period of oxygen depletion (100–400 years), the repository atmosphere becomes oxidizing and remains so thereafter. Uncertainties in CO_2 concentration are found to be implicitly propagated by the use of the THC seepage inputs as explained in Section 6.12.1. Thus, uncertainties in these inputs are propagated to TSPA-LA feeds by the random selection of the starting water and associated gas composition lookup tables.

The effects of corrosion of engineered materials on water chemistry is evaluated in Section 6.8, and found to be of low consequence. Thus, minor changes in repository design and the amounts of engineered materials have no effect on model uncertainty.

In the following sections, the ranges and distributions of the relevant uncertainties are developed, and implementation guidance is provided for propagating these uncertainties into the TSPA-LA parameter feeds.

6.12.1 Uncertainties and Variabilities in the Inputs from THC Model Calculations

The incoming seepage water and gas composition abstraction presented in Section 6.6 incorporates the range of effects due to uncertainties and variability in the THC model by including all five THC model input water compositions (w0, w4, w5, w6, and w7) in the abstraction. The choice of input water compositions covers the natural variability of pore-water compositions in the repository units, so the relative spread in predicted water compositions, and in the CO_2 partial pressures in equilibrium with them, is in most cases larger than the spread introduced by THC model and model input uncertainties. The *Drift-Scale Coupled Processes (DST and THC Seepage) Models*, (BSC 2003 [DIRS 162050]), offers the following insights:

Sect 1.3 Model Limitations, p. 32:

> "The THC Seepage Model was developed with data for the Tptpmn and Tptpll lithostratigraphic units. Although many aspects of the model are applicable to other host rock units of the repository, differences in the mineralogy, geochemistry, and thermal-hydrological (TH) properties must be considered before the results can be directly applied elsewhere. These differences, however, are expected to be reflected in the range of pore-water compositions input into the model (Section 6.2.2.1), such that results of the THC Seepage Model as a whole (i.e., including the variability introduced by using various input water compositions) could be reasonably applied to other locations within the repository footprint."

6.2.2.1 Initial Pore-Water and Pore-Gas Chemistry, p. 72:

> "The choice of input water composition must also consider the natural variability of pore-water compositions in the repository units. This natural variability is illustrated in Figure 6.2-4."

and p. 74:

> "Given these considerations, initial water compositions were selected for REV02 simulations based on the following criteria:
>
> (1) Capture the spread of pore-water compositions shown on Figure 6.2-3 and include, to the extent practicable, waters that may yield different end-brine compositions…"

6.9.2 Evaluation of Model Result Uncertainty, p. 241:

> "In this study, the spread in predicted concentrations of aqueous species and CO_2 (i.e., Figures 6.8-12–6.8-21 and 6.8-25–6.8-38) is related to:
>
> - The natural variability of input water compositions (Sections 6.2.2.1)
> - The various investigated model conceptualizations (vapor-pressure model, drift location, stratigraphic columns, open versus closed drift wall) (Table 6-1)
> - Ranges of input parameters other than water composition (in this case infiltration rates and CO_2 diffusion coefficients) (Section 6.8.5.3).
>
> The relative spread caused by the variability of input water compositions (computed as standard deviation) is shown as a function of time in Table 6.9-2. This spread is up to around one order of magnitude and in many cases much less. As shown by comparing Figures 6.8-25a–6.8-38a with Figures 6.8-25b–6.8-38b, this spread is, in most cases, larger than the spread introduced by the various model conceptualizations and ranges of other input data considered in the model. Further evaluations of the spread in model result, as it directly ties to uncertainty, will be presented in the upcoming revision of *Abstraction of Drift-Scale Coupled Processes* (CRWMS M&O 2000 [123916])."

Sect 8.1 Modeled Coupled Processes and Uncertainty, p. 338:

> "These THC Seepage Model simulations covered a wide range of the most important uncertainties from the standpoint of model validation, bounding analyses, conservatism, their impact on model results, and their propagation to other models. Based on the natural variability in input water composition and the resulting spread in simulation results, the uncertainties in predicted concentrations of aqueous species and of CO_2 gas are estimated to be up to about one order of

magnitude (Section 6.9.2), with implications for downstream use examined below in Section 8.4."

A follow-on evaluation concerning the THC seepage model results used in this document was conducted (see *Abstraction of Drift-Scale Coupled Processes*, BSC 2003, Section 8.1 [DIRS 164888]). This report evaluates the uncertainties directly associated with the five different input waters and compares them to uncertainties associated with all other factors. This report concludes that the uncertainty associated with the five input waters is generally greater than those of the other evaluated THC seepage model uncertainties.

6.12.2 Uncertainties in the In-Drift Precipitates/Salts Model that Affect Characterization and Binning of Seepage Water Compositions

The in-drift precipitates/salts model is used to predict the changing compositions of potential seepage waters as they evaporatively evolve to concentrated brines (BSC 2003 [DIRS 166031]). The output of this model is a set of lookup tables that describe the chemical compositions of these waters as a function of relative humidity. As relative humidity decreases, the degree of evaporation increases, which in turn causes an increase in the salinities of these waters. The lowest relative humidity predicted by the model corresponds to the deliquescence point (*DRH*) of the water at the specified temperature and fugacity of carbon dioxide. At relative humidity values below this deliquescence point, the brine is no longer stable and only dry salts remain. The output parameters used in TSPA-LA are pH, ionic strength (I), *DRH*, the total concentrations of chloride and nitrate, and the $Cl:NO_3$ ratio. The uncertainty in the values of these output parameters due to model uncertainty is addressed in this section. Model uncertainties result from uncertainties in the conceptual model, model equations, the choice of mineral suppressions, and constraints in the thermodynamic database.

The uncertainty that is readily quantifiable and useful to the TSPA-LA is the uncertainty in the EBS Physical and Chemical Environment model output parameter values for pH, ionic strength, *DRH*, the total concentrations of chloride and nitrate, and the $Cl:NO_3$ ratio. The in-drift precipitates/salts model uncertainty contributes to this, and is determined by comparing in-drift precipitates/salts model evaporation predictions to experimentally measured data.

The overall in-drift precipitates/salts model uncertainty in these outputs is quantified in the *In-Drift Precipitates/Salts Model* (BSC 2003 [DIRS 166031]). They are presented in Table 6.12-1.

The values for *I*, Cl, and $Cl:NO_3$ ratio (as Cl, NO_3 and $Cl:NO_3$ are not independent parameters, only two of these three must be passed to the TSPA-LA) are in units of relative percent difference. The units for pH and *DRH* are standard pH units and standard percent *RH* units, respectively.

Table 6.12-1. Estimated Model Uncertainty Ranges for In-Drift Precipitates/Salts Model Outputs

Parameter	Units	RH Range 100% - 85%	RH Range 85% - 65%	RH Range 65% - 60%	RH Range 60% - 40%	RH Range 40% - 0%
pH	pH units	+/- 1	+/- 1	+/- 1	+/- 2	+/- 2
Ionic Strength	log molal	+/- 0.1	not used[a]	not used[a]	not used[a]	not used[a]
Cl	log molal	+/- 0.0	+/- 0.2	+/- 0.5	+/- 0.7	+/- 0.7
$Cl:NO_3$	log mole ratio	+/- 0.0	+/- 0.2	+/- 0.5	+/- 0.7	+/- 1
DRH.	%RH units	+/- 5%	+/- 10%	+/- 10%	+/- 10%[b]	+/- 15%[c]

Source: DTN: MO0312SPAESMUN.002 [DIRS 166329]

NOTES: These uncertainties are defined as uniform distributions encompassing ~95 percent probability.

Uncertainties between 85 percent RH and 40 percent RH are based primarily on ternary systems involving Na, K, and Ca.

Uncertainties below 40 percent are primarily based on binary and ternary systems involving Mg and Ca.

[a] Prediction of ionic strength is for colloids model. At RH<85 percent, ionic strength exceeds 3 molal, which is far above the critical ionic strength where colloids are stable.

[b] Exceptions:

1. Predicted DRH for $Ca(NO_3)_2$ is 20-25 percent RH units higher than data: error NOT conservative
2. Predictions likely more than 10 percent RH too high for $Mg(NO_3)_2$ at T>100°C: error NOT conservative
3. DRH likely not predicted well for carbonate brines.

[c] Exceptions:

1. Predicted DRH for $Ca(NO_3)_2$ is 20-25 percent RH units higher than data
2. 15% is greater than the established model validation criteria.

6.12.3 Discretization Error Associated with Binning Abstractions

This section examines the uncertainty tied to the binning abstractions for THC seepage (Section 6.12.3.1) and dust leachate (Section 6.12.3.2), where the variability in each of the bins is considered to quantify the largest amount of uncertainty possible within a bin during the evaporative process. The variability is examined at four different relative humidity (or activity of water) conditions: unevaporated, 98 percent, 85 percent, and 65 percent. These four snapshot modeling points represent locations that capture the effects of major chemical divides that may occur, such as the precipitation of calcite and halite. At the four locations along the evaporative pathway, the objective is to see where the variability is greatest within the bin. The largest amount of variability along this pathway is the uncertainty that can be applied to any given parameter on THC seepage or dust leachate chemistry lookup tables. The probability distribution for the within-bin uncertainty is defined to be log-uniform. This designation is conservative because the probability of realizing an extreme value is higher than it is for triangular or normal distributions. A uniform distribution is also generally apparent from Figures 6.6-9 through 6.6-19.

6.12.3.1 THC Seepage Lookup Tables

The bin histories for each water (see Tables 6.6-8 through 6.6-12) were mapped back to the five unevaporated THC seepage model time history chemistries (see Table 6.6-1) in Excel spreadsheet “New Non Evaporated Binning Statistics02.xls” which is archived in DTN: MO0310SPAEBSUE.002. The standard functions of Excel (median, minimum, maximum, standard deviation (s), and 2s (where s is multiplied by 2)) were used to calculate the

statistics. This is done to determine the variability within the bins before the chemistries were evaporated. The variability of the unevaporated waters was not included in estimates of binning variability because it decreases rapidly as the waters are "normalized" by even small degrees of evaporation.

For the 98 percent and 85 percent relative humidity conditions, two Excel spreadsheets entitled "Checked 98% RH EBS THC Seepage Binning Abstraction REV03.xls" and "Checked 85% RH EBS THC Seepage Binning Abstraction REV03.xls" were developed to show the variability of seepage water chemistry due to evaporation to brine water activities corresponding to 98 and 85 percent RH. These spreadsheets and associated EQ6 input and output files are archived in DTN: MO0310SPAEBSSB.002. Recalculating the EQ6 input files listed in Table 6.6-1 at 98 percent and 85 percent relative humidity generates the EQ6 input files used in this calculation. GETEQData software was used to extract the final equilibration results from each output file. Standard Excel functions (median, minimum, maximum, standard deviation (s), and 2s) are used to calculate the statistics to determine the variability within the bins after the chemistries were evaporated. The extracted output variables, found on the "Data & Plots" worksheet in both spreadsheets, include pH, activity of water ($a_w \approx 0.98$ or 0.85), ionic strength (I), and total molalities of the aqueous constituents (Al, C, Ca, Cl, F, K, Mg, N, Na, S, Si). The waters in the "Data & Plots" worksheet are sorted by bin and the chemistries for each of the 11 bins were copied and pasted into separate abstraction bin worksheets. Two standard deviations (2s) are considered reasonable for an estimate of the 95 percent distribution about the mean for normally distributed chemistries. These variability distributions were not used in the calculations below because the values are log normally distributed.

These spreadsheets along with the binning spreadsheet (Final Checked EBS THC Seepage Binning Abstraction REV 4.xls, DTN: MO0310SPAEBSCB.003) documented in Section 6.6.4 were then used as input into a new set of spreadsheets where the parameter data was log transformed so that the statistics would be log normally distributed. These spreadsheets are listed on Table 6.12-2. Within each spreadsheet, statistics for the log-transformed data can be referenced.

Table 6.12-2 Spreadsheets Containing Log Transformed Data and Statistics for Each of the Uncertainty RH Locations Evaluated

RH Location	Spreadsheet Name
98%	checked 98% RH EBS THC Seepage Binning Abstraction REV03 log transform.xls
85%	checked 85% RH EBS THC Seepage Binning Abstraction REV03 Log transform.xls
65%	Final Checked EBS THC Seepage Binning Abstraction REV 4 log transform.xls

Source: DTN: MO0310SPAPCELT.000

A review of the 65 percent RH data indicated that in many instances the uncertainty values were skewed because the evaporative evolution had passed beyond the halite divide, causing larger uncertainty than should be present for the uncertainty caused by bin or lookup table variability. Therefore, only the data from 98 and 85 percent RH were used to develop Tables 6.12-3 and 6.12-4. Table 6.12-3 provides the relative humidity location (e.g., 98 or 85 percent RH) with the most uncertainty (largest 2s value). Only the uncertainties for the parameters of interest to the TSPA-LA are presented in the following tables; uncertainties for all other species of interest can be found in the spreadsheets listed in Table 6.12-2. Ionic Strength is not included in this table as its uncertainty is only considered at 98 percent RH (ionic strength is above 1 M at this RH). This is because the ionic strength values (I) will only be utilized by the TSPA-LA when I is less than 1 M (e.g., for colloid stability modeling, the colloids are unstable when $I > 0.05$ M (BSC 2003 [DIRS 161620], Section 5.11).

Table 6.12-3. Relative Humidity Point with the Most Variability for Bins 1 through 11 for pH, Cl, and $Cl:NO_3$

Species	Bin 1	Bin 2	Bin 3	Bin 4	Bin 5	Bin 6	Bin 7	Bin 8	Bin 9	Bin 10	Bin 11
pH	85	98	85	85	85	98	85	98	98	85	85
Cl	98	98	98	98	98	98	98	98	98	85	98
$Cl:NO_3$*	85/98	85/98	85/98	85/98	85/98	85/98	85/98	85/98	85/98	85/98	85/98

NOTES: Ionic strength was only considered at the 98 percent RH level.

*$Cl:NO_3$ ratio is the same for 85 percent and 98 percent RH.

Given the 2s statistics presented in the spreadsheets on Table 6.12-2 and the RH location where the most variability lies (Table 6.12-3), Table 6.12-4 has been developed to give the uncertainty that can be applied to any given discrete parameter used in the TSPA-LA.

Table 6.12-4. The Error Applied to the THC Seepage Lookup Tables for pH, I, Cl, and $Cl:NO_3$ Based on the RH with the Highest Variability in Bins 1 through 11 (Errors are Based on 2s Values)

Species	Bin 1	Bin 2	Bin 3	Bin 4	Bin 5	Bin 6	Bin 7	Bin 8	Bin 9	Bin 10	Bin 11
±pH	0.13	0.25	0.42	0.65	0.49	0.77	0.28	0.33	0.46	0.12	1.05
±Log I*	0.04	0.06	0.03	0.08	0.07	0.11	0.04	0.04	0.07	0.03	0.05
±Log Cl	0.13	0.10	0.03	0.30	0.13	0.17	0.48	0.50	0.38	0.11	0.43
±Log $Cl:NO_3$	0.92	0.67	0.43	1.10	0.57	0.97	0.56	0.73	0.53	0.75	0.32

Source: DTN: MO0311SPAEPMUT.000

NOTE: *Based on 98 percent RH results only.

6.12.3.2 Dust Leachate Lookup Tables

The statistical data for the 98 percent and 85 percent RH are calculated in a similar manner to the calculations performed in Section 6.12.3.1. Table 6.12-5 lists the spreadsheets and DTN for the EQ6 files that are used to develop the tables. For the unevaporated spreadsheet, the EQ6 output files that are generated for the 65 percent RH condition are also used.

Table 6.12-5. Dust Leachate Variability Calculations at 85 and 98 Percent RH

RH location	Excel File	Location of EQ6 input and output Files
98%	EBS Dust Leachate 98% RH uncert anal.xls	DTN: SN0310T0510102.010, directory /98rh
85%	EBS Dust Leachate 85% RH uncert anal.xls	DTN: SN0310T0510102.010, directory /85rh

Source: DTN: MO0310SPADLBU4.001

Two of these spreadsheets along with the binning spreadsheet (EBS Dust Leachate Binning Abstraction Rev 01.xls) documented in Section 6.10.5.2 are then used as input into a new set of spreadsheets where the statistics are applied to the log-transformed parameter data. These spreadsheets are listed on Table 6.12-6. Within each spreadsheet, statistics for the log-transformed data can be referenced.

Table 6.12-6. Spreadsheets Containing Log Transformed Data and Statistics for Each of the RH Locations Evaluated for Uncertainty

RH Location	Spreadsheet Name
98%	EBS Dust Leachate 98% RH uncert anal log transform.xls
85%	EBS Dust Leachate 85% RH uncert anal log transform.xls
65%	EBS Dust Leachate Binning Abstraction Rev 01 log transform.xls

Source: DTN: MO0310SPAPCELT.000

As with the seepage waters, a review of the 65 percent RH data indicated that in many instances the evaporative evolution had passed beyond the halite divide, causing larger uncertainty than should be present for the uncertainty caused by bin or lookup table variability. Therefore, only the data from 98 and 85 percent RH were used to develop Tables 6.12-7 and 6.12-8. Table 6.12-7 lists the relative humidity with the most uncertainty within the bins. Table 6.12-8 presents only the uncertainties for the parameters of interest to the TSPA-LA are presented in the following tables; uncertainties for all other species of interest can be found in the spreadsheets listed in Table 6.12-6.

Table 6.12-7. Table Giving the Relative Humidity with the Most Uncertainty in Bins 1 through 5 for pH, Cl, and Cl:NO_3

Species	Bin 1	Bin 2	Bin 3	Bin 4	Bin 5
pH	85	85	98	85	85
Cl	85	85	98	98	98
Cl:NO_3	98	98	85	85	85

NOTE: Bin 6 has no lookup table uncertainty.

The median and 2s statistics presented in the spreadsheets listed in Table 6.12-6 and the RH condition for which the most variability occurs (see Table 6.12-7) were used to develop Table 6.12-8, which gives the uncertainty that can be applied to any given discrete parameter used in the TSPA-LA.

Table 6.12-8. The Error Applied to the Dust Leachate Lookup Tables for pH, I, Cl, and Cl:NO_3, Based on the RH with the Highest Uncertainty within Bins 1 through 5 (Errors are Based on 2s Values)

Species	Bin 1	Bin 2	Bin 3	Bin 4	Bin 5
±pH	0.44	0.10	0.38	0.19	0.25
±Log I*	0.03	0.07	0.06	0.04	0.05
±Log Cl	0.16	0.19	0.27	0.19	0.21
±Log Cl:NO_3	0.23	0.28	0.33	0.35	0.44

Source: MO0311SPAEPMUT.000

NOTES: Bin 6 has no lookup table uncertainty.

*Based on 98 percent RH results only.

6.12.4 Factors Showing No Significant Impact on Water Chemistry

Several potential sources of perturbation to the predicted water chemistries contained within the lookup tables have been evaluated in sensitivity studies. These include:

- Degradation of stainless steel in the ground support material
- Inclusion of bromide in the seepage water compositions
- Look-up table extrapolation as a function of $P\text{co}_2$
- Use of alternate mineral suppressions.

Analyses performed on the first two of these sources demonstrate that there is no increase in overall model uncertainty, except in the case where Cr(VI) is designated as the stable chromium oxidation state. For $P\text{co}_2$, it is shown that extrapolation outside the lookup table values ($P\text{co}_2$ at 10^{-2}, 10^{-3}, and 10^{-4} bar.) is valid within the modeling error, with the only significant effect upon pH being ~0.15 pH units at $P\text{co}_2 = 2\cdot10^{-2}$ bar, which is the highest $P\text{co}_2$ found in the lookup tables. Alternate mineral suppressions are also examined, and in general are found to have no significant effect upon lookup table values, with the largest deviation being ~0.2 pH units.

These studies show that variations due to these factors fall well within the model uncertainty ranges and demonstrate that any additional errors caused by their exclusion from the lookup table calculations are subsumed by other modeling uncertainties (see Section 6.12.5.2 for uncertainty values determined for the TSPA-LA lookup tables).

For the calculations produced in this section, two general base cases are selected. This is done to characterize the uncertainty that is possible within the preceding model calculations. These cases represent the most likely (based on actual number of data points available) seepage water bin (Bin 11 in Table 6.6-6) and the most likely dust leachate water bin (Bin 5 in Table 6.10-7). The base case files are listed on Table 6.12-9.

Table 6.12-9. Base Case EQ3/6 Input Files for Uncertainty Analysis

Seepage Water Bin 11EQ3 input File	Seepage Water Bin 11EQ6 input File	Dust Leachate Water Bin 5 EQ3 input File	Dust Leachate Water Bin 5 EQ6 input File
bin11.3i	11c3t7e.6i	p26_25b.3i	d5c3t07.6i
DTN: MO0304MWDSAB11.001	DTN: MO0304MWDEBSSA.000	DTN: SN0310T0510102.010	DTN: SN0310T0510102.011

6.12.4.1 Degradation of Stainless Steel in Ground Support Components

A range of possible sources of uncertainty in the abstracted seepage-ground support interactions for 316L stainless steel is examined here. All but one was found to have no effect on the values of the lookup table results, with all deviations less than 0.04 for pH and 0.01 molal for ionic strength. Usage of Cr(VI) resulted in a large drop in pH (to 2.7 unevaporated) and increased ionic strength by 0.56 molal when evaporated. Comparisons are primarily made to the base case scenario of evaporated seepage waters, whose files are labeled as "Run" number 2 in Table 6.8-2. Some of the uncertainty cases required their own "base case" calculation run for comparative purposes, included in Sections 6.12.4.1.3 through 6.12.4.1.4, as there are changes in their basic chemical parameters (e.g., $P\mathrm{co}_2$).

All calculation runs utilized a modified Data0.YMP.R2 thermodynamic database as was described in Section 6.8.3; this modification is contained within DTN: SN0312T0510102.013 in filename Cr-database.zip.

6.12.4.1.1 Alternate Corrosion Rates

A sensitivity analysis has been performed with a corrosion rate ten times greater than the base case value. This higher corrosion rate is investigated to evaluate the base case model results and determine the effect upon seepage water chemistries. This analysis is implemented by increasing the abstracted SS316L species dissolved into the Bin 11 crown seepage water by a factor of ten, resulting in the addition of $4.7 \cdot 10^{-2}$ moles of SS316L. Table 6.12-10 shows the EQ6 input/output files generated for this uncertainty case. The bottom half of the pickup file from ssbin11.6p is used as the bottom half of the subsequent ssbin11e.6i evaporation run.

Table 6.12-10. EQ6 Input/Output Files for 316L Stainless Steel Corrosion Rate Uncertainty Case

Input File Names	Output File Names	Pickup File Names
SSBin11.6i	ssbin11.6o	ssbin11.6p
ssbin11e.6i	ssbin11e.6o	–

Source: DTN: SN0312T0510102.013, filename Uncertainties.zip

NOTE: These files are in directory: \ Cor Rate.

The calculated results of this uncertainty run are compared with the bounding base case model; the results are summarized in Table 6.12-11. There is no calculable difference in the aqueous water chemistry.

Table 6.12-11. Comparison of pH and Ionic Strength for Corrosion Rate Uncertainty Case

RH	Uncertainty Case		Base Case		Difference	
	pH	I (molality)	pH	I (molality)	pH	I (molality)
100	7.880	0.00606	7.879	0.00605	0.001	0.00001
98	9.462	0.7313	9.462	0.7312	0.000	0.0001

Source: DTN: SN0312T0510102.013, filename Uncertainties.zip, UncertaintyCases.xls, sheet Corrosion Rate

6.12.4.1.2 Cr VI

A sensitivity analysis is performed to examine the impact on seepage water chemistry resulting from the formation of Cr(VI), which could occur under extremely oxidizing conditions. As this case requires a completely new speciation from that of the base case, an EQ3NR calculation run is required and its pickup file is used as the bottom half of the calculated EQ6 SS316L dissolution run. Also, the bottom half of the pickup file from ssbin11.6p is used as the bottom half of the subsequent calculated ssbin11e.6i evaporation run. Table 6.12-12 contains the EQ3/6 filenames for this uncertainty case.

Table 6.12-12. EQ3/6 Input/Output Files for 316L Stainless Steel Cr(VI) Uncertainty Case

Input File Names	Output File Names	Pickup File Names
bin11.3i	bin11.3o	bin11.3p
SSBin11.6i	ssbin11.6o	ssbin11.6p
ssbin11e.6i	ssbin11e.6o	–

Source: DTN: SN0312T0510102.013, filename Uncertainties.zip
NOTE: These files are in directory: \Cr(VI).

The results of this uncertainty run are also compared with the bounding base case and are summarized in Table 6.12-13. Unlike the other stainless steel sensitivity cases, dramatic changes are seen in the predicted pH and ionic strength. This is directly due to the production of five protons for every $Cr(III)^{3+}$ converted to $Cr(VI)O_4^{2-}$, which exceeds the acid neutralizing capacity of the seepage water from $CO_{2(g)}$ buffering. As discussed in Section 6.8.3.1, it is unlikely that Cr (VI) will significantly contribute to the in-drift chemical environment.

Table 6.12-13. Comparison of pH and Ionic Strength for Cr(VI) Uncertainty Case

RH	Uncertainty Case		Base Case		Difference	
	pH	I (molality)	PH	I (molality)	pH	I (molality)
100	2.7281	0.00922	7.879	0.00605	-5.1509	0.00317
98	1.7107	1.28679	9.462	0.7312	-7.7514	0.5556

Source: DTN: SN0312T0510102.013, filename Uncertainties.zip, UncertaintyCases.xls, sheet Cr(VI)

6.12.4.1.3 Bin 07 Seepage

Another crown seepage abstracted water has been examined to determine if a different starting water chemistry would affect the SS316L interactions. Bin 07 (DTN: MO0304MWDSAB11.001) was chosen, because it represents seepage water that is likely to enter the repository during relatively long periods (i.e., 10,000 years, see Tables 6.6-8 through 6.6-12), thus being appropriate given the potentially long lifetimes of stainless steel.

The EQ3/6 input, output and pickup files are listed in Table 6.12-14. Because a different starting water composition is used, the EQ3NR speciation was redone by replacing the water chemistry description in file Bin11.3i (Section 6.8.4.1) with the descriptions residing in Bin 07. The rest of the procedure is identical to that used for the base case calculation runs described in Section 6.8.4.1.

Table 6.12-14. EQ3/6 Input/Output Files for 316L Stainless Steel Bin 07 Uncertainty Case

Input File Names	Output File Names	Pickup File Names
Bin07.3i	in07.3o	bin07.3p
Bin07e.6i	bin07e.6o	bin07e.6p
SSBin07.6i	ssbin07.6o	ssbin07.6p
ssbin07E.6i	sssbin07e.6o	–

Source: DTN: SN0312T0510102.013, filename Uncertainties.zip

NOTE: These files are in directory: \Bin 7.

The results of this uncertainty calculation run are compared with the pure Bin 07 seepage water evaporation results; these results are summarized in Table 6.12-15. As with the base case Bin 11 seepage water, there is effectively no change in the aqueous water chemistry caused by stainless steel corrosion and corrosion product formation in this case.

Table 6.12-15. Comparison of pH and Ionic Strength for Bin 07 Uncertainty Case

RH	Uncertainty Case		Base Case		Difference	
	pH	I (molality)	pH	I (molality)	pH	I (molality)
100	8.240	0.0110	8.240	0.0110	0.000	0.0000
98	9.520	0.7283	9.520	0.7284	0.000	–0.0001

Source: DTN: SN0312T0510102.013, filename Uncertainties.zip, UncertaintyCases.xls, sheet Bin 07

6.12.4.1.4 CO_2 Fugacities

Two additional fugacities for CO_2 gas are examined as uncertainty cases; these are taken at 10^{-2} and 10^{-4} bar. These fugacity uncertainty calculation runs are compared to the pure Bin 11 water chemistry results calculated at the same CO_2 fugacities.

The EQ3/6 input, output and pickup files are listed in Table 6.12-16 for the uncertainty case. As a different starting water fugacity of CO_2 is used, the EQ3NR speciation is redone and the resulting pickup file bin11.3p is fed to the bottom half of the two EQ6 calculation runs: Bin11e.6i and SSBin11.6i for the pure Bin 11 evaporation and SS316L/Bin 11 mixing

calculation runs, respectively. The bottom half of the pickup file ssbin11.6p is used by the evaporation EQ6 calculation run, ssbin11E.6i.

Table 6.12-16. EQ3/6 Input/Output Files for 316L Stainless Steel $Pco_2 = 10^{-2}$ Uncertainty Case

Input File Names	Output File Names	Pickup File Names
Bin11.3i	bin11.3o	bin11.3p
Bin11e.6i	bin11e.6o	bin11e.6p
SSBin11.6i	ssbin11.6o	ssbin11.6p
ssbin11E.6i	ssbin11e.6o	–

Source: DTN: SN0312T0510102.013

NOTE: These files are in directory: \PCO2 –2

The results of the fugacity uncertainty calculation run at 10^{-2} bar are compared with the pure Bin 11 seepage water evaporation results at the same CO_2 fugacities, summarized in Table 6.12-17. There is no significant change in the predicted water chemistry caused by stainless steel corrosion and corrosion product formation at this higher CO_2 fugacity.

Table 6.12-17. Comparison of pH and Ionic Strength for $Pco_2 = 10^{-2}$ Uncertainty Case

RH	Uncertainty Case		Base Case		Difference	
	pH	I (molality)	pH	I (molality)	Ph	I (molality)
100	6.898	0.00606	6.898	0.00605	0.000	0.00000
98	8.741	0.7015	8.741	0.7012	0.000	0.0003

Source: DTN: SN0312T0510102.013, filename Uncertainties.zip, UncertaintyCases.xls, sheet PCO2=–2

The EQ3/6 input, output and pickup files for the case with the CO_2 fugacity set at 10^{-4} bar are listed in Table 6.12-18. Because a different starting fugacity of CO_2 is used, the EQ3NR speciation was redone and the resulting pickup file bin11.3p was fed to the bottom half of the two EQ6 calculation runs: Bin11e.6i and SSBin11.6i for the pure Bin 11 evaporation and SS316L/Bin 11 mixing calculation runs, respectively. Again, the bottom half of the pickup file ssbin11.6p is used by the evaporation EQ6 calculation run, ssbin11E.6i.

Table 6.12-18. EQ3/6 Input/Output Files for 316: Stainless Steel $Pco_2 = 10^{-4}$ Uncertainty Case

Input File Names	Output File Names	Pickup File Names
Bin11.3i	bin11.3o	bin11.3p
Bin11e.6i	bin11e.6o	bin11e.6p
SSBin11.6i	ssbin11.6o	ssbin11.6p
ssbin11E.6i	ssbin11e.6o	–

Source: DTN: SN0312T0510102.013, filename Uncertainties.zip

NOTE: These files are in directory: \ PCO2 –4

The results of this fugacity uncertainty calculation run at 10^{-4} are compared with the pure Bin 11 seepage water evaporation results at the same CO_2 fugacity; these are summarized in Table 6.12-19. There is no significant change in the water chemistry caused by stainless steel corrosion and corrosion product formation at this lower CO_2 fugacity.

Table 6.12-19. Comparison of pH and Ionic Strength for $Pco_2 = 10^{-4}$ Uncertainty Case

RH	Uncertainty Case		Base Case		Difference	
	pH	I (molality)	pH	I (molality)	pH	I (molality)
100	8.726	0.00600	8.726	0.00600	0.000	0.00000
98	9.957	0.7088	9.957	0.7089	0.000	–0.0002

Source: DTN: SN0312T0510102.013, filename Uncertainties.zip, UncertaintyCases.xls, sheet Pco_2=–4

6.12.4.2 Evaporative Concentration of Br

The starting pore water compositions provided by the USGS (DTN: GS020408312272.003 [DIRS 160899]), which are used as primary inputs into the THC seepage model that is abstracted in Section 6.6, give trace quantities of many chemical components including Br^-. Bromide is a halide species that behaves conservatively in aqueous solutions, much like Cl^-, and will tend to concentrate in solution upon evaporation. Because total aqueous Br^- is not a modeled species in the THC seepage model, no direct model output for Br^- concentration is available. However, because halides are of concern to corrosion modeling, it is important to know to what level it would concentrate if present in the initial water. This sensitivity study investigates the evaporative concentration of Br^- in seepage waters and in dust leachate waters. The results show that the concentration of Br^- is small compared to the total halide concentrations in both water types. Therefore, the seepage and leachate compositions as presented in the lookup tables are adequate for the present applications.

6.12.4.2.1 Conceptual Framework

The calculation presented here compares the evaporative concentration of Br^- as a function of the Cl:Br ratio in the starting pore water compositions to the base case THC seepage bin file listed in Table 6.12-9.

6.12.4.2.2 Calculation Set Up

Three bounding evaporation cases are developed by altering the seepage water base case EQ3 input file (bin11.3i; see Table 6.12-9) through the addition of Br to the starting water composition. The Cl:Br ratio is calculated for samples collected at locations along the drift, as shown in Table 6.12-20 (from DTN: GS020408312272.003 [DIRS 160899]).

Table 6.12-20. Cl and Br Data for Pore Waters Collected in the ECRB

	Local Sample Name	SPC Number	Cl mg/L	Br mg/L	Br* mg/L	Cl:Br
1	ECRB-SYS-CS400/3.8-4.3/UC	SPC00554610	29	<1	0.5	58.00
2	ECRB-SYS-CS400/5.6-6.2/UC	SPC00554611	21	<1	0.5	42.00
3	ECRB-SYS-CS600/3.6-4.0/UC	SPC00554612	22	<1	0.5	44.00
4	ECRB-SYS-CS1000/7.3-7.7/UC	SPC00554613	21	<1	0.5	42.00
5	ECRB-SYS-CS750/6.2-6.5/UC	SPC00554614	73	<1	0.5	146.00
6	ECRB-SYS-CS2150/5.5-6.1/UC	SPC00554615	27	<0.2	0.1	270.00
7	ECRB-SYS-CS900/5.4-5.9/UC	SPC00554616	37	<0.2	0.1	370.00
8	ECRB-SYS-CS850/5.1-5.6/UC	SPC00554617	32	<0.2	0.1	320.00
9	SD-9/990.4-991.7/UC	SPC00554618	23	<0.2	0.1	230.00
10	ECRB-SYS-CS900/3.5-4.1/UC	SPC00554619	53	0.3	0.3	176.67
11	ECRB-SYS-CS1000/12.9-14.0/UC	SPC00554620	22	<0.1	0.05	440.00
12	ECRB-SYS-CS450/5.3-6.0/UC	SPC00554621	66	0.4	0.4	165.00
13	ECRB-SYS-CS2300/4.3-4.9/UC	SPC00554622	23	<0.1	0.05	460.00
14	ECRB-SYS-CS500/12.0-16.7/UC	SPC00554800	54	0.4	0.4	135.00
15	ECRB-SYS-CS2000/16.5-21.1/UC	SPC00554801	26	<0.2	0.1	260.00
16	ECRB-SYS-CS2000/16.3-16.5/UC	SPC00554802	24	<0.2	0.1	240.00
17	ECRB-SYS-CS950/5.2-5.3/UC	SPC00554803	19	<0.2	0.1	190.00
18	ECRB-SYS-CS950/4.8-5.5/UC	SPC00554804	30	<0.2	0.1	300.00
19	SD-9/991.7-992.1/UC	SPC00554805	26	0.1	0.1	260.00
20	ECRB-SYS-CS1250/5.0-5.7/UC	SPC00554806	50	0.2	0.2	250.00
21	ECRB-SYS-CS1250/3.4-4.0/UC	SPC00554807	25	M		
22	SD-9/670.5-670.6/UC	SPC00554808	46	0.3	0.3	153.33
23	ECRB-SYS-CS800/4.9-5.6/UC	SPC00554809	20	M		
24	ECRB-SYS-CS700/5.5-5.8/UC	SPC00554810	64	<0.1	0.05	1280.00
25	NRG-7/7A/839.3-839.8/UC	SPC00554811	31	0.1	0.1	310.00

Source: DTN: GS020408312272.003 [DIRS 160899]

NOTE: M indicates not measured.

The concentration of Cl in each sample is divided by the value of Br (both in units of mg/L) to obtain the Cl:Br ratio. For concentrations of Br below the detection limit, the value of Br used for the calculation is one half of the detection limit and is indicated in the column labeled Br* mg/L. From the ratios calculated, the mean, maximum, and minimum values are obtained using the built-in functions in Excel from *Cl:Br.xls* file (see Table 6.12-21).

Table 6.12-21. Mean, Minimum, and Maximum Cl:Br Ratios Present in Drift Samples, Calculated from the Data in DTN: GS020408312272.003 [DIRS 160899]

Parameter	Cl:Br
Avg	267.04
Min	42.00
Max	1280.00

Source: DTN: MO0310SPAPCEUA.002

The ratios found from this calculation are then used to calculate the amount of bromide to be added to the base case3i file (bin11.3i; see Table 6.12-9). By dividing the chloride constraint value in bin11 ($1.30 \cdot 10^{-3}$ molal) from the base case 3i file (bin11.3i; see Table 6.12-9) by the Cl:Br ratio, as calculated in the *Cl_BrREV2.xls* file, we obtain the three bromide concentrations presented in Table 6.12-22.

Table 6.12-22. Bromide Values Used as Input into EQ3 Input Files

Parameter	Bromide Constraint Value
Median	4.87E-06
Low	1.02E-06
High	3.10E-05

Source: DTN: MO0310SPAPCEUA.002

Each Br value found in Table 6.12-22 is then inserted into the base case EQ3 input file and run in EQ3 using the Data0.ypf database file, generating the EQ3 input and output files listed in Table 6.12-23. Once the new values for Br are added to the three 3i files, they are run using EQ3 v8.0 software. The pickup files replaced the bottom half of the base case 6i file. Then, the 6i files are run at three temperatures (40, 70, and 100°C) using EQ6 v8.0 to obtain the final results of the alternative evaporation reaction. Lookup tables are generated using GETEQDATA to compare the results of the three Br-added evaporation runs to the base case.

Table 6.12-23. Br Uncertainty Analysis EQ3/6 Input and Output Files

File Type	High Br	Median Br	Low Br
EQ3 input File Name	B11Mxbr.3i	B11Avgbr.3i	B11Mnbr.3i
EQ3 Output File Name	b11mxbr.3o	B11avgbr.3o	b11mnbr.3o
Pick Up File Name	b11mxbr.3p	B11avgbr.3p	b11mnbr.3p
EQ6 Input File Name	B11Mxbr.6i 11Mxbr1.6i 11Mxbr4.6i	B11Avgbr.6i 11Avgbr1.6i 11Avgbr4.6i	B11Mnbr.6i 11Mnbr1.6i 11Mnbr4.6i
EQ6 Output File Name	b11mxbr.6o 11mxbr1.6o 11mxbr4.6o	B11avgbr.6o 11avgbr1.6o 11avgbr4.6o	b11mnbr.6o 11mnbr1.6o 11mnbr4.6o
Look Up Table File Name	bin11mxbrLT.xls	Bin11avgbrLT.xls	bin11mnbrLT.xls

Source: DTN: MO0310SPAPCEUA.002

6.12.4.2.3 Results of Bromide in Seepage Waters

Figure 6.12-1 depicts the total Br concentration as the seepage water is evaporated: when added to the starting waters in concentrations found in the pore waters it is used as inputs to the THC seepage model. Concentrations of Br can become large as evaporation progresses and brines become more and more concentrated. Below a relative humidity of approximately 70 percent, the results start to show the temperature dependency of KBr saturation; higher Br concentrations tend to be possible at lower temperatures. At very low relative humidity, the Br concentrations in solution can become rather high, on the order of 1 to 3 molal. These concentrations are similar to those found in the dust leachate samples (see following Section 6.12.4.2.4). At the lowest lookup table RH of 65 percent, the maximum Br concentration is 0.4 molal, and is typically much lower.

Also shown in this section are the effects of Br addition on predicted pH and ionic strength (see Figures 6.12-2 and 6.12-3). Over the entire RH range examined, the presence of Br in solution causes no noticeable change in the predicted pH values. The effect on ionic strength is small but increases with evaporation. It is greatest at low relative humidity, where the uncertainty can be as large as 1 to 5 molal. At 65 percent RH, only the 40°C data show a significant deviation—in the high Br case, the predicted ionic strength is lowered by ~1 molal (~8 percent relative).

Figure 6.12-4 shows the effect on molar ratios that are of importance to waste package corrosion. The ratios only deviate significantly at lower relative humidity, where there would be an increase in halide concentration with respect to NO_3^- and SO_4^{2-}, and these are below the lowest RH values reported in the TSPA-LA lookup table and therefore of negligible impact.

6.12.4.2.4 Results of Bromide in Dust Leachate

The presence of Br in the dust leachate waters may be due to the addition of small amounts of LiBr as a tracer in construction water (Peterman et al. 2003 [DIRS 162819]). In waters above the halite divide, halides (Br and Cl) are present in the natural environment in consistent ratios (Cl:Br ~ 3.3×10^2) (see Krauskopf 1979, Table 12-4 [DIRS 105909]; White et al. 1963, p. F13 and Tables 13 to 18 [DIRS 163752]; and Table 6.12-20 in this report). Chlorine:bromine ratios in the dust leachate waters are much lower that this (Table 6.12-24), and are as much as 10-fold lower than the seepage water ratios from Table 6.12-21, suggesting that as much as 90 percent of the Br in the dust is from construction water. Whether the Br source is the construction water or is from seepage water interacting with dusts in the ESF, we can say, by analogy with the calculation results shown on Figure 6.12-1 for seepage water, that the concentration of Br in the dust leachate brines will increase as a result of evaporation, even after the solution reaches saturation with respect to halite. The evaporative concentration of Br beyond the halite divide is confirmed by Hem (1985 [DIRS 115670] p. 146).

Comparing Figure 6.12-1 with Figure 6.12-5 shows the evaporative concentration of Br for the pore waters in the mountain is consistent with this same 10-fold increase in the dust leachate results. This suggests that the concentrations of chloride and other species of interest are reasonably accurate even though there could be some impact from construction waters. There is some uncertainty in the Data0.ypf database with respect to Br species, especially Ca and Mg

bromide solids (BSC 2003 [DIRS 162529]). However, these chemical species are extremely soluble and do not affect the results shown in Figure 6.12-5 in a significant way. Therefore, this section reports the actual values calculated in Section 6.10.

Table 6.12-24. Cl:Br Ratios of Dust Leachate Samples

Data From Table 4.1-20				
Lab No.	**Field No.**	**Cl (ppm)**	**Br (ppm)**	**Cl:Br**
C-186077	SPC00573607	260	14	18.57
C-186080	SPC00573610	162	34	4.76
C-186081	SPC00573611	200	56	3.57
C-186082	SPC00573612	154	50	3.08
C-186084	SPC00573614	130	24	5.42
C-186085	SPC00573615	162	22	7.36
C-186086	SPC00573616	130	26	5.00
C-186087	SPC00573617	140	20	7.00
C-186088	SPC00573618	114	16	7.13
C-186089	SPC00573619	200	22	9.09
C-186090	SPC00573620	56	6	9.33
C-186091	SPC00573622	182	10	18.20
C-186092	SPC00573623	180	22	8.18
C-186093	SPC00573624	240	54	4.44
C-186094	SPC00573625	300	26	11.54
C-186095	SPC00573626	200	26	7.69
C-186096	SPC00573627	260	34	7.65
C-186097	SPC00573628	160	18	8.89
C-186098	SPC00573629	184	38	4.84
C-186099	SPC00573630	196	28	7.00
C-186100	SPC00573631	220	64	3.44
C-186101	SPC00573632	220	28	7.86
C-186102	SPC00573633	114	22	5.18
Data From Table 4.1-21				
Lab. No./ Sample No.	**Mesh Size**			
C-203116/ 00574980B	200-325	98	4	24.50
C-203117/ 00574980C	<325	154	8	19.25
C-203118/ 00574981A	60-200	74	4	18.50
C-203119/ 00574981B	200-325	280	44	6.36
C-203120/ 00574981C	<325	320	6	53.33
C-203121/ 00574982A	60-200	86	4	21.50
C-203122/ 00574982B	200-325	118	6	19.67
C-203123/ 00574982C	<325	170	12	14.17
C-203124/ 00574983A	60-200	114	8	14.25
C-203125/ 00574983B	200-325	260	10	26.00
C-203126/ 00574983C	<325	360	10	36.00
C-203127/ 00574984A	60-200	128	10	12.80
C-203128/ 00574984B	200-325	-	-	

Table 6.12-24. Cl:Br Ratios of Dust Leachate Samples (Continued)

Data From Table 4.1-21				
Lab No.	**Field No.**	**Cl (ppm)**	**Br (ppm)**	**Cl:Br**
C-203129/ 00574984C	<325	220	18	12.22
C-203130/ 00574985A	60-200	170	20	8.50
C-203131/ 00574985B	200-325	168	14	12.00
C-203132/ 00574985C	<325	166	16	10.38
C-203133/ 00574986A	60-200	96	6	16.00
C-203134/ 00574986B	200-325	170	10	17.00
C-203135/ 00574986C	<325	220	14	15.71
C-203136/ 00574987A	60-200	188	2	94.00
C-203137/ 00574987B	200-325	360	42	8.57
C-203138/ 00574987C	<325	320	32	10.00
C-203139/ 00574990A	60-200	88	10	8.80
C-203140/ 00574990B	200-325	102	16	6.38
C-203141/ 00574990C	<325	136	22	6.18
C-203142/ 00574991A	60-200	88	12	7.33
C-203143/ 00574991B	200-325	76	10	7.60
C-203144/ 00574991C	<325	82	12	6.83
C-203145/ 00574992A	60-200	98	6	16.33
C-203146/ 00574992B	200-325	82	<1.6	
C-203147/ 00574992C	<325	166	2	83.00
			Avg	14.88
			Min	3.08
			Max	94.00

Source: DTN: MO0310SPAPCEUA.002

All 52 of the calculated EQ6 output files listed on Table 6.10-12 were extracted using GETEQDATA software thus creating spreadsheet "newDustMOALT.xls" (archived in DTN: MO0310SPAPCELA.002). This file was then used to create Figure 6.12-5, which shows the evaporative concentration of Br as a function of relative humidity. For many of the 52 waters, Br can concentrate to values above 1 molal reaching up to ~8 molal in some cases. The 9 to 12 waters exceeding 5 molal Br are taken from dust leachate Bins 2, 3, 4 and 6, calculated at 40ºC. Examination of the results in the "newDustMOALT.xls" spreadsheet indicates that the higher Br concentrations are associated with the lower temperature calculation runs, and are not likely to occur because at low temperatures the relative humidity in the drifts should be high, and concentrated brines would not be stable.

In order to account for potential Br contamination due to construction water, Br concentrations in the dust leachates were reduced by a factor of 10 and a sensitivity calculation run was made to investigate the impacts of this reduction. The factor of ten reduction was determined by comparing the average statistics on the Cl:Br ratio for the dust leachate (14.88) calculated from the data in Table 4.1-20 and 4.1-21 as shown on Table 6.12-24 with the average Cl:Br ratio for the seepage water (267.04) shown in Table 6.12-21.

Table 6.12-25 lists the base case file and the file names for the adjusted EQ3/6 calculations. The adjusted EQ3 3i file Br concentration is reduced by a factor of 10 and the EQ6 evaporation calculation is rerun using the appended EQ3 pickup file.

Table 6.12-25. Br Dust Leachate Uncertainty Analysis EQ3/6 Input and Output Files

Base Case File	Adjusted Input and Output Files	GetEQData OutputSpreadsheet File
d1c3t07.6o (see Table 6.10-14)	Bin1_Br.3i, Bin1_Br.3p, Bin1_Br.3o, Bin1_Br.6I, Bin1_Br.6o	Dust Br sensitivity study Bin 1.xls

Source: DTN: MO0310SPAPCEUA.002

Figures 6.12-6 through 6.12-10 show the results of the sensitivity study. The results indicate that there is no significant difference in pH, ionic strength, Cl or N concentration above an activity of water of approximately 0.47. However, some differences in these values are evident below a water activity of 0.47. Still, the endpoint composition of the two calculations is essentially the same. This suggests that including the effects of Br from traced construction water does not significantly impact the results of the chemistry provided in the lookup tables.

6.12.4.3 Extrapolating Pco_2 Values Beyond Lookup Tables

As discussed in Section 6.13.3, extrapolation can be made when Pco_2 is outside the given range of the EBS seepage and dust leachate lookup tables. This sensitivity study gives the predictive range to which the lookup tables can be extrapolated. Results indicate that valid linear extrapolation as a function of Pco_2 can be performed for values of ionic strength, and chloride and nitrogen (mostly nitrate) concentrations, and log scale extrapolations for pH.

6.12.4.3.1 Calculation Framework

Two calculation cases are run for each of the base case files (see Table 6.12-15) to bound the effects of the possible range of Pco_2. Based on the total possible range of in-drift Pco_2 ($1.75 \cdot 10^{-2}$ to $2.29 \cdot 10^{-5}$ atmospheres) discussed in Section 6.7.2.2, there is a possibility that the lookup tables used in the TSPA-LA model could be outside the 10^{-2} to 10^{-4} bar range specified for the creation of the seepage lookup tables (see Section 6.9). A sensitivity calculation run is made using $Pco_2 = 10^{-5}$ bar and a sensitivity run using $Pco_2 = 10^{-1}$ bar. These input and output files are listed on Tables 6.12-26 and 6.12-27 for the seepage water and dust leachate water, respectively.

Table 6.12-26. Input and Output Files for Seepage Bin 11 Analysis of Pco_2

Pco_2	Input Files	Output Files
10^{-1} bar	11c1t7e.6i	11c1t7e.6o
10^{-5} bar	11c5t7e.6i	11c5t7e.6o

Source: DTN: MO0310SPAPCEUA.002

Table 6.12-27. Input and Output Files for Dust Leachate Bin 5 Analysis of Pco_2

Pco_2	Input Files	Output Files
10^{-1} bar	d5c1t07.6i	d5c1t07.6o
10^{-5} bar	d5c5t07.6i	d5c5t07.6o

Source: DTN: MO0310SPAPCEUA.002

6.12.4.3.2 Seepage Water Results

GETEQDATA software has been used to extract the appropriate output from the output files. The resulting spreadsheet "Seepage CO_2 uncert.xls" is used to create Figures 6.12-11 through 6.12-14. This spreadsheet is archived in DTN: MO0310SPAPCEUA.002.

Figure 6.12-11 shows the variation in pH when Pco_2 gas values fall outside the normal range of the provided lookup tables. The trend is about half a pH unit increase for every order of magnitude decrease in Pco_2 below 10^{-4} bar, and nearly one pH unit decrease when increasing Pco_2 above 10^{-2} bar. High pressure Pco_2 extrapolation of pH could result in an additional error of nearly half a pH unit, but only at this extreme Pco_2 of 10^{-1} bar. This error would at most scale log linearly with Pco_2, and therefore at $Pco_2 = 2 \cdot 10^{-2}$ bar (high end of in-drift range); this error can be at most 0.15 pH and is thus small compared to total uncertainty.

For ionic strength and N, there is only a small dependence upon Pco_2 and only at low RH (see Figures 6.12-12 and 6.12-14). Cl shows some linearly predictable trends; however, the values at 10^{-1} bar show more variation as the predictable trends are not as uniform; this is shown in Figure 6.12-13. These trends are strongly associated with the activity at which calcite and halite precipitate.

6.12.4.3.3 Dust Leachate Water Results

GETEQDATA software is used to extract the appropriate output from the output files. The resulting spreadsheet "Dust CO_2 uncert.xls" is used to create the following figures (see Figures 6.12-15 through 6.12-18). This spreadsheet is archived in DTN: MO0310SPAPCEUA.002.

Figure 6.12-15 shows the range of uncertainty that needs to be applied to the pH results when Pco_2 gas values fall outside the normal range of the provided lookup tables. This range is about half a pH unit when decreasing Pco_2 below 10^{-4} bar, and about half a pH unit when increasing Pco_2 above 10^{-2} bar. Results within this large range of Pco_2 are very regular and any interpolation errors are expected to be negligible.

For the other three lookup table parameters, there are negligible dependencies upon the Pco_2. Figures 6.12-16 through 6.12-18 show ionic strength, chloride, and nitrogen molalities, respectively, are insensitive to Pco_2. These parameters therefore add no measurable uncertainty or error to any extrapolations based upon Pco_2.

6.12.4.4 Mineral Suppressions

Three minerals, cryolite, glaserite and magnesite, have been identified as candidates for sensitivity studies to document the impact of mineral suppressions on our analyses (see Table 6.5-2). This is based on their inclusion or exclusion in the thermodynamic modeling approach that is used, as discussed in Section 6.5.

Table 6.12-28 documents the base case input files and associated output files used to investigate the suppression or inclusion of these minerals. The base case input file is modified by either including or removing the mineral in the "Alter/Suppress Options" input block of the EQ6 *.6i data file. The results are extracted into a Microsoft Excel spreadsheet using the GETEQDATA software. This spreadsheet (Mineral suppressions.xls archived in DTN: MO0310SPAPCEUA.002) is used to create the figures and determine the results shown in the following subsections.

Table 6.12-28. Traceability Roadmap for Mineral Suppression EQ6 Sensitivity Cases

Suppression Case	Base Case input file	Altered Input File	Output file
Cryolite	11c2t4e.6i (see Table 6.9-5)	11crysup.6i	11crysup.6o
Glaserite	11c3t7e.6I (see Table 6.12-9)	11glas.6i	11glas.6o
Magnesite	11c3t7e.6I (see Table 6.12-9)	11mag.6i	11mag.6o

Source: DTN: MO0310SPAPCEUA.002

6.12.4.4.1 Cryolite

In the modeling work performed to establish the mineral suppression tables (see Tables 6.5-2 and 6.6.5-1), cryolite did not precipitate; therefore, it was not suppressed when creating the seepage lookup tables (see Sections 6.5, 6.6, and 6.9), yet it precipitated in a few cases (see Table 6.13-6). Cryolite (Na_3AlF_6) is a halide mineral that is associated with pegmatite veins in granite and gneiss (Palache et al. 1951 [DIRS 162280] p. 113); it commonly forms at higher temperature and pressure conditions not relevant to the repository and would have normally been suppressed on this basis. However, during the literature review that was performed, cryolite was also found to precipitate in fluid inclusions where the end member solutions are Na-K-Ca-Cl-HCO_3 brines. The minerals associated with cryolite in these fluid inclusions are nahcolite, halite, sylvite and fluorite (Buhn and Rankin 1999 [DIRS 163753]). These minerals are commonly found in evaporite deposits and are present in many of the lookup table results as precipitates. The naturally occurring association with common evaporite minerals would justify the inclusion of cryolite as a potential precipitate in our system. Therefore, this sensitivity analysis was conducted to determine the potential impact to the lookup tables.

Total aqueous concentrations for Na, Al and F are shown on Figure 6.12-19. Also plotted are pH and the moles of cryolite precipitated in the base case results. Figure 6.12-19 also shows that with the exception of the Al concentrations, there is no major impact to the base case files from the precipitation of cryolite. The Al concentrations are affected by approximately two orders of magnitude, but because Al concentrations are less than 10^{-10} molal, the pH and other parameters of interest are unaffected.

6.12.4.4.2 Glaserite

As reported in Table 6.5-2, glaserite ($NaK_3(SO_4)_2$) is suppressed due to the uncertain nature of the values reported in the Data0.ypf thermodynamic database. This sensitivity calculation run documents the potential changes that could occur if glaserite is allowed to precipitate in the analyses. The Data0.ypf database includes two sets of data; the set that was used is the single 25ºC log K value of -3.8027. Therefore, the modeling calculation runs done at 70ºC are not fully representative, but do indicate the potential changes to the output results that could occur with inclusion.

Figure 6.12-20 shows the comparative results of the base case with the inclusion of glaserite for pH, S, Na and K. The largest change is the difference in endpoint water activity. With the glaserite present, the endpoint of the calculated model run is lowered by about 15 percent. The pH change is less than half a unit when the base-case calculation run ends. The aqueous solute concentrations do not vary much (less than 1 order of magnitude). The pH shift at the lowest water activity used in the lookup tables (a_w = 0.65) is just under 0.2 pH units.

6.12.4.4.3 Magnesite

As reported on Table 6.5-2, according to Eugster and Hardie (1978 [DIRS 100743]) magnesite can be associated with salt deposits. However, it is uncertain whether it is associated with the diagenesis of salt deposits at higher temperatures and pressures higher than 100°C and 1 atmosphere respectively, or with lower temperatures and pressures such as those anticipated in the repository. The sensitivity analysis is conducted to evaluate the possible effects to our model results. The results indicate that even with the inclusion of magnesite in the modeling calculation run, it does not precipitate in the base case file. Therefore, with this limited sensitivity study, it is concluded that there is no impact to the results.

6.12.5 Implementing Uncertainties in the TSPA-LA Abstraction Look-Up Tables

EBS chemical environments abstractions are documented for use by the TSPA-LA in the form of lookup tables that are identified in Sections 6.7, 6.9, 6.10, 6.15.1.1 and 6.15.1.2. Seepage evaporation and condensation lookup tables and deliquescence lookup tables are archived in DTNs: MO0304SPACSALT.000, MO0310SPADLALT.001, and DTN: MO0310SPADLHTL.000.

The subsequent sections provide the details on the determination and guidelines on the treatment of uncertainties by the TSPA-LA.

6.12.5.1 Uncertainties that Are Negligible and Not Included

Degradation of stainless steel in ground support components, treatment of bromide in the abstraction, extrapolation of Pco_2 values outside the range of the lookup tables, and alternate mineral suppressions are all shown to have a negligible effect on the uncertainties in EBS chemical environments abstractions. Evidence for the relative insignificance of those processes is presented in previous Section 6.12.4.

6.12.5.2 Uncertainty Distributions for TSPA-LA Lookup Tables

As shown on Table 6.12-1, 6.12-4 and 6.12-8, uncertainty in the model output stems from two sources, in-drift precipitates/salts model uncertainty and the uncertainty due to binning (or lookup table) variability. These two types of uncertainty have to be accounted for in the TSPA-LA. The in-drift precipitates/salts model uncertainties in chemical parameters relevant to the TSPA-LA, and in deliquescence RH, are summarized in Table 6.12-1. Binning uncertainties for seepage and dust can be found on Tables 6.12-4 and 6.12-8, respectively.

The lookup table results in Section 6.13 (see Figures 6.13-29 and 6.13-38) indicate that, in all cases, once the halite divide is crossed, the $Cl:NO_3$ ratio can only decrease. These results indicate that there is a maximum limit that can be placed on the uncertainty of this value at relative humidities below the halite divide. In most lookup table cases, there is another divide (sylvite) that further ensures this limit. Tables 6.12-29 and 6.12-30 are a compilation of the $Cl:NO_3$ ratio at the halite divide for all simulations. These tables were created by extracting the relevant information from the lookup table DTNs (see MO0304SPACSALT.000, DTN: MO0310SPADLALT.001, and DTN: MO0310SPADLHTL.000) and calculating the ratios.

6.12.5.3 Specific Guidance for TSPA-LA Implementation

The lookup tables summarizing seepage waters and dust deliquescence chemistries must be implemented in the TSPA-LA with the associated uncertainties. Carbon dioxide partial pressure lookup tables, as taken from the THC model results, are shown in Tables 6.7-1 through 6.7-5 and are archived in DTN: MO0308SPACO2GL.001. Seepage lookup tables and low and high temperature dust lookup tables are archived in DTN: MO0304SPACSALT.000 (see DTN: MO0310SPAPCEGS.000 for the TSPA-LA model use), DTN: MO0310SPADLALT.001, and DTN: MO0310SPADLHTL.000, respectively.

Quantification of the uncertainties in parameters that will feed the TSPA-LA is developed above and includes the following parameters:

- Ionic strength
- Chloride concentration
- Chloride to nitrate ratio
- pH
- Deliquescence Relative Humidity point.

Nitrate uncertainty is calculated using the chloride and chloride to nitrate ratio uncertainties as discussed in the following paragraphs.

Because distinct water compositions are provided in the lookup tables along an evolutionary evaporative path using the in-drift precipitates/salts model, any uncertainty distribution selected at the beginning of the evaporative path can be maintained throughout any given TSPA-LA model realization.

Table 6.12-29. Cl:NO_3 Molal Ratio for Seepage at the Halite Chemical Divide

Bin Number	Temp (°C)	Pco_2 (bar)	Halite Divide Cl:N Molal Ratio	Halite Divide Log Cl:N Molal Ratio
1	70	0.0001	15.46	1.19
	40	0.0001	15.46	1.19
	100	0.0001	15.46	1.19
	70	0.001	15.46	1.19
	40	0.001	15.46	1.19
	100	0.001	15.46	1.19
	70	0.01	15.46	1.19
	40	0.01	15.46	1.19
	100	0.01	15.46	1.19
2	70	0.0001	9.19	0.96
	40	0.0001	9.19	0.96
	100	0.0001	9.19	0.96
	70	0.001	9.19	0.96
	40	0.001	9.19	0.96
	100	0.001	9.19	0.96
	70	0.01	9.19	0.96
	40	0.01	9.19	0.96
	100	0.01	9.19	0.96
3	70	0.0001	18.30	1.26
	40	0.0001	18.30	1.26
	100	0.0001	18.30	1.26
	70	0.001	18.30	1.26
	40	0.001	18.30	1.26
	100	0.001	18.30	1.26
	70	0.01	18.30	1.26
	40	0.01	18.30	1.26
	100	0.01	18.30	1.26
4	70	0.0001	7.74	0.89
	40	0.0001	7.74	0.89
	100	0.0001	7.74	0.89
	70	0.001	7.74	0.89
	40	0.001	7.74	0.89
	100	0.001	7.74	0.89
	70	0.01	7.74	0.89
	40	0.01	7.74	0.89
	100	0.01	7.74	0.89

Table 6.12-29. Cl:NO_3 Molal Ratio for Seepage at the Halite Chemical Divide (Continued)

Bin Number	Temp (°C)	Pco_2 (bar)	Halite Divide Cl:N Molal Ratio	Halite Divide Log Cl:N Molal Ratio
5	70	0.0001	14.77	1.17
	40	0.0001	14.77	1.17
	100	0.0001	14.77	1.17
	70	0.001	14.77	1.17
	40	0.001	14.77	1.17
	100	0.001	14.77	1.17
	70	0.01	14.77	1.17
	40	0.01	14.77	1.17
	100	0.01	14.77	1.17
6	70	0.0001	31.91	1.50
	40	0.0001	31.91	1.50
	100	0.0001	31.91	1.50
	70	0.001	31.91	1.50
	40	0.001	31.91	1.50
	100	0.001	31.91	1.50
	70	0.01	31.91	1.50
	40	0.01	31.91	1.50
	100	0.01	31.91	1.50
7	70	0.0001	31.70	1.50
	40	0.0001	31.70	1.50
	100	0.0001	31.70	1.50
	70	0.001	31.70	1.50
	40	0.001	31.70	1.50
	100	0.001	31.70	1.50
	70	0.01	31.70	1.50
	40	0.01	31.70	1.50
	100	0.01	31.70	1.50
8	70	0.0001	14.12	1.15
	40	0.0001	14.12	1.15
	100	0.0001	14.12	1.15
	70	0.001	14.12	1.15
	40	0.001	14.12	1.15
	100	0.001	14.12	1.15
	70	0.01	14.12	1.15
	40	0.01	14.12	1.15
	100	0.01	14.12	1.15

Table 6.12-29. Cl:NO_3 Molal Ratio for Seepage at the Halite Chemical Divide (Continued)

Bin Number	Temp (°C)	Pco_2 (bar)	Halite Divide Cl:N Molal Ratio	Halite Divide Log Cl:N Molal Ratio
9	70	0.0001	2.37	0.37
	40	0.0001	2.37	0.37
	100	0.0001	2.37	0.37
	70	0.001	2.37	0.37
	40	0.001	2.37	0.37
	100	0.001	2.37	0.37
	70	0.01	2.37	0.37
	40	0.01	2.37	0.37
	100	0.01	2.37	0.37
10	70	0.0001	14.11	1.15
	40	0.0001	14.11	1.15
	100	0.0001	14.11	1.15
	70	0.001	14.11	1.15
	40	0.001	14.11	1.15
	100	0.001	14.11	1.15
	70	0.01	14.11	1.15
	40	0.01	14.11	1.15
	100	0.01	14.11	1.15
11	70	0.0001	10.31	1.01
	40	0.0001	10.31	1.01
	100	0.0001	10.31	1.01
	70	0.001	10.31	1.01
	40	0.001	10.31	1.01
	100	0.001	10.31	1.01
	70	0.01	10.31	1.01
	40	0.01	10.31	1.01
	100	0.01	10.31	1.01

DTN: MO0311SPAEPMUT.000 / FILE: HALITE DIVIDE RATIO FOR SEEPAGE.XLS

Table 6.12-30. Cl:NO_3 Molal Ratio for Dust at the Halite Chemical Divide

Bin Number	Temperature (Deg C)	Pco_2 (bar)	Halite Divide Cl:N Molal Ratio	Halite Divide Log Cl:N Molal Ratio
1	40	0.01	0.47	-0.33
	40	0.001	0.47	-0.32
	40	0.0001	0.47	-0.32
	70	0.01	0.42	-0.38
	70	0.001	0.42	-0.38
	70	0.0001	0.42	-0.38
	100	0.01	0.42	-0.38
	100	0.001	0.42	-0.38
	100	0.0001	0.42	-0.38
	120	0.01	0.42	-0.38
	120	0.001	0.42	-0.38
	120	0.0001	0.42	-0.38
	140	0.0001	0.42	-0.38
	140	0.001	0.42	-0.38
	140	0.01	0.42	-0.38
2	40	0.01	0.81	-0.09
	40	0.001	0.81	-0.09
	40	0.0001	0.81	-0.09
	70	0.01	0.81	-0.09
	70	0.001	0.81	-0.09
	70	0.0001	0.81	-0.09
	100	0.01	0.81	-0.09
	100	0.001	0.81	-0.09
	100	0.0001	0.81	-0.09
	120	0.01	0.81	-0.09
	120	0.001	0.81	-0.09
	120	0.0001	0.81	-0.09
	140	0.0001	0.81	-0.09
	140	0.001	0.80	-0.09
	140	0.01	0.81	-0.09

Table 6.12-30. Cl:NO_3 Molal Ratio for Dust at the Halite Chemical Divide. (Continued)

Bin Number	Temperature (Deg C)	Pco_2 (bar)	Halite Divide Cl:N Molal Ratio	Halite Divide Log Cl:N Molal Ratio
3	40	0.01	1.14	0.06
	40	0.001	1.15	0.06
	40	0.0001	1.06	0.03
	70	0.01	1.15	0.06
	70	0.001	1.15	0.06
	70	0.0001	1.15	0.06
	100	0.01	1.15	0.06
	100	0.001	1.15	0.06
	100	0.0001	1.15	0.06
	120	0.01	1.15	0.06
	120	0.001	1.15	0.06
	120	0.0001	1.15	0.06
	140	0.0001	1.01	0.00
	140	0.001	1.00	0.00
	140	0.01	1.15	0.06
4	40	0.01	0.77	-0.11
	40	0.001	0.77	-0.11
	40	0.0001	0.77	-0.11
	70	0.01	0.77	-0.11
	70	0.001	0.77	-0.11
	70	0.0001	0.77	-0.11
	100	0.01	0.77	-0.11
	100	0.001	0.77	-0.11
	100	0.0001	0.77	-0.11
	120	0.01	0.77	-0.11
	120	0.001	0.77	-0.11
	120	0.0001	0.77	-0.11
	140	0.0001	0.77	-0.11
	140	0.001	0.77	-0.11
	140	0.01	0.77	-0.11

Table 6.12-30. Cl:NO_3 Molal Ratio for Dust at the Halite Chemical Divide. (Continued)

Bin Number	Temperature (Deg C)	Pco_2 (bar)	Halite Divide Cl:N Molal Ratio	Halite Divide Log Cl:N Molal Ratio
5	40	0.01	0.87	-0.06
	40	0.001	0.87	-0.06
	40	0.0001	0.87	-0.06
	70	0.01	0.87	-0.06
	70	0.001	0.87	-0.06
	70	0.0001	0.87	-0.06
	100	0.01	0.87	-0.06
	100	0.001	0.87	-0.06
	100	0.0001	0.87	-0.06
	120	0.01	0.87	-0.06
	120	0.001	0.87	-0.06
	120	0.0001	0.87	-0.06
	140	0.0001	0.87	-0.06
	140	0.001	0.87	-0.06
	140	0.01	0.87	-0.06
6	40	0.01	2.18	0.34
	40	0.001	2.34	0.37
	40	0.0001	2.39	0.38
	70	0.01	2.45	0.39
	70	0.001	2.45	0.39
	70	0.0001	2.45	0.39
	100	0.01	2.45	0.39
	100	0.001	2.45	0.39
	100	0.0001	2.45	0.39
	120	0.0001	1.52	0.18
	120	0.001	1.15	0.06
	120	0.01	2.19	0.34
	140	0.0001	0.76	-0.12
	140	0.001	0.76	-0.12
	140	0.01	0.52	-0.28

DTN: MO0311SPAEPMUT.000/ FILE: HALITE DIVIDE RATIO FOR DUST.XLS

Implementation of Ionic Strength and Chloride Concentration Uncertainties–Quantifying and implementing uncertainties for the chemical parameters of ionic strength and chloride concentration are to be carried out as explained in the steps directly below. The two distributions for ionic strength and chloride concentration ($[Cl^-]$) should be co-varied using same-scaled random uncertainty factor (i.e., the two parameters can use the same sampled distribution), as the ionic strength directly depends upon the often-dominant chloride concentration.

1. Look up the appropriate parameter value (ionic strength or $[Cl^-]$) from the relevant TSPA-LA lookup table, for either dust deliquescence or seepage. Convert this value to its $\log_{10}$-base quantity; this becomes the value for which the subsequent distribution will be developed.

2. Create a uniform parameter uncertainty range that extends from the $\log_{10}$-base quantity calculated in Step 1 by adding and subtracting the parameter binning uncertainty (Table 6.12-4 or 6.12-8) for each parameter.

3. Randomly choose a parameter value within this range (thereby producing a log uniform probability of occurrence) to obtain the log $[Cl^-]$ or ionic strength that includes the binning uncertainty.

4. Combine the $[Cl^-]$ or ionic strength log value from Step 3 which includes the binning uncertainty with the model uncertainty by adding and subtracting the model uncertainty tabulated as a function of RH in Table 6.12-1). This will establish upper and lower bounds for the log $[Cl^-]$ and ionic strength.

5. Randomly choose a parameter value within this range (thereby producing a log uniform probability of occurrence) to obtain the log $[Cl^-]$ or ionic strength that includes both binning uncertainty and model variability.

6. Take the adjusted uncertainty log value and convert this back to non-log units.

Implementation of Chloride:Nitrate Ratio Uncertainties–Quantifying uncertainties for the chemical parameter of chloride to nitrate concentration is to be carried out as explained in the steps directly below:

1. Using the chloride and nitrate concentrations from the lookup table determinations (without uncertainty), compute the chloride to nitrate ratio without uncertainty. Calculate the chloride to nitrate ratio from the appropriate TSPA-LA lookup table, either for dust deliquescence or seepage, then convert this value to its $\log_{10}$-base quantity. This becomes the nominal value for which the subsequent distribution will be developed.

2. Create a uniform parameter uncertainty range that extends from the $\log_{10}$-base quantity calculated in Step 1 by adding and subtracting the bin uncertainty from Table 6.12-4 or 6.12-8 to account for bin uncertainty.

3. Randomly choose a parameter value within this range (thereby producing a uniform probability of occurrence) to obtain a $Cl:NO_3$ that includes the binning uncertainty.

Note the difference between this step and the nominal log $Cl:NO_3$ ratio (Step 1). Call this difference delta because it will be used in Step 4 to adjust the theoretical log upper limit for $Cl:NO_3$. Delta can be a positive or negative value.

4. From the $Cl:NO_3$ halite divide molal ratio lookup table (Table 6.12-29 or 6.12-30), find the nominal theoretical upper limit as a function of bin, temperature, and Pco_2. Adjust this upper limit for binning uncertainty by adding the delta determined in Step 3.

5. Combine the $Cl:NO_3$ log value from Step 3, which includes the binning uncertainty, with the model uncertainty by adding and subtracting the log of the model uncertainty tabulated as a function of RH in Table 6.12-1. This will establish a lower and a preliminary upper bound for the log $Cl:NO_3$ ratio.

6. Compare the preliminary upper bound established in Step 5 with the theoretical upper bound established in Step 4. If the upper bound of Step 4 is more than the value of Step 5, then set the final log upper bound to equal the value of Step 5. If the value of Step 4 is less than the value of Step 5, use the theoretical upper limit of Step 4 as the final value for the log upper bound.

7. Sample randomly from the range of log $Cl:NO_3$ ratio established in Steps 5 and 6 to obtain a value that includes both binning and modeling uncertainties (i.e., log uniform distribution). If the preferred ratio is nitrate to chloride (NO_3:Cl) proceed with the negative value of this resulting log_{10}-base quantity. Convert this log_{10}-base quantity back to a ratio of non-log units.

Calculation of Nitrate Concentration and Uncertainty–To obtain a consistent and correlated nitrate concentration value it must be calculated from the two previously determined chemical conditions of chloride concentration and chloride to nitrate ratio.

Take the value for the chloride concentration and divide it by the chloride to nitrate ratio, where both of these values have already been adjusted to their uncertainty ranges.

Implementation of pH Uncertainties–Quantifying and implementing uncertainties for the pH is to be carried out as explained in the steps directly below. This will yield a uniform distribution centered on the pH value initially selected from the TSPA-LA lookup table.

1. Choose the appropriate pH value from the relevant TSPA-LA lookup table (dust deliquescence or seepage). This will become the nominal pH value for a subsequent distribution to be developed for this parameter.

2. Create a uniform parameter uncertainty range that extends from the nominal pH in Step 1 by adding and subtracting the bin uncertainty from either Table 6.12-4 or 6.12-8.

3. Randomly select a value from the range established in Step 2 to produce a pH adjusted for binning uncertainty.

4. Create a uniform parameter uncertainty range that extends from the pH in Step 3, which includes binning uncertainty by adding and subtracting the model uncertainty of Table 6.12-1.

5. Randomly select a value from the range established in Step 4 to produce a pH adjusted for both binning and modeling uncertainty.

Implementation of Deliquescence Relative Humidity Point Uncertainties–There is uncertainty in the deliquescence relative humidity (DRH), the value of the relative humidity below-which no stable aqueous solution exists. That is to say, at RH levels lower than those in the tables, stable aqueous solutions do not exist and therefore no values for solution composition parameters are given. The uncertainty range of the DRH point is given on Table 6.12-1.

The TSPA-LA dust deliquescence lookup tables provide, except for Bin 1, aqueous solution compositions down to values of RH that define the deliquescence point. Bin 1 is characterized by Na-$CaNO_3$ salts and a DRH is not predicted; this bin should be treated as having a DRH of 0 percent RH, that is, aqueous conditions would exist at all temperatures and RHs.

The TSPA-LA seepage evaporation lookup tables approach, but do not always predict the deliquescence RH point. When seepage chemistry is to be predicted, the conservative modeling decision of always having aqueous conditions should be made regardless of RH.

Quantifying and implementing uncertainties associated with the DRH point for dust leachate chemistries on the waste packages are to be carried out as explained in the steps directly below.

1. The DRH point is to be determined by selecting the appropriate nominal value from the TSPA-LA lookup table for dust deliquescence or seepage (the lowest RH point for a given bin selection subsequently referred to as DRH_{nominal}).

2. Add and subtract the amount of RH uncertainty found in Table 6.12-1 to the DRH_{nominal} to establish the upper and lower bounds of a DRH uncertainty range.

3. Randomly select a value from the range established in Step 2 between the estimated bounding values. This will yield the DRH adjusted to account for uncertainty.

4. For dust deliquescence, once the RH of the emplacement drift exceeds the value of $DRH_{\text{wUncertainty}}$, aqueous conditions are assumed to exist except for dust Bin 1 where aqueous conditions should always be assumed. Under seepage conditions, wet conditions should always be assumed. The composition of the aqueous solution that exists is taken from the suitable lookup table with the following rules:

   a) If the $DRH_{\text{wUncertainty}}$ value is below that of the *DRH* in the lookup tables, then once the emplacement drift RH is at or just above $DRH_{\text{wUncertainty}}$, the chemical composition is taken as being that at the lookup table *DRH* until the drift RH reaches the next highest RH value given in the lookup table.

b) If the $DRH_{\mathrm{wUncertainty}}$ value is above that of the *DRH* in the lookup table, then dry conditions exist until the emplacement drift RH equals or exceeds the value of $DRH_{\mathrm{wUncertainty}}$. At this point, the aqueous composition at the *DRH* from the lookup table is used. At drift RH values above $DRH_{\mathrm{wUncertainty}}$, the lookup table is to be accessed directly.

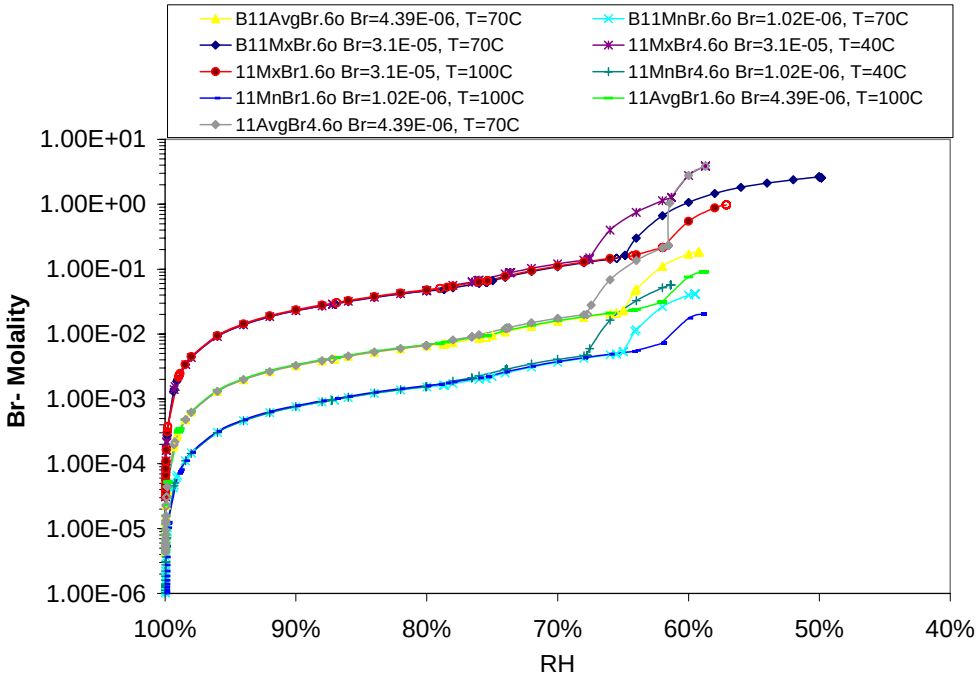

DTN: MO0310SPAPCEUA.002

Figure 6.12-1. Uncertainty in Bin 11 Br Concentrations Using the Br Values from Pore Water

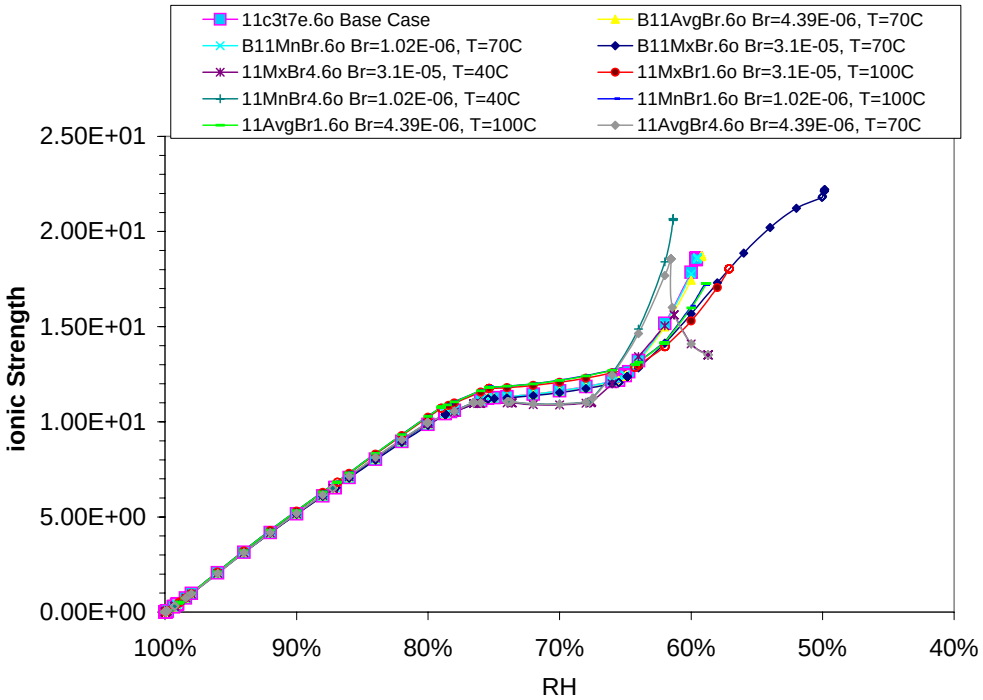

DTN: MO0310SPAPCEUA.002

Figure 6.12-2. Uncertainty in Bin 11 Ionic Strength Due to Adding Br

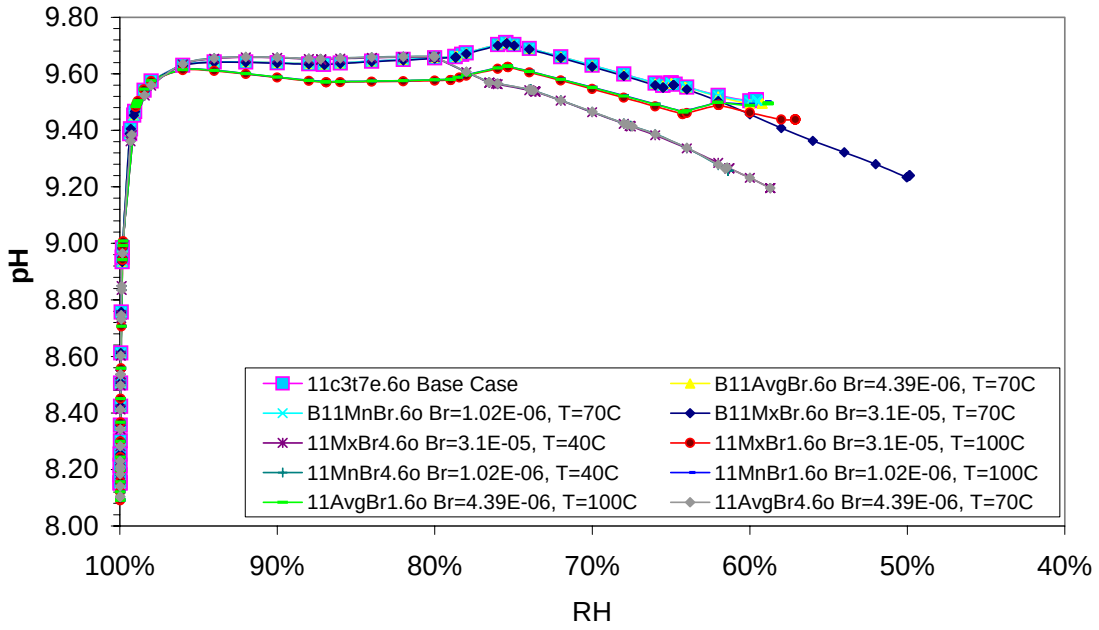

DTN: MO0310SPAPCEUA.002

Figure 6.12-3. Uncertainty in Bin 11 pH Due to Adding Br

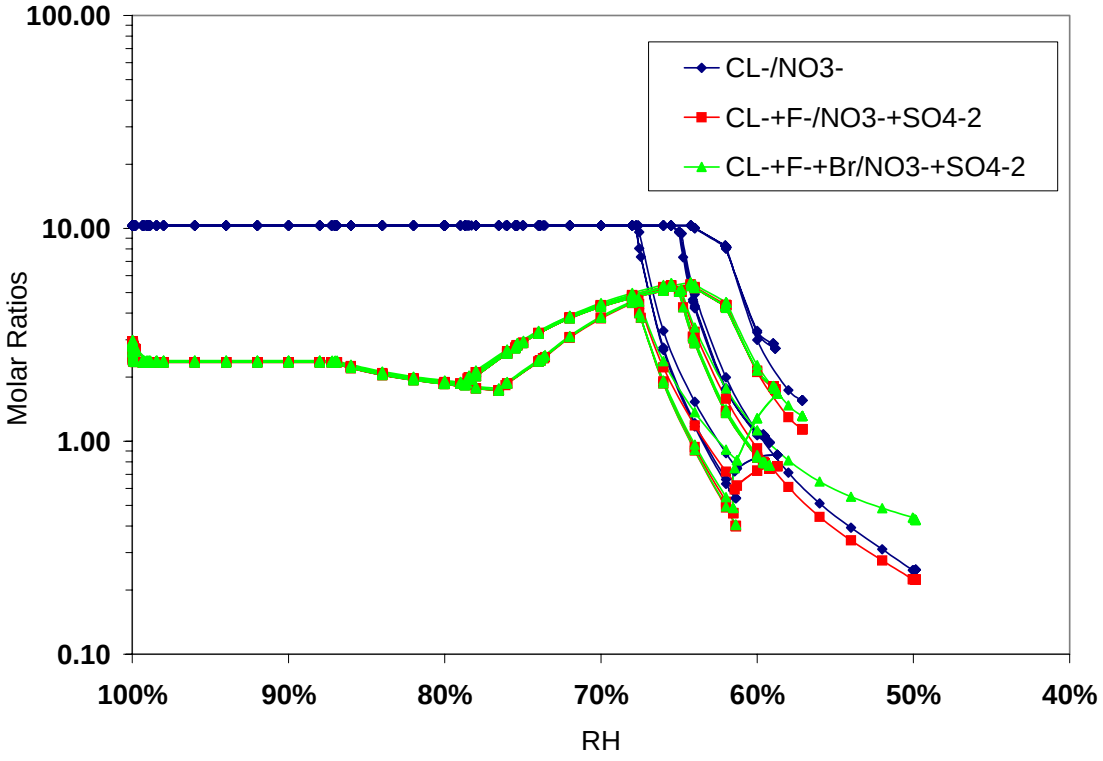

DTN: MO0310SPAPCEUA.002

Figure 6.12-4. Uncertainty in Bin 11 Molar Ratios Due to Adding Br

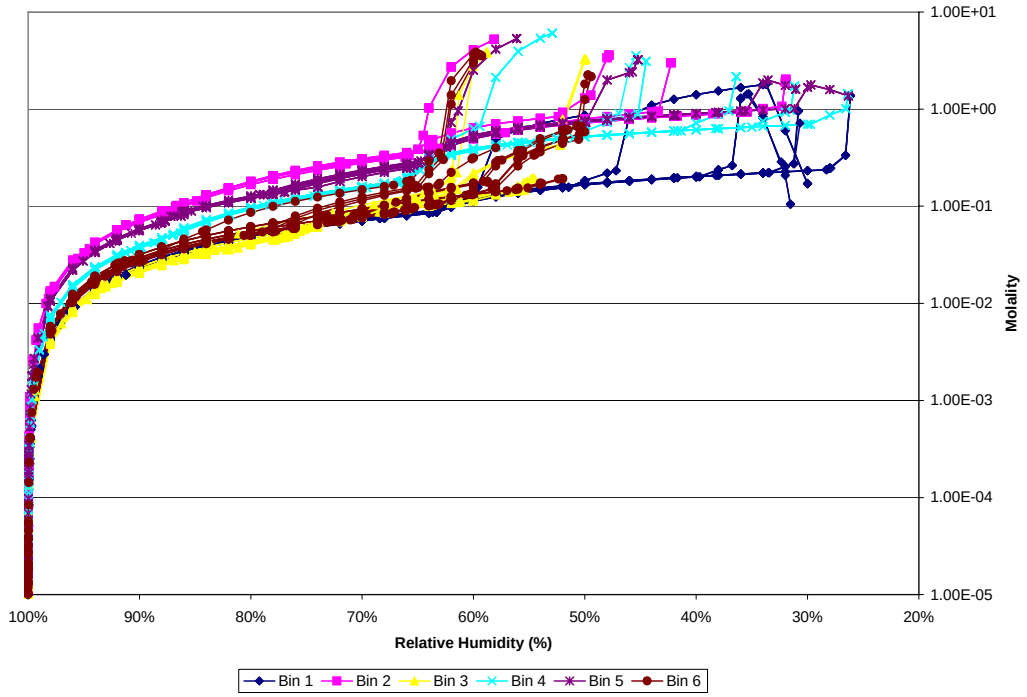

DTN: MO0310SPAPCELA.002

Figure 6.12-5. Comparative Evaporative Concentration of Br in Dust Leachate Water Lookup Tables

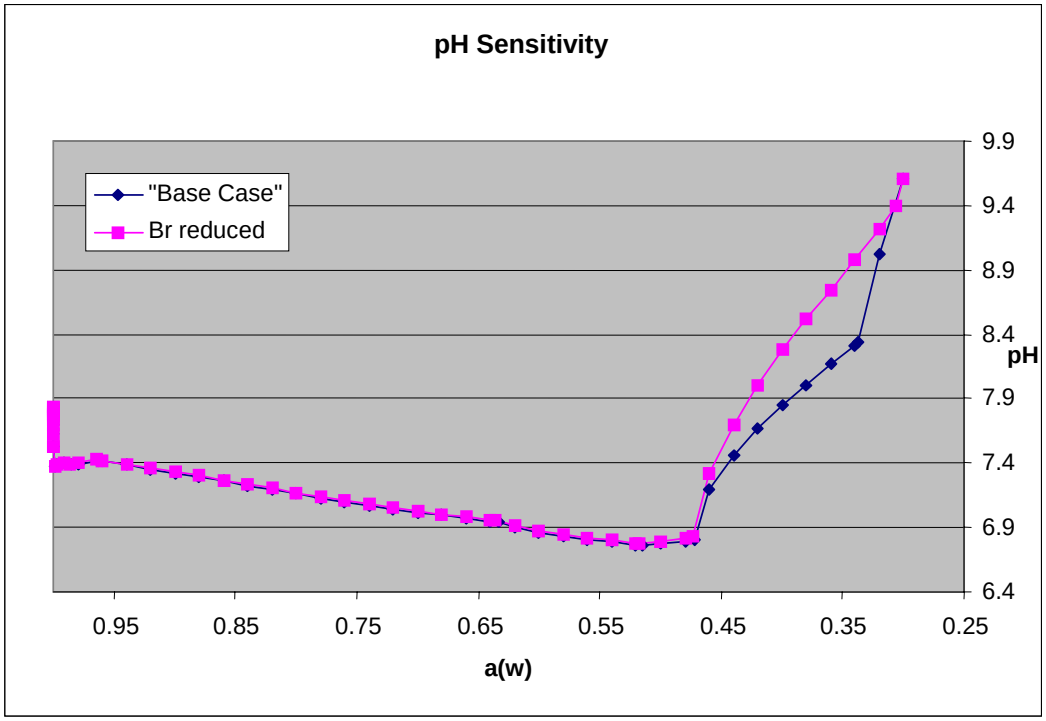

DTN: MO0310SPAPCEUA.002

Figure 6.12-6. Change in Predicted pH Due to Adjustment of Dust Leachate Bin 1 Br Concentration

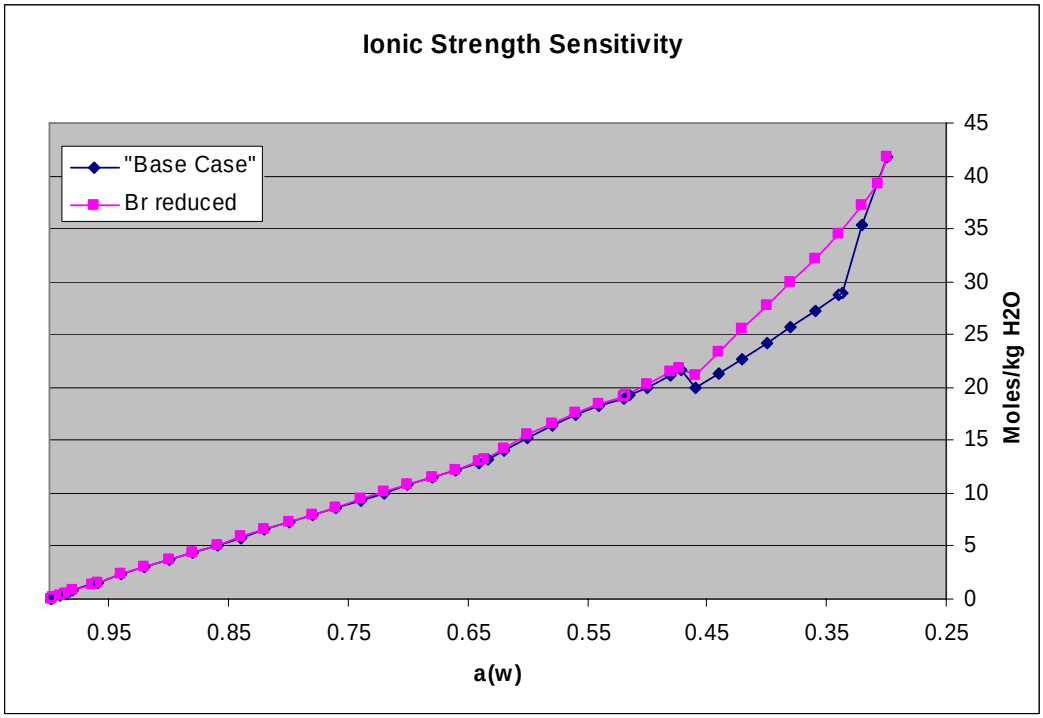

DTN: MO0310SPAPCEUA.002

Figure 6.12-7. Change in Predicted Ionic Strength Due to Adjustment of Dust Leachate Bin 1 Br Concentration

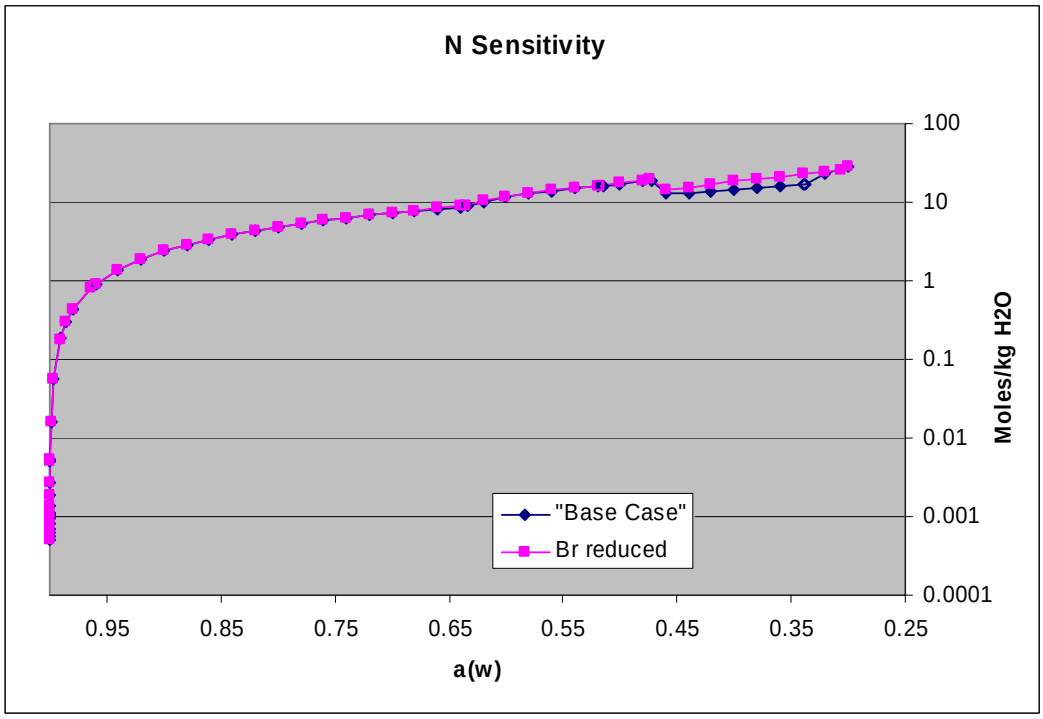

DTN: MO0310SPAPCEUA.002

Figure 6.12-8. Change in Predicted N Concentrations Due to Adjustment of Dust Leachate Bin 1 Br Concentration

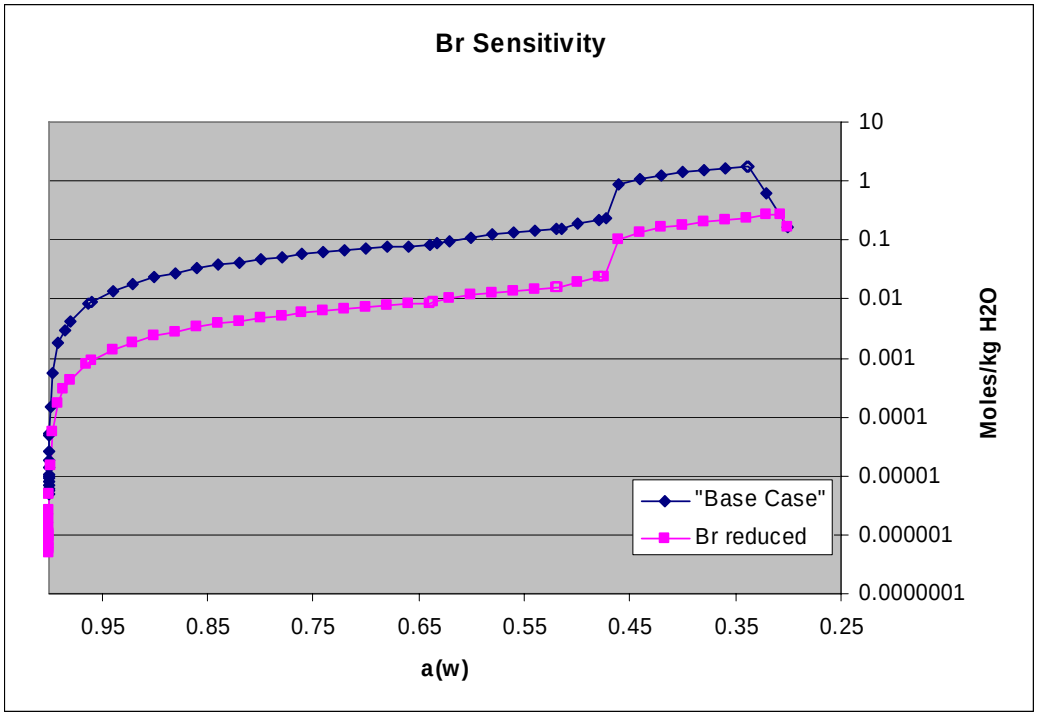

DTN: MO0310SPAPCEUA.002

Figure 6.12-9. Change in Predicted Br Concentrations Due to Adjustment of Dust Leachate Bin 1 Br Concentration

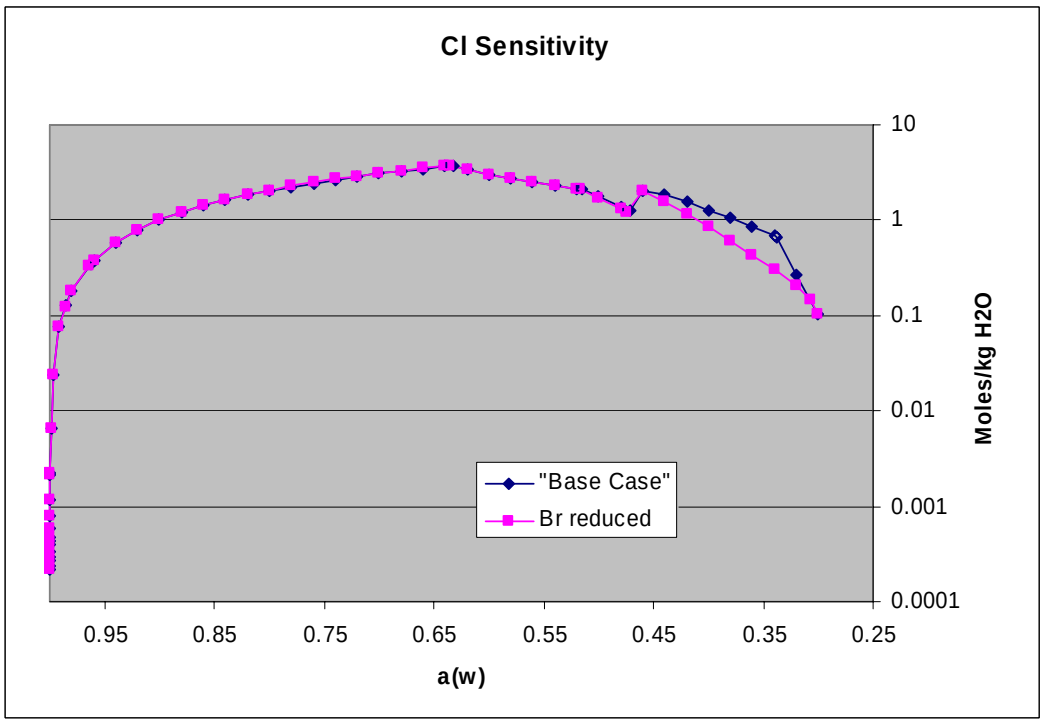

DTN: MO0310SPAPCEUA.002

Figure 6.12-10. Change in Predicted Cl Concentrations Due to Adjustment of Dust Leachate Bin 1 Br Concentration

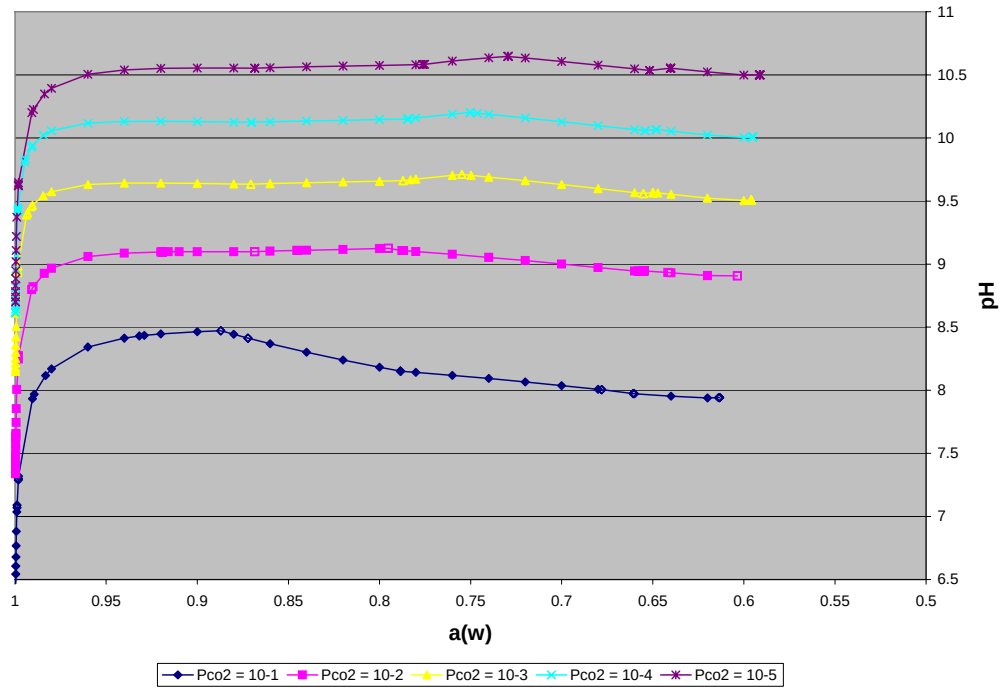

DTN: MO0310SPAPCEUA.002

Figure 6.12-11. Variation in Bin 11 Base Case pH as a Function of Pco_2

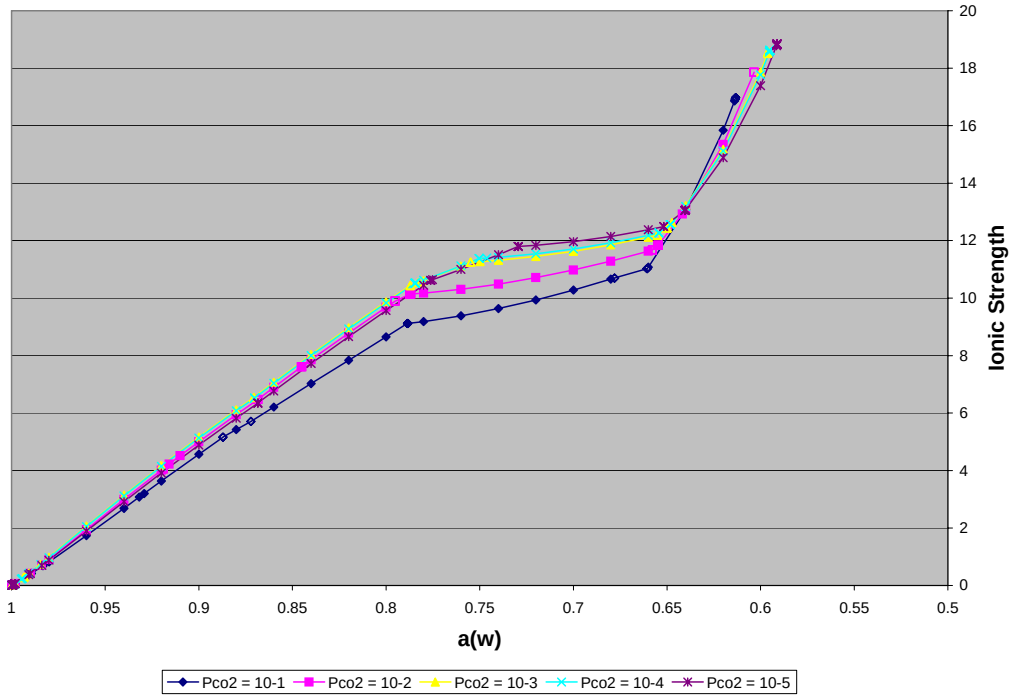

DTN: MO0310SPAPCEUA.002

Figure 6.12-12. Variation in Bin 11 Base Case Ionic Strength as a Function of Pco_2

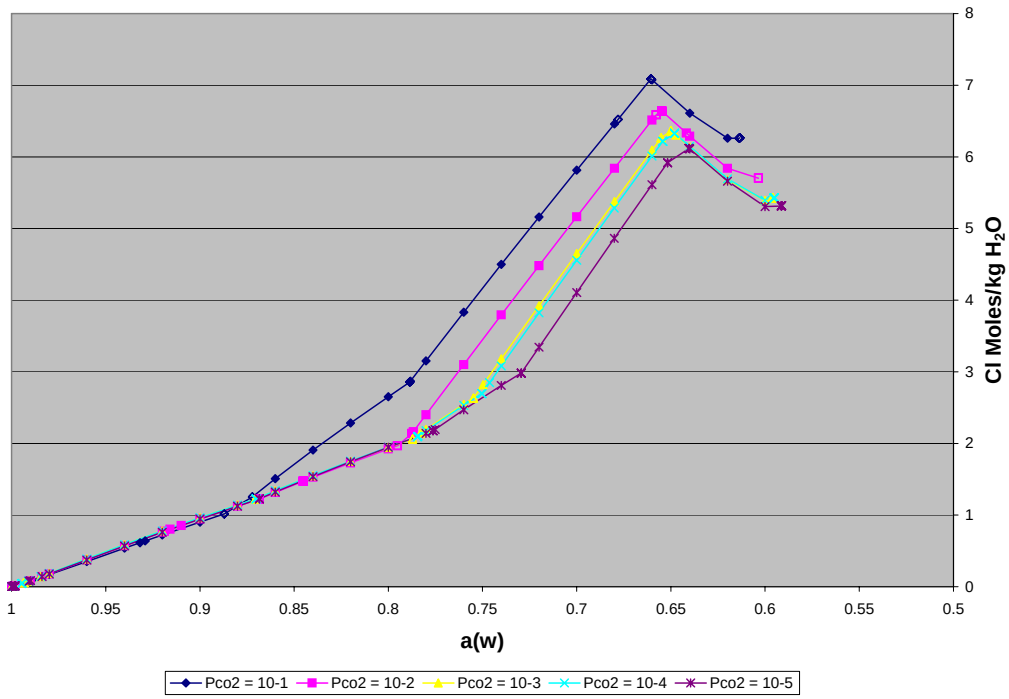

DTN: MO0310SPAPCEUA.002

Figure 6.12-13. Variation in Bin 11 Base Case Total Elemental Cl as a Function of Pco_2

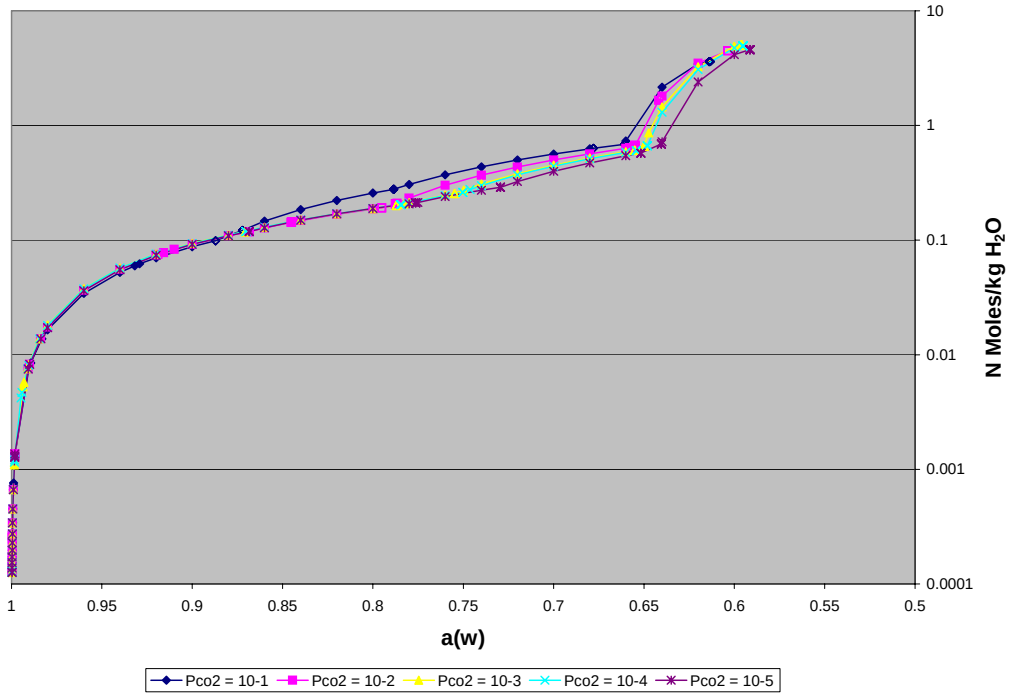

DTN: MO0310SPAPCEUA.002

Figure 6.12-14. Variation in Bin 11 Base Case Total Elemental N as a Function of Pco_2

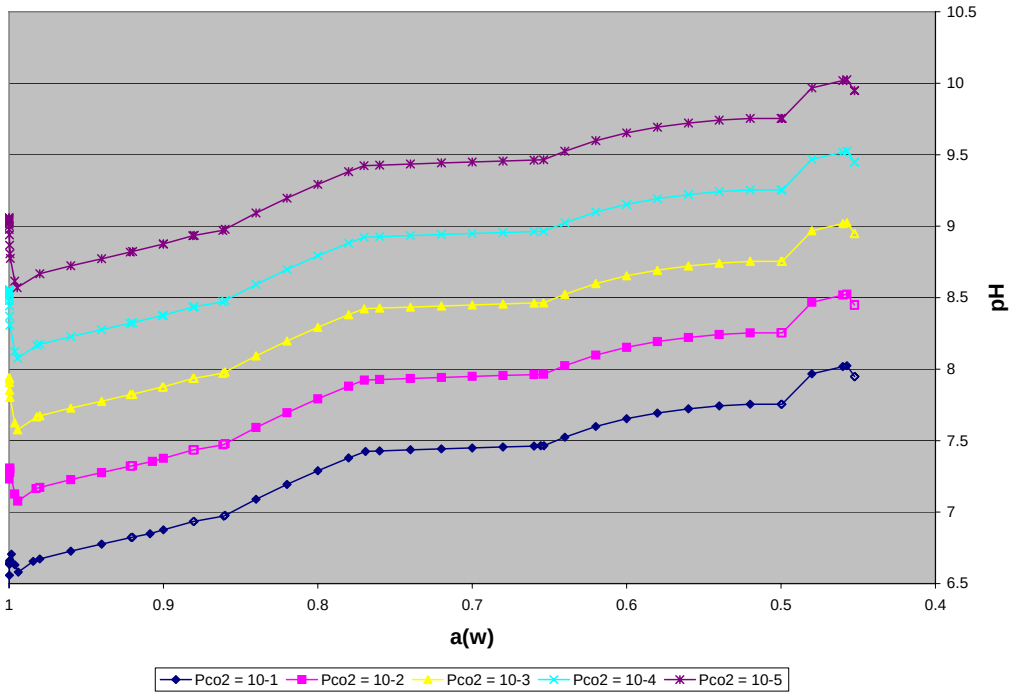

DTN: MO0310SPAPCEUA.002

Figure 6.12-15. Variation in Bin 5 Base Case pH as a Function of Pco_2

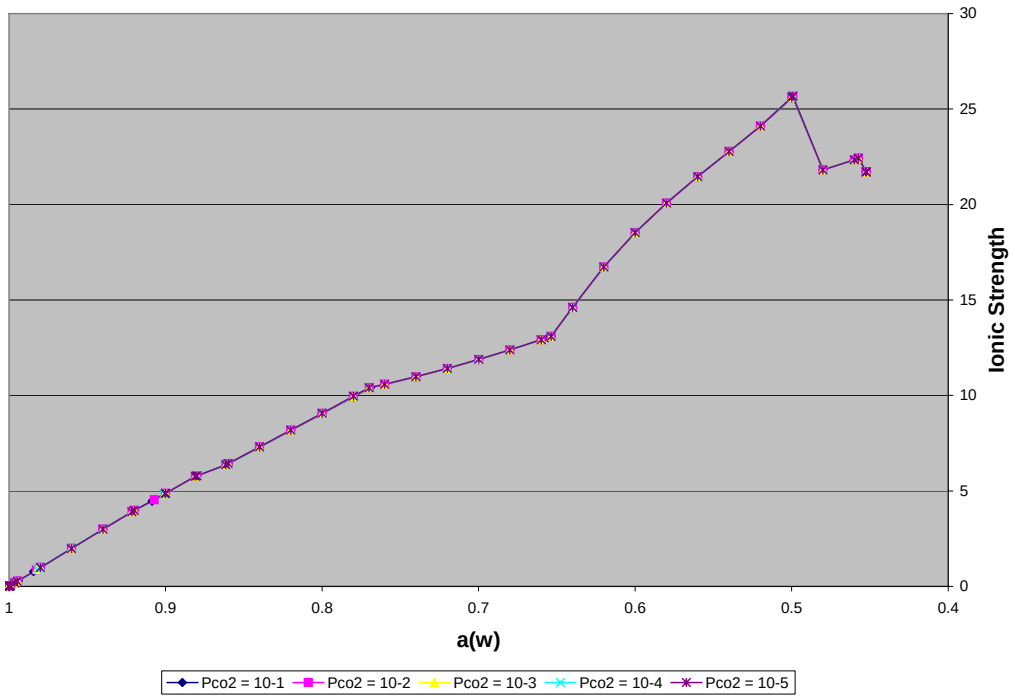

DTN: MO0310SPAPCEUA.002

Figure 6.12-16. Variation in Bin 5 Base Case Ionic Strength as a Function of Pco_2

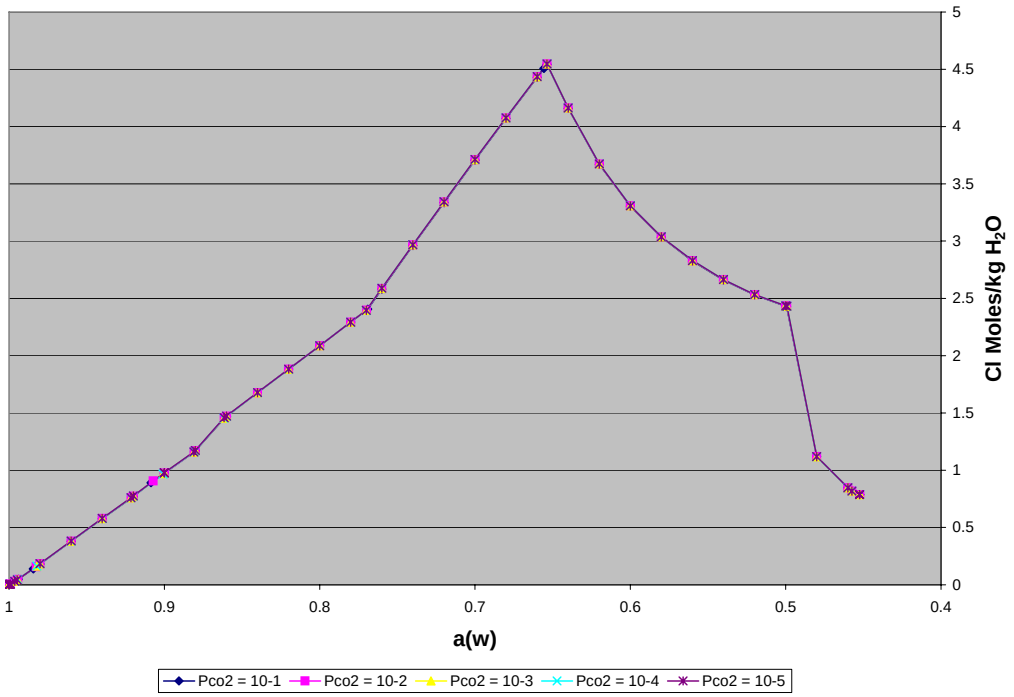

DTN: MO0310SPAPCEUA.002

Figure 6.12-17. Variation in Bin 5 Base Case Total Elemental Cl as a Function of Pco_2

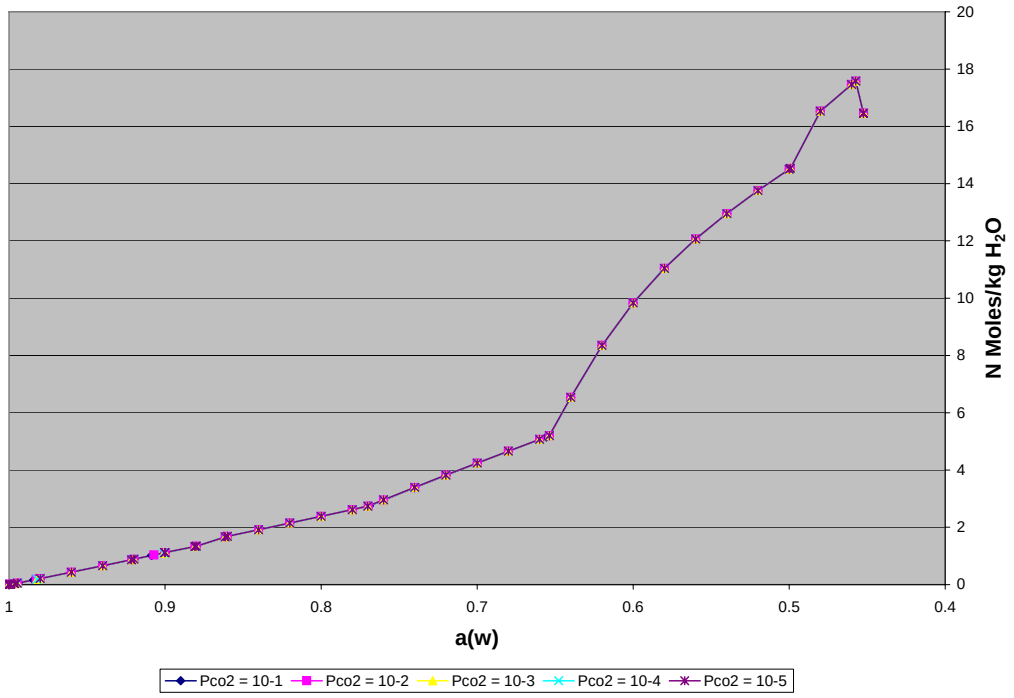

DTN: MO0310SPAPCEUA.002

Figure 6.12-18. Variation in Bin 5 Base Case Total Elemental N as a Function of Pco_2

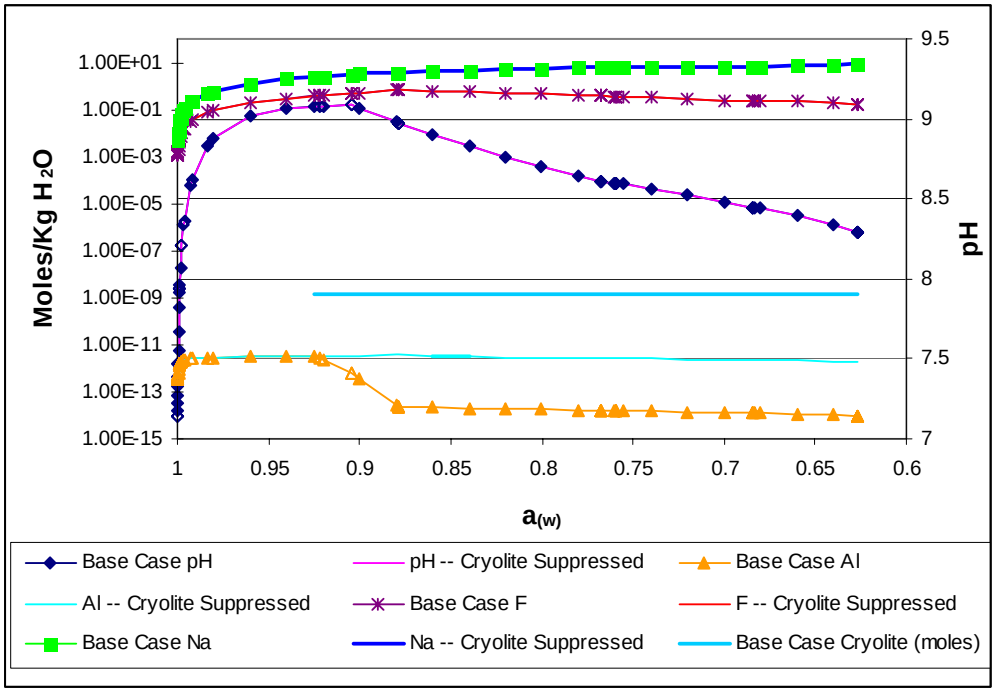

DTN: MO0310SPAPCEUA.002

Figure 6.12-19. Comparison of Base Case EQ6 Results with those of the Cryolite-Suppressed Modeling Run

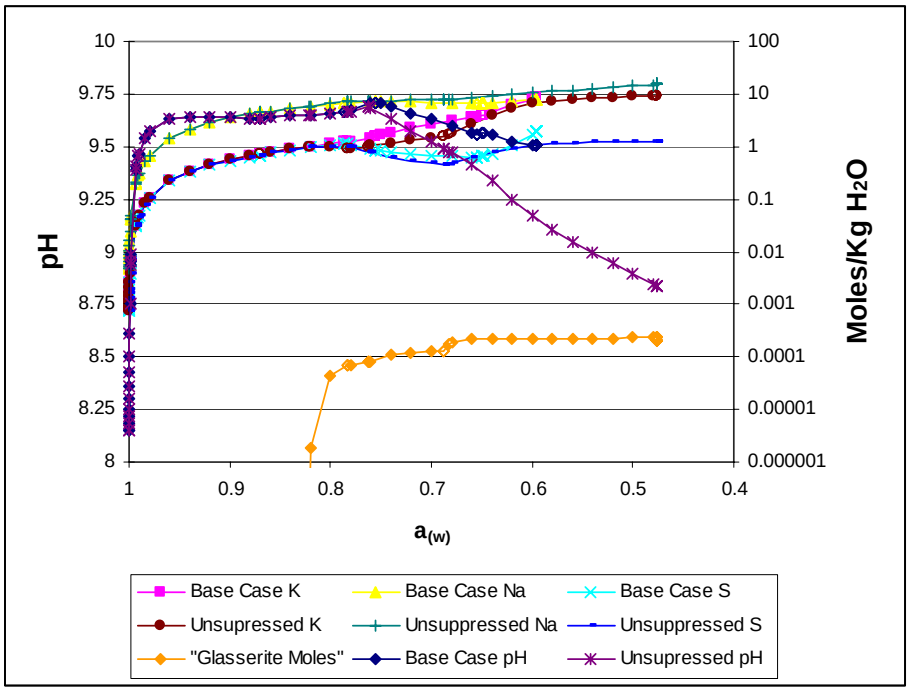

DTN: MO0310SPAPCEUA.002

Figure 6.12-20. Comparison of Base Case Results to those of the Same Modeling Run with Glaserite Unsuppressed

6.13 ENGINEERED BARRIER SYSTEM CHEMICAL ENVIRONMENT

The engineered barrier system chemical environment analyses focus on a quantitative description of the pH, ionic strength (I), and major ionic and elemental compositions of waters in contact with the waste package and drip shield and the invert. The brines that form by evaporative concentration from the crown seepage over time can potentially affect localized corrosion rates on the waste package and drip shield, and influence radionuclide mobility in the invert. Corrosion of the C-22 alloy forming the waste package may lead to premature release of radionuclides from the waste form. Elemental ratios such as Cl:N are important in assessing the potential for localized corrosion of the waste package in the engineered barrier system environment (BSC 2003 [DIRS 161235] and BSC 2003 [DIRS 161236]). Acidic or alkaline pH values of water in the invert can enhance the solubility of radionuclides. The ionic strength of water in the invert will control the mobility of colloidal material transporting sorbed radionuclides.

In addition, dust that accumulates on waste packages or drip shields during the operational and ventilation time periods may contain soluble salts, which will cause water condensation if the in-drift humidity is higher than the minimum deliquescent point of the salts. The resulting concentrated solution can potentially affect the degradation of the waste package outer barrier and drip shield.

This section summarizes the results of the P&CE model described in this document, establishing the magnitude and range of chemical variables in the processes involved, and establishing the foundation for the TSPA-LA modeling approach for the engineered barrier system environment.

Two terms, widely used in this document, are defined again here to ensure that the reader understands the material presented in this section. “Bin” is defined as a group of THC seepage model output waters with physical and chemical characteristics (listed in Section 6.6.4), that fall within a single geochemical group as determined by chemical divides or precipitated minerals upon evaporation. A “bin history” is defined as the discretized version of the evolution curves (developed in Section 6.6.6) of the five THC seepage model starting water compositions, for both invert and crown seepage waters, in which the water compositions at each time interval are mapped to the compositional bins to which they belong.

As calculated in Section 6.8.4, the quantifiable effects of 316L stainless steel active corrosion on seepage water for pH and ionic strength are insignificant at 100 percent relative humidity and negligible at 98 percent relative humidity. Based on these results and the results of the uncertainty calculations presented in Section 6.12.4, it has been concluded that active corrosion of the ground support will not appreciably influence the composition of the seepage waters in the drift.

To determine the most likely water chemistries for both the waste package surface and the invert over a given time interval, a time-integrated bin probability is calculated for both the crown seepage and dust leachate waters from the bin histories. This provides a quantitative probability of occurrence for a given “binned” water type over the time interval of interest, and enables determination of which water compositions and concentrations are likely to occur in a given period.

Figure 6.13-1 has been created from the bin history maps (see Section 6.6.6) and other work prepared for model validation (see Section 7.2). This work is documented in spreadsheet "Time integration20013.xls" (archived in DTN: MO0312SPAPCESA.002). Figure 6.13-1 shows the bin history maps for each of the five waters in a color-coded scheme. Also calculated in this spreadsheet is the time-integrated bin probability for waters entering the crown of the drift and the invert. The probability is calculated by determining the relative percent of time each bin occurs for the five different waters. The relative weighting for a bin at a given time step is calculated by dividing the time step by the total length of the time interval examined. By totaling the relative weighting of the individual time steps according to bin, the percent of time the waters from each bin occur is calculated for each of the five different starting waters. This total is, for the specified time interval, the time-integrated probability of occurrence for each bin, for the five different waters entering the crown of the drift and the invert.

It should be noted that the bin history maps show the composition of most-likely seepage waters—the liquid water existing closest to the drift in any given time step. They do not necessarily represent water present at the drift face. At early times (<~1800 years), when temperatures exceed the boiling point of water at the drift wall, the vaporization barrier should prevent water from entering the drift. In these early time steps, the most proximal liquid water may be meters into the drift wall. Only after temperatures have cooled below boiling (96ºC at the elevation of the repository) will the given compositions correspond to waters at the drift face.

The resulting time-integrated bin probabilities for the first 20,000 years after closure are shown in Table 6.13-1 (crown seepage waters) and Table 6.13-2 (invert wicking waters), where each of the five starting waters are equally likely to occur and the normalized values reflect the sum total of all five starting waters. These probabilities represent the percent of time that each bin water is expected to enter the drift at the given location. For instance, in the first 20,000 years, if W0 is the chosen starting water, Bin 3 water will be present at the drift crown for 1.12 percent of the time, or 224 years. However, since all five waters are equally probable, Bin 3 water will be present at the crown, on the average, for 0.22 percent of the time, or 44 years. These probabilities are only applicable for the time interval 0-20,000 years, as the bin occurrences are not randomly distributed through time (see Figure 6.13-1).

Table 6.13-1. Time Integrated Bin Probability for Any Given Crown Seepage Bin (20,000 Year Case)

Water	W0 %	W4 %	W5 %	W6 %	W7 %	Sum %	Norm %
Bin 1	0.00%	0.00%	0.00%	0.00%	0.00%	0.00%	0.00%
Bin 2	0.00%	0.00%	0.00%	0.00%	0.00%	0.00%	0.00%
Bin 3	1.12%	0.00%	0.00%	0.00%	0.00%	1.12%	0.22%
Bin 4	2.62%	1.00%	1.00%	1.00%	1.50%	7.12%	1.42%
Bin 5	0.56%	1.87%	1.00%	0.00%	0.50%	3.93%	0.79%
Bin 6	25.82%	0.00%	0.00%	1.50%	0.00%	27.32%	5.46%
Bin 7	31.75%	26.48%	32.01%	0.25%	45.25%	135.74%	27.15%
Bin 8	12.50%	31.03%	12.50%	12.50%	12.50%	81.02%	16.20%
Bin 9	0.00%	12.50%	13.00%	39.75%	12.50%	77.75%	15.55%

Table 6.13-1. Time Integrated Bin Probability for Any Given Crown Seepage Bin (20,000 Year Case) (Continued)

Water	W0 %	W4 %	W5 %	W6 %	W7 %	Sum %	Norm %
Bin 10	0.00%	0.25%	13.24%	45.00%	0.00%	58.49%	11.70%
Bin 11	25.63%	26.88%	27.25%	0.00%	27.75%	107.50%	21.50%
Sum	100.00	100.00	100.00	100.00	100.00	500.00	100.00

Source: DTN: MO0312SPAPCESA.002

NOTE: W0 through W7 refer to the THC seepage model outputs as listed in Section 4.1.3.1.

Table 6.13-2. Time Integrated Bin Probability for Any Given Invert Wicking Seepage Bin (20,000 Year Case)

Water	W0 %	W4 %	W5 %	W6 %	W7 %	Sum %	Norm %
Bin 1	0.29%	0.00%	0.10%	0.10%	0.10%	0.59%	0.12%
Bin 2	2.17%	0.00%	0.19%	0.24%	0.69%	3.29%	0.66%
Bin 3	0.62%	0.00%	0.05%	0.00%	1.30%	1.97%	0.39%
Bin 4	1.37%	1.92%	1.87%	1.87%	1.46%	8.50%	1.70%
Bin 5	5.01%	1.37%	0.87%	0.00%	0.66%	7.92%	1.58%
Bin 6	12.50%	0.00%	0.00%	0.00%	1.00%	13.50%	2.70%
Bin 7	45.00%	26.48%	32.01%	0.25%	45.25%	148.99%	29.80%
Bin 8	12.50%	31.03%	12.50%	12.50%	12.50%	81.02%	16.20%
Bin 9	1.00%	12.50%	12.50%	40.04%	12.50%	78.53%	15.71%
Bin 10	0.00%	0.25%	13.24%	45.00%	0.00%	58.49%	11.70%
Bin 11	19.53%	26.45%	26.66%	0.00%	24.54%	97.18%	19.44%
Sum	100.00	100.00	100.00	100.00	100.00	500.00	100.00

Source: DTN: MO0312SPAPCESA.002

NOTE: W0 through W7 refer to the THC seepage model outputs as listed in Section 4.1.3.1.

The results in Table 6.13-1 show that for the drift crown, the probability of waters from Bins 1 and 2 coming in contact with the waste package and drip shield is zero. The bin waters most likely to be present as crown seepage through the critical time period (701 to 7000 years), when the repository is cooling down, are Bins 4, 9, and 11, with small amounts of time with waters from Bins 5 and 6. For the invert, during 701 to 7,000 years, waters from Bins 4, 5, 9, and 11 are dominant, with small amounts of time when Bin 6 water is most likely. However, from 7,001 to 20,000 years at both the crown and the invert, waters from Bins 7 and 8 are the most likely bins, with Bin 10 waters also occurring in both the crown and the invert, and Bin 6 only in the crown. For periods beyond 20,000 years, only Bin 8 waters will be present. Only during the high-temperature period (from 51 to 700 years) do the more corrosive Bin 1, 2, and 3 waters potentially enter the repository, with Bin 3 water possibly occurring in both the crown and the invert, and Bin 1 and 2 waters possibly occurring in the invert. This high temperature period is precisely the time when there is the least potential for liquid water to enter the drift, due to the heat energy generated within the waste packages.

These observations have been included in Table 6.13-3, which associates the bins with five general periods of repository time. These periods are associated with general thermal or operational constraints. They include the preclosure period (0-50 years), the boiling period (51-700 years), a hot period (701-2,000 years), a cool down period (2,001-7,000 years), and a return to ambient period (7,001-20,000) years. Although the chemistry is similar, the hot and cool-down periods are generally separated by a short, chemically distinct period that is shown both in the bin histories (Tables 6.6-8 through 6.6-12 and Figure 6.13-1) and the THC seepage results (Figures 6.6-20 through 6.6-29). It corresponds to the period in which the fractures in the drift wall start to rewet (see Figures 6.6-2 through 6.6-4).

Table 6.13-3. Water Bins Associated with Different Periods in the Repository Thermal History

Water Location	0-50 years (Preclosure)	51-700 years (Boiling)	701-2000 years (Hot)	2001-5000 years (Cool Down)	5001-20,000 years (Return to Ambient)
Crown	4,**7**,10	3,**4**,5,6,**9**,**11**	4,5,6,**9**,**11**	6,**9**,**11**	6,**7**,**8**,9,**10**
Invert	4,**7**,10	1,**2**,**3**,**4**,5,9,11	**4**,**5**,6,**9**,**11**	6,**9**,**11**	6,**7**,**8**,9,**10**

NOTE: Bins marked in bold are the most likely for each period, based on Figure 6.13-1.

At the edges of the repository, the duration of the heat pulse will be much shorter. The net effect of this distance on the "center of repository" results that are reported in this section would be to shorten the boiling and hot periods and result in reaching the cool down period sooner (see Table 6.13-3 for the associated bins).

Additional time integrated probability calculations are done for the period beyond 20,000 years (archived in DTN: MO0312SPAPCESA.002) exactly as described for the 20,000-year case, with the upper bound changed to 35,024, 50,034, and 100,000 years. These calculations demonstrate that for times greater than 20,000 years, Bin 8 waters increasingly become the most likely water type. Only the probabilities calculated at 20,000 years, the regulatory time interval, are used throughout the remainder of this document.

In addition to the time integrated bin probabilities previously discussed, a second discrete probability distribution is also presented. This approach looks at the probability of the occurrence of the waters from any given bin at any given time.

As described in Section 6.6, the abstraction of the THC model incoming seepage waters resulted in the definition of eleven groups of waters based on water type. Single median waters were chosen from these groups (or bins) to represent the bin in the abstraction. Bin histories were developed to mimic the incoming water compositions predicted by the THC model to be the most likely waters to seep into the drift.

Because there were five THC model runs, each with a different starting water composition (w0, w4, w5, w6, and w7), five bin histories are mapped for the crown seepage and five bin histories are mapped for the invert seepage (Section 6.6.6). These five THC starting water compositions are determined to be equally probable. Therefore, each bin has a 0 percent, 20 percent, 40 percent, 60 percent, 80 percent, or 100 percent probability of occurring in the TSPA-LA model at any given time.

The bin probabilities are calculated for the crown and invert seepage for the time intervals defined in the bin histories. They are presented in Tables 6.13-4 and 6.13-5. Time intervals are approximated where noted in the tables. Approximations have been made where time intervals did not exactly match between bin histories.

Table 6.13-4. Bin Probabilities for Crown Seepage as a Function of Time

Start (yr)	End (yr)	Bin 1	Bin 2	Bin 3	Bin 4	Bin 5	Bin 6	Bin 7	Bin 8	Bin 9	Bin 10	Bin 11
0.0	30.5	—	—	—	20%	—	—	60%	—	—	20%	—
30.5	52.0	—	—	—	—	20%	—	—	—	20%	—	60%
52.0	54.0	—	—	—	—	20%	—	—	—	20%	—	60%
54.0	57.5	—	—	—	—	—	20%	—	—	20%	—	60%
57.5	67.5	—	—	—	—	—	20%	—	—	20%	—	60%
67.5	87.5	—	—	—	—	20%	—	—	—	20%	—	60%
87.5	125.0	—	—	—	—	20%	—	—	—	20%	—	60%
125.0	175.0	—	—	—	20%	—	—	—	—	20%	—	60%
175.0	225.0	—	—	—	20%	—	—	—	—	20%	—	60%
225.0	275.0	—	—	20%	—	—	—	—	—	20%	—	60%
275.0	325.0	—	—	20%	—	20%	—	—	—	20%	—	40%
325.0	375.0	—	—	20%	20%	—	—	—	—	20%	—	40%
375.0	450.0	—	—	20%	20%	—	—	—	—	20%	—	40%
450.0	550.0	—	—	—	40%	20%	20%	—	—	20%	—	—
550.0	625.0	—	—	—	40%	20%	—	—	—	20%	—	20%
625.0	675.0	—	—	—	—	40%	—	—	—	20%	—	40%
675.0	725.0	—	—	—	—	—	—	—	—	20%	—	80%
725.0	775.0	—	—	—	—	—	—	—	—	20%	—	80%
775.0	900.0	—	—	—	—	—	—	—	—	20%	—	80%
900.0	1100.0	—	—	—	—	—	—	—	—	20%	—	80%
1100.0	1300.0	—	—	—	—	—	—	—	—	20%	—	80%
1300.0	1500.5	—	—	—	—	—	—	—	—	20%	—	80%
1500.5	1701.0	—	—	—	—	—	—	—	—	20%	—	80%
1701.0	1901.0	—	—	—	—	40%	20%	—	—	—	—	40%
1901.0	2101.0	—	—	—	80%	—	—	—	—	—	—	20%
2101.0	2301.0	—	—	—	—	—	—	—	—	20%	—	80%
2301.0	2701.5	—	—	—	—	—	—	—	—	20%	—	80%
2701.5	4002.5	—	—	—	—	—	—	—	—	20%	—	80%
4002.5	6003.5	—	—	—	—	—	—	—	—	20%	—	80%
6003.5	8505.0	—	—	—	—	—	20%	—	—	80%	—	—
8505.0	11289.0 [a]	—	—	—	—	—	20%	40%	—	—	40%	—
11289.0[a]	13791.0 [a]	—	—	—	—	—	—	80%	—	—	20%	—
13791.0 [a]	17511.5	—	—	—	—	—	—	60%	20%	—	20%	—
17511.5	35023.5	—	—	—	—	—	—	—	100%	—	—	—
35023.5	100000.0	—	—	—	—	—	—	—	100%	—	—	—

Source: DTN: MO0310SPAEBSCB.003

NOTE: [a] Approximated time interval cutoff to accommodate all bin histories.

Table 6.13-5. Bin Probabilities for Invert Seepage as a Function of Time

Start (yr)	End (yr)	Bin 1	Bin 2	Bin 3	Bin 4	Bin 5	Bin 6	Bin 7	Bin 8	Bin 9	Bin 10	Bin 11
0.0	30.5	—	—	—	20%	—	—	60%	—	—	20%	—
30.5	52.0	—	—	—	—	20%	—	—	—	20%	—	60%
52.0	54.0	—	—	—	—	—	—	—	—	20%	—	80%
54.0	57.5	—	—	—	—	—	—	—	—	20%	—	80%
57.5	67.5	—	40%	40%	20%	—	—	—	—	—	—	—
67.5	87.5	60%	—	—	20%	—	—	—	—	—	—	20%
87.5	125.0	20%	60%	—	—	—	—	—	—	—	—	20%
125.0	175.0	—	20%	—	80%	—	—	—	—	—	—	—
175.0	225.0	—	20%	—	80%	—	—	—	—	—	—	—
225.0	275.0	—	20%	—	20%	40%	—	—	—	20%	—	—
275.0	325.0	—	20%	20%	60%	—	—	—	—	—	—	—
325.0	375.0	—	20%	20%	40%	20%	—	—	—	—	—	—
375.0	450.0	—	20%	20%	20%	20%	—	—	—	20%	—	—
450.0	550.0	—	40%	—	60%	—	—	—	—	—	—	—
550.0	625.0	—	—	40%	40%	20%	—	—	—	—	—	—
625.0	675.0	—	—	20%	40%	20%	—	—	—	20%	—	—
675.0	725.0	—	—	—	40%	20%	—	—	—	20%	—	20%
725.0	767.0 [a]	—	—	—	40%	20%	—	—	—	20%	—	20%
767.0 [a]	792.0 [a]	—	—	—	20%	20%	—	—	—	20%	—	40%
792.0 [a]	900.0	—	—	—	20%	20%	—	—	—	20%	—	40%
900.0	1100.0	—	—	—	—	20%	20%	—	—	20%	—	40%
1100.0	1300.0	—	—	—	—	20%	—	—	—	20%	—	60%
1300.0	1500.5	—	—	—	—	20%	—	—	—	20%	—	60%
1500.5	1701.0	—	—	—	—	20%	—	—	—	20%	—	60%
1701.0	1901.0	—	—	—	—	20%	—	—	—	20%	—	60%
1901.0	2101.0	—	—	—	—	—	—	—	—	40%	—	60%
2101.0	2301.0	—	—	—	—	—	—	—	—	20%	—	80%
2301.0	2701.5	—	—	—	—	—	—	—	—	20%	—	80%
2701.5	4002.5	—	—	—	—	—	—	—	—	20%	—	80%
4002.5	6003.5	—	—	—	—	—	—	—	—	20%	—	80%
6003.5	8505.0	—	—	—	—	—	20%	—	—	80%	—	—
8505.0	11228.3 [a]	—	—	—	—	—	—	60%	—	—	40%	—
11228.3 [a]	13730.3 [a]	—	—	—	—	—	—	80%	—	—	20%	—
13730.3 [a]	17511.5	—	—	—	—	—	—	60%	20%	—	20%	—
17511.5	35023.5	—	—	—	—	—	—	—	100%	—	—	—

Source: DTN: MO0310SPAEBSCB.003

NOTE: [a]Approximated time interval cutoff to accommodate all bin histories.

6.13.1 Engineered Barrier System Seepage Chemistry

Section 6.9 describes the development of seepage evaporation model lookup tables that represent the pH, I, and chemical compositions (Ca, Na, K, Mg, Al, F, S, Si, N, Cl, and C) of crown seepage and seepage wicking into the invert. Attachment II contains figures that show the various chemical parameters as a function of relative humidity and concentration factor as well as the results from any of the 99 individual evaporation lookup tables. The results from all of the lookup tables are summarized as follows:

- Section 6.13.1.1 describes the distribution of starting water that would define which set of bin history maps could be used at any given time.
- Section 6.13.1.2 discusses what these lookup tables represent and the ranges of outputs associated with these tables.

6.13.1.1 Engineered Barrier System Seepage Chemistry Constraints

The THC Seepage model output (Table 4.1-13) is calculated at a discrete location in the repository associated with the Topopah Spring tuff lower lithophysal zone (Tptpll, BSC 2003 [DIRS 162050]). The assumption is made for this report, as discussed in Section 5.2.2, that the starting waters taken from the THC model, and their subsequent abstraction, can be applied throughout the repository as representing the full range of possible seepage water chemistries.

In Figure 5.2-1, the five starting waters selected by the THC seepage model for use in their model (the same five waters used in this P&CE model), represent the range of chemistries in the plotted data. Therefore, each of the five starting waters (w0, w4, w5, w6, and w7) is assigned a 20 percent probability of being selected as the starting water for a given realization. The selection of a starting water also dictates the bin history that a given model realization uses. The bin histories are located in Section 6.6.6 (see Tables 6.6-8 through 6.6-12). Selecting a starting water also establishes what the starting Pco_2 lookup table is for a given model realization. These lookup tables are found in Section 6.7.2.1 (see Tables 6.7-1 through 6.7-5). Both the bin history maps and Pco_2 lookup tables are produced for two source locations: crown seepage and invert wicking.

In-drift temperatures and relative humidity are calculated in another YMP process modeling document (see *Multiscale Thermohydrologic Model*, BSC 2003 [DIRS 166463]). As this data is not available currently, the model results presented here are generalized, and results are discussed in terms of ranges. Aside from the overall calculated ranges, specific ranges are discussed in Sections 6.13.4 and 6.13.5 for the five periods that are reported in Table 6.13-3. This provides the reader with compositional trends through time.

6.13.1.2 Engineered Barrier System Seepage Chemistry Response Surface Ranges

The set of seepage evaporation lookup tables developed and described in Section 6.9 are combined into one large lookup table to assess the overall ranges of model outputs. This combined lookup table, documented in DTN: MO0304SPACPSLT.000, defines 11 multidimensional response surfaces, one for each of the representative bin seepage waters. From these response surfaces, in-drift precipitates/salts model outputs can be interpolated for

water temperatures ranging from 40ºC to 100ºC, fugacities of CO_2 from 10^{-4} to 10^{-2} atmospheres, and relative humidity in the drift from 0 to 100 percent.

Figures 6.13-2 through 6.13-12 show the seepage evaporation lookup tables for each of the 11 bins. These figures are meant only to illustrate the general output trends. The actual values are provided in the specific lookup tables listed in Table 6.9-6. For each bin, there are nine evaporation runs represented, one for each combination of temperature (40ºC, 70ºC, and 100ºC) and CO_2 fugacity (10^{-4}, 10^{-3}, and 10^{-2} bar).

The combination of the nine individual lookup tables for each bin represents a response surface for the chemistry in that bin, so they suggest the potential ranges of outputs for the ranges of inputs simulated. These figures provide the entire range of values for each compositional variable. However, in the TSPA-LA simulations, the potential range of values is constrained to a single evolution path for each variable by the choice of P_{CO_2} and temperature. The predicted relative humidity will further constrains the possible value of each parameter to a narrow range on each curve.

For example, the Bin 1 results shown in Figure 6.13-2 indicate that pH could vary from 8 or 9 to 3.5 for the ranges of temperature, CO_2 fugacity, and relative humidity modeled. However, according to the bin maps in Section 6.6.6, Bin 1 water only occurs in the invert between 57.5 years and 125 years. During this period, the temperature will be high and the CO_2 fugacity and relative humidity will be relatively low. The most likely Bin 1 output values used in the TSPA-LA will correspond to those predicted at low relative humidity for the high temperature, low CO_2 fugacity simulation (01c4t1e). The pH curve that corresponds to this case in Figure 6.13-2 is that with the highest pH values at a relative humidity of less than 35 percent. Consequently, if the relative humidity is less than 60 percent during this time period, which is reasonable, then the most likely pH range for TSPA-LA Bin 1 output is approximately 5 to 6, a much smaller range than the pH response surface represented in Figure 6.13-2.

Figure 6.13-13 displays the all-bin response surface for two molar ratios: Cl/NO_3 which is potentially important to corrosion, and $(Cl+F)/(NO_3+SO_4)$, which provides information on additional ions that potentially inhibit corrosion. As is the case for the response surfaces for the individual components displayed in the previous figures in this section, the ranges for the ratios that are relevant to the TSPA-LA in any given time step are much smaller than the ranges plotted. In other words, many of the points plotted in Figure 6.13-13 (perhaps a majority based on an extrapolation of the analysis in the previous paragraph) have a TSPA-LA probability of occurrence that approaches zero.

6.13.1.3 Evaporative Brine Precipitate Mineralogy and Chemical Divide Phenomena

Each lookup table developed in Section 6.9 has an associated precipitating mineral assemblage. Mineral precipitation as a function of relative humidity and degree of evaporative concentration is presented for each individual lookup table in Attachment II. Table 6.13-6 summarizes the characteristic mineral assemblages for each of the 11 bins.

Table 6.13-6. Summary Table of Precipitating Minerals in Each of the Eleven Bins

Bin	Precipitating Minerals at the Start of EQ6 Runs	Additional Precipitating Minerals (Roman Numerals Represent the Precipitation Sequence)	Occurrence Notes
Bin 1	$SiO_{2(am)}$, Stellerite	Fluorite (I), Calcite (II), Anhydrite (III), Sepiolite (IV), Halite (V), Ca(NO3)2 (VI_a), $Ca(NO_3)_2{:}3H_2O$ (VI_b), $Ca(NO_3)_2{:}4H_2O$ (VI_c),	Sepiolite does not form at $Pco_2 = 10^{-2}$; Calcium Nitrates are strongly temperature dependant; a = 100ºC; b = 70ºC; c = 40ºC.
Bin 2	$SiO_{2(am)}$, Stellerite	Calcite (I), Fluorite (II), Anhydrite (III), Sepiolite (IV), Halite (V), Soda Niter (VI)	Soda Niter only forms at 40ºC.
Bin 3	Stellerite, $SiO_{2(am)}$	Fluorite (I), Calcite (II), Anhydrite (III), Sepiolite (IV), Halite (V), Sylvite (VI), Niter (VII)	$SiO_{2(am)}$ in one lookup table did not form at the start of the run; Niter only forms at 40ºC.
Bin 4	$SiO_{2(am)}$, Stellerite	Calcite (I), Fluorite (II), Anhydrite (III), Sepiolite (IV), Phillipsite (V), Glauberite (VI), Halite (VII), Pentasalt (VIII), Erionite (IX), Niter (X)	Zeolite minerals evolve in this bin in the following general manner: Stellerite to Phillipsite to Erionite; niter does not show up in the 100°C-simulations tables; erionite does not show up in the 40ºC modeling runs.
Bin 5	$SiO_{2(am)}$, Stellerite, Fluorite	Calcite (I), Sepiolite (II), Glauberite (III), Thenardite (IV), Erionite (V), Halite (VI), Syngenite (VII), Niter (VIII)	Syngenite does not form at 100ºC; Niter only forms in the 40ºC, $Pco_2 = 10^{-4}$ modeling runs.
Bin 6	Stellerite, Calcite, Sepiolite	$SiO_{2(am)}$ (I), Fluorite (II), Erionite (III), Thenardite (IV), Halite (V), Arcanite (VI), Natrite (VII_a), Nahcolite (VII_b), [Pirssonite, Burkeite, Trona] (VII_c)	Calcite and Sepiolite do not precipitate at the start of the run in one model simulation (06c2t4e); natrite does not form at 40ºC; nahcolite does not form at 100ºC or at $Pco_2 = 10^{-4}$; burkeite, pirssonite and trona only form at 40ºC and Pco_2 10^{-4}.
Bin 7	Calcite, Sepiolite, Stellerite	$SiO_{2(am)}$ (I), Fluorite (II), Erionite (III), Thenardite (IV), Halite (V), Arcanite (VI), Natrite (VII_a), Nahcolite (VII_b), [Pirssonite, Burkeite, Trona] (VII_c)	Calcite and Sepiolite do not precipitate at the start of the run in one model simulation (07c2t4e); stellerite does not precipitate at start of run in two of the three 100ºC runs; natrite does not form at 40ºC; nahcolite does not form at 100ºC or at $Pco_2 = 10^{-4}$; burkeite, pirssonite and trona only form at 40ºC and Pco_2 10^{-4}.
Bin 8	Calcite, Sepiolite	Stellerite (I), $SiO_{2(am)}$ (II), Erionite (III), Fluorite (IV), Natrite (V_a), Nahcolite (V_b), [Pirssonite, Trona, Burkeite, Niter] (V_c), Thenardite (VI), Halite (VII), Arcanite (VIII)	Sepiolite does not form at the start in one model run (08c2t4e); stellerite does not form at all in three modeling runs; natrite does not form at 40ºC, nahcolite does not form at 100ºC or at $Pco_2 = 10^{-4}$; burkeite, pirssonite, niter and trona only form at 40ºC and Pco_2 10^{-4}. When these 4 minerals form, thenardite does not.
Bin 9	Stellerite	Calcite (I), Sepiolite (II), $SiO_{2(am)}$ (III), Fluorite (IV), Erionite (V), Villiaumite (VI), Natrite (VII_a), [Nahcolite, Sellaite, Cryolite] (VII_b), [Trona, Burkeite] (VII_c), Halite (VIII), Arcanite (IX)	Calcite does not form in two model runs (09c2t4e, 09c2t7e); natrite does not form at 40ºC, nahcolite does not form at 100ºC or at $Pco_2 = 10^{-4}$; arcanite does not form at 100ºC; sellaite only appears at $Pco_2 = 10^{-2}$; cryolite, burkeite, and trona only form at 40ºC and Pco_2 10^{-4}; nahcolite, trona, burkeite, niter, sellaite and cryolite only form when natrite does not. Trona and burkeite form when natrite and nahcolite do not.

Table 6.13-6. Summary Table of Precipitating Minerals in Each of the Eleven Bins (Continued)

Bin	Precipitating Minerals at the Start of EQ6 Runs	Additional Precipitating Minerals (Roman Numerals Represent the Precipitation Sequence)	Occurrence Notes
Bin 10	Calcite, Sepiolite	Stellerite (I), $SiO_{2(am)}$ (II), Fluorite (III), Erionite (IV), Natrite (V_a), [Nahcolite, Sellaite, Cryolite] (V_b), [Trona, Burkeite, Niter] (V_c), Thenardite (VI), Villiaumite (VII) Arcanite (VIII), Halite (IX)	Sepiolite does not form at the start in one model run (10c4t1e); natrite does not form at 40ºC; nahcolite does not form at 100ºC or at $Pco_2 = 10^{-4}$, sellaite and cryolite only appear at $Pco_2 = 10^{-2}$; nahcolite, trona, burkeite, niter, sellaite and cryolite only form when natrite does not; trona, burkeite and niter only form when thenardite does not.
Bin 11	Fluorite, $SiO_{2(am)}$, Stellerite, Sepiolite	Calcite (I), Erionite (II), Villiaumite (III), Thenardite (IV_a), [Burkeite, Trona, Niter] (IV_b), Natrite (V_a), [Sellaite, Cryolite, Nahcolite] (V_b), [Sellaite, Nahcolite], (V_c), Nahcolite (V_d), Halite (VI), Arcanite (VII)	Sepiolite does not form at the start in two model runs (11c2t7e, 11c2t4e); calcite does not form in some model runs (11c2t4e, 11c4t1e, and 11c2t7e); burkeite, trona and niter only form when thenardite and natrite do not form; Vc and Vb only form when no calcite is present.

Source: DTN: MO0312SPAPCESA.002

Based on the discussion of chemical divides in Section 6.2, an analysis of the lookup table mineralogy is provided in the following paragraphs, linking each of the bins to the precipitation of a particular sequence of minerals. The analysis is performed by extracting the mineral data from the EQ6 output files listed on Table 6.9-5 into Excel spreadsheet *11 bin mineral assemblage.xls* using GETEQDATA software. This spreadsheet is archived in DTN: MO0312SPAPCESA.002. Within the spreadsheet, a simplified paragenetic sequence is constructed for each bin based on the order of mineral appearance, the temperature, and Pco_2 of each evaporated brine. This worksheet is the source of the information found on Table 6.13-6.

Using the information on Table 6.13-6, Figure 6.13-14 is constructed to illustrate which precipitating minerals control the trajectory of brine evolution as the seepage waters are evaporated.

Although not directly equivalent to the classical chemical divides, as shown in Drever (1988, p. 236 [DIRS 118564]) (see Figure 6.2-1), Figure 6.13-14 does show the mineral phases that precipitate as the THC seepage waters evaporate, and that are associated with the 11 Bins. The presence or absence of anhydrite in the precipitated mineral assemblage separates the evaporative brine evolution of Bins 1 through 4 from Bins 5 through 11. Combined with the comparative pH results of all bins shown in Figures 6.13-15 and 6.13-16, three major groupings of brine chemistry and mineral precipitation can be seen, where not only the presence or absence of anhydrite but the presence or absence of glauberite is associated with the distribution of the pH. In general, the sequencing of natrite, thenardite, and villiaumite characterizes the evolution of Bins 6 through 11. Bins 1 through 3 are characterized by early precipitation of halite and Bins 4 and 5 by the precipitation of glauberite. Bins 6 and 7 are a result of the binning criterion shown in Figure 6.13-14. In no cases do any calcium chloride, magnesium chloride, or calcium-magnesium chloride minerals, such as bischofite and tachyhydrite, precipitate.

6.13.2 Engineered Barrier System Dust Deliquescence Chemistry

Section 6.10 describes the development of lookup tables that represent the chemical compositions of dust leachate and brines forming by deliquescence on the waste package and drip shield surfaces. Attachment III contains figures for each individual lookup table that show the various chemical parameters as a function of relative humidity and concentration factor as well as the results of any individual lookup tables. The combined results from all lookup tables are discussed in the following paragraphs. Section 6.13.2.1 describes the distribution of starting waters and other initial modeling constraints that should be imposed on the results. Section 6.13.2.2 discusses what the dust leachate lookup tables represent and the ranges of outputs associated with these lookup tables.

6.13.2.1 Engineered Barrier System Dust Deliquescence Chemistry Constraints

When seepage into the repository does not occur, deliquescence of salts in dust deposited on the waste package and drip shield will control the chemistry of in-drift waters that affect corrosion. As shown on Table 6.10-6, the six dust leachate bins have a discrete probability of occurrence. The bin probabilities listed in Table 6.10-6 will serve as the likely distribution of waters formed by deliquescence (equivalent to assigning an equal probability of occurrence to all sampled waters; see Assumption 5.2.3). To determine the value for $P\mathrm{co}_2$ in the drift, it is necessary to utilize a $P\mathrm{co}_2$ lookup table. As stated in Section 6.13.1.1, the probability for any given $P\mathrm{co}_2$ lookup table is tied to the probability of the starting water associated with that table. In the absence of seepage, each of the five lookup tables is given an equal probability of occurrence. These lookup tables are provided in Section 6.7.2.1 (see Tables 6.7-1 through 6.7-5).

Figure 6.13-17 shows the H_2O vapor pressure curves associated with the activity of water (or *RH*) for all lookup tables at or above 100°C. Also plotted (orange line) is the pressure that is reported by the THC seepage model for in-drift pressures through time (0.89 bars; see THC CO2 GAS& TEMP COMPARE.xls archived in DTN: MO0308SPACO2GL.001 developed in Section 6.7). The intersection of these two values indicates the maximum value of water activity at which aqueous solutions can deliquesce on waste packages, given the drift pressure conditions. Essentially, any temperature and pressure condition above the orange line will not be able to sustain liquid water. These conditions indicate that there is no liquid water in the drift above 140°C, and limited liquid water at 120°C (water present below 44 percent *RH*) and 100°C (water present below 88 percent *RH*). However, uncertainties in the deliquescence relative humidity may shift the endpoints in these curves, so the possibility of liquid water at somewhat higher temperatures cannot be ruled out.

In-drift temperatures and relative humidity are calculated in other YMP process modeling documents. As these data are not available currently, the model presented here is generalized, in which its results are discussed in terms of ranges.

6.13.2.2 Engineered Barrier System Dust Deliquescence Chemistry Response Surface Ranges

The set of dust leachate lookup tables developed and described in Section 6.10 are combined into one large lookup table to assess the overall ranges of model outputs. This combined lookup

table, which is documented in DTN: MO0310SPAPCELA.002, defines six multidimensional response surfaces, one for each of the representative dust bin waters. From these response surfaces, the model outputs can be interpolated for temperatures ranging from 40ºC to 140ºC, fugacities of CO_2 from 10^{-4} to 10^{-2} atmospheres, and relative humidity from 0 to 100 percent.

Figures 6.13-18 through 6.13-23 show the water chemistries contained in the dust leachate lookup tables for each of the six bins. These figures are meant only to illustrate the general output trends. The actual values are provided in the specific lookup tables listed in Table 6.10-14. For each bin, there are fifteen evaporation runs represented, one for each combination of temperature (40ºC, 70ºC, 100°C, 120°C, and 140ºC) and CO_2 fugacity (10^{-4}, 10^{-3}, and 10^{-2} bar).

The combination of the 15 individual lookup tables for each bin represents a response surface for the chemistry in that bin, so they suggest the potential ranges of outputs for the ranges of inputs simulated. These figures provide the entire range of values for each compositional variable, but in the TSPA-LA simulations, the potential range of values are constrained by the choice of P_{CO_2} and temperature to a single evolution path for each variable. The predicted relative humidity will further constrains the possible value of each parameter to a narrow range on each curve.

For example, the Bin 1 results shown in Figure 6.13-18 indicate that the range in possible pH values range from 6.3 – 8 in the initial waters, up to 10 for specific values of temperature, CO_2 fugacity, and relative humidity modeled. However, according to the bin distribution in Section 6.10.5.3.2 (see Table 6.10-6), Bin 1 water only occurs about 5.8 percent of the time. The most likely bin (Bin 5) occurs about 44.2 percent of the time. The range of pH covered by this bin is 8 to 11.5, as shown on Figure 6.13-23.

Figure 6.13-24 displays the all-dust bin response surface for the two molar ratios Cl/NO_3 and $(Cl+F)/(NO_3+SO_4)$. As was the case with the seepage waters, the ranges for these ratios that are relevant to the TSPA-LA may be smaller than the ranges plotted.

6.13.2.3 Dust Leachate Evaporative Brine Precipitate Mineralogy and Chemical Divide Phenomena

Each lookup table developed in Section 6.10 has associated with it a precipitating mineral assemblage. Mineral precipitation as a function of relative humidity and degree of evaporative concentration is presented for each individual lookup table in Attachment III. Table 6.13-7 summarizes the characteristic mineral assemblages for each of the six bins.

Based on the discussion of chemical divides in Section 6.2, an analysis of the lookup table mineralogy is provided below, linking each of the six bins to the precipitation of a particular sequence of minerals. The analysis is performed by extracting the mineral data from the EQ6 output files listed on Table 6.10-12 into Excel spreadsheet *Modified Dust Mineral Assemblage Spreadsheet.xls* using GETEQDATA. This spreadsheet is archived in DTN: MO0310SPAPCELA.002. Within the spreadsheet, a simplified paragenetic sequence is constructed for each bin based on the order of mineral appearance, the temperature, and Pco_2 of each evaporated brine. This worksheet is the source of the information found on Table 6.13-7.

Using the information on Table 6.13-7, Figure 6.13-25 has been constructed to provide an understanding as to which precipitating minerals are associated with the trajectory of brine evolution as the dust leachate waters are evaporated.

Table 6.13-7. Summary Table of Precipitating Minerals in Each of the Six Dust Leachate Evaporation Bins

Bin	Precipitating Minerals at the Start of EQ6 Runs	Additional Precipitating Minerals (Numerals Represent Precipitation Sequence) [Brackets Represent Limited Precipitation]	Occurrence Notes
Bin 1	Calcite, Sepiolite, [Brucite]	Anhydrite (I), Sellaite (II), Halite (III), [Fluorite (IV)], Huntite (V), Niter (VI), Soda Niter (VII), KBr (VIII), [Ca $(NO_3)_2$]	Brucite forms only at or above 100°C and $Pco_2 = 10^{-3}$ or higher; calcite always precipitates at the start of a run except at $Pco_2 = 10^{-2}$ and temperature =100°C; sepiolite always forms first or second in sequence for all Pco_2 and temperature conditions; fluorite only forms at 100°C or higher at $Pco_2 = 10^{-4}$; $Ca(NO_3)_2$ only forms in one model simulation (d1c4t14.6o).
Bin 2	Calcite, [Brucite]	Sepiolite (I), Anhydrite(II), Sellaite (III) [Fluorite (IV)], Huntite (V), Glauberite (VI), Pentasalt (VII), Halite (VIII), [Sylvite (IX)], Niter (X), KBr (XI)	Calcite always precipitates first in sequence for all Pco_2 and temperature conditions; sepiolite always forms either second or third in sequence; brucite forms only at or above 100°C and Pco_2 of 10^{-3} or higher. Niter and KBr always form late in sequence when present; fluorite only forms at $Pco_2 = 10^{-4}$ and temperatures =100°C or higher; pentasalt never forms above 100°C; sylvite only forms at 140°C; anhydrite usually forms after calcite or after sepiolite in sequence.
Bin 3	Calcite, [Brucite]	Sepiolite (I), Sellaite (II), Fluorite (III), Huntite (IV), Arcanite (V), Thenardite (VI), [Nahcolite (VIIa), Hallite (VIIIa)], [Thermonatrite (VIIb), Hallite (VIIIb)], [Natrite (VIIc), Hallite (VIIIc)], [Niter (VIId) KBr (VIIId)]	Calcite always precipitates first in sequence for all Pco_2 and temperature conditions; sepiolite always forms either second or third in sequence; sellaite usually forms after sepiolite; brucite forms only at or above 100°C and $Pco_2 = 10^{-3}$ or higher; niter and KBr form late in sequence when present; thermonatrite only precipitates at 100°C; villiaumite, pirssonite and burkeite precipitate in one calculation each.
Bin 4	Calcite, [Brucite]	Sepiolite (I), Anhydrite (II), [Sellaite (III)], [Huntite (IV)], [Fluorite (V)], Glauberite (VI), Halite (VII), Niter (VIII), Soda Niter (IX), KBr (X)	The first few minerals to precipitate at 70°C or higher usually are calcite (or brucite), sepiolite, anhydrite (or sellaite); brucite forms only at or above 100°C and $Pco_2 = 10^{-3}$ or higher; niter and KBr always form late in sequence when present; fluorite only precipitates at $Pco_2 = 10^{-4}$ and temperatures at 100°C or above.
Bin 5	Calcite, [Brucite]	Sepiolite(I), Fluorite (II), Sellaite (III), Glauberite (IV), Thenardite (V), Halite (VI), Niter (VII), KBr (VIII), [Soda Niter (IXa), Darapskite (IXb)]	Calcite always precipitates at the start of a run, usually followed by sepiolite; commonly, after sepiolite forms, fluorite, sellaite, and glauberite form; brucite forms only at or above 100°C and $Pco_2 = 10^{-3}$ or higher; niter, KBr, soda niter, and darapskite form late in sequence when they are present.
Bin 6	Calcite, [Brucite]	Sepiolite (I), $SiO_{2(am)}$ (II), Fluorite (III), Arcanite (IV), [Villiaumite (V), Thenardite (VI), Natrite (VII), Nahcolite (VIII), Halite (IX), Pirssonite (X), Sylvite (XI), Niter (XII), KBr (XIII)]	Calcite usually precipitates first in sequence and sepiolite second; after sepiolite precipitates, either fluorite, arcanite, or $SiO_{2(am)}$ usually form; brucite forms only at or above 120°C and $Pco_2 = 10^{-3}$ or higher; halite never forms above 100°C; nahcolite only forms at 40°C; sylvite never forms above 100°C; niter never forms above 70°C.

Source: DTN: MO0310SPAPCELA.002

Although not directly equivalent to Figure 6.2-1 in its chemical divides, Figure 6.13-25 does show the mineral phases associated with the brine evolution of the dust leachate waters as they are associated with the six leachate evaporation bins. The presence or absence of anhydrite divides Bins 1, 2, and 5 from Bins 3, 4, and 6. Comparing the results shown on Figure 6.13-26, three major groupings of brine chemistry evolution can be seen where not only the presence or absence of anhydrite but the presence or absence of glauberite is associated with the general trajectory of the pH. In general, the precipitation of glauberite is associated with waters in Bins 2, 4, and 5. Bins 3 and 6 are associated with arcanite. Bin 2 is characterized by the early precipitation of halite. In no cases do any calcium chloride, magnesium chloride or calcium-magnesium chloride minerals, such as bischofite and tachyhydrite, precipitate.

6.13.3 Lookup Table Interpolation for Seepage and Deliquescence Conditions

Aside from the general modeling uncertainty discussed in Section 6.12, this section considers the interpolation requirements associated with implementing the lookup tables within the TSPA-LA. The lookup tables contain two types of parameters, independent and dependent. The independent parameters are relative humidity, temperature, and carbon dioxide fugacity. Values for these parameters are needed to determine the values of the dependent parameters, such as the pH, or the total concentration of a dissolved chemical component (chloride, for example).

The independent variables in the lookup tables (i.e., relative humidity, temperature, and CO_2 fugacity) have their own uncertainty in the TSPA-LA realizations. The uncertainties for temperature and relative humidity are defined outside the physical and chemical environment model and are not addressed here. As for CO_2 fugacity, tables are generated from the THC model results in Section 6.7.2, and overall statistics on CO_2 fugacity are reported. When a given water type is selected for any given TSPA-LA model realization, the $P\mathrm{co}_2$ value becomes a discrete value over the time interval in the given lookup table designation. Therefore, the interpolation range over that given time period is established by looking at the previous time step's value and the next time step's value. This gives the total range that is associated with that period. For example, when using Table 6.7-1 for the interval from 200 to 250 years, the drift $P\mathrm{co}_2$ is set at $4.34 \cdot 10^{-4}$ bar. The $P\mathrm{co}_2$ for that period would range between $5.28 \cdot 10^{-4}$ (the value for the preceding period) and $3.18 \cdot 10^{-4}$ bar (the value for the following period). This range is far smaller than the overall range that is associated with in-drift $P\mathrm{co}_2$, as discussed in Section 6.7.2.

The lookup tables provide direct results only for select combinations of independent variables. That is, they provide results at temperatures of 40ºC, 70ºC, 100ºC (for both seepage and dust leachates), 120ºC and 140ºC for dust leachates, CO_2 fugacities of 10^{-2}, 10^{-3}, and 10^{-4} bar, and relative humidity at intervals up to 2 percent. Most humidity intervals are less than 2 percent. The TSPA-LA model is designed to interpolate and extrapolate ($P\mathrm{co}_2$ parameter only) dependent variable outputs for other combinations of these parameters (except for temperatures above 140ºC and below 40ºC, see Section 6.7.2.2). By interpolating and extrapolating, the lookup tables provide a set of smooth and continuous response surfaces. Although some error may be introduced by interpolation and extrapolation, this error is negligible compared to model uncertainty and uncertainty in the predicted values of the independent variables (see Section 6.12 for uncertainty analysis).

6.13.4 Chemical Environments on the Drip Shield and Waste Package

In addition to pH and ionic strength, the main parameter of interest for drip shield performance is the concentration of F in the solution, because fluoride has a strong influence on titanium corrosion rates. For the waste package environment, the primary aqueous components of concern include Cl, N, and S, and to some extent other halides such as Br, because high concentrations of these elements enhance corrosion of Alloy 22. In addition to these chemical parameters, other particular parameters of interest are deliquescence points, brine compositions, and brine evolution. Each of these is discussed in terms of the two major outputs of this model, the composition of in-drift seepage and dust leachate type waters.

In order to develop an argument that supports the use of probabilities and distributions for the seepage water inputs, an assumption is made (see Assumption 5.2.2 for basis and further discussion), that the 368 waters used to initiate this abstraction and their bin percentages (see Table 6.6-4), as discussed in Section 6.6, represent a reasonable distribution of all waters entering the drift through all time.

6.13.4.1 Seepage

From Tables 6.13-1 through 6.13-3, waters from Bins 1 and 2 are not deemed to be relevant for the waste package or drip shield, and there is some correlation through time for which bins are most likely. For pH, Figure 6.13-15 shows that the seepage pH range varies from bin to bin as a function of relative humidity. The overall pH range is approximately 10.5 to 4.5. For Bin 3, the range is from about 8 to 4.5. As shown on Table 6.13-1, the time-integrated percentage of all of the 368 starting waters represented by this bin is less than 1 percent. For Bins 4 and 5, the pH range is between 6.5 and 8.5. These two bins account for about 20 percent of the locations on the bin history map (see Table 6.6-4), but only have a time-integrated probability of occurrence, in the first 20,000 years, of about 1.5 percent. For the remaining 70 percent of the starting waters (Bins 6 through 11) used in the abstraction, the pH range is from about 8 to 10.5. Therefore, the most likely pH range of seepage water on the waste package is from approximately 8 to 10.5. Bins 6 through 11 also represent 98 percent of the time-integrated bin probability (for the 20,000-year regulatory time interval).

Figure 6.13-27 shows the predicted concentrations of F for the lookup tables representing Bins 3 through 11. The figure indicates that the maximum molality that could be present is about 1. This occurs at a drift relative humidity above about 90 percent. The maximum values fall within Bins 9 and 6. Bin 9 has a high probability of occurrence in the boiling, hot, and cool down periods. Possible Cl concentrations are much higher, up to about 10 molal at low relative humidity (see Figure 6.13-28), and are relatively insensitive to bin choice.

Table 6.13-8 shows the brine compositions that develop during evaporative concentration of the engineered barrier system seepage waters, as presented in the TSPA-LA lookup tables. Also shown is the endpoint relative humidity of the brines represented by the 11 bins. Under most conditions, the seepage waters can be classified as one of three brine types: sodium chloride, sodium carbonate, or calcium chloride. Bins 1 through 3 show the accumulation of Ca and Cl is sufficient to make them the dominant cation and anion, respectively, as relative humidity decreases. Under these conditions, the potential for aggressive localized corrosion exists.

However, based on the bin history maps (Figure 6.13-1) bins 1 and 2 are not possible as crown seepage and the time integrated bin probability for Bin 3 over the 20,000-year regulatory timeframe is 0.22 percent (Table 6.13-1). In fact, Bin 3 waters only occur during the first several hundred years (Figure 6.13-1) when drift temperatures are high and liquid water is least likely to enter the drift. With the exception of Bins 8 through 10, the dominant anion is Cl, which could provide for corrosion potential (~72 percent), yet Bins 4 through 7 and 11 are not expected to be as aggressive as Bin 3 because of the absence of $CaCl_2$. Also evident from Figure 6.13-29 is the potential for six of the bins to have a Cl:N ratio above 10 at relative humidity conditions above 70 percent. In Bins 6 and 7, Cl:N ratios above 30 are possible. Bin 7 is associated with the cool down and preclosure periods and has a relatively high probability of occurrence in the 10,000 to 20,000 year interval (Figure 6.13-1). Bin 6 is associated with the hotter waste package temperatures that occur early in the repository history, and waters in this bin are much less likely to occur.

Additional plots have been included in the following figures to show the ranges in Bins 3 through 11 for total Ca, S, and C (Figures 6.13-30 through 6.13-32). Plots for Si, N, K, Mg, and Na are provided in spreadsheet "checked MOALT R0d2.xls" archived in DTN: MO0312SPAPCESA.002.

Somewhere between 100 and 95 percent relative humidity in the drift, the ionic strength of the evaporating solutions will go above 1 molal (see Figure 6.13-33). At lower relative humidity conditions, concentrations of well over 10 molal are possible. EQ6 results report the relative loss of water mass through the evaporative process. Figure 6.13-34 plots this water loss against the ionic strength. This figure shows that when the brines are very concentrated, the relative mass of water becomes extremely small. For example, when 1 kg of seepage water is concentrated to ionic strengths of 10 or greater, the mass of remaining water has become a gram or less. In some cases, the remaining brine is 10^{-4} grams or less. This indicates that the overall corrosion capability of the brines reacting with the waste package or drip shield should decrease as evaporation increases due to the substantial reduction in seepage water mass.

The mineral assemblages associated with Bins 3 through 11 are provided on Table 6.13-6. These minerals are likely to form on drip shield and waste package surfaces as seepage evaporites.

6.13.4.2 Dust Leachate

For a given set of temperatures, Pco_2, and humidity values, the chemical parameters that are most relevant to waste package degradation include pH, Cl, Cl/ NO_3, and (Cl + F)/(NO_3 + SO_4). From the lookup table calculations, it is determined that the brine pH is more sensitive to the in-drift temperature and Pco_2 changes than to the other parameters. Figure 6.13-26 shows that a decrease in Pco_2 from 10^{-2} to 10^{-4} bar would systematically increase pH by one unit over the whole evaporation range. To illustrate this effect, Figure 6.13-26 shows three groupings of curves for each bin. These three groupings reflect the Pco_2 concentrations trending downward from lowest to highest. As a result of the decrease of Pco_2, carbonate minerals precipitate, and the concentrations of Ca and Mg decrease. However, the effect of temperature on brine pH is more complicated and varies with humidity. Temperature effects are shown on Figure 6.13-26 by examining each bundle of five lines that is associated with a given Pco_2 group.

A change in temperature from 40 to 140°C generally results in pH variations of less than one-half a pH unit.

Table 6.13-8. Engineered Barrier System Seepage Lookup Table End Point Relative Humidity and Brine Evolution

Lookup Table File Name	Number of 6o Binning Files Matching this Sensitivity Run (number of waters in bin)	% of 368 Binning Output Runs	Bin	Temp.	Pco_2	Endpoint RH	98% RH Brine	85% RH Brine	65% RH Brine	Endpoint Brine
01c2t1e.xls.xls	5	1.4%	1	100	1.00E-02	20.0%	Ca-Cl	Ca-Cl	Ca-Cl	Ca-Cl
01c2t4e.xls.xls			1	40	1.00E-02	18.1%	Ca-Cl	Ca-Cl	Ca-Cl	Ca-Cl
01c2t7e.xls.xls			1	70	1.00E-02	18.7%	Ca-Cl	Ca-Cl	Ca-Cl	Ca-Cl
01c3t1e.xls.xls			1	100	1.00E-03	20.0%	Ca-Cl	Ca-Cl	Ca-Cl	Ca-Cl
01c3t4e.xls.xls			1	40	1.00E-03	18.1%	Ca-Cl	Ca-Cl	Ca-Cl	Ca-Cl
01c3t7e.xls.xls			1	70	1.00E-03	18.7%	Ca-Cl	Ca-Cl	Ca-Cl	Ca-Cl
01c4t1e.xls.xls			1	100	1.00E-04	20.0%	Ca-Cl	Ca-Cl	Ca-Cl	Ca-Cl
01c4t4e.xls.xls			1	40	1.00E-04	18.2%	Ca-Cl	Ca-Cl	Ca-Cl	Ca-Cl
01c4t7e.xls.xls			1	70	1.00E-04	18.7%	Ca-Cl	Ca-Cl	Ca-Cl	Ca-Cl
02c2t1e.xls.xls	13	3.5%	2	100	1.00E-02	24.0%	Na-Cl	Na-Cl	Na-Cl	Ca-Cl
02c2t4e.xls.xls			2	40	1.00E-02	23.1%	Na-Cl	Na-Cl	Na-Cl	Ca-Cl
02c2t7e.xls.xls			2	70	1.00E-02	23.4%	Na-Cl	Na-Cl	Na-Cl	Ca-Cl
02c3t1e.xls.xls			2	100	1.00E-03	24.0%	Na-Cl	Na-Cl	Na-Cl	Ca-Cl
02c3t4e.xls.xls			2	40	1.00E-03	23.1%	Na-Cl	Na-Cl	Na-Cl	Ca-Cl
02c3t7e.xls.xls			2	70	1.00E-03	24.0%	Na-Cl	Na-Cl	Na-Cl	Ca-Cl
02c4t1e.xls.xls			2	100	1.00E-04	24.0%	Na-Cl	Na-Cl	Na-Cl	Ca-Cl
02c4t4e.xls.xls			2	40	1.00E-04	23.1%	Na-Cl	Na-Cl	Na-Cl	Ca-Cl
02c4t7e.xls.xls			2	70	1.00E-04	24.0%	Na-Cl	Na-Cl	Na-Cl	Ca-Cl
03c2t1e.xls.xls	12	3.3%	3	100	1.00E-02	43.9%	Na-Cl	Na-Cl	Na-Cl	K-Cl
03c2t4e.xls.xls			3	40	1.00E-02	38.9%	Na-Cl	Na-Cl	Na-Cl	Ca-Cl
03c2t7e.xls.xls			3	70	1.00E-02	42.3%	Na-Cl	Na-Cl	Na-Cl	K-Cl
03c3t1e.xls.xls			3	100	1.00E-03	44.0%	Na-Cl	Na-Cl	Na-Cl	K-Cl
03c3t4e.xls.xls			3	40	1.00E-03	39.8%	Na-Cl	Na-Cl	Na-Cl	Ca-Cl
03c3t7e.xls.xls			3	70	1.00E-03	42.5%	Na-Cl	Na-Cl	Na-Cl	K-Cl
03c4t1e.xls.xls			3	100	1.00E-04	44.0%	Na-Cl	Na-Cl	Na-Cl	K-Cl
03c4t4e.xls.xls			3	40	1.00E-04	40.0%	Na-Cl	Na-Cl	Na-Cl	Ca-Cl
03c4t7e.xls.xls			3	70	1.00E-04	42.5%	Na-Cl	Na-Cl	Na-Cl	K-Cl
04c2t1e.xls.xls	43	11.7%	4	100	1.00E-02	47.4%	Na-Cl	Na-Cl	K-Cl	K-N
04c2t4e.xls.xls			4	40	1.00E-02	65.0%	Na-Cl	Na-Cl	Na-N	Na-N
04c2t7e.xls.xls			4	70	1.00E-02	52.9%	Na-Cl	Na-Cl	Na-N	Na-N
04c3t1e.xls.xls			4	100	1.00E-03	47.4%	Na-Cl	Na-Cl	K-Cl	K-N
04c3t4e.xls.xls			4	40	1.00E-03	65.0%	Na-Cl	Na-Cl	Na-N	Na-N
04c3t7e.xls.xls			4	70	1.00E-03	52.9%	Na-Cl	Na-Cl	Na-N	Na-N
04c4t1e.xls.xls			4	100	1.00E-04	47.4%	Na-Cl	Na-Cl	K-Cl	K-N
04c4t4e.xls.xls			4	40	1.00E-04	65.0%	Na-Cl	Na-Cl	Na-N	Na-N
04c4t7e.xls.xls			4	70	1.00E-04	52.9%	Na-Cl	Na-Cl	Na-N	Na-N
05c2t1e.xls.xls	27	7.3%	5	100	1.00E-02	60.1%	Na-Cl	Na-Cl	Na-Cl	Na-Cl
05c2t4e.xls.xls			5	40	1.00E-02	69.1%	Na-Cl	Na-Cl	No Brine	Na-Cl
05c2t7e.xls.xls			5	70	1.00E-02	62.1%	Na-Cl	Na-Cl	Na-Cl	K-Cl
05c3t1e.xls.xls			5	100	1.00E-03	60.1%	Na-Cl	Na-Cl	Na-Cl	Na-Cl
05c3t4e.xls.xls			5	40	1.00E-03	69.9%	Na-Cl	Na-Cl	No Brine	Na-Cl
05c3t7e.xls.xls			5	70	1.00E-03	62.1%	Na-Cl	Na-Cl	Na-Cl	K-Cl
05c4t1e.xls.xls			5	100	1.00E-04	60.1%	Na-Cl	Na-Cl	Na-Cl	Na-Cl
05c4t4e.xls.xls			5	40	1.00E-04	62.4%	Na-Cl	Na-Cl	Na-N	Na-N
05c4t7e.xls.xls			5	70	1.00E-04	62.1%	Na-Cl	Na-Cl	Na-Cl	K-Cl
06c2t1e.xls.xls	8	2.2%	6	100	1.00E-02	59.1%	Na-Cl	Na-Cl	Na-Cl	K-Cl
06c2t4e.xls.xls			6	40	1.00E-02	63.0%	Na-Cl	Na-Cl	Na-Cl	Na-N
06c2t7e.xls.xls			6	70	1.00E-02	60.5%	Na-Cl	Na-Cl	Na-Cl	K-Cl
06c3t1e.xls.xls			6	100	1.00E-03	59.1%	Na-Cl	Na-Cl	Na-Cl	Na-Cl
06c3t4e.xls.xls			6	40	1.00E-03	61.7%	Na-Cl	Na-Cl	Na-Cl	Na-N
06c3t7e.xls.xls			6	70	1.00E-03	59.7%	Na-Cl	Na-Cl	Na-Cl	K-Cl
06c4t1e.xls.xls			6	100	1.00E-04	58.9%	Na-Cl	Na-Cl	Na-Cl	Na-Cl
06c4t4e.xls.xls			6	40	1.00E-04	64.1%	Na-Cl	Na-Cl	Na-Cl	Na-Cl
06c4t7e.xls.xls			6	70	1.00E-04	59.6%	Na-Cl	Na-Cl	Na-Cl	K-Cl

Table 6.13-8. Engineered Barrier System Seepage Lookup Table End Point Relative Humidity and Brine Evolution (Continued)

07c2t1e.xls.xls	25	6.8%	7	100	1.00E-02	59.1%	Na-Cl	Na-Cl	Na-Cl	K-Cl
07c2t4e.xls.xls			7	40	1.00E-02	63.0%	Na-Cl	Na-Cl	Na-Cl	Na-N
07c2t7e.xls.xls			7	70	1.00E-02	60.5%	Na-Cl	Na-Cl	Na-Cl	K-Cl
07c3t1e.xls.xls			7	100	1.00E-03	59.1%	Na-Cl	Na-Cl	Na-Cl	Na-Cl
07c3t4e.xls.xls			7	40	1.00E-03	61.7%	Na-Cl	Na-Cl	Na-Cl	Na-N
07c3t7e.xls.xls			7	70	1.00E-03	59.7%	Na-Cl	Na-Cl	Na-Cl	K-Cl
07c4t1e.xls.xls			7	100	1.00E-04	60.0%	Na-Cl	Na-Cl	Na-Cl	Na-Cl
07c4t4e.xls.xls			7	40	1.00E-04	66.2%	Na-Cl	Na-Cl	No Brine	Na-Cl
07c4t7e.xls.xls			7	70	1.00E-04	59.6%	Na-Cl	Na-Cl	Na-Cl	K-Cl
08c2t1e.xls.xls	22	6.0%	8	100	1.00E-02	59.1%	Na-C	Na-C	Na-Cl	K-Cl
08c2t4e.xls.xls			8	40	1.00E-02	63.0%	Na-C	Na-Cl	Na-N	Na-N
08c2t7e.xls.xls			8	70	1.00E-02	60.5%	Na-C	Na-C	Na-Cl	K-Cl
08c3t1e.xls.xls			8	100	1.00E-03	59.1%	Na-C	Na-C	Na-Cl	Na-Cl
08c3t4e.xls.xls			8	40	1.00E-03	61.7%	Na-C	Na-C	Na-Cl	Na-N
08c3t7e.xls.xls			8	70	1.00E-03	59.7%	Na-C	Na-C	Na-Cl	K-Cl
08c4t1e.xls.xls			8	100	1.00E-04	58.9%	Na-C	Na-C	Na-Cl	Na-Cl
08c4t4e.xls.xls			8	40	1.00E-04	62.2%	Na-C	Na-C	Na-Cl	Na-Cl
08c4t7e.xls.xls			8	70	1.00E-04	59.6%	Na-C	Na-C	Na-Cl	K-Cl
09c2t1e.xls.xls	58	15.8%	9	100	1.00E-02	50.9%	Na-C	Na-C	Na-Cl	K-Cl
09c2t4e.xls.xls			9	40	1.00E-02	62.0%	Na-C	Na-Cl	Na-Cl	K-N
09c2t7e.xls.xls			9	70	1.00E-02	50.0%	Na-C	Na-C	Na-Cl	K-N
09c3t1e.xls.xls			9	100	1.00E-03	50.9%	Na-C	Na-C	Na-Cl	K-Cl
09c3t4e.xls.xls			9	40	1.00E-03	61.3%	Na-C	Na-C	Na-Cl	K-N
09c3t7e.xls.xls			9	70	1.00E-03	57.5%	Na-C	Na-C	Na-Cl	K-N
09c4t1e.xls.xls			9	100	1.00E-04	52.3%	Na-Si	Na-C	Na-Cl	K-N
09c4t4e.xls.xls			9	40	1.00E-04	62.1%	Na-C	Na-C	Na-Cl	K-N
09c4t7e.xls.xls			9	70	1.00E-04	49.8%	Na-C	Na-C	Na-Cl	K-N
10c2t1e.xls.xls	10	2.7%	10	100	1.00E-02	59.0%	Na-C	Na-C	Na-Cl	Na-Cl
10c2t4e.xls.xls			10	40	1.00E-02	66.1%	Na-C	Na-Cl	No Brine	Na-Cl
10c2t7e.xls.xls			10	70	1.00E-02	60.3%	Na-C	Na-C	Na-Cl	K-Cl
10c3t1e.xls.xls			10	100	1.00E-03	59.0%	Na-C	Na-C	Na-Cl	Na-Cl
10c3t4e.xls.xls			10	40	1.00E-03	61.5%	Na-C	Na-C	Na-Cl	Na-N
10c3t7e.xls.xls			10	70	1.00E-03	59.6%	Na-C	Na-C	Na-Cl	K-Cl
10c4t1e.xls.xls			10	100	1.00E-04	58.8%	Na-Si	Na-C	Na-Cl	Na-Cl
10c4t4e.xls.xls			10	40	1.00E-04	62.1%	Na-C	Na-C	Na-Cl	Na-N
10c4t7e.xls.xls			10	70	1.00E-04	59.5%	Na-C	Na-C	Na-Cl	K-Cl
11c2t1e.xls.xls	145	39.4%	11	100	1.00E-02	59.0%	Na-Cl	Na-Cl	Na-Cl	Na-Cl
11c2t4e.xls.xls			11	40	1.00E-02	62.7%	Na-Cl	Na-Cl	Na-Cl	Na-N
11c2t7e.xls.xls			11	70	1.00E-02	60.4%	Na-Cl	Na-Cl	Na-Cl	K-Cl
11c3t1e.xls.xls			11	100	1.00E-03	59.0%	Na-Cl	Na-Cl	Na-Cl	Na-Cl
11c3t4e.xls.xls			11	40	1.00E-03	61.5%	Na-Cl	Na-Cl	Na-Cl	Na-N
11c3t7e.xls.xls			11	70	1.00E-03	59.6%	Na-Cl	Na-Cl	Na-Cl	K-Cl
11c4t1e.xls.xls			11	100	1.00E-04	58.8%	Na-Cl	Na-Cl	Na-Cl	Na-Cl
11c4t4e.xls.xls			11	40	1.00E-04	62.1%	Na-Cl	Na-Cl	Na-Cl	Na-N
11c4t7e.xls.xls			11	70	1.00E-04	59.5%	Na-Cl	Na-Cl	Na-Cl	K-Cl

Source: DTN: MO0312SPAPCESA.002

NOTE: Shown on the table is the percentage of all waters the bins represent. To see the time normalized percentages for the crown and invert, see Tables 6.13-1 and 6.13-2.

The variations of brine chemistry among the six representative dusts are shown in Figure 6.13-26 and Figures 6.13-35 through 6.13-40. Figure 6.13-26 indicates that the maximum pH that can occur in deliquescing water on the waste packages is 11.7, ranging down to a value slightly greater than 6. Figure 6.13-35 shows that F concentrations are less than one molal for all samples during evaporation because of the precipitation of CaF. Figure 6.13-36 indicates that the ionic strength ranges from 10^{-3} molal to values as great as ~50 molal at low humidities. Figure 6.13-37 shows at low humidity, the brine condensed on dust could have Cl concentrations as high as 9 molal. The NO_3 concentrations can be as high as ~20 molal (Figure 6.13-39). Figure 6.13-24 and 6.13-38 show that high ratios of Cl/NO_3 and $(Cl + F)/(NO_3 + SO_4)$ occur only for dust leachate Bin 6, at relative humidity values greater than 50 percent. At least 81 percent of waste packages will never be exposed to deliquescent brine with a Cl/NO_3 ratio higher than one (see Figure 6.13-38 and Table 6.13-9). This value does not account for uncertainty. The difference between Figure 6.13-24 and Figure 6.13-38 is mainly due to SO_4 concentrations, which could be as high as 2 molal.

Figure 6.12-5 shows the concentrations of Br that can occur in brines formed by dust deliquescence. These values can get as high as ~6 molal. Although the presence of relatively high Br concentrations could be an artifact of the bromide in the dusts being derived from LiBr-containing construction water (Peterman et al. 2003 [DIRS 162819]), the fact that high Br concentrations can occur in the seepage water (see Figure 6.12.4-1) indicates that this may be a real effect. See Section 6.12.4.2.4 for further discussion on the uncertainty associated with Br in dust samples.

Figure 6.13-40 shows how the mass of solvent and ionic strength vary with relative humidity. The mass of solvent becomes less than 10^{-4} kg H_2O/20 grams of dust before the evaporation reaches the minimum deliquescence point. At such low water/solid ratios, there is sufficient liquid water to only form a few molecular layers on the dust surface. This very small amount of water is insufficient to form a continuous water film on waste packages.

Additional plots can be found for aqueous concentrations of C, S, and Ca in newDustMOALT.xls archived in DTN: MO0310SPAPCELA.002.

Table 6.13-9 shows the brine compositions that develop by evaporative concentration of the dust leachate, using the data in the dust leachate lookup tables. Also shown in this figure is the endpoint relative humidity of the brines represented by the six dust leachate bin waters. Under most conditions, the dust leachate waters tend to be classified as sodium nitrate, sodium sulfate, potassium nitrate, sodium chloride, or calcium nitrate brines. Only Bin 1 shows sufficient accumulation of Ca to make it the dominant cation, yet the dominant anion in this bin at all relative humidities is nitrate, which inhibits corrosion. Bins 3 and 6 are the only bins that show any generation of a chloride-type brine. Based on the given distribution, this could occur about 19.2 percent of the time (see Table 6.13-9). However, the N concentration in these waters is fairly high and could limit any potential corrosion at low relative humidity. Bin 3 and 6 waters also have the highest pH values. In the most likely case (Bin 5), the evolution of the brine is from a sodium nitrate water to a potassium nitrate or a sodium bromide type water.

Table 6.13-7 contains the mineral assemblages that are likely to comprise the soluble dust mineral phases sitting on the waste packages and drip shield.

6.13.5 The Chemical Environment in the Invert

The chemical environment in the invert is important for two key TSPA-LA parameters, radionuclide solubility and colloid stability. In general, the chemical parameters of interest are pH and ionic strength. All 11 sets of bin chemistries are possible in the invert, whereas the drip shield and waste package environment discussed in Section 6.13.4 did not consider Bins 1 and 2, as they do not occur in the crown seepage waters. To establish the chemical environment in the invert, multiple sources of water must be considered. These include waters that have wicked into the invert from below, dripped from the crown, drip shield, or outer surface of the waste package, or exited from a breached waste package after interacting with the waste form.

Table 6.13-9. Dust Leachate Lookup Table End Point Relative Humidity and Brine Evolution

Lookup Table File Name	Number of 6o Binning Files Matching this Sensitivity Run	% of 52 Binning Output Runs	Bin	Temp.	Pco_2	Endpoint RH	98% RH Brine	85% RH Brine	65% RH Brine	Endpoint Brine
d1c2t04.xls			1	40	1.00E-02	50.0%	Na-N	Na-N	Na-N	Ca-N
d1c2t07.xls			1	70	1.00E-02	30.0%	Na-N	Na-N	Na-N	Ca-N
d1c2t10.xls			1	100	1.00E-02	31.5%	Na-N	Na-N	Na-N	Ca-N
d1c2t12.xls			1	120	1.00E-02	30.8%	Na-N	Na-N	Na-N	K-N
d1c2t14.xls			1	140	1.00E-02	26.2%	Na-N	Na-N	Na-N	Na-N
d1c3t04.xls			1	40	1.00E-03	50.0%	Na-N	Na-N	Na-N	Ca-N
d1c3t07.xls			1	70	1.00E-03	30.0%	Na-N	Na-N	Na-N	Ca-N
d1c3t10.xls	3	5.8	1	100	1.00E-03	31.5%	Na-N	Na-N	Na-N	Ca-N
d1c3t12.xls			1	120	1.00E-03	30.7%	Na-N	Na-N	Na-N	K-N
d1c3t14.xls			1	140	1.00E-03	26.2%	Na-N	Na-N	Na-N	Na-N
d1c4t04.xls			1	40	1.00E-04	50.0%	Na-N	Na-N	Na-N	Ca-N
d1c4t07.xls			1	70	1.00E-04	30.0%	Na-N	Na-N	Na-N	Ca-N
d1c4t10.xls			1	100	1.00E-04	32.4%	Na-N	Na-N	Na-N	Ca-N
d1c4t12.xls			1	120	1.00E-04	30.8%	Na-N	Na-N	Na-N	K-N
d1c4t14.xls			1	140	1.00E-04	26.2%	Na-N	Na-N	Na-N	Na-N
d2c2t04.xls			2	40	1.00E-02	58.1%	Na-N	Na-N	Na-N	Na-Br
d2c2t07.xls			2	70	1.00E-02	47.8%	Na-N	Na-N	Na-N	Na-N
d2c2t10.xls			2	100	1.00E-02	42.2%	Na-N	Na-N	K-N	K-N
d2c2t12.xls			2	120	1.00E-02	35.4%	Na-N	Na-N	K-N	K-N
d2c2t14.xls			2	140	1.00E-02	32.0%	Na-N	Na-N	K-N	K-N
d2c3t04.xls			2	40	1.00E-03	58.1%	Na-N	Na-N	Na-N	Na-Br
d2c3t07.xls			2	70	1.00E-03	47.8%	Na-N	Na-N	Na-N	Na-N
d2c3t10.xls	4	7.7	2	100	1.00E-03	42.2%	Na-N	Na-N	K-N	K-N
d2c3t12.xls			2	120	1.00E-03	35.4%	Na-N	Na-N	K-N	K-N
d2c3t14.xls			2	140	1.00E-03	32.0%	Na-N	Na-N	K-N	K-N
d2c4t04.xls			2	40	1.00E-04	58.1%	Na-N	Na-N	Na-N	Na-Br
d2c4t07.xls			2	70	1.00E-04	47.8%	Na-N	Na-N	Na-N	K-N
d2c4t10.xls			2	100	1.00E-04	42.2%	Na-N	Na-N	K-N	K-N
d2c4t12.xls			2	120	1.00E-04	35.4%	Na-N	Na-N	K-N	K-N
d2c4t14.xls			2	140	1.00E-04	32.0%	Na-N	Na-N	K-N	K-N
d3c2t04.xls			3	40	1.00E-02	60.5%	Na-S	Na-Cl	Na-Cl	Na-N
d3c2t07.xls			3	70	1.00E-02	49.9%	Na-S	Na-S	Na-Cl	K-N
d3c2t10.xls			3	100	1.00E-02	42.8%	Na-S	Na-S	Na-Cl	K-N
d3c2t12.xls			3	120	1.00E-02	38.4%	Na-S	Na-S	Na-Cl	K-N
d3c2t14.xls			3	140	1.00E-02	32.4%	Na-S	Na-S	Na-Cl	K-N
d3c3t04.xls			3	40	1.00E-03	58.8%	Na-S	Na-S	Na-Cl	Na-Br
d3c3t07.xls			3	70	1.00E-03	50.0%	Na-S	Na-S	Na-Cl	Na-N
d3c3t10.xls	9	17.3	3	100	1.00E-03	43.2%	Na-S	Na-S	Na-Cl	K-N
d3c3t12.xls			3	120	1.00E-03	38.5%	Na-S	Na-S	Na-Cl	K-N
d3c3t14.xls			3	140	1.00E-03	32.6%	Na-S	Na-S	Na-Cl	K-N
d3c4t04.xls			3	40	1.00E-04	58.8%	Na-S	Na-S	Na-Cl	Na-Br
d3c4t07.xls			3	70	1.00E-04	50.0%	Na-S	Na-S	Na-Cl	Na-N
d3c4t10.xls			3	100	1.00E-04	43.4%	Na-S	Na-S	Na-Cl	K-N
d3c4t12.xls			3	120	1.00E-04	38.6%	Na-S	Na-S	Na-Cl	K-N
d3c4t14.xls			3	140	1.00E-04	32.6%	Na-S	Na-S	Na-Cl	K-N

Table 6.13-9. Dust Leachate Lookup Table End Point Relative Humidity and Brine Evolution (Continued)

d4c2t04.xls			4	40	1.00E-02	52.9%	Na-N	Na-N	Na-N	Na-Br
d4c2t07.xls			4	70	1.00E-02	45.4%	Na-N	Na-N	Na-N	Na-N
d4c2t10.xls			4	100	1.00E-02	36.4%	Na-N	Na-N	Na-N	Na-N
d4c2t12.xls			4	120	1.00E-02	31.2%	Na-N	Na-N	Na-N	Na-N
d4c2t14.xls			4	140	1.00E-02	26.4%	Na-N	Na-N	Na-N	Na-N
d4c3t04.xls			4	40	1.00E-03	52.9%	Na-N	Na-N	Na-N	Na-Br
d4c3t07.xls			4	70	1.00E-03	44.5%	Na-N	Na-N	Na-N	Na-N
d4c3t10.xls	12	23.1	4	100	1.00E-03	36.4%	Na-N	Na-N	Na-N	Na-N
d4c3t12.xls			4	120	1.00E-03	31.2%	Na-N	Na-N	Na-N	Na-N
d4c3t14.xls			4	140	1.00E-03	26.4%	Na-N	Na-N	Na-N	Na-N
d4c4t04.xls			4	40	1.00E-04	52.9%	Na-N	Na-N	Na-N	Na-Br
d4c4t07.xls			4	70	1.00E-04	44.5%	Na-N	Na-N	Na-N	Na-N
d4c4t10.xls			4	100	1.00E-04	36.4%	Na-N	Na-N	Na-N	Na-N
d4c4t12.xls			4	120	1.00E-04	31.2%	Na-N	Na-N	Na-N	Na-N
d4c4t14.xls			4	140	1.00E-04	26.4%	Na-N	Na-N	Na-N	Na-N
d5c2t04.xls			5	40	1.00E-02	56.1%	Na-N	Na-N	Na-N	Na-Br
d5c2t07.xls			5	70	1.00E-02	45.2%	Na-N	Na-N	Na-N	Na-N
d5c2t10.xls			5	100	1.00E-02	41.8%	Na-N	Na-N	Na-N	K-N
d5c2t12.xls			5	120	1.00E-02	31.1%	Na-N	Na-N	Na-N	Na-N
d5c2t14.xls			5	140	1.00E-02	26.3%	Na-N	Na-N	Na-N	Na-N
d5c3t04.xls			5	40	1.00E-03	56.1%	Na-N	Na-N	Na-N	Na-Br
d5c3t07.xls			5	70	1.00E-03	45.2%	Na-N	Na-N	Na-N	Na-N
d5c3t10.xls	23	44.2	5	100	1.00E-03	41.8%	Na-N	Na-N	Na-N	K-N
d5c3t12.xls			5	120	1.00E-03	31.1%	Na-N	Na-N	Na-N	Na-N
d5c3t14.xls			5	140	1.00E-03	26.3%	Na-N	Na-N	Na-N	Na-N
d5c4t04.xls			5	40	1.00E-04	56.1%	Na-N	Na-N	Na-N	Na-Br
d5c4t07.xls			5	70	1.00E-04	45.2%	Na-N	Na-N	Na-N	Na-N
d5c4t10.xls			5	100	1.00E-04	41.8%	Na-N	Na-N	Na-N	K-N
d5c4t12.xls			5	120	1.00E-04	31.1%	Na-N	Na-N	Na-N	Na-N
d5c4t14.xls			5	140	1.00E-04	26.3%	Na-N	Na-N	Na-N	Na-N
d6c2t04.xls			6	40	1.00E-02	59.8%	Na-C	Na-Cl	Na-Cl	Na-Br
d6c2t07.xls			6	70	1.00E-02	55.9%	Na-C	Na-C	Na-Cl	K-N
d6c2t10.xls			6	100	1.00E-02	42.8%	Na-C	Na-Cl	Na-Cl	K-N
d6c2t12.xls			6	120	1.00E-02	38.4%	Na-C	Na-Cl	Na-Cl	K-N
d6c2t14.xls			6	140	1.00E-02	32.3%	Na-Cl	Na-Cl	Na-Cl	K-N
d6c3t04.xls			6	40	1.00E-03	59.4%	Na-C	Na-Cl	Na-Cl	Na-Cl
d6c3t07.xls			6	70	1.00E-03	49.7%	Na-Cl	Na-Cl	Na-Cl	K-N
d6c3t10.xls	1	1.9	6	100	1.00E-03	43.2%	Na-Cl	Na-Cl	Na-Cl	K-N
d6c3t12.xls			6	120	1.00E-03	38.5%	Na-Cl	Na-Cl	Na-Cl	K-N
d6c3t14.xls			6	140	1.00E-03	32.6%	Na-Cl	Na-Cl	Na-Cl	K-N
d6c4t04.xls			6	40	1.00E-04	59.3%	Na-Cl	Na-Cl	Na-Cl	Na-Cl
d6c4t07.xls			6	70	1.00E-04	49.4%	Na-Cl	Na-Cl	Na-Cl	K-N
d6c4t10.xls			6	100	1.00E-04	43.4%	Na-Cl	Na-Cl	Na-Cl	K-N
d6c4t12.xls			6	120	1.00E-04	38.6%	Na-Cl	Na-Cl	Na-Cl	K-N
d6c4t14.xls			6	140	1.00E-04	32.7%	Na-Cl	Na-Cl	Na-Cl	K-N

SOURCE: DTN: MO0310SPAPCELA.002

Figure 6.13-1 shows the bin history maps for each of the five waters in a color-coded scheme. This figure illustrates that the waters being wicked into the invert are chemically distinct from the waters seeping from the crown over significant portions during the early periods (i.e., the boiling and hot periods; see Table 6.13-3). In addition, the temperature, Pco_2, and relative humidity will not be the same in the drift as in the invert throughout time (see Section 6.7.2). This indicates that, even though the waters wicking into the invert and seeping into the invert from the crown of the drift come from the same bin, the chemistry parameters that are obtained from a given lookup table could be different. During certain time periods there is also the possibility that seepage that has entered the waste package and become chemically modified due to reactions with the waste form and in-package components can leave the waste package and introduce yet a third type of water into the invert. Figure 6.13-41 shows the potential sources of water that can enter the invert. These three sources of water are discussed independently in the following paragraphs.

6.13.5.1 Crown Seepage Chemistry

Seepage chemistry is previously discussed in detail in Section 6.13.4. That section provides a description of the ranges of crown seepage waters that could enter the invert.

6.13.5.2 Invert Wicking Chemistry

In addition to the range of possible water chemistries available from crown seepage (Bins 3 through 11), waters entering the invert by wicking waters include Bins 1 and 2, as shown on Figure 6.13-1. Although the potentially corrosive waters in Bins 1 and 2 are rare over the long term (thousands of years), they are common in the invert during the boiling period, as shown on Table 6.13-3. Figure 6.13-16 and Figures 6.13-42 through 6.13-47 show the compositional (pH, F, Cl, Ca, S, C, and ionic strength) evolution of Bin 1 and 2 waters that occurs during evaporation. Plots for Si, N, K, Mg, Na, and Cl:N ratio are not shown here but are provided in the spreadsheet "checked MOALT R02d2.xls" archived in DTN: MO0312SPAPCESA.002.

In contrast to crown seepage, during the boiling period the overall pH range of the waters in the invert increases, extending from ~ 8.5 down to 3.5 (Figure 6.13-16). The total range in ionic strength during this time interval, however, is similar for both crown seepage and invert wicking waters. In the hot period, Bin 4 and 5 waters are more dominant in the invert than in the crown waters and the predicted pH range extends from 6 to 10.5, as opposed to approximately 8 to 10.5 for the crown waters. For all other periods, the ranges in pH and ionic strength in the invert waters are similar to those reported for the crown seepage waters in Section 6.13.4 (pH approximately 8 to 10.5). The differences in water chemistry between the crown of the drift and the base of the invert during the boiling and hot periods are due to the temperature difference at these two localities.

6.13.5.3 Chemistry of Waste Package Leakage

The compositions of water produced in the waste package by interactions of seepage or condensate water with waste package materials and waste is documented in another process model report (BSC 2003 [DIRS 161962]). The *In-Package Chemistry Abstraction* (BSC 2003 [DIRS 161962]) provides datasets containing the parameters of interest. A review of Sections 6 and 8 of the *In-Package Chemistry Abstraction* indicates that pH and ionic strengths through time are generally much different than those reported for the crown seepage and invert wicking chemistries.

W0

Time	Invert	Crown
10	4	4
51	5	5
53	11	5
55	11	6
60	2	6
75	1	5
100	1	5
150	2	4
200	2	4
250	2	3
300	2	3
350	2	3
400	2	3
500	2	4
600	3	4
650	3	5
700	4	11
751	4	11
790	4	11
801	4	11
1001	5	11
1201	5	11
1401	5	11
1601	5	11
1801	5	11
2001	9	4
2202	11	11
2402	11	11
3002	11	11
5003	11	11
7005	6	6
10007	7	6
12310	7	7
15010	7	7
20013	8	8
50035	8	8

W4

Time	Invert	Crown
10	10	10
51	11	11
53	11	11
55	11	11
60	4	11
75	11	11
100	11	11
150	4	11
200	4	11
250	5	11
300	4	11
350	5	11
400	5	11
500	4	5
600	4	5
650	4	11
700	5	11
751	5	11
801	11	11
804	11	11
1001	11	11
1201	11	11
1401	11	11
1601	11	11
1801	11	5
2001	11	4
2202	11	11
2402	11	11
2597	11	11
3002	11	11
5003	11	11
7005	9	9
10007	7	7
12598	7	7
15010	8	8
20013	8	8
50035	8	8

W5

Time	Invert	Crown
10	7	7
51	11	11
53	11	11
55	11	11
60	3	11
75	1	11
100	2	11
150	4	11
200	4	11
250	5	11
300	4	11
350	4	11
400	4	11
500	4	9
600	5	11
650	5	11
700	11	11
751	11	11
785	11	11
801	11	11
1001	11	11
1201	11	11
1401	11	11
1601	11	11
1801	11	5
2001	11	4
2202	11	11
2392	11	11
2402	11	11
3002	11	11
5003	11	11
7005	9	9
10007	10	10
12304	7	7
15010	7	7
20013	8	8
50035	8	8

W6

Time	Invert	Crown
10	7	7
51	9	9
53	9	9
55	9	9
60	2	9
75	1	9
100	2	9
150	4	9
200	4	9
250	9	9
300	4	9
350	4	9
400	9	9
500	4	6
600	4	9
650	9	9
700	9	9
751	9	9
801	9	9
865	9	9
1001	9	9
1201	9	9
1401	9	9
1601	9	9
1801	9	6
2001	9	4
2202	9	9
2402	9	9
3002	9	9
3049	9	9
5003	9	9
7005	9	9
10007	10	10
13054	10	10
15010	10	10
20013	8	8
50035	8	8

W7

Time	Invert	Crown
10	7	7
51	11	11
53	11	11
55	11	11
60	3	11
75	1	11
100	2	11
150	4	11
200	4	11
250	4	11
300	3	5
350	3	4
400	3	4
500	2	4
600	3	4
650	4	5
700	4	11
751	4	11
784	5	11
801	5	11
1001	6	11
1201	11	11
1401	11	11
1601	11	11
1801	11	11
2001	11	11
2202	11	11
2402	11	11
2592	11	11
3002	11	11
5003	11	11
7005	9	9
10007	7	7
12596	7	7
15010	7	7
20013	8	8
50035	8	8

DTN: MO0312SPAPCESA.002

Figure 6.13-1. Color Coded Bin History Maps Showing Differences Between Crown Seepage and Invert Wicking

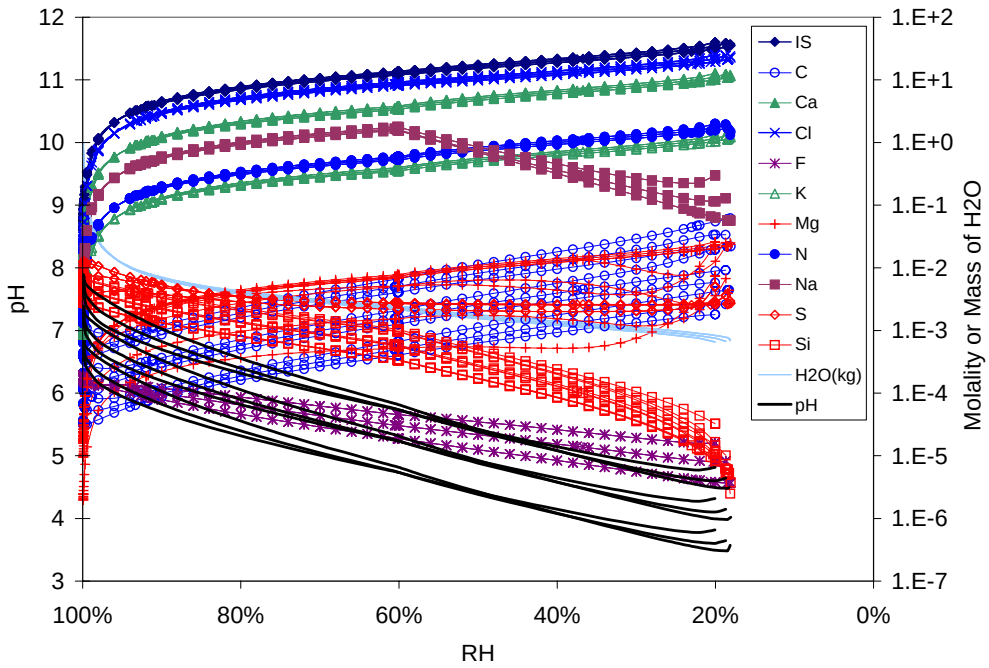

DTN: MO0304SPACPSLT.000

Figure 6.13-2. Aqueous Composition Predictions Versus Relative Humidity for All Seepage Evaporation Lookup Tables for Bin 1 (IS = Ionic Strength)

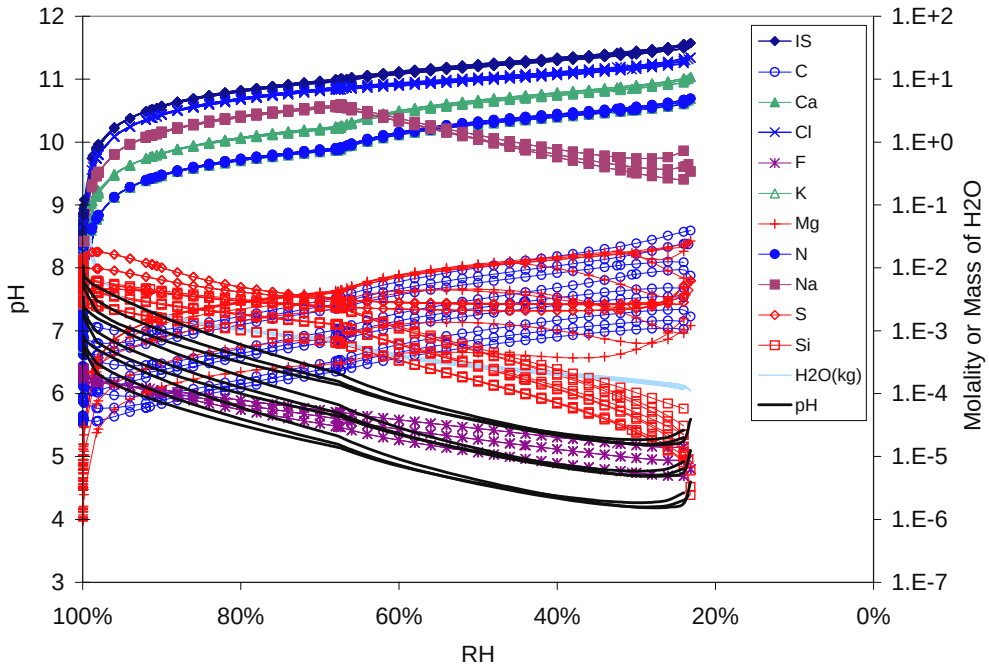

DTN: MO0304SPACPSLT.000

Figure 6.13-3. Aqueous Composition Predictions Versus Relative Humidity for All Seepage Evaporation Lookup Tables for Bin 2 (IS = Ionic Strength)

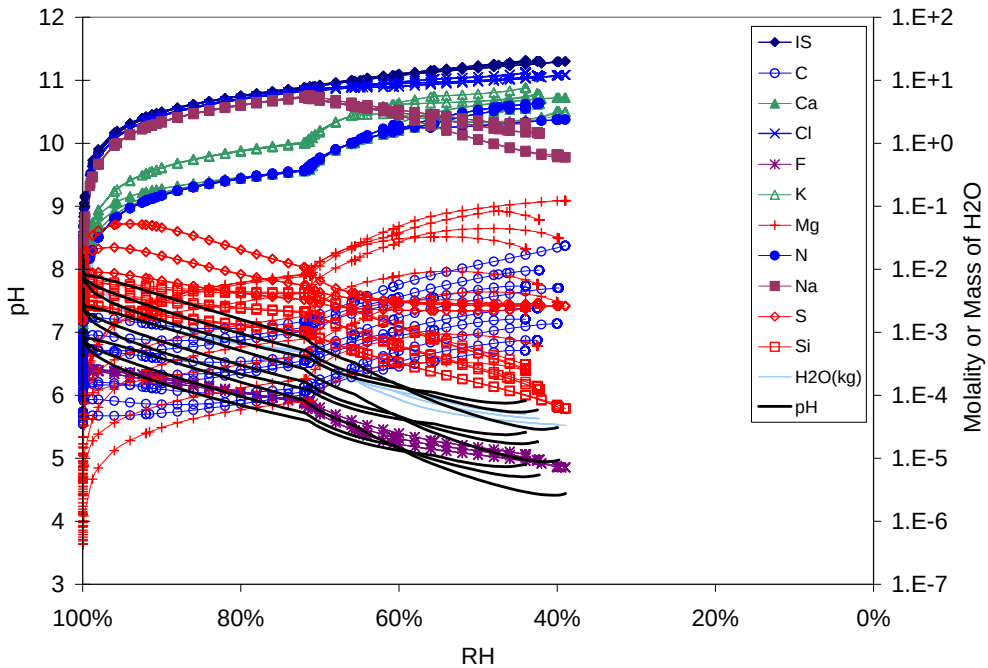

DTN: MO0304SPACPSLT.000

Figure 6.13-4. Aqueous Composition Predictions Versus Relative Humidity for All Seepage Evaporation Lookup Tables for Bin 3 (IS = Ionic Strength)

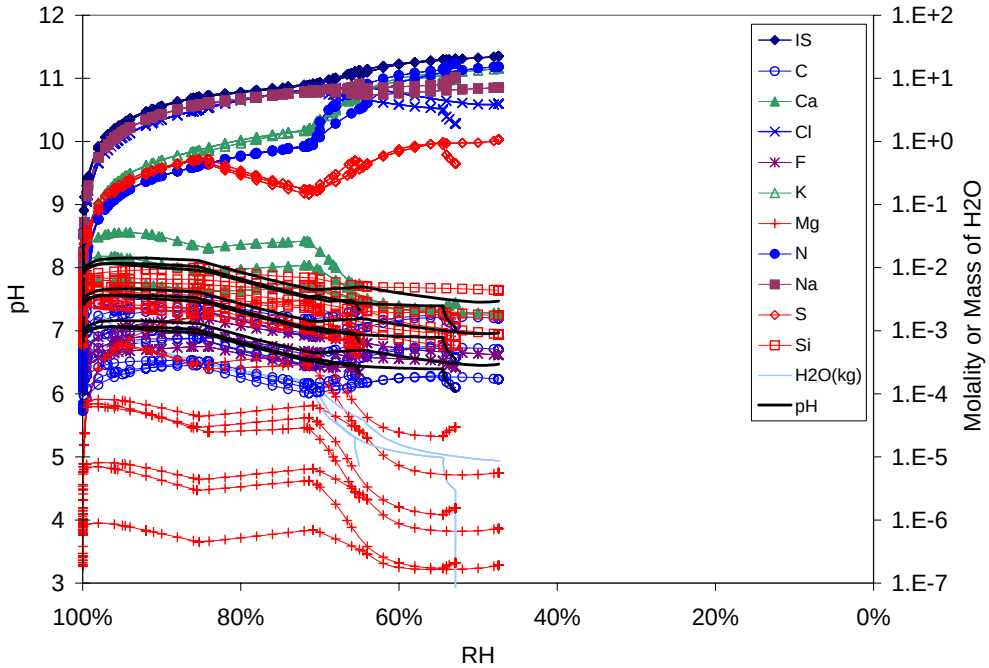

DTN: MO0304SPACPSLT.000

Figure 6.13-5. Aqueous Composition Predictions Versus Relative Humidity for All Seepage Evaporation Lookup Tables for Bin 4 (IS = Ionic Strength)

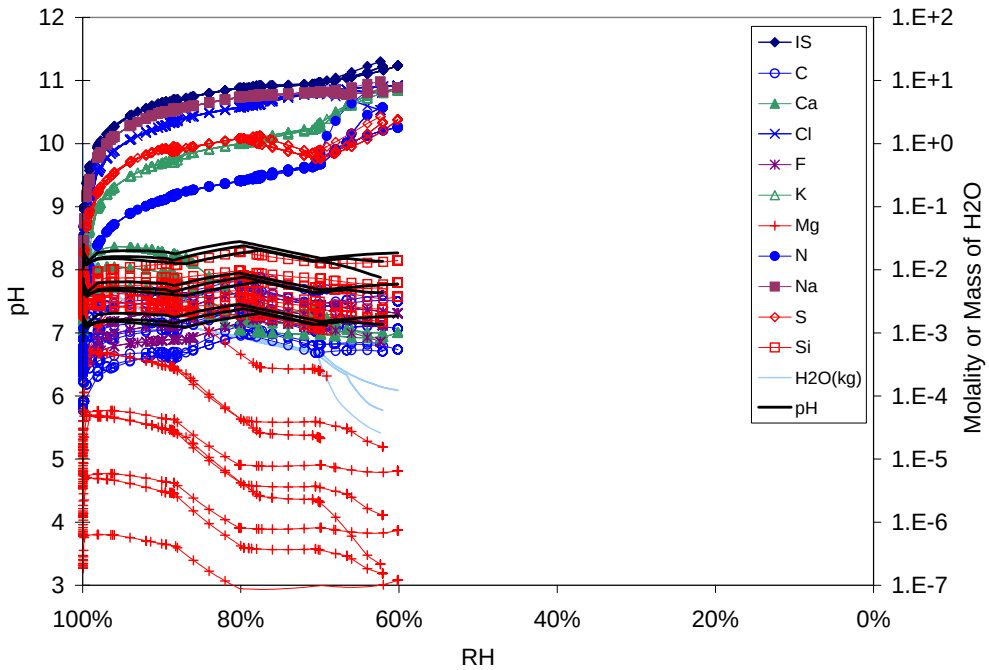

DTN: MO0304SPACPSLT.000

Figure 6.13-6. Aqueous Composition Predictions Versus Relative Humidity for All Seepage Evaporation Lookup Tables for Bin 5 (IS = Ionic Strength)

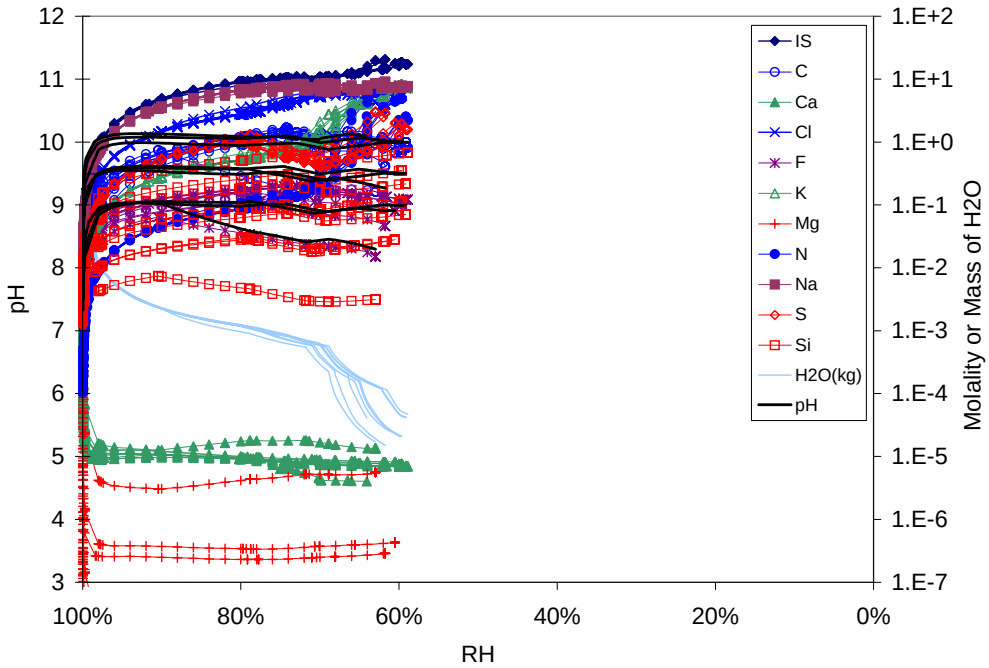

DTN: MO0304SPACPSLT.000

Figure 6.13-7. Aqueous Composition Predictions Versus Relative Humidity for All Seepage Evaporation Lookup Tables for Bin 6 (IS = Ionic Strength)

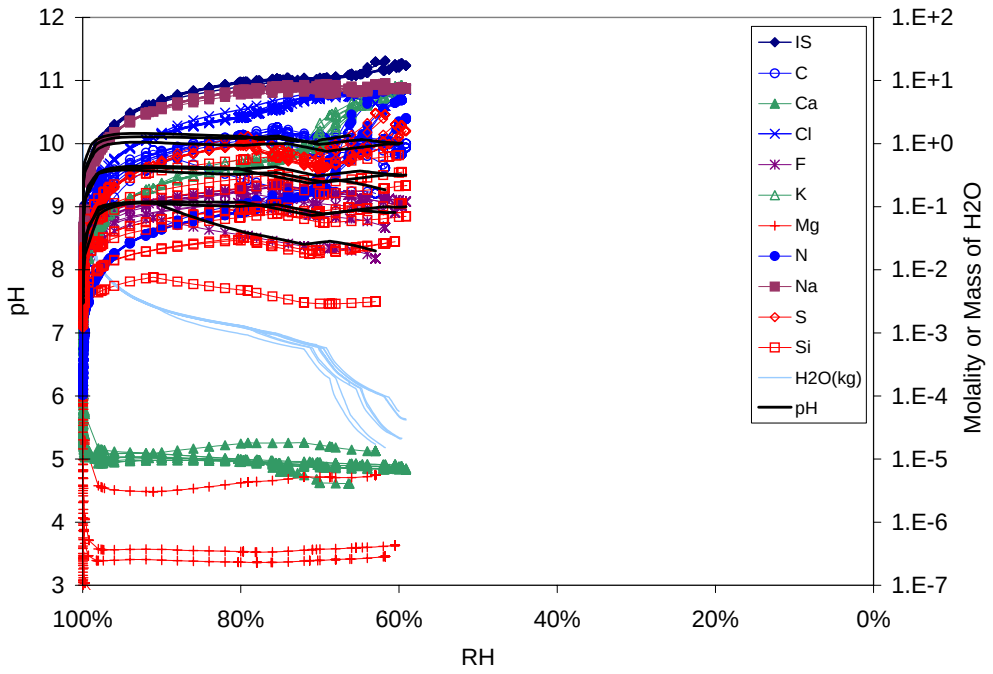

DTN: MO0304SPACPSLT.000

Figure 6.13-8. Aqueous Composition Predictions Versus Relative Humidity for All Seepage Evaporation Lookup Tables for Bin 7 (IS = Ionic Strength)

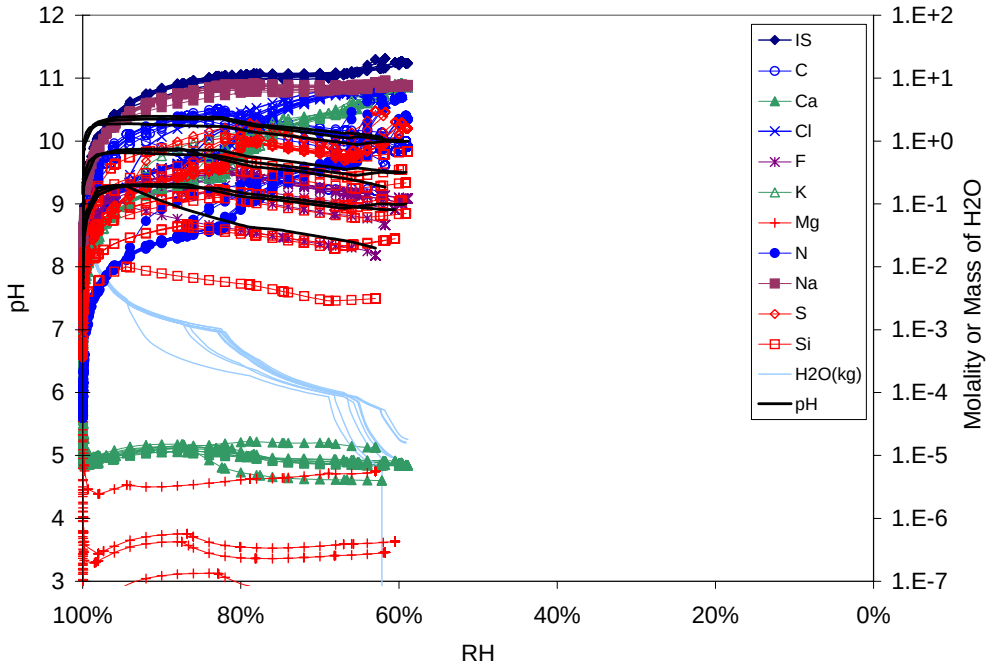

DTN: MO0304SPACPSLT.000

Figure 6.13-9. Aqueous Composition Predictions Versus Relative Humidity for All Seepage Evaporation Lookup Tables for Bin 8 (IS = Ionic Strength)

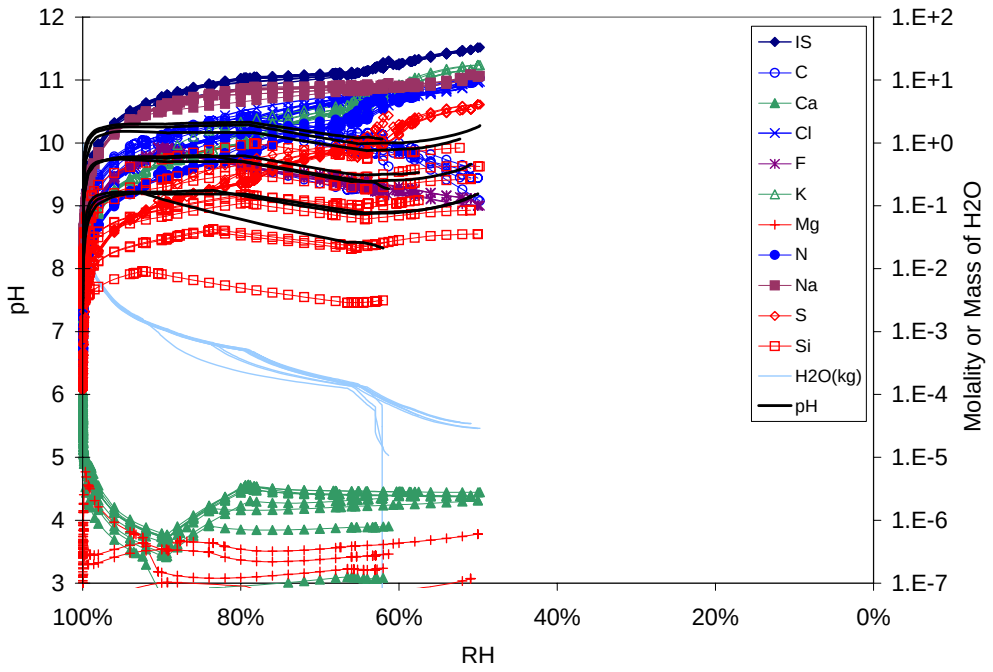

DTN: MO0304SPACPSLT.000

Figure 6.13-10. Aqueous Composition Predictions Versus Relative Humidity for All Seepage Evaporation Lookup Tables for Bin 9 (IS = Ionic Strength)

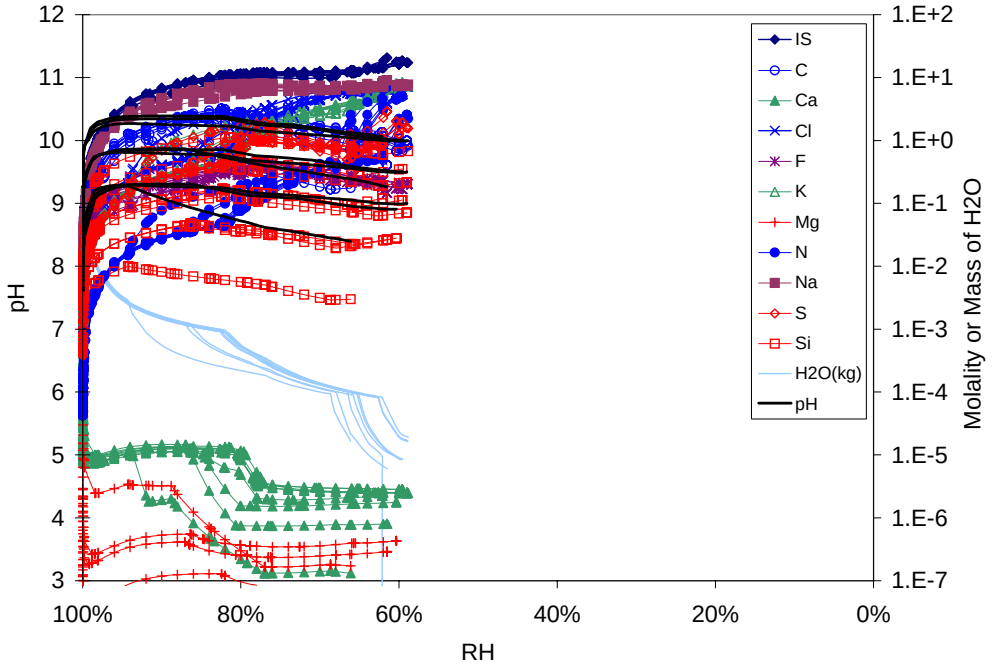

DTN: MO0304SPACPSLT.000

Figure 6.13-11. Aqueous Composition Predictions Versus Relative Humidity for All Seepage Evaporation Lookup Tables for Bin 10 (IS = Ionic Strength)

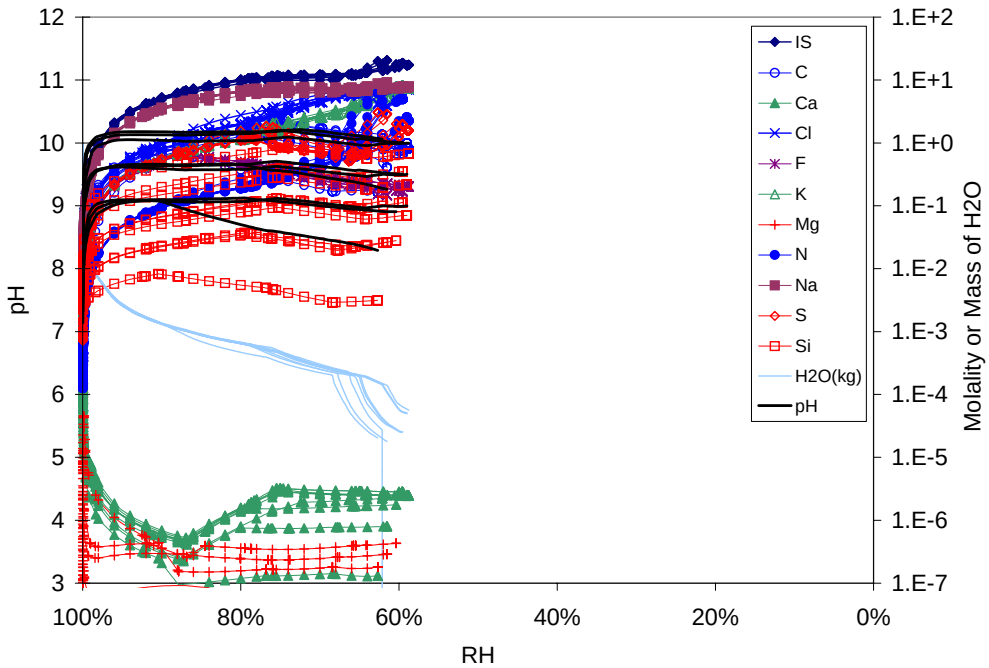

DTN: MO0304SPACPSLT.000

Figure 6.13-12. Aqueous Composition Predictions Versus Relative Humidity for All Seepage Evaporation Lookup Tables for Bin 11 (IS = Ionic Strength)

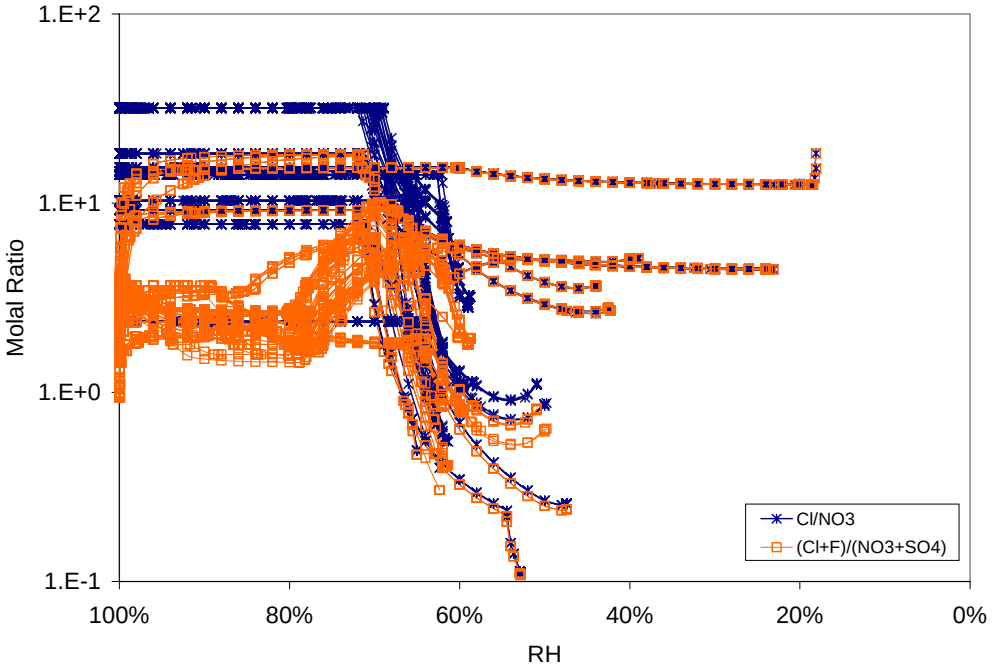

DTN: MO0304SPACPSLT.000

Figure 6.13-13. Selected Aqueous Molal Ratios Useful for Corrosion Analysis Versus Relative Humidity for All Seepage Evaporation Lookup Tables for All Bins

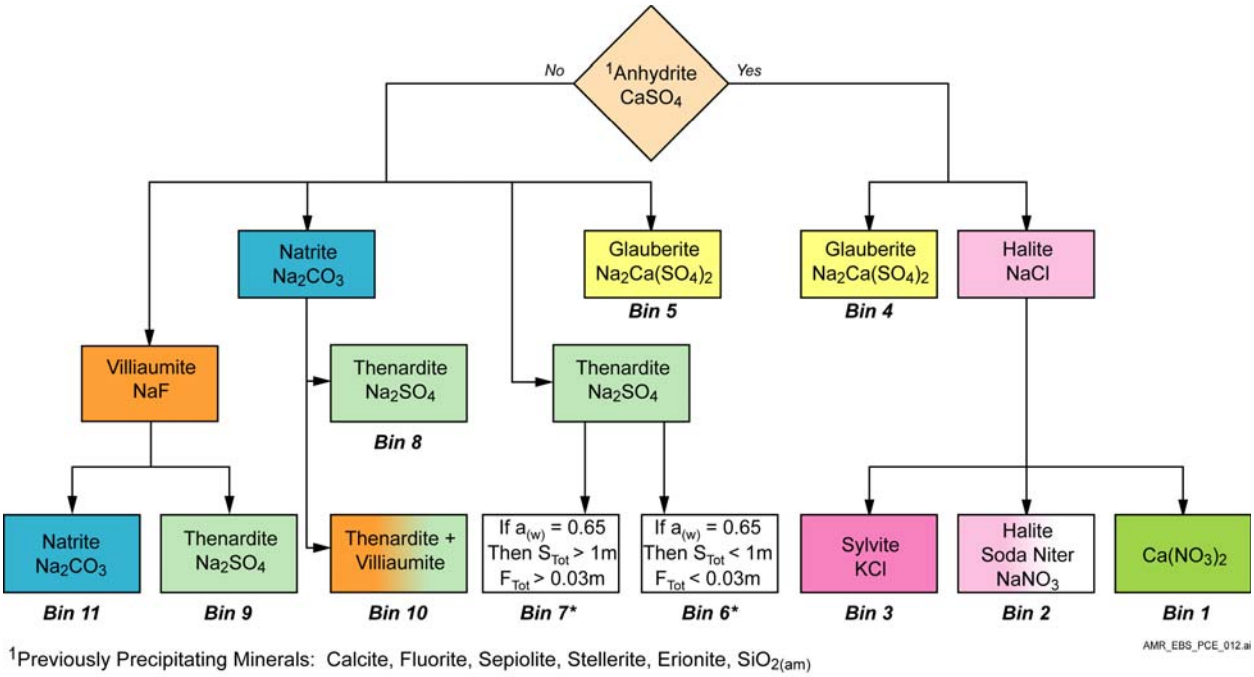

[1]Previously Precipitating Minerals: Calcite, Fluorite, Sepiolite, Stellerite, Erionite, $SiO_{2(am)}$

*Bin 6 and Bin 7 do not tie directly to a precipitating mineral that defines the bin.

Figure 6.13-14. Flow Diagram Showing Some of the Precipitating Minerals that are Associated with Each of the 11 Seepage Bins

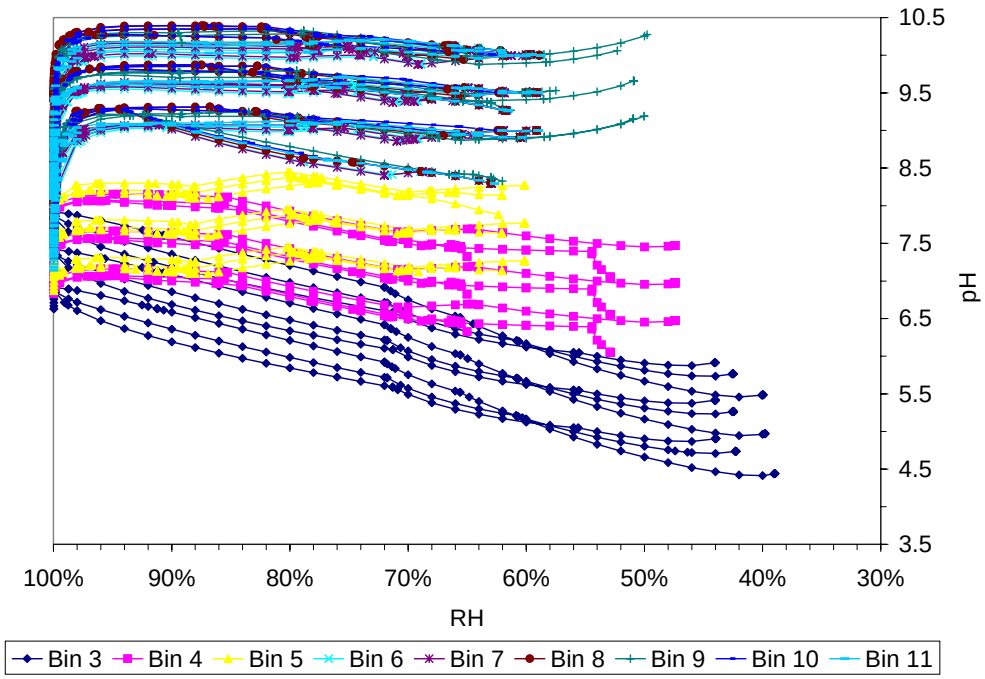

DTN MO0312SPAPCESA.002

Figure 6.13-15. Range of pH Versus Relative Humidity for the Seepage Evaporation Lookup Tables Representing Bins 3 through 11

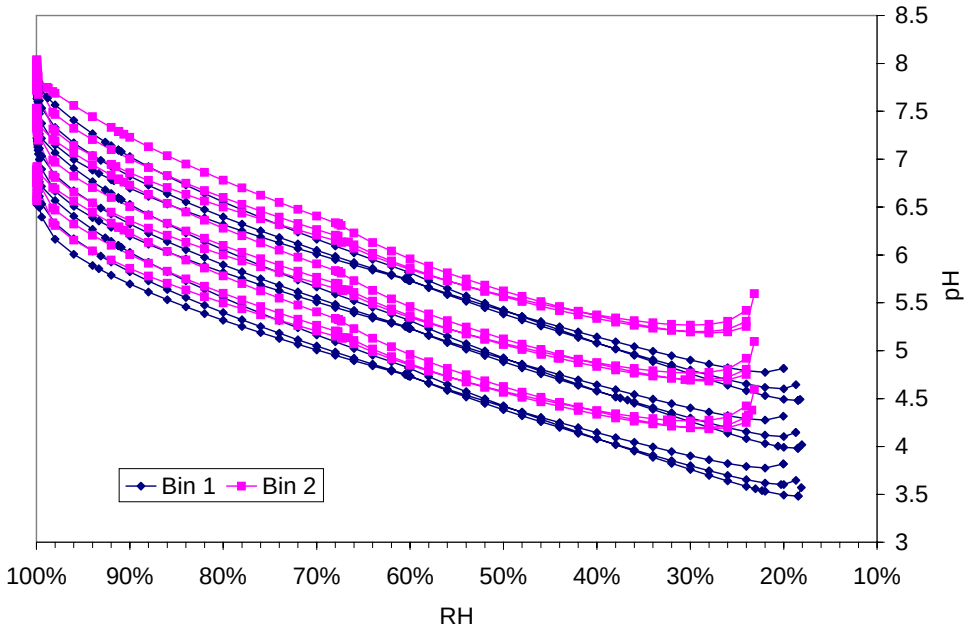

DTN MO0312SPAPCESA.002

Figure 6.13-16. Range of pH Versus Relative Humidity for the Seepage Evaporation Lookup Tables Representing Bins 1 and 2

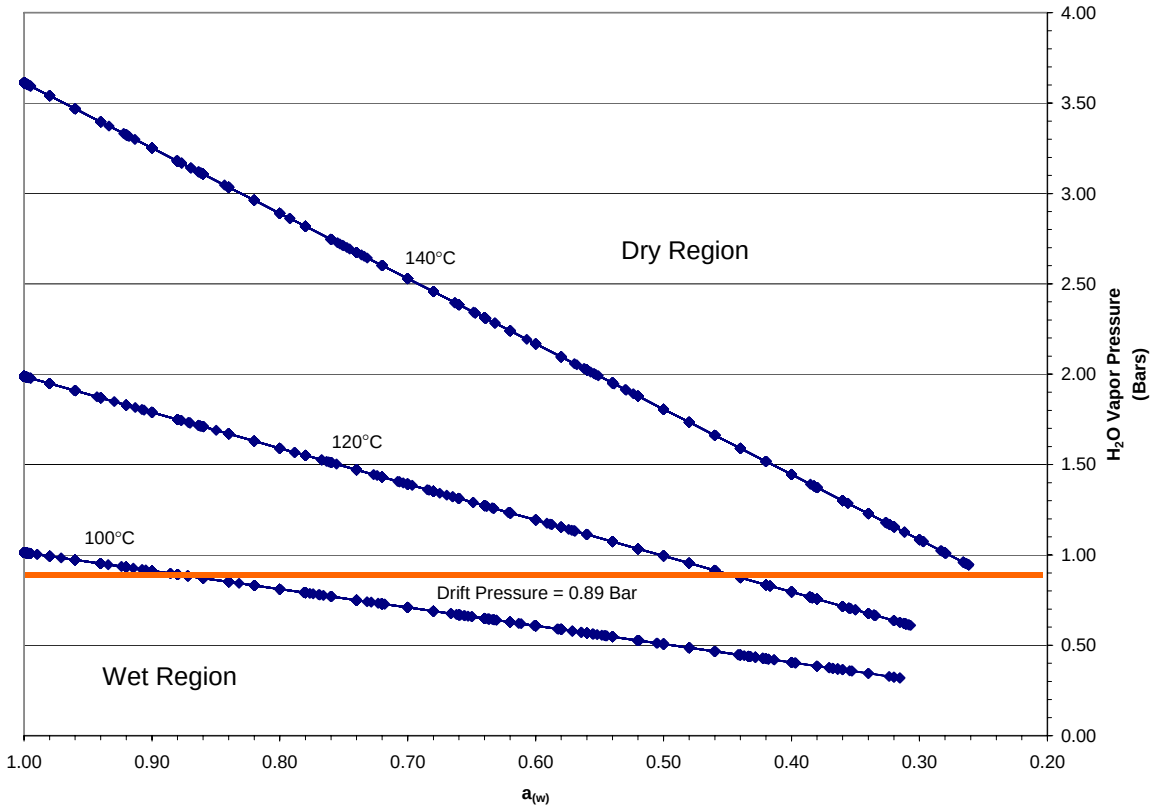

DTN MO0310SPAPCELA.002

Figure 6.13-17. Range of H_2O Vapor Pressure Versus Activity of Water Resulting in Wet Conditions for All Dust Leachate Lookup Tables at or above 100°C

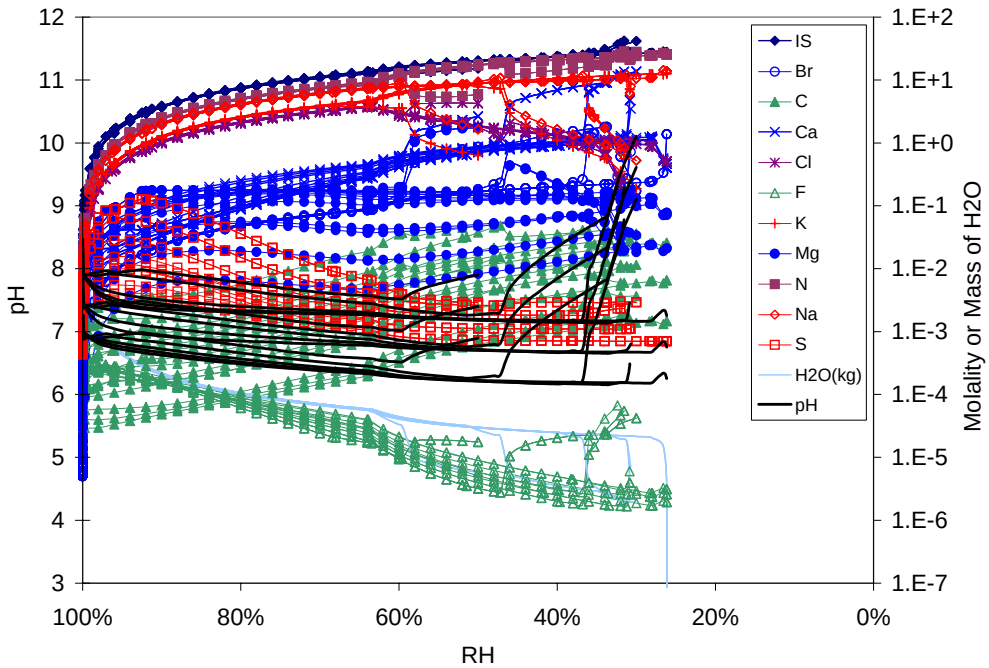

DTN: MO0310SPAPCELA.002

Figure 6.13-18. Aqueous Composition Predictions Versus Relative Humidity for All Dust Leachate Lookup Tables for Bin 1 (IS = Ionic Strength)

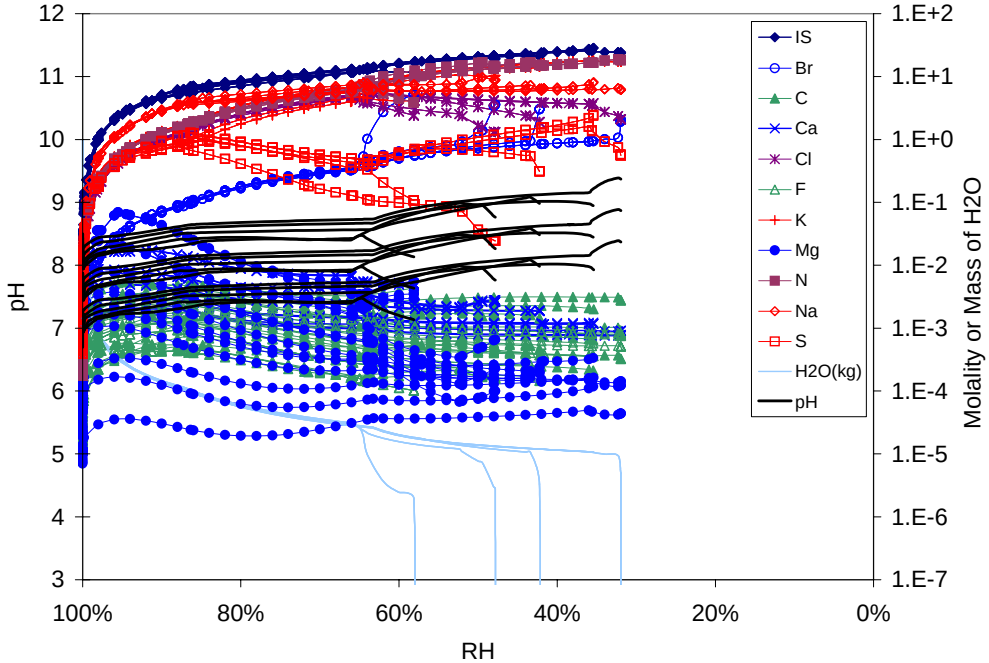

DTN: MO0310SPAPCELA.002

Figure 6.13-19. Aqueous Composition Predictions Versus Relative Humidity for All Dust Leachate Lookup Tables for Bin 2 (IS = Ionic Strength)

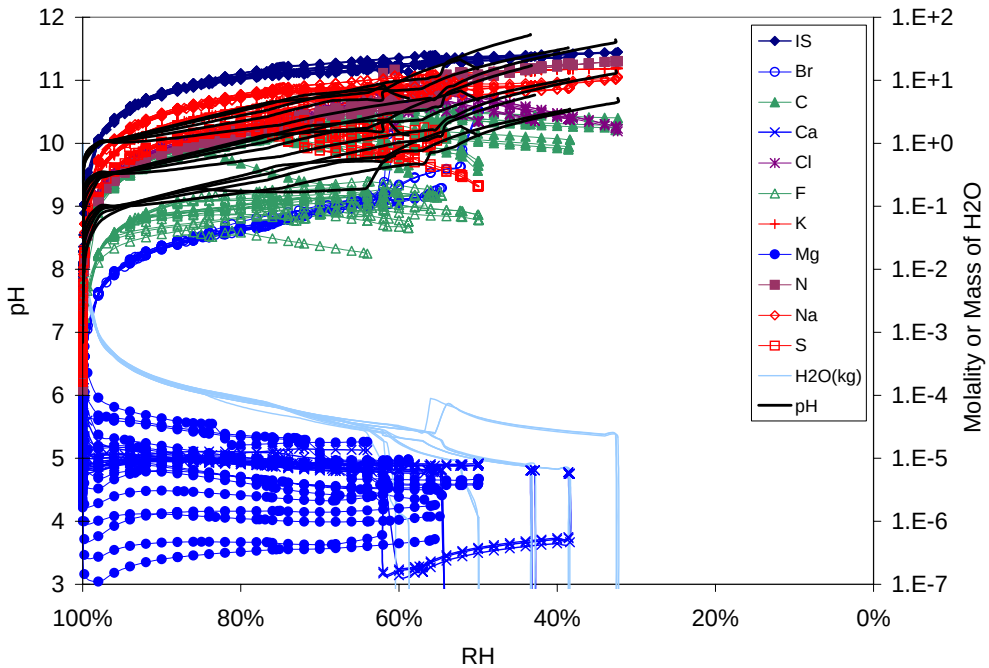

DTN: MO0310SPAPCELA.002

Figure 6.13-20. Aqueous Composition Predictions Versus Relative Humidity for All Dust Leachate Lookup Tables for Bin 3 (IS = Ionic Strength)

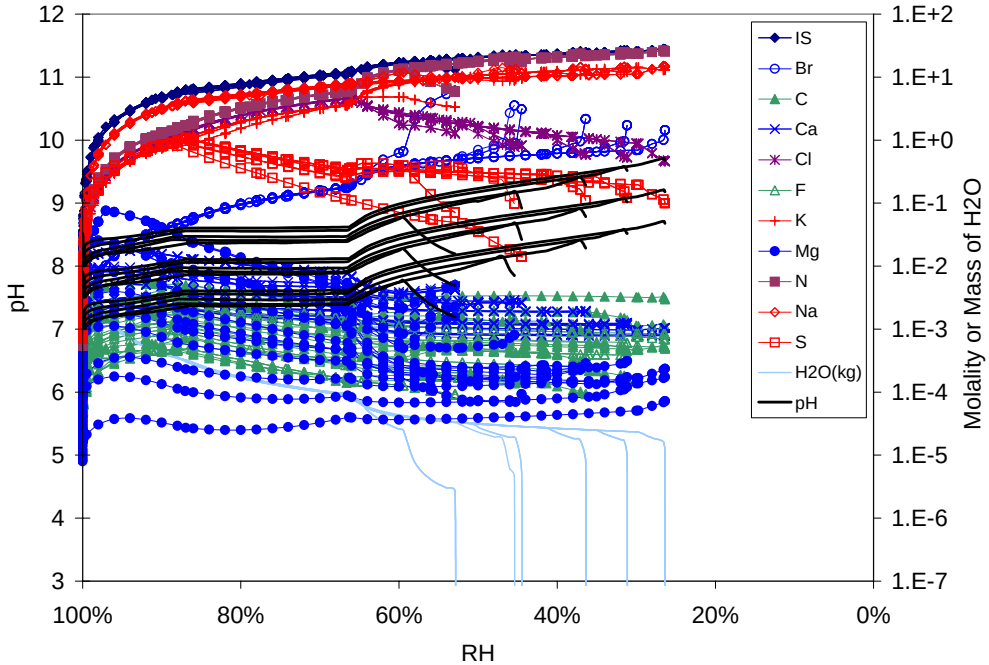

DTN: MO0310SPAPCELA.002

Figure 6.13-21. Aqueous Composition Predictions Versus Relative Humidity for All Dust Leachate Lookup Tables for Bin 4 (IS = Ionic Strength)

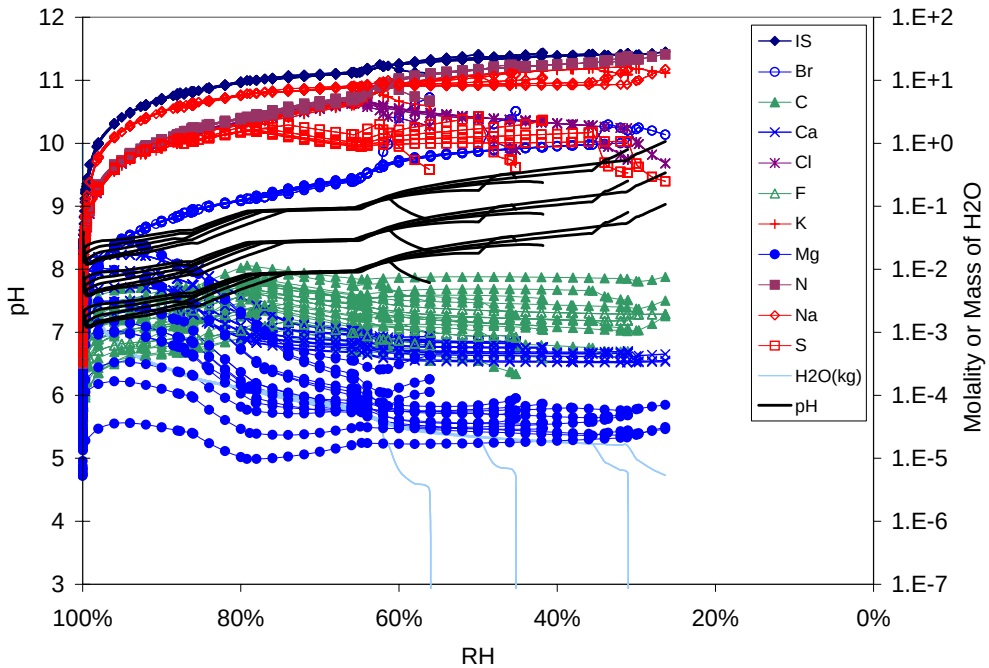

DTN: MO0310SPAPCELA.002

Figure 6.13-22. Aqueous Composition Predictions Versus Relative Humidity for All Dust Leachate Lookup Tables for Bin 5 (IS = Ionic Strength)

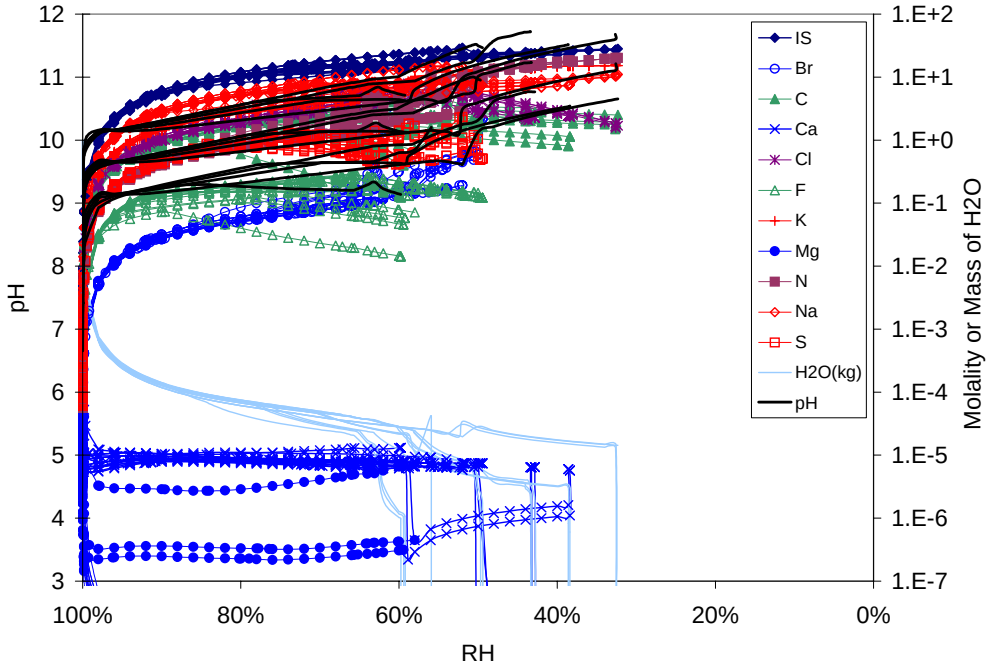

DTN: MO0310SPAPCELA.002

Figure 6.13-23. Aqueous Composition Predictions Versus Relative Humidity for All Dust Leachate Lookup Tables for Bin 6 (IS = Ionic Strength)

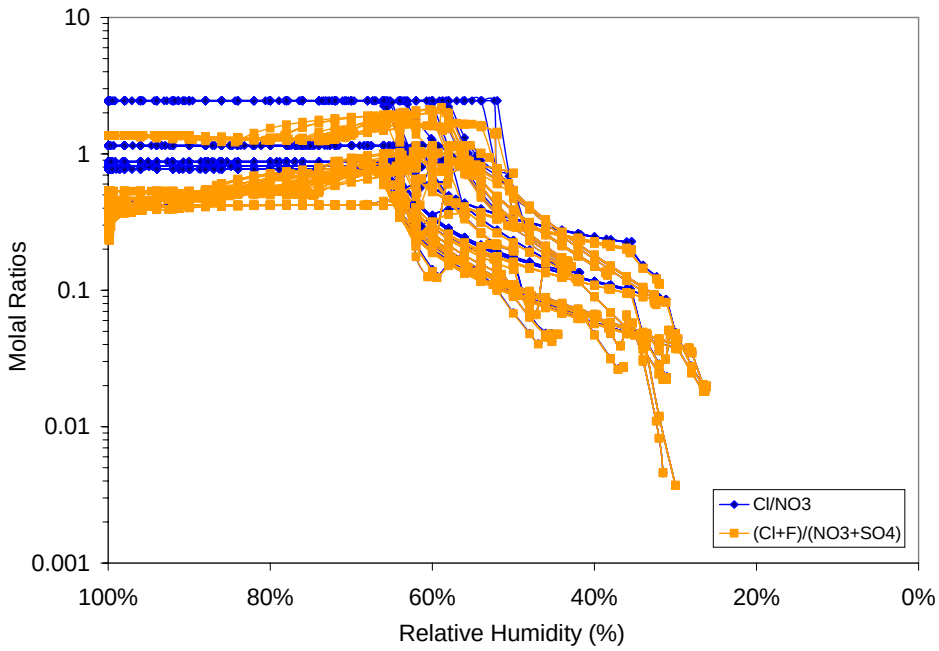

DTN: MO0310SPAPCELA.002

Figure 6.13-24. Selected Aqueous Molal Ratios Versus Relative Humidity for All Dust Leachate Lookup Tables for All Bins

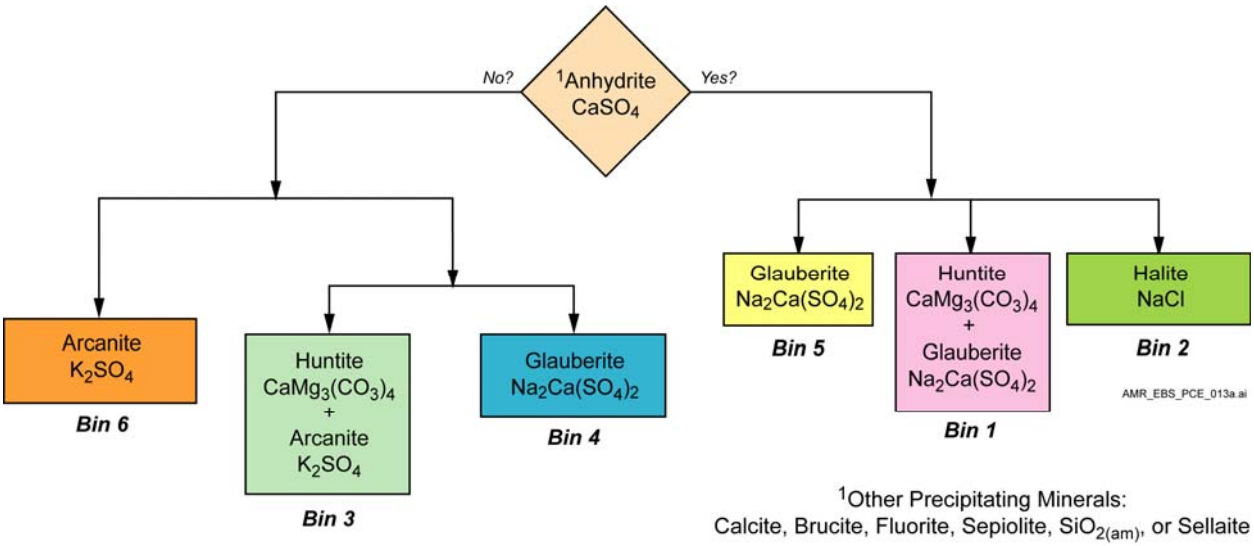

Figure 6.13-25. Flow Diagram Showing Some of the Precipitating Minerals that are Associated with Each of the 6 Dust Leachate Brine Evaporation Bins

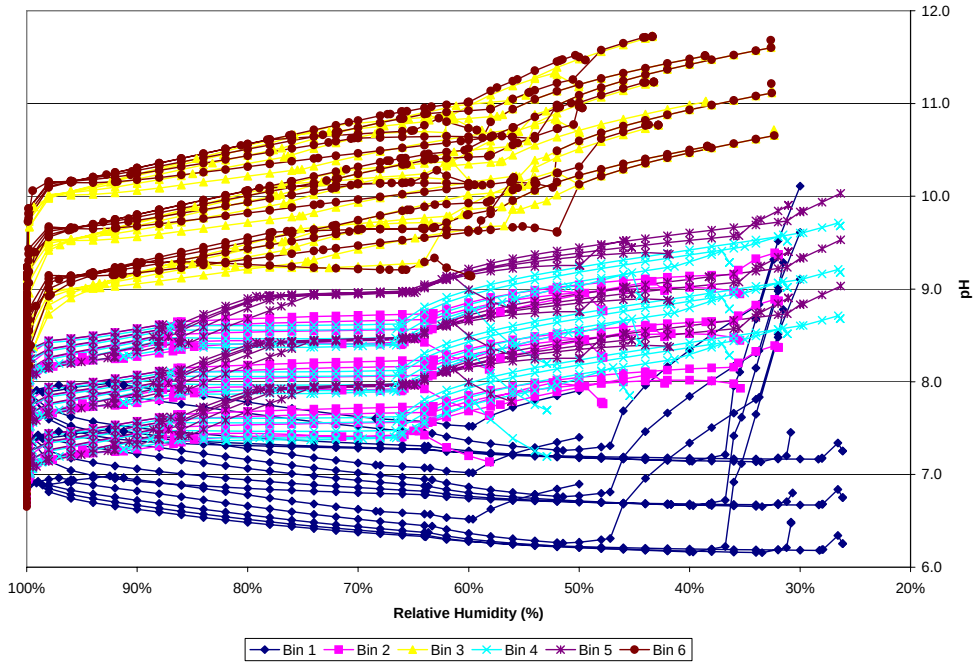

DTN: MO0310SPAPCELA.002

Figure 6.13-26. Variation of pH with Relative Humidity for All Six Dust Leachate Bins

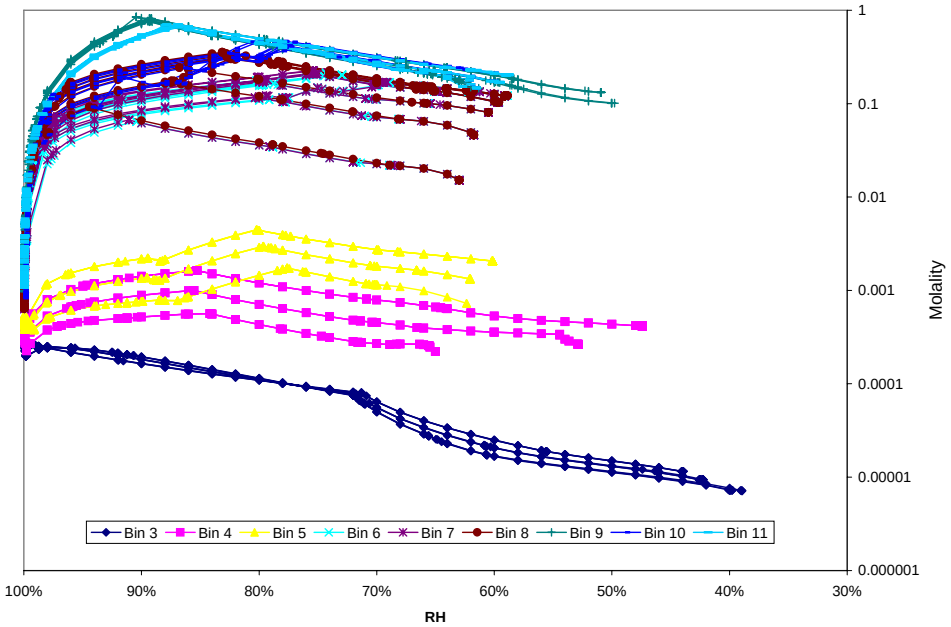

DTN MO0312SPAPCESA.002

Figure 6.13-27. Range of F Versus Relative Humidity for the Seepage Evaporation Lookup Tables Representing Bins 3 through 11

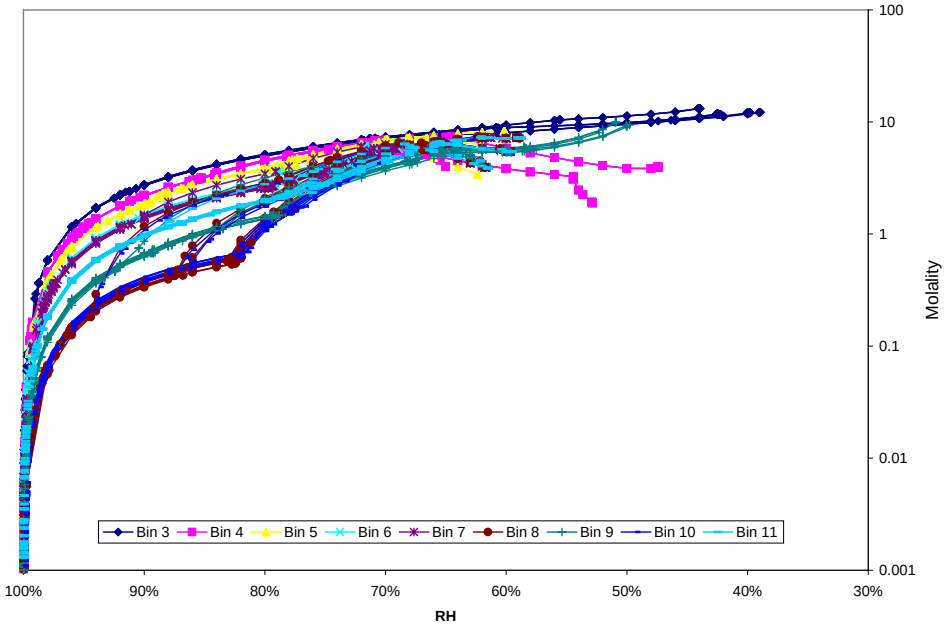

DTN MO0312SPAPCESA.002

Figure 6.13-28. Range of Cl Versus Relative Humidity for the Seepage Evaporation Lookup Tables Representing Bins 3 through 11

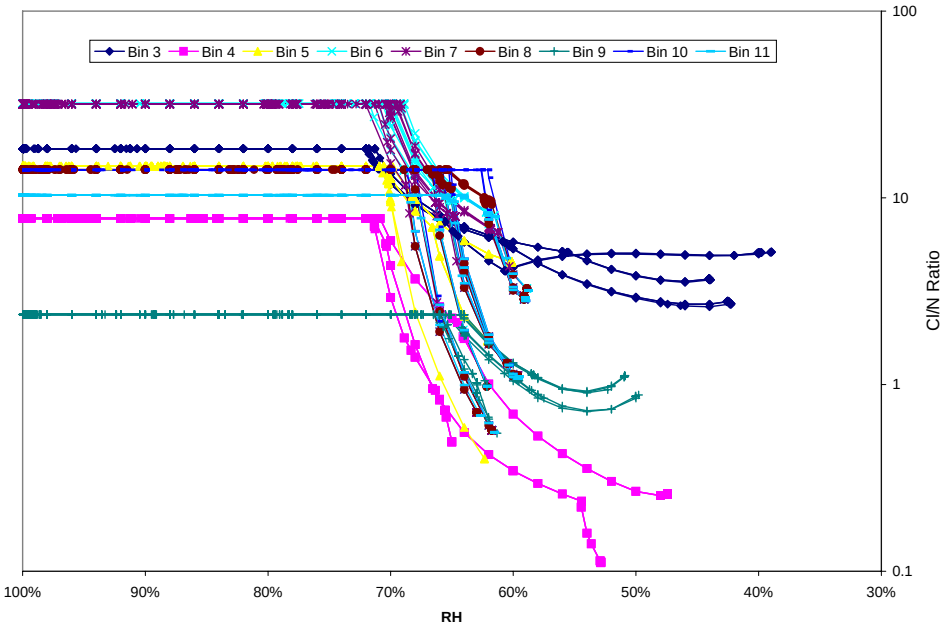

DTN MO0312SPAPCESA.002

Figure 6.13-29. Range of Cl to N Molal Ratios for the Seepage Evaporation Lookup Tables Representing Bins 3 through 11

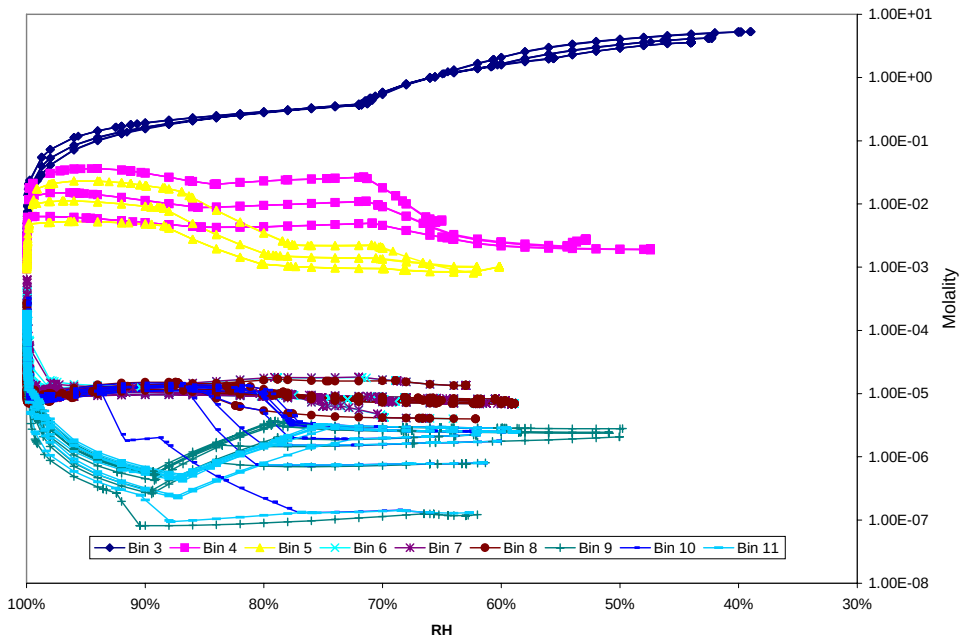

DTN MO0312SPAPCESA.002

Figure 6.13-30. Range of Total Elemental Ca for the Seepage Evaporation Lookup Tables Representing Bins 3 through 11

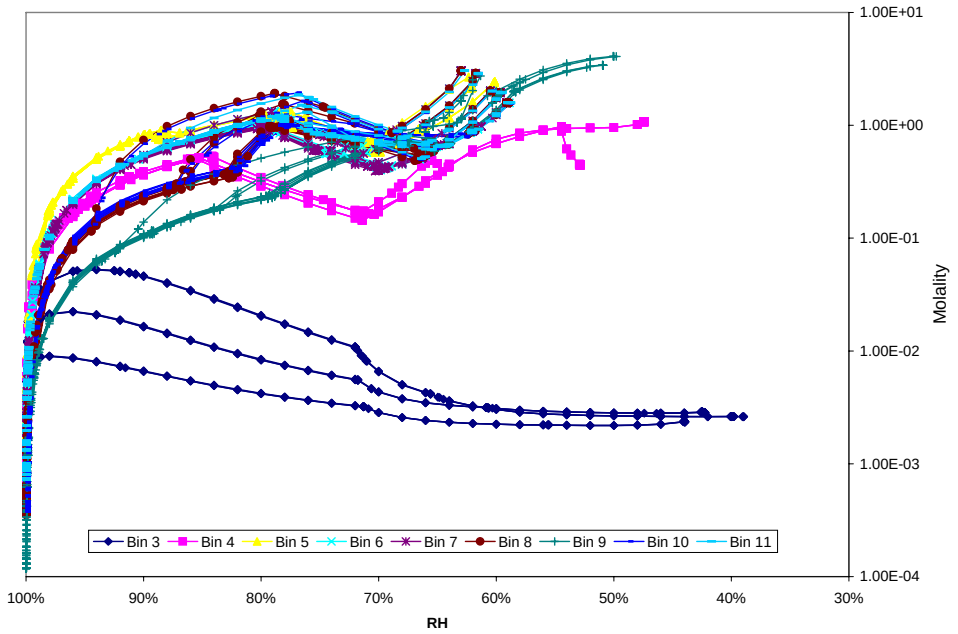

DTN MO0312SPAPCESA.002

Figure 6.13-31. Range of Total Elemental S for the Seepage Evaporation Lookup Tables Representing Bins 3 through 11

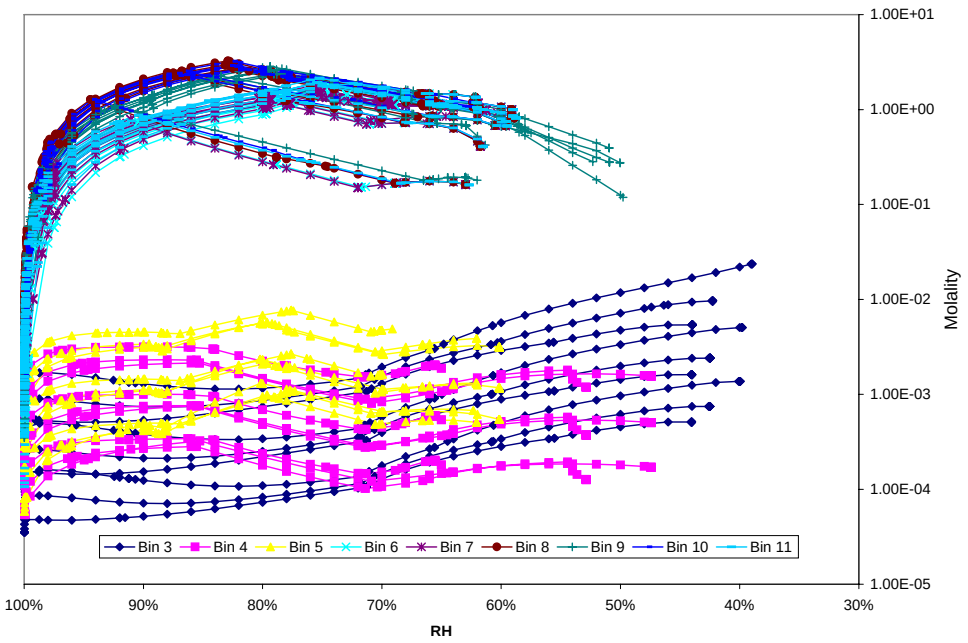

DTN MO0312SPAPCESA.002

Figure 6.13-32. Range of Total Elemental C for the Seepage Evaporation Lookup Tables Representing Bins 3 through 11

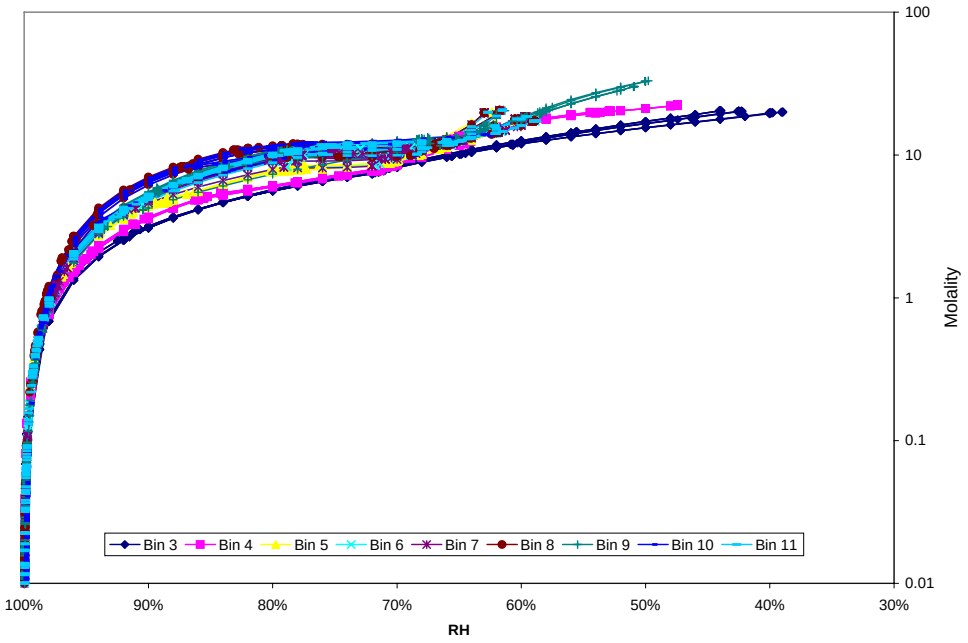

DTN MO0312SPAPCESA.002

Figure 6.13-33. Range of Ionic Strength Versus Relative Humidity for the Seepage Evaporation Lookup Tables Representing Bins 3 through 11

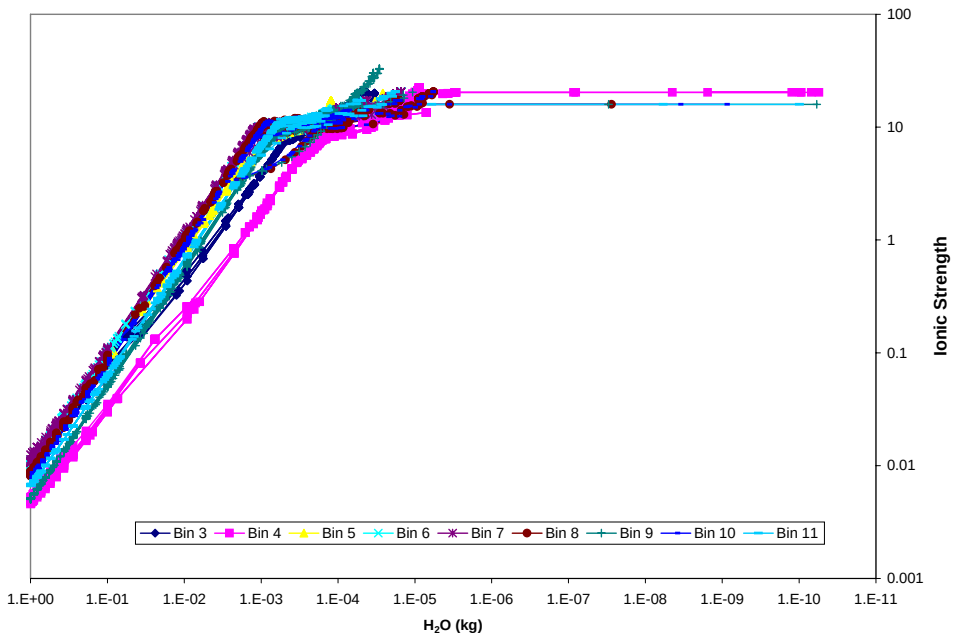

DTN MO0312SPAPCESA.002

Figure 6.13-34. Mass of Water Versus Ionic Strength for the Seepage Evaporation Lookup Tables Representing Bins 3 through 11

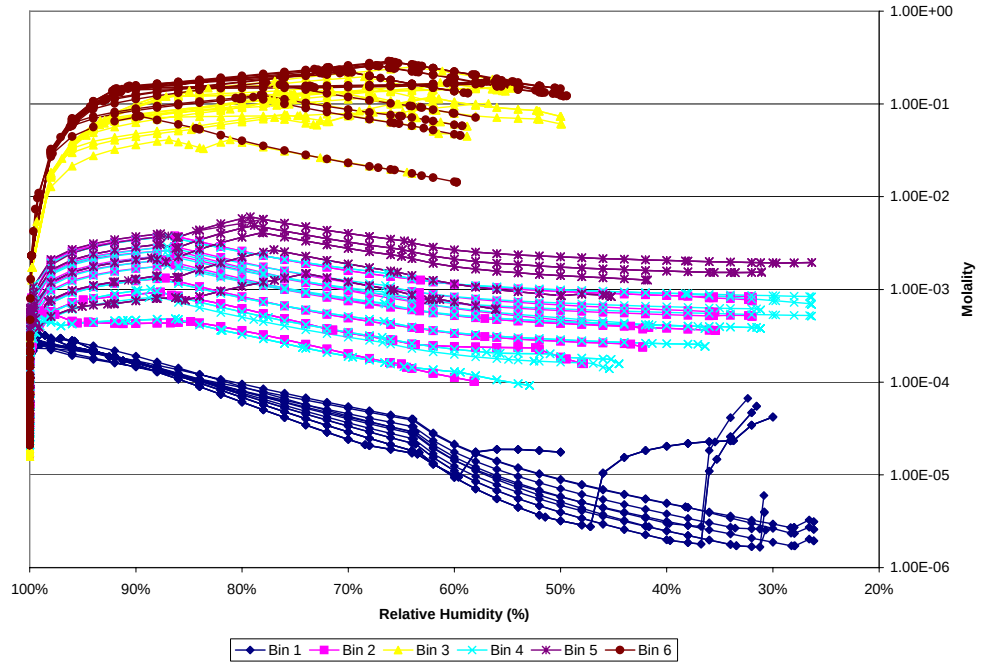

DTN MO0310SPAPCELA.002

Figure 6.13-35. Variation of F Concentration with Relative Humidity for All Six Dust Leachate Bins

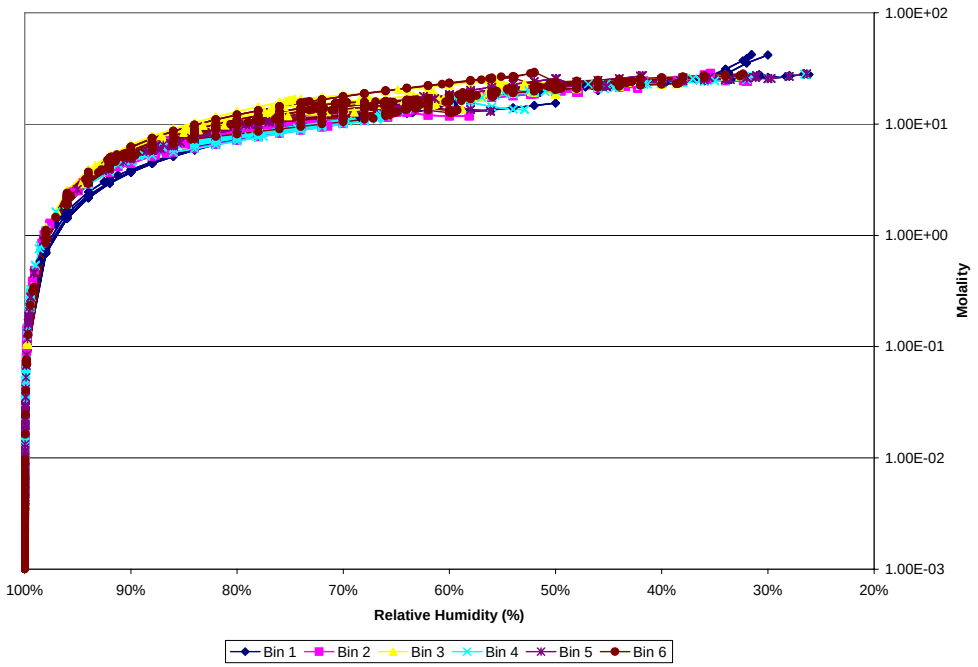

DTN MO0310SPAPCELA.002

Figure 6.13-36. Variation of Ionic Strength with Relative Humidity for All Six Dust Leachate Bins

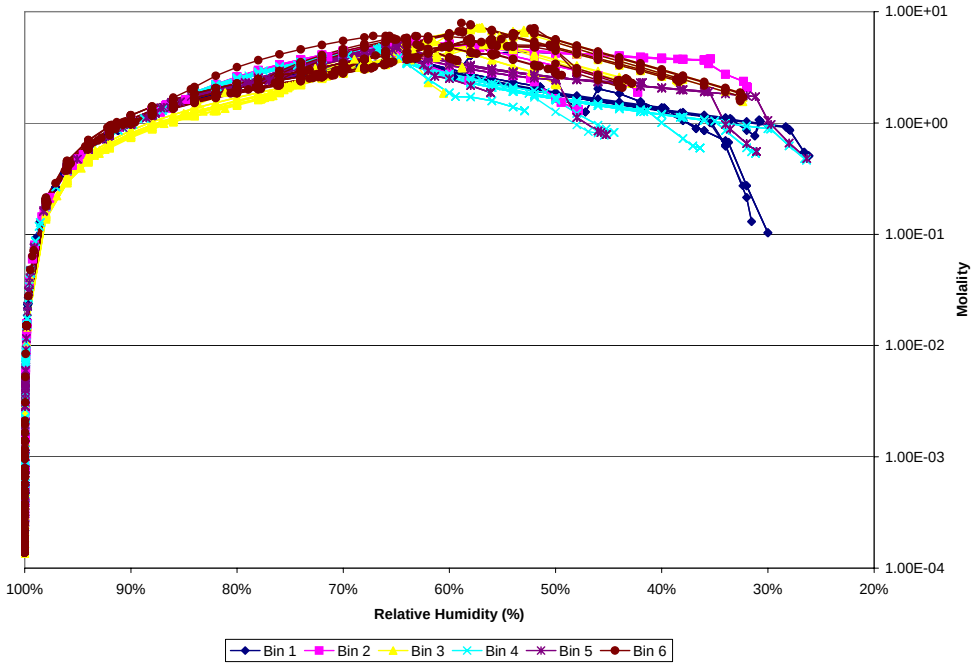

DTN MO0310SPAPCELA.002

Figure 6.13-37. Variation of Cl Concentration with Relative Humidity for All Six Dust Leachate Bins

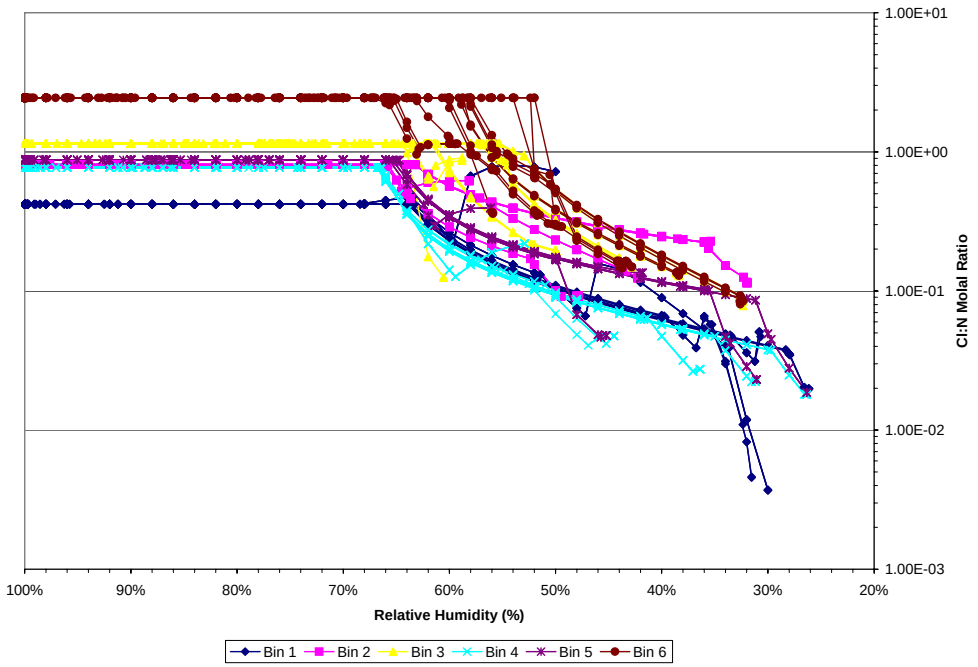

DTN: MO0310SPAPCELA.002

Figure 6.13-38. Variation of Cl/NO_3 with Relative Humidity for All Six Dust Leachate Bins

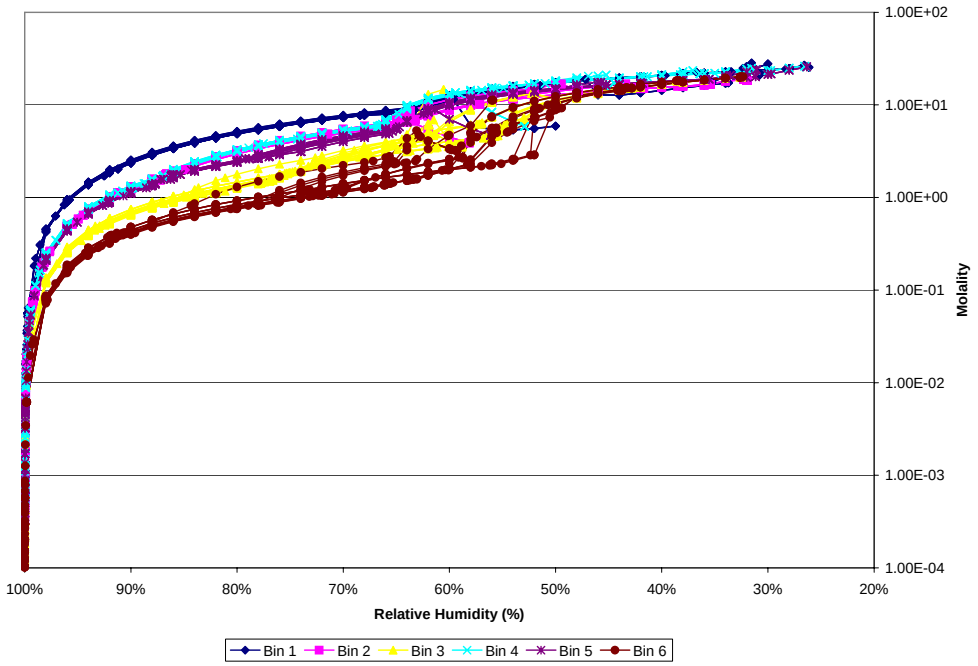

DTN: MO0310SPAPCELA.002

Figure 6.13-39. Variation of NO_3 with Relative Humidity for All Six Dust Leachate Bins

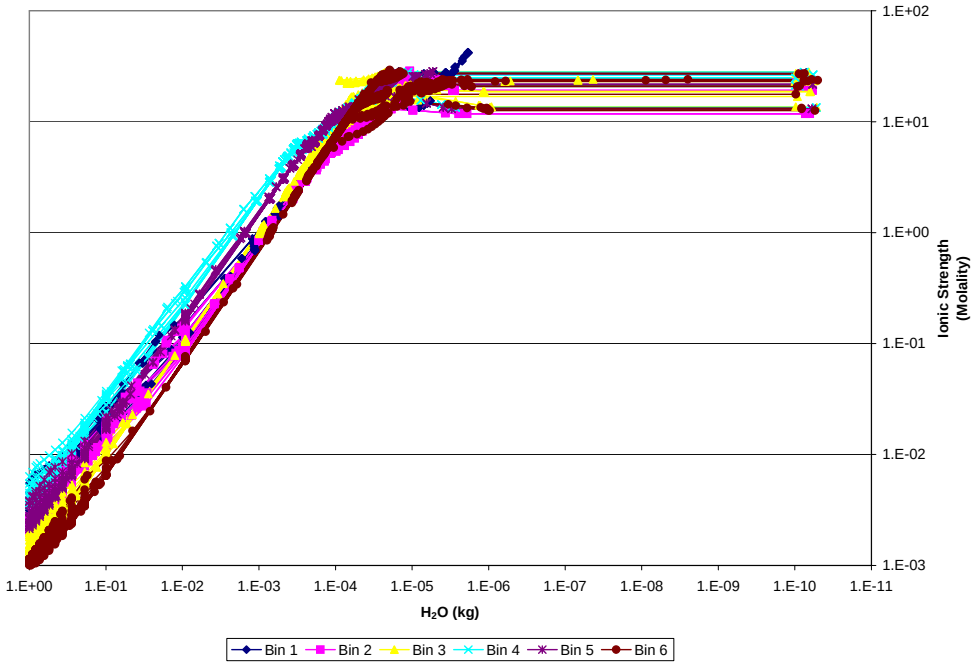

DTN: MO0310SPAPCELA.002

Figure 6.13-40. Mass of Water Versus Ionic Strength for All 6 Dust Leachate Bins

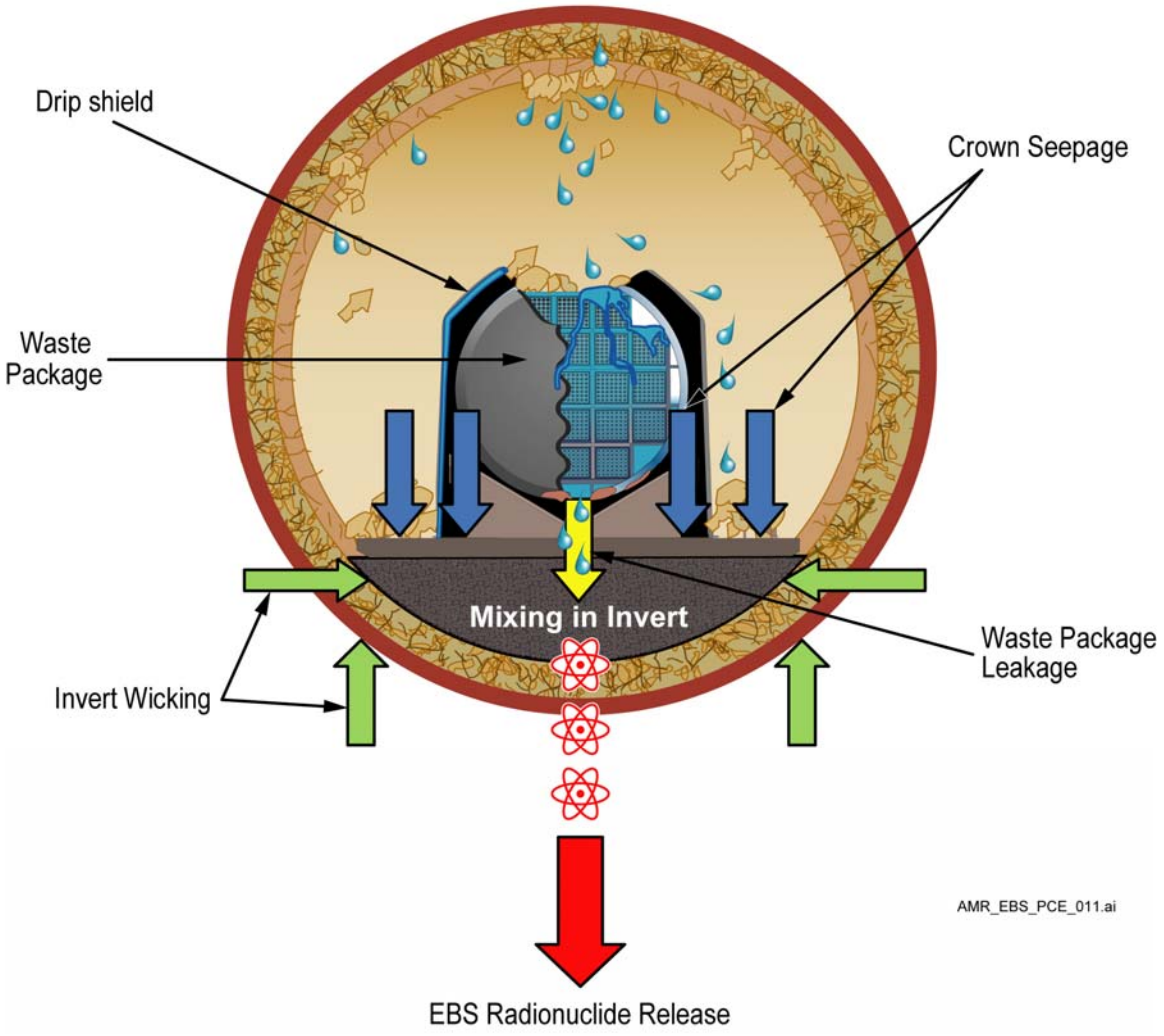

Figure 6.13-41. Schematic Representation of the Sources of Different Chemical Fluxes Into the Invert and Subsequent Radionculide Release from the Engineered Barrier System

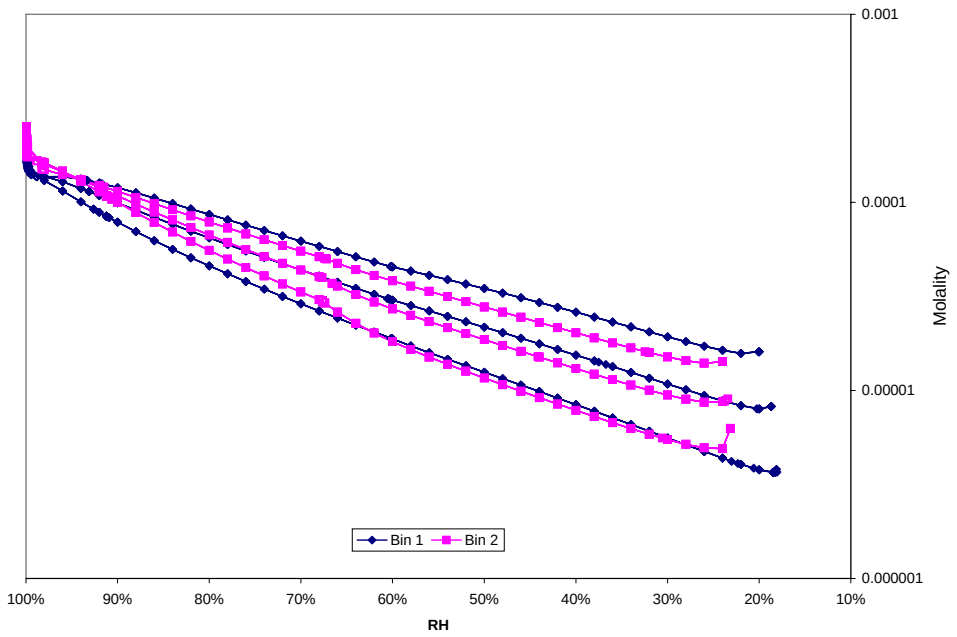

DTN MO0312SPAPCESA.002

Figure 6.13-42. Range of F Versus Relative Humidity for the Seepage Evaporation Lookup Tables Representing Bins 1 and 2

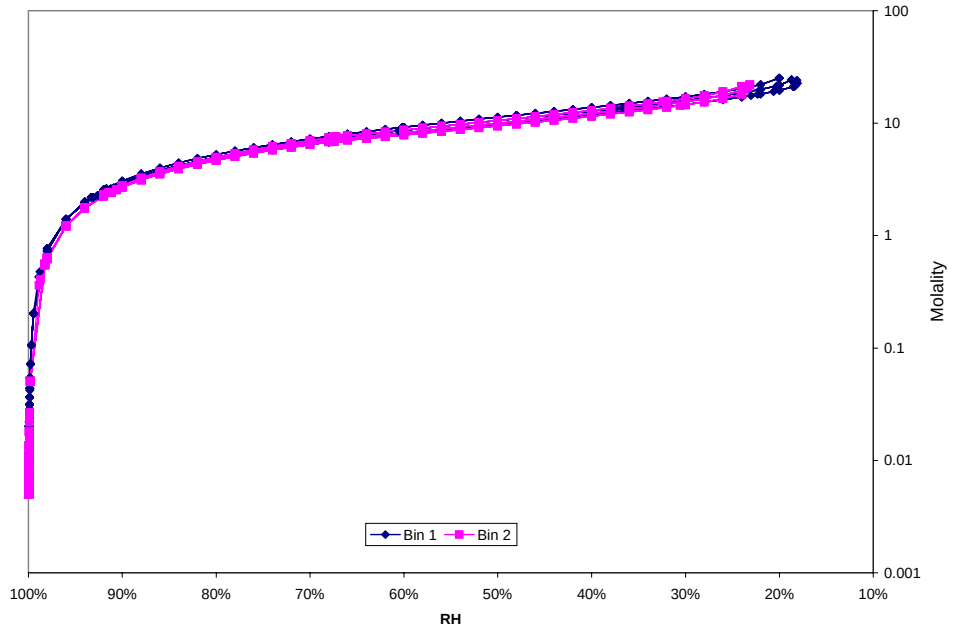

DTN MO0312SPAPCESA.002

Figure 6.13-43. Range of Cl Versus Relative Humidity for the Seepage Evaporation Lookup Tables Representing Bins 1 and 2

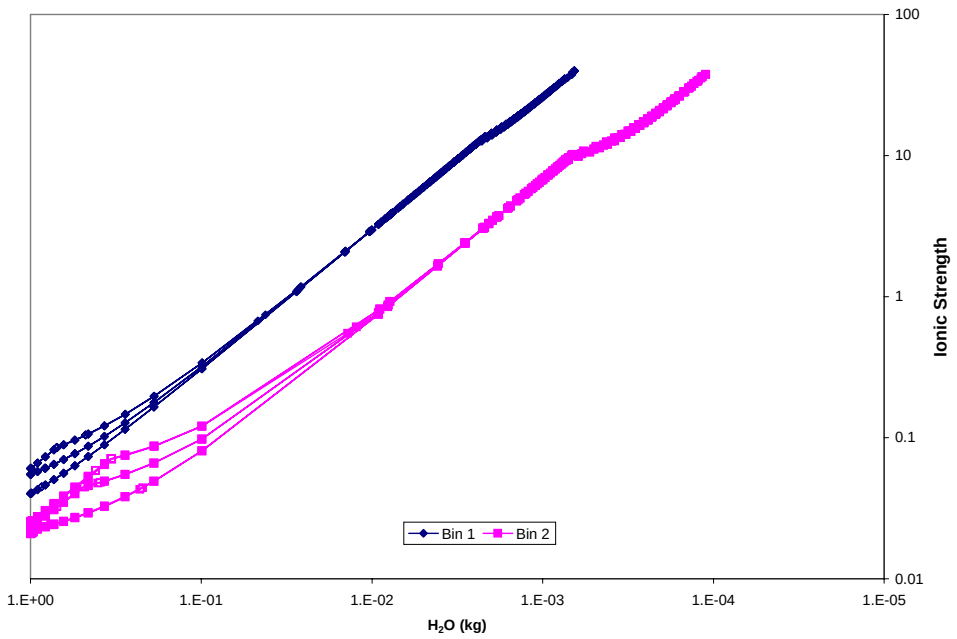

DTN MO0312SPAPCESA.002

Figure 6.13-44. Range of Ionic Strength Versus Mass of Water (kg) for the Seepage Evaporation Lookup Tables Representing Bins 1 and 2

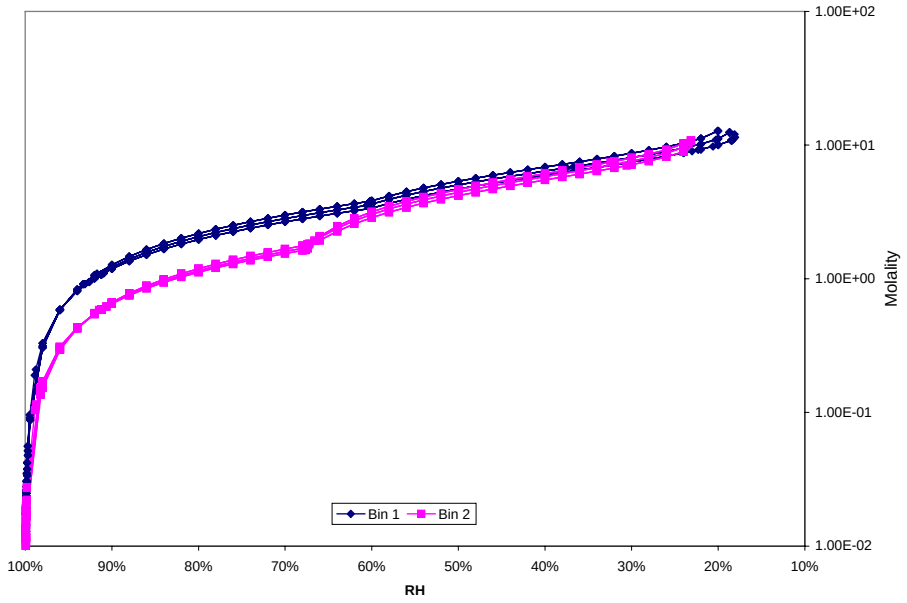

DTN MO0312SPAPCESA.002

Figure 6.13-45. Range of Total Elemental Ca for the Seepage Evaporation Lookup Tables Representing Bins 1 and 2

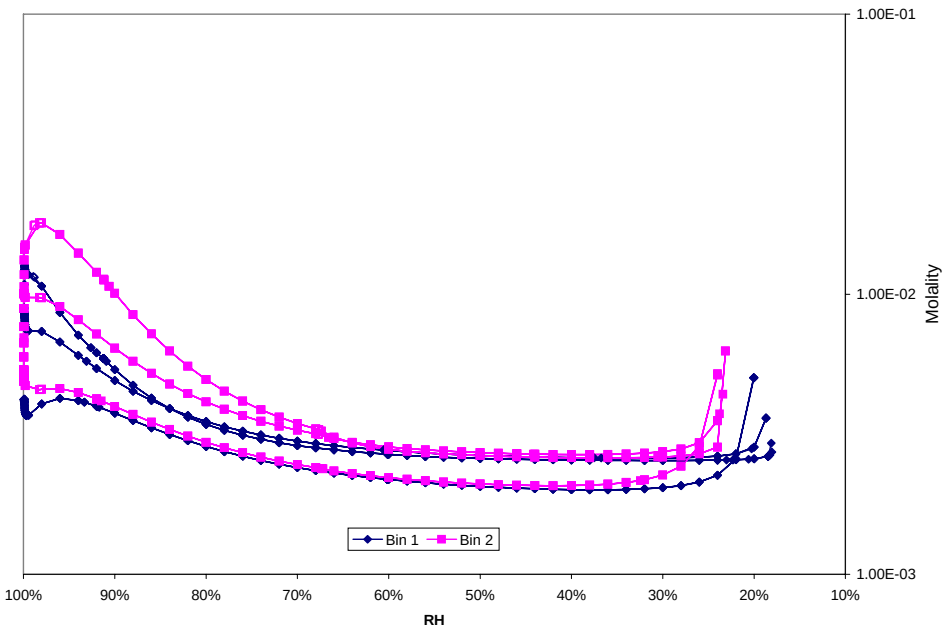

DTN MO0312SPAPCESA.002

Figure 6.13-46. Range of Total Elemental S for the Seepage Evaporation Lookup Tables Representing Bins 1 and 2

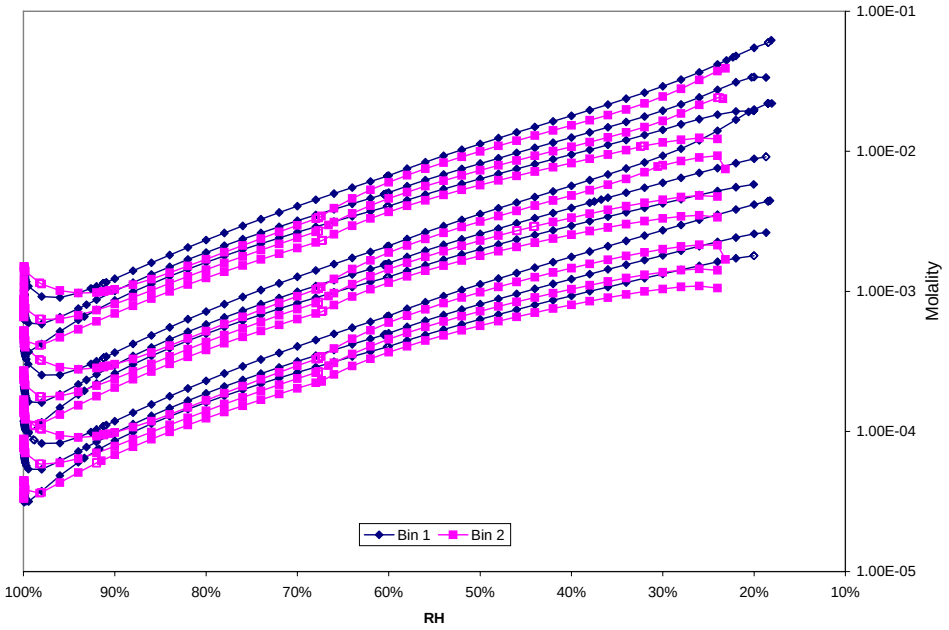

DTN MO0312SPAPCESA.002

Figure 6.13-47. Range of Total Elemental C for the Seepage Evaporation Lookup Tables Representing Bins 1 and 2

6.14 FEATURES, EVENTS AND PROCESSES EVALUATION

Section 1.2.1.2 of the technical work plan (BSC 2004, Table 1 [DIRS 166519]), lists the features, events, and processes (FEPs) related to the EBS physical and chemical environment. FEPs evaluation due to the presence of microbial communities has not been evaluated in this report. FEPs associated with microbial activity will be addressed in BSC 2003 [DIRS 166464]. Although FEP 1.1.02.00.0A is listed in the technical work plan as a FEP to be addressed in this report (BSC 2004, Table 1 [DIRS 166519]), because of integration and disposition purposes, this FEP will only be addressed in BSC 2003 [DIRS 166464].

The disposition of included FEPs is discussed in Table 6.14-1; excluded FEPs are discussed in Table 6.14-2. In addition to the EBS FEPs listed in Tables 6.14-1 and 6.14-2, several other FEPs that are explicitly incorporated in the *Abstraction of Drift-Scale Coupled Processes* report (BSC 2003 [DIRS 164888], Table 6.1-1) are implicitly included in this analysis as part of model input (water and gas compositions) and/or boundary conditions. However, these additional FEPs are adequately addressed in the *Abstraction of Drift-Scale Coupled Processes* report (BSC 2003 [DIRS 164888], Table 6.1-1) and are not repeated here.

Table 6.14-1. Features, Events and Processes Included in This Model Report and Their Disposition in Total Systems Performance Assessment - License Application

FEP Number	LA-FEP Title	Section Where Disposition is Described
2.1.08.06.0A	**Capillary effects (wicking) in EBS**	6.6, 6.9, 6.13
	Description: Capillary rise, or wicking, is a potential mechanism for water to move through the waste and EBS.	
	Summary of Disposition in TSPA-LA: The composition of water entering the drift by wicking in the invert or by crown seepage is model input. Possible incoming water compositions were determined using a complex algorithm. 368 THC water compositions, representing the chemical evolution of 5 starting waters at each location (the invert and the crown) through time, are model inputs. These waters were grouped into 11 bins, according to a “normalized” chemistry determined by using geochemical modeling (EQ3/6) to simulate evaporation of the waters to a fixed activity of water. A representative water composition for each bin was chosen using a ranking algorithm. Look-up tables were then created for each of the five starting waters. The lookup tables are “bin history” maps; the evolving water compositions for the 5 starting waters (sampled to produce 368 water compositions) are mapped to the 11 bins through time. These lookup tables are then used to determine an incoming crown and invert water compositions by randomly choosing one of the 5 starting waters and using the appropriate bin history map to determine the applicable bin. The representative water for that bin is then used as the invert or crown water composition (Sections 6.6 and 6.13). Evaporative concentration of the chosen water for each location is then simulated by geochemical modeling to produce a suite of possible water compositions (Section 6.9) that are passed to the TSPA-LA in the form of lookup tables. Chemical parameters used by the TSPA-LA are pH, ionic strength, and total aqueous Cl and N. This document only discusses the chemical effects on water composition due to wicking. For discussion on the flow and transport issues related to this FEP, see BSC (2003 [DIRS 166466]).	

Table 6.14-1 Features, Events and Processes Included in This Model Report and Their Disposition in Total Systems Performance Assessment - License Application (Continued)

FEP Number	LA-FEP Title	Section Where Disposition is Described
2.1.08.07.0A	**Unsaturated flow in the EBS**	6.6, 6.9, 6.13
	Description: Unsaturated flow may occur along preferential pathways in the waste and EBS. Physical and chemical properties of the EBS and waste form, in both intact and degraded states, should be considered in evaluating pathways.	
	Summary of Disposition in TSPA-LA: One pathway for water entering the drift is by wicking upwards through the invert. The composition of water entering the drift by wicking in the invert or by crown seepage is model input. Possible incoming water compositions were determined using a complex algorithm. 368 THC water compositions, representing the chemical evolution of 5 starting waters at each location (the invert and the crown) through time, are model inputs. These waters were grouped into 11 bins, according to a "normalized" chemistry determined by using geochemical modeling (EQ3/6) to simulate evaporation of the waters to a fixed activity of water. A representative water composition for each bin was chosen using a ranking algorithm. Look-up tables were then created for each of the five starting waters. The lookup tables are "bin history" maps; the evolving water compositions for the 5 starting waters (sampled to produce 368 water compositions) are mapped to the 11 bins through time. These lookup tables are then used to determine an incoming crown and invert water compositions by randomly choosing one of the 5 starting waters and using the appropriate bin history map to determine the applicable bin. The representative water for that bin is then used as the invert or crown water composition (Sections 6.6 and 6.13). Evaporative concentration of the chosen water for each location is then simulated by geochemical modeling to produce a suite of possible water compositions(Section 6.9) that are passed to the TSPA-LA in the form of lookup tables. Chemical parameters used by the TSPA-LA are pH, ionic strength, and total aqueous Cl and N. This document only discusses the chemical effects on water composition due to wicking. For discussion on the flow and transport issues related to this FEP, see BSC (2003 [DIRS 166466]).	

Table 6.14-1 Features, Events and Processes Included in This Model Report and Their Disposition in Total Systems Performance Assessment - License Application (Continued)

FEP Number	LA-FEP Title	Section Where Disposition is Described
2.1.09.01.0A	**Chemical characteristics of water in drifts**	6.4, 6.6, 6.7, 6.8, 6.9, 6.10, 6.12, 6.13
	Description: When flow in the drifts is re-established following the peak thermal period, water may have chemical characteristics influenced by the near-field host rock and EBS. Specifically, the water chemistry (pH and dissolved species in the groundwater) may be affected by interactions with cementitious materials or steel used in the disposal region. These point source contaminated waters may coalesce to form a larger volume of contaminated water. This altered groundwater is referred to as the carrier plume because dissolution and transport will occur in this altered chemical environment as contaminants move through the EBS, and down into the unsaturated zone. (Note: there is no defining limit as to what volume of contaminated water constitutes a plume.)	
	Summary of Disposition in TSPA-LA: The composition of water entering the drift by wicking in the invert or by crown seepage is model input. Possible incoming water compositions were determined using a complex algorithm. 368 THC water compositions, representing the chemical evolution of 5 starting waters at each location (the invert and the crown) through time, are model inputs. These waters were grouped into 11 bins, according to a “normalized” chemistry determined by using geochemical modeling (EQ3/6) to simulate evaporation of the waters to a fixed activity of water. A representative water composition for each bin was chosen using a ranking algorithm. Look-up tables were then created for each of the five starting waters. The lookup tables are “bin history” maps; the evolving water compositions for the 5 starting waters (sampled to produce 368 water compositions) are mapped to the 11 bins through time. These lookup tables are then used to determine an incoming crown and invert water compositions by randomly choosing one of the 5 starting waters and using the appropriate bin history map to determine the applicable bin. The representative water for that bin is then used as the invert or crown water composition (Sections 6.6 and 6.13). Evaporative concentration of the chosen water for each location is then simulated by geochemical modeling to produce a suite of possible water compositions that are passed to the TSPA-LA in the form of lookup tables. Also included in these results is the precipitation of likely mineral phases in equilibrium with each water composition. Interactions from the abstracted time dependent THC seepage model compositions with in-drift committed materials were evaluated in Section 6.8, and found to be of low consequence with respect to water chemistry. Cement grout is no longer part of the repository drift design (Section 6.4). Spatial heterogeneity is captured in the THC model results and abstraction where the 11 bins represent the probable seepage waters that could enter the drift through time as discussed in Section 6.6 and 6.12. Sorption is not discussed in this report. A discussion of sorption issues are contained in BSC 2003 [DIRS 161620] and BSC 2003 [DIRS 166466]. The composition of brines formed by deliquescence of salt minerals in dust on the drip shield and waste package is modeled in Section 6.10, and passed to the TSPA-LA in the form of lookup tables. Parameters extracted from the water chemistries and used by the TSPA-LA are pH, ionic strength, and total aqueous Cl and N.	

Table 6.14-1 Features, Events and Processes Included in This Model Report and Their Disposition in Total Systems Performance Assessment - License Application (Continued)

FEP Number	LA-FEP Title	Section Where Disposition is Described
2.1.09.02.0A	**Chemical interaction with corrosion products**	6.7, 6.8
	Description: Corrosion products produced during degradation of the waste form, metallic portions of the waste package, and metals in the drift (rock bolts, steel in invert, gantry rails) may affect the mobilization and transport of radionuclides. Corrosion products may facilitate sorption/desorption and coprecipitation/dissolution processes. Corrosion products may form a “rind” around the fuel that could (1) restrict the availability of water for dissolution of radionuclides or (2) inhibit advective or diffusive transport of water and radionuclides from the waste form to the EBS. Corrosion products also have the potential to retard the transport of radionuclides to the EBS. Finally, corrosion products may alter the local chemistry, possibly enhancing dissolution rates for specific waste forms, or altering radionuclide solubility.	
	Summary of Disposition in TSPA-LA: The effects of corrosion product formation on in-drift water chemistry and gas composition are evaluated in Sections 6.8 and 6.7, respectively. THC seepage model abstracted water compositions are reacted with the 316L stainless steel ground support at the drift wall in Section 6.8. Results indicate that the active corrosion of these ground support components have a negligible effect on water chemistry contacting the waste package or flowing into the invert. Oxygen consumption due to corrosion of ground support materials and other committed materials is evaluated in the in-drift gas composition calculations in Section 6.7. Modeling suggests that oxygen consumption due to corrosion may result in oxygen-depleting conditions for a short period after closure (a few hundred years), primarily due to the corrosion of mild steel; there is no long-term effect on repository atmosphere. However, the repository is not expected to develop anoxic conditions. The oxygen-depleting period also corresponds to the “hot” period, during which seepage inflow is minimal or nonexistent. The effects of the buildup of corrosion products on metal surfaces were simulated by reducing the corrosion rates—this resulted in a somewhat longer period of oxygen depletion, but still not significant relative to regulatory time periods. Thus, all geochemical modeling for this report was carried out using a partial pressure of oxygen corresponding to that of the Earth’s atmosphere (~0.2), and a the partial pressure of CO_2 matching that of the THC model inputs. A discussion of colloid issues are is contained in BSC 2003 [DIRS 161620]. In-package and waste form chemistry issues are addressed in BSC (2003 [DIRS 161962]).	

Table 6.14-1 Features, Events and Processes Included in This Model Report and Their Disposition in Total Systems Performance Assessment - License Application (Continued)

FEP Number	LA-FEP Title	Section Where Disposition is Described
2.1.09.06.0A	**Reduction-Oxidation potential in EBS**	6.7
	Description: The redox potential in the waste and EBS influences the oxidation of barrier and waste-form materials and the solubility of radionuclide species. Local variations in the redox potential can occur.	
	Summary of Disposition in TSPA-LA: Redox conditions in the repository were addressed in the Section 6.7, where in-drift gas composition calculations evaluated oxygen consumption due to corrosion of ground support materials and other committed. Calculations show that oxygen consumption due to corrosion may result in oxygen-depleting conditions for a short period after closure (a few hundred years), primarily due to the corrosion of mild steel, but there is no long-term effect on repository atmosphere. The repository is not expected to develop anoxic conditions. Reduced oxygen availability would result in a lower corrosion rate, this results in a somewhat longer period of oxygen depletion, but still not significant relative to regulatory time periods. Thus, all geochemical modeling for this report was carried out using a partial pressure of oxygen corresponding to that of the Earth's atmosphere (~0.2).	
2.1.09.07.0A	**Reaction kinetics in EBS**	6.5, 6.6, 6.7, 6.8, 6.9, 6.10, 6.13
	Description: Chemical reactions, such as radionuclide dissolution/ precipitation reactions and reactions controlling the reduction-oxidation state, may not be at equilibrium in the drift and waste environment.	
	Summary of Disposition in TSPA-LA: The effects of reaction kinetics are implicitly included in each geochemical submodel of the P&CE model report. In reaction path geochemical modeling calculations using EQ3/6 of the water compositions resulting from seepage evaporation (section 6.9) or dust deliquescence (Section 6.10), individual mineral phases were suppressed if those phases are kinetically inhibited from forming under repository conditions. A list of minerals inhibited during the modeling, including justification for the decision to inhibit each mineral, is present in Section 6.5. The choice of mineral suppressions directly affects the modeled evolution of the in-drift waters, and hence the water compositions that are passed to the TSPA-LA in the form of lookup tables. In addition, the kinetics of corrosion of committed materials was examined with respect to its effect on in-drift water and atmosphere compositions. Seepage water interactions with rock bolts and 316L stainless steel mesh in the drift wall is evaluated in Section 6.8 and found to be of low consequence. In Section 6.12, a sensitivity analysis shows that increasing corrosion rates by an order of magnitude has no significant effect. Oxygen consumption due to corrosion of ground support materials and other committed materials is evaluated in the in-drift gas composition calculations in Section 6.7. Although the repository may have oxygen-depleting conditions for a short period after closure (a few hundred years), primarily due to the corrosion of mild steel, there is no long-term effect on repository atmosphere. The repository is not expected to develop anoxic conditions. The effects of corrosion kinetics were evaluated by reducing the corrosion rates—this resulted in a somewhat longer period of oxygen depletion, but still not significant relative to regulatory periods. For this reason, all geochemical modeling for this report was carried out using a partial pressure of oxygen corresponding to that of the Earth's atmosphere (~0.2). . The choice of Po_2 directly affects the modeled evolution of the in-drift waters, and hence the water compositions that are passed to the TSPA-LA in the form of lookup tables. Parameters that are extracted from the lookup tables and used by the TSPA-LA are pH, ionic strength, and total aqueous Cl and N.	

Table 6.14-1 Features, Events and Processes Included in This Model Report and Their Disposition in Total Systems Performance Assessment - License Application (Continued)

FEP Number	LA-FEP Title	Section Where Disposition is Described
2.1.09.28.0A	**Deliquescence on waste package outer surface**	6.4, 6.7, 6.8, 6.10, 6.13
	Description: Salt-containing dust, which would have accumulated on the waste package surface during the pre-closure ventilation period, can absorb moisture from the drift atmosphere, even at low RH, dissolving the salt and creating concentrated aqueous solutions. This deliquescence process may result in 1) moisture contacting the waste package surface earlier than predicted by general seepage and relative humidity considerations, 2) a localized surface chemistry that might be more corrosive than seepage waters or concentrated solutions created by evaporation of seepage waters.	
	Summary of Disposition in TSPA-LA: The composition of moisture forming by deliquescence and dissolution of salts in dust on the exterior of the waste package is explicitly modeled in the in-drift dust leachate analysis submodel (Section 6.10). The potential compositions of fluids forming on the waste package are estimated from the experimentally determined soluble components in dust samples from the Experimental Drift. Evaporation to dryness of water leachate from the dust samples was simulated using EQ3/6 calculations; the predicted fluid compositions at low water activity correspond to the fluids that would form by deliquescence at the relative humidities corresponding to those water activities. The compositions of brines formed by deliquescence as a function or relative humidity are provided to the TSPA-LA as model output in the form of lookup tables. Parameters extracted from the water chemistries and used by the TSPA-LA are pH, ionic strength, and total aqueous Cl and N. In addition, this water chemistry is used as a basis for estimating committed materials corrosion rates in Section 6.4. These corrosion rates were used to evaluate the effects of corrosion on in-drift water and atmosphere compositions (Sections 6.8 and 6.7, respectively). The effects on water composition were found to be negligible; atmosphere compositions were sensitive to corrosion only in the short term (conditions potentially became oxygen-depleted for the first few hundred years) but were excluded from long-term repository performance on the basis of low consequence.	
2.1.09.28.0B	**Deliquescence on drip shield outer surface**	6.4, 6.7, 6.8, 6.10, 6.13
	Description: Salt-containing dust, which would have accumulated on the drip shield surface during the pre-closure ventilation period, can absorb moisture from the drift atmosphere, even at low RH, dissolving the salt and creating concentrated aqueous solutions. This deliquescence process may result in 1) moisture contacting the drip shield surface earlier than predicted by general seepage and relative humidity considerations, 2) a localized surface chemistry that might be more corrosive than seepage waters or concentrated solutions created by evaporation of seepage waters.	
	Summary of Disposition in TSPA-LA: The composition of moisture forming by deliquescence and dissolution of salts in dust on the drip shield is explicitly modeled in the in-drift dust leachate analysis submodel (Section 6.10). The potential compositions of fluids forming on the waste package are estimated from the experimentally determined soluble components in dust samples from the Experimental Drift. Evaporation to dryness of water leachate from the dust samples was simulated using EQ3/6 calculations; the predicted fluid compositions at low water activity correspond to the fluids that would form by deliquescence at the relative humidities corresponding to those water activities. The compositions of brines formed by deliquescence as a function or relative humidity are provided to the TSPA-LA as model output in the form of lookup tables. Parameters extracted from the water chemistries and used by the TSPA-LA are pH, ionic strength, and total aqueous Cl and N. In addition, this water chemistry is used as a basis for estimating committed materials corrosion rates in Section 6.4. These corrosion rates were used to evaluate the effects of corrosion on in-drift water and atmosphere compositions (Sections 6.8 and 6.7, respectively). The effects on water composition were found to be negligible; atmosphere compositions were sensitive to corrosion only in the short term (conditions potentially became oxygen-depleted for the first few hundred years) but were excluded from long-term repository performance on the basis of low consequence.	

Table 6.14-1 Features, Events and Processes Included in This Model Report and Their Disposition in Total Systems Performance Assessment - License Application (Continued)

FEP Number	LA-FEP Title	Section Where Disposition is Described
2.1.11.01.0A	**Heat generation in EBS**	6.7, 6.8, 6.9, 6.10, 6.12, 6.13
	Description: Temperature in the waste and EBS will vary through time. Heat from radioactive decay will be the primary cause of temperature change, but other factors to be considered in determining the temperature history include the in-situ geothermal gradient, thermal properties of the rock, EBS, and waste materials, hydrological effects, and the possibility of exothermic reactions. Considerations of the heat generated by radioactive decay should take different properties of different waste types, including Defense SNF, into account.	
	Summary of Disposition in TSPA-LA: Heat generation in the EBS controls predicted in-drift temperatures in the THC model. . In-drift temperature is model input, taken from the THC model at each time step. The effects of temperature on mineral stabilities and chemical reaction rates are implicitly included in each geochemical submodel of the P&CE model report. In geochemical modeling of the water compositions resulting from seepage evaporation (section 6.9) or dust deliquescence (Section 6.10), the temperature range over which individual mineral phases are stable is a function of the thermodynamic data used in the modeling. By controlling the stability of some mineral phases, the in-drift temperature directly affects the modeled evolution of the in-drift waters, and hence the water compositions that are passed to the TSPA-LA in the form of lookup tables. In addition, temperature will affect reaction kinetics for corrosion of committed materials. This was examined with respect to its effect on in-drift water and atmosphere compositions. Seepage water interactions with rock bolts and 316L stainless steel mesh in the drift wall is evaluated in Section 6.8 and found to be of low consequence. In Section 6.12, a sensitivity analysis shows that increasing corrosion rates by an order of magnitude has no significant effect. Oxygen consumption due to corrosion of ground support materials and other committed materials is evaluated in the in-drift gas composition calculations in Section 6.7. Although the repository may go oxygen-depleted for a short period after closure (a few hundred years), primarily due to the corrosion of mild steel, there is no long-term effect on repository atmosphere. The repository is not expected to develop anoxic conditions. The effects of corrosion kinetics were evaluated by reducing the corrosion rates—this resulted in a somewhat longer period of oxygen depletion, but still not significant relative to regulatory periods. For this reason, all geochemical modeling for this report was carried out using a partial pressure of oxygen corresponding to that of the Earth's atmosphere (~0.2). The choice of Po_2 directly affects the modeled evolution of the in-drift waters, and hence the water compositions that are passed to the TSPA-LA in the form of lookup tables. Parameters that are extracted from the lookup tables and used by the TSPA-LA are pH, ionic strength, and total aqueous Cl and N. Within the TSPA-LA model, temperature and RH conditions that are derived from the *Multiscale Thermohydrologic Model* BSC (2003 [DIRS 166463]) are used to define the environmental conditions on the lookup tables (Section 6.9 and 6.10) so that the chemistry can be determined through time. The multiscale thermohydrologic model accounts for radioactive decay (the dominant source of heat in the drift), different waste types, natural thermal gradients and thermal properties of EBS components. Heat generated by other exothermic reactions (e.g., mineral precipitation), is insignificant compared to the heat generated from radioactive decay (see FEP 2.1.11.03.0A).	

Table 6.14-1 Features, Events and Processes Included in This Model Report and Their Disposition in Total Systems Performance Assessment - License Application (Continued)

FEP Number	LA-FEP Title	Section Where Disposition is Described
2.1.11.08.0A	**Thermal effects on chemistry and microbial activity in the EBS**	6.4, 6.7, 6.9, 6.10,
	Description: Temperature changes may affect chemical and microbial processes in the waste and EBS.	
	Summary of Disposition in TSPA-LA: Heat generation in the EBS controls predicted in-drift temperatures in the THC model. . In-drift temperature is model input, taken from the THC model at each time step. The effects of temperature on mineral stabilities and chemical reaction rates are implicitly included in each geochemical submodel of the P&CE model report. In geochemical modeling of the water compositions resulting from seepage evaporation (section 6.9) or dust deliquescence (Section 6.10), the temperature range over which individual mineral phases are stable is a function of the thermodynamic data used in the modeling. By controlling the stability of some mineral phases, the in-drift temperature directly affects the modeled evolution of the in-drift waters, and hence the water compositions that are passed to the TSPA-LA in the form of lookup tables. In addition, temperature will affect reaction kinetics for corrosion of committed materials. This was examined with respect to its effect on in-drift water and atmosphere compositions. Seepage water interactions with rock bolts and 316L stainless steel plate in the drift wall is evaluated in Section 6.8 and found to be of low consequence. In Section 6.12, a sensitivity analysis on the corrosion rate of the stainless steel ground support shows that increasing corrosion rates (simulating a change in the reaction kinetics) by an order of magnitude has no significant effect on seepage water chemistries. Oxygen consumption due to corrosion of ground support materials and other committed materials is evaluated in the in-drift gas composition calculations in Section 6.7. Although the repository may go oxygen-depleted for a short period after closure (a few hundred years), primarily due to the corrosion of mild steel and the increase in drift temperature, which drives out gas from the drift, there is no long-term effect on repository atmosphere. The repository is not expected to develop anoxic conditions. The effects of corrosion kinetics were evaluated by reducing the corrosion rates—this resulted in a somewhat longer period of oxygen depletion, but still not significant relative to regulatory periods. For this reason, all geochemical modeling for this report was carried out using a partial pressure of oxygen corresponding to that of the Earth's atmosphere (~0.2). The choice of P_{O_2} directly affects the modeled evolution of the in-drift waters, and hence the water compositions that are passed to the TSPA-LA in the form of lookup tables. FEPS associated with microbial activity will be addressed in BSC 2003 [166464]. Parameters that are extracted from the lookup tables and used by the TSPA-LA are pH, ionic strength, and total aqueous Cl and N.	

Table 6.14-1 Features, Events and Processes Included in This Model Report and Their Disposition in Total Systems Performance Assessment - License Application (Continued)

FEP Number	LA-FEP Title	Section Where Disposition is Described
2.2.08.04.0A	**Redissolution of precipitates directs more corrosive fluids to containers**	6.6, 6.9, 6.10, 6.13
	Description: Redissolution of precipitates which have plugged pores as a result of evaporation of groundwater in the dry-out zone, produces a pulse of fluid reaching the waste packages when gravity-driven flow resumes, which is more corrosive than the original fluid in the rock.	
	Summary of Disposition in TSPA-LA: The process of redissolution of mineral precipitates is explicitly included in the drift-scale THC model as part of the unsaturated zone analysis. This effect is included as part of the boundary condition to the EBS analysis, and the chemical properties of water inflow are model input. Possible incoming water compositions were determined using a complex algorithm. 368 THC water compositions, representing the chemical evolution of 5 starting waters at each location (the invert and the crown) through time, are model inputs. These waters were grouped into 11 bins, according to a “normalized” chemistry determined by using geochemical modeling (EQ3/6) to simulate evaporation of the waters to a fixed activity of water. A representative water composition for each bin was chosen using a ranking algorithm. Look-up tables were then created for each of the five starting waters. The lookup tables are “bin history” maps; the evolving water compositions for the 5 starting waters (sampled to produce 368 water compositions) are mapped to the 11 bins through time. These lookup tables are then used to determine an incoming crown and invert water compositions by randomly choosing one of the 5 starting waters and using the appropriate bin history map to determine the applicable bin. The representative water for that bin is then used as the invert or crown water composition (Sections 6.6 and 6.13). Evaporative concentration of the chosen water for each location is then simulated by geochemical modeling to produce a suite of possible water compositions (Section 6.9) that are passed to the TSPA-LA as model output in the form of lookup tables. The 11 bin waters that represent the abstraction of the THC seepage waters capture the effects of redissolution of precipitates in the host rock after the thermal dryout and how they evolve by dissolution and further evaporation (see Sections 6.6, 6.9 and 6.13). The composition of moisture forming by deliquescence and dissolution of salts in dust on the dust shield is explicitly modeled in the in-drift dust leachate analysis submodel (Section 6.10). The potential compositions of fluids forming on the waste package are estimated from the experimentally determined soluble components in dust samples from the Experimental Drift. Evaporation to dryness of water leachate from the dust samples was simulated using EQ3/6 calculations; the predicted fluid compositions at low water activity correspond to the fluids that would form by deliquescence at the relative humidities corresponding to those water activities. The compositions of brines formed by deliquescence as a function or relative humidity are model output, and are provided to the TSPA-LA in the form of lookup tables. In both cases, parameters extracted from the water chemistries and used by the TSPA-LA are pH, ionic strength, and total aqueous Cl and N.	

Table 6.14-2. Features, Events and Processes Excluded in This Model Report and Their Disposition in Total Systems Performance Assessment - License Application

FEP Number	LA-FEP Title	Section Where Disposition is Described
2.1.06.01.0A	**Chemical effects of rock reinforcement and cementitious materials**	6.4, 6.7, 6.8
	Description: Degradation of ground support material (cement, rock bolts, wire mesh) used for any purpose in the disposal region may affect long-term performance through both chemical and physical processes. Degradation may occur by physical, chemical, and microbial processes.	
	Rationale for Exclusion: Seepage water entering the drift may react with rock bolts and 316L stainless steel mesh in the drift wall. The impact of bolt and mesh corrosion on the chemistry of seepage entering the drift is evaluated in Section 6.8, and determined to be of low consequence. Oxygen consumption due to corrosion of ground support materials and other committed materials is evaluated in the in-drift gas composition calculations in Section 6.7. Although the repository may go oxygen-depleted for a short period after closure (a few hundred years), primarily due to the corrosion of mild steel, there is no long-term effect on repository atmosphere. These sensitivity analyses indicate that the chemical effects of ground support materials can be excluded on the basis of low consequence. Cement grout is no longer part of the repository drift design (Section 6.4).	
2.1.06.05.0C	**Chemical degradation of emplacement pallet**	6.4, 6.7, 6.8
	Description: Degradation of the materials used in the pedestal supporting the waste package may occur by chemical or microbial processes, and may affect the long-term performance of the repository.	
	Rationale for Exclusion: The waste package emplacement pallet contains components composed of 316L stainless steel and Alloy 22. The effects of corrosion of the stainless steel components on the chemistry of seepage entering the drift is evaluated and determined to be of low consequence in Section 6.8. Oxygen consumption due to corrosion of pallet materials and other committed materials is evaluated in the in-drift gas composition calculations in Section 6.7. Although the repository may go oxygen-depleted for a short period after closure (a few hundred years), primarily due to the corrosion of mild steel in the invert, there is no long-term effect on repository atmosphere. Uncertainties in the seepage water chemistry lookup tables passed to the TSPA-LA are adequately bounded without including these effects. Because the corrosion rate for Alloy 22 is much slower than that of other metals and alloys comprising the drift materials and waste package (Section 6.4.1), it was not included in model calculations. This document only discusses the chemical effects on water composition due to the presence of the emplacement pallet. For discussion on the flow and transport issues related to this FEP see BSC (2003 [DIRS 166466]).	

Table 6.14-2. Features, Events and Processes Excluded in This Model Report and Their Disposition in Total Systems Performance Assessment - License Application (Continued)

FEP Number	LA-FEP Title	Section Where Disposition is Described
2.1.06.05.0D	**Chemical degradation of invert**	6.4, 6.7,
	Description: Degradation of the materials used in the invert may occur by chemical or microbial processes, and may affect the long-term performance of the repository.	
	Rationale for Exclusion: The invert is composed of mild carbon steel components and crushed tuff. The carbon steel components are predicted to corrode very rapidly, within a few hundred years (Section 6.4.2.2). Because of the high corrosion rates for carbon steel, the effects of seepage interactions with these components were screened out with respect to long-term drift chemistry. Oxygen consumption due to corrosion of mild steel in the invert and other committed materials is evaluated in the in-drift gas composition calculations in Section 6.7. Although the repository may go oxygen-depleted for a short period after closure (a few hundred years), primarily due to the corrosion of mild steel, there is no long-term effect on repository atmosphere. Ground water seeping into the crushed tuff in the invert is assumed to be in equilibrium with the tuff host rock, and hence to interact little with the crushed material. For these reasons, the chemical effects of degradation of invert materials is are excluded from this model on the basis of low consequence. Radiological effects on the invert should be of little consequence due to the short lifetime of the invert materials This document only discusses the chemical effects on water composition due to chemical degradation of the emplacement pallet. FEPs associated with microbial activity will be addressed in BSC 2003 [166464]	

INTENTIONALLY LEFT BLANK

6.15 IMPLEMENTATION INSTRUCTIONS FOR TOTAL SYSTEM PERFORMANCE ASSESSMENT-LICENSE APPLICATION MODEL

This section describes how the chemistry and, more specifically, the lookup tables developed in Sections 6.6, 6.7, 6.9, and 6.10, and uncertainty instructions developed in Sections 6.12, are to be implemented in the TSPA-LA. This section provides roadmap figures for implementation of the lookup tables established in this report for the parameters of interest on the waste package surface and within the invert, during the development of the TSPA-LA model. Although the processes used to ascertain these parameters for the two locations are similar, the resulting chemical environments are different.

A general rule that applies to the seepage scenarios discussed in the following subsection is that once a starting water is selected (i.e., w0, w4, w5, w6, or w7, see Section 4.1.3), the associated Pco_2 gas lookup tables for that given water should also be selected for that given realization (see Section 6.7.3.1). The TSPA-LA model should not select these two tables independently. This also means that the Pco_2 lookup table applied in the drift for waste package chemistry should be from the same starting water (e.g. w0, w4, etc.,) as the selected crown seepage water entering the invert. In addition, the gas applied in the invert should be associated with the same starting water that is specified to select the gas in the drift. The only time that this rule does not apply is in the dust deliquescence scenario on the waste package surface scenario, because no seepage is present. In this case, any of the five Pco_2 lookup tables can be randomly selected for any given waste package.

6.15.1 Implementation of Engineered Barrier System Chemistry on Waste Package Surfaces

Two primary scenarios are envisioned for the use of the chemical parameters from the lookup tables on the waste package surface:

- When crown seepage is directly dripping onto the drip shields and waste packages.
- When there is no seepage flowing onto the waste packages or drip shields and the deliquescent dust and salt minerals that have accumulated on the waste package surface absorb water due to the local relative humidity in the drift.

These two scenarios are independently discussed in the following subsection.

6.15.1.1 Seepage or "Dripping Scenario"

This scenario, in which crown seepage drips directly onto the waste package or drip shield surface, is modeled in the TSPA-LA by using the roadmap given in Figure 6.15-1 and described further here.

For each TSPA-LA realization, in order to represent the uncertainty of seepage water entering the drift, the starting water (w0, w4, w5, w6 and w7, see Section 4.1.3) must be randomly selected. All five of these waters have an equal probability of selection for any given TSPA-LA realization. Therefore, the probability of any given water being selected is 20 percent.

Once the starting water is selected, the corresponding "bin history map" tables and Pco_2 lookup tables associated with that water are selected. This map gives the bin history across time for that particular starting water (see Section 6.6 for the development of these maps). These "bin history map" tables are archived in DTN: MO0310SPAEBSCB.003 and are provided on Tables 6.6-8 through 6.6-12. The Pco_2 lookup tables are provided in Tables 6.7-1 through 6.7-5 and are archived in DTN: MO0308SPACO2GL.001. Each bin history map table and Pco_2 lookup table is unique to the particular starting water.

Next, for any given TSPA-LA model time step, the appropriate seepage water bin (Table 6.9-6 provides file names of lookup tables) and Pco_2 are determined (in the bin history map table, use the column labeled "Bin for Crown Seepage," and in each Pco_2 lookup table, use the column labeled "Drift"). Concurrently, temperature and relative humidity values for the same time step, are obtained from other process models lookup tables.

The selected in-drift relative humidity value is used to determine whether the evaporative or condensate lookup tables are used. The condensate lookup tables are used if the selected relative humidity is greater than the relative humidity boundary condition values found in Table 6.9-7. In all other cases, the evaporative lookup tables are used. Table 6.9-6 lists the files that are part of DTN: MO0304SPACSALT.000, along with the 99 lookup tables for evaporative conditions and 99 lookup tables for condensate conditions. This DTN has been modified slightly for TSPA-LA use (see Section 8.2.1 for discussion) resulting in a DTN for use in the TSPA-LA model archived in MO0310SPAPCEGS.000.

The lookup table file nomenclature is ??c#t%$.xls.xls where:

- "??" is the two-digit bin number (01, 02 03 etc.),
- "#" is 2, 3, or 4 for fugacity of CO_2 equal to 10^{-2}, 10^{-3} or 10^{-4} bar, respectively,
- "%" is 4, 7, or 1 for temperature equal to 40, 70, or 100ºC, respectively, and
- "$" is e or c for evaporation or dilution.

The chemistries from the lookup tables are shown in Section 6.9.4 and in Attachment II.

To select the appropriate chemistry from a selected lookup table, the nearest drift relative humidity value row is used. When selecting chemical parameters that fall between lookup tables, the parameters should be estimated using liner interpolation on temperature and log linear for Pco_2 parameters. Chemistry values should be extrapolated for pH, I, Cl, and N if the Pco_2 exceeds the range of 10^{-4} to 10^{-2} bar, established in the lookup tables (up to $2 \cdot 10^{-2}$ and down to $1 \cdot 10^{-5}$ bar). This is based on the uncertainty results documented in Section 6.12.4.3. For temperatures above 100ºC and below 40ºC, extrapolation may not be used and the values to be used should be taken from the 100ºC or 40ºC lookup tables, respectively. If the RH is greater than the highest value in the lookup tables, use the highest value. Additional discussion of the use of extrapolation is included in Section 6.13.3. Implementation of uncertainty on any parameter should be done in accordance with the instructions found in Section 6.12.5.

The EQ3/6 calculation runs used to produce the seepage lookup tables did not always converge on the eutectic point associated with the deliquescence RH value for very low water to solute

ratios (this occurs at relatively low RH values). An appropriately conservative method to deal with this limitation is to specify that aqueous conditions exist at all times when seepage is occurring, regardless of the in-drift RH. For TSPA-LA purposes, the selection of chemical parameters below the reported DRH in the lookup tables (row with lowest RH value on the lookup table) can be done, because the chemistries should be conservative with respect to NO_3 (i.e., NO_3 should only increase with respect to Cl with decreasing RH due to the presence of the halite chemical divide). The basis for this modeling decision is illustrated in Figure 6.13-29, where at low RH the NO_3 concentration climbs in comparison to Cl ion, indicating that no matter where the DRH is predicted for the seepage, nitrate will continue to dominate the brine chemistry. The exception to this general rule is bin 1, where $Ca(NO_3)_2$ is precipitating and NO_3 is being removed from the aqueous system. This occurs around an RH of 20 percent. However, at lower RH values, the Cl:NO_3 ratio remains relatively constant because of the continued precipitation of halite and the lowest value taken from the lookup table will result in a conservative estimate of the Cl:NO_3 ratio.

6.15.1.2 Deliquescence or "No Drip Scenario"

This scenario is to be modeled in the TSPA-LA using the roadmap of Figure 6.15-2.

The identical Pco_2, temperature and RH histories that were selected based on the starting water composition are utilized for these no drip scenarios, as per Section 6.15.1.1.

The relative proportion of waste packages exposed to each dust leachate bin from Table 6.10-14 is determined by applying the probability distribution of the bins (representing the percentage of dust leachate samples in each bin), as shown on Table 6.10-6. Thus, in any given TSPA-LA realization, all dust bins will be represented.

The dust leachate lookup tables are archived in DTNs: MO0310SPADLALT.001 and MO0310SPADLHTL.000 and the chemistries contained in them are shown in Section 6.10.7 and in Attachment III.

The lookup table file nomenclature is d?c#t%.xls.xls where:

- "??" is the bin number (1, 2, 3 etc.),
- "#" is 2, 3, or 4 for fugacity of CO_2 equal to 10^{-2}, 10^{-3} or 10^{-4} bar, respectively, and
- "%" is 04, 07, 10, 12, or 14 for temperature equal to 40, 70, 100, 120, or 140ºC, respectively.

Because atmospheric pressure conditions are imposed in the repository through all time, there are conditions under which no water can be present (the existence of an aqueous liquid would require pressurized conditions). In order to determine when deliquescence water can be present in the repository environment, the TSPA-LA model should check to see when the RH conditions are possible for water to be present. This is done by comparing the lookup table H_2O vapor pressure value against the value of atmospheric pressure at the repository level (0.89 Bar). If the required pressure conditions of the chemistry are greater than this value, then no water can

deliquesce until the RH rises (see Figure 6.13-17). However, because of the uncertainty on deliquesce relative humidity (DRH), liquid water at or above 140°C is possible. The chemistry from the last data point on each of the 140°C lookup tables will be sufficient to predict the chemistry of the system in these sections of the lookup tables.

To select the appropriate chemistry from a lookup table, the nearest waste package relative humidity value row is used. When selecting chemical parameters that fall between lookup tables, the parameters should be estimated using linear interpolation on temperature and log linear interpolation on Pco_2 parameters. Chemistry values should be extrapolated for pH, I, Cl, and N if the Pco_2 exceeds the range of 10^{-4} to 10^{-2} bar, established in the lookup tables (up to $2 \cdot 10^{-2}$ and down to $1 \cdot 10^{-5}$ bar). This is based on the uncertainty results documented in Section 6.12. For temperatures above 140ºC and below 40ºC, no extrapolation may be performed and values to be used must be taken from the 140ºC or 40ºC lookup table chemistry results respectively. If the RH is greater than the highest value in the lookup tables, use the highest value. Additional discussion of the use of extrapolation discussion is included in Section 6.13.3. Implementation of uncertainty on any parameter should be done in accordance with the instructions found in Section 6.12.5.

The in-drift precipitates/salts model predictions for DRH below 40 percent RH are outside the range of the in-drift precipitates/salts model validation (see Table 6.12-1). Therefore, for TSPA-LA purposes the dust on the waste packages should be considered wet at all times when the DRH (last value on the lookup table) occurs below 40 percent RH (without uncertainty applied). Even though the DRH is not a valid parameter at these low RHs, the solubility results from the lookup table are well within the appropriate in-drift precipitates/salts model validation criteria and results (see BSC 2003 [DIRS 166031]). This means that, although we do not know with confidence where along the evaporative path the final dryout point is, we do have confidence that the chemistries predicted at low RH are reasonable. Dust Bin 1 should also be considered wet at all times. According to Table 6.12-1, the uncertainty in the DRH for $Ca(NO_3)_2$ also goes beyond the validation criteria established by the in-drift precipitates/salts. Bin 1 is the only dust bin to precipitate $Ca(NO_3)_2$ (see Table 6.13-7). Selection of chemical parameters below the reported DRH in the lookup tables (row with lowest RH value on the lookup table) can be done, as these chemistries should be conservative with respect to NO_3 (i.e., NO_3 should only increase or remain constant with respect to Cl with decreasing RH due to the initial encounter with halite chemical divide). The basis for this modeling decision can be seen from Figure 6.13-38, where at low RH the NO_3 concentration climbs in comparison to Cl, indicating that no matter where the DRH is predicted for the deliquescent dusts, nitrate will continue to dominate the brine chemistry. One exception to this is the values in dust bin 1 (which contains the highest ratio of nitrate) below 70°C where soda niter is encountered prior to halite, precipitating NO_3 from the aqueous system. This occurs briefly around a RH of 60 percent, just before the halite divide is reached. In this case, the $Cl:NO_3$ ratio briefly increases and then remains relatively constant once the halite divide has been crossed.

6.15.2 Implementation of Engineered Barrier System Chemistry in the Invert

The following instructions are imposed to ensure that the appropriate parameters are selected for lookup tables (crown seepage or invert wicking) that may be used in the invert cell of the TSPA-LA model.

For each TSPA-LA realization, one of the five starting seepage waters (w0, w4, w5, w6 and w7) must be selected randomly. All starting waters are equally probable and, therefore, the probability of any given water being selected is 20 percent.

Once the starting water is selected, the ”bin history map” and $P\mathrm{co}_2$ lookup tables (invert only) are to be selected. There are two separate maps, one for crown seepage and one for invert wicking water. These “bin history maps” are archived in DTN: MO0310SPAEBSCB.003 and can be found on Tables 6.6-8 through 6.6-12. The next set of lookup tables that are used is the $P\mathrm{co}_2$ lookup tables. The invert $P\mathrm{co}_2$ lookup tables are archived in DTN: MO0308SPACO2GL.001 and can be found on Tables 6.7-1 through 6.7-5. Whether the incoming water originates in the crown as seepage or from invert wicking, all evaluations of invert chemistry should apply the invert $P\mathrm{co}_2$ tables to select appropriate chemical values. The drift $P\mathrm{co}_2$ tables should not be used in the invert. Each bin history map table and $P\mathrm{co}_2$ lookup table is unique to a particular starting water.

Next, for any given TSPA-LA model time step, the appropriate seepage water bin (Table 6.9-6 provides file names of lookup tables) and $P\mathrm{co}_2$ are to be selected (see Table 6.9-7). In addition, temperature and relative humidity input for the same time step, which is available from other process models lookup tables, must be selected.

The selected in-drift relative humidity value should be used to determine whether the evaporative or condensate lookup tables are to be used. The condensate lookup tables are to be used if the selected relative humidity is greater than the relative humidity boundary condition values found in Table 6.9-7. In all other cases, the chemistries on the evaporative lookup tables are to be used. (Table 6.9-6 is part of DTN: MO0304SPACSALT.000, along with the 99 lookup tables for evaporative conditions and 99 lookup tables for condensate conditions.) This DTN has been modified slightly for TSPA-LA use (see Section 8.2.1 for discussion) resulting in a DTN for use in the TSPA-LA model archived in MO0310SPAPCEGS.000.

The lookup table file nomenclature is ??c#t%$.xls.xls where:

- “??” is the two-digit bin number (01, 02 03 etc.),
- “#” is 2, 3, or 4 for fugacity of CO_2 equal to 10^{-2}, 10^{-3} or 10^{-4} bar, respectively,
- “%” is 4, 7, or 1 for temperature equal to 40, 70, or 100ºC, respectively, and
- “$” is e or c for evaporation or dilution.

The chemistries from the lookup tables are shown in Section 6.9.4 and in Attachment II.

To select the appropriate chemistry from a lookup table, the nearest invert relative humidity value row is used. When selecting chemical parameters that fall between lookup tables, the parameters can be estimated using liner interpolation on temperature and log linear interpolation

on Pco_2 parameters. Chemistry values can be extrapolated for pH, I, Cl, and N if the Pco_2 exceeds the range of 10^{-4} to 10^{-2} established in the lookup tables (up to $2 \cdot 10^{-2}$ and down to $1 \cdot 10^{-5}$ bar). This is based on the uncertainty results documented in Section 6.12. For temperatures above 100ºC and below 40ºC, no extrapolation is allowed and values should be taken from the 100ºC or 40ºC lookup tables. If the RH is greater than the highest value in the lookup tables, use the highest value. Additional extrapolation discussion is included in Section 6.13.3. Implementation of uncertainty on any parameter should be done in accordance with the instructions found in Section 6.12.5.

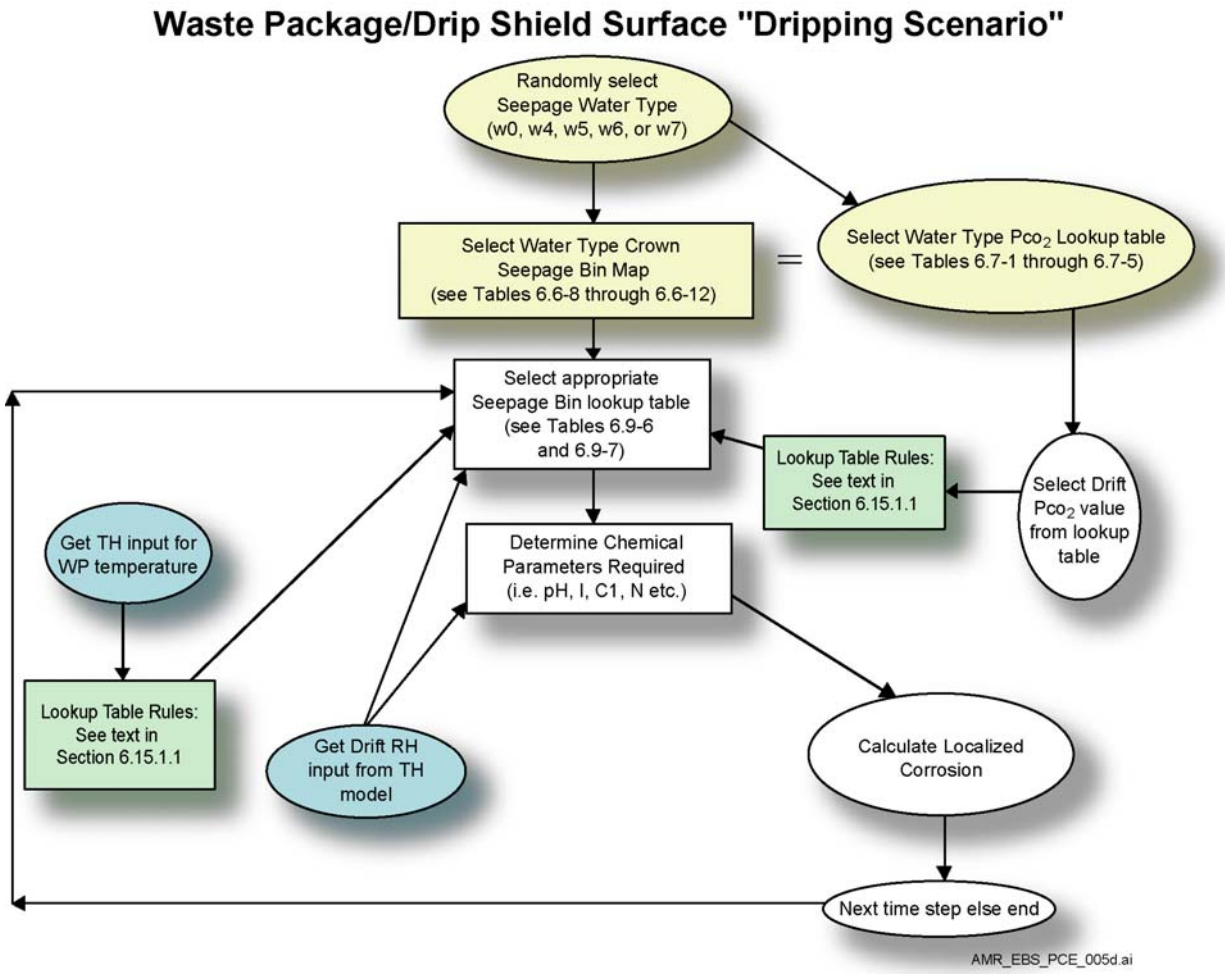

NOTE: The equal sign indicates that the bin map and Pco_2 lookup table have to be associated with the same seepage water type (w0,w4,w5,w6 or w7).

Figure 6.15-1. Roadmap for Total Systems Performance Assessment - License Application Implementation of Engineered Barrier System Chemistry on the Waste Package Surface Under the "Dripping Scenario"

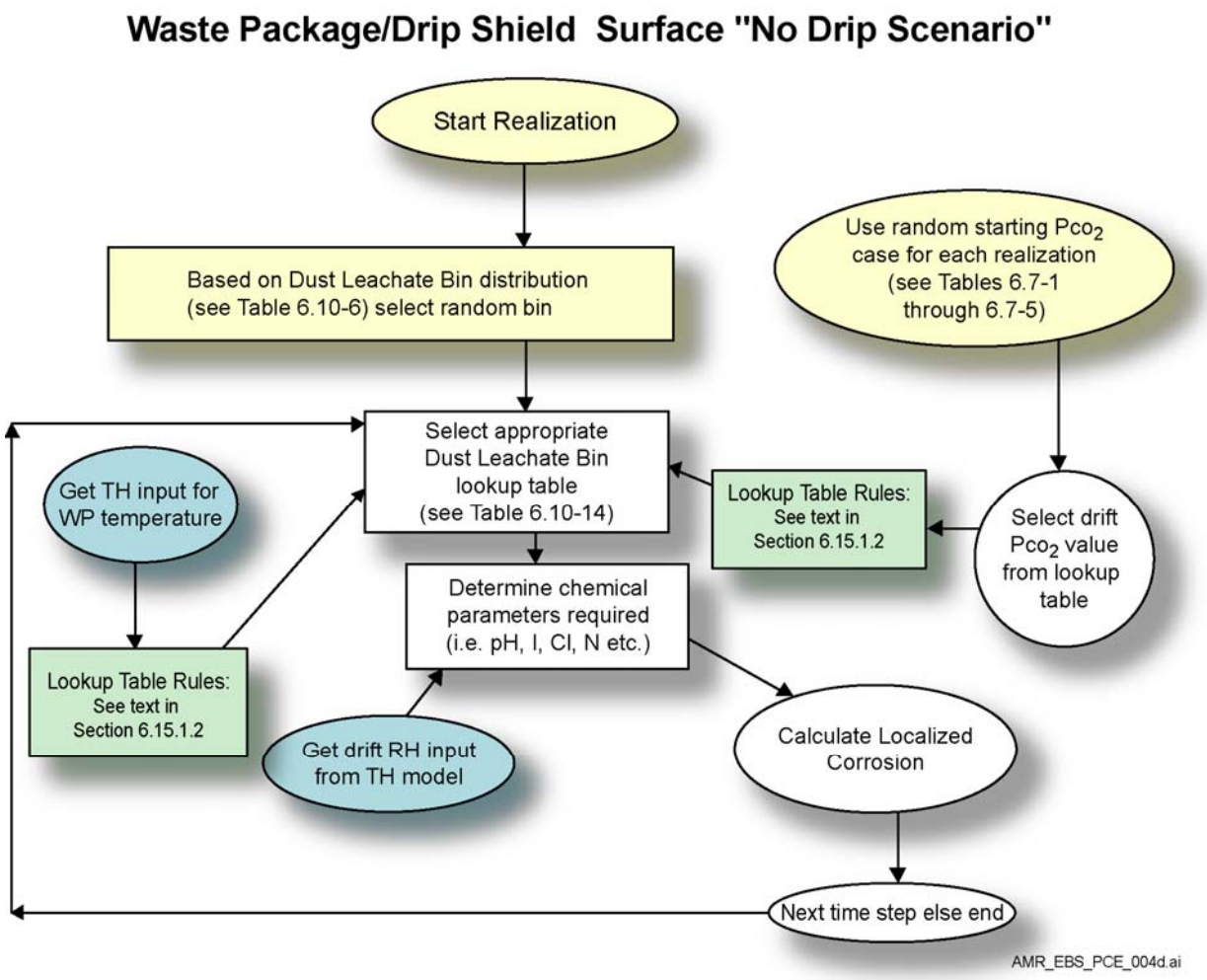

Figure 6.15-2. Roadmap for Total Systems Performance Assessment - License Application Implementation of Engineered Barrier System Chemistry on the Waste Package Surface Under the "No Dripping Scenario"

7. VALIDATION

This section summarizes the validation of models detailed in Section 6, and summarizes and further develops the validation discussions in other external model reports that affect the engineered barrier system (EBS) environment. The validation discussions identify an appropriate level of confidence by demonstrating that the models conform to generally accepted physical and chemical principles.

Section 7.1 specifies the validation criteria for this document. Section 7.2 compares thermal-hydrological-chemical (THC) reactive transport seepage abstraction model results with THC seepage model output to ensure that the abstractions described in Section 6.6 represents their intended use. Section 7.3 provides details of validation for the in-drift precipitates/salts model that quantifies the processes by which waters in the drift can evaporate, concentrate, deliquesce, or precipitate mineral solids that affect the aqueous chemistry and resulting environment. Section 7.4 enhances the validation of the in-drift precipitates salts model by considering evaporation of mountain spring water to a concentrated alkaline brine.

Section 7.5 compares deliquescence point comparisons with predictions derived from model evaporations using the EQ3/6 Version 8.0 software with the data0.ypf Pitzer database (for high ionic strength calculations) to experimental data taken from the literature. Section 7.6 includes mineral suppression sensitivity analyses for two minerals that additional natural analog information suggested should be handled differently than in the original EQ3/6 calculation runs. The sensitivity of this study's calculations to such changes is discussed, along with the natural analog suppression information, for other minerals with potential for occurrence in evaporative concentration EQ3/6 model calculation runs.

Section 7.7 is the validation of chromium equilibria for metal dissolution.

7.1 VALIDATION CRITERIA

Several models used directly in this document are validated within their corresponding model reports (e.g., precipitates/salts, THC seepage). However, validation efforts for several models that are developed in or for this document, or efforts which validation has been updated, are provided below. These models include the THC seepage abstraction model (Section 6.6), further validation for the implemented use of the in-drift precipitates salts model as it applies to dust leachate analyses (Section 6.10), and the implementation of the chemical divide phenomenon described in the literature (as described in Sections 6.2.2.2 and 6.6).

The following validation criteria are based on the technical work plan (BSC 2004, Section 2.1 [DIRS 166519]) and are applied in this validation study.

Criterion 1–Comparison of abstraction results with process model results, where the comparisons are within the uncertainty range, are established with past and planned model uncertainty and sensitivity studies. This applies to the abstraction of the THC seepage model discussed in Sections 6.6 and 6.7.

Criterion 2–Comparison of model results with alternative models from the literature, where the comparisons are within the uncertainty range, are established with model uncertainty and

sensitivity studies. This applies to the additional corroboration of the in-drift precipitates salts model and Pitzer database as it applies to the chemical divide phenomena described in Sections 6.6, 6.9, and the dust leachate analyses discussed in Section 6.10.

Criterion 3–Comparison of model results with data published in refereed journals, where the comparisons are within the uncertainty range, were established with model uncertainty and sensitivity studies. This applies to the additional corroboration of the in-drift precipitates salts model and Pitzer database as it applies to the implementation of the chemical divide phenomena described in Sections 6.6, 6.9, and the dust leachate analyses discussed in Section 6.10. This criterion is also used to validate the model for aqueous chromium species used in calculations made for seepage-steel ground support interactions discussed in Section 6.8.

7.2 MODEL ABSTRACTION VALIDATION CASES

Two sets of abstraction comparisons are discussed in this section. The first set (Section 7.2.1) compares the binning abstraction to that of the actual THC seepage model output. The second comparison uses a set of lookup tables and performs an interpolation between the lookup tables in a similar manner as is described in Sections 6.15.1.1 and 6.15.1.2.

7.2.1 Comparison of THC Seepage Abstraction with THC Seepage Model Output

In accordance with Criterion 1, the THC seepage abstraction results are compared to the actual THC seepage model output results to insure that the original THC model output results are within the bounds of the abstractions uncertainty range.

These comparisons are documented in the "THC Seepage Validation Spreadsheet LOG distributions.xls" (DTN: MO0312SPAPCESA.002) that contains the output values developed in Section 6.6. This spreadsheet was constructed using the THC Starting Chemistry Tables worksheet (copied from "Final Checked EBS THC Seepage Binning Abstraction REV 4xls" archived in DTN: MO0310SPAEBSCB.003), the All Data worksheet and the 11 bin worksheets copied from "New Non Evaporated Binning Statistics.xls" archived in DTN: MO0310SPAEBSUE.002.

For each comparison (see Figures 7.2-1 through 7.2-20), four series of data were plotted:

- First, the "THC Seepage," the actual water chemistry found on the "all data" worksheet. These data are the THC model values of the waters identified to potentially seep into the drift from the crown ("tf4") or from the invert ("bf4") for the various THC model starting waters (w0, w4, w5, w6, and w7). These values change as a function of time.

- Second, the "Bin Median Water Abstraction," the median water chemistry parameter found on the "THC starting chemistry" tables. These are the THC model values of the 11 waters chosen to represent the water chemistry in each of the bins. These values do *not* change as a function of time. Thus, they are *not* exposed in this validation exercise to the same conditions (temperature, relative humidity, and fugacity of carbon dioxide) as the "THC Seepage." As a result, differences between these data and the "THC Seepage" compositions may be considerably larger than they would be had these median bin waters been normalized for the same set of conditions. Therefore, the differences

observed in this validation should not be interpreted as error. These non-normalized differences are used in this report for model validation only. Uncertainty in the THC model abstraction is evaluated under normalized conditions in Section 6.12.

- Third, the "Median Parameter." These values are the medians of the THC model values in each bin. They also do *not* change as a function of time and are *not* normalized to the same conditions of temperature, relative humidity, and fugacity of carbon dioxide as the "THC Seepage." These are best compared to the second data set, the "Bin Median Water Abstraction," though these comparisons also are non-normalized for environmental conditions. Note also that these median parameters are strictly statistical and that taken together for a given bin they do not represent any actual water compositions that could exist.

- Fourth, the 2s error bars. The 2s values used to generate the error bars are twice the standard deviations calculated from the set of THC seepage waters in each bin. Thus, these values are bin-specific, do not change as a function of time, and are not normalized for environmental conditions of temperature, relative humidity, and fugacity of carbon dioxide. These 2s values are applied to the "Bin Median Water Abstraction" in the figures to generate +/-2s error bars. These error bars should not be interpreted as uncertainty in the THC abstraction. These non-normalized values are used here for model validation only. Uncertainty in the THC model abstraction is evaluated under normalized conditions in Section 6.12.

Figures 7.2-1 through 7.2-20 show abstracted values versus the original THC input. As an example, the abstraction bin information for Figures 7.2-9 and 7.2-10 is mapped in Figure 6.13-1 for water 5, "w5," in the invert. The THC seepage water represents the explicit temporal evolution of water 5 (matrix water at the base of the invert, for the wetting front at node four - w5bf4). To limit the comparisons to a reasonable number, the results for pH and one other parameter are presented for each water type and location. Each non-pH parameter was picked in an unbiased manner.

The abstraction reduces fluctuations in the THC seepage outputs. With the exception of a few cases, all values plotted fall within the 2s error bar values. Those that fall outside the error bars are THC seepage waters that would actually fall much closer to the median values upon equilibration with the same temperature, relative humidity, and fugacity of carbon dioxide as the median waters. Based on comparisons of this type, the abstraction is considered a valid representation of the THC seepage model results. An evaluation of the uncertainty in the THC model abstraction under normalized conditions is presented in Section 6.12.

7.2.2 Comparison of Lookup Table Interpolations with P&CE Model Results

In accordance with Criterion 1, the lookup table interpolation results are compared with an actual model output to ensure that the interpolation results are within the bounds of the uncertainty range on the actual model output.

The inputs selected for this validation calculation were from Bin 11 seepage lookup table EQ6 calculations found in DTN: MO0304MWDEBSSA.000. These include the following input and output files:

- 11c3t4e.6i
- 11c3t7e.6o
- 11c3t4e.6o
- 11c4t7e.6o
- 11c4t4e.6o.

The input file 11c3t4e.6i was modified to replace the temperature and CO_2 partial pressure and renamed bin11val.6i. The selected temperature and Pco_2 for the actual model calculation run was 56°C and $10^{-3.2}$ bars of CO_2.

Software application EQ3/6 version 8.0 was used to run bin11val.6i along with Data0.ypf (DTN: SN0302T0510102.002 [DIRS 162572]) to create bin11val.6o. GetEQData was then used to extract the results from bin11val.6o along with the results of the four lookup table output files listed above into a spreadsheet entitled "bin11val.xls". This spreadsheet was then used to create Figures 7.2-21 through 7.2-24.

In the validation, values for pH, ionic strength, Cl, and NO_3 were first interpolated with respect to CO_2 partial pressure at 40°C and 70°C, the two nearest temperatures in the set of lookup tables. Interpolation for $10^{-3.2}$ bars of CO_2 partial pressure is accomplished by linearly interpolating the logarithms of CO_2 partial pressure. In this case, the two nearest logarithms of CO_2 partial pressure in the lookup tables are -3 and -4. The interpolated values were then plotted at 40°C and 70°C and connected by a straight line (in yellow in the figures) to determine the interpolated value at 56°C and $10^{-3.2}$ bars of CO_2. This interpolation is compared in the figures to the directly modeled result, shown as pink squares. The uncertainty data for the error bars shown were taken from Table 6.12-1. These files can be found in DTN: MO0312SPAPMVIC.000.

The actual model results when compared to the interpolation results indicate that the interpolated values fall well within the model uncertainty and are almost identical to the actual model results. This indicates that the interpolation method performed in this validation provides adequate abstractions of the lookup table results.

7.3 IN DRIFT PRECIPITATES/SALTS MODEL VALIDATION DISCUSSION

The in-drift precipitates salts model is validated for its intended use in Section 7 of BSC (2003 [DIRS 162529]). The intended use of the in-drift precipitates salts model in this report is:

- To estimate, within an appropriate level of confidence, the effects of evaporation and deliquescence on the presence and composition of water occurring within the proposed repository during the postclosure period (specifically, pH, ionic strength, deliquescence relative humidity, total concentrations of dissolved components in the system Na-K-H-Mg-Ca-Al-Cl-F-NO_3-SO_4-Br-CO_3-SiO_2-CO_2-O_2-H_2O, and concentrations of

the following aqueous species that potentially affect acid neutralizing capacity: HCO_3^-, CO_3^{-2}, OH^-, H^+, HSO_4^-, Ca^{+2}, Mg^{+2}, $CaHCO_3^+$, $MgHCO_3^+$, $HSiO_3^-$, and $MgOH^+$).

- To estimate, within an appropriate level of confidence, mineral precipitation resulting from the evaporation of water occurring within the proposed repository during the postclosure period (specifically, minerals of the system Na-K-H-Mg-Ca-Al-Cl-F-NO_3-SO_4-Br-CO_3-SiO_2-CO_2-O_2-H_2O).

- To provide a means for abstracting these effects and incoming seepage compositions (including seepage waters potentially modified by introduced materials such as 316L stainless steel wire mesh) into a set of lookup tables that provide input to downstream models used for performance assessment, such as in Section 6.6.

As stated in Section 2.1 of the technical work plan (BSC 2004 [DIRS 166519]), the criterion for validation of the in-drift precipitates salts model is the agreement of model results to the past and ongoing evaporation tests results and to the independent published data. In accordance with the technical work plan, the criterion for model validation is an agreement with the above comparisons within the uncertainty range established by past and planned model uncertainty and sensitivity studies. In addition to these criteria, results using the Pitzer database are compared in Section 7.3 of the in-drift precipitates salts model report (BSC 2003 [DIRS 162529]) to those generated using a separately qualified thermodynamic database over applicable ranges common to both databases.

In accordance with the overall criteria for model validation, individual validation objectives were developed in BSC (2003 [DIRS 162529]) for specific in-drift precipitates salts model output parameters, as presented in Table 7.3-1.

The results of the validation, briefly summarized below, demonstrate that the in-drift precipitates salts model is valid for its intended use. Sections 7.3.1 through 7.3.3 of this report summarize model validation runs corroborating the results of multi-component evaporation experiments, handbook aqueous solubilities of simple salts, and predictions using an independent database. These sections focus primarily on the validation of the aqueous outputs of the in-drift precipitates salts model. Section 7.3.4 summarizes the validation for mineral outputs. Additional validation simulations, such as the evaporation of seawater and the prediction of deliquescent relative humidity, eutectic points, and solubilities of salts in binary and ternary systems, can be found in BSC (2003 [DIRS 162529]) and/or REV 01 ICN 01 of BSC (2003 [DIRS 162529]), in progress.

7.3.1 Experimental Evaporation Data

Several sources of experimental laboratory data were used in model validation in BSC (2003 [DIRS 162529]), including Rosenberg et al. (1999 [DIRS 125338] and [DIRS 125339]), and *Environment on the Surfaces of the Drip Shield and Waste Package Outer Barrier* (CRWMS M&O 2000 [DIRS 146460]). The first and third sources involved monitoring the evaporation of synthetic average J-13 well water or a synthetic solution that approximated J-13 well water at a concentration factor of 100 (100x). The second involved a synthetic solution designed to simulate Topopah Spring pore water. In each of these experiments, the solutions were evaporated from a beaker open to the atmosphere at elevated temperatures. Experimental details

are summarized in Section 7.1 of *In-Drift Precipitates/Salts Model* (BSC 2003 [DIRS 162529]), and provided in full in the source documents.

Figure 7.3-1 compares the measured concentrations in the evaporated synthetic average J-13 well water (Rosenberg et al. 1999 [DIRS 125338]), to in-drift precipitates salts model predictions at three different concentration factors. This figure shows that the predictions approximate the Na, F, HCO_3, Cl, K, Mg, NO_3, SO_4, and SiO_2 concentrations within a factor of 10 when compared to the laboratory measurements. Ca predictions are within a factor of 100 of the measurements. The differences are within the acceptable ranges established by the model validation objectives listed in Table 7.3-1.

Table 7.3-1. Specific In-Drift Precipitates Salts Model Output Validation Objectives

Category of Model Output	Related Components	Related ANC Species	Related Minerals	Experimental Agreement for Aqueous Components and ANC Species	Experimental Agreement for Minerals
pH	H	H^+, OH^-	not applicable	pH within 1 pH unit; Concentration within 1 order of magnitude (factor of 10)	not applicable
Ionic Strength	Al, Br, Ca, CO_3, Cl, F, K, Mg, Na, NO_3, SiO_2, SO_4	not applicable	not applicable	Concentration within 1 order of magnitude (factor of 10)	not applicable
Deliquescence Relative Humidity (RH_d)	H_2O	not applicable	Highly soluble minerals in the system Al-Br-Ca-CO_3-Cl-F-K-Mg-Na-NO_3-SO_4-SiO_2-H-H_2O at potential repository temperatures and pressures	Activity of water within 0.1 of deliquescence relative humidity (RH_d)	Solubility within 1 order of magnitude (factor of 10)
Rapidly equilibrated components and their associated ANC species and minerals	Al, Br, CO_3, Cl, F, K, Na, NO_3, SO_4	HCO_3^-, CO_3^{2-}, HSO_4^-	Unsuppressed potential minerals of the system Al-Br-CO_3-Cl-F-K-Na-NO_3-SO_4-H-H_2O at potential repository temperatures and pressures	Concentration within 1 order of magnitude (factor of 10)	Solubility within 1 order of magnitude (factor of 10)
Less rapidly equilibrated components and their associated ANC species and minerals	Ca, Mg, SiO_2	Ca^{2+}, Mg^{2+}, $CaHCO_3^+$, $MgHCO_3^+$, $MgOH^+$, $HSiO_3^-$	Unsuppressed potential Ca, Mg, and SiO_2 minerals of the system Al-Br-Ca-CO_3-Cl-F-K-Mg-Na-NO_3-SO_4-SiO_2-H-H_2O at potential repository temperatures and pressures	Concentration within 2 orders of magnitude (factor of 100)	Solubility within 1 order of magnitude (factor of 10)

Figure 7.3-2 compares the pH predictions for this same experiment with laboratory measurements. The experimental pH is predicted within a pH unit thereby meeting the validation objective (Table 7.3-1).

In the 100x synthetic J-13 evaporation experiment (CRWMS M&O 2000 [DIRS 146460]), predicted concentrations of Na, F, Cl, K, NO_3, HCO_3, and SO_4 closely approximate the measured concentrations (Figure 7.3-3). The model underestimates Ca and Mg by about 1 to 2 orders of magnitude when compared to the laboratory measurements. However, these differences are within the required accuracy ranges specified by the objectives (Table 7.3-1).

The in-drift precipitates/salts model also simulated the synthetic Topopah Spring pore water evaporation experiment (Rosenberg et al. 1999 [DIRS 125339]) with sufficient accuracy to meet model validation objectives. Figure 7.3-4 compares the measured and predicted total aqueous concentrations, and Figure 7.3-5 compares the measured and predicted pH values. These comparisons (and those for the other evaporation experiments) are discussed in detail in Section 7.1 of *In-Drift Precipitates/Salts Model* (BSC 2003 [DIRS 162529]).

7.3.2 Evaporation of Dilute Salt Solutions

To demonstrate model validation for simple salt systems, the in-drift precipitates salts model and Pitzer database were used to evaporate dilute solutions (0.0001 molal) of simple Na, K, Ca, and Mg salts to mineral saturation at 25°C and 100°C. The final aqueous compositions were then compared to salt solubilities reported in *CRC Handbook of Chemistry and Physics* (Lide 2000, pp. 8-102 to 8-110 [DIRS 162229]). The results are shown in Figures 7.3-6 and 7.3-7.

The salts include all binary combinations of the system Na-K-Ca-Mg-CO_3-Cl-F-Br-SO_4-NO_3 documented in the handbook. The comparisons show that the in-drift precipitates salts model predicts solubility of each salt within a factor of 10 of the handbook values, satisfying the model validation criteria in Table 7.3-1. Most predictions are within 20 percent of the handbook values. Details of this analysis are presented in Section 7.2 of *In-Drift Precipitates/Salts Model* (BSC 2003 [DIRS 162529]).

The following three nitrate salts did not reach saturation before the end of the run: $Ca(NO_3)_2$ (100°C), $Mg(NO_3)_2$ (25°C and 100°C), and KNO_3 (100°C). In the event that one or more of these salts become supersaturated in a particular application, the model tends to overestimate the aqueous concentrations of the components. For these salts, this could only happen at low relative humidity (e.g., below 50 percent) and for those incoming waters whose chemical divides allow extensive concentration of these salts' components. In all cases, however, the model is validated for these nitrate salts, as explained in detail in BSC (2003 [DIRS 162529]).

7.3.3 Comparison of Data0.ypf and Data0.ymp.R2 Database Predictions

The in-drift precipitates salts model was further validated in Section 7.3 of *In-Drift Precipitates/Salts Model* (BSC 2003 [DIRS 162529]) by comparing model predictions using the Pitzer database to those generated using the YMP.R2 thermodynamic database (DTN: MO0302SPATHDYN.000 [DIRS 161756]). An in situ J-13 water composition was evaporated to an ionic strength of 1 molal using each database. The B-dot equation option was

chosen for calculating the activity coefficients for the YMP.R2 simulation. This option is generally valid for solutions having ionic strength values up to 1 molal (SNL 2003, p. B-31 [DIRS 162494]).

Two sets of results were generated using the YMP.R2 database. In the first set, only the minerals identified in Section 6.6.2.6.4 of *In-Drift Precipitates/Salts Model* (BSC 2003 [DIRS 162529] in process) were suppressed from forming. The results for this set are compared to the Pitzer database predictions in Figures 7.3-8 and 7.3-9. Because the YMP.R2 database contains many more minerals than the Pitzer database, two minerals not included in the Pitzer database (tridymite and dolomite-ord) precipitated in this set of results. These minerals are not likely to form under the conditions of the repository. Nevertheless, the comparisons in Figures 7.3-8 and 7.3-9 show strong agreement between the two databases in the values of the aqueous output parameters.

In the second set of YMP.R2 results, only the minerals that precipitated in the Pitzer results (calcite, amorphous silica, and sepiolite) were allowed to precipitate. The results for this set are compared to the Pitzer database predictions in Figures 7.3-10 and 7.3-11. Except for Si, these results are almost identical to the Pitzer results. These simulations demonstrate that the in-drift precipitates salts model produces similar aqueous output (up to an ionic strength of 1 molal), regardless of whether the Pitzer database or the YMP.R2 database is used.

7.3.4 Validation for Mineral Outputs

A major feature of the in-drift precipitates salts model is the selection of minerals that are allowed (or not allowed) to precipitate upon saturation. Each precipitating mineral creates a new chemical divide that has important consequences on the evolution of the aqueous phase. Thus, mineral precipitation in the model determines the aqueous evolution of the evaporating solution. In the in-drift precipitates salts model, the minerals allowed to precipitate are those in the Pitzer thermodynamic database that are not suppressed in the input file. The minerals that are allowed to precipitate in the model reflect natural analog information and confirm the presence of the precipitating minerals in evaporative geological environments (Table 6.5-3).

Because of the strong relationship between the evolution of the aqueous and mineral phases due to the conservation of mass, validation of the aqueous phase evolution (as shown in Sections 7.3.1 through 7.3.3) indicates validation of the model for predicting bulk compositions of precipitated minerals. The bulk mineral composition is the set of the total masses of each elemental component in the total precipitation. While model validation for predicting the bulk mineral composition does not imply the model predicts exactly which minerals precipitate, at least it implies that the minerals predicted by the model to precipitate are adequate for predicting the evaporative evolution of the aqueous phase.

For TSPA-LA, predicting the specific mineral assemblage that would be generated by evaporation of a given water is not required. What is required, however, is predicting a mineral assemblage that will generate sufficiently accurate aqueous solutions upon deliquescence or dissolution. As Sections 7.3.1 through 7.3.3 show, the mineral assemblages predicted by the model accomplish this objective, thereby validating the mineral outputs for their intended use.

Additional discussion on this topic is provided in Section 7.4 of *In-Drift Precipitates/Salts Model* (BSC 2003 [DIRS 162529]).

7.4 EVAPORATION OF SIERRA NEVADA SPRING WATERS TO FORM CONCENTRATED BRINES

The EBS Seepage Evaporation Model Calculations also can be evaluated by comparison with alternative classical models, which employ evaporative concentration of dissolved species in solution (including precipitation). One such example is the classical study of the isothermal evaporation, at 25°C and $P_{CO2} = 10^{-3.5}$ atm, of Sierra Nevada spring waters by Garrels and Mackenzie (1967, pp. 222-242 [DIRS 123636]), which has been cited by Drever (1988, pp. 232-234 [DIRS 118564]) as "a simulation of what might happen if streams from the Sierra Nevada flowed out into one of the arid basins of Nevada" to form saline lake water.

Drever (1988, p. 233 [DIRS 118564]) suggests that the resulting brine "chemistry of these lakes could be explained by simple evaporation of dilute spring waters whose chemistry was, in turn, controlled by reactions between rainwater and igneous rock." In an analogous way, several Yucca Mountain waters can concentrate into alkaline carbonate brines by evaporation of initial crown seepage, invert wicking, or condensate that has reacted with volcanic tuff. It is useful to explore the similarities and differences between this classical study's graphical display of pH and major ions as a function of up to 1000-fold evaporation concentration (Figure 7.4.1), compared to the same concentration developed using the methodology of the present work (Figure 7.4.2).

Before detailing the results of the Sierra Nevada Spring evaporation calculations, the difference in databases, mineral suppression during speciation calculations, and the number of chemical species is evaluated. Garrels and Mackenzie (1967, p. 234 [DIRS 123636]) originally considered 11 major aqueous species and seven minerals that could precipitate during evaporative concentration: calcite, gypsum, brucite, magnesite, hydromagnesite, sepiolite, and amorphous silica (Garrels and Mackenzie 1967, p. 234 [DIRS 123636]).

In this validation, at least 50 aqueous species whose concentrations were greater than 10^{-100} molal are considered (this concentration limit is constrained by the EQ3/6 software to prevent concentrations that could affect the reactions) (File:val3bdot.6o archived in DTN: MO0306SPAPCEVC.000). Saturation values for at least 53 minerals minus 15 mineral suppressions are evaluated.

Further, the molecular formula of sepiolite and hydromagnesite has been revised. Sepiolite's common molecular formula has been changed from $MgSi_3O_6(OH)_2$ (Garrels and Mackenzie 1967, p. 234 [DIRS 123636]) to $Mg_4Si_6O_{15}(OH)_2{\cdot}6H_2O$. Hydromagnesite's common molecular formula has been changed from $Mg_4(CO_3)_3(OH)_2$ (Garrels and Mackenzie 1967, p. 234) to $Mg_5(CO_3)_4(OH)_2{\cdot}4H_2O$. The Debye-Huckel activity coefficients used by Garrels and Mackenzie are accurate up to an ionic strength of (I) = 0.05 molal (Garrels and Christ 1990, p. 64 [DIRS 144877]), and the B-dot activity coefficients calculated with the current EQ3/6 version 8.0 software values are accurate to I = 1.0 molal. However, the final brine after evaporation contains 8×10^{-8} grams of water at greater than 5 molal ionic strength (File:val3bdot.6o archived in DTN: MO0306SPAPCEVC.000 [DIRS 165031]). Garrels and Mackenzie (1967, p. 240) were aware of the problem in using in brines activity coefficients

derived for use in low ionic strength solutions, and emphasized that using their results carried increasing uncertainty with ionic strength: "Using the Debye-Huckel activity coefficients obviously leads to an increasing uncertainty in $gamma_i$ (activity coefficient) values with increasing ionic strength, and the values calculated for 1000X concentration should be regarded as rough approximations."

Figures 7.4-1 and 7.4-2 are similar, despite the differences in how they were derived. The evaporative concentration starts with a near neutral pH, Na-Ca-HCO_3 water and concentrates it to highly alkaline Na-HCO_3-CO_3 water. Calcium and magnesium are removed by early mineral precipitation. Na^+, K^+, Cl^-, and SO_4^{-2} are concentrated without forming solids. Bicarbonate and carbonate ions deviate from the rates of log-linear concentration by mineral precipitation, in contrast to Na^+, K^+, Cl^-, and SO_4^{-2}. Because the Sierra Spring waters are originally low in SO_4^{-2}, gypsum doesn't precipitate. Many waters in the repository are expected to concentrate by evaporation in a similar manner (Section 6.9).

The major difference between the classical model results and the present validation arises from a change in the log K value for the solubility of amorphous silica, which is based on more recent experimental and thermodynamic data reviews than were available to Garrels and Mackenzie (1967, pp. 222-242 [DIRS 123636]). In brief, during the intervening four decades the amorphous silica log K value at 25°C (and above) has been revised as a result of laboratory experiments and field validation tests.

The difference in these results demonstrates the generally accepted change from the so-called "Fournier" silica paradigm to the "Rimstidt" silica paradigm, as outlined in the development of the data0.ymp R2 database, and as detailed under uncertainties in log K values by Steinborn et al. (2003 [DIRS 161956]). In Figure 7.4-1, amorphous silica precipitates up to a concentration factor of approximately 10X, and reaches a saturation solubility limit for the rest of the evaporative concentration that is shown to be at a concentration above what is currently used (Steinborn et al. 2003). In contrast, the graphic plot of Figure 7.4-2 shows that amorphous silica is constant throughout the evaporative concentration range shown, because the modern "Rimstidt" paradigm log K value at 25°C is saturated at the start of the concentration calculation and remains so throughout the calculation.

For the accuracy needed in the present work, the Figure 7.4-2 graphically plotted data is well validated by the evaporative concentration documented by Garrels and Mackenzie in their classic study (1967, pp. 222-242 [DIRS 123636]) in the Figure 7.4-1 graphical data plot.

7.5 DELIQUESCENCE POINT COMPARISON

Validation of equilibrium salt deliquescence points is conducted by comparing predictions made by the use of the EQ3/6 software with the data0.ypf Pitzer database, and experimental data for simple and mixed electrolytes reported by Greenspan (1977 [DIRS 104945]) and Pabalan et al. (2002 [DIRS 163067]). Greenspan (1977) presents a compilation of equilibrium relative humidity values for binary salts as a function of temperature. Pabalan et al. (2002 [DIRS 163067]) reports salt deliquescence point experiments for selected binary and mixed salts as a function of temperature. This validation effort follows both Criterion 2 and Criterion 3 defined in Section 7.1.

Each validation run predicts a water activity (equivalent to relative humidity) at the deliquescence point for a set of highly soluble salts at a temperature range of 23°C to 86 °C. In the EQ3/6 calculation runs, the salt deliquescence point corresponds to the equilibrium of the electrolyte solution with respect to the salt solid. At this equilibrium point, EQ3/6 calculates the activity of water (or relative humidity) using the Pitzer activity model. The selected simple and mixed salt compositions for which deliquescence data are considered in the validation are $NaNO_3$, $MgCl_2$, NaCl + $NaNO_3$, and NaCl + $NaNO_3$ + KNO_3.

Input and output files used in the EQ3/6 calculations are listed in Table 7.5-1. The computed equilibrium relative humidity values for a given salt composition using the EQ3/6 and the data0.ypf Pitzer databases are given as a function of temperature in Table 7.5-2.

Table 7.5-1. Input/Output Files EQ3/6 (Version 8.0) Used to Calculate the Equilibrium Deliquescence Points of Binary and Mixed Salts

Temperature	Salt Composition	EQ3/6 (Version 8.0) Input Files	EQ3/6 (Version 8.0) Output Files
23.0	$CaCl_2$	CaCl2_23.3i	CaCl2_23.3o
38.1	$CaCl_2$	CaCl2_38.3i	CaCl2_38.3o
48.0	$CaCl_2$	CaCl2_48.3i	CaCl2_48.3o
69.0	$CaCl_2$	CaCl2_69.3i	CaCl2_69.3o
85.8	$CaCl_2$	CaCl2_86.3i	CaCl2_86.3o
23.0	$MgCl_2$	MgCl2_23b.3i	MgCl2_23b.3o
38.1	$MgCl_2$	MgCl2_38b.3i	MgCl2_38b.3o
48.0	$MgCl_2$	MgCl2_48b.3i	MgCl2_48b.3o
69.0	$MgCl_2$	MgCl2_69b.3i	MgCl2_69b.3o
85.8	$MgCl_2$	MgCl2_86b.3i	MgCl2_86b.3o
23.0	$NaNO_3$	NaNO_23b.3i	NaNO_23b.3o
38.1	$NaNO_3$	NaNO_38b.3i	NaNO_38b.3o
48.0	$NaNO_3$	NaNO_48b.3i	NaNO_48b.3o
69.0	$NaNO_3$	NaNO_69b.3i	NaNO_69b.3o
85.8	$NaNO_3$	NaNO_86b.3i	NaNO_86b.3o
23.0	NaCl + $NaNO_3$	naclno3_23.3i	naclno3_23.3o
38.1	NaCl + $NaNO_3$	naclno3_38.3i	naclno3_38.3o
48.0	NaCl + $NaNO_3$	naclno3_48.3i	naclno3_48.3o
69.0	NaCl + $NaNO_3$	naclno3_69.3i	naclno3_69.3o
85.8	NaCl + $NaNO_3$	naclno3_86.3i	naclno3_863.3o

Table 7.5-1. Input/Output Files EQ3/6 (Version 8.0) Used to Calculate the Equilibrium Deliquescence Points of Binary and Mixed Salts (Continued)

Temperature	Salt Composition	EQ3/6 (Version 8.0) Input Files	EQ3/6 (Version 8.0) Output Files
23.0	$NaCl + NaNO_3 + KNO_3$	nakclno3_23.3i	nakclno3_23.3o
38.1	$NaCl + NaNO_3 + KNO_3$	nakclno3_38.3i	nakclno3_38.3o
48.0	$NaCl + NaNO_3 + KNO_3$	nakclno3_48.3i	nakclno3_48.3o
69.0	$NaCl + NaNO_3 + KNO_3$	nakclno3_69.3i	nakclno3_69.3o
85.8	$NaCl + NaNO_3 + KNO_3$	nakclno3_86.3i	nakclno3_86.3o

Source: DTN: SN0303T0510102.004

Table 7.5-2. Comparisons of Relative Humidity Values for Equilibrium Deliquescence Points of Selected Salts Between EQ3/6 (Version 8.0–data0.ypf Pitzer Database) and Experimental Data

Salt Composition	Code or Source	Temperature (°C)					[c] EQ3NR/EQ6 vs. Others
		23.0	38.1	48.0	69.0	85.8	
$NaNO_3$	EQ3NR/EQ6 (Version 8.0)	74.3	70.8	68.6	64.3	61.1	-
	Greenspan (1977 [DIRS 104945])	74.7	71.4	69.4	66.2	65.0	-0.5(23), -0.8(38.1), -1.1(48), -2.9(69), -6(86)
	Pabalan, et al. (2002 [DIRS 163067])	74.9	—	69.7	62.7	—	-0.8(23), -1.6(48), -2.5(69)
[a] $MgCl_2$	EQ3NR/EQ6 (Version 8.0)	37.0	35.8	34.8	31.9	28.4	-
	Greenspan (1977 [DIRS 104945])	32.9	31.8	30.8	27 .9	25.0	12.5(23), 12.6(38.1), 13(48), 14.3(69), 13.6(86)
	Pabalan, et al. (2002 [DIRS 163067])	33.9	31.7	31.0	29.1	—	9.1(23), 12.9(38.1), 12.3(48), 9.6(69)
$NaCl + NaNO_3$	EQ3NR (Version 8.0)	68.7	66.9	65.6	62.7	60.1	
	Pabalan, et al. (2002 [DIRS 163067])	74.7	66.4	67.2	59.6	56.0	-8.0(23), -0.7(38.1), -2.4(48), 5.2(69), 7.3(86)
[b] $NaCl + NaNO_3 + KNO_3$	EQ3NR/EQ6 (Version 8.0)	66.2	61.4	57.5	48.0	39.0	
	Pabalan, et al. (2002 [DIRS 163067])	67.8	60.7	61.3	51.8	43.4	-2.4(23), 1.1(38.1), -6.2(48), -7.3(69), -10.1(86)

Source: DTN: SN0303T0510102.004

NOTES: [a] $MgCl_2$ salt solid used in equilibrium calculation is $MgCl_2*6H_2O$.
[b] Pitzer interaction parameters for K^+ and NO_3^- pair are only available at 25°C.
[c] Numbers represent percent difference, those in parenthesis represent temperature.

The resulting percent differences between relative humidity values from EQ3/6 calculation predictions and experimental data for salt deliquescence points range from less than a percent to approximately 14.3 percent (Table 7.5-2). The highest values for percent differences are largely restricted to the $MgCl_2$ salt when compared to the other salts. The reason for this larger discrepancy could be related to the solubility constant value used for the $MgCl_2 \cdot 6H_2O$ solid in the data0.ypf database. For mixed electrolytes, the maximum percent difference is approximately 10.1 percent, which suggests the applicability of the Pitzer model in modeling mixed salts. In the mixed salt case, NaCl + $NaNO_3$ + KNO_3, the Pitzer parameter for KNO_3 is only available at 25°C.

Overall, percent differences between predicted and experimental values of less than approximately 15 percent are acceptable for model applications, given the combined inherent uncertainties present in both experiments and code calculations using the Pitzer model. In addition, these results easily fall within the 0.1 activity of water validation objective of the in-drift precipitates salts model (see Table 7.3-1). Therefore, the present comparisons between two different sets of experimental data and code predictions validate the application of the computational method to predict salt deliquescence points to an acceptable level of accuracy. Additional information on the validation of deliquescence relative humidity can be found in the in-drift precipitates/salts model documentation as shown on Table 6.12-1.

7.6 MINERAL PRECIPITATION

In addition to the information found on Table 6.5-3, Table 7.6-1 includes natural analog information and the mineral inclusion (or suppression) criteria as discussed in Section 6.5.5. As indicated, all minerals listed on Tables 6.5-3 and 7.6-1 have analog information that allows for their precipitation in this model. Using model validation Criterion 3 stated in Section 7.1, this result corroborates the minerals that are precipitating in this model.

Cryolite (Table 6.10-1), which was included in the seepage modeling runs, but suppressed in the dust leachate runs, has analog information that suggests mineral suppression indicated in EQ3/6 calculations would be warranted. It may be possible for cryolite to precipitate under repository conditions.

Section 6.12.4.4.1 documents an uncertainty calculation that indicates a suppression of cryolite has virtually no impact on the seepage lookup table results except for the Al output (see Figure 6.12-19). This portion of the output can be affected by two orders of magnitude as the water activity decreases. Cryolite formation is indicated in some of the lookup tables representing bins 9, 10 and 11. As shown in Figure 6.12-19, the impact is not significant, as the Al concentrations are less than 10^{-10} molal.

Table 7.6-1. Natural Analog Information for the Inclusion of Minerals Not Reported in Section 6.5

Mineral	Formula	Criteria Selected	Rationale	References
$Ca(NO_3)_2$	$Ca(NO_3)_2$	Criterion 3	Less hydrated phase of nitrocalcite	See below
$Ca(NO_3)_2{:}3H_2O$	$Ca(NO_3)_2{:}3H_2O$	Criterion 3	Less hydrated phase of nitrocalcite	See below
$Ca(NO_3)_2{:}4H_2O$ (Nitrocalcite)	$Ca(NO_3)_2{:}4H_2O$	Criterion 3	Water soluble salt associated with niter deposits in caves and lake beds	Palache et al. 1951, pp. 306-307 [DIRS 162280]
Erionite	$K_{1.5}Na_{0.9}Ca_{0.9}Al_{4.2}Si_{13.8}O_{36}{:}13H_2O$	Criterion 3	Zeolite mineral known to form in sedimentary saline, nonmarine environments	Frye 1981, p. 524 [DIRS 161804] Hay 1966, Table 4 [DIRS 105965]
Nahcolite	$NaHCO_3$	Criterion 3	Associated with trona and other playa or salt bed minerals	Palache et al. 1951, p. 135 [DIRS 162280]
Pirssonite	$Na_2Ca(CO_3)_2{:}2H_2O$	Criterion 3	Associated with trona and thenardite and is found in clays in dry lake beds	Palache et al. 1951, p. 233 [DIRS 162280]
KBr	KBr	Criterion 3	Deliquescent mineral that maintains a saturated solution at 84% RH at 20ºC and 69%RH at 100ºC	Weast 1984, p. E-42 [DIRS 106170]
Kalicinite	$KHCO_3$	Criterion 3	Associated with trona	Palache et al. 1951, p. 136 [DIRS 162280]
Brucite	$Mg(OH)_2$	Criterion 3	Associated with contact metamorphosed limestones in association with calcite, dolomite and magnesite. This would be analogous to calcite alteration on the surface of the hot waste packages. In the modeling runs brucite only forms in one dust leachate lookup table at 100ºC Brucite is also found in crystalline limestones; the chief component of which is calcite	Frye 1981, p. 568 [DIRS 161804] Klein and Hurlbut 1977, p. 316 [DIRS 105907]
Darapskite	$Na_3(NO_3)(SO_4){:}H_2O$	Criterion 3	Associated soda-niter, niter, halite, and anhydrite. Also occurs in nitrate and sulfate deposits	Palache et al. 1951, p. 310 [DIRS 162280]
Thermonatrite	$Na_2CO_3{:}H_2O$	Criterion 3	Associated with trona and is found as an efflorescence on soil in arid regions and as a deposit from saline lakes	Palache et al. 1951, p. 224 [DIRS 162280]
Villiaumite	NaF	Criterion 3	Deliquescent mineral that maintains a saturated solution at 96% RH at 100ºC	Weast, 1984, p. E-42 [DIRS 106170]

7.7 CHROMIUM CALCULATIONS

After determining that the most common aqueous chromium oxidation state will be Cr(III) [and not Cr(VI) (Section 6.8.1.3)], all Cr(VI) related species are suppressed in the EQ3/6 chemical model calculations. Detailed examination of the remaining Cr(III) aqueous species is performed.

Five aqueous species in the EQ3/6 data input files are suppressed from the data0.ymp.R2 database (DTN: MO0302SPATHDYN.000 [DIRS 161756]) prior to finalizing the model runs: three have undesired oxidation states (+6 and +5) and the other two had recently been characterized as relatively unimportant polynuclear Cr(III) species (these aqueous suppressions are listed in Table 6.8-4). The polynuclear species in the data0.ymp.R2 database (DTN: MO0302SPATHDYN.000 [DIRS 161756]) are derived from the thermodynamic data compiled by Baes and Mesmer (1976 [DIRS 157860]). More recent experimental analysis by Rai et al. (1987 [DIRS 163369]) have cast doubt upon the importance of these polynuclear Cr(III) species, which the thermodynamic data (Baes and Mesmer 1976 [DIRS 157860]) predicts as becoming the dominant aqueous species at pH < 6. This has the effect of raising the solubility of $Cr(OH)_3$ "unrealistically high and is completely at odds with the long-known descriptive solubility of $Cr(OH)_3(s)$" (Rai et al. 1987, p. 346 [DIRS 163369]).

The remaining Cr(III) aqueous species are based upon thermodynamic estimates by Shock et al. (1997 [DIRS 127953]) who based their estimations upon the enthalpy of Cr^{3+} determined by Dellien et al. (1976 [DIRS 151392]). Though differing in their water content from the comprehensive review speciation equations of Ball & Nordstrom (1998, Table 10 [DIRS 163015]) (e.g., CrO^+ in the database and not $Cr(OH)_2^+$), they are retained unaltered as they represent the same basic species and make no numerical difference in calculation of formation constants using them. With the remaining aqueous chromium(III) species and the solubility constant of amorphous chromium(III) hydroxide (from Ball and Nordstrom 1998, [DIRS 163015], Table 8) that resulted from the experimental work of Rai et al. (1987 [DIRS 163369]), the solubility of the amorphous chromium(III) hydroxide is calculated as a function of pH (4 through 13). The results of these calculations are compared to the Rai et al. results (Figure 2 in Rai et al. (1987 [DIRS 163369])) plotted in Figure 7.7-1.

In this comparison, the detection limit reported by Rai et al. probably overestimates solubility in the pH range of 6 through 11. Their raw data show measurements well below their detection limits with values approaching those of the calculations (e.g., ~4 10^{-9} molar aqueous Cr in Figure of Rai et al. (1987 [DIRS 163369]), compared to a calculated $3.6 \cdot 10^{-9}$ molal at pH of 9 shown in the Figure 7.7-1 plot of this report. At these concentrations, solution density is very close to 1.0 gm/cm^3, making molar and molal concentrations effectively equivalent).

This favorable comparison provides an independent validation of the remaining unsuppressed chromium(III) aqueous species in the data0.ymp.R2 database (DTN: MO0302SPATHDYN.000 [DIRS 161756]), which were derived from independent thermodynamic data sources, as they reproduce chromium(III) solubility based on the log K value of hydroxide ($Cr(OH)_3(am)$) obtained from Ball and Nordstrom (1998 [DIRS 163015]) (derived from Rai et al. 1987 [DIRS 163369]).

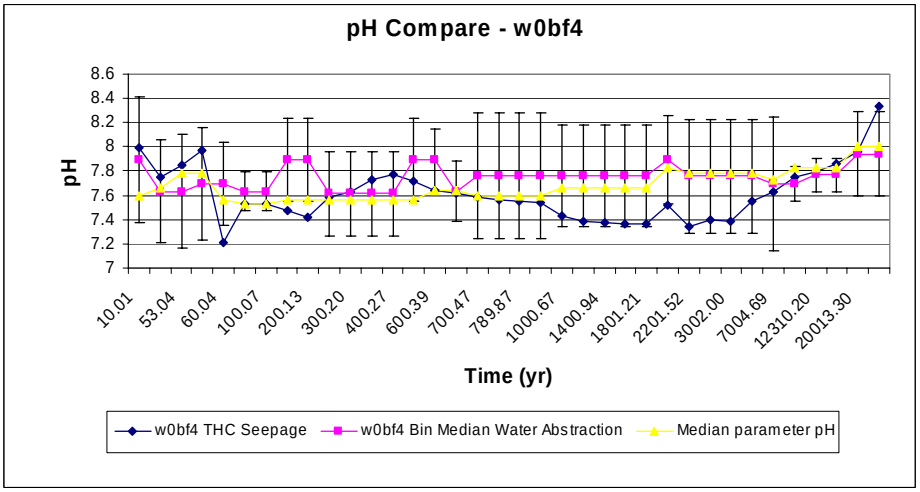

DTN: MO0312SPAPCESA.002

Figure 7.2-1. Comparison of Thermal-Hydrological-Chemical Seepage pH with Abstraction Results for w0bf4

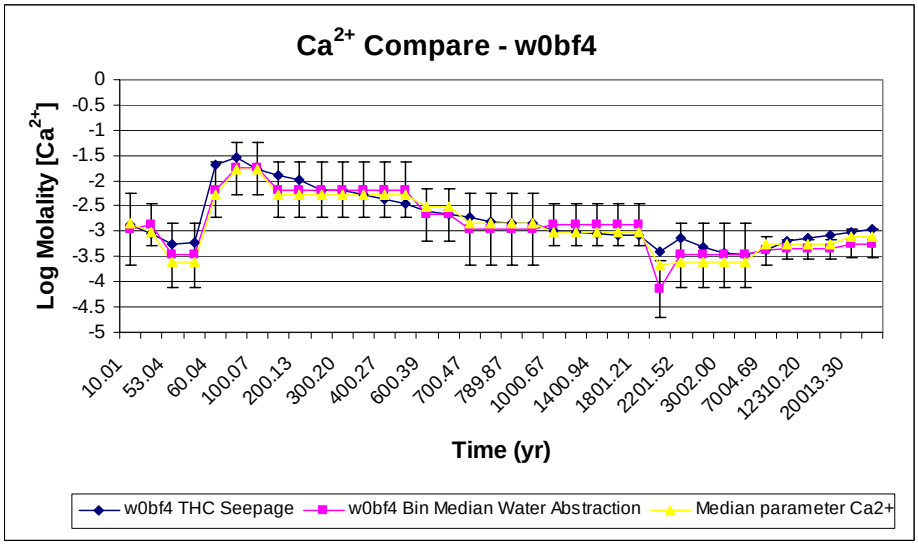

DTN: MO0312SPAPCESA.002

Figure 7.2-2. Comparison of Thermal-Hydrological-Chemical Seepage Ca^{2+} with Abstraction Results for w0bf4

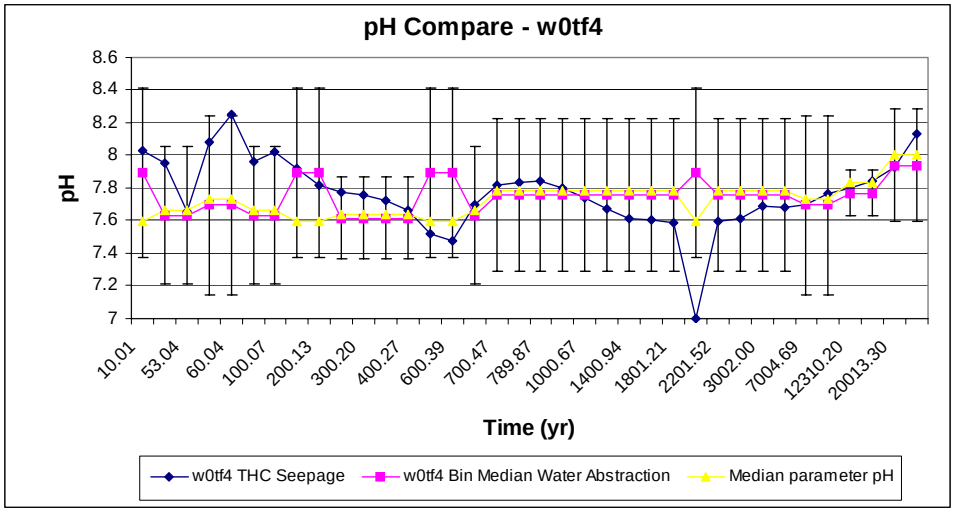

DTN: MO0312SPAPCESA.002

Figure 7.2-3. Comparison of Thermal-Hydrological-Chemical Seepage pH with Abstraction Results for w0tf4

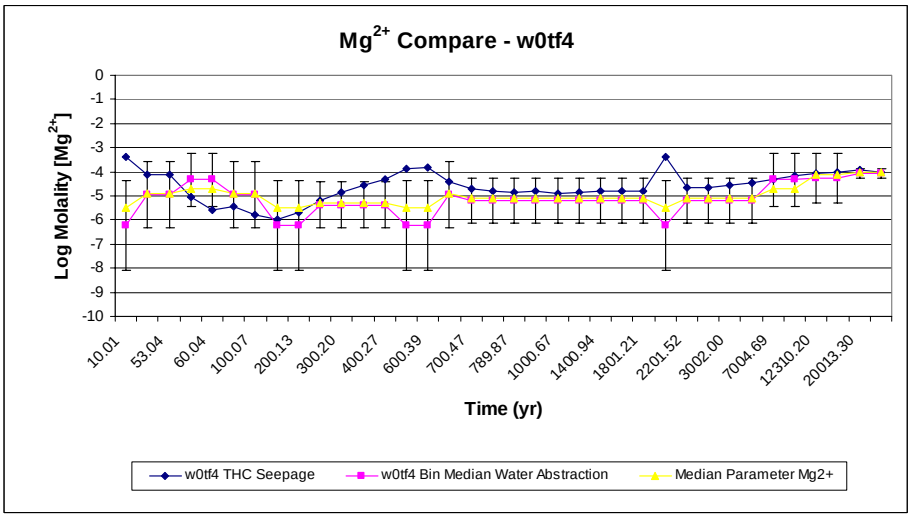

DTN: MO0312SPAPCESA.002

Figure 7.2-4. Comparison of Thermal-Hydrological-Chemical Seepage Mg^{2+} with Abstraction Results for w0tf4

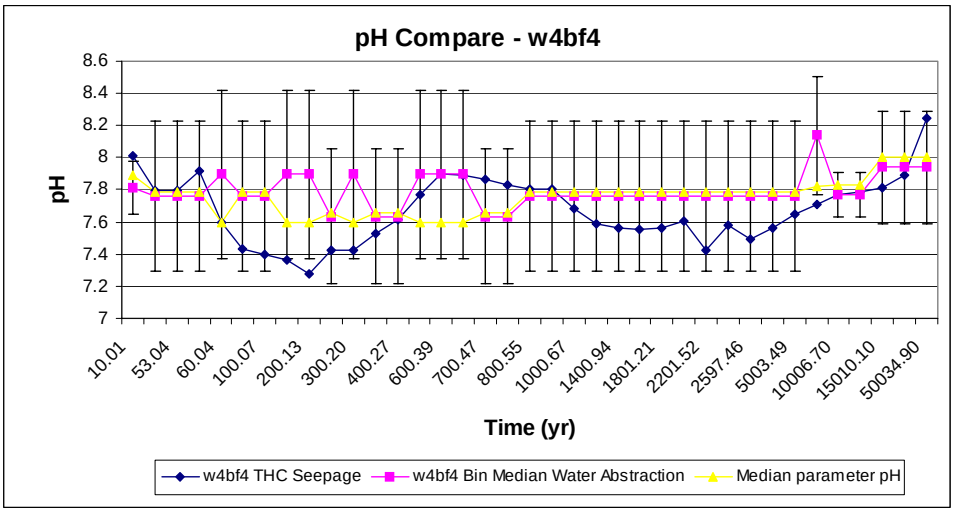

DTN: MO0312SPAPCESA.002

Figure 7.2-5. Comparison of Thermal-Hydrological-Chemical Seepage pH with Abstraction Results for w4bf4

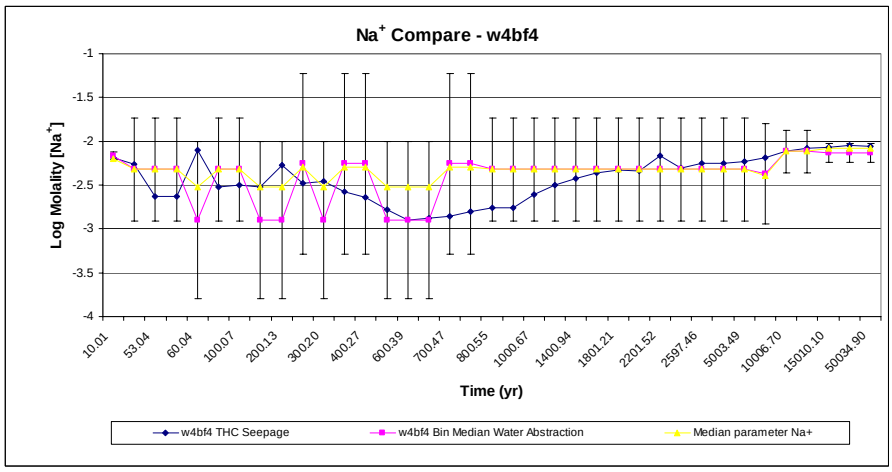

DTN: MO0312SPAPCESA.002

Figure 7.2-6. Comparison of Thermal-Hydrological-Chemical Seepage Na^+ with Abstraction Results for w4bf4

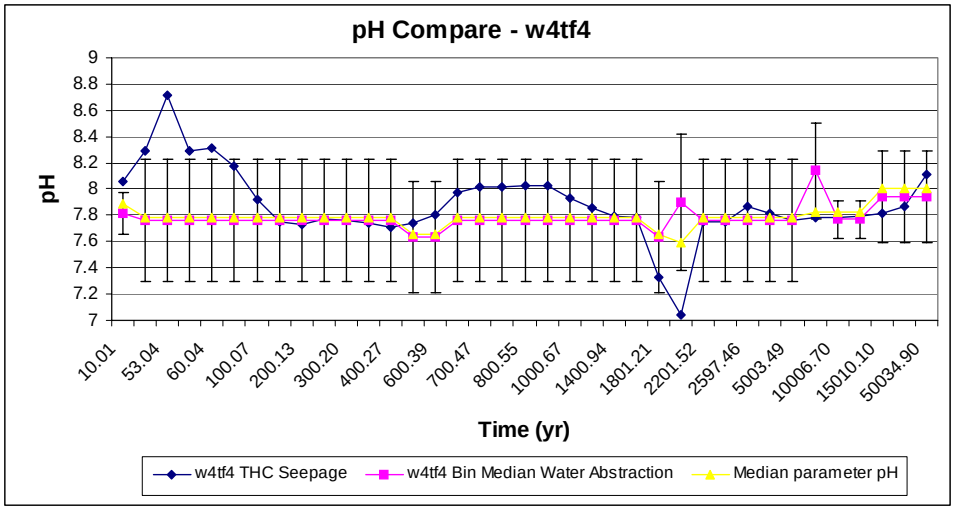

DTN: MO0312SPAPCESA.002

Figure 7.2-7. Comparison of Thermal-Hydrological-Chemical Seepage pH with Abstraction Results for w4tf4

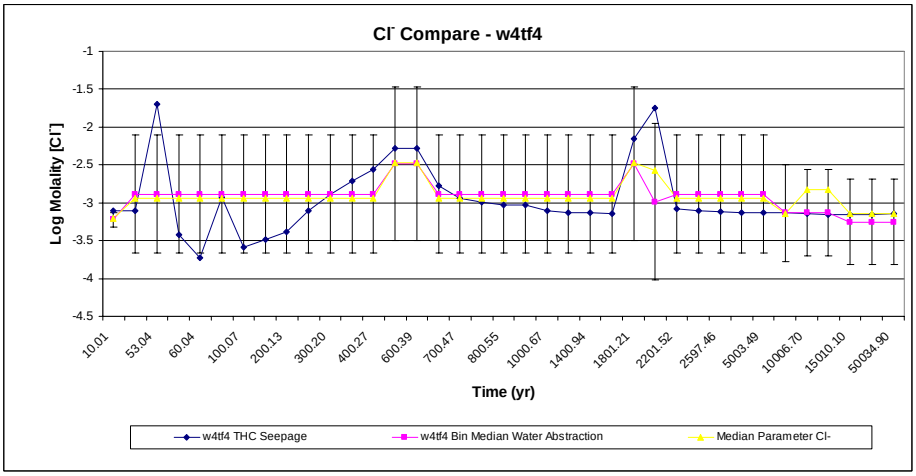

DTN: MO0312SPAPCESA.002

Figure 7.2-8. Comparison of Thermal-Hydrological-Chemical Seepage Cl^- with Abstraction Results for w4tf4

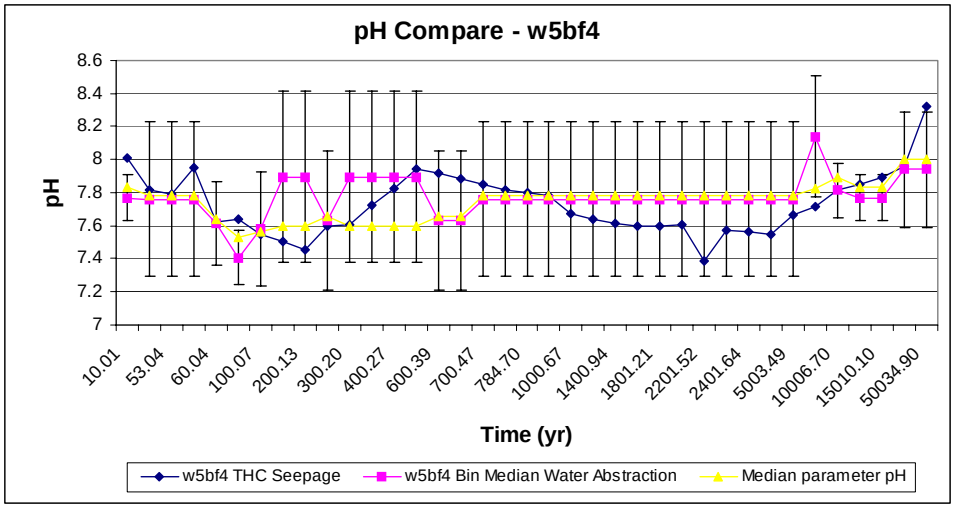

DTN: MO0312SPAPCESA.002

Figure 7.2-9. Comparison of Thermal-Hydrological-Chemical Seepage pH with Abstraction Results for w5bf4

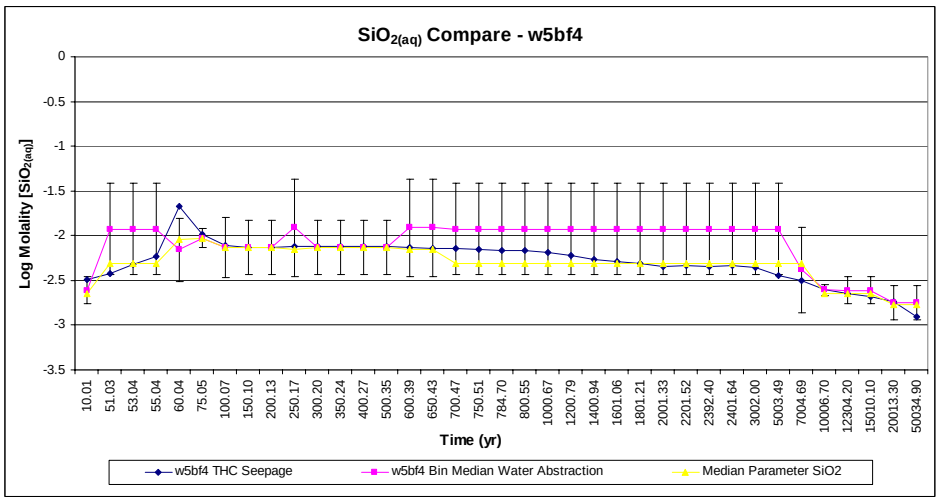

DTN: MO0312SPAPCESA.002

Figure 7.2-10. Comparison of Thermal-Hydrological-Chemical Seepage $SiO_{2(aq)}$ with Abstraction Results for w5bf4

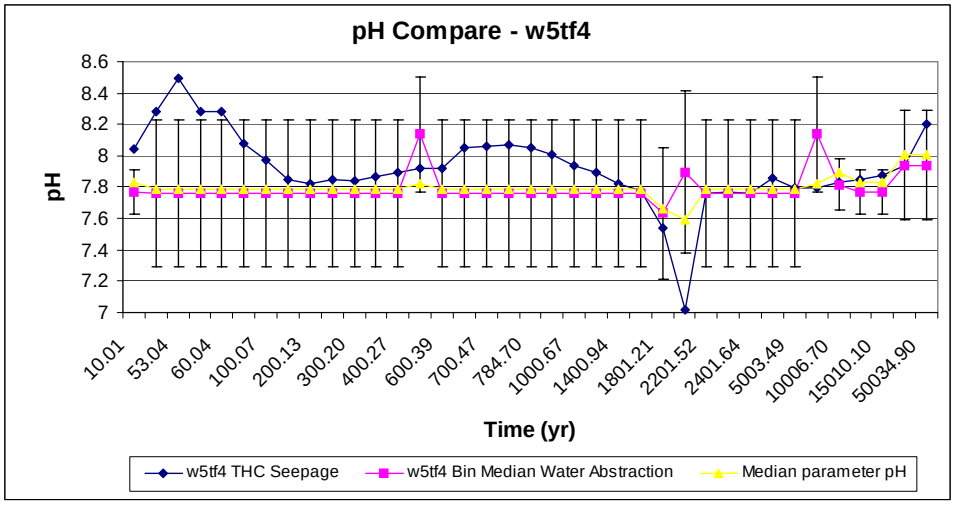

DTN: MO0312SPAPCESA.002

Figure 7.2-11. Comparison of Thermal-Hydrological-Chemical Seepage pH with Abstraction Results for w5tf4

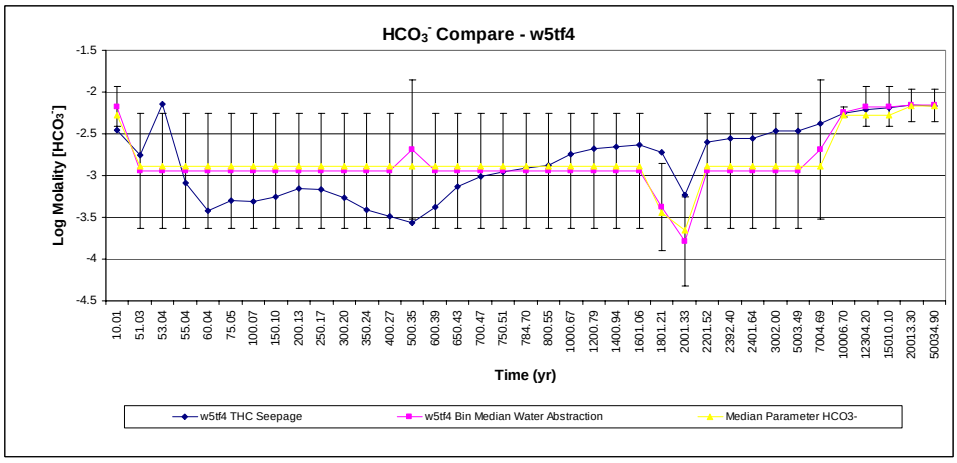

DTN: MO0312SPAPCESA.002

Figure 7.2-12. Comparison of Thermal-Hydrological-Chemical Seepage HCO_3^- with Abstraction Results for w5tf4

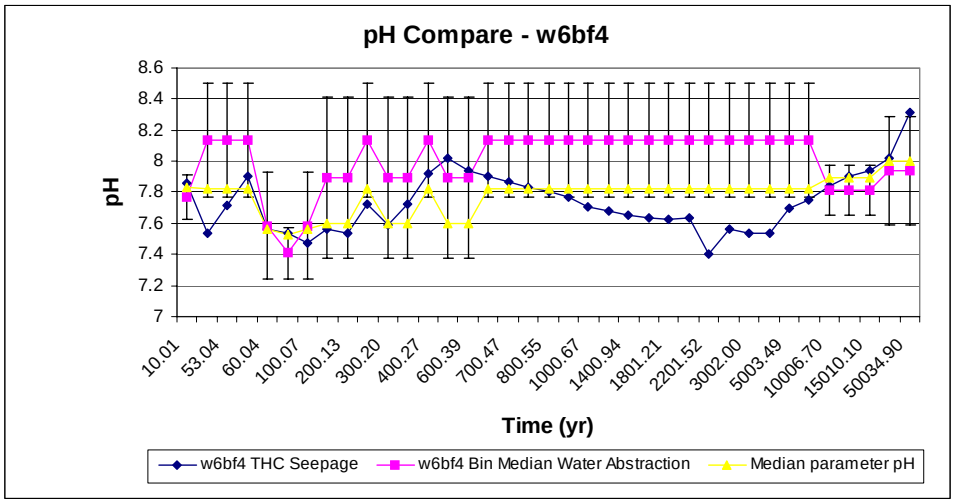

DTN: MO0312SPAPCESA.002

Figure 7.2-13. Comparison of Thermal-Hydrological-Chemical Seepage pH with Abstraction Results for w6bf4

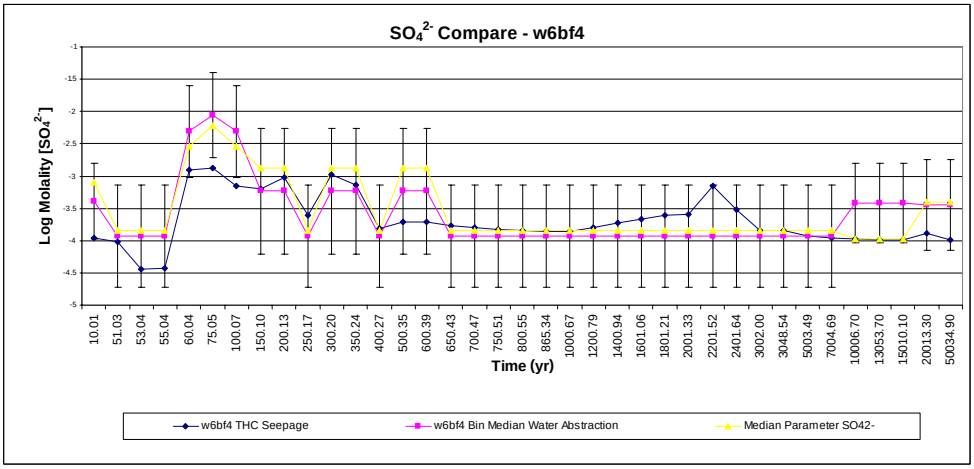

DTN: MO0312SPAPCESA.002

Figure 7.2-14. Comparison of Thermal-Hydrological-Chemical Seepage SO_4^{2-} with Abstraction Results for w6bf4

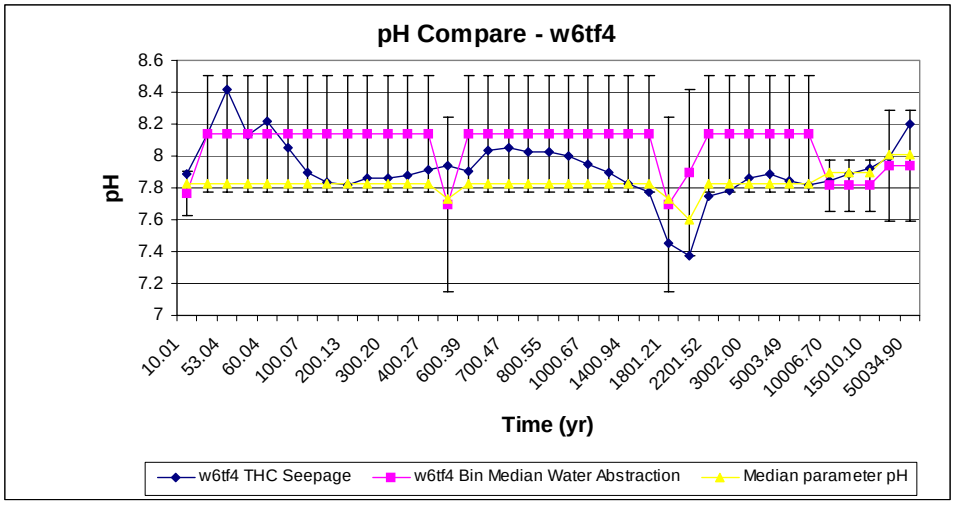

DTN: MO0312SPAPCESA.002

Figure 7.2-15. Comparison of Thermal-Hydrological-Chemical Seepage pH with Abstraction Results for w6tf4

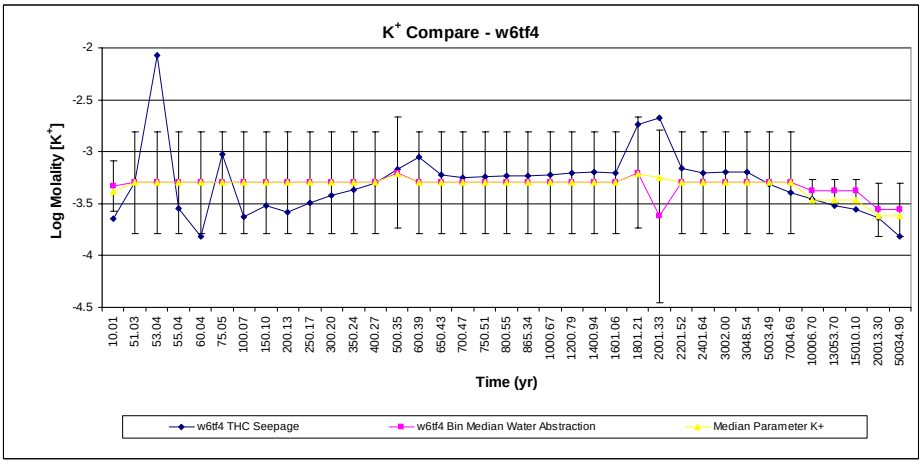

DTN: MO0312SPAPCESA.002

Figure 7.2-16. Comparison of Thermal-Hydrological-Chemical Seepage K^+ with Abstraction Results for w6tf4

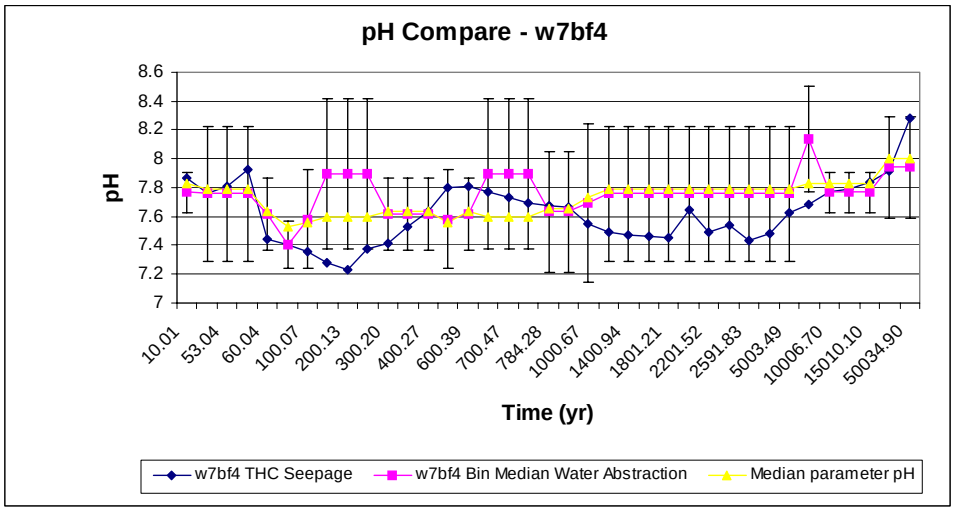

DTN: MO0312SPAPCESA.002

Figure 7.2-17. Comparison of Thermal-Hydrological-Chemical Seepage pH with Abstraction Results for w7bf4

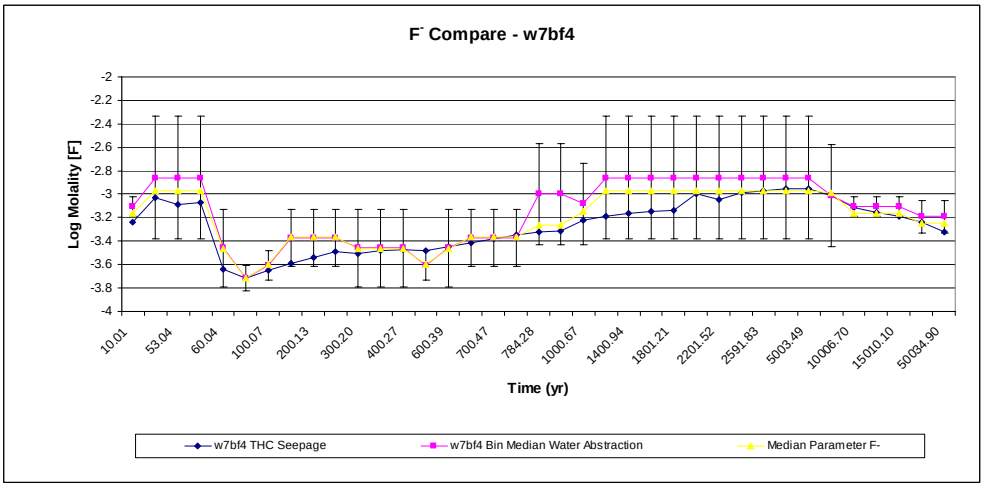

DTN: MO0312SPAPCESA.002

Figure 7.2-18. Comparison of Thermal-Hydrological-Chemical Seepage F^- with Abstraction Results for w7bf4

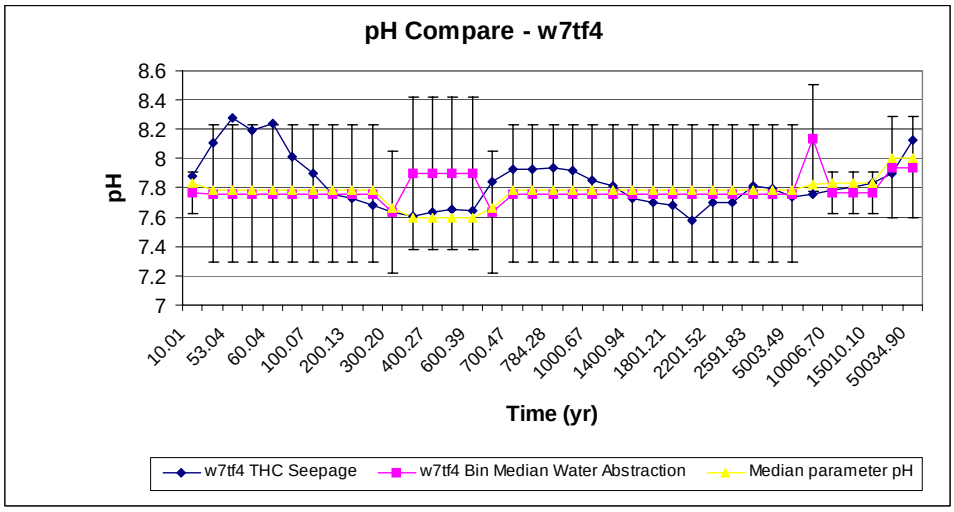

DTN: MO0312SPAPCESA.002

Figure 7.2-19. Comparison of Thermal-Hydrological-Chemical Seepage pH with Abstraction Results for w7tf4

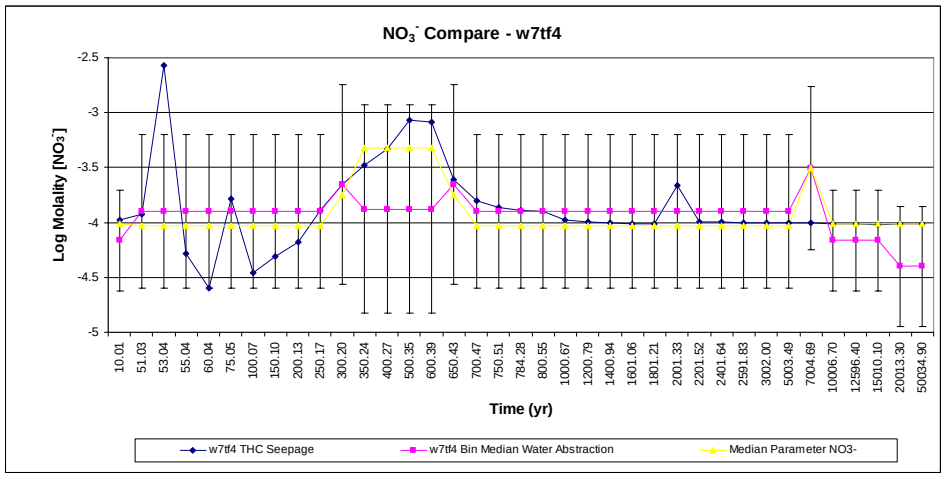

DTN: MO0312SPAPCESA.002

Figure 7.2-20. Comparison of Thermal-Hydrological-Chemical Seepage NO_3^- with Abstraction Results for w7tf4

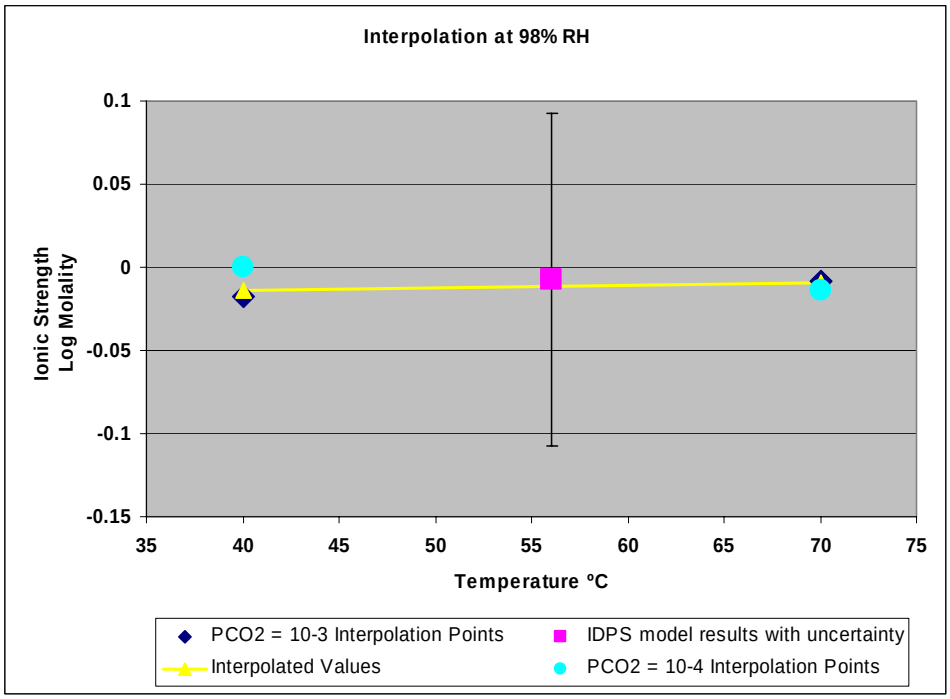

DTN: MO0312SPAPMVIC.000

Figure 7.2-21. Comparison of Model Results (Ionic Strength at 98% RH) with Look-up Table Interpolation Values ($Pco_2 = 10^{-3.2}$ Bars and Temperature = 56°C)

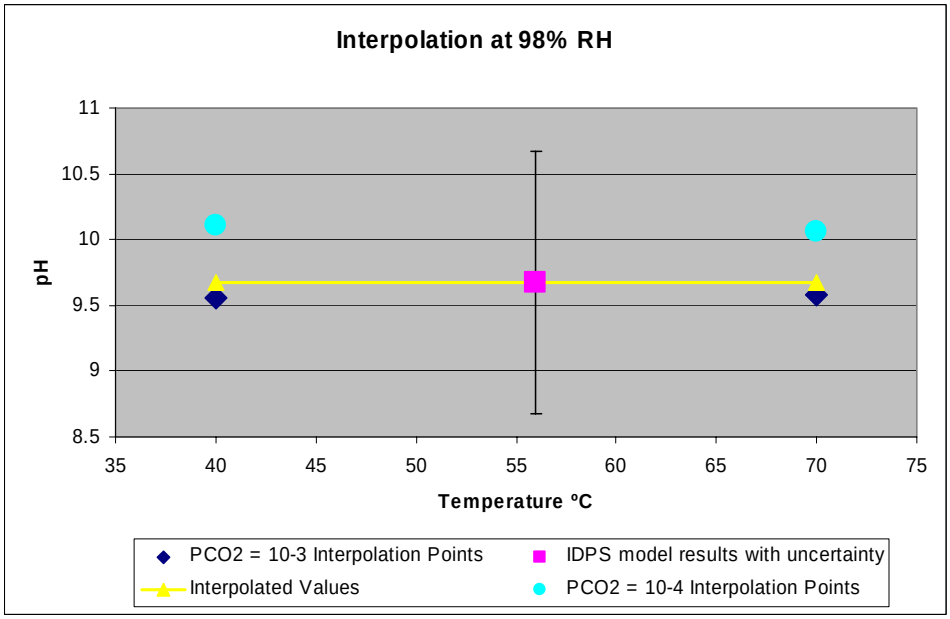

DTN: MO0312SPAPMVIC.000

Figure 7.2-22. Comparison of Model Results (pH at 98% RH) with Look-up Table Interpolation Values ($Pco_2 = 10^{-3.2}$ Bars and Temperature = 56°C)

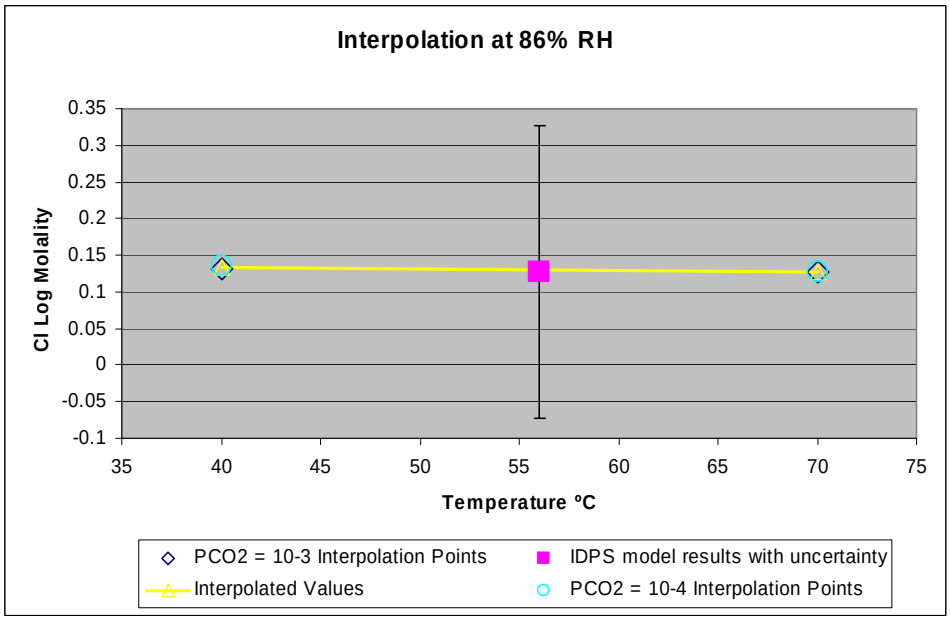

DTN: MO0312SPAPMVIC.000

Figure 7.2-23. Comparison of Model Results (Cl^- at 86% RH) with Look-up Table Interpolation Values ($Pco_2 = 10^{-3.2}$ Bars and Temperature = 56°C)

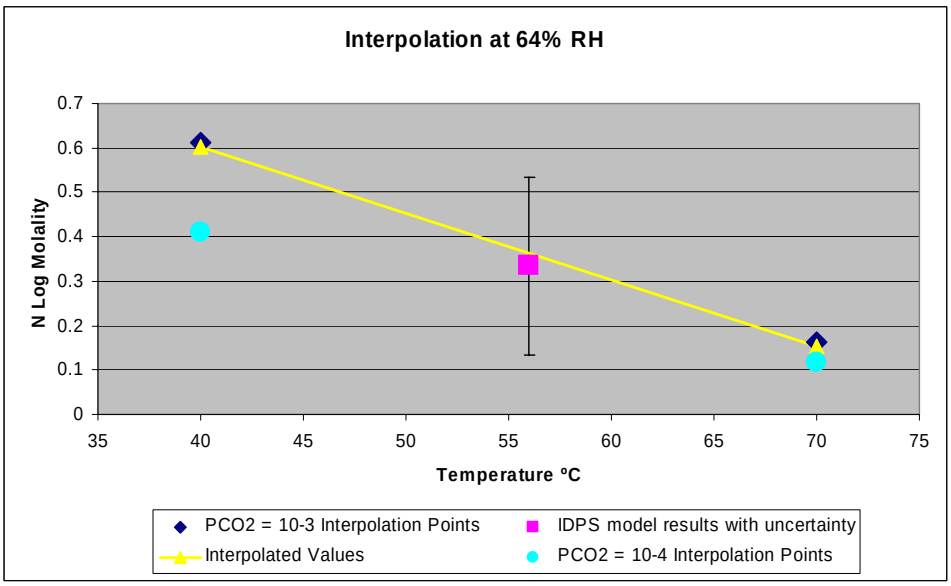

DTN: MO0312SPAPMVIC.000

Figure 7.2-24. Comparison of Model Results (NO_3^- at 64% RH) with Look-up Table Interpolation Values ($Pco_2 = 10^{-3.2}$ Bars and Temperature = 56°C)

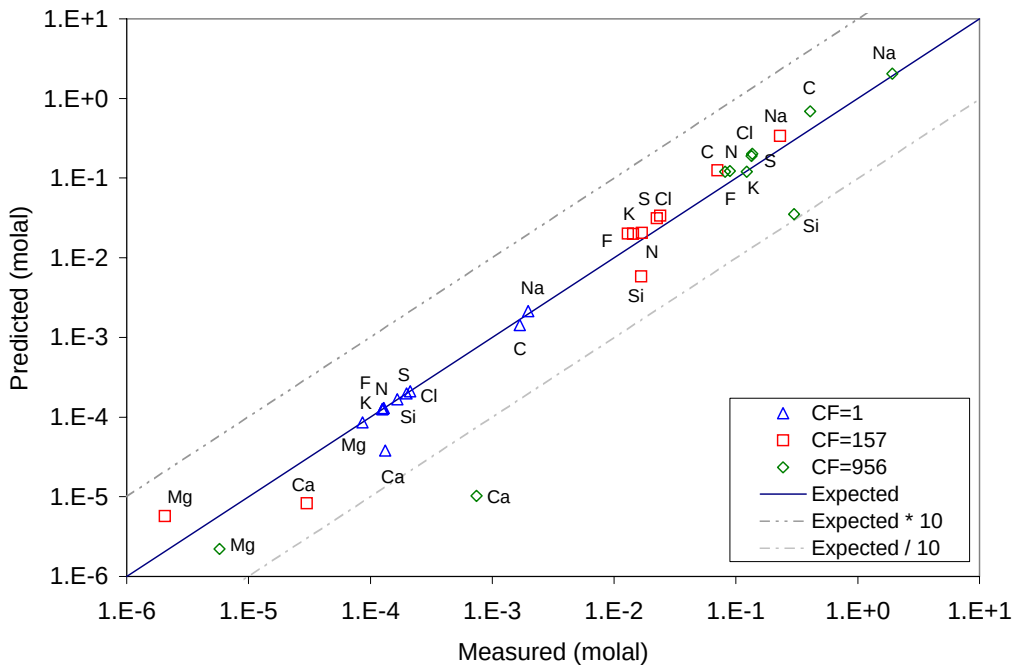

DTN: MO0303MWDJ13RB.000 [DIRS 163884]

Figure 7.3-1. Predicted Versus Measured Concentrations for Synthetic J-13 Water Evaporation Experiments of Rosenberg et al. (1999 [125338])

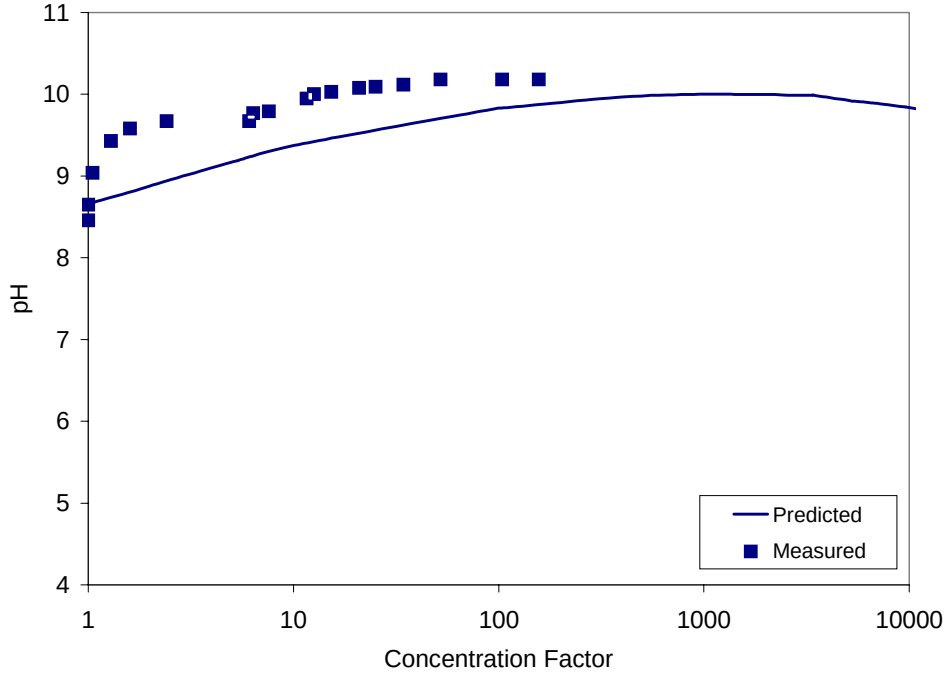

DTN: MO0303MWDJ13RB.000 [DIRS 163884]

Figure 7.3-2. Predicted Versus Measured pH Values for Synthetic J-13 Water Evaporation Experiments of Rosenberg et al. (1999 [125338])

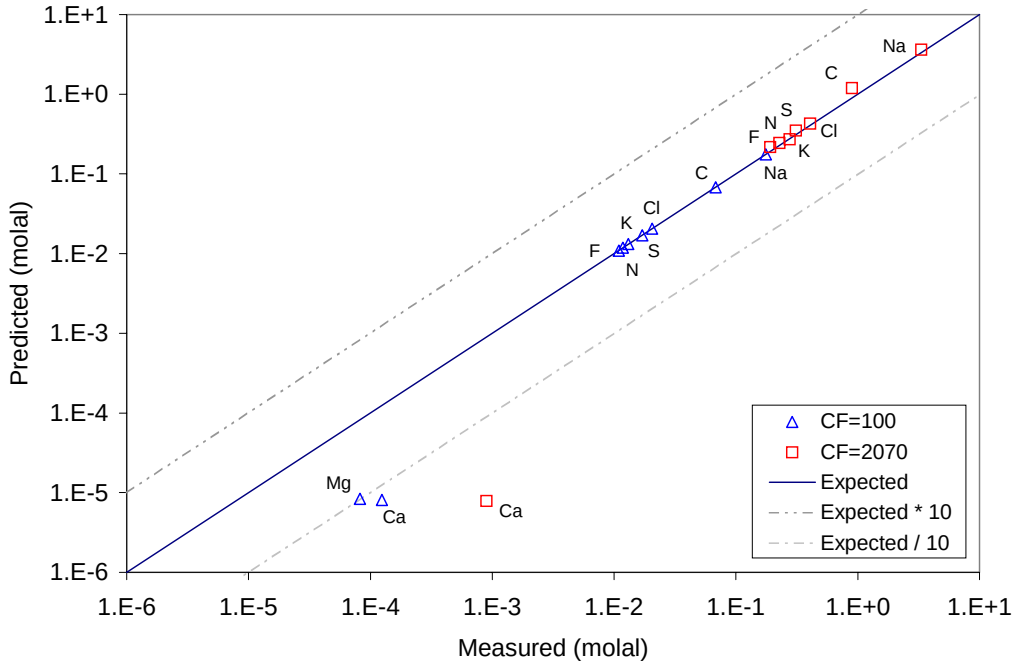

DTN: MO0303MWDJ13GD.000 [DIRS 164886]

Figure 7.3-3. Predicted Versus Measured Concentrations for 100x Synthetic J-13 Water Evaporation Experiments of CRWMS M&O (2000 [146460])

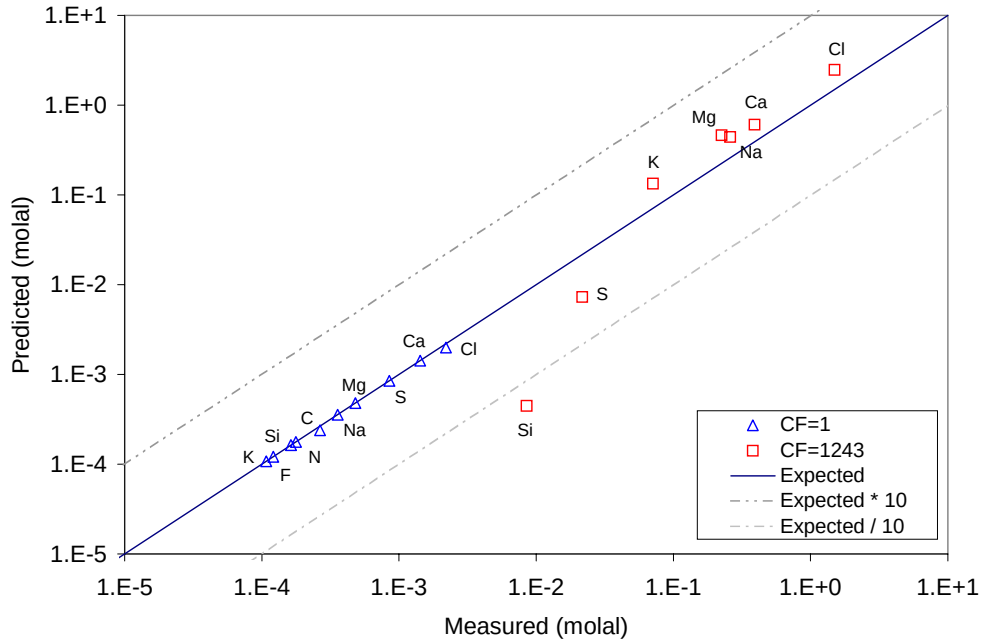

DTN: MO0303MWDTSWRB.000 [DIRS 164885]

Figure 7.3-4. Predicted Versus Measured Concentrations for Synthetic Topopah Spring Tuff Pore Water from Evaporation Experiments of Rosenberg et al. (1999 [125339])

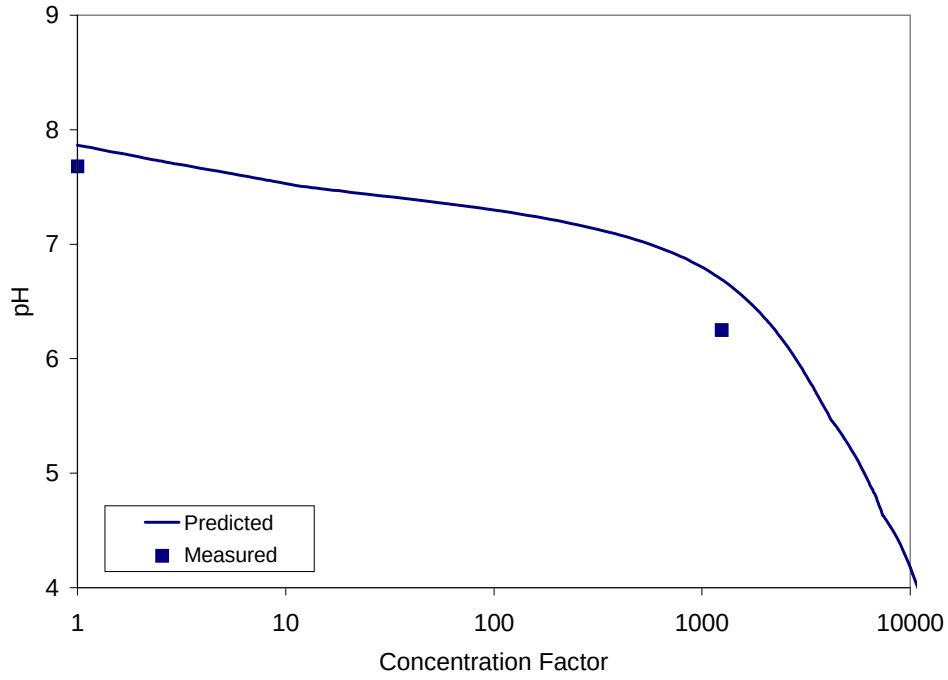

DTN: MO0303MWDTSWRB.000 [DIRS 164885]

Figure 7.3-5. Predicted Versus Measured pH Values for Synthetic Topopah Spring Tuff Pore Water from Evaporation Experiments of Rosenberg et al. (1999 [125339])

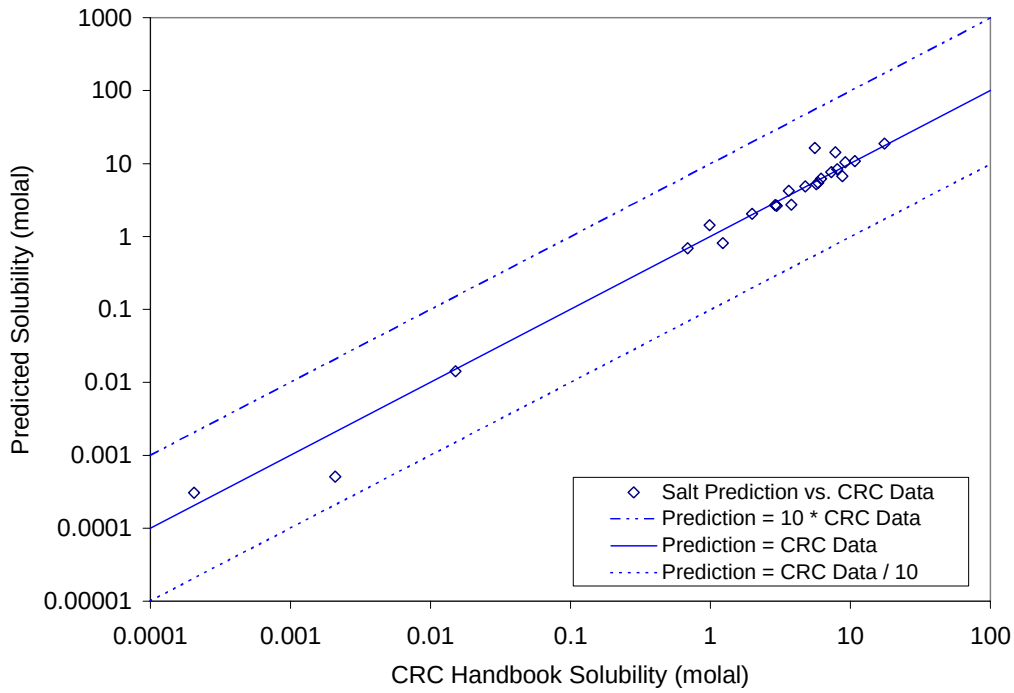

DTN: MO0303MWDSEDSS.000 [DIRS 163882]

Figure 7.3-6. Predicted Versus CRC Handbook Mineral Solubilities at 25°C

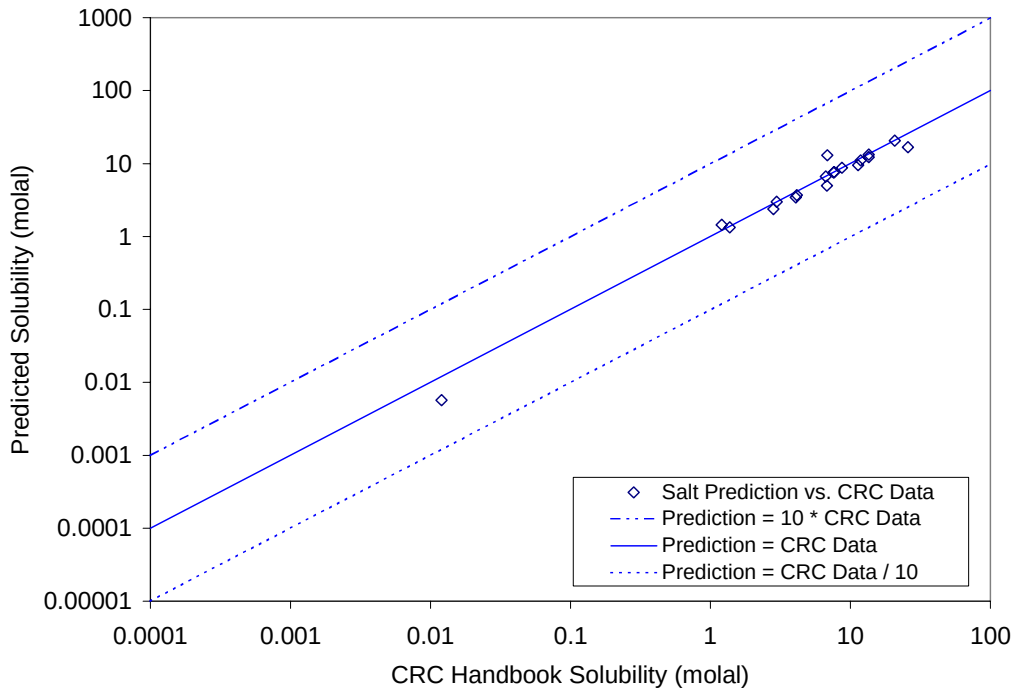

DTN: MO0303MWDSEDSS.000 [DIRS 163882]

Figure 7.3-7. Predicted Versus CRC Handbook Mineral Solubilities at 100°C

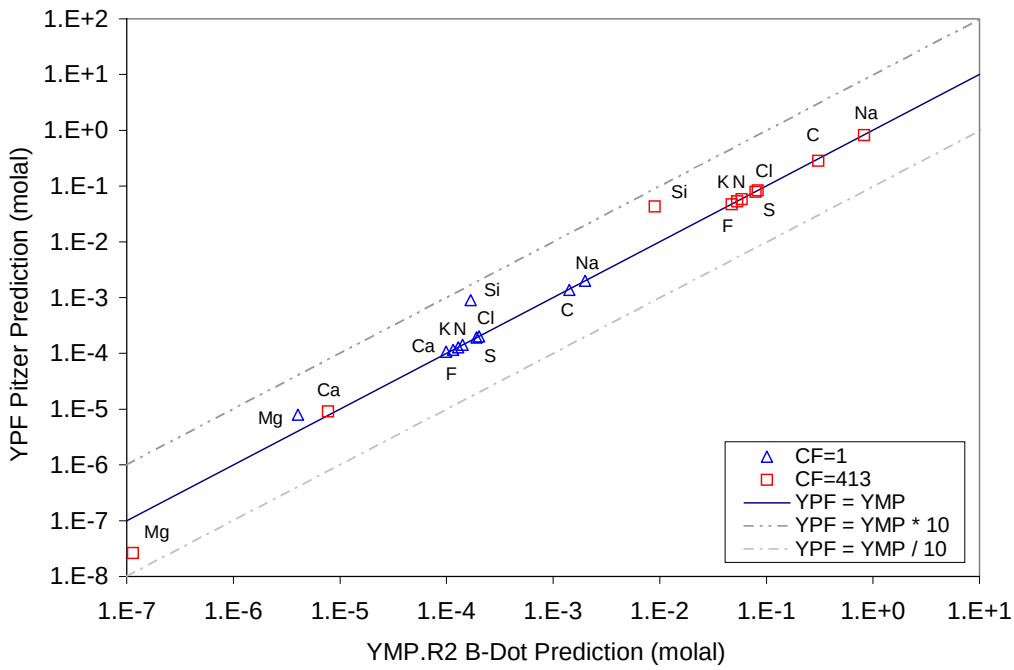

DTN: MO0303MWDINJ13.000 [DIRS 163881]

Figure 7.3-8. YPF Versus Set 1 YMP.R2 Aqueous Predictions for Average In Situ J-13 Well Water at 70°C and $CO_{2(g)}$ Fugacity of 10^{-3} Bar

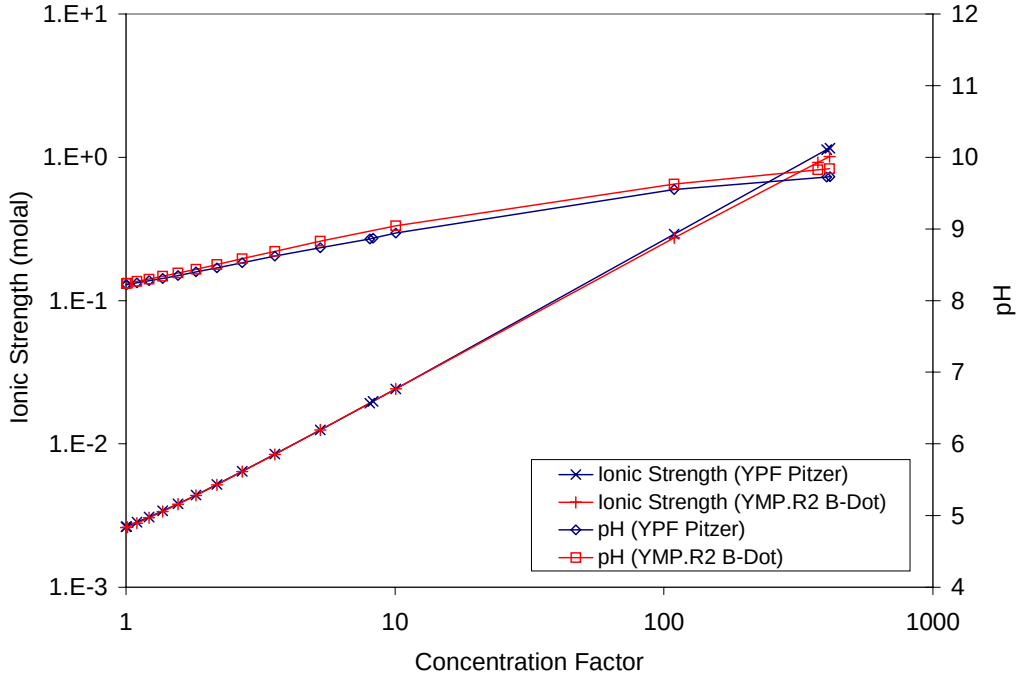

DTN: MO0303MWDINJ13.000 [DIRS 163881]

Figure 7.3-9. YPF Versus Set 1 YMP pH and Ionic Strength Predictions for Average In Situ J-13 Well Water at 70°C and $CO_{2(g)}$ Fugacity of 10^{-3} Bar

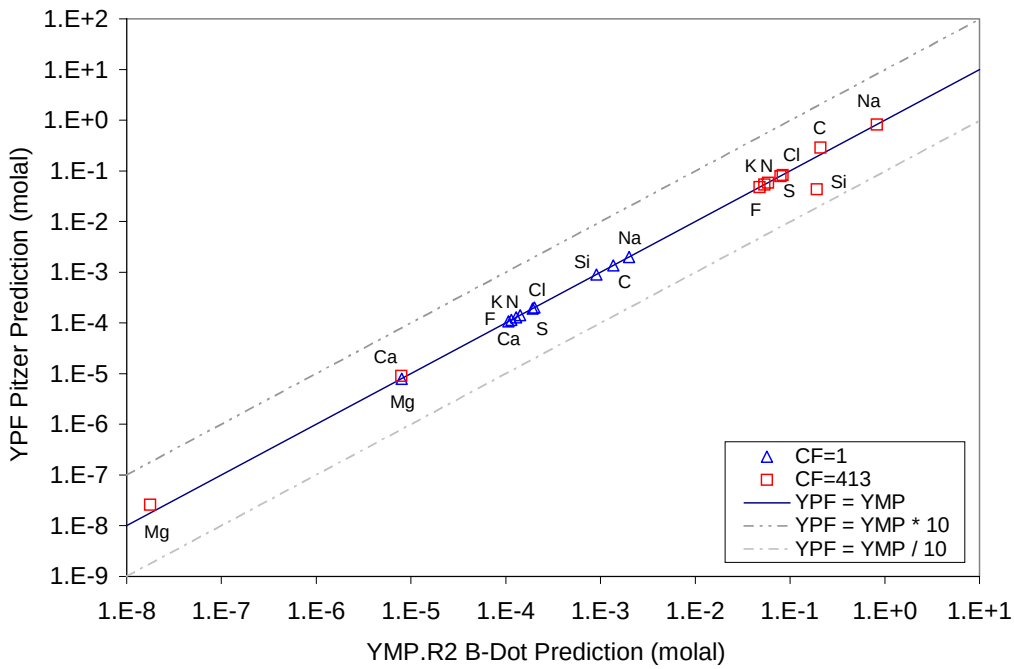

DTN: MO0303MWDINJ13.000 [DIRS 163881]

Figure 7.3-10. YPF Versus Set 2 YMP Aqueous Predictions for Average In Situ J-13 Well Water at 70°C and $CO_{2(g)}$ Fugacity of 10^{-3} Bar

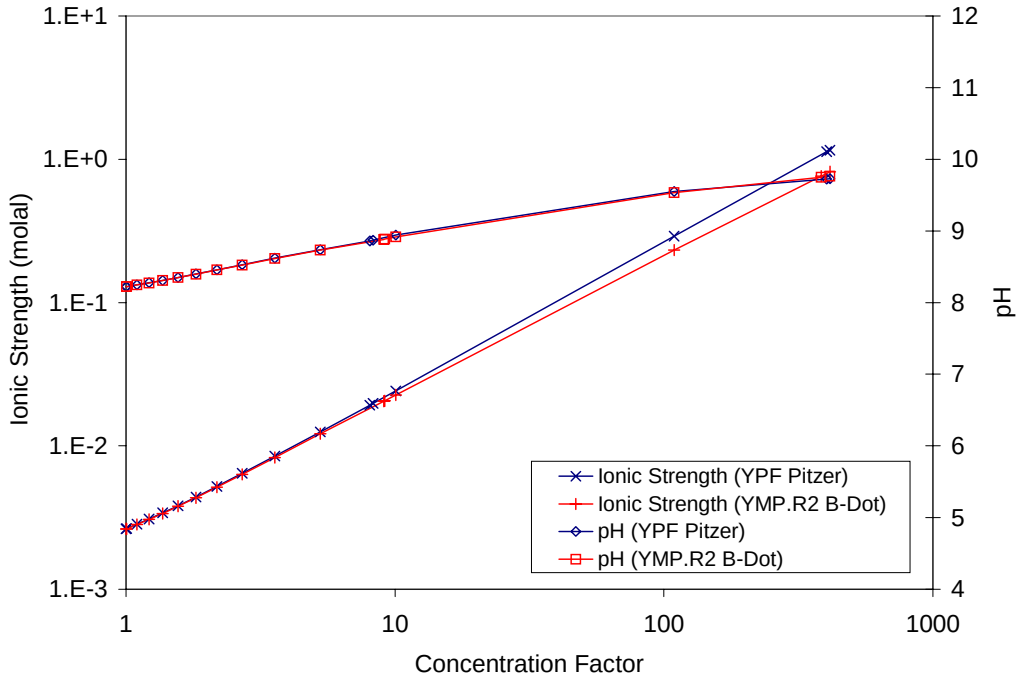

DTN: MO0303MWDINJ13.000 [DIRS 163881]

Figure 7.3-11. YPF Versus Set 2 YMP pH and Ionic Strength Predictions for Average In Situ J-13 Well Water at 70°C and $CO_{2(g)}$ Fugacity of 10^{-3} Bar

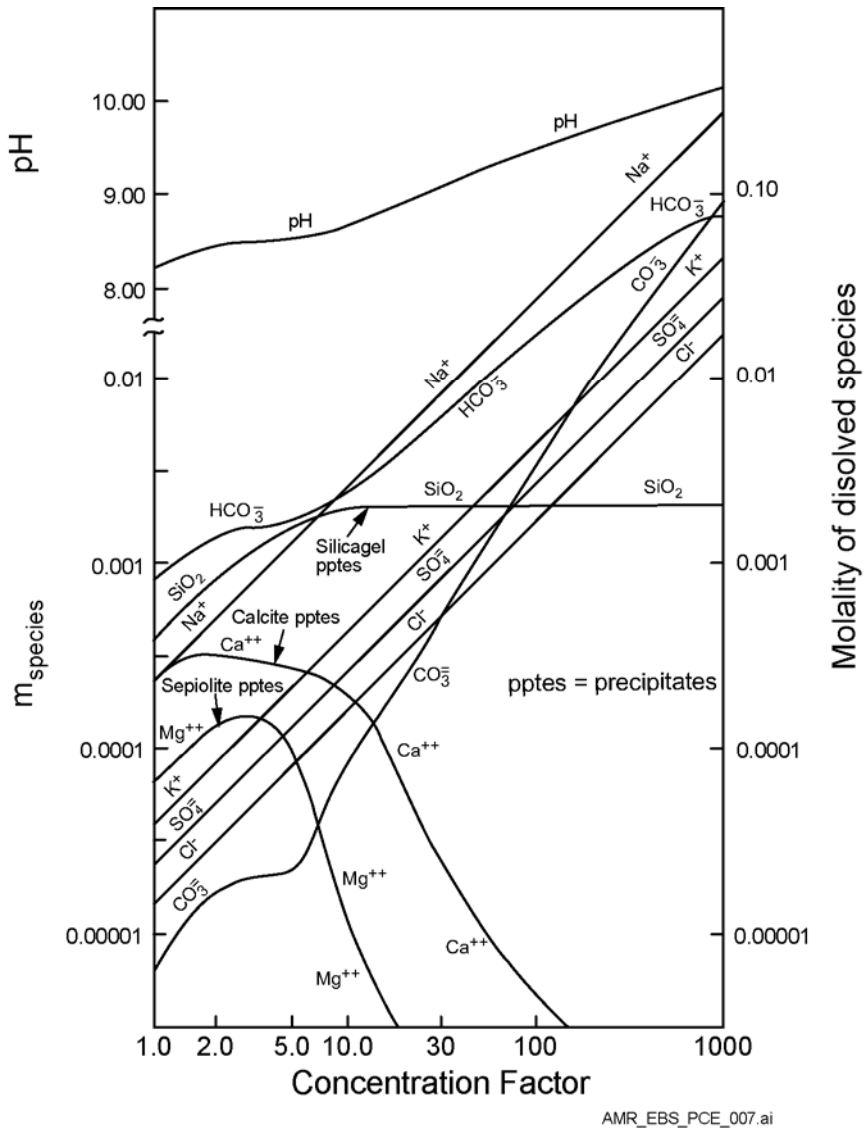

Source: Garrels and Mackenzie 1967 [DIRS 123636], page 239

Figure 7.4-1. Published Results (Garrels and Mackenzie 1967 [DIRS 123626]) for Modeled Evaporation of Typical Sierra Nevada Spring Water at 25°C in Equilibrium with Atmospheric CO_2 at $10^{-3.5}$ Bar

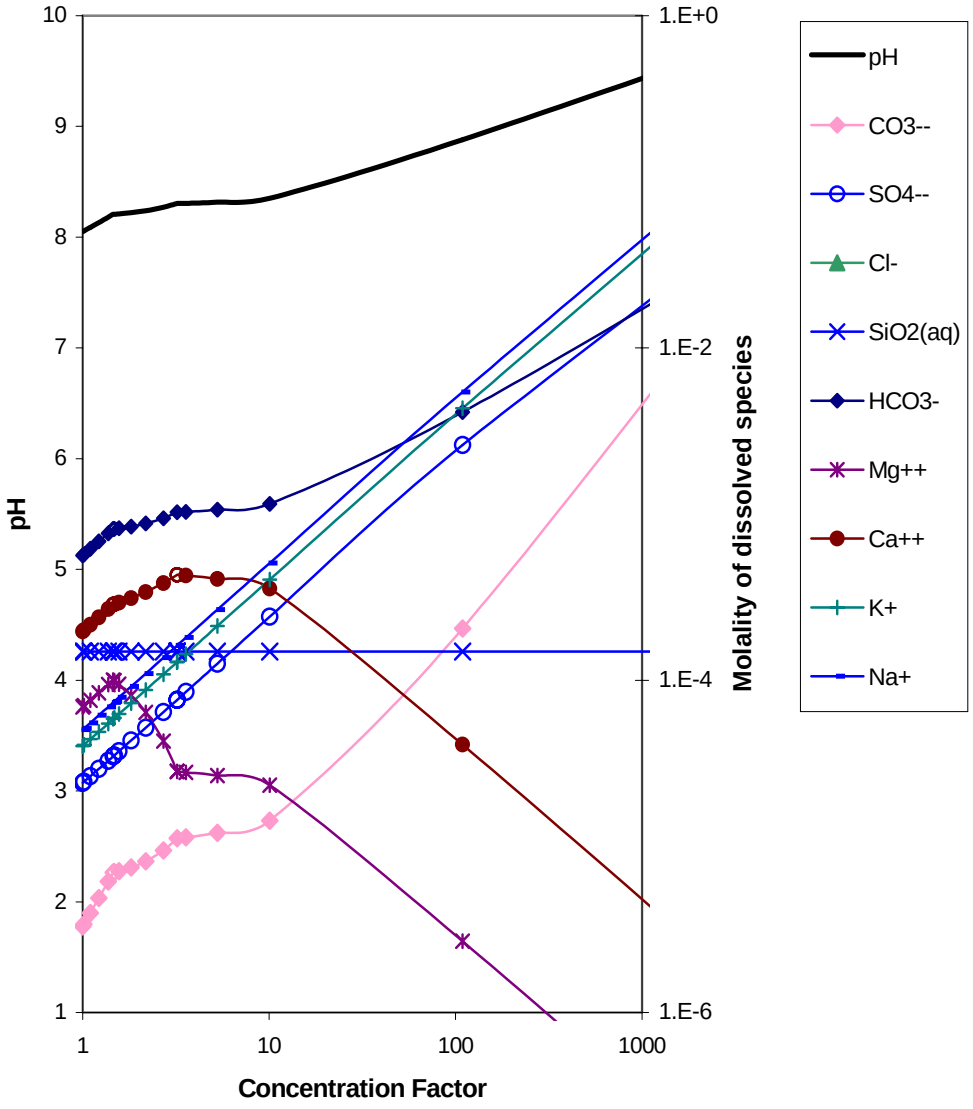

Source: DTN: MO0306SPAPCEVC.000 (File:val3bdot.6o)

Figure 7.4-2. IDPS Model Results for Evaporation of Typical Sierra Nevada Spring Water at 25°C in Equilibrium with Atmospheric CO_2 at $10^{-3.5}$ Bar

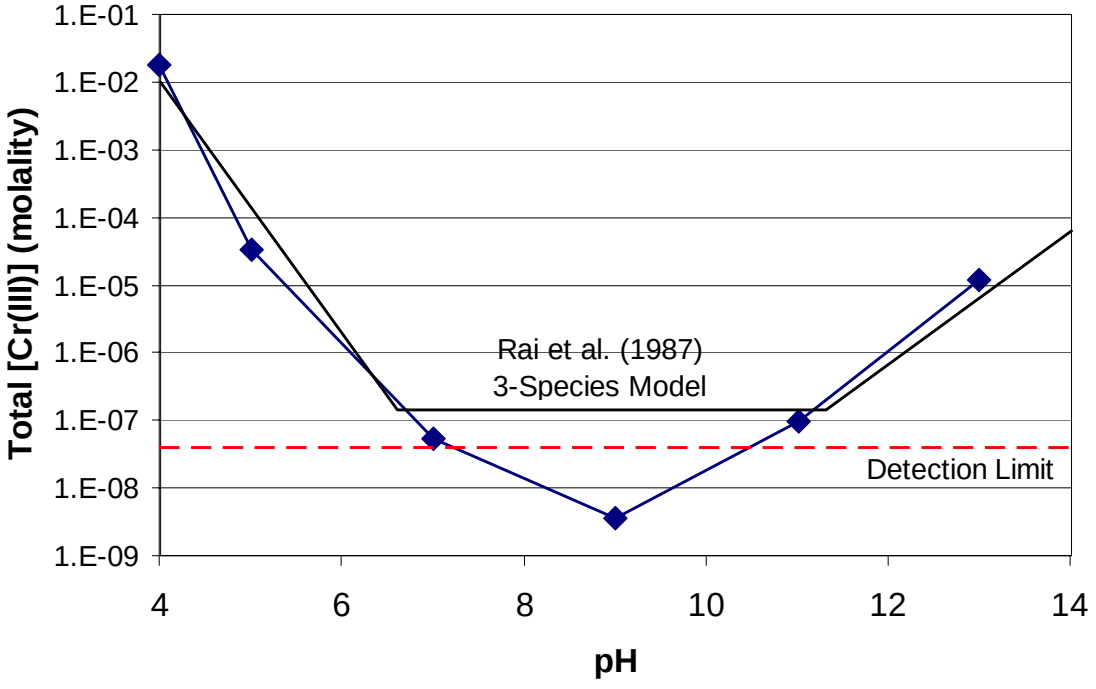

DTN: MO0306SPAPCESS.000

Figure 7.7-1. EQ3/6 Calculated Chromium Solubility in Equilibrium with $Cr(OH)_{3(am)}$ (Blue Diamonds with Lines) Compared to the 3-Species Model of Rai et al. (1987 [163369], Figure 2, Solid Black Lines) with Their Detection Limit Shown by the Red Dashed Line

8. CONCLUSIONS

8.1 SUMMARY OF MODEL FINDINGS

The engineered barrier system chemical environment analyses focus on a quantitative description of the pH, ionic strength (I), and major ionic and elemental compositions of waters in contact with the waste package and drip shield, and the invert. The brines that form by evaporative concentration of the crown seepage over time, by heating or drying out, can potentially affect localized corrosion on the waste package and drip shield, and influence radionuclide mobility in the invert. Compositional parameters in the waters contacting the drip shield and waste package, such as pH, or the ratio of chloride to nitrate are important in assessing potential localized corrosion (BSC 2003 [DIRS 161235], and BSC 2003 [DIRS 161236]). Acidic or alkaline pH values in the water of the invert may enhance the solubility of radionuclides. Increasing ionic strength of the water in the invert may reduce the mobility of colloidal particles transporting sorbed radionuclides.

Potential water compositions of crown seepage from the thermal-hydrological-chemical (THC) seepage model are abstracted into 11 possible waters that represent different brine types upon evaporation (see Section 6.6). These abstracted waters are used to generate a set of 198 look-up tables to represent evaporated crown seepage and invert wicked waters. The look-up tables represent a response surface for each bin covering a range of temperatures (100°C to 40°C), $P\mathrm{co}_2$ (10^{-4} to 10^{-2} bars) and relative humidities. The generation of these tables is discussed in Section 6.9. The total range in chemistry of the crown seepage and invert wicked waters (e.g., pH, I, Cl, N), as predicted by the look-up tables, is discussed in Section 6.13.

The EBS P&CE model predicts that corrosive calcium and magnesium chloride brines are unlikely to form on waste packages and drip shields (see Tables 6.13-1 and 6.13-8), and, if they do form, persist for only very short times soon after closure of the repository. The most likely brines to form are sodium chloride or sodium carbonate type brines (see Table 6.13-8, Bins 7 through 11), which are far less aggressive with respect to corrosion of engineered barrier materials. Cl:N ratios for all bins expected to contact drip shields and waste packages are shown in Figure 6.13-29. The mineral assemblages that precipitate during evaporation of the brines in the 99 crown seepage evaporative look-up table brines are reported in Table 6.13-6.

Lookup tables that represent both seepage water and invert wicking water have been provided with instructions (see Section 6.15) on how to select the appropriate chemical values from the lookup tables. These lookup tables can be used as source chemistry for waters fluxing into the invert.

Introduced materials were evaluated for longevity and chemical composition in Section 6.4. Short-lived materials, such as mild carbon steel, corrode rapidly in the environment of the drift and do not persist long enough to affect the chemistry of seepage waters. Others, such as the Alloy 22 that comprises the engineered barrier pallet, are resistant enough to prevent the engineered barrier from falling to the invert during the regulatory time frame. Oxygen gas fugacities (about equivalent to partial pressures) in the atmosphere of the drift are expected to be sufficient to maintain an oxygen-rich environment during the corrosion of the mild carbon steels

(see Section 6.7). Two important material longevity outputs are provided as a result of this evaluation:

1. Representative ranges of corrosion rates for all design materials that are planned to be placed into the repository drifts (see Table 6.4-18)

2. Selected compositions for each of the planned design materials (see Table 6.4-20).

These two outputs allowed for the selection of a long-lasting material that provided the bounding case for ground support interactions with seepage. This material is 316L stainless steel that comprised the wire mesh ground support component. Abstracted modeling and sensitivity studies of crown seepage interacting with 316L stainless steel as calculated in Section 6.8.4, indicate that the effects of the active corrosion of 316L stainless steel, on crown seepage water for pH and ionic strength is insignificant at 100 percent relative humidity and negligible at 98 percent relative humidity. Based on these results and the results of the uncertainty calculations presented in Section 6.12.4, it is reasonable to believe that the active corrosion of ground support will not appreciably influence the composition of the seepage over the interval examined for the TSPA-License Application (LA).

Dust that settles onto the waste package and drip shield from natural sources and repository construction processes generally is of little consequence with respect to corrosion. In the short term, when temperatures are above 105°C, no liquid water is expected to flow in the drift (Section 6.2). Thus, the only waters that are likely to be present are those that forms by deliquescence of the dust. Most of the dust is derived from the volcanic tuff host rock and most brines that form by dust deliquescence are not aggressive with respect to corrosion of titanium or C-22 alloy. The potential for corrosive brines to form is very low and if they do form they will not persist long (Section 6.13).

To quantitatively investigate the effect of deliquesced brines, measured compositions of dust leachate water were abstracted into 6 possible waters that represent dust leachate compositions upon evaporation (see Section 6.10). These abstracted waters were used to generate a set of 90 look-up tables to represent deliquescence on settled dust. The look-up tables represent a response surface for each bin covering a range of temperatures (140°C to 40°C), $P\mathrm{co}_2$ (10^{-4} to 10^{-2} bars) and relative humidity values. The total range of dust leachate chemistry (e.g., pH, I, Cl, N) covered in the generation of the look-up tables is discussed in Section 6.13. Minerals that precipitate as the 6 look-up table brines evaporate are reported in Table 6.13-7.

8.2 SUMMARY OF MODEL ABSTRACTION FOR TOTAL SYSTEM PERFORMANCE ASSESSMENT

8.2.1 Summary of the Total System Performance Assessment Look-up Tables

Fold out F/O 8.2-1 summarizes the recommended usage of the look-up tables developed in Sections 6.6, 6.7, 6.9 and, 6.10 for use on the engineered barrier surface. The instructions and restrictions for use of the scenarios depicted by this foldout is summarized in Sections 6.13 and 6.15. The foldout describes the use of this model by the TSPA to determine water chemistries during active seepage and deliquescence of dust on the waste packages and drip

shields. Section 6.15.2 gives the instructions for implementing look-up tables to determine chemistry in the invert. Section 8.2.2 lists the look-up table data tracking numbers (DTNs).

During preliminary implementation of the seepage lookup tables in the TSPA, it was discovered that the Goldsim software (BSC 2003 [DIRS 161572]) duplicate values for the independent parameter in the tables. This occurs in the look-up tables when mineral precipitation occurs. In order to provide a set of lookup tables to the TSPA that could be utilized, the lookup tables in MO0304SPACSALT.000 were modified; in cases where the independent parameter (RH) was duplicated, the value was modified slightly to eliminate the duplication without removing chemical parameter values from the dataset. The modified versions of the files in MO0304SPACSALT.000 are found in a new DTN (MO0310SPAPCEGS.000); modifications are indicated in the lookup table by red text. All other users of data from this report should use the original files archived in MO0304SPACSALT.000.

8.2.2 Data Tracking Numbers for Data Generated in This Report

Tables 8.2-1 and 8.2-2 list the DTNs for data generated in this report. Table 8.2-1 is for data generated to feed the TSPA-LA and Table 8.2-2 is for supporting data used in development of the TSPA-LA data feeds. These data are also summarized in Attachment I.

Table 8.2-1. Engineered Barrier System Physical and Chemical Environment Model Output DTNs Derived for use in the Total System Performance Assessment-License Application Model

Data Tracking Number	Location In Text	Description of TSPA Parameters
MO0310SPAEBSCB.003	Tables 6.6-3 to 6.6-14 Section 6.6.4 Section 6.6.5 Section 6.6.7.1 Section 6.6.7.2 Section 6.11.1 Tables 6.13-4 and 6.13-5 Section 6.15.1.1 Section 6.15.2 Section 7.2	Bin History Maps for each of the 5 starting THC waters for both crown seepage and invert wicking.
MO0308SPACO2GL.001	Tables 6.7-1 to 6.7-5 Section 6.7.2.1 Section 6.7.2.2 Section 6.12.5.3 Section 6.13.2.1 Section 6.15.1.1 Section 6.15.2	Pco_2 time history look-up tables for each of the 5 starting THC waters for both crown seepage and invert wicking.
MO0310SPAPCEGS.000 These values are for TSPA Goldsim software implementation. All other users should use the lookup tables archived in MO0304SPACSALT.000	Tables 6.9-6 and 6.9-7 Section 6.9.3 Section 6.12.5 Section 6.12.5.3 Section 6.15.1.1 Section 6.15.2 Section 8.2.1	198 THC seepage look-up tables containing pH, I, Cl, F, N, and other ions as a function of drift relative humidity, associated with the 11 abstraction bins, three starting temperatures (100ºC, 70ºC and 40ºC) and three Pco_2 values (10^{-4}, 10^{-3} and 10^{-2} atmospheres) – in all 99 tables for evaporation and 99 tables for condensation. Also included is a relative humidity map to interface between the evaporation look-up tables and the condensation look-up tables.

Table 8.2-1. Engineered Barrier System Physical and Chemical Environment Model Output DTNs Derived for use in the Total System Performance Assessment-License Application Model (Continued)

Data Tracking Number	Location In Text	Description of TSPA Parameters
MO0310SPADLALT.001	Table 6.10-14 Section 6.10.6.5 Section 6.12.5 Section 6.12.5.3 Section 6.15.1.2	54 Dust Leachate look-up tables containing pH, I, Cl, F, N, Cl:N ratio, and other ions as a function of relative humidity, associated with the 6 abstraction bins, three starting temperatures (100ºC, 70ºC and 40ºC) and three Pco_2 values (10^{-4}, 10^{-3} and 10^{-2} atmospheres).
MO0310SPADLHTL.000	Table 6.10-14 Section 6.10.6.5 Section 6.12.5 Section 6.12.5.3 Section 6.15.1.2	36 Dust Leachate look-up tables containing pH, I, Cl, F, N, Cl:N ratio, and other ions as a function of relative humidity, associated with the 6 abstraction bins, three starting temperatures (120ºC, 140ºC) and three Pco_2 values (10^{-4}, 10^{-3} and 10^{-2} atmospheres).
MO0310SPADLBU4.001	Table 6.7-7 Section 6.7.5 Tables 6.10-5 to, 6.10-10 Section 6.10.4 Section 6.10.5.2 Section 6.10.5.3 Section 6.10.5.5	Percentage of waters in each of the 6 dust leachate bins.
MO0311SPAEPMUT.000	Table 6.12-4, Table 6.12-8, Table 6.12-29, and Table 6.12-30	Uncertainty Values for pH, Ionic Strength, Cl, and $Cl:NO_3$ parameters .

EBS Environment Water Chemistry Derivations by Source and Location for TSPA:

I. Crown Seepage and Dust Leachate Effects on Waste Package and Drip Shield

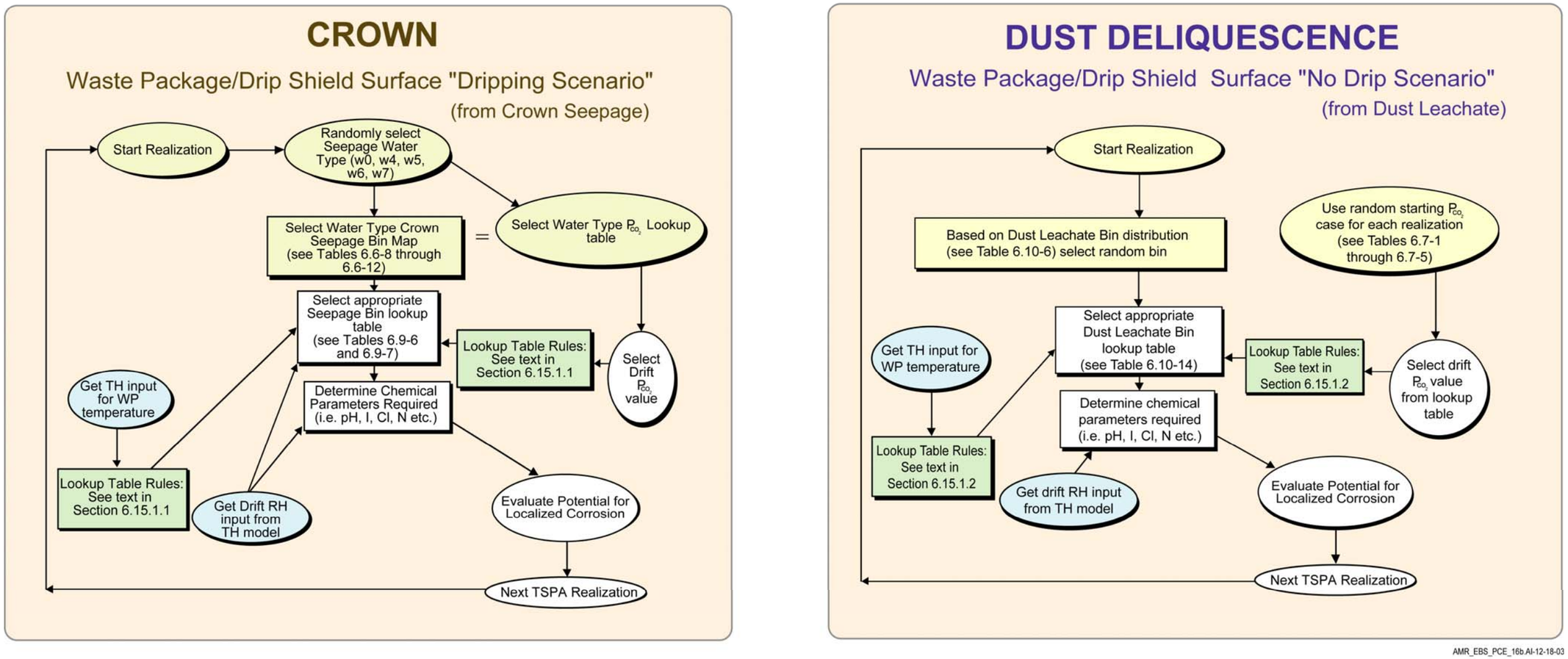

F/O 8.2-1. Engineered Barrier System Environment Water Chemistry Derivations for Total System Performance Assessment-License Application on the Waste Package and Drip Shield

INTENTIONALLY LEFT BLANK

Table 8.2-2. Engineered Barrier System Physical and Chemical Environment Model Supplemental Output DTNs

Output DTN	Location In Text	Title
SN0310T0510102.010	Section 6.10 Table 6.10-3, Section 6.10.3 Section 6.10.4 Section 6.10.5.1 Section 6.10.5.2 Section 6.10.5.5 Section 6.10.6.1 Table 6.12-9	Analysis of In-Drift Dust Leachates at 25 Degrees C to Various Evaporation Relative Humidity (RH) Levels
MO0304SPAA11GC.000	Tables 6.7-6 Tables 6.9-1 and 6.9-2 Section 6.9.1	EBS THC Seepage Abstraction 11 Bin EQ3 3o File Water and Gas Chemistry Extraction
SN0310T0510102.011	Table 6.10-13 Section 6.10.6.2 Section 6.10.6.3	Dust Leachate Abstraction TSPA-LA Lookup Table Eq3/6 Input and Output Files, Low Temperature
SN0310T0510102.012	Table 6.10-13 Section 6.10.6.2 Section 6.10.6.3	Dust Leachate Abstraction TSPA-LA Lookup Table Eq3/6 Input and Output Files, High Temperature
MO0304MWDSAB11.001	Section 6.8.2 Section 6.8.4.1 Tables 6.9-3 and 6.9-4 Section 6.9.1 Table 6.12-9 Section 6.12.4.1.3	EBS THC Seepage Abstraction 11 Bin EQ3 3i, 3p, and 3o Files
MO0303MWDSCMAB.000	Table 6.6-1 Section 6.6.3 Section 6.7.3 Section 6.9.1	THC Seepage Chemistry Model Abstraction Binning EQ3 Input, Pickup and Output Files
MO0303MWDEBSSM.000	Tables 6.6-1, 6.6-13, and 6.6-14 Section 6.6.3 Section 6.6.4 Section 6.7.3	EBS Abstraction of the THC Seepage Model: Binning Analysis Evaporation to 65% RH EQ6 Input and Output Files
MO0310SPAEBSUE.002	Section 6.12.3.1	EBS Chemistry Unevaporated Binning Abstraction Statistics
MO0304MWDEBSSA.000	Table 6.9-5 Section 6.9.2 Table 6.12-9	EBS THC Seepage Abstraction TSPA-LA Look-up Table EQ6 Input and Output Files
MO0312SPAPCEML.003	Tables 6.4-2, 6.4-3, 6.4-5, 6.4-8, 6.4-11, 6.4-15, 6.4-18 to 6.4-20 Section 6.4.1 Section 6.4.2.2 Section 6.8.2 Section 6.8.3	EBS P&CE Model Longevity of Materials Evaluation
MO0310SPAPCEUA.002	Tables 6.12-21 to 6.12-28 Section 6.12.4.3.2 Section 6.12.4.3.3 Section 6.12.4.4	EBS P&CE Uncertainty Analyses for Pco_2, Br, and Mineral Suppressions

Table 8.2-2. Engineered Barrier System Physical and Chemical Environment Model Supplemental Output DTNs (Continued)

Output DTN	Location In Text	Title
SN0303T0510102.004	Tables 7.5-1 and 7.5-2	EQ3/6 (Version 8.0) Input/Output Data Files – Salt Deliquescence Point Modeling as A Function of Temperature
MO0310SPAPCEAC.002	Tables 6.11-1 to 6.11-13 Section 6.11.1	EBS P&CE Alternate Conceptual Model Calculations
MO0312SPAPCEGF.002	Table 4.1-17 Section 4.1.2 Section 4.1.3 Section 6.7.1 Section 6.7.2	EBS P&CE Model Gas Flux Evaluation
SN0312T0510102.013	Section 4.1.7 Tables 6.8-2 and 6.8-5 Section 6.8.3 Section 6.8.4.1 Section 6.8.4.3 Tables 6.12-10 to 6.12-19	EBS P&CE Model Stainless Steel Abstraction
MO0310SPAPCELA.002	Section 6.12.4.2.4 Table 6.13-7 and 6.13-9 Section 6.13.2.2 Section 6.13.2.3	EBS P&CE Model Dust Leachate Analyses Spreadsheets and Data
MO0312SPAPCESA.002	Tables 6.13-1, 6.13-2, 6.13-6, and 6.13-8 Section 6.13 Section 6.13.1.3 Section 6.13.4.1 Section 6.13.5.2 Section 7.2	EBS P&CE Model THC Seepage Analysis Spreadsheets
MO0304SPACPSLT.000	Section 6.13.1.2	Combined In-Drift Precipitates/Salts Model Look-up Table for Seepage Evaporation Abstractions for All Bins
MO0310SPAEBSSB.002	Section 6.12.3.1	EBS P&CE Model THC Seepage Bin Uncertainty Analyses
MO0306SPAPCEVC.000	Section 7.4	EBS P&CE Model Validation Calculations, Spreadsheets, and Data.
MO0310SPAPCELT.000	6.12.3	EBS P&CE Log Transform Of Uncertainty Data
MO0311SPASADLS.000	6.10.8	EBS P&CE Sensitivity Analyses On Dust Leachate Silica Values
MO0312SPAPMVIC.000	Section 7.2.2	EBS P&CE Model Validation Interpolation Calculations

8.3 MODEL UNCERTAINTY AND RESTRICTIONS

Uncertainties in the output from the EBS physical and chemical environment (P&CE) model are summarized in this section. Direct inputs to the model are tabulated and discussed in Section 4.1, but the uncertainties associated with those inputs are discussed in the subsections of Section 6 where they are used. The effects of input uncertainties are discussed in more detail in Section 6.12. Limitations and constraints on the use of the model and its outputs are discussed in Section 6.13 with the discussions of the various components and features of the overall EBS P&CE model. Specific limitations involved in the model are listed in Section 1.3.

The EBS P&CE model uses five primary inputs, and each has uncertainty associated with it. These inputs are:

- Composition of water entering the drift
- Composition of dust predicted to settle on repository surfaces
- *In Drift Precipitates/Salts Model* (BSC 2003 [DIRS 162529 in progress]) and its associated data bases (thermodynamic data and other technical information not specific to the site used in the geochemical modeling that results in the model output)
- Composition and flux of in-drift gases
- Amounts and characteristics of engineered materials to be placed in the drift (ground support, emplacement rails, etc.).

For evaluating repository performance, five parameters have been identified as output from this model that will be used as direct input to TSPA calculations: 1) chloride ion concentration, 2) chloride/nitrate molar ratio, 3) ionic strength, 4) pH, and 5) relative humidity point at which salt minerals deliquesce and an aqueous phase appears.

As explained in Section 6.12, of the five inputs, only three were found to have uncertainties that would propagate into the output parameters that feed the TSPA: 1) the In-Drift Precipitates/Salts model (IDPS), 2) the abstracted incoming seepage waters, and 3) aqueous solutions that could result from deliquescence of salts in dust.

An evaluation of the In-Drift Precipitates/Salts model was conducted to determine its contribution to error in predicting all of the parameters of interest as explained in Section 6.12.2. A statistical evaluation of the TSPA parameter feeds (except relative humidity which was not relevant to this evaluation) in the 11 bins of seepage water and the 6 bins of deliquescent dust solutions was conducted as explained in Section 6.12.3. This evaluation demonstrated that there is a sufficiently large variability within the bins to warrant the creation of a discretization error band around the median values of parameters that need be propagated by the TSPA process.

Uncertainties from these three sources were combined to create total error bands for the parameters of interest to TSPA, an appropriate distribution for the error ranges was selected, and instructions for how to sample the errors were developed in Section 6.12.5.

8.4 YUCCA MOUNTAIN REVIEW PLAN CRITERIA ASSESSMENT

8.4.1 Degradation of Engineered Barriers Acceptance Criteria

These criterion are from the *Yucca Mountain Review Plan, Final Report* (NRC 2003, Section 2.2.1.3.1.3 [DIRS 163274] which are from 10 CFR 63.114(a)–(c) and (e)–(g) [DIRS 156605]).

8.4.1.1 Acceptance Criterion 1–System Description and Model Integration Are Adequate

(1) The total system performance assessment adequately incorporates important design features, physical phenomena, and couplings, and uses consistent and appropriate assumptions throughout the degradation of engineered barriers abstraction process;

Analyses addressed in this report use current design information (see Section 4.1), and are based on physical phenomena expected within repository drifts (see Section 6.2). The effects of coupled processes (Section 6.3) have been considered in part of the development of this model. For example, thermal-hydrological-chemical effects on input water compositions are incorporated in the THC model output (Section 4.1.3) used as input to the P&CE model. Coupled processes that are not addressed in this report are considered, and their rationale for exclusion presented, in the *Engineered Barrier System Features, Events, And Processes* report (BSC 2003 [DIRS 166464]). Efforts have been made to ensure that the assumptions (Section 5) contained in this report are consistent with similar assumptions in related documents. These factors are included in the analyses leading to the output parameters (Section 6.13) which will be used to assess engineered barrier performance.

(2) Assessment abstraction of the degradation of engineered barriers uses assumptions, technical bases, data, and models that are appropriate and consistent with other related U.S. Department of Energy abstractions. For example, the assumptions used for degradation of engineered barriers should be consistent with the abstractions of quantity and chemistry of water contacting waste packages and waste forms (Section 2.2.1.3.3), climate and infiltration (Section 2.2.1.3.5), mechanical disruption of waste packages (Section 2.2.1.3.2). The descriptions and technical bases provide transparent and traceable support for the abstraction of the degradation of engineered barriers;

This report uses the same technical bases and other information as are used in other LA supporting documents concerned with engineered barrier performance. The conceptual model (Section 6.2) that forms the basis for this report and its assumptions (Section 5) are consistent with other engineered system models and repository design. Primary input (Section 4.1) is taken from the unsaturated zone (UZ) THC model and uses the in-drift precipitates salts (IDPS) model to generate in-drift water chemistry. Section 6.2 provides details of these model interfaces.

(3) The descriptions of engineered barriers, design features, degradation processes, physical phenomena, and couplings that may affect the degradation of the engineered barriers are adequate. For example, materials and methods used to construct the engineered barriers are included, and degradation processes, such as uniform corrosion, pitting corrosion, crevice corrosion, stress corrosion cracking, intergranular corrosion, microbially influenced corrosion, dry-air oxidation, hydrogen embrittlement, and the effects of wet and dry cycles, material aging and phase stability, welding,

and initial defects on the degradation modes for the engineered barriers are considered.

This model is based on descriptions of the components (see Sections 4.1 and 6.4) and predicted behavior of the engineered barrier system (see Section 6.2) in response to various design features, degradation processes, physical phenomena, and couplings as documented in this report, Project design documents and in other barrier-specific models and abstractions. For example, this model uses information on the materials and construction of engineered barriers (Sections 4.1 and 6.4) to assess the chemical effects of corrosion on engineered materials (see Sections 6.7 and 6.8).

(4) Boundary and initial conditions used in the total system performance assessment abstractions are propagated consistently throughout the abstraction approaches. For example, the conditions and assumptions used in the degradation of engineered barriers abstraction are consistent with those used to model the quantity and chemistry of water contacting waste packages and waste forms (Section 2.2.1.3.3); climate and infiltration (Section 2.2.1.3.5); and mechanical disruption of waste packages (Section 2.2.1.3.2);

The boundary and initial conditions used in the P&CE model are consistent with other Project subsystem models supporting total system performance assessment. For example, the P&CE model uses initial and boundary conditions dictated in part by the THC model outputs that are used to develop the chemistry of water within the drifts (Section 6.9). These THC outputs, in turn, reflect natural system initial and boundary conditions (see Section 6.6) common to other drift-scale hydrological models. Another example consists of the initial and boundary conditions pertinent to the corrosion analyses of engineered materials (Section 6.4 and 6.8). These conditions are common to other Project models and analyses involving degradation of engineered barriers.

(5) Sufficient technical bases for the inclusion of features, events, and processes related to degradation of engineered barriers in the total system performance assessment abstractions are provided;

FEPs specific to this document, including FEPs related to degradation of engineered barriers, are discussed with their technical bases in Section 6.14. This section also lists FEPs screened out of the P&CE model as well the exclusion rationale. Additional details about included and excluded FEPs are discussed in various FEPs reports such as the *Engineered Barrier System Features, Events, And Processes* report (BSC 2003 [DIRS 166464]).

(7) Guidance in NUREG–1297 (Altman et al. 1988 [DIRS 103597]) and NUREG–1298 (Altman et al. 1988 [DIRS 103750]), or other acceptable approaches is followed.

Inputs were selected and documented according to applicable YMP procedures, which comply with NUREG-1297 and NUREG-1298 (see Section 4.1).

8.4.1.2 Acceptance Criterion 2–Data Are Sufficient for Model Justification

(1) Parameters used to evaluate the degradation of engineered barriers in the license application are adequately justified (e.g., laboratory corrosion tests, site-specific data such as data from drift-scale tests, in-service experience in pertinent industrial applications, and test results not specifically performed for the Yucca Mountain site, etc.). The U.S. Department of Energy describes how the data were used, interpreted, and appropriately synthesized into the parameters;

While the P&CE model does not evaluate engineered barrier performance, it does provide information to other Project models for that purpose (see Sections 6.13 and 6.15). The selection justification of input used in this model is contained in Section 4.1 and tabulated in the Document Input Reference System (DIRS). Further details of model development as it relates to the use, interpretation, and synthesis of founding data into parameters are presented throughout Section 6, especially in Section 6.6. Site-specific are embodied in the water chemistries delivered to this model from the THC model (see Section 6.6) and dust taken from the ESF and adjoining facilities. Environmental conditions were selected consistent with the underground design as envisioned to exist and as confirmed by results from the Drift-Scale Test and other tests.

(2) Sufficient data have been collected on the characteristics of the engineered components, design features, and the natural system to establish initial and boundary conditions for abstraction of degradation of engineered barriers;

Data and technical information collected from field and experimental sources and from literature searches for the P&CE model are discussed for engineered materials in Section 4.1 (engineered components), Section 6.4 (design features) and for natural system characteristics in Section 6.5 (mineralogical information) and in Section 6.6 (THC model). Natural system data are used to develop the THC model, which is a major input to the P&CE model (Section 6.6). The results of the P&CE model are provided to Project models to evaluate engineered barrier performance.

8.4.1.3 Acceptance Criterion 3–Data Uncertainty Is Characterized and Propagated Through the Model Abstraction

(1) Models use parameter values, assumed ranges, probability distributions, and/or bounding assumptions that are technically defensible, reasonably account for uncertainties and variabilities, and do not result in an under-representation of the risk estimate;

This model used parameter values that are representative of the natural and engineered system (see Sections 4.1, 6.4, 6.5, 6.6, and 6.10). Ranges, probability distributions, and bounding assumptions were considered in assessing boundary conditions and input uncertainties and variabilities, which were propagated through the model as described in Section 6.12. Further propagation through TSPA-LA implementation is described in Section 6.15. When modeling decisions were necessary, the choices were made to result in conservative outcomes that avoid an under-representation of risk (as in Sections 6.9, 6.10 and 6.12). In some cases, sensitivity

analyses enabled exclusion of some phenomena and provided a technical basis to enable selective extrapolation outside the nominal bounding ranges.

(2) For those degradation processes that are significant to the performance of the engineered barriers, the U.S. Department of Energy provides appropriate parameters, based on techniques that may include laboratory experiments, field measurements, industrial analogs, and process-level modeling studies conducted under conditions relevant to the range of environmental conditions within the waste package emplacement drifts. The U.S. Department of Energy also demonstrates the capability to predict the degradation of the engineered barriers in laboratory and field tests;

This model assesses in-drift water and gas chemistry under conditions relevant to those expected within the emplacement drifts; its parameter output is used by others to model engineered barrier degradation. The parameters (Section 4.1) upon which the P&CE model is based are themselves based upon laboratory experiments, field measurements, industrial analogs and process-level modeling studies. Examples include the thermodynamic databases, discussed in Section 4.1.4 with additional discussion in *Data Qualification: Update and Revision of the Geochemical Thermodynamic Database, Data0.ymp* (Steinborn et al. 2003 [DIRS 161956]) and *In-Drift Precipitates/Salts Model* (BSC 2003 [DIRS 162529]); corrosion data, discussed in Sections 6.4 and 6.8; and mineralogy data discussed in Attachment IV. Much of the data founding model development was collected in the ESF and adjoining facilities. This included seepage water samples and dust samples. Environmental conditions imposed on model development (temperatures, RH, and moisture contents) were consistent with data collected from the Drift-Scale test and other related tests. The validation for the THC seepage abstraction has been performed against results from the THC seepage model, which was validated against data from the Drift Scale Test. Other laboratory and natural analog information was used for validation of portions of the model (see Section 7).

(3) For the selection of parameters used in conceptual and process-level models of engineered barrier degradation that can be expected under repository conditions, assumed range of values and probability distributions are not likely to underestimate the actual degradation and failure of engineered barriers as a result of corrosion;

Parameters developed by the P&CE model are presented in the form of look-up tables to the TSPA-LA and others for the analysis of engineered barrier degradation (see Section 6.15). These look-up tables incorporate parameter uncertainty and, used appropriately, allow that uncertainty to be propagated through engineered barrier performance analyses (see Section 6.15). When modeling decisions regarding the range of parameter values and probability distributions were necessary, choices were made to result in conservative outcomes as in Sections 6.9, 6.10 and 6.12.

8.4.1.4 Acceptance Criterion 4–Model Uncertainty Is Characterized and Propagated Through the Model Abstraction

(1) Alternative modeling approaches of features, events, and processes are considered and are consistent with available data and current scientific understanding, and the results and limitations are appropriately considered in the abstraction;

The evaluation of FEPs documented in Section 6.14 is based on the model results developed in this report, including the alternative modeling discussed in Section 6.11. This alternative modeling is consistent with available data and scientific understanding. The results and limitations of the alternative FEPs modeling and their impact on engineered barrier performance are presented in Section 6.14.

(2) Consideration of conceptual model uncertainty is consistent with available site characterization data, laboratory experiments, field measurements, natural analog information and process-level modeling studies; and the treatment of conceptual model uncertainty does not result in an under-representation of the risk estimate; and

Uncertainties in inputs and in analytical methodology are considered in the development of the conceptual model (see Section 6.2) and output parameters (see Section 6.15). Discussion of uncertainty in the conceptual model appears in various places throughout the report. One example is Section 6.12.1, where quotations from Section 6.9.2 of The *Drift-Scale Coupled Processes (DST and THC Seepage) Models*, (BSC 2003 [DIRS 162050]) discuss the uncertainty of model conceptualizations involving the THC abstraction. The uncertainty evaluation is consistent with available site-specific data, laboratory experiments, field studies, natural analog data and process-level modeling studies. In addition, model validation is based on available site characterization data, laboratory experiments and natural analogues (see Section 7). The treatment of conceptual model uncertainty described in this report does not under-represent risk.

(3) The U.S. Department of Energy uses alternative modeling approaches, consistent with available data and current scientific understanding, and evaluates the model results and limitations, using tests and analyses that are sensitive to the processes modeled. For example, for processes such as uniform corrosion, localized corrosion, and stress corrosion cracking of the engineered barriers, the U.S. Department of Energy considers alternative modeling approaches, to develop its understanding of environmental conditions and material factors significant to these degradation processes.

Alternate modeling approaches are considered in Section 6.11. As previously discussed, these approaches are consistent with available data and current scientific understanding. Results and limitations of these alternative modeling approaches were evaluated using tests and analyses that reflect the processes and conditions being modeled. This model does not directly address engineered barrier performance, but it does provide information for use in understanding of barrier performance.

8.4.1.5 Acceptance Criterion 5–Model Abstraction Output Is Supported by Objective Comparisons

(1) Models implemented in this total system performance assessment abstraction provide results consistent with output from detailed process-level models and/or empirical observations (laboratory and field testings and/or natural analogs);

Information provided to the TSPA-LA (see Section 6.15) depends on the output from detailed process-level models. The resulting abstracted model output provided for implementation in the TSPA-LA is consistent with the related process-level output (Section 7). For appropriate cases, validation has been done against empirical observations as shown in Section 7.

(5) Accepted and well-documented procedures are used to construct and test the numerical models that simulate the engineered barrier chemical environment and degradation of engineered barriers; and

Accepted and well-documented procedures contained in the quality assurance program (Section 2) governed the development of this report and the work it documents. This model has been constructed and documented according to AP-SIII.10Q, *Models*. Test and validation methods (Section 7) comply with AP-SIII.10Q and applicable guidance. This report was generated according to the requirements of the *Technical Work Plan For: In-Drift Geochemistry Modeling* (BSC 2004 [DIRS 166519]) as directed by AP-2.27Q, *Planning for Science Activities*.

(6) Sensitivity analyses or bounding analyses are provided to support the abstraction of degradation of engineered barriers that cover ranges consistent with the site data, field or laboratory experiments and tests, and industrial analogs.

In developing output to support the analysis of engineered barrier performance, the P&CE model considers a number of sensitivity or bounding analyses that cover ranges consistent with site data, field and laboratory experiments and tests, and industrial analogs. For example, sensitivity studies associated with the potential effects of ground support degradation are developed in Section 6.8. The relevant ranges in material lifetimes (Section 6.4) and oxygen demand (Section 6.7.1) are consistent with laboratory experimental data and industrial experience. The sensitivity of water chemistry evolution to changing environmental conditions is discussed in Section 6.12. Other sensitivity studies done as part of alternative modeling are discussed in Section 6.11.

8.4.2 Quantity and Chemistry of Water Contacting Engineered Barriers and Waste Forms–Acceptance Criteria

These criterion are from the *Yucca Mountain Review Plan, Final Report* (NRC 2003, Section 2.2.1.3.3.3 [DIRS 163274] which is from 10 CFR 63.114(a)–(c) and (e)–(g) [DIRS 156605]).]

8.4.2.1 Acceptance Criterion 1–System Description and Model Integration are Adequate

(1) Total system performance assessment adequately incorporates important design features, physical phenomena, and couplings, and uses consistent and appropriate assumptions throughout the quantity and chemistry of water contacting engineered barriers and waste forms abstraction process;

The effects of coupled processes (Section 6.3) have been considered in part in the development of this model. For example, thermal-hydrological-chemical effects on input water compositions are incorporated in the THC model output (Section 4.1.3) used as input to the P&CE model. Thermal-hydrological-chemical processes are at the heart of the in-drift water chemistry evolution presented in this report. The analyses presented in this report use current design information (Sections 4.1 and 6.4), and are based on physical phenomena expected within repository drifts (Section 6.2). Coupled processes that are not addressed in this report are considered, and their rational for exclusion presented, in the *Engineered Barrier System Features, Events, And Processes* report (BSC 2003 [DIRS 166464]). Efforts have been made to ensure that the assumptions (Section 5) contained in this report are consistent with similar assumptions in related documents. These factors are included in the analyses leading to the output parameters (Section 6.13), which may be used to assess engineered barrier and waste form degradation.

(2) The abstraction of the quantity and chemistry of water contacting engineered barriers and waste forms uses assumptions, technical bases, data, and models, that are appropriate and consistent with other related U.S. Department of Energy abstractions. For example, the assumptions used for the quantity and chemistry of water contacting engineered barriers and waste forms are consistent with the abstractions of "Degradation of Engineered Barriers" (Section 2.2.1.3.1); "Mechanical Disruption of Engineered Barriers" (Section 2.2.1.3.2); "Radionuclide Release Rates and Solubility Limits" (Section 2.2.1.3.4); "Climate and Infiltration" (Section 2.2.1.3.5); and "Flow Paths in the Unsaturated Zone" (Section 2.2.1.3.6). The descriptions and technical bases provide transparent and traceable support for the abstraction of quantity and chemistry of water contacting engineered barriers and waste forms;

This report uses the same technical bases and other information as are used in other LA supporting documents concerned with engineered barrier and waste form performance. The conceptual model that forms the basis for this report (see Section 6.2) and its assumptions (see Section 5) are consistent with other engineered system models and repository design. Primary input (see Section 4.1) is taken from the UZ THC model to develop both the in-drift water and gas chemistry. The IDPS model is used in conjunction with the THC model output to generate in-drift water chemistry. Section 6.2 provides details of these model interfaces. The P&CE model does not consider input water fluxes, which are dealt with in *Seepage Model for PA Including Drift Collapse* (BSC 2003 [DIRS 163226]).

(3) Important design features, such as waste package design and material selection, backfill, drip shield, ground support, thermal loading strategy, and degradation processes, are adequate to determine the initial and boundary conditions for calculations of the quantity and chemistry of water contacting engineered barriers and waste forms;

Initial and boundary conditions for this model are based on descriptions of design features (see Section 6.4) and predicted behavior of the engineered barrier system (see Section 6.2) as documented in Project design documents and in other barrier-specific models and abstractions. This model includes consideration of the chemical effects of corrosion on engineered materials (see Sections 6.7 and 6.8).

(4) Spatial and temporal abstractions appropriately address physical couplings (thermal-hydrologic-mechanical-chemical). For example, the U.S. Department of Energy evaluates the potential for focusing of water flow into drifts, caused by coupled thermal-hydrologic-mechanical-chemical processes;

The abstractions in the P&CE model incorporate the effects of a number of different coupled processes in its evaluation of in-drift water chemistry. For example, thermal-hydrological-chemical effects are included implicitly through the THC model output as well as through the abstraction methodology. Another example is the analysis addressing the impact of corrosion of ground support materials impact. This analysis takes into account various thermal-hydrological-mechanical-chemical effects, as do the corrosion rates used in the analysis. Coupled processes formally classified as FEPs are discussed briefly in Section 6.14 and documented in more detail in various FEPs reports such as the *Engineered Barrier System Features, Events, And Processes* report (BSC 2003 [DIRS 166464]). These reports contain straightforward screening arguments if the FEP is excluded from further consideration and a description of the TSPA disposition if it is included.

(5) Sufficient technical bases and justification are provided for total system performance assessment assumptions and approximations for modeling coupled thermal-hydrological-mechanical-chemical effects on seepage and flow, the waste package chemical environment, and the chemical environment for radionuclide release. The effects of distribution of flow on the amount of water contacting the engineered barriers and waste forms are consistently addressed, in all relevant abstractions;

Assumptions (Section 5) and approximations pertaining to coupled processes in the P&CE model as well as the associated technical bases and justification are provided throughout the report. FEPs involving coupled processes are discussed with their technical bases in Section 6.14. This model report is not concerned with distribution of flow within the drift. However, the seepage abstraction is consistent with the THC seepage model and the look-up tables are designed to couple the thermal hydrology of the drift with the chemical environment in drift.

(6) The expected ranges of environmental conditions within the waste package emplacement drifts, inside of breached waste packages, and contacting the

waste forms and their evolution with time are identified. These ranges may be developed to include:

(i) the effects of the drip shield and backfill on the quantity and chemistry of water (e.g., the potential for condensate formation and dripping from the underside of the shield);

(ii) conditions that promote corrosion of engineered barriers and degradation of waste forms;

(iii) irregular wet and dry cycles;

(iv) gamma-radiolysis; and

(v) size and distribution of penetrations of engineered barriers;

This report develops and presents the expected ranges of environmental conditions within the drifts (Section 6.7, 6.9 and 6.10). This model does not consider the effect of the drip shield or backfill (current design does not include backfill) on the quantity and chemistry of water, but it does characterize conditions that affect corrosion of engineered barriers (see Section 6.13). Wet and dry cycles, gamma radiolysis, and size and distribution of engineered barriers are not the subject of this report, although information from it may be used to assess those factors.

(7) The model abstraction for quantity and chemistry of water contacting engineered barriers and waste forms is consistent with the detailed information on engineered barrier design and other engineered features. For example, consistency is demonstrated for:

(i) dimensionality of the abstractions;

(ii) various design features and site characteristics; and

(iii) alternative conceptual approaches.

Analyses are adequate to demonstrate that no deleterious effects are caused by design or site features that the U.S. Department of Energy does not take into account in this abstraction;

This report does not address dimensionality of the abstractions as they relate to water contacting engineered barriers. The chemistry of water contacting engineered barriers was developed using detailed information on various designed (engineered) features and site characteristics (see Section 4.1). This report includes consideration of potential impacts of design features such as ground support degradation on in-drift water composition (see Section 6.8). In addition, treatment of alternative conceptual approaches (e.g., Section 6.11) is consistent with engineered barrier design and other engineered features. For those design or site features not incorporated in the P&CE model, analyses were done to ensure that there were no adverse impacts caused by their exclusion (see Section 6.14 as well as the relevant FEPs report for further details).

(12) Guidance in NUREG–1297 (Altman et al. 1988 [DIRS 103597]) and NUREG–1298 (Altman et al. 1988 [DIRS 103750]), or other acceptable approaches, is followed.

Inputs were selected and documented according to applicable BSC procedures, which comply with NUREG-1297 and 1298 (see Section 4.1).

8.4.2.2 Acceptance Criterion 2–Data are Sufficient for Model Justification

(1) Geological, hydrological, and geochemical values used in the license application are adequately justified. Adequate description of how the data were used, interpreted, and appropriately synthesized into the parameters is provided;

The selection justification of geological, hydrological, and geochemical values for use and sources of input data are contained in Section 4.1 and tabulated in the DIRS. Further details of model development as relates to the use, interpretation, and synthesis of founding data into parameters are presented throughout Section 6, especially in Section 6.6. The model was developed using water chemistry and dust data collected in the ESF and adjoining facilities. The geochemical analyses presented in this report are based on a chemical thermodynamic database developed for this use from internationally accepted thermodynamic data (see Sections 6.2 and Section 6.5).

(2) Sufficient data were collected on the characteristics of the natural system and engineered materials to establish initial and boundary conditions for conceptual models of thermal-hydrological-mechanical-chemical coupled processes, that affect seepage and flow and the engineered barrier chemical environment;

Data and technical information collected from field and experimental sources, and from literature searches for this model are discussed for engineered materials in Section 4.1 (engineered components) and Section 6.4 (design features) and for natural system characteristics in Section 6.5 (mineralogical information) and in Section 6.6 (THC model). Natural system data are used to develop the THC model, which is a major input to this model (see Section 6.6). The natural system data are used to establish initial and boundary conditions that affect seepage and flow and are discussed in Section 6.6. The discussion of the initial and boundary conditions that affect seepage and flow for the engineered material data is discussed in Section 6.8. The affects on the chemical environment in the waste package from collected data are discussed in the *In-Package Chemistry Abstraction* (BSC 2003 [DIRS 161962]).

8.4.2.3 Acceptance Criterion 3–Data Uncertainty Is Characterized and Propagated Through the Model Abstraction

(1) Models use parameter values, assumed ranges, probability distributions, and bounding assumptions that are technically defensible, reasonably account for uncertainties and variabilities, and do not result in an under-representation of the risk estimate;

The model parameter values were selected based on the characteristics of the input and are considered representative of the natural and engineered systems (see Sections 4.1, 6.4, 6.5, 6.6, and 6.10). Ranges, probability distributions, and bounding assumptions were considered in assessing boundary conditions and input uncertainties and variabilities, which were propagated through the model as described in Section 6.12. Further propagation through TSPA-LA implementation is described in Section 6.15. When modeling decisions were necessary, the choices were made to result in conservative outcomes that avoid dilution of overall risk (as in Sections 6.9, 6.10 and 6.12).

(2) Parameter values, assumed ranges, probability distributions, and bounding assumptions used in the total system performance assessment calculations of quantity and chemistry of water contacting engineered barriers and waste forms are technically defensible and reasonable, based on data from the Yucca Mountain region (e.g., results from large block and drift-scale heater and niche tests), and a combination of techniques that may include laboratory experiments, field measurements, natural analog research, and process-level modeling studies;

The parameter values, assumed ranges, probability distributions, and bounding assumptions developed by other models based on site-specific data are discussed in Sections 6.6 and 6.11. Values, ranges, and distributions obtained from other techniques mentioned above include such information as the thermodynamic databases, discussed in Section 4.1.4 with additional discussion in Data Qualification: *Update and Revision of the Geochemical Thermodynamic Database, Data0.ymp* (Steinborn et al. 2003 [DIRS 161956]) and *In-Drift Precipitates/Salts Model* (BSC 2003 [DIRS 162529]); corrosion data, discussed in Sections 6.4 and 6.8; and mineralogy data discussed in Attachment IV. Much of the data founding model development was collected in the ESF and adjoining facilities. This included seepage water samples and dust samples. Environmental conditions imposed on model development (temperatures, RH, and moisture contents) were consistent with data collected from the Drift-Scale test and other related tests. The validation for the THC seepage abstraction has been performed against results from the THC seepage model, which was validated against data from the Drift Scale Test. Other laboratory and natural analog information was used for validation of portions of the model (see Section 7).

(3) Input values used in the total system performance assessment calculations of quantity and chemistry of water contacting engineered barriers (e.g., drip shield and waste package) are consistent with the initial and boundary conditions and the assumptions of the conceptual models and design concepts for the Yucca Mountain site. Correlations between input values are appropriately established in the U.S. Department of Energy total system performance assessment. Parameters used to define initial conditions, boundary conditions, and computational domain in sensitivity analyses involving coupled thermal-hydrological-mechanical-chemical effects on seepage and flow, the waste package chemical environment, and the chemical environment for radionuclide release, are consistent with available data. Reasonable or conservative ranges of parameters or functional relations are established;

The input values (Section 4.1) were developed using initial and boundary conditions and assumptions (Section 5) common to other conceptual models and compatible with design concepts. Sensitivity studies involving coupled effects on the chemical environment were conducted (e.g., Section 6.12). The initial and boundary conditions and computational domain for these sensitivity analyses were determined using parameters that are consistent with available data. This report uses the same technical bases and other information as are used in other LA supporting documents concerned with engineered barrier and waste form performance. The conceptual model that forms the basis for this report is consistent with other engineered system models and repository design. Primary input is taken from the UZ THC model and uses the IDPS model to generate in-drift water chemistry. Sections 6.2 and 6.6 provide details of these model interfaces.

Correlations between input values were established and used at various points in the P&CE model (e.g., Section 6.6, 6.7, and 6.13). For example, the input water and gas chemistries through time are correlated to each other, to temperature, and to relative humidity. The ranges of parameters and functional relations developed in this report, primarily as look-up tables (Section 6.13), are considered reasonable or conservative. Section 6.15 discusses the appropriate use of these tables, which are response surfaces that relate water chemistry to relative humidity, temperature, Pco_2 and time.

(4) Adequate representation of uncertainties in the characteristics of the natural system and engineered materials is provided in parameter development for conceptual models, process-level models, and alternative conceptual models. The U.S. Department of Energy may constrain these uncertainties using sensitivity analyses or conservative limits. For example, the U.S. Department of Energy demonstrates how parameters used to describe flow through the engineered barrier system bound the effects of backfill and excavation-induced changes;

Uncertainties in natural system characteristics are included in the THC model output, which is used as direct input to this model. Uncertainties in the Pitzer (natural system) and the data0.ymp.R2 (engineered systems) thermodynamic databases used as direct input to this model are discussed in Section 6.12, with additional mineralogy discussion in Attachment IV. Engineered materials uncertainties are specifically considered in Section 6.12, with further extensive discussions on the effects of dust in Section 6.10 and the effects of microbiology in Section 6.11. Those uncertainties are evaluated using sensitivity analyses as discussed in Section 4.1.8 and 6.12. Section 6.12 discusses five key uncertainties including both engineered materials and natural systems parameters.

8.4.2.4 Acceptance Criterion 4–Model Uncertainty Is Characterized and Propagated Through the Model Abstraction

(1) Alternative modeling approaches of features, events, and processes are considered and are consistent with available data and current scientific understanding, and the results and limitations are appropriately considered in the abstraction;

The evaluation of FEPs documented in Section 6.14 is based on the model results developed in this report, including the alternative modeling discussed in Section 6.11. This alternative modeling is consistent with available data and scientific understanding. The results and limitations of the alternative FEP modeling and their impact on the engineered barrier chemical environment are presented in Section 6.14.

(2) Alternative modeling approaches are considered and the selected modeling approach is consistent with available data and current scientific understanding. A description that includes a discussion of alternative modeling approaches not considered in the final analysis and the limitations and uncertainties of the chosen model is provided;

Section 6.11 describes several alternative modeling approaches considered for various P&CE submodels. None of these alternative models were selected for further use. For all but one of them, brief descriptions and the rationale for exclusion are included as well as references to other reports and/or sections within this report for further detail. These references also contain information about the models that were selected including their technical bases, limitations and uncertainties. Section 6.11 also provides an investigation of a single model involving an alternative method for clustering waters during the abstraction of THC seepage waters. The exclusion rationale is based upon a comparison of results from the alternative model with those from the selected approach (Section 6.6). The selected approach is consistent with available data and current scientific understanding. The uncertainties and limitations of various selected approaches are discussed throughout the report, e.g., Sections 1.3, 6.6, 6.12, and 8.3.

(3) Consideration of conceptual model uncertainty is consistent with available site characterization data, laboratory experiments, field measurements, natural analog information and process-level modeling studies; and the treatment of conceptual model uncertainty does not result in an under-representation of the risk estimate;

Uncertainties in inputs and in analytical methodology are considered in the development of the conceptual model (see Section 6.2) and output parameters (see Section 6.15). Discussion of uncertainty in the conceptual model appears in various places throughout the report. One example is Section 6.12.1, where quotations from Section 6.9.2 of The *Drift-Scale Coupled Processes (DST and THC Seepage) Models*, (BSC 2003 [DIRS 162050]) discuss the uncertainty of model conceptualizations involving the THC abstraction. The uncertainty evaluation is consistent with available site-specific data, laboratory experiments, field studies, natural analog data and process-level modeling studies. In addition, model validation is based on available site characterization data, laboratory experiments and natural analogues (see Section 7). The treatment of conceptual model uncertainty described in this report does not under-represent risk.

(4) Adequate consideration is given to effects of thermal-hydrological-mechanical-chemical coupled processes in the assessment of alternative conceptual models. These effects may include:

(i) thermal-hydrologic effects on gas, water, and mineral chemistry;

(ii) effects of microbial processes on the engineered barrier chemical environment and the chemical environment for radionuclide release;

(iii) changes in water chemistry that may result from the release of corrosion products from the waste package and interactions between engineered materials and ground water; and

(iv) changes in boundary conditions (e.g., drift shape and size) and hydrologic properties, relating to the response of the geomechanical system to thermal loading;

The effects of coupled processes were considered during the assessment of alternative conceptual models (Section 6.11). The descriptions in Section 6.11 are brief because the primary evaluation of most of these alternative models (e.g., effects of microbial processes on the in-drift chemical environment) was outside the scope of this report. References are provided to the other pertinent reports. However, Section 6.11 does provide details on an investigation of an alternative method for clustering waters during the abstraction of THC seepage waters. This alternative method does incorporate coupled thermal-hydrological-chemical processes.

8.4.2.5 Acceptance Criterion 5–Model Abstraction Output is Supported by Objective Comparisons

(1) The models implemented in this total system performance assessment abstraction provide results consistent with output from detailed process-level models and/or empirical observations (laboratory and field testings and/or natural analogs);

Information provided to the TSPA-LA was developed using detailed process-level models (see Section 6.2). The resulting abstracted model output provided for implementation in the TSPA-LA is consistent with the related process-level model output (Section 7). For appropriate cases, validation against empirical observation is also provided (see Section 7).

(2) Abstracted models for coupled thermal-hydrological-mechanical-chemical effects on seepage and flow and the engineered barrier chemical environment, as well as on the chemical environment for radionuclide release, are based on the same assumptions and approximations demonstrated to be appropriate for process-level models or closely analogous natural or experimental systems. For example, abstractions of processes, such as thermally induced changes in hydrological properties, or estimated diversion of percolation away from the drifts, are adequately justified by comparison to results of process-level modeling, that are consistent with direct observations and field studies; and

The abstracted model is based on the same assumptions and approximations demonstrated to be appropriate for process-level models. Coupled thermal-hydrological-chemical considerations are the dominant factor in the development of this model abstraction. The output of this model is a tabulation of chemical conditions as a function of physical environmental conditions that is

consistent with process-level modeling as demonstrated by model validation results (Section 7), which are in turn consistent with direct observations from laboratory and field studies.

(3) Accepted and well-documented procedures are used to construct and test the numerical models that simulate coupled thermal-hydrological-mechanical-chemical effects on seepage and flow, engineered barrier chemical environment, and the chemical environment for radionuclide release. Analytical and numerical models are appropriately supported. Abstracted model results are compared with different mathematical models, to judge robustness of results.

Accepted and well-documented procedures contained in the quality assurance program (see Section 2) governed the development of this report and the work it documents. The PC&E model was constructed, supported, and documented according to AP-SIII.10Q. Test and validation methods (Section 7), including comparison of abstracted output with that of other relevant models, also comply with AP-SIII.10Q as well as with applicable written guidance. This report was generated according to the requirements of the *Technical Work Plan For: In-Drift Geochemical Modeling* (BSC 2004 [DIRS 166519]) as directed by AP-2.27Q.

9. INPUTS AND REFERENCES

9.1 DOCUMENTS CITED

100033 Flint, L.E. 1998. *Characterization of Hydrogeologic Units Using Matrix Properties, Yucca Mountain, Nevada*. Water-Resources Investigations Report 97-4243. Denver, Colorado: U.S. Geological Survey. ACC: MOL.19980429.0512.

100051 Langmuir, D. 1997. *Aqueous Environmental Geochemistry*. Upper Saddle River, New Jersey: Prentice Hall. TIC: 237107.

100097 Wolery, T.J. and Daveler, S.A. 1992. EQ6, A *Computer Program for Reaction Path Modeling of Aqueous Geochemical Systems: Theoretical Manual, User's Guide, and Related Documentation (Version 7.0).* UCRL-MA-110662 PT IV. Livermore, California: Lawrence Livermore National Laboratory. ACC: MOL.19980701.0459.

100743 Eugster, H.P. and Hardie, L.A. 1978. "Saline Lakes." *Lakes, Chemistry, Geology,* Physics. Lerman, A., ed. Pages 237-293. New York, New York: Springer-Verlag. TIC: 240782.

100829 Stumm, W. and Morgan, J.J. 1981. *Aquatic Chemistry, An Introduction Emphasizing Chemical Equilibria in Natural Waters*. 2nd Edition. New York, New York: John Wiley & Sons. TIC: 208448.

100836 Wolery, T.J. 1992. EQ3NR, *A Computer Program for Geochemical Aqueous Speciation-Solubility Calculations: Theoretical Manual, User's Guide, and Related Documentation (Version 7.0).* UCRL-MA-110662 PT III. Livermore, California: Lawrence Livermore National Laboratory. ACC: MOL.19980717.0626.

100883 Brasher, D.M. and Mercer, A.D. 1968. "Comparative Study of Factors Influencing the Action of Corrosion Inhibitors for Mild Steel in Neutral Solution, I. Sodium Benzoate." *British Corrosion Journal, 3,* 120-129. London, England: British Joint Corrosion Group. TIC: 236434.

100895 Guttman, H. and Sereda, P.J. 1968. " Measurement of Atmospheric Factors Affecting the Corrosion of Metals." *Metal Corrosion in the Atmosphere, A Symposium Presented at the Seventieth Annual Meeting, Boston, Massachusetts, June 25-30, 1967*. ASTM Special Technical Publication 435. 326-359. Philadelphia, Pennsylvania: American Society for Testing and Materials. TIC: 239410.

100899 Haynie, F.H. and Upham, J.B. 1971. "Effects of Atmospheric Pollutants on Corrosion Behavior of Steels." *Materials Protection and Performance, 10,* (11), 18-21. Houston, Texas: National Association of Corrosion Engineers. TIC: 236590.

100900 Haynie, F. H. and Upham, J. B. 1974. "Correlation Between Corrosion Behavior of Steel and Atmospheric Pollution Data." *Corrosion in Natural Environments, Three Symposia Presented at the 76th Annual Meeting, Philadelphia, Pennsylvania, June 24-29, 1973.* ASTM STP 558. Pages 33-51. Philadelphia, Pennsylvania: American Society for Testing and Materials. TIC: 223374.

100908 Komp, M.E. 1987. "Atmospheric Corrosion Ratings of Weathering Steels-Calculation and Significance." *Materials Performance, 26,* (7), 42-44. Houston, Texas: National Association of Corrosion Engineers. TIC: 236725.

100927 Southwell, C.R.; Bultman, J.D.; and Alexander, A.L. 1976. "Corrosion of Metals in Tropical Environments - Final Report of 16-Year Exposures." *Materials Performance, 15,* (7), 9-25. Houston, Texas: National Association of Corrosion Engineers. TIC: 224022.

100928 Southwell, C.R. and Bultman, J.D. 1982. "Atmospheric Corrosion Testing in the Tropics." Chapter 64 of *Atmospheric* Corrosion. The Corrosion Monograph Series. Ailor, W.H., ed. New York, New York: John Wiley and Sons. TIC: 240907.

100937 Townsend, H.E. and Zoccola, J.C. 1982. "Eight-Year Atmospheric Corrosion Performance of Weathering Steel in Industrial, Rural, and Marine Environments." *Atmospheric Corrosion of Metals, A Symposium on Corrosion of Metals, Denver, Colorado, 19-20 May 1980.* Dean, S.W., Jr., and Rhea, E.C., eds. ASTM Special Technical Publication 767. Pages 45-59. Philadelphia, Pennsylvania: American Society for Testing and Materials. TIC: 243129.

100945 Wei, F.I. 1991. "Atmospheric Corrosion of Carbon Steels and Weathering Steels in Taiwan." *British Corrosion Journal, 26,* (3), 209-214. London, England: Metals Society. TIC: 212462.

100948 Van Konynenburg, R.A.; Curtis, P.G.; and Summers, T.S.E. 1998. *Scoping Corrosion Tests on Candidate Waste Package Basket Materials for the Yucca Mountain Project*. UCRL-ID-130386. Livermore, California: Lawrence Livermore National Laboratory. ACC: MOL.19980727.0385.

101941 USN (U.S. Department of the Navy) 1996. *Department of the Navy Final Environmental Impact Statement for a Container System for the Management of Naval Spent Nuclear Fuel*. DOE/EIS-0251. Washington, D.C.: U.S. Department of Energy. ACC: MOL.20010724.0299.

102010 Jury, W.A.; Gardner, W.R.; and Gardner, W.H. 1991. Soil Physics. 5th Edition. New York, New York: John Wiley & Sons. TIC: 241000.

102865 Weast, R.C. and Astle, M.J., eds. 1979. CRC Handbook of Chemistry and Physics. 60th Edition. 2nd Printing 1980. Boca Raton, Florida: CRC Press. TIC: 245312.

103441 Smith, R.J.; Loomis, G.W.; and Deltete, C. P. 1992. *Borated Stainless Steel Application in Spent-Fuel Storage Racks.* TR-100784. Palo Alto, California: Electric Power Research Institute. TIC: 225730.

103597 Altman, W.D.; Donnelly, J.P.; and Kennedy, J.E. 1988. *Peer Review for High-Level Nuclear Waste Repositories: Generic Technical Position.* NUREG-1297. Washington, D.C.: U.S. Nuclear Regulatory Commission. TIC: 200651.

103750 Altman, W.D.; Donnelly, J.P.; and Kennedy, J.E. 1988. *Qualification of Existing Data for High-Level Nuclear Waste Repositories: Generic Technical Position.* NUREG-1298. Washington, D.C.: U.S. Nuclear Regulatory Commission. TIC: 200652.

103896 Parrington, J.R.; Knox, H.D.; Breneman, S.L.; Baum, E.M.; and Feiner, F. 1996. *Nuclides and Isotopes, Chart of the Nuclides*. 15th Edition. San Jose, California: General Electric Company and KAPL, Inc. TIC: 233705.

104945 Greenspan, L. 1977. "Humidity Fixed Points of Binary Saturated Aqueous Solutions." *Journal of Research of the National Bureau of Standards, 81A*, (1), 89-96. Washington, D.C.: U.S. Department of Commerce. TIC: 241138.

105092 Brookins, D.G. 1988. *Eh-pH Diagrams for Geochemistry*. New York, New York: Springer-Verlag. TIC: 237943.

105213 Carlos, B.A.; Chipera, S.J.; Bish, D.L.; and Raymond, R. 1995. "Distribution and Chemistry of Fracture-Lining Zeolites at Yucca Mountain, Nevada." *Natural Zeolites '93: Occurrence, Properties, Use, Proceedings of the 4th International Conference on the Occurrence, Properties, and Utilization of Natural Zeolites, June 20-28, 1993,* Boise, Idaho. Ming, D.W. and Mumpton, F.A., eds. Pages 547-563. Brockport, New York: International Committee on Natural Zeolites. TIC: 243086.

105701 Amonette, J.E. and Rai, D. 1990. "Identification of Noncrystalline (Fe,Cr)(OH)3 by Infrared Spectroscopy." *Clays and Clay Minerals*, 38, (2), 129-136. Boulder, Colorado: Clay Minerals Society. TIC: 243615.

105730 Baron, D. and Palmer, C.D. 1996. "Solubility of KFe3(CrO4)2(OH)6 at 4 to 35[degrees]C." *Geochimica et Cosmochimica Acta*, 60, (20), 3815-3824. New York, New York: Elsevier. TIC: 243731.

105732 Cotton, F.A. and Wilkinson, G. 1988. *Advanced Inorganic Chemistry*. 5th Edition. New York, New York: John Wiley & Sons. TIC: 236867.

105778 Deng, Y.; Stjernstrom, M.; and Banwart S. 1996. "Accumulation and Remobilization of Aqueous Chromium (VI) at Iron Oxide Surfaces: Application of a Thin-film Continuous Flow-through Reactor." *Journal of Contaminant Hydrology, 21*, 141-151. Amsterdam, The Netherlands: Elsevier. TIC: 243062.

105780 Eary, L.E. and Rai, D. 1987. "Kinetics of Chromium(III) Oxidation to Chromium(VI) by Reaction with Manganese Dioxide." Environmental Science & Technology, 21, (12), 1187-1193. Washington, D.C.: American Chemical Society. TIC: 243224.

105784 Eary, L.E. and Rai, D. 1988. "Chromate Removal from Aqueous Wastes by Reduction with Ferrous Ion." *Environmental Science & Technology, 22*, (8), 972-977. Washington, D.C.: American Chemical Society. TIC: 243600.

105788 Eary, L.E. and Rai, D. 1989. "Kinetics of Chromate Reduction by Ferrous Ions Derived from Hematite and Biotite at 25C." *American Journal of Science, 289*, 180-213. New Haven, Connecticut: Yale University. TIC: 243614.

105795 Fitzpatrick, R.W.; Le Roux, J.; and Schwertmann, U. 1978. "Amorphous and Crystalline Titanium and Iron-Titanium Oxides in Synthetic Preparations, at Near Ambient Conditions, and in Soil Clays." *Clays and Clay Minerals, 26*, (3), 189-201. Boulder, Colorado: Clay Minerals Society. TIC: 242847.

105854 Hem, J.D.; Lind, C.J.; and Roberson, C.E. 1989. "Coprecipitation and Redox Reactions of Manganese Oxides with Copper and Nickel." *Geochimica et Cosmochimica Acta, 53*, 2811-2822. New York, New York: Pergamon Press. TIC: 243113.

105878 Johnson, C.A. and Xyla, A.G. 1991. "The Oxidation of Chromium (III) to Chromium (VI) on the Surface of Manganite (MnOOH*)." Geochimica et Cosmochimica Acta, 55*, 2861-2866. New York, New York: Pergamon Press. TIC: 243616.

105907 Klein, C. and Hurlbut, C.S., Jr. 1985. *Manual of Mineralogy*. 20th Edition. New York, New York: John Wiley & Sons. TIC: 242818.

105909 Krauskopf, K.B. 1979. Introduction to Geochemistry. 2nd Edition. New York, New York: McGraw-Hill. TIC: 242816.

105952 Pankow, J.F. 1991. Aquatic Chemistry Concepts. Chelsea, Michigan: Lewis Publishers. TIC: 242999.

105955 Pettine, M.; D'Ottone, L.; Campanella, L.; Millero, F.J.; and Passino, R. 1998. "The Reduction of Chromium(VI) by Iron(II) in Aqueous Solutions." *Geochimica et Cosmochimica Acta, 62*, (9), 1509-1519. New York, New York: Pergamon Press. TIC: 243059.

105957 Sass, B.R. and Rai, D. 1987. "Solubility of Amorphous Chromium(III)-Iron(III) Hydroxide Solid Solutions." Inorganic Chemistry, 26, (13), 2228-2232. Washington, D.C.: American Chemical Society. TIC: 243717.

105959 Schwertmann, U. and Taylor, R.M. 1995. "Iron Oxides." Chapter 8 of *Minerals in Soil Environments.* 2nd Edition. Dixon, J.B. and Weed, S.B., eds. SSSA Book Series, No. 1. Madison, Wisconsin: Soil Science Society of America. TIC: 237222.

105960 Tebo, B.M.; Ghiorse, W.C.; van Wassbergen, L.G.; Siering, P.L.; and Caspi, R. 1997. "Bacterially Mediated Mineral Formation: Insights into Manganese(II) Oxidation from Molecular Genetic and Biochemical Studies." Chapter 7 of *Geomicrobiology: Interactions Between Microbes and Minerals.* Banfield, J.F. and Nealson, K.H., eds. Reviews in Mineralogy, Volume 35. Washington, D.C.: Mineralogical Society of America. TIC: 236757.

105963 Zachara, J.M.; Girvin, D.C.; Schmidt, R.L.; and Resch, C.T. 1987. "Chromate Adsorption on Amorphous Iron Oxyhydroxide in the Presence of Major Groundwater Ions." *Environmental Science & Technology, 21*, (6), 589-594. Easton, Pennsylvania: American Chemical Society. TIC: 243613.

105964 Sedlak, D.L. and Chan, P.G. 1997. "Reduction of Hexavalent Chromium by Ferrous Iron." *Geochimica et Cosmochimica Acta, 61*, (11), 2185-2192. New York, New York: Elsevier. TIC: 243064.

105965 Hay, R.L. 1966. *Zeolites and Zeolitic Reactions in Sedimentary Rocks*. Special Paper 85. Boulder, Colorado: Geological Society of America. TIC: 238294.

106170 Weast, R.C., ed. 1984. *CRC Handbook of Chemistry and Physics*. 65th Edition. Boca Raton, Florida: CRC Press. TIC: 206666.

107060 Rai, D. and Zachara, J.M. 1984. *A Critical Review*. Volume 1 of *Chemical Attenuation Rates, Coefficients, and Constants in Leachate Migration*. EPRI EA-3356. Palo Alto, California: Electric Power Research Institute. TIC: 237846.

107066 Vaniman, D.T.; Ebinger, M.H.; Bish, D.L.; and Chipera, S. 1992. "Precipitation of Calcite, Dolomite, Sepiolite, and Silica from Evaporated Carbonate and Tuffaceous Waters of Southern Nevada, USA." *Proceedings of the 7th International Symposium on Water-Rock Interaction, Park City, Utah, July 13-18, 1992*. Kharaka, Y.K. and Maest, A., eds. 1, 687-691. Brookfield, Vermont: A.A. Balkema. TIC: 208527.

107105 Roberts, W.L.; Campbell, T.J.; and Rapp, G.R., Jr. 1990. *Encyclopedia of Minerals*. 2nd Edition. New York, New York: Van Nostrand Reinhold. TIC: 242976.

107760 Kügler, A. 1996. *Böhler Neutronit A976 Sheet and Plate for Nuclear Engineering*. Murzzuschlag, Austria: Böhler Bleche GmbH. TIC: 240558.

108954 McLean, J.E. and Bledsoe, B.E. 1992. *Behavior of Metals in Soils*. EPA/540/S-92/018. Washington, D.C.: U.S. Environmental Protection Agency. TIC: 243412.

108991 Palmer, C.D. and Puls, R.W. 1994. *Natural Attenuation of Hexavalent Chromium in Ground Water and Soils.* EPA/540/S-94/505. Washington, D.C.: U.S. Environmental Protection Agency. TIC: 243413.

110969 Bruno, J.; Duro, L.; de Pablo, J.; Casas, I.; Ayora, C.; Delgado, J.; Gimeno, M.J.; Peña, J.; Linklater, C.; Pérez del Villar, L.; and Gómez, P. 1998. "Estimation of the Concentrations of Trace Metals in Natural Systems. The Application of Codissolution and Coprecipitation Approaches to El Berrocal (Spain) and Poços de Caldas (Brazil)." *Chemical Geology, 151,* 277 291. Amsterdam, The Netherlands: Elsevier. TIC: 246492

112147 Schutz, R.W. and Thomas, D.E. 1987. "Corrosion of Titanium and Titanium Alloys." In Corrosion, Volume 13, Pages 669-706 of *ASM Handbook*. Formerly 9th Edition, Metals Handbook. Materials Park, Ohio: ASM International. TIC: 240704.

114637 McCright, R.D. 1998. *Corrosion Data and Modeling, Update for Viability Assessment.* Volume 3 of *Engineered Materials Characterization Report.* UCRL-ID-119564, Rev. 1.1. Livermore, California: Lawrence Livermore National Laboratory. ACC: MOL.19980806.0177.

115670 Hem, J.D. 1985. *Study and Interpretation of the Chemical Characteristics of Natural Water*. 3rd Edition. Geological Survey Water-Supply Paper 2254. Washington, D.C.: U.S. Government Printing Office. ACC: NNA.19940427.0181.

118564 Drever, J.I. 1988. The *Geochemistry of Natural Waters*. 2nd Edition. Englewood Cliffs, New Jersey: Prentice-Hall. TIC: 242836.

119530 Pitzer, K.S. 1979. "Theory: Ion Interaction Approach." Volume 1, Chapter 7 of *Activity Coefficients in Electrolyte Solutions.* Pytkowicz, R.M., ed. Boca Raton, Florida: CRC Press. TIC: 239527.

123636 Garrels, R.M. and Mackenzie, F.T. 1967. "Origin of the Chemical Compositions of Some Springs and Lakes?" *Equilibrium Concepts in Natural Water Systems*. American Chemical Society Advances in Chemistry Series 67. Pages 222-242. Washington, D.C.: American Chemical Society. TIC: 246519.

123916 CRWMS M&O 2000. *Abstraction of Drift-Scale Coupled Processes*. ANL-NBS-HS-000029 REV 00. Las Vegas, Nevada: CRWMS M&O. ACC: MOL.20000525.0371.

125329 Koorevaar, P.; Menelik, G.; and Dirksen, C. 1983. *Elements of Soil Physics*. Developments in Soil Science 13. New York, New York: Elsevier. TIC: 246286.

125338 Rosenberg, N.D.; Knauss, K.G.; and Dibley, M.J. 1999. *Evaporation of J13* Water: *Laboratory Experiments and Geochemical Modeling*. UCRL-ID-134852. Livermore, California: Lawrence Livermore National Laboratory. TIC: 246322.

125339 Rosenberg, N.D.; Knauss, K.G.; and Dibley, M.J. 1999. *Evaporation of Topopah Spring Tuff Pore Water*. UCRL-ID-135765. Livermore, California: Lawrence Livermore National Laboratory. TIC: 246231.

127454 Walton, J.C. 1994. "Influence of Evaporation on Waste Package Environment and Radionuclide Release from a Tuff Repository." *Water Resources Research, 30*, (12), 3479-3487. Washington, D.C.: American Geophysical Union. TIC: 246921.

127953 Shock, E.L.; Sassani, D.C.; Willis, M.; and Sverjensky, D.A. 1997. "Inorganic Species in Geologic Fluids: Correlations Among Standard Molal Thermodynamic Properties of Aqueous Ions and Hydroxide Complexes." *Geochimica et Cosmochimica Acta, 61*, (5), 907-950. New York, New York: Pergamon Press. TIC: 246451.

137246 Helgeson, H.C. 1969. "Thermodynamics of Hydrothermal Systems at Elevated Temperatures and Pressures." *American Journal of Science, 267*, (6), 729-804. New Haven, Connecticut: Scholarly Publications. TIC: 241817.

142177 Parkhurst, D.L. 1995. *User's Guide to PHREEQC—A Computer Program for Speciation, Reaction-Path, Advective-Transport, and Inverse Geochemical Calculations*. Water-Resources Investigations Report 95-4227. Lakewood, Colorado: U.S. Geological Survey. TIC: 248314.

144877 Garrels, R.M. and Christ, C.L. 1990. *Solutions, Minerals, and Equilibria*. Boston, Massachusetts: Jones and Barlett Pulishers. TIC: 223483.

146460 CRWMS M&O 2000. *Environment on the Surfaces of the Drip Shield and Waste Package Outer Barrier*. ANL-EBS-MD-000001 REV 00. Las Vegas, Nevada: CRWMS M&O. ACC: MOL.20000328.0590.

150095 DOE 2000. *N Reactor (U-Metal) Fuel Characteristics for Disposal Criticality Analysis*. DOE/SNF/REP-056, Rev. 0. Washington, D.C.: U.S. Department of Energy, Office of Environmental Management. TIC: 247956.

151102 Covington, L.C. and Schutz, R.W. 1981. "Resistance of Titanium to Atmospheric Corrosion." *Corrosion/81, International Corrosion Forum, April 6-10, 1981, Toronto, Ontario,* Canada. Pages 113/1-113/7. Houston, Texas: National Association of Corrosion Engineers. TIC: 248534.

151162 Schutz, R.W. 1986. "Titanium." *Process Industries Corrosion.* Pages 503-527. Houston, Texas: National Association of Corrosion Engineers. TIC: 226189.

151392 Dellien, I.; Hall, F.M.; and Hepler, L.G. 1976. "Chromium, Molybdenum, and Tungsten: Thermodynamic Properties, Chemical Equilibria, and Standard Potentials." *Chemical Reviews, 76*, (3), 283-310. Washington, D.C.: American Chemical Society. TIC: 248458.

151561 CRWMS M&O 2000. In-Drift Microbial Communities. ANL-EBS-MD-000038 REV 00 ICN 01. Las Vegas, Nevada: CRWMS M&O. ACC: MOL.20001213.0066.

152738 Pitzer, K.S. 1973. "Thermodynamics of Electrolytes. I. Theoretical Basis and General Equations." *Journal of Physical Chemistry, 77,* (2), 268–277. Washington, D.C.: American Chemical Society. TIC: 239503.

152740 Pitzer, K.S. 1975. "Thermodynamics of Electrolytes. V. Effects of Higher-Order Electrostatic Terms." *Journal of Solution Chemistry*, 4, (3), 249–265. New York, New York: Plenum Publishing. TIC: 248997.

155318 Boyer, H.E. and Gall, T.L., eds. 1984. *Metals Handbook*. Desk Edition. 10th Printing 1997. Metals Park, Ohio: American Society for Metals. TIC: 250192.

156276 BSC 2001. *Repository Multiple Waste Package Thermal Calculation.* CAL-WIS-TH-000010 REV 00. Las Vegas, Nevada: Bechtel SAIC Company. ACC: MOL.20010814.0330.

156639 Borchardt, G. 1995. "Smectites." Chapter 14 of *Minerals in Soil Environments*. 2nd Edition. Dixon J.B. and Weed, S.B., eds. SSSA Book Series, No. 1. Madison, Wisconsin: Soil Science Society of America. TIC: 237222.

157860 Baes, C.F., Jr. and Mesmer, R.E. 1976. The Hydrolysis of Cations. Pages 1, 6, 7, 176, 177, 180, 181, 184-191. New York, New York: John Wiley & Sons. TIC: 217440.

158974 HydroGeoLogic and Allison Geoscience Consultants. 1999. *MINTEQA2/PRODEFA2, A Geochemical Assessment Model for Environmental Systems: User Manual Supplement for Version 4.0.* Athens, Georgia: U.S. Environmental Protection Agency, National Exposure Research Laboratory. TIC: 252456.

159034 Li, G.; Peacor, D.R.; Coombs, D.S.; and Kawachi, Y. 1997. "Solid Solution in the Celadonite Family: The New Minerals Ferroceladonite, $K_2Fe^2{}_2{+}Fe^3{}_2{+}Si_8O_{20}(OH)_4$, and Ferroaluminoceladonite, $K_2Fe^2{}_2{+}Al_2Si_8O_{20}(OH)_4$" *American Mineralogist, 82,* (5-6), 503-511. Washington, D.C.: Mineralogical Society of America. TIC: 252472.

159336 McCright, R.D.; Halsey, W.G.; and Van Konynenburg, R.A. 1987. *Progress Report on the Results of Testing Advanced Conceptual Design Metal Barrier Materials Under Relevant Environmental Conditions for a Tuff Repository.* UCID-21044. Livermore, California: Lawrence Livermore National Laboratory. ACC: HQX.19880201.0016.

159341 Beavers, J.A. and Durr, C.L. 1991. *Immersion Studies on Candidate Container Alloys for the Tuff Repository*. NUREG/CR-5598. Washington, D.C.: U.S. Nuclear Regulatory Commission. TIC: 209162.

159343 Forgeson, B.W.; Southwell, C.R.; Alexander, A.L.; Mundt, H.W.; and Thompson, L.J. 1958. "Corrosion of Metals in Tropical Environments, (Part 1—Five Non-Ferrous Metals and a Structural Steel)." *Corrosion, 14*, (2), 73t-81t. Houston, Texas: National Association of Corrosion Engineers. TIC: 223373.

159367 EPRI (Electric Power Research Institute) 1986. *Behavior of High-Density Spent-Fuel Storage Racks*. EPRI NP-4724. Palo Alto, California: Electric Power Research Institute. TIC: 252124.

159368 Butler, F.E. 1963. *Corrosion Studies on 304 Stainless Steel Containing One Percent Boron-10*. RFP-307. Washington, D.C.: U.S. Atomic Energy Commission. TIC: 252108.

159369 Cole, H.S. 1976. *Corrosion of Stainless Steel Type 304 Alloyed with Boron or Gadolinium by Plant Process Solutions Containing* HNO_3 and HF. ICP-1097. [Idaho Falls], Idaho: Idaho National Engineering Laboratory. TIC: 252106.

161235 BSC (Bechtel SAIC Company) 2003. *General Corrosion and Localized Corrosion of Waste Package Outer Barrier*. ANL-EBS-MD-000003 REV 01. Las Vegas, Nevada: Bechtel SAIC Company. ACC: DOC.20030916.0010.

161236 BSC 2003. *General Corrosion and Localized Corrosion of the Drip Shield*. ANL-EBS-MD-000004 REV 01. Las Vegas, Nevada: Bechtel SAIC Company. ACC: DOC.20030626.0001.

161317 BSC 2003. *WAPDEG Analysis of Waste Package and Drip Shield Degradation*. ANL-EBS-PA-000001 REV 01. Las Vegas, Nevada: Bechtel SAIC Company. ACC: DOC.20031208.0004.

161602 Smith, W.R. and Missen, R.W. 1991. *Chemical Reaction Equilibrium Analysis: Theory and Algorithms*. Malabar, Florida: Krieger Publishing Company. TIC: 252885.

161603 Van Zeggeren, F. and Storey, S.H. 1970. The *Computation of Chemical Equilibria*. New York, New York: Cambridge University Press. TIC: 252891.

161606 Kerr, P.F. 1977. *Optical Mineralogy*. 4th Edition. New York, New York: McGraw-Hill. TIC: 252886.

161620 BSC 2003. *Waste Form and In-Drift Colloids-Associated Radionuclide Concentrations: Abstraction and Summary*. MDL-EBS-PA-000004 REV 00. Las Vegas, Nevada: Bechtel SAIC Company. ACC: DOC.20030626.0006.

161752 DOE (U.S. Department of Energy) 2002. *SNF Canister Characteristics for Criticality Analysis of a Dual Canister/Waste Package Disposal Strategy*. DOE/SNF/REP-074, Rev. 0. Idaho Falls, Idaho: U.S. Department of Energy. TIC: 253869.

161804 Frye, K. 1981. *Encyclopedia of Mineralogy*. Encyclopedia of Earth Sciences, Volume 4B. Stroudsburg, Pennsylvania: Hutchinson Ross. TIC: 252977.

161956 Steinborn, T.L.; Wolery, T.J.; Alcorn, S.R.; Arthur, S.E.; Bernot, P.A.; Brady, P.V.; Chen, Y.; Domski, P.S.; Jolley, D.M.; Metcalf, R.C.; and Thomas, E. 2003. *Data Qualification: Update and Revision of the Geochemical Thermodynamic Database, Data0.ymp*. TDR-EBS-MD-000022 REV 00. Las Vegas, Nevada: Bechtel SAIC Company. ACC: DOC.20030331.0003.

161962 BSC 2003. *In-Package Chemistry Abstraction*. ANL-EBS-MD-000037 REV 02. Las Vegas, Nevada: Bechtel SAIC Company. ACC: DOC.20030723.0003.

162050 BSC 2003. *Drift-Scale Coupled Processes (DST and THC Seepage) Models*. MDL-NBS-HS-000001 REV 02. Las Vegas, Nevada: Bechtel SAIC Company. ACC: DOC.20030804.0004.

162069 Grønvold, F. and Meisingset, K.K. 1983. "Thermodynamic Properties and Phase Transitions of Salt Hydrates between 270 and 400 K. II. $Na_2CO_3 \cdot H_2O$ and $Na_2CO_3 \cdot 10H_2O$." *Journal of Chemical Thermodynamics, 15,* (9), 881-889. New York, New York: Academic Press. TIC: 253936.

162229 Lide, D.R., ed. 2000. *CRC Handbook of Chemistry and Physics*. 81st Edition. Boca Raton, Florida: CRC Press. TIC: 253056.

162265 Alexander, A.L.; Southwell, C.R.; and Forgeson, B.W. 1961. "Corrosion of Metals in Tropical Environments." Corrosion, 17, 97-104. Houston, Texas: National Association of Corrosion Engineers. TIC: 223352.

162266 Dutra, A.C. and Vianna, R.de O. 1982. "*Atmospheric Corrosion* Testing in Brazil." Chapter 53 of Atmospheric Corrosion. The Corrosion Monograph Series. Ailor, W.H., ed. New York, New York: John Wiley and Sons. TIC: 240907.

162270 Bethke, C.M. 1996. *Geochemical Reaction Modeling, Concepts and Applications*. New York, New York: Oxford University Press. TIC: 252884.

162274 Papke, K.G. 1976. *Evaporites and Brines in Nevada Playas*. Nevada Bureau of Mines and Geology Bulletin 87. Reno, Nevada: University of Nevada, Reno, Mackay School of Mines. TIC: 211869.

162280 Palache, C.; Berman, H.; and Frondel, C. 1951. *Halides, Nitrates, Borates, Carbonates, Sulfates, Phosphates, Arsenates, Tungstates, Molybdates, Etc. Volume II of The System of Mineralogy of James Dwight Dana and Edward Salisbury Dana, Yale University 1837–1892.* 7th Edition. New York, New York: John Wiley & Sons. TIC: 209332.

162281 Hay, R.L. and Wiggins, B. 1980. "Pellets, Ooids, Sepiolite and Silica in Three Calcretes of the Southwestern United States." Sedimentology, 27, 559-576. Malden, Massachusetts: Blackwell Publishing. TIC: 222806.

162282 Faust, G.T. 1953. "Huntite, $Mg_3Ca(CO_3)_4$, a New Mineral." American Mineralogist, 38, (1-2), 4-24. Washington, D.C.: Mineralogical Society of America. TIC: 252888.

162283 Walling, E.M.; Rock, P.A.; and Casey, W.H. 1995. "The Gibbs Energy of Formation of Huntite, $CaMg_3(CO_3)_4$, at 298 K and 1 Bar from Electrochemical Cell Measurements." *American Mineralogist, 80*, (3-4), 355-360. Washington, D.C.: Mineralogical Society of America. TIC: 252890.

162284 Fleischer, M. and Pabst, A. 1983. "New Mineral Names." *Journal of the Mineralogical Society of America, 68*, (1-2), 281-283. Washington, D.C.: Mineralogical Society of America. TIC: 252898.

162288 Larrabee, C.P. and Coburn, S.K. 1962. "The Atmospheric Corrosion of Steels as Influenced by Changes in Chemical Composition." *First International Congress on Metallic Corrosion, London, England, April 10-15, 1961*. Pages 276-285. London, England: Butterworths. TIC: 223384. Copyright Requested

162290 Merz, M.D. 1982. *State-of-the-Art Report on Corrosion Data Pertaining to Metallic Barriers for Nuclear Waste Repositories.* PNL-4474. Richland, Washington: Pacific Northwest Laboratory. ACC: NNA.19891215.0033.

162292 Johnson, M.J. and Pavlik, P.J. 1982. "Atmospheric Corrosion of Stainless Steel." Chapter 32 of *Atmospheric Corrosion*. The Corrosion Monograph Series. Ailor, W.H., ed. New York, New York: John Wiley and Sons. TIC: 240907.

162312 Fleischer, M. and Efremov, N. 1954. "New Mineral Names." *American Mineralogist, 39*, (3-4), 402-408. Washington, D.C.: Mineralogical Society of America. TIC: 252897.

162338 Deer, W.A.; Howie, R.A.; and Zussman, J. 1967. *An Introduction to the Rock-Forming Minerals*. New York, New York: John Wiley and Sons. TIC: 234769.

162451 Copson, H.R. 1955. "Atmospheric Corrosion Behavior of Some Nickel Alloys." *Symposium on Atmospheric Corrosion of Non-Ferrous Metals, Prestented at the Fifty-Eighth Annual meeting Ameri an Society for Testing Materials, Atlantic City, N.J., June 29, 1955*. 175, 141-158. Philadelphia, Pennsylvania: American Society for Testing and Materials. TIC: 226997. Copyright Requested

162479 Jenne, E.A. 1981. *Waste/Rock Interactions Technology Program, Geochemical Modeling:* A Review. PNL-3574. Richland, Washington: Pacific Northwest Laboratory. TIC: 229656.

162480 Nordstrom, D.K. and Jenne, E.A. 1977. "Fluorite Solubility Equilibria in Selected Geothermal Waters." *Geochimica et Cosmochimica Acta*, 41, (2), 175-188. New York, New York: Pergamon Press. TIC: 253587.

162481 Pitzer, K.S. 1987. "A *Thermodynamic Model for Aqueous Solutions of Liquid-Like Density." Thermodynamic Modeling of Geological Materials: Minerals, Fluids and Melts.* Carmichael, I.S.E. and Eugster, H.P., eds. Reviews in Mineralogy Volume 17. Pages 97-142. [Washington, D.C.]: Mineralogical Society of America. TIC: 253653.

162482 Davies, C.W. 1962. *Ion Association*. Washington, D.C.: Butterworths. TIC: 244840.

162494 SNL (Sandia National Laboratories) 2003. *Software User's Manual, EQ3/6, Version 8.0.* SDN: 10813-UM-8.0-00. Albuquerque, New Mexico: Sandia National Laboratories. ACC: MOL.20030312.0084.

162508 Nordstrom, D.K.; Jenne, E.A.; and Ball, J.W. 1979. "Redox Equilibria of Iron in Acid Mine Waters." Chapter 3 *of Chemical Modeling in Aqueous Systems, Specification, Sorption, Solubility, and Kinetics*. Jenne, E.A., ed. ACS Symposium Series 93. Washington, D.C.: American Chemical Society. TIC: 208922.

162529 BSC (Bechtel SAIC Company) 2003. *In-Drift Precipitates/Salts Model.* ANL-EBS-MD-000045 REV 01. Las Vegas, Nevada: Bechtel SAIC Company. ACC: DOC.20031028.0003.

162576 Peterman, Z.E. and Cloke, P.L. 2002. "Geochemistry of Rock Units at the Potential Repository Level, Yucca Mountain, Nevada (includes Erratum)." *Applied Geochemistry, 17,* ([6, 7]), 683-698, 955-958. New York, New York: Pergamon. TIC: 252516; 252517.

162819 Peterman, Z.E.; Paces, J.B.; Neymark, L.A.; and Hudson, D. 2003. "Geochemistry of Dust in the Exploratory Studies Facility, Yucca Mountain, Nevada." *Proceedings of the 10th International High-Level Radioactive Waste Management Conference (IHLRWM), March 30-April 2, 2003, Las Vegas, Nevada.* Pages 637-645. La Grange Park, Illiniois: American Nuclear Society. TIC: 254559.

162970 Sequeira, C.A.C. 2000. "Corrosion of Copper and Copper Alloys." Chapter 42 of Uhlig's *Corrosion Handbook*. 2nd Edition. Revie, R.W., ed. New York, New York: John Wiley & Sons. TIC: 248360.

162971 Davison, R.M.; DeBold, T.; and Johnson, M.J. 1987. "Corrosion of Stainless Steels." In *Corrosion*, Volume 13, Pages 547-565 of *ASM Handbook*. Formerly 9th Edition, Metals Handbook. [Materials Park, Ohio]: ASM International. TIC: 240704.

162976 Smith, W.H. and Purdy, G.M. 1995. "Chromium in Aqueous Nitrate Plutonium Process Streams: Corrosion of 316 Stainless Steel and Chromium Speciation." Waste Management, 15, (7), 477-484. New York, New York: Pergamon. TIC: 254034.

163007 Money, K.L. 1987. "Corrosion Testing in the Atmosphere." In *Corrosion*, Volume 13, Pages 204-206 of *ASM Handbook*. Formerly 9th Edition, Metals Handbook. [Materials Park, Ohio]: ASM International. TIC: 240704.

163015 Ball, J.W. and Nordstrom, D.K. 1998. "Critical Evaluation and Selection of Standard State Thermodynamic Properties for Chromium Metal and its Aqueous Ions, Hydrolysis Species, Oxides, and Hydroxides." *Journal of Chemical & Engineering Data*, *43*, (6), 895-918. Washington, D.C.: American Chemical Society. TIC: 254015.

163030 Perez, J.M., Jr.; Bickford, D.F.; Day, D.E.; Kim, D.S.; Lambert, S.L.; Marra, S.L.; Peeler, D.K.; Strachan, D.M.; Triplett, M.B.; Vienna, J.D.; and Wittman, R.S. 2001. *High-Level Waste Melter Study Report*. PNNL-13582. Richland, Washington: Pacific Northwest National Laboratory. TIC: 254062.

163031 Hrma, P.; Piepel, G.F.; Vienna, J.D.; Cooley, S.K.; Kim, D.S.; and Russell, R.L. 2001. *Database and Interim Glass Property Models for Hanford HLW Glasses*. PNNL-13573. Richland, Washington: Pacific Northwest National Laboratory. TIC: 254061.

163034 Agarwal, D.C. 2000. "Nickel and Nickel Alloys." Chapter 45 of *Uhlig's Corrosion Handbook*. 2nd Edition. Revie, R.W., ed. New York, New York: John Wiley & Sons. TIC: 248360.

163067 Pabalan, R.T.; Yang, L.; and Browning, L. 2002. *Effects of Salt Formation on the Chemical Environment of Drip Shields and Waste Packages at the Proposed Nuclear Waste Repository at Yucca Mountain, Nevada*. CNWRA 2002-03. San Antonio, Texas: Center for Nuclear Waste Regulatory Analyses. TIC: 254207.

163132 Reheis, M.C.; Budahn, J.R.; and Lamothe, P.J. 2002. "Geochemical Evidence for Diversity of Dust Sources in the Southwestern United States." *Geochimica et Cosmochimica Acta*, *66*, (9), 1569-1587. New York, New York: Pergamon. TIC: 254213.

163152 BSC 2003. *Dissolved Concentration Limits of Radioactive Elements*. ANL-WIS-MD-000010 REV 02. Las Vegas, Nevada: Bechtel SAIC Company. ACC: DOC.20030624.0003.

163226 BSC 2003. *Seepage Model for PA Including Drift Collapse.* MDL-NBS-HS-000002 REV 02. Las Vegas, Nevada: Bechtel SAIC Company. ACC: DOC.20030709.0001.

163274 NRC (U.S. Nuclear Regulatory Commission) 2003. *Yucca Mountain Review Plan, Final Report.* NUREG-1804, Rev. 2. Washington, D.C.: U.S. Nuclear Regulatory Commission, Office of Nuclear Material Safety and Safeguards. TIC: 254568.

163286 Deer, W.A.; Howie, R.A.; and Zussman, J. 1992. *An Introduction to the Rock-Forming Minerals*. 2nd Edition. New York, New York: Prentice Hall. TIC: 221918.

163369 Rai, D.; Sass, B.M.; and Moore, D.A. 1987. "Chromium(III) Hydrolysis Constants and Solubility of Chromium(III) Hydroxide." *Inorganic Chemistry, 26*, (3), 345-349. [Washington, D.C.]: American Chemical Society. TIC: 254060.

163377 DOE 2003. *Source Term Estimates for DOE Spent Nuclear Fuels.* DOE/SNF/REP-078, Rev. 0. Idaho Falls, Idaho: U.S. Department of Energy, Idaho Operations Office. TIC: 254275.

163693 BSC (Bechtel SAIC Company) 2003. *DSNF and Other Waste Form Degradation Abstraction.* ANL-WIS-MD-000004 REV 02. Las Vegas, Nevada: Bechtel SAIC Company. ACC: DOC.20030711.0002

163699 Bomberger, H.B.; Cambourelis, P.J.; and Hutchinson, G.E. 1954. "Corrosion Properties of Titanium in Marine Environments." *Journal of the Electrochemical Society, 101*, (9), 442-447. New York, New York: Electrochemical Society. TIC: 254366.

163705 Gilbert, R.O. 1987. *Statistical Methods for Environmental Pollution Monitoring*. New York, New York: John Wiley & Sons. TIC: 252619.

163728 Niki, K. 1985. "Chromium." In *Standard Potentials in Aqueous Solution, Monographs in Electroanalytical Chemistry and Electrochemistry*. Bard, A.J.; Parsons, R.; and Jordan, J.; eds. New York, New York: Marcel Dekker. TIC: 254232.

163752 White, D.E.; Hem, J.D.; and Waring, G.A. 1980. "Chemical Composition of Subsurface Waters." Chapter F of *Data of Geochemistry*. 6th Edition. Geological Survey Professional Paper 440-F. Washington, D.C.: U.S. Government Printing Office. TIC: 249975.

163753 Bühn B. and Rankin A.H. 1999. "Composition of Natural, Volatile-Rich Na-Ca-REE-Sr Carbonatitic Fluids Trapped in Fluid Inclusions." *Geochimica et Cosmochimica Acta*, 63, (22), 3781-3797. New York, New York: Elsevier. TIC: 254299.

163754 Kracek, F.C. and Clark, S.P., Jr. 1966. "Melting and Transformation Points in Oxide and Silicate Systems at Low Pressure." Section 13 of *Handbook of Physical Constants*. Clark, S.P., Jr., ed. Memoir 97. New York, New York: Geological Society of America. TIC: 244868.

163817 Campbell, A.N. and Smith, N.O. 1951. *The Phase Rule and its Applications*. 9th Edition. New York, New York: Dover Publications. TIC: 254360.

163824 BSC 2003. *CSNF Waste Form Degradation: Summary Abstraction*. ANL-EBS-MD-000015 REV 01. Las Vegas, Nevada: Bechtel SAIC Company. ACC: DOC.20030708.0004.

163855 BSC 2003. *Repository Design Project, RDP/PA IED Typical Waste Package Components Assembly (2).* 800-IED-WIS0-00202-000-00A. Las Vegas, Nevada: Bechtel SAIC Company. ACC: ENG.20030702.0002.

164052 BSC (Bechtel SAIC Company) 2003. *Repository Design Project, Repository/PA IED Emplacement Drift Committed Materials 1 of 2.* 800-IED-WIS0-00301-000-00A. Las Vegas, Nevada: Bechtel SAIC Company. ACC: ENG.20030627.0003.

164069 BSC 2003. *Repository Design Project, Repository/PA IED Emplacement Drift Configuration 1 of 2.* 800-IED-EBS0-00201-000-00A. Las Vegas, Nevada: Bechtel SAIC Company. ACC: ENG.20030630.0002.

164101 BSC (Bechtel SAIC Company) 2003. *Repository Design Project, Repository/PA IED Emplacement Drift Committed Materials (2).* 800-IED-WIS0-00302-000-00A. Las Vegas, Nevada: Bechtel SAIC Company. ACC: ENG.20030627.0004.

164872 BSC (Bechtel SAIC Company) 2003. *Environment on the Surfaces of the Drip Shield and Waste Package Outer Barrier.* ANL-EBS-MD-000001 REV 01D. Las Vegas, Nevada: Bechtel SAIC Company. ACC: MOL.20030825.0151. TBV-5638

164888 BSC (Bechtel SAIC Company) 2003. *Abstraction of Drift-Scale Coupled Processes.* MDL-NBS-HS-000018 REV 00C. Las Vegas, Nevada: Bechtel SAIC Company. ACC: MOL.20031118.0182. TBV-5640

165179 BSC (Bechtel SAIC Company) 2003. *Q-List.* TDR-MGR-RL-000005 REV 00. Las Vegas, Nevada: Bechtel SAIC Company. ACC: DOC.20030930.0002.

165304 BSC (Bechtel SAIC Company) 2003. *Design and Engineering, D&E / PA/C IED Interlocking Drip Shield and Emplacement Pallet.* 800-IED-WIS0-00401-000-00B. Las Vegas, Nevada: Bechtel SAIC Company. ACC: ENG.20030929.0008.

165406 BSC (Bechtel SAIC Company) 2003. *Design and Engineering, D&E/PA/C IED Typical Waste Package Components Assembly 1 of 9.* 800-IED-WIS0-00201-000-00C. Las Vegas, Nevada: Bechtel SAIC Company. ACC: ENG.20030917.0002.

166031 BSC 2003. *In-Drift Precipitates/Salts Model.* ANL-EBS-MD-000045 REV 01 ICN 01B. Las Vegas, Nevada: Bechtel SAIC Company. ACC: MOL.20031215.0159. TBV-5622

166275 Canori, G.F. and Leitner, M.M. 2003. *Project Requirements Document.* TER-MGR-MD-000001 REV 02. Las Vegas, Nevada: Bechtel SAIC Company. ACC: DOC.20031222.0006.

166463 BSC (Bechtel SAIC Company) 2003. *Multiscale Thermohydrologic Model.* ANL-EBS-MD-000049 REV 01G. Las Vegas, Nevada: Bechtel SAIC Company. ACC: MOL.20031212.0037. TBV-5641

166464 BSC (Bechtel SAIC Company) 2003. *Engineered Barrier System Features, Events, and Processes.* ANL-WIS-PA-000002 REV 02E. Las Vegas, Nevada: Bechtel SAIC Company. ACC: MOL.20031212.0038. TBV-5642

166466 BSC (Bechtel SAIC Company) 2003. *EBS Radionuclide Transport Abstraction.* ANL-WIS-PA-000001 REV 01F. Las Vegas, Nevada: Bechtel SAIC Company. ACC: MOL.20031210.0361. TBV-5644

166512 BSC (Bechtel SAIC Company) 2003. *Drift-Scale Coupled Processes (DST and TH Seepage) Models.* MDL-NBS-HS-000015 REV 00C. Las Vegas, Nevada: Bechtel SAIC Company. ACC: MOL.20030910.0160. TBV-5666

166519 BSC 2003. *Technical Work Plan for*: *In-Drift Geochemistry Modeling.* TWP-MGR-PA-000013 REV 00. Las Vegas, Nevada: Bechtel SAIC Company. ACC: DOC.20040128.0002.

9.2 CODES, STANDARDS, AND REGULATIONS

103515 ASTM G 1-90 (Reapproved 1999). 1999. *Standard Practice for Preparing, Cleaning, and Evaluating Corrosion Test Specimens.* West Conshohocken, Pennsylvania: American Society for Testing and Materials. TIC: 238771.

103753 ASM International. 1987. *Corrosion*. Volume 13 of *Metals Handbook*. 9th Edition. Metals Park, Ohio: ASM International. TIC: 209807.

105725 ASTM C 1174-97. 1998. *Standard Practice for Prediction of the Long-Term Behavior of Materials, Including Waste Forms, Used in Engineered Barrier Systems (EBS) for Geological Disposal of High-Level Radioactive Waste*. West Conshohocken, Pennsylvania: American Society for Testing and Materials. TIC: 246015.

107063 AISC (American Institute of Steel Construction) 1997. *Manual of Steel Construction, Allowable Stress Design.* 9th Edition, 2nd Revision, 2nd Impression. Chicago, Illinois: American Institute of Steel Construction. TIC: 240772.

145103 ASME (American Society of Mechanical Engineers) 1998. *1998 ASME Boiler and Pressure Vessel Code.* 1998 Edition with 1999 and 2000 Addenda. New York, New York: American Society of Mechanical Engineers. TIC: 247429.

147465 ASTM B 575-99a. 1999. *Standard Specification for Low-Carbon Nickel-Molybdenum-Chromium, Low-Carbon Nickel-Chromium-Molybdenum, Low-Carbon Nickel-Chromium-Molybdenum-Copper, Low-Carbon Nickel-Chromium-Molybdenum-Tantalum, and Low-Carbon Nickel-Chromium-Molybdenum-Tungsten Alloy Plate, Sheet, and Strip.* West Conshohocken, Pennsylvania: American Society for Testing and Materials. TIC: 247534.

156605 10 CFR 63. Energy: Disposal of High-Level Radioactive Wastes in a Geologic Repository at Yucca Mountain, Nevada. Readily available.

158661 ASTM A 572/A 572M-01. 2001. *Standard Specification for High-Strength Low-Alloy Columbium-Vanadium Structural Steel.* West Conshohocken, Pennsylvania: American Society for Testing and Materials. TIC: 252605.

158937 ASTM A 490-02. 2002. *Standard Specification for Structural Bolts, Alloy Steel, Heat Treated, 150 ksi Minimum Tensile Strength*. West Conshohocken, Pennsylvania: American Society for Testing and Materials. TIC: 252766.

159971 ASTM A 759-00. 2001. *Standard Specification for Carbon Steel Crane Rails*. West Conshohocken, Pennsylvania: American Society for Testing and Materials. TIC: 253176.

162719 ASTM A 53/A 53M-02. 2002. *Standard Specification for Pipe, Steel, Black and Hot-Dipped, Zinc-Coated, Welded and Seamless*. West Conshohocken, Pennsylvania: American Society for Testing and Materials. TIC: 253988.

162720 ASTM A 240/A 240M-02a. 2002. *Standard Specification for Chromium and Chromium-Nickel Stainless Steel Plate, Sheet, and Strip for Pressure Vessels and for General* Applications. West Conshohocken, Pennsylvania: American Society for Testing and Materials. TIC: 253994.

162722 ASTM A 307-02. 2002. *Standard Specification for Carbon Steel Bolts and Studs, 60 000 PSI Tensile Strength.* West Conshohocken, Pennsylvania: American Society for Testing and Materials. TIC: 253996.

162723 ASTM A 516/A 516M-01. 2001. *Standard Specification for Pressure Vessel Plates, Carbon Steel, for Moderate- and Lower-Temperature Service.* West Conshohocken, Pennsylvania: American Society for Testing and Materials. TIC: 253997.

162724 ASTM A 588/A 588M-01. 2001. *Standard Specification for High-Strength Low-Alloy Structural Steel with 50 ksi [345 MPa] Minimum Yield Point to 4–in. [100–mm] Thick.* West Conshohocken, Pennsylvania: American Society for Testing and Materials. TIC: 253998.

162726 ASTM B 265-02. 2002. *Standard Specification for Titanium and Titanium Alloy Strip, Sheet, and Plate.* West Conshohocken, Pennsylvania: American Society for Testing and Materials. TIC: 254000.

162727 ASTM B 209M-02. 2002. *Standard Specification for Aluminum and Aluminum-Alloy Sheet and Plate [Metric].* West Conshohocken, Pennsylvania: American Society for Testing and Materials. TIC: 253985.

165006 ASTM A 276-03. 2003. *Standard Specification for Stainless Steel Bars and Shapes.* West Conshohocken, Pennsylvania: American Society for Testing and Materials. TIC: 254842.

9.3 DATA, LISTED BY DIRS

113644 MO9807DSTSET01.000. Drift Scale Test (DST) Temperature, Power, Current, Voltage Data for November 7, 1997 through May 31, 1998. Submittal date: 07/09/1998.

113662 MO9810DSTSET02.000. Drift Scale Test (DST) Temperature, Power, Current, Voltage Data for June 1 through August 31, 1998. Submittal date: 10/09/1998.

113673 MO9906DSTSET03.000. Drift Scale Test (DST) Temperature, Power, Current, and Voltage Data for September 1, 1998 through May 31, 1999. Submittal date: 06/08/1999.

144913 LL000202905924.117. Environment on the Surfaces of the Drip Shield and Waste Package Outer Barrier. Submittal date: 02/18/2000.

147298 LL980704605924.035. Engineering Material Characterization Report, Volume 3. Submittal date: 07/17/1998.

147299 MO0003SPASUP02.003. Supporting Media for Calculation of General Corrosion Rate of Drip Shield and Waste Package Outer Barrier to Support WAPDEG Analysis. Submittal date: 03/02/2000.

151049 MO0004SPASMA05.004. Supporting Media for Abstraction of Models for Stainless Steel Structural Material Degradation. Submittal date: 04/05/2000.

153044 MO0003RIB00076.000. Physical and Chemical Characteristics of Type 316N Grade. Submittal date: 03/14/2000.

153707 MO0007SEPDSTPC.001. Drift Scale Test (DST) Temperature, Power, Current, and Voltage Data for November 1, 1999 through May 31, 2000. Submittal date: 07/13/2000.

153836 MO0001SEPDSTPC.000. Drift Scale Test (DST) Temperature, Power, Current, and Voltage Data for June 1, 1999 through October 31, 1999. Submittal date: 01/12/2000.

155964 MO0109RIB00049.001. Waste Package Material Properties: Neutron Absorbing Materials. Submittal date: 09/17/2001.

159551 LL020710223142.024. Moisture Content of Rock from Neutron Logging Activities in the Drift Scale Test (DST): August 1997 through May 2002. Submittal date: 08/20/2002.

160899 GS020408312272.003. Collection and Analysis of Pore Water Samples for the Period from April 2001 to February 2002. Submittal date: 04/24/2002.

161756 MO0302SPATHDYN.000. Thermodynamic Data Input Files - Data0.YMP.R2. Submittal date: 02/05/2003.

161976 LB0302DSCPTHCS.002. Drift-Scale Coupled Processes (THC Seepage) Model: Data Summary. Submittal date: 02/11/2003.

162549 MO0303SPAMEQ36.000. General Formats of In-Drift Precipitates/Salts Model EQ3/6 Input Files. Submittal date: 03/04/2003.

162556 MO0207EBSDUSTS.020. Geochemical Composition of Dust Samples. Submittal date: 07/11/2002.

162557 MO0209EBSDUST2.030. Geochemical Composition of Dust Samples (Phase II). Submittal date: 09/30/2002.

162572 SN0302T0510102.002. Pitzer Thermodynamic Database (data0.ypf, Revision 1). Submittal date: 02/06/2003.

162841 MO0303MWDIOJ13.000. Example EQ3/6 In-Drift Precipitates/Salts Model Input/Output Files for In Situ J-13 Well Water. Submittal date: 03/04/2003.

163531 MO0210MWDEXC01.008. CSNF Results in Excel Spreadsheets - CSNF_Spreadsheets. Submittal date: 10/22/2002.

163881 MO0303MWDINJ13.000. Comparison of In-Drift Precipitates/Salts Model Simulations of Evaporation of In Situ J-13 Well Water Using Different Databases (YPF Pitzer vs. YMP.R2). Submittal date: 03/04/2003.

163882 MO0303MWDSEDSS.000. In-Drift Precipitates/Salts Model Simulations of Evaporation of Dilute Salt Solutions at 25C and 100C. Submittal date: 03/04/2003.

163884 MO0303MWDJ13RB.000. In-Drift Precipitates/Salts Model Simulation of Synthetic J-13 Water Evaporation Experiments Documented in Rosenberg et al. 1999. Submittal date: 03/04/2003.

164885 MO0303MWDTSWRB.000. In-Drift Precipitates/Salts Model Simulation of Synthetic Topopah Spring Tuff Pore Water Evaporation Experiments Documented In Rosenberg et al. 1999. Submittal date: 03/04/2003.

164886 MO0303MWDJ13GD.000. In-Drift Precipitates/Salts Model Simulation of Synthetic J-13 Water Evaporation Experiments Documented in ANL-EBS-MD-000001. Submittal date: 03/04/2003.

166329 MO0312SPAESMUN.002. Estimated Model Uncertainties In IDPS Model Outputs. Submittal date: 12/03/2003.

166801 MO0401SPAMCRAE.000. Materials Corrosion Rates In Aqueous Environments. Submittal date: 01/16/2004.

9.4 PROJECT SOFTWARE SOURCES

161572 BSC (Bechtel SAIC Company) 2003. *Software Code: GoldSim.* V7.50.100. PC. 10344-7.50.100-00.

161900 BSC 2003. *Software Code: GetEQData.* V1.0.1. PC w/Windows 2000 and Windows NT. 10809-1.0.1-0.

162228 BSC 2003. *Software Code: EQ3/6.* V8.0. PC w/ Windows 95/98/2000/NT 4.0. 10813-8.0-00.

9.5 OUTPUT DATA, LISTED BY DATA TRACKING NUMBER

MO0303MWDEBSSM.000. EBS Abstraction of the THC Seepage Model: Binning Analysis Evaporation to 65% RH EQ6 Input and Output Files. Submittal date: 03/12/2003.

MO0303MWDSCMAB.000. THC Seepage Chemistry Model Abstraction Binning EQ3 Input, Pickup and Output Files. Submittal date: 03/06/2003.

MO0304MWDEBSSA.000. EBS THC Seepage Abstraction TSPA-LA Lookup Table EQ6 Input and Output Files. Submittal date: 04/01/2003.

MO0304MWDSAB11.001. EBS THC Seepage Abstraction 11 Bin EQ3 3i, 3p, and 3o Files. Submittal date: 04/08/2003.

MO0304SPAA11GC.000. EBS THC Seepage Abstraction 11 Bin EQ3 3o File Water and Gas Chemistry Extraction. Submittal date: 04/10/2003.

MO0308SPACO2GL.001. EBS Environment In-Drift CO2 Gas Lookup Tables for TSPA-LA. Submittal date: 08/04/2003.

MO0304SPACPSLT.000. Combined In-Drift Precipitates/Salts Model Lookup Table for Seepage Evaporation Abstractions for All Bins. Submittal date: 04/18/2003.

MO0304SPACSALT.000. EBS Chemistry THC Seepage Model Abstraction Lookup Tables for TSPA-LA. Submittal date: 04/14/2003.

MO0310SPAEBSCB.003. EBS Chemistry Binning Abstraction Results of the THC Seepage Model. Submittal date: 10/15/2003.

MO0310SPAEBSUE.002. EBS Chemistry Unevaporated Binning Abstraction Statistics. Submittal date: 10/15/2003.

MO0310SPAPCEAC.002. EBS P&CE Alternate Conceptual Model Calculations. Submittal date: 10/15/2003.

MO0310SPAPCELA.002. EBS P&CE Model Dust Leachate Analyses Spreadsheets and Data. Submittal date: 10/16/2003.

MO0310SPAEBSSB.002. EBS P&CE Model THC Seepage Within and Without Bin Uncertainty Analyses. Submittal date: 10/15/2003.

MO0310SPAPCEUA.002. EBS P&CE Uncertainty Analyses for Pco2, Br, and Mineral Suppressions. Submittal date: 10/15/2003.

MO0306SPAPCEVC.000. EBS P&CE Model Validation Calculations, Spreadsheets, and Data. Submittal date: 06/05/2003.

MO0310SPAPCEGS.000. EBS P&CE “Goldsim Friendly” THC Seepage Look-Up Tables For TSPA-LA. Submittal date: 10/16/2003.

MO0310SPADLALT.001. Dust Leachate Low Temperature Lookup Tables For TSPA-LA. Submittal date: 10/15/2003.

MO0310SPADLHTL.000. Dust Leachate High Temperature Lookup Tables For TSPA-LA. Submittal date: 10/15/2003.

MO0310SPADLBU4.001. Dust Leachate Binning And Uncertainty Analysis Spreadsheets. Submittal date: 10/08/2003.

MO0310SPAPCELT.000. EBS P&CE Log Transform of Uncertainty Data. Submittal date: 10/28/2003.

MO0311SPAEPMUT.000. EBS P&CE Model Uncertainty Tables For TSPA-LA. Submittal date: 11/05/2003.

MO0311SPASADLS.000. EBS P&CE Sensitivity Analyses On Dust Leachate Silica Values. Submittal date: 11/05/2003.

MO0312SPAPCEGF.002. EBS P&CE Model Gas Flux Evaluation. Submittal date: 12/11/2003.

MO0312SPAPCEML.003. EBS P&CE Model Longevity of Materials Evaluation. Submittal date: 12/18/2003.

MO0312SPAPCESA.002. EBS P&CE Model THC Seepage Analysis Spreadsheets. Submittal date: 12/10/2003.

MO0312SPAPMVIC.000. EBS P&CE Model Validation Interpolation Calculations. Submittal date: 12/10/2003.

SN0303T0510102.004. EQ3/6 (Version 8.0) Input/Output Data Files - Salt Deliquescence Point Modeling as A Function of Temperature. Submittal date: 04/29/2003.

SN0310T0510102.010. Analysis Of In-Drift Dust Leachates At 25 Degrees C To Various Evaporation Relative Humidity (RH) Levels. Submittal date: 10/08/2003.

SN0310T0510102.011. Dust Leachate Abstraction TSPA-LA Lookup Table EQ3/6 Input And Output Files, Low Temperature. Submittal date: 10/14/2003.

SN0310T0510102.012. Dust Leachate Abstraction TSPA-LA Lookup Table EQ3/6 Input And Output Files, High Temperature. Submittal date: 10/14/2003.

SN0312T0510102.013. EBS P&CE Model Stainless Steel Abstraction. Submittal date: 12/15/2003.

ATTACHMENT I
SUPPORTING FILES ON CD ROM

TABLE

Page

I-1. Traceability of Output DTNs to the Section or Table from Which They Were Developed and Their Associated Zip Files That are Archived on Attachment I.....I-1

INTENTIONALLY LEFT BLANK

ATTACHMENT I
SUPPORTING FILES ON CD ROM

Table I-1 documents the output DTNs created by this document and lists the zipped datafiles containing the information listed on the tables. These zip files are found in the attached CD ROM.

Table I-1. Traceability of Output DTNs to the Section or Table from Which They Were Developed and Their Associated Zip Files That are Archived on Attachment I

Output DTN	Associated File Traceability Table or Section	Zip File(s) Name(s)	File Date/Time	File Size
SN0310T0510102.010	Tables 6.10-3, 6.10-4, 6.10-6, and 6.10-13 Section 6.10.3 Section 6.10.4 Section 6.10.5.1 Section 6.10.5.2 Section 6.10.5.5 Section 6.10.6.1 Tables 6.12-5 and 6.12-9 Table 8.2-2	Dust-25c.zip	12/22/2003/ 12:31	12,628 KB
MO0303MWDEBSSM.000	Tables 6.6-1, 6.6-13, and 6.6-14 Section 6.6.3 Section 6.6.4 Section 6.7.3 Table 8.2-2	W0_THCabstractionRH65_6i_6o_files.zip; W4_THCabstractionRH65_6i_6o_files.zip; W5_THCabstractionRH65_6i_6o_files.zip; W6_THCabstractionRH65_6i_6o_files.zip; W7_THCabstractionRH65_6i_6o_files.zip	12/22/2003/ 12:32; 12/22/2003/ 12:32; 12/22/2003/ 12:32; 12/22/2003/ 12:32; 12/22/2003/ 12:33	8,783 KB; 8,999 KB; 9,214 KB; 8,994 KB; 9,076 KB
MO0310SPADLBU4.001	Table 6.7-7 Section 6.7.4 Tables 6.10-5, 6.10-7 to 6.10-12 Section 6.10.4 Section 6.10.5.2 Section 6.10.5.3 Section 6.10.5.5 Table 8.2-1	DustLeachateBinning_Uncertainty.zip	12/22/2003/ 12:34	232 KB

Table I-1. Traceability of Output DTNs to the Section or Table from Which They Were Developed and Their Associated Zip Files That are Archived on Attachment I (Continued)

Output DTN	Associated File Traceability Table or Section	Zip File(s) Name(s)	File Date/Time	File Size
MO0303MWDSCMAB.000	Table 6.6-1 Section 6.6.3 Section 6.7.3 Section 6.9.1 Table 8.2-2	W0_THCabstraction3i3o3pfiles.zip; W4_THCabstraction3i3o3pfiles.zip; W5_THCabstraction3i3o3pfiles.zip; W6_THCabstraction3i3o3pfiles.zip; W7_THCabstraction3i3o3pfiles.zip	12/22/2003/ 12:35; 12/22/2003/ 12:35; 12/22/2003/ 12:35; 12/22/2003/ 12:35; 12/22/2003/ 12:35	1,232 KB; 1,260 KB; 2,488 KB; 2,464 KB; 2,522 KB
MO0310SPAEBSUE.002	Section 6.12.3.1 Section 7.2 Table 8.2-2	New Non Evaporated Binning Statistics02.zip	12/22/2003/ 12:36	283 KB
SN0310T0510102.011	Table 6.10-14 Section 6.10.6.2 Table 8.2-2	Dust_040C.zip Dust_070.zip Dust_100C.zip	12/22/2003/ 12:37; 12/22/2003/ 12:37; 12/22/2003/ 12:37	1,664 KB; 1,745 KB; 2,305 KB
SN0310T0510102.012	Table 6.10-14 Section 6.10.6.2 Table 8.2-2	Dust_120C.zip Dust_140C.zip Dust_150C.zip	12/22/2003/ 12:38; 12/22/2003/ 12:38; 12/22/2003/ 12:38	2,204 KB; 1,955 KB; 1,189 KB
MO0304MWDEBSSA.000	Table 6.9-5 Section 6.9.2 Table 6.12-9 Table 8.2-2	EQ6_Cond.zip; EQ6_EVAP.zip	12/22/2003/ 12:39; 12/22/2003/ 12:39	5,387 KB; 17,658 KB
MO0304MWDSAB11.001	Section 6.8.2 Section 6.8.4.1 Tables 6.9-3 and 6.9-4 Section 6.9.1 Table 6.12-9 Section 6.12.4.1.3 Table 8.2-2	11_Bin3i3p3o_files.zip	12/22/2003/ 12:40	183 KB

Table I-1. Traceability of Output DTNs to the Section or Table from Which They Were Developed and Their Associated Zip Files That are Archived on Attachment I (Continued)

Output DTN	Associated File Traceability Table or Section	Zip File(s) Name(s)	File Date/Time	File Size
MO0304SPAA11GC.000	Tables 6.7-6 and 6.7-7 Tables 6.9-1 and 6.9-2 Section 6.9.1 Table 8.2-2	11_bin_EQ3_file_dataExtract.zip	12/22/2003/ 12:40	12 KB
MO0308SPACO2GL.001	Tables 6.7-1 to 6.7-5 Section 6.7.2.1 Section 6.7.2.2 Section 6.7.3 Section 6.12.5 Section 6.12.5.3 Section 6.13.2.1 Section 6.15.1.1 Section 6.15.1.2 Section 6.15.2 Table 8.2-1	CO2 Look-up Tables.zip	12:22/2003/ 12:41	48 KB
MO0304SPACPSLT.000	Section 6.13.1.2 Table 8.2-2	checked_MOALT_r1.zip	12/22/2003/ 12:42	6,799 KB
MO0304SPACSALT.000	Table 6.9-6 Table 6.9-7 Section 6.9.3 Section 6.12.5 Section 6.12.5.3 Section 6.15.1.1 Section 6.15.2 Table 8.2-1 Section 8.2.1	Cond_Look-up-Tables.zip; Evap_Look-up-Tables.zip	12/22/2003/ 12:42; 12/22/2003/ 12:42	1,900 KB; 10,179 KB
MO0310SPADLALT.001	Table 6.10-15 Section 6.10.6.3 Section 6.12.5 Section 6.12.5.3 Section 6.15.1.2 Table 8.2-1	Low Temp Dust Lookup Tables.zip	12/22/2003/ 12:43	4,956 KB

Table I-1. Traceability of Output DTNs to the Section or Table from Which They Were Developed and Their Associated Zip Files That are Archived on Attachment I (Continued)

Output DTN	Associated File Traceability Table or Section	Zip File(s) Name(s)	File Date/Time	File Size
MO0310SPAEBSCB.003	Tables 6.6-3 to 6.6-14 Section 6.6.4 Section 6.6.5 Section 6.6.7.1 Section 6.6.7.2 Section 6.11.1 Tables 6.13-4 and 6.13-5 Section 6.15.1.1 Section 6.15.2 Section 7.2 Table 8.2-1	incomplete 65% RH EQ6 files.zip; pCO2 & 65% RH Bin Abstraction Reruns.zip; Final Checked EBS THC Seepage Binning Abstraction REV 4.zip	12/22/2003/ 12:44; 12/22/2003/ 12:44; 12/22/2003/ 12:44	624 KB; 1,763 KB; 585 KB
MO0310SPAPCEAC.002	Tables 6.11-1 to 6.11-13 Section 6.11.1 Table 8.2-2	Alternative Conceptual Model Statistics.zip	12/22/2003/ 12:45	533 KB
MO0312SPAPCEGF.002	Table 4.1-17 Section 4.1.2 Section 4.1.3 Section 6.7.1 Table 8.2-2	GasFluxandOxygenDemand.zip	12/22/2003/ 7:51	130 KB
MO0310SPAPCELA.002	Section 6.13.2 Tables 6.12-24 to 6.12-26 Section 6.12.4.2.4 Tables 6.13-7 and 6.13-9 Section 6.13.2.2 Section 6.13.2.3 Section 6.13.4.2 Table 8.2-2	Dust_Leach_anal_spreadsheets.zip	12/22/2003/ 12:46	7,275 KB
MO0312SPAPCEML.003	Tables 6.4-2, 6.4-3, 6.4-5, 6.4-8, 6.4-11, 6.4-15, 6.4-18 to 6.4-20 Section 6.4.1 Section 6.4.2.2 Section 6.8.2 Section 6.8.3 Table 8.2-2	Longevity.zip	12/22/2003/ 12:49	241 KB

Table I-1. Traceability of Output DTNs to the Section or Table from Which They Were Developed and Their Associated Zip Files That are Archived on Attachment I (Continued)

Output DTN	Associated File Traceability Table or Section	Zip File(s) Name(s)	File Date/Time	File Size
MO0312SPAPCESA.002	Tables 6.13-1, 6.13-2, 6.13-6, and 6.13-8 Section 6.13 Section 6.13.1.3 Section 6.13.4.1 Section 6.13.5.2 Section 7.2 Table 8.2-2	THCSeepageModelAnalysis.zip	12/22/2003/ 12:50	8,110 KB
MO0310SPAEBSSB.002	Tables 6.12-3 and 6.12-4 Section 6.12.3.1 Table 8.2-2	RH98andRH85EQ6filesW4.zip; RH98andRH85EQ6filesW5.zip; RH98andRH85EQ6filesW6.zip; RH98andRH85EQ6filesW0.zip; RH98andRH85EQ6filesW7.zip; THC Seepage Bin Uncertainty.zip	12/22/2003/ 12:51; 12/22/2003/ 12:51; 12/22/2003/ 12:50; 12/22/2003/ 12:51; 12/22/2003/ 12:51; 12/22/2003/ 12:51	11,193 KB; 11,165 KB; 11,202 KB; 10,464 KB; 10,879 KB; 771 KB
SN0312T0510102.013	Section 4.18 Tables 6.8-2 and 6.8-5 Section 6.8.3 Section 6.8.4.1 Section 6.8.4.3 Tables 6.12-10 to 6.12-19 Table 8.2-2	DegradationMolality.zip; Cr-database.zip; Cr-validation.zip; Base case.zip, Uncertainties.zip	12/22/2003-12:52; 12/22/2003-12:52; 12/22/2003-12:52; 12/22/2003-12:52 12/22/2003-12:52	9 KB 2 KB 81 KB 376 KB 1758 KB
MO0310SPAPCEUA.002	Tables 6.12-21 to 6.12-28 Section 6.12.4.3.2 Section 6.12.4.3.3 Section 6.12.4.4 Table 8.2-2	DustLeachBrSensitivity.zip MineralSuppressions.zip PCO2DustLeachSensitivity.zip seepage_pco2uncertcalcs.zip SeepageBrSensitivityStudy.zip	12/22/2003/ 12:53; 12/22/2003/ 12:53; 12/22/2003/ 12:53; 12/22/2003/ 12:53; 12/22/2003/ 12:53	289 KB; 675 KB; 666 KB; 972 KB; 4,075 KB

Table I-1. Traceability of Output DTNs to the Section or Table from Which They Were Developed and Their Associated Zip Files That are Archived on Attachment I (Continued)

Output DTN	Associated File Traceability Table or Section	Zip File(s) Name(s)	File Date/Time	File Size
MO0306SPAPCEVC.000	Section 7.4 Table 8.2-2	Sierra Spring Water Validation.zip	12/22/2003/ 1:15	907 KB
SN0303T0510102.004	Tables 7.5-1 and 7.5-2 Table 8.2-2	Salt_Deliq_EQ36_IO_files.zip	12/22/2003/ 12:55	363 KB
MO0310SPADLHTL.000	Table 6.10-15 Section 6.10.6.3 Section 6.12.5 Section 6.12.5.3 Section 6.15.1.2 Table 8.2-1	High T Dust Lookup Tables.zip	12/22/2003/ 12:56	3,459 KB
MO0310SPAPCEGS.000	Table 8.2-1 Section 8.2.1	seepage_lookup_cond.zip seepage_lookup_evap.zip	12/22/2003/ 12:56; 12/22/2003/ 12:56	1,927 KB; 10,238 KB
MO0310SPAPCELT.000	Section 6.12.3	Logtransform.zip	12/22/2003/ 12:57	1,494 KB
MO0311SPAEPMUT.000	Table 6.12-4, Table 613-8, Table 6.12-29, and Table 6.12-30	TSPA_LA_UncertaintyTables.zip	12/22/2003/ 12:58	461 KB
MO0311SPASADLS.000	Section 6.10.8	EQ36_SiO2_sensitivity_analysis.zip	12/22/2003/ 12:58	777 KB
MO0312SPAPMVIC.000	Section 7.2.2	InterpolationCalc.zip	12/22/2003/ 12:59	167 KB

ATTACHMENT II
T-H-C SEEPAGE LOOKUP TABLE RESULTS

FIGURES

Page

II-01-1. Bin 01 Aqueous Composition Evaporation Predictions vs. Relative Humidity at 100ºC and 10^{-2} CO_2 Fugacity II-6
II-01-2. Bin 01 Mineral Precipitation Evaporation Predictions vs. Relative Humidity at 100ºC and 10^{-2} CO_2 Fugacity II-6
II-01-3. Bin 01 Aqueous Composition Evaporation Predictions vs. Relative Humidity at 100ºC and 10^{-3} CO_2 Fugacity II-6
II-01-4. Bin 01 Mineral Precipitation Evaporation Predictions vs. Relative Humidity at 100ºC and 10^{-3} CO_2 Fugacity II-6
II-01-5. Bin 01 Aqueous Composition Evaporation Predictions vs. Relative Humidity at 100ºC and 10^{-4} CO_2 Fugacity II-7
II-01-6. Bin 01 Mineral Precipitation Evaporation Predictions vs. Relative Humidity at 100ºC and 10^{-4} CO_2 Fugacity II-7
II-01-7. Bin 01 Aqueous Composition Evaporation Predictions vs. Relative Humidity at 70ºC and 10^{-2} CO_2 Fugacity II-7
II-01-8. Bin 01 Mineral Precipitation Evaporation Predictions vs. Relative Humidity at 70ºC and 10^{-2} CO_2 Fugacity II-7
II-01-9. Bin 01 Aqueous Composition Evaporation Predictions vs. Relative Humidity at 70ºC and 10^{-3} CO_2 Fugacity II-8
II-01-10. Bin 01 Mineral Precipitation Evaporation Predictions vs. Relative Humidity at 70ºC and 10^{-3} CO_2 Fugacity II-8
II-01-11. Bin 01 Aqueous Composition Evaporation Predictions vs. Relative Humidity at 70ºC and 10^{-4} CO_2 Fugacity II-8
II-01-12. Bin 01 Mineral Precipitation Evaporation Predictions vs. Relative Humidity at 70ºC and 10^{-4} CO_2 Fugacity II-8
II-01-13. Bin 01 Aqueous Composition Evaporation Predictions vs. Relative Humidity at 40ºC and 10^{-2} CO_2 Fugacity II-9
II-01-14. Bin 01 Mineral Precipitation Evaporation Predictions vs. Relative Humidity at 40ºC and 10^{-2} CO_2 Fugacity II-9
II-01-15. Bin 01 Aqueous Composition Evaporation Predictions vs. Relative Humidity at 40ºC and 10^{-3} CO_2 Fugacity II-9
II-01-16. Bin 01 Mineral Precipitation Evaporation Predictions vs. Relative Humidity at 40ºC and 10^{-3} CO_2 Fugacity II-9
II-01-17. Bin 01 Aqueous Composition Evaporation Predictions vs. Relative Humidity at 40ºC and 10^{-4} CO_2 Fugacity II-10
II-01-18. Bin 01 Mineral Precipitation Evaporation Predictions vs. Relative Humidity at 40ºC and 10^{-4} CO_2 Fugacity II-10
II-02-1. Bin 02 Aqueous Composition Evaporation Predictions vs. Relative Humidity at 100ºC and 10^{-2} CO_2 Fugacity II-10
II-02-2. Bin 02 Mineral Precipitation Evaporation Predictions vs. Relative Humidity at 100ºC and 10^{-2} CO_2 Fugacity II-10
II-02-3. Bin 02 Aqueous Composition Evaporation Predictions vs. Relative Humidity at 100ºC and 10^{-3} CO_2 Fugacity II-11
II-02-4. Bin 02 Mineral Precipitation Evaporation Predictions vs. Relative Humidity at 100ºC and 10^{--3} CO_2 Fugacity II-11
II-02-5. Bin 02 Aqueous Composition Evaporation Predictions vs. Relative Humidity at 100ºC and 10^{-4} CO_2 Fugacity II-11
II-02-6. Bin 02 Mineral Precipitation Evaporation Predictions vs. Relative Humidity at 100ºC and 10^{-4} CO_2 Fugacity II-11
II-02-7. Bin 02 Aqueous Composition Evaporation Predictions vs. Relative Humidity at 70ºC and 10^{-2} CO_2 Fugacity II-12

FIGURES (CONTINUED)

Page

II-02-8. Bin 02 Mineral Precipitation Evaporation Predictions vs. Relative Humidity at 70ºC and 10^{-2} CO_2 Fugacity II-12
II-02-9. Bin 02 Aqueous Composition Evaporation Predictions vs. Relative Humidity at 70ºC and 10^{-3} CO_2 Fugacity II-12
II-02-10. Bin 02 Mineral Precipitation Evaporation Predictions vs. Relative Humidity at 70ºC and 10^{-3} CO_2 Fugacity II-12
II-02-11. Bin 02 Aqueous Composition Evaporation Predictions vs. Relative Humidity at 70ºC and 10^{-4} CO_2 Fugacity II-13
II-02-12. Bin 02 Mineral Precipitation Evaporation Predictions vs. Relative Humidity at 70ºC and 10^{-4} CO_2 Fugacity II-13
II-02-13. Bin 02 Aqueous Composition Evaporation Predictions vs. Relative Humidity at 40ºC and 10^{-2} CO_2 Fugacity II-13
II-02-14. Bin 02 Mineral Precipitation Evaporation Predictions vs. Relative Humidity at 40ºC and 10^{-2} CO_2 Fugacity II-13
II-02-15. Bin 02 Aqueous Composition Evaporation Predictions vs. Relative Humidity at 40ºC and 10^{-3} CO_2 Fugacity II-14
II-02-16. Bin 02 Mineral Precipitation Evaporation Predictions vs. Relative Humidity at 40ºC and 10^{-3} CO_2 Fugacity II-14
II-02-17. Bin 02 Aqueous Composition Evaporation Predictions vs. Relative Humidity at 40ºC and 10^{-4} CO_2 Fugacity II-14
II-02-18. Bin 02 Mineral Precipitation Evaporation Predictions vs. Relative Humidity at 40ºC and 10^{-4} CO_2 Fugacity II-14
II-03-1. Bin 03 Aqueous Composition Evaporation Predictions vs. Relative Humidity at 100ºC and 10^{-2} CO_2 Fugacity II-15
II-03-2. Bin 03 Mineral Precipitation Evaporation Predictions vs. Relative Humidity at 100ºC and 10^{-2} CO_2 Fugacity II-15
II-03-3. Bin 03 Aqueous Composition Evaporation Predictions vs. Relative Humidity at 100ºC and 10^{-3} CO_2 Fugacity II-15
II-03-4. Bin 03 Mineral Precipitation Evaporation Predictions vs. Relative Humidity at 100ºC and 10^{-3} CO_2 Fugacity II-15
II-03-5. Bin 03 Aqueous Composition Evaporation Predictions vs. Relative Humidity at 100ºC and 10^{-4} CO_2 Fugacity II-16
II-03-6. Bin 03 Mineral Precipitation Evaporation Predictions vs. Relative Humidity at 100ºC and 10^{-4} CO_2 Fugacity II-16
II-03-7. Bin 03 Aqueous Composition Evaporation Predictions vs. Relative Humidity at 70ºC and 10^{-2} CO_2 Fugacity II-16
II-03-8. Bin 03 Mineral Precipitation Evaporation Predictions vs. Relative Humidity at 70ºC and 10^{-2} CO_2 Fugacity II-16
II-03-9. Bin 03 Aqueous Composition Evaporation Predictions vs. Relative Humidity at 70ºC and 10^{-3} CO_2 Fugacity II-17
II-03-10. Bin 03 Mineral Precipitation Evaporation Predictions vs. Relative Humidity at 70ºC and 10^{-3} CO_2 Fugacity II-17
II-03-11. Bin 03 Aqueous Composition Evaporation Predictions vs. Relative Humidity at 70ºC and 10^{-4} CO_2 Fugacity II-17
II-03-12. Bin 03 Mineral Precipitation Evaporation Predictions vs. Relative Humidity at 70ºC and 10^{-4} CO_2 Fugacity II-17
II-03-13. Bin 03 Aqueous Composition Evaporation Predictions vs. Relative Humidity at 40ºC and 10^{-2} CO_2 Fugacity II-18
II-03-14. Bin 03 Mineral Precipitation Evaporation Predictions vs. Relative Humidity at 40ºC and 10^{-2} CO_2 Fugacity II-18

II-03-15. Bin 03 Aqueous Composition Evaporation Predictions vs. Relative Humidity at 40ºC and 10^{-3} CO_2 Fugacity II-18
II-03-16. Bin 03 Mineral Precipitation Evaporation Predictions vs. Relative Humidity at 40ºC and 10^{-3} CO_2 Fugacity II-18
II-03-17. Bin 03 Aqueous Composition Evaporation Predictions vs. Relative Humidity at 40ºC and 10^{-4} CO_2 Fugacity II-19
II-03-18. Bin 03 Mineral Precipitation Evaporation Predictions vs. Relative Humidity at 40ºC and 10^{-4} CO_2 Fugacity II-19
II-04-1. Bin 04 Aqueous Composition Evaporation Predictions vs. Relative Humidity at 100ºC and 10^{-2} CO_2 Fugacity II-19
II-04-2. Bin 04 Mineral Precipitation Evaporation Predictions vs. Relative Humidity at 100ºC and 10^{-2} CO_2 Fugacity II-19
II-04-3. Bin 04 Aqueous Composition Evaporation Predictions vs. Relative Humidity at 100ºC and 10^{-3} CO_2 Fugacity II-20
II-04-4. Bin 04 Mineral Precipitation Evaporation Predictions vs. Relative Humidity at 100ºC and 10^{-3} CO_2 Fugacity II-20
II-04-5. Bin 04 Aqueous Composition Evaporation Predictions vs. Relative Humidity at 100ºC and 10^{-4} CO_2 Fugacity II-20
II-04-6. Bin 04 Mineral Precipitation Evaporation Predictions vs. Relative Humidity at 100ºC and 10^{-4} CO_2 Fugacity II-20
II-04-7. Bin 04 Aqueous Composition Evaporation Predictions vs. Relative Humidity at 70ºC and 10^{-2} CO_2 Fugacity II-21
II-04-8. Bin 04 Mineral Precipitation Evaporation Predictions vs. Relative Humidity at 70ºC and 10^{-2} CO_2 Fugacity II-21
II-04-9. Bin 04 Aqueous Composition Evaporation Predictions vs. Relative Humidity at 70ºC and 10^{-3} CO_2 Fugacity II-21
II-04-10. Bin 04 Mineral Precipitation Evaporation Predictions vs. Relative Humidity at 70ºC and 10^{-3} CO_2 Fugacity II-21
II-04-11. Bin 04 Aqueous Composition Evaporation Predictions vs. Relative Humidity at 70ºC and 10^{-4} CO_2 Fugacity II-22
II-04-12. Bin 04 Mineral Precipitation Evaporation Predictions vs. Relative Humidity at 70ºC and 10^{-4} CO_2 Fugacity II-22
II-04-13. Bin 04 Aqueous Composition Evaporation Predictions vs. Relative Humidity at 40ºC and 10^{-2} CO_2 Fugacity II-22
II-04-14. Bin 04 Mineral Precipitation Evaporation Predictions vs. Relative Humidity at 40ºC and 10^{-2} CO_2 Fugacity II-22
II-04-15. Bin 04 Aqueous Composition Evaporation Predictions vs. Relative Humidity at 40ºC and 10^{-3} CO_2 Fugacity II-23
II-04-16. Bin 04 Mineral Precipitation Evaporation Predictions vs. Relative Humidity at 40ºC and 10^{-3} CO_2 Fugacity II-23
II-04-17. Bin 04 Aqueous Composition Evaporation Predictions vs. Relative Humidity at 40ºC and 10^{-4} CO_2 Fugacity II-23
II-04-18. Bin 04 Mineral Precipitation Evaporation Predictions vs. Relative Humidity at 40ºC and 10^{-4} CO_2 Fugacity II-23
II-05-1. Bin 05 Aqueous Composition Evaporation Predictions vs. Relative Humidity at 100ºC and 10^{-2} CO_2 Fugacity II-24
II-05-2. Bin 05 Mineral Precipitation Evaporation Predictions vs. Relative Humidity at 100ºC and 10^{-2} CO_2 Fugacity II-24
II-05-3. Bin 05 Aqueous Composition Evaporation Predictions vs. Relative Humidity at 100ºC and 10^{-3} CO_2 Fugacity II-24
II-05-4. Bin 05 Mineral Precipitation Evaporation Predictions vs. Relative Humidity at 100ºC and 10^{-3} CO_2 Fugacity II-24
II-05-5. Bin 05 Aqueous Composition Evaporation Predictions vs. Relative Humidity at 100ºC and 10^{-4} CO_2 Fugacity II-25
II-05-6. Bin 05 Mineral Precipitation Evaporation Predictions vs. Relative Humidity at 100ºC and 10^{-4} CO_2 Fugacity II-25

II-05-7. Bin 05 Aqueous Composition Evaporation Predictions vs. Relative Humidity at 70ºC and 10^{-2} CO_2 Fugacity II-25
II-05-8. Bin 05 Mineral Precipitation Evaporation Predictions vs. Relative Humidity at 70ºC and 10^{-2} CO_2 Fugacity II-25
II-05-9. Bin 05 Aqueous Composition Evaporation Predictions vs. Relative Humidity at 70ºC and 10^{-3} CO_2 Fugacity II-26
II-05-10. Bin 05 Mineral Precipitation Evaporation Predictions vs. Relative Humidity at 70ºC and 10^{-3} CO_2 Fugacity II-26
II-05-11. Bin 05 Aqueous Composition Evaporation Predictions vs. Relative Humidity at 70ºC and 10^{-4} CO_2 Fugacity II-26
II-05-12. Bin 05 Mineral Precipitation Evaporation Predictions vs. Relative Humidity at 70ºC and 10^{-4} CO_2 Fugacity II-26
II-05-13. Bin 05 Aqueous Composition Evaporation Predictions vs. Relative Humidity at 40ºC and 10^{-2} CO_2 Fugacity II-27
II-05-14. Bin 05 Mineral Precipitation Evaporation Predictions vs. Relative Humidity at 40ºC and 10^{-2} CO_2 Fugacity II-27
II-05-15. Bin 05 Aqueous Composition Evaporation Predictions vs. Relative Humidity at 40ºC and 10^{-3} CO_2 Fugacity II-27
II-05-16. Bin 05 Mineral Precipitation Evaporation Predictions vs. Relative Humidity at 40ºC and 10^{-3} CO_2 Fugacity II-27
II-05-17. Bin 05 Aqueous Composition Evaporation Predictions vs. Relative Humidity at 40ºC and 10^{-4} CO_2 Fugacity II-28
II-05-18. Bin 05 Mineral Precipitation Evaporation Predictions vs. Relative Humidity at 40ºC and 10^{-4} CO_2 Fugacity II-28
II-06-1. Bin 06 Aqueous Composition Evaporation Predictions vs. Relative Humidity at 100ºC and 10^{-2} CO_2 Fugacity II-28
II-06-2. Bin 06 Mineral Precipitation Evaporation Predictions vs. Relative Humidity at 100ºC and 10^{-2} CO_2 Fugacity II-28
II-06-3. Bin 06 Aqueous Composition Evaporation Predictions vs. Relative Humidity at 100ºC and 10^{-3} CO_2 Fugacity II-29
II-06-4. Bin 06 Mineral Precipitation Evaporation Predictions vs. Relative Humidity at 100ºC and 10^{-3} CO_2 Fugacity II-29
II-06-5. Bin 06 Aqueous Composition Evaporation Predictions vs. Relative Humidity at 100ºC and 10^{-4} CO_2 Fugacity II-29
II-06-6. Bin 06 Mineral Precipitation Evaporation Predictions vs. Relative Humidity at 100ºC and 10^{-4} CO_2 Fugacity II-29
II-06-7. Bin 06 Aqueous Composition Evaporation Predictions vs. Relative Humidity at 70ºC and 10^{-2} CO_2 Fugacity II-30
II-06-8. Bin 06 Mineral Precipitation Evaporation Predictions vs. Relative Humidity at 70ºC and 10^{-2} CO_2 Fugacity II-30
II-06-9. Bin 06 Aqueous Composition Evaporation Predictions vs. Relative Humidity at 70ºC and 10^{-3} CO_2 Fugacity II-30
II-06-10. Bin 06 Mineral Precipitation Evaporation Predictions vs. Relative Humidity at 70ºC and 10^{-3} CO_2 Fugacity II-30
II-06-11. Bin 06 Aqueous Composition Evaporation Predictions vs. Relative Humidity at 70ºC and 10^{-4} CO_2 Fugacity II-31
II-06-12. Bin 06 Mineral Precipitation Evaporation Predictions vs. Relative Humidity at 70ºC and 10^{-4} CO_2 Fugacity II-31
II-06-13. Bin 06 Aqueous Composition Evaporation Predictions vs. Relative Humidity at 40ºC and 10^{-2} CO_2 Fugacity II-31
II-06-14. Bin 06 Mineral Precipitation Evaporation Predictions vs. Relative Humidity at 40ºC and 10^{-2} CO_2 Fugacity II-31
II-06-15. Bin 06 Aqueous Composition Evaporation Predictions vs. Relative Humidity at 40ºC and 10^{-3} CO_2 Fugacity II-32
II-06-16. Bin 06 Mineral Precipitation Evaporation Predictions vs. Relative Humidity at 40ºC and 10^{-3} CO_2 Fugacity II-32

II-06-17. Bin 06 Aqueous Composition Evaporation Predictions vs. Relative Humidity at 40ºC and 10^{-4} CO_2 Fugacity II-32
II-06-18. Bin 06 Mineral Precipitation Evaporation Predictions vs. Relative Humidity at 40ºC and 10^{-4} CO_2 Fugacity II-32
II-07-1. Bin 07 Aqueous Composition Evaporation Predictions vs. Relative Humidity at 100ºC and 10^{-2} CO_2 Fugacity II-33
II-07-2. Bin 07 Mineral Precipitation Evaporation Predictions vs. Relative Humidity at 100ºC and 10^{-2} CO_2 Fugacity II-33
II-07-3. Bin 07 Aqueous Composition Evaporation Predictions vs. Relative Humidity at 100ºC and 10^{-3} CO_2 Fugacity II-33
II-07-4. Bin 07 Mineral Precipitation Evaporation Predictions vs. Relative Humidity at 100ºC and 10^{-3} CO_2 Fugacity II-33
II-07-5. Bin 07 Aqueous Composition Evaporation Predictions vs. Relative Humidity at 100ºC and 10^{-4} CO_2 Fugacity II-34
II-07-6. Bin 07 Mineral Precipitation Evaporation Predictions vs. Relative Humidity at 100ºC and 10^{-4} CO_2 Fugacity II-34
II-07-7. Bin 07 Aqueous Composition Evaporation Predictions vs. Relative Humidity at 70ºC and 10^{-2} CO_2 Fugacity II-34
II-07-8. Bin 07 Mineral Precipitation Evaporation Predictions vs. Relative Humidity at 70ºC and 10^{-2} CO_2 Fugacity II-34
II-07-9. Bin 07 Aqueous Composition Evaporation Predictions vs. Relative Humidity at 70ºC and 10^{-3} CO_2 Fugacity II-35
II-07-10. Bin 07 Mineral Precipitation Evaporation Predictions vs. Relative Humidity at 70ºC and 10^{-3} CO_2 Fugacity II-35
II-07-11. Bin 07 Aqueous Composition Evaporation Predictions vs. Relative Humidity at 70ºC and 10^{-4} CO_2 Fugacity II-35
II-07-12. Bin 07 Mineral Precipitation Evaporation Predictions vs. Relative Humidity at 70ºC and 10^{-4} CO_2 Fugacity II-35
II-07-13. Bin 07 Aqueous Composition Evaporation Predictions vs. Relative Humidity at 40ºC and 10^{-2} CO_2 Fugacity II-36
II-07-14. Bin 07 Mineral Precipitation Evaporation Predictions vs. Relative Humidity at 40ºC and 10^{-2} CO_2 Fugacity II-36
II-07-15. Bin 07 Aqueous Composition Evaporation Predictions vs. Relative Humidity at 40ºC and 10^{-3} CO_2 Fugacity II-36
II-07-16. Bin 07 Mineral Precipitation Evaporation Predictions vs. Relative Humidity at 40ºC and 10^{-3} CO_2 Fugacity II-36
II-07-17. Bin 07 Aqueous Composition Evaporation Predictions vs. Relative Humidity at 40ºC and 10^{-4} CO_2 Fugacity II-37
II-07-18. Bin 07 Mineral Precipitation Evaporation Predictions vs. Relative Humidity at 40ºC and 10^{-4} CO_2 Fugacity II-37
II-08-1. Bin 08 Aqueous Composition Evaporation Predictions vs. Relative Humidity at 100ºC and 10^{-2} CO_2 Fugacity II-37
II-08-2. Bin 08 Mineral Precipitation Evaporation Predictions vs. Relative Humidity at 100ºC and 10^{-2} CO_2 Fugacity II-37
II-08-3. Bin 08 Aqueous Composition Evaporation Predictions vs. Relative Humidity at 100ºC and 10^{-3} CO_2 Fugacity II-38
II-08-4. Bin 08 Mineral Precipitation Evaporation Predictions vs. Relative Humidity at 100ºC and 10^{-3} CO_2 Fugacity II-38
II-08-5. Bin 08 Aqueous Composition Evaporation Predictions vs. Relative Humidity at 100ºC and 10^{-4} CO_2 Fugacity II-38
II-08-6. Bin 08 Mineral Precipitation Evaporation Predictions vs. Relative Humidity at 100ºC and 10^{-4} CO_2 Fugacity II-38
II-08-7. Bin 08 Aqueous Composition Evaporation Predictions vs. Relative Humidity at 70ºC and 10^{-2} CO_2 Fugacity II-39
II-08-8. Bin 08 Mineral Precipitation Evaporation Predictions vs. Relative Humidity at 70ºC and 10^{-2} CO_2 Fugacity II-39

II-08-9. Bin 08 Aqueous Composition Evaporation Predictions vs. Relative Humidity at 70ºC and 10^{-3} CO_2 Fugacity II-39
II-08-10. Bin 08 Mineral Precipitation Evaporation Predictions vs. Relative Humidity at 70ºC and 10^{-3} CO_2 Fugacity II-39
II-08-11. Bin 08 Aqueous Composition Evaporation Predictions vs. Relative Humidity at 70ºC and 10^{-4} CO_2 Fugacity II-40
II-08-12. Bin 08 Mineral Precipitation Evaporation Predictions vs. Relative Humidity at 70ºC and 10^{-4} CO_2 Fugacity II-40
II-08-13. Bin 08 Aqueous Composition Evaporation Predictions vs. Relative Humidity at 40ºC and 10^{-2} CO_2 Fugacity II-40
II-08-14. Bin 08 Mineral Precipitation Evaporation Predictions vs. Relative Humidity at 40ºC and 10^{-2} CO_2 Fugacity II-40
II-08-15. Bin 08 Aqueous Composition Evaporation Predictions vs. Relative Humidity at 40ºC and 10^{-3} CO_2 Fugacity II-41
II-08-16. Bin 08 Mineral Precipitation Evaporation Predictions vs. Relative Humidity at 40ºC and 10^{-3} CO_2 Fugacity II-41
II-08-17. Bin 08 Aqueous Composition Evaporation Predictions vs. Relative Humidity at 40ºC and 10^{-4} CO_2 Fugacity II-41
II-08-18. Bin 08 Mineral Precipitation Evaporation Predictions vs. Relative Humidity at 40ºC and 10^{-4} CO_2 Fugacity II-41
II-09-1. Bin 09 Aqueous Composition Evaporation Predictions vs. Relative Humidity at 100ºC and 10^{-2} CO_2 Fugacity II-42
II-09-2. Bin 09 Mineral Precipitation Evaporation Predictions vs. Relative Humidity at 100ºC and 10^{-2} CO_2 Fugacity II-42
II-09-3. Bin 09 Aqueous Composition Evaporation Predictions vs. Relative Humidity at 100ºC and 10^{-3} CO_2 Fugacity II-42
II-09-4. Bin 09 Mineral Precipitation Evaporation Predictions vs. Relative Humidity at 100ºC and 10^{-3} CO_2 Fugacity II-42
II-09-5. Bin 09 Aqueous Composition Evaporation Predictions vs. Relative Humidity at 100ºC and 10^{-4} CO_2 Fugacity II-43
II-09-6. Bin 09 Mineral Precipitation Evaporation Predictions vs. Relative Humidity at 100ºC and 10^{-4} CO_2 Fugacity II-43
II-09-7. Bin 09 Aqueous Composition Evaporation Predictions vs. Relative Humidity at 70ºC and 10^{-2} CO_2 Fugacity II-43
II-09-8. Bin 09 Mineral Precipitation Evaporation Predictions vs. Relative Humidity at 70ºC and 10^{-2} CO_2 Fugacity II-43
II-09-9. Bin 09 Aqueous Composition Evaporation Predictions vs. Relative Humidity at 70ºC and 10^{-3} CO_2 Fugacity II-44
II-09-10. Bin 09 Mineral Precipitation Evaporation Predictions vs. Relative Humidity at 70ºC and 10^{-3} CO_2 Fugacity II-44
II-09-11. Bin 09 Aqueous Composition Evaporation Predictions vs. Relative Humidity at 70ºC and 10^{-4} CO_2 Fugacity II-44
II-09-12. Bin 09 Mineral Precipitation Evaporation Predictions vs. Relative Humidity at 70ºC and 10^{-4} CO_2 Fugacity II-44
II-09-13. Bin 09 Aqueous Composition Evaporation Predictions vs. Relative Humidity at 40ºC and 10^{-2} CO_2 Fugacity II-45
II-09-14. Bin 09 Mineral Precipitation Evaporation Predictions vs. Relative Humidity at 40ºC and 10^{-2} CO_2 Fugacity II-45
II-09-15. Bin 09 Aqueous Composition Evaporation Predictions vs. Relative Humidity at 40ºC and 10^{-3} CO_2 Fugacity II-45
II-09-16. Bin 09 Mineral Precipitation Evaporation Predictions vs. Relative Humidity at 40ºC and 10^{-3} CO_2 Fugacity II-45
II-09-17. Bin 09 Aqueous Composition Evaporation Predictions vs. Relative Humidity at 40ºC and 10^{-4} CO_2 Fugacity II-46
II-09-18. Bin 09 Mineral Precipitation Evaporation Predictions vs. Relative Humidity at 40ºC and 10^{-4} CO_2 Fugacity II-46

II-10-1. Bin 10 Aqueous Composition Evaporation Predictions vs. Relative Humidity at 100ºC and 10^{-2} CO_2 Fugacity II-46
II-10-2. Bin 10 Mineral Precipitation Evaporation Predictions vs. Relative Humidity at 100ºC and 10^{-2} CO_2 Fugacity II-46
II-10-3. Bin 10 Aqueous Composition Evaporation Predictions vs. Relative Humidity at 100ºC and 10^{-3} CO_2 Fugacity II-47
II-10-4. Bin 10 Mineral Precipitation Evaporation Predictions vs. Relative Humidity at 100ºC and 10^{-3} CO_2 Fugacity II-47
II-10-5. Bin 10 Aqueous Composition Evaporation Predictions vs. Relative Humidity at 100ºC and 10^{-4} CO_2 Fugacity II-47
II-10-6. Bin 10 Mineral Precipitation Evaporation Predictions vs. Relative Humidity at 100ºC and 10^{-4} CO_2 Fugacity II-47
II-10-7. Bin 10 Aqueous Composition Evaporation Predictions vs. Relative Humidity at 70ºC and 10^{-2} CO_2 Fugacity II-48
II-10-8. Bin 10 Mineral Precipitation Evaporation Predictions vs. Relative Humidity at 70ºC and 10^{-2} CO_2 Fugacity II-48
II-10-9. Bin 10 Aqueous Composition Evaporation Predictions vs. Relative Humidity at 70ºC and 10^{-3} CO_2 Fugacity II-48
II-10-10. Bin 10 Mineral Precipitation Evaporation Predictions vs. Relative Humidity at 70ºC and 10^{-3} CO_2 Fugacity II-48
II-10-11. Bin 10 Aqueous Composition Evaporation Predictions vs. Relative Humidity at 70ºC and 10^{-4} CO_2 Fugacity II-49
II-10-12. Bin 10 Mineral Precipitation Evaporation Predictions vs. Relative Humidity at 70ºC and 10^{-4} CO_2 Fugacity II-49
II-10-13. Bin 10 Aqueous Composition Evaporation Predictions vs. Relative Humidity at 40ºC and 10^{-2} CO_2 Fugacity II-49
II-10-14. Bin 10 Mineral Precipitation Evaporation Predictions vs. Relative Humidity at 40ºC and 10^{-2} CO_2 Fugacity II-49
II-10-15. Bin 10 Aqueous Composition Evaporation Predictions vs. Relative Humidity at 40ºC and 10^{-3} CO_2 Fugacity II-50
II-10-16. Bin 10 Mineral Precipitation Evaporation Predictions vs. Relative Humidity at 40ºC and 10^{-3} CO_2 Fugacity II-50
II-10-17. Bin 10 Aqueous Composition Evaporation Predictions vs. Relative Humidity at 40ºC and 10^{-4} CO_2 Fugacity II-50
II-10-18. Bin 10 Mineral Precipitation Evaporation Predictions vs. Relative Humidity at 40ºC and 10^{-4} CO_2 Fugacity II-50
II-11-1. Bin 11 Aqueous Composition Evaporation Predictions vs. Relative Humidity at 100ºC and 10^{-2} CO_2 Fugacity II-51
II-11-2. Bin 11 Mineral Precipitation Evaporation Predictions vs. Relative Humidity at 100ºC and 10^{-2} CO_2 Fugacity II-51
II-11-3. Bin 11 Aqueous Composition Evaporation Predictions vs. Relative Humidity at 100ºC and 10^{-3} CO_2 Fugacity II-51
II-11-4. Bin 11 Mineral Precipitation Evaporation Predictions vs. Relative Humidity at 100ºC and 10^{-3} CO_2 Fugacity II-51
II-11-5. Bin 11 Aqueous Composition Evaporation Predictions vs. Relative Humidity at 100ºC and 10^{-4} CO_2 Fugacity II-52
II-11-6. Bin 11 Mineral Precipitation Evaporation Predictions vs. Relative Humidity at 100ºC and 10^{-4} CO_2 Fugacity II-52
II-11-7. Bin 11 Aqueous Composition Evaporation Predictions vs. Relative Humidity at 70ºC and 10^{-2} CO_2 Fugacity II-52
II-11-8. Bin 11 Mineral Precipitation Evaporation Predictions vs. Relative Humidity at 70ºC and 10^{-2} CO_2 Fugacity II-52
II-11-9. Bin 11 Aqueous Composition Evaporation Predictions vs. Relative Humidity at 70ºC and 10^{-3} CO_2 Fugacity II-53
II-11-10. Bin 11 Mineral Precipitation Evaporation Predictions vs. Relative Humidity at 70ºC and 10^{-3} CO_2 Fugacity II-53

II-11-11. Bin 11 Aqueous Composition Evaporation Predictions vs. Relative Humidity at 70ºC and 10^{-4} CO_2 Fugacity II-53
II-11-12. Bin 11 Mineral Precipitation Evaporation Predictions vs. Relative Humidity at 70ºC and 10^{-4} CO_2 Fugacity II-53
II-11-13. Bin 11 Aqueous Composition Evaporation Predictions vs. Relative Humidity at 40ºC and 10^{-2} CO_2 Fugacity II-54
II-11-14. Bin 11 Mineral Precipitation Evaporation Predictions vs. Relative Humidity at 40ºC and 10^{-2} CO_2 Fugacity II-54
II-11-15. Bin 11 Aqueous Composition Evaporation Predictions vs. Relative Humidity at 40ºC and 10^{-3} CO_2 Fugacity II-54
II-11-16. Bin 11 Mineral Precipitation Evaporation Predictions vs. Relative Humidity at 40ºC and 10^{-3} CO_2 Fugacity II-54
II-11-17. Bin 11 Aqueous Composition Evaporation Predictions vs. Relative Humidity at 40ºC and 10^{-4} CO_2 Fugacity II-55
II-11-18. Bin 11 Mineral Precipitation Evaporation Predictions vs. Relative Humidity at 40ºC and 10^{-4} CO_2 Fugacity II-55

TABLES

Page

II-1. Excel File Names for each Look-up Table in DTN: MO0304SPACSALT.000 2
II-2. Deliquescence Point Relative Humidity and Associated Chemical Parameters Taken from the THC Seepage Look-up Tables in DTN: MO0304SPACSALT.000 3

INTENTIONALLY LEFT BLANK

ATTACHMENT II

T-H-C SEEPAGE LOOKUP TABLE RESULTS

The graphs presented in this document are representative of the information available in DTN: MO0304SPACSALT.000. Two graphs from each excel file are shown here, they are: Aqueous Composition Evaporation Predictions vs. Relative Humidity and Mineral Precipitation Evaporation Predictions vs. Relative Humidity. Also available in this DTN: MO0304SPACSALT.000 is the condensation information: Aqueous Composition Condensation Predictions vs. Relative Humidity, Aqueous Composition Condensation Predictions vs. Concentration Factor, ANC Species Concentration Condensation Predictions vs. Relative Humidity, and ANC Species Concentration Condensation Predictions vs. Concentration Factor. This information is provided for each respective bin and parameter setting. Also available in the respective excel files, but not shown here, are: ANC Species Concentration Evaporation Predictions vs. Relative Humidity, ANC Species Concentration Evaporation Predictions vs. Concentration Factor, Aqueous Composition Evaporation Predictions vs. Concentration Factor, and Mineral Precipitation Evaporation Predictions vs. Concentration.

The graphs given in this document are referenced only by the bin number and parameter settings. Table II-1 gives the associated excel source file name for the graphs in this document. Each excel file header contains the traceability back to the specific input data used in the calculation. The file nomenclature is d?c#t%$.xls, where d represents the dust bin, ? is the 1-digit bin number (01, 02, etc.), # = 2, 3, or 4 (for $Pco_2 = 10^{-\#}$), % = 4, 7, or 1 (for temp = 40, 70, or 100°C, respectively). FILE NAME EXAMPLE (d1c2t1.xls) dust bin 01 at a Pco_2 of 10^{-2} at 100°C.

For the figures shown below, two terms need to be defined:

1. IS: Ionic Strength
2. RH: Relative Humidity

The values in Table II-2 correspond to the given parameters extracted from the excel files in DTN: MO0304SPACSALT.000. Given in this table are deliquescence point relative humidity and the associated chemical parameters of interest to TSPA.

Table II-1. Excel File Names for each Look-up Table in DTN: MO0304SPACSALT.000

Bin	Evaporation Lookup Tables	Condensation Lookup Tables
1	01c2t1e.xls.xls, 01c3t1e.xls.xls, 01c4t1e.xls.xls, 01c2t4e.xls.xls, 01c3t4e.xls.xls, 01c4t4e.xls.xls, 01c2t7e.xls.xls, 01c3t7e.xls.xls, 01c4t7e.xls.xls	01c2t1c.xls.xls, 01c3t1c.xls.xls, 01c4t1c.xls.xls, 01c2t4c.xls.xls, 01c3t4c.xls.xls, 01c4t4c.xls.xls, 01c2t7c.xls.xls, 01c3t7c.xls.xls, 01c4t7c.xls.xls
2	02c2t1e.xls.xls, 02c3t1e.xls.xls, 02c4t1e.xls.xls, 02c2t4e.xls.xls, 02c3t4e.xls.xls, 02c4t4e.xls.xls, 02c2t7e.xls.xls, 02c3t7e.xls.xls, 02c4t7e.xls.xls	02c2t1c.xls.xls, 02c3t1c.xls.xls, 02c4t1c.xls.xls, 02c2t4c.xls.xls, 02c3t4c.xls.xls, 02c4t4c.xls.xls, 02c2t7c.xls.xls, 02c3t7c.xls.xls, 02c4t7c.xls.xls
3	03c2t1e.xls.xls, 03c3t1e.xls.xls, 03c4t1e.xls.xls, 03c2t4e.xls.xls, 03c3t4e.xls.xls, 03c4t4e.xls.xls, 03c2t7e.xls.xls, 03c3t7e.xls.xls, 03c4t7e.xls.xls	03c2t1c.xls.xls, 03c3t1c.xls.xls, 03c4t1c.xls.xls, 03c2t4c.xls.xls, 03c3t4c.xls.xls, 03c4t4c.xls.xls, 03c2t7c.xls.xls, 03c3t7c.xls.xls, 03c4t7c.xls.xls
4	04c2t1e.xls.xls, 04c3t1e.xls.xls, 04c4t1e.xls.xls, 04c2t4e.xls.xls, 04c3t4e.xls.xls, 04c4t4e.xls.xls, 04c2t7e.xls.xls, 04c3t7e.xls.xls, 04c4t7e.xls.xls	04c2t1c.xls.xls, 04c3t1c.xls.xls, 04c4t1c.xls.xls, 04c2t4c.xls.xls, 04c3t4c.xls.xls, 04c4t4c.xls.xls, 04c2t7c.xls.xls, 04c3t7c.xls.xls, 04c4t7c.xls.xls
5	05c2t1e.xls.xls, 05c3t1e.xls.xls, 05c4t1e.xls.xls, 05c2t4e.xls.xls, 05c3t4e.xls.xls, 05c4t4e.xls.xls, 05c2t7e.xls.xls, 05c3t7e.xls.xls, 05c4t7e.xls.xls	05c2t1c.xls.xls, 05c3t1c.xls.xls, 05c4t1c.xls.xls, 05c2t4c.xls.xls, 05c3t4c.xls.xls, 05c4t4c.xls.xls, 05c2t7c.xls.xls, 05c3t7c.xls.xls, 05c4t7c.xls.xls
6	06c2t1e.xls.xls, 06c3t1e.xls.xls, 06c4t1e.xls.xls, 06c2t4e.xls.xls, 06c3t4e.xls.xls, 06c4t4e.xls.xls, 06c2t7e.xls.xls, 06c3t7e.xls.xls, 06c4t7e.xls.xls	06c2t1c.xls.xls, 06c3t1c.xls.xls, 06c4t1c.xls.xls, 06c2t4c.xls.xls, 06c3t4c.xls.xls, 06c4t4c.xls.xls, 06c2t7c.xls.xls, 06c3t7c.xls.xls, 06c4t7c.xls.xls
7	07c2t1e.xls.xls, 07c3t1e.xls.xls, 07c4t1e.xls.xls, 07c2t4e.xls.xls, 07c3t4e.xls.xls, 07c4t4e.xls.xls, 07c2t7e.xls.xls, 07c3t7e.xls.xls, 07c4t7e.xls.xls	07c2t1c.xls.xls, 07c3t1c.xls.xls, 07c4t1c.xls.xls, 07c2t4c.xls.xls, 07c3t4c.xls.xls, 07c4t4c.xls.xls, 07c2t7c.xls.xls, 07c3t7c.xls.xls, 07c4t7c.xls.xls
8	08c2t1e.xls.xls, 08c3t1e.xls.xls, 08c4t1e.xls.xls, 08c2t4e.xls.xls, 08c3t4e.xls.xls, 08c4t4e.xls.xls, 08c2t7e.xls.xls, 08c3t7e.xls.xls, 08c4t7e.xls.xls	08c2t1c.xls.xls, 08c3t1c.xls.xls, 08c4t1c.xls.xls, 08c2t4c.xls.xls, 08c3t4c.xls.xls, 08c4t4c.xls.xls, 08c2t7c.xls.xls, 08c3t7c.xls.xls, 08c4t7c.xls.xls
9	09c2t1e.xls.xls, 09c3t1e.xls.xls, 09c4t1e.xls.xls, 09c2t4e.xls.xls, 09c3t4e.xls.xls, 09c4t4e.xls.xls, 09c2t7e.xls.xls, 09c3t7e.xls.xls, 09c4t7e.xls.xls	09c2t1c.xls.xls, 09c3t1c.xls.xls, 09c4t1c.xls.xls, 09c2t4c.xls.xls, 09c3t4c.xls.xls, 09c4t4c.xls.xls, 09c2t7c.xls.xls, 09c3t7c.xls.xls, 09c4t7c.xls.xls
10	10c2t1e.xls.xls, 10c3t1e.xls.xls, 10c4t1e.xls.xls, 10c2t4e.xls.xls, 10c3t4e.xls.xls, 10c4t4e.xls.xls, 10c2t7e.xls.xls, 10c3t7e.xls.xls, 10c4t7e.xls.xls	10c2t1c.xls.xls, 10c3t1c.xls.xls, 10c4t1c.xls.xls, 10c2t4c.xls.xls, 10c3t4c.xls.xls, 10c4t4c.xls.xls, 10c2t7c.xls.xls, 10c3t7c.xls.xls, 10c4t7c.xls.xls
11	11c2t1e.xls.xls, 11c3t1e.xls.xls, 11c4t1e.xls.xls, 11c2t4e.xls.xls, 11c3t4e.xls.xls, 11c4t4e.xls.xls, 11c2t7e.xls.xls, 11c3t7e.xls.xls, 11c4t7e.xls.xls	11c2t1c.xls.xls, 11c3t1c.xls.xls, 11c4t1c.xls.xls, 11c2t4c.xls.xls, 11c3t4c.xls.xls, 11c4t4c.xls.xls, 11c2t7c.xls.xls, 11c3t7c.xls.xls, 11c4t7c.xls.xls

Source: DTN: MO0304SPACSALT.000

Table II-2. Deliquescence Point Relative Humidity and Associated Chemical Parameters Taken from the THC Seepage Look-up Tables in DTN: MO0304SPACSALT.000

Bin	Temperature (Celsius)	Pco_2 (atm)	Deliquescence Point Relative Humidity*	pH	Ionic Strength (Moles/kg. H_2O)	Cl (Moles/kg. H_2O)	N (Moles/kg. H_2O)
1	100	0.0100	20.037%	3.817	3.985E+01	2.513E+01	1.989E-00
	40		18.119%	3.572	3.736E+01	2.406E+01	1.313E-00
	70		18.692%	3.646	3.864E+01	2.431E+01	1.938E-00
	100	0.0010	20.038%	4.317	3.985E+01	2.512E+01	1.990E-00
	40		18.062%	4.018	3.556E+01	2.266E+01	1.485E-00
	70		18.704%	4.146	3.866E+01	2.432E+01	1.937E-00
	100	0.0001	20.013%	4.816	3.984E+01	2.511E+01	1.989E-00
	40		18.245%	4.493	3.441E+01	2.174E+01	1.607E-00
	70		18.685%	4.645	3.864E+01	2.430E+01	1.937E-00
2	100	0.0100	24.000%	4.423	3.624E+01	2.126E+01	4.690E-00
	40		23.135%	4.597	3.763E+01	2.192E+01	4.904E-00
	70		23.412%	4.381	3.540E+01	2.066E+01	4.619E-00
	100	0.0010	24.000%	4.921	3.620E+01	2.123E+01	4.684E-00
	40		23.137%	5.096	3.762E+01	2.191E+01	4.905E-00
	70		24.000%	4.806	3.358E+01	1.959E+01	4.383E-00
	100	0.0001	24.000%	5.420	3.618E+01	2.122E+01	4.682E-00
	40		23.141%	5.596	3.763E+01	2.191E+01	4.902E-00
	70		24.000%	5.306	3.358E+01	1.958E+01	4.382E-00
3	100	0.0100	43.947%	4.906	2.038E+01	1.317E+01	3.620E-00
	40		38.942%	4.441	2.000E+01	1.221E+01	2.382E-00
	70		42.259%	4.736	2.024E+01	1.166E+01	4.312E-00
	100	0.0010	44.004%	5.415	2.039E+01	1.323E+01	3.597E-00
	40		39.781%	4.972	1.975E+01	1.208E+01	2.373E-00
	70		42.471%	5.265	2.024E+01	1.180E+01	4.237E-00
	100	0.0001	44.020%	5.915	2.039E+01	1.323E+01	3.595E-00
	40		39.953%	5.488	1.973E+01	1.209E+01	2.373E-00
	70		42.492%	5.767	2.024E+01	1.181E+01	4.230E-00
4	100	0.0100	47.411%	6.473	2.239E+01	3.936E-00	1.523E+01
	40		65.012%	6.325	1.346E+01	3.994E-00	8.100E-00
	70		52.860%	6.049	2.029E+01	1.904E-00	1.705E+01
	100	0.0010	47.412%	6.973	2.239E+01	3.937E-00	1.523E+01
	40		65.014%	6.825	1.346E+01	3.994E-00	8.101E-00
	70		52.861%	6.549	2.029E+01	1.902E-00	1.705E+01
	100	0.0001	47.414%	7.473	2.239E+01	3.936E-00	1.523E+01
	40		65.014%	7.325	1.346E+01	3.994E-00	8.101E-00
	70		52.861%	7.048	2.029E+01	1.900E-00	1.705E+01
5	100	0.0100	60.130%	7.270	1.727E+01	8.186E-00	1.802E-00
	40		69.130%	7.119	1.001E+01	5.998E-00	1.321E-00
	70		62.053%	7.136	1.660E+01	6.375E-00	3.728E-00
	100	0.0010	60.129%	7.770	1.728E+01	8.186E-00	1.801E-00
	40		69.943%	7.637	9.368E-00	6.267E-00	7.024E-01
	70		62.066%	7.636	1.658E+01	6.375E-00	3.726E-00
	100	0.0001	60.131%	8.269	1.727E+01	8.182E-00	1.801E-00
	40		62.351%	7.880	1.996E+01	3.406E-00	8.532E-00
	70		62.059%	8.136	1.659E+01	6.376E-00	3.726E-00
6	100		59.117%	8.999	1.719E+01	7.213E-00	2.518E-00

Table II-2. Deliquescence Point Relative Humidity and Associated Chemical Parameters Taken from the THC Seepage Look-up Tables in DTN: MO0304SPACSALT.00 (Continued)

Bin	Temperature (Celsius)	Pco_2 (atm)	Deliquescence Point Relative Humidity*	pH	Ionic Strength (Moles/kg. H_2O)	Cl (Moles/kg. H_2O)	N (Moles/kg. H_2O)
	40	0.0100	62.976%	8.298	1.979E+01	4.304E-00	6.088E-00
	70		60.500%	8.910	1.782E+01	5.750E-00	4.430E-00
	100		59.123%	9.503	1.717E+01	7.269E-00	2.440E-00
	40	0.0010	61.745%	9.266	2.055E+01	3.930E-00	6.918E-00
	70		59.703%	9.510	1.854E+01	5.458E-00	5.018E-00
	100		58.888%	9.999	1.730E+01	7.200E-00	2.207E-00
	40	0.0001	64.071%	10.096	1.404E+01	5.033E-00	2.567E-00
	70		59.630%	10.010	1.856E+01	5.458E-00	4.897E-00
	100		59.108%	8.999	1.720E+01	7.215E-00	2.519E-00
	40	0.0100	62.976%	8.298	1.979E+01	4.304E-00	6.088E-00
	70		60.501%	8.910	1.781E+01	5.750E-00	4.430E-00
	100		59.123%	9.503	1.717E+01	7.269E-00	2.440E-00
7	40	0.0010	61.745%	9.266	2.054E+01	3.930E-00	6.918E-00
	70		59.704%	9.510	1.854E+01	5.458E-00	5.018E-00
	100		60.000%	9.992	1.607E+01	7.120E-00	1.835E-00
	40	0.0001	66.234%	10.126	1.237E+01	5.606E-00	7.012E-01
	70		59.634%	10.010	1.855E+01	5.457E-00	4.896E-00
	100		59.112%	8.999	1.720E+01	7.214E-00	2.518E-00
	40	0.0100	62.977%	8.298	1.978E+01	4.304E-00	6.088E-00
	70		60.498%	8.910	1.782E+01	5.751E-00	4.430E-00
	100		59.116%	9.503	1.718E+01	7.270E-00	2.441E-00
8	40	0.0010	61.744%	9.266	2.055E+01	3.930E-00	6.918E-00
	70		59.701%	9.510	1.854E+01	5.458E-00	5.019E-00
	100		58.884%	9.999	1.730E+01	7.200E-00	2.208E-00
	40	0.0001	62.162%	10.061	1.594E+01	4.489E-00	4.609E-00
	70		59.624%	10.010	1.857E+01	5.459E-00	4.898E-00
	100		50.935%	9.157	3.012E+01	9.899E-00	8.991E-00
	40	0.0100	62.013%	8.327	1.923E+01	4.532E-00	6.774E-00
	70		50.023%	9.191	3.284E+01	9.339E-00	1.075E+01
	100		50.905%	9.661	3.017E+01	9.977E-00	8.948E-00
9	40	0.0010	61.329%	9.270	2.041E+01	3.934E-00	7.178E-00
	70		57.507%	9.530	2.168E+01	5.656E-00	6.710E-00
	100		52.305%	10.061	2.794E+01	8.008E-00	8.526E-00
	40	0.0001	62.119%	10.060	1.593E+01	4.479E-00	4.590E-00
	70		49.783%	10.274	3.307E+01	9.401E-00	1.070E+01
	100		58.991%	8.997	1.724E+01	7.175E-00	2.556E-00
	40	0.0100	66.105%	8.399	1.247E+01	5.578E-00	2.558E-00
	70		60.345%	8.907	1.787E+01	5.704E-00	4.485E-00
	100		59.008%	9.501	1.721E+01	7.229E-00	2.477E-00
10	40	0.0010	61.525%	9.262	2.061E+01	3.879E-00	7.010E-00
	70		59.598%	9.508	1.857E+01	5.428E-00	5.056E-00
	100		58.844%	9.996	1.725E+01	7.147E-00	2.235E-00
	40	0.0001	62.119%	10.060	1.593E+01	4.480E-00	4.589E-00
	70		59.542%	10.008	1.856E+01	5.424E-00	4.932E-00
11	100		58.995%	8.997	1.723E+01	7.174E-00	2.555E-00
	40	0.0100	62.683%	8.292	1.995E+01	4.227E-00	6.213E-00
	70		60.351%	8.907	1.786E+01	5.703E-00	4.484E-00

Table II-2. Deliquescence Point Relative Humidity and Associated Chemical Parameters Taken from the THC Seepage Look-up Tables in DTN: MO0304SPACSALT.00 (Continued)

Bin	Temperature (Celsius)	Pco_2 (atm)	Deliquescence Point Relative Humidity*	pH	Ionic Strength (Moles/kg. H_2O)	Cl (Moles/kg. H_2O)	N (Moles/kg. H_2O)
	100	0.0010	59.004%	9.501	1.721E+01	7.229E-00	2.477E-00
	40		61.524%	9.262	2.062E+01	3.879E-00	7.011E-00
	70		59.596%	9.508	1.858E+01	5.428E-00	5.056E-00
	100	0.0001	58.768%	9.997	1.734E+01	7.160E-00	2.245E-00
	40		62.119%	10.060	1.593E+01	4.476E-00	4.593E-00
	70		59.511%	10.008	1.862E+01	5.430E-00	4.936E-00

DTN: MO0304SPACSALT.000

NOTE: *Deliquescence Point Relative Humidity can not be confirmed in all cases (see Table 6.12-1).

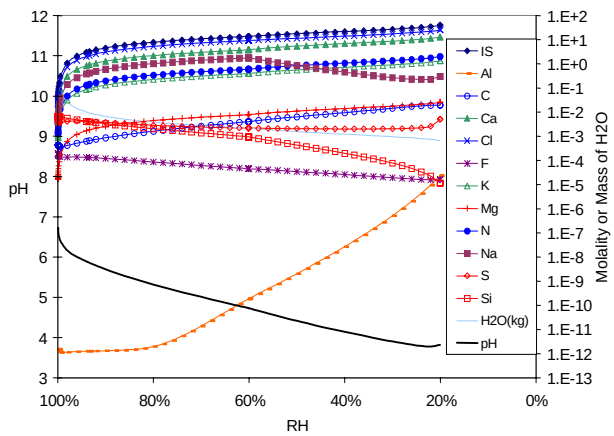

DTN: MO0304SPACSALT.000\01c2t1e.xls.xls

Figure II-01-1. Bin 01 Aqueous Composition Evaporation Predictions vs. Relative Humidity at 100ºC and 10^{-2} CO_2 Fugacity

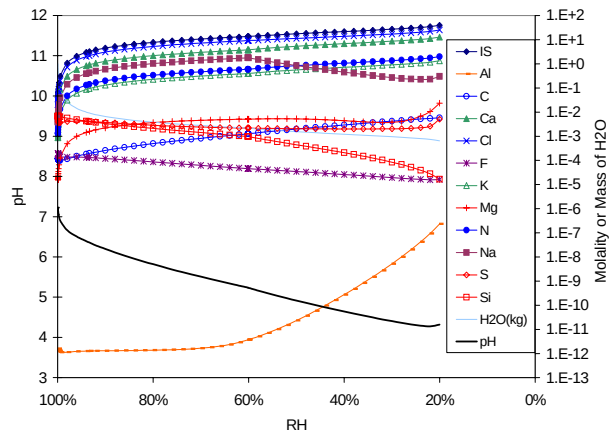

DTN: MO0304SPACSALT.000\01c3t1e.xls.xls

Figure II-01-3. Bin 01 Aqueous Composition Evaporation Predictions vs. Relative Humidity at 100ºC and 10^{-3} CO_2 Fugacity

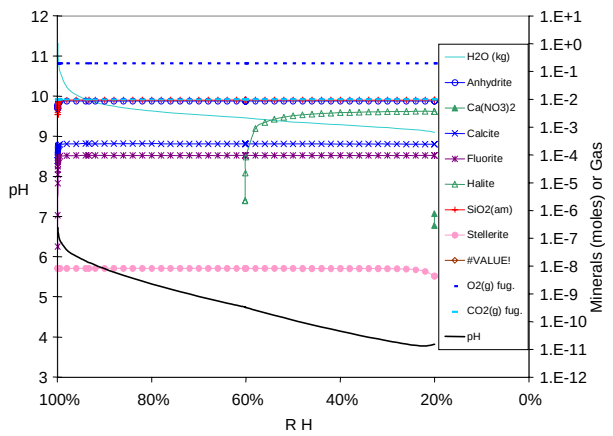

DTN: MO0304SPACSALT.000\01c2t1e.xls.xls

Figure II-01-2. Bin 01 Mineral Precipitation Evaporation Predictions vs. Relative Humidity at 100ºC and 10^{-2} CO_2 Fugacity

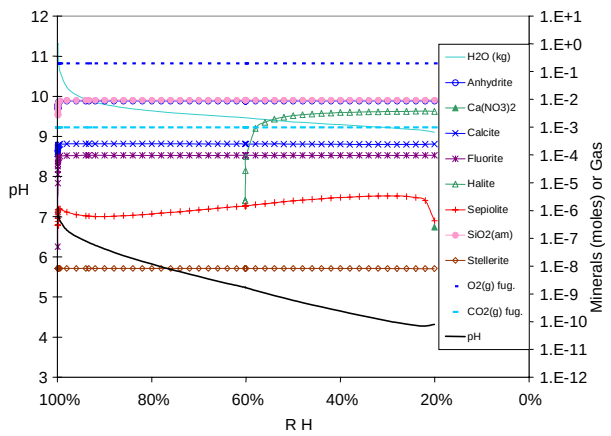

DTN: MO0304SPACSALT.000\01c3t1e.xls.xls

Figure II-01-4. Bin 01 Mineral Precipitation Evaporation Predictions vs. Relative Humidity at 100ºC and 10^{-3} CO_2 Fugacity

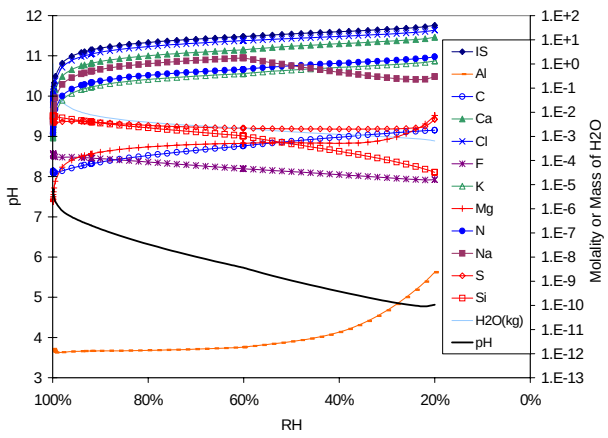

DTN: MO0304SPACSALT.000\01c4t1e.xls.xls

Figure II-01-5. Bin 01 Aqueous Composition Evaporation Predictions vs. Relative Humidity at 100ºC and 10^{-4} CO_2 Fugacity

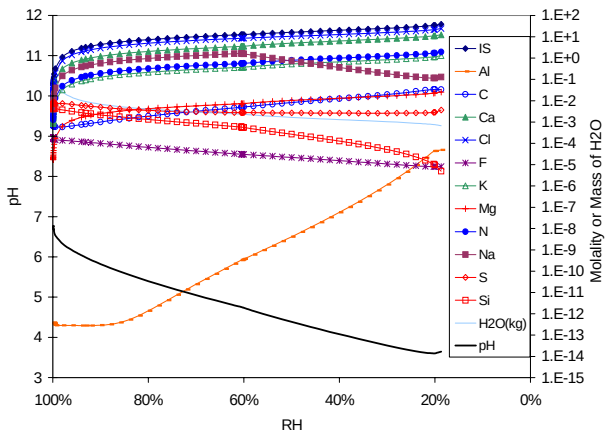

DTN: MO0304SPACSALT.000\01c2t7e.xls.xls

Figure II-01-7. Bin 01 Aqueous Composition Evaporation Predictions vs. Relative Humidity at 70ºC and 10^{-2} CO_2 Fugacity

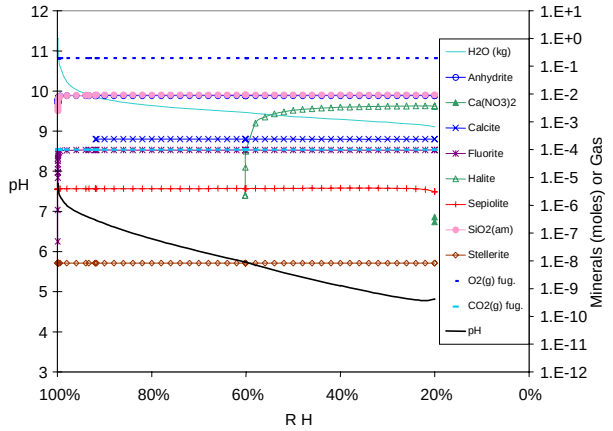

DTN: MO0304SPACSALT.000\01c4t1e.xls.xls

Figure II-01-6. Bin 01 Mineral Precipitation Evaporation Predictions vs. Relative Humidity at 100ºC and 10^{-4} CO_2 Fugacity

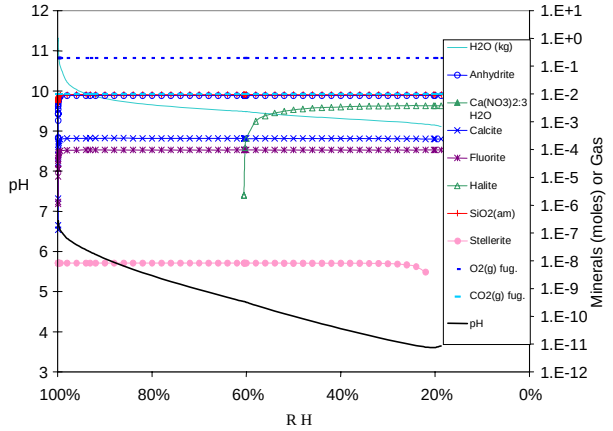

DTN: MO0304SPACSALT.000\01c2t7e.xls.xls

Figure II-01-8. Bin 01 Mineral Precipitation Evaporation Predictions vs. Relative Humidity at 70ºC and 10^{-2} CO_2 Fugacity

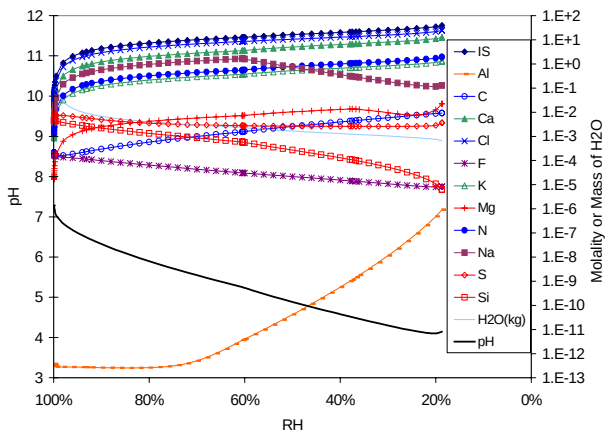

DTN: MO0304SPACSALT.000\01c3t7e.xls.xls

Figure II-01-9. Bin 01 Aqueous Composition Evaporation Predictions vs. Relative Humidity at 70ºC and 10^{-3} CO_2 Fugacity

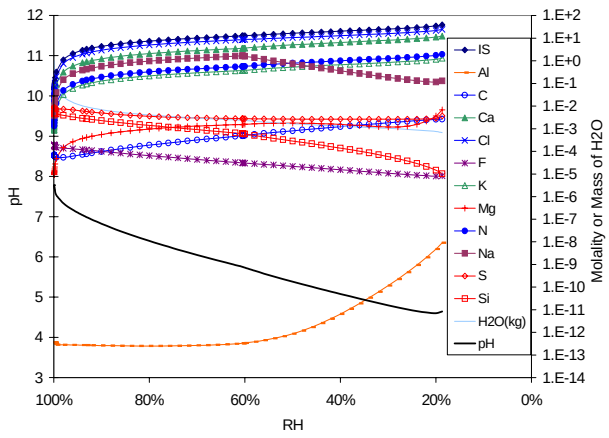

DTN: MO0304SPACSALT.000\01c4t7e.xls.xls

Figure II-01-11. Bin 01 Aqueous Composition Evaporation Predictions vs. Relative Humidity at 70ºC and 10^{-4} CO_2 Fugacity

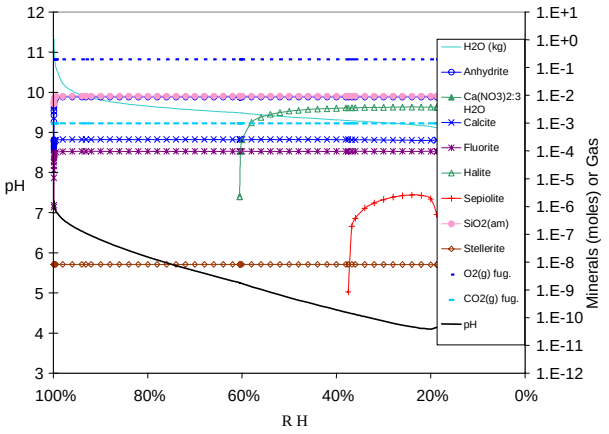

DTN: MO0304SPACSALT.000\01c3t7e.xls.xls

Figure II-01-10. Bin 01 Mineral Precipitation Evaporation Predictions vs. Relative Humidity at 70ºC and 10^{-3} CO_2 Fugacity

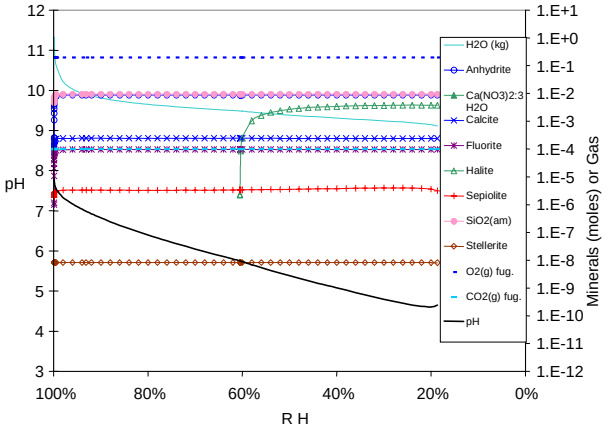

DTN: MO0304SPACSALT.000\01c4t7e.xls.xls

Figure II-01-12. Bin 01 Mineral Precipitation Evaporation Predictions vs. Relative Humidity at 70ºC and 10^{-4} CO_2 Fugacity

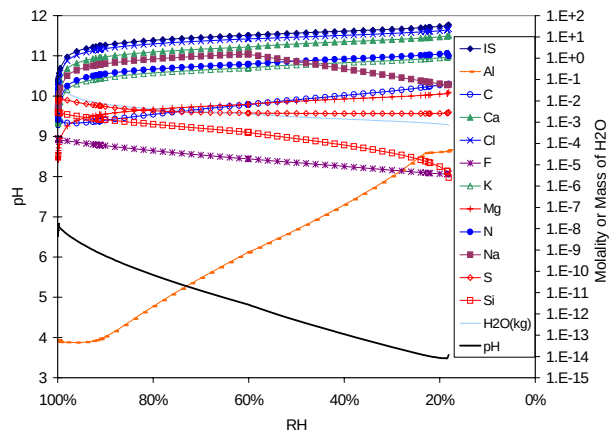

DTN: MO0304SPACSALT.000\01c2t4e.xls.xls

Figure II-01-13. Bin 01 Aqueous Composition Evaporation Predictions vs. Relative Humidity at 40ºC and 10^{-2} CO_2 Fugacity

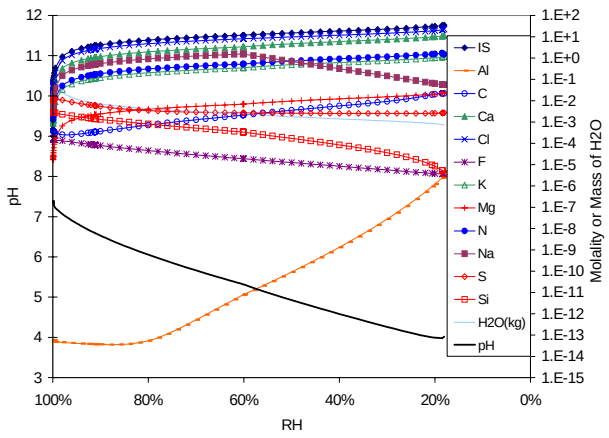

DTN: MO0304SPACSALT.000\01c3t4e.xls.xls

Figure II-01-15. Bin 01 Aqueous Composition Evaporation Predictions vs. Relative Humidity at 40ºC and 10^{-3} CO_2 Fugacity

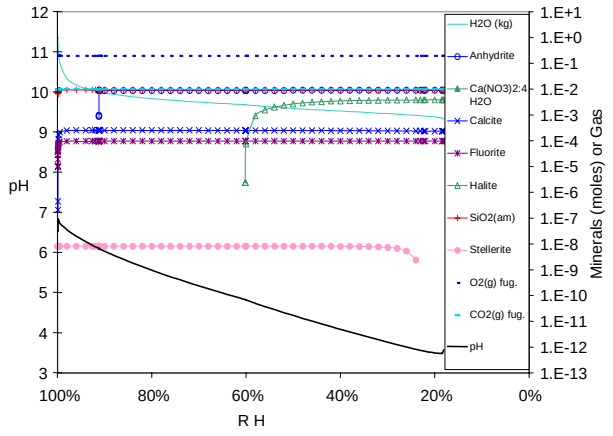

DTN: MO0304SPACSALT.000\01c2t4e.xls.xls

Figure II-01-14. Bin 01 Mineral Precipitation Evaporation Predictions vs. Relative Humidity at 40ºC and 10^{-2} CO_2 Fugacity

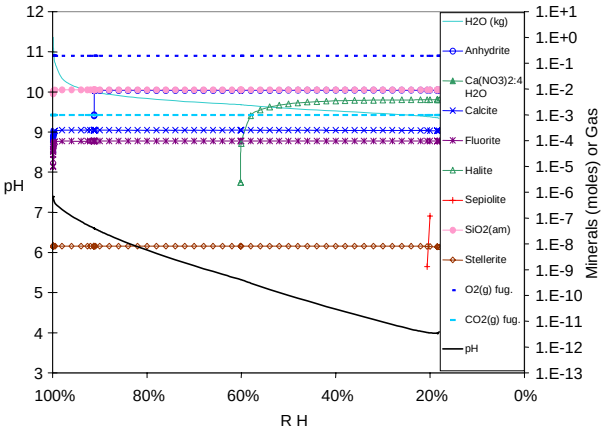

DTN: MO0304SPACSALT.000\01c3t4e.xls.xls

Figure II-01-16. Bin 01 Mineral Precipitation Evaporation Predictions vs. Relative Humidity at 40ºC and 10^{-3} CO_2 Fugacity

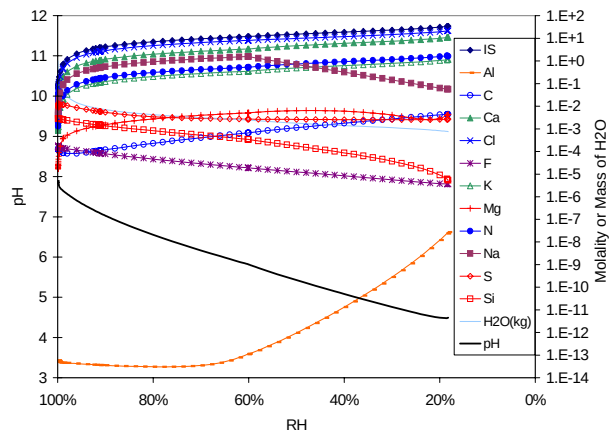

DTN: MO0304SPACSALT.000\01c4t4e.xls.xls

Figure II-01-17. Bin 01 Aqueous Composition Evaporation Predictions vs. Relative Humidity at 40ºC and 10^{-4} CO_2 Fugacity

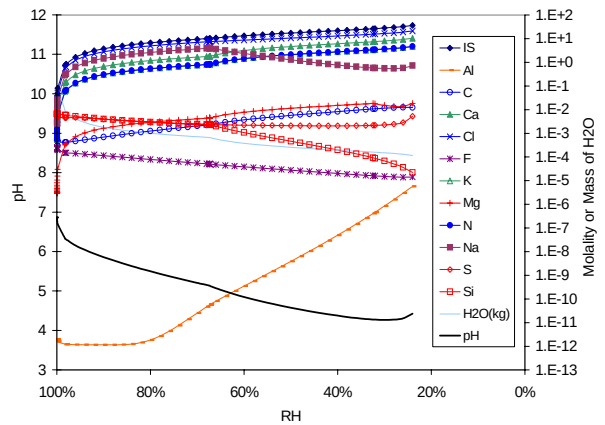

DTN: MO0304SPACSALT.000\02c2t1e.xls.xls

Figure II-02-1. Bin 02 Aqueous Composition Evaporation Predictions vs. Relative Humidity at 100ºC and 10^{-2} CO_2 Fugacity

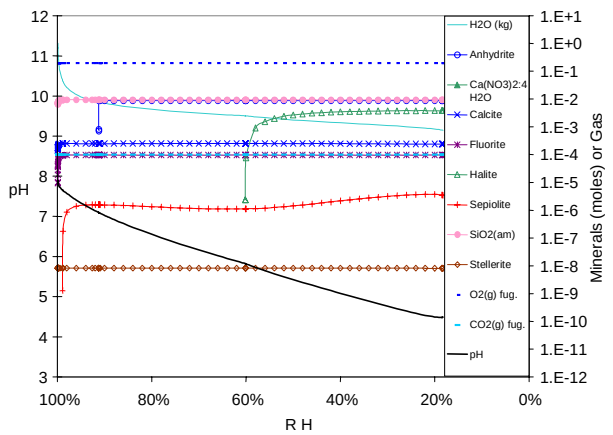

DTN: MO0304SPACSALT.000\01c4t4e.xls.xls

Figure II-01-18. Bin 01 Mineral Precipitation Evaporation Predictions vs. Relative Humidity at 40ºC and 10^{-4} CO_2 Fugacity

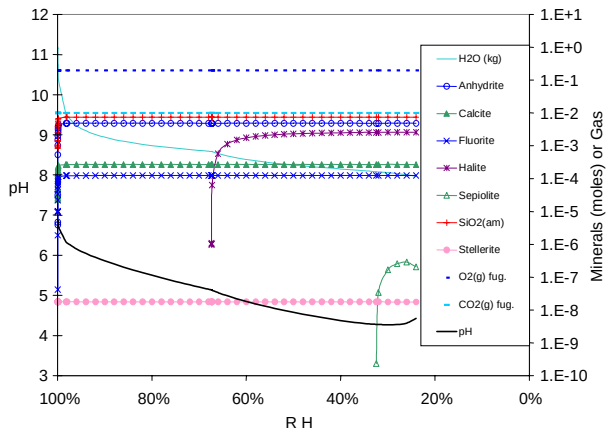

DTN: MO0304SPACSALT.000\02c2t1e.xls.xls

Figure II-02-2. Bin 02 Mineral Precipitation Evaporation Predictions vs. Relative Humidity at 100ºC and 10^{-2} CO_2 Fugacity

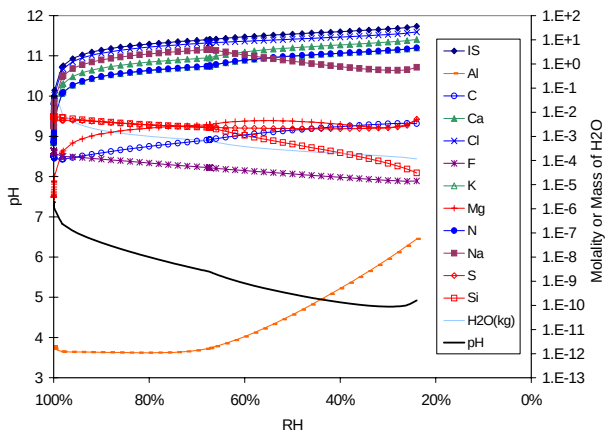

DTN: MO0304SPACSALT.000\02c3t1e.xls.xls

Figure II-02-3. Bin 02 Aqueous Composition Evaporation Predictions vs. Relative Humidity at 100ºC and 10^{-3} CO_2 Fugacity

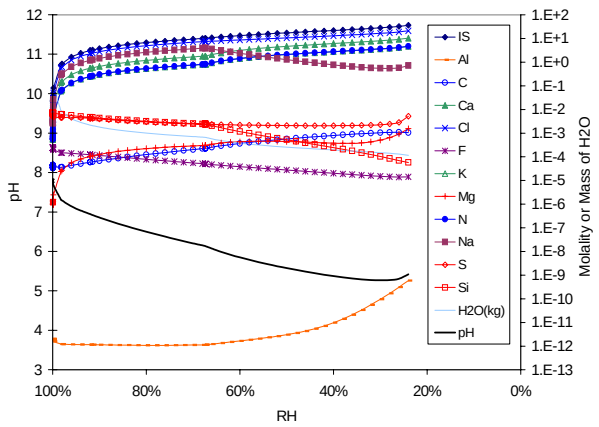

DTN: MO0304SPACSALT.000\02c4t1e.xls.xls

Figure II-02-5. Bin 02 Aqueous Composition Evaporation Predictions vs. Relative Humidity at 100ºC and 10^{-4} CO_2 Fugacity

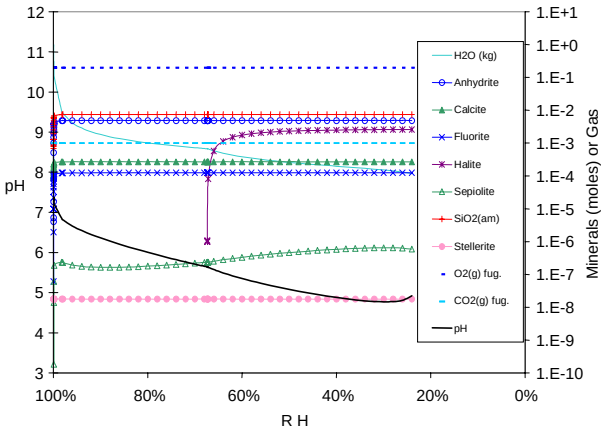

DTN: MO0304SPACSALT.000\02c3t1e.xls.xls

Figure II-02-4. Bin 02 Mineral Precipitation Evaporation Predictions vs. Relative Humidity at 100ºC and 10^{-3} CO_2 Fugacity

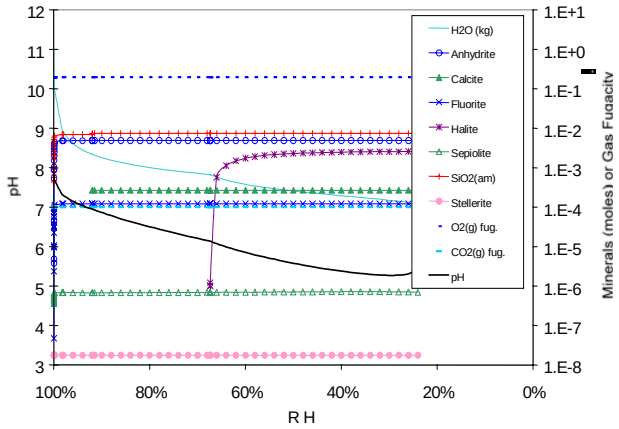

DTN: MO0304SPACSALT.000\02c4t1e.xls.xls

Figure II-02-6. Bin 02 Mineral Precipitation Evaporation Predictions vs. Relative Humidity at 100ºC and 10^{-4} CO_2 Fugacity

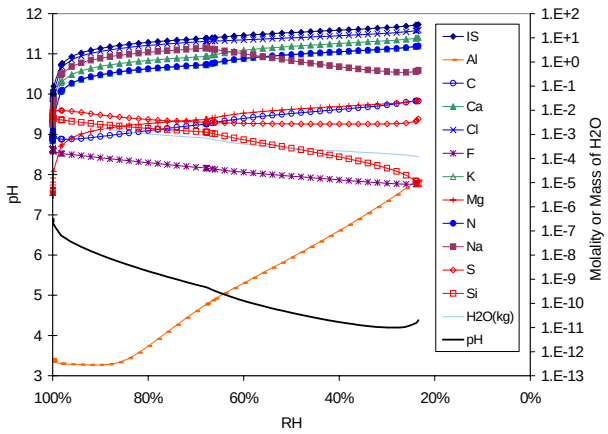

DTN: MO0304SPACSALT.000\02c2t7e.xls.xls

Figure II-02-7. Bin 02 Aqueous Composition Evaporation Predictions vs. Relative Humidity at 70ºC and 10^{-2} CO_2 Fugacity

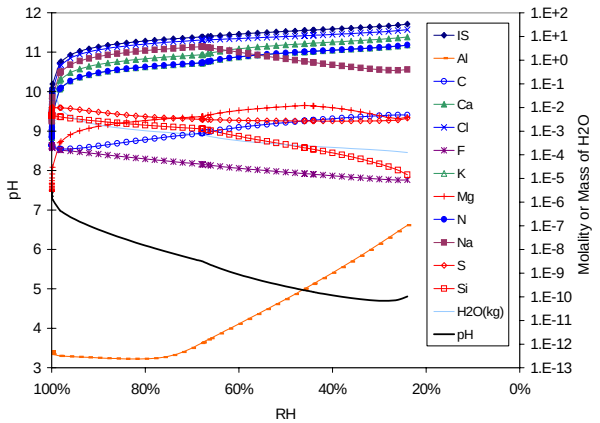

DTN: MO0304SPACSALT.000\02c3t7e.xls.xls

Figure II-02-9. Bin 02 Aqueous Composition Evaporation Predictions vs. Relative Humidity at 70ºC and 10^{-3} CO_2 Fugacity

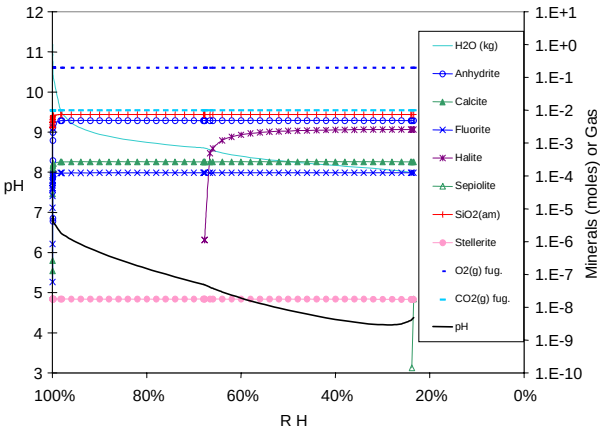

DTN: MO0304SPACSALT.000\02c2t7e.xls.xls

Figure II-02-8. Bin 02 Mineral Precipitation Evaporation Predictions vs. Relative Humidity at 70ºC and 10^{-2} CO_2 Fugacity

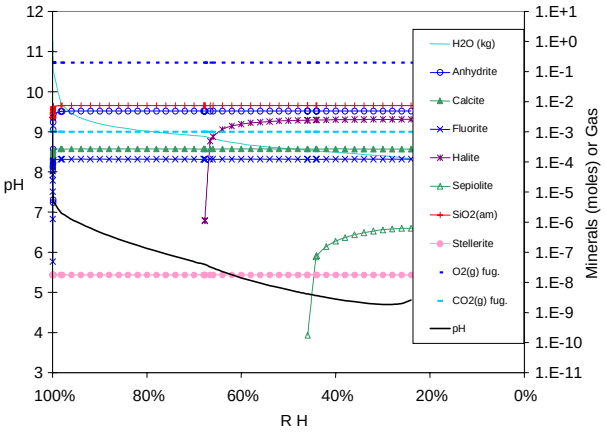

DTN: MO0304SPACSALT.000\02c3t7e.xls.xls

Figure II-02-10. Bin 02 Mineral Precipitation Evaporation Predictions vs. Relative Humidity at 70ºC and 10^{-3} CO_2 Fugacity

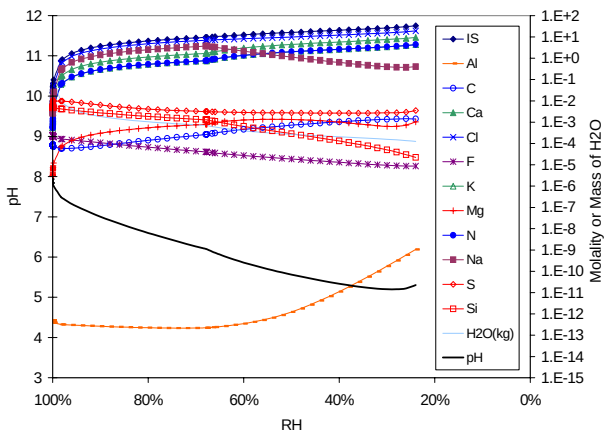

DTN: MO0304SPACSALT.000\02c4t7e.xls.xls

Figure II-02-11. Bin 02 Aqueous Composition Evaporation Predictions vs. Relative Humidity at 70ºC and 10^{-4} CO_2 Fugacity

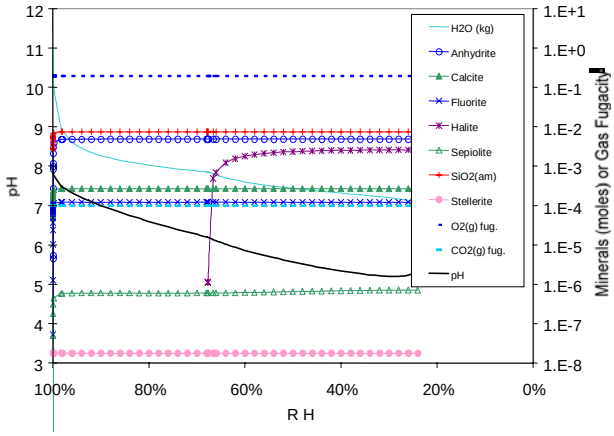

DTN: MO0304SPACSALT.000\02c4t7e.xls.xls

Figure II-02-12. Bin 02 Mineral Precipitation Evaporation Predictions vs. Relative Humidity at 70ºC and 10^{-4} CO_2 Fugacity

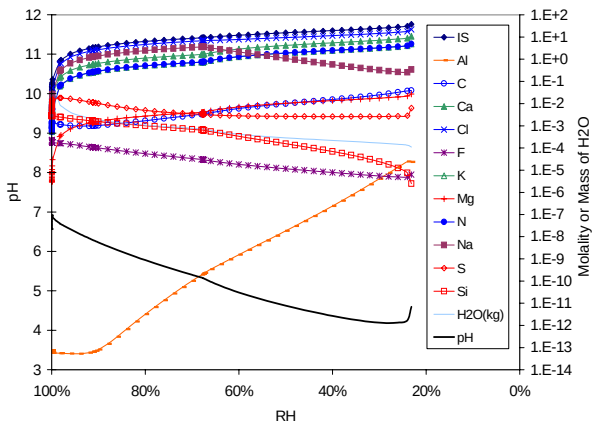

DTN: MO0304SPACSALT.000\02c2t4e.xls.xls

Figure II-02-13. Bin 02 Aqueous Composition Evaporation Predictions vs. Relative Humidity at 40ºC and 10^{-2} CO_2 Fugacity

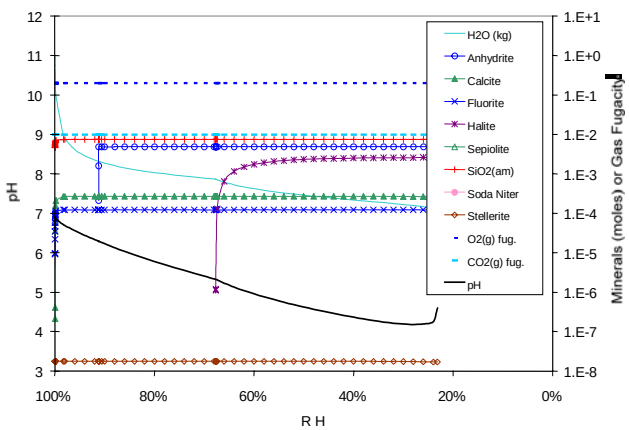

DTN: MO0304SPACSALT.000\02c2t4e.xls.xls

Figure II-02-14. Bin 02 Mineral Precipitation Evaporation Predictions vs. Relative Humidity at 40ºC and 10^{-2} CO_2 Fugacity

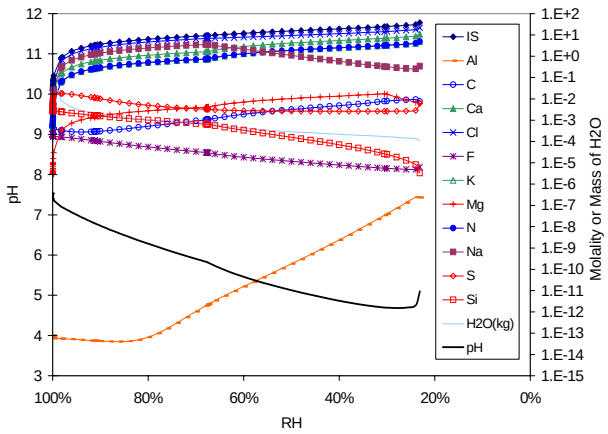

DTN: MO0304SPACSALT.000\02c3t4e.xls.xls

Figure II-02-15. Bin 02 Aqueous Composition Evaporation Predictions vs. Relative Humidity at 40ºC and 10^{-3} CO_2 Fugacity

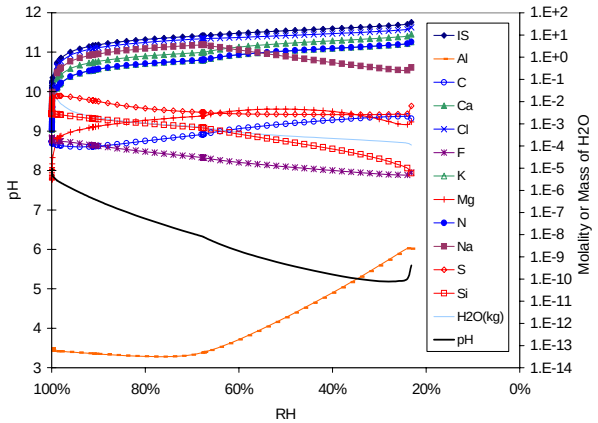

DTN: MO0304SPACSALT.000\02c4t4e.xls.xls

Figure II-02-17. Bin 02 Aqueous Composition Evaporation Predictions vs. Relative Humidity at 40ºC and 10^{-4} CO_2 Fugacity

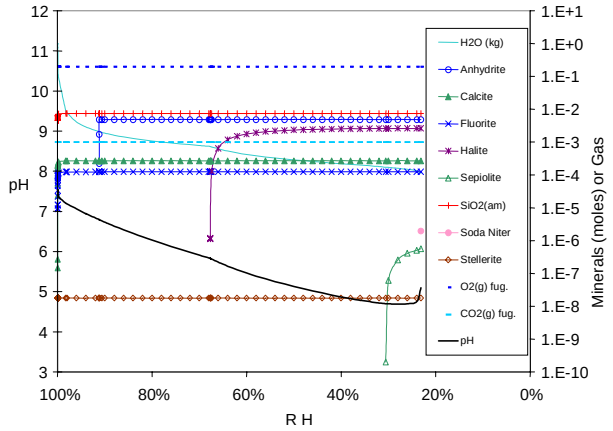

DTN: MO0304SPACSALT.000\02c3t4e.xls.xls

Figure II-02-16. Bin 02 Mineral Precipitation Evaporation Predictions vs. Relative Humidity at 40ºC and 10^{-3} CO_2 Fugacity

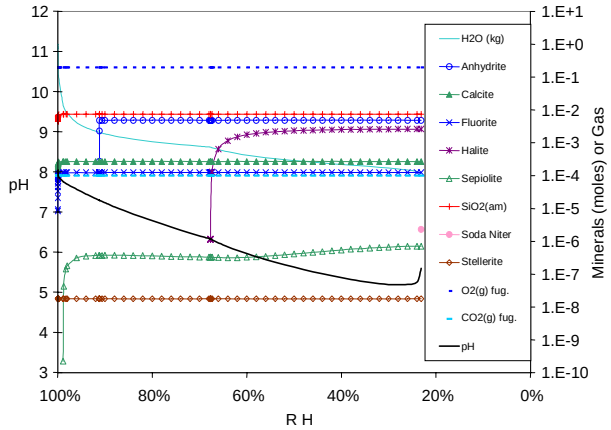

DTN: MO0304SPACSALT.000\02c4t4e.xls.xls

Figure II-02-18. Bin 02 Mineral Precipitation Evaporation Predictions vs. Relative Humidity at 40ºC and 10^{-4} CO_2 Fugacity

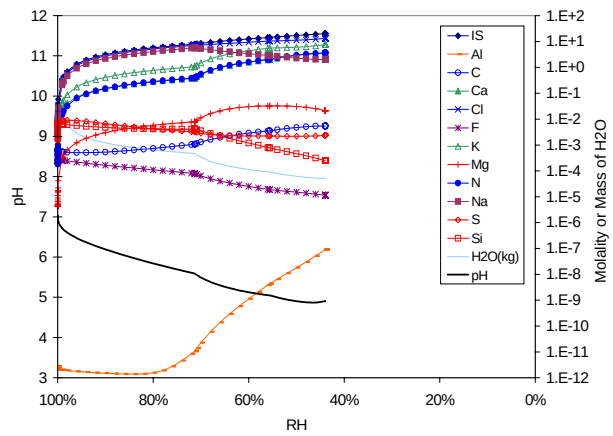

DTN: MO0304SPACSALT.000\03c2t1e.xls.xls

Figure II-03-1. Bin 03 Aqueous Composition Evaporation Predictions vs. Relative Humidity at 100ºC and 10^{-2} CO_2 Fugacity

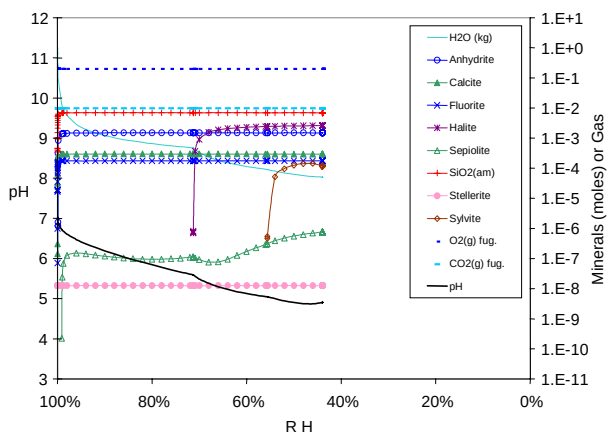

DTN: MO0304SPACSALT.000\03c2t1e.xls.xls

Figure II-03-2. Bin 03 Mineral Precipitation Evaporation Predictions vs. Relative Humidity at 100ºC and 10^{-2} CO_2 Fugacity

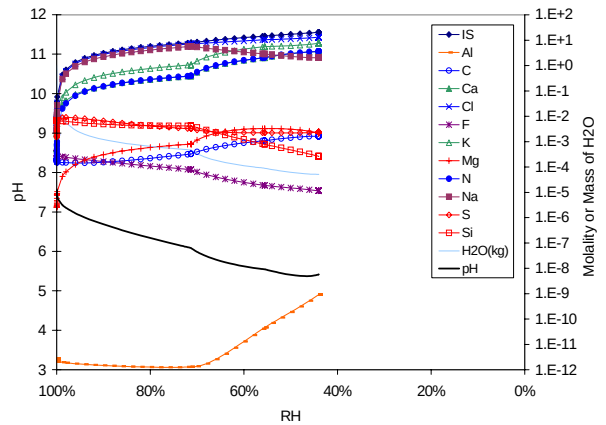

DTN: MO0304SPACSALT.000\03c3t1e.xls.xls

Figure II-03-3. Bin 03 Aqueous Composition Evaporation Predictions vs. Relative Humidity at 100ºC and 10^{-3} CO_2 Fugacity

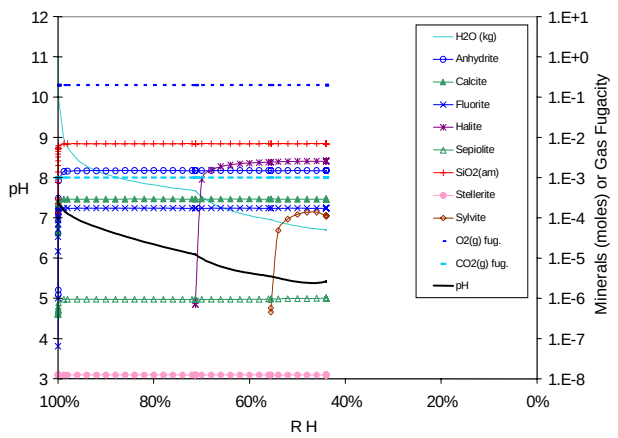

DTN: MO0304SPACSALT.000\03c3t1e.xls.xls

Figure II-03-4. Bin 03 Mineral Precipitation Evaporation Predictions vs. Relative Humidity at 100ºC and 10^{-3} CO_2 Fugacity

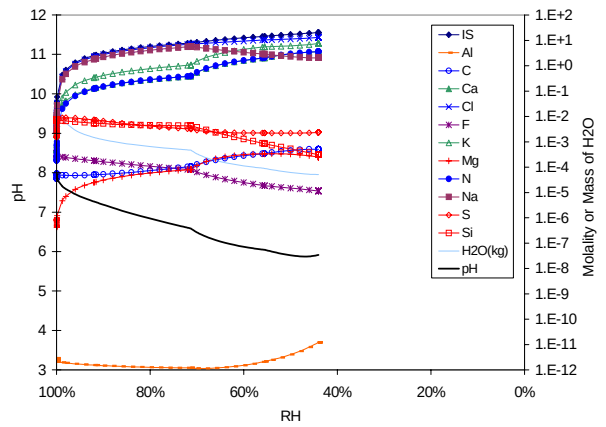

DTN: MO0304SPACSALT.000\03c4t1e.xls.xls

Figure II-03-5. Bin 03 Aqueous Composition Evaporation Predictions vs. Relative Humidity at 100ºC and 10^{-4} CO_2 Fugacity

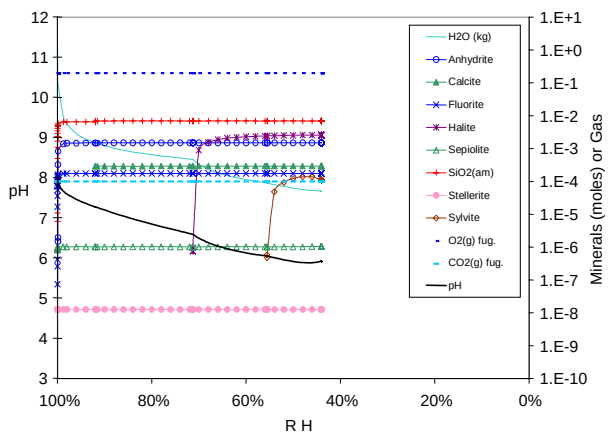

DTN: MO0304SPACSALT.000\03c4t1e.xls.xls

Figure II-03-6. Bin 03 Mineral Precipitation Evaporation Predictions vs. Relative Humidity at 100ºC and 10^{-4} CO_2 Fugacity

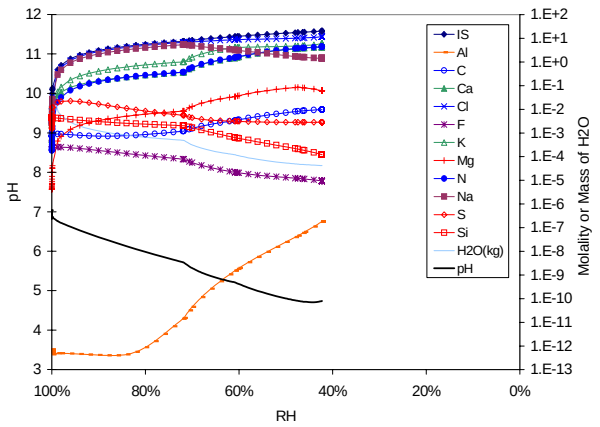

DTN: MO0304SPACSALT.000\03c2t7e.xls.xls

Figure II-03-7. Bin 03 Aqueous Composition Evaporation Predictions vs. Relative Humidity at 70ºC and 10^{-2} CO_2 Fugacity

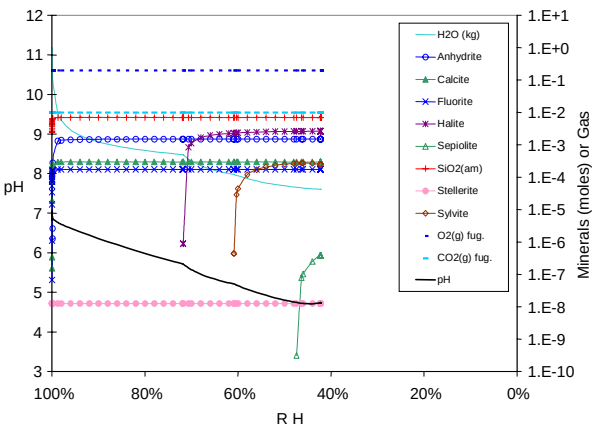

DTN: MO0304SPACSALT.000\03c2t7e.xls.xls

Figure II-03-8. Bin 03 Mineral Precipitation Evaporation Predictions vs. Relative Humidity at 70ºC and 10^{-2} CO_2 Fugacity

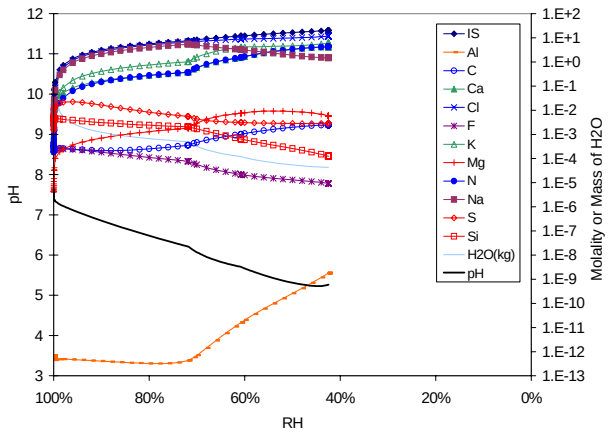

DTN: MO0304SPACSALT.000\03c3t7e.xls.xls

Figure II-03-9. Bin 03 Aqueous Composition Evaporation Predictions vs. Relative Humidity at 70ºC and 10^{-3} CO_2 Fugacity

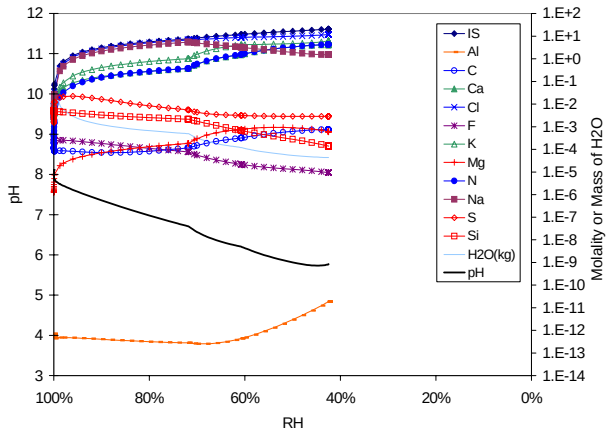

DTN: MO0304SPACSALT.000\03c4t7e.xls.xls

Figure II-03-11. Bin 03 Aqueous Composition Evaporation Predictions vs. Relative Humidity at 70ºC and 10^{-4} CO_2 Fugacity

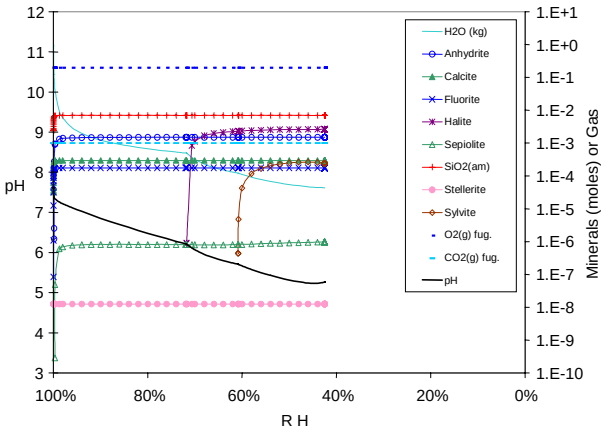

DTN: MO0304SPACSALT.000\03c3t7e.xls.xls

Figure II-03-10. Bin 03 Mineral Precipitation Evaporation Predictions vs. Relative Humidity at 70ºC and 10^{-3} CO_2 Fugacity

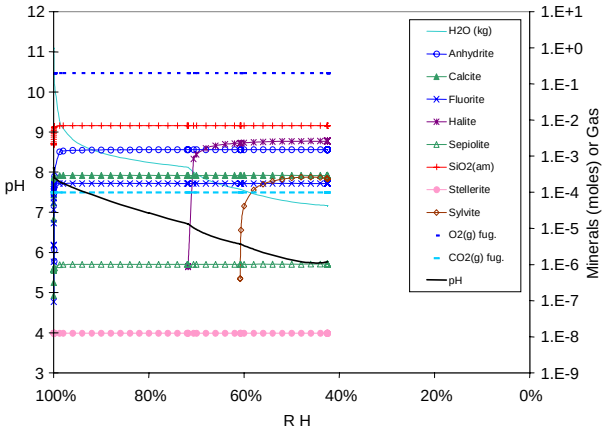

DTN: MO0304SPACSALT.000\03c4t7e.xls.xls

Figure II-03-12. Bin 03 Mineral Precipitation Evaporation Predictions vs. Relative Humidity at 70ºC and 10^{-4} CO_2 Fugacity

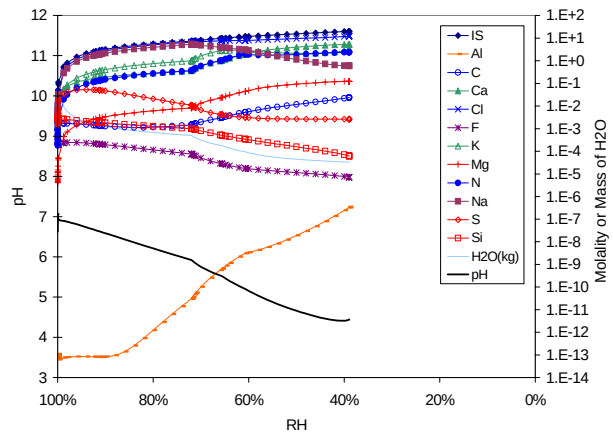

DTN: MO0304SPACSALT.000\03c2t4e.xls.xls

Figure II-03-13. Bin 03 Aqueous Composition Evaporation Predictions vs. Relative Humidity at 40ºC and 10^{-2} CO_2 Fugacity

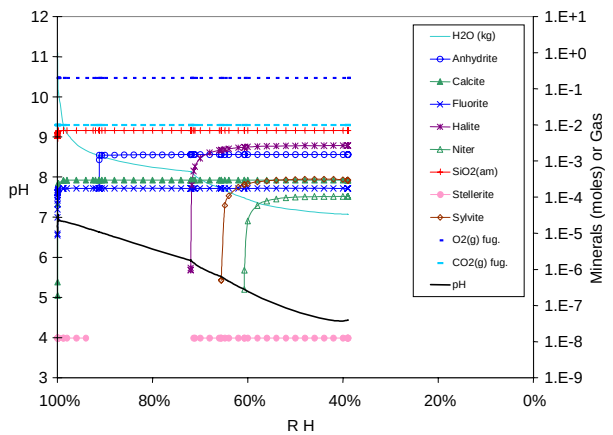

DTN: MO0304SPACSALT.000\03c2t4e.xls.xls

Figure II-03-14. Bin 03 Mineral Precipitation Evaporation Predictions vs. Relative Humidity at 40ºC and 10^{-2} CO_2 Fugacity

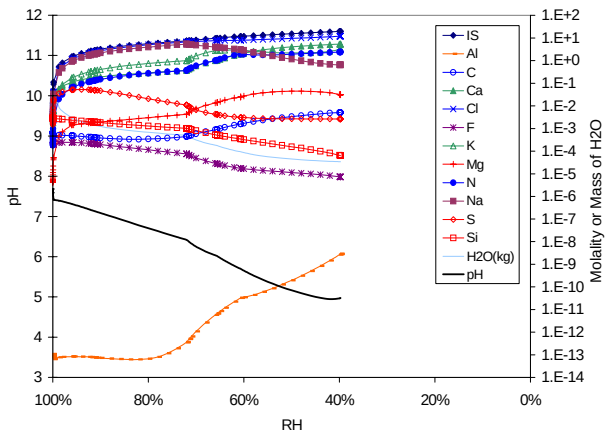

DTN: MO0304SPACSALT.000\03c3t4e.xls.xls

Figure II-03-15. Bin 03 Aqueous Composition Evaporation Predictions vs. Relative Humidity at 40ºC and 10^{-3} CO_2 Fugacity

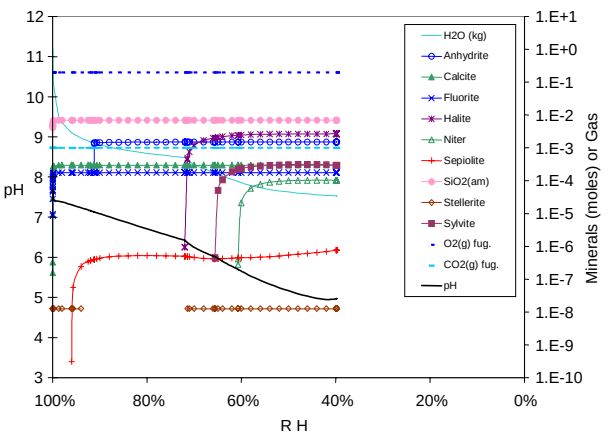

DTN: MO0304SPACSALT.000\03c3t4e.xls.xls

Figure II-03-16. Bin 03 Mineral Precipitation Evaporation Predictions vs. Relative Humidity at 40ºC and 10^{-3} CO_2 Fugacity

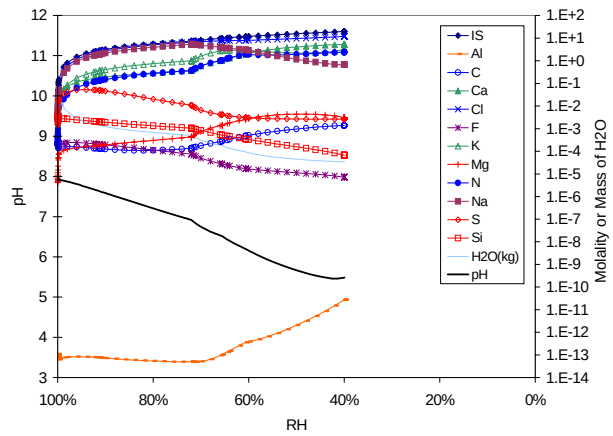

DTN: MO0304SPACSALT.000\03c4t4e.xls.xls

Figure II-03-17. Bin 03 Aqueous Composition Evaporation Predictions vs. Relative Humidity at 40ºC and 10^{-4} CO_2 Fugacity

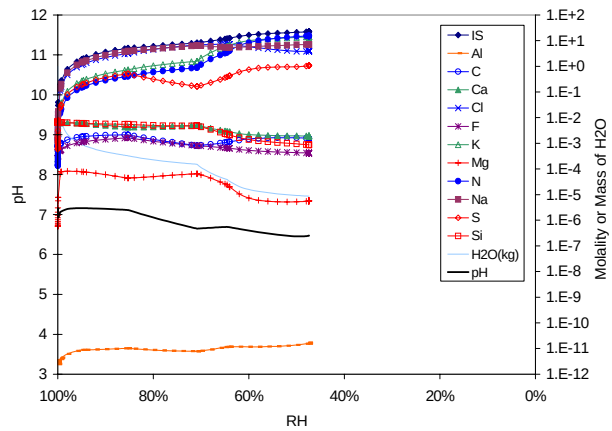

DTN: MO0304SPACSALT.000\04c2t1e.xls.xls

Figure II-04-1. Bin 04 Aqueous Composition Evaporation Predictions vs. Relative Humidity at 100ºC and 10^{-2} CO_2 Fugacity

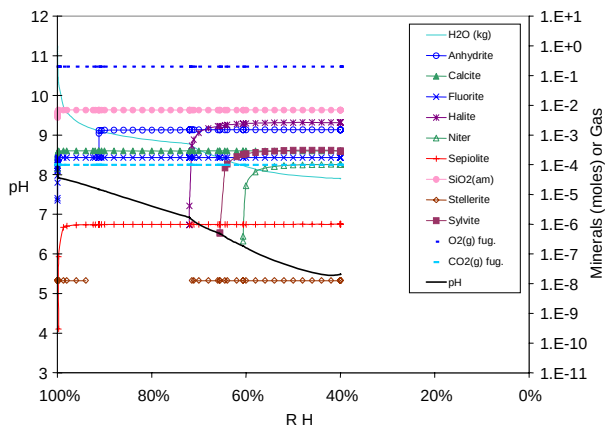

DTN: MO0304SPACSALT.000\03c4t4e.xls.xls

Figure II-03-18. Bin 03 Mineral Precipitation Evaporation Predictions vs. Relative Humidity at 40ºC and 10^{-4} CO_2 Fugacity

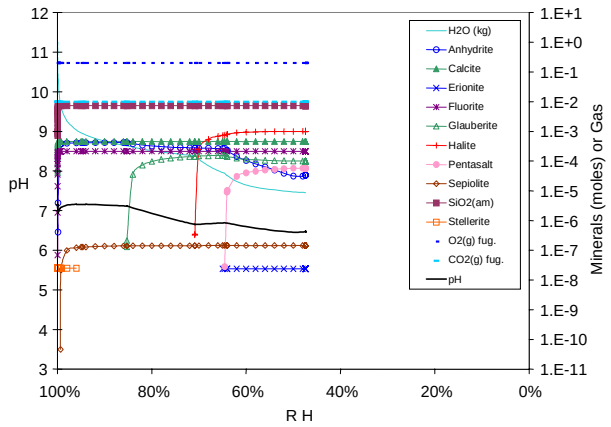

DTN: MO0304SPACSALT.000\04c2t1e.xls.xls

Figure II-04-2. Bin 04 Mineral Precipitation Evaporation Predictions vs. Relative Humidity at 100ºC and 10^{-2} CO_2 Fugacity

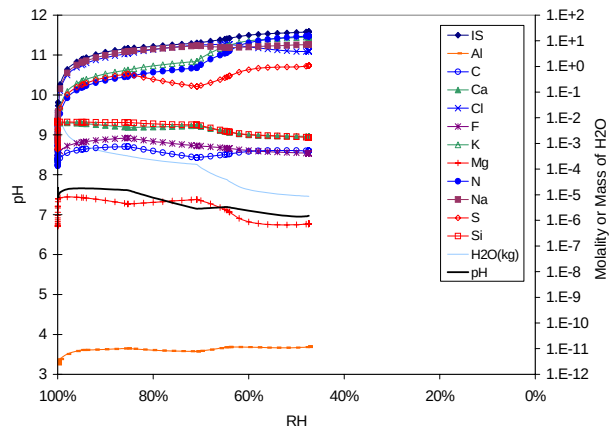

DTN: MO0304SPACSALT.000\04c3t1e.xls.xls

Figure II-04-3. Bin 04 Aqueous Composition Evaporation Predictions vs. Relative Humidity at 100ºC and 10^{-3} CO_2 Fugacity

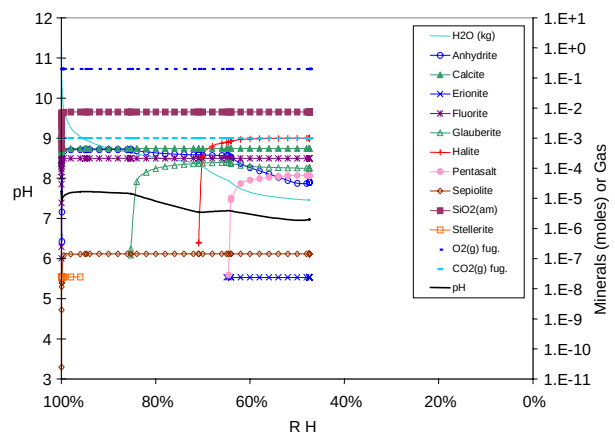

DTN: MO0304SPACSALT.000\04c3t1e.xls.xls

Figure II-04-4. Bin 04 Mineral Precipitation Evaporation Predictions vs. Relative Humidity at 100ºC and 10^{-3} CO_2 Fugacity

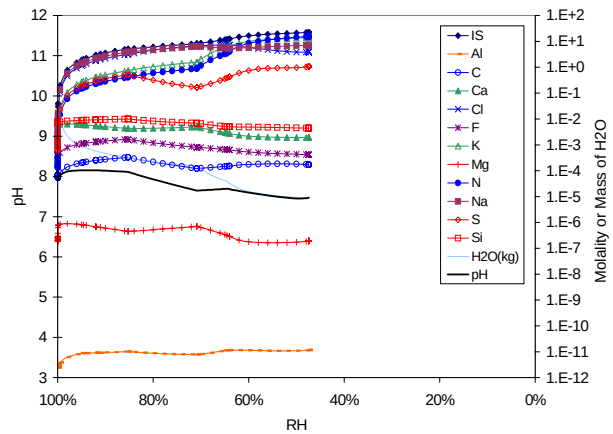

DTN: MO0304SPACSALT.000\04c4t1e.xls.xls

Figure II-04-5. Bin 04 Aqueous Composition Evaporation Predictions vs. Relative Humidity at 100ºC and 10^{-4} CO_2 Fugacity

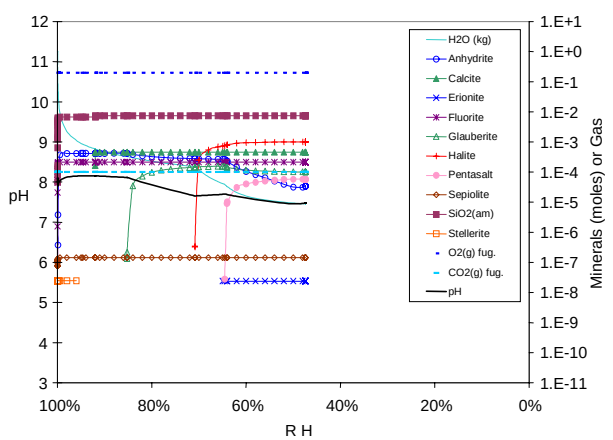

DTN: MO0304SPACSALT.000\04c4t1e.xls.xls

Figure II-04-6. Bin 04 Mineral Precipitation Evaporation Predictions vs. Relative Humidity at 100ºC and 10^{-4} CO_2 Fugacity

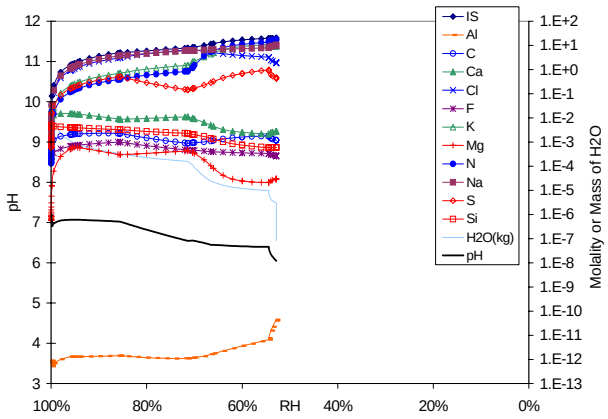

DTN: MO0304SPACSALT.000\04c2t7e.xls.xls

Figure II-04-7. Bin 04 Aqueous Composition Evaporation Predictions vs. Relative Humidity at 70ºC and 10^{-2} CO_2 Fugacity

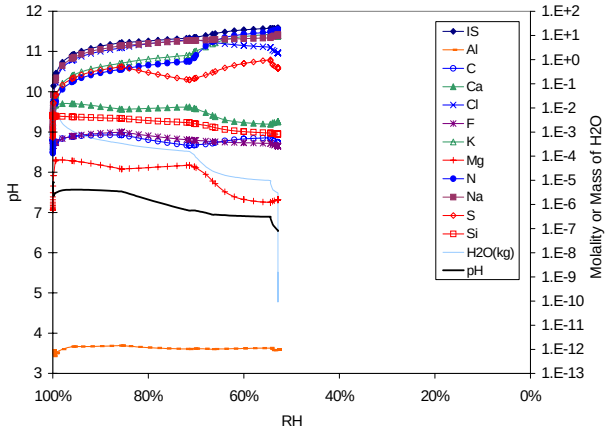

DTN: MO0304SPACSALT.000\04c3t7e.xls.xls

Figure II-04-9. Bin 04 Aqueous Composition Evaporation Predictions vs. Relative Humidity at 70ºC and 10^{-3} CO_2 Fugacity

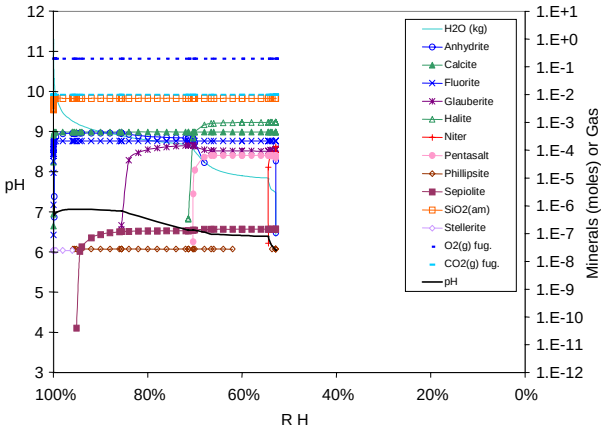

DTN: MO0304SPACSALT.000\04c2t7e.xls.xls

Figure II-04-8. Bin 04 Mineral Precipitation Evaporation Predictions vs. Relative Humidity at 70ºC and 10^{-2} CO_2 Fugacity

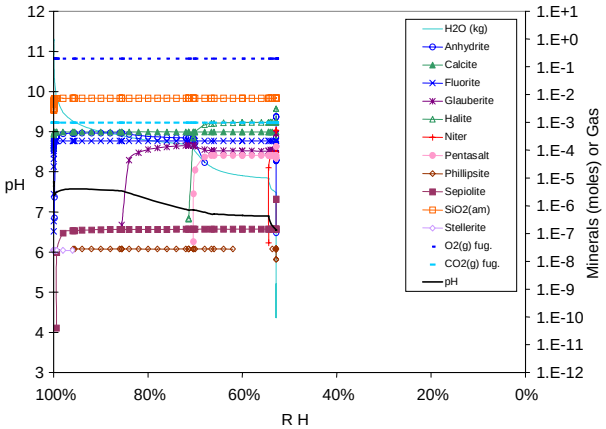

DTN: MO0304SPACSALT.000\04c3t7e.xls.xls

Figure II-04-10. Bin 04 Mineral Precipitation Evaporation Predictions vs. Relative Humidity at 70ºC and 10^{-3} CO_2 Fugacity

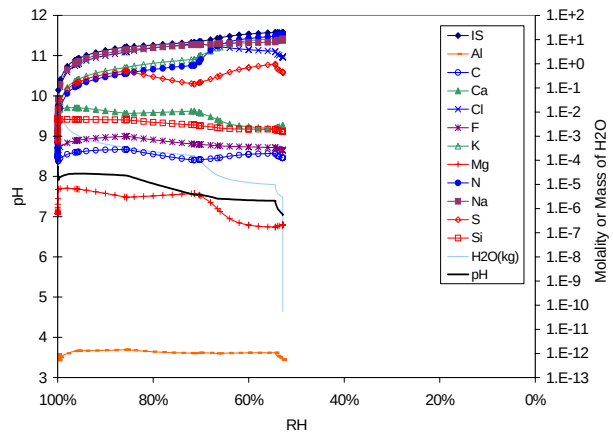

DTN: MO0304SPACSALT.000\04c4t7e.xls.xls

Figure II-04-11. Bin 04 Aqueous Composition Evaporation Predictions vs. Relative Humidity at 70ºC and 10^{-4} CO_2 Fugacity

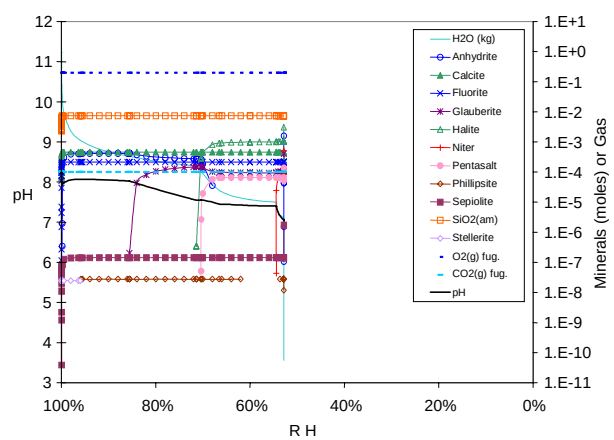

DTN: MO0304SPACSALT.000\04c4t7e.xls.xls

Figure II-04-12. Bin 04 Mineral Precipitation Evaporation Predictions vs. Relative Humidity at 70ºC and 10^{-4} CO_2 Fugacity

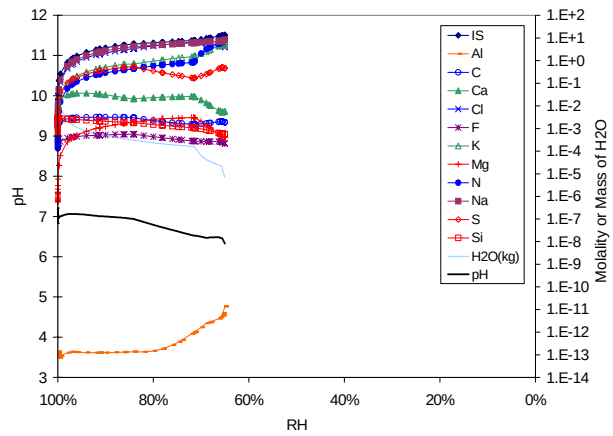

DTN: MO0304SPACSALT.000\04c2t4e.xls.xls

Figure II-04-13. Bin 04 Aqueous Composition Evaporation Predictions vs. Relative Humidity at 40ºC and 10^{-2} CO_2 Fugacity

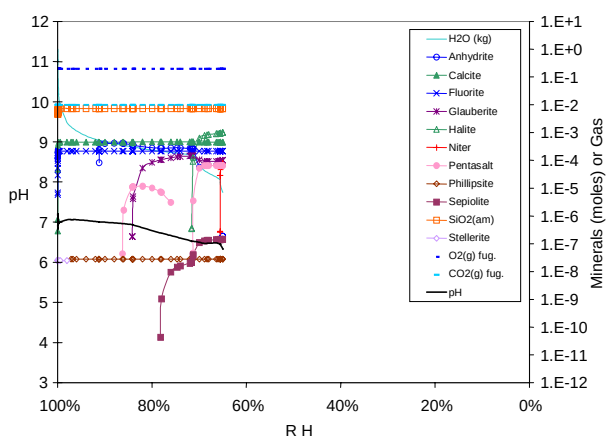

DTN: MO0304SPACSALT.000\04c2t4e.xls.xls

Figure II-04-14. Bin 04 Mineral Precipitation Evaporation Predictions vs. Relative Humidity at 40ºC and 10^{-2} CO_2 Fugacity

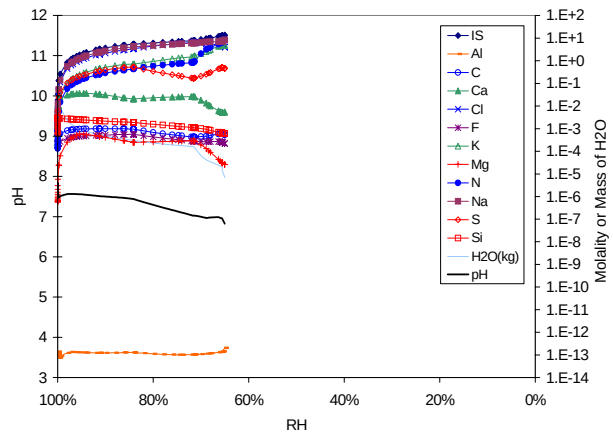

DTN: MO0304SPACSALT.000\04c3t4e.xls.xls

Figure II-04-15. Bin 04 Aqueous Composition Evaporation Predictions vs. Relative Humidity at 40ºC and 10^{-3} CO_2 Fugacity

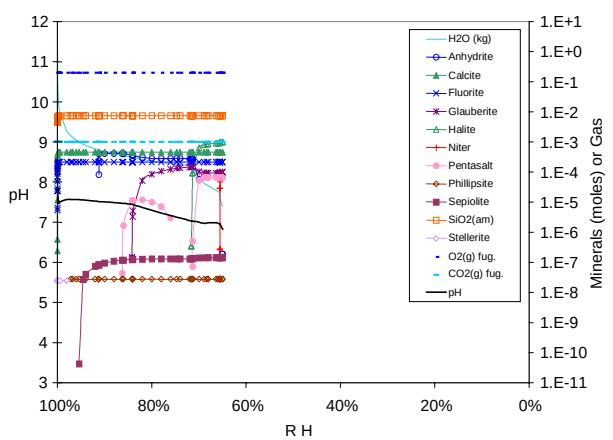

DTN: MO0304SPACSALT.000\04c3t4e.xls.xls

Figure II-04-16. Bin 04 Mineral Precipitation Evaporation Predictions vs. Relative Humidity at 40ºC and 10^{-3} CO_2 Fugacity

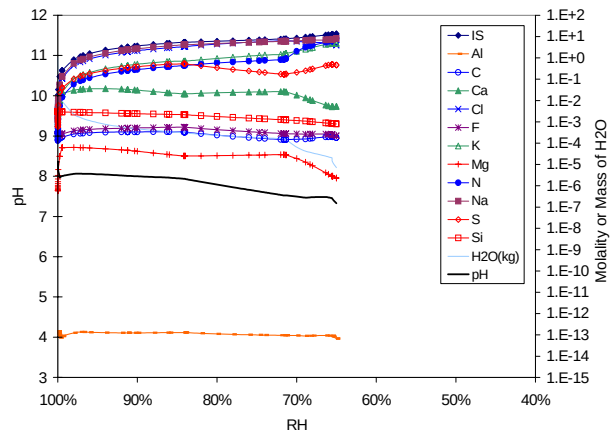

DTN: MO0304SPACSALT.000\04c4t4e.xls.xls

Figure II-04-17. Bin 04 Aqueous Composition Evaporation Predictions vs. Relative Humidity at 40ºC and 10^{-4} CO_2 Fugacity

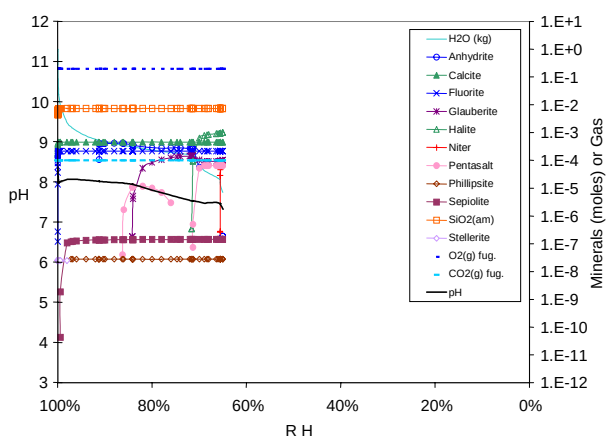

DTN: MO0304SPACSALT.000\04c4t4e.xls.xls

Figure II-04-18. Bin 04 Mineral Precipitation Evaporation Predictions vs. Relative Humidity at 40ºC and 10^{-4} CO_2 Fugacity

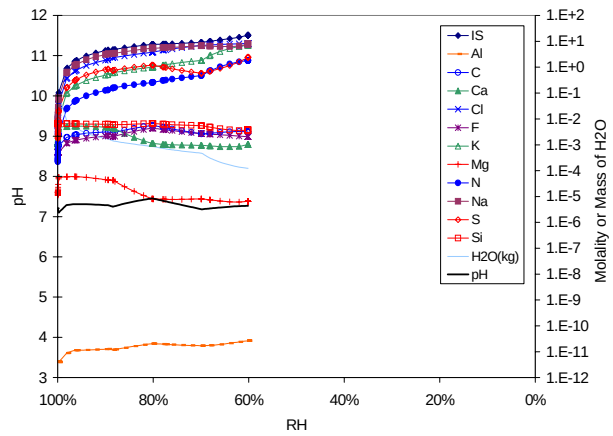

DTN: MO0304SPACSALT.000\05c2t1e.xls.xls

Figure II-05-1. Bin 05 Aqueous Composition Evaporation Predictions vs. Relative Humidity at 100ºC and 10^{-2} CO_2 Fugacity

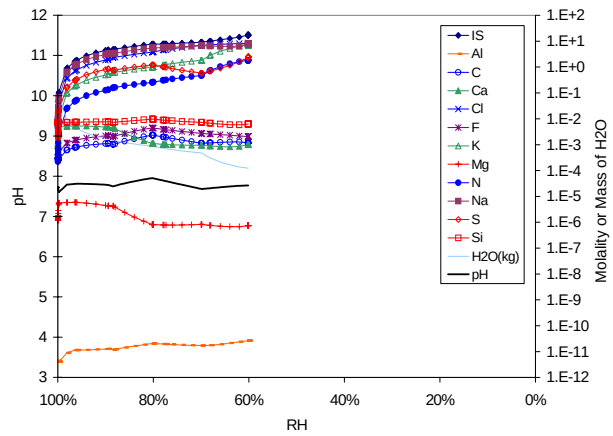

DTN: MO0304SPACSALT.000\05c3t1e.xls.xls

Figure II-05-3. Bin 05 Aqueous Composition Evaporation Predictions vs. Relative Humidity at 100ºC and 10^{-3} CO_2 Fugacity

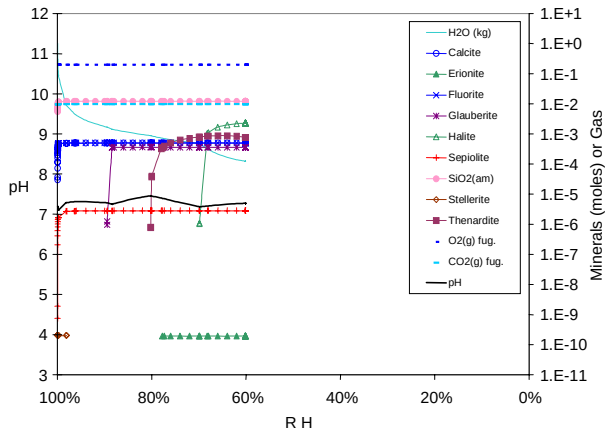

DTN: MO0304SPACSALT.000\05c2t1e.xls.xls

Figure II-05-2. Bin 05 Mineral Precipitation Evaporation Predictions vs. Relative Humidity at 100ºC and 10^{-2} CO_2 Fugacity

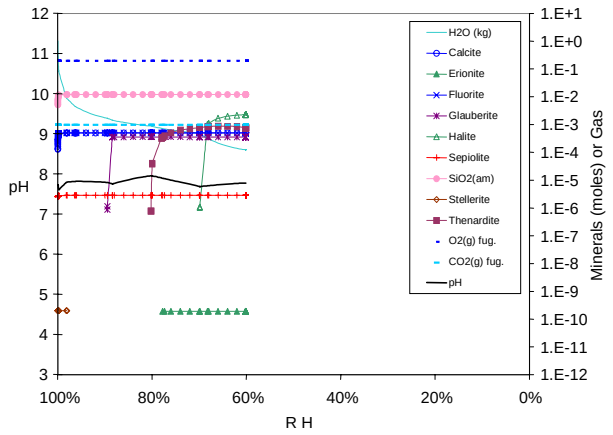

DTN: MO0304SPACSALT.000\05c3t1e.xls.xls

Figure II-05-4. Bin 05 Mineral Precipitation Evaporation Predictions vs. Relative Humidity at 100ºC and 10^{-3} CO_2 Fugacity

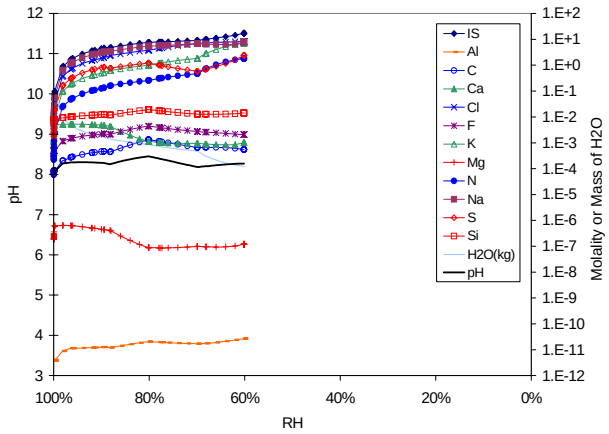

DTN: MO0304SPACSALT.000\05c4t1e.xls.xls

Figure II-05-5. Bin 05 Aqueous Composition Evaporation Predictions vs. Relative Humidity at 100ºC and 10^{-4} CO_2 Fugacity

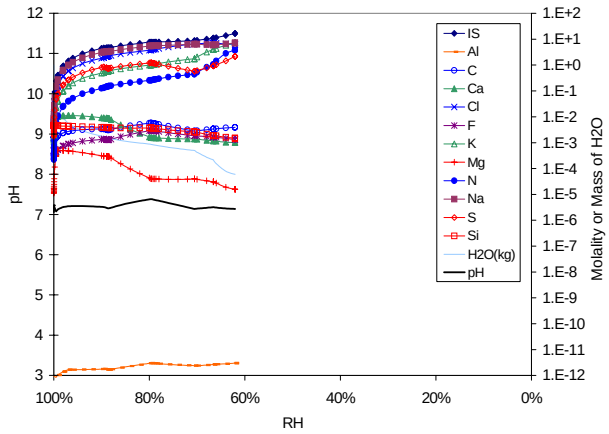

DTN: MO0304SPACSALT.000\05c2t7e.xls.xls

Figure II-05-7. Bin 05 Aqueous Composition Evaporation Predictions vs. Relative Humidity at 70ºC and 10^{-2} CO_2 Fugacity

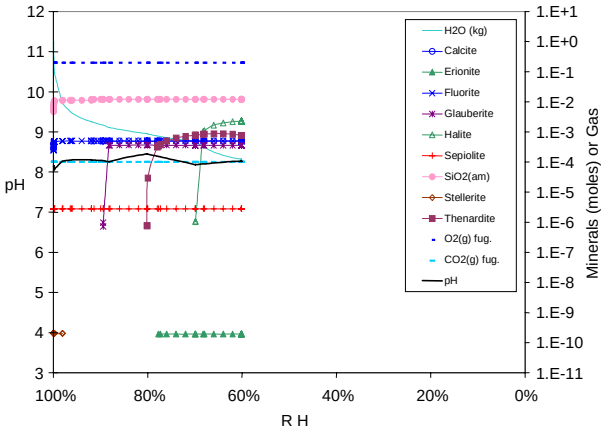

DTN: MO0304SPACSALT.000\05c4t1e.xls.xls

Figure II-05-6. Bin 05 Mineral Precipitation Evaporation Predictions vs. Relative Humidity at 100ºC and 10^{-4} CO_2 Fugacity

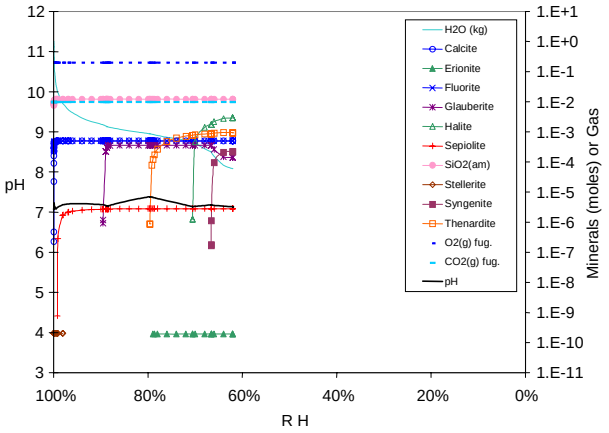

DTN: MO0304SPACSALT.000\05c2t7e.xls.xls

Figure II-05-8. Bin 05 Mineral Precipitation Evaporation Predictions vs. Relative Humidity at 70ºC and 10^{-2} CO_2 Fugacity

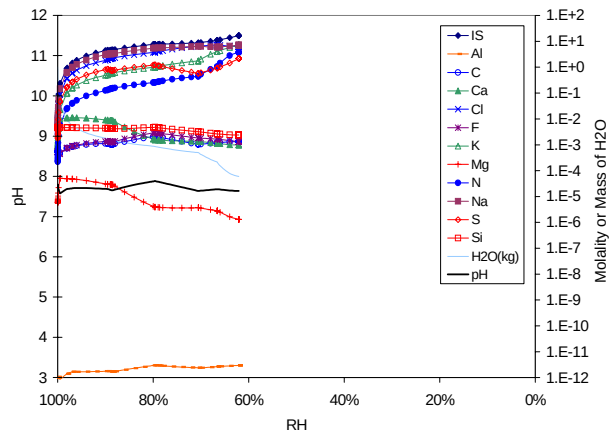

DTN: MO0304SPACSALT.000\05c3t7e.xls.xls

Figure II-05-9. Bin 05 Aqueous Composition Evaporation Predictions vs. Relative Humidity at 70ºC and 10^{-3} CO_2 Fugacity

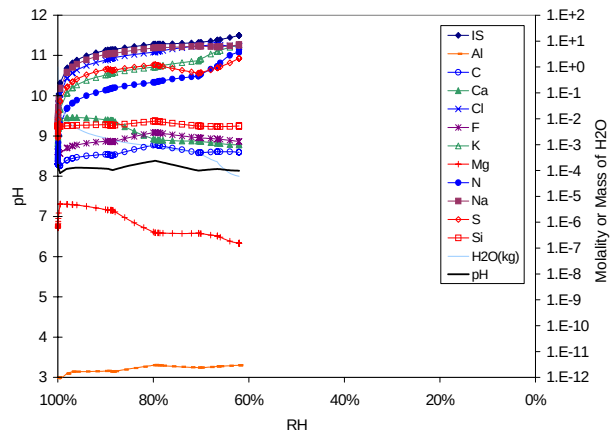

DTN: MO0304SPACSALT.000\05c4t7e.xls.xls

Figure II-05-11. Bin 05 Aqueous Composition Evaporation Predictions vs. Relative Humidity at 70ºC and 10^{-4} CO_2 Fugacity

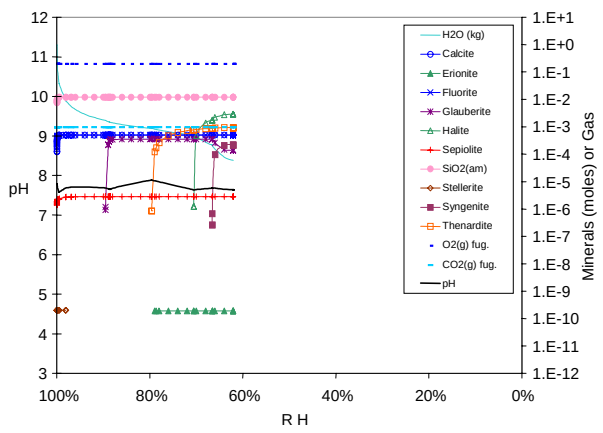

DTN: MO0304SPACSALT.000\05c3t7e.xls.xls

Figure II-05-10. Bin 05 Mineral Precipitation Evaporation Predictions vs. Relative Humidity at 70ºC and 10^{-3} CO_2 Fugacity

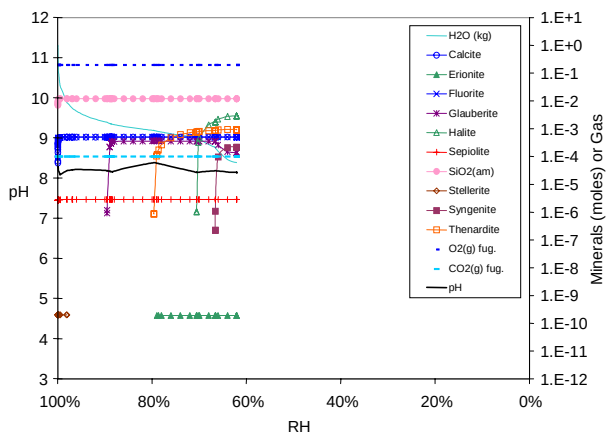

DTN: MO0304SPACSALT.000\05c4t7e.xls.xls

Figure II-05-12. Bin 05 Mineral Precipitation Evaporation Predictions vs. Relative Humidity at 70ºC and 10^{-4} CO_2 Fugacity

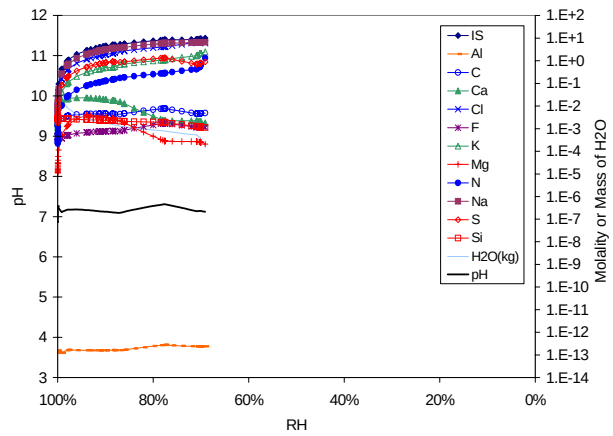

DTN: MO0304SPACSALT.000\05c2t4e.xls.xls

Figure II-05-13. Bin 05 Aqueous Composition Evaporation Predictions vs. Relative Humidity at 40ºC and 10^{-2} CO_2 Fugacity

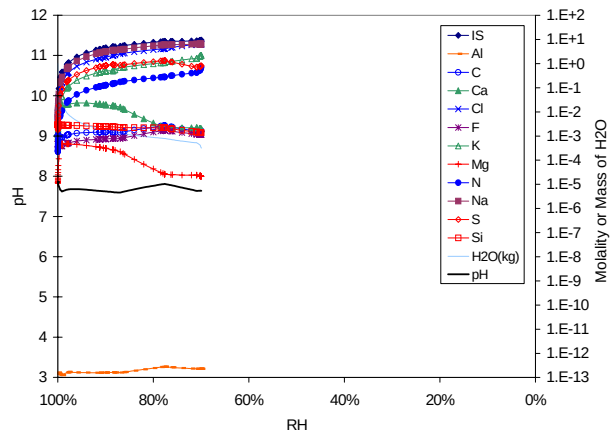

DTN: MO0304SPACSALT.000\05c3t4e.xls.xls

Figure II-05-15. Bin 05 Aqueous Composition Evaporation Predictions vs. Relative Humidity at 40ºC and 10^{-3} CO_2 Fugacity

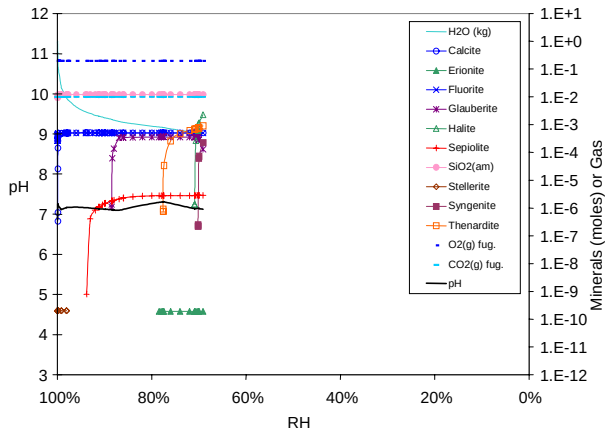

DTN: MO0304SPACSALT.000\05c2t4e.xls.xls

Figure II-05-14. Bin 05 Mineral Precipitation Evaporation Predictions vs. Relative Humidity at 40ºC and 10^{-2} CO_2 Fugacity

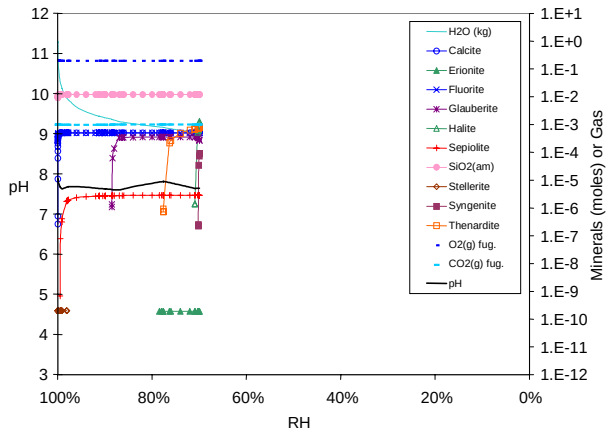

DTN: MO0304SPACSALT.000\05c3t4e.xls.xls

Figure II-05-16. Bin 05 Mineral Precipitation Evaporation Predictions vs. Relative Humidity at 40ºC and 10^{-3} CO_2 Fugacity

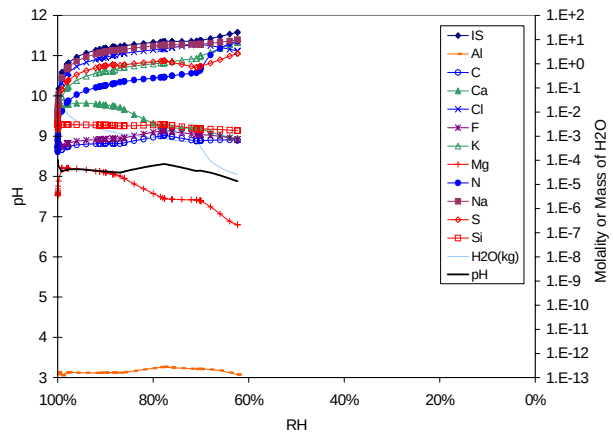

DTN: MO0304SPACSALT.000\05c4t4e.xls.xls

Figure II-05-17. Bin 05 Aqueous Composition Evaporation Predictions vs. Relative Humidity at 40ºC and 10^{-4} CO_2 Fugacity

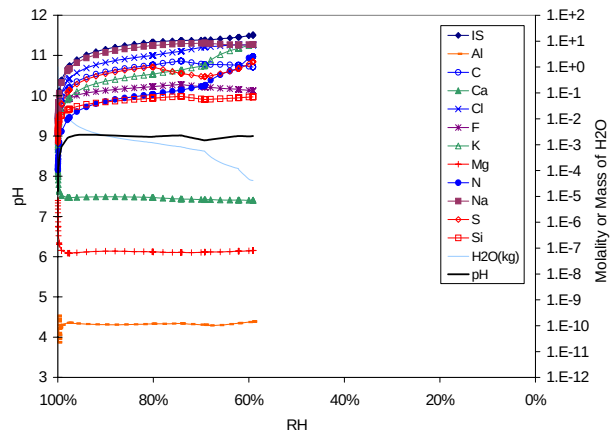

DTN: MO0304SPACSALT.000\06c2t1e.xls.xls

Figure II-06-1. Bin 06 Aqueous Composition Evaporation Predictions vs. Relative Humidity at 100ºC and 10^{-2} CO_2 Fugacity

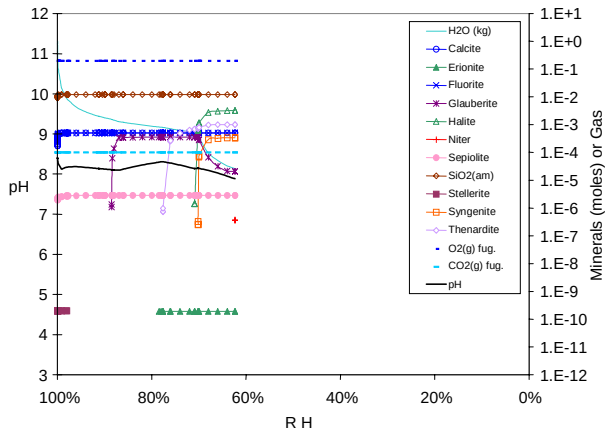

DTN: MO0304SPACSALT.000\05c4t4e.xls.xls

Figure II-05-18. Bin 05 Mineral Precipitation Evaporation Predictions vs. Relative Humidity at 40ºC and 10^{-4} CO_2 Fugacity

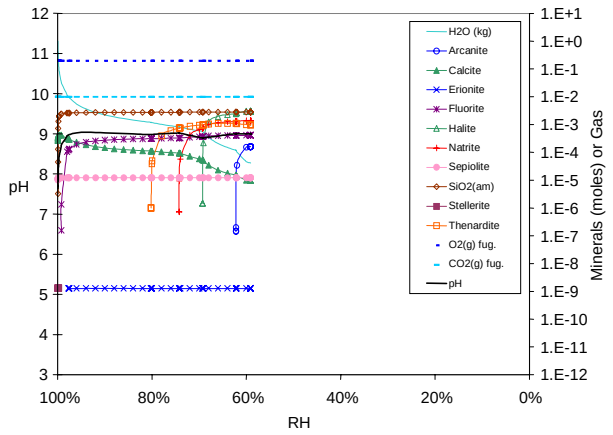

DTN: MO0304SPACSALT.000\06c2t1e.xls.xls

Figure II-06-2. Bin 06 Mineral Precipitation Evaporation Predictions vs. Relative Humidity at 100ºC and 10^{-2} CO_2 Fugacity

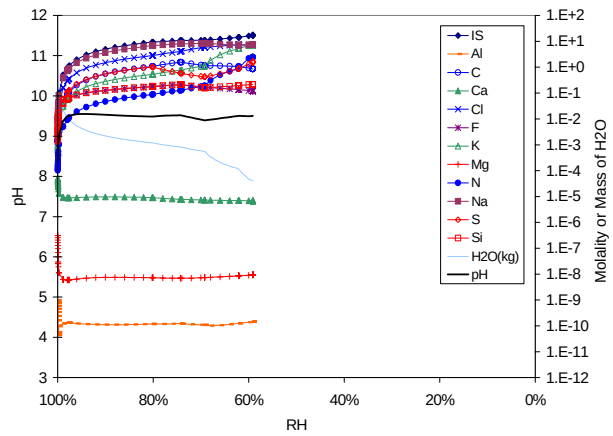

DTN: MO0304SPACSALT.000\06c3t1e.xls.xls

Figure II-06-3. Bin 06 Aqueous Composition Evaporation Predictions vs. Relative Humidity at 100ºC and 10^{-3} CO_2 Fugacity

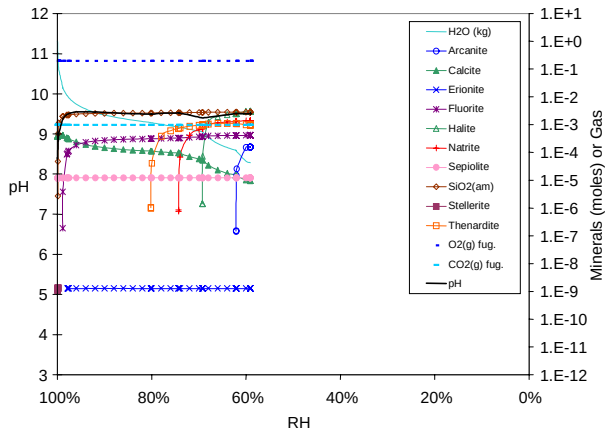

DTN: MO0304SPACSALT.000\06c3t1e.xls.xls

Figure II-06-4. Bin 06 Mineral Precipitation Evaporation Predictions vs. Relative Humidity at 100ºC and 10^{-3} CO_2 Fugacity

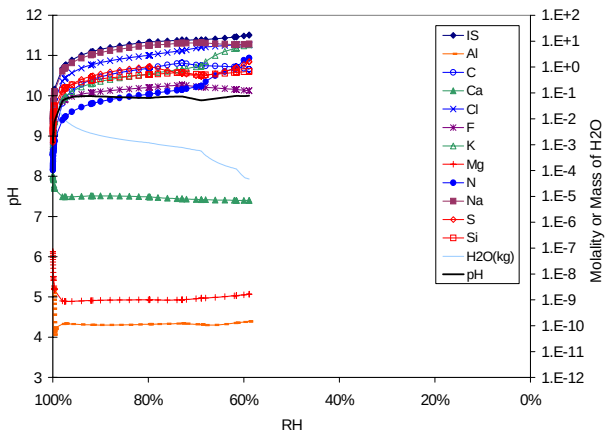

DTN: MO0304SPACSALT.000\06c4t1e.xls.xls

Figure II-06-5. Bin 06 Aqueous Composition Evaporation Predictions vs. Relative Humidity at 100ºC and 10^{-4} CO_2 Fugacity

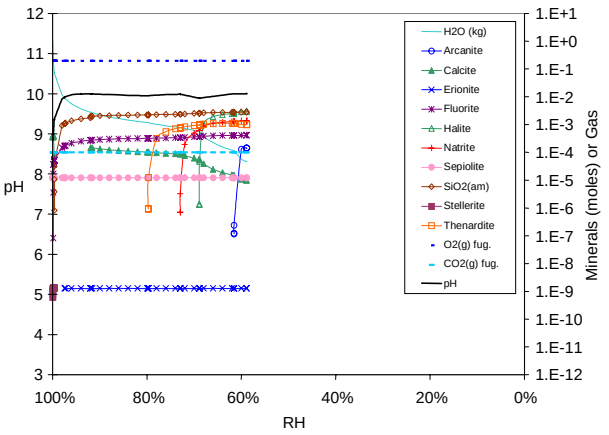

DTN: MO0304SPACSALT.000\06c4t1e.xls.xls

Figure II-06-6. Bin 06 Mineral Precipitation Evaporation Predictions vs. Relative Humidity at 100ºC and 10^{-4} CO_2 Fugacity

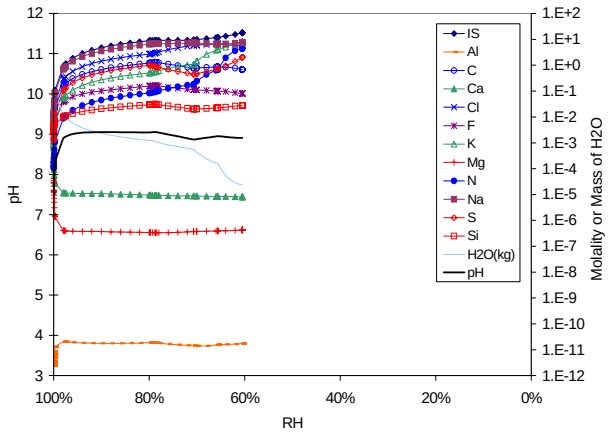

DTN: MO0304SPACSALT.000\06c2t7e.xls.xls

Figure II-06-7. Bin 06 Aqueous Composition Evaporation Predictions vs. Relative Humidity at 70ºC and 10^{-2} CO_2 Fugacity

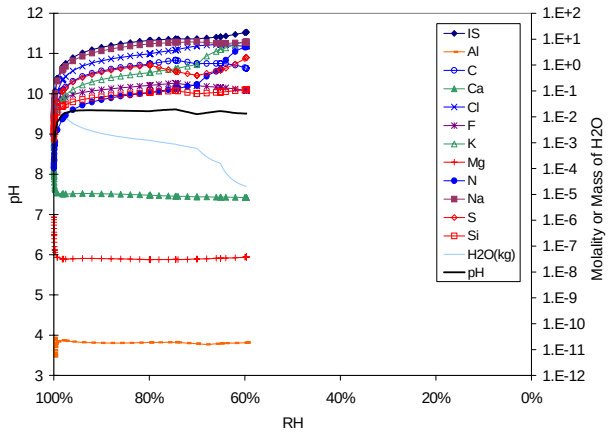

DTN: MO0304SPACSALT.000\06c3t7e.xls.xls

Figure II-06-9. Bin 06 Aqueous Composition Evaporation Predictions vs. Relative Humidity at 70ºC and 10^{-3} CO_2 Fugacity

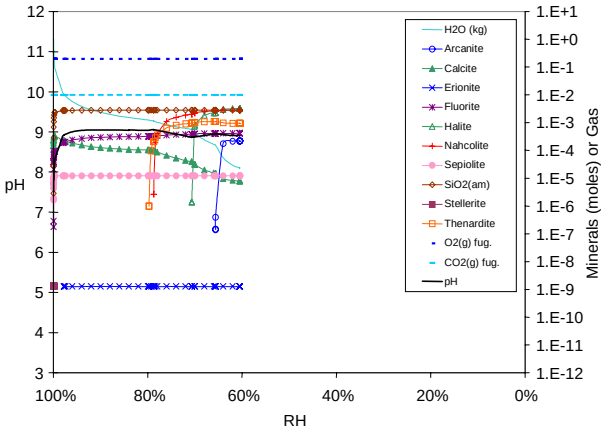

DTN: MO0304SPACSALT.000\06c2t7e.xls.xls

Figure II-06-8. Bin 06 Mineral Precipitation Evaporation Predictions vs. Relative Humidity at 70ºC and 10^{-2} CO_2 Fugacity

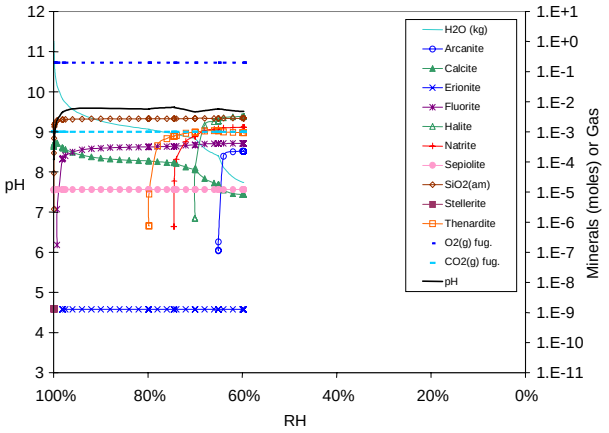

DTN: MO0304SPACSALT.000\06c3t7e.xls.xls

Figure II-06-10. Bin 06 Mineral Precipitation Evaporation Predictions vs. Relative Humidity at 70ºC and 10^{-3} CO_2 Fugacity

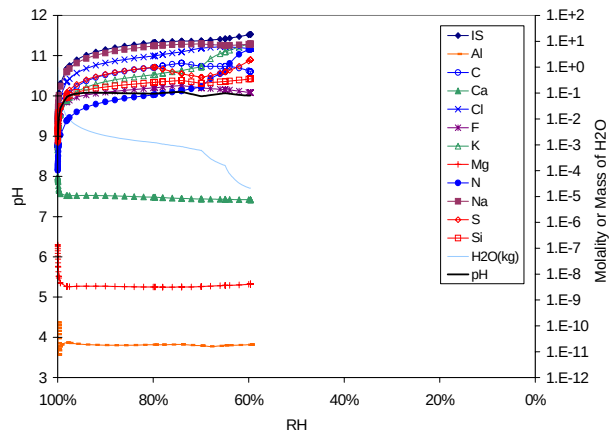

DTN: MO0304SPACSALT.000\06c4t7e.xls.xls

Figure II-06-11. Bin 06 Aqueous Composition Evaporation Predictions vs. Relative Humidity at 70ºC and 10^{-4} CO_2 Fugacity

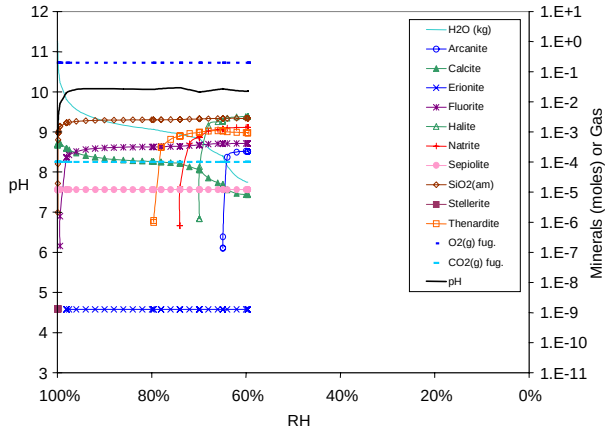

DTN: MO0304SPACSALT.000\06c4t7e.xls.xls

Figure II-06-12. Bin 06 Mineral Precipitation Evaporation Predictions vs. Relative Humidity at 70ºC and 10^{-4} CO_2 Fugacity

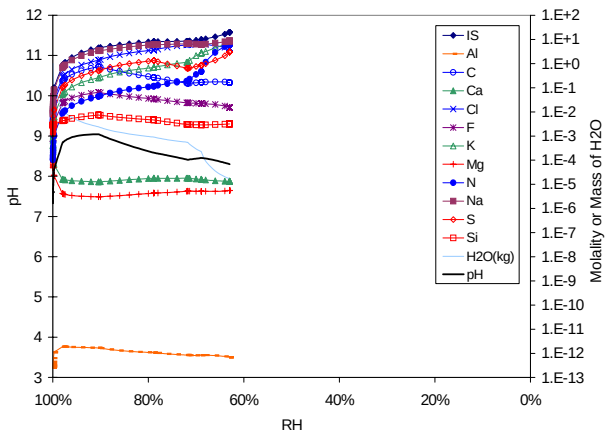

DTN: MO0304SPACSALT.000\06c2t4e.xls.xls

Figure II-06-13. Bin 06 Aqueous Composition Evaporation Predictions vs. Relative Humidity at 40ºC and 10^{-2} CO_2 Fugacity

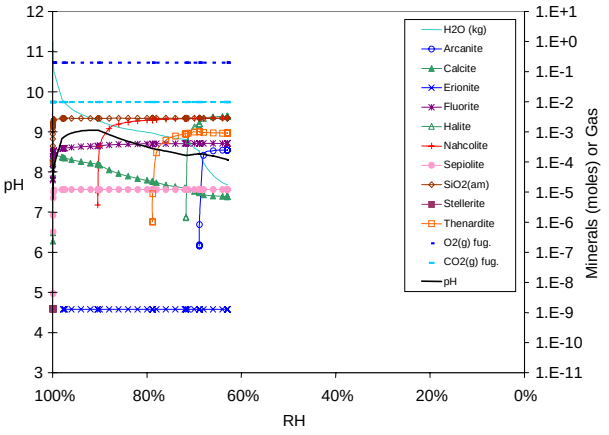

DTN: MO0304SPACSALT.000\06c2t4e.xls.xls

Figure II-06-14. Bin 06 Mineral Precipitation Evaporation Predictions vs. Relative Humidity at 40ºC and 10^{-2} CO_2 Fugacity

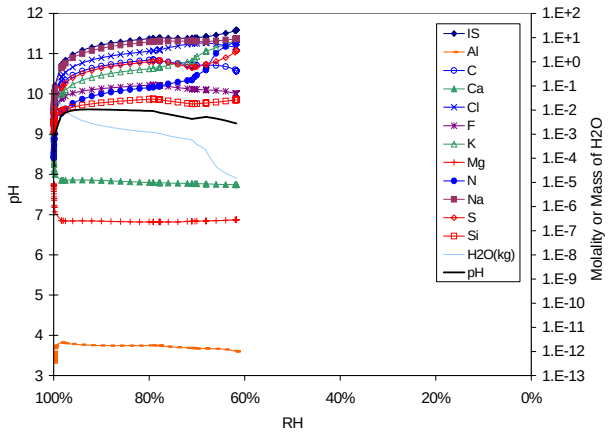

DTN: MO0304SPACSALT.000\06c3t4e.xls.xls

Figure II-06-15. Bin 06 Aqueous Composition Evaporation Predictions vs. Relative Humidity at 40ºC and 10^{-3} CO_2 Fugacity

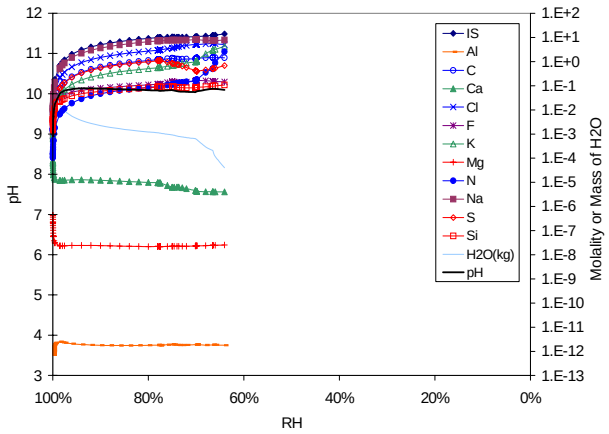

DTN: MO0304SPACSALT.000\06c4t4e.xls.xls

Figure II-06-17. Bin 06 Aqueous Composition Evaporation Predictions vs. Relative Humidity at 40ºC and 10^{-4} CO_2 Fugacity

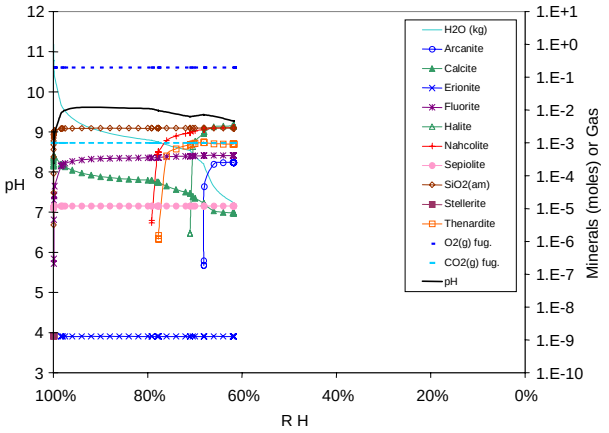

DTN: MO0304SPACSALT.000\06c3t4e.xls.xls

Figure II-06-16. Bin 06 Mineral Precipitation Evaporation Predictions vs. Relative Humidity at 40ºC and 10^{-3} CO_2 Fugacity

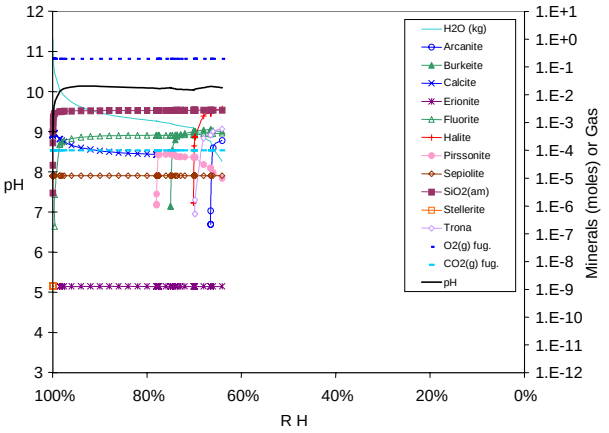

DTN: MO0304SPACSALT.000\06c4t4e.xls.xls

Figure II-06-18. Bin 06 Mineral Precipitation Evaporation Predictions vs. Relative Humidity at 40ºC and 10^{-4} CO_2 Fugacity

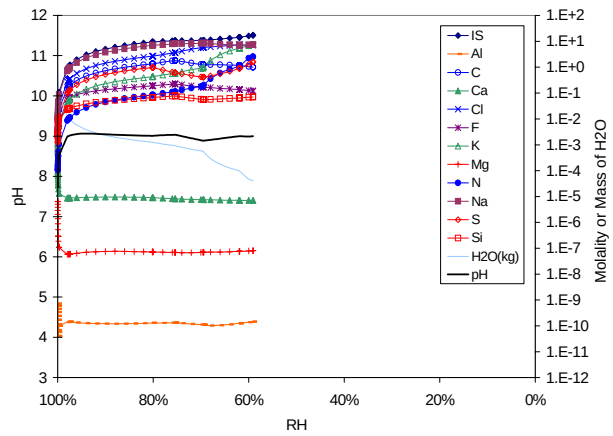

DTN: MO0304SPACSALT.000\07c2t1e.xls.xls

Figure II-07-1. Bin 07 Aqueous Composition Evaporation Predictions vs. Relative Humidity at 100ºC and 10^{-2} CO_2 Fugacity

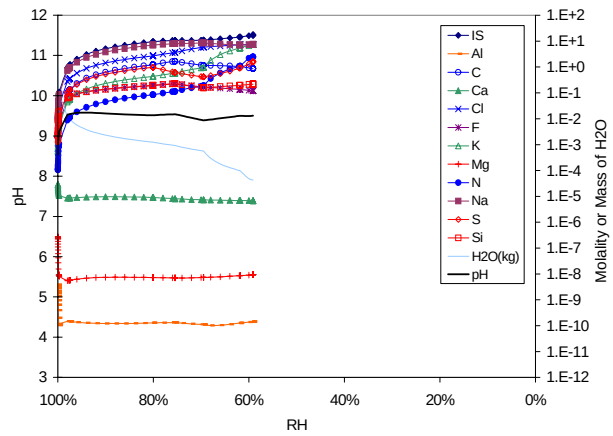

DTN: MO0304SPACSALT.000\07c3t1e.xls.xls

Figure II-07-3. Bin 07 Aqueous Composition Evaporation Predictions vs. Relative Humidity at 100ºC and 10^{-3} CO_2 Fugacity

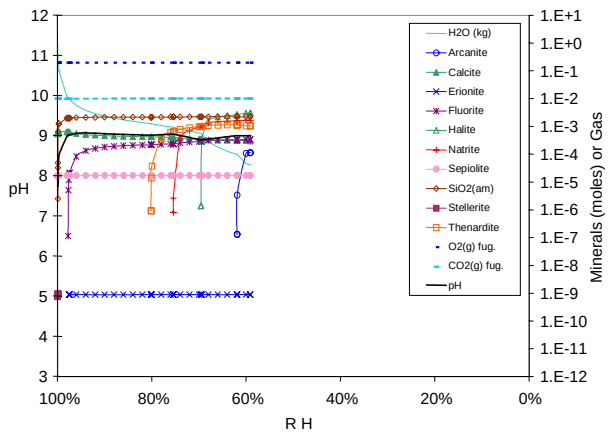

DTN: MO0304SPACSALT.000\07c2t1e.xls.xls

Figure II-07-2. Bin 07 Mineral Precipitation Evaporation Predictions vs. Relative Humidity at 100ºC and 10^{-2} CO_2 Fugacity

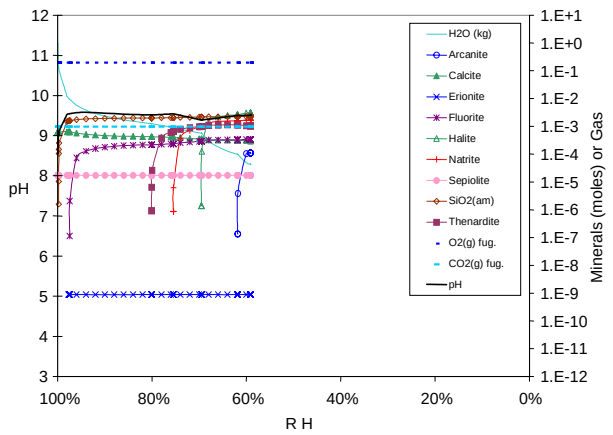

DTN: MO0304SPACSALT.000\07c3t1e.xls.xls

Figure II-07-4. Bin 07 Mineral Precipitation Evaporation Predictions vs. Relative Humidity at 100ºC and 10^{-3} CO_2 Fugacity

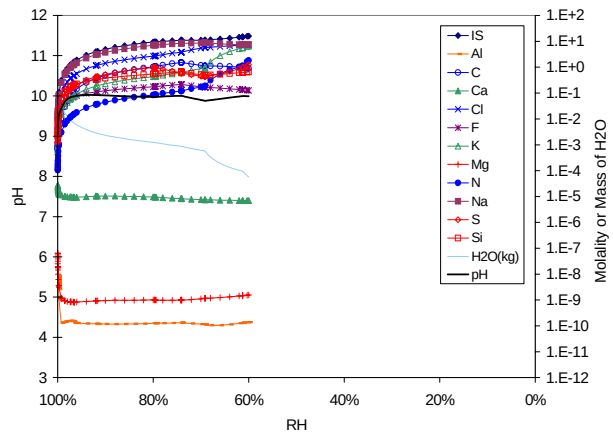

DTN: MO0304SPACSALT.000\07c4t1e.xls.xls

Figure II-07-5. Bin 07 Aqueous Composition Evaporation Predictions vs. Relative Humidity at 100ºC and 10^{-4} CO_2 Fugacity

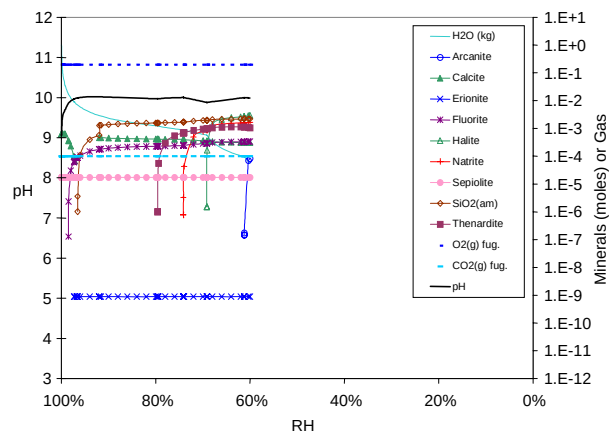

DTN: MO0304SPACSALT.000\07c4t1e.xls.xls

Figure II-07-6. Bin 07 Mineral Precipitation Evaporation Predictions vs. Relative Humidity at 100ºC and 10^{-4} CO_2 Fugacity

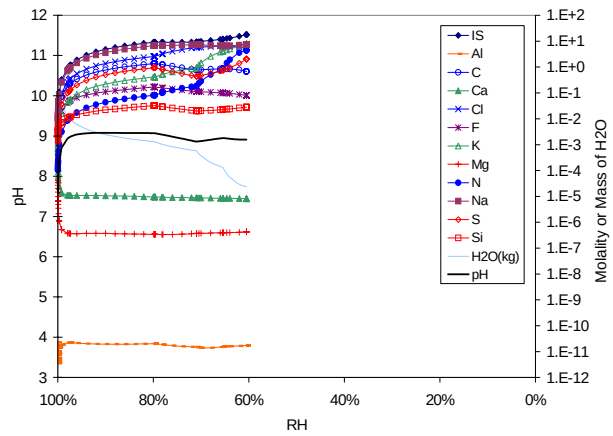

DTN: MO0304SPACSALT.000\07c2t7e.xls.xls

Figure II-07-7. Bin 07 Aqueous Composition Evaporation Predictions vs. Relative Humidity at 70ºC and 10^{-2} CO_2 Fugacity

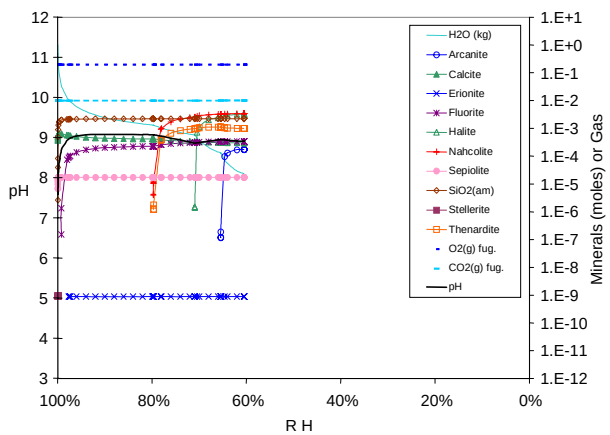

DTN: MO0304SPACSALT.000\07c2t7e.xls.xls

Figure II-07-8. Bin 07 Mineral Precipitation Evaporation Predictions vs. Relative Humidity at 70ºC and 10^{-2} CO_2 Fugacity

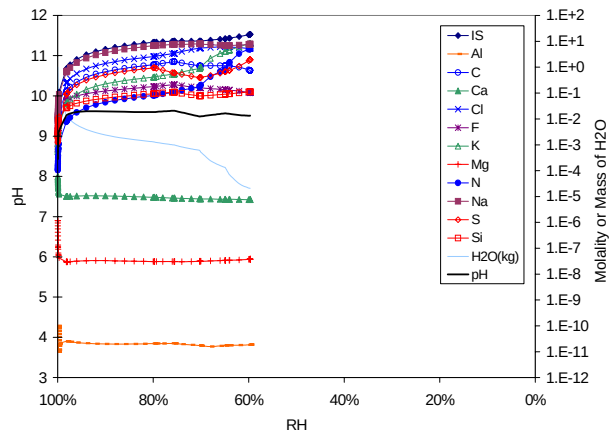

DTN: MO0304SPACSALT.000\07c3t7e.xls.xls

Figure II-07-9. Bin 07 Aqueous Composition Evaporation Predictions vs. Relative Humidity at 70ºC and 10^{-3} CO_2 Fugacity

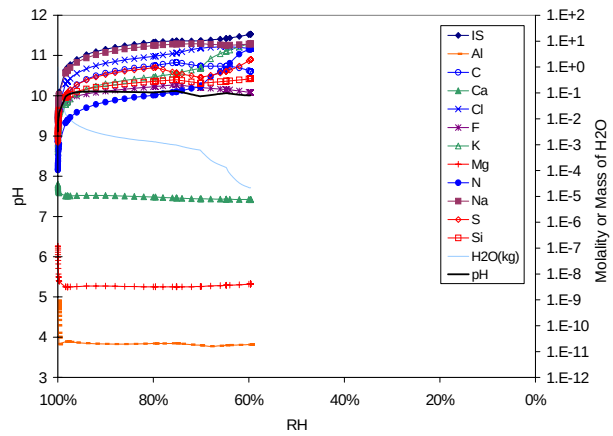

DTN: MO0304SPACSALT.000\07c4t7e.xls.xls

Figure II-07-11. Bin 07 Aqueous Composition Evaporation Predictions vs. Relative Humidity at 70ºC and 10^{-4} CO_2 Fugacity

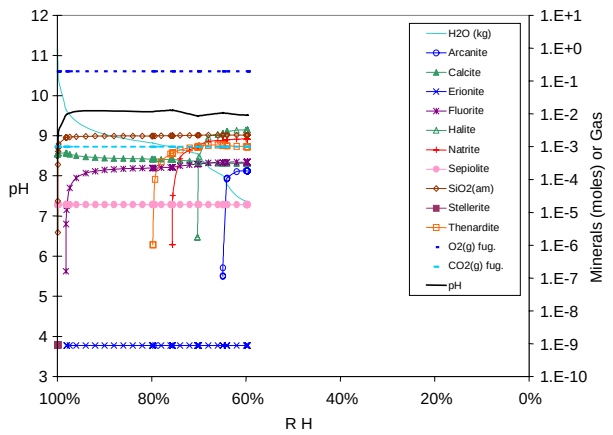

DTN: MO0304SPACSALT.000\07c3t7e.xls.xls

Figure II-07-10. Bin 07 Mineral Precipitation Evaporation Predictions vs. Relative Humidity at 70ºC and 10^{-3} CO_2 Fugacity

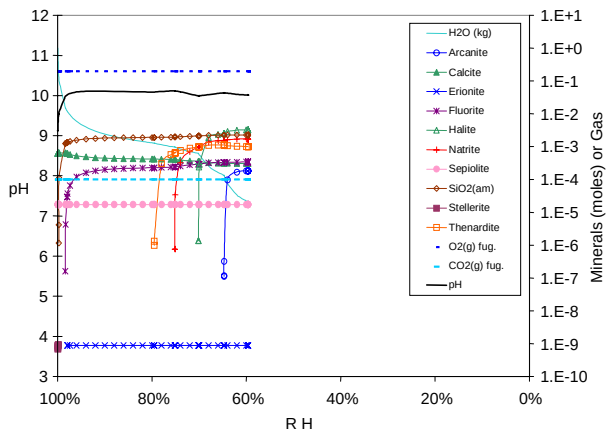

DTN: MO0304SPACSALT.000\07c4t7e.xls.xls

Figure II-07-12. Bin 07 Mineral Precipitation Evaporation Predictions vs. Relative Humidity at 70ºC and 10^{-4} CO_2 Fugacity

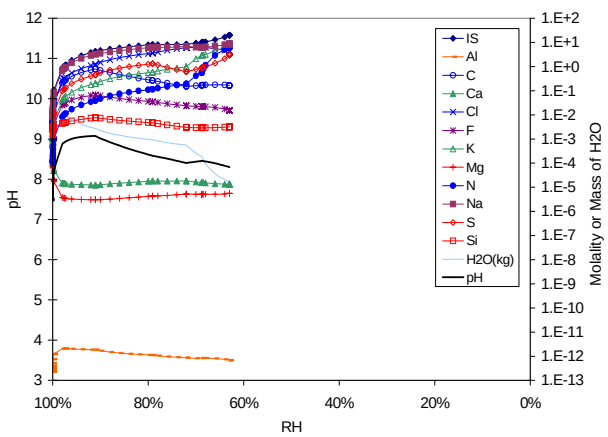

DTN: MO0304SPACSALT.000\07c2t4e.xls.xls

Figure II-07-13. Bin 07 Aqueous Composition Evaporation Predictions vs. Relative Humidity at 40ºC and 10^{-2} CO_2 Fugacity

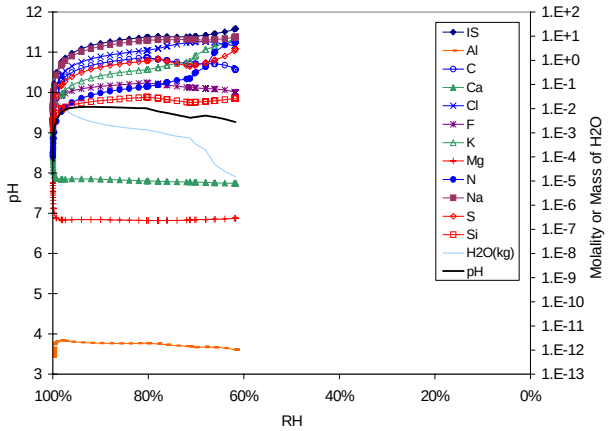

DTN: MO0304SPACSALT.000\07c3t4e.xls.xls

Figure II-07-15. Bin 07 Aqueous Composition Evaporation Predictions vs. Relative Humidity at 40ºC and 10^{-3} CO_2 Fugacity

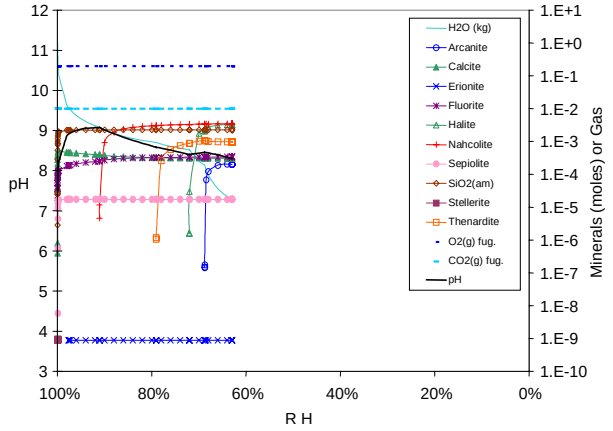

DTN: MO0304SPACSALT.000\07c2t4e.xls.xls

Figure II-07-14. Bin 07 Mineral Precipitation Evaporation Predictions vs. Relative Humidity at 40ºC and 10^{-2} CO_2 Fugacity

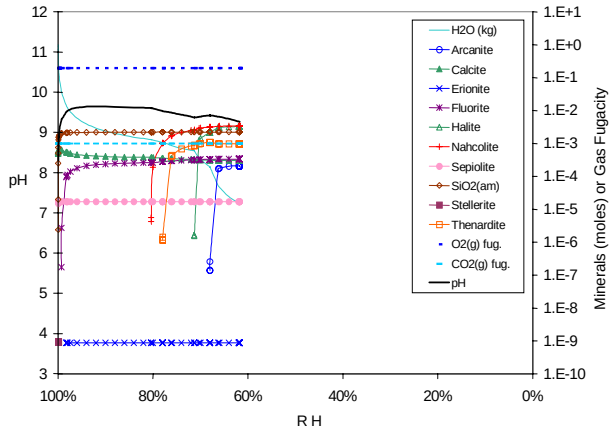

DTN: MO0304SPACSALT.000\07c3t4e.xls.xls

Figure II-07-16. Bin 07 Mineral Precipitation Evaporation Predictions vs. Relative Humidity at 40ºC and 10^{-3} CO_2 Fugacity

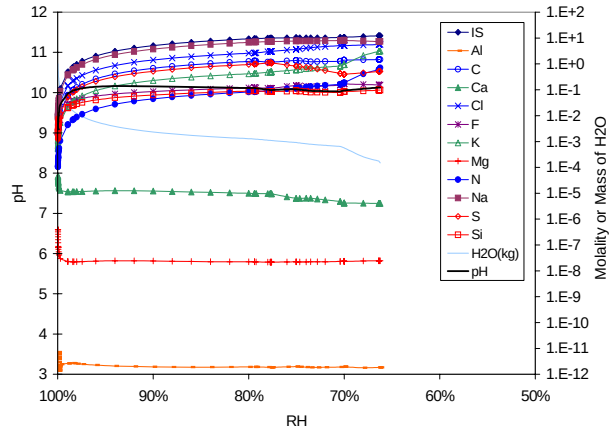

DTN: MO0304SPACSALT.000\07c4t4e.xls.xls

Figure II-07-17. Bin 07 Aqueous Composition Evaporation Predictions vs. Relative Humidity at 40ºC and 10^{-4} CO_2 Fugacity

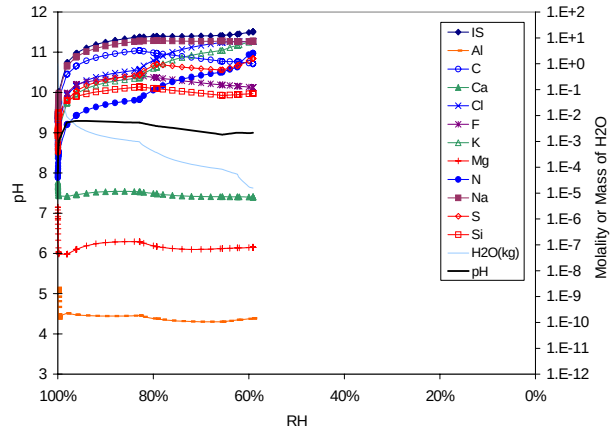

DTN: MO0304SPACSALT.000\08c2t1e.xls.xls

Figure II-08-1. Bin 08 Aqueous Composition Evaporation Predictions vs. Relative Humidity at 100ºC and 10^{-2} CO_2 Fugacity

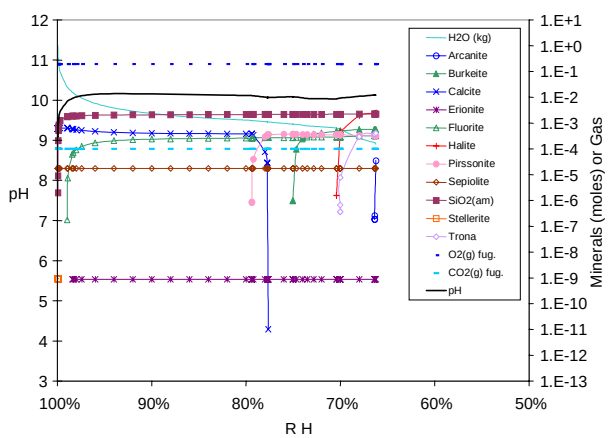

DTN: MO0304SPACSALT.000\07c4t4e.xls.xls

Figure II-07-18. Bin 07 Mineral Precipitation Evaporation Predictions vs. Relative Humidity at 40ºC and 10^{-4} CO_2 Fugacity

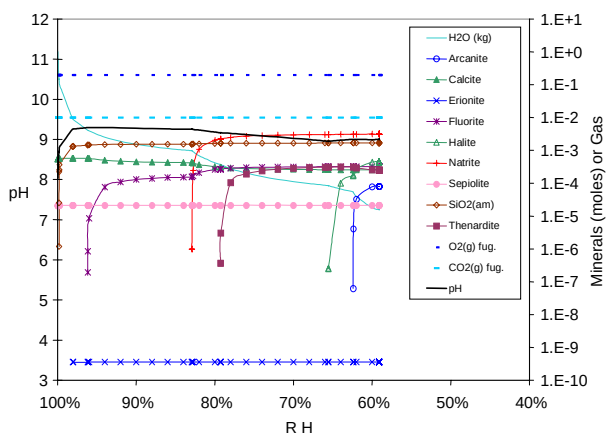

DTN: MO0304SPACSALT.000\08c2t1e.xls.xls

Figure II-08-2. Bin 08 Mineral Precipitation Evaporation Predictions vs. Relative Humidity at 100ºC and 10^{-2} CO_2 Fugacity

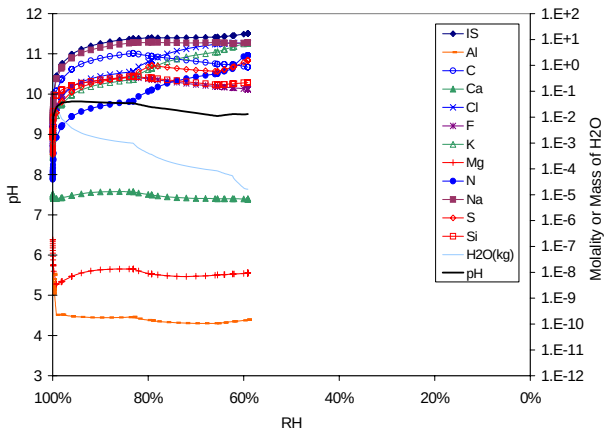

DTN: MO0304SPACSALT.000\08c3t1e.xls.xls

Figure II-08-3. Bin 08 Aqueous Composition Evaporation Predictions vs. Relative Humidity at 100ºC and 10^{-3} CO_2 Fugacity

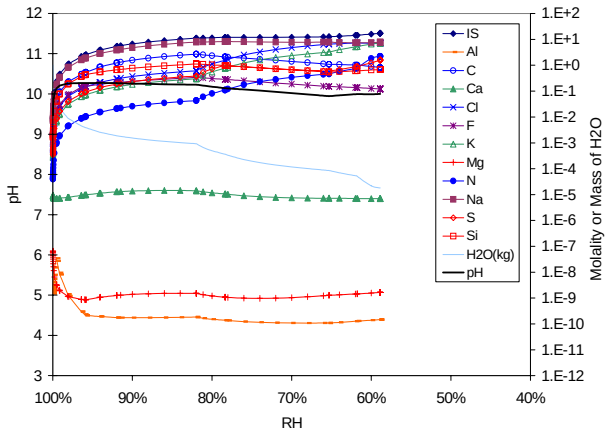

DTN: MO0304SPACSALT.000\08c4t1e.xls.xls

Figure II-08-5. Bin 08 Aqueous Composition Evaporation Predictions vs. Relative Humidity at 100ºC and 10^{-4} CO_2 Fugacity

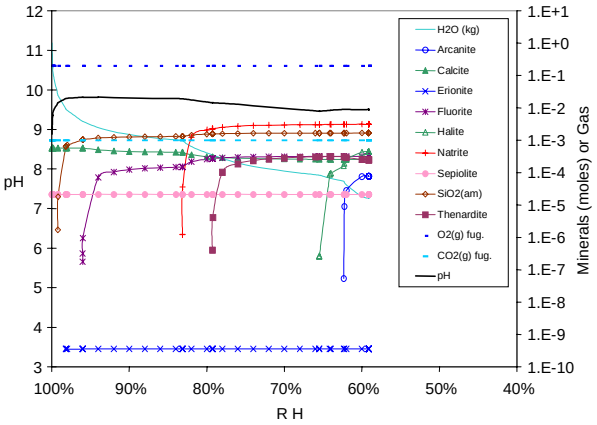

DTN: MO0304SPACSALT.000\08c3t1e.xls.xls

Figure II-08-4. Bin 08 Mineral Precipitation Evaporation Predictions vs. Relative Humidity at 100ºC and 10^{-3} CO_2 Fugacity

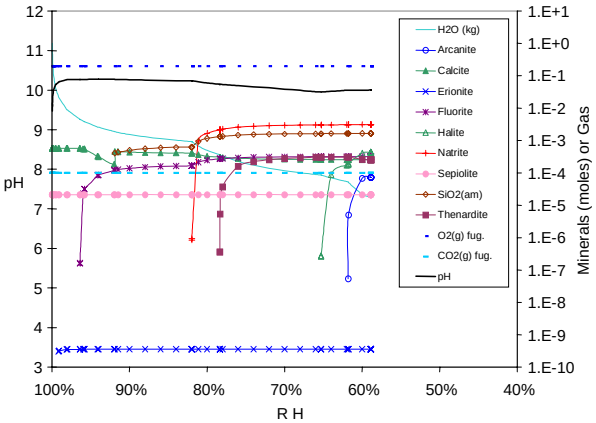

DTN: MO0304SPACSALT.000\08c4t1e.xls.xls

Figure II-08-6. Bin 08 Mineral Precipitation Evaporation Predictions vs. Relative Humidity at 100ºC and 10^{-4} CO_2 Fugacity

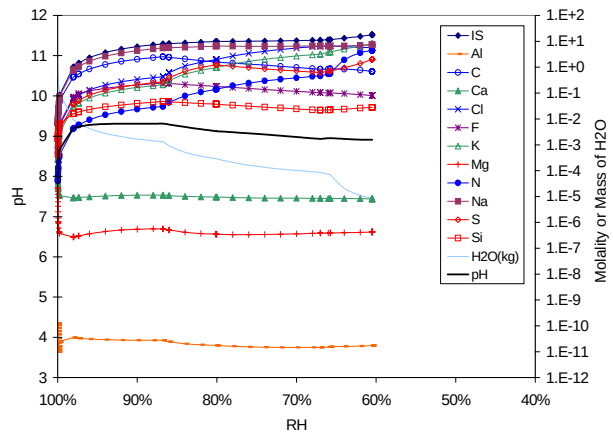

DTN: MO0304SPACSALT.000\08c2t7e.xls.xls

Figure II-08-7. Bin 08 Aqueous Composition Evaporation Predictions vs. Relative Humidity at 70ºC and 10^{-2} CO_2 Fugacity

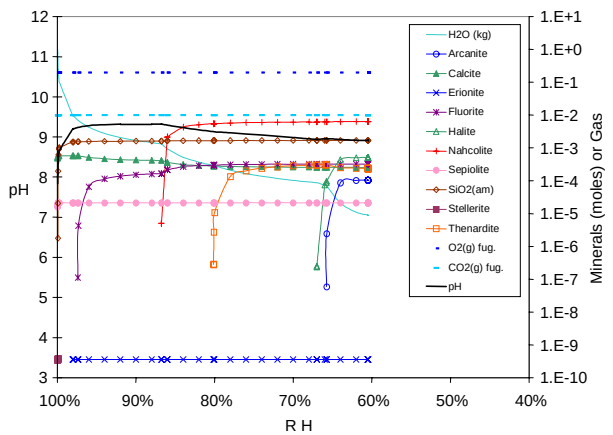

DTN: MO0304SPACSALT.000\08c2t7e.xls.xls

Figure II-08-8. Bin 08 Mineral Precipitation Evaporation Predictions vs. Relative Humidity at 70ºC and 10^{-2} CO_2 Fugacity

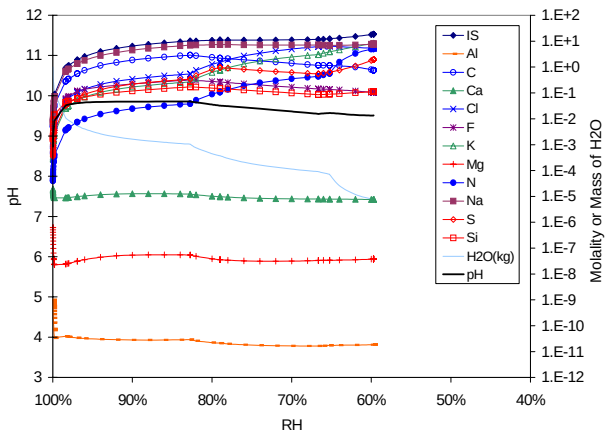

DTN: MO0304SPACSALT.000\08c3t7e.xls.xls

Figure II-08-9. Bin 08 Aqueous Composition Evaporation Predictions vs. Relative Humidity at 70ºC and 10^{-3} CO_2 Fugacity

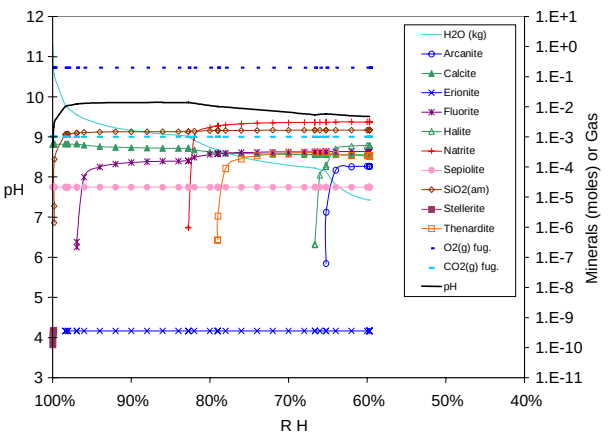

DTN: MO0304SPACSALT.000\08c3t7e.xls.xls

Figure II-08-10. Bin 08 Mineral Precipitation Evaporation Predictions vs. Relative Humidity at 70ºC and 10^{-3} CO_2 Fugacity

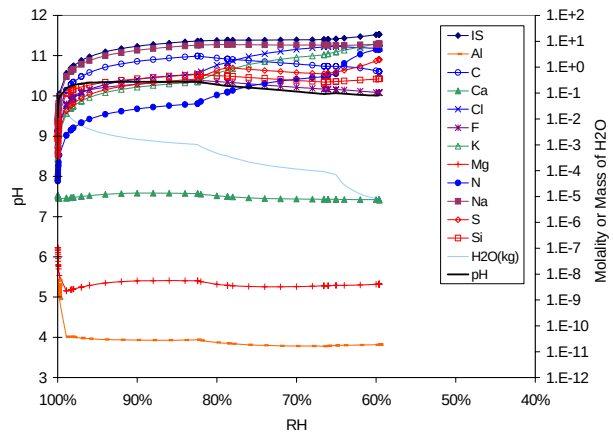

DTN: MO0304SPACSALT.000\08c4t7e.xls.xls

Figure II-08-11. Bin 08 Aqueous Composition Evaporation Predictions vs. Relative Humidity at 70ºC and 10^{-4} CO_2 Fugacity

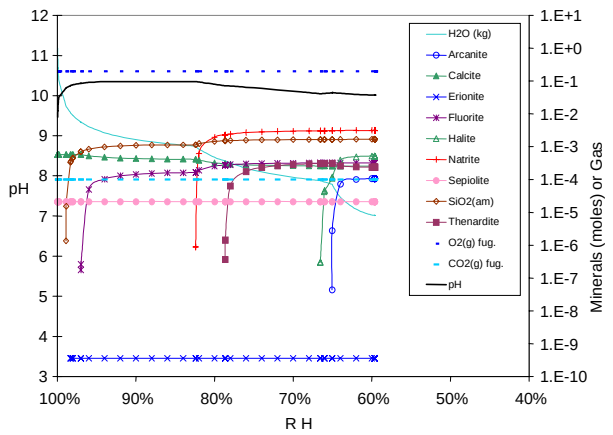

DTN: MO0304SPACSALT.000\08c4t7e.xls.xls

Figure II-08-12. Bin 08 Mineral Precipitation Evaporation Predictions vs. Relative Humidity at 70ºC and 10^{-4} CO_2 Fugacity

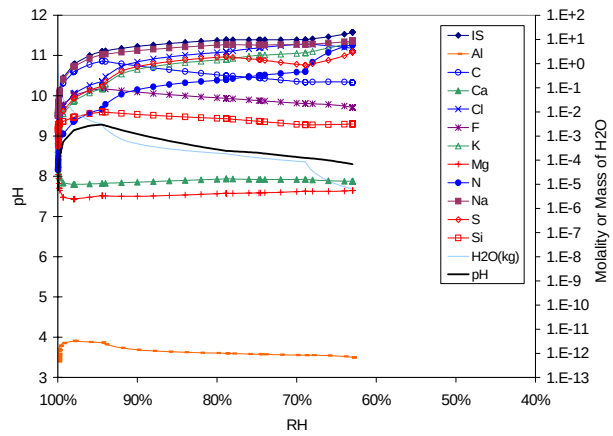

DTN: MO0304SPACSALT.000\08c2t4e.xls.xls

Figure II-08-13. Bin 08 Aqueous Composition Evaporation Predictions vs. Relative Humidity at 40ºC and 10^{-2} CO_2 Fugacity

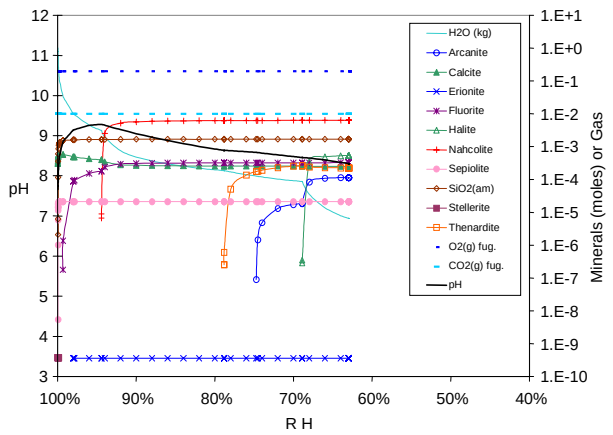

DTN: MO0304SPACSALT.000\08c2t4e.xls.xls

Figure II-08-14. Bin 08 Mineral Precipitation Evaporation Predictions vs. Relative Humidity at 40ºC and 10^{-2} CO_2 Fugacity

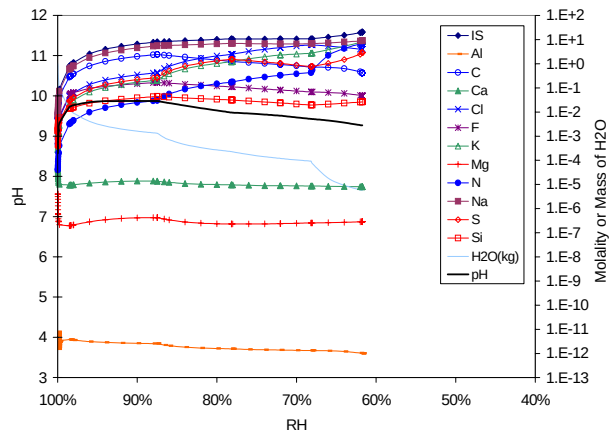

DTN: MO0304SPACSALT.000\08c3t4e.xls.xls

Figure II-08-15. Bin 08 Aqueous Composition Evaporation Predictions vs. Relative Humidity at 40ºC and 10^{-3} CO_2 Fugacity

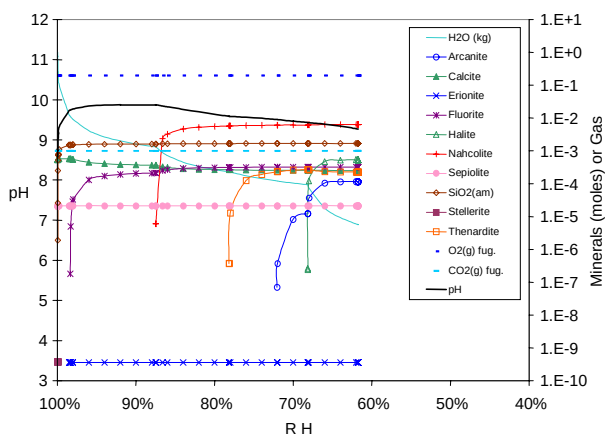

DTN: MO0304SPACSALT.000\08c3t4e.xls.xls

Figure II-08-16. Bin 08 Mineral Precipitation Evaporation Predictions vs. Relative Humidity at 40ºC and 10^{-3} CO_2 Fugacity

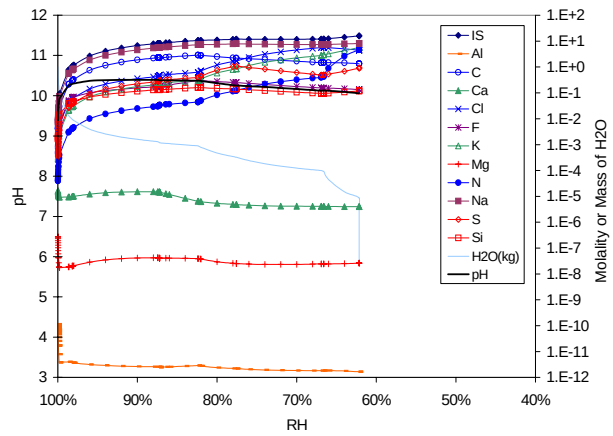

DTN: MO0304SPACSALT.000\08c4t4e.xls.xls

Figure II-08-17. Bin 08 Aqueous Composition Evaporation Predictions vs. Relative Humidity at 40ºC and 10^{-4} CO_2 Fugacity

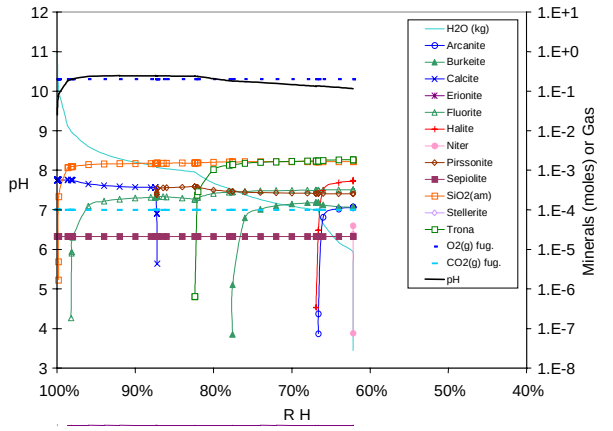

DTN: MO0304SPACSALT.000\08c4t4e.xls.xls

Figure II-08-18. Bin 08 Mineral Precipitation Evaporation Predictions vs. Relative Humidity at 40ºC and 10^{-4} CO_2 Fugacity

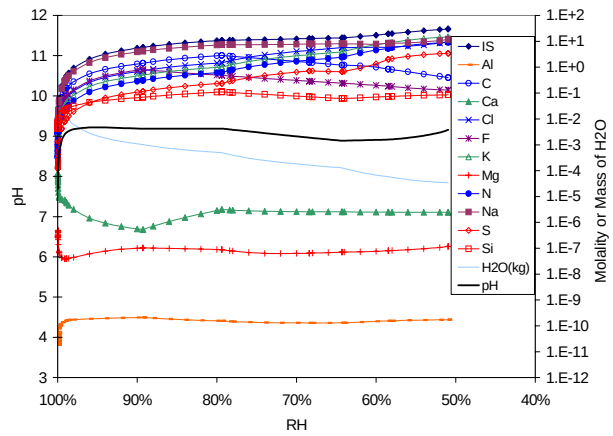

DTN: MO0304SPACSALT.000\09c2t1e.xls.xls

Figure II-09-1. Bin 09 Aqueous Composition Evaporation Predictions vs. Relative Humidity at 100ºC and 10^{-2} CO_2 Fugacity

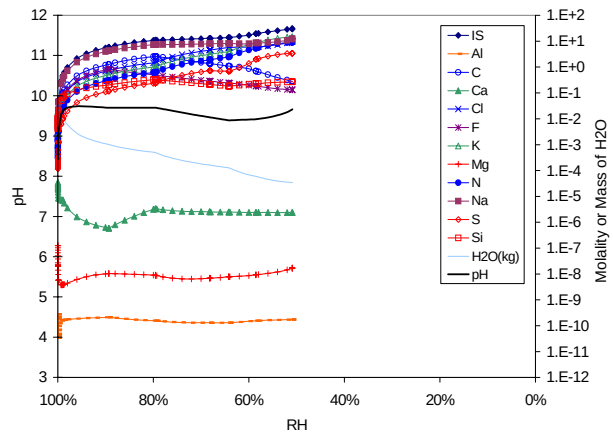

DTN: MO0304SPACSALT.000\09c3t1e.xls.xls

Figure II-09-3. Bin 09 Aqueous Composition Evaporation Predictions vs. Relative Humidity at 100ºC and 10^{-3} CO_2 Fugacity

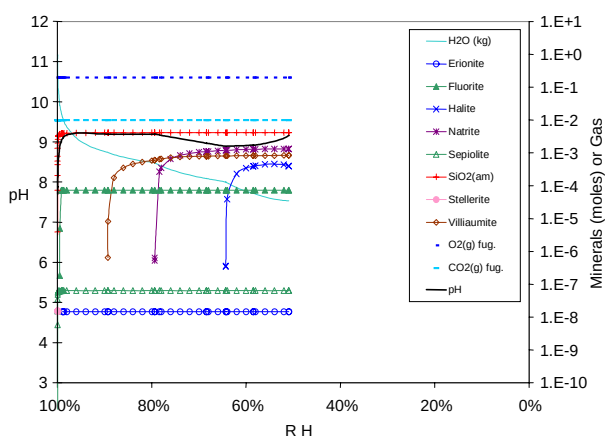

DTN: MO0304SPACSALT.000\09c2t1e.xls.xls

Figure II-09-2. Bin 09 Mineral Precipitation Evaporation Predictions vs. Relative Humidity at 100ºC and 10^{-2} CO_2 Fugacity

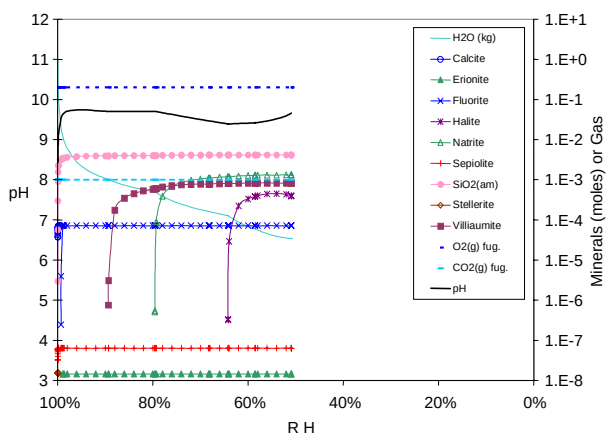

DTN: MO0304SPACSALT.000\09c3t1e.xls.xls

Figure II-09-4. Bin 09 Mineral Precipitation Evaporation Predictions vs. Relative Humidity at 100ºC and 10^{-3} CO_2 Fugacity

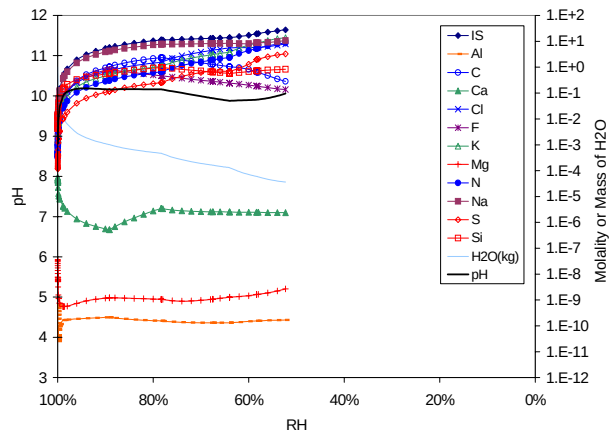

DTN: MO0304SPACSALT.000\09c4t1e.xls.xls

Figure II-09-5. Bin 09 Aqueous Composition Evaporation Predictions vs. Relative Humidity at 100ºC and 10^{-4} CO_2 Fugacity

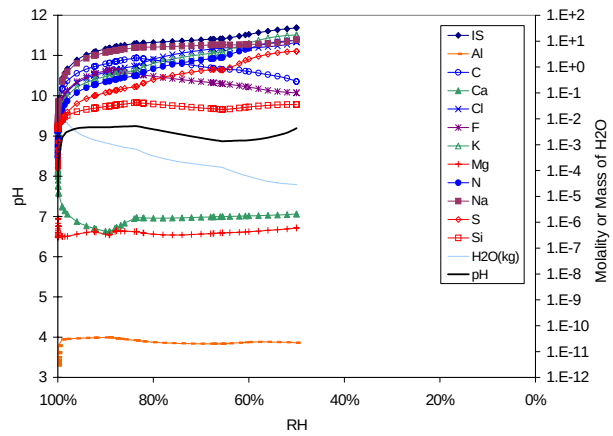

DTN: MO0304SPACSALT.000\09c2t7e.xls.xls

Figure II-09-7. Bin 09 Aqueous Composition Evaporation Predictions vs. Relative Humidity at 70ºC and 10^{-2} CO_2 Fugacity

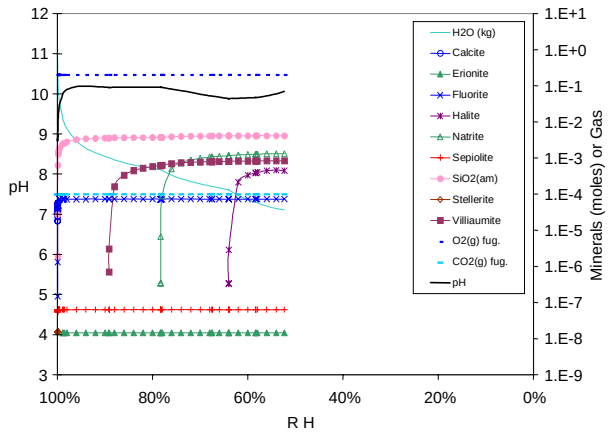

DTN: MO0304SPACSALT.000\09c4t1e.xls.xls

Figure II-09-6. Bin 09 Mineral Precipitation Evaporation Predictions vs. Relative Humidity at 100ºC and 10^{-4} CO_2 Fugacity

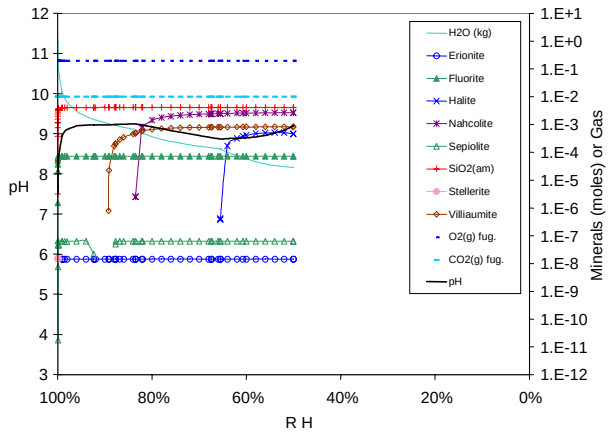

DTN: MO0304SPACSALT.000\09c2t7e.xls.xls

Figure II-09-8. Bin 09 Mineral Precipitation Evaporation Predictions vs. Relative Humidity at 70ºC and 10^{-2} CO_2 Fugacity

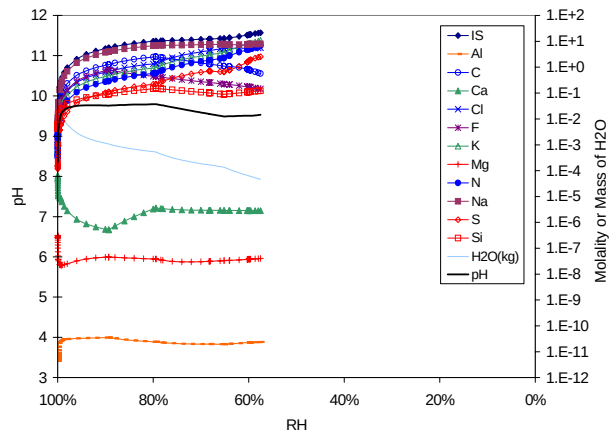

DTN: MO0304SPACSALT.000\09c3t7e.xls.xls

Figure II-09-9. Bin 09 Aqueous Composition Evaporation Predictions vs. Relative Humidity at 70ºC and 10^{-3} CO_2 Fugacity

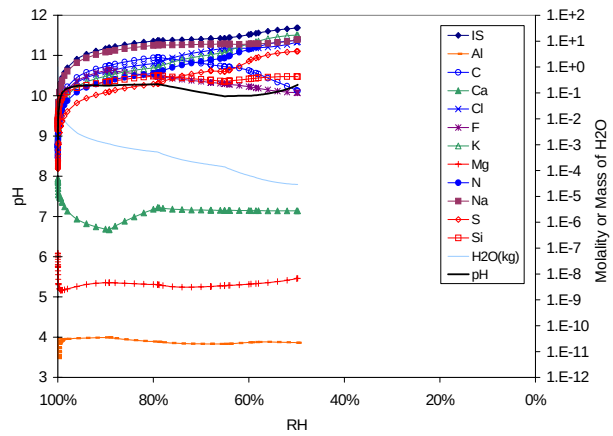

DTN: MO0304SPACSALT.000\09c4t7e.xls.xls

Figure II-09-11. Bin 09 Aqueous Composition Evaporation Predictions vs. Relative Humidity at 70ºC and 10^{-4} CO_2 Fugacity

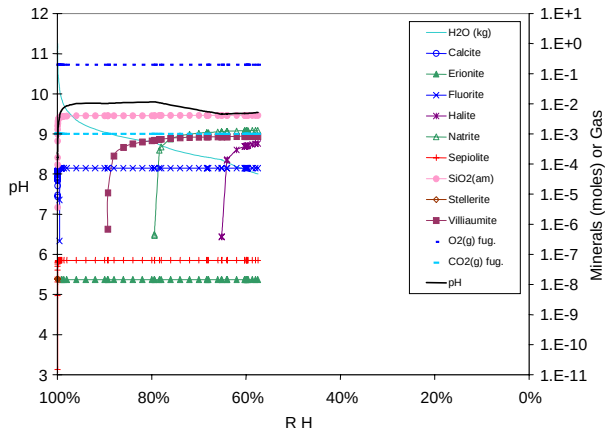

DTN: MO0304SPACSALT.000\09c3t7e.xls.xls

Figure II-09-10. Bin 09 Mineral Precipitation Evaporation Predictions vs. Relative Humidity at 70ºC and 10^{-3} CO_2 Fugacity

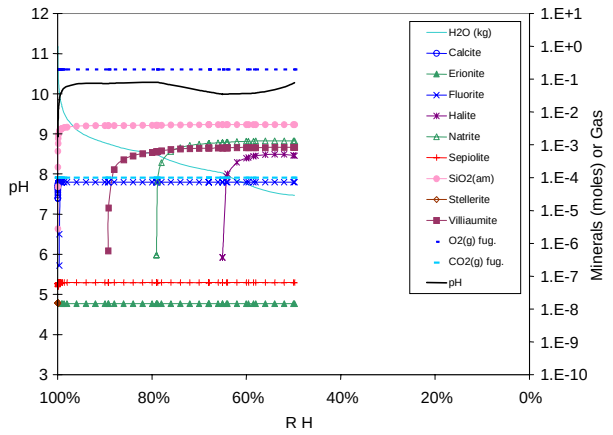

DTN: MO0304SPACSALT.000\09c4t7e.xls.xls

Figure II-09-12. Bin 09 Mineral Precipitation Evaporation Predictions vs. Relative Humidity at 70ºC and 10^{-4} CO_2 Fugacity

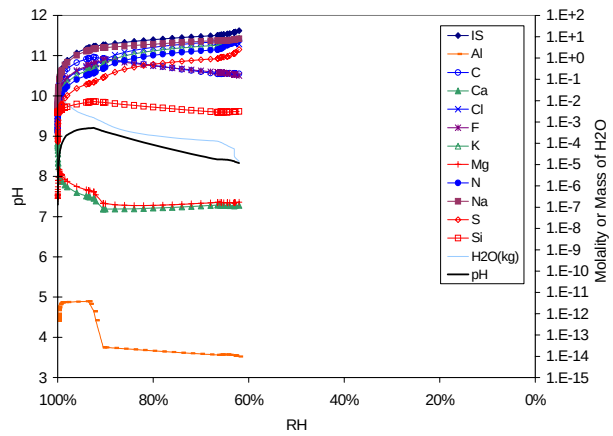

DTN: MO0304SPACSALT.000\09c2t4e.xls.xls

Figure II-09-13. Bin 09 Aqueous Composition Evaporation Predictions vs. Relative Humidity at 40ºC and 10^{-2} CO_2 Fugacity

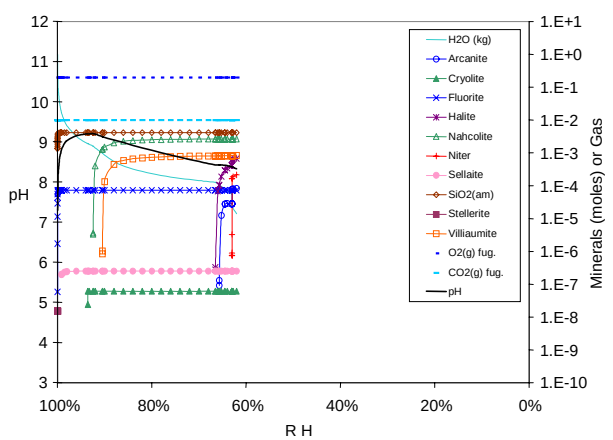

DTN: MO0304SPACSALT.000\09c2t4e.xls.xls

Figure II-09-14. Bin 09 Mineral Precipitation Evaporation Predictions vs. Relative Humidity at 40ºC and 10^{-2} CO_2 Fugacity

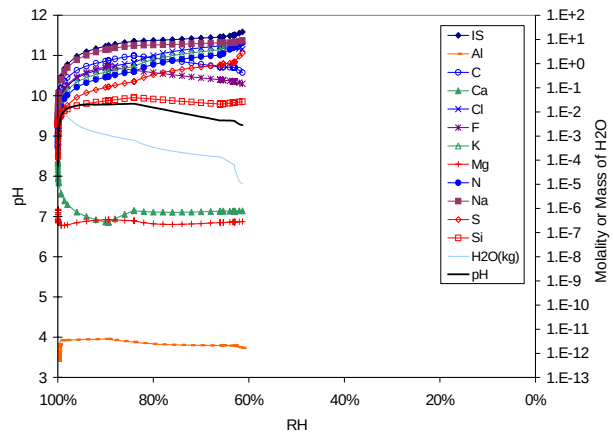

DTN: MO0304SPACSALT.000\09c3t4e.xls.xls

Figure II-09-15. Bin 09 Aqueous Composition Evaporation Predictions vs. Relative Humidity at 40ºC and 10^{-3} CO_2 Fugacity

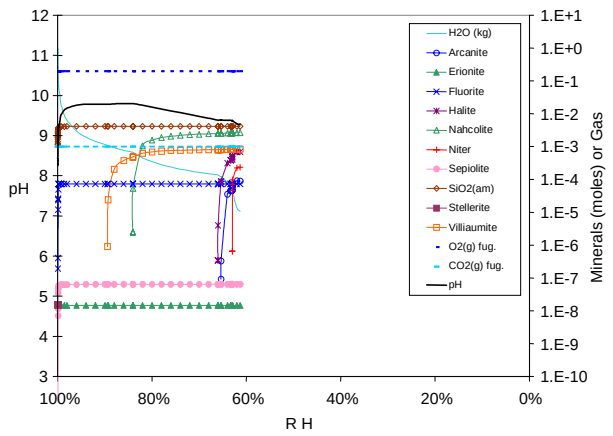

DTN: MO0304SPACSALT.000\09c3t4e.xls.xls

Figure II-09-16. Bin 09 Mineral Precipitation Evaporation Predictions vs. Relative Humidity at 40ºC and 10^{-3} CO_2 Fugacity

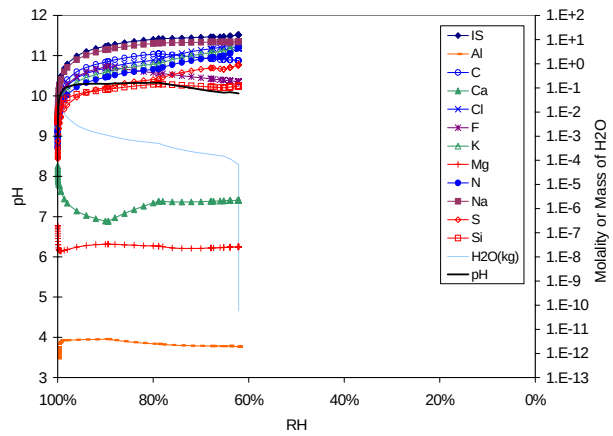

DTN: MO0304SPACSALT.000\09c4t4e.xls.xls

Figure II-09-17. Bin 09 Aqueous Composition Evaporation Predictions vs. Relative Humidity at 40ºC and 10^{-4} CO_2 Fugacity

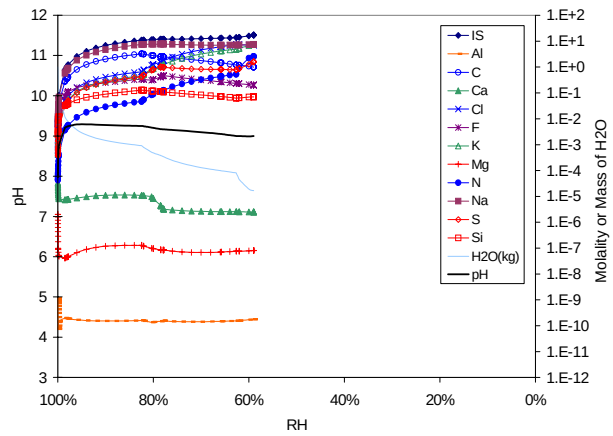

DTN: MO0304SPACSALT.000\10c2t1e.xls.xls

Figure II-10-1. Bin 10 Aqueous Composition Evaporation Predictions vs. Relative Humidity at 100ºC and 10^{-2} CO_2 Fugacity

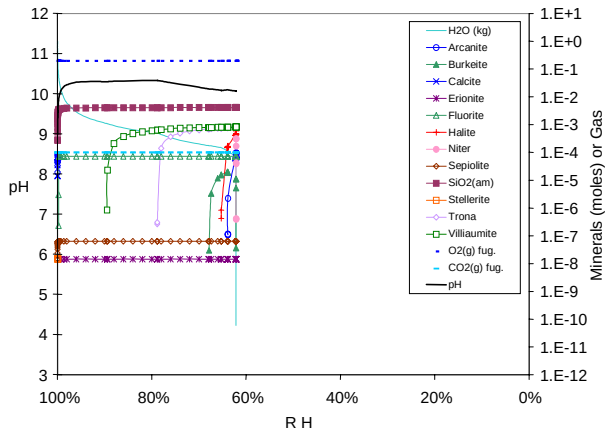

DTN: MO0304SPACSALT.000\09c4t4e.xls.xls

Figure II-09-18. Bin 09 Mineral Precipitation Evaporation Predictions vs. Relative Humidity at 40ºC and 10^{-4} CO_2 Fugacity

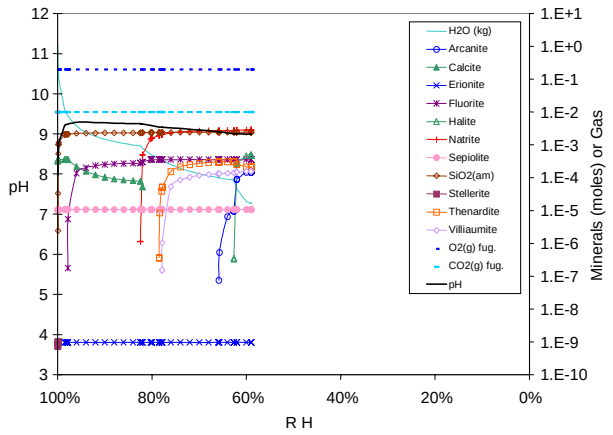

DTN: MO0304SPACSALT.000\10c2t1e.xls.xls

Figure II-10-2. Bin 10 Mineral Precipitation Evaporation Predictions vs. Relative Humidity at 100ºC and 10^{-2} CO_2 Fugacity

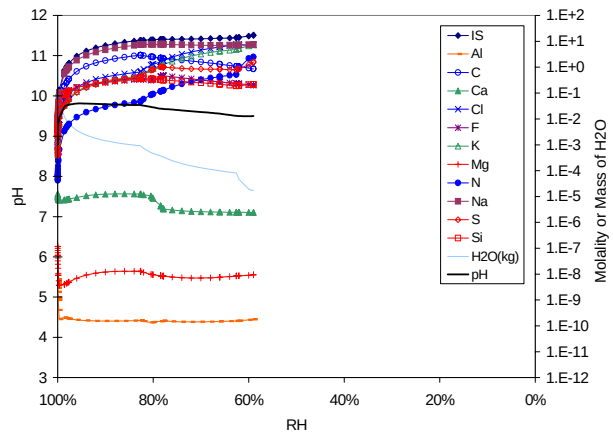

DTN: MO0304SPACSALT.000\10c3t1e.xls.xls

Figure II-10-3. Bin 10 Aqueous Composition Evaporation Predictions vs. Relative Humidity at 100ºC and 10^{-3} CO_2 Fugacity

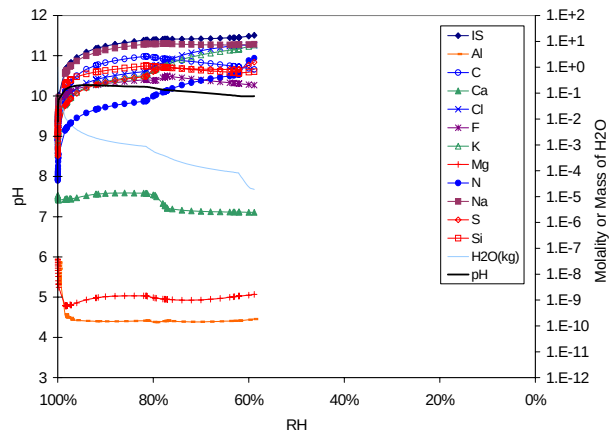

DTN: MO0304SPACSALT.000\10c4t1e.xls.xls

Figure II-10-5. Bin 10 Aqueous Composition Evaporation Predictions vs. Relative Humidity at 100ºC and 10^{-4} CO_2 Fugacity

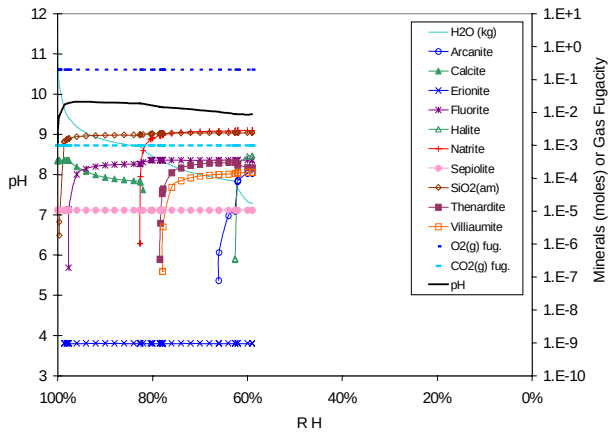

DTN: MO0304SPACSALT.000\10c3t1e.xls.xls

Figure II-10-4. Bin 10 Mineral Precipitation Evaporation Predictions vs. Relative Humidity at 100ºC and 10^{-3} CO_2 Fugacity

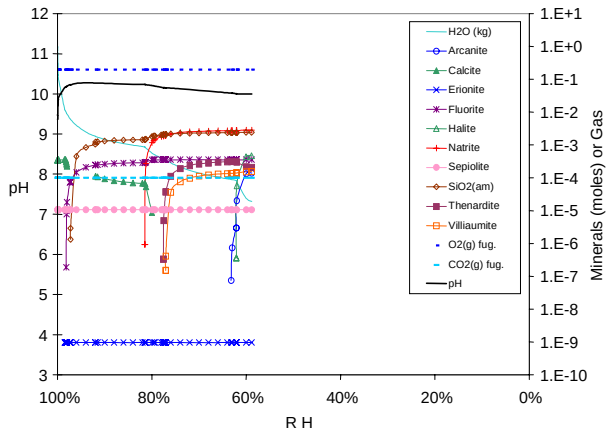

DTN: MO0304SPACSALT.000\10c4t1e.xls.xls

Figure II-10-6. Bin 10 Mineral Precipitation Evaporation Predictions vs. Relative Humidity at 100ºC and 10^{-4} CO_2 Fugacity

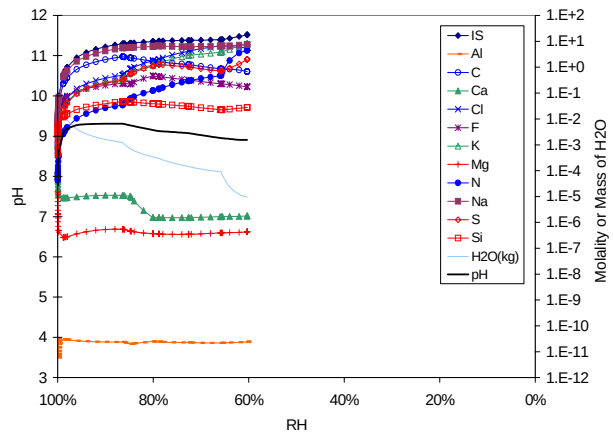

DTN: MO0304SPACSALT.000\10c2t7e.xls.xls

Figure II-10-7. Bin 10 Aqueous Composition Evaporation Predictions vs. Relative Humidity at 70ºC and 10^{-2} CO_2 Fugacity

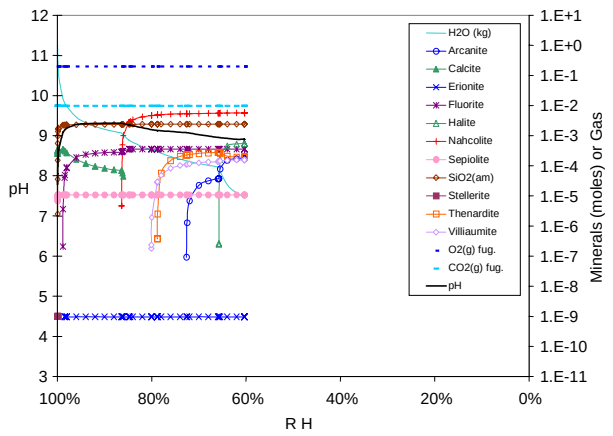

DTN: MO0304SPACSALT.000\10c2t7e.xls.xls

Figure II-10-8. Bin 10 Mineral Precipitation Evaporation Predictions vs. Relative Humidity at 70ºC and 10^{-2} CO_2 Fugacity

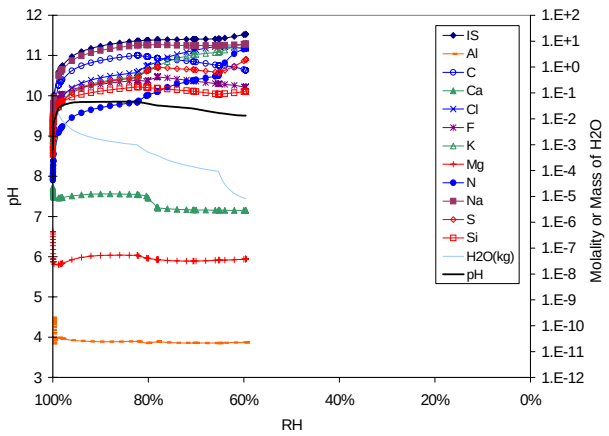

DTN: MO0304SPACSALT.000\10c3t7e.xls.xls

Figure II-10-9. Bin 10 Aqueous Composition Evaporation Predictions vs. Relative Humidity at 70ºC and 10^{-3} CO_2 Fugacity

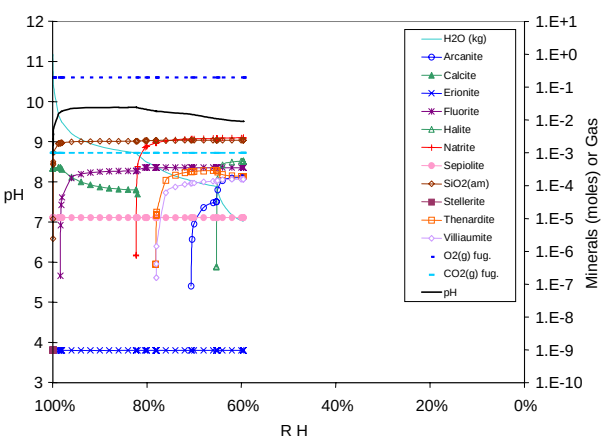

DTN: MO0304SPACSALT.000\10c3t7e.xls.xls

Figure II-10-10. Bin 10 Mineral Precipitation Evaporation Predictions vs. Relative Humidity at 70ºC and 10^{-3} CO_2 Fugacity

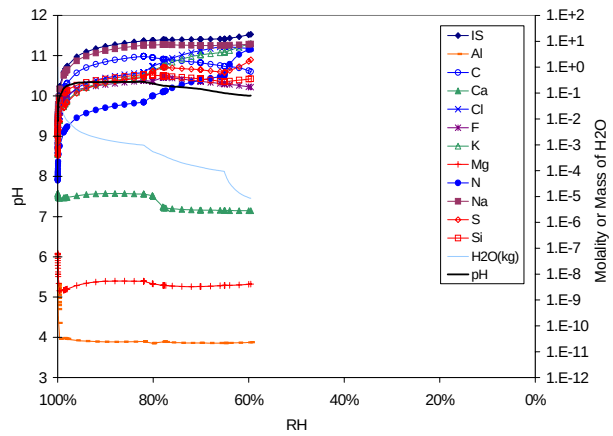

DTN: MO0304SPACSALT.000\10c4t7e.xls.xls

Figure II-10-11. Bin 10 Aqueous Composition Evaporation Predictions vs. Relative Humidity at 70ºC and 10^{-4} CO_2 Fugacity

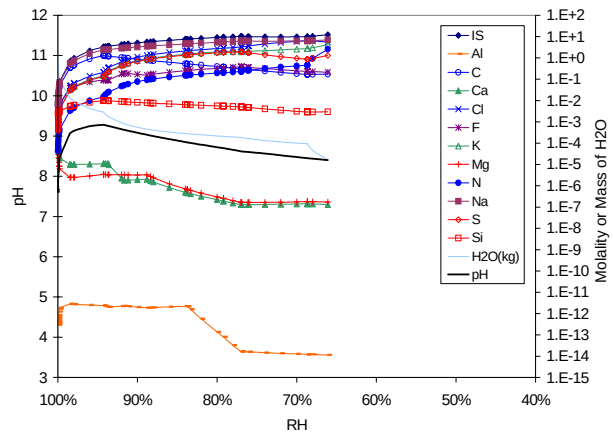

DTN: MO0304SPACSALT.000\10c2t4e.xls.xls

Figure II-10-13. Bin 10 Aqueous Composition Evaporation Predictions vs. Relative Humidity at 40ºC and 10^{-2} CO_2 Fugacity

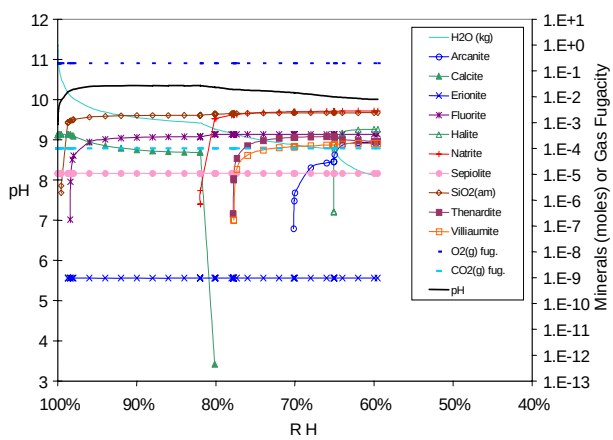

DTN: MO0304SPACSALT.000\10c4t7e.xls.xls

Figure II-10-12. Bin 10 Mineral Precipitation Evaporation Predictions vs. Relative Humidity at 70ºC and 10^{-4} CO_2 Fugacity

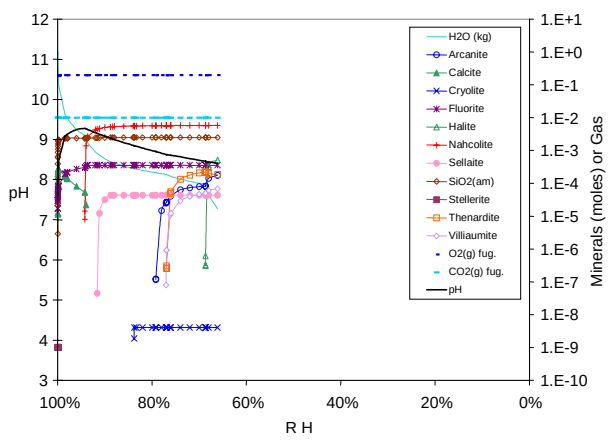

DTN: MO0304SPACSALT.000\10c2t4e.xls.xls

Figure II-10-14. Bin 10 Mineral Precipitation Evaporation Predictions vs. Relative Humidity at 40ºC and 10^{-2} CO_2 Fugacity

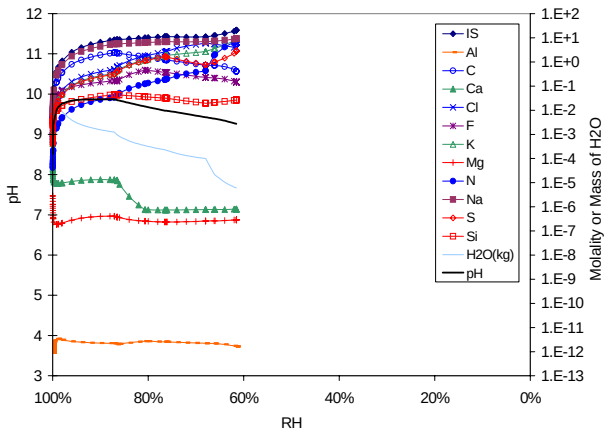

DTN: MO0304SPACSALT.000\10c3t4e.xls.xls

Figure II-10-15. Bin 10 Aqueous Composition Evaporation Predictions vs. Relative Humidity at 40ºC and 10^{-3} CO_2 Fugacity

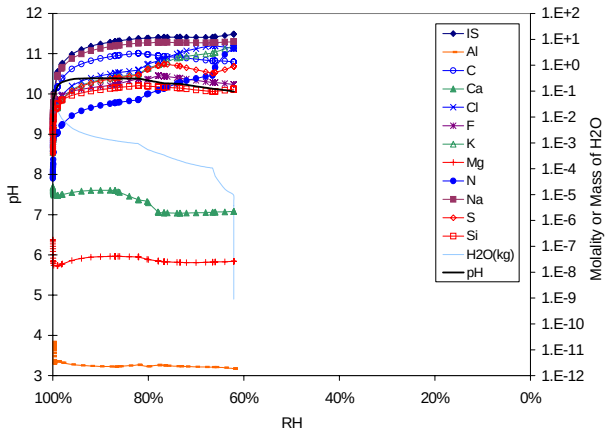

DTN: MO0304SPACSALT.000\10c4t4e.xls.xls

Figure II-10-17. Bin 10 Aqueous Composition Evaporation Predictions vs. Relative Humidity at 40ºC and 10^{-4} CO_2 Fugacity

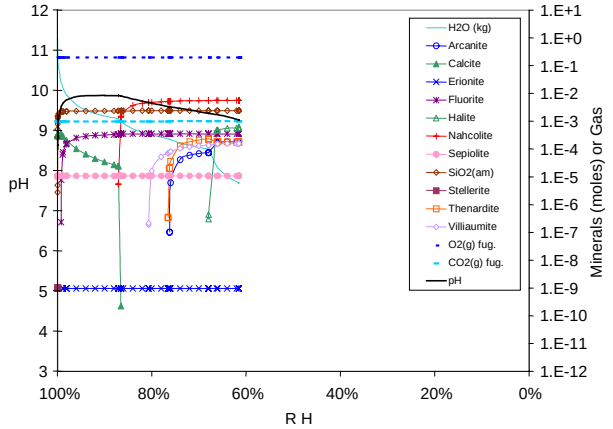

DTN: MO0304SPACSALT.000\10c3t4e.xls.xls

Figure II-10-16. Bin 10 Mineral Precipitation Evaporation Predictions vs. Relative Humidity at 40ºC and 10^{-3} CO_2 Fugacity

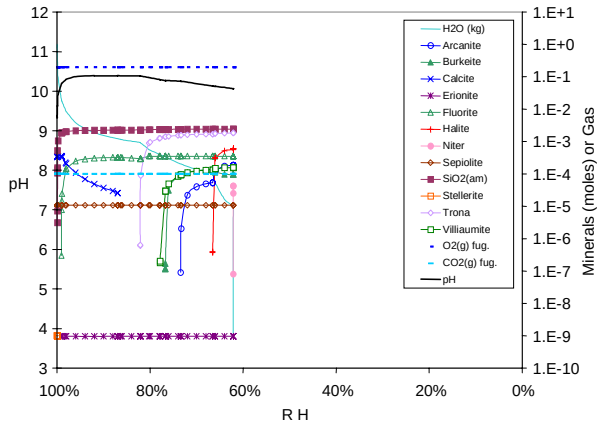

DTN: MO0304SPACSALT.000\10c4t4e.xls.xls

Figure II-10-18. Bin 10 Mineral Precipitation Evaporation Predictions vs. Relative Humidity at 40ºC and 10^{-4} CO_2 Fugacity

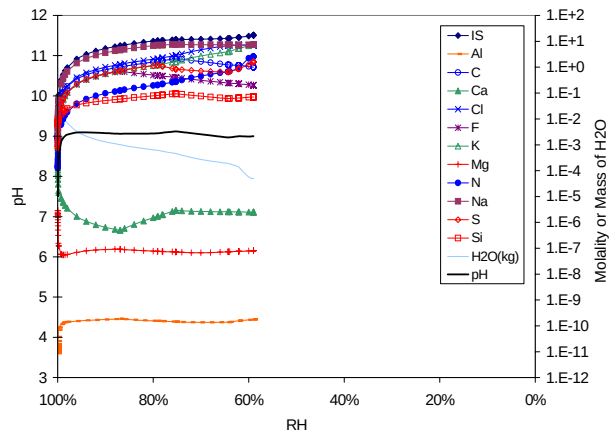

DTN: MO0304SPACSALT.000\11c2t1e.xls.xls

Figure II-11-1. Bin 11 Aqueous Composition Evaporation Predictions vs. Relative Humidity at 100ºC and 10^{-2} CO_2 Fugacity

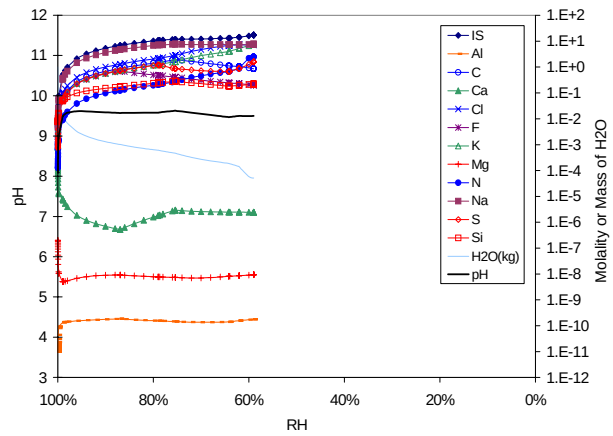

DTN: MO0304SPACSALT.000\11c3t1e.xls.xls

Figure II-11-3. Bin 11 Aqueous Composition Evaporation Predictions vs. Relative Humidity at 100ºC and 10^{-3} CO_2 Fugacity

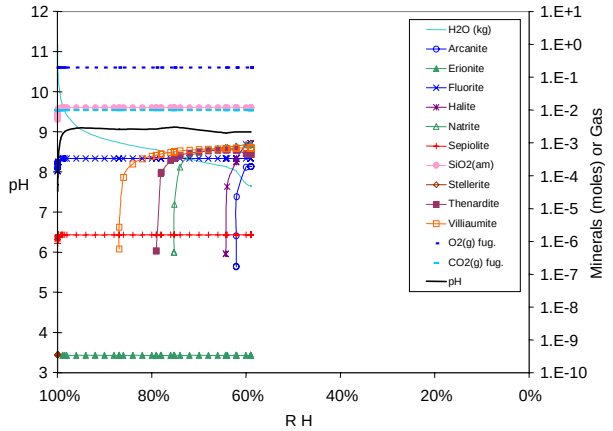

DTN: MO0304SPACSALT.000\11c2t1e.xls.xls

Figure II-11-2. Bin 11 Mineral Precipitation Evaporation Predictions vs. Relative Humidity at 100ºC and 10^{-2} CO_2 Fugacity

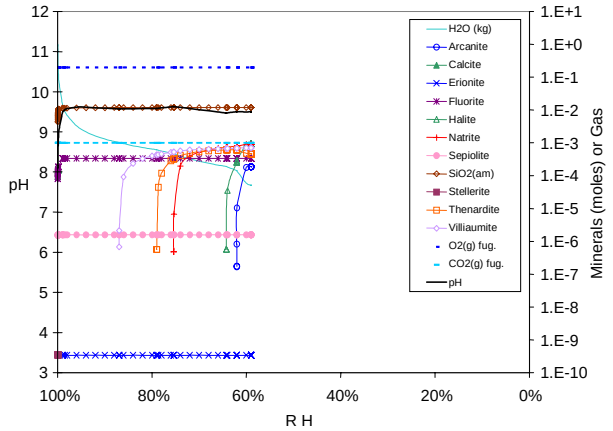

DTN: MO0304SPACSALT.000\11c3t1e.xls.xls

Figure II-11-4. Bin 11 Mineral Precipitation Evaporation Predictions vs. Relative Humidity at 100ºC and 10^{-3} CO_2 Fugacity

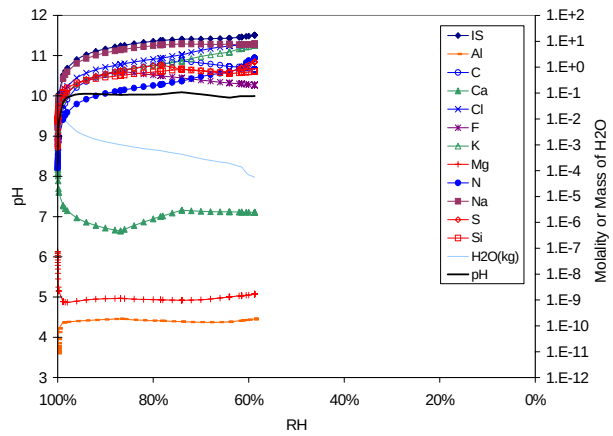

DTN: MO0304SPACSALT.000\11c4t1e.xls.xls

Figure II-11-5. Bin 11 Aqueous Composition Evaporation Predictions vs. Relative Humidity at 100ºC and 10^{-4} CO_2 Fugacity

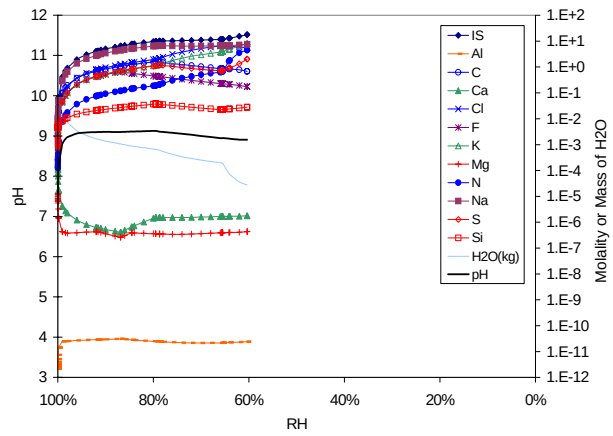

DTN: MO0304SPACSALT.000\11c2t7e.xls.xls

Figure II-11-7. Bin 11 Aqueous Composition Evaporation Predictions vs. Relative Humidity at 70ºC and 10^{-2} CO_2 Fugacity

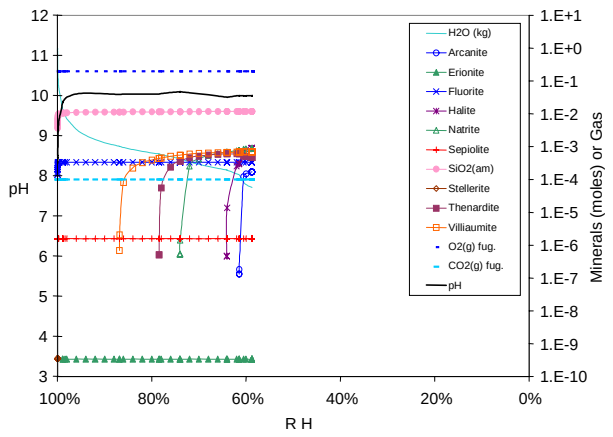

DTN: MO0304SPACSALT.000\11c4t1e.xls.xls

Figure II-11-6. Bin 11 Mineral Precipitation Evaporation Predictions vs. Relative Humidity at 100ºC and 10^{-4} CO_2 Fugacity

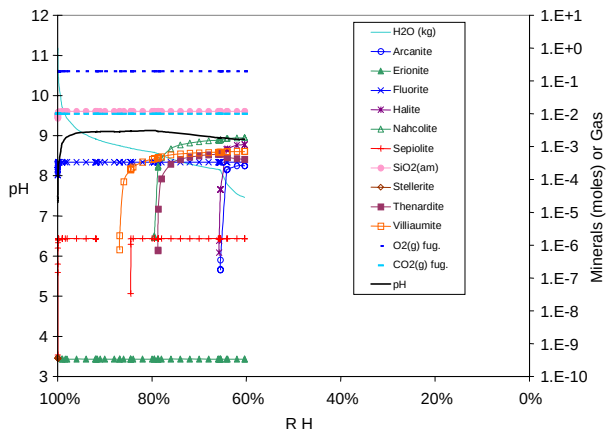

DTN: MO0304SPACSALT.000\11c2t7e.xls.xls

Figure II-11-8. Bin 11 Mineral Precipitation Evaporation Predictions vs. Relative Humidity at 70ºC and 10^{-2} CO_2 Fugacity

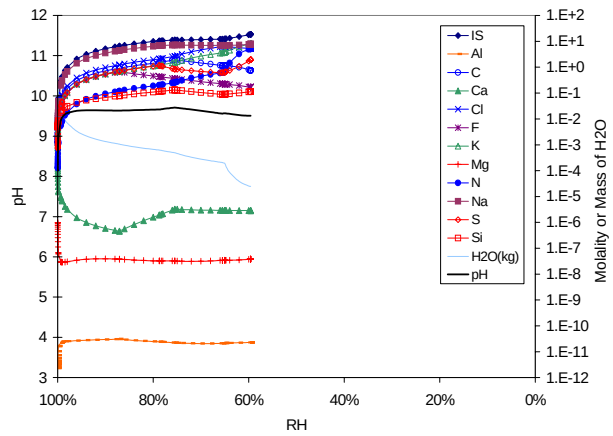

DTN: MO0304SPACSALT.000\11c3t7e.xls.xls

Figure II-11-9. Bin 11 Aqueous Composition Evaporation Predictions vs. Relative Humidity at 70ºC and 10^{-3} CO_2 Fugacity

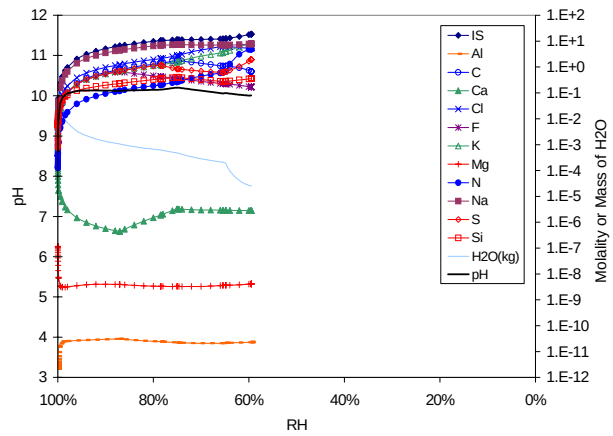

DTN: MO0304SPACSALT.000\11c4t7e.xls.xls

Figure II-11-11. Bin 11 Aqueous Composition Evaporation Predictions vs. Relative Humidity at 70ºC and 10^{-4} CO_2 Fugacity

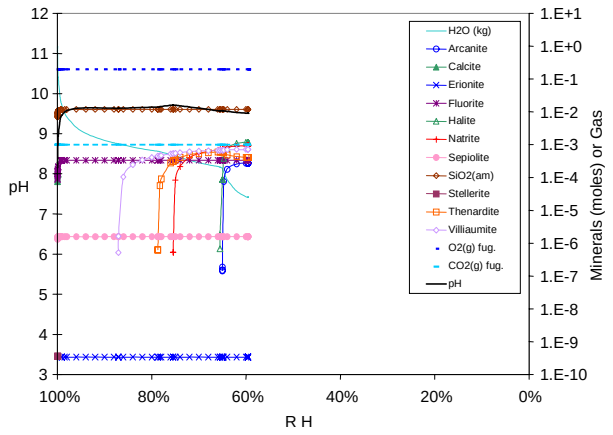

DTN: MO0304SPACSALT.000\11c3t7e.xls.xls

Figure II-11-10. Bin 11 Mineral Precipitation Evaporation Predictions vs. Relative Humidity at 70ºC and 10^{-3} CO_2 Fugacity

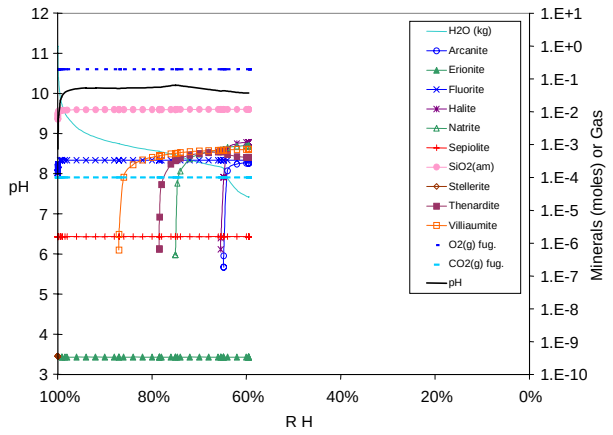

DTN: MO0304SPACSALT.000\11c4t7e.xls.xls

Figure II-11-12. Bin 11 Mineral Precipitation Evaporation Predictions vs. Relative Humidity at 70ºC and 10^{-4} CO_2 Fugacity

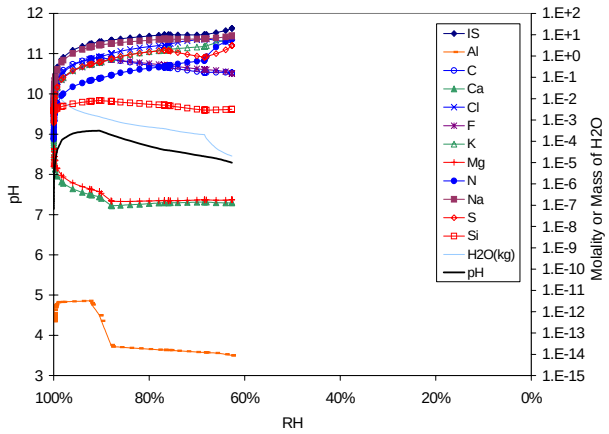

DTN: MO0304SPACSALT.000\11c2t4e.xls.xls

Figure II-11-13. Bin 11 Aqueous Composition Evaporation Predictions vs. Relative Humidity at 40ºC and 10^{-2} CO_2 Fugacity

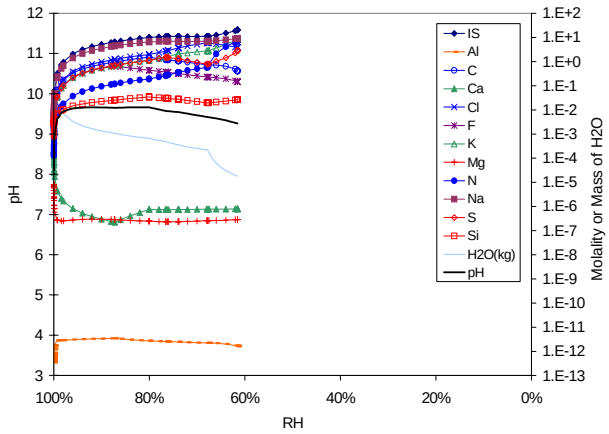

DTN: MO0304SPACSALT.000\11c3t4e.xls.xls

Figure II-11-15. Bin 11 Aqueous Composition Evaporation Predictions vs. Relative Humidity at 40ºC and 10^{-3} CO_2 Fugacity

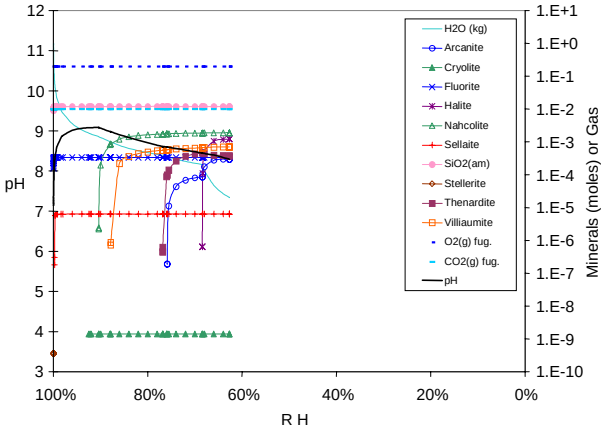

DTN: MO0304SPACSALT.000\11c2t4e.xls.xls

Figure II-11-14. Bin 11 Mineral Precipitation Evaporation Predictions vs. Relative Humidity at 40ºC and 10^{-2} CO_2 Fugacity

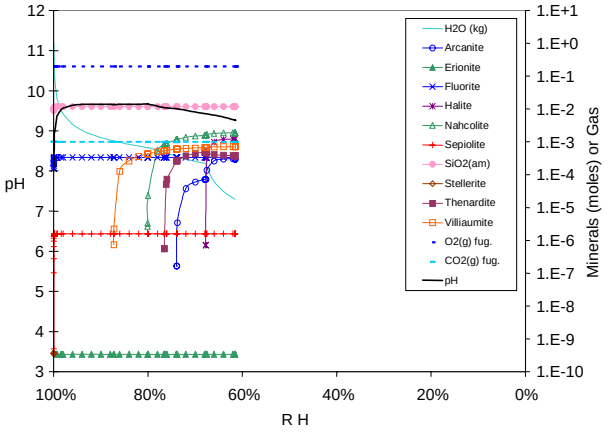

DTN: MO0304SPACSALT.000\11c3t4e.xls.xls

Figure II-11-16. Bin 11 Mineral Precipitation Evaporation Predictions vs. Relative Humidity at 40ºC and 10^{-3} CO_2 Fugacity

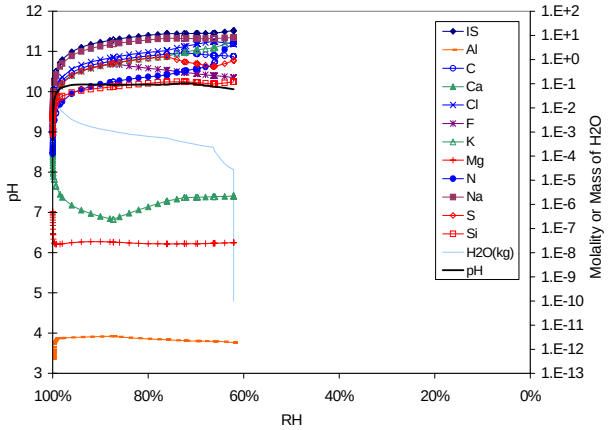

DTN: MO0304SPACSALT.000\11c4t4e.xls.xls

Figure II-11-17. Bin 11 Aqueous Composition Evaporation Predictions vs. Relative Humidity at 40ºC and 10^{-4} CO_2 Fugacity

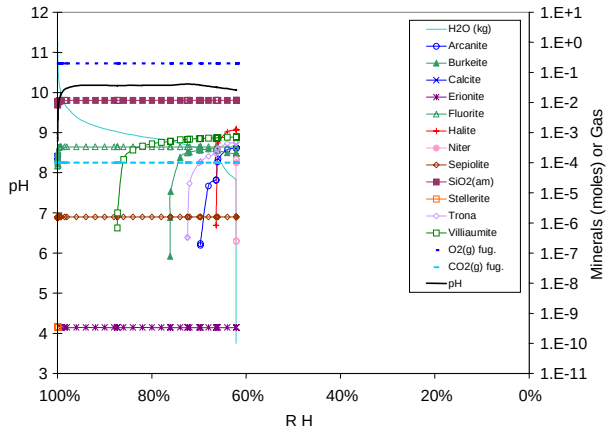

DTN: MO0304SPACSALT.000\11c4t4e.xls.xls

Figure II-11-18. Bin 11 Mineral Precipitation Evaporation Predictions vs. Relative Humidity at 40ºC and 10^{-4} CO_2 Fugacity

INTENTIONALLY LEFT BLANK

ATTACHMENT III
DUST LEACHATE LOOKUP TABLE RESULTS

FIGURES

Page

III-01-1. Bin 01 Aqueous Composition Evaporation Predictions vs. Relative Humidity at 40ºC and 10^{-2} CO_2 Fugacity III-6
III-01-2. Bin 01 Mineral Precipitation Evaporation Predictions vs. Relative Humidity at 40ºC and 10^{-2} CO_2 Fugacity III-6
III-01-3. Bin 01 Aqueous Composition Evaporation Predictions vs. Relative Humidity at 70ºC and 10^{-2} CO_2 Fugacity III-6
III-01-4. Bin 01 Mineral Precipitation Evaporation Predictions vs. Relative Humidity at 70ºC and 10^{-2} CO_2 Fugacity III-6
III-01-5. Bin 01 Aqueous Composition Evaporation Predictions vs. Relative Humidity at 100ºC and 10^{-2} CO_2 Fugacity III-7
III-01-6. Bin 01 Mineral Precipitation Evaporation Predictions vs. Relative Humidity at 100ºC and 10^{-2} CO_2 Fugacity III-7
III-01-7. Bin 01 Aqueous Composition Evaporation Predictions vs. Relative Humidity at 120ºC and 10^{-2} CO_2 Fugacity III-7
III-01-8. Bin 01 Mineral Precipitation Evaporation Predictions vs. Relative Humidity at 120ºC and 10^{-2} CO_2 Fugacity III-7
III-01-9. Bin 01 Aqueous Composition Evaporation Predictions vs. Relative Humidity at 140ºC and 10^{-2} CO_2 Fugacity III-8
III-01-10. Bin 01 Mineral Composition Evaporation Predictions vs. Relative Humidity at 140ºC and 10^{-2} CO_2 Fugacity III-8
III-01-11. Bin 01 Aqueous Composition Evaporation Predictions vs. Relative Humidity at 40ºC and 10^{-3} CO_2 Fugacity III-8
III-01-12. Bin 01 Mineral Precipitation Evaporation Predictions vs. Relative Humidity at 40ºC and 10^{-3} CO_2 Fugacity III-8
III-01-13. Bin 01 Aqueous Composition Evaporation Predictions vs. Relative Humidity at 70ºC and 10^{-3} CO_2 Fugacity III-9
III-01-14. Bin 01 Mineral Precipitation Evaporation Predictions vs. Relative Humidity at 70ºC and 10^{-3} CO_2 Fugacity III-9
III-01-15. Bin 01 Aqueous Composition Evaporation Predictions vs. Relative Humidity at 100ºC and 10^{-3} CO_2 Fugacity III-9
III-01-16. Bin 01 Mineral Precipitation Evaporation Predictions vs. Relative Humidity at 100ºC and 10^{-3} CO_2 Fugacity III-9
III-01-17. Bin 01 Aqueous Composition Evaporation Predictions vs. Relative Humidity at 120ºC and 10^{-3} CO_2 Fugacity III-10
III-01-18. Bin 01 Mineral Precipitation Evaporation Predictions vs. Relative Humidity at 120ºC and 10^{-3} CO_2 Fugacity III-10
III-01-19. Bin 01 Aqueous Composition Evaporation Predictions vs. Relative Humidity at 140ºC and 10^{-3} CO_2 Fugacity III-10
III-01-20. Bin 01 Mineral Precipitation Evaporation Predictions vs. Relative Humidity at 140ºC and 10^{-3} CO_2 Fugacity III-10
III-01-21. Bin 01 Aqueous Composition Evaporation Predictions vs. Relative Humidity at 40ºC and 10^{-4} CO_2 Fugacity III-11
III-01-22. Bin 01 Mineral Precipitation Evaporation Predictions vs. Relative Humidity at 40ºC and 10^{-4} CO_2 Fugacity III-11
III-01-23. Bin 01 Aqueous Composition Evaporation Predictions vs. Relative Humidity at 70ºC and 10^{-4} CO_2 Fugacity III-11
III-01-24. Bin 01 Mineral Precipitation Evaporation Predictions vs. Relative Humidity at 70ºC and 10^{-4} CO_2 Fugacity III-11
III-01-25. Bin 01 Aqueous Composition Evaporation Predictions vs. Relative Humidity at 100ºC and 10^{-4} CO_2 Fugacity III-12
III-01-26. Bin 01 Mineral Precipitation Evaporation Predictions vs. Relative Humidity at 100ºC and 10^{-4} CO_2 Fugacity III-12

FIGURES (Continued)

Page

III-01-27. Bin 01 Aqueous Composition Evaporation Predictions vs. Relative Humidity at 120ºC and 10^{-4} CO_2 Fugacity III-12
III-01-28. Bin 01 Mineral Precipitation Evaporation Predictions vs. Relative Humidity at 120ºC and 10^{-4} CO_2 Fugacity III-12
III-01-29. Bin 01 Aqueous Composition Evaporation Predictions vs. Relative Humidity at 140ºC and 10^{-4} CO_2 Fugacity III-13
III-01-30. Bin 01 Mineral Precipitation Evaporation Predictions vs. Relative Humidity at 140ºC and 10^{-4} CO_2 Fugacity III-13
III-02-1. Bin 02 Aqueous Composition Evaporation Predictions vs. Relative Humidity at 40ºC and 10^{-2} CO_2 Fugacity III-13
III-02-2. Bin 02 Mineral Precipitation Evaporation Predictions vs. Relative Humidity at 40ºC and 10^{-2} CO_2 Fugacity III-13
III-02-3. Bin 02 Aqueous Composition Evaporation Predictions vs. Relative Humidity at 70ºC and 10^{-2} CO_2 Fugacity III-14
III-02-4. Bin 02 Mineral Precipitation Evaporation Predictions vs. Relative Humidity at 70ºC and 10^{-2} CO_2 Fugacity III-14
III-02-5. Bin 02 Aqueous Composition Evaporation Predictions vs. Relative Humidity at 100ºC and 10^{-2} CO_2 Fugacity III-14
III-02-6. Bin 02 Mineral Precipitation Evaporation Predictions vs. Relative Humidity at 100ºC and 10^{-2} CO_2 Fugacity III-14
III-02-7. Bin 02 Aqueous Composition Evaporation Predictions vs. Relative Humidity at 120ºC and 10^{-2} CO_2 Fugacity III-15
III-02-8. Bin 02 Mineral Precipitation Evaporation Predictions vs. Relative Humidity at 120ºC and 10^{-2} CO_2 Fugacity III-15
III-02-9. Bin 02 Aqueous Composition Evaporation Predictions vs. Relative Humidity at 140ºC and 10^{-2} CO_2 Fugacity III-15
III-02-10. Bin 02 Mineral Precipitation Evaporation Predictions vs. Relative Humidity at 140ºC and 10^{-2} CO_2 Fugacity III-15
III-02-11. Bin 02 Aqueous Composition Evaporation Predictions vs. Relative Humidity at 40ºC and 10^{-3} CO_2 Fugacity III-16
III-02-12. Bin 02 Mineral Precipitation Evaporation Predictions vs. Relative Humidity at 40ºC and 10^{-3} CO_2 Fugacity III-16
III-02-13. Bin 02 Aqueous Composition Evaporation Predictions vs. Relative Humidity at 70ºC and 10^{-3} CO_2 Fugacity III-16
III-02-14. Bin 02 Mineral Precipitation Evaporation Predictions vs. Relative Humidity at 70ºC and 10^{-3} CO_2 Fugacity III-16
III-02-15. Bin 02 Aqueous Composition Evaporation Predictions vs. Relative Humidity at 100ºC and 10^{-3} CO_2 Fugacity III-17
III-02-16. Bin 02 Mineral Precipitation Evaporation Predictions vs. Relative Humidity at 100ºC and 10^{-3} CO_2 Fugacity III-17
III-02-17. Bin 02 Aqueous Composition Evaporation Predictions vs. Relative Humidity at 120ºC and 10^{-3} CO_2 Fugacity III-17
III-02-18. Bin 02 Mineral Precipitation Evaporation Predictions vs. Relative Humidity at 120ºC and 10^{-3} CO_2 Fugacity III-17
III-02-19. Bin 02 Aqueous Composition Evaporation Predictions vs. Relative Humidity at 140ºC and 10^{-3} CO_2 Fugacity III-18
III-02-20. Bin 02 Mineral Precipitation Evaporation Predictions vs. Relative Humidity at 140ºC and 10^{-3} CO_2 Fugacity III-18
III-02-21. Bin 02 Aqueous Composition Evaporation Predictions vs. Relative Humidity at 40ºC and 10^{-4} CO_2 Fugacity III-18
III-02-22. Bin 02 Mineral Precipitation Evaporation Predictions vs. Relative Humidity at 40ºC and 10^{-4} CO_2 Fugacity III-18

FIGURES (Continued)

Page

III-02-23. Bin 02 Aqueous Composition Evaporation Predictions vs. Relative Humidity at 70ºC and 10^{-4} CO_2 Fugacity III-19
III-02-24. Bin 02 Mineral Precipitation Evaporation Predictions vs. Relative Humidity at 70ºC and 10^{-4} CO_2 Fugacity III-19
III-02-25. Bin 02 Aqueous Composition Evaporation Predictions vs. Relative Humidity at 100ºC and 10^{-4} CO_2 Fugacity III-19
III-02-26. Bin 02 Mineral Precipitation Evaporation Predictions vs. Relative Humidity at 100ºC and 10^{-4} CO_2 Fugacity III-19
III-02-27. Bin 02 Aqueous Composition Evaporation Predictions vs. Relative Humidity at 120ºC and 10^{-4} CO_2 Fugacity III-20
III-02-28. Bin 02 Mineral Precipitation Evaporation Predictions vs. Relative Humidity at 120ºC and 10^{-4} CO_2 Fugacity III-20
III-02-29. Bin 02 Aqueous Composition Evaporation Predictions vs. Relative Humidity at 140ºC and 10^{-4} CO_2 Fugacity III-20
III-02-30. Bin 02 Mineral Precipitation Evaporation Predictions vs. Relative Humidity at 140ºC and 10^{-4} CO_2 Fugacity III-20
III-03-1. Bin 03 Aqueous Composition Evaporation Predictions vs. Relative Humidity at 40ºC and 10^{-2} CO_2 Fugacity III-21
III-03-2. Bin 03 Mineral Precipitation Evaporation Predictions vs. Relative Humidity at 40ºC and 10^{-2} CO_2 Fugacity III-21
III-03-3. Bin 03 Aqueous Composition Evaporation Predictions vs. Relative Humidity at 70ºC and 10^{-2} CO_2 Fugacity III-21
III-03-4. Bin 03 Mineral Precipitation Evaporation Predictions vs. Relative Humidity at 70ºC and 10^{-2} CO_2 Fugacity III-21
III-03-5. Bin 03 Aqueous Composition Evaporation Predictions vs. Relative Humidity at 100ºC and 10^{-2} CO_2 Fugacity III-22
III-03-6. Bin 03 Mineral Precipitation Evaporation Predictions vs. Relative Humidity at 100ºC and 10^{-2} CO_2 Fugacity III-22
III-03-7. Bin 03 Aqueous Composition Evaporation Predictions vs. Relative Humidity at 120ºC and 10^{-2} CO_2 Fugacity III-22
III-03-8. Bin 03 Mineral Composition Evaporation Predictions vs. Relative Humidity at 120ºC and 10^{-2} CO_2 Fugacity III-22
III-03-9. Bin 03 Aqueous Composition Evaporation Predictions vs. Relative Humidity at 140ºC and 10^{-2} CO_2 Fugacity III-23
III-03-10. Bin 03 Mineral Composition Evaporation Predictions vs. Relative Humidity at 140ºC and 10^{-2} CO_2 Fugacity III-23
III-03-11. Bin 03 Aqueous Composition Evaporation Predictions vs. Relative Humidity at 40ºC and 10^{-3} CO_2 Fugacity III-23
III-03-12. Bin 03 Mineral Precipitation Evaporation Predictions vs. Relative Humidity at 40ºC and 10^{-3} CO_2 Fugacity III-23
III-03-13. Bin 03 Aqueous Composition Evaporation Predictions vs. Relative Humidity at 70ºC and 10^{-3} CO_2 Fugacity III-24
III-03-14. Bin 03 Mineral Precipitation Evaporation Predictions vs. Relative Humidity at 70ºC and 10^{-3} CO_2 Fugacity III-24
III-03-15. Bin 03 Aqueous Composition Evaporation Predictions vs. Relative Humidity at 100ºC and 10^{-3} CO_2 Fugacity III-24
III-03-16. Bin 03 Mineral Precipitation Evaporation Predictions vs. Relative Humidity at 100ºC and 10^{-3} CO_2 Fugacity III-24
III-03-17. Bin 03 Aqueous Composition Evaporation Predictions vs. Relative Humidity at 120ºC and 10^{-3} CO_2 Fugacity III-25
III-03-18. Bin 03 Mineral Precipitation Evaporation Predictions vs. Relative Humidity at 120ºC and 10^{-3} CO_2 Fugacity III-25

FIGURES (Continued)

Page

III-03-19. Bin 03 Aqueous Composition Evaporation Predictions vs. Relative Humidity at 140ºC and 10^{-3} CO_2 Fugacity III-25
III-03-20. Bin 03 Mineral Precipitation Evaporation Predictions vs. Relative Humidity at 140ºC and 10^{-3} CO_2 Fugacity III-25
III-03-21. Bin 03 Aqueous Composition Evaporation Predictions vs. Relative Humidity at 40ºC and 10^{-4} CO_2 Fugacity III-26
III-03-22. Bin 03 Mineral Precipitation Evaporation Predictions vs. Relative Humidity at 40ºC and 10^{-4} CO_2 Fugacity III-26
III-03-23. Bin 03 Aqueous Composition Evaporation Predictions vs. Relative Humidity at 70ºC and 10^{-4} CO_2 Fugacity III-26
III-03-24. Bin 03 Mineral Precipitation Evaporation Predictions vs. Relative Humidity at 70ºC and 10^{-4} CO_2 Fugacity III-26
III-03-25. Bin 03 Aqueous Composition Evaporation Predictions vs. Relative Humidity at 100ºC and 10^{-4} CO_2 Fugacity III-27
III-03-26. Bin 03 Mineral Precipitation Evaporation Predictions vs. Relative Humidity at 100ºC and 10^{-4} CO_2 Fugacity III-27
III-03-27. Bin 03 Aqueous Composition Evaporation Predictions vs. Relative Humidity at 120ºC and 10^{-4} CO_2 Fugacity III-27
III-03-28. Bin 03 Mineral Precipitation Evaporation Predictions vs. Relative Humidity at 120ºC and 10^{-4} CO_2 Fugacity III-27
III-03-29. Bin 03 Aqueous Composition Evaporation Predictions vs. Relative Humidity at 140ºC and 10^{-4} CO_2 Fugacity III-28
III-03-30. Bin 03 Mineral Precipitation Evaporation Predictions vs. Relative Humidity at 140ºC and 10^{-4} CO_2 Fugacity III-28
III-04-1. Bin 04 Aqueous Composition Evaporation Predictions vs. Relative Humidity at 40ºC and 10^{-2} CO_2 Fugacity III-28
III-04-2. Bin 04 Mineral Precipitation Evaporation Predictions vs. Relative Humidity at 40ºC and 10^{-2} CO_2 Fugacity III-28
III-04-3. Bin 04 Aqueous Composition Evaporation Predictions vs. Relative Humidity at 70ºC and 10^{-2} CO_2 Fugacity III-29
III-04-4. Bin 04 Mineral Precipitation Evaporation Predictions vs. Relative Humidity at 70ºC and 10^{-2} CO_2 Fugacity III-29
III-04-5. Bin 04 Aqueous Composition Evaporation Predictions vs. Relative Humidity at 100ºC and 10^{-2} CO_2 Fugacity III-29
III-04-6. Bin 04 Mineral Precipitation Evaporation Predictions vs. Relative Humidity at 100ºC and 10^{-2} CO_2 Fugacity III-29
III-04-7. Bin 04 Aqueous Composition Evaporation Predictions vs. Relative Humidity at 120ºC and 10^{-2} CO_2 Fugacity III-30
III-04-8. Bin 04 Mineral Precipitation Evaporation Predictions vs. Relative Humidity at 120ºC and 10^{-2} CO_2 Fugacity III-30
III-04-9. Bin 04 Aqueous Composition Evaporation Predictions vs. Relative Humidity at 140ºC and 10^{-2} CO_2 Fugacity III-30
III-04-10. Bin 04 Mineral Precipitation Evaporation Predictions vs. Relative Humidity at 140ºC and 10^{-2} CO_2 Fugacity III-30
III-04-11. Bin 04 Aqueous Composition Evaporation Predictions vs. Relative Humidity at 40ºC and 10^{-3} CO_2 Fugacity III-31
III-04-12. Bin 04 Mineral Precipitation Evaporation Predictions vs. Relative Humidity at 40ºC and 10^{-3} CO_2 Fugacity III-31
III-04-13. Bin 04 Aqueous Composition Evaporation Predictions vs. Relative Humidity at 70ºC and 10^{-3} CO_2 Fugacity III-31
III-04-14. Bin 04 Mineral Precipitation Evaporation Predictions vs. Relative Humidity at 70ºC and 10^{-3} CO_2 Fugacity III-31

FIGURES (Continued)

Page

III-04-15. Bin 04 Aqueous Composition Evaporation Predictions vs. Relative Humidity at 100ºC and 10^{-3} CO_2 Fugacity III-32
III-04-16. Bin 04 Mineral Precipitation Evaporation Predictions vs. Relative Humidity at 100ºC and 10^{-3} CO_2 Fugacity III-32
III-04-17. Bin 04 Aqueous Composition Evaporation Predictions vs. Relative Humidity at 120ºC and 10^{-3} CO_2 Fugacity III-32
III-04-18. Bin 04 Mineral Precipitation Evaporation Predictions vs. Relative Humidity at 120ºC and 10^{-3} CO_2 Fugacity III-32
III-04-19. Bin 04 Aqueous Composition Evaporation Predictions vs. Relative Humidity at 140ºC and 10^{-3} CO_2 Fugacity III-33
III-04-20. Bin 04 Mineral Precipitation Evaporation Predictions vs. Relative Humidity at 140ºC and 10^{-3} CO_2 Fugacity III-33
III-04-21. Bin 04 Aqueous Composition Evaporation Predictions vs. Relative Humidity at 40ºC and 10^{-4} CO_2 Fugacity III-33
III-04-22. Bin 04 Mineral Precipitation Evaporation Predictions vs. Relative Humidity at 40ºC and 10^{-4} CO_2 Fugacity III-33
III-04-23. Bin 04 Aqueous Composition Evaporation Predictions vs. Relative Humidity at 70ºC and 10^{-4} CO_2 Fugacity III-34
III-04-24. Bin 04 Mineral Precipitation Evaporation Predictions vs. Relative Humidity at 70ºC and 10^{-4} CO_2 Fugacity III-34
III-04-25. Bin 04 Aqueous Composition Evaporation Predictions vs. Relative Humidity at 100ºC and 10^{-4} CO_2 Fugacity III-34
III-04-26. Bin 04 Mineral Precipitation Evaporation Predictions vs. Relative Humidity at 100ºC and 10^{-4} CO_2 Fugacity III-34
III-04-27. Bin 04 Aqueous Composition Evaporation Predictions vs. Relative Humidity at 120ºC and 10^{-4} CO_2 Fugacity III-35
III-04-28. Bin 04 Mineral Precipitation Evaporation Predictions vs. Relative Humidity at 120ºC and 10^{-4} CO_2 Fugacity III-35
III-04-29. Bin 04 Aqueous Composition Evaporation Predictions vs. Relative Humidity at 140ºC and 10^{-4} CO_2 Fugacity III-35
III-04-30. Bin 04 Mineral Precipitation Evaporation Predictions vs. Relative Humidity at 140ºC and 10^{-4} CO_2 Fugacity III-35
III-05-1. Bin 05 Aqueous Composition Evaporation Predictions vs. Relative Humidity at 40ºC and 10^{-2} CO_2 Fugacity III-36
III-05-2. Bin 05 Mineral Precipitation Evaporation Predictions vs. Relative Humidity at 40ºC and 10^{-2} CO_2 Fugacity III-36
III-05-3. Bin 05 Aqueous Composition Evaporation Predictions vs. Relative Humidity at 70ºC and 10^{-2} CO_2 Fugacity III-36
III-05-4. Bin 05 Mineral Precipitation Evaporation Predictions vs. Relative Humidity at 70ºC and 10^{-2} CO_2 Fugacity III-36
III-05-5. Bin 05 Aqueous Composition Evaporation Predictions vs. Relative Humidity at 100ºC and 10^{-2} CO_2 Fugacity III-37
III-05-6. Bin 05 Mineral Precipitation Evaporation Predictions vs. Relative Humidity at 100ºC and 10^{-2} CO_2 Fugacity III-37
III-05-7. Bin 05 Aqueous Composition Evaporation Predictions vs. Relative Humidity at 120ºC and 10^{-2} CO_2 Fugacity III-37
III-05-8. Bin 05 Mineral Precipitation Evaporation Predictions vs. Relative Humidity at 120ºC and 10^{-2} CO_2 Fugacity III-37
III-05-9. Bin 05 Aqueous Composition Evaporation Predictions vs. Relative Humidity at 140ºC and 10^{-2} CO_2 Fugacity III-38
III-05-10. Bin 05 Mineral Precipitation Evaporation Predictions vs. Relative Humidity at 140ºC and 10^{-2} CO_2 Fugacity III-38

FIGURES (Continued)

Page

III-05-11. Bin 05 Aqueous Composition Evaporation Predictions vs. Relative Humidity at 40ºC and 10^{-3} CO_2 Fugacity III-38
III-05-12. Bin 05 Mineral Precipitation Evaporation Predictions vs. Relative Humidity at 40ºC and 10^{-3} CO_2 Fugacity III-38
III-05-13. Bin 05 Aqueous Composition Evaporation Predictions vs. Relative Humidity at 70ºC and 10^{-3} CO_2 Fugacity III-39
III-05-14. Bin 05 Mineral Precipitation Evaporation Predictions vs. Relative Humidity at 70ºC and 10^{-3} CO_2 Fugacity III-39
III-05-15. Bin 05 Aqueous Composition Evaporation Predictions vs. Relative Humidity at 100ºC and 10^{-3} CO_2 Fugacity III-39
III-05-16. Bin 05 Mineral Precipitation Evaporation Predictions vs. Relative Humidity at 100ºC and 10^{-3} CO_2 Fugacity III-39
III-05-17. Bin 05 Aqueous Composition Evaporation Predictions vs. Relative Humidity at 120ºC and 10^{-3} CO_2 Fugacity III-40
III-05-18. Bin 05 Mineral Precipitation Evaporation Predictions vs. Relative Humidity at 120ºC and 10^{-3} CO_2 Fugacity III-40
III-05-19. Bin 05 Aqueous Composition Evaporation Predictions vs. Relative Humidity at 140ºC and 10^{-3} CO_2 Fugacity III-40
III-05-20. Bin 05 Mineral Precipitation Evaporation Predictions vs. Relative Humidity at 140ºC and 10^{-3} CO_2 Fugacity III-40
III-05-21. Bin 05 Aqueous Composition Evaporation Predictions vs. Relative Humidity at 40ºC and 10^{-4} CO_2 Fugacity III-41
III-05-22. Bin 05 Mineral Precipitation Evaporation Predictions vs. Relative Humidity at 40ºC and 10^{-4} CO_2 Fugacity III-41
III-05-23. Bin 05 Aqueous Composition Evaporation Predictions vs. Relative Humidity at 70ºC and 10^{-4} CO_2 Fugacity III-41
III-05-24. Bin 05 Mineral Precipitation Evaporation Predictions vs. Relative Humidity at 70ºC and 10^{-4} CO_2 Fugacity III-41
III-05-25. Bin 05 Aqueous Composition Evaporation Predictions vs. Relative Humidity at 100ºC and 10^{-4} CO_2 Fugacity III-42
III-05-26. Bin 05 Mineral Precipitation Evaporation Predictions vs. Relative Humidity at 100ºC and 10^{-4} CO_2 Fugacity III-42
III-05-27. Bin 05 Aqueous Composition Evaporation Predictions vs. Relative Humidity at 120ºC and 10^{-4} CO_2 Fugacity III-42
III-05-28. Bin 05 Mineral Precipitation Evaporation Predictions vs. Relative Humidity at 120ºC and 10^{-4} CO_2 Fugacity III-42
III-05-29. Bin 05 Aqueous Composition Evaporation Predictions vs. Relative Humidity at 140ºC and 10^{-4} CO_2 Fugacity III-43
III-05-30. Bin 05 Mineral Precipitation Evaporation Predictions vs. Relative Humidity at 140ºC and 10^{-4} CO_2 Fugacity III-43
III-06-1. Bin 06 Aqueous Composition Evaporation Predictions vs. Relative Humidity at 40ºC and 10^{-2} CO_2 Fugacity III-43
III-06-2. Bin 06 Mineral Precipitation Evaporation Predictions vs. Relative Humidity at 40ºC and 10^{-2} CO_2 Fugacity III-43
III-06-3. Bin 06 Aqueous Composition Evaporation Predictions vs. Relative Humidity at 70ºC and10^{-2} CO_2 Fugacity III-44
III-06-4. Bin 06 Mineral Precipitation Evaporation Predictions vs. Relative Humidity at 70ºC and 10^{-2} CO_2 Fugacity III-44
III-06-5. Bin 06 Aqueous Composition Evaporation Predictions vs. Relative Humidity at 100ºC and 10^{-2} CO_2 Fugacity III-44
III-06-6. Bin 06 Mineral Precipitation Evaporation Predictions vs. Relative Humidity at 100ºC and 10^{-2} CO_2 Fugacity III-44

FIGURES (Continued)

Page

III-06-7. Bin 06 Aqueous Composition Evaporation Predictions vs. Relative Humidity at 120ºC and 10^{-2} CO_2 Fugacity III-45
III-06-8. Bin 06 Mineral Precipitation Evaporation Predictions vs. Relative Humidity at 120ºC and 10^{-2} CO_2 Fugacity III-45
III-06-9. Bin 06 Aqueous Composition Evaporation Predictions vs. Relative Humidity at 140ºC and 10^{-2} CO_2 Fugacity III-45
III-06-10. Bin 06 Mineral Precipitation Evaporation Predictions vs. Relative Humidity at 140ºC and 10^{-2} CO_2 Fugacity III-45
III-06-11. Bin 06 Aqueous Composition Evaporation Predictions vs. Relative Humidity at 40ºC and 10^{-3} CO_2 Fugacity III-46
III-06-12. Bin 06 Mineral Precipitation Evaporation Predictions vs. Relative Humidity at 40ºC and 10^{-3} CO_2 Fugacity III-46
III-06-13. Bin 06 Aqueous Composition Evaporation Predictions vs. Relative Humidity at 70ºC and 10^{-3} CO_2 Fugacity III-46
III-06-14. Bin 06 Mineral Precipitation Evaporation Predictions vs. Relative Humidity at 70ºC and 10^{-3} CO_2 Fugacity III-46
III-06-15. Bin 06 Aqueous Composition Evaporation Predictions vs. Relative Humidity at 100ºC and 10^{-3} CO_2 Fugacity III-47
III-06-16. Bin 06 Mineral Precipitation Evaporation Predictions vs. Relative Humidity at 100ºC and 10^{-3} CO_2 Fugacity III-47
III-06-17. Bin 06 Aqueous Composition Evaporation Predictions vs. Relative Humidity at 120ºC and 10^{-3} CO_2 Fugacity III-47
III-06-18. Bin 06 Mineral Precipitation Evaporation Predictions vs. Relative Humidity at 120ºC and 10^{-3} CO_2 Fugacity III-47
III-06-19. Bin 06 Aqueous Composition Evaporation Predictions vs. Relative Humidity at 140ºC and 10^{-3} CO_2 Fugacity III-48
III-06-20. Bin 06 Mineral Precipitation Evaporation Predictions vs. Relative Humidity at 140ºC and 10^{-3} CO_2 Fugacity III-48
III-06-21. Bin 06 Aqueous Composition Evaporation Predictions vs. Relative Humidity at 40ºC and 10^{-3} CO_2 Fugacity III-48
III-06-22. Bin 06 Mineral Precipitation Evaporation Predictions vs. Relative Humidity at 40ºC and 10^{-4} CO_2 Fugacity III-48
III-06-23. Bin 06 Aqueous Composition Evaporation Predictions vs. Relative Humidity at 70ºC and 10^{-4} CO_2 Fugacity III-49
III-06-24. Bin 06 Mineral Precipitation Evaporation Predictions vs. Relative Humidity at 70ºC and 10^{-4} CO_2 Fugacity III-49
III-06-25. Bin 06 Aqueous Composition Evaporation Predictions vs. Relative Humidity at 100ºC and 10^{-4} CO_2 Fugacity III-49
III-06-26. Bin 06 Mineral Precipitation Evaporation Predictions vs. Relative Humidity at 100ºC and 10^{-4} CO_2 Fugacity III-49
III-06-27. Bin 06 Aqueous Composition Evaporation Predictions vs. Relative Humidity at 120ºC and 10^{-4} CO_2 Fugacity III-50
III-06-28. Bin 06 Mineral Precipitation Evaporation Predictions vs. Relative Humidity at 120ºC and 10^{-4} CO_2 Fugacity III-50
III-06-29. Bin 06 Aqueous Composition Evaporation Predictions vs. Relative Humidity at 140ºC and 10^{-4} CO_2 Fugacity III-50
III-06-30. Bin 06 Mineral Precipitation Evaporation Predictions vs. Relative Humidity at 140ºC and 10^{-4} CO_2 Fugacity III-50

TABLES

Page

III-1. Excel File Names for each Look-up Table.....2
III-2. Deliquescence Point Relative Humidity and Associated Chemical Parameters Taken from the Dust Leachate Look-up Tables.....3

ATTACHMENT III

DUST LEACHATE LOOKUP TABLE RESULTS

The graphs presented in this document are representative of the information available in DTN: MO0310SPADLALT.001 and DTN: MO0310SPADLHTL.000. Two graphs from each excel file are shown here, they are: Aqueous Composition Evaporation Predictions vs. Relative Humidity and Mineral Precipitation Evaporation Predictions vs. Relative Humidity. This information is provided for each respective bin and parameter setting. Also available in the respective excel files, but not shown here, are: ANC Species Concentration Evaporation Predictions vs. Relative Humidity, ANC Species Concentration Evaporation Predictions vs. Concentration Factor, Aqueous Composition Evaporation Predictions vs. Concentration Factor, and Mineral Precipitation Evaporation Predictions vs. Concentration.

The graphs given in this document are referenced only by the Bin number and parameter settings. Table III-1 gives the associated excel source file name for the graphs in this document. Each excel file header contains the tractability back to the specific input data used in the calculation. The file nomenclature is d?c#t%$.xls, where d represents the dust bin, "?" is the 1-digit bin number (1, 2, etc.), "#" is 2, 3, or 4 (for $Pco_2 = 10^{-\#}$), "%" is 04, 07, 10, 12, or 14 (for temp = 40, 70, 100, 120, or 140°C, respectively). FILE NAME EXAMPLE (d1c2t10.xls) is dust bin 1 at a Pco_2 of 10^{-2} at 100°C.

For the figures shown below, three terms need to be defined:

1. IS: Ionic Strength
2. RH: Relative Humidity
3. a(w) = Activity of Water

The values in Table III-2 correspond to the given parameters extracted from the excel files in DTN: MO0310SPADLALT.001 and DTN: MO0310SPADLHTL.000. Given in this table are deliquescence point relative humidity and the associated chemical parameters of interest to the TSPA.

Table III-1. Excel File Names for each Look-up Table

Bin	Look-up Tables
1	d1c2t04.xls, d1c3t04.xls, d1c4t04.xls, d1c2t07.xls, d1c3t07.xls, d1c4t07.xls, d1c2t10.xls, d1c3t10.xls, d1c4t10.xls, d1c2t12.xls, d1c3t12.xls, d1c4t12.xls, d1c2t14.xls, d1c3t14.xls, d1c4t14.xls
2	d2c2t04.xls, d2c3t04.xls, d2c4t04.xls, d2c2t07.xls, d2c3t07.xls, d2c4t07.xls, d2c2t10.xls, d2c3t10.xls, d2c4t10.xls, d2c2t12.xls, d2c3t12.xls, d2c4t12.xls, d2c2t14.xls, d2c3t14.xls, d2c4t14.xls
3	d3c2t04.xls, d3c3t04.xls, d3c4t04.xls, d3c2t07.xls, d3c3t07.xls, d3c4t07.xls, d3c2t10.xls, d3c3t10.xls, d3c4t10.xls, d3c2t12.xls, d3c3t12.xls, d3c4t12.xls, d3c2t14.xls, d3c3t14.xls, d3c4t14.xls
4	d4c2t04.xls, d4c3t04.xls, d4c4t04.xls, d4c2t07.xls, d4c3t07.xls, d4c4t07.xls, d4c2t10.xls, d4c3t10.xls, d4c4t10.xls, d4c2t12.xls, d4c3t12.xls, d4c4t12.xls, d4c2t14.xls, d4c3t14.xls, d4c4t14.xls
5	d5c2t04.xls, d5c3t04.xls, d5c4t04.xls, d5c2t07.xls, d5c3t07.xls, d5c4t07.xls, d5c2t10.xls, d5c3t10.xls, d5c4t10.xls, d5c2t12.xls, d5c3t12.xls, d5c4t12.xls, d5c2t14.xls, d5c3t14.xls, d5c4t14.xls
6	d6c2t04.xls, d6c3t04.xls, d6c4t04.xls, d6c2t07.xls, d6c3t07.xls, d6c4t07.xls, d6c2t10.xls, d6c3t10.xls, d6c4t10.xls, d6c2t12.xls, d6c3t12.xls, d6c4t12.xls, d6c2t14.xls, d6c3t14.xls, d6c4t14.xls

Source: DTN: MO0310SPADLALT.001 and MO0310SPADLHTL.000

Table III-2. Deliquescence Point Relative Humidity and Associated Chemical Parameters Taken from the Dust Leachate Look-up Tables

Bin	Temperature (Celsius)	P_{CO_2} (atm)	Deliquescence Point Relative Humidity	pH	Ionic Strength (Moles/kg. H_2O)	Cl (Moles/kg. H_2O)	NO_3 (Moles/kg. H_2O)
1	40	0.0100	50.0%	6.896	1.541E+01	4.269E+00	5.921E+00
	70		30.0%	9.106	4.17E+01	1.04E-01	2.78E+01
	100		31.5%	8.780	4.219E+01	1.306E-01	2.837E+01
	120		30.8%	6.486	2.782E+01	1.065E+00	2.089E+01
	140		26.2%	6.255	2.780E+01	5.061E-01	2.552E+01
	40	0.0010	50.0%	7.402	1.541E+01	4.262E+00	5.912E+00
	70		30.0%	9.612	4.178E+01	1.027E-01	2.782E+01
	100		31.5%	9.286	4.227E+01	1.294E-01	2.842E+01
	120		30.7%	6.801	2.732E+01	1.031E+00	2.199E+01
	140		26.2%	6.752	2.782E+01	5.078E-01	2.554E+01
	40	0.0001	50.0%	7.903	1.541E+01	4.261E+00	5.908E+00
	70		30.0%	10.110	4.178E+01	1.030E-01	2.782E+01
	100		32.4%	9.318	3.715E+01	2.727E-01	2.490E+01
	120		30.8%	7.454	2.782E+01	1.066E+00	2.106E+01
	140		26.2%	7.253	2.783E+01	5.038E-01	2.557E+01
2	40	0.0100	58.1%	7.135	1.181E+01	2.404E+00	3.881E+00
	70		47.8%	7.763	1.918E+01	1.306E+00	1.423E+01
	100		42.2%	7.984	2.108E+01	1.893E+00	1.524E+01
	120		35.4%	7.929	2.869E+01	3.784E+00	1.656E+01
	140		32.0%	8.369	2.406E+01	2.088E+00	1.827E+01
	40	0.0010	58.1%	7.635	1.181E+01	2.404E+00	3.881E+00
	70		47.8%	8.263	1.918E+01	1.306E+00	1.423E+01
	100		42.2%	8.484	2.108E+01	1.893E+00	1.524E+01
	120		35.4%	8.445	2.840E+01	3.752E+00	1.655E+01
	140		32.0%	8.869	2.406E+01	2.088E+00	1.827E+01
	40	0.0001	58.1%	8.135	1.181E+01	2.404E+00	3.882E+00
	70		47.8%	8.763	1.918E+01	1.306E+00	1.423E+01
	100		42.2%	8.984	2.108E+01	1.893E+00	1.524E+01
	120		35.4%	8.947	2.836E+01	3.749E+00	1.654E+01
	140		32.0%	9.369	2.406E+01	2.088E+00	1.827E+01

Table III-2. Deliquescence Point Relative Humidity and Associated Chemical Parameters Taken from the Dust Leachate Look-up Tables (Continued)

Bin	Temperature (Celsius)	P_{CO_2} (atm)	Deliquescence Point Relative Humidity	pH	Ionic Strength (Moles/kg. H_2O)	Cl (Moles/kg. H_2O)	NO_3 (Moles/kg. H_2O)
3	40	0.0100	60.5%	9.802	1.683E+01	1.857E+00	1.469E+01
	70		49.9%	10.121	1.866E+01	2.207E+00	1.151E+01
	100		42.8%	10.768	2.408E+01	2.265E+00	1.521E+01

	120		38.4%	10.544	2.332E+01	2.343E+00	1.821E+01
	140		32.4%	10.717	2.810E+01	1.554E+00	1.986E+01
	40		58.8%	10.125	1.351E+01	3.128E+00	3.618E+00
	70		50.0%	10.685	1.870E+01	2.235E+00	1.146E+01
	100	0.0010	43.2%	11.237	2.376E+01	2.425E+00	1.525E+01
	120		38.5%	11.027	2.313E+01	2.418E+00	1.821E+01
	140		32.6%	11.152	2.732E+01	1.732E+00	1.995E+01
	40		58.8%	10.714	1.360E+01	3.181E+00	3.508E+00
	70		50.0%	11.180	1.866E+01	2.253E+00	1.145E+01
	100	0.0001	43.4%	11.731	2.365E+01	2.469E+00	1.525E+01
	120		38.6%	11.519	2.307E+01	2.451E+00	1.822E+01
	140		32.6%	11.644	2.707E+01	1.758E+00	1.992E+01
	40		52.9%	7.195	1.343E+01	1.288E+00	5.884E+00
	70		45.4%	7.850	2.082E+01	7.776E-01	1.620E+01
	100	0.0100	36.4%	8.286	2.481E+01	5.950E-01	2.172E+01
	120		31.2%	8.518	2.646E+01	5.313E-01	2.384E+01
	140		26.4%	8.680	2.794E+01	4.657E-01	2.574E+01
	40		52.9%	7.695	1.343E+01	1.288E+00	5.886E+00
	70		44.5%	8.422	2.123E+01	8.213E-01	1.727E+01
4	100	0.0010	36.4%	8.786	2.481E+01	5.950E-01	2.172E+01
	120		31.2%	9.018	2.646E+01	5.314E-01	2.384E+01
	140		26.4%	9.180	2.794E+01	4.658E-01	2.574E+01
	40		52.9%	8.195	1.343E+01	1.288E+00	5.887E+00
	70		44.5%	8.922	2.123E+01	8.213E-01	1.727E+01
	100	0.0001	36.4%	9.286	2.481E+01	5.950E-01	2.172E+01
	120		31.2%	9.518	2.646E+01	5.314E-01	2.384E+01
	140		26.4%	9.680	2.794E+01	4.658E-01	2.574E+01

Table III-2. Deliquescence Point Relative Humidity and Associated Chemical Parameters Taken from the Dust Leachate Look-up Tables (Continued)

Bin	Temperature (Celsius)	P_{CO_2} (atm)	Deliquescence Point Relative Humidity	pH	Ionic Strength (Moles/kg. H_2O)	Cl (Moles/kg. H_2O)	NO_3 (Moles/kg. H_2O)
5	40		56.1%	7.787	1.307E+01	1.867E+00	4.724E+00
	70		45.2%	8.448	2.171E+01	7.877E-01	1.646E+01
	100	0.0100	41.8%	8.374	2.728E+01	2.307E+00	1.709E+01
	120		31.1%	8.904	2.709E+01	5.534E-01	2.392E+01
	140		26.3%	9.031	2.836E+01	4.801E-01	2.576E+01
	40		56.1%	8.286	1.307E+01	1.868E+00	4.725E+00
	70		45.2%	8.948	2.171E+01	7.878E-01	1.646E+01
	100	0.0010	41.8%	8.870	2.736E+01	2.315E+00	1.709E+01
	120		31.1%	9.403	2.709E+01	5.536E-01	2.392E+01
	140		26.3%	9.531	2.836E+01	4.803E-01	2.576E+01
	40		56.1%	8.786	1.307E+01	1.868E+00	4.725E+00

	70	0.0001	45.2%	9.448	2.171E+01	7.879E-01	1.646E+01
	100		41.8%	9.374	2.725E+01	2.307E+00	1.708E+01
	120		31.1%	9.903	2.709E+01	5.536E-01	2.392E+01
	140		26.3%	10.030	2.836E+01	4.804E-01	2.576E+01
6	40	0.0100	59.8%	9.139	1.262E+01	3.751E+00	3.274E+00
	70		55.9%	10.203	1.768E+01	4.049E+00	1.126E+01
	100		42.8%	10.767	2.409E+01	2.268E+00	1.521E+01
	120		38.4%	10.542	2.333E+01	2.351E+00	1.822E+01
	140		32.3%	10.654	2.830E+01	1.701E+00	2.020E+01
	40	0.0010	59.4%	10.124	1.304E+01	3.676E+00	3.226E+00
	70		49.7%	10.952	2.074E+01	2.687E+00	9.194E+00
	100		43.2%	11.233	2.377E+01	2.436E+00	1.525E+01
	120		38.5%	10.118	1.906E+01	6.655E+00	2.718E+00
	140		32.6%	11.215	2.717E+01	1.575E+00	1.959E+01
	40	0.0001	59.3%	10.714	1.329E+01	3.644E+00	3.190E+00
	70		49.4%	11.469	2.102E+01	2.693E+00	9.262E+00
	100		43.4%	11.724	2.366E+01	2.487E+00	1.525E+01
	120		38.6%	11.518	2.307E+01	2.456E+00	1.822E+01
	140		32.7%	11.683	2.697E+01	1.658E+00	1.970E+01

DTNs: MO0310SPADLALT.001 and MO0310SPADLHTL.000

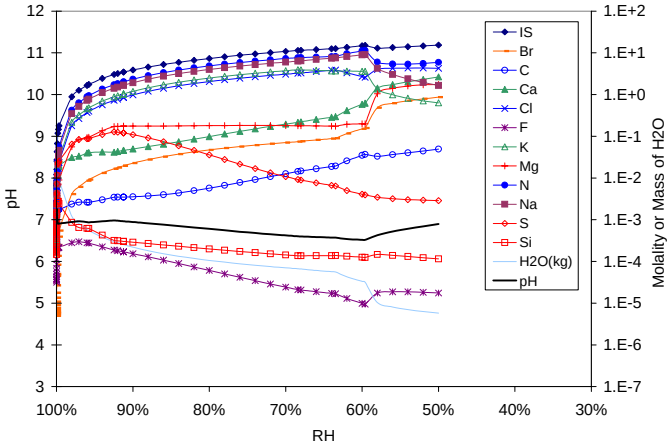

DTN: MO0310SPADLALT.001\d1c2t04.xls

Figure III-01-1. Bin 01 Aqueous Composition Evaporation Predictions vs. Relative Humidity at 40ºC and 10^{-2} CO_2 Fugacity

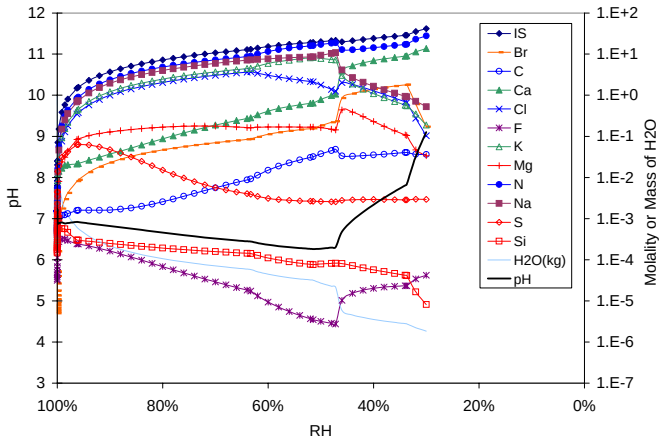

DTN: MO0310SPADLALT.001\d1c2t07.xls

Figure III-01-3. Bin 01 Aqueous Composition Evaporation Predictions vs. Relative Humidity at 70ºC and 10^{-2} CO_2 Fugacity

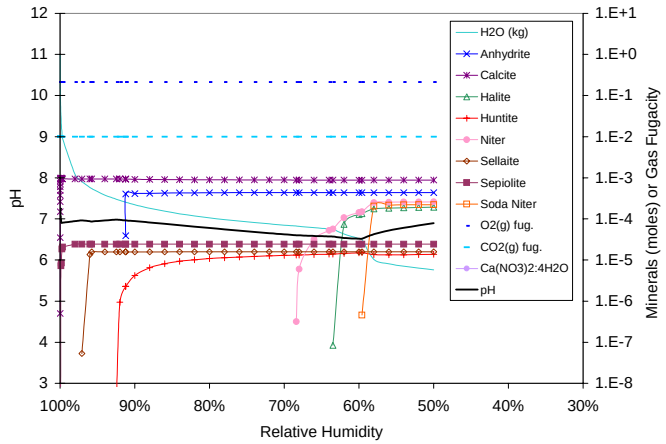

DTN: MO03104SPADLALT.001\d1c2t04.xls

Figure III-01-2. Bin 01 Mineral Precipitation Evaporation Predictions vs. Relative Humidity at 40ºC and 10^{-2} CO_2 Fugacity

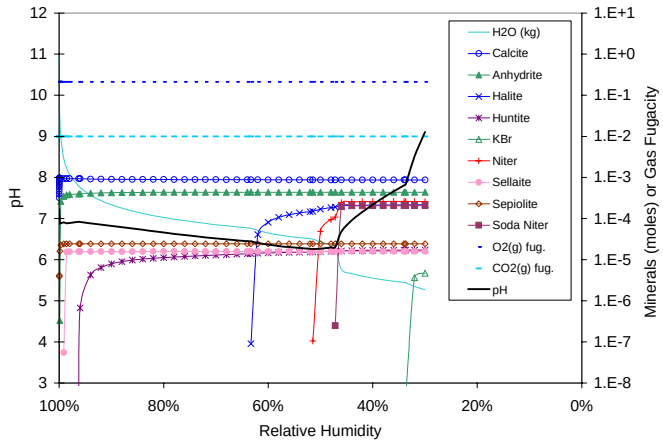

DTN: MO0304SPADLALT.000\d1c2t07.xls

Figure III-01-4. Bin 01 Mineral Precipitation Evaporation Predictions vs. Relative Humidity at 70ºC and 10^{-2} CO_2 Fugacity

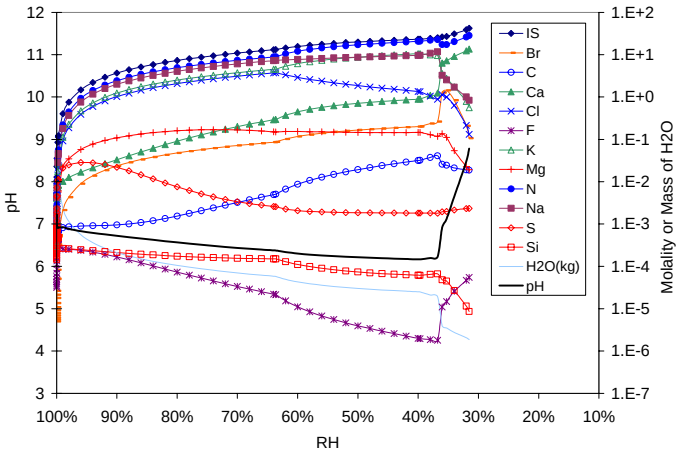

DTN: MO0310SPADLALT.001\d1c2t10.xls

Figure III-01-5. Bin 01 Aqueous Composition Evaporation Predictions vs. Relative Humidity at 100ºC and 10^{-2} CO_2 Fugacity

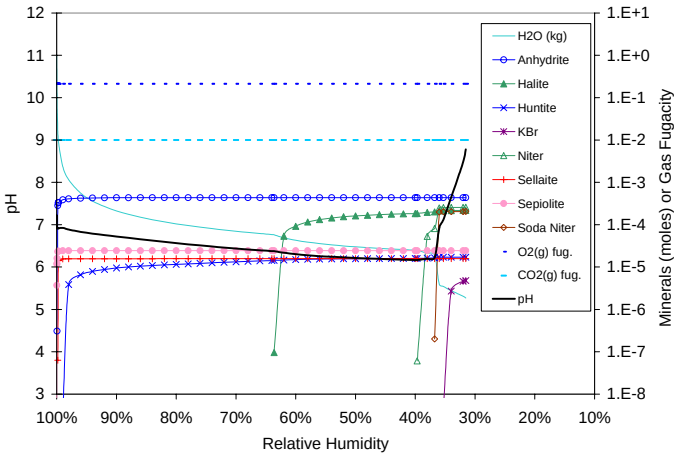

DTN: MO0304SPADLALT.000\d1c2t10.xls

Figure III-01-6. Bin 01 Mineral Precipitation Evaporation Predictions vs. Relative Humidity at 100ºC and 10^{-2} CO_2 Fugacity

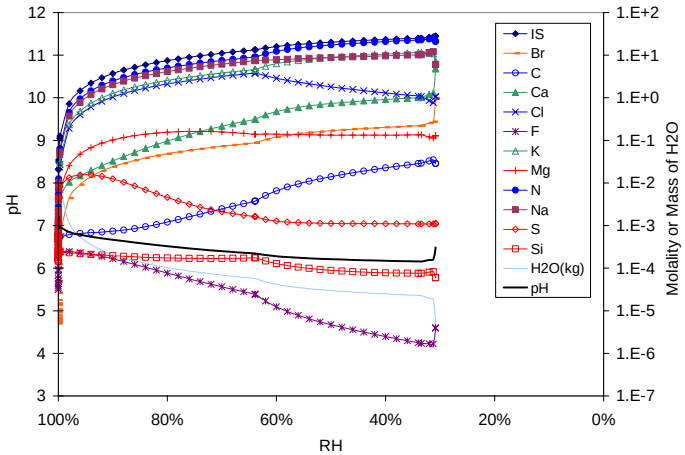

DTN: MO0310SPADLHTL.000\d1c2t12.xls

Figure III-01-7. Bin 01 Aqueous Composition Evaporation Predictions vs. Relative Humidity at 120ºC and 10^{-2} CO_2 Fugacity

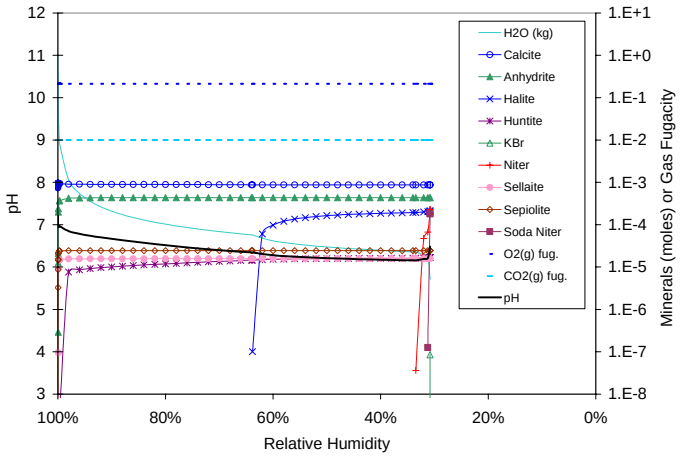

DTN: MO0310SPADLHTL.000\d1c2t12.xls

Figure III-01-8. Bin 01 Mineral Precipitation Evaporation Predictions vs. Relative Humidity at 120ºC and 10^{-2} CO_2 Fugacity

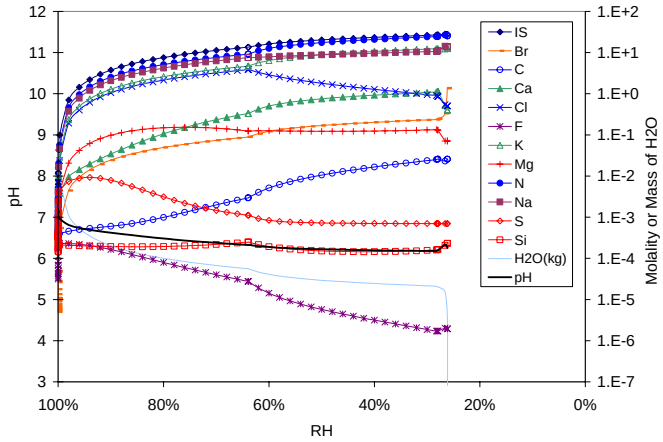

DTN: MO0310SPADLHTL.000\d1c2t14.xls

Figure III-01-9. Bin 01 Aqueous Composition Evaporation Predictions vs. Relative Humidity at 140ºC and 10^{-2} CO_2 Fugacity

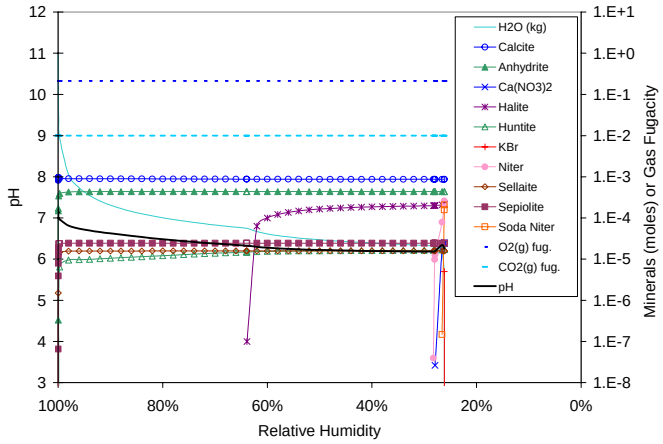

DTN: MO0310SPADLHTL.000\d1c2t14.xls

Figure III-01-10. Bin 01 Mineral Precipitation Evaporation Predictions vs. Relative Humidity at 140ºC and 10^{-2} CO_2 Fugacity

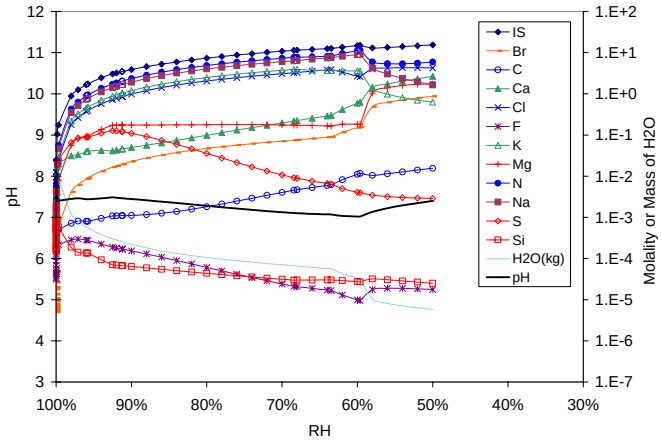

DTN: MO03010SPADLALT.001\d1c3t04.xls

Figure III-01-11. Bin 01 Aqueous Composition Evaporation Predictions vs. Relative Humidity at 40ºC and 10^{-3} CO_2 Fugacity

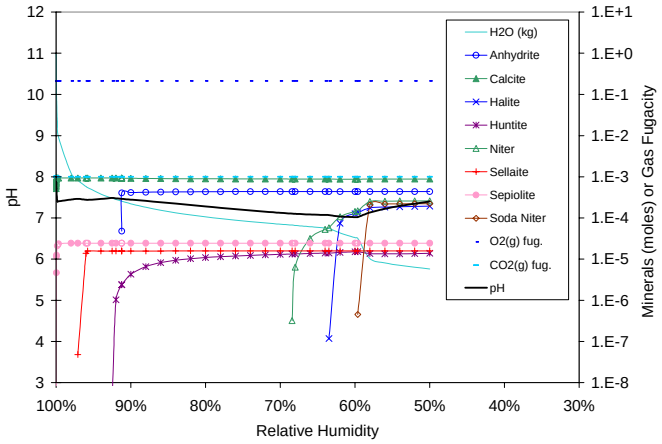

DTN: MO0310SPADLALT.001\d1c3t04.xls

Figure III-01-12. Bin 01 Mineral Precipitation Evaporation Predictions vs. Relative Humidity at 40ºC and 10^{-3} CO_2 Fugacity

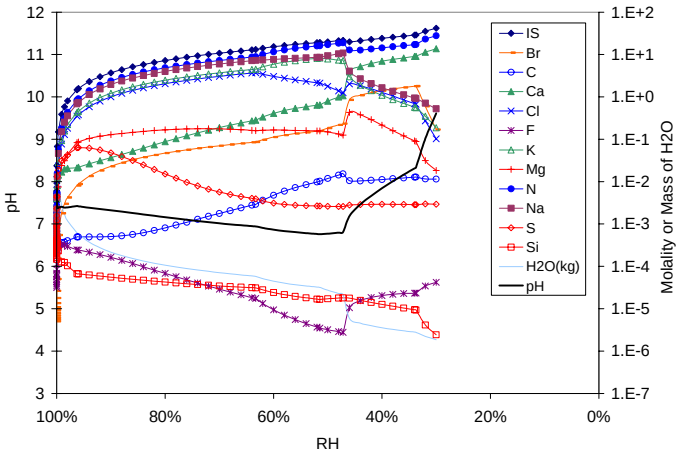

DTN: MO0310SPADLALT.001\d1c3t07.xls

Figure III-01-13. Bin 01 Aqueous Composition Evaporation Predictions vs. Relative Humidity at 70ºC and 10^{-3} CO_2 Fugacity

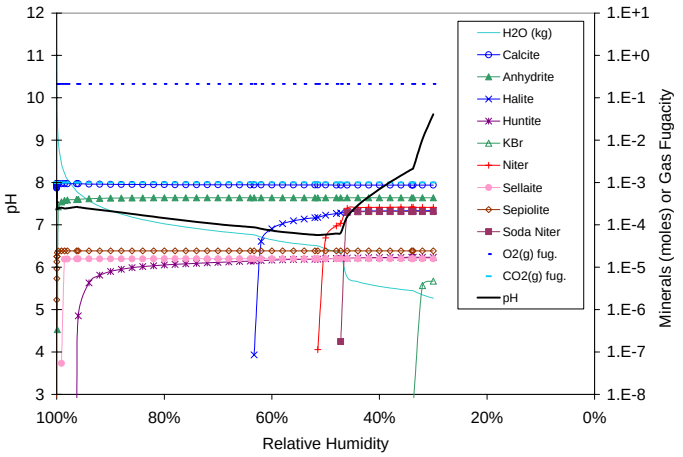

DTN: MO0310SPADLALT.001\d1c3t07.xls

Figure III-01-14. Bin 01 Mineral Precipitation Evaporation Predictions vs. Relative Humidity at 70ºC and 10^{-3} CO_2 Fugacity

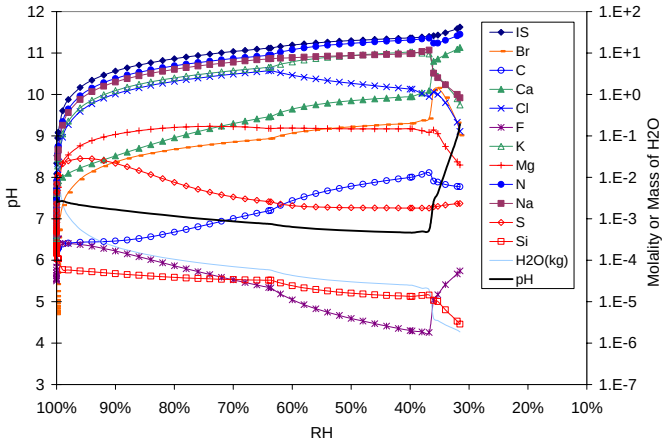

DTN: MO0310SPADLALT.001\d1c3t10.xls

Figure III-01-15. Bin 01 Aqueous Composition Evaporation Predictions vs. Relative Humidity at 100ºC and 10^{-3} CO_2 Fugacity

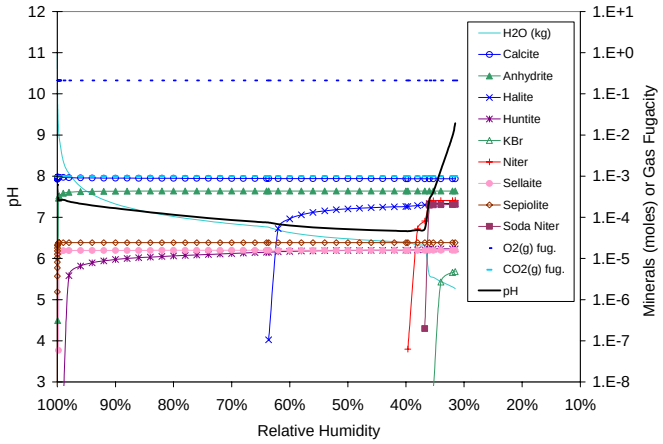

DTN: MO0310SPADLALT.001\d1c3t10.xls

Figure III-01-16. Bin 01 Mineral Precipitation Evaporation Predictions vs. Relative Humidity at 100ºC and 10^{-3} CO_2 Fugacity

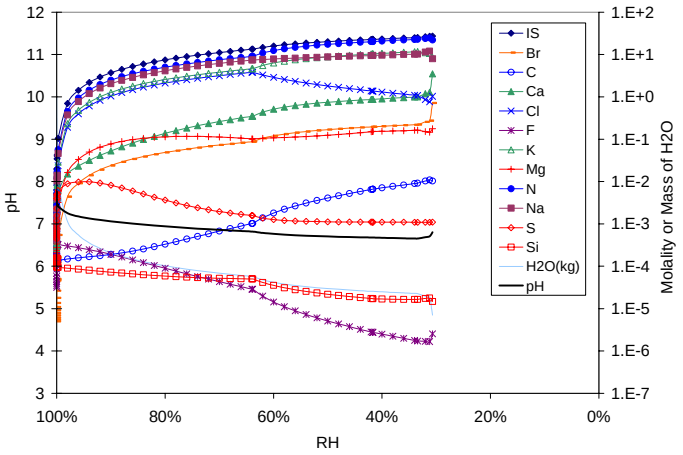

DTN: \ MO0310SPADLHTL.000\d1c3t12.xls

Figure III-01-17. Bin 01 Aqueous Composition Evaporation Predictions vs. Relative Humidity at 120ºC and 10^{-3} CO_2 Fugacity

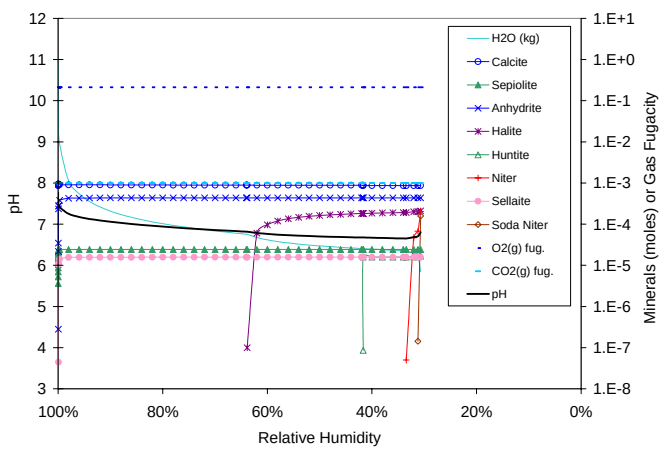

DTN: MO0310SPADLHTL.000\d1c3t12.xls

Figure III-01-18. Bin 01 Mineral Precipitation Evaporation Predictions vs. Relative Humidity at 120ºC and 10^{-3} CO_2 Fugacity

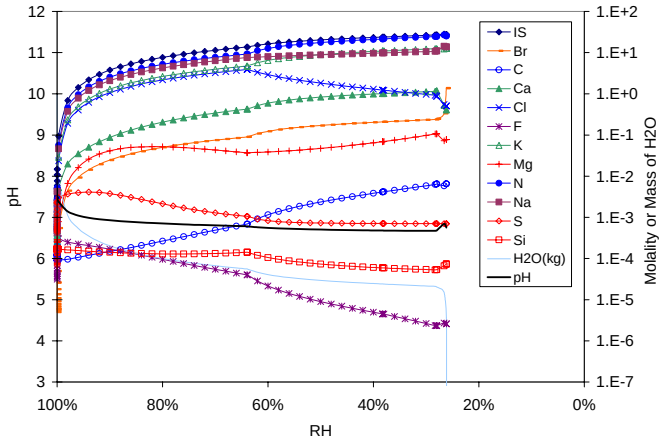

DTN: MO0310SPADLHTL.000\d1c3t14.xls

Figure III-01-19. Bin 01 Aqueous Composition Evaporation Predictions vs. Relative Humidity at 140ºC and 10^{-3} CO_2 Fugacity

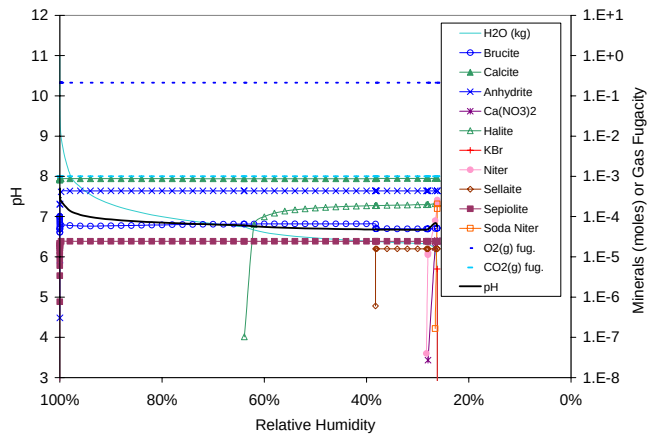

DTN: MO0310SPADLHTL.000\d1c3t14.xls

Figure III-01-20. Bin 01 Mineral Precipitation Evaporation Predictions vs. Relative Humidity at 140ºC and 10^{-3} CO_2 Fugacity

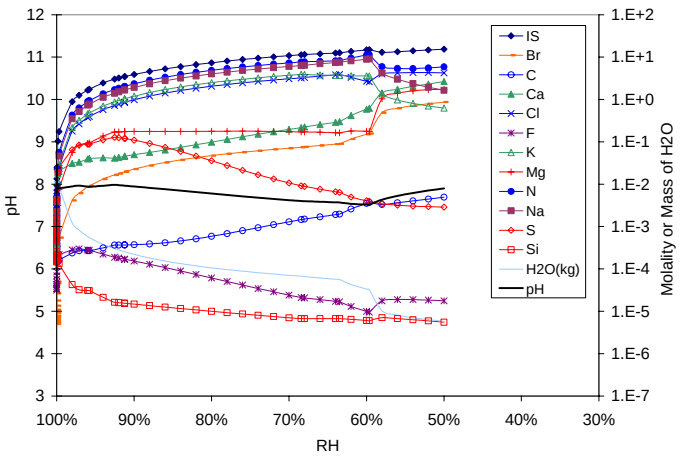

DTN: MO0310SPADLALT.001\d1c4t04.xls

Figure III-01-21. Bin 01 Aqueous Composition Evaporation Predictions vs. Relative Humidity at 40ºC and 10^{-4} CO_2 Fugacity

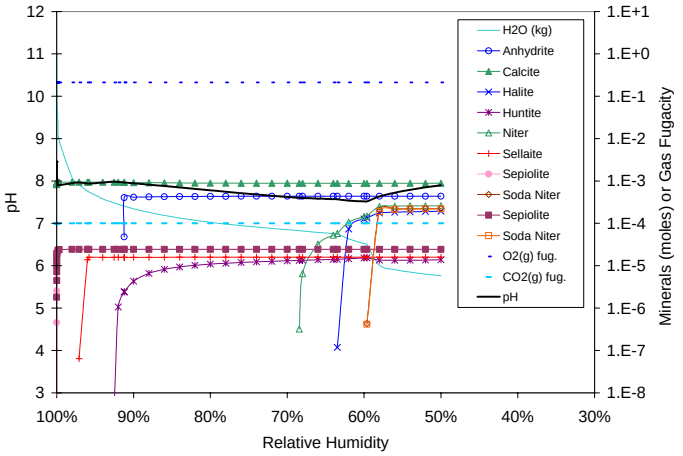

DTN: MO0310SPADLALT.001\d1c4t04.xls

Figure III-01-22. Bin 01 Mineral Precipitation Evaporation Predictions vs. Relative Humidity at 40ºC and 10^{-4} CO_2 Fugacity

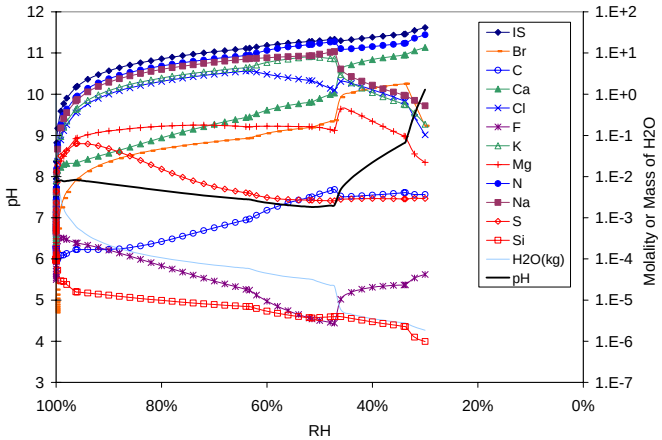

DTN: MO0310SPADLALT.001\d1c4t07.xls

Figure III-01-23. Bin 01 Aqueous Composition Evaporation Predictions vs. Relative Humidity at 70ºC and 10^{-4} CO_2 Fugacity

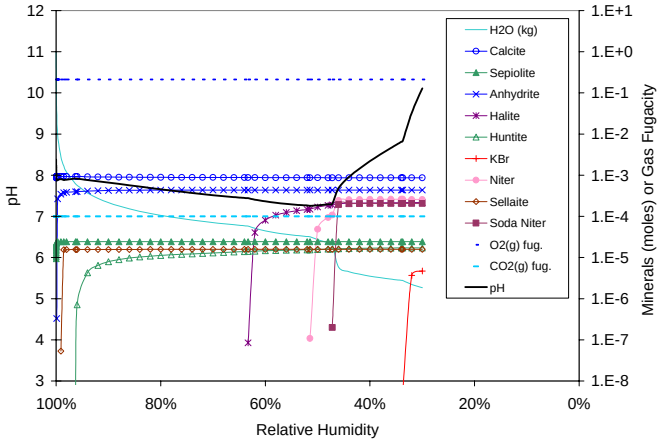

DTN: MO0310SPADLALT.001\d1c4t07.xls

Figure III-01-24. Bin 01 Mineral Precipitation Evaporation Predictions vs. Relative Humidity at 70ºC and 10^{-4} CO_2 Fugacity

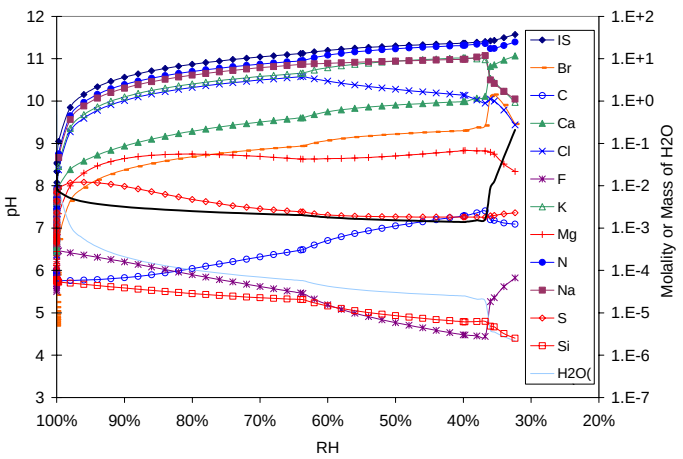

DTN: MO0310SPADLALT.001\d1c4t10.xls

Figure III-01-25. Bin 01 Aqueous Composition Evaporation Predictions vs. Relative Humidity at 100ºC and 10^{-4} CO_2 Fugacity

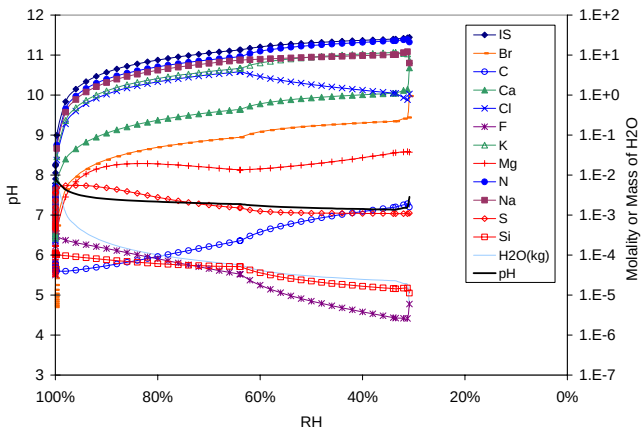

DTN: MO0310SPADLHTL.000\d1c4t12.xls

Figure III-01-27. Bin 01 Aqueous Composition Evaporation Predictions vs. Relative Humidity at 120ºC and 10^{-4} CO_2 Fugacity

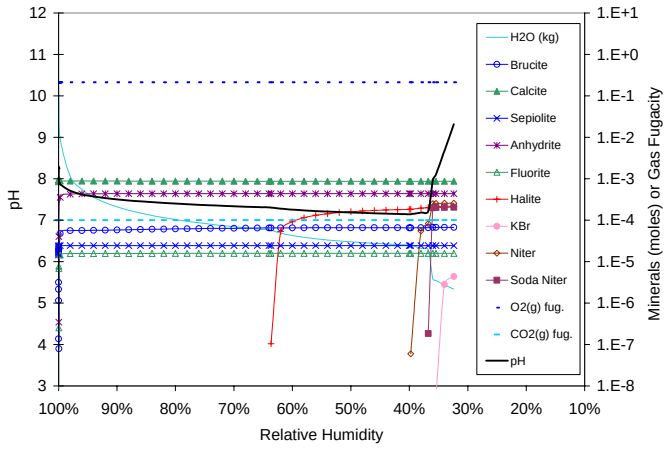

DTN: MO0310SPADLALT.001\d1c4t10.xls

Figure III-01-26. Bin 01 Mineral Precipitation Evaporation Predictions vs. Relative Humidity at 100ºC and 10^{-4} CO_2 Fugacity

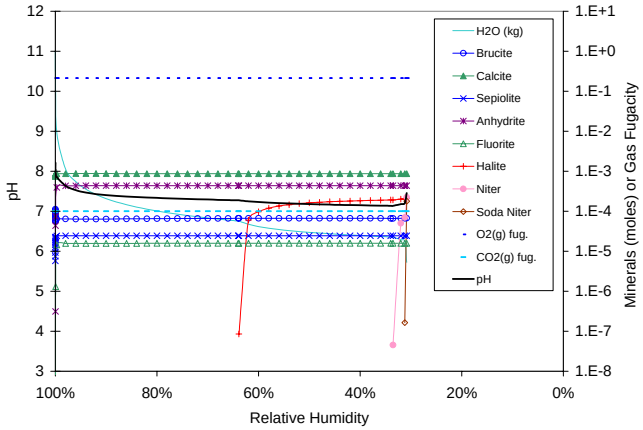

DTN: MO0310SPADLHTL.000\d1c4t12.xls

Figure III-01-28. Bin 01 Mineral Precipitation Evaporation Predictions vs. Relative Humidity at 120ºC and 10^{-4} CO_2 Fugacity

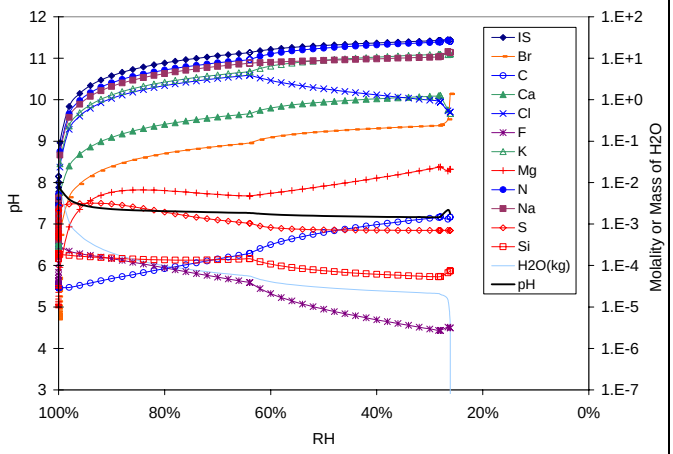

DTN: MO0310SPADLHTL.000\d1c4t14.xls

Figure III-01-29. Bin 01 Aqueous Composition Evaporation Predictions vs. Relative Humidity at 140ºC and 10^{-4} CO_2 Fugacity

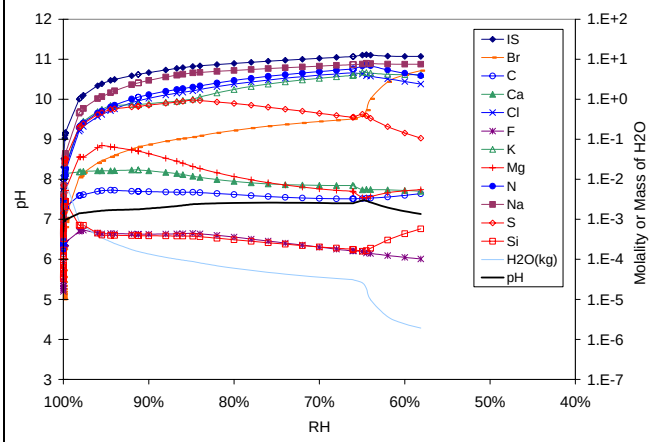

DTN: MO0310SPADLALT.001\d2c2t04.xls

Figure III-02-1. Bin 02 Aqueous Composition Evaporation Predictions vs. Relative Humidity at 40ºC and 10^{-2} CO_2 Fugacity

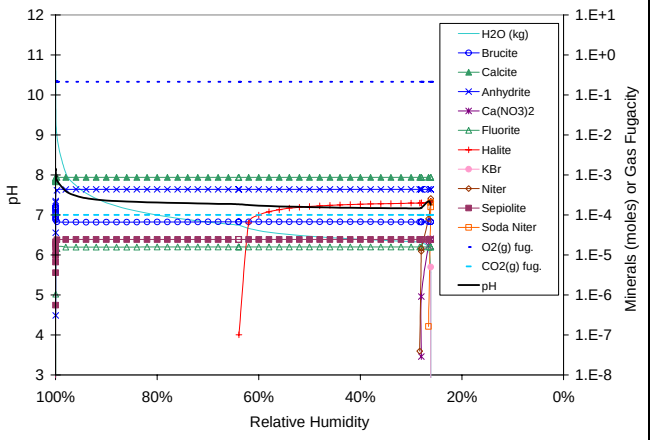

DTN: MO0310SPADLHTL.000\d1c4t14.xls

Figure III-01-30. Bin 01 Mineral Precipitation Evaporation Predictions vs. Relative Humidity at 140ºC and 10^{-4} CO_2 Fugacity

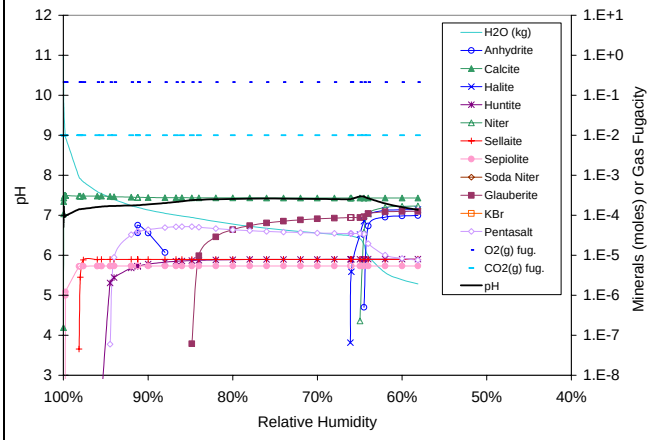

DTN: MO0310SPADLALT.001\d2c2t04.xls

Figure III-02-2. Bin 02 Mineral Precipitation Evaporation Predictions vs. Relative Humidity at 40ºC and 10^{-2} CO_2 Fugacity

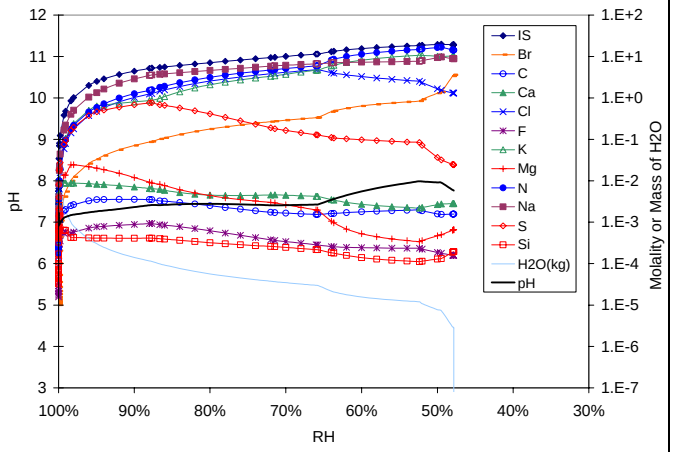

DTN: MO0310SPADLALT.000\d2c2t07.xls

Figure III-02-3. Bin 02 Aqueous Composition Evaporation Predictions vs. Relative Humidity at 70ºC and 10^{-2} CO_2 Fugacity

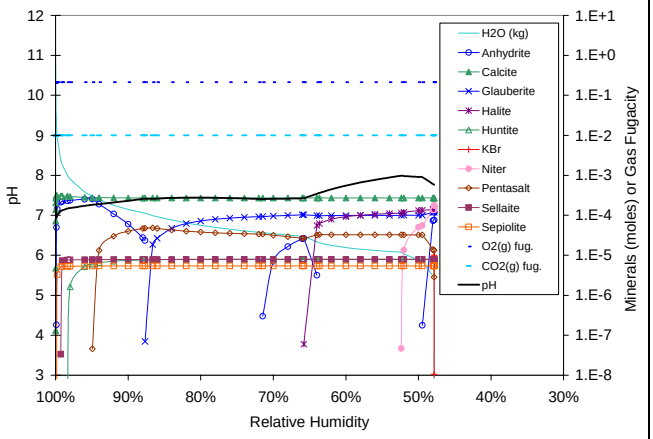

DTN: MO0310SPADLALT.001\d2c2t07.xls

Figure III-02-4. Bin 02 Mineral Precipitation Evaporation Predictions vs. Relative Humidity at 70ºC and 10^{-2} CO_2 Fugacity

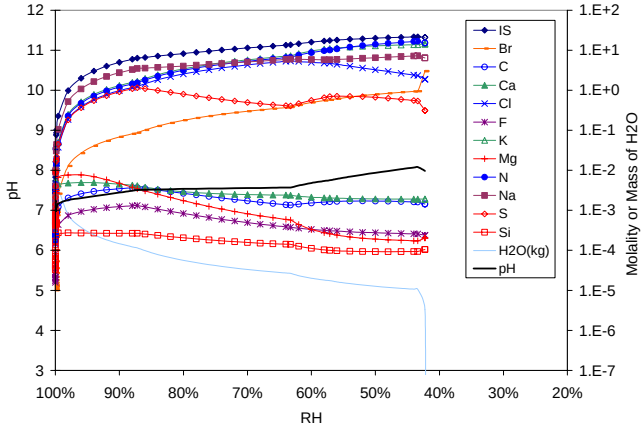

DTN: MO0310SPADLALT.001\d2c2t10.xls

Figure III-02-5. Bin 02 Aqueous Composition Evaporation Predictions vs. Relative Humidity at 100ºC and 10^{-2} CO_2 Fugacity

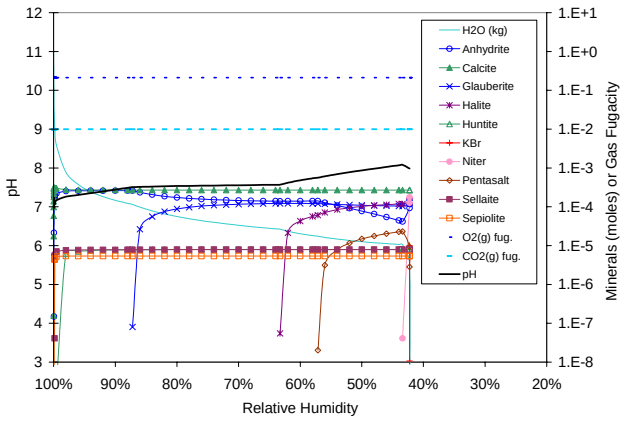

DTN: MO0310SPADLALT.000\d2c2t10.xls

Figure III-02-6. Bin 02 Mineral Precipitation Evaporation Predictions vs. Relative Humidity at 100ºC and 10^{-2} CO_2 Fugacity

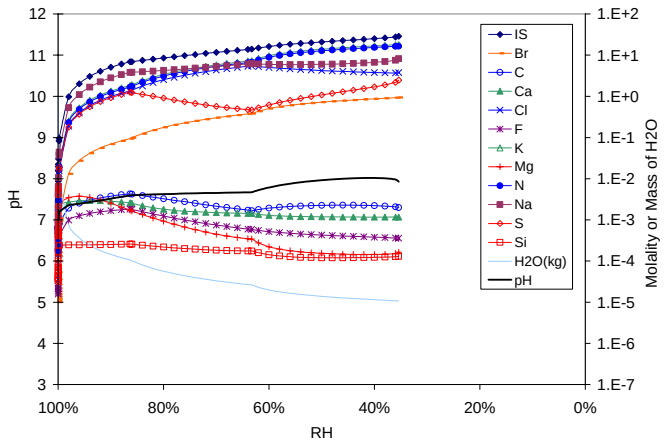

DTN: MO0310SPADLHTL.000\d2c2t12.xls

Figure III-02-7. Bin 02 Aqueous Composition Evaporation Predictions vs. Relative Humidity at 120ºC and 10^{-2} CO_2 Fugacity

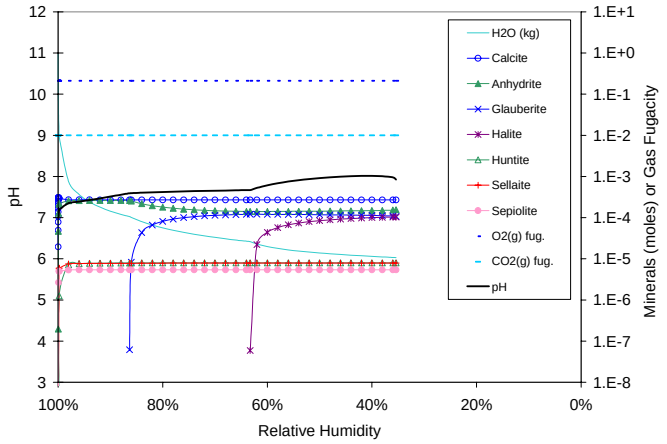

DTN: MO0310SPADLHTL.000\d2c2t12.xls

Figure III-02-8. Bin 02 Mineral Precipitation Evaporation Predictions vs. Relative Humidity at 120ºC and 10^{-2} CO_2 Fugacity

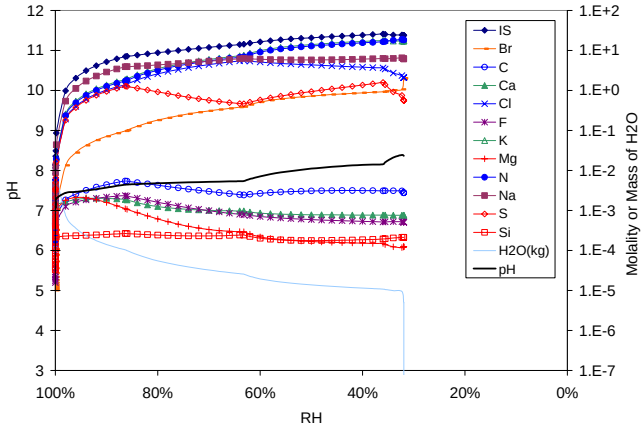

DTN: MO0310SPADLHTL.000\d2c2t14.xls

Figure III-02-9. Bin 02 Aqueous Composition Evaporation Predictions vs. Relative Humidity at 140ºC and 10^{-2} CO_2 Fugacity

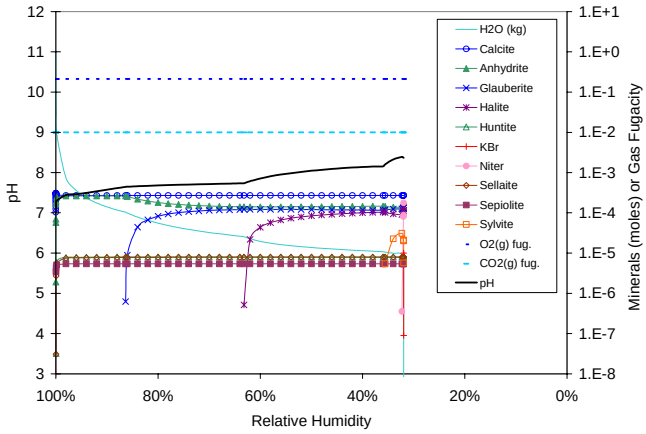

DTN: MO0310SPADLHTL.000\d2c2t14.xls

Figure III-02-10. Bin 02 Mineral Precipitation Evaporation Predictions vs. Relative Humidity at 140ºC and 10^{-2} CO_2 Fugacity

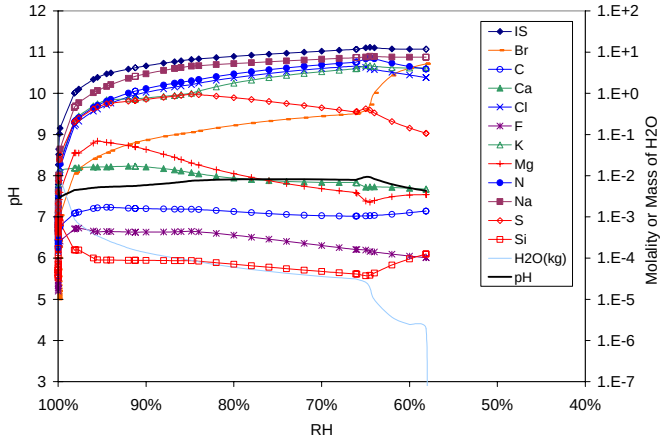

DTN: MO0310SPADLALT.001\d2c3t04.xls

Figure III-02-11. Bin 02 Aqueous Composition Evaporation Predictions vs. Relative Humidity at 40ºC and 10^{-3} CO_2 Fugacity

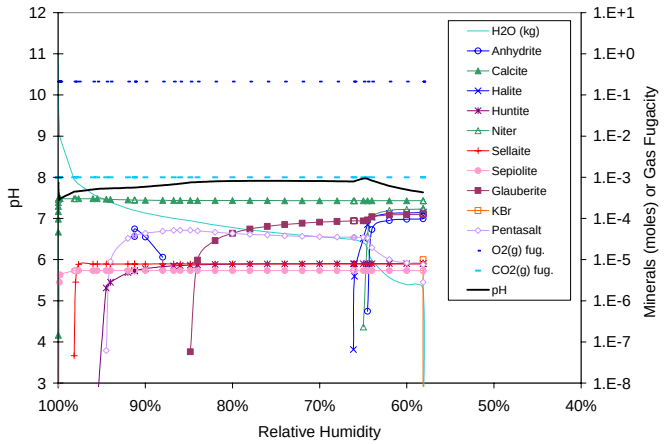

DTN: MO0310SPADLALT.001\d2c3t04.xls

Figure III-02-12. Bin 02 Mineral Precipitation Evaporation Predictions vs. Relative Humidity at 40ºC and 10^{-3} CO_2 Fugacity

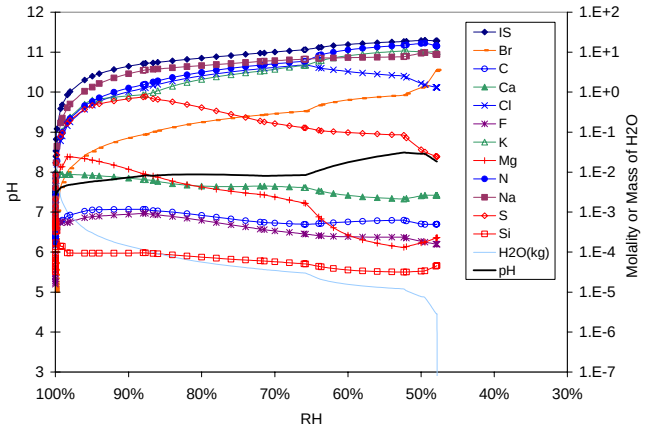

DTN: MO0310SPADLALT.001\d2c3t07.xls

Figure III-02-13. Bin 02 Aqueous Composition Evaporation Predictions vs. Relative Humidity at 70ºC and 10^{-3} CO_2 Fugacity

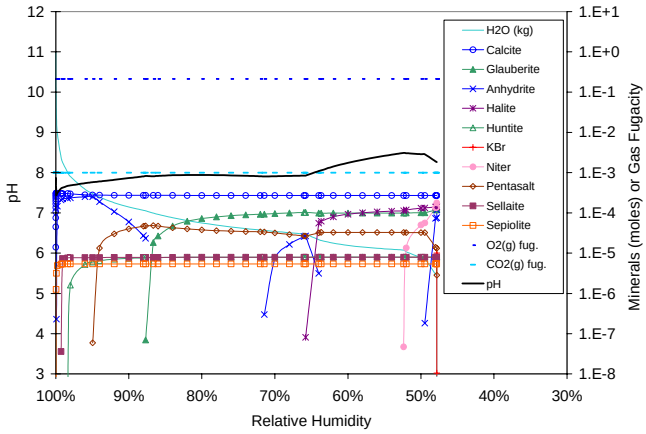

DTN: MO0310SPADLALT.001\d2c3t07.xls

Figure III-02-14. Bin 02 Mineral Precipitation Evaporation Predictions vs. Relative Humidity at 70ºC and 10^{-3} CO_2 Fugacity

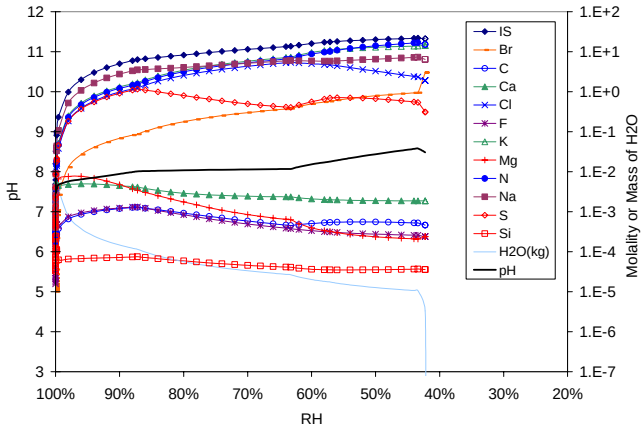

DTN: MO0310SPADLALT.001\d2c3t10.xls

Figure III-02-15. Bin 02 Aqueous Composition Evaporation Predictions vs. Relative Humidity at 100ºC and 10^{-3} CO_2 Fugacity

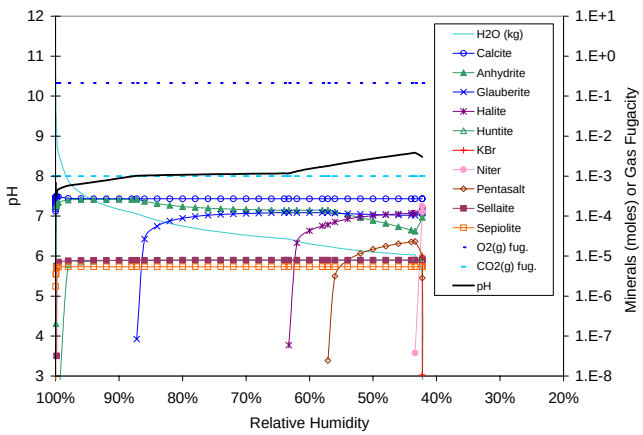

DTN: MO0310SPADLALT.001\d2c3t10.xls

Figure III-02-16. Bin 02 Mineral Precipitation Evaporation Predictions vs. Relative Humidity at 100ºC and 10^{-3} CO_2 Fugacity

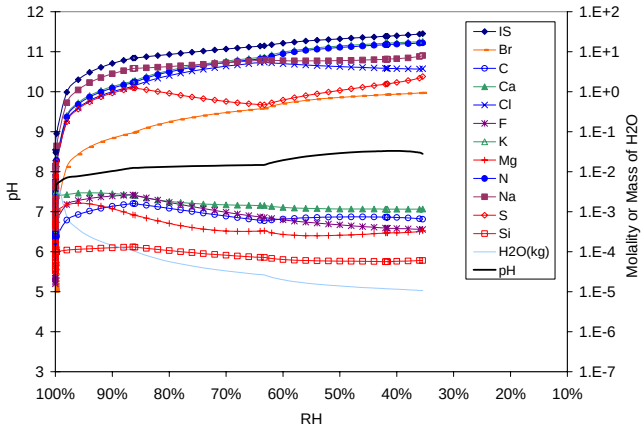

DTN: MO0310SPADLHTL.000\d2c3t12.xls

Figure III-02-17. Bin 02 Aqueous Composition Evaporation Predictions vs. Relative Humidity at 120ºC and 10^{-3} CO_2 Fugacity

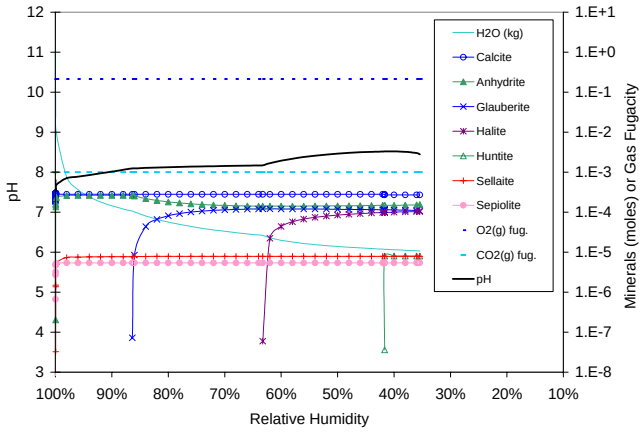

DTN: MO0310SPADLHTL.000\d2c3t12.xls

Figure III-02-18. Bin 02 Mineral Precipitation Evaporation Predictions vs. Relative Humidity at 120ºC and 10^{-3} CO_2 Fugacity

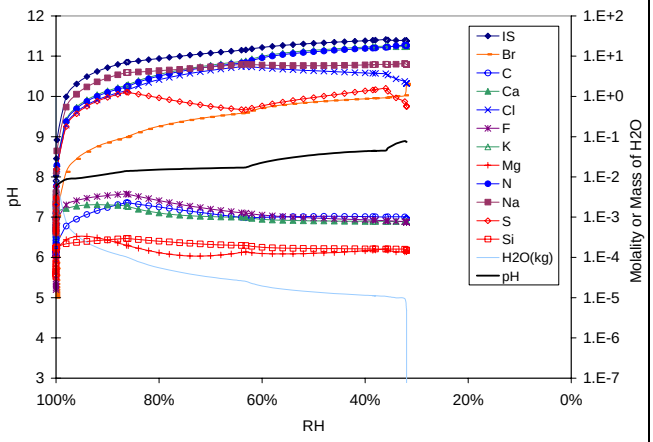

DTN: MO0310SPADLHTL.000\d2c3t14.xls

Figure III-02-19. Bin 02 Aqueous Composition Evaporation Predictions vs. Relative Humidity at 140ºC and 10^{-3} CO_2 Fugacity

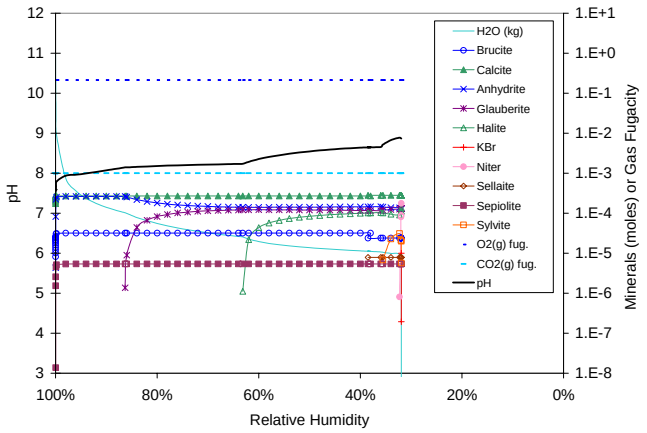

DTN: MO0310SPADLHTL.000\d2c3t14.xls

Figure III-02-20. Bin 02 Mineral Precipitation Evaporation Predictions vs. Relative Humidity at 140ºC and 10^{-3} CO_2 Fugacity

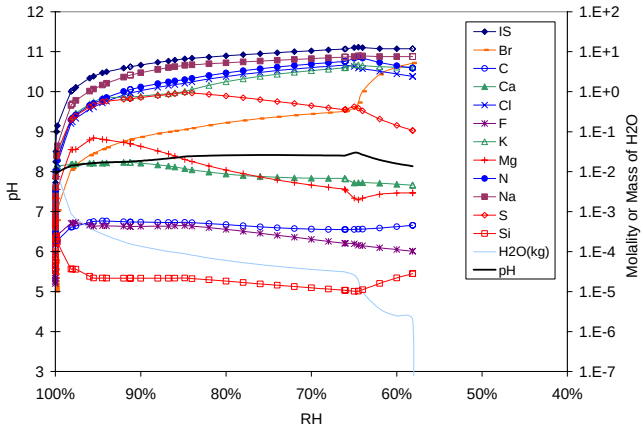

DTN: MO0310SPADLALT.001\d2c4t04.xls

Figure III-02-21. Bin 02 Aqueous Composition Evaporation Predictions vs. Relative Humidity at 40ºC and 10^{-4} CO_2 Fugacity

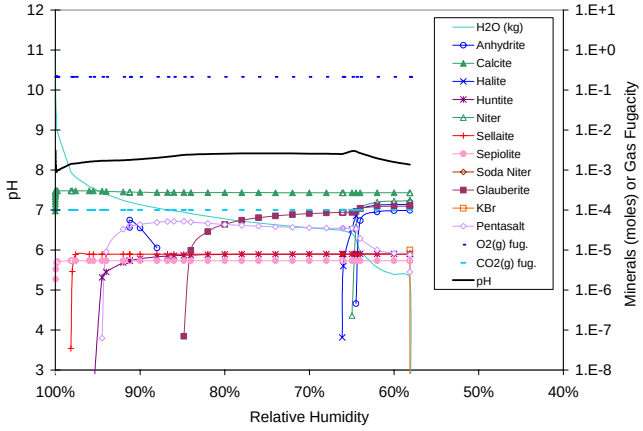

DTN: MO0310SPADLALT.001\d2c4t04.xls

Figure III-02-22. Bin 02 Mineral Precipitation Evaporation Predictions vs. Relative Humidity at 40ºC and 10^{-4} CO_2 Fugacity

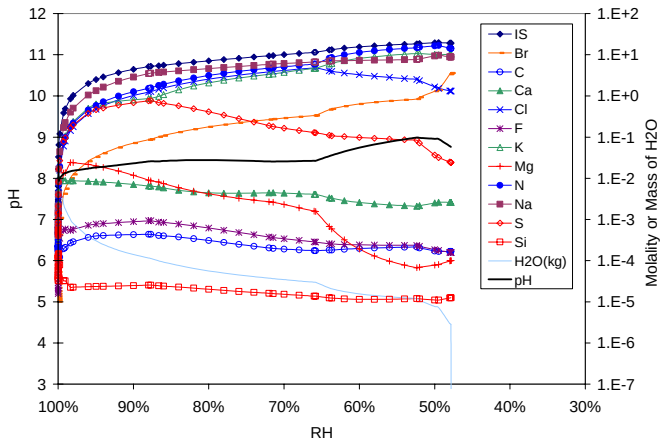

DTN: MO0310SPADLALT.001\d2c4t07.xls

Figure III-02-23. Bin 02 Aqueous Composition Evaporation Predictions vs. Relative Humidity at 70ºC and 10^{-4} CO_2 Fugacity

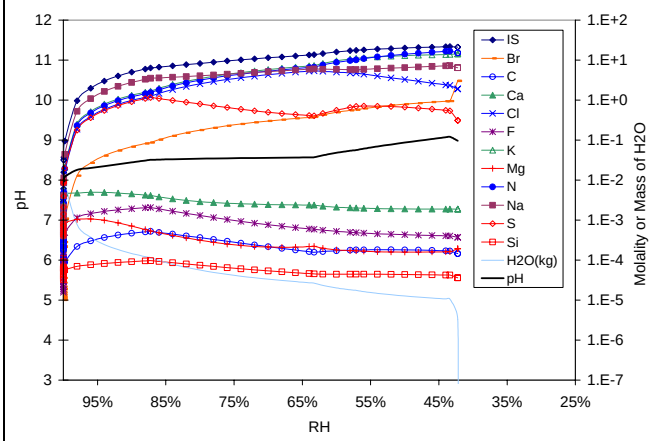

DTN: MO0310SPADLALT.001\d2c4t10.xls

Figure III-02-25. Bin 02 Aqueous Composition Evaporation Predictions vs. Relative Humidity at 100ºC and 10^{-4} CO_2 Fugacity

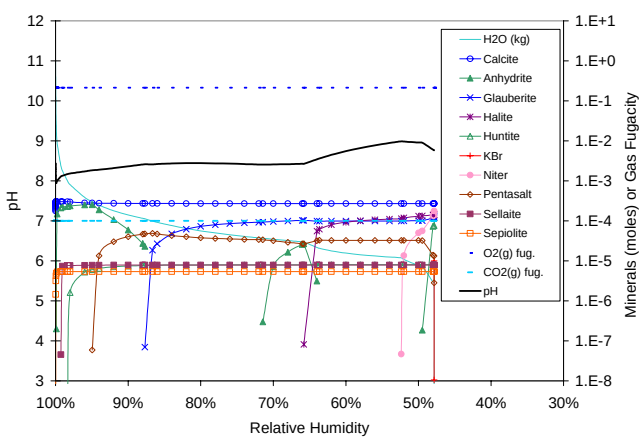

DTN: MO0310SPADLALT.001\d2c4t07.xls

Figure III-02-24. Bin 02 Mineral Precipitation Evaporation Predictions vs. Relative Humidity at 70ºC and 10^{-4} CO_2 Fugacity

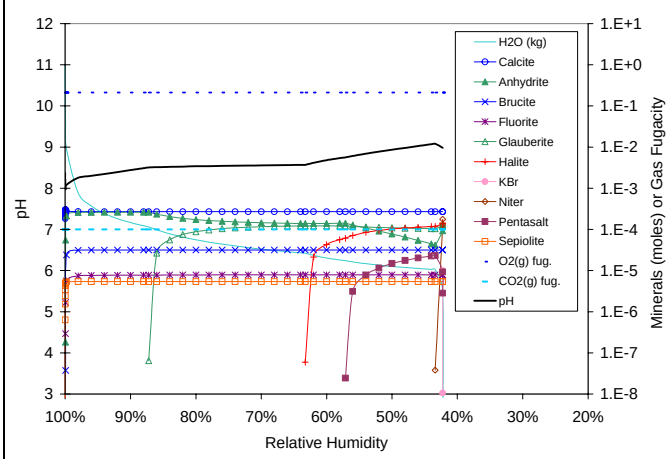

DTN: MO0310SPADLALT.001\d2c4t10.xls

Figure III-02-26. Bin 02 Mineral Precipitation Evaporation Predictions vs. Relative Humidity at 100ºC and 10^{-4} CO_2 Fugacity

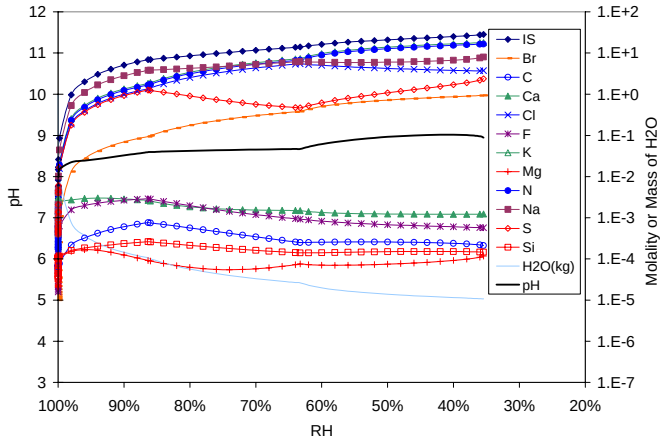

DTN: MO0310SPADLHTL.000\d2c4t12.xls

Figure III-02-27. Bin 02 Aqueous Composition Evaporation Predictions vs. Relative Humidity at 120ºC and 10^{-4} CO_2 Fugacity

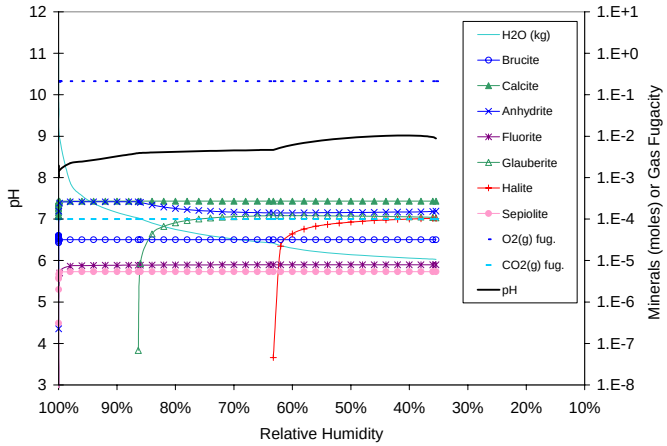

DTN: MO0310SPADLHTL.000\d2c4t12.xls

Figure III-02-28. Bin 02 Mineral Precipitation Evaporation Predictions vs. Relative Humidity at 120ºC and 10^{-4} CO_2 Fugacity

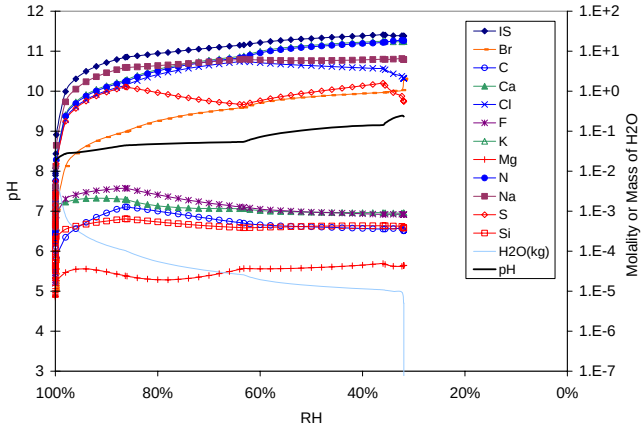

DTN: MO0310SPADLHTL.000\d2c4t14.xls

Figure III-02-29. Bin 02 Aqueous Composition Evaporation Predictions vs. Relative Humidity at 140ºC and 10^{-4} CO_2 Fugacity

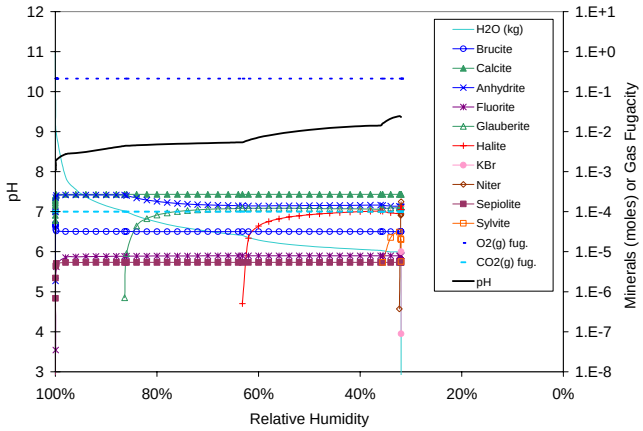

DTN: MO0310SPADLHTL.000\d2c4t14.xls

Figure III-02-30. Bin 02 Mineral Precipitation Evaporation Predictions vs. Relative Humidity at 140°C and 10^{-4} CO_2 Fugacity

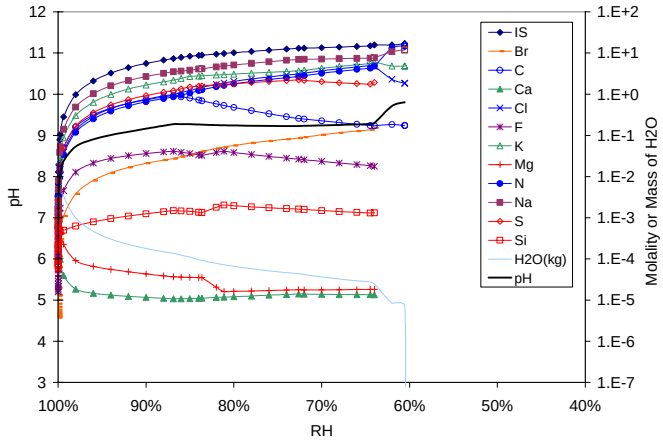

DTN: MO03100SPADLALT.001\d3c2t04.xls

Figure III-03-1. Bin 03 Aqueous Composition Evaporation Predictions vs. Relative Humidity at 40ºC and 10^{-2} CO_2 Fugacity

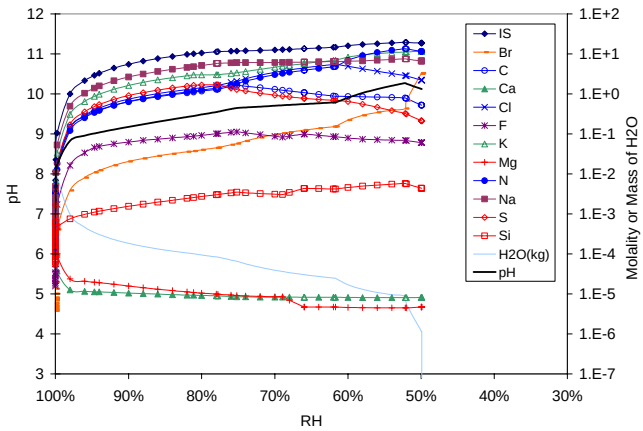

DTN: MO0310SPADLALT.001\d3c2t07.xls

Figure III-03-3. Bin 03 Aqueous Composition Evaporation Predictions vs. Relative Humidity at 70ºC and 10^{-2} CO_2 Fugacity

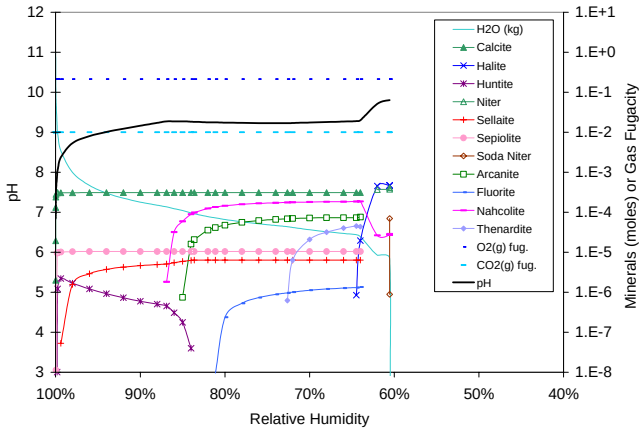

DTN: MO0310SPADLALT.001\d3c2t04.xls

Figure III-03-2. Bin 03 Mineral Precipitation Evaporation Predictions vs. Relative Humidity at 40ºC and 10^{-2} CO_2 Fugacity

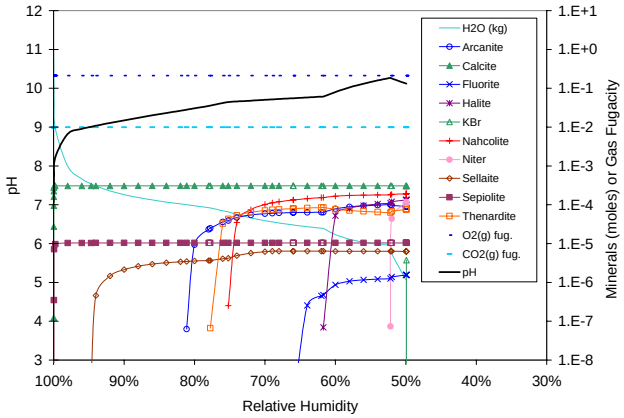

DTN: MO0310SPADLALT.001\d3c2t07.xls

Figure III-03-4. Bin 03 Mineral Precipitation Evaporation Predictions vs. Relative Humidity at 70ºC and 10^{-2} CO_2 Fugacity

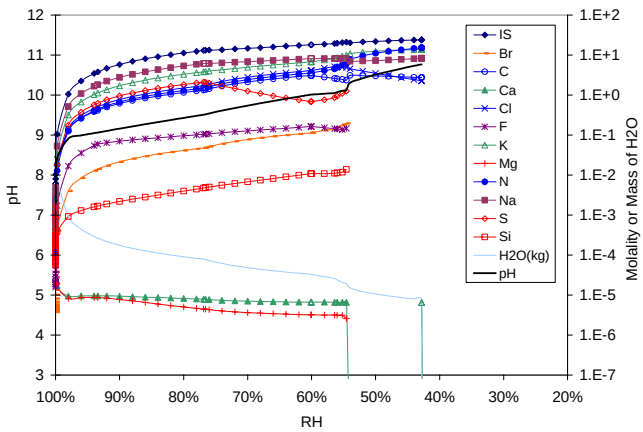

DTN: MO0310SPADLALT.001\d3c2t10.xls

Figure III-03-5. Bin 03 Aqueous Composition Evaporation Predictions vs. Relative Humidity at 100ºC and 10^{-2} CO_2 Fugacity

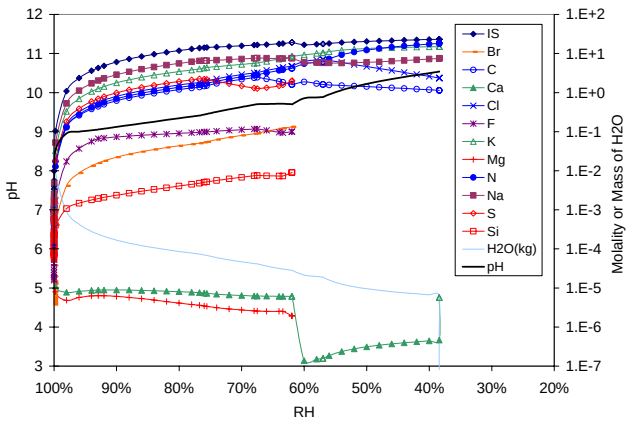

DTN: MO0310SPADLHTL.000\d3c2t12.xls

Figure III-03-7. Bin 03 Aqueous Composition Evaporation Predictions vs. Relative Humidity at 120ºC and 10^{-2} CO_2 Fugacity

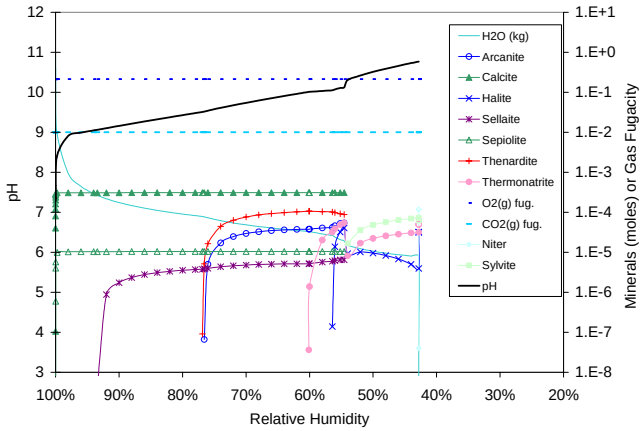

DTN: MO0310SPADLALT.001\d3c2t10.xls

Figure III-03-6. Bin 03 Mineral Precipitation Evaporation Predictions vs. Relative Humidity at 100ºC and 10^{-2} CO_2 Fugacity

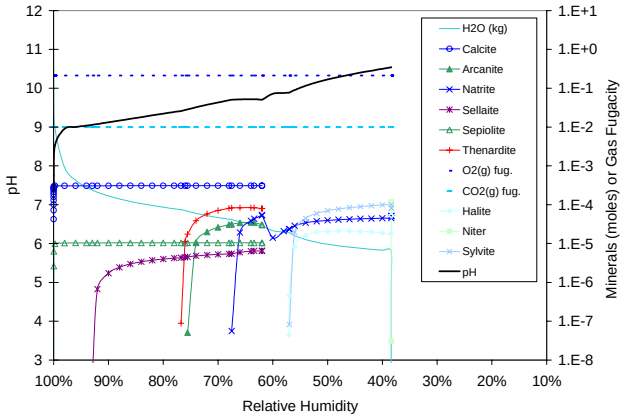

DTN: MO0310SPADLHTL.000\d3c2t12.xls

Figure III-03-8. Bin 03 Mineral Precipitation Evaporation Predictions vs. Relative Humidity at 120ºC and 10^{-2} CO_2 Fugacity

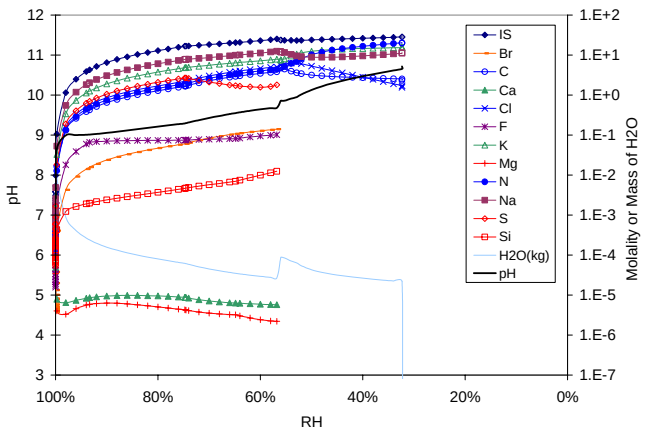

DTN: MO0310SPADLHTL.000\d3c2t14.xls

Figure III-03-9. Bin 03 Aqueous Composition Evaporation Predictions vs. Relative Humidity at 140ºC and 10^{-2} CO_2 Fugacity

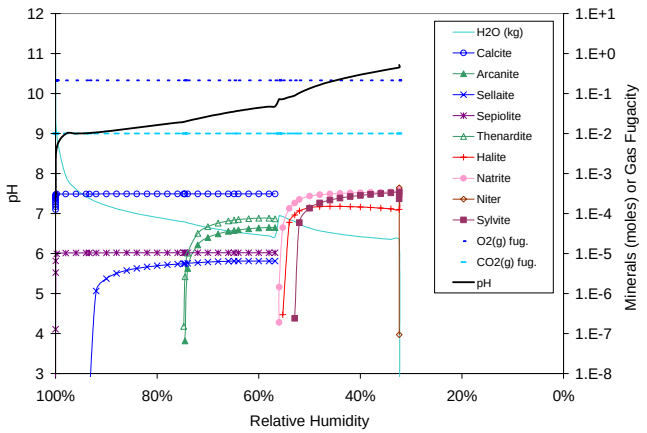

DTN: MO0310SPADLHTL.000\d3c2t14.xls

Figure III-03-10. Bin 03 Mineral Precipitation Evaporation Predictions vs. Relative Humidity at 140ºC and 10^{-2} CO_2 Fugacity

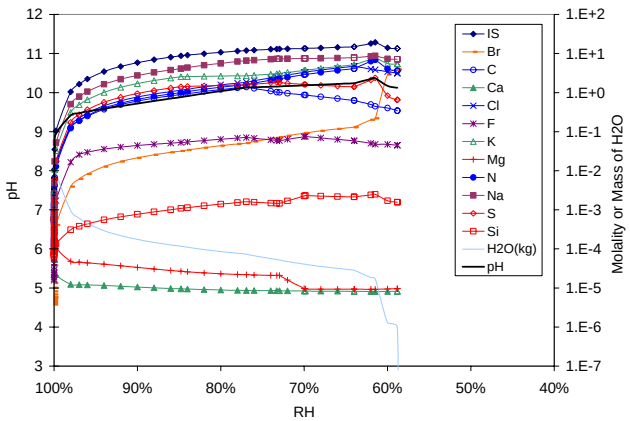

DTN: MO0310SPADLALT.001\d3c3t04.xls

Figure III-03-11. Bin 03 Aqueous Composition Evaporation Predictions vs. Relative Humidity at 40ºC and 10^{-3} CO_2 Fugacity

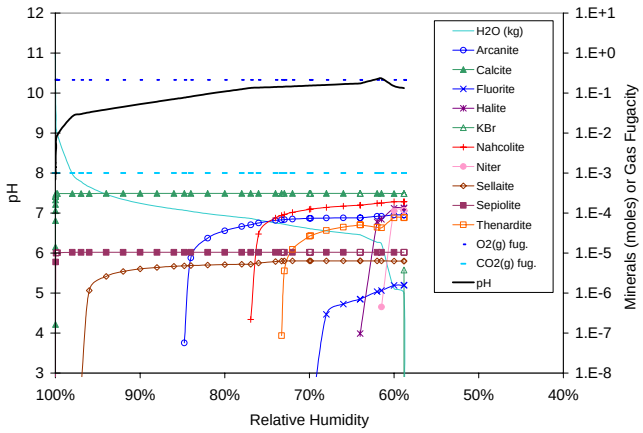

DTN: MO0310SPADLALT.001\d3c3t04.xls

Figure III-03-12. Bin 03 Mineral Precipitation Evaporation Predictions vs. Relative Humidity at 40ºC and 10^{-3} CO_2 Fugacity

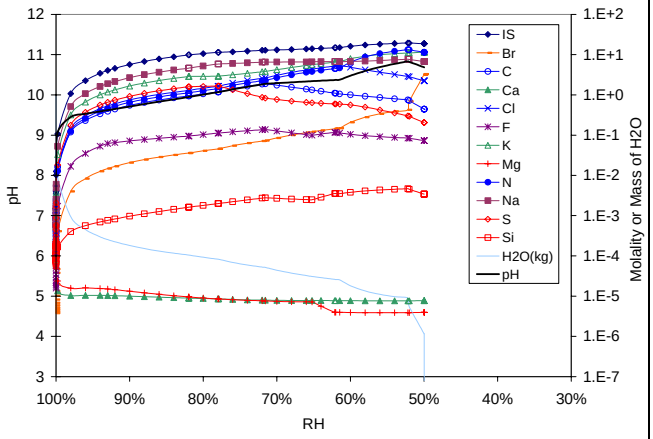

DTN: MO0310SPADLALT.0010\d3c3t07.xls

Figure III-03-13. Bin 03 Aqueous Composition Evaporation Predictions vs. Relative Humidity at 70ºC and 10^{-3} CO_2 Fugacity

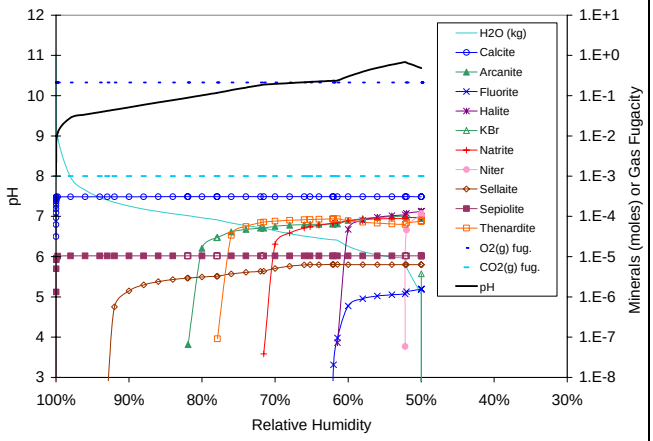

DTN: MO0310SPADLALT.001\d3c3t07.xls

Figure III-03-14. Bin 03 Mineral Precipitation Evaporation Predictions vs. Relative Humidity at 70ºC and 10^{-3} CO_2 Fugacity

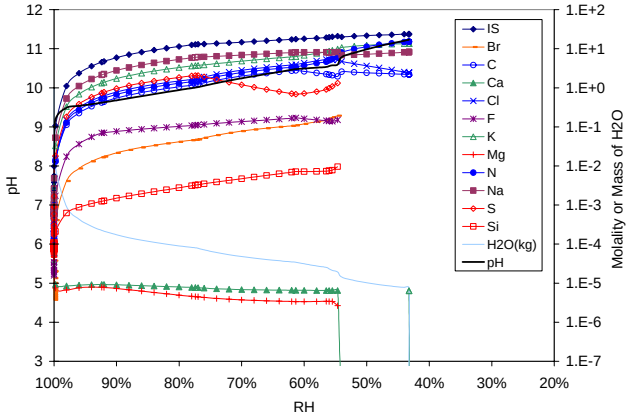

DTN: MO0310SPADLALT.001\d3c3t10.xls

Figure III-03-15. Bin 03 Aqueous Composition Evaporation Predictions vs. Relative Humidity at 100ºC and 10^{-3} CO_2 Fugacity

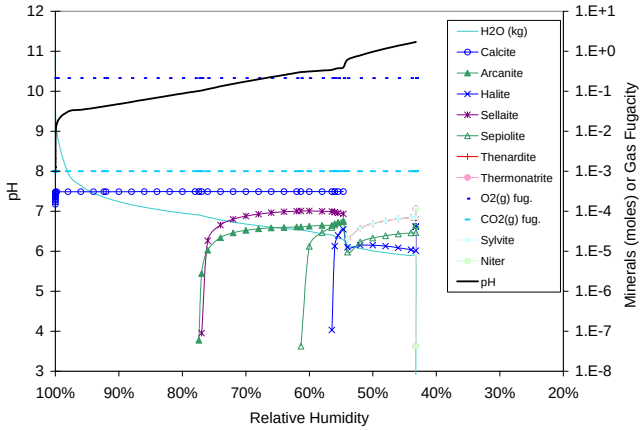

DTN: MO0310SPADLALT.001\d3c3t10.xls

Figure III-03-16. Bin 03 Mineral Precipitation Evaporation Predictions vs. Relative Humidity at 100ºC and 10^{-3} CO_2 Fugacity

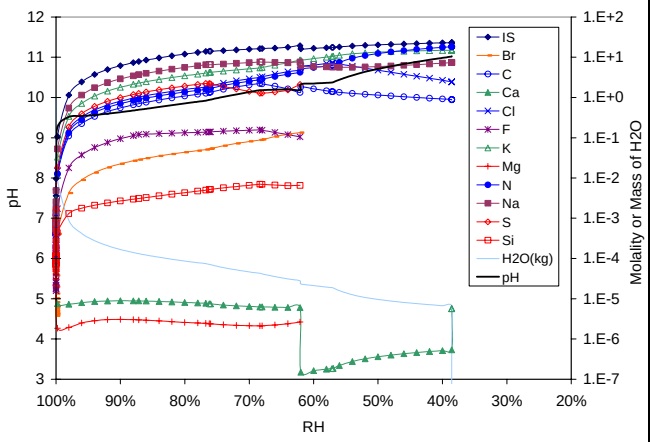

DTN: MO0310SPADLHTL.000\d3c3t12.xls

Figure III-03-17. Bin 03 Aqueous Composition Evaporation Predictions vs. Relative Humidity at 120ºC and 10^{-3} CO_2 Fugacity

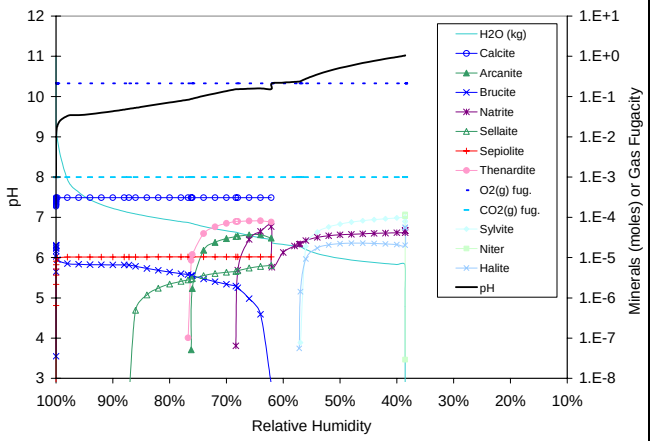

DTN: MO0310SPADLHTL.000\d3c3t12.xls

Figure III-03-18. Bin 03 Mineral Precipitation Evaporation Predictions vs. Relative Humidity at 120ºC and 10^{-3} CO_2 Fugacity

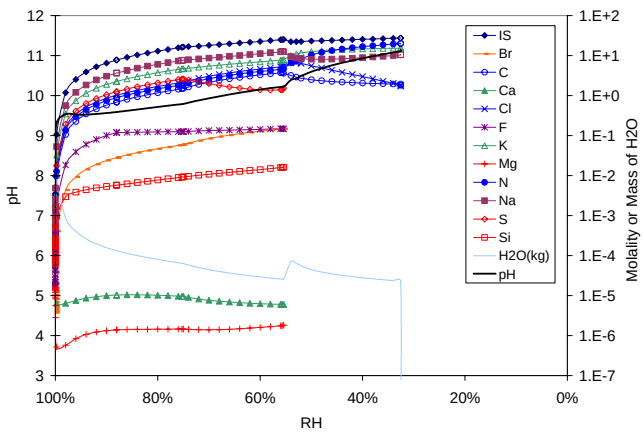

DTN: MO0310SPADLHTL.000\d3c3t14.xls

Figure III-03-19. Bin 03 Aqueous Composition Evaporation Predictions vs. Relative Humidity at 140ºC and 10^{-3} CO_2 Fugacity

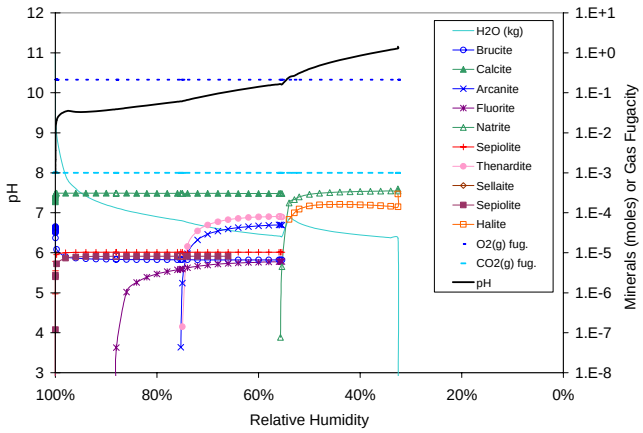

DTN: MO0310SPADLHTL.000\d3c3t14.xls

Figure III-03-20. Bin 03 Mineral Precipitation Evaporation Predictions vs. Relative Humidity at 140ºC and 10^{-3} CO_2 Fugacity

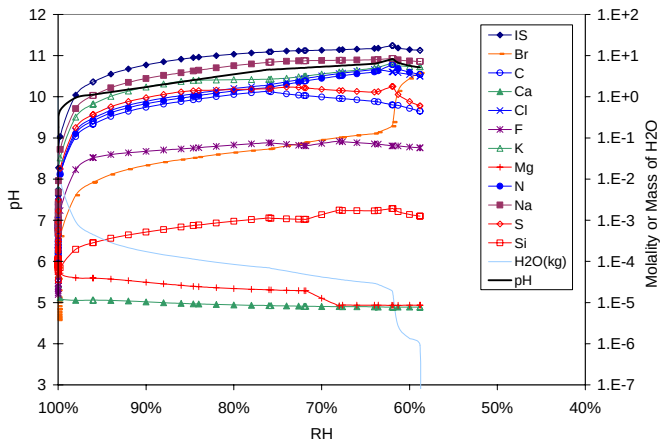

DTN: MO0310SPADLALT.001\d3c4t04.xls

Figure III-03-21. Bin 03 Aqueous Composition Evaporation Predictions vs. Relative Humidity at 40ºC and 10^{-4} CO_2 Fugacity

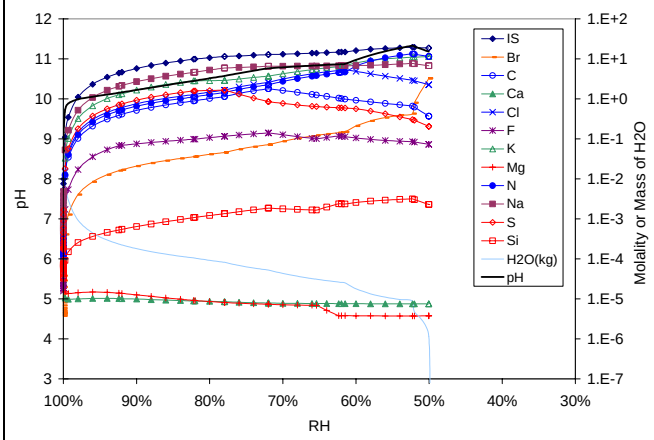

DTN: MO0310SPADLALT.001\d3c4t07.xls

Figure III-03-23. Bin 03 Aqueous Composition Evaporation Predictions vs. Relative Humidity at 70ºC and 10^{-4} CO_2 Fugacity

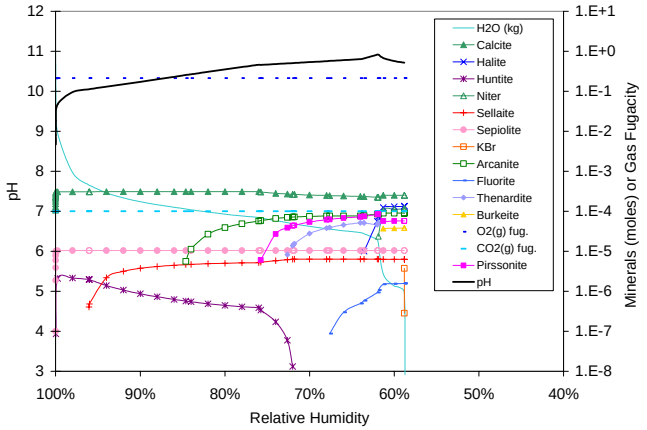

DTN: MO0310SPADLALT.001\d3c4t04.xls

Figure III-03-22. Bin 03 Mineral Precipitation Evaporation Predictions vs. Relative Humidity at 40ºC and 10^{-4} CO_2 Fugacity

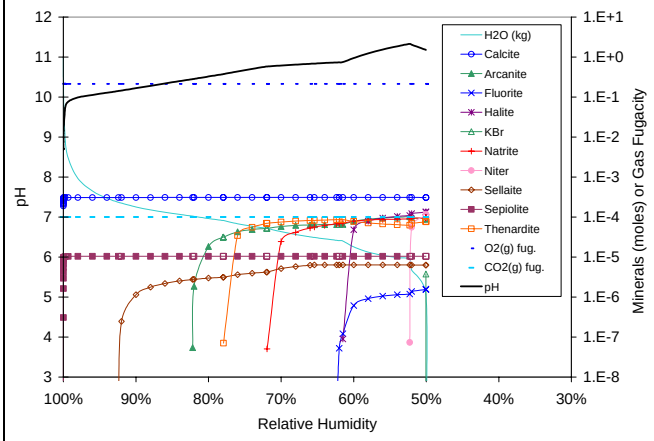

DTN: MO0310SPADLALT.001\d3c4t07.xls

Figure III-03-24. Bin 03 Mineral Precipitation Evaporation Predictions vs. Relative Humidity at 70ºC and 10^{-4} CO_2 Fugacity

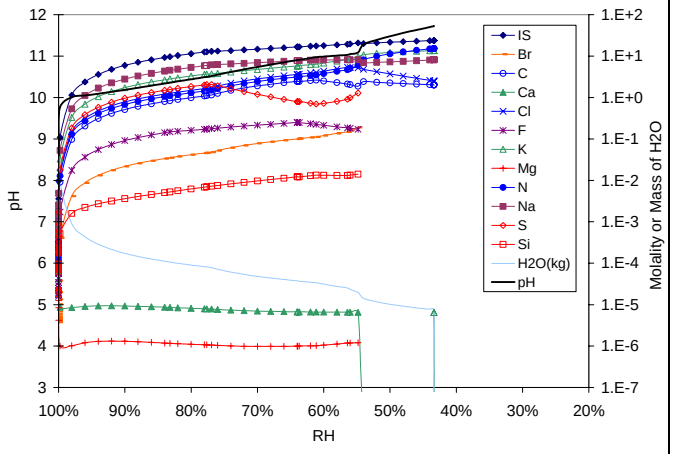

DTN: MO0310SPADLALT.001\d3c4t10.xls

Figure III-03-25. Bin 03 Aqueous Composition Evaporation Predictions vs. Relative Humidity at 100ºC and 10^{-4} CO_2 Fugacity

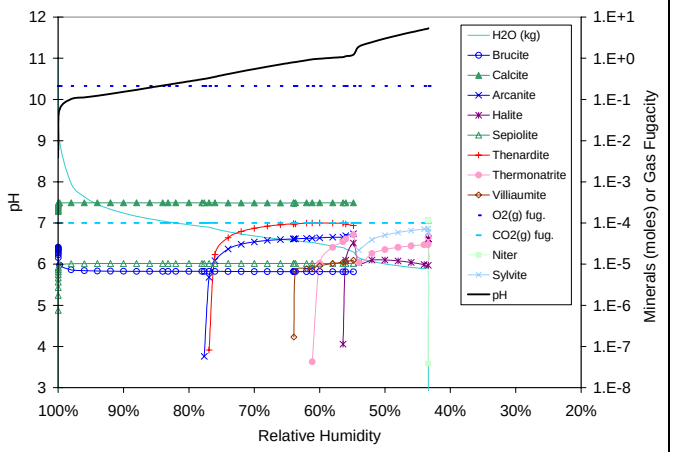

DTN: MO0310SPADLALT.001\d3c4t10.xls

Figure III-03-26. Bin 03 Mineral Precipitation Evaporation Predictions vs. Relative Humidity at 100ºC and 10^{-4} CO_2 Fugacity

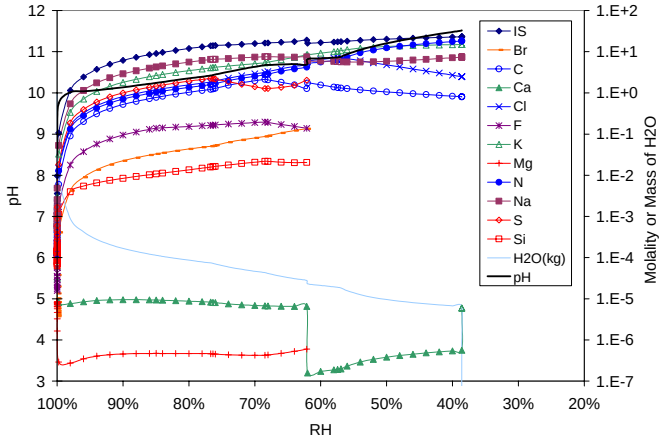

DTN: MO0310SPADLHTL.000\d3c4t12.xls

Figure III-03-27. Bin 03 Aqueous Composition Evaporation Predictions vs. Relative Humidity at 120ºC and 10^{-4} CO_2 Fugacity

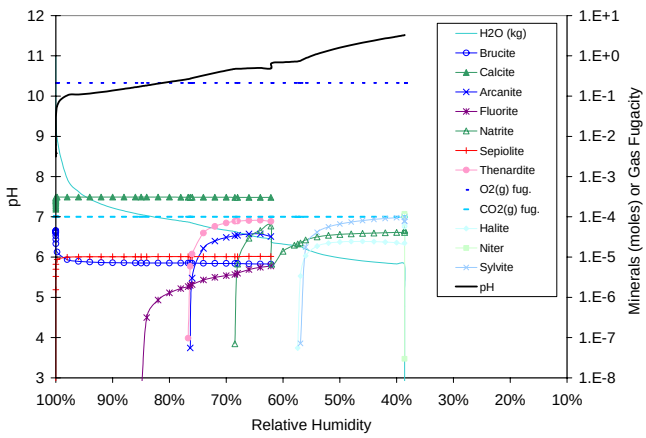

DTN: MO0310SPADLHTL.000\d3c4t12.xls

Figure III-03-28. Bin 03 Mineral Precipitation Evaporation Predictions vs. Relative Humidity at 120ºC and 10^{-4} CO_2 Fugacity

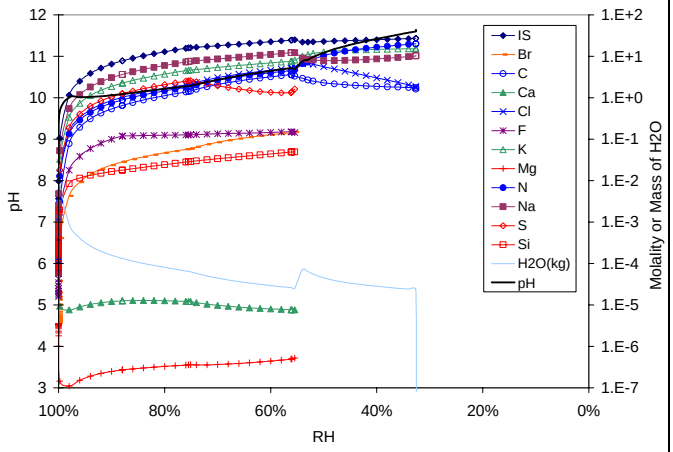

DTN: MO0310SPADLHTL.000\d3c4t14.xls

Figure III-03-29. Bin 03 Aqueous Composition Evaporation Predictions vs. Relative Humidity at 140ºC and 10^{-4} CO_2 Fugacity

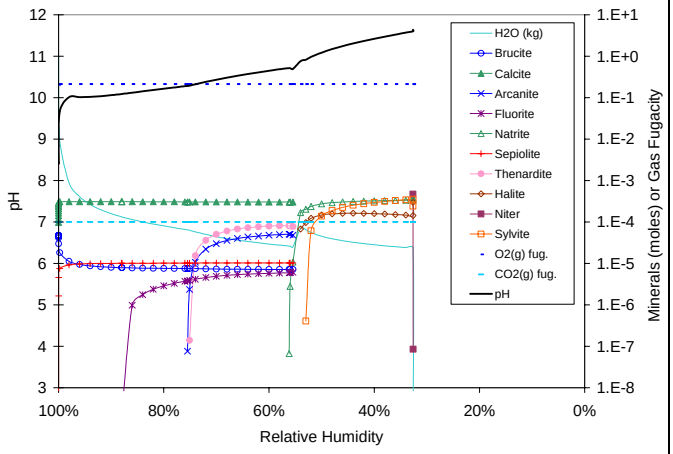

DTN: MO0310SPADLHTL.000\d3c4t14.xls

Figure III-03-30. Bin 03 Mineral Precipitation Evaporation Predictions vs. Relative Humidity at 140ºC and 10^{-4} CO_2 Fugacity

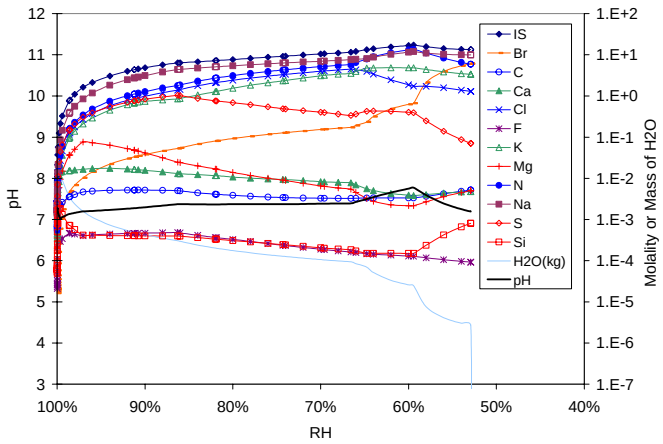

DTN: MO0310SPADLALT.001\d4c2t04.xls

Figure III-04-1. Bin 04 Aqueous Composition Evaporation Predictions vs. Relative Humidity at 40ºC and 10^{-2} CO_2 Fugacity

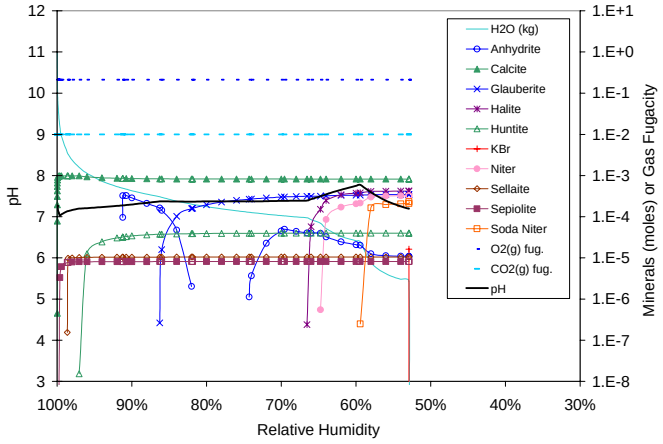

DTN: MO0310SPADLALT.001\d4c2t04.xls

Figure III-04-2. Bin 04 Mineral Precipitation Evaporation Predictions vs. Relative Humidity at 40ºC and 10^{-2} CO_2 Fugacity

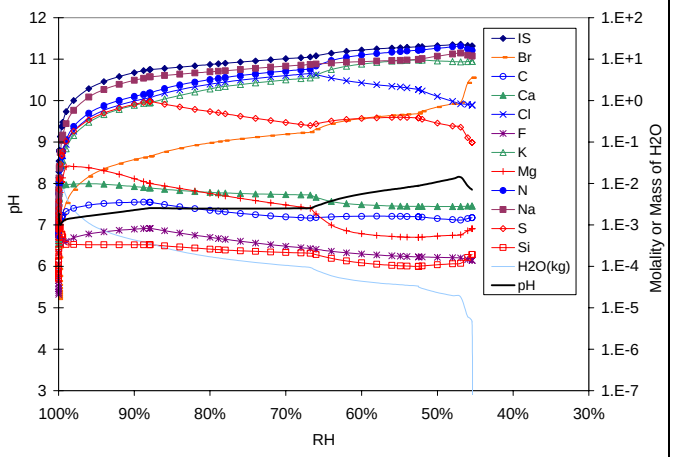

DTN: MO0310SPADLALT.001\d4c2t07.xls

Figure III-04-3. Bin 04 Aqueous Composition Evaporation Predictions vs. Relative Humidity at 70ºC and 10^{-2} CO_2 Fugacity

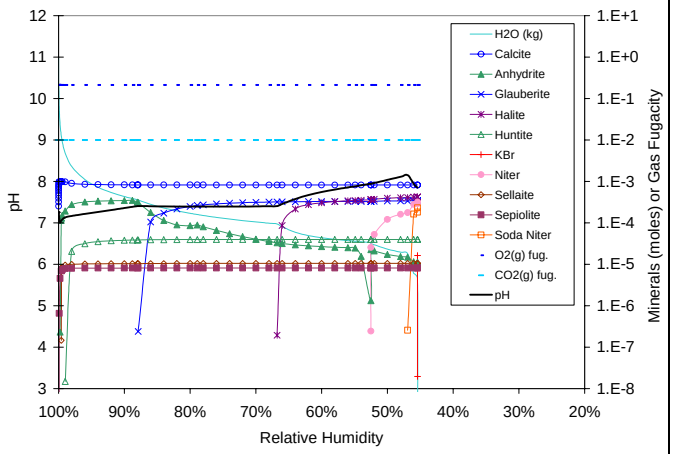

DTN: MO0310SPADLALT.001\d4c2t07.xls

Figure III-04-4. Bin 04 Mineral Precipitation Evaporation Predictions vs. Relative Humidity at 70ºC and 10^{-2} CO_2 Fugacity

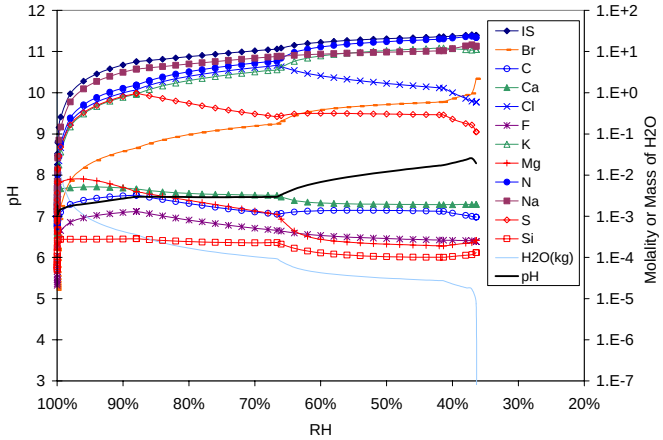

DTN: MO0310SPADLALT.001\d4c2t10.xls

Figure III-04-5. Bin 04 Aqueous Composition Evaporation Predictions vs. Relative Humidity at 100ºC and 10^{-2} CO_2 Fugacity

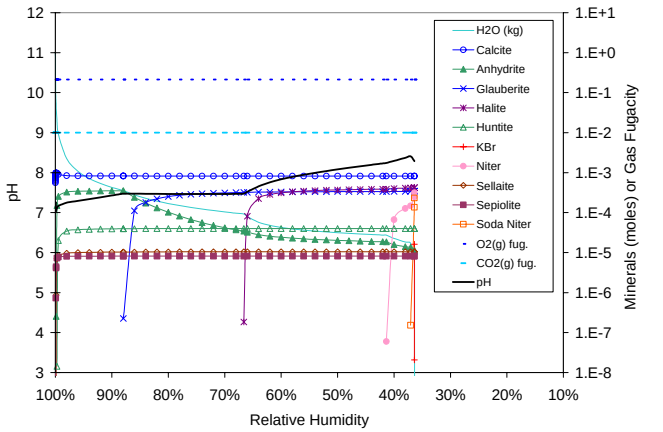

DTN: MO0310SPADLALT.001\d4c2t10.xls

Figure III-04-6. Bin 04 Mineral Precipitation Evaporation Predictions vs. Relative Humidity at 100ºC and 10^{-2} CO_2 Fugacity

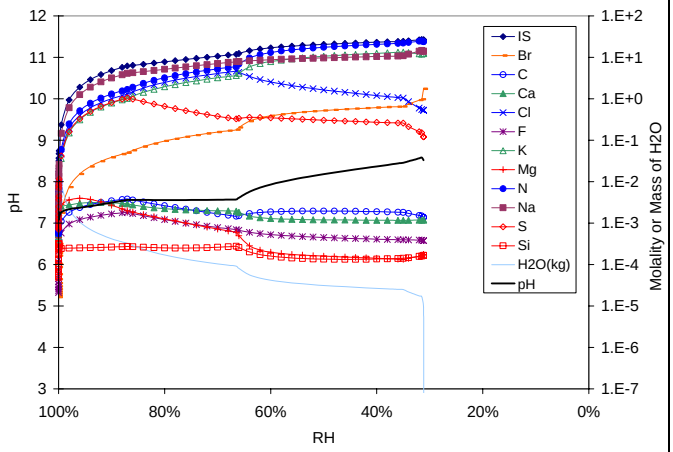

DTN: MO0310SPADLHTL.000\d4c2t12.xls

Figure III-04-7. Bin 04 Aqueous Composition Evaporation Predictions vs. Relative Humidity at 120ºC and 10^{-2} CO_2 Fugacity

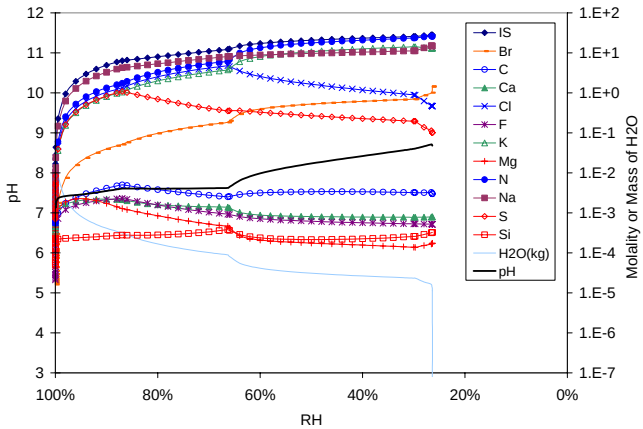

DTN: MO0310SPADLHTL.000\d4c2t14.xls

Figure III-04-9. Bin 04 Aqueous Composition Evaporation Predictions vs. Relative Humidity at 140ºC and 10^{-2} CO_2 Fugacity

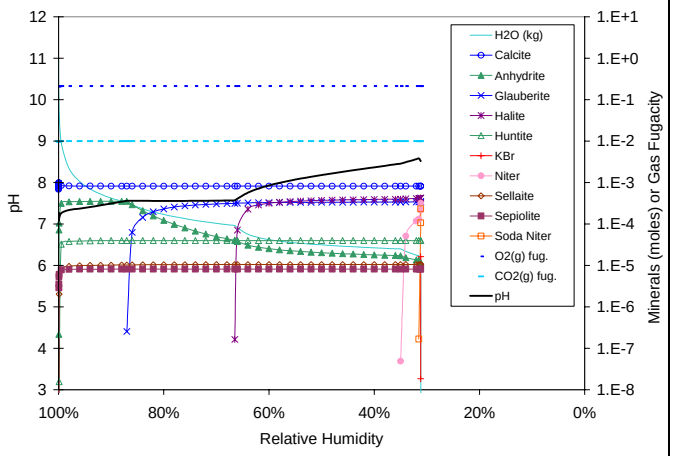

DTN: MO0310SPADLHTL.000\d4c2t12.xls

Figure III-04-8. Bin 04 Mineral Precipitation Evaporation Predictions vs. Relative Humidity at 120ºC and 10^{-2} CO_2 Fugacity

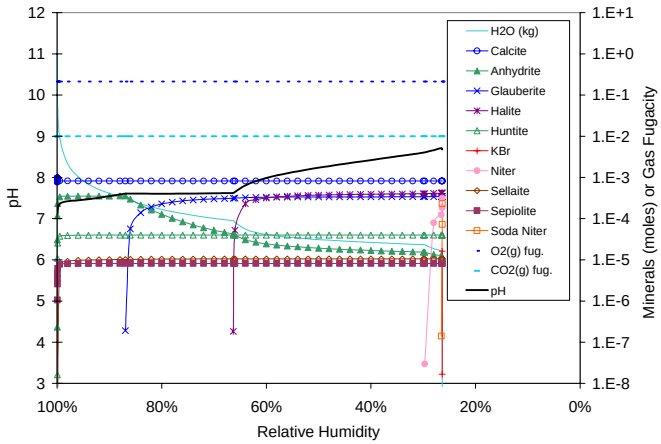

DTN: MO0310SPADLHTL.000\d4c2t14.xls

Figure III-04-10. Bin 04 Mineral Precipitation Evaporation Predictions vs. Relative Humidity at 140ºC and 10^{-2} CO_2 Fugacity

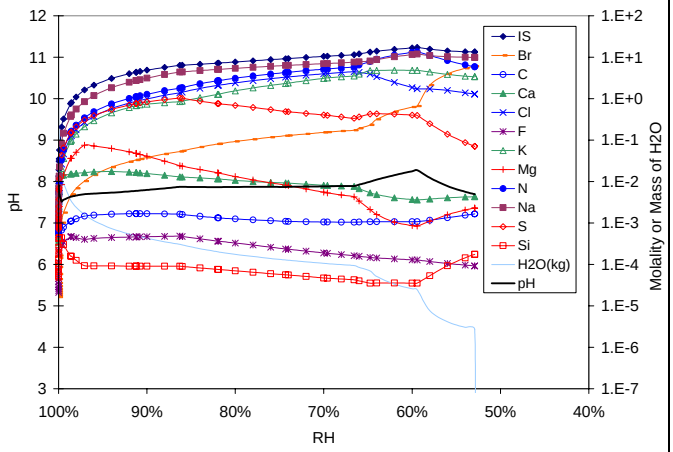

DTN: MO0310SPADLALT.001\d4c3t04.xls

Figure III-04-11. Bin 04 Aqueous Composition Evaporation Predictions vs. Relative Humidity at 40ºC and 10^{-3} CO_2 Fugacity

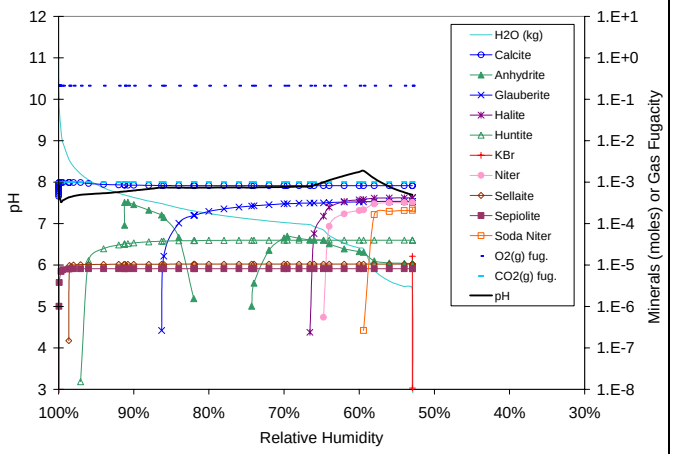

DTN: MO0310SPADLALT.001\D4C3T04.XLS

Figure III-04-12. Bin 04 Mineral Precipitation Evaporation Predictions vs. Relative Humidity at 40ºC and 10^{-3} CO_2 Fugacity

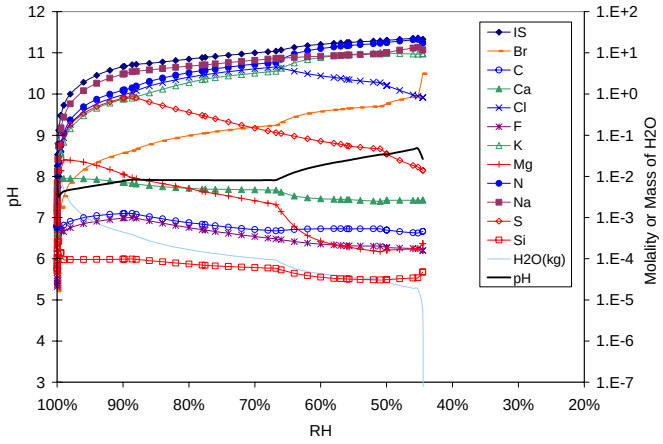

DTN: MO0310SPADLALT.001\d4c3t07.xls

Figure III-04-13. Bin 04 Aqueous Composition Evaporation Predictions vs. Relative Humidity at 70ºC and 10^{-3} CO_2 Fugacity

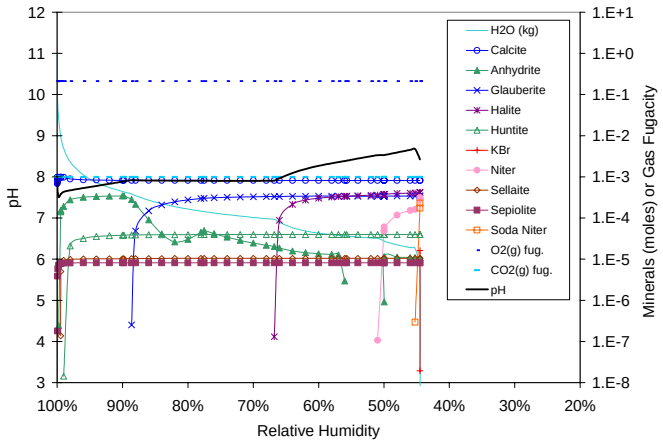

DTN: MO0310SPADLALT.001\d4c3t07.xls

Figure III-04-14. Bin 04 Mineral Precipitation Evaporation Predictions vs. Relative Humidity at 70ºC and 10^{-3} CO_2 Fugacity

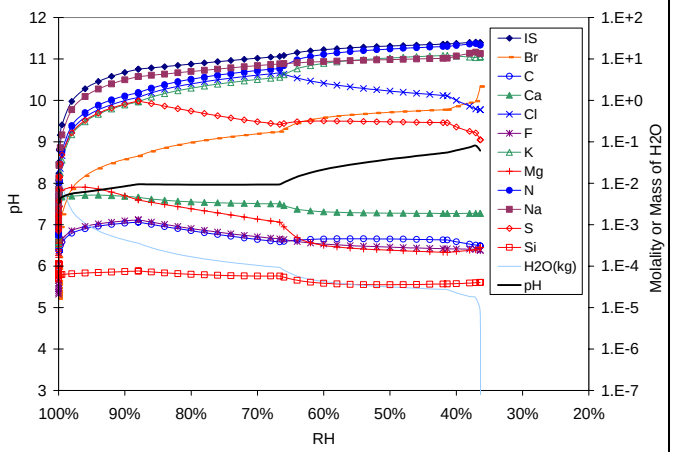

DTN: MO0310SPADLALT.001\d4c3t10.xls

Figure III-04-15. Bin 04 Aqueous Composition Evaporation Predictions vs. Relative Humidity at 100ºC and 10^{-3} CO_2 Fugacity

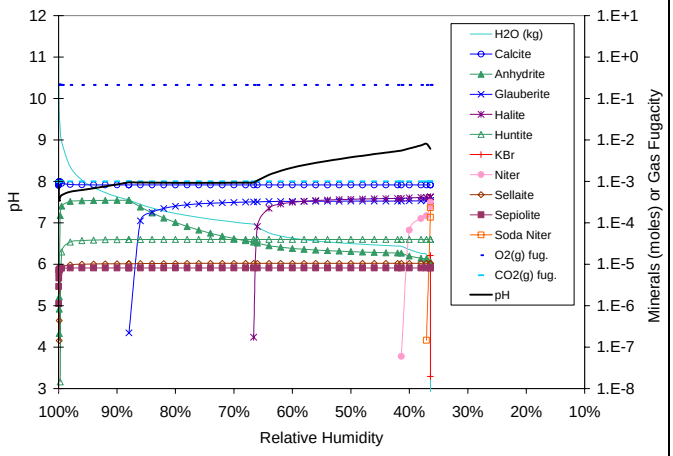

DTN: MO0310SPADLALT.001\d4c3t10.xls

Figure III-04-16. Bin 04 Mineral Precipitation Evaporation Predictions vs. Relative Humidity at 100ºC and 10^{-3} CO_2 Fugacity

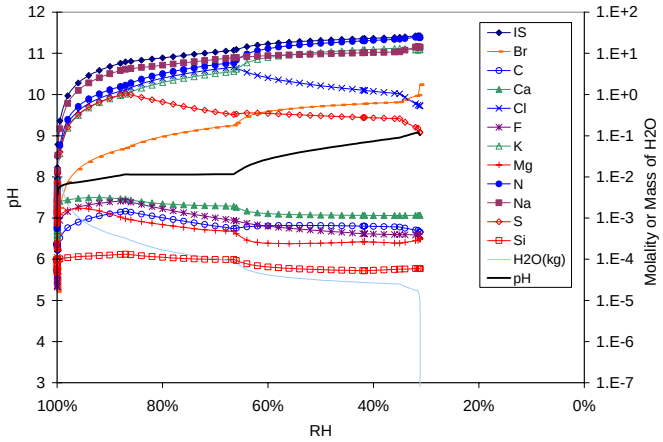

DTN: MO0310SPADLHTL.000\d4c3t12.xls

Figure III-04-17. Bin 04 Aqueous Composition Evaporation Predictions vs. Relative Humidity at 120ºC and 10^{-3} CO_2 Fugacity

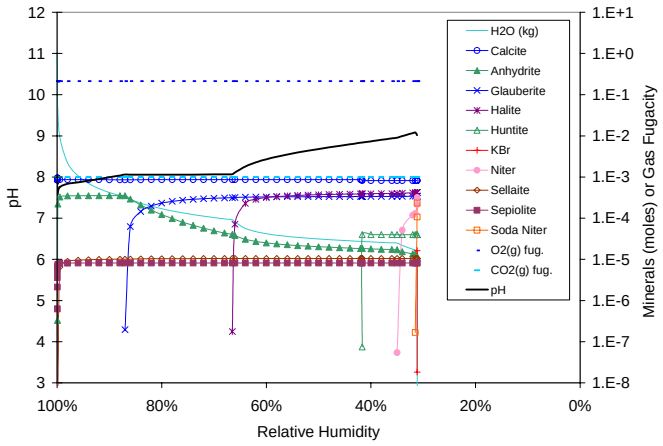

DTN: MO0310SPADLHTL.000\d4c3t12.xls

Figure III-04-18. Bin 04 Mineral Precipitation Evaporation Predictions vs. Relative Humidity at 120ºC and 10^{-3} CO_2 Fugacity

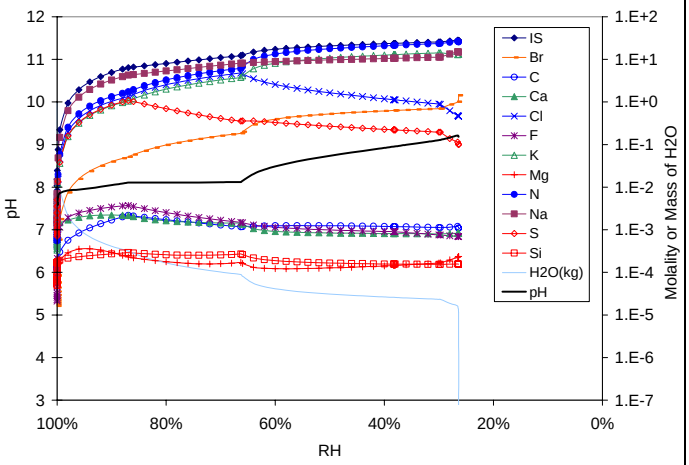

DTN: MO0310SPADLHTL.000\d4c3t14.xls

Figure III-04-19. Bin 04 Aqueous Composition Evaporation Predictions vs. Relative Humidity at 140ºC and 10^{-3} CO_2 Fugacity

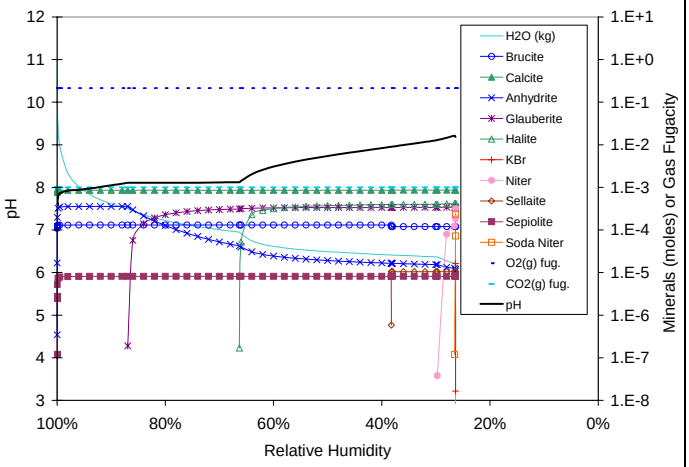

DTN: MO0310SPADLHTL.000\d4c3t14.xls

Figure III-04-20. Bin 04 Mineral Precipitation Evaporation Predictions vs. Relative Humidity at 140ºC and 10^{-3} CO_2 Fugacity

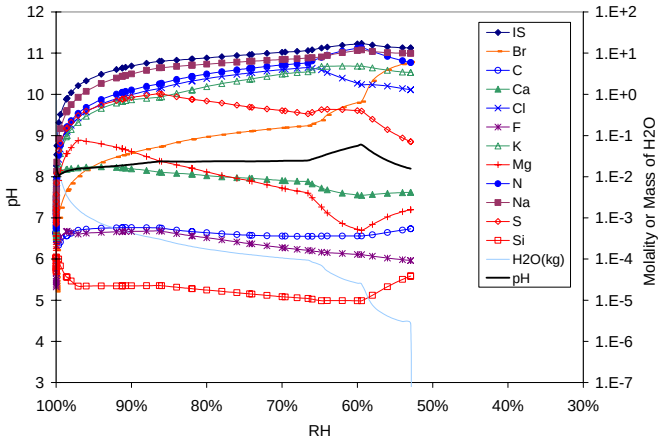

DTN: MO0310SPADLALT.001\d4c4t04.xls

Figure III-04-21. Bin 04 Aqueous Composition Evaporation Predictions vs. Relative Humidity at 40ºC and 10^{-4} CO_2 Fugacity

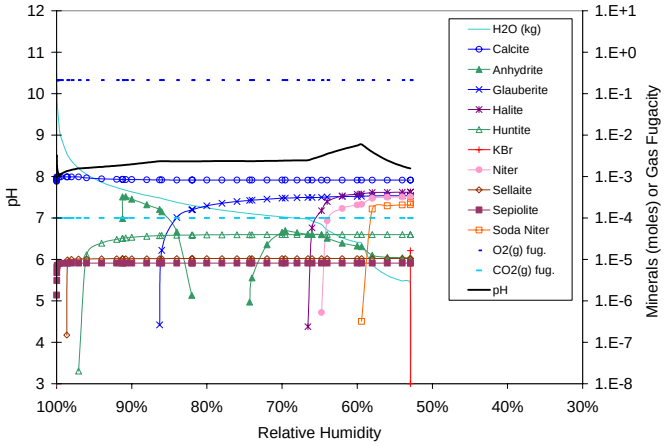

DTN: MO0310SPADLALT.001\d4c4t04.xls

Figure III-04-22. Bin 04 Mineral Precipitation Evaporation Predictions vs. Relative Humidity at 40ºC and 10^{-4} CO_2 Fugacity

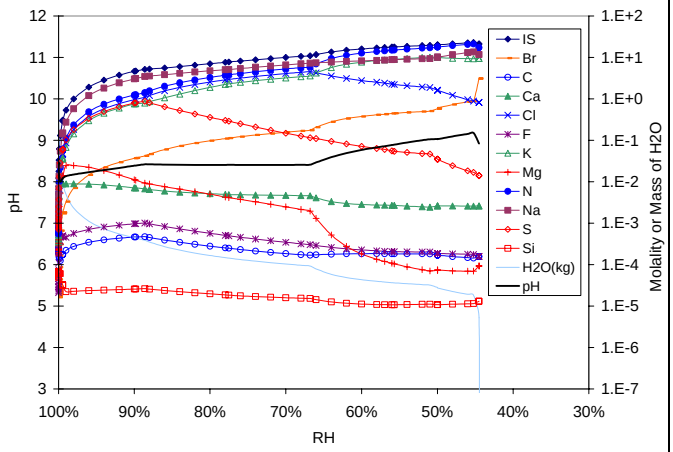

DTN: MO0310SPADLALT.001\d4c4t07.xls

Figure III-04-23. Bin 04 Aqueous Composition Evaporation Predictions vs. Relative Humidity at 70ºC and 10^{-4} CO_2 Fugacity

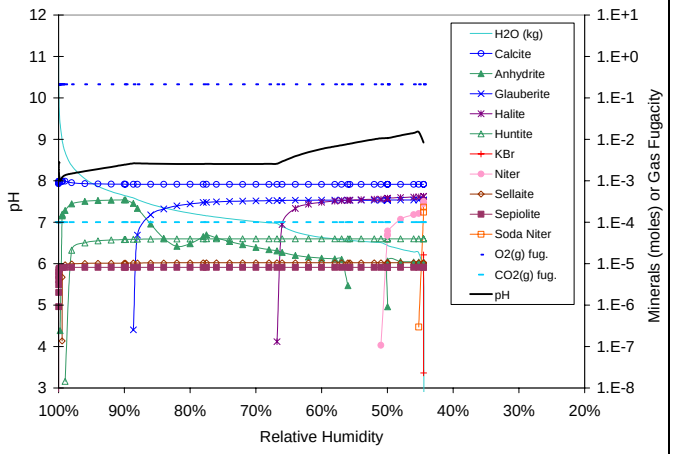

DTN: MO0310SPADLALT.001\d4c4t07.xls

Figure III-04-24. Bin 04 Mineral Precipitation Evaporation Predictions vs. Relative Humidity at 70ºC and 10^{-4} CO_2 Fugacity

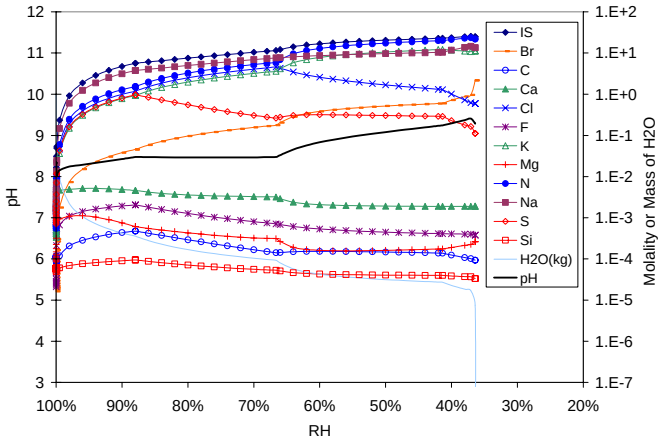

DTN: MO0310SPADLALT.001\d4c4t10.xls

Figure III-04-25. Bin 04 Aqueous Composition Evaporation Predictions vs. Relative Humidity at 100ºC and 10^{-4} CO_2 Fugacity

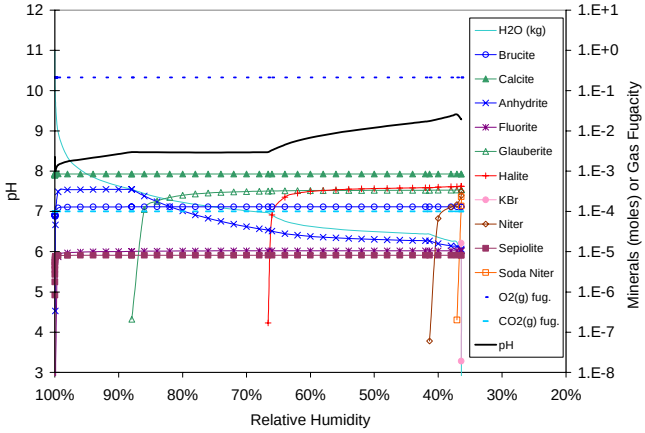

DTN: MO0310SPADLALT.001\d4c4t10.xls

Figure III-04-26. Bin 04 Mineral Precipitation Evaporation Predictions vs. Relative Humidity at 100ºC and 10^{-4} CO_2 Fugacity

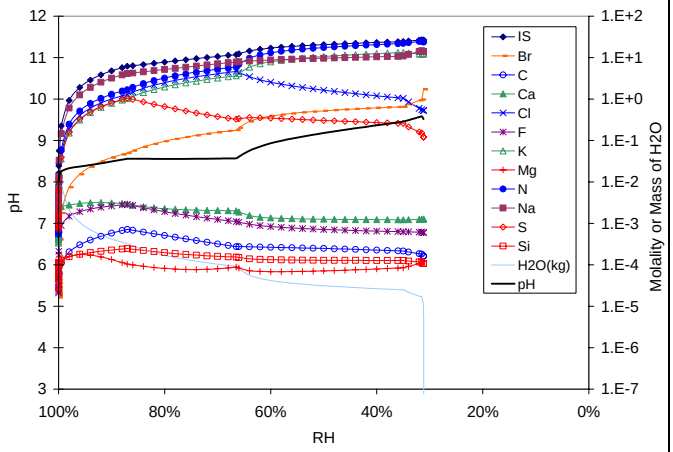

DTN: MO0310SPADLHTL.000\d4c4t12.xls

Figure III-04-27. Bin 04 Aqueous Composition Evaporation Predictions vs. Relative Humidity at 120ºC and 10^{-4} CO_2 Fugacity

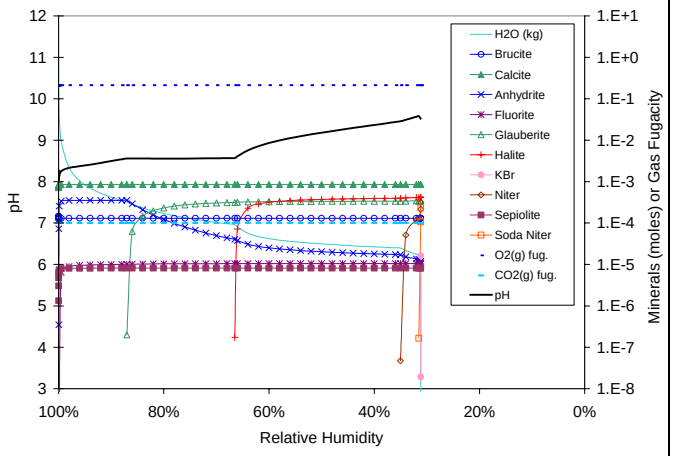

DTN: MO0310SPADLHTL.000\d4c4t12.xls

Figure III-04-28. Bin 04 Mineral Precipitation Evaporation Predictions vs. Relative Humidity at 120ºC and 10^{-4} CO_2 Fugacity

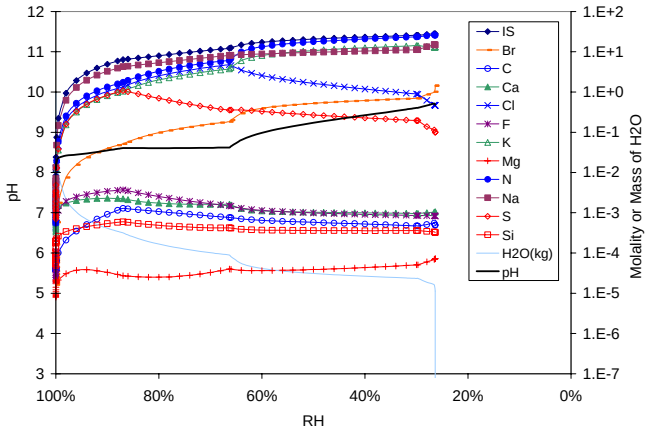

DTN: MO0310SPADLHTL.000\d4c4t14.xls

Figure III-04-29. Bin 04 Aqueous Composition Evaporation Predictions vs. Relative Humidity at 140ºC and 10^{-4} CO_2 Fugacity

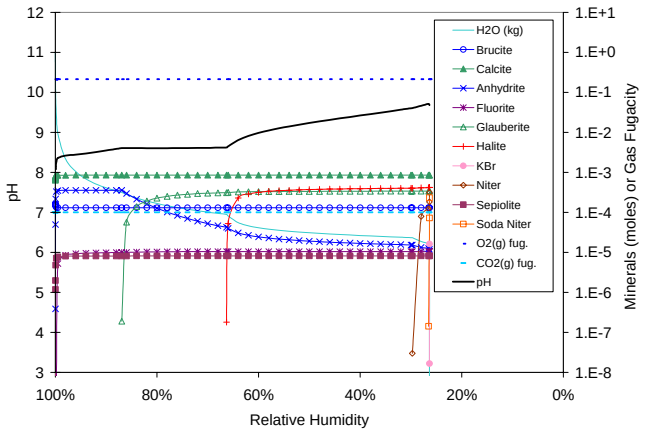

DTN: MO0310SPADLHTL.000\d4c4t14.xls

Figure III-04-30. Bin 04 Mineral Precipitation Evaporation Predictions vs. Relative Humidity at 140ºC and 10^{-4} CO_2 Fugacity

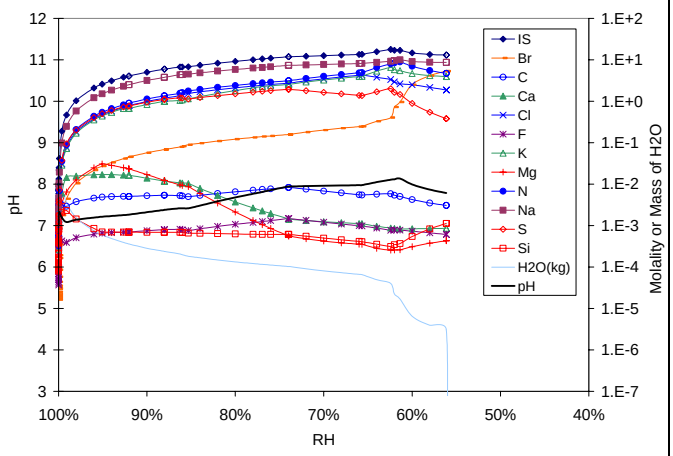

DTN: MO0310SPADLALT.001\d5c2t04.xls

Figure III-05-1. Bin 05 Aqueous Composition Evaporation Predictions vs. Relative Humidity at 40ºC and 10^{-2} CO_2 Fugacity

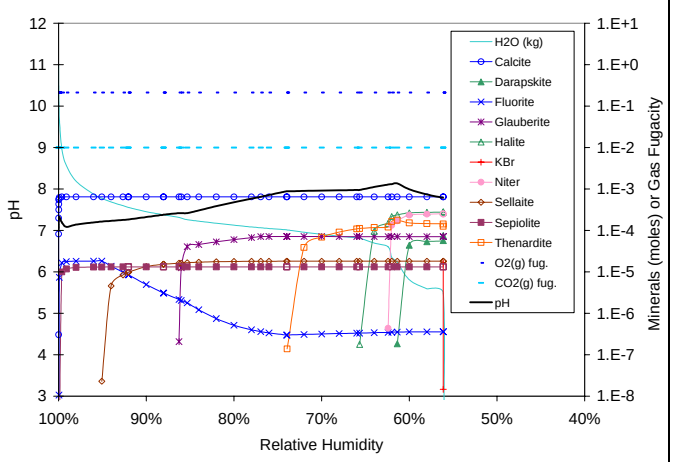

DTN: MO0310SPADLALT.000\d5c2t04.xls

Figure III-05-2. Bin 05 Mineral Precipitation Evaporation Predictions vs. Relative Humidity at 40ºC and 10^{-2} CO_2 Fugacity

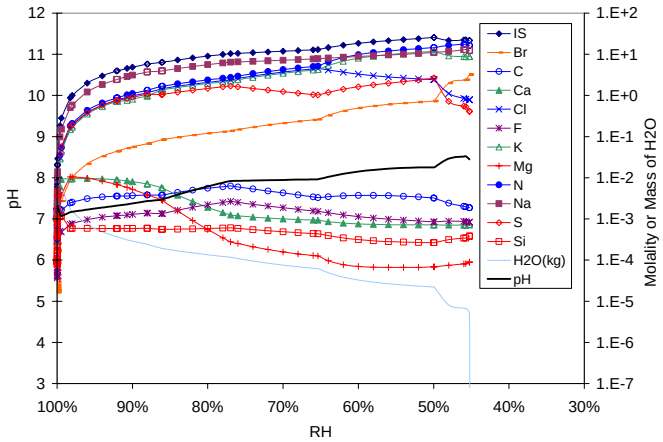

DTN: MO0310SPADLALT.001\d5c2t07.xls

Figure III-05-3. Bin 05 Aqueous Composition Evaporation Predictions vs. Relative Humidity at 70ºC and 10^{-2} CO_2 Fugacity

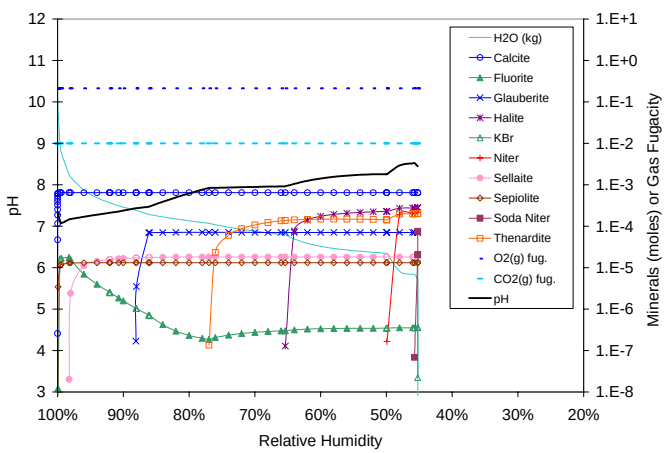

DTN: MO0310SPADLALT.001\d5c2t07.xls

Figure III-05-4. Bin 05 Mineral Precipitation Evaporation Predictions vs. Relative Humidity at 70ºC and 10^{-2} CO_2 Fugacity

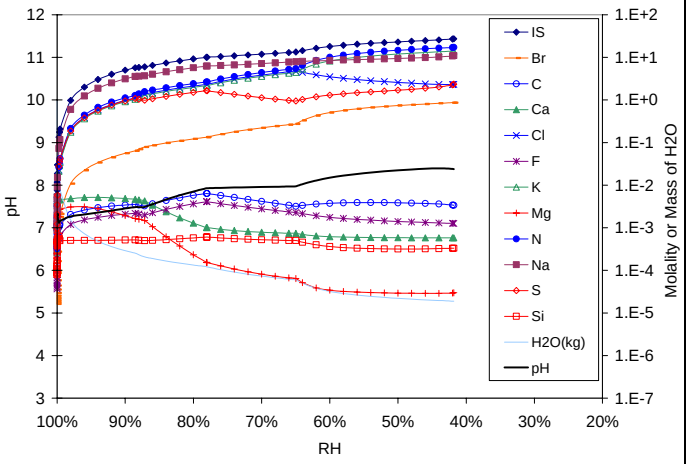

DTN: MO0310SPADLALT.001\d5c2t10.xls

Figure III-05-5. Bin 05 Aqueous Composition Evaporation Predictions vs. Relative Humidity at 100ºC and 10^{-2} CO_2 Fugacity

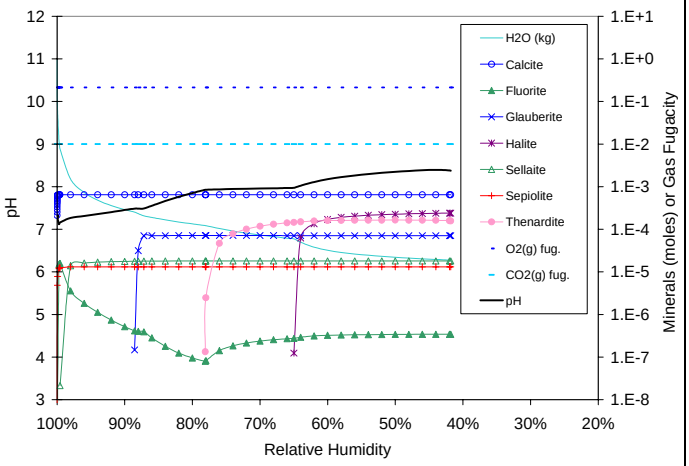

DTN: MO0310SPADLALT.001\d5c2t10.xls

Figure III-05-6. Bin 05 Mineral Precipitation Evaporation Predictions vs. Relative Humidity at 100ºC and 10^{-2} CO_2 Fugacity

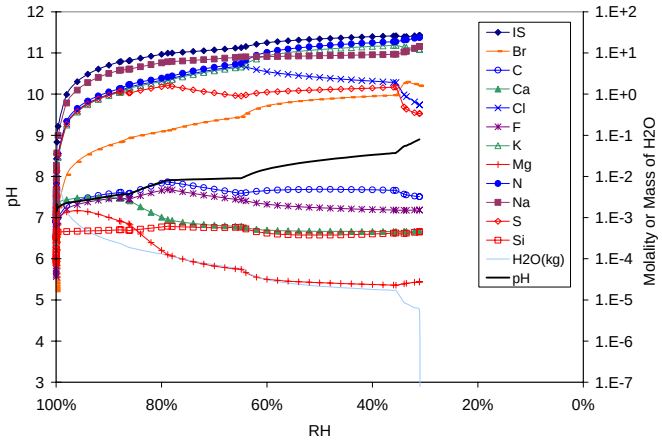

DTN: MO0310SPADLHTL.000\d5c2t12.xls

Figure III-05-7. Bin 05 Aqueous Composition Evaporation Predictions vs. Relative Humidity at 120ºC and 10^{-2} CO_2 Fugacity

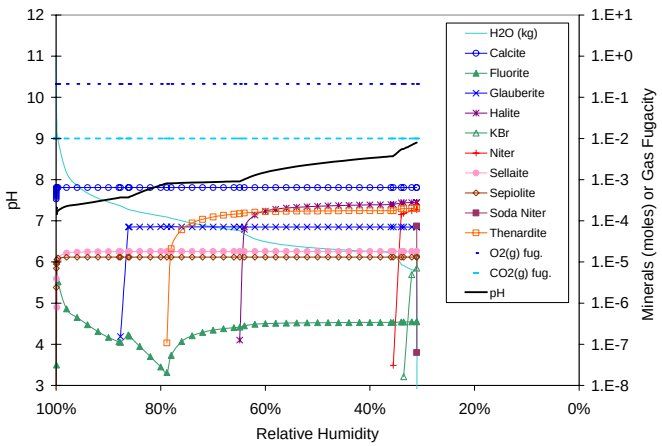

DTN: MO0310SPADLHTL.000\d5c2t12.xls

Figure III-05-8. Bin 05 Mineral Precipitation Evaporation Predictions vs. Relative Humidity at 120ºC and 10^{-2} CO_2 Fugacity

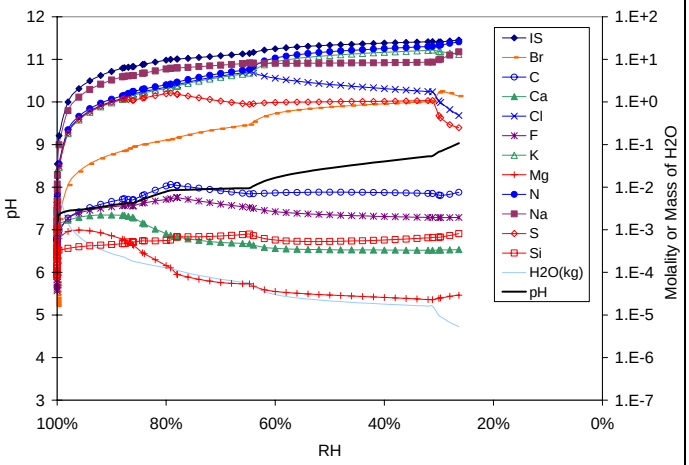

DTN: MO0310SPADLHTL.000\d5c2t14.xls

Figure III-05-9. Bin 05 Aqueous Composition Evaporation Predictions vs. Relative Humidity at 140ºC and 10^{-2} CO_2 Fugacity

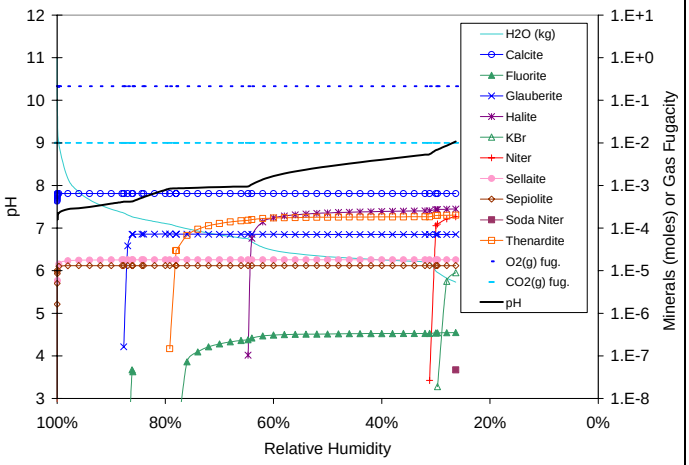

DTN: MO0310SPADLHTL.000\d5c2t14.xls

Figure III-05-10. Bin 05 Mineral Precipitation Evaporation Predictions vs. Relative Humidity at 140ºC and 10^{-2} CO_2 Fugacity

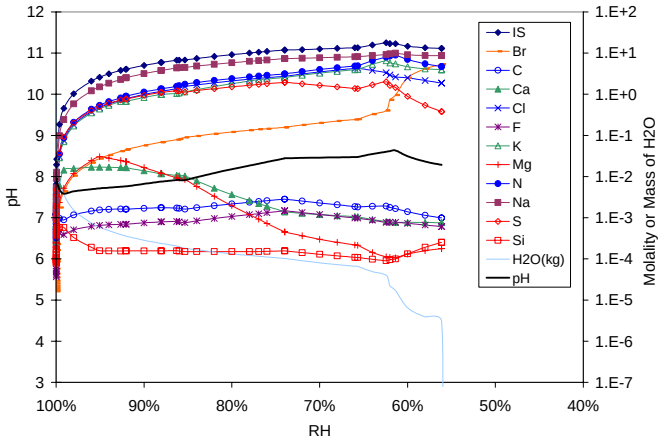

DTN: MO0310SPADLALT.001\d5c3t04.xls

Figure III-05-11. Bin 05 Aqueous Composition Evaporation Predictions vs. Relative Humidity at 40ºC and 10^{-3} CO_2 Fugacity

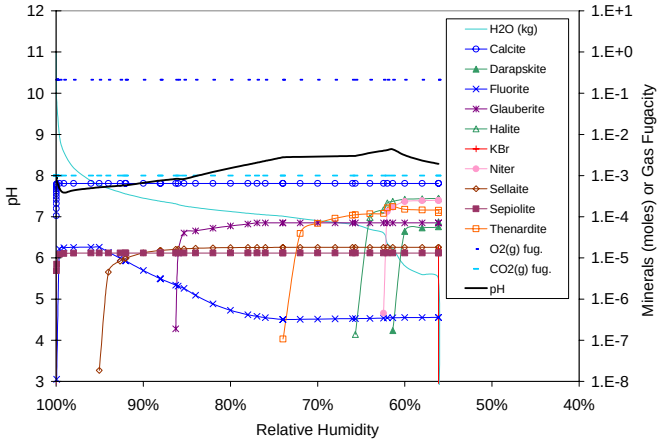

DTN: MO0310SPADLALT.001\d5c3t04.xls

Figure III-05-12. Bin 05 Mineral Precipitation Evaporation Predictions vs. Relative Humidity at 40ºC and 10^{-3} CO_2 Fugacity

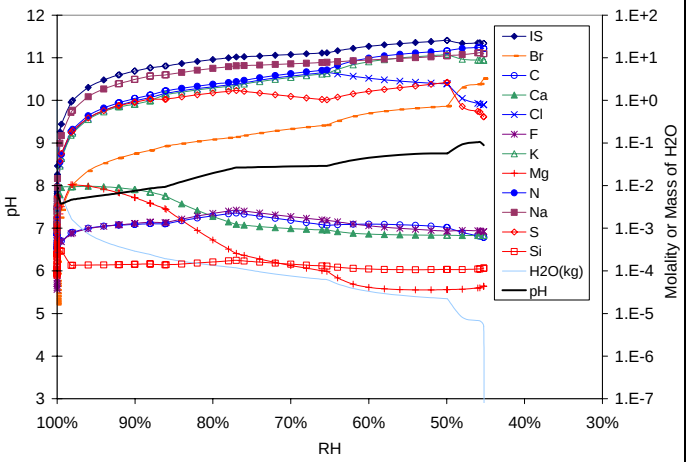

DTN: MO0310SPADLALT.001\d5c3t07.xls

Figure III-05-13. Bin 05 Aqueous Composition Evaporation Predictions vs. Relative Humidity at 70ºC and 10^{-3} CO_2 Fugacity

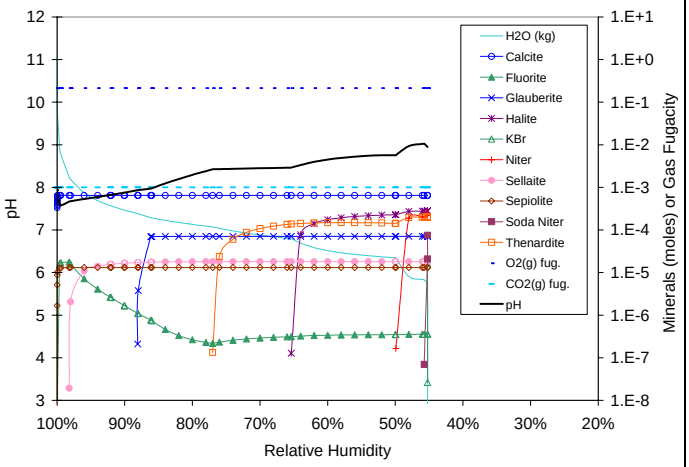

DTN: MO0310SPADLALT.001\d5c3t07.xls

Figure III-05-14. Bin 05 Mineral Precipitation Evaporation Predictions vs. Relative Humidity at 70ºC and 10^{-3} CO_2 Fugacity

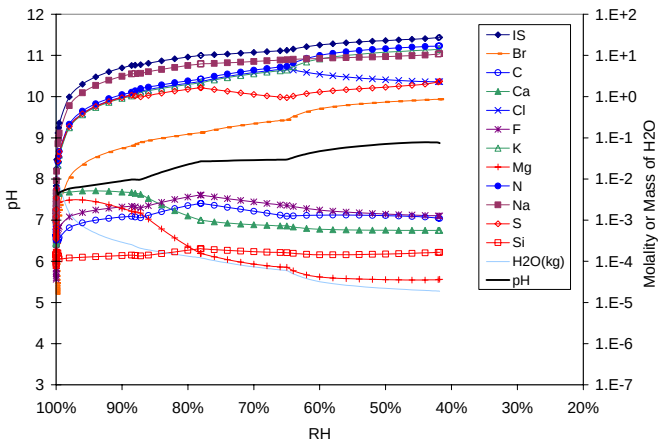

DTN: MO0310SPADLALT.001\d5c3t10.xls

Figure III-05-15. Bin 05 Aqueous Composition Evaporation Predictions vs. Relative Humidity at 100ºC and 10^{-3} CO_2 Fugacity

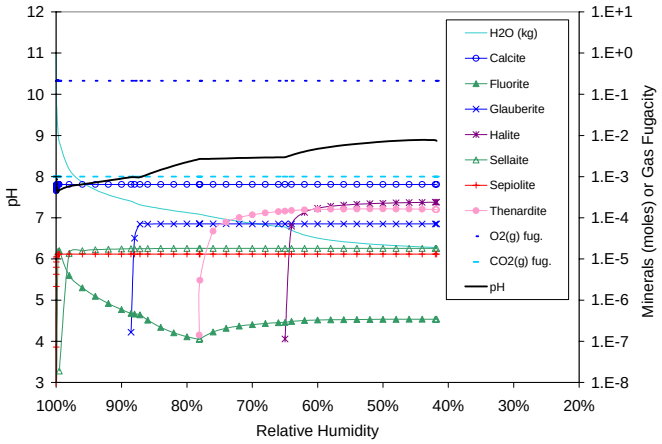

DTN: MO0310SPADLALT.001\d5c3t10.xls

Figure III-05-16. Bin 05 Mineral Precipitation Evaporation Predictions vs. Relative Humidity at 100ºC and 10^{-3} CO_2 Fugacity

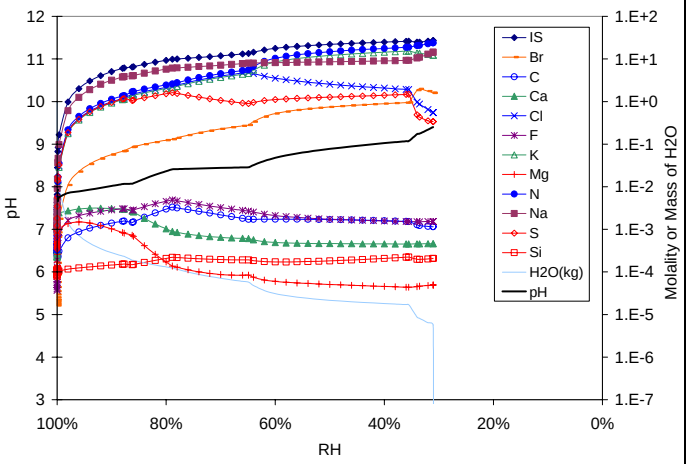

DTN: MO0310SPADLHTL.000\d5c3t12.xls

Figure III-05-17. Bin 05 Aqueous Composition Evaporation Predictions vs. Relative Humidity at 120ºC and 10^{-3} CO_2 Fugacity

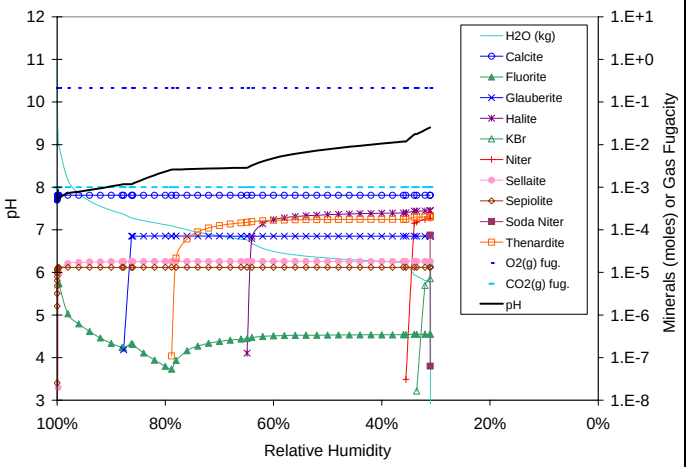

DTN: MO0310SPADLHTL.000\d5c3t12.xls

Figure III-05-18. Bin 05 Mineral Precipitation Evaporation Predictions vs. Relative Humidity at 120ºC and 10^{-3} CO_2 Fugacity

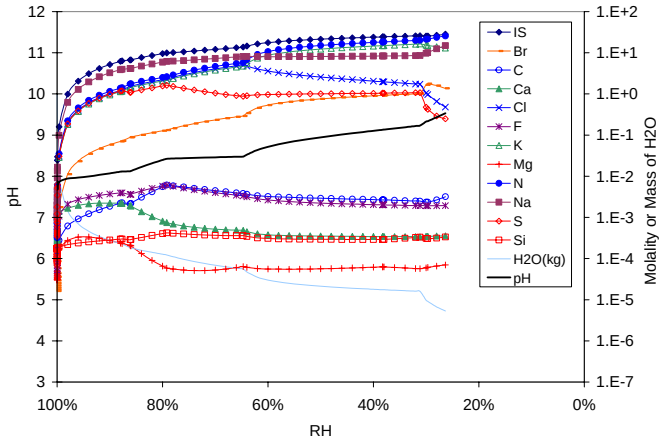

DTN: MO0310SPADLHTL.000\d5c3t14.xls

Figure III-05-19. Bin 05 Aqueous Composition Evaporation Predictions vs. Relative Humidity at 140ºC and 10^{-3} CO_2 Fugacity

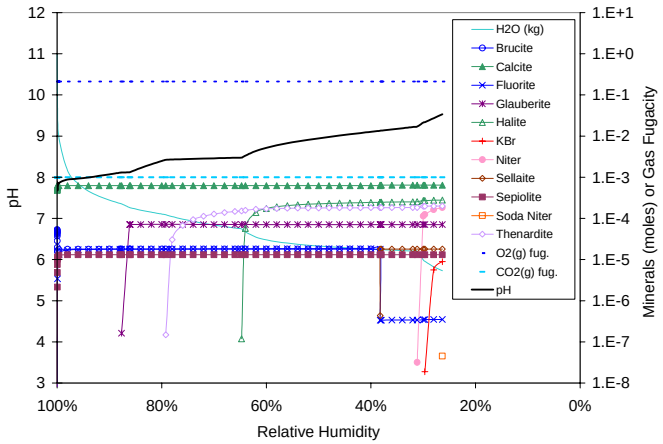

DTN: MO0310SPADLHTL.000\d5c3t14.xls

Figure III-05-20. Bin 05 Mineral Precipitation Evaporation Predictions vs. Relative Humidity at 140ºC and 10^{-3} CO_2 Fugacity

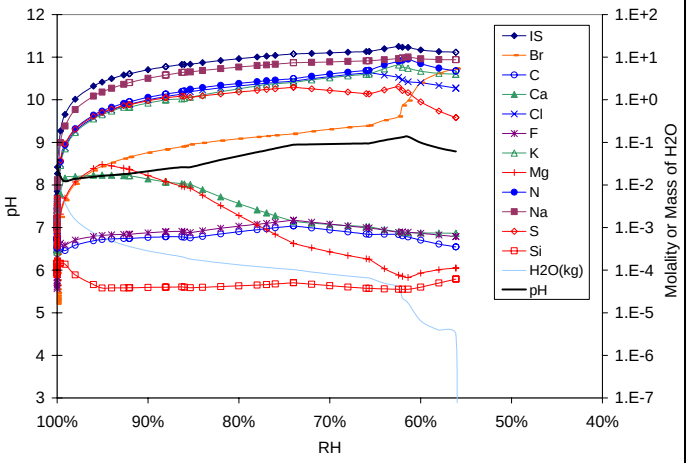

DTN: MO0310SPADLALT.001\d5c4t04.xls

Figure III-05-21. Bin 05 Aqueous Composition Evaporation Predictions vs. Relative Humidity at 40ºC and 10^{-4} CO_2 Fugacity

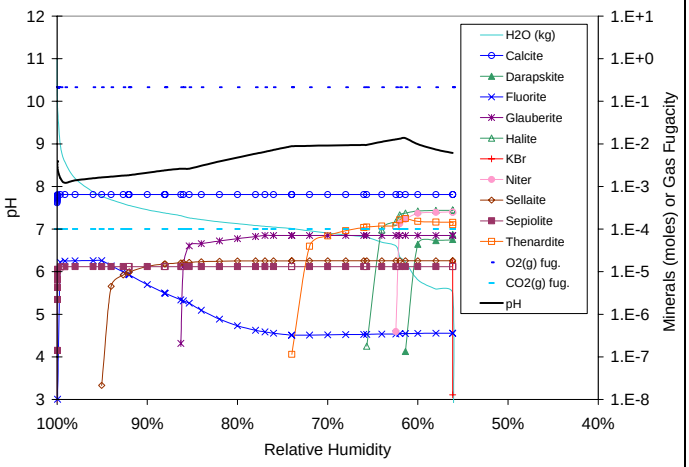

DTN: MO0310SPADLALT.001\d5c4t04.xls

Figure III-05-22. Bin 05 Mineral Precipitation Evaporation Predictions vs. Relative Humidity at 40ºC and 10^{-4} CO_2 Fugacity

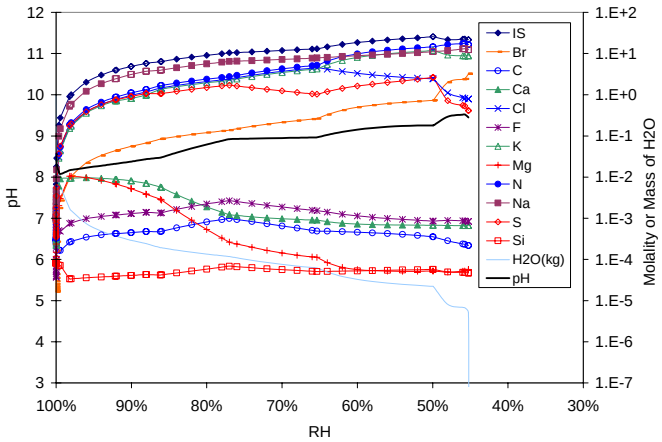

DTN: MO0310SPADLALT.001\d5c4t07xls

Figure III-05-23. Bin 05 Aqueous Composition Evaporation Predictions vs. Relative Humidity at 70ºC and 10^{-4} CO_2 Fugacity

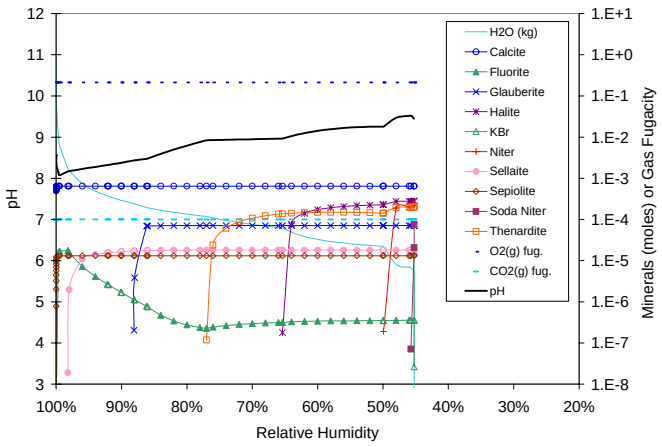

DTN: MO0310SPADLALT.001\d5c4t07.xls

Figure III-05-24. Bin 05 Mineral Precipitation Evaporation Predictions vs. Relative Humidity at 70ºC and 10^{-4} CO_2 Fugacity

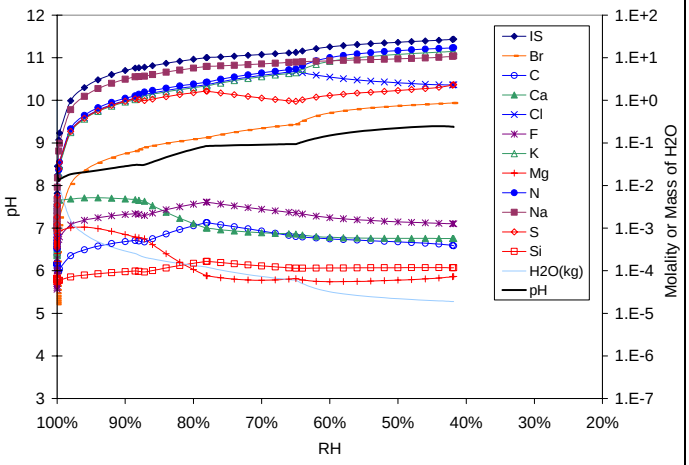

DTN: MO0310SPADLALT.001\d5c4t10.xls

Figure III-05-25. Bin 05 Aqueous Composition Evaporation Predictions vs. Relative Humidity at 100ºC and 10^{-4} CO_2 Fugacity

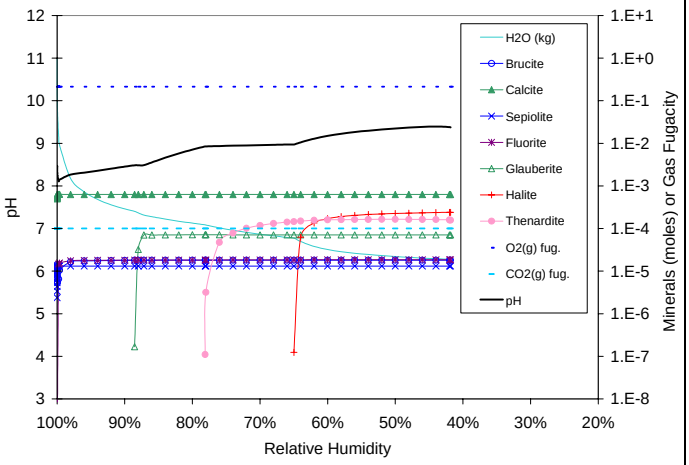

DTN: MO0310SPADLALT.001\d5c4t10.xls

Figure III-05-26. Bin 05 Mineral Precipitation Evaporation Predictions vs. Relative Humidity at 100ºC and 10^{-4} CO_2 Fugacity

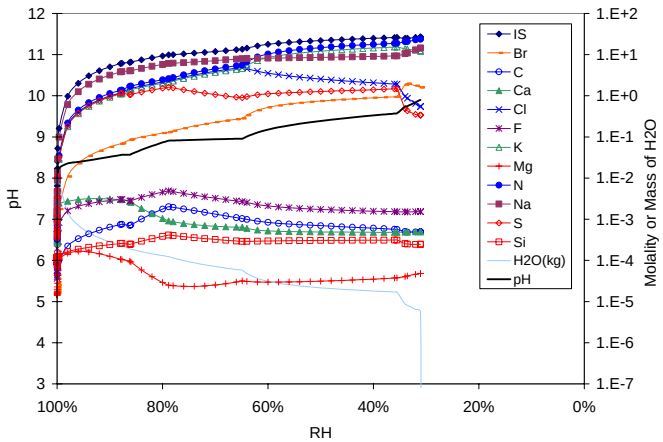

DTN: MO0310SPADLHTL.000\d5c4t12.xls

Figure III-05-27. Bin 05 Aqueous Composition Evaporation Predictions vs. Relative Humidity at 120ºC and 10^{-4} CO_2 Fugacity

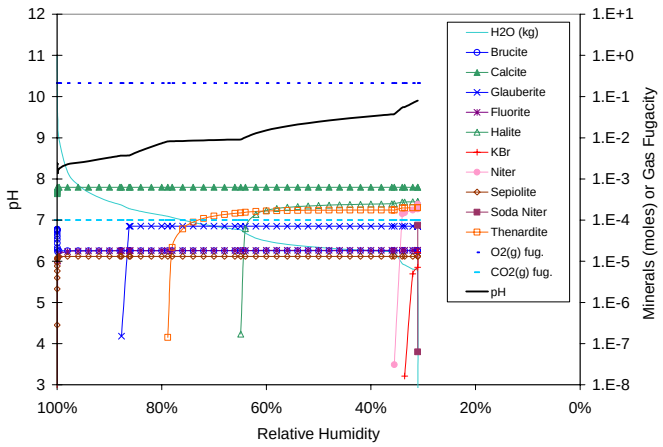

DTN: MO0310SPADLHTL.000\d5c4t12.xls

Figure III-05-28. Bin 05 Mineral Precipitation Evaporation Predictions vs. Relative Humidity at 120ºC and 10^{-4} CO_2 Fugacity

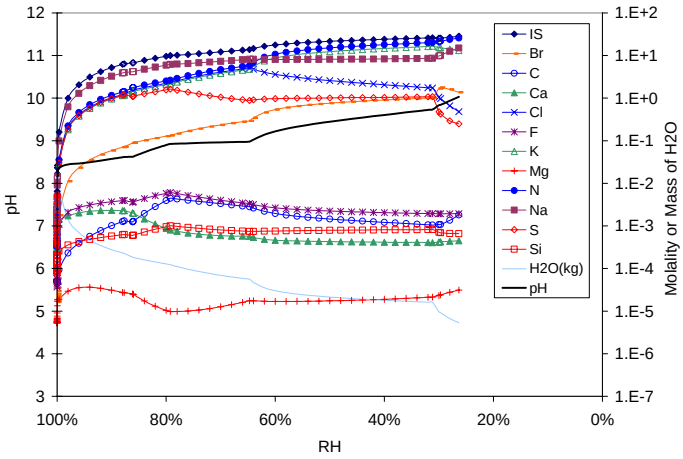

DTN: MO0310SPADLHTL.000\d5c4t14.xls

Figure III-05-29. Bin 05 Aqueous Composition Evaporation Predictions vs. Relative Humidity at 140ºC and 10^{-4} CO_2 Fugacity

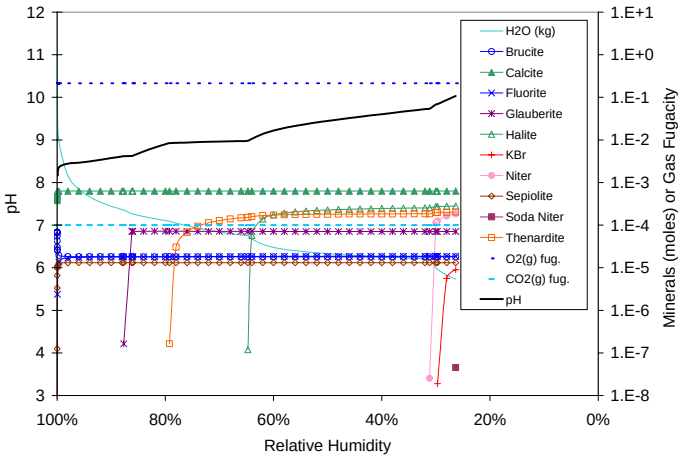

DTN: MO0310SPADLHTL.000\d5c4t14.xls

Figure III-05-30. Bin 05 Mineral Precipitation Evaporation Predictions vs. Relative Humidity at 140ºC and 10^{-4} CO_2 Fugacity

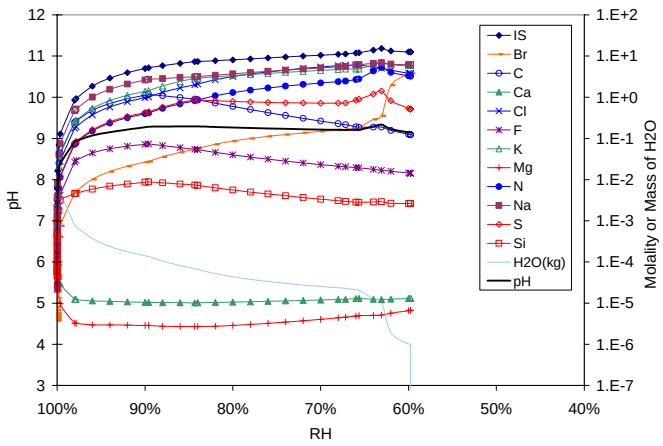

DTN: MO0310SPADLALT.001\d6c2t04.xls

Figure III-06-1. Bin 06 Aqueous Composition Evaporation Predictions vs. Relative Humidity at 40ºC and 10^{-2} CO_2 Fugacity

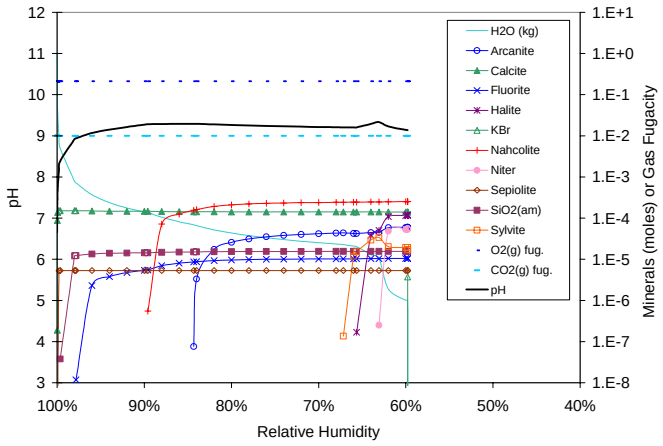

DTN: MO0310SPADLALT.001\d6c2t04.xls

Figure III-06-2. Bin 06 Mineral Precipitation Evaporation Predictions vs. Relative Humidity at 40ºC and 10^{-2} CO_2 Fugacity

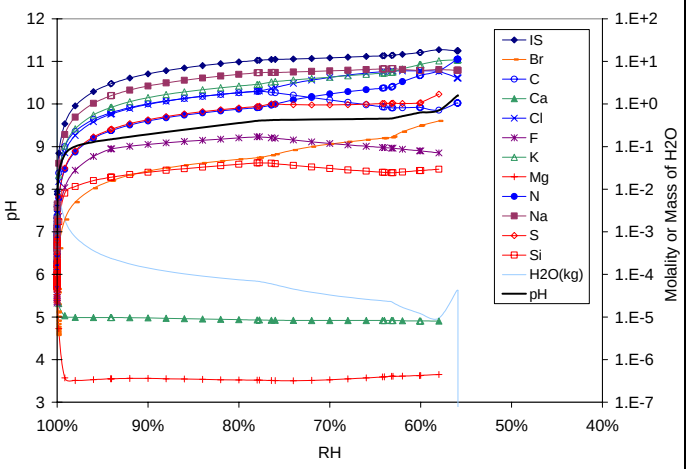

DTN: MO0310SPADLALT.001\d6c2t07.xls

Figure III-06-3. Bin 06 Aqueous Composition Evaporation Predictions vs. Relative Humidity at 70ºC and 10^{-2} CO_2 Fugacity

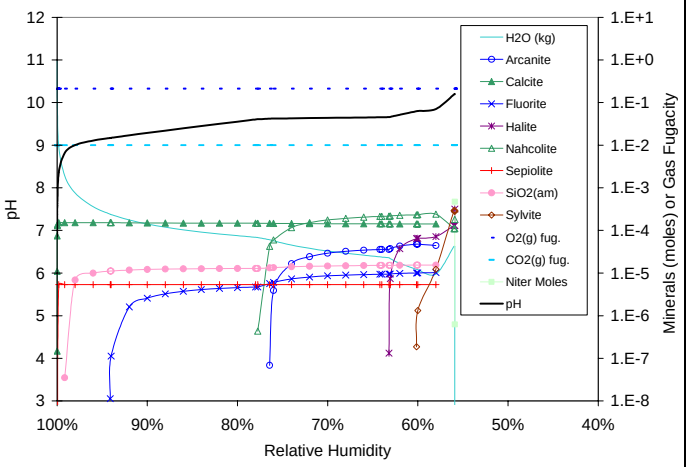

DTN: MO0310SPADLALT.001\d6c2t07.xls

Figure III-06-4. Bin 06 Mineral Precipitation Evaporation Predictions vs. Relative Humidity at 70ºC and 10^{-2} CO_2 Fugacity

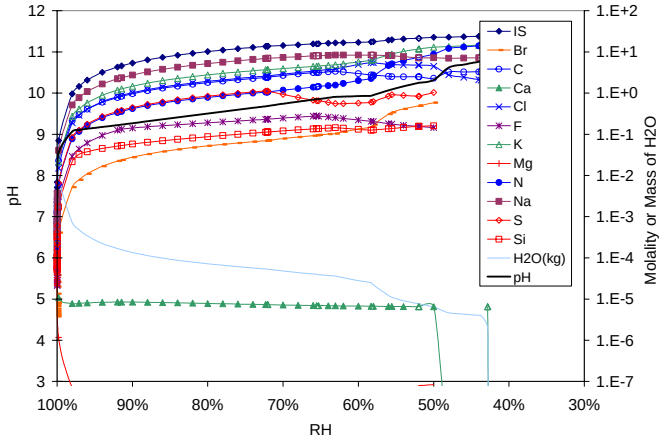

DTN: MO0310SPADLALT.001\d6c2t10.xls

Figure III-06-5. Bin 06 Aqueous Composition Evaporation Predictions vs. Relative Humidity at 100ºC and 10^{-2} CO_2 Fugacity

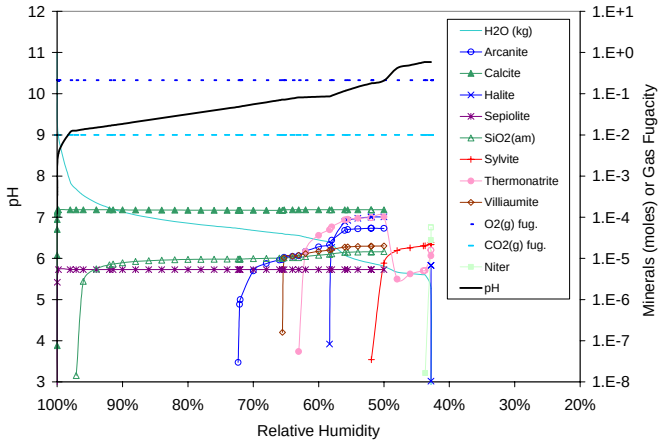

DTN: MO0310SPADLALT.001\d6c2t10.xls

Figure III-06-6. Bin 06 Mineral Precipitation Evaporation Predictions vs. Relative Humidity at 100ºC and 10^{-2} CO_2 Fugacity

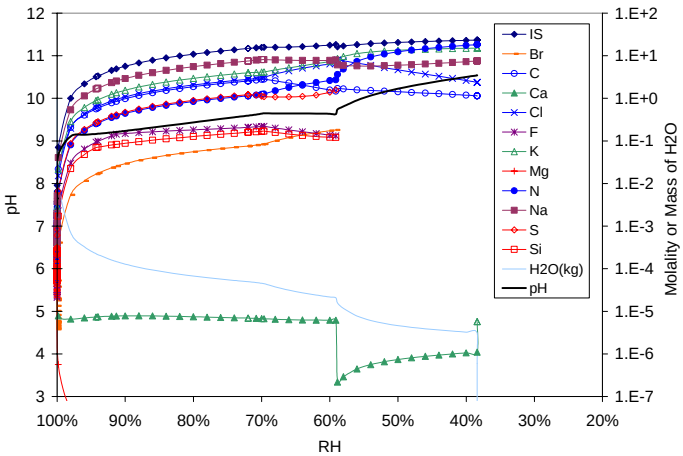

DTN: MO0310SPADLHTL.000\d6c2t12.xls

Figure III-06-7. Bin 06 Aqueous Composition Evaporation Predictions vs. Relative Humidity at 120ºC and 10^{-2} CO_2 Fugacity

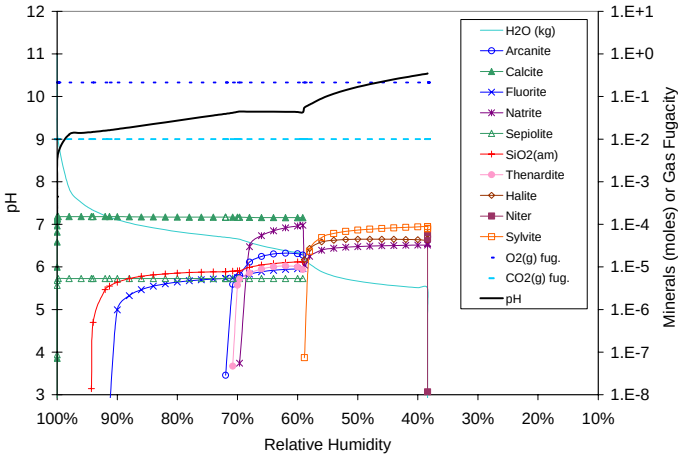

DTN: MO0310SPADLHTL.000\d6c2t12.xls

Figure III-06-8. Bin 06 Mineral Precipitation Evaporation Predictions vs. Relative Humidity at 120ºC and 10^{-2} CO_2 Fugacity

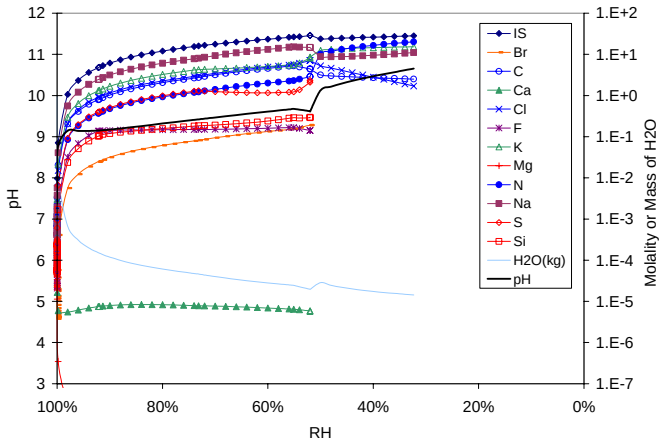

DTN: MO0310SPADLHTL.000\d6c2t14.xls

Figure III-06-9. Bin 06 Aqueous Composition Evaporation Predictions vs. Relative Humidity at 140ºC and 10^{-2} CO_2 Fugacity

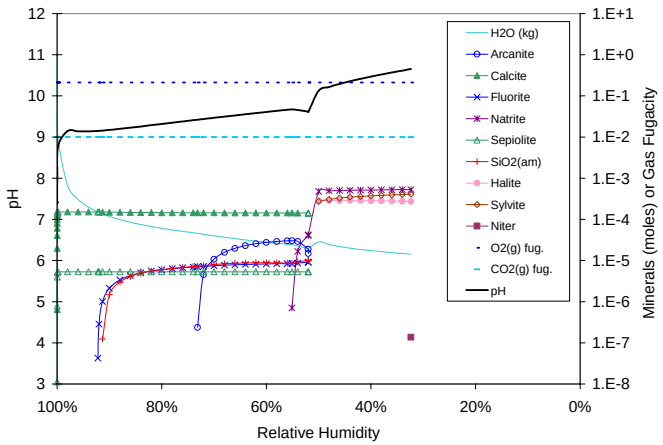

DTN: MO0310SPADLHTL.000\d6c2t14.xls

Figure III-06-10. Bin 06 Mineral Precipitation Evaporation Predictions vs. Relative Humidity at 140ºC and 10^{-2} CO_2 Fugacity

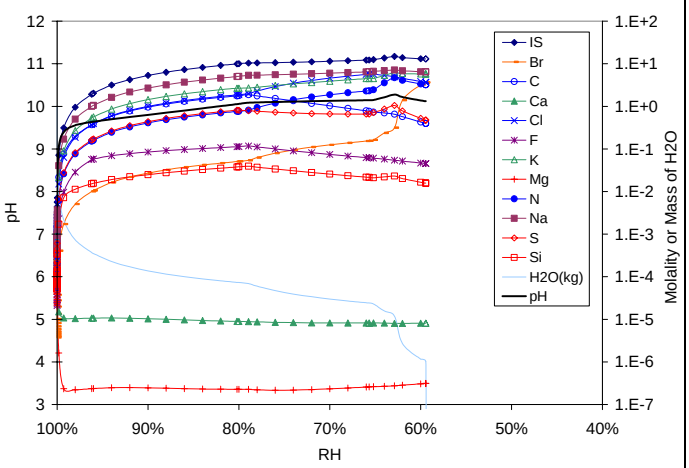

DTN: MO0310SPADLALT.001\d6c3t04.xls

Figure III-06-11. Bin 06 Aqueous Composition Evaporation Predictions vs. Relative Humidity at 40ºC and 10^{-3} CO_2 Fugacity

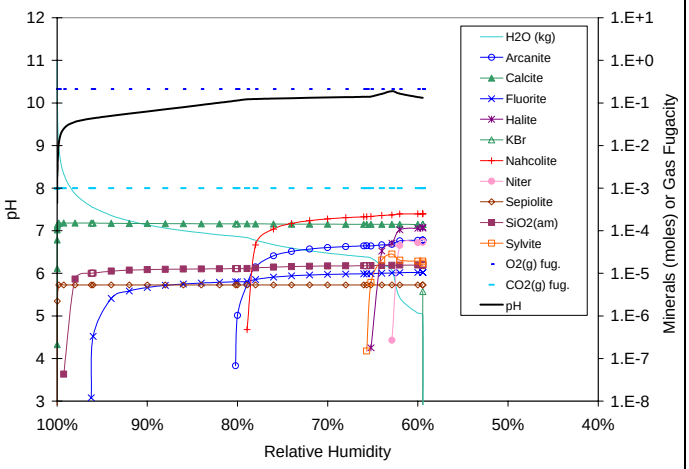

DTN: MO0310SPADLALT.001\d6c3t04.xls

Figure III-06-12. Bin 06 Mineral Precipitation Evaporation Predictions vs. Relative Humidity at 40ºC and 10^{-3} CO_2 Fugacity

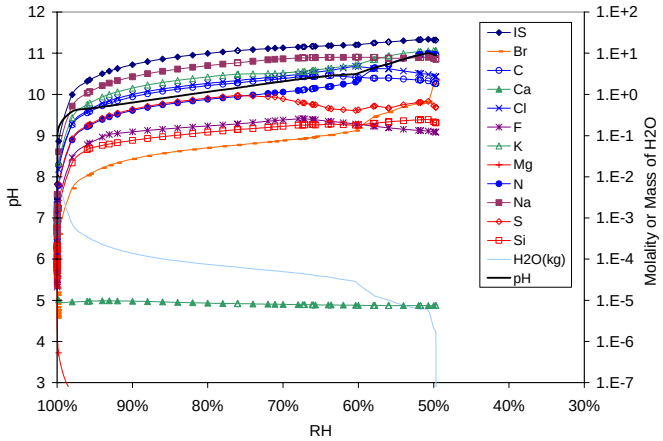

DTN: MO0310SPADLALT.001\d6c3t07.xls

Figure III-06-13. Bin 06 Aqueous Composition Evaporation Predictions vs. Relative Humidity at 70ºC and 10^{-3} CO_2 Fugacity

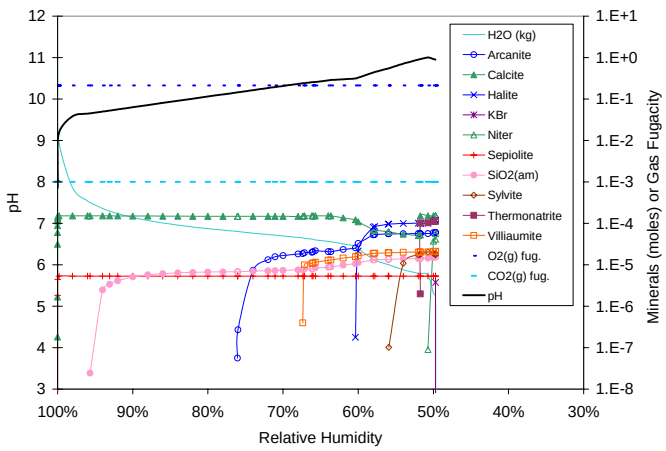

DTN: MO0310SPADLALT.001\d6c3t07.xls

Figure III-06-14. Bin 06 Mineral Precipitation Evaporation Predictions vs. Relative Humidity at 70ºC and 10^{-3} CO_2 Fugacity

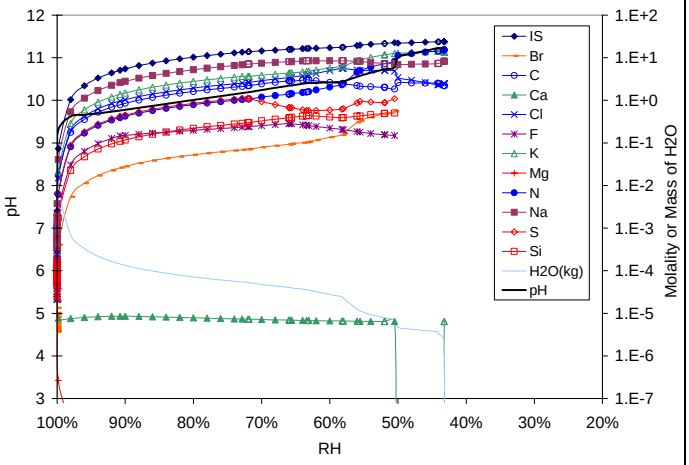

DTN: MO0310SPADLALT.001\d6c3t10.xls

Figure III-06-15. Bin 06 Aqueous Composition Evaporation Predictions vs. Relative Humidity at 100ºC and 10^{-3} CO_2 Fugacity

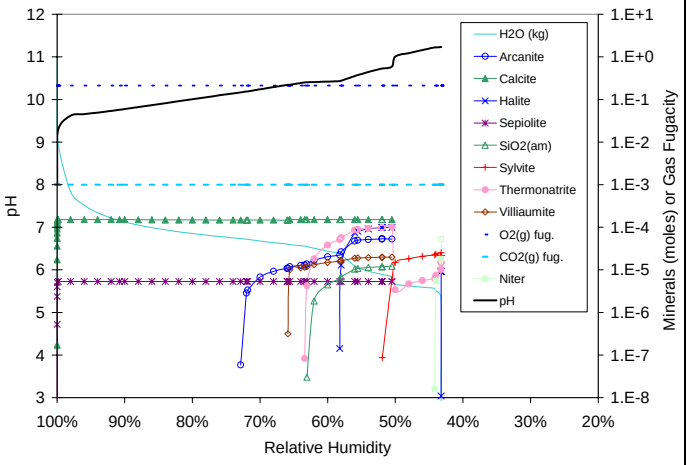

DTN: MO0310SPADLALT.001\d6c3t10.xls

Figure III-06-16. Bin 06 Mineral Precipitation Evaporation Predictions vs. Relative Humidity at 100ºC and 10^{-3} CO_2 Fugacity

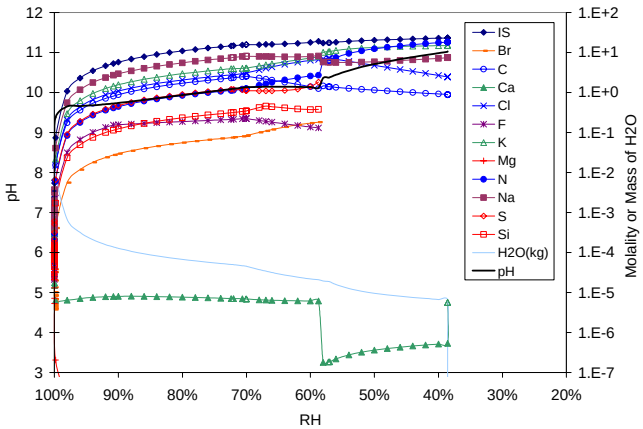

DTN: MO0310SPADLHTL.000\d6c3t12.xls

Figure III-06-17. Bin 06 Aqueous Composition Evaporation Predictions vs. Relative Humidity at 120ºC and 10^{-3} CO_2 Fugacity

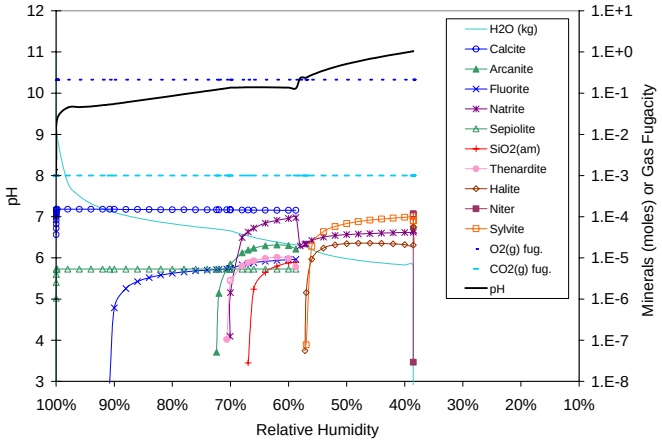

DTN: MO0310SPADLHTL.000\d6c3t12.xls

Figure III-06-18. Bin 06 Mineral Precipitation Evaporation Predictions vs. Relative Humidity at 120ºC and 10^{-3} CO_2 Fugacity

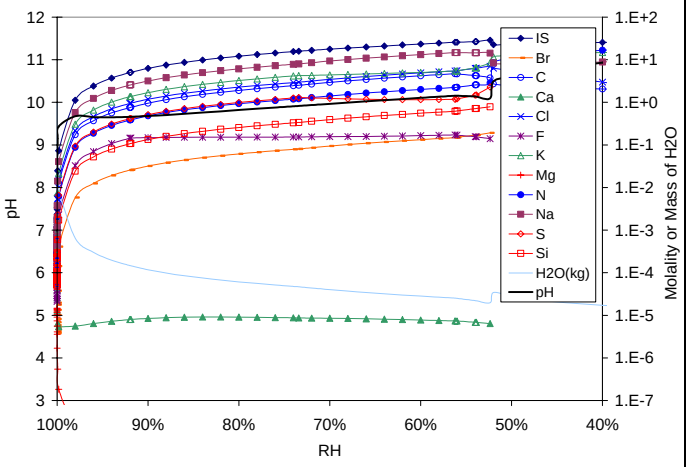

DTN: MO0310SPADLHTL.000\d6c3t14.xls

Figure III-06-19. Bin 06 Aqueous Composition Evaporation Predictions vs. Relative Humidity at 140ºC and 10^{-3} CO_2 Fugacity

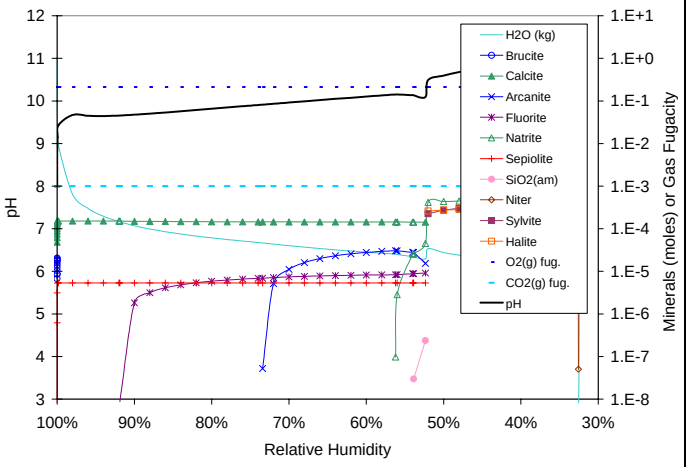

DTN: MO0310SPADLHTL.000\d6c3t14.xls

Figure III-06-20. Bin 06 Mineral Precipitation Evaporation Predictions vs. Relative Humidity at 140ºC and 10^{-3} CO_2 Fugacity

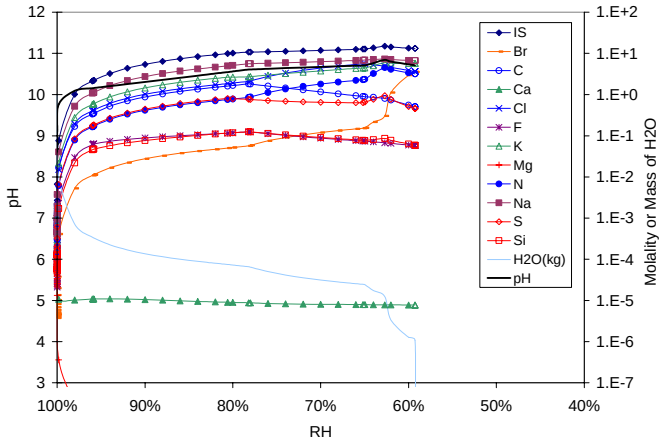

DTN: MO0310SPADLALT.001\d6c4t04.xls

Figure III-06-21. Bin 06 Aqueous Composition Evaporation Predictions vs. Relative Humidity at 40ºC and 10^{-4} CO_2 Fugacity

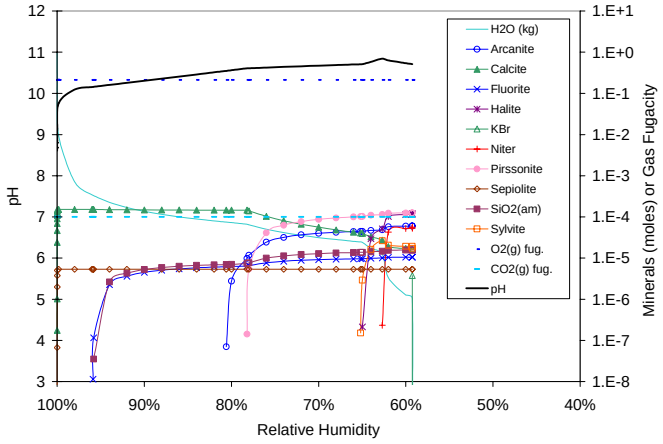

DTN: MO0310SPADLALT.001\d6c4t04.xls

Figure III-06-22. Bin 06 Mineral Precipitation Evaporation Predictions vs. Relative Humidity at 40ºC and 10^{-4} CO_2 Fugacity

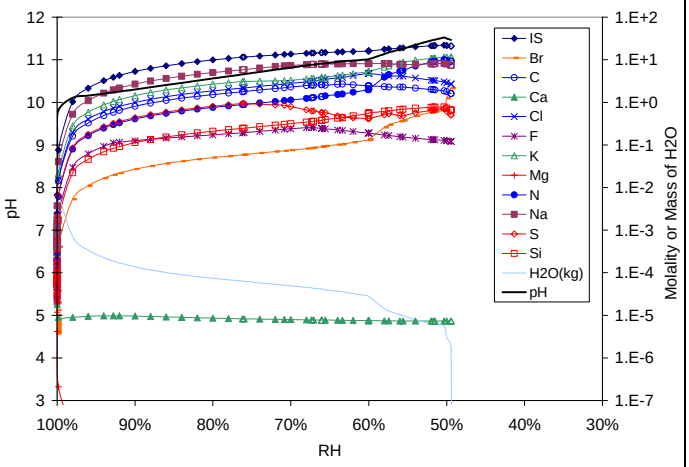

DTN: MO0310SPADLALT.001\d6c4t07.xls

Figure III-06-23. Bin 06 Aqueous Composition Evaporation Predictions vs. Relative Humidity at 70ºC and 10^{-4} CO_2 Fugacity

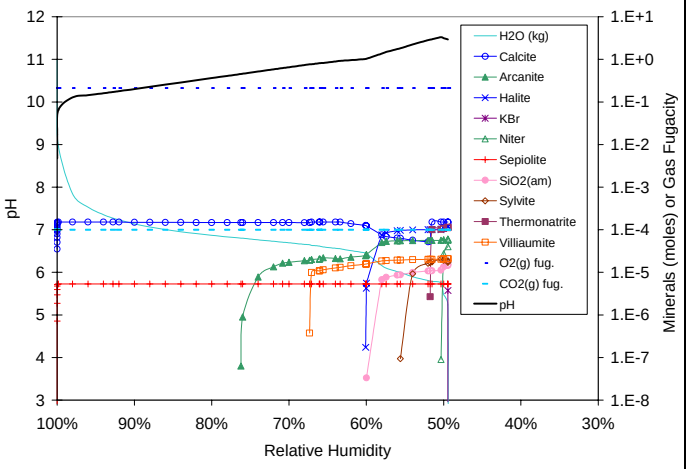

DTN: MO0310SPADLALT.001\d6c4t07.xls

Figure III-06-24. Bin 06 Mineral Precipitation Evaporation Predictions vs. Relative Humidity at 70ºC and 10^{-4} CO_2 Fugacity

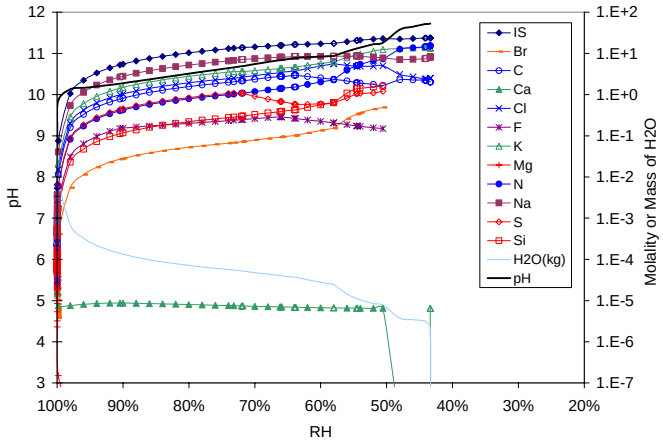

DTN: MO0310SPADLALT.001\d6c4t10xls

Figure III-06-25. Bin 06 Aqueous Composition Evaporation Predictions vs. Relative Humidity at 100ºC and 10^{-4} CO_2 Fugacity

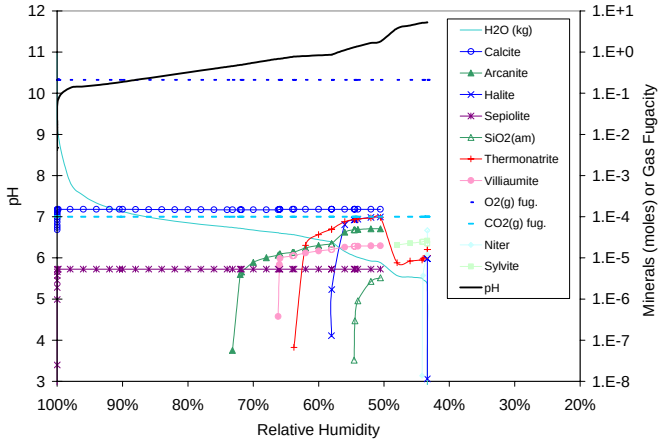

DTN: MO0310SPADLALT.001\d6c4t10.xls

Figure III-06-26. Bin 06 Mineral Precipitation Evaporation Predictions vs. Relative Humidity at 100ºC and 10^{-4} CO_2 Fugacity

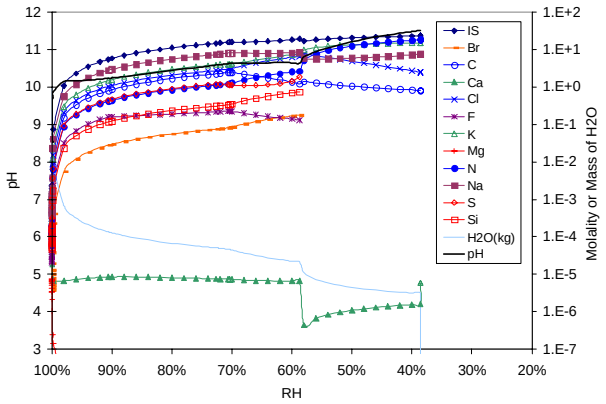

DTN: MO0310SPADLHTL.000\d6c4t12xls

Figure III-06-27. Bin 06 Aqueous Composition Evaporation Predictions vs. Relative Humidity at 120ºC and 10^{-4} CO_2 Fugacity

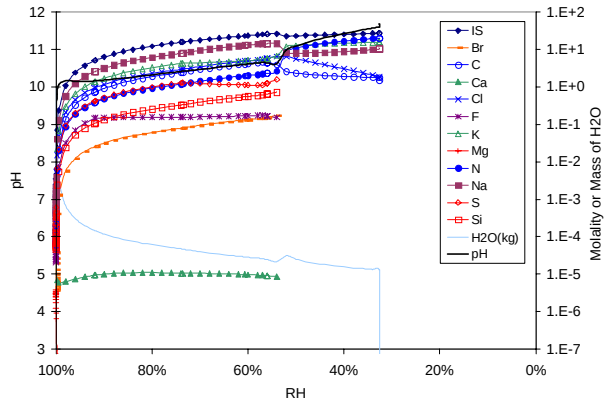

DTN: MO0310SPADLHTL.000\d6c4t14.xls

Figure III-06-29. Bin 06 Aqueous Composition Evaporation Predictions vs. Relative Humidity at 140ºC and 10^{-4} CO_2 Fugacity

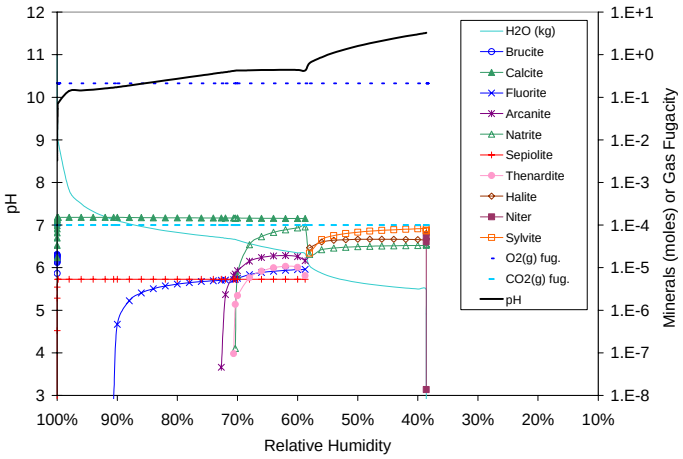

DTN: MO0310SPADLHTL.000\d6c4t12xls

Figure III-06-28. Bin 06 Mineral Precipitation Evaporation Predictions vs. Relative Humidity at 120ºC and 10^{-4} CO_2 Fugacity

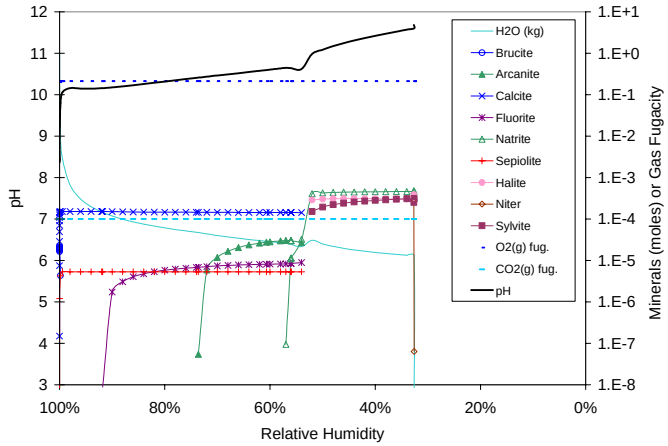

DTN: MO0310SPADLHTL.000\d6c4t14.xls

Figure III-06-30. Bin 06 Mineral Precipitation Evaporation Predictions vs. Relative Humidity at 140ºC and 10^{-4} CO_2 Fugacity

ATTACHMENT IV
CRITIQUE OF EXCLUDED MINERALS

ATTACHMENT IV
CRITIQUE OF EXCLUDED MINERALS

To evaluate as comprehensively as possible what solids need to be included in the database entries all minerals in Roberts, et al., *Encyclopedia of Minerals, 2nd Ed.* (1990 [DIRS 107105]), have been examined in respect to the anticipated physicochemical system. Table IV-1 provides the results of this evaluation. Minerals known to form only at temperatures outside the anticipated range of temperature for seepage to enter the drift, (0º to 100º C; see Section 6.2.2.5), are excluded from the table. Specifically, this means that, if the only occurrences noted in Roberts, et al., (1990 [DIRS 107105]) are for hydrothermal, metamorphic, or igneous conditions the mineral is not included in the table. Similarly, minerals that form only at elevated pressure are omitted. Limits have been placed on chemical conditions. Specifically, the minerals that contain Na, Mg, Al, Si, K, Ca, Mn, and Fe were included, if they did not also contain Li, Be, B, Sc, V, Cr, or elements heavier than Fe, and if they were not already included in data0.ymp.R2 or in data0.ypf. This excludes minerals that contain ferroalloy metals other than iron. To the extent that they will occur in the repository, they are included in analyses and models of metal corrosion and need not be included here. Similarly, the various elements of concern in respect to radioactivity are considered separately. The scope of the chemical range for minerals included in Table IV-1 does not include: reducing conditions; the oxidizing zone of ore deposits (especially sulfide ore bodies); those minerals that formed within the range, 0º to 100º C, that form only as weathering products on basic and ultrabasic rocks, pegmatites, or metamorphic rocks; environments in which the rocks consist largely or dominantly of iron, manganese, or phosphate minerals; meteorites; deep sea minerals; or minerals that are known to form, by alteration or epitaxial growth, only on preexisting minerals that are unexpected to be present or to form in the repository (often in Table IV-1 the comment "precursor absent" is used to designate this situation). As noted above, training in mineralogy and petrology is required in making these evaluations. For the purposes of Table IV-1, metamorphic rocks include those formed by regional metamorphism, contact metamorphism, and metasomatism. Serpentine is considered metamorphic rather than igneous. Pegmatites are considered igneous, and in many cases minerals formed by alteration of pegmatite minerals are, also; it is often not clear whether these minerals formed during late stage hydrothermal alteration or by weathering.

Many igneous and metamorphic minerals vary in chemical composition and include varieties that are unusually rich in Fe, Mn, Mg, or Na. The occurrences of these enriched minerals have been examined and generally excluded from the listing in Table IV-1 because their conditions of formation were either essentially the same as for the corresponding non-enriched varieties or would be excluded on other bases. Thus, most minerals beginning with the prefixes, ferri-, ferro-magnesio-, magnesium- mangan-, natro-, and sodium-, were not included. In similar fashion, minerals that differ only slightly, e.g., in amount of water of hydration, or small differences in structure, prefixes meta-, ortho-, and para-, were excluded. Minerals identified as consisting of interstratified sheet silicates with intercalated layers characteristic of different minerals, have been excluded as well as a few inadequately described rare minerals.

Except for the exclusions noted above, all minerals listed in Roberts et al. (1990 [DIRS 107105]), are included in Table IV-1.

The criteria used to construct Table IV-1 resemble those given for suppression of minerals in Section 6.5.4, but some either differ slightly or are not used. They are:

Criterion 1. The conditions for formation of the mineral lie outside the defined physicochemical system.

Criterion 2. There is evidence that the precipitation of the mineral in nature is likely slow within the defined temperature range. For example, authigenic minerals, which typically form very slowly, fall in this category.

Criterion 3. Another mineral with the same, or nearly the same, chemical composition is in one of the databases, e.g., one with a difference only in the degree of hydration.

Criterion 4. The mineral is not needed to test uncertainty or sensitivity. Not evaluated.

Criterion 5. Exclusion of the mineral does not make the model less conservative. Used only for rare minerals.

Criterion 6. Other minerals that are in a database provide an adequate surrogate or proxy for the mineral.

This criterion is used globally for those lacustrine borate evaporate minerals not included in data0.ymp.R2. A large number of minerals containing boron occur in lacustrine evaporites. If those that also contain Al, As, Be, Ce, Cu, Cs, Fe, La, Mn, Nb, NH4, Ni, Si, Sn, or Sr are excluded, because all are expected to have very low concentrations in solution either due to their rarity or their insolubility, the only remaining cations in these borate minerals are Ca, Na, and Mg. Some of these minerals also contain carbonate, chloride, sulfate, or phosphate. Consequently, the minerals, borax, colemanite, hydroboracite, calcite, gypsum, apatite, and halite, that are incorporated into data0.ymp.R2, include all the elements in any of the borate minerals that might reasonably be expected to form as a consequence of evaporation of water in the repository. Because these minerals (and others in the data base, including boehmite, for Al, SiO2(am) for Si, goethite for Fe) in one proportion or another encompass the anticipated compositional range in respect to boron, there is no need to include the approximately 85 additional borate minerals in the database and they are not further evaluated in Table IV-1.

The first column in Table IV-1 gives the mineral name, and the second the corresponding chemical formula. The third states whether the mineral is known to form in nature within the temperature range, 0º to 100º C. The fourth uniformly states that these minerals are not needed for the geochemical models on the basis of the criteria in column 5 and comments in column 7. Column 6 provides a more general evaluation of whether or not the mineral is known to, or may, form within both the chemical and physical scopes applicable to the repository. So long as a suitable surrogate is available within the databases in the form or one or more minerals, a yes in this column does not mean that the mineral must be a database. In all cases, such surrogates appear adequate.

For those minerals whose conditions for formation lie within the physicochemical system for the repository, but are not in a database, one or more minerals is listed or referred to by category, in the comments section for that mineral. These minerals are in data0.ymp.R2 or data0.ypf, include

all or most of the elements in the mineral, and tend to precipitate under conditions resembling those for formation of the mineral in question. These lists are not intended to be comprehensive, but merely to show that minerals of the same general nature are in at least one of the databases. During geochemical modeling a combination of these minerals, possibly including others not listed, that corresponds approximately to the composition of the mineral may precipitate. If instead the mineral should have precipitated, the modeled result will leave more of at least some of the elements involved in solution than would be the case, if the mineral itself precipitated. Because the concentrations would be higher, the modeled results are more conservative. In any event, the evolution of the water chemistry would be similar because the amounts and proportions of precipitated components would largely correspond.

The principal reference for all entries is Roberts, et al. (1990 [DIRS 107105]). In addition Stumm, W., and Morgan, J. J., *Aquatic Chemistry, An Introduction Emphasizing Chemical Equilibria in Natural Waters, 2nd Edition,* (1981 [DIRS 100829], pp. 284-285) used for the mineral, carbonate-apatite.

Table IV-1 Critique of Minerals not Included in Project Databases

Mineral	Chemical Formula	Precipitates from 0-100ºC and at 1 ATM	Needed	Criterion	Within Defined Physico-chemical System	Comments on Occurrence or Formation
actinolite	$Ca_2(Mg,Fe^{+2})_5Si_8O_{22}(OH)_2$	No	No	1	No	Metamorphic mineral
aegirine(Acmite)	$NaFe^{+3}Si_2O_6$	Yes	No	2	Yes	Igneous, metamorphic & authigenic mineral. Not needed because authigenic minerals form very slowly.
aenigmatite	$Na_2Fe_5TiSi_6O_{20}$	No	No	1	No	Igneous mineral
afghanite	$(Na,Ca,K)_8(Si,Al)_{12}O_{24}(Cl,SO_4,CO_3)_{3-4}\cdot H_2O$	No	No	1	No	Igneous mineral
afwillite	$Ca_3Si_2O_4(OH)_6$	No	No	1	No	Igneous or metamorphic mineral
agrellite	$NaCa_2Si_4O_{10}F$	No	No	1	No	Metamorphic mineral
akaganéite	β-FeO(OH,Cl)	?	No	6	Yes	Other FeOOH minerals suffice for conservatism
akatoreite	$Mn_9(Si,Al)_{10}O_{23}(OH)_9$	No	No	1	No	Metamorphic mineral
akdalaite	$4Al_2O_3\cdot H_2O$	No	No	1	No	Hydrothermal & metasomatic
aldermanite	$Mg_5Al_{12}(PO_4)_8(OH)_{22}\cdot 32H_2O$	Yes?	No	1	No	Associated with phosphate deposits
alleghanyite	$Mn_5Si_2O_8(OH)_2$	No	No	1	No	Metamorphic mineral, occurs in Mn deposits
allophane	$Al_2SiO_5\cdot nH_2O$	No	No	1	No	Hydrothermal mineral & in coal
alluaudite	$(Na,Ca)Fe^{+2}(Mn,Fe^{+2},Fe^{+3},Mg)_2(PO_4)_3$	No	No	1	No	Igneous mineral
almandine	$Fe^{+2}{}_3Al_2(SiO_4)_3$	No	No	1	No	Igneous & metamorphic mineral
alstonite	$CaBa(CO_3)_2$	No	No	1	No	Hydrothermal mineral
althausite	$Mg_2(PO_4)(OH,F,O)$	No	No	1	No	Igneous or hydrothermal mineral
aluminite	$Al_2(SO_4)(OH)_4\cdot 7H_2O$	Yes	No	5	Possibly	Rare, in limestone. Other minerals, e.g. alum-K, gypsum, boehmite, provide adequate conservatism for elements in this mineral

Table IV-1 Critique of Minerals not Included in Project Databases (Continued)

Mineral	Chemical Formula	Precipitates from 0-100ºC and at 1 ATM	Needed	Criterion	Within Defined Physico-chemical System	Comments on Occurrence or Formation
aluminocopiapite	$AlFe^{+3}{}_4(SO_4)_6O(OH)\cdot 20H_2O$	Yes	No	5	Possibly	Rare,Other minerals, e.g., ettringite, jarosite, provide adequate conservatism for elements in this mineral
alumohydrocalcite	$CaAl_2(CO_3)_2(OH)_4\cdot 3H_2O$	Yes	No	5	No	Rare, alteration of allophane, precursor absent. Other solids, e.g., cement phases hemi- & mono carboaluminate in data0.ypf, as well as boehmite & calcite, provide adequate conservatism for elements in this mineral.
alunogen	$Al_2(SO_4)_3\cdot 17H_2O$	Yes	No	1	No	Uncommon in shale, slate, coal
amakinite	$(Fe^{+2},Mg)(OH)_2$	No?	No	5	No	Rare, in kimberlite
amarantite	$Fe^{+3}(SO_4)(OH)\cdot 3H_2O$	Yes	No	1	No	Forms in sulfide mines and dumps
amarillite	$NaFe^{+3}(SO_4)_2\cdot 6H_2O$	Yes	No	1	No	Forms in sulfide mines and dumps
amicite	$K_2Na_2Al_4Si_4O_{16}\cdot 5H_2O$	No	No	1	No	Igneous or hydrothermal mineral
ammoniojarosite	$(NH_4)Fe^{+3}{}_3(SO_4)_2(OH)_6$	?	No	1	No	Associated with geysers & hot springs, requires reducing conditions.
ammonioleucite	$(NH_4)AlSi_2O_6$	Yes?	No	1	No	Occurs in dolomitized schist, requires reducing conditions.
anapaite	$Ca_2Fe^{+2}(PO_4)_2\cdot 4H_2O$	?	No	1	No	Associated with phosphates, iron ore, clay, in pegmatite
andradite	$Ca_3Fe^{+3}{}_2(SiO_4)_3$	No	No	1	No	Igneous & metamorphic mineral
ankerite	$Ca(Fe^{+2},Mg)(CO_3)_2$	No	No	1	No	Hydrothermal mineral
anthophyllite	$(Mg,Fe^{+2})_7Si_8O_{22}(OH)_2$	No	No	1	No	Metamorphic mineral
antigorite	$(Mg,Fe^{+2})_3Si_2O_5(OH)_4$	No?	No	1	No	Associated with ultramafic rocks

Table IV-1 Critique of Minerals not Included in Project Databases (Continued)

Mineral	Chemical Formula	Precipitates from 0-100ºC and at 1 ATM	Needed	Criterion	Within Defined Physico-chemical System	Comments on Occurrence or Formation
apjohnite	$Mn^{+2}Al_2(SO_4)_4 \cdot 22H_2O$	Yes	No	5	No	Rare. Probably requires high Mn content in environment.
archerite	$(K,NH_4)H_2PO_4$	Yes	No	1	No	Requires reducing conditions
arctite	$Na_2Ca_4(PO_4)_3F$	No	No	1	No	Igneous mineral
ardealite	$Ca_2HPO_4SO_4 \cdot 4H_2O$	?	No	1	No	Occurs in phosphate rocks
arfvedsonite	$Na_3(Fe^{+2},Mg)_4Fe^{+3}Si_8O_{22}(OH)_2$	No	No	1	No	Igneous mineral
armalcolite	$(Mg,Fe^{+2})Ti_2O_5$	No	No	1	No	Igneous mineral and in meteorites
arrojadite	$KNa_4CaMn^{+2}{}_4Fe^{+2}{}_{10}Al(PO_4)_{12}(OH,F)_2$	No	No	1	No	Igneous mineral
astrophyllite	$(K,Na)_3(Fe,Mn)_7Ti_2Si_8O_{24}(O,OH)_7$	No	No	1	No	Igneous mineral
attakolite	$(Ca,Mn,Sr)_3Al_6(PO_4,SiO_4)_7 \cdot 3H_2O$	No?	No	1	No	Occurs in an iron mine
augelite	$Al_2(PO_4)(OH)_3$	No	No	1	No	Igneous & metamorphic mineral
augite	$(Ca,Na)(Mg,Fe,Al)(Si,Al)_2O_6$	No	No	1	No	Igneous & metamorphic mineral
babingtonite	$Ca_2Fe^{+2}Fe^{+3}Si_5O_{14}(OH)$	No?	No	1	No	Secondary mineral in cavities and fractures in igneous and metamorphic rocks
balangeroite	$(Mg,Fe^{+2},Fe^{+3},Mn^{+2})_{42}Si_{16}O_{54}(OH)_{40}$	No	No	1	No	Igneous or metamorphic mineral
bannisterite	$Ca(K,Na)(Mn,Fe^{+2})_{21}(Si,Al)_{32}O_{76}(OH)_{16} \cdot 12H_2O$	No	No	1	No	Metamorphic mineral
bararite	$(NH_4)_2SiF_6$	No	No	1	No	Fumarolic mineral
barbosalite	$Fe^{+2}Fe^{+3}{}_2(PO_4)_2(OH)_2$	No	No	1	No	Igneous mineral
barentsite	$Na_7AlH_2(CO_3)_4F_4$	No	No	1	No	Hydrothermal mineral
baricite	$(Mg,Fe^{+2})_3(PO_4)_2 \cdot 8H_2O$	?	No	1	No	Associated with iron formation
barrerite	$(Na,K,Ca)_2Al_2Si_7O_{18} \cdot 7H_2O$	?	No	5	?	Rare zeolite. Other zeolites provide adequate conservatism for elements in this mineral.

Table IV-1 Critique of Minerals not Included in Project Databases (Continued)

Mineral	Chemical Formula	Precipitates from 0-100ºC and at 1 ATM	Needed	Criterion	Within Defined Physico-chemical System	Comments on Occurrence or Formation
barringtonite	$MgCO_3 \cdot 2H_2O$ (?)	Yes	No	1	No	Alteration from basalt, precursor absent in repository.
bartonite	$K_3Fe_{10}S_{14}$	No	No	1	No	Requires reducing conditions
basaluminite	$Al_4SO_4(OH)_{10} \cdot 5H_2O$	Yes	No	1	No	Associated with coal, gypsum, siderite
bassanite	$CaSO_4 \cdot 0.5H_2O$	No	No	1	No	Igneous or fumarolic mineral
bayerite	$Al(OH)_3$	Yes	No	6	Yes	Gibbsite provides adequate substitute. Occurs with calcite, gypsum, portlandite
baylissite	$K_2Mg(CO_3) \cdot 4H_2O$	?	No	5	No?	Rare mineral. Other minerals, e.g., kalicinite, hydromagnesite, provide adequate conservatism for elements in this mineral.
bementite	$Mn_8Si_6O_{15}(OH)_{10}$	Yes?	No	1	No	Occurs in Mn ore deposits
beraunite	$Fe^{+2}Fe^{+3}{}_5(PO_4)_4(OH)_5 \cdot 4H_2O$	Yes	No	1	No	Alteration product in phosphatic rocks and of iron phosphate minerals
berlinite	$AlPO_4$	No?	No	1	No?	Associated with iron formation
bermanite	$Mn^{+2}Mn^{+3}{}_2(PO_4)_2(OH)_2 \cdot 4H_2O$	No	No	1	No	Igneous mineral
berthierine	$(Fe^{+2},Fe^{+3},Mg)_{2-3}(Si,Al)_2O_5(OH)_4$	Yes?	No	6	Possibly	Other Fe-Mg aluminosilicates provide adequate conservatism for elements in this mineral.
beusite	$(Mn,Fe,Ca,Mg)_3(PO_4)_2$	No	No	1	No	Igneous mineral
bicchulite	$Ca_2Al_2SiO_6(OH)_2$	No	No	1	No	Metamorphic mineral
bilinite	$Fe^{+2}Fe^{+3}{}_2(SO_4)_4 \cdot 22H_2O$	Yes	No	1	No	Alters from sulfides, absent in repository
biphosphammite	$(NH_4,K)H_2PO_4$	Yes	No	1	No	Occurs in bat guano
birnessite	$Na_4Mn_{14}O_{27} \cdot 9H_2O$	Yes	No	1	No	Probably requires high Mn content in environment. Other Mn minerals provide adequate conservatism for elements in

Table IV-1 Critique of Minerals not Included in Project Databases (Continued)

Mineral	Chemical Formula	Precipitates from 0-100ºC and at 1 ATM	Needed	Criterion	Within Defined Physico-chemical System	Comments on Occurrence or Formation
						this mineral.
bobfergusonite	$Na_2Mn_5Fe^{+3}Al(PO_4)_6$	No	No	1	No	Igneous mineral
bobierrite	$Mg_3(PO_4)_2 \cdot 8H_2O$	Yes	No	1	No	Rare, in guano, etc., also in pegmatite
bolivarite	$Al_2(PO_4)(OH)_3 \cdot 4\text{-}5H_2O$	Yes	No	1	No	Occurs in weathered phosphatic pegmatite, granite
bonshtedtite	$Na_3Fe(PO_4)(CO_3)$	No	No	1	No	Igneous or metamorphic mineral
borcarite	$Ca_4MgH_6(BO_3)_4(CO_3)_2$	No	No	1	No	Metamorphic mineral
borickite	$CaFe_3(PO_4)_2(OH)_{11} \cdot 3H_2O$	?	No	6	Unknown	Other minerals, e.g., apatite, goethite, provide adequate conservatism for elements in this mineral.
bostwickite	$CaMn^{+3}{}_6Si_3O_{16} \cdot 7H_2O$	No	No	1	No	Hydrothermal mineral
botryogen	$MgFe^{+3}(SO_4)_2(OH) \cdot 7H_2O$	?	No	1	No	Associated with oxidized sulfides
boussingaultite	$(NH_4)_2Mg(SO_4)_2 \cdot 6H_2O$	Yes?	No	1	No	Associated with hot springs, shale, coal
bradleyite	$Na_3Mg(PO_4)(CO_3)$	Yes	No	1	No	Found in oil shale
brammallite	$(Na,H_3O)(Al,Mg,Fe)_2(Si,Al)_4O_{10}[(OH)_2,H_2O]$	Yes?	No	1	No	Occurs in shale overlying coal
braunite	$Mn^{+2}Mn^{+3}{}_6SiO_{12}$	Yes	No	1	No	Occurs in Mn ore deposits
brazilianite	$NaAl_3(PO_4)_2(OH)_4$	No	No	1	No	Pegmatitic & hydrothermal mineral
bredigite	$(Ca,Ba)Ca_{13}Mg_2Si_8O_{32}$	No	No	1	No	Contact metamorphic mineral
brenkite	$Ca_2(CO_3)F_2$	?	No	6	?	Other minerals, e.g., calcite, fluorite, provide adequate conservatism for elements in this mineral.
brianite	$Na_2CaMg(PO_4)_2$	No	No	1	No	Found in a meteorite

Table IV-1 Critique of Minerals not Included in Project Databases (Continued)

Mineral	Chemical Formula	Precipitates from 0-100ºC and at 1 ATM	Needed	Criterion	Within Defined Physico-chemical System	Comments on Occurrence or Formation
brownmillerite	$Ca_2(Al,Fe)_2O_5$	No	No	1	No	Metamorphic mineral
brugnatellite	$Mg_6FeCO_3(OH)_{13}\cdot 4H_2O$	No	No	1	No	Hydrothermal mineral in serpentine; in igneous rock
buchwaldite	$NaCaPO_4$	No	No	1	No	Found in a meteorite
buddingtonite	$(NH_4)AlSi_3O_8\cdot 0.5H_2O$	No	No	1	No	Hydrothermal mineral, reducing condition
buergerite	$NaFe^{+3}{}_3Al_6Si_6B_3O_{30}F$	No	No	1	No	Igneous mineral
buetschliite	$K_2Ca(CO_3)_2$	No	No	1	No	Occurs as clinkers in wood ash
bultfonteinite	$Ca_2SiO_2(OH,F)_4$	?	No	1	No	Rare, metamorphic mineral
burangaite	$(Na,Ca)_2(Fe^{+2},Mg)_2Al_{10}(PO_4)_8(OH,O)_{12}\cdot 4H_2O$	No	No	1	No	Igneous mineral
bustamite	$(Ca,Mn)Si_2O_6$	No	No	1	No	Metamorphic mineral
butlerite	$Fe^{+3}SO_4(OH)\cdot 2H_2O$	?	No	1	No	Associated with oxidized sulfides
cacoxenite	$Fe^{+3}{}_4(PO_4)_3(OH)_3\cdot 12H_2O$	Yes	No	1	No	In phosphatic rocks
cadwaladerite	$Al(OH)_2Cl\cdot 4H_2O$	Yes?	No	6	Possibly	Occurs in a sulfate deposit. Other evaporite minerals and boehmite provide adequate conservatism for elements in this mineral.
cafetite	$Ca(Fe^{+3},Al)_2Ti_4O_{12}\cdot 4H_2O$	No	No	1	No	Igneous mineral
calciocopiapite	$CaFe_4(SO_4)_6(OH)_2\cdot 19H_2O$	Yes	No	1	No	Weathering product of pyritic magnetite
calcioferrite	$Ca_4Fe^{+2}(Fe^{+3},Al)_4(PO_4)_6(OH)_4\cdot 12H_2O$	Yes	No	1	No	Nodules in clay
calclacite	$CaC_2H_3ClO_2\cdot 5H_2O$	Yes	No	1	No	Occurs on pottery and museum specimens in oak cabinets
calderite	$(Mn^{+2},Ca)_3(Fe^{+3},Al)_2(SiO_4)_3$	?	No	1	?	A garnet, hence, likely metamorphic. Other minerals, e.g., wollastonite, fayalite, provide adequate conservatism for elements in this mineral.

Table IV-1 Critique of Minerals not Included in Project Databases (Continued)

Mineral	Chemical Formula	Precipitates from 0-100ºC and at 1 ATM	Needed	Criterion	Within Defined Physico-chemical System	Comments on Occurrence or Formation
canaphite	$CaNa_2H_2(PO_4)_2 \cdot 3H_2O$	?	No	5	?	Rare, on stilbite. Zeolites and apatite provide adequate conservatism for elements in this mineral.
canasite	$(Na,K)_6Ca_5Si_{12}O_{30}(OH,F)_4$	No	No	1	No	Igneous mineral
cancrinite	$Na_6Ca_2Al_6Si_6O_{24}(CO_3)_2$	No?	No	1	No	Igneous mineral or alteration of nepheline
carbonate-hydroxylapatite	$Ca_5(PO_4,CO_3)_3(OH,F)$	Yes	No	6	No?	Replacement of calcite, probably absent in repository. Other minerals, e.g., hydroxylapatite, calcite, provide adequate conservatism for elements in this mineral.
carletonite	$KNa_4Ca_4Si_8O_{18}(CO_3)_4(OH,F) \cdot H_2O$	No	No	1	No	Metamorphosed inclusions in igneous rock
carlhintzeite	$Ca_2AlF_7 \cdot H_2O$	No	No	1	No	Igneous mineral
carpholite	$MnAl_2Si_2O_6(OH)_4$	?	No	1	No	Probably requires high Mn content in environment.
caryopilite	$(Mn,Mg)_3Si_2O_5(OH)_4$	Yes?	No	1	No	Probably requires high Mn content in environment. Replacement of rhodonite, which is absent in the repository.
cebollite	$Ca_4Al_2Si_3O_{12}(OH)_2$	Yes?	No	1	No	Alters from melilite, precursor absent in repository. Also, igneous mineral.
cesanite	$Na_3Ca_2(SO_4)_3(OH)$	?	No	1	Possibly	Other minerals, e.g. glauberite, provide adequate conservatism for elements in this mineral.
chantalite	$CaAl_2SiO_4(OH)_4$	No	No	1	No	Igneous mineral
charoite	$K(Ca,Na)_2Si_4O_{10}(OH,F) \cdot H_2O$	No	No	1	No	Contact metamorphic mineral
chesterite	$(Mg,Fe^{+2})_{17}Si_{20}O_{54}(OH)_6$	No	No	1	No	Metamorphic mineral

Table IV-1 Critique of Minerals not Included in Project Databases (Continued)

Mineral	Chemical Formula	Precipitates from 0-100ºC and at 1 ATM	Needed	Criterion	Within Defined Physico-chemical System	Comments on Occurrence or Formation
childrenite	$(Fe,Mn)AlPO_4(OH)_2 \cdot H_2O$	No	No	1	No	Hydrothermal & igneous mineral
chiolite	$Na_5Al_3F_{14}$	No	No	1	No	Igneous mineral
chloraluminite	$AlCl_3 \cdot 6H_2O$	No	No	1	No	Igneous or fumarolic mineral
chlorapatite	$Ca_5(PO_4)_3Cl$	No	No	1	No	Igneous or metamorphic mineral
chloritoid	$(Fe^{+2},Mg,Mn)_2Al_4Si_2O_{10}(OH)_4$	No	No	1	No	Metamorphic & hydrothermal mineral
chlormagaluminite	$(Mg,Fe^{+2})_4Al_2(OH)_{12}(Cl_2,CO_3)_2 \cdot 2H_2O$	No	No	1	No	Metamorphic mineral
chlormanganokalite	K_4MnCl_6	No?	No	1	No	Fumarolic mineral and associated with halite, sylvite, and hematite.
chondrodite	$Mg_5(SiO_4)_2(F,OH)_2$	No	No	1	No	Metamorphic or igneous mineral
clairite	$(NH_4)_2Fe_3(SO_4)_4(OH)_3 \cdot 3H_2O$	Yes	No	1	No	Altered from pyrite under reducing conditions
clinohumite	$(Mg,Fe)_9(SiO_4)_4(F,OH)_2$	No	No	1	No	Metamorphic mineral
clinojimthompsonite	$(Mg,Fe^{+2})_5Si_6O_{16}(OH)_2$	No	No	1	No	Metamorphic mineral
clinophosinaite	$Na_3CaPSiO_7$	No	No	1	No	Igneous mineral
clinoungemachite	probably near $K_3Na_9Fe(SO_4)_6(OH)_3 \cdot 9H_2O$	Yes	No	1	No	Oxidation product at copper mine. Jarosite and natrojarosite provide adequate conservatism.
clintonite	$Ca(Mg,Al)_3(Al_3Si)O_{10}(OH)_2$	No	No	1	No	Metamorphic mineral
coalingite	$Mg_{10}Fe^{+3}{}_2(CO_3)(OH)_{24} \cdot 2H_2O$	Yes	No	1	No	Weathering product of serpentine, which is absent in repository.
coesite	SiO_2	No	No	1	No	In meteorite craters
collinsite	$Ca_2(Mg,Fe)(PO_4)_2 \cdot 2H_2O$	Yes?	No	5	No	Rare, associated with phosphate nodules or asphaltum, pegmatites
combeite	$Na_2Ca_2Si_3O_9$	No	No	1	No	Igneous mineral

Table IV-1 Critique of Minerals not Included in Project Databases (Continued)

Mineral	Chemical Formula	Precipitates from 0-100ºC and at 1 ATM	Needed	Criterion	Within Defined Physico-chemical System	Comments on Occurrence or Formation
copiapite	$(Fe^{+2},Mg)Fe^{+3}_4(SO_4)_6(OH)_2 \cdot 20H_2O$	Yes	No	1	No	Alters from sulfides, absent in repository
coquimbite	$Fe^{+3}_2(SO_4)_3 \cdot 9H_2O$	Yes	No	1	No	Alters from sulfides, absent in repository
cordierite	$(Mg,Fe^{+3})_2Al_4Si_5O_{18}$	No	No	1	No	Igneous & metamorphic mineral
cowlesite	$CaAl_2Si_3O_{10} \cdot 5\text{-}6H_2O$	Yes?	No	1	No	Associated with zeolites in basalt
crandallite	$CaAl_3(PO_4)(OH)_5 \cdot H_2O$	Yes	No	1	No	Associated with phosphate deposits
creedite	$Ca_3Al_2(SO_4)(F,OH)_{10} \cdot 2H_2O$	No	No	1	No	Hydrothermal mineral
crossite	$Na_2(Mg,Fe^{+2})_3(Al,Fe^{+3})_2Si_8O_{22}(OH)_2$	No	No	1	No	Metamorphic mineral
cryptohalite	$(NH_4)_2SiF_6$	No	No	1	No	Fumarolic mineral or sublimation product
cryptomelane	$K(Mn^{+2},Mn^{+4})_8O_{16}$	Yes	No	6	No	Other minerals,e.g., pyrolusite, provide adequate conservatism for elements in this mineral.
cummingtonite	$(Mg,Fe^{+2})_7Si_8O_{22}(OH)_2$	No	No	1	No	Metamorphic mineral
cuspidine	$Ca_4Si_2O_7(F,OH)_2$	No	No	1	No	Metamorphic mineral
cyrilovite	$NaFe^{+3}_3(PO_4)_2(OH)_4 \cdot 2H_2O$	Yes?	No	1	No	Alteration mineral in pegmatites, and in phosphate deposit.
dachiardite	$(Ca,Na_2,K_2)_5Al_{10}Si_{38}O_{96} \cdot 25H_2O$	No?	No	1	No	Found in pegmatites
dannemorite	$Mn_2(Fe^{+2},Mg)_5Si_8O_{22}(OH)_2$	No	No	1	No	Metamorphic or igneous mineral
d'Ansite	$Na_{21}Mg(SO_4)_{10}Cl_3$	Yes	No	6	Yes	Other minerals, e.g. bloedite, halite, provide adequate conservatism for elements in this mineral.
davanite	$K_2TiSi_6O_{15}$	No	No	1	No	Contact metamorphic mineral
davreuxite	$Mn_2Al_{12}(SiO_4)_7O_3(OH)_6$	?	No	1	No	Hydrothermal mineral

Table IV-1 Critique of Minerals not Included in Project Databases (Continued)

Mineral	Chemical Formula	Precipitates from 0-100ºC and at 1 ATM	Needed	Criterion	Within Defined Physico-chemical System	Comments on Occurrence or Formation
davyne	$(Na,Ca,K)_8Al_6Si_6O_{24}(Cl,SO_4,CO_3)_{2-3}$	No	No	1	No	Igneous mineral
deerite	$(Fe^{+2},Mn)_6(Fe^{+3},Al)_3Si_6O_{20}(OH)_5$	No	No	1	No	Metamorphic mineral
defernite	$Ca_6(CO_3)_2(OH,Cl)_8 \cdot nH_2O$	No	No	1	No	Contact metamorphic mineral
delhayelite	$(Na,K)_{10}Ca_5Al_6Si_{32}O_{80}(Cl_2,F_2,SO_4)_3 \cdot 18H_2O$	No	No	1	No	Igneous mineral
dellaite	$Ca_6Si_3O_{11}(OH)_2$	No	No	1	No	Hydrothermal mineral
delvauxite	$(Ca,Mg)(Fe^{+3},Al)_3(PO_4,SO_4,CO_3)_2(OH)_8 \cdot 4\text{-}6H_2O$	Yes?	No	6	Possibly	Other minerals, e.g., hydroxylapatite, strengite, provide adequate conservatism for elements in this mineral.
denisovite	$(K,Na)Ca_2Si_3O_8(F,OH)$	No	No	1	No	Igneous or metamorphic mineral
desautelsite	$Mg_6Mn^{+3}{}_2(CO_3)(OH)_{16} \cdot 4H_2O$	No?	No	6	No?	Other minerals, hydromagnesite, rhodochrosite, provide adequate conservatism for elements in this mineral.
despujolsite	$Ca_3Mn^{+4}(SO_4)_2(OH)_6 \cdot 3H_2O$	Yes?	No	1	No	Associated only with other Mn minerals
diadochite	$Fe^{+3}{}_9(PO_4)(SO_4)(OH) \cdot 5H_2O$	Yes	No	1	No	Associated with (sulfide?) mine workings
dickite	$Al_2Si_2O_5(OH)_4$	No?	No	3	No	Hydrothermal mineral; properties close to kaolinite, which provides adequate conservatism for this mineral.
dittmarite	$(NH_4)Mg(PO_4) \cdot H_2O$	Yes	No	1	No	Occurs in guano, etc.
donpeacorite	$(Mn,Mg)MgSi_2O_6$	No	No	1	No	Metamorphic mineral
dorfmanite	$Na_2H(PO_4) \cdot 2H_2O$	Yes	No	1	No	Alteration mineral in akalic pegmatite
douglasite	$K_2Fe^{+2}Cl_4 \cdot 2H_2O$	Yes?	No	1	No	Occurs in marine evaporites; ferous iron requires reducing conditions
doyleite	$Al(OH)_3$	No	No	1	No	Igneous (& metamorphic?)

Table IV-1 Critique of Minerals not Included in Project Databases (Continued)

Mineral	Chemical Formula	Precipitates from 0-100ºC and at 1 ATM	Needed	Criterion	Within Defined Physico-chemical System	Comments on Occurrence or Formation
						mineral
dufrenite	$Fe^{+2}Fe^{+3}{}_4(PO_4)_3(OH)_5 \cdot 2H_2O$	Yes?	No	1	No	Associated with pegmatites & phosphate deposits
dypingite	$Mg_5(CO_3)_4(OH)_2 \cdot 5H_2O$	Yes?	No	1	No	Metamorphic mineral (& on serpentine)
earlandite	$Ca_3(C_6H_5O_7)_2 \cdot 4H_2O$	Yes	No	1	No	In oceanic bottom sediments, Antarctica
earlshannonite	$MnFe^{+3}{}_2(PO_4)_2(OH)_2 \cdot 4H_2O$	No	No	1	No	Igneous mineral
eckermannite	$Na_3(Mg,Fe^{+2})_4(Al,Fe^{+3})Si_8O_{22}(OH)_2$	No	No	1	No	Igneous mineral
edenite	$NaCa_2(Mg,Fe^{+2})_5Si_7AlO_{22}(OH)_2$	No	No	1	No	Igneous and metamorphic mineral
eggletonite	$(Na,K,Ca)_2(Mn,Fe)_8(Si,Al)_{12}O_{29}(OH)_7 \cdot 11H_2O$	No	No	1	No	Occurs in cavities in igneous rock
eifelite	$KNa_3Mg_4Si_{12}O_{30}$	No	No	1	No	Metamorphic mineral
eitelite	$Na_2Mg(CO_3)_2$	Yes?	No	6	Yes	Associated with lacustrine evaporites. Other minerals, e.g., natron, hydromagnesite, provide adequate conservatism for elements in this mineral.
elpasolite	K_2NaAlF_6	No	No	1	No	Igneous mineral
endellite	$Al_2Si_2O_5(OH)_4 \cdot 2H_2O$	Yes?	No	3	No	Resembles kaolinite, which suffices for conservatism.
englishite	$K_3Na_2Ca_{10}Al_{15}(PO_4)_{21}(OH)_7 \cdot 26H_2O$	Yes?	No	1	No	Igneous or in phosphate deposits
eosphorite	$(Mn,Fe)Al(PO_4)(OH)_2 \cdot H_2O$	No	No	1	No	Igneous mineral
epistilbite	$CaAl_2Si_6O_{16} \cdot 5H_2O$	No?	No	1	No	Cavities in basalt; in pegmatites
erdite	$NaFeS_2 \cdot 2H_2O$	No	No	1	No	Igneous or hydrothermal mineral
ernstite	$(Mn_{1-x}Fe_x)Al(PO_4)(OH)_{2-x}O_x$	Yes	No	1	No	Alters from eosphorite, precursor absent
ertixiite	$Na_2Si_4O_9$	No	No	1	No	Igneous mineral

Table IV-1 Critique of Minerals not Included in Project Databases (Continued)

Mineral	Chemical Formula	Precipitates from 0-100ºC and at 1 ATM	Needed	Criterion	Within Defined Physico-chemical System	Comments on Occurrence or Formation
erythrosiderite	$K_2Fe^{+3}Cl_5 \cdot H_2O$	Yes	No	6	No	Efflorescence on marine evaporites. Other minerals, e.g., sylvite, molysite, provide adequate conservatism for elements in this mineral.
essenite	$CaFe^{+3}AlSiO_6$	No	No	1	No	Occurs in fused sedimentary rock
eugsterite	$Na_4Ca(SO_4)_3 \cdot 2H_2O$	Yes	No	6	Yes	Occurs in lacustrine evaporites. Other minerals, e.g., glauberite, provide adequate conservatism for elements in this mineral.
evansite	$Al_3(PO_4)(OH)_6 \cdot 6H_2O$ (?)	Yes	No	1	No	In Al and phosphate rich settings
fairchildite	$K_2Ca(CO_3)_2$	No	No	1	No	In clinkers in wood ash
fairfieldite	$Ca_2(Mn^{+2},Fe^{+2})(PO_4)_2 \cdot 2H_2O$	No	No	1	No	Igneous mineral
farringtonite	$Mg_3(PO_4)_2$	No	No	1	No	In a meteorite
faujasite	$(Na_2,Ca)Al_2Si_4O_{12} \cdot 8H_2O$	No?	No	1	No	Associated with augite and other zeolites
fedorite	$(K,Na)_2(Ca,Na)_7Si_{16}O_{38}(OH,F)_2 \cdot H_2O$	No	No	1	No	Metasomatic mineral
feitknechtite	β-MnO(OH)	Yes	No	1	No	Alters from pyrochroite, precursor absent
felsöbanyaite	$Al_4(SO_4)(OH)_{10} \cdot 5H_2O$	No	No	1	No	Hydrothermal mineral
fenaksite	$(K,Na,Ca)_4(Fe^{+2},Fe^{+3},Mn)_2Si_8O_{20}(OH,F)$	No	No	1	No	Igneous mineral
ferdisilicite	$FeSi_2$	No	No	1	No	Found in amphibolite & placers
feroxyhyte	δ-$Fe^{+3}O(OH)$	Yes	No	1	No	Occurs in Fe-Mn deep sea nodules
ferrierite	$(Na,K)_2MgAl_3Si_{15}O_{36}(OH) \cdot 9H_2O$	No?	No	1	No	Associated with andesites & basalt
ferrihydrite	$5Fe^{+3}{}_2O_3 \cdot 9H_2O$	Yes	No	1	Possibly	Goethite and $Fe(OH)_3$ provide adequate conservatism for this mineral.

Table IV-1 Critique of Minerals not Included in Project Databases (Continued)

Mineral	Chemical Formula	Precipitates from 0-100ºC and at 1 ATM	Needed	Criterion	Within Defined Physico-chemical System	Comments on Occurrence or Formation
ferrinatrite	$Na_3Fe^{+3}(SO_4)_3 \cdot 3H_2O$	Yes	No	6	Possibly	With other sulfates in Atacama desert & in furmaroles. Other minerals, e.g., natrojarosite, provide adequate conservatism for elements in this mineral.
ferrohexahydrite	$Fe^{+2}SO_4 \cdot 6H_2O$	Yes	No	6	No	Alters from melanterite, which, while unlikely to occur in the repository, provides adequate conservatism. Also a fumarolic mineral.
ferrohornblende	$Ca_2(Fe^{+2},Mg)_4Al(Si_7Al)O_{22}(OH,F)_2$	No	No	1	No	Igneous & metamorphic mineral
fersilicite	FeSi	No	No	1	No	Found in amphibolite & placers
fibroferrite	$Fe^{+3}(SO_4)(OH) \cdot 5H_2O$	Yes	No	1	No	Alters from sulfides, absent in repository
fillowite	$Na_2Ca(Mn,Fe^{+2})_7(PO_4)_6$	No	No	1	No	Igneous mineral
fluellite	$Al_2(PO_4)F_2(OH) \cdot 7H_2O$	No	No	1	No	Igneous and, possibly, hydrothermal mineral
fluorapophyllite	$KCa_4Si_8O_{20}(F,OH) \cdot 8H_2O$	No	No	1	No?	Associated with basalts or low-temperature hydrothermal deposits.
fluorellestadite	$Ca_5(SiO_4,PO_4,SO_4)_3(F,OH,Cl)$	No	No	1	No	Contact metamorphic mineral
foggite	$CaAl(PO_4)(OH)_2 \cdot H_2O$	No	No	1	No	Igneous mineral
foshagite	$Ca_4Si_3O_9(OH)_2$	No	No	1	No	Hydrothermal mineral
foshallasite	$Ca_3Si_2O_7 \cdot 3H_2O$ (?)	No	No	1	No	Hydrothermal mineral
francoanellite	$H_6(K,Na)_3(Al,Fe^{+3})_5(PO_4)_8 \cdot 13H_2O$	Yes	No	1	No	Associated with bat guano
franzinite	$(Na,Ca)_7(Si,Al)_{12}O_{24}(SO_4,CO_3,OH,Cl)_3 \cdot H_2O$	No	No	1	No	Occurs in pumice in Italy
friedelite	$(Mn,Fe)_8Si_6O_{15}(OH,Cl)_{10}$	No	No	1	No	Hydrothermal mineral
frondelite	$(Mn^{+2},Fe^{+2})Fe^{+3}{}_4(PO_4)_3(OH)_5$	Yes	No	1	No	Alters from triphylite in pegmatites, precursor absent
fukalite	$Ca_4Si_2O_6(CO_3)(OH,F)_2$	No	No	1	No	Metamorphic mineral

Table IV-1 Critique of Minerals not Included in Project Databases (Continued)

Mineral	Chemical Formula	Precipitates from 0-100ºC and at 1 ATM	Needed	Criterion	Within Defined Physico-chemical System	Comments on Occurrence or Formation
galaxite	$(Mn,Fe^{+2},Mg)(Al,Fe^{+3})_2O_4$	?	No	1	No	Occurs in vein with other Mn minerals
galeite	$Na_{15}(SO_4)_5F_4Cl$	Yes?	No	6	Possibly	Occurs in lacustrine evaporites. Other minerals, e.g., thenardite, halite, villiaumite, provide adequate conservatism for elements in this mineral
ganophyllite	$(Na,K)(Mn,Fe^{+2},Al)_5(Si,Al)_6O_{15}(OH)_5 \cdot 2H_2O$	No	No	1	No	Hydrothermal mineral
garronite	$Na_2Ca_5Al_{12}Si_{20}O_{64} \cdot 27H_2O$	No?	No	1	No	Zeolite found in basalts
garyansellite	$(Mg,Fe^{+3})_6(PO_4)_4(OH)_3 \cdot 3H_2O$	No?	No	1	No	Occurs in iron formation
gatumbaite	$CaAl_2(PO_4)_2(OH)_2 \cdot H_2O$	No	No	1	No	Igneous mineral
gearksutite	$CaAlF_4(OH) \cdot H_2O$	No	No	1	No	Hydrothermal mineral
gedrite	$(Mg,Fe^{+2})_5Al_2(Si_6Al_2)O_{22}(OH)_2$	No	No	1	No	Metamorphic
geikielite	$MgTiO_3$	No	No	1	No	Metamorphic
giniite	$Fe^{+2}Fe^{+3}{}_4(PO_4)_4(OH)_2 \cdot 2H_2O$	No	No	1	No	Igneous mineral
giorgiosite	$Mg_5(CO_3)_4(OH)_2 \cdot 5H_2O$	Yes	No	1	Possibly	Weathering product on lava
giuseppettite	$(Na,K,Ca)_{7\text{-}8}(Si,Al)_{12}O_{24}(SO_4,Cl)_{1\text{-}2}$	No	No	1	No	Veinlets in feldspar rich igneous rock
glaucochroite	$CaMnSiO_4$	No	No	1	No	Metamorphic mineral
glauconite	$(K,Na)(Fe^{+3},Al,Mg)_2(Si,Al)_4O_{10}(OH)_2$	Yes	No	1	No	Forms in marine sands & sedimentary rocks
glaucophane	$Na_2(Mg,Fe^{+2})_3Al_2Si_8O_{22}(OH)_2$	No	No	1	No	Metamorphic
glushinskite	$MgC_2O_4 \cdot 2H_2O$	Yes	No	1	No	Occurs with lichen
gmelinite	$(Na_2,Ca)Al_2Si_4O_{12} \cdot 6H_2O$	No?	No	1	No	Zeolite found in basalts
goldichite	$KFe^{+3}(SO_4)_2 \cdot 4H_2O$	Yes	No	1	No	In talus below a pyritic deposit
gonnardite	$Na_2CaAl_4Si_6O_{20} \cdot 7H_2O$	No?	No	1	No	Zeolite found in basalts & in pyritic metamorphic rock.
gonyerite	$(Mn,Mg)_5Fe^{+3}(Si_3Fe^{+3})O_{10}(OH)_8$	No	No	1	No	Hydrothermal mineral
goosecreekite	$CaAl_2Si_6O_{16} \cdot 10H_2O$	No?	No	1	No	Associated with diabase
gordonite	$MgAl_2(PO_4)_2(OH)_2 \cdot 8H_2O$	?	No	1	No	Associated with variscite

Table IV-1 Critique of Minerals not Included in Project Databases (Continued)

Mineral	Chemical Formula	Precipitates from 0-100ºC and at 1 ATM	Needed	Criterion	Within Defined Physico-chemical System	Comments on Occurrence or Formation
görgeyite	$K_2Ca_5(SO_4)_6 \cdot H_2O$	Yes?	No	6	No	In marine evaporite. Syngenite provides adequate conservatism for this mineral.
gormanite	$Fe^{+2}{}_3Al_4(PO_4)_4(OH)_6 \cdot 2H_2O$	?	No	1	No	Associated with phosphate deposits
graftonite	$(Fe^{+2},Mn^{+2},Ca)_3(PO_4)_2$	Yes	No	1	No	Igneous mineral
gregoryite	$(Na_2,K_2,Ca)CO_3$	No	No	1	No	Igneous mineral
greigite	$Fe^{+2}Fe^{+3}{}_2S_4$	Yes	No	1	No	Forms under reducing conditions
groutite	$Mn^{+3}O(OH)$	?	No	1	No	Occurs in Fe & talc deposits, probably metamorphic
grunerite	$(Fe,Mg)_7Si_8O_{22}(OH)_2$	No	No	1	No	Metamorphic
gupeiite	Fe_3Si	No	No	1	No	Probably extraterrestrial
hagendorfite	$(Na,Ca)Mn(Fe^{+2},Fe^{+3},Mg)_2(PO_4)_3$	No	No	1	No	Igneous mineral
halloysite	$Al_2Si_2O_5(OH)_4$	Yes	No	3	Yes	Kaolinite provides adequate proxy for this mineral
halotrichite	$Fe^{+2}Al_2(SO_4)_4 \cdot 22H_2O$	Yes	No	1	No	Alteration product of pyrite, precursor absent. Also, a fumarolic & hydrothermal mineral.
hanksite	$KNa_{22}(SO_4)_9(CO_3)_2Cl$	Yes?	No	6	Possibly	Occurs in lacustrine evaporites. Other minerals, e.g., glaserite, burkeite, sylvite, provide adequate conservatism for elements in this mineral.
hannayite	$(NH_4)_2Mg_3H_4(PO_4)_4 \cdot 8H_2O$	Yes	No	1	No	Occurs with bat guano
hastingsite	$NaCa_2(Fe^{+2},Mg)_4Fe^{+3}(Al_2Si_6)O_{22}(OH)_2$	No	No	1	No	Igneous & metamorphic mineral
hatrurite	Ca_3SiO_5	No	No	1	No	Metamorphic mineral
hauerite	MnS_2	Yes	No	1	No	Sulfide mineral, requires reducing conditions.
haüyne	$(Na,Ca)_{4-8}Al_6Si_6(O,S)_{24}(SO_4,Cl)_{1-2}$	No	No	1	No	Igneous mineral

Table IV-1 Critique of Minerals not Included in Project Databases (Continued)

Mineral	Chemical Formula	Precipitates from 0-100ºC and at 1 ATM	Needed	Criterion	Within Defined Physico-chemical System	Comments on Occurrence or Formation
henritermierite	$Ca_3(Mn^{+3},Al)_2(SiO_4)_2(OH)_4$	No?	No	1	No	Occurs in Mn deposits
herschelite	$(Na,Ca,K)AlSi_2O_6 \cdot 3H_2O$	No?	No	1	No	Occurs in cavities in basalt
heterosite	$(Fe^{+3},Mn^{+3})PO_4$	Yes?	No	1	No	Alters from triphylite, precursor absent.
hieratite	K_2SiF_6	No	No	1	No	Fumarolic mineral
hillebrandite	$Ca_2SiO_3(OH)_2$	No	No	1	No	Metamorphic mineral
hisingerite	$Fe^{+3}{}_2Si_2O_5(OH)_4 \cdot 2H_2O$	Yes	No	6	Possibly	Weathering product, but may be slow to form. Greenalite provides a reasonable proxy for this mineral.
högbomite	$Mg(Al,Fe,Ti)_4O_7$	No?	No	1	No	Occurs with emery, magnetite, & corundum, hence is metamorphic.
hohmannite	$Fe^{+3}{}_2(SO_4)_2(OH)_2 \cdot 7H_2O$	No	No	1	No	Hydrothermal or alteration product at sulfide mines.
holtedahlite	$Mg_2(PO_4)(OH)$	No	No	1	No	Igneous or metamorphic mineral
hotsonite	$Al_{11}(PO_4)_2(SO_4)_3(OH)_{21} \cdot 16H_2O$	No	No	1	No	Metamorphic mineral
howieite	$Na(Fe^{+2},Mn)_{10}(Fe^{+3},Al)_2Si_{12}O_{31}(OH)_{13}$	No	No	1	No	Metamorphic mineral
humberstonite	$Na_7K_3Mg_2(SO_4)_6(NO_3)_2 \cdot 6H_2O$	Yes	No	6	No	Associated with nitrates in Atacama desert. Other minerals, e.g., bloedite, picromerite, niter, soda niter, provide adequate conservatism for elements in this mineral.
humboldtine	$Fe^{+2}C_2O_4 \cdot 2H_2O$	Yes	No	1	No	Associated with coal, outside redox range
humite	$(Mg,Fe^{+2})_7(SiO_4)_3(F,OH)_2$	No	No	1	No	Metamorphic mineral
hureaulite	$Mn_5(PO_4)_2[PO_3(OH)]_2 \cdot 4H_2O$	No	No	1	No	Alters from triphylite in pegmatites, precursor absent
hydroastrophyllite	$(H_3O,K,Ca)_3(Fe^{+2},Mn)_{5-6}Ti_2Si_6(O,OH)_{31}$	Yes	No	1	No	Weathering product in an alkalic pegmatite

Table IV-1 Critique of Minerals not Included in Project Databases (Continued)

Mineral	Chemical Formula	Precipitates from 0-100ºC and at 1 ATM	Needed	Criterion	Within Defined Physico-chemical System	Comments on Occurrence or Formation
hydrobasaluminite	$Al_4(SO_4)(OH)_{10}\cdot 12\text{-}36H_2O$	Yes	No	1	No	Weathering product in siderite & clay deposits
hydrocalumite	$Ca_2Al(OH)_6[Cl_{1-x}(OH)_x]\cdot 3H_2O$	No	No	1	No	In vugs in a metamorphic rock
hydroglauberite	$Na_4Ca(SO_4)_3\cdot 2H_2O$	Yes	No	6	Yes	Other minerals, notably glauberite, provide adequate conservatism for elements in this mineral.
hydrogrossular	$Ca_3Al_2(SiO_4)_{3-x}(OH)_{4x}$	No?	No	1	No?	Dominantly a metamorphic mineral. Grossular provides adequate conservatism.
hydrohalite	$NaCl\cdot 2H_2O$	No	No	1	No	Stable only below 0º C.
hydromolysite	$FeCl_3\cdot 6H_2O$	Yes	No	1	No	Alteration of pyrite, precursor absent
hydronium jarosite	$(H_3O)Fe^{+3}{}_3(SO_4)_2(OH)_6$	Yes	No	1	No	Alteration of pyrite, precursor absent, or in similar settings.
hydroscarbroite	$Al_{14}(CO_3)_3(OH)_{36}\cdot nH_2O$	?	No	1	Unlikely	Little detail available, Formation would require unusual conditions, such as repression of gibbsite precipitation.
hydrotalcite	$Mg_6Al_2(CO_3)(OH)_{16}\cdot 4H_2O$	?	No	6	No	Occurs in rocks with high Mg, such as serpentine. Other minerals provide adequate conservatism for elements in this mineral.
hydrougrandite	$(Ca,Mg,Fe^{+2})_3(Fe^{+3},Al)_2(SiO_4)_{3-x}(OH)_{4x}$	No	No	1	No	Igneous mineral
hydroxyapophyllite	$KCa_4Si_8O_{20}(OH,F)\cdot 8H_2O$	No?	No	1	No?	Reported occurrences in mines. Probably similar settings as fluorapophyllite.
hydroxylellestadite	$Ca_{10}(SiO_4)_3(SO_4)_3(OH,Cl,F)_2$	No	No	1	No	Occurs in metamorphic rocks
ikaite	$CaCO_3\cdot 6H_2O$	No?	No	1	No	Occurs in a fjord in Greenland
ilvaite	$CaFe^{+2}{}_2Fe^{+3}(SiO_4)_2(OH)$	No	No	1	No	Igneous & metamorphic mineral
imandrite	$Na_{12}Ca_3Fe^{+3}{}_2(Si_6O_{18})_2$	No	No	1	No	Igneous mineral

Table IV-1 Critique of Minerals not Included in Project Databases (Continued)

Mineral	Chemical Formula	Precipitates from 0-100ºC and at 1 ATM	Needed	Criterion	Within Defined Physico-chemical System	Comments on Occurrence or Formation
indialite	$(Mg,Fe)_2Al_4Si_5O_{18}$	No	No	1	No	Metamorphic mineral (e.g., in fused rock)
indigirite	$Mg_2Al_2(CO_3)_4(OH)_2 \cdot 15H_2O$	Yes	No	1	No	Occurs in oxidized zone of a Au-Sb deposit
inesite	$Ca_2Mn_7Si_{10}O_{28}(OH)_2 \cdot 5H_2O$	No	No	1	No	Occurs in Mn ore deposits
iowaite	$Mg_4Fe^{+3}(OH)_8OCl \cdot 2\text{-}4H_2O$	No	No	1	No	Occurs in ultramafic rocks
iron	Fe	No	Yes	2	Yes	Iron needed as a component of reactants in geochemical models.
isoclasite	$Ca_2(PO_4)(OH) \cdot 2H_2O$	?	No	6	Possibly	Other minerals, e.g., apatite, provide adequate conservatism for elements in this mineral.
isokite	$CaMg(PO_4)F$	No	No	1	No	Igneous mineral
iwakiite	$Mn^{+2}(Fe^{+3},Mn^{+3})_2O_4$	No?	No	1	No	Occurs in Mn ores
jacobsite	$(Mn^{+2},Fe^{+2},Mg)(Fe^{+3},Mn^{+3})_2O_4$	No	No	1	No	Associated with Mn minerals
jahnsite	$CaMn(Mg,Fe^{+2})_2Fe^{+3}{}_2(PO_4)_4(OH)_2 \cdot 8H_2O$	No	No	1	No	Igneous & metamorphic mineral
janggunite	$Mn^{+4}{}_{5-x}(Mn^{+2},Fe^{+3})_{1+x}O_8(OH)_6$	Yes	No	1	No	Supergene Mn mineral
jasmundite	$Ca_{11}(SiO_4)_4O_2S$	No	No	1	No	Metamorphic mineral
jennite	$Ca_9H_2Si_6O_{18}(OH)_8 \cdot 6H_2O$	No	No	1	No	Metamorphic mineral
jerrygibbsite	$Mn_9(SiO_4)_4(OH)_2$	No	No	1	No	Hydrothermal mineral
jimthompsonite	$(Mg,Fe^{+2})_5Si_6O_{16}(OH)_2$	No	No	1	No	Metamorphic mineral
johannsenite	$Ca(Mn,Fe^{+2})Si_2O_6$	No	No	1	No	Metasomatic mineral; associated with Mn minerals
johnsomervilleite	$Na_{10}Ca_6Mg_{18}(Fe,Mn)_{25}(PO_4)_{36}$	No	No	1	No	Metamorphic mineral
jokokuite	$MnSO_4 \cdot 5H_2O$	Yes	No	1	Yes	Occurs in caves. Associated minerals indicate a reducing environment, outside of redox range.
jouravskite	$Ca_3Mn^{+4}(SO_4)(CO_3)(OH)_6 \cdot 13H_2O$	No?	No	1	No	Associated with Mn minerals on mine dump

Table IV-1 Critique of Minerals not Included in Project Databases (Continued)

Mineral	Chemical Formula	Precipitates from 0-100ºC and at 1 ATM	Needed	Criterion	Within Defined Physico-chemical System	Comments on Occurrence or Formation
juanite	$Ca_{10}Mg_4Al_2Si_{11}O_{39}\cdot 4H_2O$ (?)	Yes	No	1	No	Alters from melilite, precursor absent
julgoldite	$Ca_2Fe^{+2}(Fe^{+3},Al)_2(SiO_4)(Si_2O_7)(OH)_2\cdot H_2O$	No?	No	1	No	Occurs in Fe ore.
jurbanite	$Al(SO_4)(OH)\cdot 5H_2O$	Yes	No	6	No	Post-mining deposit in a Cu mine. Other minerals, e.g., alum-K, gypsum, boehmite, provide adequate conservatism for elements in this mineral.
kaersutite	$NaCa_2(Mg,Fe^{+2})_4Ti(Si_6Al_2)O_{22}(OH)_2$	No	No	1	No	Igneous mineral
kafehydrocyanite	$K_4Fe^{+2}(CN)_6\cdot 3H_2O$	No	No	1	No	Metamorphic mineral
kalinite	$KAl(SO_4)_2\cdot 11H_2O$	?	No	6	?	Alum-K and other K-Al sulfates in data0.ypf provide adequate conservatism for elements in this mineral.
kaliophilite	$KAlSiO_4$	No	No	1	No	Igneous mineral
kalsilite	$KAlSiO_4$	No	No	1	No	Igneous mineral
kamaishilite	$Ca_2Al_2SiO_6(OH)_2$	No	No	1	No	Metamorphic mineral
kanemite	$NaHSi_2O_4(OH)_2\cdot 2H_2O$	Yes	No	6	Yes	Occurs in lacustrine evaporites. Other minerals, e.g., nahcolite, trona, SiO_2(am), provide adequate conservatism for elements in this mineral.
kanoite	$(Mn^{+2},Mg)_2Si_2O_6$	No	No	6	No	A pyroxene, hence probably metamorphic or igneous. Other solids, e.g., SiO_2(am), $Mn(OH)_2$, boehmite, manganite, provide adequate conservatism for elements in this mineral.
kanonaite	$(Mn^{+3},Al)AlSiO_5$	No	No	1	No	Metamorphic mineral
kassite	$CaTi_2O_4(OH)_2$	No	No	1	No	Igneous mineral
katoite	$Ca_3Al_2(SiO_4)_{3-x}(OH)_{4x}$	No	No	1	No	Igneous mineral

Table IV-1 Critique of Minerals not Included in Project Databases (Continued)

Mineral	Chemical Formula	Precipitates from 0-100ºC and at 1 ATM	Needed	Criterion	Within Defined Physico-chemical System	Comments on Occurrence or Formation
kazakovite	$Na_6(Mn,H_2)TiSi_6O_{18}$	No	No	1	No	Igneous mineral
kellyite	$(Mn^{+2},Mg,Al)_3(Si,Al)_2O_5(OH)_4$	No?	No	1	No	Occurs with sulfides in a Mn mine. Requires reducing conditions
kempite	$Mn_2Cl(OH)_3$	?	No	5	No	Rare. Found in a Mn rich boulder.
kennedyite	$MgFe^{+3}{}_2Ti_3O_{10}$	No	No	1	No	Igneous mineral
kenyaite	$Na_2Si_{22}O_{41}(OH)_8 \cdot 6H_2O$	Yes	No	6	Yes	Occurs in lacustrine evaporites. Other minerals, e.g., nahcolite, trona, SiO_2(am), provide adequate conservatism for elements in this mineral.
kidwellite	$NaFe^{+3}{}_9(PO_4)_6(OH)_{10} \cdot 5H_2O$	?	No	6	No?	Found in a few mines, but reference provides no other data on type of occurrence. Other minerals, e.g., strengite, nahcolite, natron, provide adequate conservatism for elements in this mineral.
kilchoanite	$Ca_3Si_2O_7$	No	No	1	No	Metamorphic mineral
killalaite	$Ca_6(Si_2O_7)_2 \cdot H_2O$	No	No	1	No	Metamorphic mineral
kingite	$Al_3(PO_4)_2(OH,F)_3 \cdot 9H_2O$	No?	No	1	No	Associated with a metamorphic, Fe, and phosphate minerals.
kingsmountite	$(Ca,Mn^{+2})_4(Fe^{+2},Mn^{+2})Al_4(PO_4)_6(OH)_4 \cdot 12H_2O$	No	No	1	No	Igneous mineral
kirschsteinite	$CaFe^{+2}SiO_4$	No	No	1	No	Igneous mineral
kittatinnyite	$Ca_4Mn^{+3}{}_4Mn^{+2}{}_2Si_4O_{16}(OH)_8 \cdot 18H_2O$	No	No	1	No	Hydrothermal mineral
kleberite	$FeTi_6O_{13} \cdot 4H_2O$ (?)	?	No	5,6	Unlikely	Rare. Found in Tertiary sediments, Germany. Other minerals, e.g., rutile, goethite, provide adequate conservatism for elements in this mineral.

Table IV-1 Critique of Minerals not Included in Project Databases (Continued)

Mineral	Chemical Formula	Precipitates from 0-100ºC and at 1 ATM	Needed	Criterion	Within Defined Physico-chemical System	Comments on Occurrence or Formation
koashvite	$Na_6(Ca,Mn)(Ti,Fe)Si_6O_{18}\cdot H_2O$	No	No	1	No	Igneous mineral
koenenite	$Na_4Mg_9Al_4Cl_{12}(OH)_{22}$	Yes	No	6	Yes?	Marine evaporite. Other minerals, e.g., bischofite, halite, gibbsite, provide adequate conservatism for elements in this mineral.
kogarkoite	$Na_3(SO_4)F$	No	No	1	No	Igneous and sublimated mineral
koktaite	$(NH_4)_2Ca(SO_4)_2\cdot H_2O$	Yes	No	1	No	Requires reducing conditions
koninckite	$Fe^{+3}PO_4\cdot 3H_2O$ (?)	Yes	No	6	Yes	Other minerals, e.g., strengite, provide adequate conservatism for elements in this mineral.
konyaite	$Na_2Mg(SO_4)_2\cdot 5H_2O$	Yes	No	6	Yes	Other minerals, e.g., bloedite, provide adequate conservatism for elements in this mineral.
kornelite	$Fe^{+3}{}_2(SO_4)_3\cdot 7H_2O$	Yes	No	6	No?	Oxidation product at Cu mines. Other minerals, e.g., jarosite, provide adequate conservatism for elements in this mineral.
korshunovskite	$Mg_2Cl(OH)_3\cdot nH_2O$	No?	No	1	No	Found in a veinlet in metamorphic rock in Fe ore.
kovdorskite	$Mg_5(PO_4)_2(CO_3)(OH)_2\cdot 9/2H_2O$	No	No	1	No	Igneous mineral
kozulite	$Na_3Mn_4(Fe^{+3},Al)Si_8O_{22}(OH,F)_2$	No	No	1	No	Metamorphic mineral
krausite	$KFe^{+3}(SO_4)_2\cdot H_2O$	Yes?	No	6	Possibly	Other minerals, e.g., jarosite, provide adequate conservatism for elements in this mineral.
kremersite	$(NH_4,K)_2Fe^{+3}Cl_5\cdot H_2O$	No	No	1	No	Fumarolic mineral
kribergite	$Al_5(PO_4)_3(SO_4)(OH)_4\cdot 2H_2O$ (?)	No?	No	1	No	Occurs within a sulfide, outside redox range.

Table IV-1 Critique of Minerals not Included in Project Databases (Continued)

Mineral	Chemical Formula	Precipitates from 0-100ºC and at 1 ATM	Needed	Criterion	Within Defined Physico-chemical System	Comments on Occurrence or Formation
kryzhanovskite	$MnFe^{+3}{}_2(PO_4)_2(OH)_2 \cdot H_2O$	No	No	1	No	Alters from pegmatitic phosphates, which are absent.
kulkeite	$Mg_8Al(AlSi_7)O_{20}(OH)_{10}$	No	No	1	No	Metamorphic mineral
kutnohorite	$Ca(Mn,Mg,Fe^{+2})(CO_3)_2$	No	No	1	No	Metamorphic mineral
kvanefjeldite	$Na_4(Ca,Mn)Si_6O_{14}(OH)_2$	No	No	1	No	Igneous mineral
lacroixite	$NaAl(PO_4)(F,OH)$	No	No	1	No	Igneous mineral
laihunite	$Fe^{+2}Fe^{+3}{}_2(SiO_4)_2$	No	No	1	No	Metamorphic mineral
landesite	$(Mn,Mg)_9Fe^{+3}{}_3(PO_4)_8(OH)_3 \cdot 9H_2O$	No	No	1	No	Igneous mineral
langbeinite	$K_2Mg_2(SO_4)_3$	Yes?	No	6	Yes?	In marine evaporites. Other minerals, e.g., picromerite, provide adequate conservatism for elements in this mineral.
lannonite	$HCa_4Mg_2Al_4(SO_4)_8F_9 \cdot 32H_2O$	Yes	No	1	No	Most mine product with other F minerals
latiumite	$(Ca,K)_8(Al,Mg,Fe)(Si,Al)_{10}O_{25}(SO_4)$	No	No	1	No	Metamorphic mineral
laubmannite	$Fe^{+2}{}_3Fe^{+3}{}_6(PO_4)_4(OH)_{12}$	Yes	No	6	No?	Found in gossan. Other minerals, e.g., strengite, provide adequate conservatism for elements in this mineral.
laueite	$Mn^{+2}Fe^{+3}{}_2(PO_4)_2(OH)_2 \cdot 8H_2O$	No	No	1	No	Igneous mineral
lausenite	$Fe^{+3}{}_2(SO_4)_3 \cdot 6H_2O$	No	No	1	No	Occurs in fire zone in a mine.
lazulite	$(Mg,Fe^{+2})Al_2(PO_4)_2(OH)_2$	No	No	1	No	Igneous, metamorphic, & hydrothermal mineral
lazurite	$(Na,Ca)_8(Al,Si)_{12}(O,S)_{24}[(SO_4),Cl_2,(OH)_2]$	No	No	1	No	Metamorphic mineral
lechatelierite	SiO_2	No	No	1	No	Natural fused silica
lecontite	$Na(NH_4,K)(SO_4) \cdot 2H_2O$	Yes	No	1	No	Occurs in bat guano
lepidocrocite	γ-FeO(OH)	Yes	No	3	Yes	Goethite provides adequate conservatism for this mineral

Table IV-1 Critique of Minerals not Included in Project Databases (Continued)

Mineral	Chemical Formula	Precipitates from 0-100ºC and at 1 ATM	Needed	Criterion	Within Defined Physico-chemical System	Comments on Occurrence or Formation
letovicite	$(NH_4)_3H(SO_4)_2$	No?	No	1	No	Rare. Found as product in burning coal mine and at a hot spring.
leucite	$KAlSi_2O_6$	No	No	1	No	Igneous mineral
leucophoenicite	$Mn_7(SiO_4)_3(OH)_2$	No	No	1	No	Hydrothermal & metamorphic mineral
leucophosphite	$KFe^{+3}{}_2(PO_4)_2(OH)\cdot 2H_2O$	No	No	1	No	Igneous mineral
levyne	$(Ca,Na_2,K_2)_3Al_6Si_{12}O_{36}\cdot 18H_2O$	No	No	1	No	Occurs in cavities in basalt.
liottite	$(Ca,Na,K)_8(Si,Al)_{12}O_{24}(SO_4,CO_3,Cl,OH)_4\cdot H_2O$	No?	No	1	No	Member of cancrinite group, all members of which are related to alkalic igneous or metamorphic rocks.
lipscombite	$(Fe^{+2},Mn)Fe^{+3}{}_2(PO_4)_2(OH)_2$	No	No	1	No	Igneous mineral
lithosite	$K_6Al_4Si_8O_{25}\cdot 2H_2O$	No	No	1	No	Igneous mineral
lizardite	$Mg_3Si_2O_5(OH)_4$	No	No	1	No	Metamorphic mineral
loeweite	$Na_{12}Mg_7(SO_4)_{13}\cdot 15H_2O$	Yes?	No	6	Yes?	Other minerals, e.g., bloedite, provide adequate conservatism for elements in this mineral.
lomonosovite	$Na_2Ti_2Si_2O_9\cdot Na_3PO_4$	No	No	1	No	Igneous mineral
lonecreekite	$(NH_4)FeSO_4)_2\cdot 2H_2O$	Yes	No	1	No	Found as alteration of pyrite in presence of organics. Requires reducing conditions
lorenzenite	$Na_2Ti_2Si_2O_9$	No	No	1	No	Igneous mineral
loughlinite	$Na_2Mg_3Si_6O_{16}\cdot 8H_2O$	No	No	1	No	Hydrothermal(?) mineral; occurs in veins in oil shale
ludlamite	$(Fe^{+2})_3(PO_4)_2\cdot 4H_2O$	Yes	No	1	No	Occurs in oxidation zone of ore deposits and in igneous rocks (pegmatites; alteration of Fe phosphates)
lun'okite	$(Mn,Ca)(Mg,Fe,Mn)Al(PO_4)_2(OH)\cdot 4H_2O$	No	No	1	No	Igneous mineral

Table IV-1 Critique of Minerals not Included in Project Databases (Continued)

Mineral	Chemical Formula	Precipitates from 0-100ºC and at 1 ATM	Needed	Criterion	Within Defined Physico-chemical System	Comments on Occurrence or Formation
macaulayite	$(Fe^{+3},Al)_{24}Si_4O_{43}(OH)_2$	Yes	No	5,6	Unlikely	Very rare in deeply weathered granite. Other minerals, e.g., hematite, kaolinite, provide adequate conservatism for elements in this mineral.
macfallite	$Ca_2Mn^{+3}{}_3(SiO_4)(Si_2O_7)(OH)_3$	Yes?	No	1	No	Associated with replacement of calcite in fissures in basalt. Rare
magadiite	$NaSi_7O_{13}(OH)_3 \cdot 4H_2O$	Yes	No	6	Yes	Occurs in lacustrine evaporites. Other minerals, e.g., nahcolite, trona, SiO_2(am), provide adequate conservatism for elements in this mineral.
maghagendorfite	$NaMgMn(Fe^{+2},Fe^{+3})_3(PO_4)_3$	No?	No	6	No?	Other minerals, e.g., strengite, nahcolite, natron, manganite, provide adequate conservatism for elements in this mineral. Mineral contains reduced Fe & Mn, implying reducing conditions needed.
maghemite	γ-Fe_2O_3	Yes	No	6	Possibly	Found in gossans. Other minerals, e.g., goethite, hematite, provide adequate conservatism for elements in this mineral.
magnesiohornblende	$Ca_2(Mg,Fe^{+2})_4Al(Si_7Al)O_{22}(OH,F)_2$	No	No	1	No	Igneous & metamorphic mineral
magnesioriebeckite	$Na_2(Mg,Fe^{+2})_3Fe^{+3}{}_2Si_8O_{22}(OH)_2$	No	No	1	No	Igneous & metamorphic mineral
magniotriplite	$(Mg,Fe^{+2},Mn)_2(PO_4)F$	No	No	1	No	Igneous mineral
majorite	$Mg_3(Fe,Al,Si)_2(SiO_4)_3$	No	No	1	No	Found in meteorites
makatite	$Na_2Si_4O_8(OH)_2 \cdot 4H_2O$	Yes	No	6	Yes	Evaporite mineral. Other minerals, e.g., trona, SiO_2(am), provide adequate conservatism for elements in

Table IV-1 Critique of Minerals not Included in Project Databases (Continued)

Mineral	Chemical Formula	Precipitates from 0-100ºC and at 1 ATM	Needed	Criterion	Within Defined Physico-chemical System	Comments on Occurrence or Formation
						this mineral.
malladrite	Na_2SiF_6	No	No	1	No	Igneous mineral (fumarolic?)
mallardite	$MnSO_4 \cdot 7H_2O$	Yes	No	1	No	Oxidation product in mines
manasseite	$Mg_6Al_2(CO_3)(OH)_{16} \cdot 4H_2O$	No	No	1	No	Metamorphic mineral
manganpyrosmalite	$(Mn,Fe^{+2})_8Si_6O_{15}(OH,Cl)_{10}$	No	No	1	No	Hydrothermal mineral
manjiroite	$(Na,K)(Mn^{+4},Mn^{+2})_8O_{16} \cdot nH_2O$	Yes	No	1	No	Found in oxidation zone of Mn deposits
mantienneite	$KMg_2Al_2Ti(PO_4)_4(OH)_3 \cdot 15H_2O$	Yes	No	1	No	In black shales. Requires reducing conditions
marcasite	FeS_2	Yes	No	1	No	Occurs under acidic conditions. Pyrite provides adequate conservatism
marialite	$3NaAlSi_3O_8 \cdot NaCl$	No	No	1	No	Metamorphic mineral
maricite	$NaFePO_4$	Yes	No	1	No	Occurs in shales with pyrite, etc. Requires reducing conditions
marokite	$CaMn_2O_4$	No	No	1	No	Hydrothermal mineral
marsturite	$NaCaMn_3Si_5O_{14}(OH)$	No	No	1	No	Metamorphic mineral
matteuccite	$NaHSO_4 \cdot H_2O$	Yes?	No	1	No	In stalactites from 1933 Vesuvius eruption
matulaite	$CaAl_{18}(PO_4)_{12}(OH)_{20} \cdot 28H_2O$	No?	No	1	No	Occurs in an Fe-phosphate mine and a pegmatite
maufite	$(Mg,Ni)Al_4Si_3O_{13} \cdot 4H_2O$ (?)	No	No	1	No	Metamorphic mineral
mazzite	$K_2CaMg_2(Al,Si)_{36}O_{72} \cdot 28H_2O$	No?	No	1	No	Occurs in cavities in basalt
mcgillite	$Mn_8Si_6O_{15}(OH)_8Cl_2$	No	No	1	No	Hydrothermal mineral
meionite	$3CaAl_2Si_2O_8 \cdot CaCO_3$	No	No	1	No	Metamorphic mineral
meixnerite	$Mg_6Al_2(OH)_{18} \cdot 4H_2O$	No	No	1	No	Metamorphic mineral
melanophlogite	SiO_2	No?	No	1	No	Occurs with sulfur or as a metamorphic mineral

Table IV-1 Critique of Minerals not Included in Project Databases (Continued)

Mineral	Chemical Formula	Precipitates from 0-100ºC and at 1 ATM	Needed	Criterion	Within Defined Physico-chemical System	Comments on Occurrence or Formation
mellite	$Al_2(C_6(COO)_6)\cdot 18H_2O$	Yes	No	1	No	Secondary mineral in coal & lignite
melonjosephite	$Ca(Fe^{+2},Mg)Fe^{+3}(PO_4)_2(OH)$	No	No	1	No	Igneous mineral
mendozite	$NaAl(SO_4)_2\cdot 11H_2O$	?	No	6	?	Other solids, e.g., Na_2SO_4, alunite, provide adequate conservatism for elements in this mineral
merrihueite	$(K,Na)_2(Fe,Mg)_5Si_{12}O_{30}$	No	No	1	No	Found in meteorites
messelite	$Ca_2(Fe^{+2},Mn^{+2})(PO_4)_2\cdot 2H_2O$	No	No	1	No	Igneous mineral (late hydrothermal stage)
microsommite	$(Na,Ca,K)_{7\text{-}8}(Si,Al)_{12}O_{24}(Cl,SO_4,CO_3)_{2\text{-}3}$	No	No	1	No	Igneous mineral
millisite	$(Na,K)CaAl_6(PO_4)_4(OH)_9\cdot 3H_2O$	Yes?	No	1	No	Occurs in phosphate rocks
millosevichite	$(Al,Fe^{+3})_2(SO_4)_3$	?	No	1	No	Single occurrence noted, evidently under reducing conditions, as color changes on exposure to air.
minamiite	$(Na,K,Ca)Al_3(SO_4)_2(OH)_6$	No	No	1	No	Hydrothermal or igneous mineral
minguzzite	$K_2Fe^{+3}(C_2O_4)_3\cdot 3H_2O$	Yes?	No	1	No	Found in limonite. Organic radical implies reducing conditions.
minyulite	$KAl_2(PO_4)_2(OH,F)\cdot 4H_2O$	Yes?	No	1	No	Occurs in phosphate deposits
mitridatite	$Ca_3Fe^{+3}{}_4(PO_4)_4(OH)_6\cdot 3H_2O$	No	No	1	No	Igneous mineral
mohrite	$(NH_4)_2Fe^{+2}(SO_4)_2\cdot 6H_2O$	No	No	1	No	Sulfataric mineral
moissanite	SiC	No?	No	1	No	Found in a meteorite, bituminous rocks, with metamorphic minerals.
monetite	$CaHPO_4$	Yes	No	6	No?	Mostly occurs in high phosphate settings. Other minerals, e.g., apatite, provide adequate conservatism for elements in this mineral.
montdorite	$(K,Na)_2(Fe^{+2},Mn,Mg)_5Si_8O_{20}(F,OH)_4$	No	No	1	No	Igneous mineral

Table IV-1 Critique of Minerals not Included in Project Databases (Continued)

Mineral	Chemical Formula	Precipitates from 0-100ºC and at 1 ATM	Needed	Criterion	Within Defined Physico-chemical System	Comments on Occurrence or Formation
montgomeryite	$Ca_4Al_4Mg(PO_4)_6(OH)_4 \cdot 12H_2O$	No?	No	1	No	Igneous mineral, or component of phosphate nodules
morinite	$NaCa_2Al_2(PO_4)_2(F,OH)_5 \cdot 2H_2O$	No	No	1	No	Igneous mineral
motukoreaite	$Na_2Mg_{38}Al_{24}(CO_3)_{13}(SO_4)_8(OH)_{108} \cdot 56H_2O$	Yes	No	6	No	Found as cement in a beach containing basalt. Cement phases included in data0,ypf have similar compositions.
mountainite	$(Ca,Na_2,K_2)_2Si_4O_{10} \cdot 3H_2O$	?	No	6	?	Other minerals, e.g., afwillite, nahcolite, SiO_2(am), provide adequate conservatism for elements in this mineral.
mullite	$Al_6Si_2O_{13}$	No	No	1	No	Found in fused argillaceous inclusions
mundrabillaite	$(NH_4)_2Ca(HPO_4)_2 \cdot H_2O$	Yes	No	1	No	Requires reducing conditions
muskoxite	$Mg_7Fe^{+3}{}_4O_{13} \cdot 10H_2O$	No	No	1	No	Metamorphic mineral
nacaphite	$Na_2Ca(PO_4)F$	No	No	1	No	Igneous mineral
nacrite	$Al_2Si_2O_5(OH)_4$	No	No	1	No	Hydrothermal mineral
nagelschmidtite	$Ca_3(PO_4)_2 \cdot 2(\alpha\text{-}Ca_2SiO_4)$	No	No	1	No	Metamorphic mineral
nahpoite	$Na_2H(PO_4)$	Yes	No	1	No	Occurs in shales with pyrite, etc. Requires reducing conditions
narsarsukite	$Na_2(Ti,Fe^{+3})Si_4(O,F)_{11}$	No	No	1	No	Igneous or metamorphic mineral
nasinite	$Na_2B_5O_8(OH) \cdot 2H_2O$	No	No	1	No	Occurs as encrustation on geothermal well tubing
natisite	$Na_2(TiO)SiO_4$	No	No	1	No	Igneous or metamorphic mineral
natroalunite	$NaAl_3(SO_4)_2(OH)_6$	No	No	1	No	Solfataric or metamorphic mineral
natrojarosite	$NaFe^{+3}(SO_4)_2(OH)_6$	Yes	No	6	No?	Alteration mineral of ores. Other minerals, jarosite, thenardite, provide adequate

Table IV-1 Critique of Minerals not Included in Project Databases (Continued)

Mineral	Chemical Formula	Precipitates from 0-100ºC and at 1 ATM	Needed	Criterion	Within Defined Physico-chemical System	Comments on Occurrence or Formation
						conservatism for elements in this mineral.
natrophilite	$NaMn(PO_4)$	No	No	1	No	Igneous mineral
natrophosphate	$Na_7H(PO_4)_2F \cdot 19H_2O$	No	No	1	No	Igneous mineral
naujakasite	$(Na,K)_6(Fe^{+2},Mn)Al_4Si_8O_{26}$	No	No	1	No	Metamorphic mineral
nefedovite	$Na_5Ca_4(PO_4)_4F$	No	No	1	No	Igneous mineral
neighborite	$NaMgF_3$	Yes	No	1	No	Found in dolomitic "oil shale", & igneous or metamorphic rocks
nekoite	$Ca_3Si_6O_{15} \cdot 7H_2O$	Yes?	No	6	No?	Other minerals, afwillite, foshagite, provide adequate conservatism for elements in this mineral.
neltnerite	$CaMn_6SiO_{12}$	No?	No	1	No	Occurs with Cu and Mn minerals
neotocite	$(Mn,Fe^{+2})SiO_3 \cdot H_2O$ (?)	Yes	No	1	No	Occurs as alteration of Mn silicates, precursors absent
newberyite	$MgHPO_4 \cdot 3H_2O$	Yes	No	1	No	Occurs in bat guano
niahite	$(NH_4)Mn(PO_4) \cdot H_2O$	Yes	No	1	No	Occurs in bat guano
niningerite	(Mg,Fe,Mn)S	No	No	1	No	Found in meteorites
nitromagnesite	$Mg(NO_3)_2 \cdot 6H_2O$	Yes	No	1	Yes	$Mg(NO_3)_2$, included in data0.ypf, provides adequate conservatism.
norbergite	$Mg_3(SiO_4)(F,OH)_2$	No	No	1	No	Metamorphic & hydrothermal mineral
nordstrandite	$Al(OH)_3$	Yes	No	3	No?	Mostly in igneous rocks. Other minerals, e.g., gibbsite, provide adequate conservatism for elements in this mineral.

Table IV-1 Critique of Minerals not Included in Project Databases (Continued)

Mineral	Chemical Formula	Precipitates from 0-100ºC and at 1 ATM	Needed	Criterion	Within Defined Physico-chemical System	Comments on Occurrence or Formation
northupite	$Na_3Mg(CO_3)_2Cl$	Yes	No	6	Yes	Other minerals, e.g., natron, hydromagnesite, halite, provide adequate conservatism for elements in this mineral.
nosean	$Na_8Al_6Si_6O_{24}(SO_4)$	No	No	1	No	Igneous mineral
nsutite	$Mn^{+2}_xMn^{+4}_{1-x}O_{2-2x}(OH)_{2x}$ (x is small)	Yes?	No	1	No	Occurs in Mn deposits
nyböite	$NaNa_2Mg_3Al_2(Si_7Al)O_{22}(OH)_2$	No	No	1	No	Metamorphic mineral
nyerereite	$Na_2Ca(CO_3)_2$	No	No	1	No	Igneous mineral
offretite	$(K_2,Ca)_5Al_{10}Si_{26}O_{72}\cdot 30H_2O$	No?	No	1	No	Associated with basalt
okenite	$Ca_{10}Si_{18}O_{46}\cdot 18H_2O$	No?	No	1	No	Associated with basalt
oldhamite	(Ca,Mn)S	No	No	1	No	Found in meteorites
olympite	Na_3PO_4	No	No	1	No	Igneous mineral
omphacite	$(Ca,Na)(Mg,Fe^{+2},Fe^{+3},Al)Si_2O_6$	No	No	1	No	Metamorphic mineral
opal	$SiO_2\cdot nH_2O$	Yes	No	6	Yes	SiO_2(am) provides adequate conservatism
orientite	$Ca_2Mn^{+2}Mn^{+3}_2Si_3O_{10}(OH)_4$	No?	No	1	No	Occurs in Mn deposits and Mn ores.
osumilite	$(K,Na)(Fe^{+2},Mg)_2(Al,Fe^{+3})_3(Si,Al)_{12}O_{30}\cdot H_2O$	No?	No	1	No	Occurs in vugs in basic igneous rocks
osumilite-(Mg)	$(K,Na)(Mg,Fe)_2(Al,Fe^{+3})_3(Si,Al)_{12}O_{30}\cdot H_2O$	No	No	1	No	Metamorphic mineral
ottrelite	$(Mn,Fe^{+2},Mg)_2Al_4Si_2O_{10}(OH)_4$	No	No	1	No	Metamorphic mineral
overite	$CaMgAl(PO_4)_2(OH)\cdot 2\text{-}4H_2O$	Yes?	No	1	No	Occurs in phosphate rocks
pachnolite	$NaCaAlF_6\cdot H_2O$	No?	No	1	No	Igneous mineral or alteration product of cryolite.
palygorskite	$(Mg,Al)_2Si_4O_{10}(OH)\cdot 4H_2O$	No?	No	6	No?	Mainly a hydrothermal mineral. Mg-montmorillonite provides adequate conservatism.
panasquieraite	$CaMg(PO_4)(OH,F)$	No	No	1	No	Hydrothermal mineral
panethite	$(Na,Ca,K)_2(Mg,Fe,Mn)_2(PO_4)_2$	No	No	1	No	Found in meteorites

Table IV-1 Critique of Minerals not Included in Project Databases (Continued)

Mineral	Chemical Formula	Precipitates from 0-100ºC and at 1 ATM	Needed	Criterion	Within Defined Physico-chemical System	Comments on Occurrence or Formation
parsettensite	$KMn_{10}Si_{12}O_{30}(OH)_{12}$	No?	No	1	No	Occurs in Mn deposits
partheite	$CaAl_2Si_2O_8 \cdot 2H_2O$	No?	No	1	No	Occurs in cavities in ultramafic rock
paulkerrite	$KTi(Mg,Mn)_2(Fe^{+2},Al,Ti,Mg)_2(PO_4)_4(OH)_3 \cdot 15H_2O)$	No	No	1	No	Occurs in phosphate rocks
pectolite	$NaCa_2Si_3O_8(OH)$	No	No	1	No	Associated with basalt
peisleyite	$Na_3Al_{16}(SO_4)_2(PO_4)_{10}(OH)_{17} \cdot 20H_2O$	Yes?	No	1	No	Occurs in phosphate rocks
penkvilksite	$Na_4Ti_2Si_8O_{22} \cdot 5H_2O$	No	No	1	No	Igneous mineral
pennantite	$Mn_5Al(Si_3Al)O_{10}(OH)_8$	No?	No	1	No	Occurs in Mn deposits
perhamite	$Ca_3Al_7(SiO_4)_3(PO_4)_4(OH)_3 \cdot 33/2H_2O$	No	No	1	No	Igneous mineral
phosphoferrite	$(Fe^{+2},Mn)_3(PO_4)_2 \cdot 3H_2O$	No?	No	1	No	Hydrothermal alteration in pegmatites.
phosphorrösslerite	$MgHPO_4 \cdot 7H_2O$	Yes	No	6	?	Other minerals, apatite, brucite, provide adequate conservatism for elements in this mineral, found in an abandoned mine.
phosphosiderite	$Fe^{+3}PO_4 \cdot 2H_2O$	No	No	1	No	Igneous mineral
pianlinite	$Al_2Si_2O_6(OH)_2$	Yes?	No	6	No?	Occurs as a monomineralic clay bed. Other minerals, e.g., kaolinite, provide adequate conservatism for elements in this mineral.
pickeringite	$MgAl_2(SO_4)_4 \cdot 22H_2O$	Yes	No	1	No	Oxidation product in mines, caves, & coal beds
piemontite	$Ca_2(Al,Mn,Fe^{+3})_3Si_3O_{12}(OH)$	No	No	1	No	Igneous & metamorphic mineral
pigeonite	$(Mg,Fe,Ca)(Mg,Fe)Si_2O_6$	No	No	1	No	Igneous mineral (& in meteorites)
plombierite	$Ca_5H_2Si_6O_{18} \cdot 6H_2O$ (?)	?	No	6	?	Other solids, e.g., cement phases included in data0.ypf, provide adequate conservatism for this mineral.

Table IV-1 Critique of Minerals not Included in Project Databases (Continued)

Mineral	Chemical Formula	Precipitates from 0-100ºC and at 1 ATM	Needed	Criterion	Within Defined Physico-chemical System	Comments on Occurrence or Formation
pokrovskite	$Mg_2(CO_3)(OH)_2 \cdot 1/2H_2O$	No?	No	1	No	Vein in ultramafic rock
preiswerkite	$NaMg_2Al_3Si_2O_{10}(OH)_2$	No?	No	1	No	Occurs in cavities in ultramafic rock
prosopite	$CaAl_2(F,OH)_8$	No	No	1	No	Igneous & metamorphic mineral
pseudobrookite	$(Fe^{+3},Fe^{+2})_2(Fe^{+3},Ti)O_5$	No	No	1	No	Igneous mineral & in cavities in basalt
pseudolaueite	$Mn^{+2}Fe^{+3}{}_2(PO_4)_2(OH)_2 \cdot 8H_2O$	No	No	1	No	Igneous mineral
pseudorulite	$Fe^{+3}{}_2Ti_3O_9$ (?)	Yes	No	1	No	Alteration product of ilmenite, precursor absent
pumpellyite	$Ca_2MgAl_2(SiO_4)(Si_2O_7)(OH)_2 \cdot H_2O$	No?	No	1	No	Occurs in cavities in basalt & metamorphic mineral
purpurite	$(Mn^{+3},Fe^{+3})PO_4$	Yes	No	1	No	Alteration product of lithiophilite, precursor absent
pyroaurite	$Mg_6Fe^{+3}{}_2(CO_3)(OH)_{16} \cdot 4H_2O$	No	No	1	No	Metamorphic or hydrothermal mineral
pyrochroite	$Mn(OH)_2$	No	No	1	No	Hydrothermal mineral
pyrope	$Mg_3Al_2(SiO_4)_3$	No	No	1	No	Igneous & metamorphic mineral
pyrophanite	$MnTiO_3$	No	No	1	No	Metamorphic mineral
pyrosmalite	$(Fe,Mn)_8Si_6O_{15}(OH,Cl)_{10}$	No?	No	1	No	Occurs in Fe deposits
pyroxferroite	$(Fe,Mn,Ca)SiO_3$	No	No	1	No	Occurs in lunar rocks
pyroxmangite	$(Mn,Fe)SiO_3$	No	No	1	No	Metamorphic mineral
qandilite	Mg_2TiO_4	No?	No	1	No	Occurs in metamorphic a Mn deposit
qingheiite	$Na_2NaMn_2Mg_2(Al,Fe^{+3})_2(PO_4)_6$	No	No	1	No	Igneous mineral
quenstedtite	$Fe^{+3}{}_2(SO_4)_3 \cdot 10H_2O$	Yes	No	1	No	Oxidation product in mines
raite	$Na_4Mn_3Si_8(O,OH)_{24} \cdot 9H_2O$ (?)	No	No	1	No	Igneous mineral
ralstonite	$Na_xMg_xAl_{2-x}(F,OH)_6 \cdot H_2O$	No	No	1	No	Igneous or metamorphic mineral
ramsdellite	MnO_2	Yes	No	1	No	Occurs in Mn deposits

Table IV-1 Critique of Minerals not Included in Project Databases (Continued)

Mineral	Chemical Formula	Precipitates from 0-100ºC and at 1 ATM	Needed	Criterion	Within Defined Physico-chemical System	Comments on Occurrence or Formation
rancieite	$(Ca,Mn^{+2})Mn^{+4}{}_4O_9 \cdot 3H_2O$	Yes	No	1	No	Occurs in Fe & Mn deposits and on a bauxite-limestone contact
rapidcreekite	$Ca_2(SO_4)(CO_3) \cdot 4H_2O$	Yes	No	1	No	Occurs in Fe deposits
rasvumite	KFe_2S_3	No	No	1	No	Igneous mineral
reddingite	$(Mn,Fe)_3(PO_4)_2 \cdot 3H_2O$	Yes	No	1	No	Secondary phosphate in pegmatites
reinhardbraunsite	$Ca_5(SiO_4)_2(OH,F)_2$	No	No	1	No	Igneous or metamorphic mineral
revdite	$Na_2Si_2O_5 \cdot 5H_2O$	No	No	1	No	Igneous or hydrothermal mineral
reyerite	$(Na,K)_4Ca_{14}(Si,Al)_{24}O_{60}(OH)_5 \cdot 5H_2O$	No	No	1	No	Occurs in cavities in basalt or within basic tuffs.
rhodesite	$(Ca,Na_2,K_2)_8Si_{16}O_{40} \cdot 11H_2O$	No?	No	6	No?	Other minerals, e.g., afwillite, nahcolite, SiO_2(am), provide adequate conservatism for elements in this mineral.
rhomboclase	$HFe^{+3}(SO_4)_2 \cdot 4H_2O$	Yes	No	1	No	Oxidation product in mines
rhönite	$Ca_2(Fe^{+2},Fe^{+3},Mg,Ti)_6(Si,Al)_6O_{20}$	No	No	1	No	Igneous mineral
ribbeite	$Mn_5(SiO_4)_2(OH)_2$	No?	No	1	No	Occurs in Mn pods in dolomite
richellite	$Ca_3Fe^{+3}{}_{10}(PO_4)_8(OH,F)_{12} \cdot nH_2O$ (?)	Yes	No	6	No?	Other minerals, e.g., apatite, goethite, provide adequate conservatism for elements in this mineral.
richterite	$Na_2Ca(Mg,Fe^{+2})_5Si_8O_{22}(OH)_2$	No	No	1	No	Igneous & metamorphic mineral
riebeckite	$Na_2(Fe^{+2},Mg)_3Fe^{+3}{}_2Si_8O_{22}(OH)_2$	No	No	1	No	Igneous & metamorphic mineral
ringwoodite	$(Mg,Fe^{+2})_2SiO_4$	No	No	1	No	Found in meteorites and veins.
rinneite	$K_3NaFe^{+2}Cl_6$	Yes	No	6	Yes	Other minerals, e.g., molysite, sylvite, halite, provide adequate conservatism for

Table IV-1 Critique of Minerals not Included in Project Databases (Continued)

Mineral	Chemical Formula	Precipitates from 0-100ºC and at 1 ATM	Needed	Criterion	Within Defined Physico-chemical System	Comments on Occurrence or Formation
						elements in this mineral.
roaldite	Fe_4N	No	No	1	No	Found in meteorites
robertsite	$Ca_3Mn^{+3}{}_4(PO_4)_4(OH)_6 \cdot 3H_2O$	No	No	1	No	Igneous mineral
rockbridgeite	$(Fe^{+2},Mn)Fe^{+3}{}_4(PO_4)_3(OH)_5$	Yes?	No	1	No	Occurs mostly in pegmatites, also in novaculite
roedderite	$(Na,K)_2(Mg,Fe^{+2})_5Si_{12}O_{30}$	No	No	1	No	Found in meteorites
roggianite	$Ca_8Al_8Si_{16}O_{44}(OH)_{16} \cdot 13H_2O$	No	No	1	No	Igneous mineral
rokühnite	$Fe^{+2}Cl_2 \cdot 2H_2O$	Yes?	No	1	No	Ferrous iron; requires reducing conditions.
römerite	$Fe^{+2}Fe^{+3}{}_2(SO_4)_4 \cdot 14H_2O$	Yes	No	1	No	Oxidation product in mines and associated with phosphates.
rosemaryite	$(Na,Ca,Mn^{+2})(Mn^{+2},Fe^{+2})(Fe^{+3},Fe^{+2},Mg)Al(PO_4)_3$	No	No	1	No	Igneous mineral
rosenhahnite	$Ca_3Si_3O_8(OH)_2$	No	No	1	No	Metamorphic mineral
rostite	$Al(SO_4)(OH) \cdot 5H_2O$	No	No	1	No	Found on burning coal dumps
rozenite	$Fe^{+2}SO_4 \cdot 4H_2O$	Yes	No	1	No	Oxidation product in mines
ruizite	$CaMn^{+3}Si_2O_6(OH) \cdot 2H_2O$	No	No	1	No	Metamorphic mineral
rustumite	$Ca_{10}(Si_2O_7)_2(SiO_4)Cl_2(OH)_2$	No	No	1	No	Metamorphic mineral
sabieite	$(NH_4)Fe^{+3}(SO_4)_2$	Yes	No	1	No	Requires reducing conditions
sacrofanite	$(Na,Ca,K)_9(Si,Al)_{12}O_{24}[(OH)_2,(SO_4),(CO_3),Cl_2]_3 \cdot nH_2O$	No	No	1	No	Igneous or metamorphic mineral
sadanagaite	$(K,Na)Ca_2(Fe^{+2},Mg,Al,Fe^{+3},Ti)_5(Si,Al)_8O_{22}(OH)_2$	No	No	1	No	Metamorphic mineral
samuelsonite	$(Ca,Ba)Fe^{+2}{}_2Mn^{+2}{}_2Ca_8Al_2(PO_4)_{10}(OH)_2$	No	No	1	No	Igneous mineral & in Fe and Mn oxides
sanderite	$MgSO_4 \cdot 2H_2O$	Yes	No	6	Yes	Other minerals, kieserite and leonhardtite, provide adequate conservatism for this mineral.

Table IV-1 Critique of Minerals not Included in Project Databases (Continued)

Mineral	Chemical Formula	Precipitates from 0-100ºC and at 1 ATM	Needed	Criterion	Within Defined Physico-chemical System	Comments on Occurrence or Formation
sanjuanite	$Al_2(PO_4)(SO_4)(OH)\cdot 9H_2O$	Yes?	No	5	No	Rare in some slates in Argentina
santaclaraite	$CaMn^{+2}{}_4Si_5O_{14}(OH)_2\cdot H_2O$	No	No	1	No	Hydrothermal mineral in Cu sulfide deposit.
sapphirine	$(Mg,Al)_8(Al,Si)_6O_{20}$	No	No	1	No	Metamorphic mineral
sarcolite	$(Ca,Na)_9Al_4Si_6O_{26}F$	No	No	1	No	Igneous mineral
sarcopside	$(Fe^{+2},Mn,Mg)_3(PO_4)_2$	No	No	1	No	Igneous mineral
sasaite	$(Al,Fe^{+3})_{14}(PO_4)_{11}(SO_4)(OH)_7\cdot 83H_2O$	Yes	No	1	No	Occurs in bat guano
satterlyite	$(Fe^{+2},Mg,Fe^{+3})_2(PO_4)(OH)$	Yes?	No	1	No	Occurs in shale with pyrite, etc.
scarbroite	$Al_5(CO_3)(OH)_{13}\cdot 5H_2O$	Yes	No	6	No?	Found in sandstone. May be hydrothermal. Other solids, boehmite, gibbsite, provide adequate conservatism for this mineral.
scawtite	$Ca_7Si_6(CO_3)O_{18}\cdot 2H_2O$	No	No	1	No	Metamorphic mineral
schairerite	$Na_2(SO_4)_7F_6Cl$	Yes	No	6	Yes	Other minerals, e.g., thenardite, halite, villiaumite, provide adequate conservatism for elements in this mineral.
schertelite	$(NH_4)_2MgH_2(PO_4)_2\cdot 4H_2O$	Yes	No	1	No	Occurs in bat guano
schorlomite	$Ca_3Ti^{+4}{}_2(Fe^{+3}{}_2Si)O_{12}$	No	No	1	No	Igneous & metamorphic mineral
scorzalite	$(Fe^{+2},Mg)Al_2(PO_4)_2(OH)_2$	No	No	1	No	Igneous or metamorphic mineral
segelerite	$CaMgFe^{+3}(PO_4)_2(OH)\cdot 4H_2O$	No	No	1	No	Igneous mineral
sekaninaite	$(Fe,Mg)_2Al_4Si_5O_{18}$	No	No	1	No	Igneous mineral
senegalite	$Al_2(PO_4)(OH)_3\cdot H_2O$	Yes	No	1	No	Oxidation zone in a mine
serandite	$Mn_2NaSi_3O_8(OH)$	No	No	1	No	Igneous mineral
serendibite	$Ca_2(Mg,Al)_6(Si,Al,B)_6O_{20}$	No	No	1	No	Metamorphic mineral

Table IV-1 Critique of Minerals not Included in Project Databases (Continued)

Mineral	Chemical Formula	Precipitates from 0-100ºC and at 1 ATM	Needed	Criterion	Within Defined Physico-chemical System	Comments on Occurrence or Formation
sergeevite	$Ca_2Mg_{11}(CO_3)_9(HCO_3)_4(OH)_4 \cdot 6H_2O$	?	No	6	Possibly	Other minerals, e.g., huntite, provide adequate conservatism for elements in this mineral.
shafranovskite	$(Na,K)_6(Mn^{+2},Fe^{+2})_3Si_9O_{24} \cdot 6H_2O$	No	No	1	No	Igneous mineral
shigaite	$Al_4Mn_7(SO_4)_2(OH)_{22} \cdot 8H_2O$	No?	No	1	No	Occurs in Mn deposits
shortite	$Na_2Ca_2(CO_3)_3$	No	No	6	No	Occurs in the Green River "oil" shale and in igneous rocks. Natron & calcite provide adequate conservatism for this mineral.
siderazot	Fe_5N_2	No?	No	1	No	Coating on lava (Mt. Vesuvius)
sideronatrite	$Na_2Fe^{+3}(SO_4)_2(OH) \cdot 3H_2O$	Yes	No	1	No	Oxidation product in mines
siderophyllite	$KFe^{+2}{}_2Al(Al_2Si_2)O_{10}(F,OH)$	?	No	6	No?	No occurrence data in reference. A mica. Other minerals, e.g., annite, provide adequate conservatism for elements in this mineral.
siderotil	$Fe^{+2}SO_4 \cdot 5H_2O$	Yes	No	6	Yes?	Other minerals, e.g., melanterite, provide adequate conservatism for this mineral.
sidorenkite	$Na_3Mn(PO_4)(CO_3)$	No	No	1	No	Igneous mineral
sigloite	$(Fe^{+3},Fe^{+2})Al_2(PO_4)_2(OH)_3 \cdot 5H_2O$	No	No	1	No	Hydrothermal mineral
silhydrite	$3SiO_2 \cdot H_2O$	Yes	No	6	No?	Alters from magadiite, which is likely absent. SiO_2(am) provides adequate conservatism.
sinjarite	$CaCl_2 \cdot 2H_2O$	Yes	No	1	Yes	Same as $CaCl_2.H_2O$ in data0.ypf
sinkankasite	$H_2MnAl(PO_4)_2(OH) \cdot 6H_2O$	No	No	1	No	Igneous mineral (secondary in pegmatite)
sinoite	Si_2N_2O	No	No	1	No	Found in meteorites
sjögrenite	$Mg_6Fe^{+3}{}_2(CO_3)(OH)_{16} \cdot 4H_2O$	No	No	1	No	Hydrothermal mineral &

Table IV-1 Critique of Minerals not Included in Project Databases (Continued)

Mineral	Chemical Formula	Precipitates from 0-100ºC and at 1 ATM	Needed	Criterion	Within Defined Physico-chemical System	Comments on Occurrence or Formation
						epitactic on pyroaurite.
slavikite	$NaMg_2Fe^{+3}{}_5(SO_4)_7(OH)_6 \cdot 33H_2O$	Yes	No	1	No	Oxidation product in mines
sobolevite	$Na_{14}Ca_2MnTi_3P_4Si_4O_{34}$	No	No	1	No	Igneous mineral
sobotkite	$(K,Ca/_2)_{0.3}(Mg_2,Al)(Si_3Al)O_{10}(OH)_2 \cdot 5H_2O$	Yes	No	6	No	Occurs in weathered serpentinite. Montmorillonite provides adequate conservatism.
sodalite	$Na_4Al_3Si_3O_{12}Cl$	No	No	1	No	Igneous & metamorphic mineral
sodium_alum	$NaAl(SO_4)_2 \cdot 12H_2O$	Yes	No	6	Yes?	Reported occurrences not authenticated. Other minerals, e.g., alum-K, thenardite, provide adequate conservatism for elements in this mineral.
sonolite	$Mn_9(SiO_4)_4(OH,F)_2$	No?	No	1	No	Occurs in Mn deposits
souzalite	$(Mg,Fe^{+2})_3(Al,Fe^{+3})_4(PO_4)_4(OH)_6 \cdot 2H_2O$	No	No	1	No	Igneous mineral (secondary in pegmatite)
spadaite	$MgSiO_2(OH)_2 \cdot H_2O$ (?)	No	No	1	No	Found in sulfide ores, igneous & metamorphic rocks
spessartine	$Mn_3Al_2(SiO_4)_3$	No	No	1	No	Igneous & metamorphic mineral
spheniscidite	$(NH_4,K)(Fe^{+3},Al)_2(PO_4)_2(OH) \cdot 2H_2O$	Yes	No	1	No	Occurs in penguin guano
spurrite	$Ca_5(SiO_4)_2(CO_3)$	No	No	1	No	Metamorphic mineral
srebrodolskite	$Ca_2Fe^{+3}{}_2O_3$	No	No	1	No	Found in petrified wood baked by burning coal
stanfieldite	$Ca_4(Mg,Fe,Mn)_5(PO_4)_6$	No	No	1	No	Found in meteorites & in veinlets in olivine
staurolite	$Fe_2Al_9(Si,Al)_4O_{22}(OH)_2$	No	No	1	No	Metamorphic mineral
stepanovite	$NaMgFe^{+3}(C_2O_4)_3 \cdot 8\text{-}9H_2O$	Yes	No	1	No	Occurs in coal
stercorite	$Na(NH_4)H(PO_4) \cdot 4H_2O$	Yes	No	1	No	Occurs in bat guano
stevensite	$Mg_3Si_4O_{10}(OH)_2$	No?	No	1	No	Occurs in basalt & dunite

Table IV-1 Critique of Minerals not Included in Project Databases (Continued)

Mineral	Chemical Formula	Precipitates from 0-100ºC and at 1 ATM	Needed	Criterion	Within Defined Physico-chemical System	Comments on Occurrence or Formation
stewartite	$MnFe^{+3}{}_2(PO_4)_2(OH)_2 \cdot 8H_2O$	No	No	1	No	Igneous mineral
stilpnomelane	$K(Fe^{+2},Fe^{+3},Al)_{10}Si_{12}O_{30}(OH)_{12}$	No	No	1	No	Metamorphic mineral
stishovite	SiO_2	No	No	1	No	Forms from meteorite impacts
strätlingite	$Ca_2Al_2SiO_7 \cdot 8H_2O$	No	No	1	No	Metamorphic mineral
strunzite	$MnFe^{+3}{}_2(PO_4)_2(OH)_2 \cdot 8H_2O$	No	No	1	No	Igneous mineral (weathering product in pegmatites), & in phosphorite
struvite	$(NH_4)MgPO_4 \cdot 6H_2O$	Yes	No	1	No	Occurs in bat guano
sudoite	$Mg_2(Al,Fe^{+3})_3Si_3AlO_{10}(OH)_8$	No?	No	1	No	Occurs in Fe deposits, and as hydrothermal mineral
suessite	Fe_3Si	No	No	1	No	Found in meteorites
sulphohalite	$Na_6(SO_4)_2FCl$	Yes	No	6	Yes	Other minerals, e.g., thenardite, halite, villiaumite, provide adequate conservatism for elements in this mineral.
suolunite	$Ca_2Si_2O_5(OH)_2 \cdot H_2O$	No	No	6	No	Occurs in veins in mafic & ultramafic rocks. Afwillite provides adequate conservatism.
sursassite	$Mn_2Al_3(SiO_4)(Si_2O_7)(OH)_3$	No?	No	1	No	Occurs in Mn & Fe deposits
sveite	$KAl_7(NO_3)_4Cl_2(OH)_{16} \cdot 8H_2O$	Yes	No	6	Possibly	Occurs in a cave. Other minerals, niter, sylvite, boehmite, provide adequate conservatism for elements in this mineral.
svetlozarite	$(Ca,K_2,Na_2)Al_2(Si,Al)_{12}O_{28} \cdot 6H_2O$	Yes?	No	1	No	Found as veinlets in andesite
svyazhinite	$(Mg,Mn,Ca)(Al,Fe^{+3})(SO_4)_2F \cdot 14H_2O$	?	No	1	No	Occurs in a mafic fenite (low silica igneous rock)
switzerite	$(Mn,Fe)_3(PO_4)_2 \cdot 7H_2O$	No	No	1	No	Igneous mineral
szmikite	$MnSO_4 \cdot H_2O$	Yes	No	1	No	Oxidation product in mines (efflorescence)
szomolnokite	$Fe^{+2}SO_4 \cdot H_2O$	Yes	No	1	No	Oxidation product in mines

Table IV-1 Critique of Minerals not Included in Project Databases (Continued)

Mineral	Chemical Formula	Precipitates from 0-100ºC and at 1 ATM	Needed	Criterion	Within Defined Physico-chemical System	Comments on Occurrence or Formation
tacharanite	$Ca_{12}Al_2Si_{18}O_{51}\cdot 18H_2O$	No?	No	1	No	Occurs in cavities in basalt & metagabbro
takanelite	$(Mn^{+2},Ca)Mn^{+4}{}_4O_9\cdot 1.3H_2O$	No?	No	1	No	Occurs in Mn deposits
tamarugite	$NaAl(SO_4)_2\cdot 6H_2O$	Yes	No	1	No?	Oxidation product in mines. Thenardite & alunite provide conservatism.
taneyamalite	$(Na,Ca)(Mn^{+2},Mg,Fe^{+3},Al)_{12}Si_{12}(O,OH)_{24}$	No?	No	1	No	Occurs in Mn deposits
taramite	$Na_2Ca(Fe^{+2},Mg)_3Al_2(Si_6Al_2)O_{22}(OH)_2$	No	No	1	No	Igneous mineral
taranakite	$(K,NH_4)Al_3(PO_4)_3(OH)\cdot 9H_2O$	Yes	No	1	No	Occurs in bat guano
tatarskite	$Ca_6Mg_2(SO_4)_2(CO_3)_2Cl_4(OH)_4\cdot 7H_2O$	Yes	No	6	Yes	Other minerals, e.g., tachyhydrite, polyhalite, calcite, provide adequate conservatism for elements in this mineral.
tauriscite	$FeSO_4\cdot 7H_2O$	Yes	No	6	No	Requires reducing conditions. Melanterite provides adequate conservatism for this mineral.
tetrakalsilite	$(K,Na)AlSiO_4$	No	No	1	No	Igneous mineral
tetranatrolite	$Na_2Al_2Si_3O_{10}\cdot 2H_2O$	No?	No	1	No	Occurs as epitactic overgrowth on natrolite, natrolite absent.
thadeuite	$Mg(Ca,Mn)(Mg,Fe,Mn)_2(PO_4)_2(OH,F)_2$	No	No	1	No	Hydrothermal mineral
thaumasite	$Ca_3Si(CO_3)(SO_4)(OH)_6\cdot 12H_2O$	No	No	1	No	Metamorphic mineral, or associated with basalts.
thomsenolite	$NaCaAlF_6\cdot H_2O$	Yes	No	1	No	Alteration product of cryolite.
thomsonite	$NaCa_2Al_5Si_5O_{20}\cdot 6H_2O$	No?	No	1	No	Occurs in cavities in basalt and as metamorphic mineral.
tilleyite	$Ca_5Si_2O_7(CO_3)_2$	No	No	1	No	Metamorphic mineral
tinaksite	$NaK_2Ca_2TiSi_7O_{19}(OH)$	No	No	1	No	Metamorphic mineral
tinsleyite	$KAl_2(PO_4)_2(OH)\cdot 2H_2O$	No	No	1	No	Igneous mineral

Table IV-1 Critique of Minerals not Included in Project Databases (Continued)

Mineral	Chemical Formula	Precipitates from 0-100ºC and at 1 ATM	Needed	Criterion	Within Defined Physico-chemical System	Comments on Occurrence or Formation
tinticite	$Fe^{+3}_6(PO_4)_4(OH)_6 \cdot 7H_2O$	Yes	No	6	Yes	Other minerals, e.g., strengite, provide adequate conservatism for elements in this mineral.
tirodite	$Mn^{+2}_2(Mg,Fe^{+2})_5Si_8O_{22}(OH)_2$	No?	No	1	No	Occurs in deposits high in Mn, Fe, or Mg.
tisinalite	$Na_3H_3(Mn,Ca,Fe)TiSi_6(O,OH)_{18} \cdot 2H_2O$	No	No	1	No	Igneous mineral
tobelite	$(NH_4,K)Al_2(Si_3Al)O_{10}(OH)_2$	No?	No	1	No	Metamorphic (and hydrothermal ?). Requires reducing conditions
tobermorite	$Ca_5Si_6O_{16}(OH)_2 \cdot 4H_2O$	No?	No	6	No?	Other minerals, e.g., zeolites, provide adequate conservatism for this mineral.
tochilinite	$6Fe_{0.9}S \cdot 5(Mg,Fe)(OH)_2$	No	No	1	No	Igneous & metamorphic mineral
todorokite	$(Mn,Ca,Mg)Mn^{+4}_3O_7 \cdot H_2O$	Yes	No	1	No	Alteration product of Mn deposits.
tokkoite	$K_4Ca_4Si_7O_{17}(O,OH,F)_4$	No	No	1	No	Igneous mineral
topaz	$Al_2SiO_4(F,OH)_2$	No	No	1	No	Igneous, metamorphic, & hydrothermal mineral
trikalsilite	$(K,Na)AlSiO_4$	No	No	1	No	Igneous mineral
triplite	$(Mn^{+2},Fe^{+2},Mg,Ca)_2(PO_4)(F,OH)$	No	No	1	No	Igneous & hydrothermal mineral
triploidite	$(Mn^{+2},Fe^{+2})_2(PO_4)(OH)$	No	No	1	No	Igneous mineral & as alteration of triplite.
trolleite	$Al_4(PO_4)_3(OH)_3$	No?	No	1	No	Found in deposits high in phosphate & at a phosphatic iron mine

Table IV-1 Critique of Minerals not Included in Project Databases (Continued)

Mineral	Chemical Formula	Precipitates from 0-100ºC and at 1 ATM	Needed	Criterion	Within Defined Physico-chemical System	Comments on Occurrence or Formation
truscottite	$(Ca,Mn)_{14}Si_{24}O_{58}(OH)_8 \cdot 2H_2O$	No?	No	6	No?	Hydrothermal (only?) mineral. Other solids, e.g., zeolites, Mn minerals, and cement phases, provide adequate conservatism for elements in this mineral.
tschermakite	$Ca_2(Mg,Fe^{+2})_3Al_2(Si_6Al_2)O_{22}(OH)_2$	No	No	1	No	Igneous & metamorphic mineral
tschermigite	$(NH_4)Al(SO_4)_2 \cdot 12H_2O$	No	No	1	No	Hydrothermal mineral & with coal. Requires reducing conditions
tuhualite	$(Na,K)Fe^{+2}Fe^{+3}Si_6O_{15}$	No	No	1	No	Igneous mineral
tungusite	$Ca_4Fe^{+2}{}_2Si_6O_{15}(OH)_6$	No?	No	1	No	Occurs in cavities in basalt
tunisite	$NaCa_2Al_4(CO_3)_4(OH)_8Cl$	No	No	1	No	Hydrothermal mineral
tuperssuatsiaite	$NaFe^{+3}{}_3Si_8O_{20}(OH)_2 \cdot 5H_2O$	Yes?	No	2	Yes?	Hydrothermal (?). Association with aegirine indicates slow rate of formation.
tuscanite	$K(Ca,Na)_6(Si,Al)_{10}O_{22}(SO_4,CO_3,(OH)_2) \cdot H_2O$	No	No	1	No	Igneous or metamorphic mineral
tychite	$Na_6Mg_2(SO_4)(CO_3)_4$	Yes	No	6	Yes	Other minerals, e.g., burkeite, kieserite, provide adequate conservatism for elements in this mineral.
uklonskovite	$NaMg(SO_4)(OH) \cdot 2H_2O$	Yes?	No	6	Yes?	Occurs in marine evaporites. Other minerals, e.g., thenardite, kieserite, villiaumite, provide adequate conservatism for elements in this mineral.
ulvöspinel	$Fe^{+2}{}_2TiO_4$	No	No	1	No	Igneous mineral
ungemachite	$K_3Na_8Fe^{+3}(SO_4)_6(OH)_2 \cdot 6H_2O$	Yes	No	1	No	Oxidation product in mines
ushkovite	$MgFe^{+3}{}_2(PO_4)_2(OH)_2 \cdot 8H_2O$	Yes	No	1	No	Alteration of triplite, not present
ussingite	$Na_2AlSi_3O_8(OH)$	No	No	1	No	Igneous mineral

Table IV-1 Critique of Minerals not Included in Project Databases (Continued)

Mineral	Chemical Formula	Precipitates from 0-100ºC and at 1 ATM	Needed	Criterion	Within Defined Physico-chemical System	Comments on Occurrence or Formation
vanthoffite	$Na_6Mg(SO_4)_4$	Yes?	No	6	Yes?	Occurs in marine evaporites. Other minerals, thenardite, natron, kieserite, provide adequate conservatism for elements in this mineral.
variscite	$AlPO_4 \cdot 2H_2O$	Yes	No	1	No	Forms from phosphatic waters altering aluminous rocks
varulite	$(Na,Ca)Mn(Mn,Fe^{+2},Fe^{+3})_2(PO_4)_3$	No	No	1	No	Igneous mineral
vashegyite	$Al_6(PO_4)_5(OH)_3 \cdot 23H_2O$	Yes	No	1	No	Forms from phosphatic waters altering aluminous rocks
vaterite	$CaCO_3$	Yes	No	1	No	Alters from larnite, which is absent.
vauxite	$Fe^{+2}Al_2(PO_4)_2(OH)_2 \cdot 6H_2O$	No	No	1	No	Occurs in hydrothermal tin deposits
vernadite	$Mn(OH)_4$	Yes	No	6	Yes	Pyrolusite provides adequate conservatism for this mineral.
vertumnite	$Ca_4Al_4Si_4O_6(OH)_{24} \cdot 3H_2O$	?	No	6	No	Found in a geode in igneous rock. Various zeolites provide adequate conservatism.
vesuvianite	$Ca_{10}Mg_2Al_4(SiO_4)_5(Si_2O_7)_2(OH)_4$	No	No	1	No	Igneous & metamorphic mineral
viitaniemiite	$Na(Ca,Mn^{+2})Al(PO_4)(F,OH)_3$	No	No	1	No	Igneous mineral
vinogradovite	$(Na,Ca,K)_4Ti_4AlSi_6O_{23}(OH) \cdot 2H_2O$	No	No	1	No	Igneous or metamorphic mineral (or altered therefrom) at alkalic pegmatite contacts.
viseite	$NaCa_2Al_{10}(SiO_4)_3(PO_4)_5(OH)_{14} \cdot 10H_2O$ (?)	Yes?	No	6	Possibly	Other minerals, e.g., zeolites & apatite, provide adequate conservatism for elements in this mineral.
vishnevite	$(Na,Ca,K)_6(Si,Al)_{12}O_{24}(SO_4,CO_3,Cl)_{2-4} \cdot nH_2O$	No	No	1	No	Igneous mineral
vivianite	$Fe^{+2}{}_3(PO_4)_2 \cdot 8H_2O$	Yes	No	1	No	Requires reducing conditions
voltaite	$K_2Fe^{+2}{}_5Fe^{+3}{}_4(SO_4)_{12} \cdot 18H_2O$	Yes	No	1	Yes	Igneous mineral or sulfide ore oxidation product

Table IV-1 Critique of Minerals not Included in Project Databases (Continued)

Mineral	Chemical Formula	Precipitates from 0-100ºC and at 1 ATM	Needed	Criterion	Within Defined Physico-chemical System	Comments on Occurrence or Formation
vuagnatite	$CaAlSiO_4(OH)$	No	No	1	No	Igneous mineral
wadsleyite	β-$(Mg,Fe^{+2})_2SiO_4$	No	No	1	No	Found in meteorites
wagnerite	$(Mg,Fe^{+2})_2PO_4F$	No	No	1	No	Igneous, metamorphic, & hydrothermal mineral
wardite	$NaAl_3(PO_4)_2(OH)_4 \cdot 2H_2O$	Yes?	No	1	No	Occurs in phosphate rocks & pegmatites
wattevillite	$Na_2Ca(SO_4)_2 \cdot 4H_2O$ (?)	Yes	No	1	No	Occurs in pyritic lignite, hence likely an oxidation product of the pyrite.
wavellite	$Al_3(PO_4)_2(OH,F)_3 \cdot 5H_2O$	Yes	No	1	No	Occurs in phosphate, hydrothermal, & metamorphic rocks
weberite	Na_2MgAlF_7	No	No	1	No	Igneous & metamorphic mineral
weddellite	$Ca(C_2O_4) \cdot 2H_2O$	No?	No	1	No	Requires reducing conditions
wegscheiderite	$Na_5(CO_3)(HCO_3)_3$	Yes	No	6	Yes	Occurs in lacustrine evaporites. Other minerals, e.g., nahcolite, natron, provide adequate conservatism for elements in this mineral.
wermlandite	$Ca_2Mg_{14}Al_4(CO_3)(OH)_{42} \cdot 29H_2O$	No	No	6	No	Occurs in an Fe deposit. Calcite, hydromagnesite, boehmite provide adequate conservatism.
whewellite	$CaC_2O_4 \cdot H_2O$	Yes	No	1	No	Occurs in coal. Requires reducing conditions.
whiteite	$Ca(Fe,Mn^{+2})Mg_2Al_2(PO_4)_4(OH)_2 \cdot 8H_2O$	No	No	1	No	Igneous mineral
whitmoreite	$Fe^{+2}Fe^{+3}{}_2(PO_4)_2(OH)_2 \cdot 4H_2O$	No	No	1	No	Igneous mineral
wicksite	$NaCa_2(Fe^{+2},Mn^{+2})_4MgFe^{+3}(PO_4)_6 \cdot 2H_2O$	?	No	1	No	Occurs in nodules with pyrite. Requires reducing conditions
wilcoxite	$MgAl(SO_4)_2F \cdot 18H_2O$	Yes	No	1	No	Oxidation product in mines
willhendersonite	$KCaAl_3Si_3O_{12} \cdot 5H_2O$	No?	No	1	No	Occurs in cavities in basalt
winchite	$NaCa(Mg,Fe^{+2})_4AlSi_8O_{22}(OH)_2$	No?	No	1	No	Occurs in Mn deposits

Table IV-1 Critique of Minerals not Included in Project Databases (Continued)

Mineral	Chemical Formula	Precipitates from 0-100ºC and at 1 ATM	Needed	Criterion	Within Defined Physico-chemical System	Comments on Occurrence or Formation
wolfeite	$(Fe^{+2},Mn)_2(PO_4)(OH)$	No	No	1	No	Igneous & hydrothermal mineral
wonesite	$(Na,K)(Mg,Fe,Al)_6(Si,Al)_8O_{20}(OH,F)_4$	No	No	1	No	Metamorphic mineral
woodhouseite	$CaAl_3(PO_4)(SO_4)(OH)_6$	Yes	No	6	Yes?	Metamorphic, and cave, mineral. Other minerals, e.g., apatite and gypsum, provide adequate conservatism for elements in this mineral.
wyllieite	$(Na,Ca,Mn^{+2})(Mn^{+2},Fe^{+2})(Fe^{+2},Fe^{+3},Mg)Al(PO_4)_3$	?	No	1	?	Mineral is high in Fe and Mn. Reference provides very little data on occurrence, but, in view of the locality, the mine is likely in a pegmatite.
xanthoxenite	$Ca_4Fe^{+3}{}_2(PO_4)_4(OH)_2 \cdot 3H_2O$	No	No	1	No	Alters from igneous mineral, triplite.
xifengite	Fe_5Si_3	No	No	1	No	Extraterrestrial origin
xitieshanite	$Fe^{+3}(SO_4)(OH) \cdot 7H_2O$	Yes	No	1	No	Oxidation product in mines
yagiite	$(Na,K)_3Mg_4(Al,Mg)_6(Si,Al)_{24}O_{60}$	No	No	1	No	Found in meteorites
yaroslavite	$Ca_3Al_2F_{10}(OH)_2 \cdot H_2O$	Yes	No	1	No	Oxidation product in mines
yavapaiite	$KFe^{+3}(SO_4)_2$	Yes	No	1	No	Oxidation product in mines
ye'elimite	$Ca_4Al_6O_{12}(SO_4)$	No	No	1	No	Metamorphic mineral
yoderite	$(Al,Mg,Fe)_2Si(O,OH)_5$	No	No	1	No	Metamorphic mineral
yofortierite	$(Mn,Mg)_5Si_8O_{20}(OH)_2 \cdot 4\text{-}5H_2O$	No	No	1	No	Igneous mineral
yugawaralite	$CaAl_2Si_6O_{16} \cdot 4H_2O$	No	No	1	No	Hydrothermal mineral
yuksporite	$KNaCa_2(Si,Ti)_4O_{11}F \cdot nH_2O$	?	No	6	?	No data on occurrence in reference. Other minerals, e.g., zeolites, rutile, provide adequate conservatism for elements in this mineral.
zaherite	$Al_{12}(SO_4)_5(OH)_{26} \cdot 20H_2O$	Yes?	No	6	No	Occurs with other Al minerals. Kaolinite & boehmite provide adequate conservatism for this mineral.

Table IV-1 Critique of Minerals not Included in Project Databases (Continued)

Mineral	Chemical Formula	Precipitates from 0-100ºC and at 1 ATM	Needed	Criterion	Within Defined Physico-chemical System	Comments on Occurrence or Formation
zakharovite	$Na_4Mn^{+2}{}_5Si_{10}O_{24}(OH)_6 \cdot 6H_2O$	No	No	1	No	Igneous or metamorphic mineral
zeophyllite	$Ca_4Si_3O_8(OH,F)_4 \cdot 2H_2O$	No?	No	1	No	Occurs in cavities in basalt
zhemchuzhnikovite	$NaMg(Al,Fe^{+3})(C_2O_4)_3 \cdot 8H_2O$	Yes	No	1	No	Requires reducing conditions, occurs in coal.
zirklerite	$(Fe,Mg,Ca)_9Al_4Cl_{18}(OH)_{12} \cdot 14H_2O$ (?)	Yes?	No	6	Yes?	Occurs in marine evaporites. Other solids, e.g., bischofite, sinjarite, portlandite, $Fe(OH)_2$, molysite, provide adequate conservatism for elements in this mineral.
zorite	$Na_3(Ti,Al)_2Si_4(O,OH)_{14} \cdot 3H_2O$	No	No	1	No	Igneous mineral
zunyite	$Al_{13}Si_5O_{20}(OH,F)_{18}Cl$	No	No	1	No	Occurs in igneous, hydrothermal, and highly aluminous deposits
zussmanite	$K(Fe^{+2},Mg,Mn)_{13}(Si,Al)_{18}O_{42}(OH)_{14}$	No	No	1	No	Metamorphic mineral
zwieselite	$(Fe^{+2},Mn^{+2},Mg,Ca)_2(PO_4)(F,OH)$	No	No	1	No	Igneous mineral

NOTE: The "?" indicates that there is not enough information in Roberts, et al., to infer or deduce the conditions under which the mineral occurs. In such cases, a conservative approach is taken that it could occur under repository conditions. "No?" means that there's enough information to conclude that the answer is probably no, but that the data given aren't definitive. This is similar for "yes?".

INTENTIONALLY LEFT BLANK